# AIC 2015 TOKYO

# Color and Image

Midterm Meeting of the International Colour Association (AIC)

19-22 May 2015 Tokyo, Japan

# Proceedings

日本色彩学会
THE COLOR SCIENCE ASSOCIATION OF JAPAN

AIC

mcs
MCS 2015

# Time Table

| 5/19 Tue | 5/20 Wed |
|---|---|

**Hour**

**8:00 - 9:00 Registration**    Reception Hall

**9:00 - 9:30 Opening ceremony**
sola city Hall

**9:30 -10:30 Keynote**
sola city Hall

**10:30-10:45 Group Photo**

**10:45-11:15 Coffee Break**

**11:15-12:45 OS1**
**Color Imaging**
(15min x 6)
sola city Hall

**11:15-12:45 OS2**
**Color Environment Design**
(15min x 6)
Room C

**9:00 -17:00**
**Exhibition**
Terrace Room

**12:45-14:15**
**Lunch**

**14:15-15:45 PS1**
**Poster 1**
Lobby / Room B

**15:45-16:00 Coffee Break**

**16:00-17:30 OS3**
**Colorimetry**
(15min x 6)
sola city Hall

**16:00-17:30 OS4**
**Color Vision, Psychophysics**
(15min x 6)
Room C

**10:00-17:30**
**EC Meeting**
Room A

**17:30-19:00**
**Study Group1**
Room A

**17:30-19:00**
**Study Group2**
Room C

**13:00-20:00**
**Registration**
Reception Hall

**18:00-20:00**
**Welcome Reception**
sola city Hall

| 5/21 Thu | 5/22 Fri | Hour |
|---|---|---|

**8:00**

8:00 - 8:30 **Registration** Reception Hall

8:30 - 9:15 **Invited Talk(MCS)**
sola city Hall

9:20 -10:40 MCS1
**Multispectral Imaging System**
(20min x 4)
sola city Hall

9:20 -10:35 OS5
**Color Education & Culture**
(15min x 5)
Room C

10:40-11:00 **Coffee Break** 10:35-11:00

11:00-12:20 MCS2
**Multispectral Color Science**
(20min x 4)
sola city Hall

11:00-12:15 OS6
**Color and Culture**
(15min x 5)
Room C

9:00 -17:00
**Exhibition**

Terrace Room

12:15-13:45
**Lunch**

13:45-15:15 PS2
**Poster 2**
Lobby / Room B

15:15-15:30 **Coffee Break**

15:30-16:30
**AIC General Assembly**
sola city Hall

16:30-17:45
**Judd Award Lecture**
sola city Hall

17:45-22:30
**Banquet**

8:00 - 8:30 **Registration** Reception Hall

8:30 - 9:15 **Invited Talk**
sola city Hall

9:20 -10:35 OS7
**Appearance, Lighting**(15min x 5)
sola city Hall

9:20 -10:35 OS8
**Color Deficiency**
(15min x 5)
Room C

9:00 -10:50
**Exhibition**

Terrace Room

10:35-10:50 **Coffee Break**

10:50-11:50 OS9
**Cosmetics, Material Perception**(15min x 4)
sola city Hall

10:50-11:50 OS10
**Color Psychology**
(15min x 4)
Room C

11:50-12:35 **Closing ceremony**
sola city Hall

12:45-18:30
**Optional Tour**

Hour
8 : 00
9 : 00
10 : 00
11 : 00
12 : 00
13 : 00
14 : 00
15 : 00
16 : 00
17 : 00
18 : 00
19 : 00
20 : 00

# Floor map  (sola city Conference Center)

## 1F

beverage vending machine

**Room A**
EC Meeting
Study Group

**Room B**

Poster

**Room C**

Oral Presentation
Study Group

To sola city Hall

Room D
Secretariat

WC

WC

To Room A,B,C

From/To subway
Shin-ochanomizu st.

EV

To 2F

Main Entrance

From/To JR ochanomizu st.

## 2F

To Room A,B,C

Staff Room

sola city Hall

Opening/Closing Ceremony

Keynote

Oral Presentation

Welcome Reception

WC

WC

Staff Room

Reception Hall

Exhibition of
Rare Books
on Chromatics

Registration

EV

↑↓

WC

Lobby

Poster

Terrace Room

Exhibition

# AIC2015 TOKYO
# Color and Image

Midterm Meeting of the International Colour Association (AIC)

19-22 May 2015, Ochanomizu sola city Conference Center, Tokyo, Japan

# Proceedings

Editors:  Hirohisa Yaguchi

Katsunori Okajima

Taiichiro Ishida

Kikuko Araki

Motonori Doi

Yoshitsugu Manabe

THE COLOR SCIENCE ASSOCIATION OF JAPAN

# Contents

## Proceedings

# AIC President's Message

For a second time the AIC is to hold a conference in Japan, in Tokyo this time, thanks to the initiative of the Color Science Association of Japan. On the first occasion, the 8th AIC Congress was held in Kyoto, and everyone remembers it as a great event. This year it is to be mid-term meeting dedicated to "Image and Color". This is a very modern issue that encompasses many fields: from acquisition and reproduction of color images to processing the images and their use in computer vision. Many other interesting topics are also included, such as color in computer graphics, colorimetry, digital archiving of art, color vision, color psychology and emotion, environmental color, design, color culture and color education. All of them in their relationship to color images. The conference will also include the 16th International Symposium on Multispectral Color Science, opening the science of color to the world of spectral imaging of large projections today.

We live in a world full of images. Communication between humans relies increasingly on the acquisition and use of images in any method of exchanging information. Optoelectronic audiovisual media of acquisition and reproduction of images and the internet have revolutionized the way we communicate and images are continuously used in color. As a result, new challenges arise: the reliability and quality of images, the development of new algorithms of image processing in order to find new applications, for example in computer vision or in medicine, etc.

Color is an added and differential value in images. We can say that it brings a great deal of transcendental information to those images that are part of our daily life. The visual images that form our eyes together with the retina and the brain processes involved, acquire a higher dimension when they are in color. We can say the same for the images obtained with a camera. I think the opportunity to discuss and exchange ideas in the field of color images at this conference will be extraordinary.

The Color Science Association of Japan is one of the most active regular members of the AIC. Proof of this is the high participation of Japanese scientists in all the AIC congresses and the participation of its members in the management of the AIC as members of the Executive Committee and as Chairs of Study Groups. From these lines I want to publicly thank these efforts that have supported the AIC since its founding and recognize the prestige of so many Japanese scientists in the field of color. I would also like to thank the great effort and work done by the organizing committee of AIC 2015 to enable this conference to be the success which I am sure it will be. The quality of the communications which are collected together in this book is sufficient proof of the magnificent meeting we are going enjoy together.

I wish all attendees a fruitful and enjoyable AIC 2015!

**Javier Romero**
President, International Colour Association

# AIC - International Colour Association

**AIC Executive Committee**

| | |
|---|---|
| President | Javier Romero |
| Past President | Berit Bergström |
| Vice President | Nick Harkness |
| Secretary/Treasurer | Tien-Rein Lee |
| Committee Members | Jin-Sook Lee |
| | Maria João Durão |
| | Nancy Kwallek |
| | Gabriela Nirino |

**AIC Regular Members**

| | |
|---|---|
| Argentina | GRUPO ARGENTINO DEL COLOR |
| Australia | COLOUR SOCIETY OF AUSTRALIA |
| Brazil | ASSOCIAÇÃO PRÓ-COR DO BRASIL |
| Bulgaria | COLOUR GROUP – BULGARIA |
| Canada | COLOUR RESEARCH SOCIETY OF CANADA |
| Chile | ASOCIACIÓN CHILENA DEL COLOR |
| China | COLOR ASSOCIATION OF CHINA |
| Finland | SUOMEN VÄRIYHDISTYS SVY RY |
| France | CENTRE FRANÇAIS DE LA COULEUR |
| Germany | DEUTSCHER VERBAND FARBE |
| Great Britain | THE COLOUR GROUP |
| Hungary | HUNGARIAN NATIONAL COLOUR COMMITTEE |
| Italy | GRUPPO DEL COLORE ASSOCIAZIONE ITALIANA COLORE |
| Japan | COLOR SCIENCE ASSOCIATION OF JAPAN |
| Korea | KOREAN SOCIETY OF COLOR STUDIES |
| Mexico | ASOCIACIÓN MEXICANA DE INVESTIGADORES DEL COLOR |
| Netherlands | NEDERLANDSE VERENIGING VOOR KLEURENSTUDIE |
| Norway | FORUM FARGE |
| Portugal | ASSOCIAÇÃO PORTUGUESA DA COR |
| Slovenia | SLOVENSKO ZDRUZENJE ZA BARVE |
| Spain | COMITÉ ESPAÑOL DEL COLOR |
| Sweden | STIFTELSEN SVENSKT FÄRGCENTRUM |
| Switzerland | PRO/COLORE |
| Taiwan | COLOR ASSOCIATION OF TAIWAN |
| Thailand | THE COLOR GROUP OF THAILAND |
| United States | INTER-SOCIETY COLOR COUNCIL |

**AIC Associate Members**

INTERNATIONAL ASSOCIATION OF COLOR CONSULTANTS/DESIGNERS, North America
COLOUR MARKETING GROUP, USA

**AIC Study Groups**

Study Group on Color Education (CE)
    Chair: Robert Hirschler (Hungary and Brazil)
Study Group on Environmental Color Design (ECD)
    Chair: Verena M. Schindler (Switzerland)
Study Group on Color Vision and Psychophysics (CVP)
    Chair: Katsunori Okajima (Japan)
Study Group on The Language of Color (LC)
    Chair: Dimitris Mylonas (United Kingdom)

# Color Science Association of Japan President's Preface

As the President of the Color Science Association of Japan I would like to welcome all of our participants to AIC2015, being held from May 19th to the 22nd in Tokyo.

Eighteen years ago in 1997 the Color Science Association of Japan held Asia's first international Congress in Japan's old capital of Kyoto, where participants from various countries had the chance to deepen friendships through lively discussions on their research, while simultaneously learning about Japan's traditions and colors. We are very happy that once again, eighteen years since then, the AIC's Midterm Meeting will once again be held in Japan.

The AIC is composed of members from more than 30 countries, and many people from various nations are gathering in Tokyo for AIC2015. We would like for this not only to be a place for research reports and scientific and technical discussions, but hope from the bottom of our hearts that it will be a chance for developing friendships which go beyond the boundaries of location or age. We, the members of the Color Science Association of Japan, have planned the program of AIC2015 Tokyo to be one that participants can enjoy. We hope you will feel happy that you participated in AIC2015 Tokyo. Additionally, to commemorate AIC2015 Tokyo, at the conference site on May 19th we will hold a symposium entitled "Considering Color and Japanese Culture from the Perspective of Food, Clothing, and Shelter" and, on the 20th, an exhibition of rare books by well-known authors such as Michel-Eugène Chevreul.

Now Tokyo is bustling with energy in preparation for the 2020 Olympic Games. We hope AIC2015 participants can observe Tokyo as it grows even more dynamically, and further develops the infrastructure to handle this major international event smoothly.

We, the members of the Color Science Association of Japan, are looking forward to meeting you in Tokyo.

**Takayoshi Fuchida**
President, The Color Science Association of Japan

# Welcome to AIC2015 TOKYO

On behalf of the Steering Committee of AIC2015 TOKYO, I would like to welcome you all to the Midterm Meeting of the International Colour Association in the exciting and traditional city of Tokyo, from May 19-22, 2015.

The meeting is organized by the International Colour Association and the Color Science Association of Japan in cooperation with Ministry of Education, Culture, Sports, Science and Technology (MEXT), Ministry of Economy, Trade and Industry, National Institute of Advanced Industrial Science and Technology, Science Council of Japan, The Tokyo Chamber of Commerce and Industry.

This meeting will provide a unique forum, bringing together researchers, academics, students, artists, architects, industrialists, engineers, designers, computer scientists, lighting experts, media types, exhibitors and business leaders. This year the 16th International Symposium on Multispectral Color Science (MCS 2015) is organized as part of AIC2015. We have chosen "Color and Image" as a theme of AIC2015. The word "image" has a very wide meaning; not only visible presentation, such as imaging devices, displays, pictures, etc., but also a presentation of anything from people's minds. So, we have called for papers from a variety of fields as follows:

Color Imaging
Color Image Processing
Computational Color Image
Color in Computer Graphics
Color Reproduction
Color Image Quality
Multispectral Color Science
Multispectral Imaging
Multispectral Image Acquisition / Display
Spectral Image Applications
Colorimetry / Colorimetric Imaging / Lighting
Digital Archiving of Art
Color Vision / Psychophysics / Physiology
Color Psychology / Emotion
Perception of Material / Surface Quality
Color Image Design
Color Environmental Design
Cosmetics
Personal Color
Color Culture
Color Education

Although as many as 324 papers have been submitted from more than 20 countries, we have to accept a limited number of papers because of limitation of time and space. Finally, we selected 60 oral and 172 papers presentations covering a diverse range of color research and applications based on peer reviews by the International Program Committee.

We have invited three speakers who all are admirable leaders in their fields. Following the opening ceremony on Wednesday, May 20, Ms. Kazuyo Sejima, the recipient of the prestigious Prizker Architecture Prize with Ryue Mishizawa of SANNA, will deliver the Keynote Lecture on the title "The Gathering Space" focusing on her recent works. She will introduce the environment and architecture enhanced by color. During the morning session, invited papers are presented. On Thursday, May 21, Professor Jon Y. Hardeberg of the Gjøvik University College, Norway will give an invited lecture, "Multispectral colour imaging: time to move out of the lab?" He has beeen recommended by MCS and will talk about his main research interests which includes multispectral color imaging, print and image quality, colorimetric device characterization, color management, and cultural heritage imaging. On Friday, May 22, the final day, Professor Hidehiko Komatsu of National Institute for Physiological Sciences talks on "Neural representation of color in visual cortex." He is currently project leader for a large research project "Brain and Information Science on shitsukan (material perception)" funded by MEXT and will talk on neural representation of color in higher visual cortex, neural mechanisms of gloss perception, texture processing, and multimodal integration in material recognition.

Following the General Assembly on Thursday, May 21, the AIC Judd Awards ceremony will be held. The 2015 Judd Award is to be received by Professor Françoise Viénot, Muséum National d'Histoire Naturelle, France. She will deliver the Judd Award Lecture on "On the dimensionality of the colour world."

Finally, I would like to note acknowledgements as the Chair of the Steering Committee. The journey today would not have been possible without a dedicated and hard working Steering Committee all of whom have devoted a considerable amount of time to ensuring that AIC2015 TOKYO will be a great success. I would like to offer my personal and sincere thanks to all of you.

I would also like to thank our sponsors whose generosity and support is greatly appreciated. I would like to ask that you all reciprocate their support when you are seeking products or services offered by our sponsors.

I hope that you all leave the AIC2015 with warm feelings for the exciting city of Tokyo, will have renewed friendships and made new friends in the global color community, and, importantly, be refreshed and stimulated with new ideas to further develop your research in the world of color.

**Hirohisa Yaguchi**
Chair, Steering Committee of AIC2015 TOKYO

# Welcome to MCS2015 TOKYO

As a MCS general chair, I would like to welcome all of you to AIC/MCS2014 TOKYO, which is held in Tokyo, Japan, during May 19–22, 2015. This year, the 16th International Symposium on Multispectral Color Science (MCS 2015) is organized as part of AIC2015 TOKYO.

Many aspects of the multi- and hyper- spectral image acquisition, analysis, and rendering have been extensively researched and studied along with the technological advances in hardware devices, software systems, and signal processing algorithms. Also, spectral imaging science and technology is more and more exploited in numerous applied technologies such as computer vision, computer graphics, biology, medicine, cosmetics, digital archiving, printing, display, and remote sensing. As a consequence, a variety of problems generally encountered have been reformulated, successfully solved, and sometimes cast into their new contexts rising new scientific challenges.

The first MCS symposium was launched at Chiba University, Japan in 1999. Since 2001 the multispectral symposium has been organized by a consortium of international researchers, mostly incorporated into larger international conferences and continues to grow. The 16th International Symposium (MCS2015 TOKYO) builds on the tradition to bring together researchers in the field of spectral color science and imaging.

We received about 40 paper submissions to the MCS group. The AIC/MCS Program Committee finally decided to accept 8 papers for MCS oral, about 20 papers for MCS poster, and some papers for AIC poster from the contributed papers, based on peer reviews by the International Program Committee. Paper presentations related on MCS are scheduled mostly on Thursday, May 21. The morning session starts with an invited lecture by Professor Jon Y. Hardeberg (Gjøvik University College, Norway), entitled "Multispectral colour imaging: time to move out of the lab," which is then followed by the Oral session. The poster presentations are in the afternoon.

I wish that all participants will successfully exchange their knowledge, technologies, and ideas with old and new friends, and enjoy the conference and the most beautiful season in Japan.

**Shoji Tominaga**
General Chair of MCS2015 Tokyo

# AIC 2015 Committees

**Organizing committee**
- Asao Komachiya, Chair
- Mitsuo Ikeda
- Takuzo Inagaki
- Naoyuki Osaka
- Hiroshi Kansaku
- Hitoshi Komatsubara
- Tsuneo Suzuki
- Shinya Takahashi
- Goro Baba
- Shoji Tominaga
- Hideaki Hayashi
- Takayoshi Fuchida
- Masao Yamagishi

**Steering committee**

| | |
|---|---|
| Chair | Hirohisa Yaguchi |
| Secretary | Yoshitsugu Manabe |
| Treasurer | Yoko Mizokami |
| | Kazuo Yamaba |
| Technical Program | |
| | Katsunori Okajima |
| | Shoji Tominaga (MCS) |
| | Taiichiro Ishida |
| | Takuzo Inagaki |
| | Shinya Takahashi |
| | Shinji Nakamura |
| | Norihiro Tanaka |
| Publicity | Motonori Doi |
| | Kohji Yoshimura |
| | Kikuko Araki |
| Local | Takahiko Horiuchi |
| | Ikuko Narita |

**Funding committee**
- Takayoshi Fuchida, Chair
- Akira Kitabatake
- Hitoshi Komatsubara
- Tsuneo Suzuki
- Takaaki Suzuki
- Yoko Matsuda
- Hiroyuki Shinoda
- Katsunori Okajima
- Shinya Takahashi
- Hiroshi Shimazaki
- Yoko Mizokami

**Local arrangements committee**
- Takahiko Horiuchi, Chair
- Ikuko Narita
- Keita Hirai
- Noriko Yata
- Shoko Isawa
- Tomoko Mitsutake
- Yoshihiko Azuma
- Wataru Iwai
- Masako Yamada

**Finance committee**
- Yoko Mizokami, Chair
- Masayuki Osumi
- Kazuo Yamaba

**International Scientific Committee**

Berit Bergstrom, Sweden

Monica Billger, Sweden

Valerie Bonnardel, United Kingdom

José Caivano, Argentina

Vien Cheung, United Kingdom

Osvaldo Da Pos, Italy

Motonori Doi, Japan

Mark Fairchild, United States

Karin Fridell Anter, Sweden

Brian Funt, Canada

Davide Gadia, Italy

Jeremie Gerhardt, Germany

Paul Green-Armytage, Australia

Helen Gurura, South Africa

Aran Hansuebsai, Thailand

Jon Hardeberg, Norway

Nick Harkness, Australia

Markku Hauta-Kasari, Finland

Javier Hernandez-Andres, Spain

Bernhard Hill, Germany

Keita Hirai, Japan

Robert Hirschler, Brazil

Takahiko Horiuchi, Japan

Po-Chieh Hung, United States

Mitsuo Ikeda, Thailand

Francisco Imai, United States

Taiichiro Ishida, Japan

Hyeon Jeongsuk, Korea

Maria Joaodurao, Portugal

Eric Kirchner, Netherlands

Michael Kriss, United States

Youngshin Kwak, Korea

Nancy Kwallek, United States

Derry Law, Hong Kong

Tien-Rein Lee, Taiwan

Wen-Yuan Lee, Taiwan

Reiner Lenz, Sweden

Lindsay  Macdonald, United Kingdom

Yoshitsugu Manabe, Japan

Alamin Mansouri, France

Gabriel Marcu, United States

John Mccann, United States

Manuel Melgosa, Spain

Yoichi Miyake, Japan

Yoko Mizokami, Japan

Nathan Moroney, United States

Judith Mottram, United Kingdom

Dimitris Mylonas, United Kingdom

Shinji Nakamura, Japan

Shigeki Nakauchi, Japan

Sérgio Nascimento, Portugal

Juan Luis Nieves, Spain

Gabriela Nirino, Argentina

Peter Nussbaum, Norway

Tomoko Obama, Japan

Katsunori Okajima, Japan

Li-Chen Ou, Taiwan

Jussi Parkkinen, Malaysia

Carinna Parraman, United Kingdom

Marius Pedersen, Norway

Katia Ripamonti, United Kingdom

Alessandro Rizzi, Italy

Javier Romero, Spain

Maurizio Rossi, Italy

Tetsuya Sato, Japan

Verena M. Schindler, France

James Shyu, Taiwan

Cecilia Sik Lanyi, Hungary

Andrew Stockman, United Kingdom

Pei-Li Sun, Taiwan

Vincent C. Sun, Taiwan

Shoji Sunaga, Japan

Shin'ya Takahashi, Japan

Norihiko Tanaka, Japan

Elza Tantcheva, United Kingdom

Kulthida Teachavorasinskun, Thailand

Shoji Tominaga, Japan

Masaru Tsuchida, Japan

Seiichi Tsujimura, Japan

Norimichi Tsumura, Japan

Eva M. Valero, Spain

Francoise Viénot, France

Yuh-Chang Wei, Taiwan

Stephen Westland, United Kingdom

Haisong Xu, China

Hirohisa Yaguchi, Japan

Sari  Yamamoto , Japan

Yasuki Yamauchi, Japan

Kohji Yoshimura, Japan

# MCS 2015 Committees

**General Chair**

Shoji Tominaga, Japan

**Program Committee of MCS 2015**

Francisco Imai, United States

Jon Yngve Hardeberg, Norway

Markku Hauta-Kasari, Finland

Bernhard Hill, Germany

Alamin Mansouri, France

Yoichi Miyake, Japan

Jussi Parkkinen, Malaysia

Norimichi Tsumura, Japan

Philipp Urban, Germany

**Local Committee of MCS 2015**

Shoji Tominaga, Japan

Masaru Tsuchida, Japan

Keita Hirai, Japan

# Cooperation & Support

**In Cooperation With:**

Ministry of Economy, Trade and Industry

Ministry of Education, Culture, Sports, Science and Technology

National Institute of Advanced Industrial Science and Technology

Science Council of Japan

The Tokyo Chamber of Commerce and Industry

**With the Support of:**

Architectural Institute of Japan

Color Universal Design Organization

Coating Equipment Manufacturers Association of Japan

The Illuminating Engineering Institute of Japan

The Imaging Society of Japan

Information Processing Society of Japan

The Institute of Electrical Engineers of Japan

The Institute of Electronics, Information and Communication Engineers

The Institute of Image Information and Television Engineers

Japan Ergonomics Society

Japanese Cosmetic Science Society

Japanese National Committee of CIE

Japanese Society for the Science of Design

The Japanese Psychological Association

The Japanese Psychonomic Society

The Japanese Society of Ophthaimological Optics

The Japanese Society of Printing Science and Technology

The Japan Paint Manufacturers Association

Japan Society of Colour Material

The Japan Society of Home Economics

Japan Society of Kansei Engineering

The Japan Society of Mechanical Engineers

The Optical Society of Japan

The Society of Cosmetic Chemists of Japan

The Society of Photography and Imaging of Japan

Vision Society of Japan

Suga Weathering Technology Foundation

# Scientific Program

## Keynote Lecture

**9:30 - 10:30   sola city Hall**

*Chair: Hirohisa Yaguchi*

The Gathering Space

*Kazuyo SEJIMA*

## Oral Papers

**11:15-12:45       (sola city Hall)**
**OS1: Color Imaging**

*Chairs: Alessandro Rizzi & Takahiko Horiuchi*

**OS1-1**   How Multi-Illuminant Scenes Affect Automatic Colour Balancing
*Liwen Xu and Brian Funt*

**OS1-2**   The Generalised Reproduction Error for Illuminant Estimation
*Graham Finlayson and Roshanak Zakizadeh*

**OS1-3**   Rank-Based Camera Spectral Sensitivity Estimation
*Graham Finlayson and Maryam Mohammadzadeh Darrodi*

**OS1-4**   Comparing Colour Camera Sensors Using Metamer Mismatch Indices
*Ben Hull and Brian Funt*

**OS1-5**   Advanced Measurement Technology for Image Clarity
*Hideo Kita and Shigeo Suga*

**OS1-6**   Painting by Numbers: Transforming Fields and Edges to Vectors
*Carinna Parraman, Paul O'Dowd and Mikaela Harding*

**11:15-12:45       (Room C)**
**OS2: Color Environment Design**

*Chairs: Taiichiro Ishida & Jin-Sook Lee*

**OS2-1**   Perception of Colours Illuminated by Coloured Light
*Shabnam Arbab and Barbara Szybinska Matusiak*

**OS2-2**   Effects of Furniture Colour on Apparent Volume of Interior Space
*Keishi Yoshida and Masato Sato*

**OS2-3**   Ideal GRID Model for Color Planning of Living Space
*Tien-Rein Lee*

**OS2-4**   Case Studies of Color Planning for Urban Renewal
*Sari Yamamoto*

**OS2-5**   Building Colours in Taipei – Taking Wanhua District as an Example
*Chia-Chi Chang, Ting-Tsung Ho and Li-Chen Ou*

**OS2-6**   Pritzker Prize Laureates' Colour Preferences
*Malvina Arrarte-Grau*

**16:00-17:30       (sola city Hall)**
**OS3: Colorimetry**

*Chairs: Haisong Xu & Yoshitsugu Manabe*

**OS3-1**   Computing Tristimulus Values: An Old Problem for a New Generation
*Zhifeng Wang, Tianyi Li, M. Ronnier Luo, Manuel Melgosa, Michael Pointer and Changjun Li*

**OS3-2**   Variability in Colour Matches between Displays
*Phil Green, Srikrishna Nuduramati and Ivar Farup*

**OS3-3**   A Comparison Study of Camera Colorimetric Characterization Models Considering Capture Settings Adjustment
*Jingyu Fang, Haisong Xu and Wei Ye*

**OS3-4**   Evaluation and Analysis of *YUTEKI-TENMOKU* Visual Effect on Traditional Ceramic Applied Gonio- Photometric Spectral Imaging and Confocal Type Laser Scanning Microscopy
*Masayuki Osumi*

**OS3-5**   Measuring Skin Colours Using Different Spectrophotometric Methods
*YuZhao Wang, Ming Ronnier Luo, Xiao Yu Liu, Haiyan Liu and BinYu Wang*

**OS3-6**   Assessing Light Appearance in Shopping Mall
*Yuteng Zhu, Ming Ye, Wenjie Huang, Muhammad Farhan Mughal, Muhammad Safdar and Ming Ronnier Luo*

**16:00-17:30       (Room C)**
**OS4: Color Vision, Psychophysics**

*Chairs: Yoko Mizokami & Li-Chen Ou*

**OS4-1**   Pupillary Light Reflex Associated with Melanopsin and Cone Photorecetors
*Seiichi Tsujimura and Katsunori Okajima*

**OS4-2**   Experimental Research on EEG Characteristics in Red, Green, Blue, and White Color Space Consequent on the Degree of Depression
*Heewon Lee, Hanna Kim, Jiseon Ryu and Jinsook Lee*

**OS4-3**   Hue-Tone Representation of the Nayatani-Theoretical Color Order System
*Hideki Sakai*

**OS4-4**   Colour Appearance in the Outdoor Environment
*Ya-Chen Liang, Li-Chen Ou and Pei-Li Sun*

**OS4-5**   Color Play: Gamification for Color Vision Study
*Shida Beigpour and Marius Pedersen*

**OS4-6**   Using Visual Illusions to Expand the Available Colors for Making Mosaics
*I-Ping Chen and Wei-Jie Chiou*

## Study Group Meetings

**17:30-19:00  (Room A)**

Study Group on Environmental Color Design
*Chair: Verena M. Schindler*

**17:30-19:00  (Room C)**

Study Group on The Language of Color
*Chair: Dimitris Mylonas*

## Poster Papers
**14:15-15:45   Poster 1   (Room B/Lobby)**
*Chairs: Shoji Sunaga & Norihiro Tanaka*

Room B  : PS1-1~64
Lobby    : PS1-65~87

**PS1-1**  Colour Image, Fashion Design and Identity
*Larissa Noury*

**PS1-2**  Contemporary Art and the Unfoldings of Colour
*Laura Carvalho*

**PS1-3**  Comparison of Slovene Colour Identities by Researchers A. Trstenjak and M. Tusak with Colors on Slovenian Municipality Flags
*Vojko Pogacar*

**PS1-4**  A Comparison of Color Schemes and Images in the Package Design of Sweets in the US and Japan
*Kyoko Hidaka*

**PS1-5**  Human Monochromatic Impressions on Multichromatic/Colorless Phenomena and Concepts
*Ayana Deguchi, Akira Asano, Chie Muraki Asano and Katsunori Okajima*

**PS1-6**  How to Create a Colour Education that Fosters Price-winning Design Students
*Ivar Jung*

**PS1-7**  Influence of Odors Function and Colors Symbolism in Odor-Color Associations: Comparative Study between Rural and Urban Regions in Lebanon
*Léa Nehmé, Reine Barbar, Yelena Maric and Muriel Jacquot*

**PS1-8**  Differences of Generation Dependences of Preferences between Colors and Styles in Women's Fashion
*Chie Muraki Asano, Kanae Tsujimoto, Akira Asano and Katsunori Okajima*

**PS1-9**  Effect of Color Appeared in Signage to Identify Gender of Thai
*Chanida Saksirikosil, Kitirochna Rattanakasamsuk and Ploy Srisuro*

**PS1-10**  Development of Three Primary-color Transparent Cubes for Learning Subtractive Color Mixing Visually
*Keiichi Miyazaki*

**PS1-11**  Multicolor LED Lighting Device with a Microprocessor for Demonstrating Effects of Lighting on Color Appearance
*Takashi Nakagawa*

**PS1-12**  The Effect of Environment Colour on Behavioural Inhibition
*Nicholas Ciccone and Stephen Westland*

**PS1-13**  Influence of Light Incident Angle and Illuminance Intensity on Visual Comfort and Clarity
*Yinqiu Yuan, Li-Ching Chuo, Hsin-Pou Huang and Ming-Shan Jeng*

**PS1-14**  Colour Terms in the Interior Design Process
*Douha Y Attiah, Vien Cheung, Stephen Westland and David Bromilow*

**PS1-15**  Effects of Classroom Wall Color on Students
*Fazila Duyan and Rengin Ünver*

**PS1-16**  A Study on the Evaluation Process of Facade Colour Parameters
*Esra Küçükkılıç Özcan and Rengin Ünver*

**PS1-17**  Correlation between Personal and Classroom color Preferences of Children
*Rengin Ünver and Fazila Duyan*

**PS1-18**  Research on the Coexistence of Color between Buildings and Exterior Advertising that Create a Cityscape  ~ focusing on the Okamoto district of Kobe ~
*Yoshifumi Takahashi and Ikuko Narita*

**PS1-19**  Colour Management in the Colour Design Process
*Per Jutterstrom*

**PS1-20**  Exploring Combinations of Color Patterns in Nature
*Akemi Yamashita and Naoko Takeda*

**PS1-21**  Visual Impressions Induced by Colours of Facial Skin and Lips
*Mei-Ting Liu, Hsing-Ju Hung, Wen-Ling Deng and Li-Chen Ou*

**PS1-22**  International Comparison of Uses of Color for Pictograms
*Yuki Akizuki, Michico Iwata and Hirotaka Suzuki*

**PS1-23**  The Influence of Color on the Perception of Cartographic Visualisations
*Zbyněk Štěrba and Jan D. Bláha*

**PS1-24**  Evaluation of Colour Appearances Displaying on Smartphones
*X. Gao, E. Khodamoradi, L. Guo, X. Yang, S. Tang, W. Guo, Y. Wang*

**PS1-25**  Colour Management for High Dynamic Range Imaging
*Keith D. M. Findlater*

**PS1-26**  Development of a Wide-Gamut Digital Image Set
*Stephen Westland, Qianqian Pan, Yuan Li and Soojin Lee*

**PS1-27**  Construction of Display Profiles Using Simplicial Maps and Application to Color Reproduction of Displays
*Masashi Yamamoto and Jinhui Chao*

**PS1-28**  "Psycolorsynthesis": An Introduction of 10-Color Communication Method
*Chiori Ohnaka*

**PS1-29**  Perceptually Inspired Gamut Mapping between Any Gamuts with Any Intersection
*Javier Vazquez-Corral and Marcelo Bertalmío*

**PS1-62** Influence of the Typical Color in Object Memory Task
*Mikuko Sasaki and Yasuhiro Kawabata*

**PS1-63** Neural Basis of Color Harmony and Disharmony Based on Two-color combination
*Takashi Ikeda and Naoyuki Osaka*

**PS1-64** Psychological Hue Circle of Blind People and Development of a Tactile Color Tag for Clothes
*Saori Okudera, Ken Sagawa, Yuko Nakajima, Natsumi Ohba and Shoko Ashizawa*

**PS1-65** Examination of Method for Decreasing Unpleasantness Caused by Strong Brightness of Smart-phone Displays in Dark Adaptation
*Itsuki Miyamae, Hyojin Jung, Saori Kitaguchi and Tetsuya Sato*

**PS1-66** A Spectral-based Color Vision Deficiency Model Compatible with Dichromat and Anomalous Trichromat
*Hiroaki Kotera*

**PS1-67** Colour Information in Design
*Seahwa Won, Stephen Westland, Kishore Budha and Bruce Carnie*

**PS1-68** Relationship between Perceived Whiteness and Color Vision Characteristics
*Ichiro Katayama, Koichi Iga, Shoko Isawa and Tsuneo Suzuki*

**PS1-69** An Experiment of Color Rendering with 3D Objects
*Laura Blaso, Cristian Bonanomi, Simonetta Fumagalli, Ornella Li Rosi and Alessandro Rizzi*

**PS1-70** Adapting and Adapted Colors under Colored Illumination
*Mitsuo Ikeda, Chanprapha Phuangsuwan and Kanwara Chunvijitra*

**PS1-71** Color Constancy Depends on Initial Visual Information
*Chanprapha Phuangsuwan, Mitsuo Ikeda and Kanwara Chunvijitra*

**PS1-72** Neighboring Color Effect on the Perception of Textile Colors
*Youngjoo Chae, John H. Xin and Tao Hua*

**PS1-73** The Impact of Light at the Perception of Colours in Architecture, State of the Art Study and Suggestions for Further Research
*Shabnam Arbab and Barbara Szybinska Matusiak*

**PS1-74** Evaluation of Cloth Roughness and Smoothness by Visual and Tactile Perceptions: Investigation of Cloth Photography Method for Online Shopping
*Tomoharu Ishikawa, Yuya Akagawa, Kazuma Shinoda, Shigeru Inui, Kazuya Sasaki, Keiko Miyatake and Miyoshi Ayama*

**PS1-75** Study of Color Preferences of Gac Fruit Blended with Mixed Mushroom Juice
*Wattana Wirivutthikorn and Somporn Jenkunawat*

**PS1-76** Luminance Contrast of Thai Letters Influencing Elderly Vision
*Kitirochna Rattanakasamsuk*

**PS1-77** Color Rendering Analysis Based on Color Pair Evaluation under Different LED Lighting Conditions
*Qing Wang, Haisong Xu, Jianqi Cai and Wei Ye*

**PS1-78** The Relationship between Whiteness Perception of Watercolor Illusions and Color Vision Characteristics
*Shoko Isawa, Koichi Iga, Ichiro Katayama and Tsuneo Suzuki*

**PS1-79** Influence of Daylight Illumination in the Visual Saliency Map of Color Scenes
*Juan Ojeda, Juan Luis Nieves and Javier Romero*

**PS1-80** Comparison between Multispectral Imaging Colors of Single Yarns and Spectrophotometric Colors of Corresponding Yarn Swatches
*Lin Luo, Hui-Liang Shen, Si-Jie Shao and John H. Xin*

**PS1-81** New Color Rendering Index Based on Color Discriminability and Its Application to Evaluate Comfortability of Illuminants
*Yasuhisa Nakano, Toshiki Nagasaki, Ryu Toyota, Jiro Kohda and Takuo Yano*

**PS1-82** Color Monitoring Method under High Temperature during Oven Cooking
*Yuji Nakamori, Hiroyuki Iyota, Hideki Sakai, Taiki Matsumoto and Shuhei Nomura*

**PS1-83** Woodblock Printing as a Means for 2.5D and 3D Surface Evaluation
*Teun Baar, Melissa Olen, Carinna Parraman and Maria Ortiz Segovia*

**PS1-84** The Relationships between Colors of Neck, Cheek, and Shaded Face Line Affects Beauty of Made-up Face
*Youhei Ishiguro, Mamiko Nakato, Erika Tokuyama, Nao Matsushita and Minori Yamahara*

**PS1-85** Experimantal Method Suggested for Optical Observation of Anisotropic Scattering
*Akio Kawaguchi and Hirofumi Ninomiya*

**PS1-86** Color Measurement of Meat in Cooking under LED Lightings with Different Spectral Distributions
*Akari Kagimoto, Risa Shiomi, Shino Okuda, Mami Masuda, Katsunori Okajima, Hideki Sakai and Hiroyuki Iyota*

**PS1-87** Color Temperature and Illuminance of Main Streets with Day and Night Illumination in the Center of Osaka, Japan
*Haruyo Ohnoh*

## Invited Talk (MCS)

**8:30 - 9:15   sola city Hall**

*Chair: Shoji Tominaga*

Multispectral colour imaging: Time to move out of the lab?

*Jon Yngve HARDEBERG*

## Oral Papers

**9:20-10:40      (sola city Hall)**
**MCS1: Multispectral Imaging System**

*Chairs: Lindsay MacDonald & Masaru Tsuchida*

**MCS1-1** Surface Spectral Reflectance Estimation with Structured Light Projection
*Grzegorz Mączkowski, Krzysztof Lech and Robert Sitnik*

**MCS1-2** Multispectral Imaging System Based On Tuneable LEDs
*Muhammad Safdar, Ming Ronnier Luo, Yuzhao Wang and Xiaoyu Liu*

**MCS1-3** Evaluation of Hyperspectral Imaging Systems for Cultural Heritage Applications Based on a Round Robin Test
*Sony George, Irina Mihaela Ciortan and Jon Yngve Hardeberg*

**MCS1-4** Spectral Gigapixel Imaging System for Omnidirectional Outdoor Scene Measurement
*Motoki Hori, Naoto Osawa, Keita Hirai, Takahiko Horiuchi and Shoji Tominaga*

**9:20-10:35      (Room C)**
**OS5: Color Education & Culture**

*Chairs: Verena M. Schindler & Kohji Yoshimura*

**OS5-1** Are There Ugly Colours?
*Ilona Huolman*

**OS5-2** A Novel Experience in Color Teaching: Master in Color Design & Technology
*Alessandro Rizzi, Maurizio Rossi, Cristian Bonanomi and Andrea Siniscalco*

**OS5-3** The Ambiguous Term of "Saturation"
*Karin Fridell Anter, Harald Arnkil and Ulf Klarén*

**OS5-4** Colour Education and Real Life Colour
*Ulf Klarén and Karin Fridell Anter*

**OS5-5** Color Universes for the Chilean Heritage
*Elisa Cordero and Eréndira Martínez*

**11:00-12:20      (sola city Hall)**
**MCS2: Multispectral Color Science**

*Chairs: Jon Yngve Hardeberg & Keita Hirai*

**MCS2-1** Handheld Hyperspectral Imaging System for the Detection of Skin Cancer
*Xana Delpueyo, Meritxell Vilaseca, Santiago Royo, Miguel Ares, Ferran Sanabria, Jorge Herrera, Francisco J. Burgos, Jaume Pujol, Susana Puig, Giovanni Pellacani, Jorge Vázquez, Giuseppe Solomita and Thierry Bosch*

**MCS2-2** Empirical Disadvantages for Color-Deficient People
*Joschua Simon-Liedtke and Ivar Farup*

**MCS2-3** Spectral Reflectance Recovery Using Natural Neighbor Interpolation with Band-Divided Linear Correction
*Tzren-Ru Chou and Tsung-Chieh Sun*

**MCS2-4** Evaluation of Gastrointestinal Tissue Oxygen Saturation Using LEDs and a Photo Detector
*Yoshitaka Minami, Takashi Ohnishi, Koki Kato, Hiroyuki Wasaki, Hiroshi Kawahira and Hideaki Haneishi*

**11:00-12:15      (Room C)**
**OS6: Color and Culture**

*Chairs: Tien-Rein Lee & Shin'ya Takahashi*

**OS6-1** Forsius' Second Colour Order Diagram of 1611 from the Iconic Point of View
*Verena M. Schindler*

**OS6-2** Five Colours - A Study of Chinese Traditional Colour
*Jie Xu*

**OS6-3** Meeting New Challenges in Colour Tendencies in Norway
*Kine Angelo and Alex Booker*

**OS6-4** The Image of the Color Red in Letters: A Study Based on the Historical Backgrounds of Russia and Japan
*Sasha Krysanova*

**OS6-5** Japanese Color Names Reflecting Dyeing: With a Focus on Their Color Terms in Brown Regions Including More than 100 Browns
*Kohji Yoshimura, Yuko Yamada and Stephen Shrader*

## Poster Papers
**13:45-15:15   Poster 2   (Room B/Lobby)**

*Chairs: Yasuki Yamauchi & Takuzi Suzuki*

**Room B : PS2-1~64**
**Lobby    : PS2-65~85**

**PS2-1** Changes of Color Names and Coloring Materials in Japan
*Norifumi Kunimoto*

**PS2-2** Differences in the Drawings and the Color of the Violence in Children from Three Different Cultures
*Georgina Ortiz Hernandez and Mabel López*

**PS2-3** Color and Image of the City in Environmental Design of Kazimir Malevich
*Yulia Griber*

**PS2-4** Comparative Study about Preference Tendency to Spatial Color Based on Color Recognitions and Emotions among Nations : Focused on Korea and Malaysia
*Ji-Young Oh, Heykyung Park, Mai Neo, Jian-Yuan Soh and Min Jae Lee*

**PS2-5** The Analysis of Door Color on the Traditional Palace of the Kingdom of Joseon
*Lu Chen and Jin Sook Lee*

**PS2-6** Comparison among Three Methods for Thai Colour Naming
*Pichayada Katemake, Dimitris Mylonas, Lindsay MacDonald and Amara Prasithrathsint*

**PS2-7** A Study on Elements Perceived as Traditional among Fabrics and Colors for Hanbok
*Ji Hyun Sung and Yung Kyung Park*

**PS2-8** The Positive Impact of Image by Colour for Vulnerable People
*Maria Elena Chagoya*

**PS2-9** Faith in the Power of Color : Spiritual Revival from the East Japan Earthquake Disaster
*Yumi Awano*

**PS2-10** Types of Smart Cities | Cities Built from the Scratch and Old Cities Transformed into Smart Cities: What Kind of Colours can We Use?
*Ana C. Oliveira*

**PS2-11** The Use of English Colour Terms in Big Data
*Dimitris Mylonas, Matthew Purver, Mehrnoosh Sadrzadeh, Lindsay MacDonald and Lewis Griffin*

**PS2-12** A Proposal of Colour Universal Design Game for Learning Dichromats' Confusion Colours
*Shigehito Katsura and Shoji Sunaga*

**PS2-13** Colour Management: Managing the Intuitive Issue, the Gamut Issue and the Engagement Issue
*Philip Henry and Stephen Westland*

**PS2-14** Suggestion for Teaching Natural Colors through Investigation and Analysis of Current Color Education for Children in Korea
*Shin Sangeun, Choi Sueran, Kim Saetbyul and Kim Yoosun*

**PS2-15** Color Mixture Learning using Personal Computer for Basic Design
*Tomoko Mitsutake, Katsuyuki Aihara and Yosuke Yoshizawa*

**PS2-16** The Art of Colour Harmony: The Enigmatic Concept of Complementary Colours
*Harald Arnkil*

**PS2-17** A Study on Influence of the Culture and Art Experience of Senior Citizens from Relationships between Culture and Art Education Space and Color Emotion Assessment
*Hyeyun Son, Yunsun Park and Jinsook Lee*

**PS2-18** Impressions of Buildings Derived from the Combined Effects of Exterior Colour, Material, and Window Shape
*Kazumi Nakayama and Masato Sato*

**PS2-19** Analysis of Current Colors of Native Plants Growing Naturally in Korea
*Yoosun Kim, Sueran Choi, Saetbyul Kim and Sangeun Shin*

**PS2-20** Effects of Accent Colour on the Apparent Distance to a Wall and the Apparent Volume of an Interior Space: The Validation Experiment in an Actual Space
*Wataru Kamijo, Keishi Yoshida and Masato Sato*

**PS2-21** Metamer Mismatching as a Measure of the Color Rendering of Lights
*Hamidreza Mirzaei and Brian Funt*

**PS2-22** Visual Impression of a Real Room Affected by Lighting Conditions and by Colour and Texture of the Walls
*Jau-Yi Wu, Henry Pan and Li-Chen Ou*

**PS2-23** Suggesting Appropriate Color Range for Indoor Space Based on EEG Measurement
*Hanna Kim, Heewon Lee, Mijin Lee and Jinsook Lee*

**PS2-24** Development of the Interior Color Coordination Recommendation System of Living Space for University Student Living Alone Using Genetic Algorithm
*Tatsunori Matsui, Keiichi Muramatsu, Kazuaki Kojima, Mai Kawashima and Miho Saito*

**PS2-25** Chromatic Integration of the Architectural Surfaces with the Environment: Analysis and Classification of Case Studies
*Alessandro Premier and Katia Gasparini*

**PS2-26** Color Appearance of Red Printing Ink for Color Vision Deficiency
*Terumi Kato, Yoko Mizokami, Masami Shishikura, Shinichiro Taniguchi, Tomomi Takeshita, Fumiko Goto and Hirohisa Yaguchi*

**PS2-27** A Study on the Utilization of Korean Saekdong Color in the Textile Arts
*Kum-Hee Ryu*

**PS2-28** Color Adjustment for an Appealing Facial Photography
*Kyeongah Jeong and Hyeon-Jeong Suk*

**PS2-61** Space Brightness Affected by a Scenic View through a Window
*Shogo Yamada, Ryousuke Tanaka, Hiroyuki Shinoda and Yasuhiro Seya*

**PS2-62** Influence of Surface Properties on Material Appearance
*Ming-Kang Lan, Tien-Rein Lee and Vincent C. Sun*

**PS2-63** Visual Evaluation of a Wooden-finish Room and the Colorimetry of Wood
*Shigeko Kitamura, Jun Tsuchiya and Shoji Sunaga*

**PS2-64** Total Appearance of Metallic Coatings using a Stereo Capture System
*Min-Ho Jung, Vien Cheung and Peter A. Rhodes*

**PS2-65** Statistical Image Analysis for Evaluating Face Shine: Cosmetic Research
*Takanori Igarashi, Takahiro Naoki, Masataka Seo and Yen-Wei Chen*

**PS2-66** High Dynamic, Spectral and Polarized Natural Light Environment Acquisition
*Philippe Porral, Patrick Callet and Philippe Fuchs*

**PS2-67** Development of Skin Reflectance Prediction Model Using a Skin Data
*Kaida Xiao, Mengmeng Wang, Tushar Chauhan, Jingjing Yin, Changjun Li, Ronnier Luo and Sophie Wuerger*

**PS2-68** Comparing CSI and PCA in Amalgamation with JPEG for Spectral Image Compression
*Muhammad Safdar, Ming Ronnier Luo and Xiaoyu Liu*

**PS2-69** A System for Analyzing Color Information with the Multi-spectral Image and Its Application
*Junyan Luo, Yoko Mizokami, Hirohisa Yaguchi, Yohei Takara, Fuminori Ando, Takahiro Fujimori and Naoki Noro*

## MCS Poster Papers

**PS2-70** Quality Comparison of Multispectral Imaging Systems Based on Real Experimental Data
*Raju Shrestha and Jon Y. Hardeberg*

**PS2-71** LED-based Gonio-hyperspectral System for the Analysis of Automotive Paintings
*Francisco J. Burgos, Meritxell Vilaseca, Esther Perales, Elísabet Chorro, Francisco M. Martínez-Verdú, José Fernández-Dorado, José L. Alvarez-Muñoz and Jaume Pujol*

**PS2-72** Multispectral Image Estimation from RGB Image Based on Digital Watermarking
*Kazuma Shinoda, Aya Watanabe, Madoka Hasegawa and Shigeo Kato*

**PS2-73** Image Correction for a Multispectral Imaging System Using Interference Filters and Its Application
*Shogo Nishi and Shoji Tominaga*

**PS2-74** Development of Multi-bands 3D Projector
*Ryotaro Miwa, Yoshitsugu Manabe and Noriko Yata*

**PS2-75** Perceived Quality of Printed Images on Fluorescing Substrates under Various Illuminations
*Steven Le Moan and Ludovic Gustafsson Coppel*

**PS2-76** To Predict Reality in Virtual Environments : Exploring the reliability of colour and light appearance in 3D-models
*Beata Stahre Wästberg, Jacqueline Forzelius and Monica Billger*

**PS2-77** Altering Perceived Depth of Objects with Colored Lighting
*Ruth Genevieve Ong and Nan-Ching Tai*

**PS2-78** A Model for Estimation of Overprinted Colors on *Nishiki-e* Printings
*Sayoko Taya, Takuzi Suzuki, Noriko Yata and Yoshitsugu Manabe*

**PS2-79** Ethical Considerations on Gene Therapy for Color-Deficient People
*Joschua Simon-Liedtke*

**PS2-80** Robust Cross-Domain Reflectance Estimation
*Christoph Godau*

**PS2-81** Colorama: Extra Color Sensation for the Color-Deficient with Gene Therapy and Modal Augmentation
*Joschua Simon-Liedtke*

**PS2-82** Benchmarking a Grating-based Spectral Imaging System
*M. James Shyu and Ting-Yun Lin*

**PS2-83** Experimental Evaluation of Chromostereopsis with Varying Spectral Power Distribution of Same Color
*Masaru Tsuchida, Minoru Mori, Kunio Kashino and Junji Yamato*

**PS2-84** Haze and Convergence Models: Experimental Comparison
*Jessica El Khoury, Jean-Baptiste Thomas and Alamin Mansouri*

**PS2-85** Hyperspectral Reflectance Reconstruction Using a Filter-based Multispectral Camera
*Wei-Chun Hung, Pei-Li Sun and Raymond Jiang*

## Judd Award Lecture

**16:30 - 17:45    sola city Hall**

*Chair: Nick Harkness*

On the dimensionality of the colour world

*Françoise VIÉNOT*

# Scientific Program

## Invited Talk

**8:30 - 9:15**      sola city Hall

*Chair: Katsunori Okajima*

Neural Representation of Color in Visual Cortex

*Hidehiko KOMATSU*

## Oral Presentation

**9:20-10:35**      (sola city Hall)
**OS7: Appearance, Lighting**

*Chairs: Ronnier Luo & Hiroyuki Shinoda*

**OS7-1**    Assessing Glare Using LED Sources Having Different Uniformity Patterns
*ShiNing Ma, Yang Yang, Ming Ronnier Luo, XiaoYu Liu and BinYu Wang*

**OS7-2**    Evaluation of the Performance of Different Colour Rendering Indices Employed in LEDs
*Haiting Gu, Xiaoyu Liu, Ming Ronnier Luo, Binyu Wang and Haiyan Liu*

**OS7-3**    A Study on the Lighting of Bathroom for the Elderly
*Jiyoung Park, Chanung Jeong, Eunji Seo and Jinsook Lee*

**OS7-4**    Sitting Posture Based Lighting System to Enhance the Desired Mood
*Hyunjoo Bae, Haechan Kim and Hyeon-Jeong Suk*

**OS7-5**    Colour Lighting Based on Chromatic Strength
*Toru Kitano, Tetsuji Yamada and Kosuke Oshima*

**9:20-10:35**      (Room C)
**OS8: Color Deficiency**

*Chairs: Youngshin Kwak & Takashi Sakamoto*

**OS8-1**    Influences to Color Constancy by Wearing the Optical Dichromatic Filter or the Aged Lens Filter under Static and Rapidly-Changed Colored Illuminations
*Mio Hashida, Ippei Negishi and Keizo Shinomori*

**OS8-2**    Spectral Functional Filters for Optical Simulation of Dichromats in Color Discrimination
*Keizo Shinomori, Kanae Miyazawa and Shigeki Nakauchi*

**OS8-3**    What Are Memory Colors for Color Deficient Persons?
*Jia-Wun Jian, Hung-Shing Chen and Ronnier Luo*

**OS8-4**    Establishment of a Model Colour Palette for Colour Universal Design
*Kei Ito, Tomomi Takeshita, Fumiko Goto, Masafumi Nishigaki, Teruo Kobayashi, Mitsumasa Hashimoto, Yosuke Tanaka, Koichi Iga, Shunsuke Watanabe, Koki Okagawa and Mitsuyoshi Maekawa*

**OS8-5**    Color Universal Design
*Yasuyo G. Ichihara*

**10:50-11:50**      (sola city Hall)
**OS9: Cosmetics, Material Perception**

*Chairs: Takanori Igarashi & Motonori Doi*

**OS9-1**    An Investigation of the Appearance Harmony Using Real Materials and Displayed Images
*Midori Tanaka and Takahiko Horiuchi*

**OS9-2**    The Colour of Gold
*Lindsay MacDonald*

**OS9-3**    Preferred LED Lighting for Wood Surfaces and Colored Surfaces
*Markus Reisinger*

**OS9-4**    Development of a Facial Imaging System and New Quantitative Evaluation Method for Pigmented Spots
*Kumiko Kikuchi, Yuji Masuda, Tetsuji Hirao, Kiyoshi Sato, Yoko Mizokami and Hirohisa Yaguchi*

**10:50-11:50**      (Room C)
**OS10: Color Psychology**

*Chairs: Osvaldo Da Pos & Shinji Nakamura*

**OS10-1**    Colour Preference and Harmony for Athletic Shoe Designs
*Wei-Hsuan Chao, Ji-Yuan Huang, Chung-Chien Lan and Li-Chen Ou*

**OS10-2**    A Study on Silver Metallic Color Preference - A Comparison of Responses by Age and Gender in Thailand -
*Kamron Yongsue, Mikiko Kawasumi, Chanprapha Phuangsuwan and Kanrawee Tawonpan*

**OS10-3**    Effects on Impression of Taste in Color Stimuli
*Masato Sakurai, Yusuke Michinaka and Takahiro Yoshikawa*

**OS10-4**    The Color Image of Dichromats and Anomalous Trichromats
*Yuria Noguchi and Muneo Mitsuboshi*

# Keynote Lecture, Invited Talks, Judd Award Lecture

# Keynote Lecture

## The Gathering Space
**Kazuyo SEJIMA**

SANAA, Japan

Focusing on her recent works, Kazuyo Sejima will introduce the environment and architecture enhanced by color.

(In Japanese, with interpreting Japanese into English)

### Kazuyo Sejima (Japan)

Kazuyo Sejima studied architecture at the Japan Women's University before going to work for Toyo Ito. She launched her own practice in 1987. In 1995, she established SANAA with Ryue Nishizawa. Her own works include, House in a Plum Grove and Inujima Art House project. SANAA's main works include the 21st Century Museum of Contemporary Art in Kanazawa, Rolex Learning Center, EPFL, the Louvre Lens, and the New Museum of Contemporary Art. SANAA's current projects include the Grace Farms Project in Connecticut, USA, and the Bezalel Academy of Arts and Design in Jerusalem, Israel. In 2010 Kazuyo Sejima was appointed director of the Venice Biennale. And in the same year, Kazuyo Sejima and Ryue Nishizawa of SANAA were the recipients of the prestigious Pritzker Architecture Prize.

*photo:Takashi Okamoto*

# Invited Talk (MCS)

## Multispectral colour imaging: Time to move out of the lab?

**Jon Yngve HARDEBERG** and Raju SHRESTHA

The Norwegian Colour and Visual Computing Laboratory
Gjøvik University College, Gjøvik, Norway

### Jon Y. Hardeberg (Norway)

He is currently Professor of Color Imaging at Faculty of Computer Science and Media Technology, Gjøvik University College, Norway and member of the Norwegian Color and Visual Computing Laboratory. His current main research interests include multispectral color imaging, print and image quality, colorimetric device characterization, color management, and cultural heritage imaging.His professional memberships include IS&T, SPIE, and ISCC. He is the Norwegian delegate to Division 8 of the CIE.

# Multispectral colour imaging:
# Time to move out of the lab?

Jon Yngve HARDEBERG and Raju SHRESTHA
The Norwegian Colour and Visual Computing Laboratory
Gjøvik University College, Gjøvik, Norway

## ABSTRACT

In this paper we present and discuss our recent research using three approaches for fast and cost-effective acquisition of multispectral colour images; using a stereoscopic camera with additional optical filters, using an extension of the traditional colour filter array beyond the conventional three channels, and using active LED illumination in conjunction with RGB or panchromatic area image sensors. An important goal for this work is to achieve faster and more practical solutions for multispectral colour imaging, paving the way for new application areas and more widespread use, beyond the scope of the resarch laboratories.

## 1. INTRODUCTION

In the past decades there has been a significant volume of research carried out in the field of multispectral colour imaging, that is, imaging systems and methodologies in which the spectral reflectance of the imaged scene is captured and processed, while one of the goals of the resulting imagery remains visual inspection; therefore precise colour information is of high importance in the imaging workflow.

The focus of much of this research has been to facilitate a type of systems that usually requires that the multispectral colour image is captured using multiple subsequent captures (e.g. systems based on filter wheels, liquid crystal tunable filters, or active lighting together with a panchromatic area imaging sensor), or a line-by-line scanning of the scene (e.g. systems based on prisms or gratings coupled with area imaging sensors). Both these approaches have serious shortcomings with regards to the usability of the systems, in particular when applied to real-world scenes with moving objects.

Multispectral colour imaging has shown its usefulness in many application domains such as cultural heritage, medical imaging, biometrics, remote sensing, food quality etc., and its scope continues to grow. Refer to Hardeberg (2001) and Shrestha (2014) for a comprehensive overview of the research field. However, the applications are so far mostly limited to research laboratories. Key obstacles to broader application include cost, user-friendliness, and speed.

Recently, new approaches for faster and more practical multispectral colour image acquisition have been proposed, including the three promising ideas of using multispectral colour filter arrays (MCFA), using two colour cameras with additional optical filters in a stereoscopic configuration, and using active LED illumination in conjunction with RGB or panchromatic area image sensors.

In this paper we present briefly our recent research using these three approaches, discuss their advantages and disadvantages, as well as directions for further research aiming for faster, cheaper, and more user friendly solutions for multispectral colour imaging.

## 2. THE MULTISPECTRAL COLOUR FILTER ARRAY APPROACH

The MCFA approach is based on an extension of the conventional colour filter array (CFA) to using more than three channels. Baone and Qi (2000) made a proposal of such an MCFA based imaging system, whose main purpose was classification, where they used four bands in the middle and low wave infrared region in addition to the conventional three in the visible spectrum. They also proposed a new demosaicking algorithm that aimed to better restore the image by maximizing a-posteriori probability. A recent work by Lu et al. (2009) also focused on constructing MCFAs to capture a NIR band along with the visible bands. The purpose of this work was the simultaneous capture of high quality visible and NIR image pair. Another work by Brauers and Aach (2006) proposes an MCFA with narrow band filters in the visible range. Here also, a demosaicking algorithm has been proposed, which attempts to make use of the inter-band correlation by low pass filtering of the channel differences.

A MCFA based multispectral camera introduces several design issues that need to be handled, even before considering possible issues related to the eventual real production of imaging sensors and systems (Lapray et al. 2014). Notable ones include the choice of the number of filters and their selection for the acquisition system, the spatial arrangement of the filters, and the demosaicking algorithm.

In (Shrestha et al. 2011a), we used the algorithm proposed by Miao and Qi (2004) to construct MCFAs of different sizes, based on the probability of appearance of the corresponding spectral bands. We simulated acquisitions of several spectral scenes using 6, 8, and 10-channel systems, and compared the results with those obtained by the conventional regular MCFA arrangement, evaluating the precision of the reconstructed scene spectral reflectances in terms of spectral RMS error, goodness-of-fit coefficient (GFC) and colorimetric CIEDE2000 colour differences. Using the proposed approach we significantly improved the precision, in particular for an eight-channel MCFA we reduced the average CIEDE2000 colour difference by up to 50%.

In (Wang et al. 2013a), we proposed to use a discrete wavelet transform (DWT) for MCFA demosaicking. In (Wang et al. 2013b), we proposed two vector based median filtering methods for MCFA demosaicking. One solved the demosaicking problems by means of vector median filters, and the other applied median filtering to the demosaicked image as a subsequent refinement process to reduce artefacts. To evaluate the performance of these algorithms, a simulation framework was constructed with the capability of simulating image acquisition, mosaicking, demosaicking and quality assessment. Through this work we have proved the feasibility of MCFA demosaicking.

## 3. THE STEREOSCOPIC CAMERA APPROACH

As the second approach towards fast and practical one-shot multispectral colour image acquisition we propose to use two colour cameras in a stereoscopic configuration, and equip them with appropriate optical filters. In a related previous work Hashimoto and Kishimoto (2008) proposed a two-shot 6-band multispectral system using a commercial digital camera and a custom colour filter. But, this still needed two subsequent shots, and custom filter needed to be constructed. Ohsawa et al. (2004) proposed a one-shot six band HDTV camera systems, and they have shown that the six band system achieved more accurate colour estimation. The system they proposed used a beam splitter and specially

designed filters, and thus construction and operation of the system was still complex and costly.

In our work (Shrestha et al. 2010; 2011b; 2011c), we have extended this idea further with a more simplified approach using a stereo camera, and a pair of filters selected from among a set of readily available filters. The best pair of filters is selected from this set such that they modify the sensitivities of the two cameras in such a way that the resulting spectral sensitivities are optimal with regards to the precision of the resulting spectral reflectance data. Depending on application, optimal filters could be selected for more accurate colour reproduction. The stereoscopic configuration of the two cameras also provides a solution to the image alignment problem by means of stereo matching algorithms. An appropriate state of the art stereo matching algorithm can be used. Furthermore, the use of a stereo camera makes the system capable of capturing three dimensional images simultaneously along with the multispectral colour images. Thus the system can be used as a "two-in-one" multispectral-stereo system.

The proposed approach has been investigated with simulations as well as experimentally. Simulations have been performed with several pairs of real as well as imaginary cameras, and a set of two hundred and sixty five optical filters from Omega Optical, Inc. And, experimental studies have been conducted with arguably the world's first modern digital 3D still camera from Fujifilm, the FinePix REAL 3D W1. The performance of the system has been evaluated both spectrally and colorimetrically based on spectral reconstruction of the scene reflectance and the scene colour reproduction respectively. Root mean square error (RMSE) and CIELAB ΔE*ab have been used as spectral and colorimetric evaluation metrics respectively for computing estimation errors. Both simulations and experiments have shown that the proposed system performed better than RGB system both spectrally and colorimetrically.

## 4. THE LED ACTIVE ILLUMINATION APPROACH

The third approach is based on multiplexed LED (Light Emitting Diode) illumination. In a typical LED illumination based multispectral imaging (LEDMSI) system, a number of narrow band LED illuminations in a certain wavelength range is used to capture images with a digital monochrome camera (Park et al. 2007, Christens-Barry et al. 2009). Since switching of LEDs can be done electronically, synchronized with the image capture by a camera through a programmable micro-controller or a computer, the imaging process is quite fast. Availability of many different colors and high intensity LEDs with peak wavelengths spanning the visible range and even infrared region has made the construction of a more effective multispectral colour imaging system possible.

We proposed a LEDMSI based multispectral film scanner for obtaining accurate digital color images from analog films (Shrestha et al. 2012). In one of our recent works, we proposed a LEDMSI system that uses an RGB camera in place of monochrome camera (RGB-LEDMSI), which increases the speed of acquisition by a factor of three (Shrestha & Hardeberg 2013a). An important step in a LEDMSI system design is the choice and number of LEDs to be used. We proposed a novel LED selection method for RGB-LEDMSI system in Shrestha et al. (2012). The method selects optimal combination of three different types of LEDs for each exposure, each type of LED lying in one of the three regions corresponding to the spectral sensitivities of the three camera channels. Simulation and experimental results have shown that the performance of the proposed RGB-LEDMSI

AIC2015 TOKYO - Color and Image

systems are comparable to the corresponding monochrome camera based LEDMSI systems both in terms of spectral and colorimetric estimations, but at a significantly higher speed.

Another important aspect in LEDMSI is uniform illumination over the imaged scene. Moreover, we strive for all the LEDs have the same intensity profile. We proposed a LED matrix design method for equal intensity and uniform illumination in a LEDMSI (Shrestha & Hardeberg 2013b). Equal intensity LEDs can be achieved by using more LEDs whose intensity is low, and fewer LEDs whose intensity is high. For a given number of different types of LEDs, the proposed method generates an optimal or near-optimal arrangement of LEDs based on probability of appearances of the LEDs, which is calculated based on the intensity profiles of the LEDs and spectral sensitivity of the camera used. The method has shown to be effective in generating LED matrix design in terms of both spatial uniformity and consistency of LED distribution.

## 6. CONCLUSIONS AND PERSPECTIVES

In conclusion, our research so far has convinced us that the three proposed approaches can be viable alternatives for affordable acquisition of multispectral colour images. However there is obviously still much work to be done, e.g. concerning algorithms for interpolation in the filter array, as well as concerning the problem of occlusion in the stereo capture. Another promising research direction is addressing the problem of determining the illuminant in uncontrolled environments, so as to be able to recover the spectral reflectances of the scene without cumbersome calibration procedures (Shrestha & Hardeberg, 2014).

## ACKNOWLEDGEMENTS

## REFERENCES

Baone, G.A., Qi, H. (2000) Demosaicking methods for multispectral cameras using mosaic focal plane array technology, in Spectral Imaging: Eighth International Symposium on Multispectral Color Science, SPIE Proceedings, 6062, 75–87

Brauers, J., Aach, T. (2006) A color filter array based multispectral camera, in Proc. 12. Workshop Farbbildverarbeitung, German Color Group, Ilmenau, Germany

Christens-Barry, W. A., et al. (2009) Camera system for multispectral imaging of documents, *in* Sensors, Cameras, and Systems for Industrial/Scientific Applications X, SPIE Proceedings, 7249, 724908

Hahshimoto, M., Kishimoto, J. (2008) Two-shot type 6-band still image capturing system using commercial digital camera and custom color filter, Fourth European Conference on Colour in Graphics, Imaging and Vision, IS&T

Hardeberg, J.Y. (2001) Acquisition and Reproduction of Color Images: Colorimetric and Multispectral approaches, Universal Publishers/dissertation.com, Parkland, FL, USA

Lapray, P.-J. et al. (2014) Multispectral Filter Arrays: Recent Advances and Practical Implementation. *Sensors*, 14(11): 21626-21659

Lu, Y.M., et al. (2009) Designing color filter arrays for the joint capture of visible and near-infrared images, in IEEE Proc. International Conference on Image Processing, pp. 3797-3800

Miao, L., Qi, H. (2004) A generic method for generating multi-spectral filter array, in IEEE Proc. International Conference on Image Processing,.

Ohsawa, K., et al. (2004) Six band HDTV camera system for spectrum-based color reproduction, *Journal of Imaging Science and Technology* 48; 85-92

Park, J. I., et al. (2007) Multispectral imaging using multiplexed illumination, *in* IEEE International Conference on Computer Vision (ICCV), pp. 1–8

Shrestha, R., Hardeberg, J.Y. (2010) Multispectral Image Capture using two RGB cameras. European Signal Processing Conference (EUSIPCO), Aalborg, Denmark

Shrestha, R., et al. (2011a) Spatial arrangement of Color Filter Array for Multispectral Image Acquisition. In Sensors, Cameras, and Systems for Industrial, Scientific, and Consumer Applications XII, SPIE Proceedings, 7875, 787502

Shrestha, R., et al. (2011b) One-Shot Multispectral Color Imaging with a Stereo Camera. Digital Photography VII, SPIE Proceedings, 7876, 787609

Shrestha, R., et al. (2011c) Multispectral imaging using a stereo camera: Concept, design and assessment, *EURASIP Journal on Advances in Signal Processing* **2011**(1), 57

Shrestha, R., et al. (2012) LED based multispectral film scanner for accurate color imaging. The 8th International Conference on Signal Image Technology and Internet based Systems (SITIS), IEEE, Pages 811-817, Sorrento, Naples, Italy

Shrestha, R., Hardeberg, J.Y. (2013a) Multispectral Imaging Using LED Illumination and an RGB Camera. The 21st Color and Imaging Conference, IS&T, pp. 8-13, Albuquerque, NM, USA

Shrestha, R. & Hardeberg, J.Y. (2013b) LED matrix design for multispectral imaging, *in* Proc. The 12th International AIC Congress, pp. 1317–1320

Shrestha, R. (2014) Multispectral imaging: Fast acquisition, capability extension, and quality evaluation, PhD dissertation, University of Oslo

Shrestha, R. & Hardeberg, J.Y. (2014) Spectrogenic imaging: A novel approach to multi-spectral imaging in an uncontrolled environment. *Optics Express*, 22(8): 9123-9133

Wang, X. et al. (2013a) Discrete wavelet transform based multispectral filter array demosaicking. Colour and Visual Computing Symposium, IEEE, Gjøvik, Norway, pp. 1-6

Wang, X.; et al. (2013b) Median filtering in multispectral filter array demosaicking. Digital Photography IX, SPIE Proceedings, 8660, 86600E

*Address: Jon Y. Hardeberg, The Norwegian Colour and Visual Computing Laboratory*
*Faculty of Computer Science and Media Technology, Gjøvik University College*
*P.O. Box 191, N-2802 Gjøvik, Norway, http://www.colourlab.no*
*E-mail: jon.hardeberg@hig.no*

# Invited Talk

## Neural Representation of Color in Visual Cortex

### Hidehiko KOMATSU

Division of Sensory and Cognitive Information, National Institute for Physiological Sciences

School of Life Science, SOKENDAI (The Graduate University for Advanced Studies)

### Hidehiko Komatsu (Japan)

He is currently Professor of Division of Sensory and Cognitive Information, National Institute for Physiological Sciences, Japan. His current main research interests include neural representation of color in higher visual cortex, neural mechanisms of gloss perception, texture processing, and multimodal integration in material recognition.

He is currently project leader for a large research project "Brain and Information Science on SHITSUKAN (material perception)" funded by the Ministry of Education of Japan.
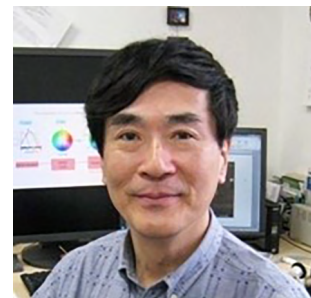
# Neural Representation of Color in Visual Cortex

Hidehiko KOMATSU,[1,2]

[1]Division of Sensory and Cognitive Information, National Institute for Physiological Sciences

[2] School of Life Science, SOKENDAI (The Graduate University for Advanced Studies)

## ABSTRACT

To understand how the object color is represented in our visual system, we need to understand at least two things: how the wavelength composition of the light is transformed to the color signal and how the surface reflectance property of the object is represented in our visual system. Numerous attempts have been made to answer to the former question, and we now know that color signal is conveyed from the retina to the higher visual cortex along a specific visual pathway through several steps of signal transformation. Attempts to answer to the latter question have emerged only recently. These studies have shown that neurons selectively responsive to specific range of gloss exist in higher ventral visual area and that these neurons encode perceptual parameters of gloss. These two lines of studies in combination will shed light on how the object color is represented in our visual system.

## 1. 'COLOR OF LIGHT' VS 'COLOR OF OBJECT'

When one says "this apple is red", he is not talking about the wavelength composition of the light coming into his eye from the apple. Instead, he is talking about some property intrinsic to an apple which makes the apple red. Numerous attempts have been previously made to understand the neural mechanisms of color vision, but most of those studies have concerned on the question about how the different wavelength compositions of the light yield different color perception. As the results of the efforts by many scientists, we are now approaching to a stage where we can make a coherent explanation about the neural mechanisms of color vision from the responses of the retinal photoreceptors to the neuron activities in the higher visual cortex. However, to what extent are we able to talk about the mechanisms of color perception with regard to the intrinsic properties of objects? In relation to the surface color, some important studies have shown the involvement of area V4 in color constancy that is related to the estimation of surface color (Zeki, 1983). However, estimation of the surface albedo is not the whole story on the surface color of objects. Surface gloss generated by the surface reflections that depends on the directions of the illumination and view point significantly affects the appearance of the object surface. For example, a matte yellow object is perceived simply as an yellow object, but if the object has a strong gloss and becomes shiny, it comes to possess golden appearance (Okazawa et al., 2011). Therefore, in order to be able to more fully talk about the object color that is associated with intrinsic properties of objects, we need to understand how gloss is represented in our visual system as well as how the wavelength composition of the light is transformed to the color signal in the visual system.

## 2. NEURAL REPRESENTATION OF 'COLOR OF LIGHT'

Neural processes to extract color from the wavelength composition of the light have been extensively studied and the processing of such color information in the early stage of the visual pathway is well established. Color signals originate by comparing signals of cones with different wavelength sensitivities (L cone, M cone, S cone) in the retina. This process yields two types of color signals, namely (L - M) and (S - (L + M)) signals (two-axes representation of color)(Komatsu, 1998). These color signals are relayed at the parvo- and konio-cellular layers of the lateral geniculate nucleus (LGN) and sent to the primary visual cortex (V1) in the cerebral cortex. In V1, these two types of color signals are combined to generate neurons that are selectively responsive for particular hues and neurons tuned for various directions in the hue circle are formed (multi-axes representation of color)(Lennie et al., 1990; Hanazawa et al., 2000; Wachtler et al., 2003).
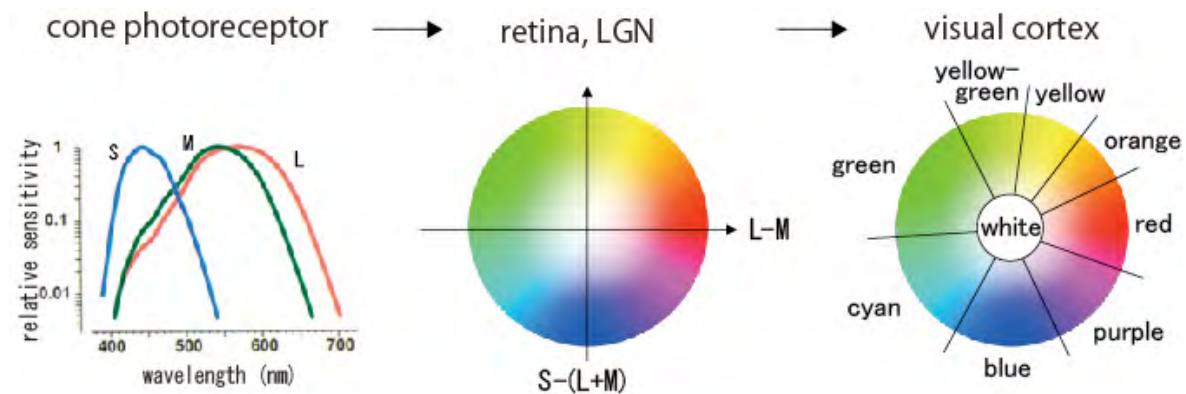
*Figure 1: Color signal transformation in the visual system.*

Color signal is transmitted from V1 through the ventral visual pathway including areas V2 and V4 to the higher ventral area (inferior temporal cortex = IT cortex in macaque monkey). IT cortex contains multiple subregions where color selective neurons are clustered. In these subregions, neurons have sharp color selectivity (Komatsu et al., 1992; Conway et al., 2007; Yasuda et al., 2010; Namima et al., 2014) and exhibit responses that are closely correlated with color perception or color related behaviors (Koida & Komatsu, 2007; Matsumora et al., 2008). In both humans and macaques, damage in the higher ventral area causes severe deficits in color perception, and it is thought that this area is responsible for color perception.
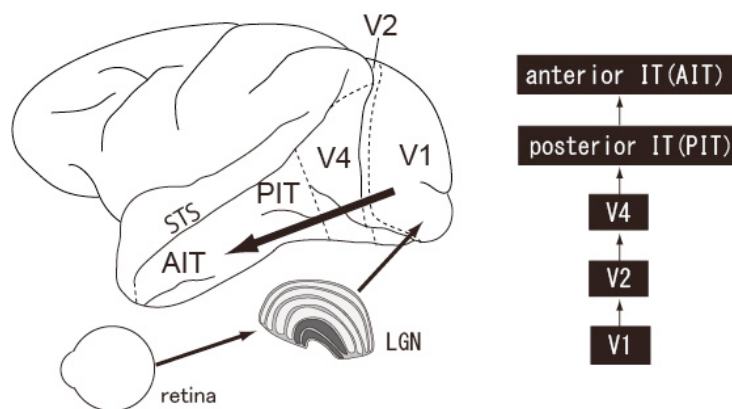
*Figure 2: Ventral visual pathway in macaque visual cortex.*

# 3. NEURAL REPRESENTATION OF GLOSS

In contrast to the accumulation of knowledge on the neural processing of 'color of light', far less is known about how 'color of object' is processed in the visual system. In the field of engineering and psychophysics, however, characterization of surface properties related to 'color of object' has made significant advancement in recent years. Especially, surface gloss has been extensively studied in terms of the directional specificity of surface reflection, and psychophysical studies have revealed the importance of the presence of the highlight and its spatial relationship with shadings (Beck & Prazdny, 1981; Kim & Anderson, 2010) as well as possible image features related to gloss perception (Nishida & Shinya, 1998; Motoyoshi et al., 2007). Based on these backgrounds, we have conducted a series of experiments to study neural representation of gloss in the visual cortex. We applied functional MRI (fMRI) to the macaque monkey, and recorded brain activities to object images with specular and matte surfaces. When we compared the responses to these images, it was found that stronger responses to the specular objects compared with the matte objects were observed in the visual areas along the ventral visual pathway (Okazawa et al., 2012). Especially, we found localized activities in restricted areas in the IT cortex including central part of the superior temporal sulcus (STS). Next, we conducted single neuron recordings from the region in the central STS, and examined the neural responses to object images with a variety of gloss. We found that neurons selectively responsive to specific range of gloss (gloss selective neurons) are accumulated in this region, and that as a population, these gloss selective neuron systematically represented a variety of gloss (Nishio et al., 2012). A previous study identified two sets of perceptual gloss parameters that form the dimensions of psychophysically uniform gloss space: contrast gloss (c) that corresponds to a non-linear combination of specular reflectance and diffuse reflectance and distinct-of-image gloss (d) that corresponds to the sharpness of highlight (Ferwerda et al., 2001). We found that responses of the gloss selective neurons are closely related to the perceptual gloss parameters (c and d), and that population activities of gloss selective neurons can precisely estimate the perceptual gloss parameters of the stimuli (Nishio et al., 2014). These results shed some light on how gloss is represented in the visual system.
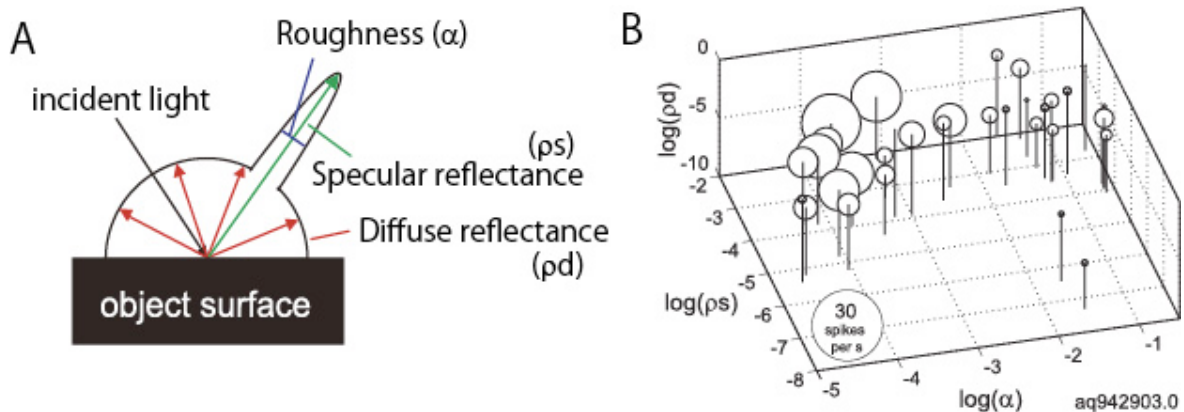


*Figure 3: (A) Physical parameters related to gloss. (B) Responses of an example of gloss selective neuron (modified from Nishio et al. 2012).*

# 4. CONCLUSIONS

Substantial knowledge has been accumulated on the neural representation of 'color of light'. Now, we are gradually learning about how gloss is represented in the visual system. We expect that by combining these knowledges, understanding on the representation of 'color of object' will be advanced. At the same time, we need to consider about new problems. For example, how are the information on the color of light and that on the surface reflection integrated when we perceive the color of object? Futhermore, there are many optical properties other than gloss such as transparency and translucency that affects the appearance of object. At this moment, we know nothing about the neural representation of those optical properties. To fully understand the mechanisms on how we perceive color of objects, development of the research in material perception or 'Shitsukan' should play a key role (Fleming et al. 2015).

## REFERENCES

Beck, J., and Prazdny, S. (1981). Highlights and the perception of glossiness. *Percept Psychophys, 30*, 407-410.

Conway, B. R., Moeller, S., and Tsao, D. Y. (2007). Specialized color modules in macaque extrastriate cortex. *Neuron, 56* (3), 560-573.

Ferwerda, J. A., Pellacini, F., and Greenberg, D. P. (2001). A psychophysically-based model of surface gloss perception. *Proceedings of SPIE Human Vision and Electronic Imaging, 4299*, 291-301.

Fleming, R.W., Nishida, S., and Gegenfurtner, K. (2015) Visual perception of Materials: the Science of Stuff. *Vis Res, in press.*

Hanazawa, A., Komatsu, H., and Murakami, I. (2000). Neural selectivity for hue and saturation of colour in the primary visual cortex of the monkey. *Eur J Neurosci, 12* (5), 1753-1763.

Kim, J., and Anderson, B. L. (2010). Image statistics and the perception of surface gloss and lightness. *J Vis, 10* (9), 3.

Koida, K., and Komatsu, H. (2007). Effects of task demands on the responses of color-selective neurons in the inferior temporal cortex. *Nat Neurosci, 10* (1), 108-116.

Komatsu, H. (1998). Mechanisms of central color vision. *Curr Opin Neurobiol, 8* (4), 503-508.

Komatsu, H., Ideura, Y., Kaji, S., and Yamane, S. (1992). Color selectivity of neurons in the inferior temporal cortex of the awake macaque monkey. *J Neurosci, 12* (2), 408-424.

Lennie, P., Krauskopf, J., and Sclar, G. (1990). Chromatic mechanisms in striate cortex of macaque. *J Neurosci, 10* (2), 649-669.

Matsumora, T., Koida, K., and Komatsu, H. (2008). Relationship between color discrimination and neural responses in the inferior temporal cortex of the monkey. *J Neurophysiol, 100* (6), 3361-3374.

Motoyoshi, I., Nishida, S., Sharan, L., and Adelson, E. H. (2007). Image statistics and the perception of surface qualities. *Nature, 447* (7141), 206-209.

Namima, T., Yasuda, M., Banno, T., Okazawa, G., and Komatsu, H. (2014). Effects of luminance contrast on the color selectivity of neurons in the macaque area V4 and inferior temporal cortex. *J Neurosci, 34* (45), 14934-14947.

Nishida, S., and Shinya, M. (1998). Use of image-based information in judgments of surface-reflectance properties. *J Opt Soc Am A Opt Image Sci Vis, 15* (12), 2951-2965.

Nishio, A., Goda, N., and Komatsu, H. (2012). Neural selectivity and representation of gloss in the monkey inferior temporal cortex. *J Neurosci, 32* (31), 10780-10793.

Nishio, A., Shimokawa, T., Goda, N., and Komatsu, H. (2014). Perceptual gloss parameters are encoded by population responses in the monkey inferior temporal cortex. *J Neurosci, 34* (33), 11143-11151.

Okazawa, G., Goda, N., and Komatsu, H. (2012). Selective responses to specular surfaces in the macaque visual cortex revealed by fMRI. *Neuroimage, 63* (3), 1321-1333.

Okazawa, G., Koida, K., and Komatsu, H. (2011). Categorical properties of the color term "GOLD". *J Vis, 11* (8), 1-19.

Wachtler, T., Sejnowski, T. J., and Albright, T. D. (2003). Representation of color stimuli in awake macaque primary visual cortex. *Neuron, 37* (4), 681-691.

Yasuda, M., Banno, T., and Komatsu, H. (2010). Color selectivity of neurons in the posterior inferior temporal cortex of the macaque monkey. *Cereb Cortex, 20* (7), 1630-1646.

Zeki, S. (1983). Colour coding in the cerebral cortex: the reaction of cells in monkey visual cortex to wavelengths and colours. *Neuroscience, 9* (4), 741-765.

*Address: Prof. Hidehiko KOMATSU, Division of Sensory and Cognitive Information, National Institute for Physiological Sciences, Nishigo-Naka 38, Myodaiji, Okazaki, Aichi, 444-8585, JAPAN*
*E-mails: komatsu@nips.ac.jp*

# Judd Award Lecture

## On the dimensionality of the colour world

**Françoise VIÉNOT**
Centre de recherche sur la conservation (CRC, USR 3224)
Muséum national d'Histoire naturelle

**Françoise Viénot (France)**

Emeritus professor, Muséum National d'Histoire Naturelle, Paris. Expert in color vision and appearance measurement, research on colorimetry, photometry, gloss metrics and LED illumination. French representative and former officer of CIE Division 1 (Vision), chair of CIE TC 1-36 "Chromaticity diagram with physiologically significant axes", vice-president of CIE-France. Newton medal (Colour Group of Great Britain) and Verriest medal (International Colour Vision Society).

# On the dimensionality of the colour world

Françoise VIÉNOT

Centre de recherche sur la conservation (CRC, USR 3224)
Muséum national d'Histoire naturelle

## ABSTRACT

Whereas, for colorimetric purpose, the three-dimensionality of colour cannot be circumvented and clearly refers to cone fundamentals, we examine situations where a reduced or expanded dimensionality could be experienced. Besides the case of individuals such as dichromats who suffer from a limited number of cone photopigments and enjoy two-dimensional colour vision, specific contexts or specific operations may require additional dimensions which could be supported by rod signals or melanopsin signals.

## 1. INTRODUCTION

Since the seminal hypothesis of Thomas Young and the studies from Maxwell and Helmholtz during the 19th century, it has been firmly established that colour is three-dimensional. Physiological, psychophysical and genetic studies have confirmed the 19th century statements so that standardization bodies, colour industry, image technology have developed tools and methods to improve numerous colour products.

It is often claimed that the three dimensions of colour originate from the presence of three families of cones in the retina. Yet, the cone signals are processed within the retina and in the brain structures so that colour construction aims at identifying objects and materials in our surrounding. Colour vision starts with the capture of photons by the long-wave sensitive (LWS) cones, the middle-wave sensitive (MWS) cones and the short-wave sensitive (SWS) cones. At the second stage, retinal ganglion cells combine the cone signals into three channels: one achromatic channel, supported by the "magno-cellular" pathway where cone signals are added, and two chromatic channels, supported by the "parvo-cellular" and the "konyo-cellular" pathways where cone signals are opposed. Retinal signals are processed in the brain in various contrasting combinations, ultimately delivering highly tuned colour responses.

Whereas the three-dimensionality of colour is consensually accepted it is of interest to examine situations where the colour dimensionality could be reduced or expanded.

## 2. THE THREE-DIMENSIONAL CIE COLOUR SPACE

### 2.1 The cone fundamentals

The three colour dimensions hypothesis has been validated by Psychophysics much earlier than Physiology and Genetics has isolated cone families and sequenced the genetic code of cone pigments (Nathans et al., 1986).

As early as 1886, König and Dieterici were able to determine accurate spectral sensitivity of the fundamental sensations. By asking colour normal observers and dichromatic observers to perform colour-matches, they were able to derive spectral sensitivity curves of the fundamental sensations that conform the most recent proposals (Stockman and Sharpe, 2000).

CIE technical committee 1-36 was established for proposing chromaticity diagrams based on the best set of colour-matching functions and cone fundamentals available nowadays. Cone fundamentals are based on Stiles and Burch (1959) experimental colour matches and validated by Physiology. A physiologically designed MacLeod-Boynton chromaticity diagram (MacLeod and Boynton, 1979) is proposed as well as a cone-fundamental-based $(x_F, y_F)$ chromaticity diagram. All data are now fixed (CIE, 2006; CIE, in press; Viénot and Walraven, 2007). Specifying colour in the LMS space will offer novel opportunities to solve problems of colour measurement and colour perception in everyday life and industry.

In the future, refinements, such as colour vision variability due to photopigment polymorphism, would not weaken the three-dimensionality hypothesis. It would secure the hypothesis.

## 2.2 Metamerism

Comparison between the richness of the spectral information available in the Physics domain and the reduced number of signals generated at the entrance of the visual system has led colour scientists to investigate at length the metamerism phenomenon.

In colorimetry, the basic experiment is a colour match between two metameric stimuli. Practically, colorimetry reduces the stimulus to a unique three component object. Indeed, the visual system is unable to finely analyse the spectral content of the stimulus. In the three-dimensional colour space, metamerism is just concealed.

Nevertheless the volume of ignored parts of the stimulus is amazing as illustrated by Kelly and Wyszecki (See figure 2(3.8.4) in Wyszecki and Stiles, 1982). It leaves room to numerous spectral power distributions with some remarkable properties.

## 3. SMALL DIMENSIONALITY COLOUR WORLDS

### 3.1 One or two photoreceptors (individual dimensionality)

#### 3.1.1 Achromatopsia

Cases of one-dimensional colour vision are rare. Achromatopsia is a very rare case of inherited total colour blindness, mainly including blue-cone monochromacy with a relative occurrence of 1:100,000 diagnosed cases (Sharpe et al., 1999).

Achromatopsia cases with total loss of all three cone opsin genes have been well documented by Nordby (he is an achromat) and Sharpe who examined the society from Guam, an island in Micronesia, known from Oliver Sacks' book entitled "The Island of the Colorblind" (1997), where about 10% of the population suffers from inherited achromatopsia.

#### 3.1.2 Dichromatism

Conversely, two-dimensional colour vision is common among mammals, apart from primates. In humans, dichromacy is well characterized. About 2% of the male population is dichromatic. Dichromacy is of genetic origin. Dichromats lack one family of cone pigments. It has been verified since 1986 by Nathans and colleagues that dichromats lack the corresponding gene sequence.

During the 20th century, dichromatic colour vision has been well documented, showing dichromatic Rayleigh matches. Hue discrimination is impaired around 590 nm for protanopes and deuteranopes, or around 490 nm for tritanopes. Colour appearance is

distorted. After a few reports from diagnosed unilateral dichromats, Judd (1948), Meyer and Greenberg (1988) and our group (Viénot et al., 1995; Brettel et al., 1997) have illustrated for the colour normal observer the colour appearance for dichromats.

The colour-blindness simulation is two-step.

In the LMS colour space, it is easy to find the colours that are confused by a dichromat. They lie on a line parallel to the axis corresponding to the missing fundamental. Our simulation was produced on a video-display, Cathode-Ray-Tube type, in which we could control the intensity of the three primaries. Yet, on a CRT, the definition of the stimulus is three-dimensional and linearly related to cone excitations.

Then we had to render a plausible appearance of the image. Reproducing how an image appears to dichromats was challenging. Given that a dichromat confuses a given red and a given green, how would these confused colours be perceived, and how should they be represented? Should the representation be red? Or green? Or yellow?

Appearance for a protanope→

Appearance for a deuteranope→



*Figure 1. Simulation, for the normal eye, of the appearance of a flower bed for the dichromat (Viénot et al., 1995).*

In his pioneer study, Judd had carefully reviewed the literature about unilateral colour defects which shows that for protanopic and deuteranopic observers, the colour perception of the spectrum is confined to two hues, yellow and blue. Judd's choice has been to represent, for a normal colour observer, all corresponding colours that are confused by dichromats by a unique sample of hue 5PB or hue 5Y of the Munsell Book of Colors. Precisely, Judd has given quantitative estimates of the colour perceptions typical of protanopic and deuteranopic observers for the whole range of Munsell colours. The same choice was retained by Meyer and Greenberg in a computer graphics simulation of dichromatic vision, prior to ours.

Our choice has been to maintain the normal colour appearance of white and greys and the same two hues of the stimuli at 475 nm and at 575 nm for protanopes, deuteranopes and normal trichromats. Finally, a photograph from a flower bed, at the Jardin des Plantes in Paris, has served to illustrate the simulation (Figure 1).

Now softwares have been written by many groups, some of them being available online. Figure 2 shows, for a trichromat, how the AIC 2015 logo (1st line) appears for a protanope (2nd line) and a deuteranope (3rd line).



*Figure 2. Colour-blind simulation of the AIC 2015 logo.*

### 3.2 Specificity of the luminance information (operational dimensionality)

The visual system network distinguishes between chromatic and achromatic pieces of information, the latter being prominent. Practically, the most efficient visual signals in nature which help the individual to localize targets and to move in the environment are based on luminance contrast.

Although the normal individual colour vision is trichromatic, behavioural responses to situations implicating resolution of high spatial and temporal frequencies depend principally on an achromatic mechanism with a spectral sensitivity much like $V(\lambda)$. Provided that the detection of high spatial frequencies or high temporal modulations depends on luminance contrast only, the chromaticity of the stimulus does not modify visual performance. Psychological evidence is obtained using the techniques of heterochromatic flicker photometry or minimally distinct border, among others. Thus, the high frequency spatial colour vision reduces to one dimension.

Lennie et al. (1993) recognize that the nature of underlying post-receptoral mechanisms is equivocal. Either LWS and MWS cone signals are directly summed into the magno-cellular pathway, or they are indistinctly processed so as issuing an additive signal.

### 3.3 The colour of illumination (contextual dimensionality)

Colour specification is well controlled by lighting engineers. With the emergence of solid-state technologies, much care is taken to correctly assess the colour of light. Indeed, for humans, the reference to qualify white light is natural daylight that needs only two variables to be qualified: the illuminance at earth level and the colour temperature.

Having measured the spectral power distribution (SPD) of real daylights, Judd and co-authors (1964) concluded, however, that distributions could be satisfactorily reconstituted by using only the first two principal components derived from principal component analysis (PCA). Later, Hernández-Andrés and colleagues (2001) concluded that more than two characteristic vectors were needed for good reconstruction. Even though they observed some departure of clear-sky colour from the CIE daylight locus, the chromaticities they measured are pretty much aligned along a unique curve.

Given the shape of the daylight locus and the dominance of the first two principal components in the analysis of daylight distribution, the question arises whether the three-dimensional colour specification that is used to specify the colour of material items is the one that should be used to scale illumination. We will see later in this paper that a specific visual channel is excited by light which might imply that the dimensions of the colour illumination world are only two.

## 4. EXPANDED DIMENSIONALITY COLOUR WORLDS

### 4.1 Additional photopigments (individual dimensionality)

Whereas the colour image domain exploits at best the three dimensions of colour, the questions arises whether the colour vision of the observer who looks at images could be more than three-dimensional.

#### 4.1.1 Tetrachromatic mothers

Anomalous trichromats possess three cone pigment families. Nevertheless, one pigment family differs from the normal's cone pigment. Men inherit the LWS and the MWS pigment genes from their mother. The likelihood that behavioural tetrachromacy exists in carriers of anomalous trichromacy was addressed by Jordan (Jordan et al., 2010). Although most carriers of colour anomaly do not exhibit four-dimensional colour vision, Jordan and colleagues found 1 of 24 female carriers who exhibited tetrachromatic behavior on a colour matching test (Rayleigh matches). Genetic analysis showed that this mother had three well-separated cone photopigments in the longwave spectral region in addition to her short-wave cone which makes the sum of cone families equal to four. Nevertheless, it may be noted that this human observer has been just able to express trichromacy in a task where the canonical normal colour observer expresses dichromacy.

#### 4.1.2 Fish and birds tetrachromatic vision

Fish and birds possess four families of cones. Although narrower tuning of the cone sensitivity might impair differential sensitivity, behavioural tests show that birds and fish enjoy tetrachromatic colour vision (Kelber and Osorio, 2010).

### 4.2 Additional receptors: rods and melanopsin (operational dimensionality)

Besides extra cone pigments, there are two photopigment families other than cone pigments, and with a different spectral sensitivity, which could be candidate to increase the dimensionality of colour vision.

### 4.2.1 Rod contribution

Rods, the spectral absorption of which, measured in the corneal plane, peaks at 507 nm, are active at mesopic levels.

Clarke (1973) and Trezona (1973) in early AIC conferences, demonstrated how to achieve a tetrachromatic colour match that holds at photopic and scotopic levels. To match every monochromatic radiation, they needed four primary matching stimuli of which they used one or another set of three. A unique match could be reached by iterative convergence. While the unique answer is recorded on the basis of the known colour sensations, this procedure ensures physiological identity of quantum absorption in four receptor responses.

### 4.2.2 Melanopsin interaction

During the past decade, it has been discovered that a few retinal ganglion cells contain a photopigment named melanopsin which can absorb photons before they reach the cone and rod layers. The melanopsin spectral sensitivity peaks at about 490 nm (estimated at the entrance of the eye), between SWS cones and rods' peak sensitivity. The so-called intrinsically photosensitive retinal ganglion cells (ipRGC) are stimulated at high mesopic and photopic illuminance levels (Dacey et al., 2005).
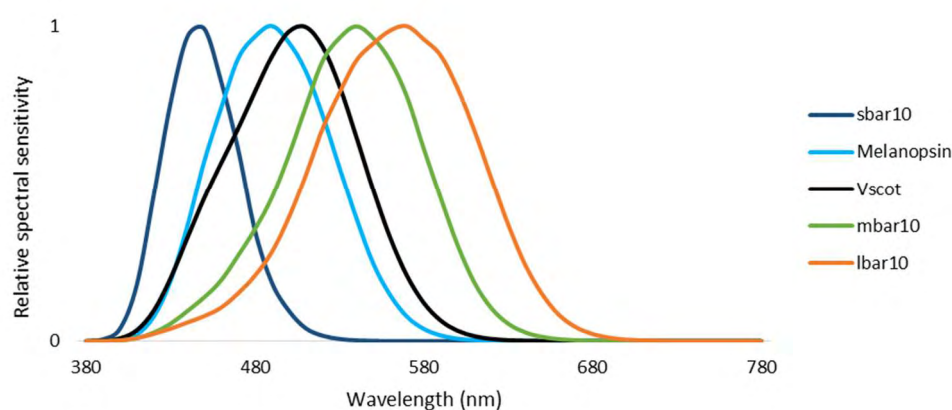


*Figure 3. Cone, rod and ipRGC spectral sensitivities.*

Using pharmacological tracers in the monkey brain, it has been shown that ipRGCs project to cortical and sub-cortical areas of the brain (Dacey et al., 2005; Hannibal et al., 2014). They convey information that is not principally devoted to image formation but mediate other visual functions such as the circadian rhythm and the pupillary reflex, and influence awareness and mood (Lucas et al. 2014).

*The effect of the spectrum on non-image forming fonctions.*

As pupil aperture is easy to record in real situations, we conducted experiments to test whether it was possible to drive the pupil response in accordance with the excitation of rods and ipRGCs (Viénot et al., 2012). Our experiments rest on the fact that metamers could differently address rods and ipRGCs. To investigate this question, at least 5 independent primaries are necessary. In a multi-LED light booth equipped with 7 types of colour LEDs, we could modulate the light spectrum, maintaining the white illumination at the same luminous level and the same CCT. Thus, the LEDs were driven so as to obtain metameric

white lights that would excite rods and ipRGCs at most or at least (Figure 4). We continuously photographed the pupil of the observers under each 7 colour LED illumination to measure the pupil diameter.
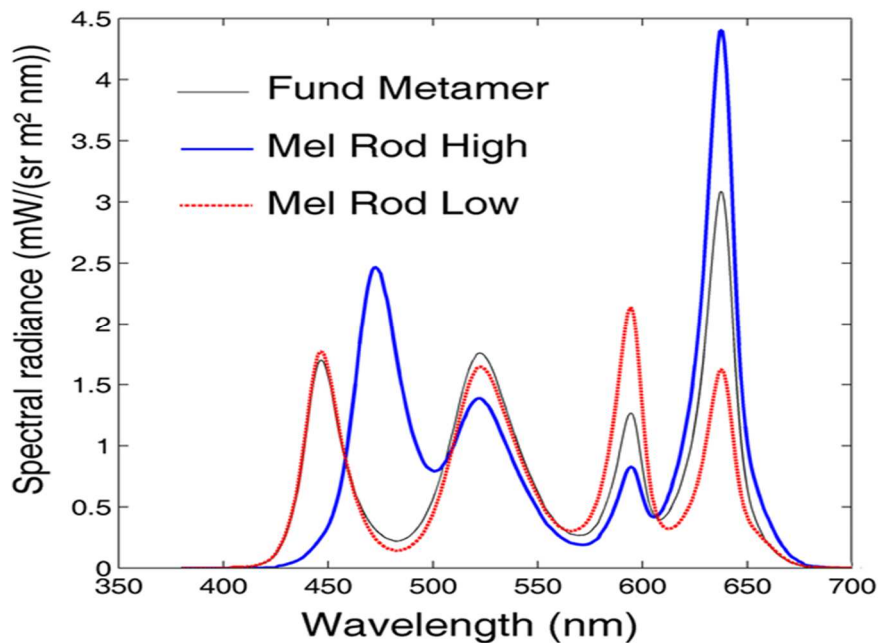


*Figure 4. Two metameric white lights that would excite rods and ipRGCs at most or at least (Viénot et al., 2012).*

Indeed, we verified that, with metameric white lights that generate identical signals in cones, the pupil diameter varies depending upon the spectral content of the light, which indicates that the light spectrum has an effect on visual functions, besides consciously seeing colours.

For domestic lighting, we draw attention to the possibility that driving the pupil reflex and possibly other non-image forming visual functions using unnatural spectrum would generate an uncomfortable behaviour.

Whether melanopsin interacts with cone colour vision is still unsolved. Brown et al. (2012) have hypothesized that ipRGCs may contribute to distinguishing brightness. Horiguchi et al. (2013) collected detection (difference) thresholds to many stimuli, using four-primary stimuli. Trichromatic theory explains foveal sensitivity, with no need to invoke a fourth photopigment. At high photopic levels where rods are not active, a fourth photopigment is required to explain peripheral sensitivity.

### 4.3 Four pigments and colour constancy (operational dimensionality)

Colour constancy is a visual phenomenon which we encounter every day. The perceived colours of reflecting surfaces remain satisfactorily stable despite changes in the spectrum of the illuminating light.

Where discounting for the illuminant change originates from is not understood yet. Simple models rely on the von Kries coefficient laws and state that the global change of illumination can be extracted from proportional changes of the cone excitations triggered by the reflecting surfaces in the scene. The gain change could operate within the retina.

However modern scientists question the complexity of colour constancy. They argue that the visual system makes a distinction between the estimation of the illuminant and the changes of surface reflectances.

Foster and colleagues (Craven and Foster, 1992; Foster, 2011) settle experiments where they introduced changes in illuminant colour and/or changes of material colour properties. They showed that subjects had been capable of correctly discriminating the two situations. They concluded that the visual system is provided with information about a changing world in "advance of the generation of a more elaborate and stable perceptual representation".

Hyperspectral images of natural scenes have revealed the occurrence of metamers in nature which indirectly means that the natural world is higher dimensional that the CIE colorimetry world (Foster et al., 2006). Of interest is the recent analysis of Barrionuevo and Cao (2014) who showed that the natural object spectra are not only discriminable by cones but that part of the spectral information can be decoded by melanopsin. Principal component analyses conducted on the excitations of rhodopsin, cone opsins, and melanopsin for natural hyperspectral images revealed that the sum of all responses ("L M S R I", with "I" for ipRGC) may contribute to the magno-cellular pathway and respond to irradiance levels. The PCA further suggests that rod and ipRGC signals also may contribute to post-receptoral pathway components that oppose LWS and MWS cone, with various combinations.

The putative role of a fourth photopigment to disambiguate the colour material factor from the colour illumination factor has been addressed in the context of colour constancy. In the future, investigation of the role of melanopsin signals might bring renewed knowledge about colour constancy as well as to the concept of colour temperature.

## 4.4 The generalized metameric approach. Metamers in the four- or five-dimensional framework

In the context of the three cones space, metameric colour stimuli have different spectral power distributions, but they excite the three families of cones similarly.

Investigation of the metamer domain has been facilitated using the concept of "metameric blacks" introduced by Gunter Wyszecki in 1953. (A simple example might be: given two real metameric stimuli, a metameric black is obtained by subtracting the SPD of one stimulus from the other.) Wyszecki presented the view that the spectral power distribution of metamers consists of two component spectral distributions: the fundamental distribution, named "fundamental metamer", that controls the three cone responses (and consequently the colour specification of the stimulus) and a secondary distribution that has no effect on cones, which he named a "metameric black". Cohen and Kappauf, in 1982, presented a procedure for accomplishing the decomposition of any visual stimulus into the fundamental metamer and the black component.

Adding a metameric black to a fundamental metamer has no effect on cone responses. However adding a metameric black to the fundamental metamer may well modify the responses of the rods and of the melanopsin cells. In order to investigate the domain of metamers in a space of higher dimensionality than the cone fundamentals', it is possible to extend Cohen and Kappauf's procedure for producing SPDs that excite or do not excite identified photoreceptors. Let us note that two metamers for a dichromat may not be metameric for the trichromat, two metamers for a trichromat may not be metameric for a four receptor visual system, two metamers for a four receptor system may not be metameric for a five receptor system, etc
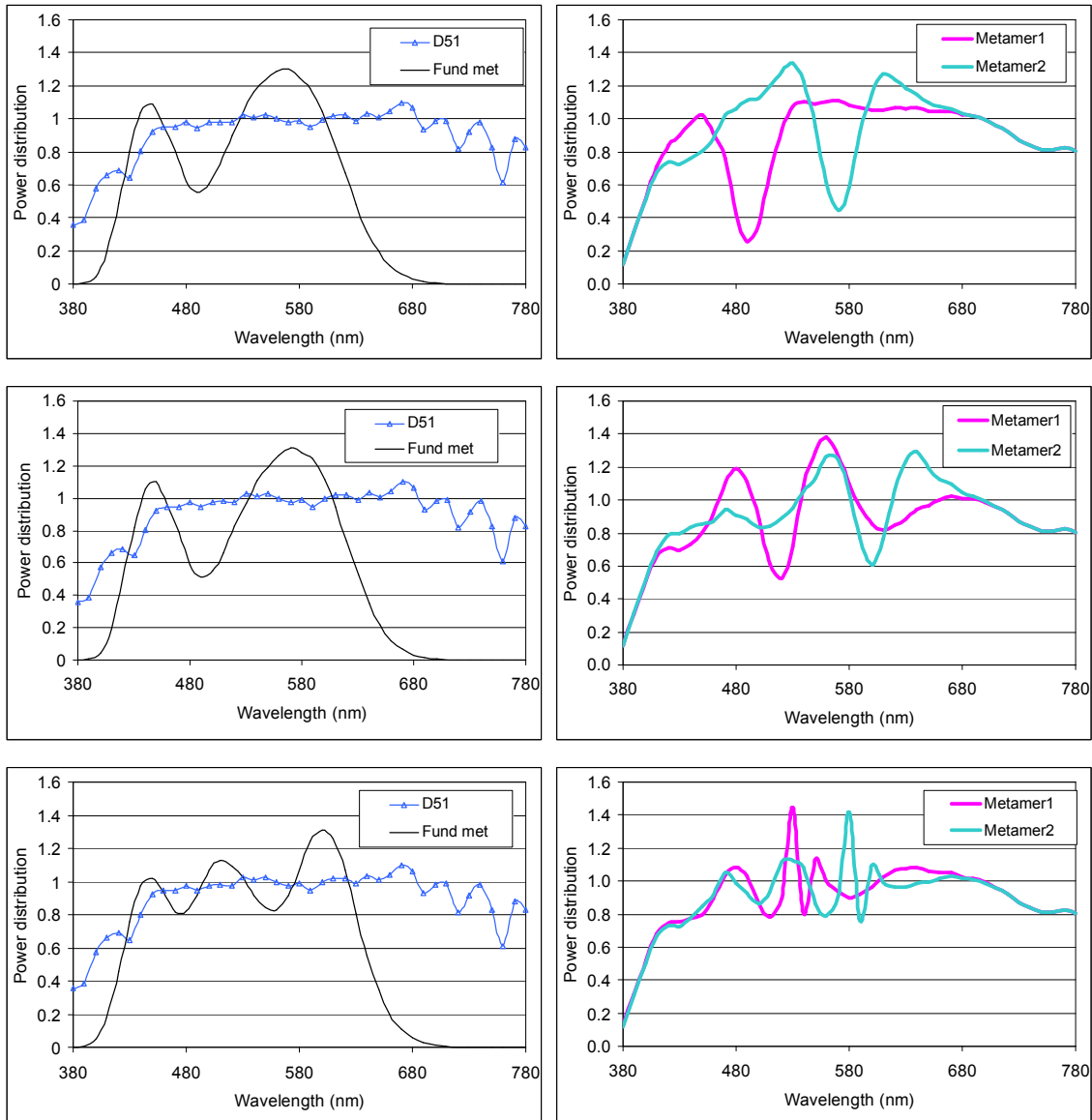
*Figure 5. Metamers of daylight at 5100 K*

Figure 5 shows examples of metamers of daylight at 5100 K for a variety of dimensionality of the visual receptor system. On the first line, the graphs show metamers for the deuteranope who lacks MWS photopigment. On the second line, the graphs show metamers for the normal trichromat. On the third line, the graphs show metamers that match for the three cone types as well as for rods and melanopsin cells. The left column presents the SPD of natural daylight at 5100 K and its fundamental metamer. In a previous paper, we already mentioned that, in the three-dimensional colour space, the fundamental metamer distribution resembles the SPD of modern light-emitting diodes. Thus while LED lighting mimics the colour of natural light it does not suit rod and melanopsin cells natural excitation. The right column presents two arbitrary chosen metamers with markedly different spectral power distribution. It can be seen that, as the dimensionality of the receptor system increases, the number of crossings of the two metameric stimulus functions increases. Note also that Metamer 1 and

AIC2015 TOKYO - Color and Image

Metamer 2 designed for the deuteranope would appear reddish and greenish to a colour normal observer.

**4.5 The necessity of categorisation (contextual dimensionality)**

Whereas receptor-level colour coding ensures continuous capture of the available information about the environment, we tend to group into categories the colour we perceive.

It is not clear whether categorization can be included in a dimensionality framework, for dividing the information into a small number of well-defined regions of the colour space tears the continuous dimensions of colour and introduces irregularities in the colour space (Jameson, 2005). Further, language, as a normative process of colour space segmentation, influences the way colour samples are grouped based on their perceptual similarities (Bonnardel, 2013).

What is accepted is that color categorization helps us to reliably and quickly identify objects and materials within a scene. It is an essential perceptual phenomenon.

## CONCLUSION

On the one hand, stating that colour vision is three-dimensional strictly applies to the cone fundamental space. It has helped the CIE to found standard colorimetry and recently to revisit the cone fundamental space (CIE, 2006).

On the other hand, the dimensionality of colour vision may vary depending on the individual, the task and the context. It is a challenge for the future to establish relationships between one or another colour space and to find the best way to define the colour of the world.

## ACKNOWLEDGMENTS

## REFERENCES

Barrionuevo, P. A. and Cao, D., 2014. Contributions of rhodopsin, cone opsins, and melanopsin to postreceptoral pathways inferred from natural image statistics. *Journal of the Optical Society of America* A, 31(4), A131.

Bonnardel, V., 2013. Color categories. In: *A Symposium on Colour Vision In Memory of Yves Le Grand*, CIE, MNHN, Paris, France.

Brettel H., Viénot F. and Mollon J. D., 1997. Computerized simulation of color appearance for dichromats. *Journal of the Optical Society of America* A 14: 2647–2655.

Brown T. M., Tsujimura S., Allen A. E., Wynne J., Bedford R., Vickery G., Vugler A., and R. J. Lucas, 2012. Melanopsin-based brightness discrimination in mice and humans, *Current Biology* 22: 1134-1141.

Clarke F. J. J., 1973. Needs and prospects for a tetrachromatic system of large field colorimetry. In: *Colour 73*, 2nd Congress of the International Colour Association, York, pp. 319-324.

Cohen J. B. and Kappauf W. E., 1982. Metameric color stimuli, fundamental metamers, and Wyszecki's metameric blacks, *American Journal of Psychology* 95: 537–564.

Commission Internationale de l'Eclairage: Fundamental Chromaticity Diagram with Physiological Axes - Part 1, CIE 170-1-2006

Craven, B. J. and Foster, D. H., 1992. An operational approach to colour constancy. *Vision Research* 32: 1359-1366.

Dacey, D. M., Liao, H.-W., Peterson, B. B., Robinson, F. R., Smith, V. C., Pokorny, J. and Gamlin, P. D., 2005. Melanopsin-expressing ganglion cells in primate retina signal colour and irradiance and project to the LGN. *Nature* 433(7027): 749–754.

Foster D. H., Amano K., Nascimento S. and Foster M. J., 2006. Frequency of metamerism in natural scenes. *Journal of the Optical Society of America* A 23: 2359–2372.

Foster, D. H., 2011. Color constancy. *Vision Research* 51(7): 674–700.

Hannibal, J., Kankipati, L., Strang, C. E., Peterson, B. B., Dacey, D., & Gamlin, P. D., 2014. Central projections of intrinsically photosensitive retinal ganglion cells in the macaque monkey: Central projections of intrinsically photosensitive RGCs in macaque. *Journal of Comparative Neurology* 522(10): 2231–2248.

Hernández-Andrés J., Romero J., Nieves J. L. and Lee Jr R. L., 2001. Color and spectral analysis of daylight in southern Europe. *Journal of the Optical Society of America* A 18(6): 1325-1335.

Horiguchi H., Winawer J., Dougherty R. F. and Wandell B. A., 2013. Human trichromacy revisited. *Proceedings of the National Academy of Science USA* 110: E260–E269.

Jameson, K., 2005. Culture and Cognition: What is Universal about the Representation of Color Experience? *Journal of Cognition and Culture*, 5(3): 293–348.

Jordan, G., Deeb, S. S., Bosten, J. M. and Mollon, J. D., 2010. The dimensionality of color vision in carriers of anomalous trichromacy. *Journal of Vision* 10(8):12, 1–19.

Judd D. B., 1948. Color perceptions of deuteranopic and protanopic observers. *J Res Nat Bur Stand (USA)* 41:247–271.

Judd D. B., MacAdam D. L. and Wyszecki G., 1964. Spectral distribution of typical daylight as a function of correlated color temperature, *Journal of the Optical Society of America* 54: 1031-1040.

Judd, D. B., Macadam, D. L., Wyszecki, G., Budde, H. W., Condit, H. R., Henderson, S. T. and Simonds, J. L., 1964. Spectral Distribution of Typical Daylight as a Function of Correlated Color Temperature. *Journal of the Optical Society of America* 54(8): 1031.

Kelber, A. and Osorio, D., 2010. From spectral information to animal colour vision: experiments and concepts. *Proceedings of the Royal Society B: Biological Sciences* 277(1688): 1617–1625.

König A. and Dieterici C., 1886. Die Grundempfindungen und ihre Intensita̎ts-Vertheilung im Spectrum. *Sitzungsberichte Akademie der Wissenschaften*, Berlin, 805–829.

Lennie, P, Pokorny, J and Smith, VC, 1993. Luminance. *Journal of the Optical Society of America* A 10: 1283-1293.

MacLeod D. I. A. and Boynton R. M., 1979. Chromaticity diagram showing cone excitation by stimuli of equal luminance. *Journal of the Optical Society of America* 69:1183-1186.

Meyer G. W. and Greenberg D. P., 1988. Color-defective vision and computer graphics displays. *IEEE Comp Graph Appl* 8: 28–40.

Nathans, J., Thomas, D. and Hogness, D., 1986. Molecular genetics of human color vision: the genes encoding blue, green, and red pigments. *Science* 232(4747): 193–202.

Report of U.S. Secretariat Committee on Colorimetry and Artificial Daylight, *CIE Proceedings*, Vol. 1, Part 7, Stockholm, 1951.

Sharpe L. TL, Stockman A., Jägle H. and Nathans J., 1999. Opsin genes, cone photopigments, color vision, and color blindness. In *Color Vision: From genes to perception*, eds : Gegenfurtner K R and Sharpe L T , Cambridge University Press, New York, pp. 3-52.

Stiles W. S. and Burch J. M., 1959. NPL colour-matching investigation: Final report (1958). *Optica Acta* 6: 1-26.

Stockman A. and Sharpe L. T., 2000. Cone spectral sensitivities and color matching. In *Color Vision: From genes to perception*, eds : Gegenfurtner K R and Sharpe L T , Cambridge University Press, New York, pp. 53-87.

Stockman A. and Sharpe L. T., 2000. Spectral sensitivities of the middle- and long-wavelength-sensitive cones derived from measurements in observers of known genotype. *Vision Research* 40: 1711–1737.

Trezona P. W., 1973. Tetrachromatic colour measurement. In: *Colour 73*, 2nd Congress oft he International Colour Association, York, pp.324-328..

Viénot F., Brettel H., Ott L., Ben M'Barek A. and Mollon J. D., 1995. What do colour-blind people see? *Nature* 376: 127-128.

Viénot, F., Brettel, H., Dang, T.-V. and Le Rohellec, J., 2012. Domain of metamers exciting intrinsically photosensitive retinal ganglion cells (ipRGCs) and rods. *Journal of the Optical Society of America* A 29(2): A366.

Viénot F., Walraven P., 2007, Colour-matching functions, physiological basis. In: Janos Schanda (Editor) *Colorimetry, Understanding the CIE system*, Wiley, pp. 219-243.

Wyszecki G. and Stiles W. S., 1982. Color science: Concepts and methods, Quantitative data and formulae, Wiley.

Wyszecki G., 1953. Valenzmetrische untersuchung des Zusammenhanges zwischen normaler und anomaler Trichromasie. *Farbe* 2:39–52.

*Address: Prof. Françoise VIÉNOT*
*Centre de recherche sur la conservation (CRC, USR 3224)*
*Sorbonne Universités*
*Muséum national d'Histoire naturelle*
*Ministère de la Culture et de la Communication, CNRS*
*CP21, 36 rue Geoffroy-Saint-Hilaire, 75005 Paris, France.*

# BIBLIOGRAPHY
# Françoise VIÉNOT

## AWARDS

VIÉNOT F., 2014, *ISCC Macbeth Award*, Inter-Society Color Council News, Issue 468, Fall 2014

VIÉNOT F., *Verriest Medal, The International Colour Vision Society*, 22nd Biennial ICVS Symposium, Winchester UK, 15 July 2013.

VIÉNOT F., "Novelty of metameric LED white lights", *Newton medal, The Colour Group of Great Britain*, London, 13th April 2012.

VIÉNOT F., "From gloss scaling to gloss constancy". Presentation of "The David Palmer lecture", *The Colour Group* (Great Britain), London, 12th January 2006.

VIÉNOT F., Prix de la meilleure communication, *LE CLUB VISU - SID-FRANCE*, 18 juin 1997.

VIÉNOT F., Prix Alfred Monnier de *l'Association Française de l'Eclairage*, 20 mars 1997.

VIÉNOT F., Médaille de l'Universidad de Granada, 1996.

## BOOKS

Commission Internationale de l'Eclairage, 2006, CIE 170-1:2006 "*Fundamental Chromaticity Diagram with Physiological Axes - Part 1*", report of CIE TC 1-36, 45 p.

ROQUE G., BODO B. & VIÉNOT F. (eds), 1997*, Michel-Eugène CHEVREUL. Un savant, des couleurs!* MNHN/EREC, Paris, 277 p.

KOWALISKI P., 2ème édition actualisée par VIÉNOT F. & SÈVE R., 1990, *Vision et mesure de la couleur*, Coll. Physique fondamentale et Appliquée, Masson, Paris.

## BOOK CHAPTERS

VIÉNOT F., 2015, Peut-on mesurer l'apparence ? Actes de l'Université européenne « Observation et pensée », *Université Paris-Diderot* (in press).

VIÉNOT F., LE ROHELLEC J., 2012, Colorimetry and physiology: the LMS specification. In : FERNANDEZ-MALOIGNE C., ROBERT-INACIO F., MACAIRE L., *Digital color. Acquisition, Perception, Coding and Rendering* Digital Signal and Image Processing Series, ISTE, Wiley, pp. 1-27.

VIÉNOT F., LE ROHELLEC J., 2012, Colorimétrie et physiologie : la spécification LMS. In : FERNANDEZ-MALOIGNE C., ROBERT-INACIO F., MACAIRE L.(Eds.), *Couleur numérique : acquisition, perception, codage et rendu (Traité Signal et Image, IC2)*, Hermès, Lavoisier, pp.19-42, planche couleur page i.

VIÉNOT F., GENDRON F., 2009, L'attrait du brillant et de la couleur. L'éclat de la pierre polie. In : M-H. Moncel et F. Fröhlich (éditeurs), *L'homme et le précieux. Matières minérales précieuses*, BAR International Series 1934, pp. 111-118. http://precieux.mnhn.fr/?page_id=250

VIÉNOT F., 2008, L'éclairage à base de LEDs. In : P. Mottier (co-ordonnateur) *Les diodes électroluminescentes pour l'éclairage* (traité EGEM), Hermes. . pp. 207-239 et IV-VI. Traduction anglaise : Quality of white light from LEDs. In: P. Mottier (editor) *LEDs for Lighting Applications*, ISTE Wiley, 2009, pp 197-232.  ISBN: 9781848211452

VIÉNOT F., WALRAVEN P., 2007, Colour-matching functions, physiological basis. In: Janos Schanda (Editor) *Colorimetry, Understanding the CIE system*, Wiley, pages 219-243.

VIÉNOT F., 2006, La vision en couleur des surfaces. In : *La couleur. Lumière, vision et matériaux*, sous la direction de Mady Elias et Jacques Lafait, Belin, collection Échelles, 27-78. www.lumilog.com

VIÉNOT F., 2001, L'usage de l'écran de visualisation dans le test de vision des couleurs. In: *Les dyschromatopsies*, rapport annuel des Sociétés d'Ophtalmologie de France, coordonnateur J. Leid, *Bull.Soc.Ophtal.Fr.* : 145-151.

RIGAUDIÈRE F.,VIÉNOT F., 2001, Quelques bases physiques, psychophysiques et neurophysiologiques de la sensation colorée. In: *Les dyschromatopsies*, rapport annuel des Sociétés d'Ophtalmologie de France, coordonnateur J. Leid, *Bull.Soc.Ophtal.Fr.* : 23-37.

VIÉNOT F., 1999, La couleur, une vue de l'esprit. In: *Mille cerveaux, mille mondes*, sous la direction de P. BUISSERET, Nathan/HER & MNHN, Paris, France, pp. 101-104.

BRETTEL H., VIÉNOT F., 1999, Web design for the colour-blind user. In: *Colour Imaging: Vision and Technology*, edited by L.W. MacDonald and M.R. Luo, John Wiley & Sons Ltd., pp.55-71.

VIÉNOT F., 1998, Perception de la couleur. In: M. BOUCART, M.-A. HÉNAFF & C. BELIN (eds.), *Vision : aspects perceptifs et cognitifs*, SOLAL, Marseille, pp. 149-168 (**Conférence invitée** à la *Société de Neuropsychologie de Langue Française*, Paris, décembre 1997)

VIÉNOT F., 1997, Parallèle entre certaines observations de Chevreul et les acquis récents sur les mécanismes visuels. In: G. ROQUE, B. BODO & F. VIÉNOT (eds.), *Michel-Eugène Chevreul. Un savant, des couleurs!* MNHN/EREC.1997. Paris, pp.147-158.

DENIEUL P., BRETTEL H., MONOT A., VIÉNOT F., 1992, Vision et visualisation. In: *Systèmes Optiques*, Les Editions de Physique, Les Ulis, France, pp.315-337. http://dx.doi.org/10.1051/bib-sfo:2002027

VIÉNOT F. & CHOUARD P., 1992, Définition des principales couleurs applicables aux végétaux. In: *Le Bon Jardinier*, 153° ed., Editions Pierre Anglade, Paris, pp.1079-1093, 2 planches couleur.

VIÉNOT F., 1991, Transition from photopic to scotopic light assessments and possible underlying processes. In: B.B.LEE & A. VALBERG (Eds.), *From Pigments to Perception,* Plenum Publishing Corporation, New York, pp.41-51. (**Conférence invitée** au colloque *Nato advanced workshop on Advances in understanding visual processes. Convergence of neurophysiological and psychophysical evidence.* Roros, Norway, 6-10 August 1990)

FLEURY P., DENIEUL P., VIÉNOT F., 1985, Vision. Dans: *Encyclopaedia Universalis,* 2° ed., pp.942-949.

VIÉNOT F., 1983, Can variation in macular pigment account for the variation of colour matches with retinal position? In: MOLLON J.D. and SHARPE L.T. (Eds), *Colour Vision: Physiology and Psychophysics,* Academic Press, London, pp.107-116. (**Conférence invitée** au colloque *Colour vision. A NATO conference*, Cambridge, August 23-27, 1982)

# ARTICLES

VIENOT F., BRETTEL H., 2014, The Verriest lecture: Visual properties of metameric blacks beyond cone vision. J. Opt. Soc. Am. A / Vol. 31, No. 4 / April 2014. A38-A46. http://dx.doi.org/10.1364/JOSAA.31.000A38 On line December 19, 2013.

COMAR A., BARRET F., OBEIN G., SIMONOT L., MENEVEAUX D., VIENOT F., DE SOLAN B., 2014, A leaf BRDF model taking into account the azimuthal anisotropy of monocotyledonous leaf surface. *Remote Sensing of Environment*, 1: 112-121.

ARNAULT E, BARRAU C, NANTEAU C, GONDOUIN P, BIGOT K, VIÉNOT F. et al., 2013, Phototoxic Action Spectrum on a Retinal Pigment Epithelium Model of Age-Related Macular Degeneration Exposed to Sunlight Normalized Conditions. PLoS ONE 8(8): e71398. doi:10.1371/journal.pone.0071398

DELPORTE, C., SAUTROT, S., BEN CHOUIKHA, M., VIÉNOT, F., ALQUIÉ, G., 2013, Biological tissue identification using a multispectral imaging system. *Sensors, Cameras, and Systems for Industrial and Scientific Applications XIV. Proceedings of the SPIE*, Volume 8659, article id. 86590H, 9 pp. (2013).

COMAR, A., BARET, F., VIÉNOT, F., YAN, L. and DE SOLAN, B., 2012. Wheat leaf bidirectional reflectance measurements: Description and quantification of the volume, specular and hot-spot scattering features. *Remote Sensing of Environment*, 121: 26-35.

VIÉNOT F., BRETTEL H., DANG T.-V., LE ROHELLEC J., 2012, Domain of metamers exciting intrinsically photosensitive retinal ganglion cells (ipRGCs) and rods, *J. Opt. Soc. Am. A* 29, Issue 2, pp. A366-A376 (2012).

DELPORTE, C., BEN CHOUIKHA, M., SAUTROT, S., VIÉNOT, F., ALQUIÉ, G., 2012, Multispectral device for help in diagnosis. In: Widenhorn, R; Nguyen, V; Dupret, A. (Eds.), Sensors, Cameras, And Systems For Industrial And Scientific Applications XIII Book Series: Proceedings of SPIE Volume: 8298, Article Number: 82980P. [hal-00671010 - version 1]

SARKAR A., F. AUTRUSSEAU, F. VIÉNOT, P LE CALLET, and L. BLONDÉ, 2011, "From CIE 2006 physiological model to improved age-dependent and average colorimetric observers," *J. Opt. Soc. Am. A* 28, 2033-2048.

BEHAR-COHEN F., MARTINSONS C., VIÉNOT F., ZISSIS G., BARLIER-SALSI A., CESARINI J.-P., ENOUF 0., GARCIA M., PICAUD S., ATTIA D., 2011, Light-emitting diodes (LED) for domestic lighting: Any risks for the eye?, *Progress in Retinal and Eye Research*, 30/ 239-257.

VIÉNOT F., CORON G., LAVÉDRINE B., 2011, LEDs as a tool to enhance faded colours of museums artefacts, *J. Cultural heritage*, Volume 12, Issue 4, Pages 431-440. doi:10.1016/j.culher.2011.03.007. https://www.em-consulte.com/revue/culher/s200/2141.

GED G., OBEIN G., SILVESTRI Z., LE ROHELLEC J., VIÉNOT F., 2010, Recognizing Real Materials from their Glossy Appearance, *Journal of Vision,* 10(9):18, 1–17. http://www.journalofvision.org/content/10/9/18

LABORIE B., VIÉNOT F., LANGLOIS S., Methodology for constructing a colour-difference acceptability scale. *Ophthalmic and Physiological Optics*, 30: 568–577, 2010.

VIÉNOT F., DURAND M.-L., MAHLER E., 2009, Kruithof's rule revisited using LED illumination. *J. Mod. Optics*, 56 : 1433-1446.

MAHLER E., EZRATI J.-J., VIÉNOT F., 2009, Testing LED Lighting for Colour Discrimination and Colour Rendering. *Color Research & Application*, 34 : 8-17.

VIÉNOT F, MAHLER E., EZRATI J.-J., BOUST C., RAMBAUD A., BRICOUNE A., 2008, Color appearance under LED illumination: The visual judgment of observers. *Journal of Light and Visual Environment*, 32 :208-213.

VIÉNOT F, SERREAULT L., PARDO FERNANDEZ P., 2006, Convergence of experimental multiple Rayleigh matches to peak L- and M- photopigment sensitivity estimates, *Visual Neuroscience*, 23: 419-427.

BOUST C., BEN CHOUIKHA C., BRETTEL H., VIÉNOT F., BERCHE S. & ALQUIÉ G., 2006, Color Enhancement of Digital Images by Experts and Preference Judgments by Observers. *The Journal of Imaging Science and Technology.* 2006, **50**: 1-11.

RIGAUDIÈRE F., LEID J., VIÉNOT F, LE GARGASSON J.-F., 2006, Comprendre et tester les déficiences de la vision des couleurs de l'enfant, en pratique. *J Fr d'Ophtalmologie*, **29** :87-102.

HARRAR M., VIÉNOT F., 2005, Regulation of chromatic induction by neighboring images. *J. Opt. Soc. Am A.*, 22: 2197−2206.

OBEIN, G., KNOBLAUCH, K., & VIÉNOT, F., 2004. Difference scaling of gloss: Nonlinearity, binocularity, and constancy. *Journal of Vision*, *4*(9), 711-720, http://journalofvision.org/4/9/4/ , doi:10.1167/4.9.4.

HARRAR, M., & VIÉNOT, F. (2004). A study on chromatic contrast regulation [Abstract]. *Journal of Vision*, *4*(11), 11a, http://journalofvision.org/4/11/11/, doi:10.1167/4.11.11.

OBEIN, G., PICHEREAU, T., HARRAR, M., MONOT, A., KNOBLAUCH, K., & VIÉNOT, F. (2004). Does binocular vision contribute to gloss perception? [Abstract]. *Journal of Vision*, *4*(11), 73a, http://journalofvision.org/4/11/73/, doi:10.1167/4.11.73.

HARRAR M., VIÉNOT F., GIRAUDET G., BAILLET G., 2003, Is glare spectrally selective ? *Perception*, Vol. 32, Suppl., p. 149.

HARRAR M., GIRAUDET G., BAILLET G., VIÉNOT F., 2003, Effet d'un éblouissement coloré sur les fonctions visuelles, *LR'O°08*, pages 6-10.

OBEIN G., KNOBLAUCH K., CHRISMENT A., VIÉNOT F., 2002, Perceptual scaling of the gloss of a one-dimensional series of painted black samples. *Perception*, Vol. 31, Suppl., p. 65.

VIÉNOT F., 2002, Michel-Eugène Chevreul: From laws and principles to the production of colour plates. *Color Research and Application :* 27 : 4-14. (**Conférence invitée** à l'*Inter-Society Color Council 2nd Panchromatic Conference,* Color in its surround, February 19-21, 2000, Savannah, U.S.A.).

VIÉNOT F., CHIRON A., 2001, Michel-Eugène Chevreul and his colour classification system. *Color Research and Application*, 26 : S20-S24. (**Conférence invitée** à l'*International Colour Vision Society*, 1999).

VIÉNOT F., 2001, Retinal distribution of the macular pigment and the cone effective optical density from colour matches of real observers. *Color Research and Application*, 26: S264-S268.

REGAN B.C., JULLIOT C., SIMMEN B., VIÉNOT F., CHARLES-DOMINIQUE P., MOLLON J.D., 2001, Fruits, foliage and the evolution of primate colour vision. *Phil. Trans. Royal Soc.*, 356: 1-55.

LE ROHELLEC J., VIÉNOT F., 2001, Interaction of luminance and spectral adaptation upon Benham subjective colours. *Color Research and Application,* 24:S174-S179.

MELGOSA M., RIVAS M.J., HITA E., VIÉNOT, 2000, Are we able to distinguish color attributes?, *Color Research and Application*, 25, 356-367.

VIÉNOT F., 1999, Le rendu des couleurs dans son contexte. Antériorité du regard des peintres sur l'analyse des scientifiques. *Techne, Centre de recherche et de restauration des musées de France*, Nos 9-10, p. 74-91.

VIÉNOT F., BRETTEL H., MOLLON J., 1999, Digital video colourmaps for checking the legibility of displays by dichromats. *Color Research and Application,* 24 : 243-252.

DIAZ NAVAS J.A., CHIRON A., VIÉNOT F., 1998, Tracing a metameric match to individual variations of colour vision. *Color Research and Application*, 23: 379-389.

BEN CHOUIKHA M., VIÉNOT F., LU G.N., 1998, Colorimetric characterization of a buried triple p-n junction photo-detector. *Displays*, vol.19, n°:30, pp. 105-110.

BÈCLE P., MONOT A., VIÉNOT F., EYQUEM D., 1998, Detecting gradient and discriminating shape from texture. *Perception*, vol.27, suppl., p.204.

LE ROHELLEC J., VIÉNOT F., 1998, The effect of luminance and spectral adaptation upon subjective colours. *Perception*, vol.27, suppl., p.174-175.

REGAN B.C., JULLIOT C., SIMMEN B., VIÉNOT F., CHARLES-DOMINIQUE P., MOLLON J.D., 1998, Frugivory and colour vision in *Alouatta seniculus*, a trichromatic platyrrhine monkey. *Vision Research*, 38: 3321-3329.

BRETTEL H., VIÉNOT F., MOLLON J., 1997, Computerized simulation of color appearance for dichromats. *J. Opt. Soc. Am.,* vol.14, 2647-2655.

PEFFERKORN S., CHIRON A., VIÉNOT F., 1996, Développement d'une méthode de photométrie visuelle mésopique. *Bull. du Bureau National de Métrologie*, vol.106, pp.19-35.

DIAZ NAVAS J.A., CHIRON A., VIÉNOT F., 1996, Tracing a metameric match to individual variations of colour vision. *Perception,* vol.25, suppl., p.15.

REGAN B.C., VIÉNOT F., CHARLES-DOMINIQUE P.C., PEFFERKORN S., SIMMEN B., JULLIOT C., MOLLON J.D., 1996, The colour signals that fruits present to primates. *Investigative Ophthalmology & Visual Science*, Vol.37, p.S648.

VIÉNOT F., BRETTEL H., OTT L., BEN M'BAREK A., MOLLON J. D., 1995, What do colour-blind people see?, *Nature*, vol. 376, pp.127-128.

LE ROHELLEC J., VIÉNOT F., 1994, Dependence of Fechner-Benham colours upon luminance adaptation, *Perception*, vol.23, suppl., p.91.

LE ROHELLEC J., VIÉNOT F., 1992, Change in the colours of Benham's top with exposure time. *Perception,* vol.21, suppl.2, p.76.

VIÉNOT F., CHIRON A., 1992, Heterochromatic flicker photometry is phase-dependent at mid-mesopic levels. *Perception,* vol.21, suppl.2, p.77.

VIÉNOT F. & LE ROHELLEC J., 1992, Reversal in the sequence of the Benham colours with a change in the wavelength of illumination. *Vision Res.*, Vol.32, pp.2369-2374.

VIÉNOT F. & CHIRON A., 1992, Brightness Matching and Flicker Photometric Data Obtained Over the Full Mesopic Range. *Vision Res.*, Vol.32, pp.533-540.

VIÉNOT F. & LE ROHELLEC J., 1990, Hue reversal in the colours of Benham's top with change in illumination wavelength. *Perception,* vol.19, pp.358-359.

VIÉNOT F., 1990, A portable apparatus for measuring wavelength discrimination in man. *J. Physiol. (Lond.),* vol.426, p.4P.

VIÉNOT F., 1987 (publié en 1989), What are observers doing when making color-matches? *Farbe,* vol.34, pp.221-228. (**Conférence invitée** au colloque *International Colour Association (AIC) interim meeting: Wyszecki and Stiles Memorial Symposium on Color Vision Models*, Florence, Italie, 10-13-juin 1987)

MORELAND J.D., VIÉNOT F., 1988, Macular pigment multiplicity. In: 11th European Conference on Visual Perception (ECVP), Bristol, G.B., *Perception,* vol.17, n°3, p.380.

CHIRON A., VIÉNOT F., 1988, Direct comparaison and flicker matches at high mesopic levels. In: 11th European Conference on Visual Perception (ECVP), Bristol, G.B., *Perception,* vol.17, n°3, p.371.

COOPER H.M., CHARLES-DOMINIQUE P., VIÉNOT F., 1986, Signification de la coloration des fruits en fonction de la vision des vertébrés consommateurs. *Mémoires du Muséum national d'Histoire naturelle ,* Série A, Zoologie, tome 132 (Entretiens du Muséum, Vertébrés et Forêts tropicales humides d'Afrique et d'Amérique), pp.131-143.

BOURDY C., VIÉNOT F., MONOT A., CHIRON A., 1985, Spatial contrast detection for colour patterns under selective chromatic  adaptation. *Displays: Technology and applications,* vol.6, n°1, pp.43-51.

BOURDY C., VIÉNOT F., MONOT A., CHIRON A., 1983, Spatial sensitivity of the human visual system under selective chromatic adaptation: shape of the contrast sensitivity curves, foveal versus peripheral vision. *J. of Optics* (Paris), vol.14, n°5, pp.225-233.

VIÉNOT F., 1983, Color-match changes between the fovea and the  perifovea. *Color Research and Application,* vol.8, n°4, pp.215-220.

BOURDY C., VIÉNOT F., MONOT A., CHIRON A., 1982, Forme des courbes de sensibilité au contraste des mécanismes colorés isolés en vision fovéale et en vision périphérique. *L'Année Psychologique,* vol.82, pp.19-27.

VIÉNOT F., 1980, Relations between inter-and intra-individual  variability of color-matching functions. Experimental results. *J. Opt. Soc. Am.,* vol.70, n°12, pp.1476-1483.

VIÉNOT F., 1977, About the statistics of color-matching functions. *Farbe,* vol.26, n°3-6, pp.205-212.

VIÉNOT F., 1977, New equipment for the measurement of color-matching functions. *Color Research and Application,* vol.2, n°4, pp.165-170.

# CONFERENCE PAPERS

VIÉNOT F., 2013, Light Emitting Diodes: quality assessment and visual comfort, Cultural heritage conservation science and sustainable development: experience, research, innovation International conference in the frame of the 50th anniversary of the Centre de recherche sur la conservation des collections – CRCC, Paris, 23, October 2013.

VIÉNOT F., 2013, Metamerism beyond colour vision. *22nd Symposium of the International Colour Vision Society*, Winchester, UK, 14-18 July 2013, p. 42. (**Verriest Medallist 2013**)

VIÉNOT F., 2013, Virtual Restoration of Faded Colours of %Museums Artefacts using LED Lighting. Proceedings of AIC2013, 12th International AIC Congress, Newcastle upon Tyne, 8 July 2013, page 101. (**Conférence invitée**)

BARRAU C., NADOLNY C., VILLETTE T., VIÉNOT F., 2013, Effects of selective blue-violet spectral subtractions on colour perception. *22nd Symposium of the International Colour Vision Society*, Winchester, UK, 14-18 July 2013, p. 123.

LE ROHELLEC J., VIÉNOT F., ANTON J.-L., NAZARIAN B., ATTIA D., MERCKEL O., ROSENFELD F., LAVÉDRINE B., 2013, A study of the sustained pupil response under a variety of LED illuminations. Proc. CIE Centenary, Paris, 15 April 2013.

VIÉNOT F., 2012, Gloss Characterization, a Cyclic Approach. In: *Predicting Perceptions: Proceedings of the 3rd International Conference on Appearance*. Lulu Press, Edinburgh UK, pp. 7-9. ISBN 978-1-4716-6869-2. (**Conférence invitée**)

DELPORTE C., BEN CHOUIKHA M., SAUTROT S., VIÉNOT F AND ALQUIÉ G, 2012, Multispectral device for help in diagnosis, *Proc. SPIE* 8298, 82980P (2012); http://dx.doi.org/10.1117/12.909107

FALKENSTERN K., BONNIER N., BRETTEL H., FELHI1 M., VIÉNOT F., 2011, Adaptively Selecting a Printer Color Workflow. *19th Color and Imaging Conference*, November 7 – 11, 2011, San Jose, CA, The Society for Imaging Science and Technology, 205-210, octobre 2011, Paris, France, 6 pages.

ROBERT-INACIO F., PERRIN M., FAVIER S., VIÉNOT F., DANG T.-V., LE ROHELLEC J. & KUSSENER E., Eye-tracking for pupil diameter extraction, ECEM 2011, 16th European Conference on Eye Movements, 21-25 August, 2011, Marseille, France.

FALKENSTERN K., BONNIER N., BRETTEL H., PEDERSEN M., VIÉNOT F., 2011, Weighing quality attributes. *21st Symposium of the International Colour Vision Society*, Kongsberg, Norway, 1-5 July 2011, p. 88.

VIÉNOT F., DANG T.-V., LE ROHELLEC J., BRETTEL H., 2011, Domain of metamers exciting melanopsin. *21st Symposium of the International Colour Vision Society*, Kongsberg, Norway, 1-5 July 2011, p. 84.

VIÉNOT F., BAILACQ S., ZOUAOUI L., LE ROHELLEC J., 2011, Variation of the pupillary reflex with the spectral power distribution of the light. Proceedings of the 27th session of the CIE, *CIE197:2011*, 940-944.

FALKENSTERN K., BONNIER N., BRETTEL H., PEDERSEN M., VIÉNOT F., 2011, Using Metrics to Assess the ICC Perceptual Rendering Intent, *Proc. SPIE*, Volume 7867 -- *Image Quality and System Performance VIII*, Burlingame, California, 2011.

ROUCHON V., ZERDOUN M., ESTÈVE J.-L., VIÉNOT F., LAVÉDRINE B., BARTHEZ J., 2010, Tonalité rouge des papiers anciens observés en lumière transmise : de l'observation à l'interprétation. In : Monique Zerdoun et Caroline Bourlet, actes du colloque "Matériaux du livre médiéval", collection Bibliologia de Brepols 30 :56-70. Turnhout, Belgique, Brepols, 55-70.

LABORIE B., LANGLOIS S., VIÉNOT F., 2010, Short-term colour discrimination: appearance and cognitive approach. *AVA CHRISTMAS MEETING 2010*, December17-18, 2010, Paris, France. *Perception*, 2011, volume 40, page 112, P2.

VIÉNOT F., LE ROHELLEC J., ZOUAOUI L., 2010, Case reports of the effect of the spectral power distribution of metamer lights on pupil aperture, *AVA CHRISTMAS MEETING 2010*, December17-18, 2010, Paris, France. *Perception*, 2011, volume 40, page 104, T1.

FALKENSTERN K., BONNIER N., BRETTEL H., PEDERSEN M., VIÉNOT F., 2010, Using Image Quality Metrics to Evaluate an ICC Printer Profile, *18th Color and Imaging Conference*, November 8 – 12, 2010, San Antonio, Texas, The Society for Imaging Science and Technology, 244-249.

LABORIE B., LANGLOIS S., VIÉNOT F., 2010, A PDP as a colorimetric tool to investigate colour vision. *15th International Workshop on Inorganic and Organic Electroluminescence & 2010 Int. Conference on the Science and Technology of Emissive Displays and Lighting & XVIII Advanced Display, Technologies* International Symposium, September 27-October 1, 2010, St. Petersburg, Russia, pp.300-301.

ATTIA D., BARLIER-SALSI A., BEHAR-COHEN F., CÉSARINI J. P., ENOUF O., GARCIA M., MARTINSONS C., MERCKEL O., PICAUD S., VIÉNOT F., ZISSIS G., 2010, Potential health impacts of LED lighting. *LS12-WhiteLED3, White LEDs and solid state lighting 3rd international conference*, July 11-16, Eindhoven, The Netherlands.

VIÉNOT F., DURAND M.-L., MAHLER E., 2009, The effect of LED lighting on performance, appearance and sensations, *Proceedings of the CIE Light and Lighting Conference,* Budapest, 27-29 May 2009. *CIE x034:2010*: 161:166.

LABORIE B., VIÉNOT F., LANGLOIS S., 2009, Construction d'un illustrateur de différence de couleur. In : ROBERT-IGNACIO F., *Cours et application industrielles de l'imagerie numérique couleur*, Toulon, France, Editions Fred Valou, 2009, p. 194-196. ISBN: 978-2-9532792-0-7. *Ecole d'Hiver sur l'Image Numérique Couleur*, Toulon, 13-16 janvier 2009, Prix du meilleur poster jeune chercheur,

VIÉNOT F., JUSTIN T., NETTER E., MILLEVILLE S., ECHARD J.-P., LAVÉDRINE B., An optical study of natural materials used in museum collections: wood and straw. *Materials & Sensations 2008*, Pau, Oct. 22–24, e-proceedings : p.117-120.

AIC2015 TOKYO - Color and Image

ECHARD, J.-P., VIÉNOT, F., BAK, A., EZRATI, J.-J., 2008, Apparence finale d'un érable ondé verni : rugosité des interfaces, in *De la peinture de chevalet à l'instrument de musique: vernis, liants et couleurs, actes du colloque, 6-7 Mars 2007. Paris Cité de la musique*, pp. 129-132.

VIÉNOT F, MAHLER E., EZRATI J.-J., BOUST C., BRICOUNE A., Color appearance under LED illumination: The visual judgment of observers. *First International Conference on White LEDs and Solid State Lighting*, Tokyo, Japan, 29 nov 2007. (**Conférence invitée**)

VIÉNOT F, LED lighting for museums, toward the highest quality of light. 3a Conferenza Nazionale del Gruppo del Colore. Torino, Italie, 25 oct 2007. (**Conférence invitée**)

VIÉNOT F, EZRATI JJ, BOUST C, MAHLER E, Grading LED illumination : from colour rendering indices to specific light quality indices. *CIE 26th session*, Beijing 2007, D1:22-25.

OBEIN G., VIÉNOT F., 2007, Modelling the BRDF of a series of matt to glossy black samples. *Proceedings of the CIE Expert Symposium on Visual Appearance, CIE publication x032:2007*, pp.67-74 (2007)

VIÉNOT F., BAK A., ECHARD J.-P., 2007, The peculiar BRDFs of flamed maple. *Proceedings of the CIE Expert Symposium on Visual Appearance, CIE publication x032:2007*, pp.230-234 (2007).

PLANTIER J., AUBRY J.P., VIÉNOT F., OSSARD G., ROUMES C., 2007, Chromatic Contrast Sensitivity Functions, *Perception*, Vol. 36, Suppl., 198.

HARRAR M., BRETTEL H., VIÉNOT, F., 2006, About the limited additive properties of colour appearance models. *Perception*, Vol. 35, Suppl., 191.

PLANTIER, J., AUBRY, J., VIÉNOT, F., OSSARD, G., & ROUMES, C., 2006, Luminance equilibrium of chromatic pairs at different eccentricities [Abstract]. *Journal of Vision*, *6*(6), 702a, http://journalofvision.org/6/6/702/, doi:10.1167/6.6.702.

VIÉNOT F., 2006, Origins and history of the Standard Observers, *CIE Expert Symposium on 75 Years of the CIE Standard Colorimetric Observer*, Ottawa, Canada, 16 May 2006, CIE x030:2006, 7p.. (**Conférence invitée**)

LAVÉDRINE B., GILLET M., VIÉNOT F., GARNIER C., MAHLER E., 2006, Évaluation de la photosensibilité et étude d'un dispositif d'éclairage à diodes électroluminescentes de photographies anciennes en couleurs. *Couleur et temps, La couleur en conservation et restauration*, Actes des 12es journées d'études de la Section française de l'institut international de conservation, 21-24 juin 2006, *SFIIC*, Champs sur Marne, pages 272-279. ISBN 2-905430-16-8.

BEN CHOUIKHA M., PLACAIS B., POULEAU G., SAUTOT S., VIÉNOT F., 2006, Benefits and Drawbacks of two Methods for Characterizing Digital Cameras, *CGIV 2006 Proceedings*, Society for Imaging science and Technology, 185-188.

VIÉNOT F., 2006, Introduction à la couleur : de l'expérience visuelle à la mesure. *Couleur et temps, La couleur en conservation et restauration*, Actes des 12es journées d'études de la Section française de l'institut international de conservation, 21-24 juin 2006, SFIIC, Champs sur Marne, pages 13-21. ISBN 2-905430-16-8. (**Conférence invitée**)

EZRATI J.-J., PÉRIGNON P., BRICOUNE A., SERREAULT L., HARRAR M., VIÉNOT F., MAHLER E., 2005, Light-emitting diodes: a future for museum lighting? *ICOM 14th Triennial Meeting 2005*, Vol. II, 26th September 2005.

VIÉNOT F., SERREAULT L., 2005, Is it possible to derive the maximum wavelength of M and L photo pigments using multiple-Rayleigh matches? *XVIIIth Symposium of the International Colour Vision Society*, Lyon, 8-12 July 2005, p. 22.

MAHLER E., EZRATI J.-J., VIÉNOT F., 2005, Designing a colour discrimination test to assess colour rendering of LED sources. *XVIIIth Symposium of the International Colour Vision Society*, Lyon, 8-12 July 2005, p. 53.

HARRAR M., BAILLET G., BOURDONCLE B., BRETTEL H., O'REGAN K., VIÉNOT F., 2005, Comparison of colour appearance changes assessed by observers versus predicted by CIECAM02, in *Proceedings of 10th Congress of the International Colour Association*, Granada (Granada, 8-13 May 2005), pp. 643-646.

VIÉNOT F., MAHLER E., SERREAULT L., HARRAR M., EZRATI J-J., PÉRIGNON P., BRICOUNE A., 2005, Discriminating colours under LED illumination, in *Proceedings of 10th Congress of the International Colour Association*, Granada (Granada, 2005), pp. 33-36.

BOUST C., CITTADINI F., BEN CHOUIKHA M., BRETTEL H., VIÉNOT F., BERCHE S., ALQUIÉ G., 2004, Does an expert use memory colors to adjust images? , *12th Color Imaging Conference IS&T*, Scottsdale, AZ, Nov. 9, 2004; p. 347-353.

VIÉNOT F., OBEIN G., 2004, Is Gloss recognized as a surface property? Proceedings of *MS 2004, 1st International Workshop on Materials and Sensations*, Pau, France, 27th to 29th October 2004, pages 77-82.

HARRAR, M., VIÉNOT F., 2004, What is controlling chromatic contrast in a complex scene? Proceedings of *CGIV 2004 - Second European Conference on Color in Graphics, Imaging and Vision*, Aachen, Germany, Volume 2, ISBN / ISSN: 0-89208-250-X, pp. 51-54.

OBEIN G., LEROUX T., KNOBLAUCH K., VIÉNOT F., 2003, Visually relevant gloss parameters. *Proceedings of 11th international Metrology congress*, Toulon, 20-23 octobre 2003, 6p.

DUMONT E., BRÉMOND R., BOUST C., DA COSTA E., VIÉNOT F., Assessment of the visual quality of tone-mapped images for visibility experiments. *CIE 152 :2003, Proc. of the 25th session of the CIE, San Diego 25 June - 2 July 2003* : D4-82-85.

BOUST C., CHAHINE H., VIÉNOT F., BRETTEL H., BEN CHOUIKHA M., ALQUIÉ G., 2003, Color correction judgements of digital images by experts and naive observers. *PICS 2003*: The PICS Conference, An International Technical Conference on The Science and Systems of Digital Photography, including the Fifth International Symposium on Multispectral Color Science, Rochester, NY; May 13, 2003; p. 4-9; ISBN / ISSN: 0-89208-245-3.

LE ROHELLEC J., BRETTEL H., VIÉNOT F., 2003, Contribution of achromatic and chromatic contrast signals to Fechner-Benham subjective colours. In : J.D. Mollon (ed.), *Normal and defective colour vision*. Oxford University Press, 2003, Proc. *International Colour Vision Society* Symposium, Cambridge, U.K. : 143-151.

VIÉNOT F., DAVID L., 2003, An algorithm to assess the detectability of spatio-temporal patterns at any illumination. Proceedings of the CIE Symposium'02 *Temporal and Spatial Aspects of Light and Colour Perception and Measurement*, 22-23 August 2002, Veszprém, Hungary, CIE x025:2003 : 73-80.

VIÉNOT F., 2002, Mesopic vision. In : *VISION (Vehicle and Infrastructure Safety Improvement in Adverse Conditions and Night Driving), Société des Ingénieurs de l'Automobile (ed.)*, Rouen, 24-25 septembre 2002, CD-ROM Proceedings : 8 p. **(Conférence invitée).**

VIÉNOT F., BOUST C., DA COSTA E., BRÉMOND R., DUMONT E., 2002, Évaluation psychométrique de la fidélité visuelle des images numériques / Psychometric assessment of the look and feel of digital images, In : *DSC 2002, Driving Simulation Conference, INRETS-RENAULT (ed.)* : 301-311.

VIÉNOT F., BOUST C., BRÉMOND R., DUMONT E., 2002, Rating tone-mapping algorithms for gradations. CGIV 2002 : In : *The First European Conference on Color in Graphics, Imaging and Vision* (CGIV), Poitiers, France, April 2002, IS&T, Springfield, USA, Volume 1 : p. 221-225.

VIÉNOT F., 2002, Report on a fundamental chromaticity diagram with physiologically significant axes, in *9th Congress of the International Colour Association,* Proceedings of SPIE Vol. 4421, 565-570 **(Conférence invitée).**

VIÉNOT F., BENHALIMA F., BRETTEL H., BOURDONCLE B., COLONNA DE LEGA A., 2002, Rating of tinted ophthalmic lenses, in *9th Congress of the International Colour Association*, Proceedings of SPIE Vol. 4421, 271-274.

VIÉNOT F., MONOT A., OBEIN G., 2001, Sensation visuelle : effets de moirés, de brillant, de lustre et de transparence. *Colloque " Jouer la lumière : le textile, la lumière et l'œil ",* Musée de la Mode et du Textile / Union centrale des arts décoratifs, 12 et 13 novembre 2001, Paris, 12 pages.

VIÉNOT F., BRETTEL H., 2001, Color display for dichromats. In: *Color imaging: Device-independent color, Color hardcopy, and Graphic arts VI,* R. Eschbach and G. G. Marcu, Eds., Proceedings of SPIE, Vol. 4300, 199-207.

OBEIN G., LEROUX T., VIÉNOT F., 2001, Bi-directional reflectance distribution factor and gloss scales. *Human vision and electronic imaging VI,* Bernice E. Rogowitz, Thrasyvoulos N. Papps, Editors, Proceedings of SPIE Vol. 4299 : 279-290.

OBEIN G., LEROUX T., VIÉNOT F., 2000, Variability of the 3d repartition of haze with the incident beam geometry. First international Conference on *Color Graphics and Image Processing*, October 1-4, 2000, Saint-Etienne, France. Pages 296-299.

OBEIN G., DOMONT S., BRETTEL H., VIÉNOT F., 2000, Contrast appearance under mesopic adaptation. A comparison between a simulation and the reality. *NPL Colour and Visual Scales 2000*, 3-5 April 2000, Egham, GB, 4 pages.

BEN CHOUIKHA M., VIÉNOT F. 1999, Colorimetric characterization of a color dedector implemented in a BiCMOS technology. *IS&T/SPIE's International Technical Group Newsletter, Vol.9, n°2, p.1&9.*

VIÉNOT F., BRETTEL H., DOMONT S., BORDENAVE E., 1999, Predictive simulation of mesopic vision. *CIE Publ.133, CIE 24rd session*, Warsaw, pp.107-111.

BÈCLE P., VIÉNOT F., MONOT A., EYQUEM D., 1998, Gradient and shape detection from texture. *1998 OSA Annual Meeting / ILS-XIV*, Baltimore, U.S.A., October 4-9, 1998, p.92.

BEN CHOUIKHA M., VIÉNOT F., LU G.N.: Temperature Effects on Colorimetric Accuracy of the BTJ Color Detector. In: *Advanced Focal Plane Arrays and Electronic Cameras II,* SPIE international sumposium on Electronic Image Capture and Publishing. Zurich 18-20 may 98. Vol: 3410. pp.204-214.

BEN CHOUIKHA M., VIÉNOT F., LU G.N., 1998, Characterization of a color sensitive photodedector implemented in a BiCMOS technology. in *Color and Document Imaging Conference, IS&T/SPIE's 10th Annual symposium: Electronic Imaging 98,* janvier 1998. Vol. 3300, pp 198-206.

BEN CHOUIKHA M., LU G.N., ALQUIÉ G., VIÉNOT F., 1997, Caractérisation d'un capteur de couleur réalisé par une technologie de circuits intégrés. In *VISU 97*, 10èmes Journées d'Etudes, Club VISU / SID-France, 3-4 avril 1997, Poitiers, France, pp.73-77.

BRUSQUE C., GANDON A., CARTA V., VIÉNOT F., 1997, Etalonnage d'une chaîne de production de diapositives par imageur numérique. In *VISU 97*, 10èmes Journées d'Etudes, Club VISU / SID-France, 3-4 avril 1997, Poitiers, France, pp.61-64.

VIÉNOT F., BRETTEL H., 1997, Palettes de couleur infographiques pour daltoniens. In *VISU 97*, 10èmes Journées d'Etudes, Club VISU / SID-France, 3-4 avril 1997, Poitiers, France, pp.65-68).

VIÉNOT F., PEFFERKORN S., CHIRON A., 1997, Photometry in the mesopic domain. *CIE x012-1997, Proc. of the NPL -CIE-UK Conference, Visual scales; photometric and colorimetric aspects*, 24-26 March 1997, Teddington, UK, pp. 52-55.

LE ROHELLEC J., VIÉNOT F., 1997, Distant colour induction on Fechner-Benham top. In: C.R.Cavonius (ed.), *Colour Vision Deficiencies XIII,* pp.459-464.

PEFFERKORN S., CHIRON A., VIÉNOT F., 1997, Effect of longitudinal chromatic aberration on photometric matches using an heterochromatic square-wave grating. In: C.R.Cavonius (ed.), *Colour Vision Deficiencies XIII,* pp.403-407.

VIÉNOT F., BEN M'BAREK A., OTT L., 1997, Screening colour vision with an LMS calibrated display. In: C.R.Cavonius (ed.), *Colour Vision Deficiencies XIII,* pp.339-349.

VIÉNOT F., 1996, Traitement de l'information chromatique dans les réseaux rétiniens. *Huitièmes Journées Neusosciences et Sciences de l'Ingénieur NSI 96*, Marly-le-Roi, 6-8 mai 1996, pp.153-160. (**Conférence invitée**)

VIÉNOT F., 1996, Fundamental chromaticity diagram with physiologically significant axes, report of the activity of CIE TC 1-36, *CIE x010-1996, Proc. of the CIE expert symposium '96 Colour standards for image technology*, 25-27 March 1996, Vienna, Austria, pp. 35-40. (**Conférence invitée**)

PEFFERKORN S., CHIRON A., VIÉNOT F.,1995, Mesopic photometry based on heterochromatic spatial contrast sensitivity measurements. *CIE 119-1995-23rd session*, New Dehli, pp.73-74.

VIÉNOT F., CHIRON A., PEFFERKORN S., 1995, Multiple approaches in heterochromatic photometry. Consequences for mesopic photometry. *CIE x009 - 1995, Proc. of the CIE Symposium on Advances in Photometry*, 1-3 December 1994, Vienna, Austria, pp.40-49. (**Conférence invitée**)

VIÉNOT F., CHIRON A., 1995, Rod and cone signal processing in mesopic heterochromatic photometry. In: B. DRUM (ed.), *Colour Vision Deficiencies XII,* Kluwer Academic Publishers, The Netherlands, pp.325-332.

LE ROHELLEC J. & VIÉNOT F., 1995, Contribution of two colour-opponent mechanisms to Fechner-Benham subjective colours. In: B. DRUM (ed), *Colour Vision Deficiencies XII*, Kluwer Academic Publishers, The Netherlands, pp. 251-258.

VIÉNOT F., OTT L., BEN M'BAREK A., 1994, LMS based colour vision test on CRT. *JERMOV, Montpellier,* p.216.

VIÉNOT F., 1994, Heterochromatic photometry. Visual capacities in the mesopic range. *IV Reunion Nacional de Optica*, Granada (Esp.), 15 Septiembre 1994, pp.XLV-L. (**Conférence invitée**)

VIÉNOT F., 1993, Fundamental chromaticity diagram with physiologically significant axes: report of the activities of CIE committee TC 1-36. *OSA Annual Meeting Technical Digest*, p.83.. (**Conférence invitée** au congrès annuel de l'Optical Society of America, Toronto, Canada, October 3-8, 1993)

PEFFERKORN S., VIÉNOT F., CHIRON A. & BRETTEL H., 1993, Problem of spectroradiometric calibration of polarized displays. In: *EURODISPLAYS '93*, proceedings of the 13th International Display Research Conference, Le Club Visu, SID - France, pp. 443-446.

VIÉNOT F. & FONTVIEILLE C., 1993, Evaluation of the "Différenciateur de Tonalité": an apparatus for measuring wavelength discrimination. In: DRUM B. and MORELAND J.D. (Eds), *Colour Vision Deficiencies XI*, Kluwer Academic Publishers, The Netherlands, pp.365-372.

BRETTEL H., CHIRON A., VIÉNOT F., GLASSER J., 1992, Etude du papillotement des écrans à cristaux liquides. In *VISU 92*, 8emes Journées d'Etudes organisées par le Club VISU / SID-France, 27-28 octobre 1992, Angers, France, pp.69-70.

VIÉNOT F., 1991, Poster session on Brightness and colour, chaired by Françoise Viénot, *CIE proceedings, 22nd session*, Vol.2, pp.105-106, Melbourne, 5 juillet 1991. (**Conférence invitée**)

VIÉNOT F. & CHIRON A., 1991, Comparison of heterochromatic flicker photometry and direct comparison brightness matching data over the spectrum. *CIE proceedings, 22nd session*, Melbourne, Vol.1, Part 1, Division 1, pp.41-42.

VIÉNOT F., CHIRON A., 1991, Mesopic luminous matches of protanopic and deuteranopic observers. In: DRUM B., MORELAND J.D. and SERRA A. (Eds), *Colour Vision Deficiencies X*, Kluwer Academic Publishers, Dordrecht, The Netherlands, pp.413-419.

VIÉNOT F., BRETTEL H., 1991, Vers une colorimétrie Physiologique. In: *VISU91*, 8emes Journées d'Etudes organisées par la SEE (Club VISU) 29-30 mai 91, Perros-Guirec, France, pp.54-55.

BRETTEL H., VIÉNOT F., MORELAND J.D., 1988, Adaptation de la méthode de photométrie par mouvement aux écrans de visualisation. In: *VISU 88,* 5èmes Journées Nationales d'Etudes organisées par le Club Visu, Gif-sur-Yvette, France, pp.53-54.

VIÉNOT F., BOUHARD F., SCHOEFFTER M., 1987, "Le différenciateur de tonalité": an apparatus for measuring wavelength discrimination. In: VERRIEST G. (ed), *Colour Vision Deficiencies VIII,* proc. of the 8th international IRGCVD symposium, Junk, the Hague, pp.253-258.

VIÉNOT F., BOUHARD F., SCHOEFFTER M., 1985, An equipment to measure wavelength discrimination. In: *Mondial Couleur 85*, actes du 5eme congrès de l'Association Internationale de la Couleur, réalisation Centre Français de la Couleur, Paris, France, p.62.

VIÉNOT F., 1985, Cone interrelations in color-matches. In: *Mondial Couleur 85*, actes du 5eme congrès de l'Association Internationale de la Couleur, réalisation Centre Français de la Couleur, Paris, France, pp.33-1,33-6.

BOURDY C., VIÉNOT F., MONOT A., CHIRON A., 1984, Spatial contrast detection for colour patterns under selective chromatic adaptation. In: GIPSON C.P. (ed), Proc. of a workshop on "*Colour coded vs monochrome electronic displays*", NATO, Farnsborough, G.B., pp.28.1-28.15.

VIÉNOT F., 1984, Color matches on large fields, changes with retinal area stimulated or with duration of presentation. in: VERRIEST G. (ed), *Colour Vision Deficiencies VII, Documenta Ophthalmologica Proc. Ser.*, Junk, The Hague, pp.121-125.

VIÉNOT F., 1981, Color match changes between the fovea end perifovea. In: *COLOR 81*, proc. of the 4th congress of the International Colour Association, Deutsche farbwissen schaftliche Gesellschaft e.V., Berlin, Deutschland, pp.B21-B23.

VIÉNOT F., 1978, Statistical study of the color-matching functions. In: *COLOR 77*, proc. 3rd congress of the International Color Association AIC, Adam Hilger, Bristol, pp.273-276.

# Proceedings

## Oral Papers

# How Multi-Illuminant Scenes Affect Automatic Colour Balancing

**Liwen XU, Brian FUNT**

School of Computing Science, Simon Fraser University

## ABSTRACT

Many illumination-estimation methods are based on the assumption that the imaged scene is lit by a single source of illumination; however, this assumption is often violated in practice. We investigate the effect this has on a suite of illumination-estimation methods by manually sorting the Gehler et al. ColorChecker set of 568 images into the 310 of them that are approximately single-illuminant and the 258 that are clearly multiple-illuminant and comparing the performance of the various methods on the two sets. The Grayworld, Spatio-Spectral-Statistics and Thin-Plate-Spline methods are relatively unaffected, but the other methods are all affected to varying degrees.

**Keywords**

Colour balancing, illumination estimation, digital photography.

## INTRODUCTION

The usual first step in automatic colour balancing of digital imagery is to estimate the chromaticity of the illumination. Although there are some recent exceptions (Beigpour 2014; Gijsenij 2012; Joze 2013), most illumination-estimation methods assume that the relative spectral power distribution of the illumination is constant throughout the scene. However, many scenes contain multiple illuminants with differing SPDs, and we investigate the effect this has on automatic colour balancing.

Somewhat surprisingly, the Gehler et al. (Gehler 2008) "Colorchecker" data set of 568 images, which is widely used in evaluating competing illumination-estimation methods, contains many images of multiple-illuminant scenes. For example, Figure 1 depicts an indoor scene that also includes a window through which daylight is clearly falling on the counter. Is the scene illuminant the light from inside the room or outside the window? Figure 2 shows an outdoor scene with at least three illuminant types: the cloudy sky, the shadowed areas, and the traffic light.

Each image in the Colorchecker dataset contains an Xrite/Macbeth ColorChecker, which is used to provide a ground-truth measure of the illumination's 'colour'. However, since many of the scenes do contain multiple illuminants, a single such measurement cannot possibly represent the colour of all the illuminants correctly, but rather must represent some sort of compromise. Whether the illumination-estimation method assumes there is a single illuminant or multiple illuminants, a single colorchecker cannot correctly represent the ground-truth illumination in a multi-illuminant scene. In this paper, we investigate how much of an effect this has on a representative set of illumination-estimation methods; namely, MaxRGB (Funt 2012), Grayworld (Weijer 2007), Shades-of-Gray (Finlayson 2004), Edge-based (Weijer 2007), N-jet (Gijsenij 2010) , Thin-Plate-Spline (Shi 2011) and Spatio-Spectral Statistics (Chakrabarti 2012).

# SCENE CLASSIFICATION

The Gehler et al. dataset (Gehler 2008) contains 568 images taken with two digital single lens reflex cameras, a Canon 5D and a Canon 1D. All images were saved in Canon RAW format. Each image contains an Xrite/Macbeth ColorChecker for reference. The image coordinates (measured by hand) of each Colorchecker square are provided with the dataset. In the tests below, we used the Shi et al. (Shi 2011) reprocessed version of the Gehler et al. data. The original dataset consists of non-linear TIFF images that were automatically generated from the RAW data. The reprocessed dataset contains PNG images that are linear and do not include any automatic white balancing or de-mosaicing.

We manually sorted the original 568 images into two groups according to whether the images were of single-illuminant or multiple-illuminant scenes. Sorting in this way is difficult because it can be hard to discern the nature of the scene illumination from the image. Figure 1 shows a typical case where the presence of multiple sources of illumination is very clear. Similarly, the traffic light in Figure 2 is an obvious additional illuminant. Figure 3 shows a situation in which it seems pretty clear that there is only a single illuminant. Figure 4 shows a somewhat ambiguous case, since there are areas in direct sun and others in shadow. The Colorchecker itself appears to be partly in sun and partly in shadow. There are also the clouds in the distance. However, this appears to be a typical outdoor scene basically dominated by sunlight/skylight and so we classified it as a single-illuminant scene. If we were to be any more strict in our interpretation of what constitutes a single-illuminant scene then almost the entire dataset would be classified as multiple-illuminant. Based on this type of analysis of each image, the 568 dataset is divided into 310 single-illuminant and 258 multiple-illuminant scenes. We denote the two images subsets as S (single) and M (multiple), and the full set of 568 images as F. The complete lists of image numbers for sets S and M are listed in the Appendix.



*Figure 1 Example of a multiple-illuminant scene with light coming both from the room and window.*



*Figure 2 Example of a multiple-illuminant scene containing a visible light source.*

*Figure 3 Example of a clearly single-illuminant scene.*



*Figure 4 Example of a somewhat ambiguous scene with sunlight and shadow but classified as single-illuminant nonetheless.*

## COMPARATIVE PERFORMANCE ON SINGLE-VERSUS MULTIPLE-ILLUMIANT SCENES

We evaluate the illumination-estimation performance of all the methods separately on subset S, subset M, and the complete set F. The illumination-estimation methods are MaxRGB (Funt 2012), Gray-World (Weijer 2007), Shades of Gray (Finlayson 2004), Edge Based (Weijer 2007), N-jet (Gijsenij 2010), TPS (Shi 2011) and Spatio-Spectral Statistics (Chakrabarti 2012). The image pixels occupied by the Colorchecker in each image areas are replaced with zeros for the tests. These methods all estimate the rg-chromaticity of the illumination. The error in a given estimate is measured relative to the measured ground-truth illumination chromaticity. The error is evaluated in terms of the angular difference in degrees between the two chromaticities after each chromaticity is converted to a 3-vector as (r, g, 1-r-g). The overall accuracy across a given test set of images is reported in terms of the mean, median, RMS and maximum errors.

*Table 1: Comparative illumination-estimation performance evaluated in terms of angular error. MaxP (MaxRGB w/o preprocessing), MaxM (MaxRGB after median filtering, GW (Grayworld), EB (Edge-Based, first and second order), 1-jet (Gamut mapping), 2-jet (Gamut mapping), SSS-ML (Spatio-Spectral Statistics with maximum likelihood, SSS-GP (Spatio-Spectral Statistics with general prior). Md (Median), Mn (Mean).*

| | Set S | | | | Set M | | | | Complete Dataset | | | |
|---|---|---|---|---|---|---|---|---|---|---|---|---|
| | Md | Mn | RMS | Max | Md | Mn | RMS | Max | Md | Mn | RMS | Max |
| MaxP | 4.6 | 7.3 | 9.9 | 27 | 16 | 14 | 16 | 50 | 9.1 | 10 | 13 | 50 |
| MaxM | 3.1 | 5.3 | 7.8 | 26 | 8.8 | 10 | 13 | 42 | 4.7 | 7.7 | 11 | 42 |
| GW | 4.0 | 5.5 | 7.3 | 25 | 3.3 | 3.8 | 4.7 | 15 | 3.6 | 4.8 | 6.2 | 25 |
| SoG (norm=6) | 2.9 | 4.8 | 6.8 | 23 | 7.4 | 8.4 | 10 | 36 | 4.5 | 6.4 | 8.7 | 36 |
| EB1 (norm=6) | 2.6 | 4.6 | 6.8 | 26 | 7.2 | 9.0 | 12 | 38 | 3.8 | 6.6 | 9.4 | 38 |
| EB1 (norm=1) | 3.8 | 4.7 | 5.6 | 17 | 3.4 | 4.1 | 4.9 | 16 | 3.6 | 4.4 | 5.3 | 17 |
| EB2 | 2.7 | 5.0 | 7.2 | 28 | 8.9 | 9.9 | 13 | 47 | 4.4 | 7.2 | 10 | 47 |
| 1-jet 3-fold | 2.8 | 4.4 | 6.2 | 24 | 6.0 | 7.7 | 9.9 | 32 | 4.1 | 5.9 | 8.1 | 32 |
| 2-jet 3-fold | 2.9 | 4.3 | 6.1 | 21 | 5.9 | 7.7 | 9.8 | 32 | 4.2 | 5.9 | 8.0 | 32 |
| TPS 3-fold | 2.6 | 3.5 | 4.5 | 17 | 3.0 | 3.6 | 4.5 | 15 | 2.7 | 3.5 | 4.5 | 17 |
| SSS-ML | 2.9 | 3.7 | 4.8 | 22 | 3.1 | 3.7 | 4.5 | 15 | 3.0 | 3.7 | 4.7 | 22 |
| SSS-GP | 2.9 | 3.6 | 4.7 | 22 | 3.0 | 3.6 | 4.4 | 15 | 3.0 | 3.6 | 4.6 | 22 |

AIC2015 TOKYO - Color and Image

The MaxRGB tests include MaxRGB without preprocessing and MaxRGB with median filtering MaxM (Funt 2012). The N-jet algorithms are tested using threefold cross-validation. Because the images are from two different cameras and the training is specific to each camera, we train and test on the images from each camera separately and then combine the results. TPS is also evaluated using threefold cross-validation.

## DISCUSSION

The results in Table 1 show that the effect of multiple scene illuminants on illumination-estimation performance varies substantially across the various methods. MaxRGB is strongly influenced by the presence of multiple illuminants. Whether MaxRGB includes image preprocessing or not, the presence of multiple illuminants seriously influences the results. As Table 1 shows, the error is approximately tripled. For example, the median error for the MaxRGB variant MaxM rises from 3.1 to 8.8 degrees for the change from subset S to subset M. In other words, MaxRGB works very well when the single-illuminant assumption holds, but fails when it is violated. Since MaxRGB is based on estimating the maximum value in each of the R, G, B channels, it is particularly vulnerable to the presence of light sources such as the traffic light in Figure 2.

Interestingly, Grayworld's performance appears to be unaffected by the presence of multiple illuminants since the median angular error on sets S, M and F is 4.0, 3.3, and 3.6, respectively. Although its overall performance is poorer than several of the other methods, it has the advantage of being stable. The Shades of Gray approach is controlled by the choice of the Minkowski norm to vary between the extremes of Grayworld and MaxRGB. A norm of 6 has been reported to work well (Finlayson 2004). As a compromise between Grayworld and MaxRGB, however, its performance is then affected by the presence of multiple illuminants, with a median angular error of 2.9, 7.4 and 4.5, on sets S, M and F, respectively.

Just as Shades of Gray is more sensitive to the presence of multiple illuminants than Grayworld, the Edge-Based method using norm = 6 is more sensitive than the Edge-Based method using norm = 1. For the norm = 1 case, Edge-Based is simply averaging derivatives within each RGB channel instead of the RGB values themselves. With norm = 6, the Edge-Based method weights the large derivatives, which are likely to arise from illumination boundaries in multiple-illuminant scenes, more heavily thus leading to a concomitant increase in angular error. The performance of the 1-jet and 2-jet Gamut Mapping methods also degrades when the single-illuminant assumption is violated. For 1-jet, the median angular on S of 2.8 degrees increases to 6.0 degrees for M. Gamut mapping assumes that the gamut of RGBs and the gamuts of their derivatives are limited by the illuminant. In the presence of multiple illuminants these image gamuts expand such that the constraint used to estimate the illuminant is no longer as strong or accurate.

The learning-based methods appear to account for the presence of multiple illuminants quite well. The performance of the Spatio-Spectral Statistics methods tends to be very good and quite unaffected by multiple illuminants. With median angular errors of 2.6 (set S), 3.0 (set M) and 2.7 (set F), the Thin-Plate Spline method (TPS) is both the least affected by multiple illuminants and also attains the minimum error of all the methods on each of the three datasets.

**REFERENCES**

Beigpour, S., C. Riess, J. van d Weijer, and E. Angelopoulou. 2014. Multi-illuminant estimation with conditional random fields. *IEEE Trans. on Image Processing* 23(1): 83-96.

Chakrabarti, A. K. Hirakawa, and T. Zickler. 2012. Color constancy with spatio-spectral statistics. *IEEE Transactions on Pattern Analysis and Machine Intelligence* 34(8): 1509-1519. Accompanying computer implementation downloaded from http://vision.seas.harvard.edu/colorconstancy/. Accessed February 23, 2015.

Finlayson, G. and E. Trezzi. 2004. Shades of gray and colour constancy. *In Proc. IS&T/SID 12$^{th}$ Color Imaging Conf.* Springfield, VA, 37-41.

Funt, B., and L. Shi. 2012. MaxRGB reconsidered. *Journal of Imaging Science and Technology* 56(2): 020501-1-020501-10.

Gehler, P., C. Rother, A. Blake, T. Minka, and T. Sharp. 2008. Bayesian color constancy revisited. In *Proc. IEEE Computer Society Conf. on Computer Vision and Patern Recognition.* Anchorage, Alaska, 1-8.

Gijsenij, A., T. Gevers, and J. van deWeijer. 2010. Generalized gamut mapping using image derivative structures for color constancy. *Int. J. Computer Vision.* 86, 127-139. Accompanying computer implementation downloaded from http://colorconstancy.com/. Accessed February 27, 2015.

Gijsenij, A., R. Lu, and T. Gevers. 2012. Color constancy for multiple light sources. *IEEE Trans. on Image Processing* 21(2): 697-707.

Joze, H.R.V. and Mark S. Drew. 2013. Exemplar-based colour constancy and multiple illumination. *IEEE Trans. on Pattern Analysis and Machine Intelligence* 36(5): 860-873.

Shi, L., W. Xiong, and B. Funt. 2011. Illumination estimation via thin-plate spline interpolation. *J. Opt. Soc. Am. A 28(5)*: 940-948. Accompanying computer implementation downloaded from http://www.cs.sfu.ca/~colour/code/. Accessed February 25, 2015.

Shi, L. and B. Funt. Re-processed version of the Gehler color constancy dataset of 568 images. Downloaded from http://www.cs.sfu.ca/~colour/data/shi_gehler/. Accessed Sept. 2014.

Weijer, J. van de, T. Gevers, and A. Gijsenij. 2007. Edge-based color constancy. *IEEE Trans. Image Processing.* 16(9): 2207-2214.
Accompanying computer implementation downloaded from http://lear.inrialpes.fr/people/vandeweijer/software. Accessed February 25, 2015.

**APPENDIX**

Image numbers of single-illuminant scenes: 1 2 3 4 7 10 11 12 14 17 18 19 21 23 27 32 33 34 35 36 37 38 39 40 41 44 45 46 47 48 49 50 52 54 56 57 58 59 63 64 65 66 67 68 69 70 71 76 77 78 79 80 81 82 83 84 85 86 87 88 89 90 91 92 93 94 95 96 99 100 101 102 103 104 105 106 107 108 109 110 111 112 113 114 115 116 117 118 119 121 122 126 127 128 129 130 131 132 134 135 136 137 139 140 141 142 143 144 147 149 150 151 152 153 154 155 156 157 158 159 160 161 162 163 164 165 166 168 169 170 171 172 173 174 176 177 178 179 180 185 186 187 188 189 191 193 196 197 199 200 203 204 206 212 219 224 225 226 227 228 229 230 232 233 234 235 248 249 250 251 253 254 255 256 257 258 259 260 261 262 264 265 266 267 268 269 270 271 273 274 275 281 282 283 285 286 287 288 289 291 292 293 295 298 299 300 301 302 303 304 305 306 307 308 309 310 342 343 344 353 355 358 359 362 364 365 367 372 377 381 384 386 394 395 396 398 401 402 407 410 411 414 416 417 418 419 420 422 423 424 425 427 428 429 430 431 432 433 434 436 437 439 441 444 449 451 453 454 455 456 458 459 461 462 463 466 473 474 475 478 479 480 482 484 487 489 490 491 493 494 496 500 502 503 504 516 522 528 530 536 537 538 541 543 546 549 560 561 562 564

Image numbers of multiple-illuminant scenes: 5 6 8 9 13 15 16 20 22 24 25 26 28 29 30 31 42 43 51 53 55 60 61 62 72 73 74 75 97 98 120 123 124 125 133 138 145 146 148 167 175 181 182 183 184 190 192 194 195 198 201 202 205 207 208 209 210 211 213 214 215 216 217 218 220 221 222 223 231 236 237 238 239 240 241 242 243 244 245 246 247 252 263 272 276 277 278 279 280 284 290 294 296 297 311 312 313 314 315 316 317 318 319 320 321 322 323 324 325 326 327 328 329 330 331 332 333 334 335 336 337 338 339 340 341 345 346 347 348 349 350 351 352 354 356 357 360 361 363 366 368 369 370 371 373 374 375 376 378 379 380 382 383 385 387 388 389 390 391 392 393 397 399 400 403 404 405 406 408 409 412 413 415 421 426 435 438 440 442 443 445 446 447 448 450 452 457 460 464 465 467 468 469 470 471 472 476 477 481 483 485 486 488 492 495 497 498 499 501 505 506 507 508 509 510 511 512 513 514 515 517 518 519 520 521 523 524 525 526 527 529 531 532 533 534 535 539 540 542 544 545 547 548 550 551 552 553 554 555 556 557 558 559 563 565 566 567 568.

*Address: Brian Funt, School of Computing Science, Simon Fraser University,*
*8888 University Drive, Burnaby, British Columbia V5A 1S6, Canada*
*E-mails: funt@sfu.ca, xuliwenx@gmail.com*

# The Generalised Reproduction Error for Illuminant Estimation

Graham FINLAYSON, Roshanak ZAKIZADEH
School of Computing Sciences, University of East Anglia, UK

## ABSTRACT

In a recent publication "Reproduction Angular Error: An Improved Performance Metric for Illuminant Estimation", British Machine Vision Conference (2014), it was argued that the commonly used Recovery angular error – the angle between the RGBs of the actual and estimated lights- is flawed when it is viewed in concert with how the illuminant estimate is used. Almost always, we use the illuminant estimate to make an image reproduction where the colour bias due to illumination is removed or reduced. It was shown that, when a single algorithm was used to estimate the light for a fixed scene viewed under a range of illuminants and where similar reproductions were produced when the estimate was 'divided out', the recovery angular error would, counterintuitively, vary widely. The Reproduction angular error introduced in that paper remedies this flaw by measuring the angle between a true white patch and the white that is reproduced when an illuminant estimate is made. In this paper we generalize the reproduction error concept to consider how well a range of colours are reproduced. We show how an illuminant estimate can be used to map the colours in a Macbeth colour checker for the actual illumination to reference lighting conditions. Then we evaluate the error of reproduction using the mean CIE Delta E. This new Generalised Reproduction error metric is used to compare the performance of a variety of different algorithms. Significantly, the rank-order of the reproduction angular error is quite similar to that established with the generalized reproduction error. Based on our experiments we propose that the simpler reproduction angular error can be used as a proxy to our generalised metric to assess the performance of illuminant estimation algorithms.

## 1. INTORODUCTION

The colours in an image captured by a digital camera are affected by the illuminant under which the scene is captured. Unlike human visual system which is able to perceive the colours constant regardless of illumination, the sensors of a camera capture a colour signal which is confounded by the illumination. To make the colours pleasant and usable by many computer vision tasks, the illuminant of the scene is estimated by reasoning about the distribution of colours in the image. In a second step, the colour of the illuminant is divided out from the colours of the image thereby removing the colour bias due to the illumination.

Illuminant estimation algorithms range from simple statistics-based methods to algorithms that use more complex statistics to learning-based methods. The *recovery error* which is the angle between the estimated and the ground-truth illuminant is commonly used to evaluate the performance of an illuminant estimation algorithm. The average (mean or median) recovery error, for a set of training set of images, is used as an index to compare and rank different algorithms.

AIC2015 TOKYO - Color and Image

However, in recent work (Finlayson & Zakizadeh 2014), a problem with the recovery error was identified. It was shown that the same scene viewed under two different colours of light where the same algorithm is used to estimate the illuminant can result in two very different angular errors. This is a problem because when each of the estimated lights are divided out from their respective images almost the same image reproduction results. Finlayson and Zakizadeh argued that the performance of illuminant estimation algorithms should be tied to how illuminant estimates are used. They are used to discount the colour bias die to illumination in making an image reproduction. Their new metric, called Reproduction Angular Error, measures the angle between the colour (RGB vector) of a white surface corrected using the estimated illuminant and the one corrected using the ground-truth illuminant (resulting in a true white patch). Significantly, this reproduction error provides a stable error for the same scene viewed under different lights and this gels with the fact that the corresponding reproductions look similar. Moreover, the new metric while broadly ranking algorithms the same as recovery angular error introduced several local changes in algorithm rank.

In this paper, we seek to measure the difference between a range of colours (not just a white patch) which are reproduced by the estimated and ground-truth illuminants. This is not as easy as it first sounds as when image data sets are compiled we often have the image and the measured white point but not the appearance of the scene under a ground truth illuminant. In out approach we first show how to make a synthetic set of Macbeth colour checkers for different illuminants for a known camera. Second we show how to make reproductions of the Macbeth colour images when the illuminant colour is discounted using the illuminants estimated by different algorithms (for the algorithm estimates we use the data provided by Gijsenij et al. 2011). Then these reproductions are compared with the actual colours in a Macbeth checker for the reference lighting condition. The CIE Lab $\Delta E$ (Sharma et al. 2005) is used to measure the colour difference between the colours of the checker reproduced by the estimated lights and those under reference lighting condition. If the correct illuminant is estimated then a very small $\Delta E$ would result. Conversely, poor estimates result in large average $\Delta E$s.

According to this new *generalised reproduction error* we can rank the performance of different algorithms. Crucially, we show that the ranking provided is almost the same as the recently introduced – and much simpler to calculate – reproduction angular error. This paper further validates the usefulness of the reproduction angular error metric.

## 2. BACKGROUND

The most commonly used metric for evaluating illuminant estimation algorithm is the recovery angular error:

$$err_{recovery} = \, cos^{-1}(\frac{\underline{E}_{est} \cdot \underline{E}_{act}}{|\underline{E}_{est}||\underline{E}_{act}|}) \qquad (1)$$

which is the angle between the estimated RGB of illuminant $\underline{E}_{act}$ and the ground-truth RGB illuminant $\underline{E}_{est}$. Recently, this recovery angular error was shown to have the problem of introducing a wide range of errors when a given algorithm estimates the illuminant for a given scene (Finlayson & Zakizadeh 2014) viewed under a wide range of illuminants. This behaviour is problematic because when the different illuminant estimates are 'divided out' similar reproductions result. It is these reproduced images that are respectively assessed in photography or used in computer vision. To solve this problem, the Reproduction Angular

Error was proposed The Reproduction angular error is defined to be the angle between the RGB of a white surface when the actual and the estimated illuminations are 'divided out'.

$$err_{recovery} = cos^{-1}(\frac{(\underline{E}_{act}/\underline{E}_{act}) * (\underline{E}_{act}/\underline{E}_{est})}{\sqrt{3}|\underline{E}_{act}/\underline{E}_{est}|}) \qquad (2)$$

## 3. GENERALISED REPRODUCTION ERROR

The Reproduction angular error assesses the performance of illuminant estimation algorithms according to how well white is reproduced when the colour bias due to illumination is removed. Here we wish to generalise this idea to consider how a range of colours are reproduced. Our idea is to provide a method for synthesising the RGB image of a Macbeth colour checker under an actual light and then use the RGB estimate of the illuminant – made by an algorithm – to correct the image colours (to remove the colour bias due to illumination). This corrected Macbeth checker is then compared with the actual reproduction (when the true illuminant is used).

In constructing our model, we use the set of spectra for 24 Macbeth colour checker patches and the 23 lights from the SFU dataset (Barnard et al. 2002). For camera sensitivity functions we use the Sony DXC-930 CCD (Barnard et al. 2002) but the sensitivities of any particular camera can be used in the problem formulation. Equation (3) teaches that the camera response ($\rho^k$) whose spectral sensitivities are denoted $R^k(\lambda)$ for the surface spectra ($S(\lambda)$) and the illuminant spectra ($E(\lambda)$) is calculated as:

$$\rho^k = \int_{380}^{700} R^k(\lambda)S(\lambda)E(\lambda)d\lambda \qquad (3)$$

For all numerical calculations, we assume the visible spectrum runs from 380 to 780 Nanometres and we use a 4 Nanometres sampling interval. For each of the 23 lights we, using (3), generate 24 RGBs. These 23 synthetic checker images encapsulate our understanding of how the checker appears under different lights. We wish to generalise this understanding so that we could, given the RGB of any target light, synthesise the appearance of the checker for any illuminant. Denoting the 24x3 RGBs for a Macbeth colour checker as *M*, we model *M* as a linear sum of three basis Macbeth colour checkers:

$$M \approx \sum_{i=1}^{3} M_i m_i \qquad (4)$$

In (4), $m_i$ denotes a scalar weight and the optimal basis in a least-squares sense are found using Characteristic Vector Analysis (Maloney 1986) (in this case of the 23 synthetic Macbeth checker images). Crucially, we found the best basis models our data extremely well with the actual and 3-basis approximation being visually almost the same in appearance.

We chose a 3-dimensional linear model because illumination is defined by 3 numbers: the RGB of the light or the RGB of the estimated light. Let us place the RGB for the white reflectance in the Macbeth checker for each basis term $M_i$ in the 3 columns of a calibration matrix $\Omega$. Denoting an RGB of a light as $\underline{E}$, the linear combination of the columns of $\Omega$ defines the weights $\underline{m}$ used in Equation (4):

$$\underline{m} = \Omega^{-1}\underline{E} \qquad (5)$$

In (5), the illuminant vector $\underline{E}$ could be the actual light or the estimate made by an algorithm. Figure 1a shows one input image and four synthetic checkers. The image is from the SFU (Barnard et al. 2002) database. For this scene a white patch was also measured. Algorithms such as pixel-based gamut mapping will attempt to infer an estimate which ideally will be close to the measured light.

With the measured and actual RGBs of the light in hand, we generated from our linear model (4) and using (5) to find our model coefficient the appearance of the actual checker (Fig. 1b) and the one that pixel based gamut mapping infers (Fig. 1c). The third checker is the correct answer (Fig. 1d). The white patch is equal to [1,1,1]. All 3 images are scaled so that the brightest pixel value across all the colour channels is 1 and a gamma of .5 is applied.



(a)                              (b)                              (c)



(d)                              (e)
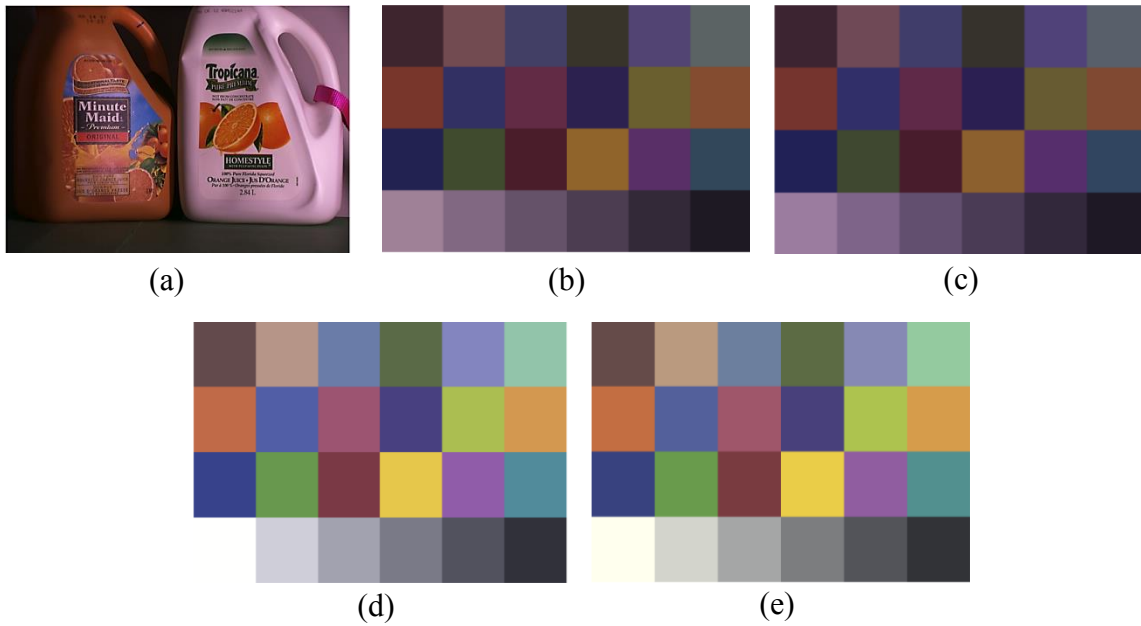
*Figure 1: (a) Image from SFU dataset, (b) Synthetic colour checker under the ground truth light under which Fig. 1a was taken, (c) Synthetic colour checker under the estimation of the same ground truth light made by pixel-based gamut mapping algorithm, (d) Synthetic colour checker under the reference light and (e) Corrected colour checker by pixel-based gamut mapping algorithm.*

So far, we have focussed on explaining how we synthesise the colours of the Macbeth colour checker for a target light. But, we ultimately seek to model the appearance of a checker under an actual light when it is corrected to the reference checker (fig. 1d) using the wrong illuminant estimate.

Denoting, respectively, the checker under the reference (white light), the actual coloured light and the estimated coloured light as $M^{ref}, M^{act}$ and $M^{est}$, the estimated reproduction, $\tilde{M}^{ref}$, is calculated as:

$$\tilde{M}^{ref} = M^{act}T \quad , \quad T = [M^{est}]^+ M^{ref} \quad (6)$$

In (6), $[M^{est}]^+$ denotes the Moore-Penrose inverse. That is, T is the least-squares fit from the checker viewed under the estimated light to the reference lighting conditions. This 3x3 matrix T is then applied to the checker under the actual light.

The *Generalised Reproduction Error* for the ith Macbeth colour checker patch is:

$$err_i = \left\| f(\widetilde{M}_i^{ref}) - f(M_i^{ref}) \right\| \quad (7)$$

where $f$ maps an RGB to CIE LAB. Note the function $f$ must map the camera values to corresponding XYZs and then the standard CIE Lab formulae can be used.

In Fig. 1e we show an actual checker under a coloured light corrected using the estimated light of pixel gamut mapping and the procedure described in (6). Note the reproduction is reasonable but there remains a slight yellowish cast.

## 4. RESULTS

Here we use the 321 images from the SFU dataset (Barnard et al. 2002). This data set has linear images and a variety of objects are imaged under 11 lights (ranging from quite yellowish to very blue). All images were captured with the SONY DXC-930. A variety of algorithms, including those listed in Table 1, were tested by Gijsenij et al. 2011 who makes all the estimated RGBs available to the community. We can thus calculate for all Macbeth colour checker images and the overall median generalised reproduction error. Then according to this global median we can rank the algorithms.

In Table 1 we list the algorithms and record the rank for the Recovery and Reproduction angular errors and the new Generalised Reproduction error.

*Table 1. Comparison of ranking of algorithms based on reproduction angular errors and generalised reproduction errors.*

| Method | Recovery angular error | | Reproduction angular error | | Generalised Reproduction Error | |
|---|---|---|---|---|---|---|
| | Median error | Rank | Median error | Rank | Median error | Rank |
| Grey-world | 7.0° | 9 | 7.49° | 9 | 7.02 | 9 |
| MaxRGB | 6.5° | 8 | 7.44° | 8 | 6.13 | 8 |
| Shades-of-gray | 3.7° | **7** | 3.94° | 6 | 3.26 | 6 |
| 1st grey-edge | 3.2° | 5 | 3.59° | 5 | 3.12 | 5 |
| 2nd grey-edge | 2.7° | 4 | 3.04° | 4 | 2.88 | 4 |
| Pixel-based gamut | 2.267° | **2** | 2.83° | 3 | 2.64 | 3 |
| Edge-based gamut | 2.278° | **3** | 2.70° | 2 | 2.59 | 2 |
| Intersection-based gamut | 2.09° | 1 | 2.48° | 1 | 2.46 | 1 |
| Heavy tailed-based | 3.45° | **6** | 4.11° | 7 | 3.74 | 7 |

AIC2015 TOKYO - Color and Image

While the rankings of all three metrics are almost similar it is clear recovery angular error ranks algorithms a little differently from reproduction angular error. Further in (Finlayson & Zakizadeh 2014) it was shown that the rankings are statistically different. And, this fact draws attention to the care the algorithm designer needs to take using the appropriate metric to assess their algorithm. The reproduction angular error assesses how well an algorithm reproduces white (i.e. when the estimated illuminant is divided out). Generalised reproduction error builds on this concept and accounts for the error for other surface colours. The ranks for the generalised reproduction error are almost identical to the reproduction angular error. Indeed – space prohibits us elucidating on this point here – the rankings are not statistically significantly different. We can conclude, for the data tested, that the simple reproduction error can be used as a proxy for the generalised reproduction error developed here.

## 5. CONCLUSION

Reproduction angular error measures the angle between a true white patch and the white patch that results when an algorithm's estimate is 'divided out' from the image. In this paper we generalised reproduction angular error to assess not only how white is reproduced but, instead, all the colours on a Macbeth colour checker. The generalised reproduction error is the CIE Lab colour difference of a reference checker and a reproduction that results when the same checker viewed under an actual coloured light is colour corrected using an estimate of that light supplied by an algorithm. Like the simple reproduction angular error the same algorithm/scene pair returns very similar error independent of the colour of the light to be estimated (because in all cases the resulting reproductions are similar). We observed that the ranking of a selection of algorithms based on the generalised reproduction error $\Delta E$s are very similar to the ranks given by the simple reproduction angular metric. Thus, while the generalised reproduction error provides a finer grained summary of the 'goodness' of an illuminant estimation algorithm, the simpler reproduction angular error can be used to assess algorithm performance.

## ACKNOWLEDGEMENTS

## REFERENCES

Barnard, K., L. Martin, B. Funt, and A. Coath. 2002. A data set for color research. *Color Research & Application, 27(3):147–151.*

Finlayson, D. G. and R. Zakizadeh. 2014. Reproduction angular error: an improved performance metric for illuminant estimation. In *Proc. British Machine Vision Confernece 2014, Nottingham, UK, September 1-5, 2014.*

Gijsenij, A., T. Gevers, and J. Van De Weijer. 2011. Computational color constancy: Survey and experiments. *IEEE Transactions on Image Processing, 20(9):2475-2489.*

Maloney, L. T. 1986. Evaluation of linear models of surface spectral reflectance with small numbers of parameters. *J. Opt. Soc. America A, 3(10), 1673-1683.*

Sharma, G., W. Wu, and E. N. Dalal. 2005. The ciede2000 color-difference formula: Implementation notes, supplementary test data, and mathematical observations. *Color Research & Application, 30(1):21-30.*

Address: School of Computing Sciences, University of East Anglia,
Norwich Research Park, Norwich, NR4 7TJ, UK
E-mails: r.zakizadeh@uea.ac.uk, g.finlayson@uea.ac.uk

# Rank-Based Camera Spectral Sensitivity Estimation

Graham Finlayson, Maryam Mohammadzadeh Darrodi
School of Computing Sciences, University of East Anglia, UK

## ABSTRACT

The spectral sensitivity function of a camera can be determined directly in the laboratory by detailed, and lengthy, measurements. Alternatively, and much more rapidly, the camera spectral sensitivities can be estimated through linear regression. However, compared with the lab based approach, the regression based estimates are not as accurate. In part, the poor performance is due some assumptions of the regression methods not holding exactly true. Indeed, prior art regression algorithms work with the assumption that a camera has a linear response. This is either not exactly the case or not the case at all. Here we develop a novel camera spectral sensitivity estimation technique that can recover the spectral sensor curves even when the camera has a non linear response. Our method assumes only that the rank-order of the final camera measurements is the same as the linear camera response. Experiments validate our method.

## 1. Introduction

The main contribution of this work is to present an estimation technique that is able to recover camera spectral sensitivity for both linear and non-linear camera responses. A camera has linear response, if when the physical signal entering the camera is scaled, the recorded RGBs scale by the same amount (e.g. double the light equals double the response). The images most people have access to (e.g. rendered jpegs from mobile phones) are the result of a long processing pipeline and are non-linear. One part of this process is the application of a color correction matrix which converts recorded sensor response to display RGBs (e.g. linear sRGB). In this scenario our method seeks to discover the linear transform of the sensor spectral sensitivities.

In this paper, we set forth an estimation technique that recovers spectral sensitivities assuming only that the recorded sensor values have the same rank order as those measured by the sensor (or of the sensor values post color correction). Importantly, almost all of the manipulations that an image undergoes preserves rank-order. For example, image gamma (approximately raising to the power of 0.5) is a monitonically increasing function. Contrast manipulation Ian S-shaped curve) also preserves rank-order. We show that the pairwise relationship between the responses of two spectral stimuli mathematically force the underlying spectral sensitivity to lie in one half of the space of all spectral sensitivity functions. Many pairs of responses induces many half-space constraints and the intersection of these is a surprisingly small set of candidate spectral sensitivity functions. One member of this intersection set is found using an appropriate optimization criteria.

We validate the results of rank-based spectral estimation for a Nikon camera using ground truth spectral data that were previously measured at National Physical Laboratory [1]. Good recovery is shown for linear raw and non-linear rendered images. We compare our recovery to that provided by a prior art linear regression method[2]. That method fails completely for the non-linear rendered image scenario.

## 2. METHODOLGY

In this paper we focus on cameras with three-channel response of red, green and blue. The typical camera response at $j$th pixel from $i$th sensor can be modelled as:

$$p_{ij} = \text{f}(\int_{\omega} E(\lambda) S_j(\lambda)Q_i(\lambda)d\lambda + N_i), \qquad\qquad i = 1,2,3 \qquad\qquad (1)$$

where $p_{ij}$ is the camera response, $E(\lambda)$ is the spectral power distribution of the scene illuminant, $S_j(\lambda)$ is the surface reflectance imaged at pixel $j$ and $Q_i(\lambda)$ is the spectral response of sensor $i$ at wavelength $\lambda$. The integral is taken over the visible spectrum $\omega$. Noise for each sensor is denoted as $N_i$ and f() denotes a non-linear rendering function. Prior art estimation algorithms ignore $N_i$ and f() to simplify Eq.1 for each channel as:

$$p_j = \int_{\omega} E(\lambda) S_j(\lambda)Q(\lambda)d\lambda = \int_{\omega} C_j(\lambda)Q(\lambda)d\lambda \equiv \underline{c_j}\underline{q}. \qquad\qquad (2)$$

Where $C(\lambda) = E(\lambda)S(\lambda)$. It is useful to translate (2) into the language of linear algebra. In (2), $\underline{c_j}$ denotes the $1 \times 31$ vector of sampled measurements (when we measure 31 wavelengths across the visible spectrum 400 to 700 Nanometres with 10Nm intervals) and $\underline{q}$ is the $31 \times 1$ single channel sensor spectral sensitivity. For $N$ colors, we can attempt to estimate $\underline{q}$, when we have the $N \times 1$ vector of single channel responses $\underline{P}$ and the corresponding $N \times 31$ matrix $C$ (with $\underline{c_j}$ being its $j$th row). Given the linear form of (2) sensor estimation can be written as a linear regression of the form below:

$$\min_{\underline{q}} \left\| C\underline{q} - \underline{P} \right\|^2 \qquad\qquad (3)$$

Solving (3) by $\underline{q} = [C^t C]^{-1}C^t\underline{P}$ according to [4], does not provide a stable solution due to the limited dimensionality of matrix $C$ [3]. Mathematically, the matrix $C^t C$ has a high condition number and, so, has a numerically unstable inverse.

Many spectral estimation algorithms begin with Equation (3) and attempt to solve for $\underline{q}$ in a more numerically robust way. Often, this is achieved by adding additional constraints into the problem formulation. For example in [2], sensors were assumed to belong to a low dimensional smooth basis and also that they should be unimodal. The resulting respective linear and linear inequality constraints led to sensor estimating being formulated as a quadratic programming problem [2]. Importantly, the constrained minimisation delivered much improved spectral sensitivity estimation. However, even this improved technique ignores the role of f() but, often, this cannot be ignored: camera responses are non linear (and when this is the case no existing method delivers good estimation performance).

Solving for $\underline{q}$ is much harder if the camera response is non-linear (i.e. when $N_i$ and f() are not ignored). In this article we also take a constraint based approach for finding $\underline{q}$ [2]. The difference is in the linear constraints that improve upon the robustness of estimation technique for non-linear data. Our key observation is that is f() is assumed to be a monotonically increasing function then this means that the ranks of the non-linear RGB

counts are the same as for their linear counterparts. Ranked single channel response for $P_1$ and $P_2$ implies:

$$f(P_1) > f(P_2) \Rightarrow P_1 > P_2 \rightarrow (\underline{c_1} - \underline{c_2}).\underline{q} > 0 \tag{4}$$

The inequality in (4) expresses the general form of a linear constraint derived from ranking the order of the single channel camera response of two colors. For $N$ color samples we can choose $\binom{N}{2}$ number of pairs to form the above linear constraint. The power of this linear constraint is in that it holds for both linear and non-linear data.

The intersection of all these 'half space' constraints results in a solution space that delimits a region of sensor space. As such, any sensor that satisfies all the ranking constraints is a possible solution to the sensor estimation problem. We choose the sensor that predicts the rank order of the response, integrates to unity, lies in a 7-dimensional Sine basis and is smoothest. This optimization is solved using Quadratic Programming.

## 3. EXPERIMENTS AND RESULTS

In this section we explain the experiments carried out for validation and evaluation of the estimated rank based spectral sensitivity functions of Nikon camera. An SG colour checker, was placed approximately in the centre of the floor of a VeriVide cabinet, facing upwards towards the D65 illuminant. The position of the camera relative to the color checker was chosen to be approximately at 45 degrees angle. For each patch in the checker, the camera signal was obtained by averaging the red, green and blue channel response over the central area of the patch resulting in matrix $P$ for the 140 colors. We took both raw and rendered images of the same scene. The matrix $C$ of colour signal measurement was obtained using a PR670 spectra radiometer.

We compare the estimated sensors $\hat{Q}$ using the ground truth spectral response functions measured (in a rigorous lab based experiment) at NPL [1]. We compare recovery for both the linear camera image and the nonlinear rendered image (the jpeg produced by the Nikon camera pipeline). In the latter case we seek to recover the camera sensitivities multiplied by the camera's 3x3 colour correction matrix T. Here, we use the work of [5] to recover the colour correction matrix $T$ and we apply it to the measured spectral sensitivities to provide ground truth for spectral estimation using a rendered (jpeg) image. Figure 1 illustrates these estimated sensors (red dashed line) and ground truth data (blue solid lines).
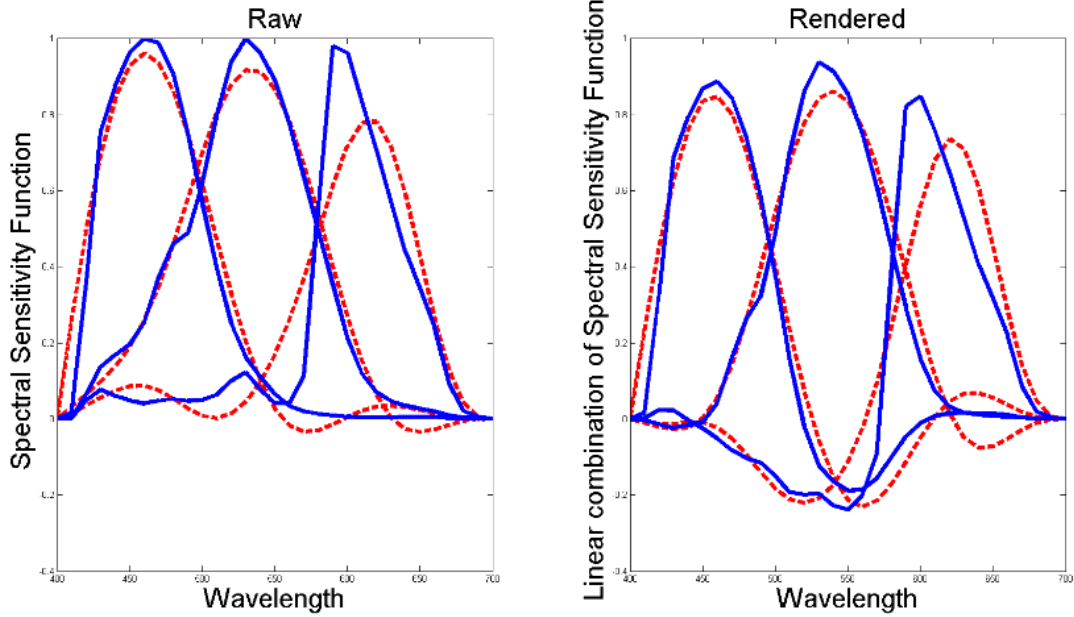
*Figure 1: Nikon spectral sensitivity function estimated using rank based technique (red-dashed) and ground truth data (blue solid) on raw (Left) and rendered (right) data.*

We also, numerically, evaluate the performance of our estimation technique by comparing it to a prior art quadratic programming estimation technique [2]. For this, we use Vora and Trusell's error [6] metric. Vora values close to 0 indicate the estimated sensors sample spectra − produce camera RGBs - close to those measured by the actual camera. The maximum Vora Value is 100. The Vora value is powerful as it teaches that two cameras with similar looking spectral profiles typically sample light in the same way. The Vora Value also capture the idea that the RGBs from a given camera can be linearly mapped to approximate measurements made by another (see [6] for a full discussion and derivation of the Vora Value).

Vora values for both raw and rendered data for the Rank-Based Spectral Estimation method (RBS) are shown in Table 1. That is, we calculate the Vora Value by comparing the estimated curves (plotted in red) in Figure 1 with the actual curves (plotted in blue). In both cases a very low Vora Value is found. That is the recovered sensors sample light very similarly to the actual sensors. The 'Rendered' results refer to the fact we are estimating the sensors multiplied by the colour correction matrix for the highly non-linear camera jpeg image.

In contrast the QP method [2] (based on assuming a camera has linear response) works well for the raw data but, as expected, terribly for the non-linear rendered data. A Vora Value of 65 teaches that the recovered sensitivities sample light nothing like the actual.

| Estimation Technique | Raw | Rendered |
|---|---|---|
| **RBS** | 5 | 6 |
| **QP** | 9 | 65 |

*Table 1: Table of Vora values. RBS: Rank based spectral estimation. QP: Prior art quadratic programming estimation technique [2].*

AIC2015 TOKYO - Color and Image

## 4. CONCLUSION

In this paper we have shown that the rank order of camera response is a powerful tool for solving the camera spectral sensitivity function (multiplied by colour correction in the case of rendered image). We have shown that this estimation technique is robust for both raw and rendered images. We validated our estimated sensors using measured spectral sensitivity functions from National Physical Laboratory. We show that prior art estimation technique fail to estimate spectral response function in the same consistent manner as our rank based technique. Experiments demonstrate that relatively good estimation is possible given a single image with known spectra.

## REFERENCES

[1]  Mohammadzadeh Darrodi M, Finlayson G.D., Goodman T., Mackiewicz M. 2014. A reference data set for camera spectral sensitivity estimation. *Journal of the Optical Society of America* (31): 381-391.

[2]  Finlayson G.D., Hordley S., and Hubel P.M. 1998. Recovering device sensitivities with quadratic programming. In *The Sixth Color Imaging Conference*: Color Science, Systems, and Applications, 90-95.

[3]  Maloney L.T. 1986. Evaluation of linear models of surface spectral reflectance with small numbers of parameters,. *Journal of the Optical Society of America* (3): 1673–1683.

[4]  Moore E. 1920. On the reciprocal of the general algebraic matrix. *Bull Am Math Soc*, (26): 394-39.

[5]  Kim S. J., Lin H. T., Lu Z., Susstrunk S., Lin S., and Brown M.S., 2012. A new in-camera imaging model for color computer vision and its application. *IEEE Transactions on Pattern Analysis and Machine Intelligence* 34(12): 2289-2302.

[6]  Vora P.L., Fareel J.E., Tietz J.D., and Brainard D., (HP, 1997). Digital color cameras - 2 Spectral response, In HP Technical Report.

Address: Dr Maryam Mohammadzadeh Darrodi, School of Computing Sciences
University of East Anglia, Norwich Research Park, Norwich, NR4 7TJ, UK
E-mails: M.Darrodi@uea.ac.uk, G.Finlayson@ uea.ac.uk

# Comparing Colour Camera Sensors Using Metamer Mismatch Indices

Ben HULL and Brian FUNT
School of Computing Science, Simon Fraser University

**ABSTRACT**

A new method of evaluating the colorimetric accuracy of a color camera is proposed that is based on the size (appropriately normalized) of the metamer mismatch volume induced by a change of 'observer' from camera to human eye and vice-versa. The degree of metamer mismatching indicates the range in the discrepancy of the colour signals that can arise and as such is a more well-founded measure of colorimetric accuracy than traditional spectral-based measures such as the root mean squared difference in fit between the camera and eye's sensitivity functions.

## 1. INTRODUCTION

It is well known that only a colour camera that satisfies the "Luther condition" (Luther 1927) can provide colorimetrically accurate colour images. Of course, colorimetric accuracy is only one issue of concern, and not necessarily the most important one, in terms of overall image quality. However, there are many situations—for example, dermatological imaging or paint and dye applications—in which it would be desirable to have a camera act as an imaging colorimeter. The Luther condition requires the camera sensitivity functions and the human eye's sensitivity functions to be within a linear transformation of one another. The problem with this condition is that it is all or none. If there is not an exact match then how is the discrepancy to be measured?

We address this question using the volume metamer mismatch index (VMMI) (Logvinenko 2014b) and compare the indices obtained for the sensitivity functions of the 28 digital cameras Jiang et al. (Jiang 2013) measured. The VMMI is a measure of the amount of metamer mismatching that can occur between two different observers for a given light. In this paper, one observer is fixed and defined by the human cone fundamentals; the other observer is defined by the spectral response functions of the colour camera being evaluated. Metamer mismatching for a pair of observers (sometimes called 'observer metamerism') refers to the fact two lights that induce an identical sensor response in one observer (i.e., match), may induce non-identical sensor responses in the second observer. The set of all possible such non-identical responses forms a convex volume in colour space referred to as the metamer mismatch volume.

The intuition behind using the degree of metamer mismatching in evaluating the colour fidelity of a digital camera is that if two lights match for the human observer, then it follows that ideally the camera should produce an identical RGB response to the two lights. If it does not, or if it produces identical RGB responses to lights that the human observer sees as distinct, then there cannot exist a one-to-one mapping between camera response and perceived colour. The greater the degree of metamer mismatching, the greater the ambiguity in the mapping between camera response and perceived colour, and hence, the less colorimetrically accurate the camera will be.

## 2. CAMERA VOLUME METAMER MISMATCH INDEX (CVMMI)

The Camera Volume Metamer Mismatch Index (CVMMI) is a measure of the amount of metamer mismatch between a particular camera sensor and the reference human observer. The CVMMI is a particular case of the VMMI in which: (*i*) the spectral response functions (Figure 1) of the reference human observer are those defined by the Govardovskii et al. model of photopigment responsivity (Govardovskii 2000) with peak photopigment optical density of 0.3 and peak absorbances of 430nm, 530nm, 560nm; and  (*ii*) the metamer mismatch volumes are computed for lights that are for the first observer metameric to the equal-energy illuminant.
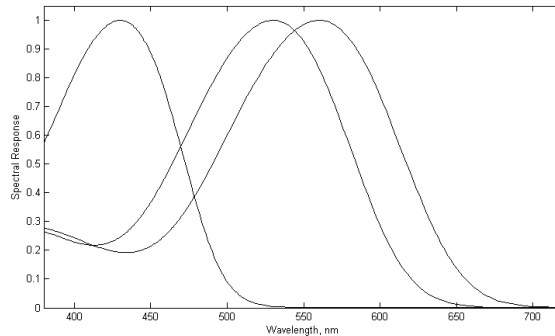


*Figure 1: The relative spectral response functions for the reference human observer based on the Govardovskii et al. model of the cone sensitivities.*

### 2.1 Calculating the Metamer Mismatch Volume

The metamer mismatch volume (MMV) for a given colour signal (i.e., XYZ, LMS or RGB, depending on the colour sensors used) recorded by the first observer in response to a given light is the set of all colour signals arising from lights that are metameric to the given colour signal that could possibly be recorded by the second observer. Logvinenko (Logvinenko 2014b) suggests that the size of the MMV can be measured in various ways, such as terms of its 'diameter', its area when projected into a 2D chromaticity space, or its three-dimensional volume. In this paper, we choose to use the cube root of its three-dimensional volume.

We calculate the MMV for the second observer given colour signal, $\Psi_1$, of the first observer using the new method Logvinenko describes (Logvinenko 2014b). This method is based on randomly choosing a set of 3 monochromatic lights and then finding a linear combination of the chosen lights that is metameric to $\Psi_1$. The response, $\Psi_2$, of the second observer to this linear combination provides a point in the MMV. Since this computation is fast, it can be repeated thousands of times with different sets of monochromatic lights thereby leading to lots of points on the boundary of the MMV. The convex hull of this set of these points provides a good approximation to the MMV.

### 2.2 Volume Metamer Mismatch index

While the volume of the MMV provides a measure of the amount of metamer mismatching, it varies in proportion to light intensity and to any linear transformation of the spectral sensitivity functions.  To obtain a measure that is unaffected by these factors, Logvinenko (Logvinenko 2014b) introduces the Volume Metamer Mismatch Index (VMMI).  The VMMI is defined as ratio of the volume of the MMV relative to the volume

of the convex hull of the spectral curve for the second observer (see Eq. 8 of Logvinenko 2014b for the formal definition). Since light intensity affects both volumes equally, as does a linear transformation of the sensitivity functions, the ratio remains unaffected.

The VMMI for the case of the reference human observer to a camera as the second observer provides a measure of how well or poorly the given camera is at representing colours as seen by the human observer. A high VMMI means that lights that look the same to the human observer can end up with significantly different RGB outputs from the camera. For the reverse case, that of the VMMI for a change from camera as the first observer to human as the second observer, the VMMI gives a measure of how well the camera preserves differences seen by the human eye. A high camera-human VMMI indicates that two lights that look very different to the human eye may be indistinguishable to the camera.

The VMMI can be computed for any colour signal $\Psi_1$ of the first observer in response to a light. In terms of using the VMMI as a measure of the colour fidelity of cameras, however, we define $\Psi_1$ to be the colour signal of the first observer in response to the equal-energy spectrum. This single case is taken as being representative of the degree of metamer mismatching for all spectra since the color signal corresponding to the equal-energy case has the largest VMMI. At the other extreme, is the colour signal of monochromatic light, for which there are no metamers.

It is possible for a camera to have a low human-camera VMMI (for colour signal of equal-energy spectrum) while having a high camera-human VMMI, and vice versa. For a camera to be colorimetrically accurate, both must be low. Therefore, we define the Camera Sensor Metamer Mismatch Index (CSMMI) as the average of the two.


## 2.3 Restricting the lights

Lights leading to colour signals on the boundary of the MMV have spectra that are non-zero at only three wavelengths. Such lights are not very representative of lights that are actually encountered by cameras in practice, although imaging a laser-based display would be a clear exception. The problem with evaluating the CSMMI for monochromatic lights is that a small difference in the camera response at a particular wavelength can lead to a high degree of potential metamer mismatching. The volume of the MMV correctly represents the range of possible responses, but this may not be what is desired in practice where monochromatic lights rarely arise, and also where the camera's sensor sensitivity functions may not have been measured all that precisely at every wavelength.

To avoid the problem of small differences in the sensor response functions leading to large differences in the CSMMI, we replace the monochromatic lights with lights having a Gaussian-shaped spectrum. Metamers are then found using linear combinations of three such lights with peaks centered at three different wavelengths. Since the set of lights is being restricted, the resulting MMVs are smaller and strictly inside the theoretical MMVs based on linear combinations of 3 monochromatic lights.

Figure 2 shows examples of the light spectra formed as a linear combination of Gaussian spectra with standard deviations of either σ=25 or σ=50. At σ=25, the Gaussian spectra are more similar the peaks in LED spectra. The spectra formed as a linear combination of three Gaussian spectra with σ=50 are closer to typical broadband light sources. We denote the CSMMI indices computed using Gaussian spectra of σ=25 and σ=50 CSMMI25 and CSMMI50, respectively.
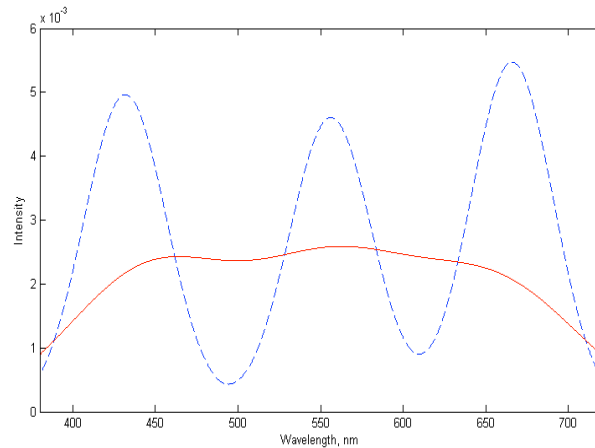
*Figure 2: Two spectra that are metameric to the equal-energy spectrum formed as linear combinations of Gaussian lights of standard deviation σ=25 (dashed blue curve) and σ=50 (solid red curve).*

## 3. RESULTS AND DISCUSSION

We computed the CSMMI25 and CSMMI50 measures for the sensor sensitivity functions of the 28 cameras measured by Jian et al. (Jiang 2013). The computation was based on finding 10,000 metameric lights as described above.

Jiang et al. rank the cameras in terms of two measures. The first is the departure from the Luther condition as measured in terms of the Root Mean Squared error in the best linear fit of the camera sensitivites to the CIE-1931 2-degree color matching functions. The second measure is the average CIEDE00 color difference taken over the 1269 Munsell reflectance spectra (Parkkinen 1989) illuminated by CIE D65 and measured between the transformed camera coordinates (i.e., best camera estimate of XYZ) and the true CIE XYZ. The RMS difference is a general measure, but using the average CIEDE00 over a set of reflectances is not. The problem is not only that the set of reflectances is limited, but that the reflectances are not lights. A general measure of camera colour fidelity must include the space of all lights, not just the space of lights reflected from surfaces under D65. In any case, Jiang et al. show that there is only a very limited correlation between the rankings that the two measures provide.

Figure 3 plots the RMS and CSMMI50 measures for the 28 cameras sorted in order of increasing CSMMI50. The two measures follow the same general trend, but there are significant disagreements between the two measures. The fact that the RMS measure can sometimes be small while the CSMMI is large is an indication of the problem with using the similarity of the camera and eye spectral sensitivity functions as a measure of colour fidelity since the CSMMI reveals that relative small differences as measured in terms of RMS can in fact lead to large colour differences between the camera and eye.

Of course, the CSMMI25 and CSMMI50 can be expected to be very correlated. Figure 4 shows that the two indices track one another closely with a few exceptions. Camera 6, for example, has a higher relative CSMMI25 than CSMMI50. This indicates that the colour fidelity of that camera will be poorer for lights with spectra having narrowband peaks than lights with strictly broadband spectra.
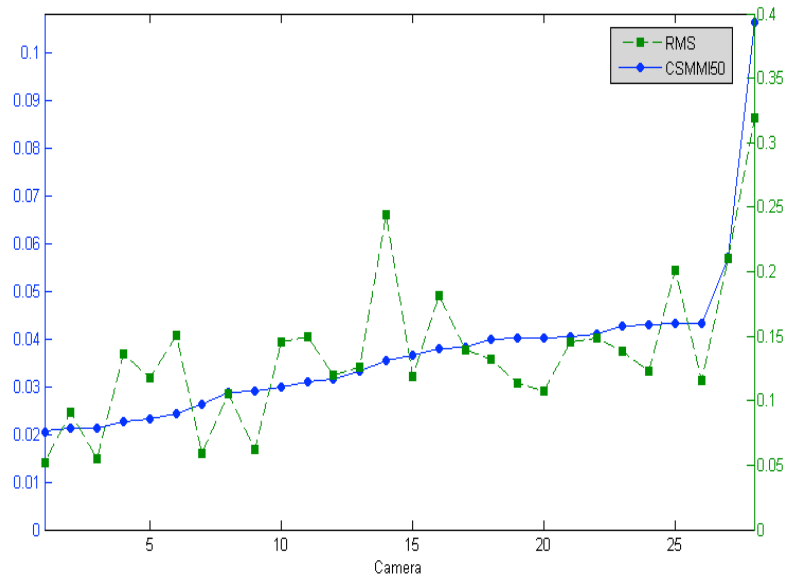
*Figure 3: The RMS (dashed green) and CSMMI50 (solid blue) measures for each of the 28 cameras with the results sorted in left−to−right order in terms increasing CSMMI50. Left axis CSMMI50 index. Right axis RMS value.*

Note that since the MMVs for the σ=50 lights are significantly smaller than the MMVs of the σ=25 lights the range of the CSMMI50 indices is always smaller than that of the CSMMI20 indices.
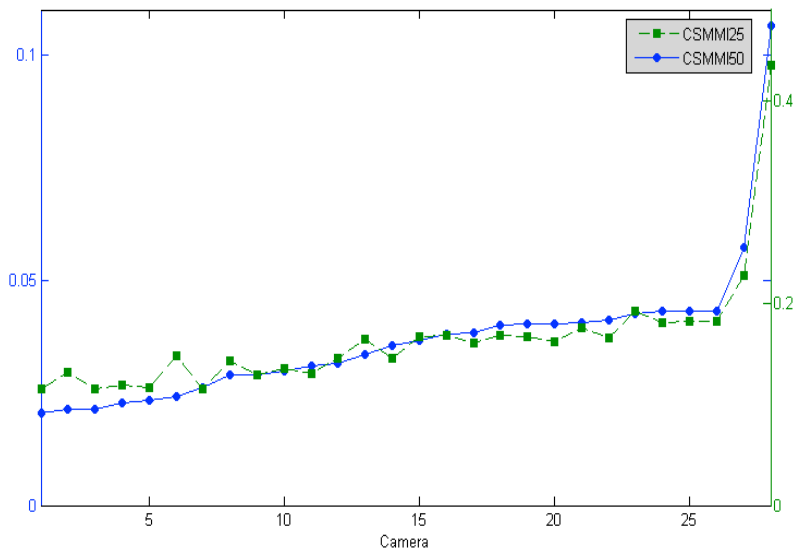


*Figure 4: Comparison of the CSMMI50 and CSMMI25 indices. Cameras are ordered in terms of increasing CSMMI50. The relative scale of the two plots has been adjusted so that they overlap for comparison.*

## 4. CONCLUSION

Digital colour cameras do not generally satisfy the Luther condition and therefore will not produce images that are entirely colorimetrically accurate. The Luther condition is all or

none. To compare the colorimetric accuracy of cameras requires a different measure, for which the RMS error in the best linear fit of the camera sensitivity functions to the human cones is often used. As an alternative, we propose a new measure, the camera sensor metamer mismatch index (CSMMI), based on Logvinenko's (Logvinenko 2014b) volume metamer mismatch index, which in turn is based on the amount of metamer mismatching that is induced by a change from the eye's sensitivity functions to a camera's and vice-versa. As such, it provides a principled measure of the colorimetric accuracy of a camera.

## ACKNOWLEDGEMENTS

## REFERENCES

Govardovskii, V., N. Fyhrquist, T. Reuter, D. Kuzmin, and K. Donner. 2000. In search of the visual pigment template. *Visual Neuroscience*. 17, 509-528.

Jiang, J., D. Liu, J. Gu, and S. Susstrunk. 2013. What is the Space of Spectral Sensitivity Functions for Digital Color Cameras? In *IEEE Workshop on Applications of Computer Vision (WAVC)* 168-179.

Logvinenko A., B. Funt B. and C. Godau. 2014a. Metamer mismatching. *IEEE Trans. on Image Processing*, 23, 34-43.

Logvinenko, A. 2014b. Colour variations arising from observer-induced metamer mismatching, *www.researchgate.net*, Accessed Oct. 2014.

Luther, R., 1927. Aus dem Gebiet der Farbreizmetrik. Zeitschrift für technische *Physik* (8) 540-558.

Parkkinen, J., J. Hallikainen, and T. Jaaskelainen. 1989. Characteristic spectra of Munsell colors. *Journal of Optical Society of America A*, 6(2) 318–322.

*Address: Brian Funt, School of Computing Science, Simon Fraser University, 8888 University Drive, Burnaby, British Columbia, Canada, V5A 1S6.*
*E-mails: bhull@sfu.ca, funt@sfu.ca*

# Advanced Measurement Technology for Image Clarity

Hideo Kita, Shigeo Suga

SUGA Test Instruments Co., Ltd.

## ABSTRACT

Evaluation of object surface structure has traditionally involved the assessment of familiar optical properties known as Gloss and Haze. More recently, the optical property attributed to object surface structure or structural internal optical effects, have gained major importance because such property can vary, while the traditional properties of gloss and haze remain constant, and vice-versa. This optical property is known as Image Clarity. We designed a test apparatus to quantify this optical phenomenon, which exists in both reflection and in transmission mode. Image Clarity is then converted to a numerical index whose values are high when the specimen reflects, or transmits the image clearly and is low when the specimen blurs the image.

## 1. FORWARD

Many have experienced this sense of quality and luxury by noticing sharp images in the form of silhouettes of surrounding trees and buildings reflected on a body panel of a stylish car, which happened to catch your eye. The overall quality perception of an object is developed by examining various optical properties of a surface; such as image sharpness, color, gloss, and haze reflecting from its surface.

Among optical properties, the degree that an image of an object can be viewed clearly without distortion is called Image Clarity. This optical property occurs in images that are either reflected or transmitted.

Viewing the image of the optical mask in reflection from two anodized aluminum plates is shown in Figure 1. The left plate is clearly defined and sharp. This plate has high Image Clarity values. The right plate is blurred and the optical mask is barely recognizable. This plate has low Image Clarity values. Image Clarity is a measure of this observed phenomenon, expressed numerically. Image Clarity values are high when the image can be seen clearly and Image Clarity values are low when the image appears blurry.
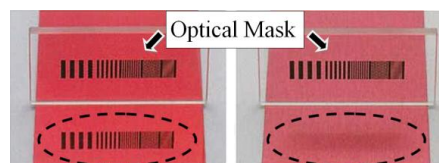


*Figure 1: Reflected Image Clarity Illustrated*

Recently, the phenomenon of Image Clarity is attracting much attention as a factor in the quantitative evaluation of how objects appear. This is occurring because the phenomenon is becoming recognized and understood. In addition to traditional measurements of Color, Gloss, and Haze, Image Clarity is being utilized in many diverse industrial fields. For example, external appearance has a significant influence on the perceived quality and value of products; such as the paint finish like piano black, orange peel or mirror finish on automobiles and other products, post cards[i], anodized aluminum, aluminum alloys and plastics whose surface is mirror finish and texturing. As a result of using Image Clarity values and controlling the manufacturing process, products are

produced that have high Image Clarity values. This means that images reflecting off surfaces or transmitted through objects can be seen clearly and distinctly. Also, for glossy post cards, Image Clarity values are used for evaluation since it enables evaluation of differences in Image Clarity even when measured Gloss values are nearly equal.

Furthermore, materials; such as packaging for electronic components, films (glass) for liquid crystal displays and smart phones require high Image Clarity values to show text and screen images clearly. Image Clarity values are used because they provide differences in visual appearance and distinctness of image, while traditional methods of analysis do not. It is interesting to note that there are cases where low Image Clarity values are a requirement; for instance, in the case of liquid crystal displays. Not only is high transmittance a requirement but so are low Image Clarity values. Low values of reflection Image Clarity are required to reduce glare by minimizing the intensity of reflection.

## 2. MEASUREMENT PRINCIPLE OF IMAGE CLARITY

Assessment of Image Clarity may be obtained by reflectance and transmittance modalities. Examples of two modalities used for these measurements are shown below. Figure 2 illustrates the Geometry for Image Clarity by Reflection and Transmission.

In Figure 2, the optical path begins with illumination from a light source and after passing through the source aperture-slit, it is collimated by the collimating lens and directed onto a specimen. Then, the image of source aperture-slit, reflected from or transmitted through a specimen, is collected and focused by the de-collimating lens on the optical mask. The light receptor detects the fractional amount of transmitted radiation passing through the optical mask.
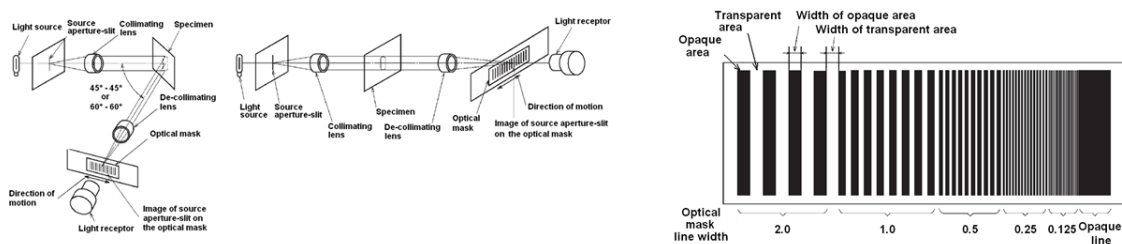


*Figure 2: Illustrates the Geometry for Image Clarity and Optical Mask*

The optical mask is illustrated in Figure 2. The geometric ratio of the opaque areas to the corresponding transparent areas is 1:1. There are 5 groups of comb patterns each having different segment widths; namely, 2.0, 1.0, 0.5, 0.25, and 0.125 mm. The data used for image analysis, which directly relates to Image Clarity, are acquired by scanning the intensity of radiation passing through the optical mask, shown as "Movement of optical mask" in Figures 3 and 4, Measurement of Image Clarity. Image Clarity, C(n)(%), is determined mathematically by the equation presented as equation (1). The largest amount of light received by the light receptor is the maximum light intensity, $M_n$. The least amount of light received by light receptor is the minimum light intensity, $m_n$. "n" is optical mask line width.

$$C_{(n)} = \frac{M_n - m_n}{M_n + m_n} \times 100 \qquad (1)$$

Referring to Figure 3, for a test specimen such as a perfect mirror, where the reflected image appears clear and distinct at the optical mask, the image of the source aperture-slit is

replicated on the optical mask perfectly within the diffraction limits of the optical system. This means that the image of the slit is fully transmitted when the optical mask is in Position 1, and blocked completely when the light is in front of the opaque part when the optical mask is in Position 2. In this case, the amount of light received by image detector is as shown in right of Figure 3. The difference between the maximum and minimum light intensities is large; therefore, the Image Clarity value is high.

Conversely, a matt surface test specimen with a dull finish causes the image to blur and distort. That distortion of the image of aperture-slit on the optical mask will be large as shown in Figure 4, Measurement of Low Image Clarity. This means that the image of aperture-slit is not fully transmitted when the optical mask is in Position 3, nor is it blocked completely when the light is in front of the opaque part of the optical mask in Position 4. The representation of the light intensities for Image Clarity having low numerical values is shown in right of Figure 4. The difference between the maximum and minimum light intensities is small; therefore, the Image Clarity value is low.
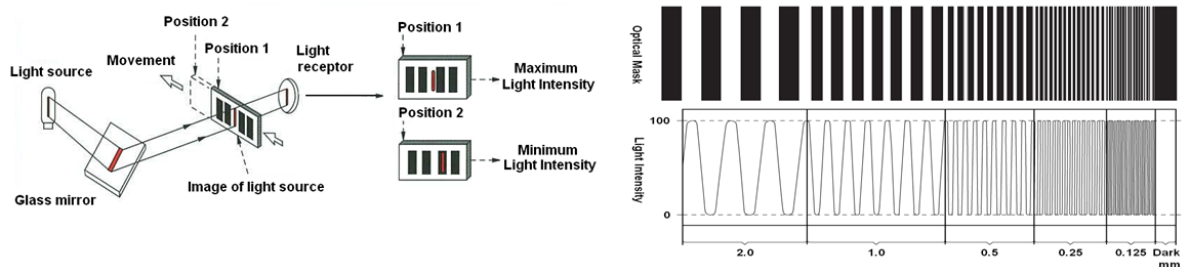


Figure 3: Measurement of High Image Clarity
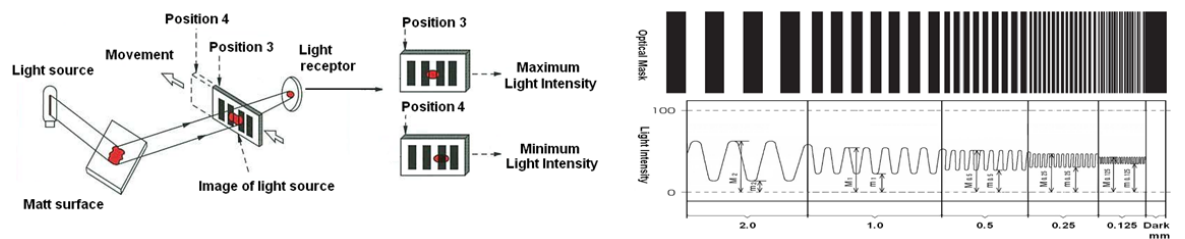


Figure 4: Measurement of Low Image Clarity

And also it is desirable to select optical mask line width depending on conformity to the visual assessment. Image Clarity values of five optical mask line widths are measured at the same time. For high Image Clarity specimens, use 0.125 mm and 0.25 mm in line width, for medium Image Clarity specimens, use 0.50 mm in line width and for low Image Clarity (matt) specimens, use 1.0 mm and 2.0 mm in line width.

## 3. A COMPARISON OF IMAGE CLARITY VERSUS GLOSS AND HAZE

### 3.1 Comparison of Measured Values for Gloss and Image Clarity

Four different tile specimens (Figure 5) that are similar in Gloss yet have different Image Clarity were selected for analysis. The tile designated A1 is a black glass, A2 is PVC, A3 is a painted plate, and A4 is a ceramic tile.

By the visual assesment, first, there is no discernable difference in Gloss among any of the specimens. Second, there are large differences in Image Clarity among all the specimens.
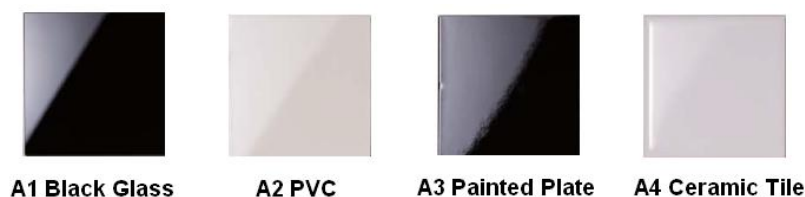
*Figure 5: Reflective Test Specimens*

The specimens were measured for Gloss at 60˚ and 20˚ in accordance with ISO 2813[ii] and Image Clarity in accordance with ISO 17221[iii] , using an Image Clarity Meter Model ICM-1T[1]. These data are presented in Table1.

One observes that the Gloss values at 60˚ are nearly the same, approximately 90 GU. Whereas the Gloss values at 20˚ and the Image Clarity values plot in descending order, A1 > A2 > A3 > A4. However the Gloss values at 20˚ do not show any obvious difference. Therefore, Gloss values at 20˚ and 60˚ do not conform to visual impressions. On the other hand, the Image Clarity C(0.25) values show large differences and those differences conform to visual impressions.

*Table1 Measured Values for Reflective Test Specimens*

| Test Specimen | A1 | A2 | A3 | A4 |
|---|---|---|---|---|
| Gloss Value GU (60˚) | 90.8 | 90.9 | 87.7 | 87.1 |
| Gloss Value GU (20˚) | 86.5 | 82.3 | 77.0 | 72.3 |
| Image Clarity C(0.25) | 99.5 | 32.0 | 18.9 | 1.6 |

**3.2 A Comparison of Haze and Image Clarity**

Four different transparent plastic specimens (Figure 6) that have different Haze values and Image Clarity values were selected for this analysis. The specimens B1 through B3 are plastic films. Specimen B4 is an anti-glare film.
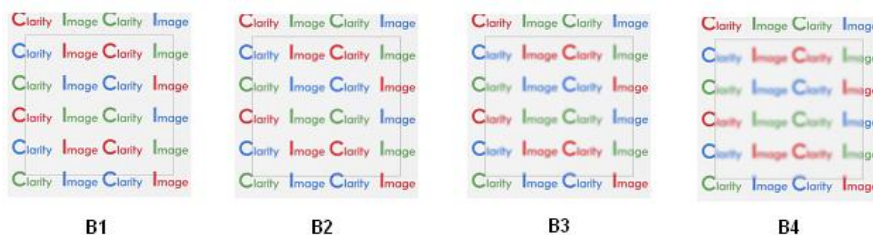


*Figure 6: Transparent Test Specimens*

By the visual assesment, specimens B1, B2 and B3 have the same high Image Clarity. The Image Clarity values of specimen B4 is distinctly lower than the grouping of the other three. The Haze of specimen B1 is barely discernable. Specimen B2 & B4 have low Haze values and specimen B3 has the highest Haze values.

The films were measured for Haze values on a Haze Meter, HZ-V3[2] in accordance with ISO 14782[iv] and Image Clarity in accordance with ISO 17221, using an Image Clarity Meter Model ICM-1T. These data are presented in Table 2.

---

[1] Manufactured by SUGA Test Instruments Co., Ltd., Shinjuku-ku, Tokyo, Japan

The Haze values increased (B1 < B2 < B3) and Image Clarity values decreased (B1 > B2 > B3), while cloudiness by visual impression increased. Therefore both sets of measured values conformed to visual impressions.

*Table2 Measured Values for Transparent Test Specimens*

| Test Specimen | B1 | B2 | B3 | B4 |
|---|---|---|---|---|
| Haze Value (%) | 1.6 | 14.1 | 33.2 | 14.7 |
| Image Clarity C(2.0) (%) | 97.1 | 90.4 | 88.5 | 38.4 |

However, in case of B4, the anti-glare film, the transmitted image is obviously hazier and appears indistinct when compared to plastic film B2. The evaluation of the Haze values gave similar values of about 14 for both specimens, but that result does not conform to visual impressions. On the other hand, the Image Clarity C(2.0) values were 90.4 for B2 and 38.4 for B4. This large difference in measured values conforms to visual impressions. From these observations and results, we conclude that the Image Clarity values are useful in the evaluation to determine the degree of glare. This is especially cogent for anti-glare films that have significant light diffusion properties.

## 4. CONSIDERATION OF DIFFERENCES IN RESULTS DUE TO DIFFERENCES IN METHODS OF EVALUATION

Differences between measured values of Gloss & Haze compared to Image Clarity are due to differences in Measurement Principles. Gloss values are determined by amount of reflected light within a small solid angle. In other words, Gloss largely depends on the amount of light reflected by an object. Haze is defined as percentage of light deviating by more than 2.5° from the incoming light transmitted through test specimen. These metrics do not access or measure image clarity.

Conversely, Image Clarity, either reflectance or transmittance measurement, is obtained by quantifying the amount of light transmitted through the optical mask at a particular spatial frequency. For example, in case of measuring Image Clarity for optical mask with 2 mm widths, the amount of light transmitted through optical mask is the greatest when image appears fully within the 2 mm transparent part of optical mask, and the detection is the smallest when image appears fully within 2 mm blocking part of optical mask. In such case, Image Clarity values will be the highest at 100 %. This phenomenon corresponds directly to the spatial frequency of the specimen texture. The degree of Image Clarity is influenced by the clearness, surface irregularities and haziness of surfaces. Gloss meters and Haze meters do not correctly access this phenomenon. Image Clarity is not the same as and should not be confused with Gloss or Haze.

## 5. PRECISION OF MEASUREMENT DATA

The confidence in a measurement system is directly related to its precision. The Image Clarity Meter was examined for its repeatability and reproducibility limit with 95% probability in accordance with ISO 5725-1[v]. The repeatability r and reproducibility R for Image Clarity by reflection measurements were performed at 6 different test laboratories for 6 different types of painted plates. For Image Clarity by transmission, measurements

---

[2] Manufactured by SUGA Test Instruments Co., Ltd., Shinjuku-ku, Tokyo, Japan

were performed at 6 different test laboratories using 4 kinds of transparent resins. The repeatability and reproducibility are presented in Table 3.

*Table3 Repeatability and Reproducibility Data for Image Clarity*

| Measurement Conditions | C(0.5) | | C(2.0) | |
|---|---|---|---|---|
| | *r* | *R* | *r* | *R* |
| **Reflectance** | 0.2〜0.3 | 0.7〜1.9 | 0.6〜0.7 | 1.0〜2.3 |
| **Transmittance** | 0.1〜0.5 | 0.4〜1.2 | 0.1〜0.9 | 0.2〜1.8 |

## 6. CONCLUSIONS

We described the significance of Image Clarity evaluation by comparisons with traditional Gloss and Haze evaluations. Image Clarity is widely used as an evaluation and analysis tool in Sensory Evaluation, since it captures differences in visual properties. This is not possible with only traditional methods of evaluation.

A new paradigm of assessing the quality of finishes using Image Clarity delivers to manufacturers the information and data that they need to perfect their materials and processes to perfect high quality finishes. This technique offers significant, valuable information that is not available from conventional sources, such as Gloss and Haze.

## ACKNOWLEDGEMENTS

## REFERENCES

[i] *Research on Paper Quality of Glossy Postcards for Inkjet Printers,* Research Paper, Institute for Posts and Telecommunications Policy (IPTP) Monthly Report 2003.1 No.172, Toyoichi Hosokawa, Mitsuyasu Kitajima

[ii] ISO 2813 *Paints and varnishes, Determination of specular gloss of non-metallic paint films at 20 degrees, 60 degrees and 85 degrees*

[iii] ISO 17221 *Plastics — Determination of image clarity (degree of sharpness of reflected or transmitted image)*

[iv] ISO 14782 Plastics, *Determination of haze for transparent materials*

[v] ISO 5725-1 *Accuracy (trueness and precision) of measurement methods and results — Part 1: General principles and definitions*

*Address: Hideo Kita, Calibration Dept, SUGA Test Instruments Co., Ltd.,*
*5-4-14, Shinjuku, Shinjuku-ku, Tokyo, 160-0022, JAPAN*
*E-mails: kita@sugatest.co.jp*

# Painting by Numbers: Transforming Fields and Edges to Vectors

Carinna Parraman, Paul O'Dowd, Mikaela Harding
The Centre for Fine Print Research, University of the West of England,
Bower Ashton Campus, Kennel Lodge Road, Bristol, BS3 2JT, UK

## ABSTRACT

This paper considers alternative approaches to image making and printing that moves from the on-screen representation of images and painting applications, to the physical generation and methods for surface deposition or *2.5D printing*. The research investigates the application of new materials and print processes, as an alternative to four-colour separation and half-toning and departs from traditional halftone screening that uses a vector approach to image construction. The first aspect of the paper describes a non-photorealistic rendering image segmentation algorithm that is used to create a series of colour texture layers. The second part of the paper describes a preparatory UV curing additive that can be used to increase the textured qualities of the brush strokes.

## 1. INTRODUCTION

The theoretical and practical objective of this research is to gain a deeper understanding of how physical artworks can be created that incorporate both analogue (paint, ink, graphite) and digital (vector); and could be described as containing textural or 2.5D qualities.

Contemporary printing has evolved as a process that is capable of printing flat areas of colour, alongside text, blends of colour and photographic images. In the emerging 2.5D and 3D print market, there is now a requirement to develop methods that can reproduce textures that have the look and feel of, for example, brushstrokes of old master paintings, or as created in a painting software. Current colour painting software tends to mimic how layers of colour are applied as if one were painting. Research so far has considered the shape of brushes, edges, opacity, pressure but less so about the textural qualities of the brush mark or the over-layering of layers of colour, or how to simulate watercolour, ink, oil paints and acrylics.

Texture is a visual attribute that enables us to distinguish the differences between materials (substances or substance out of which a thing is or is made), identify the structure and shape of objects, and discriminate edges in a complex pictorial scene. In order to gain an understanding to create verisimilitude with materials, we can study lighting techniques, drawing and painting techniques used by artists (Bayer, 2004; Hollman, 2004; Jordan, 1995; Constable, 2007) along-side scientists working on human vision and texture perception. Three main characteristics identified as useful in determining the qualities of a surface texture are: value, repetition and edges. (Landy, 1996; Klatzky, 2010) In our search for an identification of what are the basic constituents to identify, classify and reproduce texture, (Marr, 1980) differentiates between image and representation, and the use of what he describes as *primitives* to describe a shape. There are two primary classes of shape primitive: surface based (2D) and volumetric (3D). Of special interest, volumetric primitives involve the spatial distribution of a shape and vectors to describe its dimensions, along with shading and texture gradients.

In previous research, the authors considered how by observing the brush strokes of painters, (Parraman, 2012; 2013) images can be generated through the use of lines, modulation of similar strokes and a repetitive over layering of paint. Inspired by the meticulous painting methods by artists such as Van Gogh and Seurat, the objective for the experiment was to create a vector-driven painting machine that applied a brush loaded with paint to paper in a methodical and mechanical way, yet remain human analogous.

Whilst a vector approach (digital format) is highly machine repeatable, the resulting individual painted brush strokes (analogue) are not. We study the creation of non-uniform but harmonious painting effects across paper substrates through the actuation and placement of the brush, and the flow of paint. We are developing a contemporary approach that is based on vector or .SVG (Scalable Vector Graphics), which provides a set of instructions to drive CNC paths. In software programmes, a vector path is a series of mathematical elements that describe a set of lines, curves, arcs, and a combination of all to form closed shapes. A path can be *stroked* to obtain different thickness or colours, or used as input for other elements such as pressure, gradients in height, and blends to include opacity and translucency. We consider a vector-based drawing philosophy as significant to gaining an understanding of alternative approaches, which break away from pixels (digital screen resolution) and halftones (analogue print resolution).

## 2. RELATED LITERATURE

*Non-photorealistic rendering* (NPR) is a body of research which interprets digital formats (captured visual scenes or original works) and renders them with an alternate artistic expression. Typical source formats are pixel based images, although NPR can also be derived from 3D models and determined algorithmically without a prior source.

The utility in NPR can be functional, for instance 'unrealistic' shading schemes aid in the visualisation of complex parts drawn in computer-aided design (Gooch et al, 1998). The utility of NPR can also be to provide a purely artistic interpretation from a source, or to provide interactive software tools to aid in the creation of stylised digital art works. Of particular interest, a subset of NPR is stroke based rendering (SBR) which interprets pixels to strokes. We consider strokes as analogous to vectors, representing a series of movements with magnitudes and directions.

Often SPR seeks to emulate famous painterly styles, such as impressionism (Kasao, 2006; Yang, 2008), oriental ink painting (Ning, 2011; Cheok, 2007), or pen-and-ink illustration (Winkenbach, 1994). In this way SPR is motivated to model characteristics of effectors (i.e. a horsehair brush), mediums (i.e. watercolour) and substrates (i.e. canvas) to synthesise a convincing screen based render (Curtis, 1997). Our motivation is not to render the illusion of painterly styles with pixels. Rather we explore the operation of print apparatus for the tangible production of texture, which originate in painterly styles. As such the characteristics of effector, medium and substrate are inherent to the apparatus we use; we are focused on deriving the appropriate effector movement from digital sources.

We draw on NBR literature for algorithms to determine image segmentation, stroke placement and stroke characteristics that are transferable to machine control, detailed in section [3]. We intend to send a printer a sequence of movements and gestures, rather than a field of pixels to raster to a screen or to scan on to a substrate.

There are many examples of prior works that utilise a machine to produce art in more human analogous ways. Lindemeier (2013) includes a review of early painting machines

and related artists; 'eDavid' (Lindemeier, 2013), 'Paul' (Tresset, 2013) and a humanoid robot (Kudoh, 2009) are painting machines that closer approximate human movement. All three approaches utilise digital camera data to compare the working canvas against a digital source image. These three approaches therefore attempt to emulate the progressive development of paintings, stroke by stroke, by utilising predominantly 2D visual feedback during operation. In our approach we attempt to extract this chronological information from digital source images, by interpreting fields of pixels through segmentation and edges, to create a time-series composition of many-layered vectors. We develop this level of automation so that we may later experiment with controlling the generation of texture and expressive mark making.

### 3. IMAGE SEGMENTATION METHODOLOGY

We have developed a methodology inspired by the NPR algorithms for texture directionality described by Kasao et al through several papers (Kasao, 2006; Kasao 1998a; Kasao1998b). We use the convolution of a source image for texture directionality and edge detection. We implement a simpler K-Means clustering algorithm for image segmentation.

As an iterative algorithm, the K-means clustering progressively divides an image up into a predetermined number of segmentations, with a result analogous to a paint-by-numbers template. We experiment with low numbers of segmentations, such as 16 or 20, as we expect to run each segmentation as a paint layer. The segmentations do not necessarily map the spatial relationship of pixels, nor remain a fixed size of image partition. The segmentations group pixels by their similarity in calculated properties. Each segmentation is re-evaluated to generate the average characteristics of their assigned pixel grouping, thus altering the subsequent criteria for pixel assignment. The iterative algorithm ends when no more pixels are eligible to be reassigned, and therefore the segmentation averages have attained stable characteristics.

The segmentation minimises the Euclidean distance of six variables; x coordinate distance between a pixel and a possible segmentation centroid x coordinate ($D_x$), y coordinate distance between a pixel and possible segmentation y centroid coordinate ($D_y$), a pixel edge strength versus a possible segmentation average edge strength ($D_e$), a pixel texture directionality versus a possible segmentation average texture directionality ($D_d$); and the distance in colour space between a pixel hue, saturation brightness value, against the average hue, saturation brightness of a possible segmentation ($D_h$, $D_s$, and $D_b$ respectively).

The variables $D_x$, $D_y$, $D_e$, $D_d$, $D_h$, $D_s$ and $D_b$ are given weighted influence by a fixed gain value, *Kx, Ky, Ke, Kd, Kh, Ks, Kb* respectively. In this way, an image can be segmented with little regard for pixel spatial relationship ($K_x$, $K_y$ as small values, 0.01 works well), and high regard for texture directionality and edge strength ($K_e$ and $K_d$ as large values, such as 2.5). The Euclidean distance is thus calculated between each pixel and each segmentation ($D_{ps}$) as:

$$\Delta x = \sqrt{(D_x * K_x)^2}$$

$$\Delta y = \sqrt{(D_y * K_y)^2}$$

$$\Delta d = \sqrt{(D_d * K_d)^2}$$

$$\Delta e = \sqrt{(D_e * K_e)^2}$$

$$\Delta h = \sqrt{(D_h * K_h)^2}$$

$$\Delta s = \sqrt{(D_s * K_s)^2}$$

$$\Delta b = \sqrt{(D_b * K_b)^2}$$

$$D_{ps} = \sqrt{\Delta x + \Delta y + \Delta d + \Delta e + \Delta h + \Delta s + \Delta b}$$

The smallest $D_{ps}$ value assigns the pixel to the related segment cluster. We have used values Kx = , Ky = , Ke = , Kd = , Kh = , Ks = , Kb = to good effect.

The completed segmentation combined with the pixel edge strength and texture directionality provides useful data for machine control. Each segmentation provides the average hue, saturation and brightness values for the assigned pixels, creating a finite palette of colours (equal to the number of segmentations) to paint. The segment average edge strength value provides the order in which to conduct the painting, where strong edges are likely to be outlines or highlights, and performed last in the painting order. The segment average edge strength also provides a means to select a brush size, where low edge strength indicates a uniform area of an image, and so a large brush and a low density of strokes per canvas size can be adopted. Importantly, the information relating to individual pixels is preserved, so the brush stroke length and direction can be mapped from a pixel texture directionality and edge strength, creating a non-uniform characterisation of strokes within a single segmentation of pixels.

## 4. DEVELOPMENT OF INKS

The second aspect of this project is the development of a water-based UV LED curable medium that can be added to artist's inks and pigments to create a UV curable paint. In normal UV resin bases for inks and paints, the viscosity of the individual components are as low as possible to ensure satisfactory production as well as good flow behaviour of the liquid formulation. However in this application, the resin needs to be viscous in order to hold the texture of the paintbrush mark when the ink/paint is deposited.

UV LED systems potentially offer a greener alternative to conventional mercury vapour lamps used to UV cure coatings for ink, wood/furniture, electronics and other industries. The main advantages of the LED lamps are that they are more energy efficient – using up to 60% less energy than mercury UV lamps, more cost efficient – lamp lifetimes of up to 10,000 hours, and more environmentally friendly – irradiation in the near visible region (380-410 nm), no formation of ozone when curing in air and no mercury lamps to dispose of at the end of their life.

In the current formulation, the medium contains a hydrophilic aliphatic urethane acrylate solution in water, containing 50% acrylated products. This has a 95% solids content and so is easily diluted with water. Tripropylene glycol diacrylate (TPGDA) acts as a reactive dilutant monomer that also promotes adhesion to substrate, hardness and scratch resistance of the cured layer (Mashouf, 2014). Other additives are used to further increase adhesion to substrate and flow of the medium.

Because of the long wavelength absorption characteristics, which are also better suited

to commercially available LED's, acylphosphine oxides are particularly useful for the polymerization of pigmented formulations where irradiation at longer wavelength is desired. This family of photo initiators are used due to the high reactivity of the photo chemically formed phosphonyl radicals that arise from the high electron density at the phosphorus atom. Furthermore, the pyramidal structure of the radicals provide more favourable steric conditions for the unpaired radical site to react with monomers to initiate and propagate the polymerization reaction (Yagci, 2012).

A tertiary amine, N-vinyl pyrrolidinone (NVP), is used in the formulation to help in overcoming oxygen inhibition (Husar, 2014). Oxygen inhibition is due to the fact that molecular oxygen, at ambient conditions, exists as a diatomic molecule with a triplet diradical electronic ground state. Due to these triplet and radical characteristics, oxygen has high chemical reactivity towards the phosphonyl radicals created by the photo initiator, leading to the early termination of the polymerization reaction. (Miller, 2003) Therefore the free-radical photo polymerization reaction that occurs within the formulation can be inhibited significantly by oxygen in the atmosphere. The final ingredients in the UV LED formulation are mattefying silica to reduce the glossiness of the cured medium and the artist's pigment/materials to colour the formulation.

## 4. CONCLUSIONS

The paper describes methods for segmenting an image using NPR algorithms that can be exported as vector or .SVG documents that provides a set of instructions to drive CNC paths to a painting rig. Philosophically, we believe an image originally composed or acquired as vectors provides a richer description of an image, which would be especially suited to machine production. Through a process of segmentation and edges, fields of pixels are transcribed into many-layered vectors. The NPR algorithms are the starting point to transcribe the vectors into textured brushstrokes using paint and a highly experimental printer rig. The printer rig is capable of applying multilayers of artist's paints that include both traditional and UV curable inks (as described in section 4). The user is able to change the appearance of the layers ie. changes to translucency and viscosity by modifying the paints by hand, as well as change the direction of the brushstroke and the arc of the brush stroke by modifying the software, thus enabling the user to extend a greater control over the multi-layering process.

## ACKNOWLEDGEMENTS

## REFERENCES

Bayer, A. 2004. *Painters of Reality*. New York: Yale University Press.

Cheok, A.D., Z.S. Lim and R.T.K. Tan 2007. *Humanistic oriental art created using automated computer processing and non-photorealistic rendering,* Computers Graphics 31(2), 280-291.

Constable, M. 2007. *The Painted Photograph: Technical Commonality between the Digital Composite and the Pre-Modern Painting*, World Conference on Educational Multimedia, Hypermedia and Telecommunications. Vancouver: Canada.

Curtis, C.J., S.E. Anderson, J.E. Seims, K.W. Fleischer, and D.H. Salesin 1997. Computer-generated watercolour, Proc. 24th Annual Conference on Computer Graphics and Interactive Techniques, SIGGRAPH '97, pp. 421-430. ACM Press/Addison-Wesley.

Gooch, A., B. Gooch, P. Shirley, and E. Cohen 1998. A non-photorealistic lighting model for automatic technical illustration, Proc. 25th Annual Conference on Computer Graphics and Interactive Techniques, SIGGRAPH '98, pp. 447-452. ACM, NY

Hollman, E. and J. Tesch 2004. *Trick of the Eye, Trompe L'oeil Masterpieces*. Prestel.

Husar, B. 2014 *Experimental Comparison Of Various Anti-Oxygen Inhibition Strategies In LED Curing*, RadTech, Vienna University of Technology.

Jordan, W.B. and P. Cherry 1995. *Spanish Still Life from Velázquez to Goya*. London: National Gallery.

Kasao, A. and K. Miyata 2006, *Algorithmic painter: a NPR method to generate various styles of painting*, The Visual Computer 22(1), 14-27.

Kasao, A. and M. Nakajima 1998a. *A resolution independent nonrealistic imaging system for artistic use*, Proc. IEEE International Conference on Multimedia Computing and Systems, pp. 358-367 (1998a)

Kasao, A. and M. Nakajima 1998b. *K-means algorithm using texture directionality for natural image segmentation*, IEICE tech. report. Image Engineering 97(467), 17-22.

Klatzky R.L. and S. J. Lederman 2010. *Multisensory Texture Perception*, Multisensory Object Perception in the Primate Brain. Naumer, M.J. and J. Kaiser (Eds.) Springer.

Kudoh, S., K. Ogawara, M. Ruchanurucks and K. Ikeuchi 2009. *Painting robot with multi-fingered hands and stereovision,* Robotics and Autonomous Systems 57(3), 279-288.

Landy, M. 1996. *Texture Perception*, Encyclopedia of Neuroscience. Adelman, G. (Ed.) Amsterdam: Elsevier

Lindemeier, T., S. Pirk, and O. Deussen 2013. *Image stylization with a painting machine using semantic hints*, Computers Graphics 37(5), 293-301.

Marr, D. and E. Hildreth 1980. *Theory of Edge Detection*, Proc. of the Royal Society of London. Series B, Biological Sciences, Vol. 207, No. 1167: 187-217.

Mashouf, G., M. Ebrahimi, and S. Bastani. 2014. *UV curable urethane acrylate coatings formulation: experimental design approach*, Pigment & Resin Tech., 43 (2) 61-68.

Miller, C.W., C. E. Hoyle, S. Jönsson, C. Nason, T. Y. Lee, W. F. Kuang and K. Viswanathan, 2003. *N-Vinylamides and Reduction of Oxygen Inhibition in Photo polymerization of Simple Acrylate Formulations,* Photo initiated Polymerization, *ACS Symposium Series*, 847, 2–14.

Ning, X., H. Laga, S. Saito, and M. Nakajima 2011. *Contour-driven Sumi-e rendering of real photos*, Computers Graphics. 35(1), 122 -134.

Parraman, C. 2013. *The development of vector based 2.5D print methods for a painting machine*, Proc. IS&T Elec. Imaging Sci. & Tech. 8652.

Parraman, C. 2012. *Dark Texture in Artworks*, IS&T Elec. Imaging Sci. & Tech. 8292.

Tresset, P. and F.F. Leymarie 2013. *Portrait drawing by Paul the robot*, Computer Graphics 37(5), 348-363.

Winkenbach, G. and D.H. Salesin 1994. *Computer-generated pen-and-ink illustration*, Proc. 21st Annual Conference on Computer Graphics and Interactive Techniques, SIGGRAPH '94, pp. 91-100. ACM, New York.

Yagci, Y. et al, 2012. *Photoinitiated Polymerization: Advances, Challenges, and Opportunities,* Macromolecules, 43, 6245–6260.

Yang, C.K. and H.L. Yang 2008. *Realization of Seurat's pointillism via non-photorealistic rendering*, The Visual Computer 24(5), 303-322.

*E-mails: Carinna.Parraman@uwe.ac.uk¸ Paul3.O'Dowd@uwe.ac.uk,*
*Mikaela.Harding@uwe.ac.uk*

# Perception of colours illuminated by coloured light

Shabnam ARBAB, Barbara Szybinska MATUSIAK
Faculty of Architecture and Fine Art, Norwegian University of Science and Technology
(NTNU)

## ABSTRACT

The present paper reports the findings from a scale model experiment dealing with the assessment of colour under different colour temperatures of light. The data presented in this paper is a part of the findings from a large experiment. The mixed methods approach, which associates both qualitative and quantitative evaluation of the visual environment have been used to answer the following question: *How is the perception of colour influenced by the colour temperature (CT) of light?* The light in this case is a mixture of direct light from a light panel and light reflected from a coloured facade. A questionnaire was used to assess nine alternatives; each of them was a combination of one of three different colours of façade and one of three CTs of light. Forty-seven participants evaluated two different stimuli: Colour of façade and colour of light. Visitors of the exhibition participated as subjects in the experiment.

The experiment was carried out during the exhibition entitled "Colour in the city" at Trondhjems Kunstforening and it was sponsored by the Norwegian Research Council as a part of the yearly so called "research day" activities in Norway.

The results show that both, the colour temperature of light and the colour of façade, have significant impact on the colour perception; CT has stronger effect. It was also found that the nuances shift toward the same direction with the same colour temperature of light for each façade. A similar tendency was observed for the hue. The statistical analysis resulted with trustworthy and precise results that we are happy to present at the AIC-2015.

## 1. INTRODUCTION

Colour is not the property of objects, spaces or surfaces; it is the sensation caused by certain qualities of light that the eye recognizes and the brain interprets. The colours of the environment influence our experiences of light and the need for lighting – and vice versa: the qualities of light are essential for our perception and experience of colour. Therefore, light and colour are inseparable. Recent studies put the spotlight on considering simultaneously both colour and light due to their importance for architecture and their effect on the quality of life of users as well as on the minimizing energy consumption in buildings.

As it was stated above, light and colour are, however, largely two separate fields of research and most of the research deals with completely other questions than their spatial interaction (Arbab and Matusiak 2015). Considering what was mentioned, the main research question is formulated as follows:

*How is the perception of colour influenced by light?*

In order to carry out comprehensive analysis about the impact of light on colour perception there is a need to merge qualitative and qualitative approaches since the strengths of both could provide the best understanding. A mixed methods approach, which associates both qualitative and quantitative evaluation of the visual environment, will be used to answer the research questions.

## 2. METHOD

In order to answer the question, a model with two rooms in the scale 1:10 was used; Each room 50cm x 50cm x 40cm represented a living room 5m x 5m x 4m in the 1:10 scale to be large enough to allow a comfortable observation of an outdoor facade as well as the interior. The walls, ceiling and floor were constructed using 3mm MDF boards. On the outside the models were painted in black colour and on the inside they were painted in grey NCS S 5500-N.

A sample with the reference colour NCS S 1500-N was placed in the first room having large window-like opening toward the street; 14 colour samples (Table 1) were placed in the adjacent room with no opening to the street but illuminated by the white light (6500K) from translucent ceiling. The visitors could deserve if and in which way the colour perception depends on the colour temperature of light. The experiment has been repeated with three different facades, yellow, dark red and light blue; see Figure 3, something that enabled testing of the impact of the colour of the façade. The visitors were asked to assess which of the 14 colour samples looks most similar to the reference colour.

*Table 1. 14 selected colour samples*

| NCS Colour samples code | | |
|---|---|---|
| NCS S 1505-Y40R | NCS S 1510-Y90R | NCS S 1515-R90B |
| NCS S 1505-Y70R | NCS S 1502-R | NCS S 1510-B |
| NCS S 1505-Y80R | NCS S 1502-R50B | NCS S 1502-B50G |
| NCS S 1505-Y90R | NCS S 1510-R60B | NCS S 1500-N |
| NCS S 1510-Y80R | NCS S 1510-R90B | |
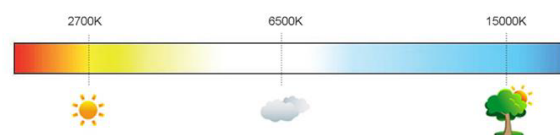




*Figure 2: Stimuli 1: Three colour temperatures of light used in the experiment.*



*Figure 1: Illustration of the model.*

*Figure 3: Stimuli 2: Three facade colouration to test. From left to right: NCS S 5030-Y80R / NCS S 2002-B / NCS S 4030-Y30R.*

The experiment was carried out during the exhibition entitled "Colour in the city" at Trondhjems Kunstforening (Group 2014) and it was sponsored by the Norwegian Research Council as a part of the yearly so called "research day" activities in Norway, and the main objective was to examine the impact of the colour temperature (CT) of light (Figure 2) on visual perception of coloured surfaces in the scale model study.

The subjects were the visitors of the exhibition and participants of the research day, some of them were artists and researchers squinted with colour design or study. The aim was to have as many participants as possible. Since all the subjects received all stimuli, this experiment had within-subject design. It was full factorial approach and all possible combinations of independent variables were distributed in a completely randomized order.

The experiment was independent of weather condition and time of the day. The light was produced by two different light sources: LED based, full-spectrum light panel and LED based Philip hue bulbs. Pilot study was done to select the colour samples from wide spectrum of hues and nuances, to provide a final check of elements and instruments and to ensure a smooth conduct of the experiment. Then analysis of pilot study was done to find out whether further refinements were needed. During the pilot study the time required for running the experiment was also estimated.

Experimental design and planning, Subject selection, Sample selection, Configuration of experimental set-up, Pilot study, Main study, Analysis and reporting were just different stages of this project necessary to make the results more reliable:
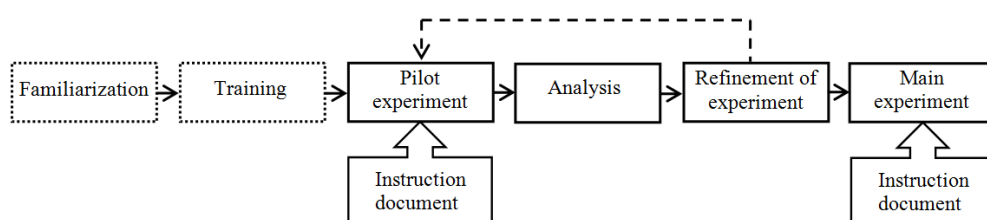


*Figure 4: Flowchart of test administration stages (Bech and Zacharov 2007).*

The colour samples were chosen from the NCS colour selection, and because of the time limitation of the experiment, it was necessary to narrow down from 71 to 14 samples. To make selection easier, the blackness of all samples was kept at the same level, namely 15%. The procedure for narrowing number of samples was the visual assessment by 5 people who were asked: which of a large number of comparison samples in the test room looked most similar to reference sample in the reference room.

To keep the same light level in both rooms, illuminance was measured in both rooms for each façade. Two Philip hue lamps and two layers of diffusing paper were used in the test room to adjust the light level and to create even light distribution.

## 3. RESULTS AND DISCUSSION

The overview of answer distribution is shown in Figure 5. The graph indicates the answer distribution on all 9 alternatives.

The effect of the CT of light and colour of façade on the responses was tested by a Stuart-Maxwell test (Stuart 1955, Trujillo-Ortiz 2005), where a computed SM value is evaluated using the chi-2 distribution. This test allows only pairwise comparisons and the

results are summed up in Table 3. As is apparent from the low probability values, both the colour of the façade and the colour temperature of light, have significant effects on the answers, with a slightly stronger effect for CT.
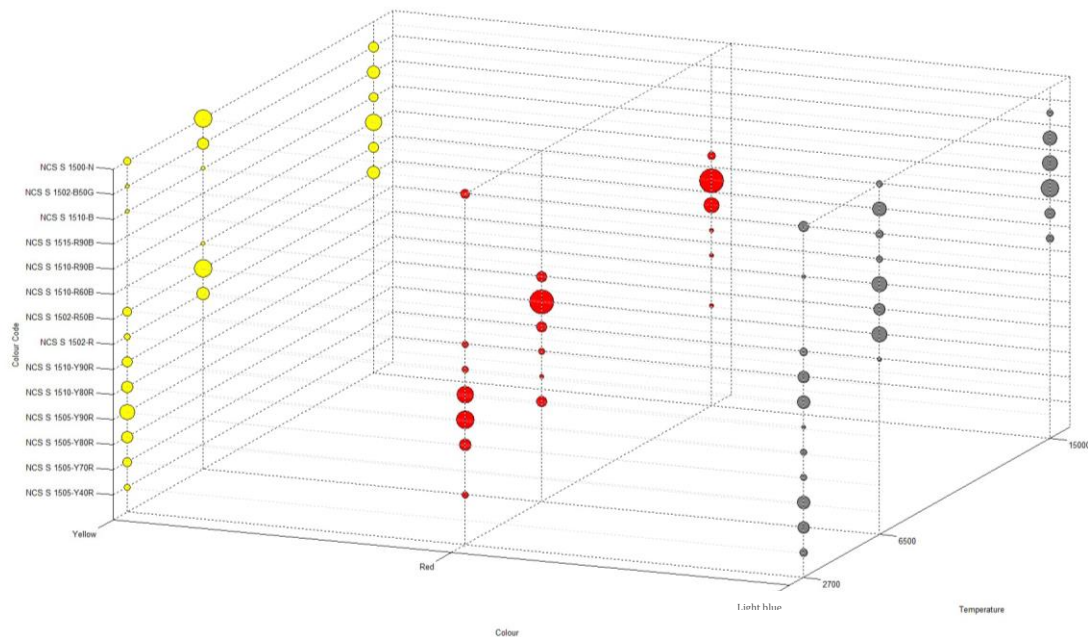


*Figure 5: General overview about answer distributions.*

In this experiment, all the colour samples had the same blackness on the nuance part but the chromaticity of colours was different. Figure 6 shows the average value of chromaticness. The differences in chromaticness of selected colour samples with different colours of façade are small and the yellow façade resulted with the lowest average of chromaticness. The differences due to different CT of light are bigger, higher temperature contributes to highest chromaticness.

Out of the three colours of façade, only yellow façade did not present in a way that we expect to have been affected by CT of light (Figure 7). See Table 4 for distribution of answers of nuances for each stimulus. Up to now, the effect of each stimulus was analysed but there is another way of analysing data, the interaction of both stimuli for 9 alternatives can be analysed separately. For example for Red façade with CT of 2700 K the tendency of answers is toward the yellowish colour with 90% red and the nuance toward the higher chromaticness. Full analysis of each alternative on NCS colour circle and triangle are available from authors upon request.

*Table 3. Stuart-Maxwell analysis (probability values < 0.05 are considered as significant).*

| Statistical Analysis | | | |
|---|---|---|---|
| Comparison | SM value | d.f. | Prob |
| 2700 K vs. 6500 K | 101.9 | 13 | 3.3e-16 |
| 2700 K vs. 15000 K | 120.1 | 13 | 0 |
| 6500 K vs. 15000 K | 79.1 | 13 | 8.2e-12 |
| Light-blue vs. red facade | 99.8 | 13 | 8.9e-16 |
| Light-blue vs. yellow facade | 59.0 | 13 | 4.0e-8 |
| Red vs. yellow facade | 67.7 | 13 | 1.1e-9 |
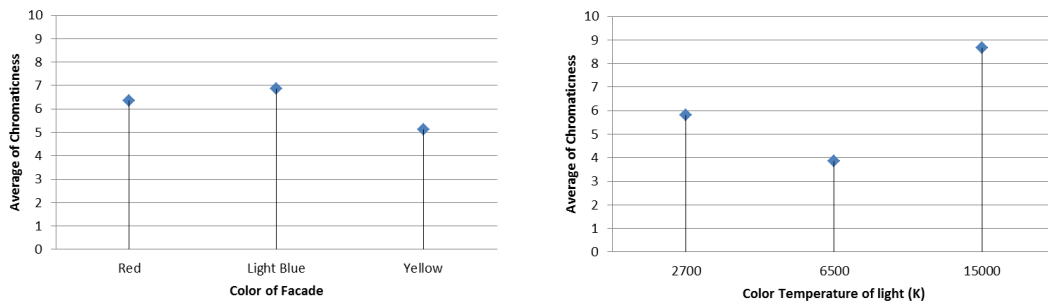
*Figure 6: average of chromaticness under different stimuli.*
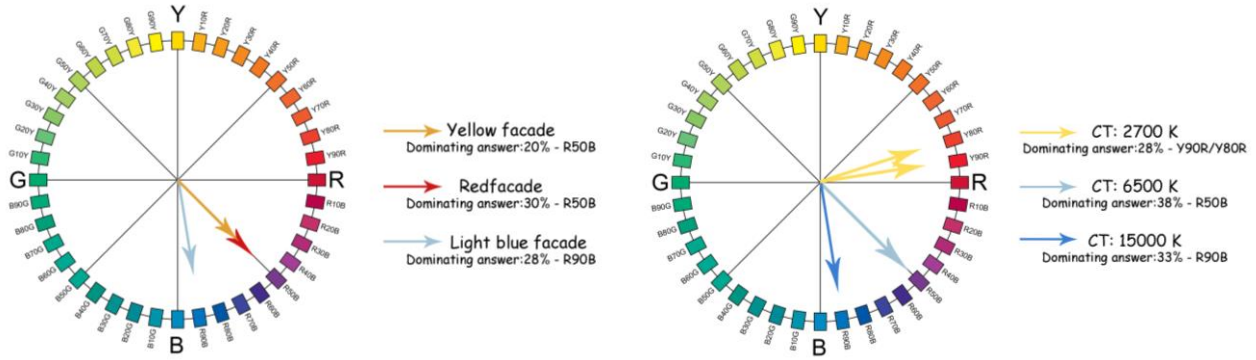


*Figure 7: Effect of two stimuli on the hue: Colour of façade and CT.*

*Table 4. Dominating answers for nuances with different stimuli*

| Stimuli | Colour of facade | | | Colour temperature of light (K) | | |
|---|---|---|---|---|---|---|
| | Yellow | Red | Light Blue | 2700 | 6500 | 15000 |
| Dominating answer (%) - Nuances | 36% - 1502 | 51% - 1510 | 42% - 1510 | 37% - 1505 | 60% - 1502 | 66% - 1510 |

Another part of the experiment was to use spectral power distribution as a visual representative of light spectrum produced by a lamp. Figure 8 shows the relative intensities of a light source at each wavelength which was measured on the reference sample for three different colour temperatures of light in the same setting as evaluated in main experiment. The quality of light created by different light sources could be compared in this graph.
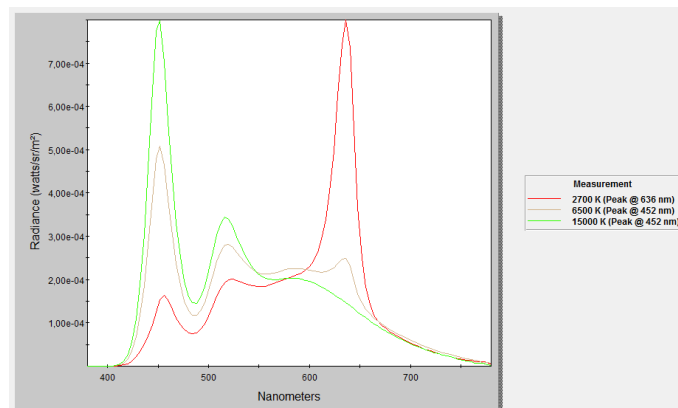


*Figure 8: Spectral power distribution of light reflected from reference sample for three colour temperatures of light.*

As expected, the results show that the effect of CT of light plays an important role in the perception rather than the façade; this coincides with the subject's answer.

*Table 5. Comparison of CT (K) in 9 alt. as well as nutural facade with CT of light panel*

| CT of light panel | CT of light on reference colour With nutral grey | CT of light on ref. colour with red facade | CT of light on ref. colour with light blue facade | CT of light on ref. colour with yellow facade |
|---|---|---|---|---|
| 2700 | 2589 | 2387 | 2743 | 2511 |
| 6500* | 6007 | 5771 | 7006 | 6054 |
| 15000* | 12425 | 12530 | 17879 | 12975 |

*After measuring spectral distribution on the light panel, it was found that the CT that was fixed on the light panel was not exactly equal with the measured by the PR-655 SpectralScan. The panel displayed 6500 and 15000 K and the measured values were respectively 6700 and 16200 K.

## 4. CONCLUSIONS

This paper discussed the interaction between light and colour on the perception of colour surfaces. Two predictors act as independent variables: Colour of façade and CT of light. In this experiment we attempted to make the model, the illumination and the outdoor environment as real as possible. The results of this study lead to the following conclusions:

If the effect of each stimulus was considered separately, the CT of light was found as most important predictor for the evaluations of all nine alternatives even though the colour of façade had effect as well.

But if the interaction of CT of light and colour of facade for each alternative were considered then the shifts from yellowish to bluish when the CT of light was increased was registered. The shift toward bluish stopped at the purple in the case of red façade, while the two other facades contributed to the shift closer to the bluish. So the effect of façade is weaker than CT of light, exactly like what we have experienced in with real overcast sky.

## ACKNOWLEDGEMENTS

## REFERENCES

Arbab, S. and Matusiak, B. S. The impact of light at the perception of colours in architecture, state of the art study and suggestions for further research. In AIC 2015, *Proceedings of Colour and image*. Tokyo.

Bech, S. and Zacharov, N. 2007. Perceptual audio evaluation-Theory, method and application, John Wiley & Sons.

Light and Colour Group. 2014. Colour in the City [Online]. Available: http://www.ntnu.no/trykk/publikasjoner/FargeiByen/

Stuart, A. 1955. A test for homogeneity of the marginal distributions in a two-way classification. Biometrika, 412-416.

Trujillo-Ortiz, A. 2005. StuMaxtest. Matlab Central.

*Address: Shabnam Arbab, Dept. of Arch. Design, Form and Colour Studies, Norwegian University of Science and Technology (NTNU), Alfred Getz vei 3, 7491 Trondheim, Norway*
*E-mails: Shabnam.arbab@ntnu.no, barbara.matusiak@ntnu.no*

# Effects of Furniture Colour on Apparent Volume of Interior Space

Keishi YOSHIDA, Masato Sato
Division of Environmental Sciences, Kyoto Prefectural University

## ABSTRACT

This study was conducted to evaluate the effects of furniture colour on the apparent volume of the interior space of a house. Psychological experiments were conducted using one-tenth scale models of a room. It was found that white solids were found to make the interior space appear more spacious compared with the other colours. As for the solids used to simulate beds, the taller the solid, the apparent volume of interior space becomes more cramped. As for the solids used to simulate cabinets, all solids except for the white solids made the interior space appear cramped, and increasingly so with increasing volume, whereas the white solids hardly made the interior space appear cramped, regardless of their volumes. In case of the solids having the same volume, interior space placed the solids used to simulate beds appeared more cramped than those placed the solids used to simulate cabinets.

## 1. INTRODUCTION

Since the concept of minimalism has become popular, the interior spaces of houses have become more compact than ever before. Therefore, it has become important issue how to make interior spaces appear spacious. Colours of interior components is one of the most successful methods for achieving this goal. There are many psychological effects of colour; advancing colour, receding colour, expanding colour, contracting colour and so on. It is evident that some of these effects play important roles in people's perceptions of interior spaces. The colours of the walls, floor, and ceiling of a room have a strong influence on the apparent volume of the room. Some studies have been conducted to evaluate the effects of the wall colour on the apparent volume of a room. One study found the effects of accent colour on the apparent distance to a front wall. Because interior spaces are usually furnished, it is clear that furniture colour must also influence the apparent volume of a room. However, only a few studies have been conducted on the effects of furniture colour on the apparent volume of a room.

The purpose of this study is to evaluate the effects of furniture colour on the apparent volume of the interior space of a house.

## 2. EXPERIMENTAL METHOD

A series of psychological experiments were conducted to evaluate the apparent volume of an interior space using a one-tenth scale model of a room measuring 2.4 m in ceiling height and 3.6 m in width and depth. The walls and floor were painted in the achromatic colour N8. A luminous ceiling comprising a milk white acrylic plate that transmitted light was included to maintain uniform interior illuminance. Fluorescent lamps of a high colour-rendering type were installed above the acrylic plate. The average interior illuminance level was approximately 250 lx. Seven types of rectangular solids were placed in the scale model of the room, one at a time, to simulate furniture pieces such as beds and cabinets. The six colours (Red, brown, blue, black, grey and white) used in the experiments were

red, blue, brown, white, grey, and black. There were 42 experimental patterns made up of combinations of the six colours and seven solids. A standard model simulating the room without a solid and a comparison model with a solid inside were presented side by side. Figure 1 shows the experimental configuration, and figure 2 shows seven comparison models, each with a solid inside, and the dimension of the solids.

The subjects consisted of 17 females and 3 males from the 20–26 years age group. The subjects had no colour-vision deficiencies. The experimental patterns were randomly presented to each subject. The magnitude estimation method was applied to evaluate the apparent volume of the room. The 20 subjects were asked to look inside each model through a viewing aperture in the rear wall and to report what they perceived to be the volume of the comparison model relative to that of the standard model. The volume of the standard model was set to a reference value of 100.
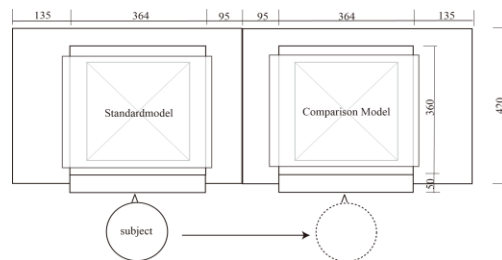


*Figure 1: Experimental configuration.*
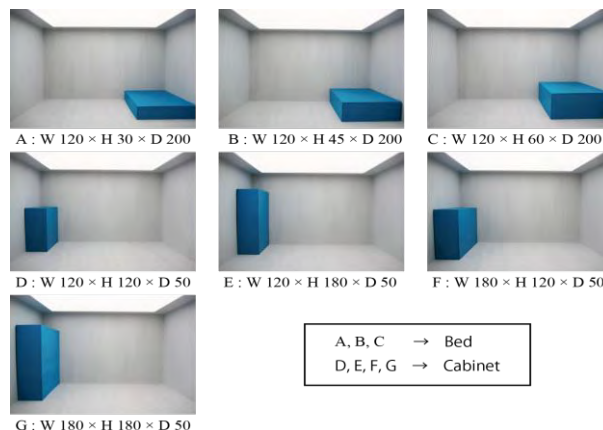


*Figure 2: Comparison models with the solids inside the model and the dimension of the solids.*

## 3. RESULTS AND DISCUSSION

### 3.1 Comparison of rectangular solids

Table 1 shows the "Magnitude average value" or "M value" for each colour and solid combination. Red coloured had the highest average value and blue coloured had the lowest average value for each solid. The white solids had the highest M values for all solids. The black, red, and brown solids had the lowest M values. The white solid brightness was N9.5, and the brightness of the scale model wall was N8. The white solid brightness was closer to the wall brightness than the brightness of any other colour, and therefore, the white solids emphasised the unity between the scaled model interior and the solid more than the other solids. This is believed to be the reason that the white solids had the highest M values. The advancing–receding phenomenon of the red and blue colours was also observed. However, some of the brown solids had M values that were not lower than the blue solids. The reason for this is that, although brown is an advancing colour like red,

brown suggests the idea of wooden furniture. Thus, the brown solids rarely produced a feeling of strangeness and were less noticeable than the red solids.

*Table 1. Magnitude average values by Solid colour and Comparison model.*

| | | Comparison model | | | | | | |
|---|---|---|---|---|---|---|---|---|
| | | A | B | C | D | E | F | G |
| Solid colour | Red | 91.57 | 86.08 | 75.68 | 91.93 | 88.6 | 87.52 | 80.98 |
| | Brown | 92.54 | 88.2 | 79.19 | 94.66 | 85.1 | 88.87 | 82.01 |
| | Blue | 96.05 | 87.85 | 78.61 | 93.19 | 92.1 | 93.19 | 83.52 |
| | Black | 94.28 | 84.3 | 78.11 | 91.13 | 88.45 | 87.27 | 80.05 |
| | Grey | 95.63 | 90.16 | 83.27 | 97.38 | 93.31 | 91.15 | 84.99 |
| | White | 101.73 | 95.04 | 83.78 | 99.66 | 95.95 | 97.3 | 93.76 |

| | Maximum value | | Minimum value |
|---|---|---|---|

## 3.2 Differences in apparent volume with differences in height

As for the solids used to simulate beds, the taller solids of all colours, the apparent volume of interior space becomes more cramped. The differences in the M values of the different colours were not significant, however, the black solids made the interior space appear more cramped than the white solids, even though the solids were 45-cm high. The results suggest that it is important to pay attention to the balance of height and colour when choosing a bed.

As for the solids used to simulate cabinets, two comparisons of the differences in apparent volume were made to assess the effect of differences in cabinet height for the same width. The results are shown in Figure 3. T-tests were conducted to clarify the relationship between the apparent volume and the colour. In the case of solids D and E, the brown and grey colours had statistically significant effects (level of significance 0.05) on the apparent volume. In the case of solids F and G, all colours except white had statistically significant effects. The wider the width of the solid, the apparent volume of interior space becomes more cramped by a solid of greater height. This means that the interior space appeared more cramped with solids of greater volume, even for the same change in height. With the white solids, however, the apparent volume of the interior space was largely unaltered by changes in the solids' heights, regardless of their width and volume, and the differences were not statistically significant.

## 3.3 Differences in apparent volume with differences in width

As for the solids used to simulate cabinets, two comparisons of the differences in apparent volume were made to assess the effect of differences in cabinet width for the same height. The results are shown in Figure 4. The t-test results showed that, in the case of solids D and F, the red, brown, and grey colours had statistically significant effects on the apparent volume. In case of solids E and G, the red, blue, black, and grey colours had statistically significant effects. However, the white did not have a statistically significant effect in any case. As with the differences in apparent volume with differences in height, for all of the solids except the white solids, the taller the solid was, the apparent volume of interior space becomes more cramped by a solid of greater width. With the white solids, however, the apparent volume of the interior space was largely unaltered by changes in the solids' heights, regardless of their width and volume. These results indicate that the greater the volume of a solid, the apparent volume of interior space becomes more cramped by increases in solid height or width. On the other hand, the white solids hardly made the interior space appear cramped at all, regardless of differences in height or width.
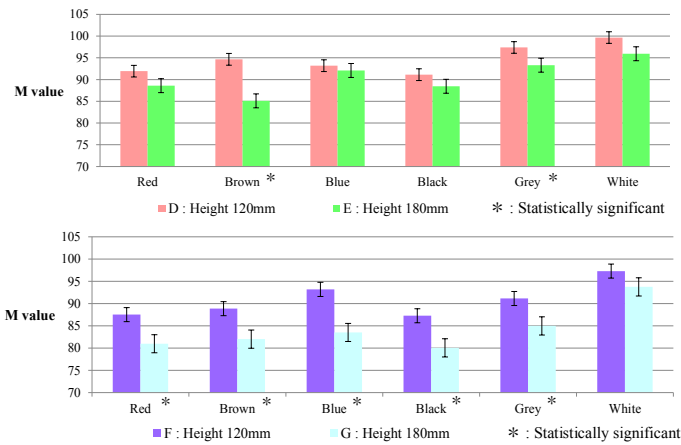
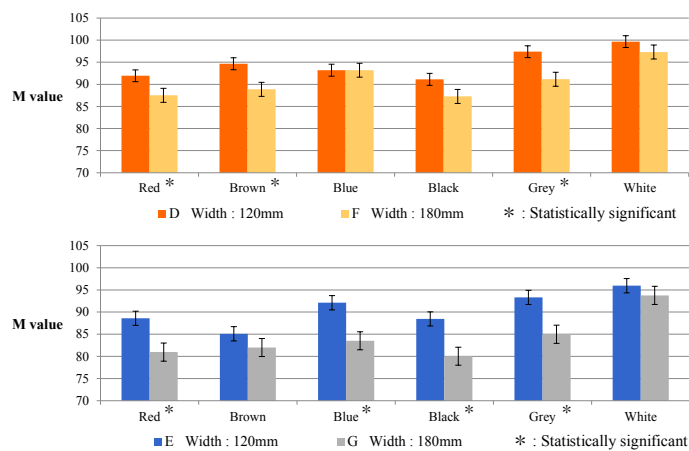*Figure 3: Differences in apparent volume with differences in height.*



*Figure 4: Differences in apparent volume with differences in width.*
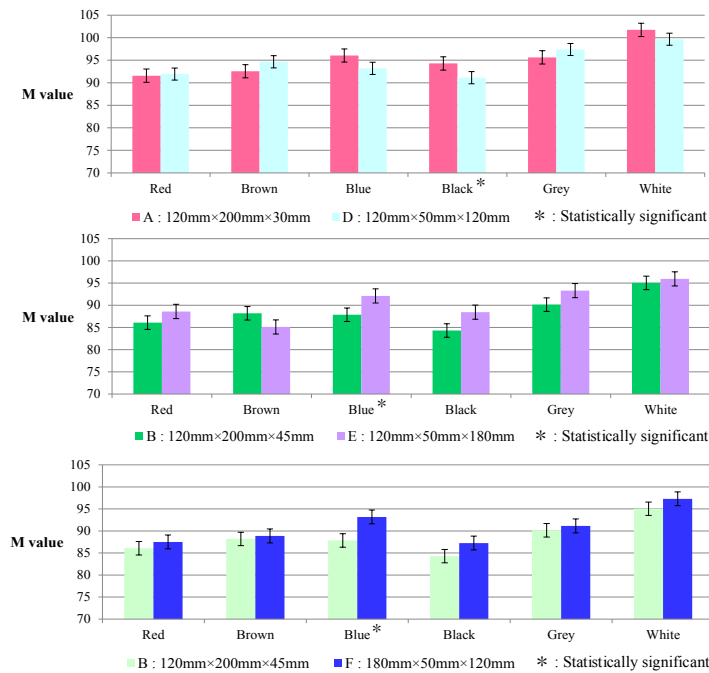


*Figure 5: Differences in apparent volume for horizontal and vertical solids
of the same volume.*

### 3.4 Differences in apparent volume for each solid volume

T-tests were conducted to clarify the relationship between the apparent volume of the interior space and the position (horizontal or vertical) of a solid of given volume in the space. In this study, the solids used to simulate beds (A, B, and C) were placed horizontally and the solids used to simulate cabinets (D, E, F, and G) were placed vertically. The results are shown in Figure 5. In the case of solids A and D, although black was statistically significant, the differences in apparent volume were small on the whole. It can be concluded that there were no differences between the horizontal solid (A) and the vertical solid (D). In the cases of B and E, and B and F, although the blue was statistically significant, the vertical solids had a tendency to make the apparent volume of interior space becomes more spacious than the horizontal solids of all colours. These results indicate that greater volumes of vertical solids tended to make the apparent volume of interior space become more spacious than greater volumes of the horizontal solids.

## 4. CONCLUSIONS

This study was conducted to evaluate the effects of furniture colour on the apparent volume of the interior space of a house. The results can be summarized as follows.

1) It was found that the white solids make interior spaces appear more spacious than any other colors. Black, red and brown solids made the interior space appear cramped.

2) As for the solids used to simulate beds, the taller the solid was, the apparent volume of the interior space becomes more cramped.

3) As for the solids used to simulate cabinets, all solids except the white solids made the interior space appear cramped, and increasingly so with increasing volume, whereas the white solids hardly made interior space appear cramped, regardless of their volumes.

4) In case of the solids having the same volume, interior space placed the solids used to simulate beds appeared more cramped than those placed the solids used to simulate cabinets.

## REFERENCES

Sato, M., 2013. *Effects of accent colour on apparent distance to a front wall and apparent volume of an interior space*, Proceedings of AIC Color' 13, Vol. 2, 555-558

Sawa, Y. 2000. *Color of various upholsteries and their desirable color coordination,* Bull. Mukogawa Women's Univ. Nat. Sci., 48, 9-17

*Address: Prof. Masato SATO, Division of Environmental Sciences,*
*Kyoto Prefectural University, 1-5 Hangi-cho, Shimogamo,*
*Sakyo-ku, Kyoto 606-8522, JAPAN*
*E-mail: ma_sato@kpu.ac.jp*

# Ideal GRID Model for Color Planning of Living Space

Tien-Rein Lee

Department of Information Communications

Chinese Culture University

## PREFACE

Color plays a key role in shaping human environments: the visual sense is an important part of human perception; it corresponds to the way people create, design and communicate their living spaces. In many cultures around the globe, different cultural traditions have made use of color for product applications of all parts of daily life, and matters of communication. Color has sometimes been described as a matter of individual perception and personal views, but this research claims to consequentially make use of color characteristics in the process of urban design and city planning. It suggests a layout for city color planning based on an overall Grid Model that uses hue, saturation and values to arrange spatial elements in a systematic way, while integrating historical and culture specific features. It also refers to three different modes of color arrangement: The Color Order System, the Chinese Five-Elements Theory, and the rainbow colors. It is assumed that color arrangements based on a grid model can be applied on micro, medium and macro levels; expanding from personal living sphere to public space, and towards a mega-level setting. While each level is marked by different characteristics, such as functional, aesthetic and symbolic meaning, a grid-based color order planning can be adjusted not just to the different levels of urban spaces, but contribute to communicating a city's color identity.

## 1. INTRODUCTION

Grid systems have been included in the methods of urban design and city planning for a long time: The old city of Chang'an (which has been called Xi'an since the Ming dynasty), in the south-western part of China (today's Sichuan province), allows insight into methods of urban design from its early beginnings. While its origins go back as far as to Neolithic times, during the Tang Dynasty (618—907), Chang'an was regarded as one of the largest cities in the world, much like Constantinople (Istanbul) and Baghdad. The structure of this early modern metropolis followed a grid pattern of 108 quarters and two large marketplaces in its eastern and western parts. This kind of model layout followed functionality regarding the placement of the Imperial Palace and its immediate administrative and urban environment; and it has served as a prototype in the city planning of several other Asian capitals, evident in the city structure of Kyoto (Japan). Looking at modern day's New York City, the island of Manhattan is called
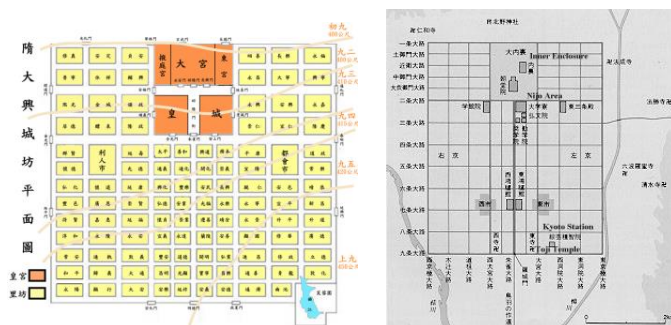


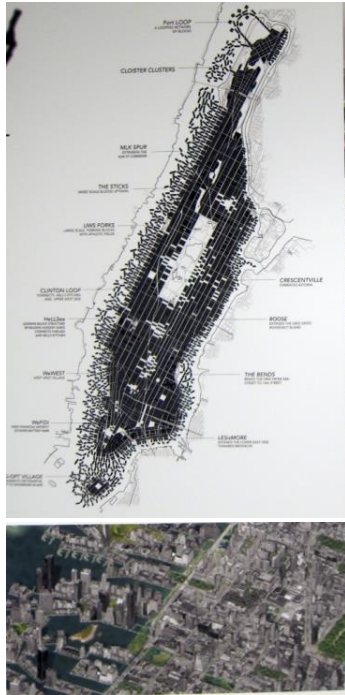*Figure 1: Grid city structures of Chang'an and Kyoto*

Figure 2: "Greatest Grid" –
urban structure of Manhattan,
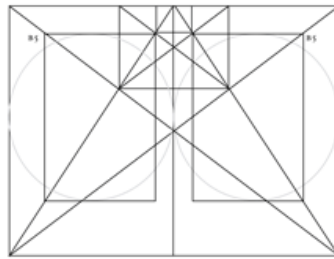New York City, U.S.A.



Figure 3: 9-parts shaped
grid by Van de Graaf
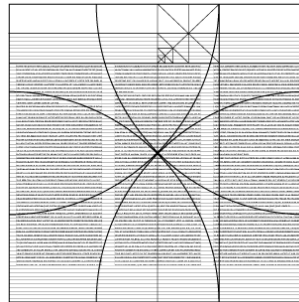


Figure 4: Grid system
applied for ancient scrolls
typography

the "Greatest Grid": Since its planning had started in 1811, these grid lines have resembled the social, architectural, financial and emotional veins of New York's urban life. In fact, grids have been applied in city planning throughout the United States (Knight, Nairn, 2013). Grid systems also play an important role in modern graphic design. A page can be divided into nine parts with the help of double diagonals and a guideline (Van de Graaf, 1946). The method results in margins with ratios of 2:3:4:6, where the original area has the ratio 2:3. In his works on typography, Tschichold appreciated this method and made it popular in his writings on the proportions and forms of books (Tschichold, 1955, 1975). Rosarivo shows how many of the classic books were designed via a module he calls MODULE 1.5.

(Rosarivo, 1948). In fact, Christian monks made use of measurements divisible by three to create books that were holy according to the Christian faith, reminding of the holy trinity, while 2000 years old scrolls have been found using 8 mm line spacing: the method of dividing something in eight parts (triangulation) was known at that time, and the number eight is a holy number within Judaism (Gärde, 2007). Modern computer graphics allow to make use of grid systems for all kinds of layouts. Grid system functions include orientation, and in a neutral, mathematical sense, they are essential in building structures for human living spheres, regardless of culturally or geographically influential factors. The grid provides a useful, efficient tool that can be applied under a variety of different conditions, for achieving clearly defined purposes of city planning in all parts of the world. But can it be utilized for color planning? How to develop a standard model of color planning based on a grid system, applicable for small scale to large scale urban space?

## 2. GRID SYSTEMS AND COLOR ARRANGEMENT

City color planning is concerned with color selection for human living spheres. But how to find the most satisfying solution for a settlement? Color order systems have been developed after the natural color spectrum, or based on the measurements of human subjects' visual responses to color. Different color order systems have been suggested by scientists throughout the centuries, with the color space of the Munsell color system specifying colors based on the three color dimensions hue, value (lightness), and chroma (color purity) being one of the most prevailing ones. Color order systems arrange color nuances based on different approaches: The Opponent Theory puts Red and Green as opposed at 180 degrees on two edges of its circle, and Blue and Yellow on the other;

while the rainbow colors follow a color order as it can be watched in the natural phenomenon. Color planning can make use of the directional functions of a grid, and add a color-coded order. Color order systems can be applied for city color planning and urban design projects by differentiating city center and districts, integrating neighborhoods and landmarks, and emphasizing directions and traffic guidance systems. A previous proposal of an urban color system for the City of Taipei, Taiwan, has included a district and neighborhood color analysis, and an overall city color layout. Three different modes of color arrangement have been proposed: The traditional Chinese Five Elements Theory, the Opponent Theory, and the rainbow colors. The Chinese Five Elements Theory is closely related to the theory of Wind and Water (Feng Shui), a traditional Chinese pattern of systematically understanding nature and natural events. The Chinese
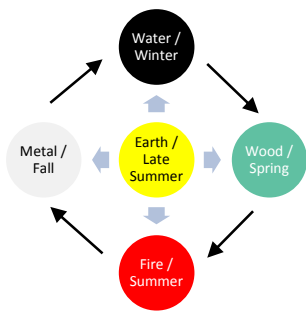
*Fig. 5: The Five Elements in the seasons*
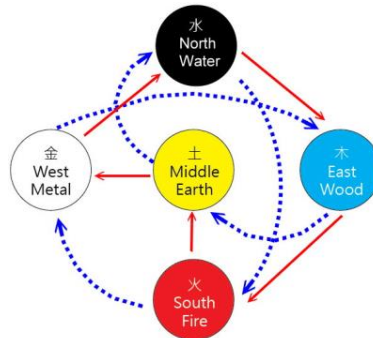
*Fig. 6: The constructive and destructive cycles*

Five Elements Theory associates the natural phenomena Wood (Blue-Green/East), Fire (Red/South), Gold/Metal (White/West), Water (Black/North), and Earth (Yellow/Center) with colors and the cardinal directions of the compass dial. Each element and its color are also associated with a range of other characteristics like taste, smell, shape, and much

more. Read in the clockwise direction, the Theory is applied following the seasonal changes of the year: Spring (Blue-Green), Summer (Red), Late Summer (Yellow), Fall (White), and Winter (Black): this order is understood as the natural "constructive cycle". A second cycle called the "destructive cycle" is defined as controlling and restricting the element considered as opposed to the prevailing one: Wood (Blue-Green/East), controls Earth (Yellow/Center); Fire (Red/South) controls Gold/Metal (White/West); Earth (Yellow/Center) controls Water (Black/North), Gold/Metal (White/West) and controls Wood (Blue-Green/East), and Water (Black/North) controls Fire (Red/South). The system is linked to a person's birthdate, so that recommendations can be given for color decisions contributing to a harmonically balanced life. This color order is very helpful for color decisions made on a personal level (regarding room colors, clothing or things of daily use), but it cannot be generalized and applied to public space. A color concept for a metropolis
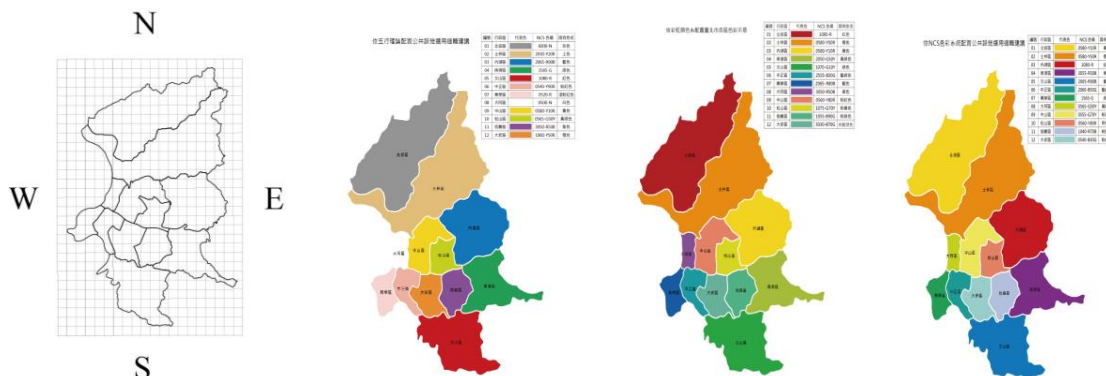
*Figure 7: Used grid system and proposed color order systems in Taipei, Taiwan.*

AIC2015 TOKYO - Color and Image

would have to use a more universally applicable system, adding an aesthetical dimension to function.

### 3. GRID SYSTEM COLOR PLANNING AND CITY IDENTITY

Color planning for public places includes functional, aesthetic and communicative goals: colors can represent city districts in the four cardinal directions, traffic systems may provide orientation by using these colors emphasizing bridges, highways, etc. Aesthetic value can be achieved by varying color shades for houses and landmarks, integrating a districts special highlights and harmonizing the general public appearance of places. The combination of grid systems and color order systems allows gradations and scaling of different sizes and ratios. It can also be adjusted to a city's layout, size, and specific proportional challenges of urban design.



Figure 8: Proposed colored Traffic Guidance System in Taipei, Taiwan.



Figure 9: Proposed colored traffic signs in Taipei, Taiwan.

It is suggested that Grid Color Systems can serve for urban design in different parts of the world, providing colorful layouts that help to identify an ideal color concept for different urban life-styles and traditions.

Cities are determining color identities related to the colors of traditional construction, or based on future-oriented tasks: geographical, climatic, and cultural influences all add individual features to the basic functions of an established common infrastructure, creating a unique appearance of the urban living sphere. These factors can constitute limitations for applying the Color Grid Model, but they can also be solved through it: The scalability and gradation of the Grid System make it a useful tool that can flexibly be adjusted to the local characteristics and circumstances. Furthermore, the flexibility of the Color Grid Model avoids creating indistinguishable neighborhoods and construction that would be leveling a city's special profile. On the contrary: The Color Grid Model can integrate a city's characteristic features and emphasize them as important parts of a city's specific identity. From small scale to medium to large scale dimensions, the Color Grid Model can serve for individual, public, and urban space color solutions.

### 4. CONCLUSION

The grid system is an ideal baseline (blue print) for rational arrangements, through thoughtful plans it matches the characteristics of color order and variations for any rational approach to utilize colors. It can create marginal effects for space planning with different needs. The proposed Grid Model for Color Planning of this research can integrate functions of communal infrastructure and suitable color components for the existing, unique local and traditional, or modern exterior design elements. It can help to develop a coherent color code that translates unique characteristics of a city into a comprehensive city color concept. The suggested Grid Model of Color Planning can be applied in all parts of urban life: starting from small scale color analysis of the neighborhood, regarding wall painting or garden architecture, street lamps and guidance systems; proceeding to medium size color recommendations of urban districts, applying color to district directions,

landmarks, bridges, etc.; towards large scale color applications in the city's total urban space, such as colored subway lines and other transportation systems, public buildings, and so on. This prototype of Grid Model Color Planning can be universally applied but adjusted to the local needs of citizens in every part of the world, by integrating basic requirements of a community, while respecting local or regional peculiarities. As the responsibility for such an important, long-term project must not be left to isolated initiatives, it should involve all public authorities and private parties concerned with the creation and design of urban color spaces: like the government, residents, architects, and others.

## REFERENCES

Gabriel, J. W. (September 1981). Color in Townscape, W. H. Freeman & Co.

Gärde, Marcus (2007) "The Way of Typography" http://www.bachgarde.com/html/works/gridsystem.html.

Glenwood (January 11, 2012). "Museum of the City of New York: the Greatest Grid & the Unfinished Grid." http://www.glenwoodnyc.com/manhattan-living/museum-city-new-york-greatest-grid-unfinished-grid/.

Knight, Paul; Nairn, Daniel(January 1, 2013). "Infographics. "http://www.thegreatamericangrid.com/infographics.

Linton, H. (January 1, 2003). Color in Architecture : Design Methods for Buildings, Interiors, and Urban Spaces, McGraw-Hill Professional Publishing.

Porter, J.-P. L. D. L. T. (2005). Doors Of The World, W. W. Norton & Co Inc.

Porter, J.-P. L. D. L. T. (2005). Windows Of The World, W. W. Norton & Co Inc.

Swirnoff, L. (February 1, 2003). The Color of Cities: An International Perspective, McGraw-Hill Professional Publishing.

Tschichold, Jan, (1955)"The Proportion of the Book (1975,)"The Form of the Book"

Van de Graaf, J. A. (1946): "Nieuwe berekening voor de vormgeving",

*Tien-Rein LEE*
*Address: Dept. of Information Communications, Chinese Culture University*
*No. 55, Hwa-Kang Rd, Shilin, Yang-Ming-Shan, Taipei 11114, Taiwan*
*Email: trlee@faculty.pccu.edu.tw,*

# Case studies of Color Planning for Urban Renewal

Sari YAMAMOTO

Faculty of Art and Design, University of Tsukuba

## ABSTRACT

Environmental color design in Japan, especially façade color, has long been considered a matter of individual choice. The Landscape Act was passed in 2004 by the Ministry of Land, Infrastructure and Transport, the purpose of which was to promote a more aesthetic approach to landscape and streetscapes, and also encourage the development of regional identity. We investigated each of these Landscape Plans, especially regarding the regulation of color, and determined that most towns use the Munsell Color System to manage façade color. 80 % of them use this system. As already mentioned, color regulation is mostly determined through restrictions regarding Chroma, however, this does not necessarily help in developing local features. We researched some unique cases in which color regulation was used in the development of streetscapes. The first case study is Girona in Spain. 30 years ago, old buildings were renovated, and street façades were renewed and colored. The second case study is the University of Tsukuba's color planning for its student accommodation facilities. The third case study is the public sign system in Tsukuba. The fourth case study is our bus color design for the town of Hitachi. Again, it is not façade color planning, but it helped to create a unique local feature for the city through the graphic design for buses and bus stops. With these case studies, I hope to have shown that color is not a minor issue and can be a useful tool in urban renewal and in creating a positive and life-affirming environment.

## 1. Background- the current status of local ordinance

Generally speaking, environmental color design in Japan, especially façade color, has long been considered a matter of individual choice. Consequently there has been little thought of coordinating façade color at a civic level. Because of this, the Landscape Act was passed in 2004 by the Ministry of Land, Infrastructure and Transport, the purpose of which was to promote a more aesthetic approach to landscape and streetscapes, and also encourage the development of regional identity. This legislation has only been partially successful.

As of January 2013 there were 568 landscape administrative organizations in Japan. "Landscape administrative organization" meaning a town or city council body tasked with managing the local landscape. Within these 568 organizations, only 384 towns have developed a "Landscape Plan" in accordance with national legislation.

We investigated each of these Landscape Plans, especially regarding the regulation of color, and determined that most towns use the Munsell Color System to manage façade color. 80 % of them use this system, with, for example, a directive like,

"within Chroma 6 in case of Hue R". In other cases recommendations are based on color palette.

Restrictions regarding color only seem to be in effect for historical towns and cities, but not for unique landscape. It may be very useful for council administrators who are not confident making aesthetic decisions. However, the current legislation can be misinterpreted to allow any color to be used within the limitations, and to organize these limitations on the basis of Chroma may be detrimental to developing design sense, and spoil the overall color harmony of a particular area.

A survey was conducted using questionnaires in each of the 384 towns in 2013/2014. We asked whether local features were thought to be enhanced by the Landscape Plan. Less than 40% answered "Yes" and 60% answered "No" or "Undecided". People were also asked to rank which points they thought were effective in developing features of the local area in the Landscape Plan. Among these points were building color, height, shape and location. The responses are shown in Table 1. Color ranked highest, indicating that local government consider color to play a crucial role in making the most of their local features.

*Table 1: Average Rank*
*(Which point is effective in developing features of the local area ?)*

| Point | Average Rank |
|---|---|
| Building Color | 1.8 |
| Building Height | 3.3 |
| Building Shape | 3.6 |
| Building Material | 4.2 |
| Outdoor advertisement | 4.6 |
| Building layout | 4.8 |
| Building greening | 4.9 |
| Others | 7.8 |

As already mentioned, color regulation is mostly determined through restrictions regarding Chroma, however, this does not necessarily help in developing local features. We researched some unique cases in which color regulation was used in the development of streetscapes.

## 2. Case study 1

The first case study is Girona in Spain. 30 years ago, old buildings were renovated, and street façades were renewed and colored. The architect, Josep Fuses Comalada, planned the color scheme, which originated from the façade colors of the old city. In general, it was usual for local governments to use white, or off-white, when repainting or coloring buildings because it is cheap. However in this case they did not do so, and used a variety of colors which would have been found in the old city, such as 'almagro', traditionally considered the color of cow's blood, 'ochre' and 'sienna-red ochre'. Figure 2 is a diagram of the color design, showing the sophistication of the color production; although not so many colors are used, there is nevertheless an impression of great

AIC2015 TOKYO - Color and Image

variety. Nowadays, there are many visitors to see the colorful streetscape of Girona. Thanks to this success, similar color planning is being applied to areas of redevelopment on the other side of the river. In Comalada's project, chemical paints were used due to cost restrictions, however, the new development uses natural paints. This is a very successful instance of urban renovation integrating streetscape color design.



*Figure 1: Girona in Spain*          *Figure 2: Diagram of the color design*

### 3. Case study 2

The second case study is the University of Tsukuba's color planning for its student accommodation facilities. The planning for this took several years. As with Girona, buildings were renovated, and at the same time, their façades were given a different color. Approximately 30 years have passed since the dormitories were built and the plumbing systems were out of date; renovation was needed. At first, it was planned that only the plumbing should be overhauled, however the university decided to recolor the façades at the same time to highlight to students the renovation of their accommodation. We have renovated approximately 5 buildings per year since 2009; there are a lot of student dormitories on our campus and it is impossible to renovate all the buildings at the same time.

Before renovation, the façades were beige or off-white. Although different colors were used to complement the concavo-convex shape of buildings or other façade features, the overall color harmony of each area was also considered. High Chroma colors were used, however these were carefully coordinated; for example, similar high Chroma colors are used for accents on adjacent buildings to give a sense of rhythm. In some cases these accent colors are designed to appear as gradation from certain angles. Mainly warm colors were used, to foster a positive and pleasant atmosphere.

The response from students is that the colored façades are cheerful and make the dormitories more appealing as habitats. This case study is a good indication of the importance of color and is informative for other renovation projects, as there are many buildings of this kind, that date back to 30 or 40 years ago.

*Figure 3: Color design for Students Accomodation in the University of Tsukuba*

## 4. Case study 3

The third case study is the public sign system in Tsukuba. This is not façade color planning as such, but sign design, which I think can also play an important role in creating unique character in an urban environment. We planned and designed a sign system for Tsukuba from 2005 to 2009, including the creation of sign guidelines, and 30 of these signs can be seen around the exits of the train station in the town center. We thought very deeply about the background color of the sign and decided on dark gray, after creating mock-ups for a field survey, so that the sign and its environment are harmonized. On the other hand, signs need to stand out, and we therefore included "art-posts" with the signs. These were made with natural materials such as stone and wood. These "art-posts" on the side of the signs, and monochrome photos on the reverse side of the signs have contributed positively to the town's environment and also give each sign a unique character. This sign system has been influential for other towns in Japan, and received an award from the Japanese Society for the Science of Design in 2009.



*Figure 4: Sign Design for Tsukuba City*

## 5. Case study 4

The fourth case study is our bus color design for the town of Hitachi. Again, it is not façade color planning, but it helped to create a unique local feature for the city through the graphic design for buses and bus stops.

Because of a decline in passenger numbers, many railway branch lines have fallen into disuse, and the routes have come to be served by bus lines. However, buses are often less punctual than trains and therefore have trouble retaining their customer base. For this reason, the government is promoting the BRT, or Bus Rapid Transit scheme, which repurposes unused railway lines as bus routes that cannot be used by other road vehicles.

In Hitachi, the railway branch line closed in 2005. Following this, the city council, in conjunction with residents who live near the old line, developed a BRT and solicited bids for the branding and graphic design. We revised the winning designs for practical application to the BRT, including the bus stops and other graphics. The concepts behind our design were:
1. To spread awareness of the BRT among Hitachi residents
2. To create a clear color scheme based on the winning design
3.To unify the graphics through the use of repeated design elements, such as color and shape
4. To respect local motifs in order to make citizens to have their attachments to our design and BRT.

The results were as follows:
1. A large BRT logo on the side and rear of the buses.
2. The use of a high chroma blue and simplified graphic design.
3. The creation of a Hitachi BRT logo, repeated on buses, bus stop signs and other PR merchandise.
4. The creation of different bus stop designs using elements that reference local culture in the immediate area.

The design has been well received by local residents, and the number of passengers has increased, making the business more profitable. This case shows that high quality design and color planning can strengthen a local population's relationship with their town and their environment, and can be a sound financial investment.



*Figure 5: Color Design for Hitachi City Bus*

## 6. Conclusion

The government has yet to devote serious attention to how color can be used in urban design, and there is a misapprehension that using more color is good, when in fact it leads to a lack of harmony. With these case studies, I hope to have shown that color is not a minor issue and can be a useful tool in urban renewal and in creating a positive and life-affirming environment. We hope that the power of the color will be used more in the process of making cities unique and beautiful.

## References

Yamamoto Sari, Seo Minjung, Maki Kiwamu and Kumazawa Takayuki, *Local Government Policy of Landscape Planning for Local Features*, Summaries of technical papers of annual meeting, Architectural Institute of Japan, E-1, pp.517-520, 2014

Seo Minjung, Yamamoto Sari, *Relationship between Color Design Standard and Local Features in Local Government Policies and Environmental Planning,* Proceeding of the Annual Conference, Japanese Society for the Science of Design, 61(61), pp.266-277, 2014

Yamamoto Sari*, Environmental Color planning in Girona, Spain,* Summaries of technical papers of annual meeting, Architectural Institute of Japan, E-1, pp.513-514, 2013

Yamamoto Sari, *A Case study of Environmental Color and Sign for Sightseeing*, Journal of Tourism Sciences, 5, pp.31-34, 2013

Sari Yamamoto, Minjung Seo, Mao Kudo and Mitsuo Seki, *Design for the Bus Rapid Transit in Hitachi City,* Proceeding of the Annual Conference, Japanese Society for the Science of Design, 60(60), pp.186-187, 2013

Nishikawa Kiyoshi and Yamamoto Sari, *Public Sign for Tsukuba City,* Annual Design Review of Japanese Society for the Science of Design, *14*(14), pp.26-31, 2009

*Address: Dr. Sari YAMAMOTO, Faculty of Art and Design, University of Tsukuba,*
*1-1-1 Tennodai, Tsukuba, Ibaraki, 305-8574, Japan*
*E-mail: y-sari@geijutsu.tsukuba.ac.jp*

# Building Colours in Taipei – Taking Wanhua District as an Example

Chia-Chi CHANG[1], Ting-Tsung HO,[2] Li-Chen OU,[1]

[1] Graduate Institute of Applied Science and Technology, National Taiwan University of Science and Technology, Taiwan

[2] Graduate Institute of Color and Illumination Technology, National Taiwan University of Science and Technology, Taiwan

## ABSTRACT

The study aims to investigate building colours in the Wanhau district of Taipei. Aims of this study include (a) to create a palette of building colours on 6 main roads in Wanhua district, (b) to analyse and improve the colour palette using CIELAB system, and (c) to develop guidelines of urban colour planing for this area. On the 6 main roads, all bulidings were measured colorimetrically, resulting in a total of 421 colours measured. According to the measurement results, most of the colours were warm colours, with high lightness and low chroma. Guidelines of building colours for this area are proposed on the basis of the colour survey results and the recent psychophysical findings of colour harmony. And a psychophysical experiment was carried out to study colours emotion and colour preference for building colours.

## 1. INTRODUCTION

Colours of urban buildings are an essential factor affecting the appearance of a landscape. Urban colours reflect a city's image and characteristics, and are related to the residents' feelings about their living environment. Due to the fast industrial development in cities of Taiwan, in addition to the lack of proper urban planning and the lack of regulations, landscapes in either urban or rural areas have become less and less attractive. As one of the most important visual factors in an architectural design, colour can easily change the impression of a landscape. Unfortunately, there has not been an urban colour system developed specifically for Taipei City using modern technologies of the CIE (International Commission of Illumination). To address the issue, this study investigated the building colour usage in Wanhua District. There are a number of historical, old buildings in Wanhua District, providing valuable cues or tendency in urban colour usage in this area.

## 2. METHODS

The present research adopted the colour matching methods developed by Lenclos (2004) for survey of building colours in Wanhua district. The NCS 1950 Index, a standard fandeck of the Natural Colour System, together with the NCS Colour Scan, a portable colour measuring device for collecting NCS values, were used during the colour survey.

Six main roads of the Wanhua District, including Zhonghua Road, Kangding Road, Wanda Road, Guilin Road, Bangka Boulevard and Xizang Road, were surveyed to cover a large range of Wanhua District. The main colour that covers 4/5 exterior surface of each

building was measured using the NCS fandeck and the NCS Colour Scan. The NCS data collected during the colour survey were converted into CIELAB values for data analysis.

In addition, in order to study perceived colour emotion of building colours for Wanhua District, this study also conducted psychophysical experiments on three main roads of this area, including Guilin Road, Zhonghua Road and Kunming Road. A total of 62 buildings were evaluated. A total of 30 observers, including 15 males and 15 females, assessed 5 colour-emotion scales: warm-cool, heavy-light, active-passive, harmony-disharmony and like-dislike. The categorical judgment method was used for data collection and analysis.

## 3. RESULTS

A total of 421 buildings were measured in colorimetric terms. As a result, most of the colours were found to have hue angles between 30 and 120 degrees, with lightness ranging between 30 and 94 (see Figure 1a) and chroma lower than 50 (see Figure 1b). Only a few colours were found to have chroma values higher than 50 for colours in the hue region from 30 to 120 degrees. In addition, the buildings in the north part of Wanhua District were found to appear darker than those located in the south of the area, suggesting a tendency related to the historical background of the region



(a)                                        (b)
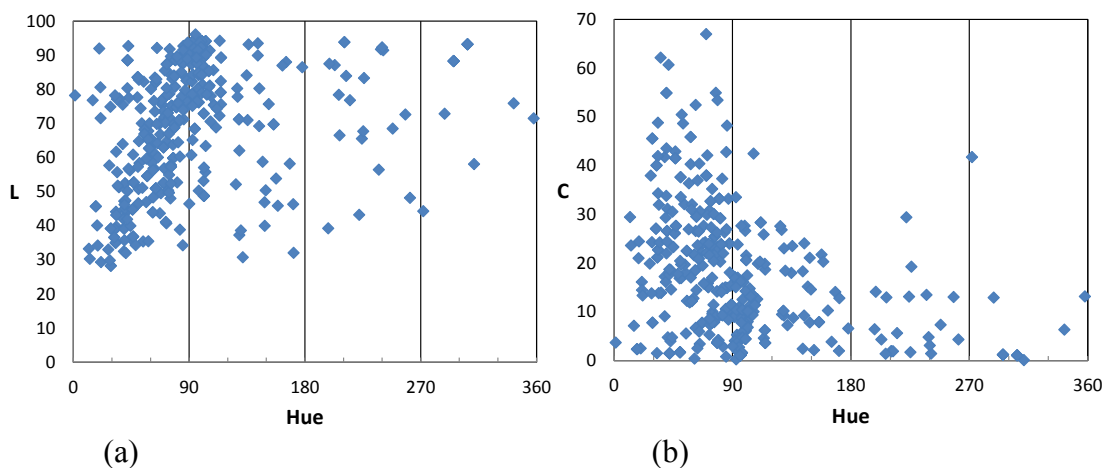
*Figure 1. Distribution of measured colours for 421 bulidings in (a) the lightness-hue diagram and (b) the chroma-hue diagram*

According to the results, most of the measured colours had a lightness ranging from 80 to 90, accounting for 24% of all colours measured, followed by the range 70 to 80 (19%), 90 to 100 (15%) and 60 to 70 (12%), as shown in Table 1 (a), suggesting that most of the building colours were light colours. In terms of chroma, most of the colours were in the range 0 to 10 (40%), followed by the range 10 to 20 (24%) and 20 to 30 (23%), as Table 1 (b) shows. This suggests that most of the colours were low-chroma colours. For hue, as Table 1 (c) demonstrates, it is clear that most of the colours were in the range 0 to 90 degrees, accounting for 56% of all colours measured, suggesting that most of the colours were warm colours.

*Table 1. Distribution of measured colours in terms of (a) lightness, (b) chroma and (c) hue*

(a)

| Lightness range | 20-30 | 30-40 | 40-50 | 50-60 | 60-70 | 70-80 | 80-90 | 90-100 |
|---|---|---|---|---|---|---|---|---|
| Percentage | 1% | 8% | 9% | 12% | 12% | 19% | 24% | 15% |

(b)

| Chroma range | 0-10 | 10-20 | 20-30 | 30-40 | 40-50 | 50-60 | 60-70 |
|---|---|---|---|---|---|---|---|
| Percentage | 40% | 24% | 23% | 6% | 5% | 1% | 1% |

(c)

| Hue range (in degree) | 0-90 | 90-180 | 180-270 | 270-360 |
|---|---|---|---|---|
| Percentage | 56% | 36% | 6% | 3% |

One of the aims of this study was to improve the colour palette according to recent psychophysical findings of colour harmony (e.g. Ou and Luo, 2006; Szabó et al., 2010). Based on these findings, a number of common principles of colour harmony have been identified:

- Equal-hue and equal-chroma. Any two colours varying only in lightness tend to appear harmonious when combined together.
- High lightness. The higher the lightness score of each constituent colour in a colour pair, the more likely it is that they will appear harmonious.
- Unequal lightness scores. Small lightness variations (i.e., less than around 15 units of CIELAB colour difference) between the constituent colours in a colour pair may reduce the harmony of that pair.

According to these principles, it is more likely to create colour harmony if the lightness of each constituent colour is enhanced (i.e. the "high lightness" principle) and chroma being reduced (the "equal chroma" principle). As Table 1 indicates, 91% of the measured colours had lightness values higher than 40. Thus, the *recommended* building colours should have lightness values higher than 40, as illustrated by the green lines in Figure 2(a). The lightness range between 30 and 40 is regarded as *tolerable*, as shown by the orange lines in the graph. Those having lightness lower than 30 are *unacceptable*, as illustrated by the red lines.

Regarding the chroma, Table 2 shows that 87% of the colours had chroma values lower than 30. Note, as Table 3 indicates, 92% of the colours had a hue range from 0 to 180 degrees, most of which were in fact in the range from 30 to 120 degrees. Thus, the *recommended* building colours are those having chroma lower than 30 for hue angle ranging from 30 to 120 degrees, or those having chroma lower than 10 for the other hue region, as illustrated by the green lines in Figure 3(b). The chroma range between 30 and 50 for hue angle ranging from 30 to 120 degrees, and chroma range between 10 and 50 for hue angle ranging from 0 to 30 and from 120 to 180 degrees, are regarded as *tolerable*, as illustrated by the orange lines. The rest of the areas shown in the graph are *unacceptable*, as illustrated by the red lines.

AIC2015 TOKYO - Color and Image
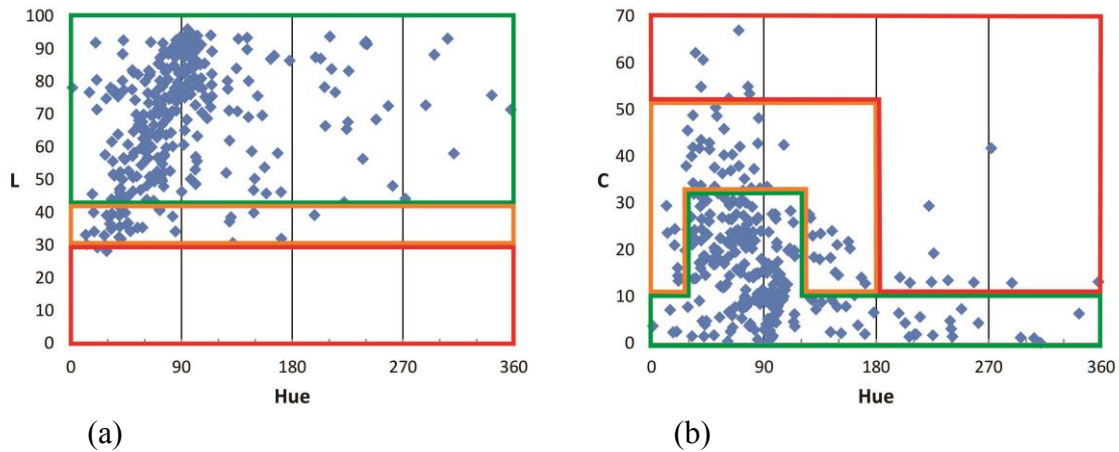
*Figure 2. Proposed guidelines in the form of (a) the lightness-hue diagram and (b) the chroma-hue diagram, where the areas divided by green, orange and red lines represent the recommended, tolerable and unacceptable building colours.*

According to the guidelines of building colour planning as illustrated in Figures 2 (a) and (b), the original palette of building colours were revised. Figures 3 (a) and (b) show the distribution of the two colour palettes, the original in grey and the revised in blue, in the lightness-hue diagram and in the chroma-hue diagram, respectively.

To see how much the revised colour palette has improved compared with the original palette, Ou and Luo's colour harmony model (2006) was used to calculate the predicted colour harmony values, also called the CH values, for both colour palettes. The higher CH value being predicted, the more harmonious the colour combination appears. As Table 2 shows, the CH values are all higher for the revised colour palette than for the original palette, for all of the 6 main roads in Wanhua district. According to the table, for both the original and the revised colour palettes, the CH value is the highest for Xizang Road and the lowest for Kangding Road. This finding is perhaps due to the fact that there were more light colours for buildings on Xizang Road than for the other areas, and that there were more dark colours for buildings on Kangding Road than for the other areas.



*Figure 3. Original colours (in grey) and of the enhanced colours (in blue) distributed in (a) the lightness-hue diagram and (b) the chroma-hue diagram*

AIC2015 TOKYO - Color and Image

*Table 2. CH values for the original and revised colour palettes for buildings on the 6 main roads in Wanhua District*
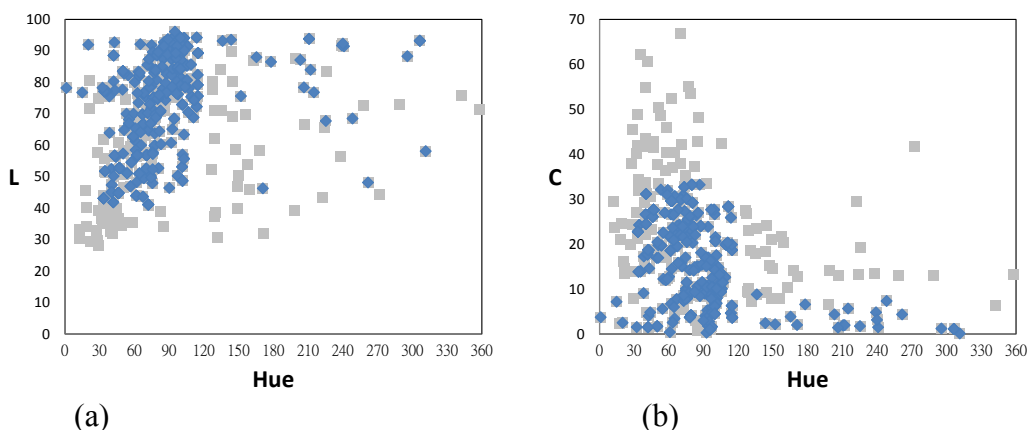
|  | Zhonghua Road | Guilin Road | Xizang Road | Bangka Boulevard | Kangding Road | Wanda Road | All areas |
|---|---|---|---|---|---|---|---|
| Original | 0.66 | 0.58 | 0.74 | 0.37 | 0.22 | 0.62 | 0.53 |
| Revised | 0.80 | 0.72 | 0.89 | 0.53 | 0.35 | 0.73 | 0.66 |

Moreover, 62 buildings of the Wanhua district were visually assessed by 30 observers. Most of the colours were found to have hue angles between 30 and 120 degrees, with lightness ranging between 20 and 95 (see Figure 4a) and chroma lower than 50 (see Figure 4b). The tendency of results is like Figure 1.



(a)                                                    (b)
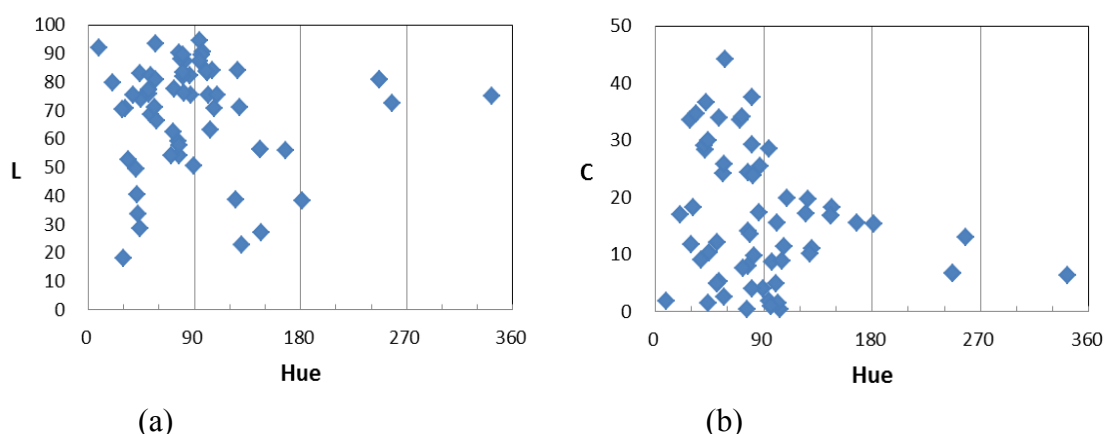
*Figure 4. Distribution of measured colours for the evaluated 62 buildings in (a) the lightness-hue diagram and (b) the chroma-hue diagram*

As Table 3 shows, the average of Like score are all minus in the 3 roads. It indicates that observers didn't like building colours in Wanhua district especially in Guilin Road. Interestingly, Heavy score indicates that observers fell a little heavy. We think probably have relations with some of old and dirty buildings. According to the result of correlation with colour emotions scales in Figures 5. Active and Harmony have high correlation ($R^2>0.7$) with Like. It indicates that building colour are the more active and harmony, the more observers like. We follow the guidelines of building colour planning as illustrated in Figures 2 (a) and (b), to calculate the average of Like scores for "recommended" and "unacceptable" building colours, as shown in Table 4. As a result, the mean "recommended" score is higher than the mean "unacceptable" score.

*Table 3. Average score of 5 colour-emotion scales for building colours on the 3 roads in Wanhua District.*

|  | Like score | Harmony score | Active score | Heavy score | Warm score |
|---|---|---|---|---|---|
| Zhonghua Road | -0.10 | 0.38 | 0.08 | 0.38 | 0.00 |
| Guilin Road | -0.25 | 0.45 | -0.07 | 0.20 | 0.00 |
| Kunming Road | -0.15 | 0.49 | -0.02 | 0.23 | 0.16 |
| All areas | -0.16 | 0.46 | -0.01 | 0.26 | 0.09 |

$y = 0.9947x - 0.1481$
$R^2 = 0.7359$

$y = 1.3375x - 0.7696$
$R^2 = 0.7893$

(a)                                   (b)

*Figure 5. Correlation between perceived colour preference and the other colour emotion scales: (a) active-passive and (b) harmony-disharmony.*

*Table 4.  Average Like scores for "recommended" and "unacceptable" building colours*
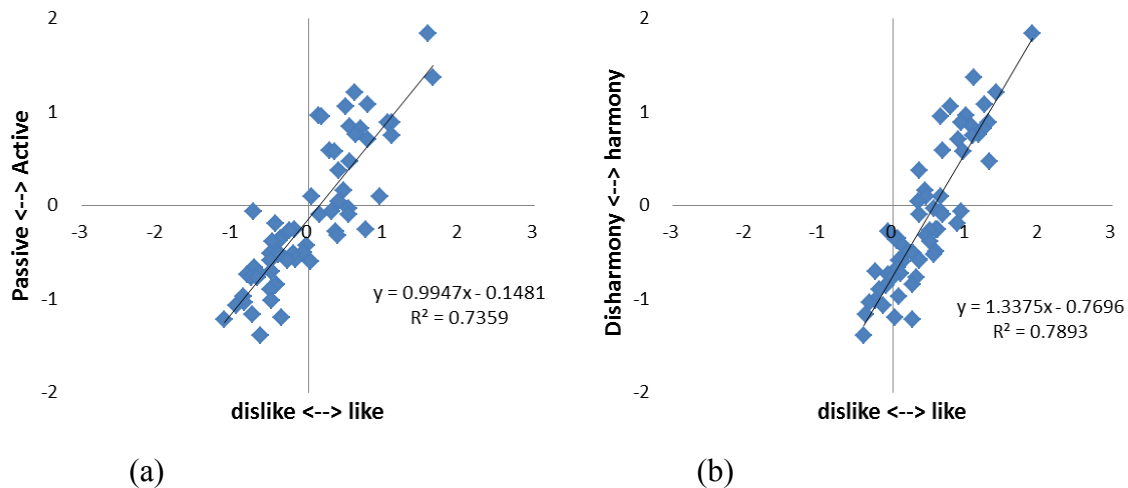
|            | All areas | recommended | unacceptable |
|------------|-----------|-------------|--------------|
| Like score | -0.13     | -0.04       | -0.31        |

## 4. CONCLUSION

This study investigated building colours in Wanhua District. According to the measurement results, most of the colours were warm colours, with high lightness and low chroma. Based on these results, together with recent colour harmony findings (Ou and Luo, 2006; Szabó et al., 2010), guidelines of building colours for Wanhua district is proposed, as illustrated in Figures 2 (a) and (b). And the result of experiment shows better Like scores for buildings using the "recommended" than the "unacceptable" colours. Future studies will focus on how the findings can generalise to other areas.

## AKNOWLEDGEMENTS

## REFERENCES

Ou, L. and Luo, M. R. 2006. A colour harmony model for two-colour combinations. *Color Research and Application* 31: 191-204.

Lenclos J. P. 2004. *Colors of the World – A Geography of Color*. W.W. Norton & Company.

Szabó, F., Bodrogi, P. and Schanda, J. 2010. Experimental modeling of colour harmony. *Color Research and Application* 35: 34-49.

*Address: Chia-Chi Chang, Graduate Institute of Applied Science and Technology,*
*National Taiwan University of Science and Technology*
*43, Section 4, Keelung Road, Taipei, Taiwan*
*E-mails: jackie7089@gmail.com, lichenou@mail.ntust.edu.tw*

# Pritzker Prize Laureates' Colour Preferences

Malvina ARRARTE-GRAU
Architect, Landscape Architect, Colour Designer
ColorARQ Lima-Peru, SG ECD

## ABSTRACT

It is unquestionable that architects dress in black, that their models are usually white and that they manifest an incomprehensible love for concrete.  Consequently, in the website of the Pritzker Architecture Prize, the profession's highest honor since 1979, the work of the laureates stands out for its colourless appearance. The reason why colour is not noticed at first might be because it acts as neutral, blending in with the compositions.

For the purpose of this study it has been important to define *achromatic* and *neutral* in the context of architecture. According to colour theory pure achromatics contain no hue or colour, but near neutrals extend to nuances of low chromaticity, as brown and tans. Applied to buildings, neutrals and near neutrals allow other tones to stand out as chromatic in the composition. Under this principle, it is possible to catalogue neutrals according to the setting.

The object of the study is a sample of projects by the Pritzker Prize winners.  The range of work which composes the portfolio of the elite is vast. The criterion for the selection is oriented towards the colour aspect of the projects.  Initially the source was the '*selected works*' section and '*official website*' of the awardees (if applicable) in the Pritzker Prize website, being later complemented by other internet sources. A general impression led to catalogue the architects according to their preference for colour usage.  Four tendencies were identified: *chromatic*; *near neutrals* for warm nuances of low chromaticity; *achromatics,* including black and gray; and *white*, as a sub-category of the achromatics. Common characteristics amongst the laureates have been pointed out, for a better understanding of their approach to colour.

## 1. INTRODUCTION

In order to find out if the preconception of non-coloured architecture amongst architects is certain, the Pritzker Prize, one of the most important international recognitions in architecture, has been used as an example of the use of colour by a select group of architects.  The Prize was first given in 1979 to Philip Johnson, author of the Glass House. The next year it was granted to Luis Barragan, renowned for his coloured buildings and exterior spaces.  The Pritzker Prize was established by Jay Pritzker and his wife Cindy to encourage and inspire creativity in the profession.  One hundred thousand dollars and a bronze medallion are granted each year by the Pritzker Foundation to honour a living architect who demonstrates talent, vision and commitment, and who has contributed to the world and to humanity through the art of architecture. Until 2014, the laureates total thirty-seven architects from four continents.

Since ancient times stone, earth, wood and vegetable fibres have been the components of buildings and the point of departure of architectural colours.  Nowadays processed construction materials and finishes come in a range of options, from those which resemble the natural to the most sterile and artificial ones. Both natural and processed materials may

serve the purpose of complementing building exteriors, delicately echoing the surroundings, reflecting, blending in, weaving a texture or making contrast. The colours of buildings may be categorized as *chromatic*, *achromatic* or *near neutral*. In theory achromatics contain very little or no chroma. These are reduced to black, white and shades of grey, allowing slight variations in tone. Near neutrals are low in saturation. Within the architectural context these are often related to local materials, climate and geology. The spectrum of near neutral colours varies from very light to dark nuances, including those of soil, mud, brick and stone, wood and rust.

## 2. METHOD

Colour tendencies amongst Pritzker awardees have been analyzed by reviewing the works of each architect, mainly through internet sources: the Pritzker Prize official website, the architects' websites -if applicable-, and complementary information. After the revision, four possibilities have been proposed as tendencies of colour use and labeled with initials: C for chromatic; N for near neutral, which include natural materials of warm hues; A for achromatic, including shades of gray, black and materials such as glass, steel and concrete; and finally, W for white, settled apart as a sub-category of the achromatics.

This study is based on the external aspect of buildings. The range of size and character of the projects by Pritzker laureates implies a degree of complexity in the selection of images. These have been limited to photos which depict the building as an object, showing its shape and finishing materials. A priori the Pritzker website displays a dominance of achromatics and near neutrals. In order to demonstrate this, the criteria for defining the colour tendency of each architect will give priority to colour: the architect will be considered in favour of colour if he uses it recurrently, even if not in the majority of his/her projects.

After reviewing the portfolio and biography of each architect, and defining his/her colour tendency, the information gathered from the websites has been conveniently ordered in Table 1. This has served to visualize common denominators amongst the architects. Additionally, a timeline (Figure 1.) and a map (Figure 2.) in relation to the use of colour have been elaborated. The results are drawn from the graphics and the four tendencies are commented in the discussion.

## 3. RESULTS AND DISCUSSION

The revision of the projects in the '*Selected Works*' section of the Pritzker Prize annual book gives a first impression of the colour tendency of each architect. Though, for a better understanding of the colour preferences of Pritzker architects it has been necessary to complement the data with google searches. Table 1. summarizes biographical information gathered in this process: year and place of birth, education, work, influences, background details and additional abilities.

It is worth mentioning that since the beginning of World War II the United States became home to many European artists and intellectuals who imparted the principles of Modernism in universities. The influence of Le Corbusier, Aalto, Kahn and Mies van der Rohe are a common denominator amongst architects, and the laureates are no exception.

The particular abilities of the architects influence their design approach. For instance, Ando, Zumthor and Wang Shu trained in woodwork and crafts. Painting is a common interest to Johnson, Meier, Hollein, Hadid and Portzamparc. Soto de Moura started to study

scupture. Jean Nouvel is inspired by cinema, as Aldo Rossi was, by theatre. Urban planning is the major of Tange, Maki, Foster, Mayne and Koolhaas. Barragan speaks of aesthetics and spirituality, as Shigueru Ban is moved by humanitarian concern. Others centered in innovative solutions, or in the context.

| AWARD YEAR | AWARDEE | YEAR OF BIRTH | ORIGIN | ARCHITECTURAL EDUCATION | TRAINING AND WORK | INFLUENCES | PERSONAL | OTHER ABILITIES | COLOUR TENDENCY |
|---|---|---|---|---|---|---|---|---|---|
| 1979 | Philip JOHNSON | 1906-1905 | Cleveland, Ohio, U.S.A. | Harvard, Architecture and Master of Architectural History | curator at MOMA, architect at 34 | Le Corbusier, Mies van der Rohe, Minimalism and Pop-Art | | critic, historian, collector of American art | A |
| 1980 | Luis BARRAGAN | 1902-1988 | Guadalajara, MEXICO | Guadalajara School of Engineering | landscape architect | Corbusier, Morocco, Guadalajara School | spiritual values | landscape architect | C |
| 1981 | James STIRLING | 1926-1992 | Glasgow, U.K. | Liverpool School of Architecture | James Gowan (London), Michael Wilford (partner) | late works of Le Corbusier | | | C |
| 1982 | Kevin ROCHE | 1922 | Dublin, Ireland/U.S.A. | Dublin, IIT (Chicago) | Eero Saarinen (Michigan), Dinkeloo (partner) | Mies van der Rohe, Eero Saarinen | | | A |
| 1983 | Ieoh MING PEI | 1917 | Canton, CHINA / U.S.A. | Pennsylvania, MIT, Harvard | U.S. planning, international | Breuer, Gropius | | | A |
| 1984 | Richard MEIER | 1935 | New Jersey, U.S.A. | Cornell University | early practice, residential | Le Corbusier, FLW, Aalto, old european masters | | expressionist painting | W |
| 1985 | Hans HOLLEIN | 1934-2014 | Vienna, AUSTRIA | Academy of Fine Arts, School of Architecture (Vienna) | U.S., Sweden, Vienna | Mies, FLW, Neutra | | artist, furniture and jewellery designer | N |
| 1986 | Gottfried BÖHM | 1929 | Offenbach-am-Main, GERMANY | Technische Hochschule and Academy of Fine Arts (Munich) | Dominicus Böhm, Rudolf Schwartz (Cologne), Cajetan Baumann (New York) | father and grandfather, Mies, Gropius | grandfather and father church designers, wife | N |
| 1987 | Kenzo TANGE | 1913-2005 | Imabari, Shikoku Island, JAPAN | University of Tokyo | Tange Laboratory, reconstuction of Hiroshima, Bologna and Catania | Le Corbusier | | urban planning | A |
| 1998 | Oscar NIEMEYER | 1906-2012 | Rio de Janeiro, BRAZIL | School of Fine Arts of Brazil | Lucio Costa, was appointed to be architect of Brasilia | Lucio Costa, Le Corbubusier | | | W |
| 1988 | Gordon BUNSHAFT | 1909-1990 | Buffalo, N.Y., U.S.A. | MIT | Worked with industrials designers, and for SOM until he became partner | Mies van der Rohe, Le Corbusier. | | | A |
| 1989 | Frank GEHRY | 1929 | Toronto, CANADA | Southern California, Harvard | André Remondet (Paris) | Corbusier, Balthasar Neumann, French Roman churches | | | C |
| 1990 | Aldo ROSSI | 1931-1997 | Milan, ITALY | Milan Polytechnic | editor of Casabella | drama, theatre | | writer, theatre | C |
| 1991 | Robert VENTURI | 1947 | Philadelphia, U.S.A. | Princeton, American Academy in Rome | Eero Saarinen, Louis Kahn, John Rauch (partner), DSB (partner) | Louis Kahn, Le Corbusier, Aalto, barroque, Palladio | Denise Scott Brown (wife and partner) | | C |
| 1992 | Alvaro SIZA | 1933 | near Oporto, PORTUGAL | Escola de Belas Artes (U. of Porto) | early practice | | father architect | | N |
| 1993 | Fumihiko MAKI | 1928 | Tokyo, JAPAN | U. of Tokyo, Cranbrook Academy of Art, Harvard | SOM and Sert Jackson. Founder of Metabolists. | Kenzo Tange, Eliel Saarinen, Post-Bauhaus internationalism, early modern in Japan, FLW | | urban design | A |
| 1994 | Christian DE PORTZAMPARC | 1944 | Casablanca, Morocco /Marseille, FRANCE | École de Beaux Arts (Paris) | New York, team of sociologists | Le Corbusier | | painter | A |
| 1995 | Tadao ANDO | 1941 | Osaka, JAPAN | self-taught (from books, trips and tradition), trained with a joiner | fired from several offices | Corbusier, Mies, Aalto and FLW | | amateur boxer, builder | A |
| 1996 | Rafael MONEO | 1937 | Tudela, SPAIN | Escuela Superior Técnica de Madrid, Spanish school in Rome | Saenz de Olsa, Utzon (Copenhague) | Nordic style, Dutch School | | | N |
| 1997 | Sverre FEHN | 1924 –2009 | Kongsberg, Buskerug, NORWAY | actual Oslo School of Architecture and Design | Jean Prouve (Paris), he met Le Corbusier. | architecture, Aalto, Korsmo, Prouve. | | | N |
| 1998 | Renzo PIANO | 1937 | Genoa, ITALY | Milan Polytechnic | Louis Kahn (Philadelphia), Makowski (London), Rice and Rogers (partners) | Le Corbusier, Prouve, Fuller, Nervi. Italian roots. | family of builders | | C |
| 1999 | Norman FOSTER | 1935 | Manchester, U.K. | University of Manchester, Yale | Buckminster Fuller, Team 4 and Richard Rogers (partners) | Paul Rudolph, Vincent Scully, Serge Chermayev, Eames | | urban planning | C |
| 2000 | Rem KOOLHAAS | 1944 | Indonesia / Rotterdam, NETHERLANDS | Architectural Association, London | founder of OMA (Madelon Vriesendorp, Elia and Zoe Zenghelis) | | father writer, grandfather architect, wife | worked in journalism, writer urbanist | A |
| 2001 | Jacques HERZOG & Pierre DE MEURON | 1950 | Basel, SWITZERLAND | Swiss Federal Institute of Technology (Zurich) | lectured, then opened their practice | Sharoun, Aalto, Rossi. No paradigms. | | | C |
| 2002 | Glenn MURCUTT | 1936 | London/ New Guinea/ Sidney, AUSTRALIA | University of South Wales, Sidney | Ancher, Mortlock, Murray and Wooley (Sidney). Now small practice. | Mies van der Rohe, David Thoureau, Aalto, Barragan, FLW | father interested in architecture | | N |
| 2003 | Jørn UTZON | 1918-2008 | Copenhague, DENMARK | Royal Academy of Fine Arts (Copenhague) | Ahlberg (Sweden), Aalto (Finland) | Aalto, Asplund, Wright. | Cousin sculptor, father naval architect | sailor, training for naval officer | N |
| 2004 | Zaha HADID | 1950 | Bagdad, Iran / London, U.K. | American U. of Beirut (Maths), Architectural Association (London) | Oma with Elia Zhengelis and Rem Koolhaas (she became partner) | Eng. Peter Rice, Niemeyer, Russian Avant-garde | | Artist; interior, furniture, clothing | A |
| 2005 | Thom MAYNE | 1944 | Connecticut, Indiana, California, U.S.A. | Pomona and Southern California, Harvard U. | Victor Gruen. Fired. Founded Morphosis (antini, Stafford, Brickler, Rotondi) and SCI Arc | | | urban planner | A |
| 2006 | Paulo MENDEZ DA ROCHA | 1928 | Vitoria, Espirito Santo, BRASIL | Mackenzie Presbiterian University | early practice, masterpiece Athletic Club of Sao Paulo | Paulist Brutalist avant garde | | urbanist | A |
| 2007 | Richard ROGERS | 1933 | Florence, Milan, London, U.K. | Architectural Association (London), Yale | Ernesto Nathan Rogers (Milan), Team 4 (partner), Renzo Piano | pupil of Rudolph and Stirling. Italy; Frank Lloyd Wright | ex-wife architect Wendy Rogers | cities | C |
| 2008 | Jean NOUVEL | 1945 | Fumel, SWFRANCE | Ecole de Beaux Arts (Paris) ÉÉ | Claude Virilio, Gilbert Lezenes, Jean-Francois Guyot and Pierre Soria | cinema, Virilio | ex-wife filmmaker; actual Swedish | | C |
| 2009 | Peter ZUMTHOR | 1943 | Basel, SWITZERLAND | Pratt Institute (N.Y.), Kunstgewerbeschule | consultant at Canton of Graubürde (monument preservation) | not influenced by global tendencies | | trained as a joiner | N |
| 2010 | Kazuyo SEJIMA & Ryue NISHIZAWA | 1956 1966 | North and South of Tokyo, JAPAN | Japan Women U. / Yokohama U. | Toyo Ito & Associates | Le Corbusier, Mies van der Rohe, Niemeyer, Koolhaas, Ghery, Siza | | | A |
| 2011 | Eduardo SOUTO DE MOURA | 1950 | Porto, PORTUGAL | School of Fine Arts (sculpture), School of Architecture, U. of Porto | Alvaro Siza | Donald Judd, Mies van der Rohe, Siza; collegues: Rossi, Herzog | wife architect | sculptor | N |
| 2012 | Wang SHU | 1963 | Urumqi, Xinjiang, CHINA | Nan Nanjing Institute of Technology | founded Amateur Architecture Studio (Hangzhou) | | wife architect Lu Wenyu | crafts, literature | N |
| 2013 | Toyo ITO | 1941 | Seul / Tokyo, JAPAN | University of Tokyo | Kiyonori Kikutake, founded URBOT, Toyo Ito & Associates | Le Corbusier, Mies van der Rohe, Isozaki, Kikutake, Koolhaas | his father liked to draw plans | | C |
| 2014 | Shigeru BAN | 1957 | Tokyo, JAPAN | Architecture Institute (S. California), Cooper Union | Arata Isozaki, NGO Voluntary Architects Network | Alvar Aalto | | paper architecture | N |

*Table 1.*

Figure 1. The timeline shows the sequence of Pritzker Laureates from 1979 until 2014 and their colour preferences.
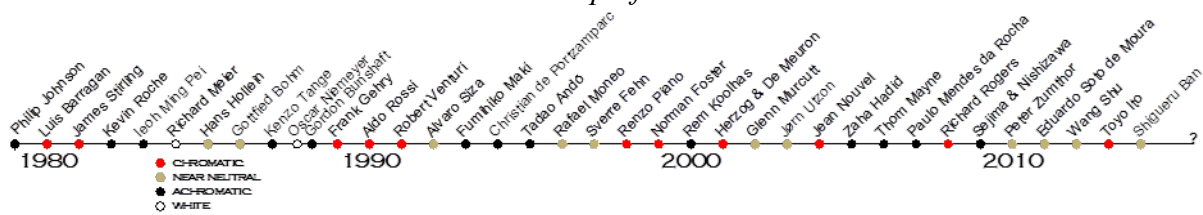
The timeline indicates the tendency of colour use by each architect, suggesting that colour has been in vogue around the 1980, 1990 and 2000. It is evidenced that during the last fifteen years, the architects who represent colour have been less frequent, giving way to more who use achromatics and near neutrals towards 2015. The immediate influence of Pritzker recipients on new generations is undeniable, but the moment of completion of each project determines available materials and technologies, and therefore, design possibilities, so there is an additional component to be considered in the former assumption.

Figure 2. Architects by zone or region
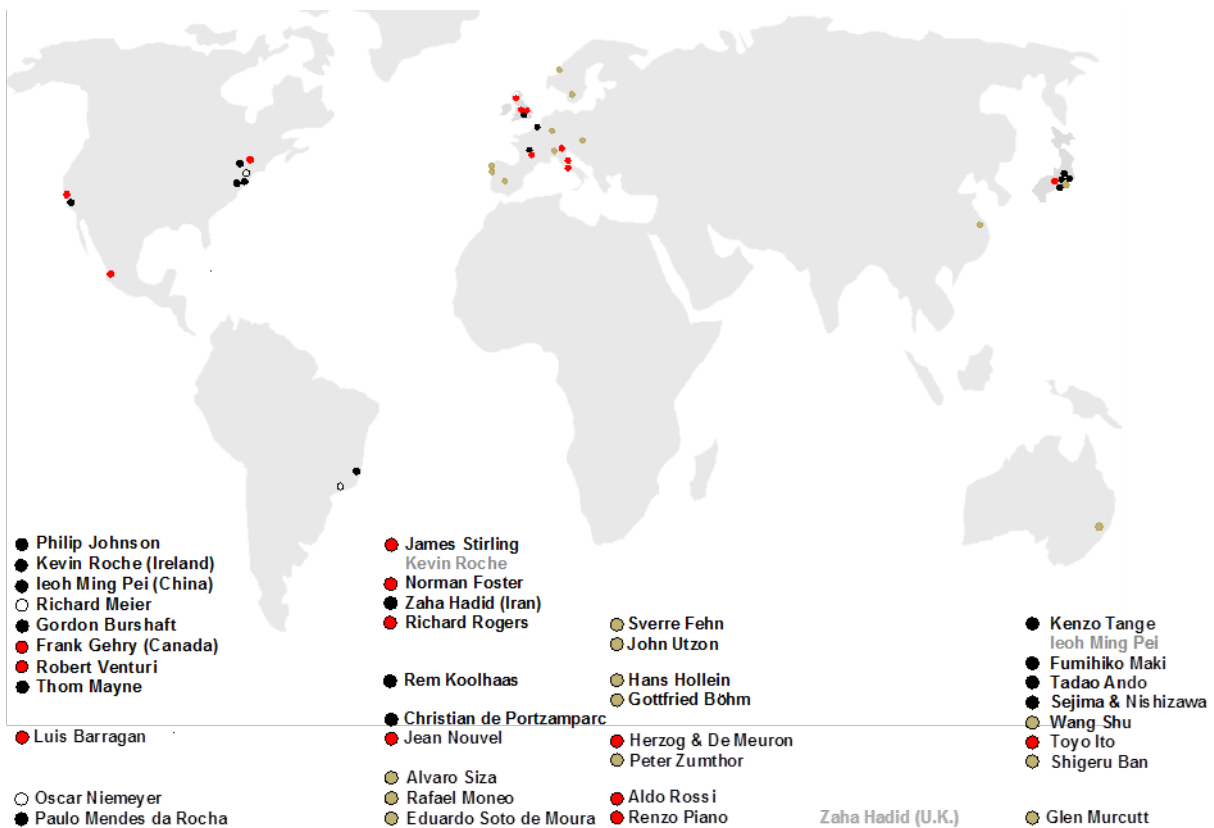


The second illustration (Figure 2.) shows the origin or main place of operation of the architects. It could be inferred that the location of each project directs, in principle, the colour possibilities of its exterior. In order to find common points as regards colour tendeny and location, the sequence of the comments follows the main country or continent from which they work.

The architects from the United States are Philip Johnson, Richard Meier, Gordon Bunshaft, Robert Venturi and Thom Mayne. Ieoh Ming Pei, Kevin Roche and Frank Gehry, who settled in the in the U.S. early in their careers, are also considered in this group. The genuine approaches of Richard Meier, who exclusively uses white, and Robert Venturi,

who publicly rejected black and white in rebelling against radical ideas of modernism, demonstrate contundency as regards colour.  Still, achromatics appear dominant in this region.  Impressive titanium façades by Frank Ghery, have made it difficult to identify him for colour, as he shows versatility in this respect.

Even if colour is part of the Mexican tradition, Luis Barragan has no less merit for being a pioneer of colour in Modern architecture. He uses it artistically in outdoor spaces and interior views in combination with white, to emphasize volume and receding planes.

In Brazil large scale developments by Oscar Niemeyer and brutalist buildings by Edoardo Mendez da Rocha, show scarce colour. Though chromatics as used to point certain elements in Niemeyer's work, it is more of an exception. White plaster and exposed concrete are used in a neutralizing mode, rendering whole buildings, giving way to the overwhelming shapes that characterize the Brazilian urban landscape.

The architects from the Iberian Peninsula Alvaro Siza and Edoardo Soto de Moura, from Portugal, and Rafael Moneo, from Spain, exhibit the use of local stone and white plaster. Rafael Moneo showcases fine projects in brick.  The predominant tendency for these architects is near neutrals.

Jean Nouvel and Christian de Portzamparc, work with avant-garde technology. Both of them employ a variety of surface materials, including plants and coloured lighting.  In the projects by Nouvel, colour is applied in innovative techniques on expressly prepared materials. The buildings by Christian Portzamparc stand out for a sophisticated achromatic appearance, complemented by textures.

The buildings by Rem Koolhaas propose original solutions with unprecedented architectural form, contributing with ideas to the built environment, but he is not fond of colour in the simplistic way, as an element that will transform a building. So far, his work stands out as achromatic.

The British architects James Stirling, Richard Rogers and Norman Foster, have used colour to characterize building parts and enhance structures, making there more human. On the other hand, the inventive use of materials by Zaha Hadid is exclusively achromatic.

From Basel, Herzog & De Meuron and Peter Zumthor, stand out for their fine craft and use of materials. Zumthor employs the textures of natural stone and wood as essential elements in his compositions.  Herzog & De Meuron apply colour in a refined manner accentuating volume and creating fabrics from structure and surface.

Aldo Rossi and Renzo Piano master colour in various ways.  Rossi uses color to emphasize volume and to codify building elements, defining façade proportions. Piano uses diverse materials and technologies, exhibiting concepts with strong colour presence.

Several houses by Glen Murcutt present metal sheets on the façade. In the Australian landscape this follows horizontal patterns perceived in the surroundings and reflect the natural elements. He also uses wood, colour and white, for specific situations, blending in with nature. The proportion of materials sets him in the near neutral tendency.

The fact that in this world selection eight architects are from Eastern Asia (22% of the total, considering that Sejima & Nishizawa work together, and that I.M. Pei settled in the U.S.), and six from Japan, is quite significative. Four of these architects have been awarded the Prize in the last five years, corroborating the consequences of globalization and substantial development in the region. Tradition in the fine craft of materials and a taste for the subtle favours the preference for achromatics and near neutrals in this group.

A selection of architects serves to exemplify each the four colour tendencies. There is a small percentage amongst the thirty-seven Pritzker winners who have been notorious for chromatic designs in the way of Luis Barragan. These are: Aldo Rossi, Herzog&De Meuron, Renzo Piano, Jean Nouvel and Robert Venturi. Colour is also an important element in projects by Norman Foster, Richard Rogers and Toyo Ito. On the other hand Jørn Utzon, Sverre Fehn, Gottfried Böhm, Wang Shu and Shigeru Ban show a marked preference for natural materials. Concrete is a favourite of Tadao Ando, Paulo Mendes da Rocha and Kenzo Tange. The achromatics have inmortalized Philip Johnson and they are main ingredients in the work of insubordinate taste of Zaha Hadid, Thom Mayne and Rem Koolhaas. The architects who rely on white for their buildings are Richard Meier and Oscar Nyemeyer. Apart from them, Alvaro Siza, Fumihiko Maki, I.M. Pei, Sejima&Nishizawa, Toyo Ito, and probably most in this elite, are authors of iconic white buildings.

## 4. CONCLUSIONS

As regards the preference for colourless designs by Pritzker architects, it is confirmed that the scale tilts towards non-colours. Even if 35% of the laureates have used chromatic colour in several projects, their joint portfolios in a span of nearly 66 years show that achromatics and natural materials recurr in their work, while colour is the exception. Although the analysis of the timetable and the world map may have an arbitrary component, history and origin are a way to understanding colour use. Architects from diferent parts of the world show inclination to similar tendencies, and this depends on the moment in time, amongst other factors. Perhaps there is no urge to look for colour as such in coloured buildings. Instead, the subtleties of achromatics and material dimensions are there to be discovered and broaden the palette.

## REFERENCES

Arrarte-Grau M. 2008. On the Bonding of Colour and Architecture: Colouring Modes. Stockholm, Sweden. In *Colour-Effects and Affects, AIC Color 2008, Proceedings*, ed. by I. Kortbawi. Stockholm: Scandinavian Colour Institute.

Koolhaas R. et al. 2001. *Colours: Rem Koolhaas/Oma, Norman Foster, Alessandro Mendini*. Basel, Berlin, Boston: Birkhäuser. 12-13

Office Profiles Architects. *Amateur Architecture Studio*. (Accessed February 27, 2015). http://www.chinese-architects.com/en/amateur.

Richard Meier & Partners Architects LLP. *Richard Meier Partners Architects Splash Comments*. (Accessed February 27, 2015). http://www.richardmeier.com/.

Home | The Pritzker Architecture Prize. *Home | The Pritzker Architecture Prize*. January 1, 2015. (Accessed February 27, 2015.). http://www.pritzkerprize.com/.

Toyo Ito & Associates, Architects. *Toyo Ito & Associates, Architects*. (Accessed February 27, 2015). http://www.toyo-ito.co.jp/.

Color Theory. *Wikipedia*. Wikimedia Foundation, n.d. Web. 27 Feb. 2015. http://en.wikipedia.org/wiki/Color_theory.

*Address: Malvina ARRARTE-GRAU / Parque José de Acosta 226, Apt. 401, San Isidro, Lima 27, PERU*
*E-mail: colorarq@gmail.com*

AIC2015 TOKYO - Color and Image

# Computing Tristimulus Values: An Old Problem for a New Generation

Zhifeng Wang,[1] Tianyi Li,[1] M Ronnier Luo,[2] Manuel Melgosa,[3] Michael Pointer,[2] Changjun Li [1]

[1] School of Electronics and Information Engineering, University of Colour and Technology Liaoning, China
[2] School of Design, University of Leeds, UK
[3] Department of Optics, University of Granada, Spain

## ABSTRACT

CIE tristimulus values (TSVs) are defined in terms of integrations and all the integrands involved have no analytical expressions: therefore accurate computation of the TSVs becomes a problem, a problem which has been noticed by scientific researchers possibly since the early 1930s. Various computational methods are available and disagreements between these methods can be large. This paper addresses this problem and shows that it becomes even worse with some current industrial applications. However, the problem is completely avoidable if a unified method is used to calculate the TSVs. The paper compares all available methods including the CIE recommended method and the ASTM weighting tables, the Oleari method and the LLR method, together with a newly developed LWL method, and it is found that this new LWL method gives the best results. It is therefore recommended for use for the computation of TSVs using data obtained at any measurement wavelength interval.

## 1. INTRODUCTION

Tristimulus values (TSVs) of object colours are defined by integrations:

$$V = \int_a^b W_V(\lambda)R(\lambda)d\lambda \text{, with } V = X \text{, } Y \text{ and } Z \tag{1}$$

where $W_X(\lambda) = \kappa S(\lambda)\bar{x}(\lambda)$, $W_Y(\lambda) = \kappa S(\lambda)\bar{y}(\lambda)$, $W_Z(\lambda) = \kappa S(\lambda)\bar{z}(\lambda)$. Here $S(\lambda)$ is the relative spectral power distribution (SPD) of an illuminant, $\bar{x}(\lambda)$, $\bar{y}(\lambda)$, $\bar{z}(\lambda)$ are the CIE 1931 (2°) or 1964 (10°) standard colorimetric observers or colour matching functions (CMFs), and $R(\lambda)$ is the reflectance (transmittance) function of a reflecting (transmitting) object colour. $(a,b)$ is the visible range of wavelengths with $a = 360$ nm and $b = 830$ nm, and $k$ is the normalizing factor defined for reflecting (transmitting) object colours and is given by $k = 100 / \int_a^b S(\lambda)\bar{y}(\lambda)d\lambda$. However, the integrands involved in Eq. (1) have no equivalent analytical expressions, hence CIE[1] recommended that the integrations should be replaced by numerical summations:

$$V = \sum_{i=0}^n W_V(\lambda_i)R(\lambda_i)\Delta\lambda \text{ , with } V = X \text{, } Y \text{ and } Z \tag{2}$$

at wavelength intervals $\Delta \lambda = 1\,\text{nm}$.

It seems that calculating TSVs using Eq. (2) should be straightforward provided that the reflectance values at 1 nm intervals are known over the full range of wavelengths. However, in practice these data are rarely available, since reflectance data are typically measured by a spectrophotometer at an interval much larger than 1 nm, for example 10, or even 20 nm, and often over a narrower wavelength range than 360 nm to 830 nm. Thus, for practical applications, there is still a problem of how to compute the TSVs. Since CIE makes has no precise recommendation on how to deal with this, there are many methods available for computing TSVs. Different methods lead to different results and the differences obtained can be large, which can cause problems in current industrial applications. Firstly, consider an example. Table 1 lists the differences in terms of CIELAB colour difference units using a number of different methods with the measured 1 nm, and then simulated 10 nm and 20 nm data, for a Munsell colour sample. In Table 1, S represents the CIE standard 1 nm summation method, which computes TSVs using the 1 nm data and 1 nm summation formula (Eq. 2) using the CIE F11 fluorescent illuminant and the CIE 1931 CMFs. This set of TSVs, denoted by XYZs, can be considered as the true TSVs of the sample. Also a number of other sets of TSVs, denoted by XYZb, were computed using the simulated 10 nm and 20 nm reflectance factors and some other available computation methods: these methods will be introduced in the next section. Ideally, XYZs and XYZb should be the same, but they are not. The values in bold and in the shaded area are the inconsistencies between different methods for 10 nm and 20 nm data respectively. Furthermore, the difference between XYZb1 obtained by method 1 and XYZb2 obtained by method 2 can be large. The values below/above the diagonal in Table 1 are for 20 nm/10 nm data and correspond to the CIELAB colour differences between the TSVs obtained using any two different methods, hence they represent the accuracies associated with the corresponding methods. It can be seen the values underlined are all greater than zero, which means no method replicates the accurate result XYZs: the smaller the value the better is the corresponding method. For the data having a 10 nm wavelength interval, the LWL, LLR and CIE-R methods are similar and are better than all the others. The worst method is the DS method which an error of 9.3 CIELAB colour difference units. For the data that has a 20 nm wavelength interval, the T6 and LLR methods are similar, and are better than all others, but they have error of 0.6 CIELAB colour difference units. The disagreements between methods can be as large as 11.1 CIELAB units for 10 nm data, and 31.8 CIELAB units for 20 nm data.

The CIE provides no recommendations for TSV computation from measured data at measurement intervals greater than 5 nm. Thus, in practice, various approaches have been used for computing TSVs, which can lead to a big discrepancy between two different methods from the same set of spectral data as shown by the above example which can cause problems. For example, a fashion designer asks a dyehouse to dye a fabric and provides spectral reflectance data at 10 nm intervals rather than a physical sample in order to save time and the cost. The requirement for the reproduction is, for example, less than 0.5 CIELAB units. If the dyehouse uses a different method for computing TSVs, it is highly possible that the dyed fabric might be rejected though the company thinks the requirement is satisfied. Another example occurs with cross media colour reproduction. In the colour reproduction chain, both the source (e.g. a camera) and destination (e.g. a printer) devices are characterized, so that the device dependent colour spaces are linked to the device independent CIE XYZ space. If the methods for computing the XYZ values are

AIC2015 TOKYO - Color and Image

different between the characterization processes of the source and destination devices, it cannot be guaranteed that the reproduction will be accurate.

*Table 1: The performance of different methods used to compute TSVs (underlined row for 20 nm interval data and underlined column for 10 nm data) for a Munsell sample under CIE illuminant F11 and the CIE 1931 standard colorimetric observer, measured as CIELAB colour differences. Values in the shaded area are for 20 nm interval data and values in bold for 10 nm interval data.*

|      | S   | T5  | T6  | LWL | LLR | CIER | OWT0 | OWT2 | DS   | T5N  | T6N  |
|------|-----|-----|-----|-----|-----|------|------|------|------|------|------|
| S    | -   | 1.8 | 0.6 | 0.7 | 0.6 | 1.5  | 5.2  | 2.2  | 26.6 | 1.7  | 2.6  |
| T5   | 0.3 | -   | 1.3 | 1.2 | 1.2 | 0.4  | 6.4  | 2.1  | 25.5 | 0.1  | 0.8  |
| T6   | 0.3 | 0   | -   | 0.1 | 0.1 | 0.9  | 5.5  | 2    | 26.3 | 1.2  | 2    |
| LWL  | 0.1 | 0.1 | 0.2 | -   | 0   | 0.8  | 5.5  | 1.9  | 26.3 | 1.1  | 2    |
| LLR  | 0.1 | 0.2 | 0.2 | 0   | -   | 0.8  | 5.5  | 1.9  | 26.3 | 1.1  | 2    |
| CIER | 0.1 | 0.1 | 0.2 | 0   | 0   | -    | 6.1  | 2    | 25.7 | 0.3  | 1.2  |
| OWT0 | 1.8 | 1.9 | 1.9 | 1.9 | 1.9 | 1.9  | -    | 4.6  | 31.8 | 6.3  | 7.1  |
| OWT2 | 0.9 | 0.9 | 0.9 | 0.9 | 0.9 | 0.9  | 1.1  | -    | 27.5 | 2.1  | 2.7  |
| DS   | 9.3 | 9.3 | 9.3 | 9.3 | 9.3 | 9.3  | 11.1 | 10.1 | -    | 25.5 | 24.9 |
| T5N  | -   | -   | -   | -   | -   | -    | -    | -    | -    | -    | 0.9  |
| T6N  | -   | -   | -   | -   | -   | -    | -    | -    | -    | -    | -    |

## 2. AVAILABLE METHODS FOR COMPUTING TSV

The various computation methods are briefly introduced in chronological order of their development; further details can be found in reference 2.

### 2.1 Direct Selection Method

Direct selection (DS) is the simplest method and it has probably been used since 1932[3]. For measured reflectance at interval $\Delta\lambda > 1$ nm, select one value from every $\Delta\lambda$ data from the spectral power distribution (SPD) and standard observer (CMF), and then carry out the corresponding summations as shown in Eq. (2).

### 2.2 ASTM E308-1985 and E308-1995 Weighting Tables

The American Society for Testing and Materials (ASTM) standardized a set of weighting tables in 1985 (E308-1985) and 1995 (E308-1995). Each set includes 36 weighting tables covering 9 illuminants (six continuous illuminants A, C, D50, D55, D65 and D75, plus the three fluorescent illuminants FL2, FL7 and FL11); each illuminant being combined with the two CIE standard colorimetric observers (1931 and 1964) and two different wavelength intervals (10 nm and 20 nm). All these tables cover a wavelength range from 360 nm to 780 nm. The ASTM E308-1985 weighting tables are denoted as Table 5 (T5) and must be used with bandpass corrected reflectance data. The E308-1995 weighting tables are denoted as Table 6 (T6) and must be used with the measured reflectance data directly.

Recently, ASTM[4] recommended that the 20 nm weighting data in both sets of tables should not be used. ASTM now recommends that, when the measured reflectance data for using T6 or the bandpass corrected reflectance for using T5, are at 20 nm intervals, they should be interpolated using the third-order Lagrange formulae to compute 10 nm reflectance data, and then the corresponding 10 nm weighting table should be used to compute TSVs. In this paper, this new recommendations are denoted T6N and T5N, respectively.

## 2.3 CIE Recommendations

For measured data with $\Delta\lambda \leq 5\,\mathrm{nm}$, CIE recommends that the DS method can be used. For $\Delta\lambda = 10\,\mathrm{nm}$ or $\Delta\lambda = 20\,\mathrm{nm}$, the measured data can be interpolated into 1 nm data and then the 1 nm summation can be used. This recommendation is named the CIE-R method in this paper. However, CIE[1] also suggested that for $\Delta\lambda = 10$ nm or $\Delta\lambda = 20$ nm, the ASTM T5 or T6 or the LLR method (which will be introduced later) may be used.

## 2.4 The Zero- and Second-Order Oleari Weighting Tables

In 2000, Oleari[5] proposed a method for the computation of TSVs based on a local power (zero or second-order) expansion for the product of the SPD of the illuminant/source and the CMFs. It was shown that the second-order method was better than ASTM T6. To avoid repeated computations, Li *et al.*[6] have derived zero- and second-order weighting tables based on Oleari's work. Henceforth, these zero- and second- order weighting tables will be termed the OWT0 and OWT2 methods, respectively.

## 2.5 LI-LUO-RIGG Method

IN 2004, Li, Luo and Rigg gave a method for computing weighting tables for calculating TSVs. The method (LLR) requires solutions to the following equations:

$$A u_V^{(\Delta\lambda)} = a_V^{(\Delta\lambda)} \text{ , with } V = X \text{ , } Y \text{ and } Z \tag{5}$$

The unknown $\mathbf{u}_V^{(\Delta\lambda)}$ are the weights in the V directions. The matrix A and the right hand vector $a_V^{(\Delta\lambda)}$ can be found in the original paper [7].

## 2.6 LI-WANG-LUO Method

Similar to the LLR method, the least square method [8] (denoted as the LWL method) also requires solving three linear systems of equations:

$$\mathbf{B} u_V^{(\Delta\lambda)} = \mathbf{a}_V^{(\Delta\lambda)} \text{ , with } V = X \text{ , } Y \text{ and } Z \tag{6}$$

Here, the right hand side vectors are the same as those of the LLR method and coefficient matrix B is also tri-diagonal. It has been shown[2] that when $\Delta\lambda$ is large, the matrix B approaches the matrix A, and therefore in this situation the LWL and LLR methods have nearly the same performance. However, when $\Delta\lambda$ is small, these two methods will perform differently, which is confirmed by the experimental results presented in the next section.

## 3. COMPARISONS OF ALL METHODS

The comparison procedure used in this paper is the same as that used in references 2 and 7. Here, the 1 nm standard reflectance factors were measured from a set of 1096 Pantone samples between 360 nm and 780 nm. Thus, TSVs can be computed using the 1 nm summation methods and this set of TSVs are considered as standard. Then, the simulated 10 nm or 20 nm reflectance factors can be obtained and the TSVs, denoted as XYZb, can be obtained using a particular method under a particular illuminant and CMF combination. Finally, the CIELAB colour differences between XYZs and XYZb are computed. Since ASTM methods are also compared, the visible range considered here is from 360 nm to 780 nm. Six CIE illuminants and the CIE 1931 and 1964 CMFs were used. The illuminants were the three continuous illuminants D65, D50, and A, plus the three CIE fluorescent illuminants FL2, FL7 and FL11. In order to save space, the computed colour differences in Table II have been grouped into continuous and fluorescent illuminant groups (C-ILLs and F-ILLs) respectively. Then the median colour difference from each group is considered as the general performance for each method.

*Table II: Median CIELAB colour differences for 10nm and 20nm using different methods under all continuous illuminants/two CMFs (C-ILLs) and Fluorescent illuminants/two CMFs (F-ILLs)*

| Method | 10nm | | 20nm | |
|--------|--------|--------|--------|--------|
| | C-ILLs | F-ILLs | C-ILLs | F-ILLs |
| T5 | 0.0111(6) | 0.035(4) | 0.1329(7) | 0.2793(6) |
| T6 | 0.0033(2) | 0.0408(5) | 0.0287(3) | 0.2199(4) |
| LWL | 0.0013(1) | 0.0095(1) | 0.0243(2) | 0.1263(2) |
| LLR | 0.0038(3) | 0.0107(2) | 0.0216(1) | 0.1238(1) |
| DS | 0.0258(8) | 7.3893(8) | 0.3306(9) | 4.6193(10) |
| CIE-R | 0.0073(4) | 0.0337(3) | 0.0644(4) | 0.1604(3) |
| OWT(0) | 0.0094(5) | 1.3594(7) | 0.1173(5) | 0.8284(7) |
| OWT(2) | 0.0197(7) | 0.5928(6) | 0.2967(8) | 0.9454(8) |
| T5N | | | 0.1184(6) | 0.2552(5) |
| T6N | | | 0.7054(10) | 0.9635(9) |

Table II lists the median results for 10 nm and 20 nm measurement interval data. Values in brackets indicate the ranking of the corresponding methods. It can be seen that the LWL method ranks first for the 10 nm interval data and second for the 20 nm interval data. The LLR method ranks first for the 20 nm interval data and second for the 10nm interval data for F-ILLs. These two methods are better than all other methods. The worst method overall is the DS method. Comparing the four ASTM methods for the 20 nm interval data, T6 is the best, T5N is the second best and the T6N is the worst. In theory, the T5 and the CIE-R method are the same if the third order interpolation method is used for the CIE-R method. However, in this test, the Sprague method is used for the interpolation not the Lagrange method. This might be the reason that the CIE-R method performs better than the T5 method, as shown in Table II.

Further tests with $\Delta\lambda$ being equal to 2, 3, 4, 5, 6 and 7 nm, respectively were also conducted. It was found that in each case the LWL method performs the best. This result is very encouraging. It was also found that the LLR method performs much worse when the measuring wavelength interval is small.

## 4. CONCLUSIONS

We have reviewed the problem of accuracy in the computation of tristimulus values. Results from different methods can be quite different which can cause problems in current industrial applications. It is highly desirable that a single optimal method be adopted by CIE. To further this aim, a comprehensive comparison has been made using 1096 Pantone samples. The results show that the method of Li-Wang-Luo (LWL) performs the best for wavelength intervals not greater than 10 nm and performs the second best when the measuring interval is 20 nm. The LWL method is simple to implement and can be recommended for the computation of CIE XYZ tristimulus values from reflectance (transmittance) data measured at any wavelength interval.

## ACKNOWLEDGEMENTS

## REFERENCES

1. CIE Publ. 15:2004. *Colorimetry*, 3rd Edition. CIE Central Bureau: Vienna; 2004.
2. Li CJ, Luo MR, Melgosa M and Pointer MR, *Testing the Accuracy of Methods for the Computation of CIE Tristimulus Values Using Weighting Tables*, Color Research and Application, 2015.
3. Hardy AC, Pineo OW. *The computation of trichromatic excitation values by the selected ordinate method*. J Opt Soc Am 1932;22:430.
4. ASTM E308-13. *Standard practice for computing the colors of objects by using the CIE system*. American Society for Testing and Materials (ASTM; 2013).
5. Oleari C. Spectral-reflectance-factor deconvolution and colorimetric calculations by local-power expansion. Color Res Appl 2000;25:176-185.5.
6. Li CJ, Oleari C, Melgosa M, Xu Y. *Methods for computing weighting tables based on local power expansion for tristimulus values computations*. J Opt Soc Am A 2011;28:2243-2252.
7. Li CJ, Luo MR, Rigg B. A new method for computing optimum weights for calculating CIE tristimulus values. Color Res Appl 2004;29:91-103.
8. Li CJ, Luo MR, Wang G. *Recent progress in computing weighting tables for calculating CIE tristimulus values*. Proc. SPIE 6033, 198-207 (2006).004;29:91-103.

*Address: Prof. Changjun Li, School of Electronics and Information Engineering, University of Science and Technology Liaoning, 185 Qianshan Road, Anshan, China*
*E-mail:cjliustl@sina.com*

# Variability in colour matches between displays

Phil GREEN,[1] Srikrishna NUDURUMATI,[2]  Ivar FARUP[1]
[1] Colour and Visual Computing Laboratory, Gjøvik University College, Norway
[2] Global Graphics Software Ltd., Cambridge, UK

## ABSTRACT

The variability between colour matches made by different observers on displays is a concern which has been addressed in several previous studies. Inter-observer variability in perceived colour matches was investigated in an experiment in which 21 observers matched a series of test colours, with the reference stimulus on a CRT and the test stimulus on an LCD display. Reference and test colour patches with a 2 degree angular subtense were presented on adjacent displays with a separation between reference and test stimuli of 7cm, and with an opaque black mask covering the remainder of the display screens. The first reference colour was a mid-tone neutral gray, followed by nine chromatic colours. Observers adjusted the test colour to produce a perceived match to the reference, and the resulting colours were measured with a Konica-Minolta CS-1000 telespectroradiometer. The results showed considerable variability in the matches in luminance. In *u'v'* chromaticity, observer variability was found to be less than in luminance, but much higher in blues than in greens and neutrals, suggesting a possible observer metamerism effect.

## 1. INTRODUCTION

The CIE 1931 Standard Colorimetric Observer was derived by pooling the colour matching functions of multiple observers. These original experiments, and subsequent ones in the following decades, recorded significant variability between matching functions of individual observers. While the typically smooth reflectance spectra of surface colours do not tend to give rise to significantly large inter-observer differences in colour matches, the nature of the spectral emission of self-luminous displays, often characterised by narrow peaks, is more likely to interact with differences in retinal spectral sensitivity to generate inter-observer variation in cross-media colour matches in cases where different colorant technologies are employed. Such inter-observer differences have been reported in previous studies (e.g. Oicherman 2007; Shaw, 2010; Sarkar 2010; Parab 2010; Sarkar 2011).

Modern displays use a variety of light-emitting technologies with very different spectral characteristics, and the goal of the present experiment was to provide experimental data on colour matches made by observers between two different types of displays.

## 2. EXPERIMENTAL

Following a small pilot study with 6 observers, 21 observers took part in the main phase of the experiment, in which 10 reference colours were matched between a CRT display (employing phosphors as the light-emitting technology) and an LCD display (with LED backlight).[1]

---

[1] The experiment was undertaken by the second author during his employment as an Early-stage Researcher in the Marie Curie Initial Training Networks (ITN) CP7.0 project.

## 2.1 Displays

The displays were a CRT (Lacie Softproofing Display) and an LED-backlit IPS-LCD (Dell U2412M). The R, G, B primaries of the two displays were measured with a Konica-Minolta CS1000 telespectroradiometer, and the spectral radiances are shown in Figure 1 below. The colour gamut of the two displays can be seen in CIE u',v' coordinates in Figure 2.
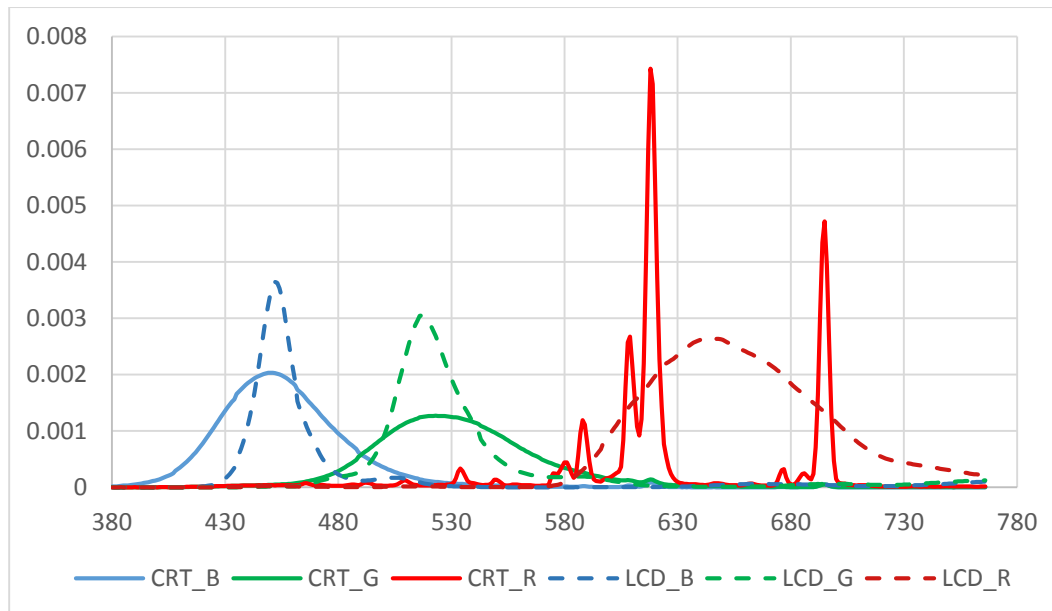


*Figure 1: Spectral radiances of CRT and LCD display primaries in the experiment.*

Since the dynamic range and colour gamut of the CRT was smaller than that of the LCD, the CRT was used to present the reference colours which observers then matched on the LCD. The neutral gray was presented first to provide an initial reference for brightness matching by observers. Display variability was evaluated by measuring a series of colours over a period of 12 hours after initial warm-up, using the K-M CS1000 TSR. The mean differences from the mean white point luminance over the period were 0.42 and 0.12 cd m$^{-2}$ for the CRT and LCD respectively.

The observer visual matches and the instrumental measurement were performed at the same location on the displays, so the matches were unaffected by any spatial non-uniformity of the displays. There was a warm-up period of at least 15 minutes for the displays and the TSR prior to measurements and observations.

## 2.2 Observers

Following a pilot study with six observers, 21 observers aged 24-55 participated in the experiment. An Isihara test was conducted prior to the experiment for those observers had not previously performed such a test, and one was found to be colour deficient. Non-expert observers were given training in colour mixing. Observer repeatability was evaluated by observers performing matches between similar patches during each run of the experiment.

## 2.2 Reference Colours

10 colours were selected in RGB coordinates and displayed on the reference (CRT) display). The resulting colours were measured with the TSR and are shown in CIE u',v' coordinates

AIC2015 TOKYO - Color and Image

in Figures 2, where the reference colours are labelled 1-10. Some of the reference colours lie close to or on the boundary of the CRT gamut, but are within the gamut of the LCD display.
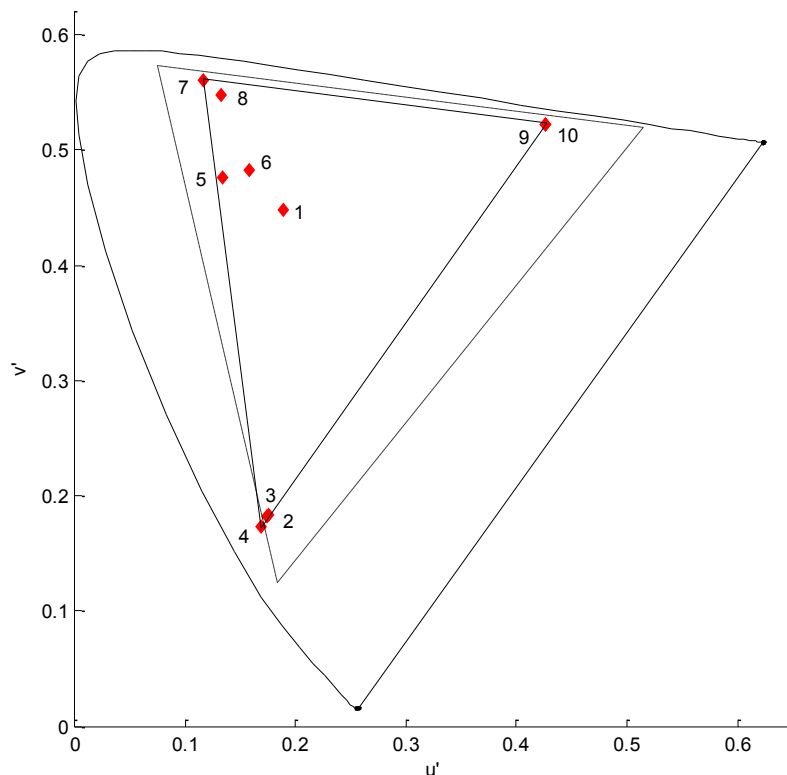


*Figure 2: Reference colours in CIE u',v' with gamut of CRT (solid) and LCD (dashed) displays*

## 2.3 Experimental Setup

The experiment was conducted in a completely dark room with the display colour patches being the only stimuli. Reference and test patches were circular and 3.5 cm in diameter. Observers were located one metre from the display faceplate, so that the colour stimulus gave an angular subtense of 2°. In order to exclude any effect due to the display backlight within the faceplate, the patches were observed through circular openings made within an opaque black sheet placed in front of the displays. The displays were placed adjacent to each other so that the reference and the test targets were located at approximately 7 cm apart. This is essentially an aperture mode rather than object mode viewing condition.

## 2.4 Experiment

In the experiment the reference colour was shown on the CRT display and the test colour shown simultaneously on the LCD display. Observers were asked to match the appearance of the test to the reference colour. To do this they were provided with three computer mice with two-way spherical scroll controlling the amounts of individual primaries (R, G & B) of the test colour, together with a keyboard control for adjustment of the brightness. Once the observer was satisfied with the match, the corresponding R, G, B values were recorded and subsequently measured with the TSR positioned at the observer location in the same viewing conditions.

## 3. RESULTS

CIE XYZ values for the reference colours and the observers matches were calculated from the measured radiances using the CIE 1931 Standard Colorimetric Observer, as shown in eqn. 1 below.

$$X = 683 \sum_{767}^{380} L(\lambda)\bar{x}(\lambda)$$

where $L(\lambda)$ is the measured spectral radiance (in W sr$^{-1}$ m$^{-2}$) at 1nm intervals and $\bar{x}(\lambda)$ is the vector of matching function values for X; and Y and Z are computed analogously. The constant 683 results in Y tristimulus values in units of cd m$^{-2}$.

Since the experiment was conducted in a dark room with no adapting white and colours were judged in aperture mode, there is no reference white or illuminant and hence the data cannot be converted to a colour space such as CIELAB. For this reason the variability between the reference colour and the observer matches is shown in terms of luminance $\Delta Y$ and chromaticity $\Delta u',v'$ (CIE 2014). The results are shown in Table 1. [We note that if the data is converted to CIELAB, using the display peak white as the reference white as is commonly done in colour management, the average CIELAB 1976 $\Delta E^*_{ab}$ colour difference from the reference is 19.5 and the inter-observer variability (expressed as the mean colour difference from the mean, or MCDM) is 10.4, which gives a misleading impression of the accuracy of the matches.]

*Table 1.Differences in luminance $\Delta Y$ and chromaticity $\Delta u',v'$ between reference colours and observer matches*

| | $\Delta Y$ | | | $\Delta u'v'$ | | |
|--------|--------|-------|-----------------|--------|--------|-----------------|
| Colour | Median | Max | 95th percentile | Median | Max | 95th percentile |
| 1 | 6.57 | 9.6 | 9.51 | 0.0107 | 0.0244 | 0.0201 |
| 2 | 0.65 | 1.27 | 1.15 | 0.0207 | 0.0543 | 0.0537 |
| 3 | 0.91 | 2.91 | 2.32 | 0.0373 | 0.1023 | 0.0819 |
| 4 | 2.46 | 5.7 | 5.5 | 0.012 | 0.0526 | 0.0491 |
| 5 | 5.31 | 14.33 | 12.85 | 0.0128 | 0.0198 | 0.0197 |
| 6 | 4.01 | 14.9 | 13.62 | 0.0178 | 0.0256 | 0.0235 |
| 7 | 9.1 | 36.43 | 30.99 | 0.0134 | 0.0572 | 0.0391 |
| 8 | 3.54 | 32.98 | 23.94 | 0.0267 | 0.1424 | 0.1421 |
| 9 | 2.32 | 9.04 | 8.52 | 0.0253 | 0.047 | 0.0469 |
| 10 | 3.17 | 13.32 | 13.21 | 0.0238 | 0.0506 | 0.0492 |
| Mean | 3.8 | 14.05 | 12.16 | 0.0201 | 0.0576 | 0.0525 |

The variability in luminance matches is very high for some colours, shown by 95th percentile $\Delta Y$ values of up to 30.99. The matches in u',v' chromaticity have smaller variability, as seen in Figures 3-5, where the reference colour is shown in red and the observer matches in black.

It should be noted that where the reference colours are close to the gamut boundary, the direction of possible matches in chromaticity space by observers was constrained.
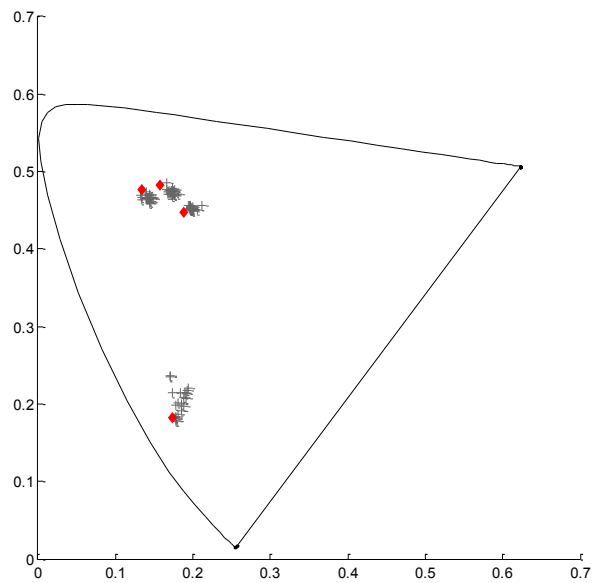


*Figure 3. CIE u',v' coordinates of reference colours (red marker) and corresponding observer matches for colours 1, 2, 5 and 6*
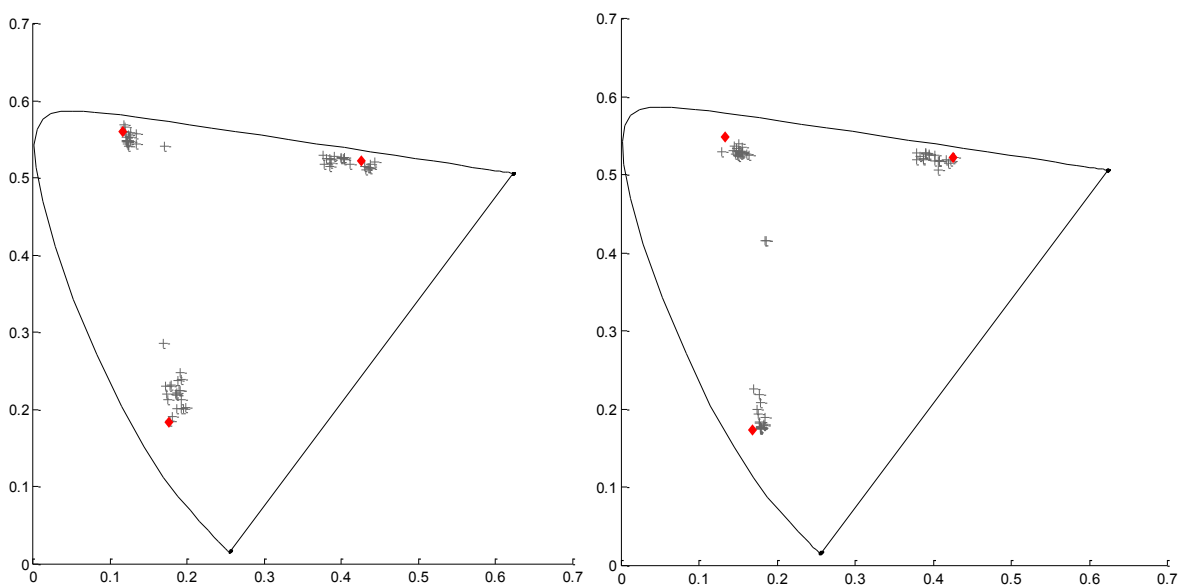


*Figure 4-5. CIE u',v' coordinates of reference colours (red marker) and corresponding observer matches for colours 3, 7 & 10 and 4, 8 & 9 respectively*

It can be seen from Figures 3-5 that observer variability in greenish and neutral colours is relatively small, while in red (colours 9-10) and blue (colours 2-4) regions it is considerably higher. The three blue reference colours are located at near-identical chromaticity coordinates, and the pattern of observer matches is very similar between the three, suggesting a possibly systematic difference in the way individual observers made the matches. A similar pattern can be seen in the two red colours, although less pronounced.

# 4. CONCLUSIONS

Observers matched a set of 10 reference colours presented on a CRT display, using an LED-backlit LCD display. Significant variability was seen in the luminance of the matches, suggesting that luminance is of less importance than chromaticity in an aperture-mode colour matching task. Variability in matching of chromaticity was small in some colours, but relatively high in certain colours, notably in blue. The similar trend seen in the matches for colours of similar chromaticity suggests there is a possible observer metamerism effect arising from different cone sensitivities of the observers. However, further analysis is needed to confirm this possibility. If present, it would be consistent with results obtained in other studies.

The results also indicate that aperture mode colour matches should be evaluated in luminance and chromaticity, with higher tolerances in luminance.

## REFERENCES

Shaw, M. and Fairchild, M. (2002) *Evaluating the 1931 CIE Color Matching Functions,* Col. Res. Appl. 27(5) 316–329

Oicherman, B. (2007) *Effects of colorimetric additivity failure and of observer metamerism on cross-media colour matching*, (PhD thesis) University of Leeds, UK

Parab, N. and Green, P. (2011) *Soft proofing of printed colours on substrates with optical brightening agents*, Proc. SPIE 7866 doi:10.1117/12.872219

Sarkar, A., L. Blondé, P. Le Callet, F. Autrusseau, J. Stauder, P. Morvan, (2010) *Toward Reducing Observer Metamerism in Industrial Applications: Colorimetric Observer Categories and Observer Classification*, Proc IS&T 18th Color Imaging Conf. 307-313

Sarkar, A., F. Autrusseau, F. Viénot, P. Le Callet, L. Blondé, (2011) *From CIE 2006 Physiological Model to Improved Age-Dependent and Average Colorimetric Observers*, J. Opt. Soc. Am. (JOSA A), 28(10) 2033-48

CIE Technical Note 001:2014 *Chromaticity Difference Specification for Light Sources*, Vienna: CIE

*Address: Prof. Phil GREEN, Colour and Visual Computing Laboratory, Gjøvik University College, Teknologivn. 22, 2815 Gjøvik, Norway*
*E-mails: philip.green@hig.no, srisrikrishna9@gmail.com, ivar.farup@hig.no*

# A comparison study of camera colorimetric characterization models considering capture settings adjustment

Jingyu Fang,[1] Haisong Xu,[1,*] Wei Ye [2]

[1] State Key Laboratory of Modern Optical Instrumentation, Department of Optical Engineering, Zhejiang University, Hangzhou 310027, China

[2] State Key Laboratory of Industrial Control Technology, Zhejiang University, Hangzhou 310027, China

## ABSTRACT

Capture settings must be fixed for colorimetric characterization models of digital camera, which greatly limits the application of the cameras. In order to overcome this disadvantage, a correction procedure for capture settings adjustment was proposed in this study. To investigate the performance of the correction comprehensively, four kinds of widely-used characterization models were employed in this correction procedure as the mapping technique, including look-up table (LUT), polynomial regression, artificial neural networks (ANN) and support vector machine (SVM). The results show that the correction procudure is applicable for all kinds of colorimetric characterizations.

## 1. INTRODUCTION

The colorimetric characterization of digital camera is of fundamental importance for its scientific applications such as image based colorimetric measurement and color communication. Color characterization of still digital camera can be divided into two methods, i.e. spectral sensitivity-based one and target-based one, in which the latter is more generally used for its low cost and convenience. Until now, there are mainly four kinds of widely-used target-based characterization models, namely LUT (Hung 1993), polynomial regression (Hong *et al.* 2001), ANN (Cheung *et al.* 2002), and SVM (Yang 2013). The mappings from device-dependent camera RGB signals to device-independent CIE XYZ values defined by the conventional characterization models can yield reasonable color accuracy. These models, however, which require camera capture settings to be fixed from sample training to practical measurement, do not make full use of the dynamic range and adaptability of the digital camera. Whenever the capture settings used in practical measurement are adjusted, the sample training process has to be performed again according to the changed settings. To overcome this inconvenience, a correction procedure was proposed in this study to compensate the error resulted from the changes of camera capture settings. Besides utilizing the mappings derived from conventional characterization models, this correction procedure introduces two processes, i.e. equivalent transformation step and scale factor step, based on the imaging system, of which the performance was validated through an experiment using the camera of Nikon D3x.

## 2. METHOD

The characterization model involves training part and testing part. The training procedure is conducted in the same way as the conventional one except that the capture settings are

recorded, while for the testing part the correction procedure is carried out to compensate the prediction error resulted by different capture settings with comparison to those in training part.

## 2.1 Capture settings correction procedure

The correction procedure for capture settings adjustment should be performed in following four steps:

1) To transform the pixel values in the image of testing targets to equivalent ones corresponding to the training stage using the Eq. (1) below. This step builds the bridge between different capture settings including ISO sensitivity, f-number and exposure time, denoted as $S$, $N$, and $T$ respectively in Eq. (1).

$$\frac{P_{ts}}{P_{eq}} = \frac{T_{ts}S_{ts} / N_{ts}}{T_{tr}S_{tr} / N_{tr}} \tag{1}$$

where the subscripts $ts$ and $tr$ stand for the testing and training ones respectively, and $eq$ represents the equivalent ones.

2) To search among training samples to find the one that is the nearest to the testing sample in $rg$ chromaticity coordinates of camera RGB color space. Then to scale the equivalent pixel values caculated by step 1 to match the values of the corresponding training sample. The scale factor, $K$, is calculated by Eq. (2)

$$K = \frac{R_{tr} + G_{tr} + B_{tr}}{R_{eq} + G_{eq} + B_{eq}} \tag{2}$$

where $R$, $G$, and $B$ are the pixel values of red, green, and blue channels.

3) To apply the scaled RGB values to the conventional colorimetric characterization models, of which the parameters are determined through training procedure. For the four models employed in this study, LUT model was modified since a regular look-up table could not be obtained by the digital camera, so the weighted mean of the 8 neighbourhood points was chosen as the predicted values. Three order polynomial expansions were adopted for the polynomial regression, resulting in the size of transform matrix being 20×3. For the popular ANN and SVM algorithms in the field of machine learning, the MATLAB neural network toolbox and an open library of libsvm (Chang *et al*. 2011) were used by default parameters without optimization for direct and effective comparison. Through the colorimetric characterization, the scaled tristimulus values XYZ could be obtained.

4) To scale back the XYZ values from step 3 to the predicted ones. The scaling factor in this step is the reciprocal of $K$ in Eq. (2).

The scale factor step is involved to reduce the error caused by the nonlinear relationship between RGB and XYZ. Following the above steps, the RGB signals of images with different capture settings can be transformed to the corresponding XYZ tristimulus values without any more training.

## 2.2 Experiments

In the experiment, a light booth of GretagMacbeth SpectraLight III was used to provide stable lighting environment, in which a GretagMacbeth DC color chart was placed as the

color target. The odd and even numbered patches of DC color checker were adopted as the training and testing samples, respectively. A Nikon D3x DSLR camera was employed to obtain the different RGB values under various capture settings. And the measuring geometry is 45/0, while the exposure time and ISO sensitivity were changed in the experiment to investigate the impact of camera settings adjustment.

## 3. RESULTS AND DISCUSSION

For the first phase of the experiment, the exposure time was the only variable while ISO and f-number were fixed as 100 and 5.6, respectively. The training samples were captured with correct exposure of 1/15s, while the testing samples were imaged with the exposure time ranged from 1/2s to 1/1000s. As the result, the comparion of the prediciton performance, in terms of $\Delta E_{ab}^*$, between different characterization models is illustrated in Figure 1.
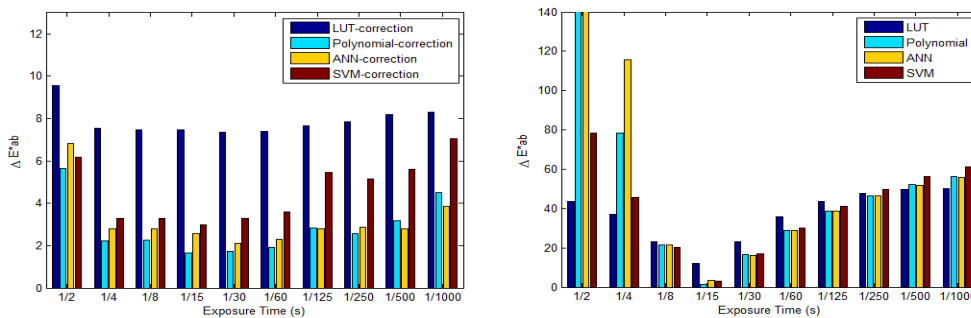


*(a) models with correction procedure*      *(b) models without correction procedure*
*Figure 1: Comparision of prediciton performance, in terms of $\Delta E_{ab}^*$, between different characterization models*

As can be seen from Figure 1, it is as expected that the prediction performance of all the four models achieve the best at the exposure time of 1/15s at which the training and testing settings are the same. The performance without correction procedure deteriorates with the camera settings being changed, while that with correction procedure remain at a stable level as the settings varies. As for the performance difference among the four models, the polynomial regression model is the best, while LUT is the worst due to the limited number and nonuniform color distribution of training samples for digital cameras. Since ANN and SVM were conducted using their default parameters, their prediction accuracies could be degraded accordingly. It could be concluded that either overexposure or underexposure should be avoided in applications as the prediction error with expsoure time at both end increases slightly.

For the second phase of the experiment, ISO sensitivity and expsoure time varied at the same time in order for right exposure, while the aperture was set as f/5.6. The training samples were captured with the ISO sensitivity of 100, while testing samples were photographed with ISO speed ranged from 100 to 6400. And the exposure time was halved when the ISO speed doubled according to the reciprocity law. The relationship between prediciton error and ISO sensitivity is shown in Figure 2, which shows that the correction procedure is applicable to ISO speed. There is a tendancy that the prediction error becomes bigger as the ISO speed increases, which results from the low signal to noise ratio for high ISO speed. Hence, it is recommended that ISO 3200 or 6400 should be avoided to set unless the lighting is too weak.
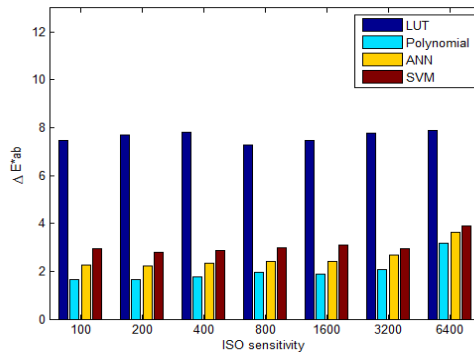
*Figure 2: Prediction error of four characterization models with correciton procedure for different levels of ISO sensitivity*

## 4. CONCLUSIONS

A correction procedure for camera colorimetric characterization was proposed in this study to compensate the prediciton error caused by capture settings adjustment. An experiment using Nikon D3x camera was conducted to validate the correction for four kinds of characterization models. It is indicated that the color prediction accuracy of all the four conventional models deteriorates badly as the gap between the image capture settings of training and testing becomes wider. On the contrary, the color differences achieved by the proposed correction based on the four models remain at a stable level with the capture settings being changed. Thereby, it can be concluded that this correction procedure for adjustable capture settings is applicable to different kinds of conventional colorimetric characterization models for camera imaging applications. In addition, the ISO sensitivity higher than the maximum of the standard ISO range (100-1600 for Nikon D3x) and the exposure value out of the dynamic range of the camera should be avoided.

## REFERENCES

Chang, C-C. and C-J. Lin. 2011. LIBSVM: a library for support vector machines. ACM Transactions on Intelligent Systems and Technology 2(3): 27.

Cheung, V.T.L. and S. Westland. 2002. Color Camera Characterization Using Artificial Neural Networks. In 10th Color and Imaging Conference: Color Science and Engineering Systems, Technologies, and Applications, ed. by P. Hubel and I. Tastl. Scottsdale: Arizona, 117-120.

Hong, G.W., M.R. Luo, and P.A. Rhodes. 2001. A study of digital camera colorimetric characterization based on polynomial modelling. Color Research and Application 26(1), 76-84.

Hung, P-C. 1993. Colorimetric calibration in electronic imaging devices using a look-up-table model and interpolations. Journal of Electronic Imaging 2(1), 53-61.

Yang, B., H.Y. Chou and T.H. Yang. 2013. Color reproduction method by support vector regression for color computer vision. OPTIK 124(22), 5649-5656

*Address: Zhejiang University, 38# Zheda Road, Hangzhou, 310027, CHINA*
*E-mails: chsxu@zju.edu.cn*

# Evaluation and Analysis of *YUTEKI-TENMOKU* Visual Effect on Traditional Ceramic Applied Gonio-Photometric Spectral Imaging and Confocal Type Laser Scanning Microscopy

Masayuki OSUMI

Office Color Science Co., Ltd.

## ABSTRACT

The object of this study was developped obsevation and everuation way combined gonio-photometric spectral imaging and conforcal type laser scanning microscopy for traditional ceramics *YUTEKI-TENMOKU*. The flat shape ceramic plate was prepared with oxidation calcinating, and the glaze was composed feldspar, lime, silica stone, kaolinate, and red iron oxide. These were typical glaze components of *YUTKI-TEMOKU*. The spectral imaging illuminant direction was 15, 45 and 75 degree from normal direction. To get highly accurate spectrum, each wavelength images were compensated to small pixel shift by black/white lattice pattern measuring. As the result, regarding distribution in CIELAB color space, the image of 15 degree angle had wide distribution of L* by metal reflection. On the other hands, images of 45 and 75 degree angle were narrow distribution and disapeared metal reflection. *YUTEKI-TENMOKU* has various visual effects depend on optics dimension. And confocal type laser scanning microscopy observation was succeeded clearly getting three dimensional orientation of metal crystalline surface.

## 1. INTRODUCTION

*TENMOKU* ceramics were produced in Zhejiang Province of Chinese Southern Sung Dynasty, and it was considered to be brought to Japan by Zen priest around 800 years ago in Kamakura period. Especially, these were prized in japanese traditional tea ceremony and one of the sought-after item in *CHANO-YU*. *YUTEKI-TENOMOKU* is kind of these type ceramic, and many traditional tea bowls were designated a national tresure. The glaze was included a lot of iron ingredient, and the visual feature is oil droplet pattern on black ground of the cermic surface. These pattern was appearanced by precipitation of iron crystaline and one of the important optical manifestation, that is gonio-apparent and anisotropic color. It is nececsary analisys corelation between changing of color appearance with various optical dimension and orientation of iron crystaline in glazing layer to clarify chractarizing about these ceramics color appearance.

## 2. METHOD

### 2.1 Sample Preparation

The flat shape plate of *YUTEKI-TENOMOKU* ceramic was prepared with oxidation calcinating, and the applied glaze was composed feldspar $(Na,K,Ca,Ba)(Si,Al)_4O_8$, lime $Ca(OH)_2$, silica stone $Si(OH)_4$, kaolinate $Al_2Si_2O_5(OH)_4$, and red iron oxide $Fe_2O_3$ ingredient. Sample size was 10cm by 10cm of square. The thcikness of glaze layer was contrloed by dipping time and prepared 10 different thickness plates. The glaze layer thickness was related size of oil droplet pattern.

## 2.2 Colorimetric way

The detail measuring way of color was applied the gonio photometric spectral imaging system which was composed liquid crystaline tunable filter, white LED illuminant, and Peltier cooling monochrome CCD image sensor. Illuminant direction was 15, 45 and 75 degree from normal direction, and detect direction was normal against sample.
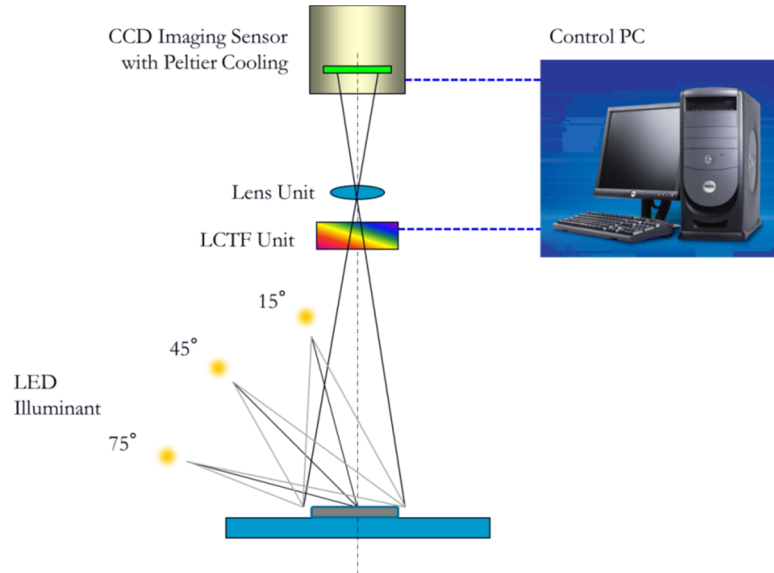


*Figure 1: Gonio-photometric spectral imaging system.*

To get highly accurate gonio-photometric reflectance spectrum and imaging information, each wavelength sample images were compensated by measuring of black/white lattice pattern to sence small shift amount of x and y direction before measuring ceramic sapmle. The lattice pattern image applied pixel shift compensation were shown in Fig. 2. Before compensation, measuring image was a lot of false color around black lattice line and reflectance profile was not horisontal. On the other hands, the image applied pixel shift compensation was disappeard false color.
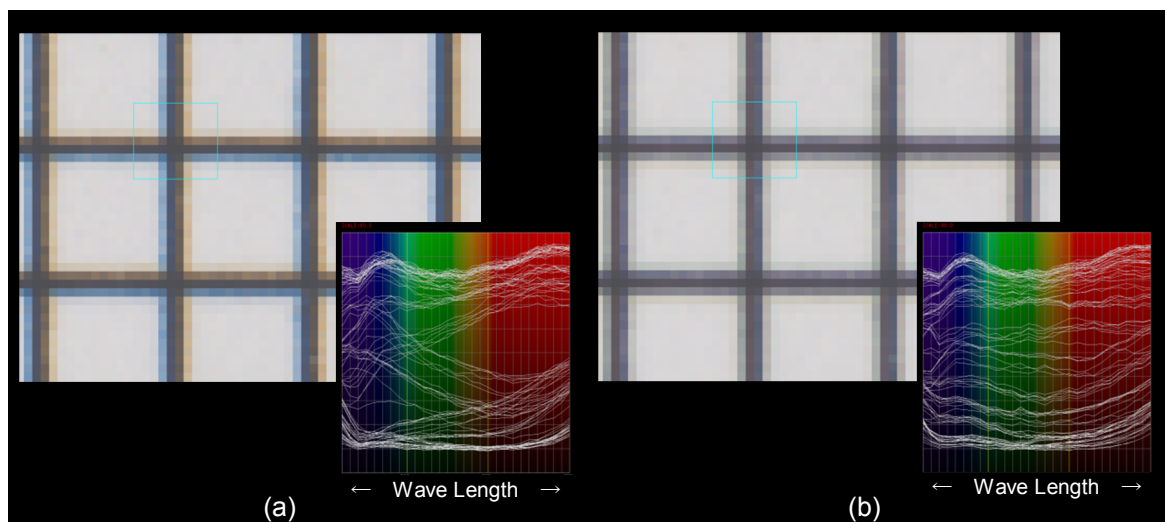


*Figure 2: Pixel shift compensation by lattice pattern.*
*(a):before compensation. (b):after compensation.*

The measuring results of sample plate by this way, three angle illuminant image were shown in Fig. 3.
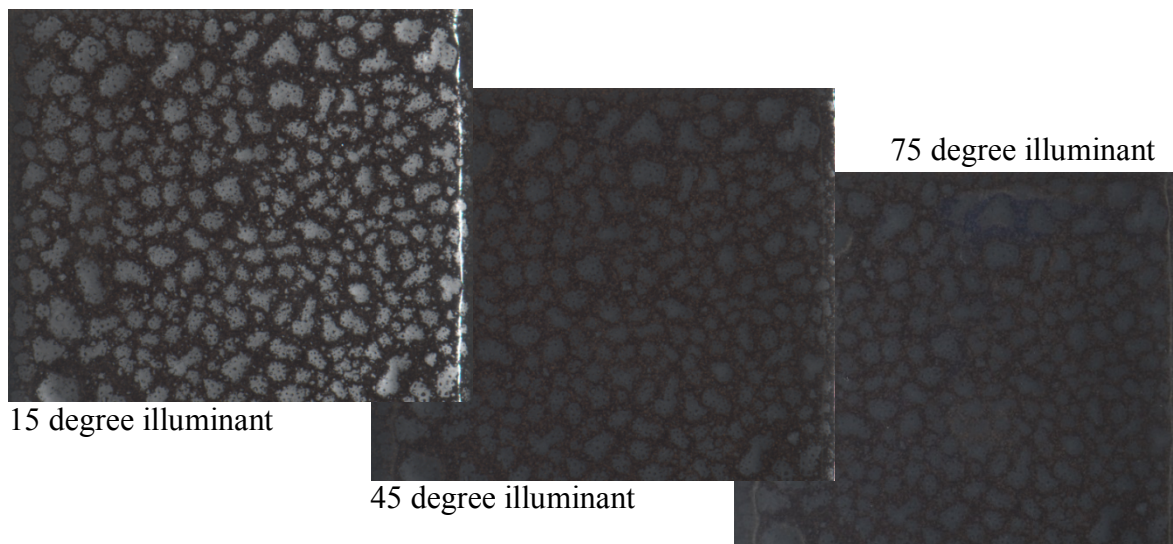
15 degree illuminant

45 degree illuminant

75 degree illuminant

*Figure 3: Measuring Image result of YUTEKITENMOKU ceramic plate*
*by gonio-photometric spectral imaging.*

## 2.3 Confocal type laser scanning microscopy observation

Also the three dimensional measuring way of iron crystaline distribution in glazing layer was applied confocal type laser scanning microscopy, and model VK-X100 made by KEYENCE was used. This microcopy was applied laser scanning technology, and allowing three dimensional reconstructions of topologically complex object by computer calculation, and can be sence interior structure with images of non-opaque specimen. In this experiment, observation magnification was 1000 times.

## 3. RESULTS AND DISCUSSION

### 3.1 Spectral Imaging observation

As the result, CIELAB coordinate value, number of color appearance and information entropy of each illuminant angle mesurements were shown in Table 1. Basically, *YUTEKI-TENMOKU* substrate color is black, and *a\**, *b\** value were almost zero, but color was slighty changed and angle dependent. The shade color, that is 75 degree illuminant angle image was bluish than the other angle. The distribution in CIELAB color space calculated from measured spectral image of each illminant angle was different. Especially, image of 15 degree angle had wide distribution of L\* direction by metal reflection. On the other hands, images of 45 and 75 degree angle were narrow distribution profile and disapeared metal reflection. *YUTEKI-TENMOKU* has various visual effects depend on optics dimension. CIELAB color space distribution of each illuminant angle is shown in Fig. 4.

*Table 1: Measuring Image result of YUTEKITENMOKU ceramic plate*
*by gonio-photometric spectral imaging.*

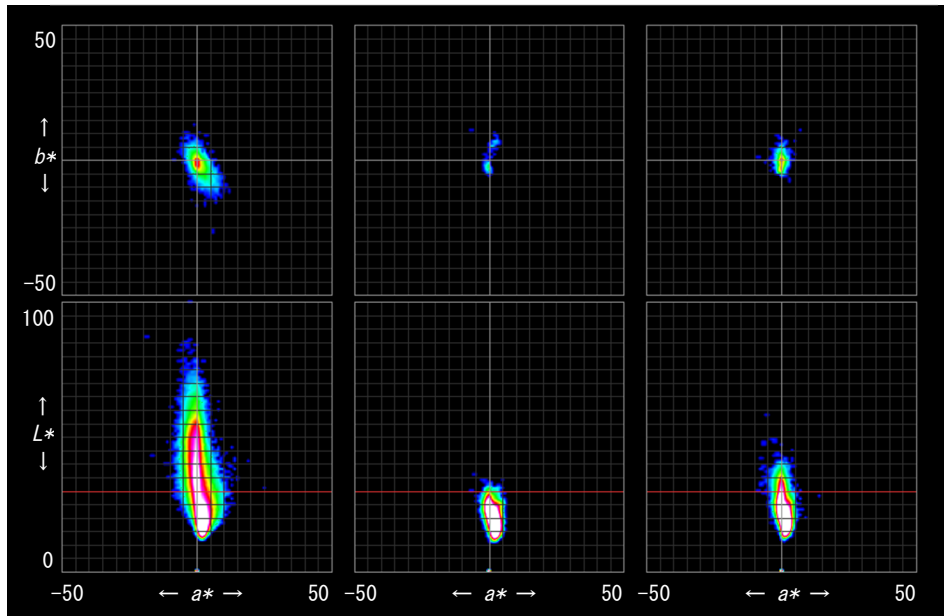|  | L* | a* | b* | Number of color appearance | Information Entropy |
|---|---|---|---|---|---|
| 15 degree | 27.63 | 1.57 | -0.52 | 785 | 5.72 |
| 45 degree | 20.26 | 1.84 | -0.48 | 120 | 4.07 |
| 75 degree | 21.65 | 1.28 | -1.75 | 233 | 4.41 |

*Figure 4: Measuring L\* distribution of YUTEKITENMOKU ceramic plate
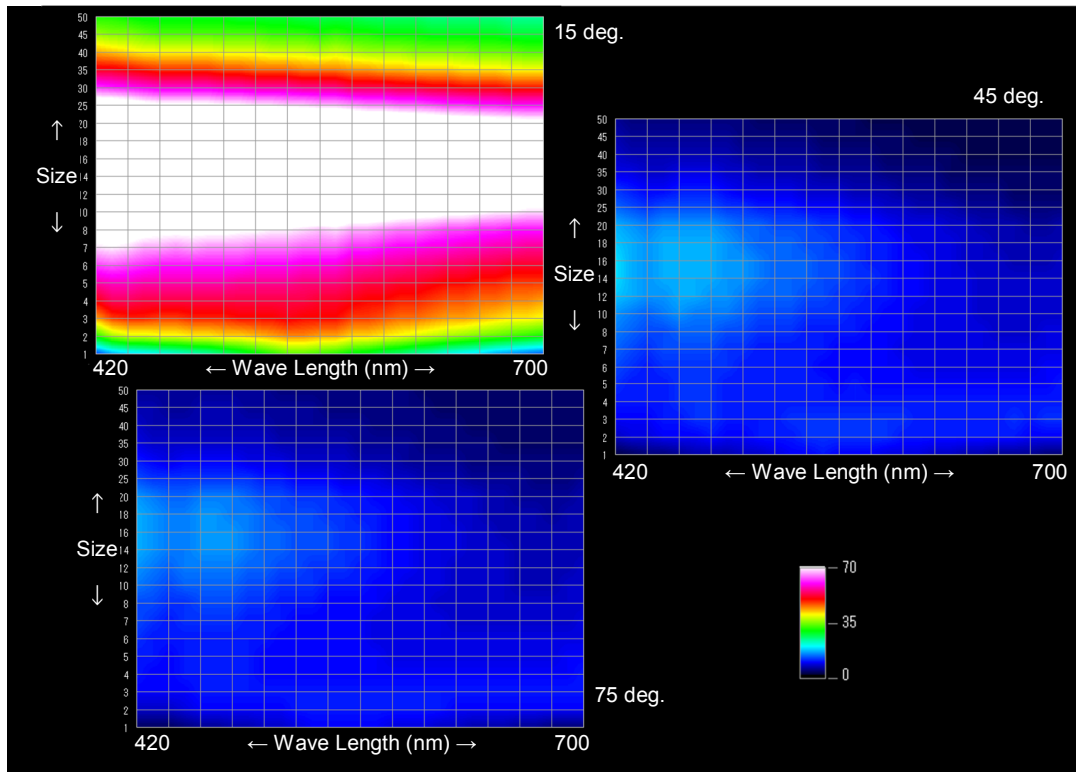by gonio-photometric spectral imaging of 15, 45 and 75 degree illuminant.*

In this figure, upper three isometric graph are distribution of each angle at *L\**=40. The *L\** distribution of each illuminant angle were shown in Fig. 5. The horizontal axis was width direction of ceramic sample plate, and vertical axis is *L\**. Figure 4 and 5 are related with number of color appearance and information entropy in Table 1. The distribution of 15 degree image is wider than the other angle distribution by metal crystalline reflection, especially, *L\** distribution is quite large.
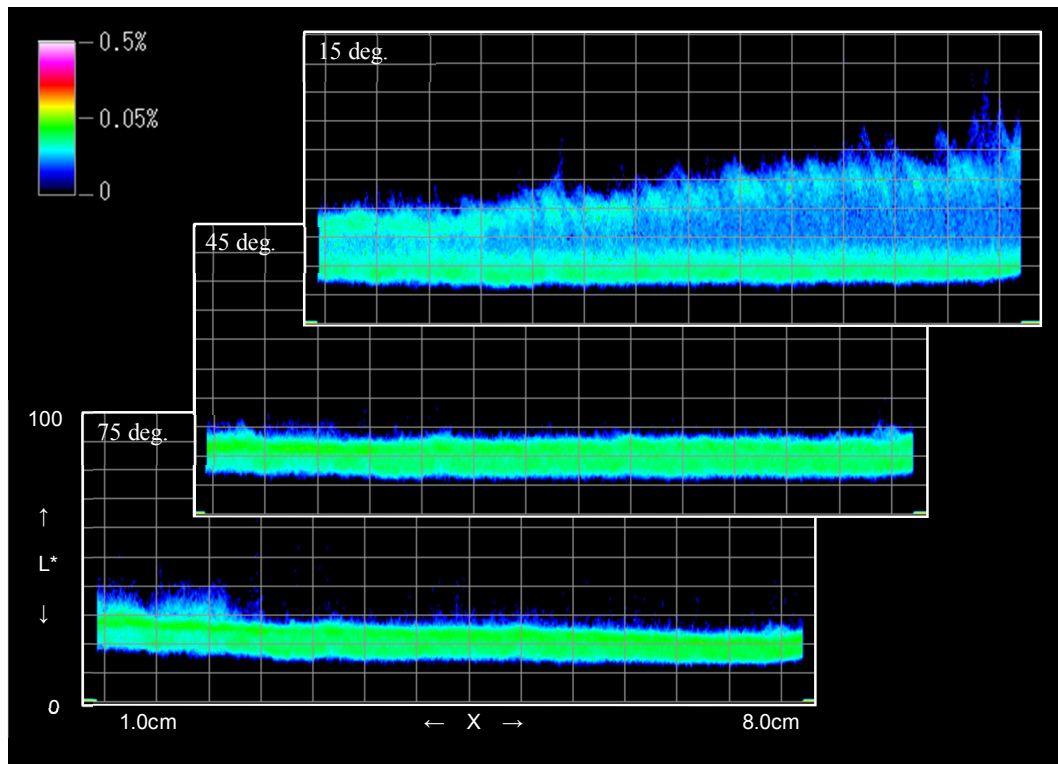


*Figure 5: Measuring L\* distribution of YUTEKITENMOKU ceramic plate
by gonio-photometric spectral imaging of 15, 45 and 75 degree illuminant.*

*Figure 6: Measuring L\* distribution of YUTEKITENMOKU ceramic plate
by gonio-photometric spectral imaging of 15, 45 and 75 degree illuminant.*

The Laplacian filter value calculation results of each angle are shown in Fig. 6. After measuring sample plate, the Laplacian filter value of each 10nm wavelength from 420 to 700nm measured spectral imaging data was calculated with various filter size by equation 1. This value is applied secondary deviation and one of the deformed contour intensifying filter. The size meaning is number of pixel and average area of filter calculation and related spatial frequency.

$$\nabla^2 f(x,y) = \frac{\partial^2 f(x,y)}{\partial x^2} + \frac{\partial^2 f(x,y)}{\partial y^2} = f_{xx}(x,y) + f_{yy}(x,y) \qquad (1)$$

The image of 15 degree illuminant, the Laplacian filter value was different and extremely huge compare with the other illuminant angle image. On the other hands, 45 and 75 illuminant image was similar and all image was not dependent on wavelength.

### 3.2 Confocal type laser scanning microscopy observation

The microscopy observation was succeeded clearly getting three dimensional orientation information of metal crystalline reflection surface. The measuring result was shown in Fig 7. The left image was laser and optics synthetic image, and recognized iron crystalline. And the glazing layer has sea island structure. The large particle crystalline was oriented almost horizontally. The non-iron crystalline area has various colors. The right image was three dimensional bird's-eye view drawing of the left side image. The iron crystalline was distributed around 2 or 3 micron of vertical direction, and glaze layer thick ness is around 5 to 10 micron. These orientation and distribution were correlated with various colors visual effects depend on optics dimension of *YUTEKI-TENMOKU*.
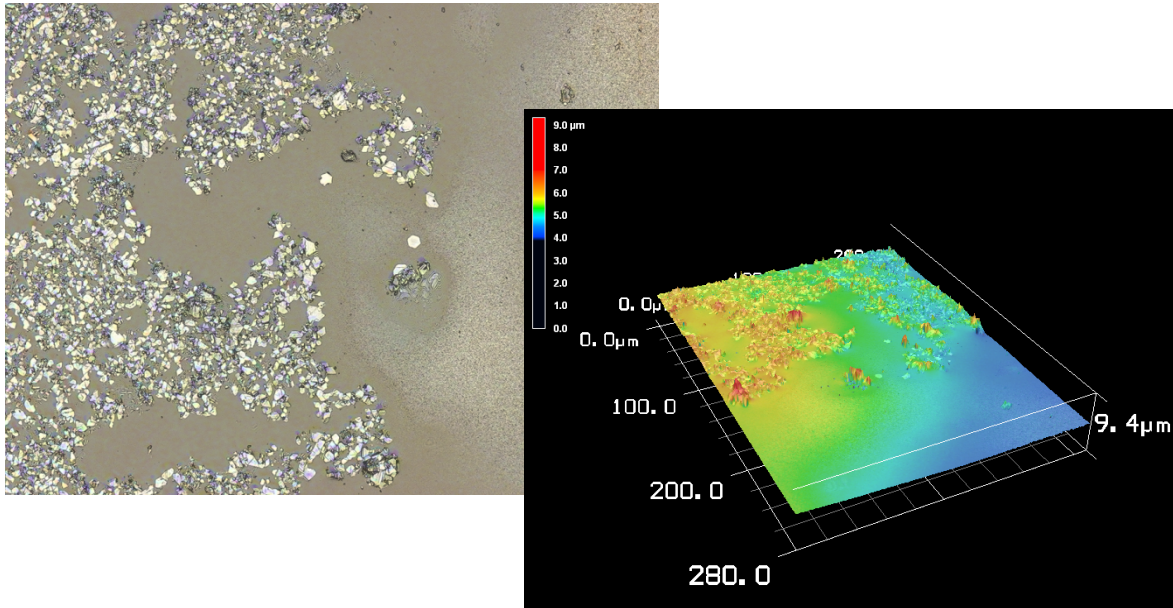
*Figure 7: Example of Confocal type laser scanning microscopy.*

## 4. CONCLUSIONS

*YUTEKI-TENMOKU* has various visual effects depend on optics dimension. And microscopy observation was succeeded clearly getting three dimensional orientation information of metal crystalline reflection surface. The benefit of combined with gonio-photometric spectral imaging and confocal type laser scanning microscopy analysis way was shown in this study. This imaging technology was quite useful for traditional ceramics characterizing.

## ACKNOWLEDGEMENTS

## REFERENCES

Takashima, H. 1994. *TOUJIKIYUU NO KAGAKU*, Uchida Rokakuho.

Seubert, C. 2013. *Measurement and Modeling of Aluminium Flake Coatings*, BYK Gardner User Meeting Presentation Document.

Taguchi, S. 2013. *Surface Structure and Color of Chogin- and Mameitagin-coins Used in the Edo Period*, AIC2013 Proceedings vol.4:1493-1496.

Robert, H. 1987. *Confocal scanning laser ophthalmoscope*. Applied Optics, vol.26, issue 6:1492-1499.

Brakenhoff, GJ. 1988. *3-dimensional imaging of biological structures by high resolution confocal scanning laser microscopy*, Scanning Microscopy, vol.2:33-40

*Address: Masayuki OSUMI, Office Color Science Co., Ltd.,*
*Shinyokohama 3-20-12 Shinyokohama Bosei Bld. 402, Kuhoku-Ku*
*Yokohama City,222-0033, JAPAN*
*E-mails: masayuki-osumi@nifty.com*

# Measuring skin colours using different spectrophotometric methods

YuZhao WANG,[1] Ming Ronnier LUO,[1,2]* XiaoYu LIU,[1,3] HaiYan LIU,[4] and BinYu WANG[4]

[1] State Key Laboratory of Modern Optical Instrumentation, Zhejiang University, Hangzhou, China

[2] School of Design, University of Leeds, UK

[3] College of science, Harbin Engineering University, Harbin, China

[4] Thousand Lights Lighting (changzhou) Limited, Changzhou, China

*m.r.luo@leeds.ac.uk

## ABSTRACT

This study investigates the skin colours. The goal is to understand the skin colour difference between different races, between genders, between different positions, and between different measuring methods. 47 observers from four skin groups were measured in terms of their spectral reflectance using 5 methods: two spectrophotometers, one tele-spectroradiometer, one camera and visual method. The data were analyzed and all the differences were successfully revealed. Also, the uncertainly of each method's uncertainty was established. Only the results of spectrophotometric data were reported. The results reveal the systematic trends between different body locations, between different genders, between skin groups and between spectrophotometers having different geometries.

## 1. INTRODUCTION

The topic of measuring skin color has long been extensively studied due to the strong interests from the photographic, digital imaging, cosmetic, medical applications. However the measuring methods and objectives of different applications are very different. For example, the contact method like spectrophotometer has been widely used for medical to detect skin related diseases and graphic applications for clour reproduction and communication. The non-contact method has been used for the appearance related application such as cosmetic, Chinese medicines, skin lighting. Also, with different illumination/viewing geometry, the measurement results could be quite different (Sun and Fairchild, 2001; Xiao, et al, 2012). However, in some of the databases such as SOCS (ISO, 1998) the measurement results were obtained using different methods. This would lead to quite different results for the same sample. In order to establish standard in this regard, basic study should be done to reveal the measuring difference between different methods. In this paper, we will discuss about the characteristics of human skin colour and the difference of different measurements.

## 2. METHOD

In the present study, four different measuring methods, five different measuring devices and tools were used. They include 3 non-contact methods (a digital camera, a skin colour chart for visual assessment, a spectroradiometer), and 2 contact methods including 2 spectrophotometers having different geometries: 45º:0º and di:8º. A D65 fluorescent simulator hand on the ceiling was used to illuminate the subject for visual assessment.

In total, 47 subjects from four skin groups participated in the experiment: 20 Chinese, 10 Pakistanis, 10 Caucasians, 5 Africans and 2 Sri Lankan. They were renamed as Chinese, Sub-Asian, Caucasian and Dark skin groups. Note the skin colours of Sri Lankan and African showed the darkest colours so that the name Dark was used. For each subject and each method except the visual match, eight locations of the body were measured: forehead, right cheek, left cheek, hand back, fist back, palm, inner forearm and outer forearm. For the visual match against a Pantone skin chart, three different observers measured only the forehead and the right cheek separately. In total, 408 data were obtained. It was found that some large difference between the contact and ono-contact methods, only the results based on the two spectrophotometers differed in illumination\viewing geometry (45º:0º and di:8º) were compared in this study. Methods from other methods will be reported elsewhere

## 3. RESULTS AND DISCUSSION

### 3.1 Colour Variation between Different body Locations

Figure 1 shows the results from the di:8º geometry. The results measured using the 45º:0º geometry were very similar. In Figure 1, the mean results from all the 20 Chinese subjects and plot them in CIELAB $a^*$-$b^*$ and $L^*$-$C_{ab}^*$.
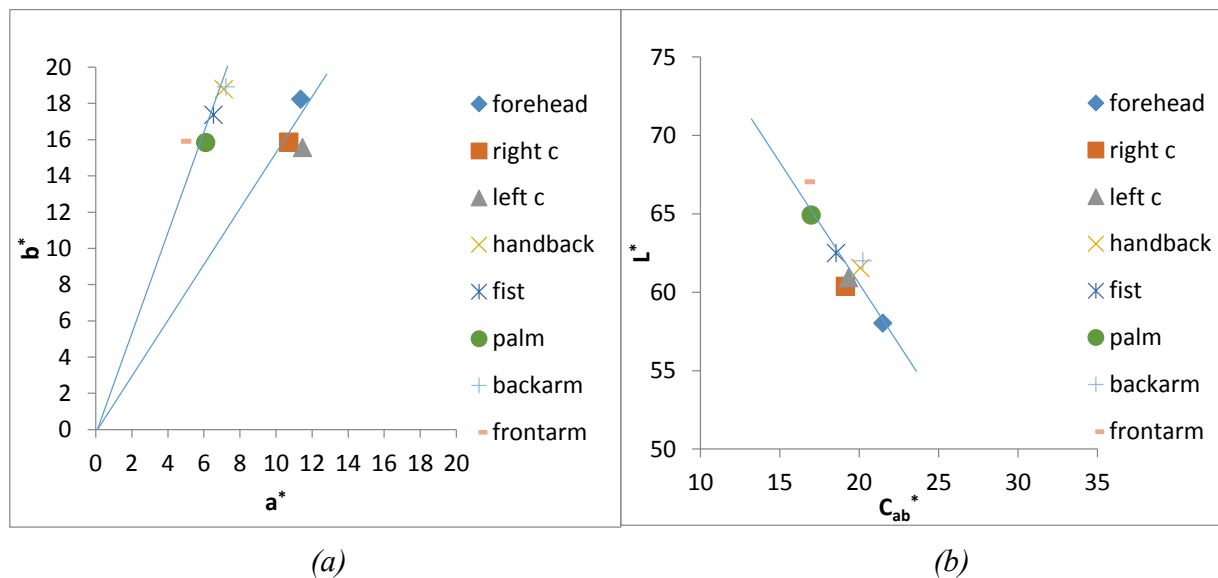


*(a)*        *(b)*

*Figure 1: Chinese averaged data in a) in $a^*$-$b^*$ plane, and b) $L^*$-$C_{ab}^*$ plane*

From Figure 1a, some systematic patterns can be seen. All the colours had hue angles red-yellow region. The data from eight locations are divided into two groups: one group contains all facial colours (forehead, right cheek and left cheek), while the other group contains all arm colours (hand back, fist, palm, outer forearm and inner forearm.) And within each group, the colours were very close in hue angle. It can be seen that arm colours are yellower than facial colours. This is expected due to the former colours are less exposed to the sun.

Figure 1b plots the same data in $L^*$-$C_{ab}^*$ plane. It can be seen that all colours lie in a more or less straight line with an intercept to the $L^*$ axis. This Line is close to the definition of

'Whiteness' as defined by NCS. Luo et al (2011) who developed whiteness and blackness model based on NCS colour atlas data. It was found that whiteness and blackness scales are visual sensations as the distance from the sample to the white and black point ($L^*$ of 100 and of 0), respectively. The shorter the distance means a whiter or blacker colour, respectively. The results in Figure 1b clearly demonstrate that the arm colours are whiter than facial colours for Chinese subjects. A whiter colours also mean lower Chroma and higher lightness colours. This systematic patterns are similar to the Caucasian and Sub-Asian groups, but not to the Dark skin group.

Figure 2 shows the averaged data of the dark skin group also from di:8° geometry. As can be seen in Figure 2b, the trend is different from that in Figure 1b. Here, all colours are located on so call blackness scale. Figure 2a shows that all colours had similar hue with facial colours slightly redder than arm colours, similar to that in Figure 1a. However, the palm colour appears the most yellower and the brightest among all colours.
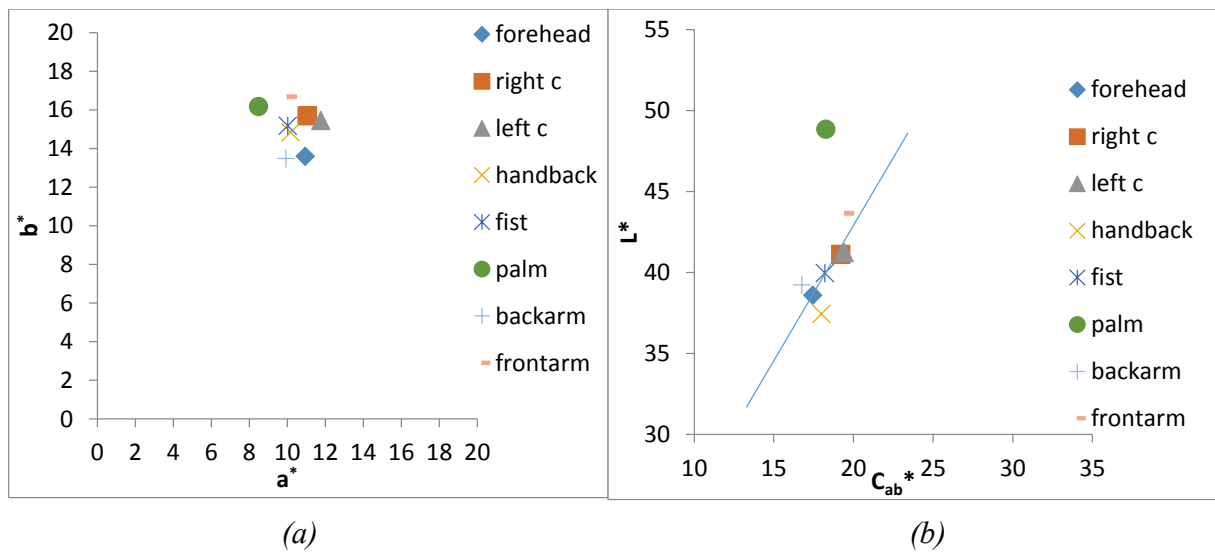


*(a)*          *(b)*

*Figure 2: Averaged data of the dark skin group in a) $a^*$-$b^*$ and b) $L^*$-$C_{ab}^*$ planes.*

## 3.2 Colour Variation between Different Subject Groups

Figure 3 plots all the colours for all subject groups in $L^*$-$C_{ab}^*$ for a) 45°:0° and b) di:8° spectrophotometers. Both figures showed the same trend, i.e. the colours following the whiteness and blackness scales. This indicates that both spectrophotometric methods gave similar results.

The most obvious trend is that Caucasian and Chinese colours have the largest lightness values, follow by Sub-Asian and the dark skin group the smallest. Also, as described earlier, the colours of the three subject groups except dark skin group, they all lie in whiteness scale. As for the dark skin group, they lie on blackness scale.
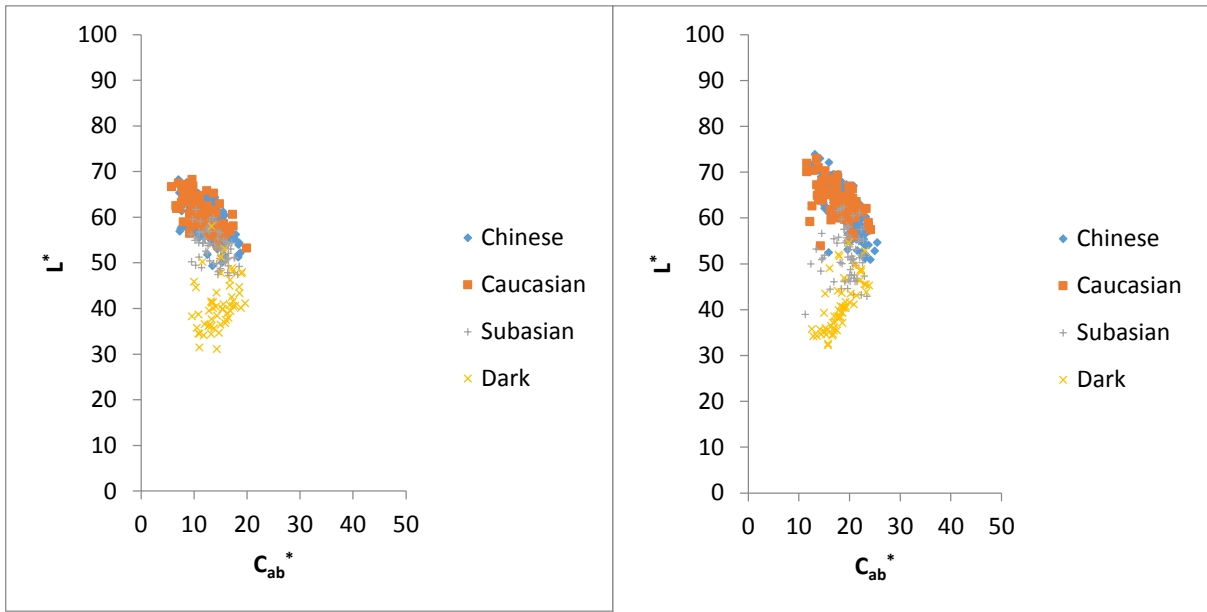
*Figure 3: All data plotted on $L^*$-$C_{ab}^*$ plane a) for $45^o$:$0^o$, and b) for di:$0^o$ instruments*

### 3.3 Colour variation between Different Genders

The results also revealed that female and male's skin colours are different. Again, same clear trend was found between the two spectrophotometric methods. Figure 4 plots the data from the Chinese group to illustrate trend in $a^*$-$b^*$ and $L^*$-$C_{ab}^*$ planes respectively. The results clearly showed that the skin colours for both genders had very similar hue but female colours are less colourful (see Figure 4a), and all data fall in the same line representing whiteness scale, with female colours whiter than male colours.
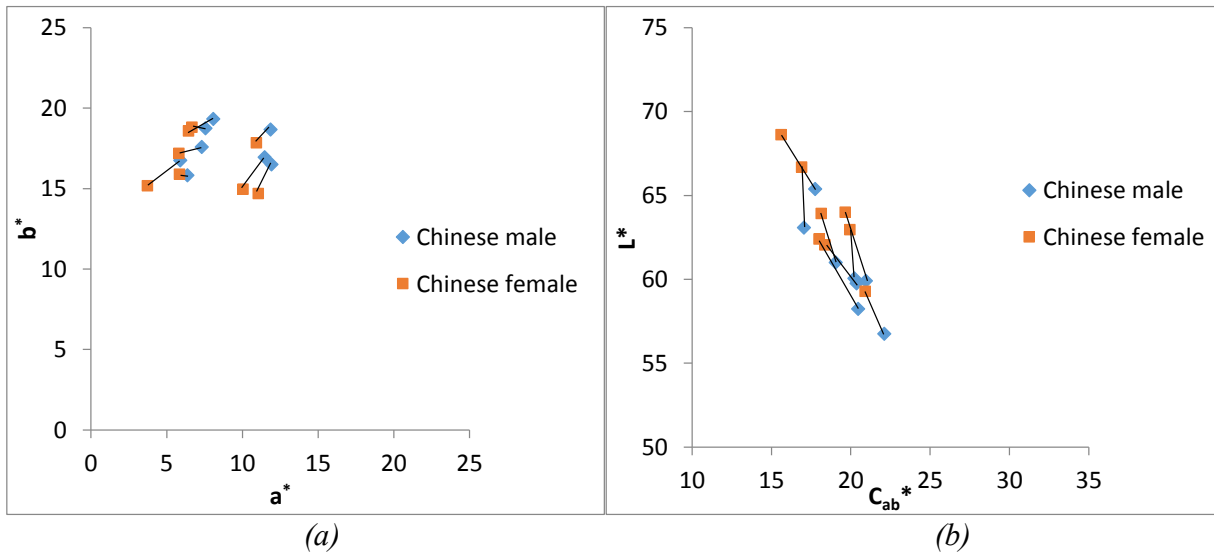


*Figure 4: Gender difference of Chinese skin colour in a) $a^*$-$b^*$ and b) $L^*$-$C_{ab}^*$ planes*

AIC2015 TOKYO - Color and Image

## 3.4 Colour variation between Different Geometry of Spectrophotometric Methods

The last comparison was made between the results from two spectrophotometers having different geometry. Figure 5 shows the mean spectral reflectance functions of all Chinese skin colours between the two spectrophotometers studied. It can be seen that the two curves agree very well until reach 550nm, for which 45°:0° are higher than di:8° geometry. Figure 6 shows the Chinese data of two measuring geometries (45°:0° and di:8°) on $a^*$-$b^*$ and $L^*$-$C_{ab}^*$ planes. Figure 6b clearly showed that the 45°:0° results are less colourful and darker than those of di:8°. This indicates that a skin colour reflecting more light in long wavelength will result in an increase in Chroma and Lightness.
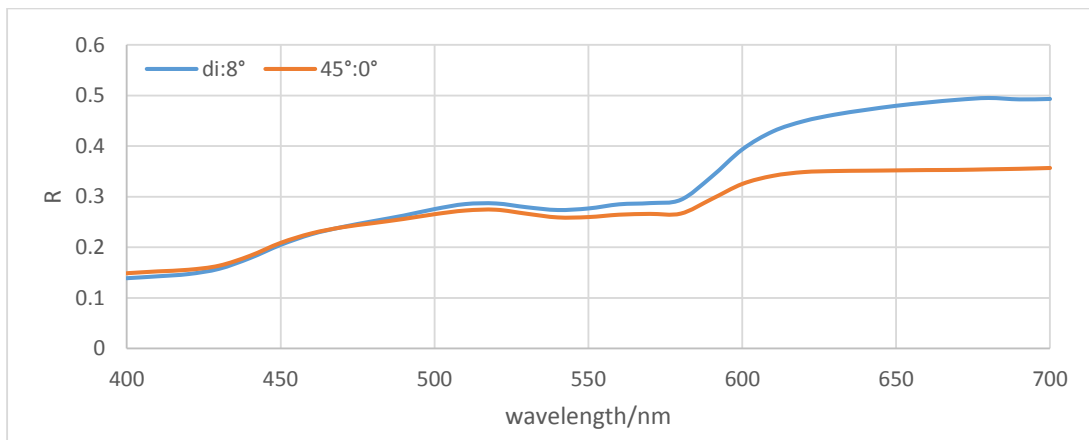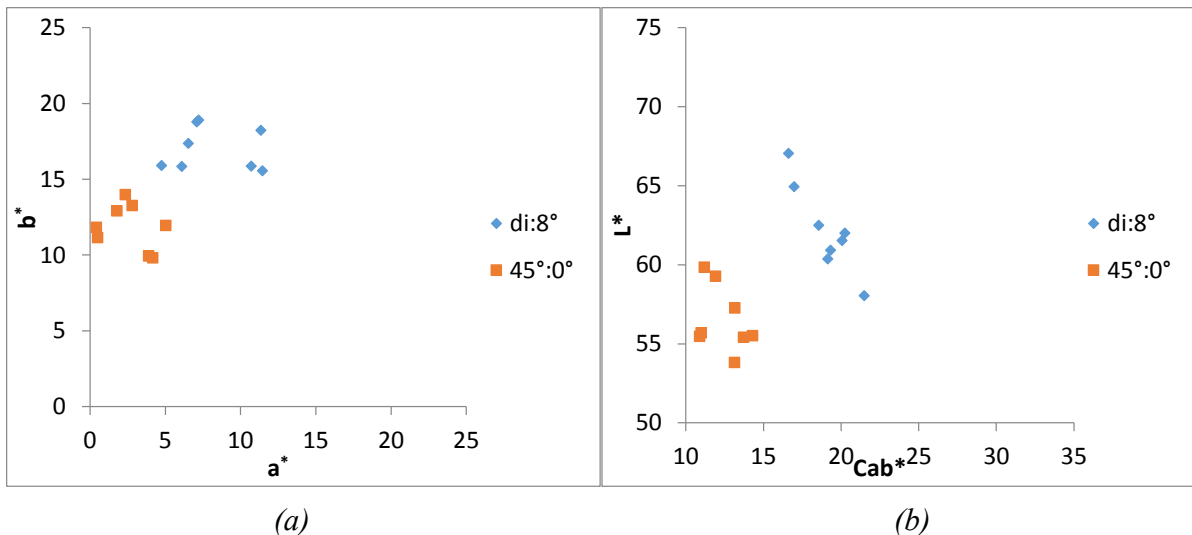


*Figure 5: Difference of two measurement*



*(a)*          *(b)*

*Figure 6: Chinese averaged data of di:8º and 45º:0º in a) $a^*$-$b^*$ plane, and b) $L^*$-$C_{ab}^*$ plane*

## 4. CONCLUSIONS

Five methods were employed to measure skin colours. It was found that the results are somewhat different. This paper is focused on the measurements based upon two spectrophotometers having geometries of 45°:0° and di:8°. The results reveal the following systematic trends:

- Comparing between different body locations, arm colours are yellower and whiter than facial colours for all skin groups except that of dark skin group, for which their colours lie in the blackness scale.

- Comparing different genders, female colours are yellower and whiter than male colours.

- Comparing different skin colours, the difference is mainly in lightness, Chinese and Caucasian gave the largest and dark group is the smallest.

- Finally, di:8° geometry data will have a higher spectral reflectance above 550nm, which results in lighter and more colourful appearance than those of 45°:0°.

## ACKNOWLEDGEMENTS

## REFERENCES

Q. Sun, and M. D. Fairchild. 2001 *Statistical Characterization of Spectral Reflectances in Spectral Imaging of Human Portraiture*, IS&T/SID Ninth Color Imaging Conference, 73-79.

Q. Sun, and M. D. Fairchild. 2001. *A New Procedure for Capturing Spectral Images of Human Portraiture*, Proceedings, AIC color01, Rochester, USA

K. Xiao, N. Liao, F. Zardawi, H. Liu, R. V. Noort, Z. Yang, M. Huang, and J. M. Yates. 2012. *Investigation of Chinese skin colour and appearance for skin colour reproduction*, Chinese optics letters, COL 10(8), 083301

M. R. Luo, G. Cui, and Y. J. Cho. *The NCS-like colour scales based on CIECAM02*, The 21th Color and Imaging Conference, 6-8 November 2013, Albuquerque, NM, USA, 177-179.

*Address: Prof. Ming Ronnier LUO, Key State Laboratory of Modern Optical Instrumentation, Zhejiang University, N.38, Zheda Road, Hangzhou, 310027, CHINA*
*E-mails: M.R.Luo@leeds.ac.uk*

# Assessing Light Appearance in Shopping Mall

Yuteng ZHU, [1] Ming YE, [1] Wenjie HUANG, [1] Muhammad Farhan Mughal, [1] Muhammad Safdar [1] and Ming Ronnier LUO, [1, 2]

[1]Key State Laboratory of Modern Optical Instrumentation, Department of Optical Engineering, Zhejiang University, Hangzhou, China

[2]School of Design, University of Leeds, Leeds, UK

## ABSTRACT

The current investigations of lighting appearance in rooms are mostly carried out in carefully controlled compartments or rooms. In order to verify the conclusions drawn from earlier studies, the lighting appearance of 21 different shops in two representative modern shopping malls in the city of Hangzhou, China, were investigated. The aim was to study the lighting appearance in real environment and eventually to establish an imaging-based method for quantifying the visual perception in real living environment, i.e. image processing software from image, via calibration, visual modelling and prediction. The CIECAM02 colour appearance model was used as a colorimetric metric to predict the room appearance. It was found that rooms with similar luminance, a light with higher CCT (Correlated Colour Temperature) appears brighter than that with lower CCT. However, as luminance levels varies from shop to shop in practical environment instead of being constant, higher CCT is perceived to be more yellowish but not occur to be brighter in our experiment. The comparison of room appearance between CIECAM02 prediction and visual assessment was shown. It was found that CIECAM02 predicts well for colorfulness and hue composition but not brightness in real rooms. An extension equation was used to adjust the brightness scale of CIECAM02 and the new model turned out to predict brightness well.

## 1. INTRODUCTION

Lighting appearance in rooms is of great importance for lighting research. Most of the previous works on lighting appearance were conducted in well-controlled environment, like Li et al. (2014) and Ohno and Fein (2014) in a room, and Rea and Freyssinier (2013) in a viewing cabinet. There is a need to investigate the earlier results in controlled environment to be agreed with those from the real environment, for which mixed lightings frequently take place. In this paper, the experimental data and analysis in scaling room appearance of modern shopping malls in city will be provided. The investigation of lighting appearance in shops can offer the basis for applying colour science in real environments.

## 2. METHOD

### 2.1 Overviews

In the current study, the experiment was conducted in 21 shops of two modern shopping malls to look into the lighting appearance. Both physical measurement and psychophysical assessment were carried out simultaneously.

## 2.2 Experimental shops

The categories of shops included costume, shoes, cosmetics, jewellery, watches and food products with different styles of decoration and ambiance. Figure 1 shows the experimental situation in a shop. A large size white cardboard ($1.2 \times 0.8$ m$^2$) attached with an Xrite Macbeth ColorChecker Chart was used to be placed in front of a region representing typical illumination area.
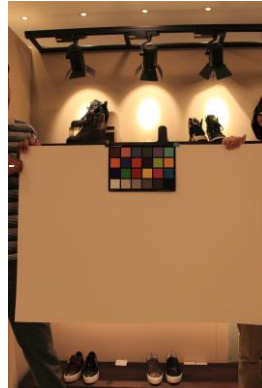


*Figure 1: An example of experimental situation in a shoes store.*

A PhotoResearch PR670 tele-spectroradiometer (denoted as TSR hereafter) was used to measure luminance, CCT, SPD, u'v' coordinates. The cardboard had L*, a*, b* values of 80.8, -0.25 and 0.19 under D65 and CIE 1964 standard colorimetric observer. Figure 2 shows the percentages in ranges of CCT, luminance, CIE-Ra and lighting technologies investigated. It can be seen that the CCTs are in the range of 2500 to 4000K. This indicates that most shops apply a yellowish and warmer ambiance to create a 'comfort' environment as reported by Liu et al. (2014).The luminance range is mainly between 80 cd/m$^2$ and 200 cd/m$^2$. The colour rendering values in CIE-R$_a$ in shops are reasonably high, i.e. mostly above 80. Many shops apply different lighting technologies to produce special ambient effect to illuminant their products. Furthermore, the LED lightings have been well populated over 65%. The concept of energy conservation has been well received by the modern shopping mall.
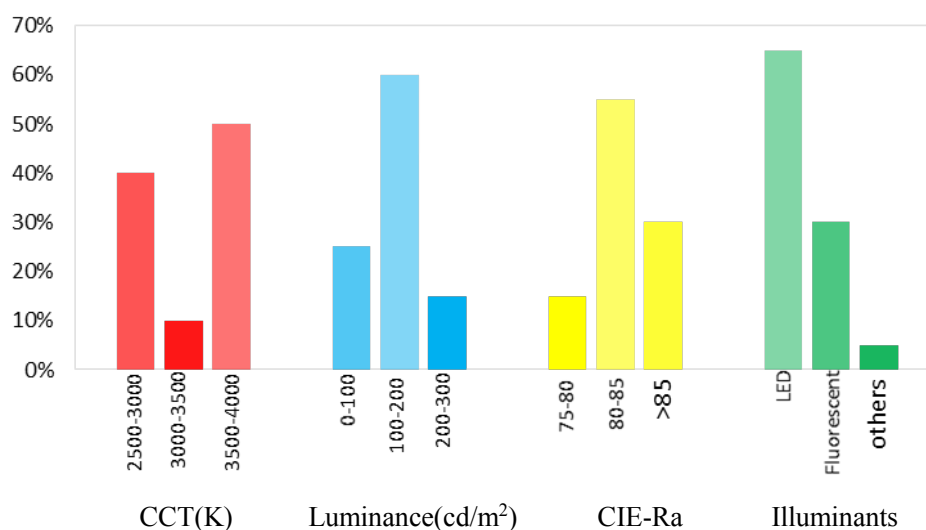


*Figure 2: The distribution of CCT, luminance, CIE-Ra and the percentages of different illumination technologies.*

## 2.3 Categorical judgement

The categorical judgement was used to describe light appearance in shops by three normal colour vision observers in the psychological experiment. The attributes of brightness and colourfulness were assessed using a 6-point categorical scale in terms of word-pairs (dark-brightness and not colourful - colourful describe for brightness and colourfulness, respectively). Taking brightness as an example, the scores are -3) 'very dark', -2) 'dark', -1) 'a little dark', 1) 'a little bright', 2) 'bright' and 3) 'very bright'.

Hue composition is an attribute for colour perception of the reflected lights from the white board (see Figure 1). A colour is described as a composition of two unique colours, red-yellow, yellow-green, green-blue or blue-red (see Figure 3). The observers were asked to give the percentage of two neighbouring unique colours to match their colour perception of light appearance in rooms.
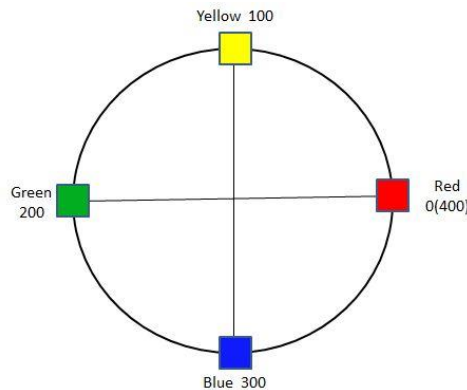


*Figure 3: Hue circle with four unique colours.*

## 2.4 Experimental Procedure

As mentioned earlier, a white cardboard having a size of 1.2×0.8 m$^2$ was used to measure the reflected lights, with a distance of 2 meters from the measuring devices or observers' position. Firstly, an image was captured by a Canon digital camera with an Xrite Macbeth ColorChecker Chart on the surface of the white cardboard. Then the lighting parameters, were measured by the TSR. In the visual assessment experiment, three normal colour vision observers scaled the brightness, colourfulness and hue composition of the light appearance after a 2 minutes' adaption.

## 3. RESULTS AND DISCUSSION

### 3.1 The effect of CCT on the attributes of appearance

Before data analysis, the scales were first transformed from -3 ~ 3 to 0 ~ 6 using an offset and the percentage of hue composition was transformed into 0 - 400 hue quadrature (see Figure 3). The relationship between CCT and appearance attributes, including brightness, colourfulness and hue composition was analysed. It can be seen that the perceived brightness is not proportional to luminance (see Figure 4a) as CCT and luminance have a combined influence on the attribute of perceived brightness. In order to study the CCT effect on perceptual brightness, data with similar luminance were selected and plotted in Figure 4b. The trend is obvious that a higher CCT makes the room appear brighter.
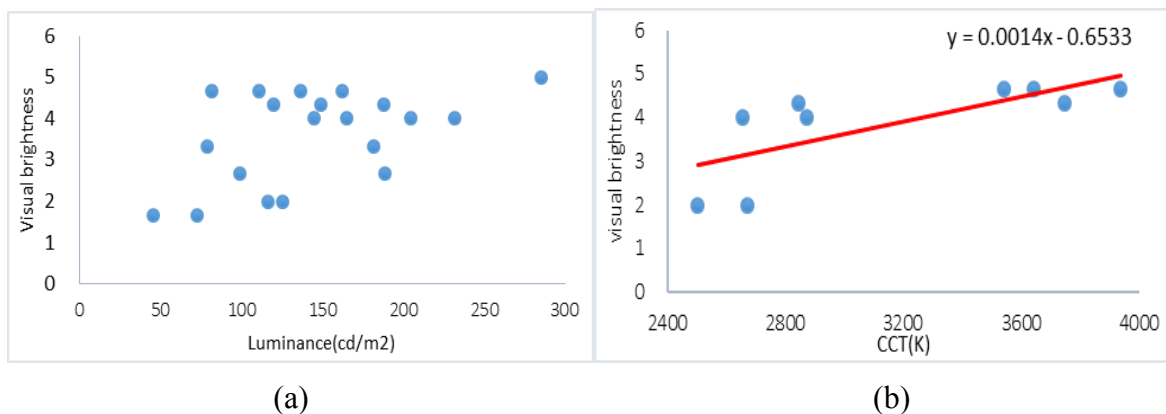
|         |         |
|:-------:|:-------:|
| (a)     | (b)     |

*Figure 4: a) The relation between luminance and visual brightness, b) CCT effect on visual brightness for similar luminance data.*

The effect of CCT on colorfulness was also analyzed (see Figure 5). The results showed that a shop with a higher CCT would appear less colorful and more likely to be perceived as neutral white. The reason can be that for CCT below 3500K, lower CCT looks more yellowish while higher CCT is closer to white and appears less colorful. This agrees with that found by Li et al (2014).
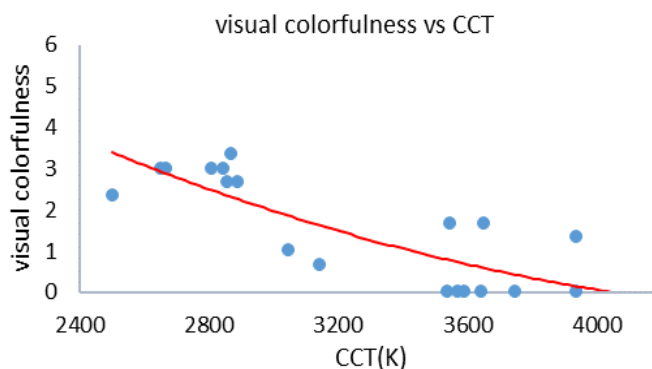


*Figure 5: The relationship between CCT and visual colorfulness.*

### 3.2 The comparison of visual perception and CIECAM02 prediction

The CIECAM02 model (CIE, 2004) was utilised to predict visual perceptions on brightness, colorfulness and hue composition as well. The comparison of the predictions and visual brightness, colorfulness and hue composition results are shown in Figures 6 and 7 respectively. It shows the CIECAM02 predicts well to the colorfulness and hue composition results but not to the brightness results.



*Figure 6: The relationship between CIECAM02 predicted and visual brightness.*

AIC2015 TOKYO - Color and Image

*Figure 7: The relationship between CIECAM02 predicted and visual colorfulness (left) and hue composition (right).*
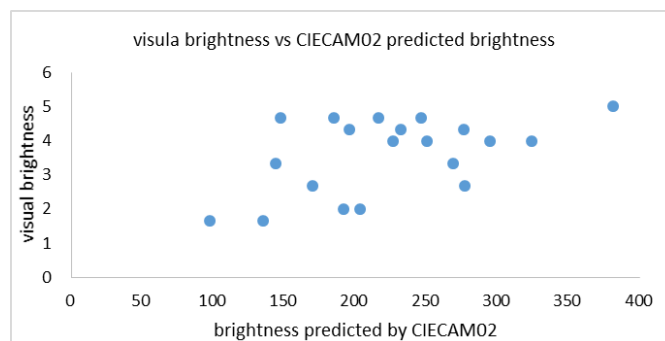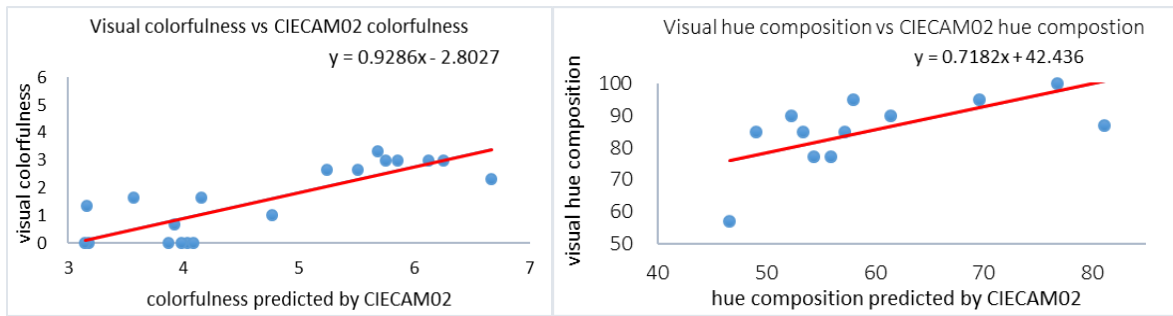
## 3.3 The modified CIECAM02 in consideration of CCT effect on visual brightness

In the CIECAM02 model, CCT has no impact on brightness prediction. However, Figure 4b strongly reveals a trend that higher CCT leads to a brighter perception. So an extension, a linear function normalized at 2850K as given in equation (1) was applied.

$$Q' = Q \times (4.2 \times 10^{-4} \times T - 0.2) \qquad (1)$$

where T means CCT value, Q is the brightness computed by the original CIECAM02 and Q' is the brightness by the modified model. According to Eq. (1), CCT was then implemented as a variable for brightness prediction. The result demonstrates that the new model predicts the brightness well against experimental visual data comparing Figures 8a and 8b.



(a)           (b)
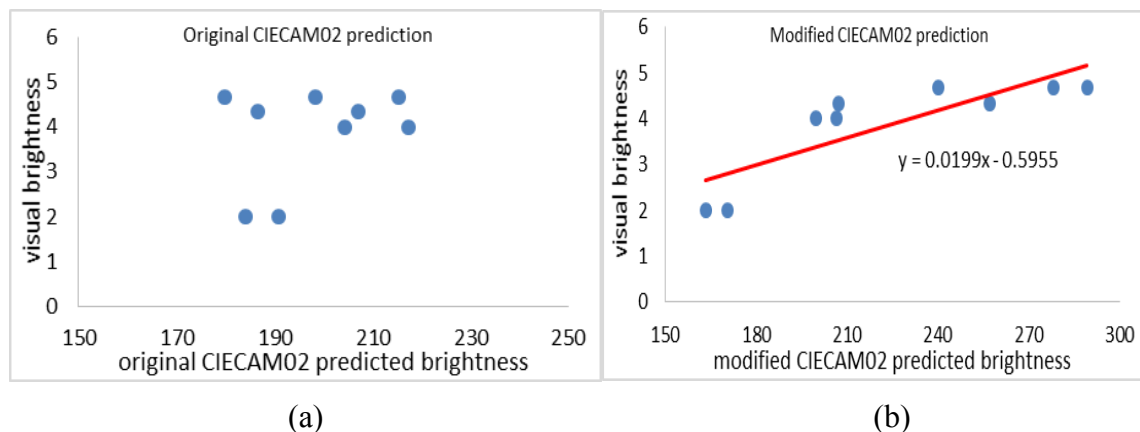
*Figure 8. a) The relation between original CIECAM02 brightness prediction and visual brightness, b) modified CIECAM02 brightness prediction against visual brightness.*

## 4. CONCLUSIONS

In this paper, the appearance of lighting in shopping malls has been investigated via physical and psychophysical measurements. The CIECAM02 model was applied to predict the perceptual attributes and a comparison of visual data and prediction data was made. The results showed that CCT and luminance had a combined effect on the perception of brightness. With similar luminance level, a light with higher CCT made the room to be perceived brighter and less colorful. The CIECAM02 model predicts well on colorfulness and hue composition but not brightness. Hence, an extension of the model was applied

considering the effect of CCT and it turned out to fit quite well with visual brightness perception.

## ACKNOWLEDGEMENTS

## REFERENCES

Liu, X. Y., M. R. Luo and H. Li. 2014. *A study of atmosphere perceptions in a living room*, Light. Res and Tech., DOI: 1477153514528934, published on line in April, 2014.

Li, H., M.R. Luo, X.Y. Liu, B.Y. Wang and H.Y. Liu. 2014. *Assessing appearance in a lite room.* Private communication.

Rea, M.S. and J.P. Freyssinier. 2013. *White lighting*, Colour Research and Application, 38(2), 82-92.

Ohno, Y. and M. Fein. 2014. *Vision experiment of acceptable and preferred white light chromaticity for lighting.* Proc., CIE 2014 Lighting Quality and Energy Efficiency, 192 – 199.

CIE. 2004. CIE 159:2004. *A colour appearance model for colour management systems: CIECAM02*, Vienna.

Hunt, R.W.G. and M.R. Pointer. 2011. *Measuring Colour.* New York: John Wiley & Sons.

Hinks, D. and S. Renzo. (2011), *Review of retail store lighting: implications for colour control of products*. Coloration Technology, 127: 121–128. doi: 10.1111/j.1478-4408.2011.00286.x

Li, H., M.R. Luo and X.Y Liu. 2014. *Scaling appearance in a room illuminated by LED sources*. CIE 2014; x039:63-72.

Muhammad, S., M.R.Luo, H. Li, L.H. Xu and Y. Yang. 2014. *An imaging method for measuring room appearance*. 7th CJK Lighting Conference.

*Address: Prof. Ming Ronnier LUO, Key State Laboratory of Modern Optical Instrumentation, Zhejiang University, N.38, Zheda Road, Hangzhou, 310027, CHINA*
*E-mails: M.R.Luo@leeds.ac.uk*

# Pupillary light reflex associated with melanopsin and cone photorecetors

Sei-ichi Tsujimura,[1] Katsunori Okajima,[2]

[1] Faculty of Sciences and Engineering, Kagoshima University, Japan

[2] Faculty of Environment and Information Sciences, Yokohama National University

## ABSTRACT

Retinal ganglion cells containing the photopigment melanopsin are intrinsically photosensitive in primates. Several studies have shown that the intrinsically photoreceptive retinal ganglion cells project to the pupillary control center in the pretectum. Here, we independently stimulated human ipRGCs and cones, and investigated how signals driven by ipRGCs and cone-mediated signals contribute to the pupillary control mechanism. A four-primary illumination system that enables independent stimulation of each photoreceptor class was used to present the following three types of test stimuli. The transient pupil responses to these stimuli were measured. It was found that the transient pupil response to ipRGC stimuli had a longer latency than the responses to the LMS-cone and light flux stimuli. The longer latency suggests that signals from ipRGCs in the non-image forming pathway travel more slowly than that of the LMS achromatic mechanism in the image forming pathway.

## 1. INTRODUCTION

The intrinsically photoreceptive retinal ganglion cells (ipRGCs), which contains photopigment melanopsin, mediate signals to the pupillary control center in the pretectum. The ganglion cell is photosensitive and receives signals from classical photoreceptors. Although both cone- and ipRGC-mediated signals contribute to pupillary light reflex it is difficult to investigate how these signals are summed. Here, we independently stimulated human cones and ipRGCs, and investigated how cone- and ipRGC-mediated signals contribute to the pupillary control mechanism.

## 2. METHODS

### 2.1 Apparatus

An eight-channel, four-primary illumination system (Brown *et al.*, 2012) that enables independent stimulation of each photoreceptor class was used to present the following three types of test stimuli: one varying L-, M- and S-cone stimulation only without change in stimulation of ipRGCs (LMS-cone stimulus), another varying radiant flux of the stimuli without change in spectral composition which reduced/increased the radiant flux uniformly at all wavelengths (Light flux stimulus) and the other varying ipRGC stimulation without change in stimulation of L-, M- and S-cones (ipRGC stimulus). The intense test and adapting fields were used which minimized the involvement of rods. The test and adapting fields had a CIE coordinate of (0.57, 0.36) and a luminance of 1,221 cd m$^{-2}$ for the test field and 355 cd m$^{-2}$ for the adapting field, respectively. The transient pupil responses to these stimuli were measured.
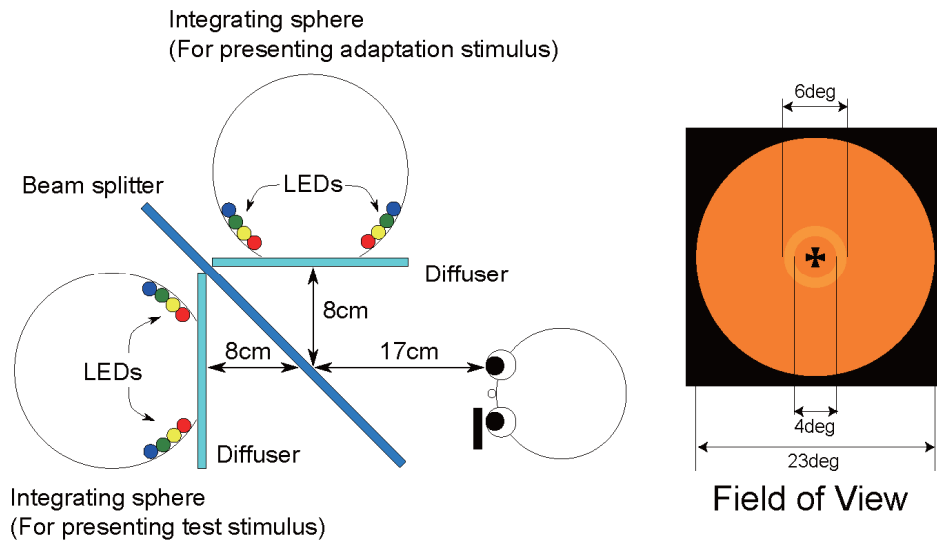
Figure 1 Eight channel, four-primary stimulation system

## 2.2 Spectral sensitivity curve for melanopsin ganglion cell

The test stimuli were generated based on the cone and ipRGC spectral sensitivities. The 10-deg cone fundamentals proposed by Stockman et al. (Stockman et al., 1999, 2000) were used to calculate the stimulation of Long-wavelength sensitive cone (L cone), Middle-wavelength sensitive cone (M cone) and Short-wavelength sensitive cone (S cone). We estimated the spectral sensitivity curve of ipRGCs based on a pigment template nomogram with a peak wavelength, $\lambda_{max}$, of 480 nm and ocular optical properties. The lens and macular pigment density spectra were those of Stockman et al. The fraction of incident light absorbed by the receptor depends on peak axial optical density ($D_{peak}$). We tentatively chose 0.1 as the $D_{peak}$ for ipRGC. We assumed that neither the S cones nor the ipRGC affect the photopic luminance efficiency function (i.e., luminance), despite using photopic luminance units (cd m$^{-2}$). Similar to S-cone stimulation (Boynton and Kambe, 1980), one ipRGC stimulation was defined as the level of ipRGC stimulation produced by an equal energy spectrum of luminance 1 cd m$^{-2}$. The resultant spectral sensitivity function of ipRGC in a 10-deg field displayed a peak of 872 at a wavelength of 493 nm. The shape of spectral sensitivity curve we estimated is similar to that proposed by Lucas and his colleagues (Enezi et al., 2011). We further considered the human macular pigment density at 10-deg for the estimation.

## 2.3 Procedure

Five visually corrected observers (age range 21–23 years) participated in the experiment. All observers had normal color vision according to the Ishihara color blindness test. All observers gave their written informed consent, and the study was approved by the local research ethics committee. The observers were seated 25 cm from the diffuser and monocularly fixated upon a black Maltese cross, which subtended 1.8° and was always present at the center of the diffuser. After an initial adaptation period of 5 min, we began a session of experimental trials. We used a ramp stimulus presented for 500 ms.

The pupil of the right eye was imaged using a video camera (Dragonfly, Point Grey Research, Canada) located 0.5 m from the observer and 28° nasal to the visual axis. The video image was fed into a personal computer and analyzed using LabVIEW and IMAQ Vision software (National Instruments) at a frequency of 60 Hz. The pupil was located using thresholding and edge detection techniques, allowing the pupil diameter to be analyzed.

## 3. RESULTS AND DISCUSSION

### 3.1 Influence of a modulation of ipRGC on amplitude of pupil response

Since both Light flux and LMS-cone stimuli modulated cones in the same way these stimuli were indistinguishable for cones. Therefore, the difference could be attributed to the difference in stimulation with or without ipRGC modulation. Pupil responses to the Light flux stimulus and to the LMS-cone stimulus were shown in Fig 2. It was found that the amplitude elicited by LMS-cone stimulus was significantly higher than that by the Light flux stimulus. The average pupil response was $0.24\pm0.06$ mm for the LMS-cone stimulus, $0.20\pm0.07$ mm for the Light flux stimulus and $010\pm0.04$ mm for the ipRGC stimulus. In other words, the modulation of ipRGC in Light flux stimulus influenced amplitude of the pupil response, suggesting that the ipRGC stimulation suppresses pupillary amplitude response.



Figure 2 Pupillary responses and its amplitudes to the LMS-cone stimulus (black), to Light flux stimulus (red) and to the ipRGC stimulus (blue).

### 3.2 Sluggish pupillary response to the ipRGC stimulus

Typical normalized pupil responses are shown in Fig. 3. The horizontal axis represents a time and the vertical axis represents pupil diameters in mm to the test stimuli. The black curve represents curves for the LMS-cone stimulus, the red curve for the Light flux stimulus and the blue curve for the ipRGC stimulus. It was found that the transient pupil response to the ipRGC stimulus had a longer latency than those to the LMS-cone and to the Light flux stimuli. The average pupil latencies were 814±39 ms for the LMS-cone stimulus, 821±41 ms for the Light flux stimulus and 1,377±618 ms for the ipRGC

stimulus. The longer latency to the ipRGC stimulus was consistent with those in the previous study (Lucas *et al*., 2001; Tsujimura *et al*., 2011), suggesting that the ipRGC-mediated signals in the non-image forming pathway travel more slowly than the LMS cone-mediated achromatic signals in the image forming pathway. These results suggested that the pupil responses to the LMS-cone stimulus and to the Light flux stimulus are mediated by cones and those to the ipRGC stimulus are mediated by ipRGCs.
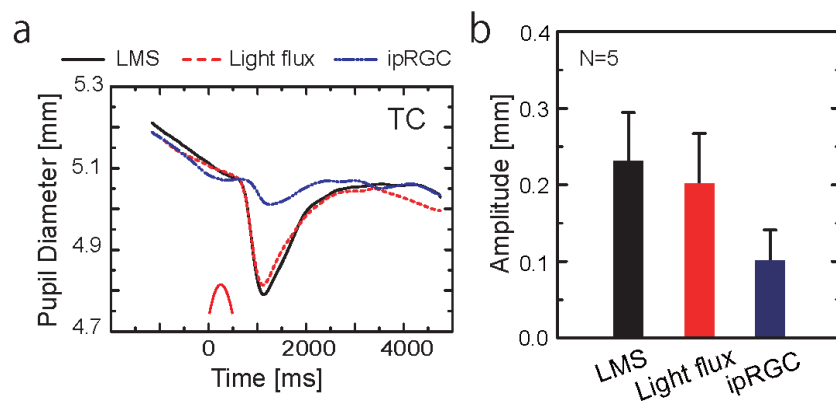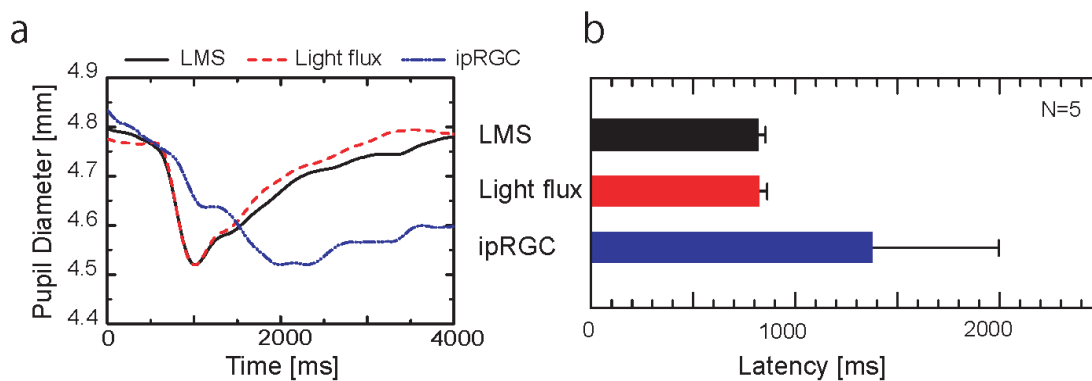


Figure 3 Normalised pupillary responses to the LMS-cone stimulus (black), to Light flux stimulus (red) and to the ipRGC stimulus (blue).

## 4. CONCLUSIONS

It was found that the transient pupil response to ipRGC stimuli had a longer latency than the responses to the LMS-cone stimulus and to the Light flux stimulus. The results indicate that we successfully demonstrated the pupillary response to ipRGCs under conditions where ipRGCs are isolated in humans. The longer latency suggests that signals from ipRGCs in the non-image forming pathway travel more slowly than that of the LMS-cone mediated signals in the image forming pathway.

## ACKNOWLEDGEMENTS

## REFERENCES

Boynton, R. M. and N. Karnbe 1980. *Chromatic Difference Steps of Moderate Size Measured along Theoretically Critical Axes*. Color Research & Application **5**(1): 13-23.

Brown, T.M.*, Tsujimura, S.*, Allen, A.E., Wynne, J., Bedford, R., Vickery, G., Vugler, A., and Lucas, R.J. 2012. *Melanopsin-Based Brightness Discrimination in Mice and Humans*. Current Biology 22, 1134-1141.*Equal contribution

Enezi, J., Revell, V., Brown, T., Wynne, J., Schlangen, L., and Lucas, R. (2011). *A "melanopic" spectral efficiency function predicts the sensitivity of melanopsin photoreceptors to polychromatic lights.* J Biol Rhythms 26, 314-323.

Lucas, R. J., R. H. Douglas, et al. 2001. *Characterization of an ocular photopigment capable of driving pupillary constriction in mice.* Nat Neurosci **4**(6): 621-626.

Stockman, A., L. T. Sharpe, et al. 1999. *The spectral sensitivity of the human short-wavelength sensitive cones derived from thresholds and color matches.* Vision Research **39**(17): 2901-2927.

Stockman, A. and L. T. Sharpe 2000. *The spectral sensitivities of the middle- and long-wavelength-sensitive cones derived from measurements in observers of known genotype.* Vision Res **40**(13): 1711-1737.

Tsujimura, S. and Tokuda, Y. 2011. *Delayed response of human melanopsin retinal ganglion cells on the pupillary light reflex.* Ophthalmic and Physiological Optics 31, 469-479.

*Address: Dr. Sei-ichi Tsujimura, Department of Information Science and Bioengineering, Kagoshima University, 1-21-40, Koorimoto, Kagoshima 890-0065 JAPAN*
*E-mail: tsujimura@ibe.kagoshima-u.ac.jp*

# Experimental Research on EEG Characteristics in Red, Green, Blue, and White Color Space consequent on the Degree of Depression

Heewon LEE[1], Hanna KIM[2], Jiseon Ryu[1], Jinsook LEE[3]

[1] Doctor Course, Dept. of Architectural Engineering, CNU, Korea

[2] Noroo Paint & Coatings Co., Ltd, NPCI, Korea

[3] Professor, Dept. of Architectural Engineering, Chungnam National University, Korea

**ABSTRACT**

This study is intending to analyze the brain wave property in color space in red, green, blue and white according to the depression level. This study conducted the experiment on 6 female subjects in their 20s~30s, and the experiment result is as follows: First, after conducting self-diagnosis check of BDI-II depression, this study divided the subjects into non-depressive group and depressive group. Then, after measuring the brain wave in color space of red, green, blue and white, this study analyzed the occurrences of RB(Relative Beta Power Spectrum), and RAB(Ratio of Alpha to Beta)indicators in the frontal lobe which has rational thought and cognitive function.

As a result of the analysis, it was found that the green and white color used in this experiment had an effect on relaxation and stability of the depressive group, but in the case of the red and blue color also used in the experiment had an inhibition effect on the depressive group's relaxation and stability; through the result, this study was able to learn that when a person makes a design of indoor color environment, the person should be careful in the use of the red, blue color.

## 1. INTRODUCTION

### 1.1 Background and Purpose of the Study

Among the factors that affect our emotions, we are living in various colors that are embedded in the spaces and objects we encounter every day. Color controls emotions and inturn changes behaviors, in addition to influencing state of mind to maintain emotional stability and impacting bodily functions including circulatory system, heartbeat, blood pressure, and tensions in the nerve system and muscles. As explained, color may provide various energy to people through its inherent wavelengths, and may maintain body and mind to be stable and balanced. Color is proactively being used in psychology, medicine, as well as marketing, emotional engineering, architecture, and industrial design, and many research are being conducted, ushering in an era of color. Such trend is especially stimulating many scientific researches to prove that color is effective in healing the body and mind. Of course, we are referring to studies on color that link human emotions to physiological reactions and brain waves.

However, looking into the preceding research works, there have been researches on depression and color, but the analytical research on brain wave in a life-size Mock-up of color space consequent on depression inventory is actually insufficient. Hereupon, this study is intending to make a comparative analysis of brain wave property in color space of

a life-size Mock-up using BDI-II(Beck Depression Inventory-II)which is the most widely used among self-report test papers developed to measure depressive symptoms.

## 1.2. Research Method & Scope

This study measured and researched the brain wave in color space consequent on the severity of depression targeting adults in their 20s~30s. This study conducted the research as shown in (Figure 1).
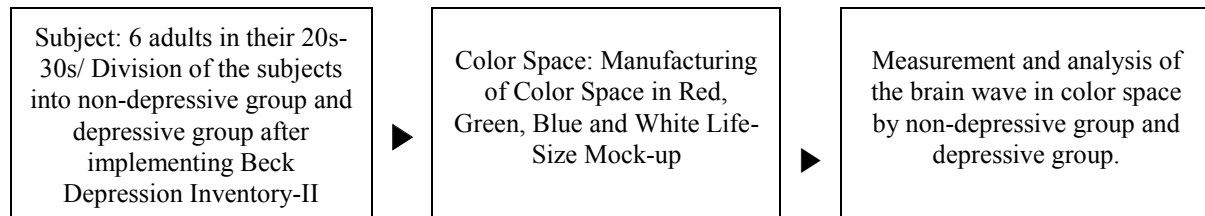
| Subject: 6 adults in their 20s-30s/ Division of the subjects into non-depressive group and depressive group after implementing Beck Depression Inventory-II | ▶ | Color Space: Manufacturing of Color Space in Red, Green, Blue and White Life-Size Mock-up | ▶ | Measurement and analysis of the brain wave in color space by non-depressive group and depressive group. |

*Figure 1. Method of the study implementation*

## 2. SPECIFICS OF THE STUDY

### 2.1 Research method

### 2.1.1 Experiment environment

This study conducted the BDI-Ⅱ Depression Inventory at a laboratory of C School. This study used the laboratory located the innermost in order to minimize interrupting factors, such as external noise at a time of testing.

The space comprised of four rooms each with 1500 ㎜×1500 ㎜×2400 ㎜ dimesions. D65 standard light source lighting devices were 600 ㎜×600 ㎜, with the light intensity of 100 ㏓. In order to minimize visual error from texture and linkage that may arise when walls are covered with colored papers, the rooms were painted in red (5R 4/14, S2070-R), green (7.5G 5/8, S2555-G), blue (7.5BG 5/8, S2555-B30G), and white(N9.5, S0500-N). By minimizing sound and light that may be distracting to the experiment, a stable environment was established, and air circulation was provided in white room in order to prevent subjects from becoming drowsy, thereby achieving an environment with minimal measurement error.

### 2.1.2. Experiment Method

At the time of BDI-Ⅱ Depression Inventory progress, this study conducted the experiment by giving subjects enough time for reading and understanding instructions related to testing before proceeding with the test on subjects.

During brain wave measurement, the subjects were guided to sit comfortably in a chair in the middle of the white room, and electrodes were attached to them. In order to reduce anxiety in an unfamiliar space, the subjects stayed in the white room for five minutes before being sent to a colored room for one minute for measurement. In order to prevent after-image effect of the previous room, they were led to the white room again for five minutes, before being sent to another colored room to have their brain wave measured as shown in (Figure 2)

*Figure 2. Brain wave measurement in each colored room*

## 2.2. Measuring Tools

### 2.2.1. Beck Depression Inventory(Beck Depression Inventory-Ⅱ: BDI-Ⅱ)

BDI-Ⅱ was created through modifying & complementing the existing BDI(which is made on the basis of depression symptoms, measuring the type and severity level of depression)according to DSM-IV's depressive disorder diagnostic criteria by Beck et al.,; there is no change in its number of questions(21) and scoring method, but most questions except a few questions were partly modified or completely changed.

In case of BDI, it evaluates the symptoms occurring during the past 1 week, whereas BDI-II is designed to evaluate the symptoms during the past 2 weeks, and each question has a sub-title specifying what is evaluated. In addition, the most noticeable change in BDI-II is that it is designed to evaluate all the decrease & increase in sleep and appetite.

### 2.2.2. Brainwave measuring test

For the brainwave measurement in this study, I used PolyG-I (Laxtha, Inc., Korea), a computerized polygraph system that can simultaneously measure the brainwave, electrocardiogram (ECG), and electromyogram (EMG) that occur in the human body. The device includes as hardware wireless brainwave measuring equipment (WEEG-8) and as software the real-time data collection and time series analysis program (Telescan). In applying electrodes for the purpose of measuring brainwave, ten-twenty electrode system of the International Federation was used to install electrodes on the pre-frontal (Fp1, Fp2), the frontal (F3, F4), the parietal (P3, P4), the Occipital (O1, O2), and the left-right earlobes (A1, A2) as shown in Table 1. To measure heartbeat, I attached a snap electrode on the wrist. The subject's brainwave signal was filtered with 0.5-50 Ηz pass filter and converted with 16bit AD (Analog-Digital converter) before the date was saved to computer for collection purpose.

### 2.3. Subject Composition

The subjects of this research included people in their twenties and thirties without a history of psychological, cranial, or optical diseases. The methodology and the goal of this research was adequately explained to them, after which they agreed to volunteer with the explicit knowledge of cautions.

After implementing Beck Depression Inventory II, this study proceeded with the brain wave experiment by dividing the subjects into non-depressive group and depressive group.

AIC2015 TOKYO - Color and Image

## 3. EXPERIMENT RESULTS AND ANALYSIS

After implementing Beck Depression Inventory II, this study proceeded with the brain wave experiment by dividing the subjects into non-depressive group and depressive group. In the brainwave experiment, brainwave variance was measured by monitoring it with the data collection and analysis program called Telescan from LAXTHA, which is a computerized polygraph system. For respective channels, the measured values were put to relative power analysis.
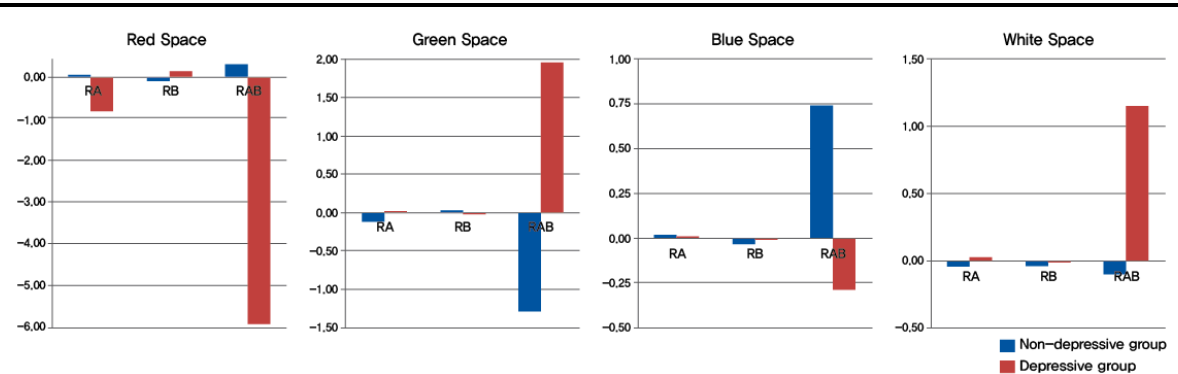


*figure 3. Graph for indicator-specific brainwave variance in different color spaces*

The analysis was performed on the brainwave indicators of RA (Relative Alpha Power Spectrum, 8-13/4-50 ㎐) that represents relaxation and stability, RB (Relative Beta Power Spectrum, 13-30/4-50 ㎐) that represents tension, alertness, and concentration, and RAB (Ratio of Alpha to Beta, 8-13/13-30 ㎐) that represents the alpha/beta ratio.

(Figure 3) shows in a graph the results of the brainwave measured in response to color spaces in the frontal that has rational thinking and cognitive ability for different indicators.

## 4. CONCLUSIONS

This study intended to look into the property of brain wave in color space in red, green, blue and white between the non-depressive group and depressive group consequent on Beck Depression Inventory-II results.

The research progress was conducted in three stages as follows:

1) In an effort to divide the subjects into non-depressive group and depressive group through Beck Depression Inventory-II, this study conducted the test on 6 adults in their 20s~30s, and measured their brain wave using PolyG-I.

2) This study conducted brain wave measurement in color space consisting of red(5R 4/14, S2070-R), green(7.5G 5/8, S2555-G), blue(7.5BG 5/8, S2555-B30G), white(N9.5, S0500-N).

The analysis result consequent on research progress is as follows:

The following is the result of the experiment, in which we measured brain wave in the frontal lobe of the subjects, which is responsible for rational thinking and cognitive abilities. In the red room, non-depression group showed increased RA and RAB indices and decreased RB index, while depression group displayed decreased RA and RAB, and increased RB index. In the green room, non-depression group had decreased RA and RAB and increased RB, while depression group had increased RA and RAB indices and decreased RB index. In the blue room, non-depression group had increased RA and RAB

indices, and decreased RB index, while depression group had increased RA index and decreased RB and RAB index. In the white room, all indices decreased for non-depression group, but depression group had increased RA and RAB indices and decreased RB index.

We learned that green and white used in the experiment had a relaxing and stabilizing effect for depression group, while red and blue used prevents such effects for depression group. We concluded that color environment designers must be wary of using red and blue for interior, and we learned that color stimulation affects brain waves depending on the degree of depression.

This study has a limit to generalization of the number of subjects. Accordingly, it is judged that there is a need for follow-up research on diverse subjects and experimental spaces in the light of the number of subjects, their age and gender, etc.

## REFERENCES

Myung-sig KIM, Im-soon LEE, Chang-seon LEE. 2007. *The Validation Study Ⅰ of Korean BDI- Ⅱ: In Female University Students Sample.* The Koeran Journal of Clinical Psychology 26(4) 997-1014.

Hyung-mo Sung, Jung-bum KIM, Young-nam PARK, Dai-seok BAI, Sun-hee LEE, Hyun-nie AHN. 2008. *A Study on the Reliability and the Validity of Korean Version of the Beck Depression Inventory- Ⅱ(BDI- Ⅱ).* Journal of the Korean Society of Biological Therapies in Psychiatry 14(2) 201-212.

Ji-A LEE. 2010. *Study on Color Preference and Color Sensibility of Depressed Patients. Master's Thesis.* Graduate School of Health Science&Welfare Management Pochon CHA University

Jin-sook LEE, Hee-won LEE, Hanna KIM, Ji-seon RYU. 2014. *A Basic Study on the Physiological Responses to the Color Stimulation in Red, Blue, Green, and White in Accordance with Youth's Concentration.* Collected Paper from Korea Society of Color Studies. 28(1) 177-86.

Heun-joo HONG, Soo-mi KIM, Beom-cheon LEE, Dong-hee LEE, and Seong-gwan AHN. 2009. *The Influence that Color Therapy Exercises on Stress and Brainwave Variation.* Journal of the Korean Society for Aesthetics and Cosmetology. 7(1) 51-59.

Beck TA, Streer RA, Brown GK. 1996. *Maunal for the BDI- Ⅱ.* The psychological corporation. San Antonio, TX

*Address : Heewon LEE, Dept. of Architectural Engineering, College of Engineering, Chungnam National University, 99 Daehak-ro, Yuseong-gu, Daejeon 305-764. Korer E-mails:bluesky4r@paran.com, hnkim@noroo.com,woman602@hanmail.net ,js_lee@cnu.ac.kr*

# Hue-Tone Representation of the Nayatani-Theoretical Color Order System

Hideki SAKAI

Graduate School of Human Life Science, Osaka City University

## ABSTRACT

The Nayatani-Theoretical (NT) color order system is a new opponent-color-type system proposed by Nayatani based on his color-appearance and color-vision studies in 2003. The NT system has color attributes, whiteness, blackness, grayness, chroma and opponent-hue; the colors with the same attributes irrespective of hues have the same perceived whiteness or blackness (i.e., perceived lightness), the same degree of vividness, and also the same color tone. However, its tones are not explicitly stated in the NT system so far. Therefore, we introduced the categorical tone representation to the NT system. This makes the NT system more useful for various purposes. The tone concept has been widely used in the artistic fields of painting and color design from the old days. The NT tone categories introduced in this paper can be used for selecting the color combinations in those artistic fields. In the color science field, the color stimuli extracted based on the tone categories are frequently used in a wide variety of sensory testing of vision. The NT tones are also suitable for such scientific purposes, because its tones are derived based on the color-appearance studies and have well-defined colorimetric values. This colorimetric background will be of help when analyzing the sensory data.

## 1. INTRODUCTION

A lot of color order or color designation systems have been proposed from past to present (Fairchild 2013). We now have various types of color systems, and some of them are widely used. However, it seems that we have not yet found an ideal one. Even widely used systems have pros and cons. There is still more room for improvement. Thus, we expect many more new candidates will be proposed in the future.

In such a situation, the Nayatani-Theoretical (NT) color order system was proposed by Nayatani based on his color-appearance and color-vision studies in 2003 as a new candidate (Nayatani 2003, 2004). The NT system designates a color with the attributes, whiteness $w$, blackness $bk$, grayness $gr$, chroma $C_{NT}$, and opponent-hue $H_{NT}$. The colors with the same NT attributes [$w, bk, gr, C_{NT}$] irrespective of hues [$H_{NT}$] have the same perceived whiteness or blackness (i.e., perceived lightness), the same degree of vividness, and also the same color tone (Nayatani and Komatsubara 2005). This is the primary feature of the NT system, that is, the inclusion of the color tone concept in it. However, its tones are not explicitly stated in the NT system so far. Therefore, in this paper, we introduced the categorical tone representation to the NT system with hue divisions. We believe that this makes the NT system more useful for various purposes.

## 2. BRIEF SUMMARY OF NT SYSTEM

### 2.1 Structure of NT system

The color solid of the NT system is shown in the Figure 1. It consists of six primary colors, red (R), green (G), yellow (Y), blue (B), white (W), and black (Bk). It adopts three opponent-colors axes, not only red-green (R-G) and yellow-blue (Y-B), but also white-black (W-Bk). It has the reference gray (Gr) in the center.
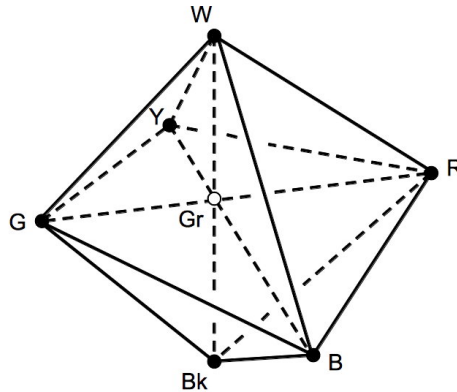


*Figure 1: The color solid of the NT color order system.*

The system has several unique features. It introduces an orthogonal coordinate using the city-block metric (Nayatani 2002) as shown in the Figure 2. It designates a color using whiteness *w*, blackness *bk*, grayness *gr*, chroma $C_{NT}$ and hue $H_{NT}$. The color P in the Figure 2 (1), for example, has the attributes [*w*=0, *bk*=0, *gr*=0, $C_{NT}$=10, $H_{NT}$=Y100]. The maximum chroma, i.e., the chroma of pure color (PC), is different for different hue $H_{NT}$ (Nayatani 2004). It clearly defines the grayness attribute, which is not defined explicitly in many other color order systems such as Munsell system and Natural Color System (Nayatani and Sakai 2014).
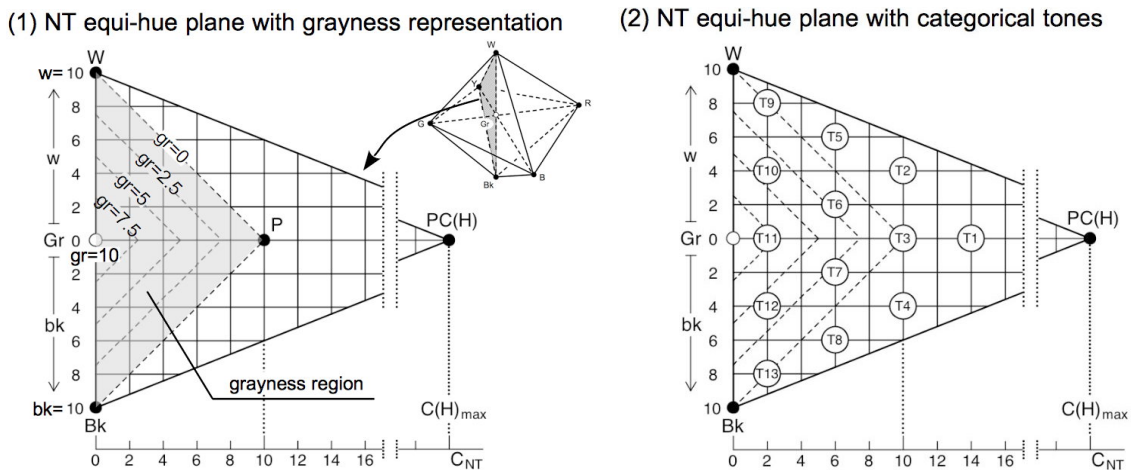


*Figure 2: Equi-hue plane of NT system. (1) Grayness region, (2) categorical tones.*

The NT system belongs to the category of Color Appearance Space (CAS) as discussed in the previous paper (Nayatani and Sakai 2007) and the name "Theoretical" comes from the fact that it can be theoretically derived from any Uniform Color Space (UCS) using the chromatic strength (CS) function and unique hue data. The concept of chromatic strength was originally proposed by Evans and Swenholt (1967) and it contains essential

AIC2015 TOKYO - Color and Image

information on color appearance. Chromatic strength function and unique hue data are the necessary elements of NT system.

## 2.2 Derivation of NT color attributes

In this paper, CIELAB with D65 white point and 2-deg. observer is used as a base UCS. For the chromatic strength function, $CS(k_1 k_2; h_{ab})$ is used (Nayatani 2004). For the primary opponent-color hues, the hue angles $h_{ab}$ = 26, 91, 162, and 262 degrees are used as shown in the Table 1, which correspond approximately to the Munsell hues 5R, 5Y, 5G, and 2.5PB, respectively. Note that, in the preceding papers, the Munsell color attributes H V/C were mainly used to describe the NT system for simplicity (Nayatani et al. 2004, 2005, 2011, 2014). For example, Munsell chroma $C$ was used as the NT chroma $C_{NT}$. We newly adopt CIELAB as the base UCS. However, no fundamental features of NT system discussed so far have changed at all. New $C_{NT}$ derived from $C^*_{ab}$ by Eq.(1) (see below) has the same meaning (Nayatani and Komatsubara 2005) and shows almost the same numerical values.

*Table 1. Correspondence among NT opponent-color hues, CIELAB $h_{ab}$, and Munsell H.*

| NT Hue $H_{NT}$ | CIELAB $h_{ab}$ [deg.] | Munsell H (approx.) | proportional coefficient $k_H$ |
|---|---|---|---|
| R100 | 26 | 5 R | 2.3015 for $26 \leq h_{ab} < 91$ |
| Y100 | 91 | 5 Y | 1.6748 for $91 \leq h_{ab} < 162$ |
| G100 | 162 | 5 G | 2.2852 for $162 \leq h_{ab} < 262$ |
| B100 | 262 | 2.5 PB | 2.4673 for $262 \leq h_{ab} < 386$ |

Transform equations from the CIELAB color attributes $[L^*, C^*_{ab}, h_{ab}]$ to NT color attributes $[w, bk, gr, C_{NT}, H_{NT}]$ are as follows:

For chroma, the following equation is used.

$$C_{NT} = k_C \cdot CS(h_{ab}) \cdot C^*_{ab} , \tag{1}$$

where $k_C = 0.14164$ is the proportional coefficient, which is determined to make $C_{NT}$ be the same scale as Munsell $C$ on average.

For hues, first, identify in which opponent-hue section a color with $h_{ab}$ is in, then, calculate the hue steps $\Delta H_{NT}$ between the two neighboring primary colors by the following equation.

$$\Delta H_{NT} = k_H \cdot \{1/CS(h_{ab})\}^2 \cdot \Delta h_{ab} , \tag{2}$$

where $k_H$ is the proportional coefficient in the fourth column of Table 1.

For whiteness and blackness, first, correct the lightness scale that becomes $L^*_{cr} = 50$ when $L^* = 55$, then, obtain the perceived lightness $L^*_{cr,eq}$, finally transform it to $w$ or $bk$.

$$L^*_{cr,eq} = k_L \cdot CS(h_{ab}) \cdot L^*_{cr} , \tag{3}$$

$$w \text{ or } bk = (1/5) \cdot (L^*_{cr,eq} - 50) , \tag{4}$$

where $k_L = 0.75029$ for $C_{NT} = 10$. For other $C_{NT}$ values, additional equations are used. See the previous paper (Nayatani and Sakai 2011) for details.

For grayness, the following equations are used (Nayatani and Sakai 2014).

$$gr = 10 - [(w \text{ or } bk) + C_{NT}] , \qquad \text{for } (w \text{ or } bk) + C_{NT} < 10 \tag{5}$$

$$gr = 0 , \qquad \text{for } (w \text{ or } bk) + C_{NT} \geq 10 \tag{6}$$

## 3. CATEGORICAL TONE DETERMINATION

In NT system, the colors with the same attributes [$w, bk, gr, C_{NT}$] irrespective of hues [$H_{NT}$] have the same tone attribute as already explained in the INTRODUCTION. Thus, It can be said that the NT system is the Hue-Tone system on its own. However, categorical tones are usually used in color design fields (Kobayashi 1981, Chung and Ou 2001, Nayatani and Komatsubara 2005). For example, Kobayashi (1981), the inventor of his Color Image Scale, defined the tone by "Colors belonging to the same tone have a common image in spite of their hue differences."

Considering these needs, we decided to introduce the categorical tone representation to the NT system. We placed the most vivid tones at [$w=0, bk=0, gr=0, C_{NT}=14, H_{NT}=$any] indicated as T1 and defined totally 13 tones from T1 to T13 as shown in the Figure 2 (2). Every tone has the definite NT attributes [$w, bk, gr, C_{NT}, H_{NT}$]. Therefore, by using the transform equations in Sec.2.2 inversely, they can be easily transformed to colorimetric values [$L^*, C^*_{ab}, h_{ab}$]. Figure 3 shows the colored image of 13 tones with eight hues, $H_{NT}=$R100, R50-Y50, Y100, Y50-G50, G100, G50-B50, B100, and B50-R50. The RGB values used in this colored image were obtained by transforming the CIELAB [$L^*, C^*_{ab}, h_{ab}$] values to the 24-bit sRGB color values (IEC 1999). Note that, however, several colors in tones T1, T2, T3, and T4 are out of sRGB range. Note also that this tone category is just an example. You can change the number of categorical tones or can adjust the interval between tones as you like by using NT system.
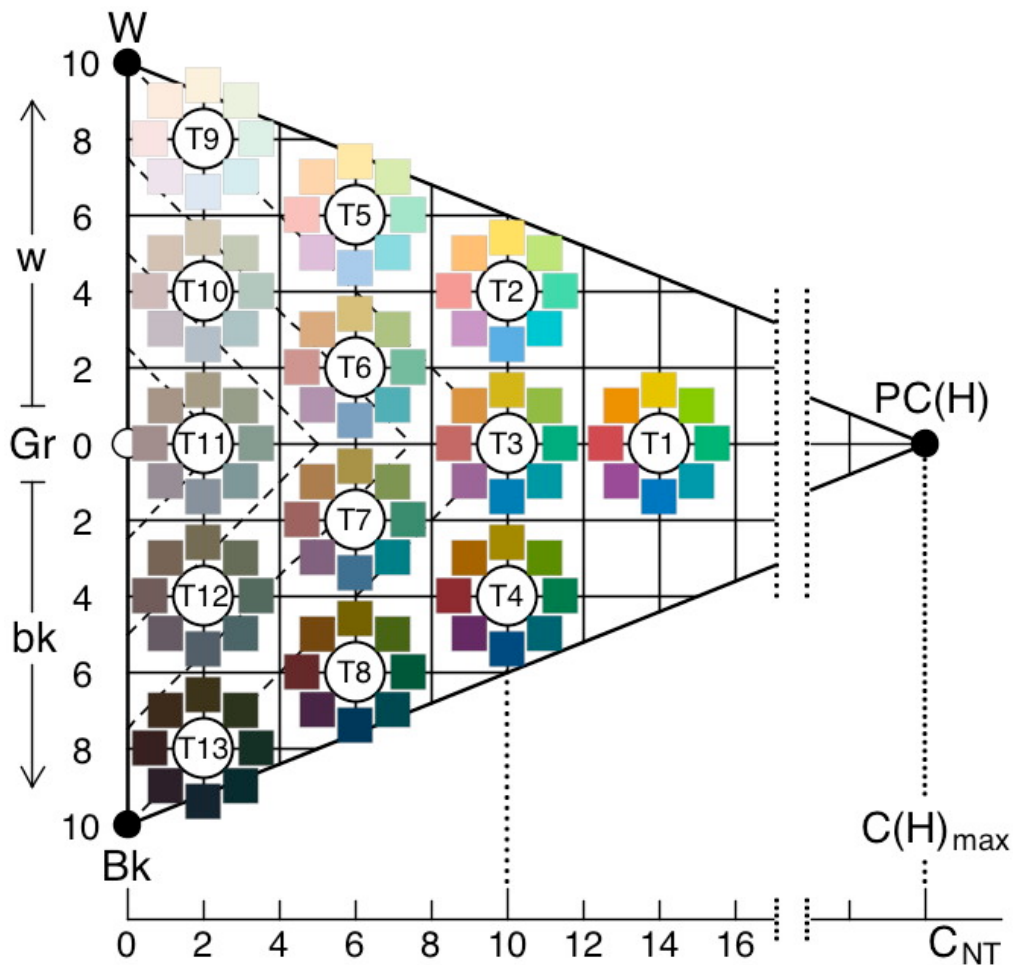


*Figure 3: Categorical tone representation of NT system (Colored image).*

## 4. CONCLUSIONS

The tone concept has been widely used in the artistic fields of painting and color design from the old days. The NT tone categories, for example, can be used for selecting the color combinations in those artistic fields (Sakai and Nayatani 2009).

In the color science field, the color stimuli extracted based on the tone categories are frequently used in a wide variety of sensory testing of vision. The NT tones are also suitable for such scientific purposes, because its tones are derived based on the color-appearance studies and have well-defined colorimetric values. This colorimetric background will be of help when analyzing the sensory data.

## REFERENCES

Chung, M.C., L.C. Ou. 2001. Influence of Holistic Color Interval on Color Harmony. *Color Research and Application* 26 (1): 29-39.

Evans, R.M., B.K. Swenholt 1967. Chromatic Strength of Colors: Dominant Wavelength and Purity. *Journal of the Optical Society of America* 57 (11): 1319-1324.

Fairchild, M.D. 2013. *Color Appearance Models, Third Edition.* Chichester: John Wiley and Sons.

IEC 61966-2-1. 1999. *Multimedia systems and equipment- Colour measurement and management - Part 2-1*: Colour management- Default RGB colour space - sRGB. International Electrotechnical Commission.

Kobayashi, S. 1981. The Aim and Method of the Color Image Scale. *Color Research and Application* 6 (2): 93-107.

Nayatani, Y. 2002. A Hue Rectangle and Its Color Metrics in a Modified Opponent-Colors System. *Color Research and Application* 27 (3): 171-179.

Nayatani, Y. 2003. A Modified Opponent-Colors Theory Considering Chromatic Strengths of Various Hues, *Color Research and Application* 28 (4): 284-297.

Nayatani, Y. 2004. Proposal of an Opponent-Colors System Based on Color-Appearance and Color-Vision Studies, *Color Research and Application* 29 (2): 135-150.

Nayatani, Y., H. Komatsubara. 2005. Relationships among Chromatic Tone, Perceived Lightness, and Degree of Vividness. *Color Research and Application* 30 (3): 221-234.

Nayatani, Y., H. Sakai. 2007. Proposal of a New Concept for Color-Appearance Modeling. *Color Research and Application* 32 (2): 113-120.

Nayatani, Y., H. Sakai. 2011. Predictions of Munsell Values with the Same Perceived Lightness at Any Specified Chroma Irrespective of Hues - Determination of Any Tonal Colors. *Color Research and Application* 36 (2): 140-147.

Nayatani, Y., H. Sakai. 2014. Gray and Grayness - its Complexities in Color Appearance of Surface Colors. *Color Research and Application* 39 (1): 37-44.

Sakai, H., Y. Nayatani. 2009. Proposal for selecting two-color combinations with various affections. Part II: Demonstration of the System. *Color Research and Application* 34 (2): 135-140.

*Address: Dr. Hideki SAKAI, Graduate School of Human Life Science,*
*Osaka City University, Sugimoto 3, Sumiyoshi-ku, Osaka, 558-8585, JAPAN*
*E-mail: hsakai@life.osaka-cu.ac.jp*

# Colour Appearance in the Outdoor Environment

Ya-Chen LIANG, Li-Chen OU, Pei-Li SUN
Graduate Institute of Color and Illumination Technology
National Taiwan University of Science and Technology, Taiwan

**ABSTRACT**

A psychophysical experiment of colour appearance, in terms of hue, lightness and colourfulness, was conducted outdoors to investigate colour appearance in the outdoor environment. The experiment was conducted outdoors on a sunny day by 14 observers at the same time, in the same place, where there was no glare in the observer's viewing field. The reference white, reference colourfulness and each test colour were all placed on a vertical panel covered with a medium grey cloth. The test colours included 42 colour patches selected randomly from the Practical Coordinate Color System to cover a wide range of hue, lightness and chroma. The 14 observers with normal colour vision were asked to estimate the lightness, colourfulness and hue for each test colour. The experimental results show high correlation between visual data and values predicted by CIECAM02 in terms of the three colour appearance scales. Although the perceived lightness also shows high correlation, experimental data suggests that the observers were more sensitive to variation in lightness for greyish colours than for highly saturated colours.

## 1. INTRODUCTION

Existing colour appearance models such as CIECAM02 (CIE Publication-159 2004) have typically been developed using displays, prints and other media. Nevertheless, these studies have been limited to indoor conditions. It has been unclear whether or not such colour appearance models also apply to the outdoor environment. CIECAM02 has defined three surround conditions, dark, dim and average. The average surround condition describing luminance level of around 1,000 cd/m$^2$ may not suffice to use in the outdoor environment, as the outdoor luminance can be easily beyond 10,000 cd/m$^2$. The luminance level of surround higher than 10,000 cd/m$^2$, also called the "bright surround condition", for which CIECAM02 did not seem to show satisfactory predictive performance (e.g. Park *et al.* 2015).

There is much greater variation in the luminance of light source outdoors (i.e. the day light) than indoor lights, due to unpredictable weather conditions. The human visual system has considerable ability to adapt to such variation. More importantly, the illumination level is way higher in the outdoor environment than indoor lighting. Colour applications for indoor conditions are quite different than those for the outdoor environment. The latter include outdoor colour measurement which is essential for architectural colour design and urban colour planning.

Several issues need to be addressed properly before a colour appearance experiment can be appropriately carried out outdoors. First, the selection of the experimental location is crucial. There should be no glare within visual range of the observer, so that the white tile serving as the reference white is the brightest in the viewing field. Moreover, outdoor luminance varies all the times due to the position of the sun and the weather conditions. To

overcome these issues, all observers in the study must assess colour appearance of each colour sample at the same time, in the same place. And this was exactly how the present study was carried out.

## 2. METHODS

### 2.1 Experimental set-up

As described above, the experiment was conducted outdoors on a sunny day (afternoon) by all observers at the same time, in the same place, where there is no glare in the observer's viewing field. The reference white, the reference colourfulness and each test colour patch were all placed on a vertical panel covered with a medium grey cloth. During the experiment, the mean luminance value of the reference white was 13,050 cd/m$^2$ (SD = 2,639), as measured using a Konica Minolta CS-100A, a portable colour meter.

As shown in Figures 1 (a) and (b), the viewing distance for all observers was about 300 to 400cm, where the locations of each observer varied in terms of both viewing distance and viewing angle. To see whether this would result in significant colour difference for different observers, the CS-100A portable colour meter was used to measure the test colours from various locations of each observer. The measurement result shows a mean CIELAB colour difference of 1.38, which was thought acceptable in such an experimental condition.



*(a)* *(b)*
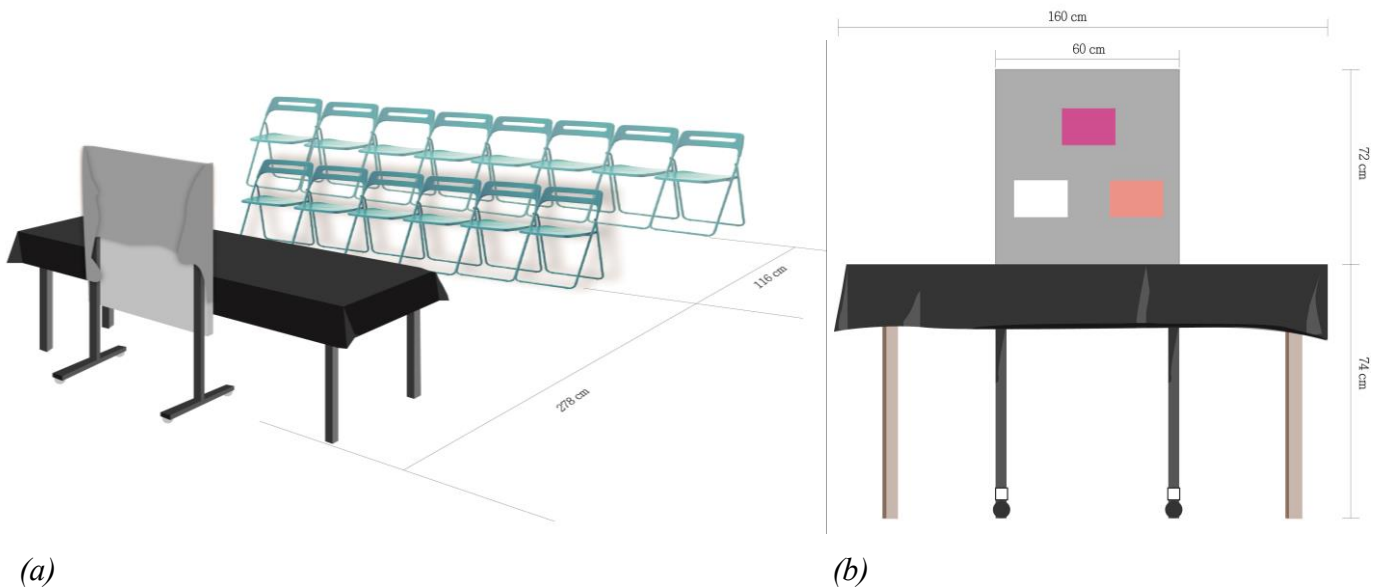
*Figure 1: Experimental set-up: (a) the 14 observers conducted the experiment simultaneously with a viewing distance of about 300-400cm, (b) each test colour, together with a reference white and a reference colourfulness, presented against a medium grey background on a black table*

### 2.2 Colour samples

The test colours included 42 colour patches selected randomly from the Practical Coordinate Color System to cover a wide range of hue, lightness and chroma. The 42 colours included 6 achromatic colours for further data analysis.

During the experiment, for each test colour, the reference white, reference colourfulness and the test colour itself were measured in terms of the tristimulus values using the CS-100A portable colour meter. Figures 2 (a) and (b) show distribution of the 42 colour samples in CIELAB colour space according to the measurement results, illustrating a wide spread of colour samples in terms of hue, lightness and chroma.
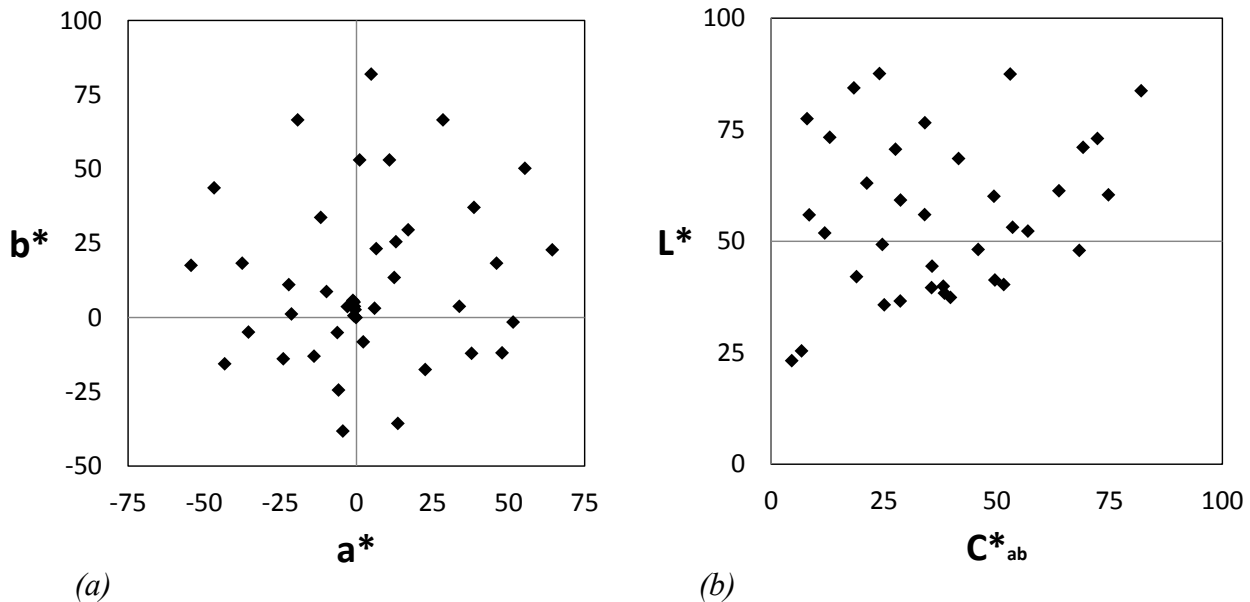


(a)                                                                                     (b)

*Figure 2: The 42 colour samples in (a) CIELAB a\*-b\* and (b) L\*-C\*$_{ab}$ diagrams*

## 2.3 Observers

A total of 14 observers with normal colour vision were asked to estimate the lightness, colourfulness and hue for each test colour. The observers were all Taiwanese citizens, and were postgraduate students at the National Taiwan University of Science and Technology. Prior to the experiment, the observers received trainings of definitions of hue, lightness and chroma using the Munsell Color Book.

The 42 colour samples were presented individually in random order. To assess lightness of each test colour, the reference white was assigned to have a lightness value of 100. To assess colourfulness, the reference colourfulness was assigned to have a colourfulness value of 40. The hue quadrature was used to assess hue of each test colour in terms of proportion of red, yellow, green and blue in colour mixture that can match the test colour.

## 3. RESULTS

To see how well CIECAM02 performed in predicting hue, lightness and colourfulness for colour patches presented in the outdoor environment, the visual results were plotted against the predicted CIECAM02 values, as shown in Figures 3 (a)-(c) for hue, lightness and colourfulness, respectively. High correlation was found for all of the three scales, with a coefficient of determination ($R^2$) of 0.99 for hue, 0.82 for lightness and 0.89 for colourfulness. The results indicate good predictive performance of CIECAM02 for colour

appearance in the outdoor environment, with the predicted values accounting for 99% of the total variance in the visual data of hue, 82% for lightness and 89% for colourfulness.



(a)

(b)

(c)
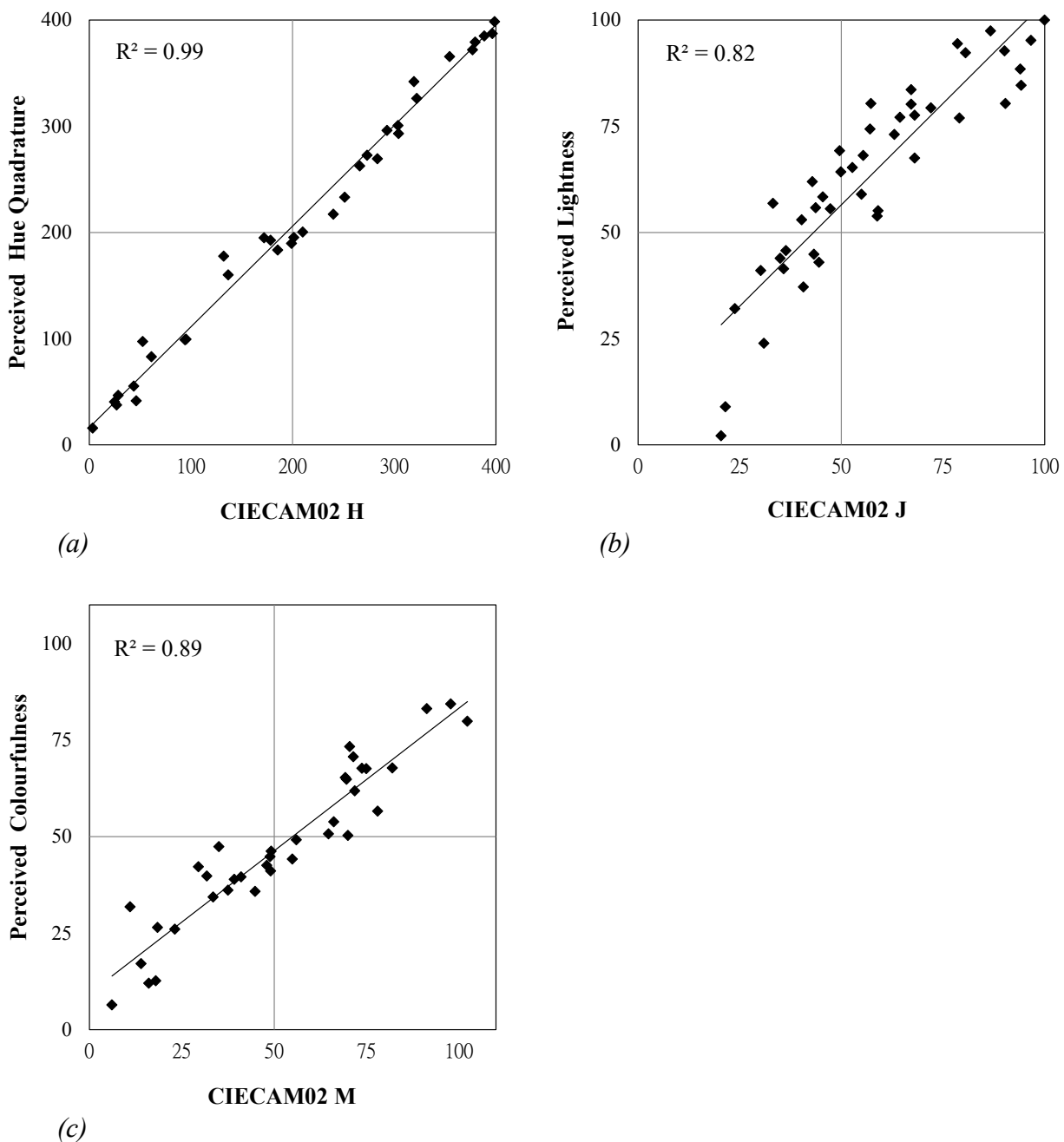
*Figure 3: Comparisons between visual results and predicted CIECAM02 values in terms of (a) hue, (b) lightness and (c) colourfulness*

Note, however, that although experimental results show a coefficient of determination of 0.82 for lightness, as demonstrated in Figure 3 (b), which seems to suggest a close correlation between the visual results and the predicted value in lightness, the scatter graph illustrated in Figure 3 (b) shows a somewhat curvy trend line; colour samples having low CIECAM02 J values tended to be rated extremely low in lightness.

It is tempting to assume that the two data points located lowest in Figure 3 (a) being the outliers. To see whether this was the case, the experimental data were separated into five groups defined by CIECAM02 M (colourfulness): those with the M values lower than 5 (i.e. the achromatic colours), those with the M values greater than 5 and lower than 30, those with the M values greater than 30 and lower than 50, those with the M values greater than 50 and lower than 70, those with the M values greater than 70. As Figure 4 demonstrates, the five colourfulness groups seem to show different tendencies in terms of slope of trend line; the higher colourfulness, the lower slope of trend line. The achromatic colour group (i.e. M < 5) shows the highest slope, while the group with the highest colourfulness values (i.e. M > 70) shows the lowest slope. This seems to suggest that the observers were more sensitive to variation in lightness for greyish colours than for highly saturated colours.
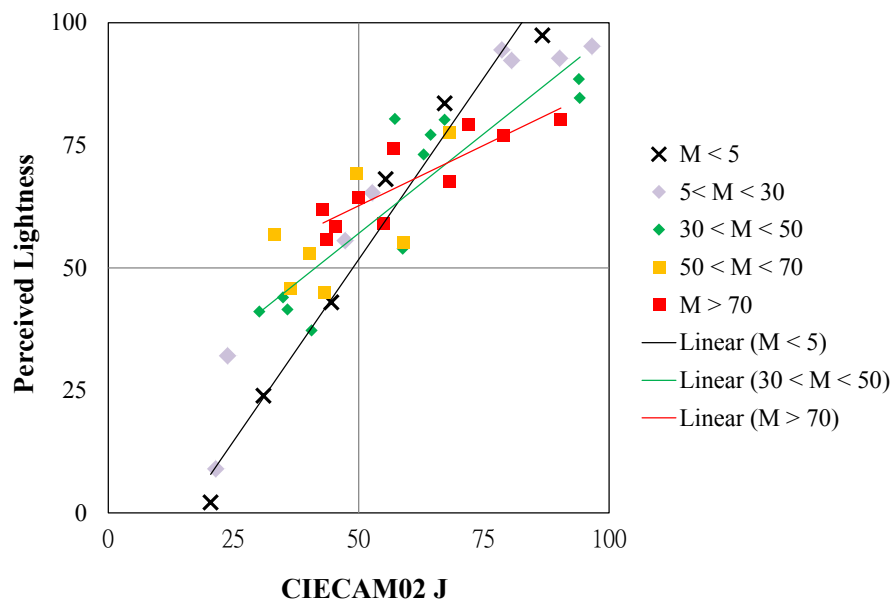


*Figure 4: Perceived lightness plotted against CIECAM02 J for five colourfulness groups defined by CIECAM02 M*

## 4. CONCLUSION

The experimental results show high correlation between the visual data and the predicted values by CIECAM02 in terms of the three colour appearance attributes: hue, lightness and colourfulness. While the perceived lightness also shows high coefficient of determination (0.82) as shown in Figure 3 (b), suggesting good predictive performance of CIECAM02 for outdoor environment, Figure 4 demonstrates different tendencies in terms of slope of trend line; the higher colourfulness, the lower slope of trend line. The result suggests that the observers were more sensitive to variation in lightness for greyish colours than for highly saturated colours. Whether the finding only applies in the outdoor environment or it may also occur in the average surround condition will require further study using more dark colour samples in the experiment.

AIC2015 TOKYO - Color and Image

## REFERENCES

CIE Publication-159. 2004. *A Colour Appearance Model for Colour Management Systems: CIECAM02*. Vienna: CIE Central Bureau.

Park, Y., Luo, M. R., Li, C. J., and Kwak, Y. 2015. *Refined CIECAM02 for bright surround conditions*, Color Research and Application 40 (2) 114-124.

*Address: Li-Chen OU, Graduate Institute of Color and Illumination Technology,*
*National Taiwan University of Science and Technology*
*43, Section 4, Keelung Road, Taipei, Taiwan*
*E-mails: lycperry@gmail.com, lichenou@mail.ntust.edu.tw, plsun@mail.ntust.edu.tw*

# Color Play: Gamification for Color Vision Study

Shida BEIGPOUR[1], Marius PEDERSEN

The Norwegian Colour and Visual Computing Laboratory, Gjøvik University College

## ABSTRACT

The study of color perception in humans is an important ongoing research which currently mainly relies on psychophysical studies. Most psychophysical studies are prune to limitations which can highly reduce the scalability and repeatability of their experiments, cause over-fitting, and fail to fully engage subjects in performing the given tasks. Gamification is becoming a popular approach in obtaining large amount of data, and making the tasks more interesting for subjects. We design a game called Color Play which consists of a series of simple color mixing and matching tasks. This game engages both the children and adults in experimenting with different colors and color spaces. Through this game, the players would learn about different color spaces while at the same time becoming subjects of our color perception study. By analyzing the players' performance we investigate the differences between the RGB and HSV color spaces, and compare the importance of luminance versus chroma.

## 1. INTRODUCTION

While the human visual system can be studied in biology using sophisticated techniques like MRI, research on human color perception as a rather cognitive process, relies mainly on the study of the human behavior given visual stimuli. These studies analyze the results and performance of human subjects which take part and perform a set of tasks manually or semi-manually (e.g., segmenting objects in an image or rating images).

Performing such experiments is often time consuming, tedious, and can involve paid subjects. This all limit the number of subjects. Moreover, the tasks can be boring for the subjects and due to tiredness they might tend to pay less attention toward the end. Repeating the experiment (especially by other scientists) is not straightforward. Often these studies use participants from one location (e.g., their university), and mostly involve adults as collecting data from children requires much more effort. Lastly, the very controlled set up and lab environment results in a less natural behavior from the users, especially when they feel that their behavior is being controlled (Heppner et al. 2007).

In the current work, we investigate "gamification" as a method to tackle all the above challenges in psychophysical studies. The main goal of our study is to investigate the intuitiveness and ease of color matching and color mixing tasks in different color spaces, namely for the widely used RGB and HSV, and for different colors. The main purpose of our gameplay framework is to take a typical color mixing/matching scenario out of the laboratory environment and bring it to the context of everyday life. We study how people interact with colors and color spaces in work and leisure. Such study would help us analyze people's relation with color spaces based on the practical scenarios like finding the desired color mixture for a room, a graphic design, website, advertisement, video game, and so on.

We briefly list our main contributions: showing the advantage of gamification in psychophysical studies to improve the subjects' experience as well as the performance and

---

[1] S. Beigpour is now with the Chair for Computer Graphics at University of Siegen, Germany.

quality of the study; designing a portable and robust system to take advantage of public spaces as a platform to reach wide variety of subjects (e.g., age, gender, nationality); using a game environment we help subjects to present more natural behavior compared to a controlled lab environment; and finally as a result we study the intuitiveness of the RGB and HSV color spaces as well the importance and contribution of chroma and luminance for human observers in daily life. We provide quantitative data analysis.

## 2. RELATED WORK

Schwarz et al. (1987) designed a study on the effect of color spaces on color matching with a large number of naive subjects (96) in which 14 pages of instructions were handed out. Each subject matched five colors six times each for a total of 30 trials. They concluded that in their study: first, subjects were faster in matching using RGB and opponent color space; second, having a lightness axis helped with matching lightness more than having a hue or chroma axis helped with matching hue or chroma; third, significant learning occurred with respect to matching time and closeness; fourth, inexperienced subjects using the RGB color model matched rapidly but inaccurately in comparison with other color models; and fifth, the opponent, LAB, YIQ, and HSV color models require learning to use effectively.

Douglas and Kirkpatrick (1996) studied the effectiveness of color models with respect to interface feedback level. The experiment was performed for four groups of naive subjects (12 in each group). Each group was tested for a combination of the color model (RGB or HSV) and one of the two interfaces with different feedback. The subjects were required to perform a color matching task (30 target colors with the time limit of maximum three minutes per color). They concluded that the color model does not play a role in time or accuracy of the matching task, while higher level of feedback results in more accuracy.

Luo et al. (2005) designed an experiment to study the sources of uncertainty in color matching experiments. They have presented quantitative results comparing each source and concluded that the observers play the main role in such uncertainty. Furthermore, they have provided solutions for various types of uncertainty.

Flatla et al. (2011) proposed a framework that simplifies the design of *calibration games* as a way to improve both the performance and the user experience while performing a tedious task like calibration. They conclude that the gamification does significantly improve the enjoyment, and that even though there are some differences in the recorded data it does not reduce the utility of the data for calibration.

## 2. METHOD

In our gamification approach, the user is provided with a tangible environment consisting of four Philips Hue color light bulbs and the Playstation3 Move™ controller to interact with the game. The *feedback* element is provided by setting the bulbs to change color based on the user's action. We also provide scores to make the game more *competitive*.

### 2.1 Technical Specifications

We use a set of Philips Hue bulbs to represent the colors since they are capable of displaying a wide range of colors and their control interface is straight forward. Three bulbs are set to represent the three primaries in the color space to be studied and a fourth bulb displays the color produced by the subject. As the bulbs use colored LEDs, they are relatively robust and consistent over time. Furthermore, they don't heat up much. On the

other hand, as they are mainly targeted for commercial use to provide household ambient lighting, their gamut is rather limited to the common indoor and outdoor illuminant colors (e.g., dark green and cyan are outside the gamut).

To overcome this limitation, we created a look-up table for the colors using a Konica Minolta CS1000 tele-spectro-radiometer mapping the values in the sRGB color gamut to their corresponding values for the bulbs. This look up table helps us find a set of colors which can be displayed by these bulbs as well as the exact values to be provided to the bulb in order to display the desired colors. Since the color reproduction function of the bulb turned out to be nonlinear and complex, using a look-up table to convert the values between the game's sRGB system and the bulb is a reasonable choice.

Furthermore, we use the open source code of Perl (2012) for tracking the PS3 Move™ controller with the help of a webcam. The tracking is quite robust to occlusions.

## 2.2 Game Setup

Figure 1 presents a schematic view of the game setup. We divide the space to equal horizontal portions, each of which is assigned to one of the three bulbs who stand for each of the primaries of a color space (i.e., Red, Green, and Blue for RGB). When the subject places the controller in each of these areas, the corresponding bulb is activated. The vertical dimension is divided to three areas, namely, *up*, *middle*, and *down*. Therefore for example placing the controller in the area assigned to the first bulb in the up or down areas will result in an increase or decrease (respectively) in the contribution of that bulb in the color mixed by users. The *middle* area is design to introduce a null state which helps users get better control of the changing bulbs, where no change occurs in the bulbs. The total number of steps in each color channel of each color space is kept constant to avoid giving more importance to chromatic and none chromatic characteristics of the color spaces.
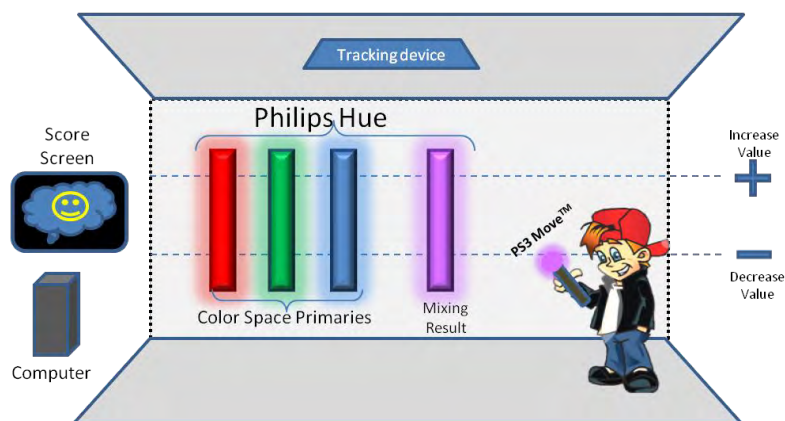


*Figure 1: Schematic view of the game setup and its components.*

The fourth bulb displays the color mixed by the player. The player needs to match this color to the color of the patch given on the screen. The screen also shows the player their score upon completing each round of the game.

At each instance of the game, one of the target colors is displayed in a large patch on the screen next to a few lines of instructions. The order of colors is random. The screen is placed in a way that the player can not see the target bulb and the patch on the monitor at the same time, so that they need to rely on their idea of that color. This way we can better study which characteristics of the color are more important for people. We setup the game

inside a dark room to avoid the effect of ambient illumination and provide better contrast for the bulbs and the monitor.

**Target Colors:** We've chosen six colors, namely: Sand (RGB:206,188,96), Pimento (230,97,69), Sapphire (88,10,226), coral Pink (244,121,129), Lemon (225,238,24), pastel Purple (216,157,237).

## 3. EXPERIMENTS AND DISSCUSSION

In this section we provide details on our data analysis. First we define our metrics. Then we present the results for supervised and unsupervised experiments. Finally we compare the contribution of chroma versus luminance using the intra-observer data analysis.

### 2.1 Metrics

We use Median Observer Time (MOT) in seconds as a notion of how intuitive it is to mix and match colors in each space. The median is chosen since it is more robust to outliers. Luo et al. (2005) define *observer accuracy* as "the closeness of the agreement between the result of each individual observer and a true value of the measurement, i.e. the mean of all the observations for each color". Following Luo et al. (2005), we define Average Inter-Observer Inaccuracy $AIOI_{CS}$ for each color $C$ and color space $S$ in CIE $\Delta E^{*}_{ab}$ as:

$$AIOI_{cs} = (1/n) \sum_{i}^{n} \Delta E^{*}_{ab} (T_{CS}, P_{CS_{i}}),$$

where $T_{CS} = (1/n) \sum_{i}^{n} P_{CS_{i}}$, and $P_{CS_{i}}$ is a player's result for each $C$ and $S$. The number of observations is $n$. We have also calculated the difference between the $T_{CS}$ and the actual match (from the look-up table explained before). We refer to this error as Average Observer Error (AOE) also in $\Delta E^{*}_{ab}$ units.

### 2.2 Supervised Experiment

For the first experiment, we asked 14 adult male and female subjects (8 expert and 6 naive subjects) with corrected to normal eye-sight to reproduce the six target colors in each of the two color spaces. They were also required to take a color deficiency test prior to the game to make sure they all have normal color vision. Two subjects repeated the experiment to provide data for the intra-observer study.

Questionnaires were provided to the participants to evaluate their experience. The subjects were asked to rate the game (on a scale of 1 to 5) based on how fun and how hard it is to play. Overall, the players rated the game as "fun" (4.1/5) and with "average difficulty" (2.98/5). On average, each color has been played about 35 times.

### 2.3 Unsupervised Experiment

In the second experiment we had the visitors voluntarily play as many colors as they like. These subjects were male and female between 22 and 27 years old and not included in the supervised experiment. The order of colors were random. On average, each color was played 5.2 times for RGB and 4.5 times for HSV.

### 2.3 Data Analysis

Figure 2 summarizes the analysis of the supervised and unsupervised experiments respectively. According to the top row, HSV is a more intuitive color space as the naive subjects were faster in mixing colors compared to RGB. On the other hand, the subjects

performed similarly in both color spaces based on their unanimity (AIOI). In average, coral pink and pastel purple were the most and least accurately mixed colors respectively (AOE). Even though, the naive group took longer time in RGB, both groups performed similarly in average regarding their AIOI and AOE.

The AOE is more than twice the AIOI, and it is quite high for a perceptual difference. This shows that the subjects' perception of the bulb color was quite far from its actual color value measured accurately using the tele-spectro-radiometer. There are several possible reasons for that, including the surround effect, and that the players did not have the screen and the bulb next to each other. This is an indication of cognitive processes affecting our perception of colors.

Based on Figure 2 bottom row, when players' task was to only play one color and space each, they were less unanimous among themselves maching in HSV (high AIOI). This indicates that as Schwarz et al. (1987) expressed, HSV requires learning to use effectively.
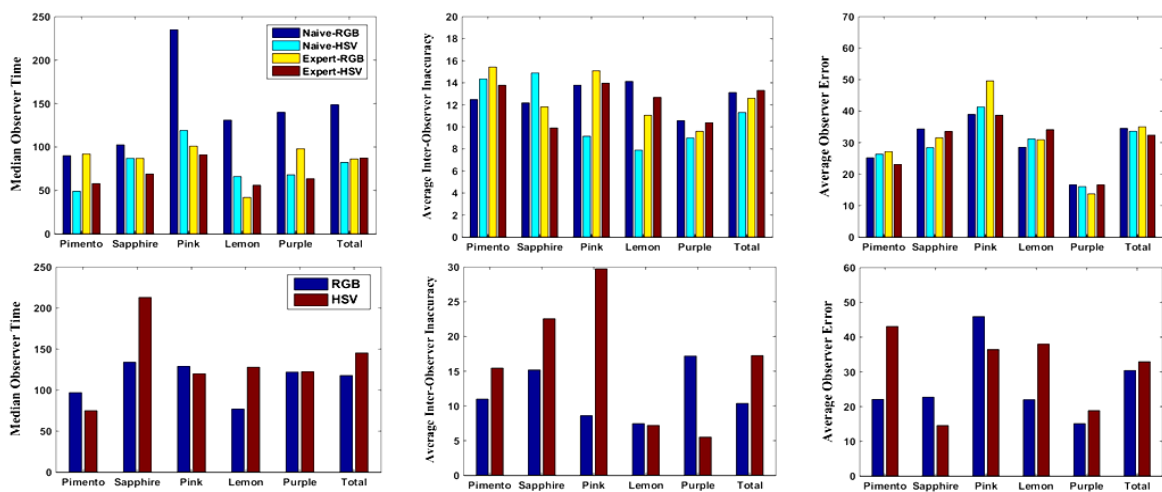


*Figure 2: Top and bottom rows present supervised and unsupervised experiments respectively. From left to right: the MOT in seconds, AIOA and AOE in $\Delta E^*_{ab}$.*

To compare the contribution of chroma versus luminance we use the intra-observer data gathered from two expert subjects. Table 1 compares the Average Intra-Observer inaccuracy (AAO), as a measure of repeatability, and Average Matching Error (AE), absolute error, between the two color spaces in Chroma and Luminance. Based on the obtained values, subjects performed better in matching luminance than chroma in both color spaces.

*Table 1. Intra-observer study:subjects matched better in Luminance than croma.*

|       | Time | Number | AAO-Chroma | AAO-Luminance | AE-Chroma | AE-Luminance |
|-------|------|--------|------------|---------------|-----------|--------------|
| RGB   | 73.5 | 32     | 8.6        | 5.5           | 41.8      | 21.3         |
| HSV   | 75.1 | 33     | 7.0        | 5.3           | 41.5      | 24.8         |

## 2.3 Challenges

An inevitable challenge in a serious game is the *meta-gaming* (McCallum 2012). For example, a player might try to intentionally play bad. But it's difficult to ensure that there

AIC2015 TOKYO - Color and Image

are no loopholes in the game rules, and restricting the game could limit the players' natural behaviour and bias the results. Having many subjects, reduces the effect of such outliers.

## 4. CONCLUSIONS

In this paper we took advantage of gamification in designing a study on human color perception. The designed game was used to gather information about the intuitiveness of mixing and matching colors in two different color spaces (i.e., RGB and HSV). The results of a supervised and controlled experiment indicate that HSV is a more intuitive colorspace as the subjects were faster in mixing colors compared to RGB. Results also indicate that subjects better matched in luminance compared to chroma. In an unsupervised experiment subjects were less unanimous matching in HSV.

Future work includes gathering data with more subjects. It can also include studies of the effect of gender, nationality, and age. The game can also be adapted for the observers to mix their favorite color, or for color memory experiments. It could also be interesting to see if one can detect color deficient players through the game.

## ACKNOWLEDGEMENTS

**REFERENCES**Douglas, S. and T. Kirkpatrick. Do color models really make a difference? *In Proceedings of the SIGCHI Conference on Human Factors in Computing Systems*, pages 399–ff. ACM, 1996.

Flatla, D.R, C. Gutwin, L.E. Nacke, S. Bateman, and R.L Mandryk. Calibration games: Making calibration tasks enjoyable by adding motivating game elements. *In Proceedings of the 24th Annual ACM Symposium on User Interface Software and Technology*, pages 403–412, New York, NY, USA, 2011. ACM.

Heppner,P., B. Wampold, and D. Kivlighan. *Research Design in Counseling*. Research, Statistics, and Program Evaluation Series. Cengage Learning, 2007.

Luo, W., MR. Luo, S. Westland, A. Tarrant, and A. Robertson. Measuring the uncertainty of colour matching. *AIC Colour 05 – 10th congress of the International Colour Association*. Pages 1087-1090. 2005 McCallum, S. Gamification and serious games for personalized health. *Studies in health technology and informatics*, 177:85–96, 2012

Perl T.. *Cross-platform tracking of a 6dof motion controller using computer vision and sensor fusion*. Master's thesis, Technischen Universität Wien, 2012.

Schwarz, M.W., W. B. Cowan, and J. C. Beatty. An experimental comparison of RGB, YIQ, LAB, HSV, and opponent color models. *ACM Transactions on Graphics*, 6(2):123–158, 1987.

*Address: Shida Beigpour, PhD, Chair for Computer Graphics, Faculty IV*
*University of Siegen, Hölderlin Street 3, 57068 Siegen, Germany*
*E-mails: shida.beigpour@uni-siegen.de, marius.pedersen@hig.no*

# Using Visual Illusions to Expand the Available Colors for Making Mosaics

I-Ping CHEN, Wei-Jei CHIOU,
Institute of Applied Arts, National Chiao Tung University

## ABSTRACT

Mosaic is an ancient art form of creating images by arranging pebbles, small pieces of ceramics, or other colored material called tesserae. One of the challenges in creating mosaics is the limited number of colors of the material. In order to create the desired colors that do not exist, mosaic artists have to make great efforts to learn principles of color mixture of tesserae which is not always intuitive. In this research, we attempt to look for other possible solutions for increasing available colors by applying two different visual illusions, Craik-O'brien-Cornsweet illusion and neon color spread illusion, to the mosaic design. To find out the optimal set of parameters to maximize the effect of illusion, we designed a series of computer-simulated experiments to examine how parameters such as the size of tesserae, the width and the color of grout, and the slope of luminance grading affect the magnitude of these two illusions. The results show that the magnitude of Craik-O'brien-Cornsweet illusion is remarkably stable across all manipulated values of parameters. The neon color spread illusion, by contrast, is sensitive to scale of tesserae, and width and color of the grout lines. Increasing the width of the grout lines will enhance the neon color spread illusion while increasing the size of tesserae would weaken the illusion. The magnitude of neon color spread varies with hues of grout. Green grout generates the strongest illusion, followed by red, blue and yellow grout in that order. We also create an Ehrenstein figure with ceramic tesserae according to the results of the experiment and the illusion effect of this physical version supports the conclusion of the experiment of neon color spread illusion.

## 1. INTRODUCTION

Mosaic is a discrete form of art. Unlike the case of painting, where the artist can produce a wide range of colors by mixing colors on his/her pallete, in mosaic making the artist has to work with a very small number of colors carried by the available tesserae. While not completely impossible, it is very difficult to achive color mixture effect by arranging colored tesserae in a specific way, the reason being that the grain size of mosaic elements is considerably larger than the color elements in a Pointillism painting. The top priority in the consideration of the arrangement of the tesserae should be given to conveying the spatial structure of the picture, not to the color mixture effect. It takes great talent and skill to make a mosaic work that excels both in form and color (Locktov & Clagett, 2002).

Given the color constraints faced by mosaic artists, we are highly motivated to seek for ways to expand the useful color range for the artists. In this study we try to make use of two color-related visual illusions, Craik-O'brien-Cornsweet illusion (Cornsweet, 1970) and the neon color spread illusion (Bressan et al., 1997), to increase the subjective number of colors in a mosaic.

In the original form of the Craik-O'brien-Cornsweet illusion, two panels of identical luminance are connected to each other by an 'amplified' luminance edge (aka. the Cornsweet edge) in the middle (Cornsweet, 1970, see Figure 2). The polarity suggested by this 'amplified edge' would bleed into these two side panels, making the panel by the dark side of the edge look darker (the right panel in Figure 1), the panel by the bright side brighter (the left panel in Figure 1).
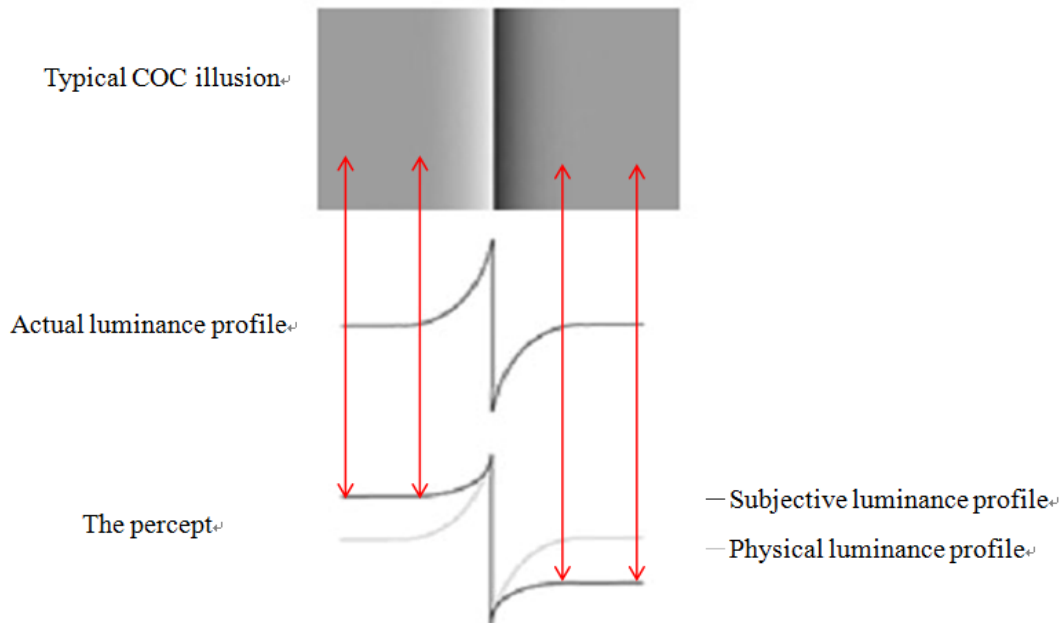


*Figure 1: Illustration of the Craik-O'brien-Cornsweet illusion.*

Several forms of the neon color spread illusion have been described in the literature (see Bressan et al., 1997 for a review ). Two of them are shown in Figure 2.
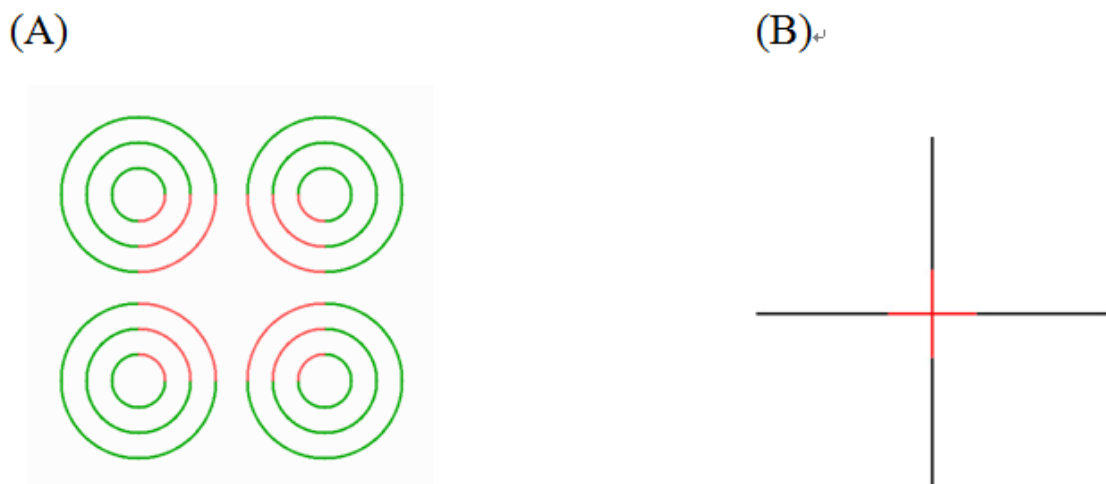


*Figure 2: The neon color spread. (A) The version by Dario Varin; (B) The version by Tuijl (Bressan et al., 1997).*

In all forms of the neon spread illusion, the color of some fine line pattern bleeds into the surrounding background, making a shaped area tinted with the color of the fine line.

We figured that the above two illusions have the potential of increasing available colors in a mosaic without having to increase the number of physical colors of the tesserae. Two sets of psychophysics experiments were carried out to determine the optimal parameters for creating the strongest color effect.

## 2. METHOD

The first set of psychophysics experiments manipulated (1) grain size of the tesserae, (2) the width of grout lines, (3) the slope of luminance grading, to map out the optimal range of these parameters. In the second of experiment, the effect of: (1) size of the tesserae, (2) the width of grout lines, (3) the color of grout lines, on the magnitude of neon color spread were measured with the method of adjustment

### 2.1 Materials for studying the discrete version of COC illusion

Figure 3 shows the discrete version of the COC illusion along with a blown up view the lluminance profile near the Cornsweet edge. To use the method of constant stimuli to gauge the magnitude of illusion, there are five levels of luminance difference spanning from significantly brighter to significantly darker between the left and the right half of the stimuli. The subjective eqality point was derived from the psychometric function as the index to the strength of the illusion.
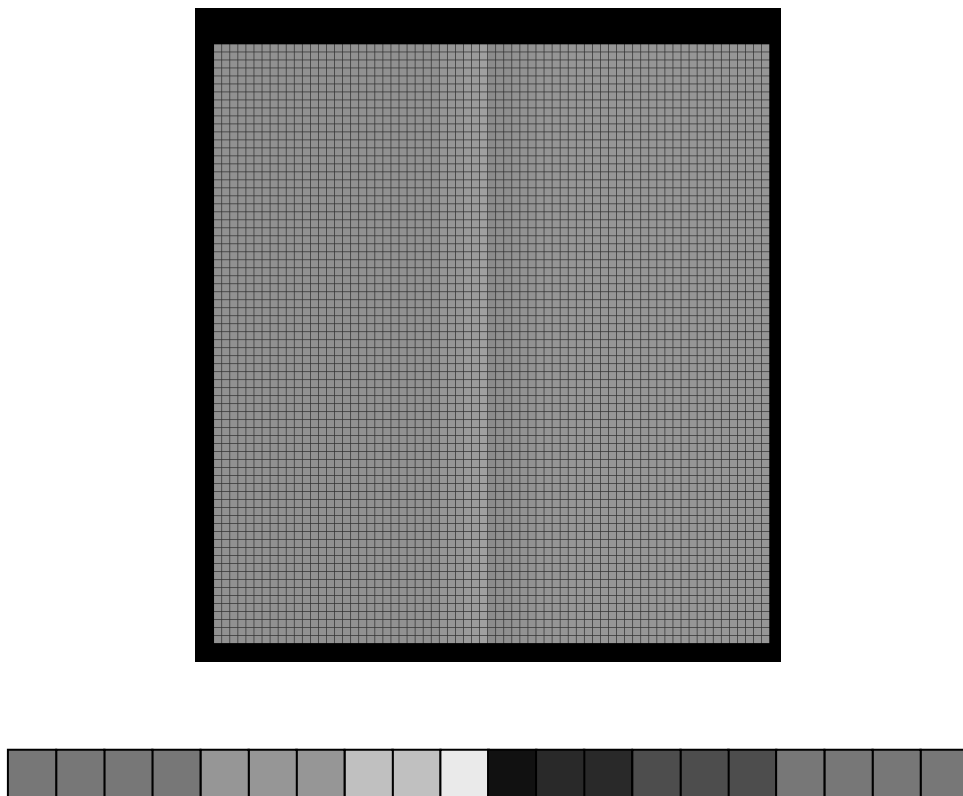
*Figure 3: The discrete COC stimulus used in the first set of experiment. Notice that the grain size, line width, and the slope of the luminance gradient were manipulated in this experiment.*

## 2.2 Experimental Procedure for studying the discrete version of the COC illusion

A typical method of constant stimuli procedure was adopted in this eperiment. The participant was asked to judge whether the left half of the stimulus looks brigher than the right half. There were 30 trials for each of the five luminance difference level, making the total number of trials 150 in a complete session.

## 2.3 Materials for measuring the magnitude of the neon color spread illusion

In the second set of experiment, we used method of adjustment to measure the effect of the neon color spread. The stimulus layout is illustrated in Figure 4.
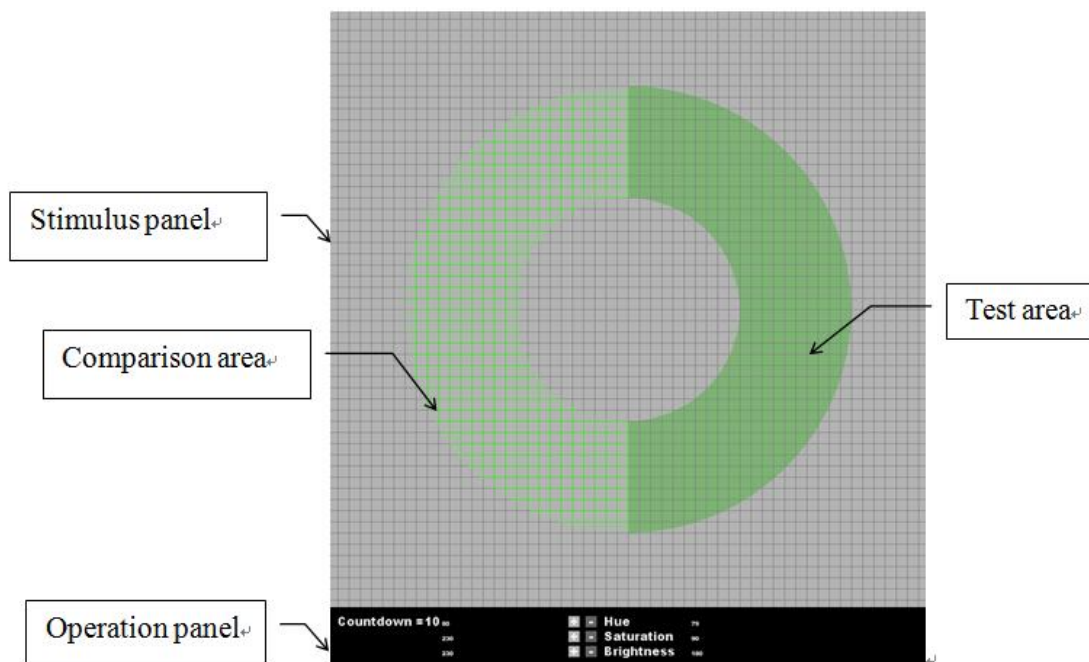


*Figure 4: Stimulus layout and the operation panel in the neon color experiment. Notice that the between-line space in the comparison area is of the identical grey of the rest background. The color of the between-line space is subject to the participant's adjustment.*

## 2.4 Experimental Procedure for neon color experiment

The participants needed to adjust the color appearance of the color of the between-line space in the test area utill it matches that of the comparison area by controlling the hue, saturation, and the brightness slide bars on the operation panel.

## 3. RESULTS

### 3.1 The COC eperiment

**Effect of Grain Size** Of the two levels of grain size used in this study (10 x 10 pixels vs. 20 x 20 pixels), we found a tendency of obtaining larger illusion effect with bigger grains. However, the difference is not statistically significant ($p=0.27 > 0.05$).

**Effect of Line Width** Of the two levels of line width used in this study (1 vs. 2 pixels), we found a clear pattern of larger line width produces stronger illusion effect ($p=0.02$).

**Effect of Luminance Slope** Of the two levels of luminance slope used in this study (on average, 15 units/step vs 22.5 units/step), we did not find significant difference in the illusion strength ($p$=0.88).

### 3.1 The neon spread eperiment

**Effect of Grain Size** The effect of grain size was very significant in the neon experiment ($p$<0.01), the bigger the grain, the stronger the sense of neon spread was iduced.

**Effect of Line Width** The effect of line width was also very significant in the neon experiment ($p$<0.01), the wider the line, the stronger the sense of neon spread was iduced.

**Effect of Hue** We tested four different hues, red, yellow, green, and blue, the results being that green was significantly more potent in inducing neon spread than all other hues, and there was no difference among red, yellow, and blue.

## 4. CONCLUSIONS

We found, in the computer simulation mode, great effect of both the COC and the neon color spread illusion in discrete forms. The magnitude of the COC illusion is relatively stable across all levels of parameters tested in this study, only significantly modulated by levels of line width.

In the case of the neon color spread, the effect is not only more dramatic but also much easier to apply to real art creation. The artist can apply chosen colors to grout lines, and the area circumscribed by the line would be tinted with the colors. The effect is somehow hue-dependent. Of the four basic colors tested in this study, green bleeds most aggressively. Both the size of tesserae and the line width affect the magnitude of the illusion.

To check whether our conclusion holds for reflective instead of illuminating surface (Bressan, 1995), we did an informal comparison with physical Ehrenstein figures (Ejima et al., 1984) as shown in Figure 5. The general patterns hold in the physical version. However, the size of illusion becomes smaller in the real version.
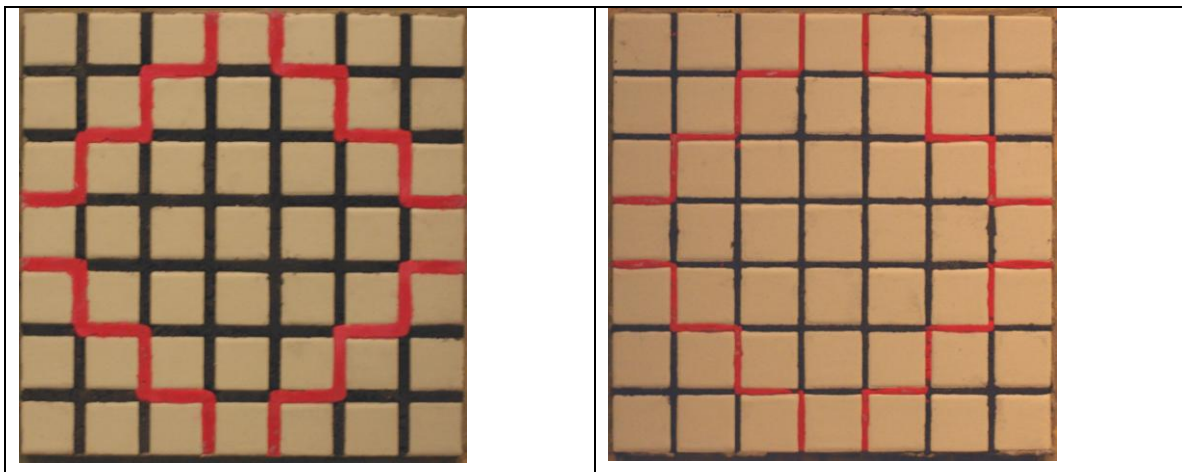


Figure 5: Two physical Ehrenstein figures of different line widths.

## ACKNOWLEDGEMENTS

AIC2015 TOKYO - Color and Image

## REFERENCES

Bressan, P. 1995. *A closer look at the dependence of neon color spreading on wavelength and illuminance*. Vision Research (35) 375-379.

Bressan, P., E. Mingolla L. Spillmann and T. Watanabe 1997. *Neon color spreading: a review*. Perception (26) 1353-1366.

Cornsweet, T. N. 1970. *Visual perception*. NY: Academic Press.

Ejima, Y., C. Redies S. Takahashi and M. Akita 1984. *The neon color effect in the Ehrenstein pattern: Dependence on wavelength and illuminance*. Vision Research ( 24) 1719-1726.

Locktov, J., & Clagett, L. P. (2002). *The art of mosaic design*. Rockport Publishers

Redies, C. and L. Spillmann 1981. *The neon color effect in the Ehrenstein illusion*. Perception (10) 667-681.

*Address: Prof. I-Ping CHEN, Institute of Applied Arts,*
*National Chiao Tung University, 1001 University Road, Hsinchu, Taiwan 300, ROC*
*E-mails: iping@faculty.nctu.edu.tw,*

# Are There Ugly Colours?

Ilona Huolman

Helsinki Metropolia University of Applied Sciences

Degree Programme in Technology and Design

## ABSTRACT

This paper presents a case study of my colour education classes, how students of Graphic-, Textile- and Industrial Design investigate and intentionally express their concepts of disharmony.

For centuries artists have asked what kinds of colour combinations are harmonic, affording aesthetic pleasure to the viewers. In the Finnish art education, teaching of colour relationships is still largely based on traditional notions of harmony. Many kinds of theories have been formed of colour harmonies. We have seen endlessly beautiful, harmonic paintings, all kinds of images in the different media. Colour harmony based on abstract and formal ordering, unity, balance or pleasantness has to a large extent ceased to motivate artists (Arnkil 2013).

What does the opposite, disharmony, mean? If harmony affords aesthetic pleasure and "tranquillity of mind", does disharmony afford aesthetic discomfort and "disturbance of mind"? How can we create aesthetic discomfort? It raises conflicting feelings when there is no visual hierarchy and equal "visual powers" are fighting with each other causing frustrations and aesthetic discomfort. If the main message is not clear nor do we even know what to look for first in the disharmonic picture that might cause the feeling there is something unknown and repulsive and something even scary to us.

The target of ugliness in the meaning of disharmony is, generally speaking, difficult for the students to achieve. Is it possible to achieve disharmony at all? It is also a kind of paradox that when students try to create chromatic harmony and beauty they fail, whereas when their primary task is to create disharmony they achieve something very interesting, fresh and good looking, something they would never have achieved, had they worked in the accustomed manner.

## 1. INTRODUCTION

In my colour education, it is most important that the students learn to develop efficiently their sensibility to make their own exact observations of colours. I use a number of exercises where students are learning by doing. This case study exercise is one of them. When they are painting and working with coloured papers (Josef Albers 2006) they have to make and analyse their own perceptions of different colour interactions in different colour comparisons. Become good visual professionals, e.g. designers, students should learn to open their eyes, understand what they see and how they react as individuals when they look at colours in any environment.

Colour harmony is the subject of endless texts offerings advice to the artists and designers and generally speaking disharmony is mentioned to be the opposite, something disturbing or unusual. If harmony is related to beauty, is disharmony related to ugliness? In

AIC2015 TOKYO - Color and Image

the exercise, their tasks were to create an as disharmonic painting as they can and make observations of their own way to solve the question of disharmony. Officially disharmony was defined as the opposite visual term of harmony. In my opinion, disharmony is a visual term which means there is no visual hierarchy and the main message is not clear nor do we even know what to look for at first in the disharmonic picture. These kinds of aspects cause frustrations and aesthetic discomfort. Here is my "theoretical" example of disharmony. It represents at the same time visual chaos: the elements are distributed randomly, there is no rhythm and no visual cohesion (Figure 1).
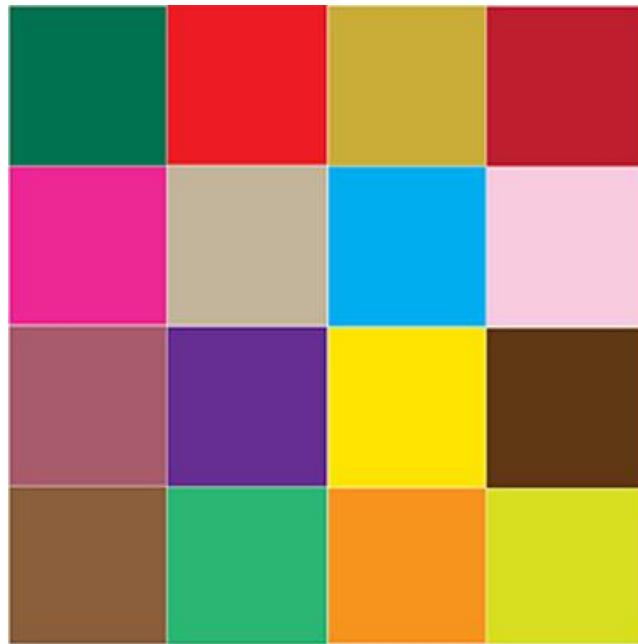


*Figure 1: Example of disharmony.*

## 2. METHOD

The exercise is simply called "Disharmonic painting". Instructions for the exercise were to discuss the visual terms "harmony" and its opposite, "disharmony". The students should think and ask themselves if harmony affords aesthetic pleasure and tranquillity of mind and what does disharmony afford? How can I create aesthetic discomfort? What does disharmony mean personally to me?

The students should not be shown examples of disharmony. Instead, they should think visually and make sketches about what kind of compositions and colours will establish disharmony in the best way in their own opinion. The topic could be approached freely. Finally, they should execute a disharmonic painting which is as disharmonic as possible in size A3 with gouache or acrylic colours.

The first reactions of the students after receiving instructions to the exercise "Disharmonic painting" are always disbelief and laughter. They think "disharmonic painting" is very easy and fast to do. It is usual that they have never tried to paint in a disharmonic way an "ugly" painting before.

In general, they begin to paint with the "ugly colours", with colours and compositions they hate. The painting processes are very interesting to follow as a teacher. When the processes approach the end, many students begin to express their amazed feelings and observations: their paintings are not so disharmonic although they tried to use "ugly colours" and imperfect compositions!

## 3. RESULTS AND DISCUSSION

The students tried in general to establish disharmony by establishing ugliness. There were two main approaches. The subject is narrative and there is something odd, disgusting and even scary about it. Another general topic is an abstract composition with a lot of colours. The students´ most common arguments for their disharmonious paintings were: disgusting topic, restless composition and ugly colours meaning for example colours with low saturation for example browns, greens with strong yellows, reds and blues. The second most common arguments had to do with "too many colours". They used more colours than what they usually do. They mixed new colours they never used before and what they had not liked at all.

It was interesting to share and discuss notions of what constitutes disharmony and ugliness after all. The students noticed that disharmony and ugliness are not always the same thing. Disharmony is a visual term and ugliness is quite a subjective and also a cultural learned matter. Disgusting topics include for example establishing instructively cultural and individual notions of ugliness. What ugliness means is more of a philosophical matter in our time and in our western culture now.

What constitutes disharmony in the picture? We drew a conclusion that all these anomalous colours, contrasts, details and compositions did not produce absolute disharmony in the meaning of totally aesthetic discomfort or chaos. Instead, disharmonic elements, anomalies created visual tension and fresh attractiveness. In that way their alleged disharmony turned into harmony in the meaning of affording aesthetic pleasure.

In the end, the students learned to understand that harmony and disharmony are equally important in art, graphic design and in all visual expression. With both harmony and disharmony highly interesting contrast can be created. The students also learn that there are no ugly colours in the absolute meaning: their ugly colours turned out to be the opposite in the way they used them.

I have had this exercise "Disharmonic painting" at my colour education now for many years. Always as the students failed in their task, finding it hard to achieve the set goal of disharmony, frustration set in.  It feels paradoxical, even absurd, to fail when you have been allowed to do just that in the beginning, to create a disharmonious or as they think in general, "an ugly picture instead of a good looking one". At the same time this exercise has encouraged the students to create something different and new to themselves. I often heard:" I would have never done anything like this without the exercise!" That has been a way to exceed themselves and has given them a strong feeling of success after all.  By giving up preference for harmony, they accepted dissonance to be as desirable as consonance (Albers 2006).

# 4. CONCLUSIONS

We achieved a kind of harmony through disharmony: A disharmoniously coloured painting can also afford aesthetic pleasure. We considered dynamic harmony in the way Josef Albers describes it: "Besides a balance through colour harmony, which is comparable to symmetry, there is equilibrium possible between colour tension, related to a more dynamic asymmetry" (Albers 2006).

Conclusions are in general that if there is no absolute colour harmony there is no absolute colour disharmony either. Also there are no absolutely ugly or beautiful colours but a very large and rich spectrum of different colour combinations. There are no absolutely failed compositions either. Everything depends on what we need in a certain actual context. Historical, cultural and individual qualities define how we understand the terms harmony and disharmony in a Western culture. These visual terms are not direct synonyms to the adjectives beauty and ugly.

Neuroscientist Beau Lotto expresses in his studies (Lotto 2013) that he learned to foresee what the next colour is people would choose when they can freely combine different colours at Lotto´s experiment. He said that we like to use side by side colours in the same way they occur in nature because we are used to that.

But we have seen in art history how new colour combinations could also be beautiful after we have become accustomed to them. Impressionism, Fauvism and Expressionism were at first badly received and their colours regarded as most disharmonious and ugly (Honour & Fleming 1992) but their works are highly valued today. These trends taught us to see a new kind of beauty and harmony. The students will be these agents of cultural evolution of colour images in the future.

# ACKNOWLEDGEMENTS

# REFERENCES

Albers, Josef  2006. *Interaction of Color* 42-43.

Arnkil, Harald 2013. *"Colour harmony: from dualism to living perception". Proceedings of the AIC 2013: 12th International AIC Congress.* Lindsay MacDonald, Stephen Westland, Sophie Wuerger (eds.)The Colour Group (Great Britain).

Honour H. & Fleming J. 1992. *A World History  of Art* 601, 652-653.

Lotto, Beau 2013. *Do you see the same than me?* Horizon, BBC/ Prisma Document, Yle Finland.

*Address: MA Ilona Huolman, Degree programme in Technology and Design, Helsinki Metropolia University of Applied Sciences, Lummetie 2, FI-01300 Vantaa, FINLAND E-mail: ilona.huolman@metropolia.fi*

# A novel experience in color teaching: Master in Color Design & Technology

Alessandro RIZZI,[1] Maurizio ROSSI,[2] Cristian BONANOMI,[1] Andrea SINISCALCO[2]

[1] Dept. of Computer Science, Università degli Studi di Milano

[2] Dept. of Design, Politecnico di Milano

## ABSTRACT

Experiences in the teaching of color are central to the AIC community. The difficulties in this goal are due to the intrinsic multidisciplinary nature of color and to its many different possible applications and related technologies. Moreover, colors have emotional, cultural and symbolic valences and designing with color can sometimes look like a matter of personal preference. In order to be able to teach all aspects related to color and make the student experience them, Università degli Studi di Milano and Politecnico di Milano have organized in the 2014-2015 the first edition of the Master in Color Design & Technology with the aim of providing in-depth training in the complex field of color design and color technology. The master aims at forming professionals able to manage the technological and design complexities of using color in creative and industrial processes and in many application domains: from industrial product design to interior architecture, from communication to fashion and entertainment, and even in designing the urban environment. The master's program is organized in two separate learning phases. The first phase is theoretical, while the second part consists of project works to make students apply what they have learned in the fundamentals in scenarios of typical color design. At the end of all these modules, students are called for an internship in one of the companies or research centers related to the master.

*Figure 1: Three moments involving the students, during the lessons: From left: practicing with a spectrophotometer, in the middle: using color atlases, at right: exercise for the Design Week about color trends.*

## 1. INTRODUCTION

The Master, organized by Politecnico di Milano and Università degli Studi di Milano, aims to provide in-depth training in the complex field of color design and technologies, to form professionals able to use color in creative and industrial processes and in numerous application domains. Before being allocated in the internship the students completed the two learning phases that constitute the training part of the Master. The first phase, conducted at the Università degli Studi di Milano, is theoretical, and it is divided in four modules: perception and color history, colorimetry and color systems, digital color and

color application. The second, held at Politecnico di Milano, part consists of five project works to make students apply what they have learned in the fundamentals in five scenarios of typical color design: color for communication, color for fashion design, color for interior design, color for industrial product design, color for urban space. In the following, details about the two phases are presented.

## 2. DIDACTIC OF THE MASTER

### 2.1 The theoretical fundamentals

*Perception and color history*

The aim of the first module was to present culture and color history, and the aspects of perception that are the basis of its complexity. The perceptual mechanisms that affect the color and vision in general have been examined in order to enable the students to recognize and design them.

*Colorimetry and color systems*

Although color is a subjective characteristic, colorimetry is needed to measure, standardize, communicate and represent in an accurate way the color of a surface or a light source. The theoretical basis of perception, colorimetry, photometric and radiometric measures have been presented in this second part as well as the color atlases, an alternative way to select, represent and communicate color. The module presented the essential technical skills that are the basis of the color designer, whatever the application areas on which it will choose to specialize in the future. The fundamentals have been presented both through frontal lessons, and practical or laboratory activities. Students have been encouraged not only to understand the laws that govern, i.e. a spectrophotometer, but also to learn how to use it correctly.

*Digital color*

With the diffusion of new technologies, more and more aspects of communication and color reproduction are becoming digital. In this module theoretical and practical fundamentals for manage, view and reproduce the digital color applied to different media have been provided, with particular attention to the limitations and problems associated with the use of different devices and color profiles.

*Color applications*

The success of a project that requires the conscious choice of colors depends on the experience, the preparation and the diligence of the designer. This module showed how the knowledge acquired in the previous modules can be applied in most professional fields and applications, through examples and case studies deriving from different contexts: marketing, visual communication, restoration of cultural heritage, photography, architecture, product and lighting design and more. A week later the beginning of the Master, in Milan started *the Design Week*, one of the most important world event related to the topic of design. Students were asked to actively participate to the event, looking for future trends in colors and finishing and reasoning about the change in the use of colors, in terms of decorations and schemes, from 1950s to now and more.

## 2.2 The project works

*Color for communication*

This module focused on the function and communicative dimension of color within the project of Communication Design. The idea focus on the fact that each communicative artifact arises from a series of choices that fit into a well-defined design process. The design and implementation of a brand start from the visual identity (name, brand, logo, lettering, packaging, integrated communication) that ensures the recognition and affirmation of the company. It is clear the importance of color in this strategy: the visual identity is built on the evocative and persuasive aspects of the chromatic language.



*Figure 2: Project Work "Color for communication" teachers Elena Caratti and Elisabetta Del Zoppo, works of Sandra Niggl, Simona Troiano, and Sara Ubaldini.*

*Color for fashion design*

This project work is dedicated to the study of the color texturing in fashion with the aim of being able to offer the same product with different color variation, in order to reach culturally different markets and to offer the sensation of a personal choice to individual consumers. The starting point is the construction of the color palette, composed by individual colors, for the fashion collection, combined in two or three main approaches in relation to the messages conveyed, their aesthetic and social characteristics. The basic concepts of pigments for dyeing and printing textiles as well as the quality standards for the marketing of fashion products have been presented: clothing, footwear and accessories.



*Figure 3: Project Work "Color for fashion design" teachers Nello Marelli and Renata Pompas. On the left work of Francis Wild. On the right, students at work.*

*Color for interior design*

The project work on interiors design is dedicated to the analysis of the application possibilities of a chromatic design, for the creation of innovative retail spaces, that can ensure a harmonious relationship, with the values from the image communicated by the brand and corporate identity. Starting from practical applications, examples of different approaches to retail design have been shown, proposing a new type of commercial space (permanent or temporary) where the color is integral part of the experience design.
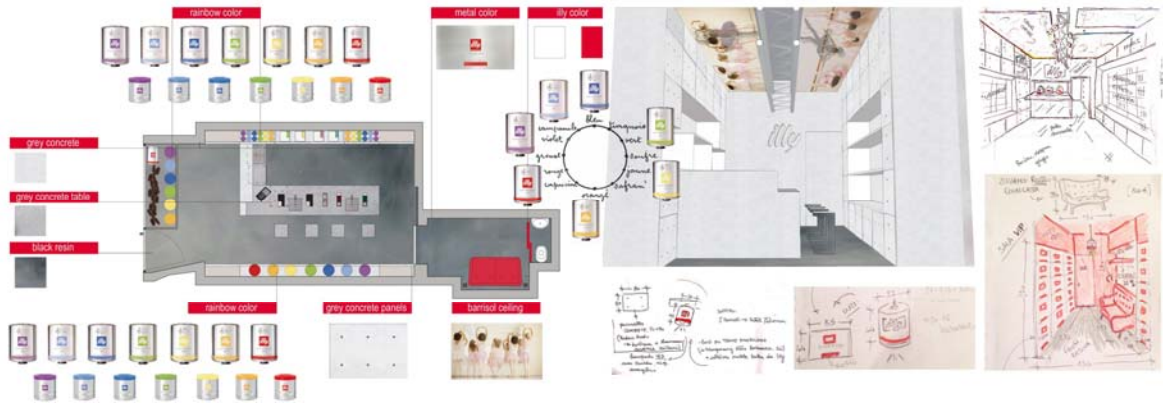


*Figure 4: Project Work "Color for interior design" teachers Arturo Dell'Acqua Bellavitis and Lorenzo Morganti. Work of Costanza Fausone and Ilaria Sarà.*

*Color for industrial product design*

The aim of this project work is to develop a methodology to design through the simulation of a CMF project (Color/Material/Finishes) of a real product (a branded coffee machine in the specific case). The students have gone through all of the methodical phases needed for the definition of the identity of the product: study of the market (position, competitors…), study and definition of the target, study of CMF trends in the sector and creation of CMF scenarios. The CMF responsible for the De Longhi group taught to the class about tendencies, brought samples of the colours used at present on the market and a new prototype ready for the commercial launch. After this first part students have gone through the proposal phase with the design of colours, materials and finishes to apply to the new product. The final output for the presentation have been shown also to the responsible from De Longhi that integrated the notes of the teachers with comments based on their experience on the real market.



*Figure 5: Project Work "Color for product design" teachers Stefania Perenich and Francesca Valan. Work of Suheir Darhouth, Beatriz Travieso and Joni Kirk.*

*Color for urban space*

This part of the master program dealt with the close relationship between architecture and urban space. The aspects related to the interaction between the human being and the natural environment has been analyzed. It will be highlighted the role of the "perceptual project" for the growth of civic and urban identities. The module analyzed the issues related to the phenomena of perception and color in the urban scale by providing theoretical and procedural tools with the support of pictures, cognitive maps and case studies.
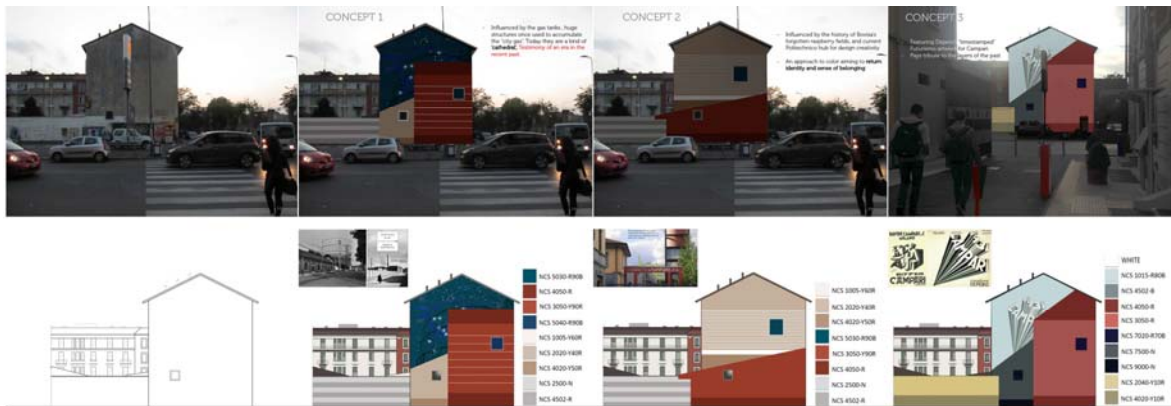


*Figure 6: Project Work "Color in urban spaces" teachers Giulio Bertagna and Aldo Bottoli. Work of Salma Hussein and Tanja Polegubic.*

Interim checks on students' learning progress are scheduled both for the theoretical part and the project works, where they have to work in group to present a final project for each module. After the internship they have to provide a final report considering goals achieved and skills developed during the experience that will be judge by the academic board during the final exam.

## 2.3 Empowerment

Some hours of the master program have been dedicated to the company empowerment: some of the companies (NCS, Barbieri, Mammafotogramma, Flukso, Barco, X-rite, Konica Minolta, Fontegrafica, Mantero, Missoni, Elementi Moda, F.lli Giovanardi, Oikos, De Longhi, Nankai Co Ltd, Merck, TIGER Coatings GmbH & Co. KG and Materis Paints) willing to host interns came in the classroom to tell their story and explain why there is the need of a color expert. They also brought devices and materials to show to the students. Moreover, were made two visits to companies that deal with color design: Clariant Color Work and Lechler, who opened us the doors of their laboratories. Empowerment supports the student's process of personal and professional growth by developing development the ability to form relationships and to work successfully in a variety of dynamics.

## 3. CONCLUSIONS

We are working to launch the second edition of the master. The teaching staff will receive useful information from the interviews that we are doing to the students, faculty, and the companies involved. Meanwhile we are writing this paper, the first edition of the Master in Color Design & Technology is ending. The students, coming from all around the world

(Italy, Australia, Germany, Egypt, Lebanon, Colombia), are engaged in the internship at one of the many companies related to the Master, in view of the final exam, in March. The hosting companies operate in various sectors: chemistry, fashion, product design, and measurement instrumentation as demonstration that color has a multidisciplinary nature and many different applications.

## ACKNOWLEDGEMENTS

## BASIC REFERENCES OF THE MASTER

Ball, P. 2003. *Bright Earth: Art and the Invention of Color*, University of Chicago Press.

Berlin, B. and P. Kay 1969. *Basic Color Terms: Their Universality and Evolution.* University of California Press.

Braddock, S.E. M O'Mahony. 1999. *Techno Textiles: Revolutionary Fabrics for Fashion and Design*. Thames & Hudson.

Fletcher, A. 2004, *Beware wet paint*, Phaidon.

Hoffman, D. 2009. *The interface theory of perception: Natural selection drives true perception to swift extinction*. In Object categorization: Computer and human vision perspectives, S. Dickinson, M. Tarr, A. Leonardis, B. Schiele (Eds.) Cambridge, UK: Cambridge University Press, 148–165.

Hunt, R. W. G. 2004. *The Reproduction of Colour. 6th Edition*. Wiley.

Lefteri, C. 2001. *Plastic, materials for inspirational design*, Rotovision.

McCann, J.J. A. Rizzi. 2011. *The Art and Science of HDR Imaging*. Wiley.

Oleari, C.1998. *Misurare il colore*, Hoepli.

Ramanath R., W. E. Snyder, Y. Yoo, M. S. Drew , 2005. *Color image processing pipeline,* IEEE Signal Processing Magazine 22(1) 34-43.

Wyszecki, G. W.S. Stiles. 2000. *Color Science: Concepts and Methods, Quantitative Data and Formulae, 2nd ed.*, Wiley.

*Address: Prof. Maurizio ROSSI, Department of Design, Politecnico di Milano,*
*Via Durando 38/A, 20158 Milano, ITALY*
*E-mails: alessandro.rizzi@unimi.it, maurizio.rossi@polimi.it,*
*cristian.bonanomi@unimi,it, andrea.siniscalco@polimi.it*

# The ambiguous term of "saturation"

Karin FRIDELL ANTER, Harald ARNKIL, Ulf KLARÉN
SYN-TES Nordic Interdisciplinary Network on Colour and Light

## ABSTRACT

Ambiguous use of colour terms creates misunderstandings in the colour classroom, among professionals and in customer services. One obvious example is the term *saturation.* *Saturation* is not a common colour term in everyday language, but is widely used in the professional languages of art, design and science. There it has got several parallel definitions. In art and design parlance it most often refers to the "intensity" or "vividness" of a colour much in the same sense as NCS *chromaticness* and Munsell *chroma.* It can also be used as an equivalent of "depth", where "deep colours" and "strong colours" are not the same. NCS uses *saturation* for the relationship between chromaticness and whiteness, a variable that cannot be perceived, where the calculated values have no logical connection to perception and which gives a totally ambiguous value to the black elementary colour. We understand the concept of *NCS-saturation* as a deviation from the NCS's solid foundations in human perception and suggest that it is reconsidered and possibly excluded from the NCS's set of parameters. *NCS-saturation* is one of many attempts to categorise colours as deep or saturated in a meaning that does not coincide with their chroma/ chromaticness. Other similar attempts have been made by, among others, Tryggve Johansson, who created a previous version of the natural colour system, and also within the NCS as a "dual attribute" called deepness. We see the need for further investigations of the perceived colour quality of depth.

## 1. INTRODUCTION

Ambiguous use of colour terms creates misunderstandings in the colour classroom, among professionals and in customer services. One obvious example is the term *saturation* (German *Sättigung*, French *saturation*, Spanish *saturación*). *Saturation* is a generic word that one nevertheless seldom comes across in casual speech about colour. It is widely used in professional languages of art, design and science, though, and there it has got several parallel definitions. To add to the confusion, the words *chroma, chromaticness*, *chromaticity*, *purity* and *colourfulness* are also used, referring to more or less the same thing.[1]

## 2. *SATURATION* IN ART AND IN EVERYDAY LANGUAGE

The word *saturation* comes from the Latin word *saturare* (*satur* full). In everyday language*, saturation* is not a common colour term, but in art and design parlance, it is widely used, most often referring to the "intensity" or "vividness" of a colour much in the same sense as NCS *chromaticness* and Munsell *chroma.*

---

[1] Arnkil et al. 2015 includes discussions on several difficulties in colour terminology.

AIC2015 TOKYO - Color and Image

The term *saturation* features in digital colour management in the colour models HSL (Hue, Saturation, Lightness) and HSV or HSB (Hue, Saturation, Value/Brightness). Both HSL and HSV/HSB are cylindrical colour spaces, but with different mappings of the colour variables, resulting in two dramatically different interpretations of *Saturation*.[2] The term *saturation* is also used in chemistry, referring to the limit where a fluid cannot resolve more of another substance. In painting it can similarly refer to the concentration of the pigment or to the relative contents of chromatic pigment and white. These relative contents affect the chromatic properties of the painted surface differently depending on the pigment. Some pigments, such as yellow ochres, yield their most intense appearance unmixed. For those, *chemical saturation* and *chromaticness* coincide. Other pigments, notably blue ones, such as deep ultramarine, become more chromatic when mixed with a little white. For those, the visual property yielded by maximum chemical saturation could be called *depth*.

## 3. *SATURATION* IN COLORIMETRIC LANGUAGE

In the context of a colorimetric colour space the saturation of a colour can be understood as its proximity to its fully chromatic outer limit (Billmayer & Saltzmann 1981 p50) In Hermann von Helmholtz's words, saturation is the proportional mixture of "white" and pure monochromatic light of equal brightness. The same thing is said by Rolf Kuehni, who also clarifies how colorimetric language makes a distinction between *saturation* and *chromaticness.* Varying the brightness of a coloured lamp in total darkness is equivalent to varying its chromaticness. The brighter a red lamp shines, the higher its chromaticness. Kuehni concludes: "Chromaticness is an absolute measure of chromatic content of a colour regardless of its brightness, while saturation is a measure of the chromatic content of colours of equal brightness" (Kuehni 1983, p39f).

## 4. NCS *SATURATION*

In the NCS system, developed by the Judd award winning researchers Hård, Sivik and Tonnquist based on the findings of Ewald Hering (Hering 1964), saturation is used in a way that clearly differs from *chromaticness*. In the following text we refer to this as *NCS-saturation*. According to the definition given in the NCS atlas, colours that lie on a straight line from *NCS black* (S) possess equal saturation; thus *NCS-saturation* is defined as the relationship between *chromaticness* and *whiteness*. The illustration in the NCS atlas gives numeric values for each of the shown three lines (m=0,25, m= 0,50, m=0,75) where *m* refers to the Swedish word *mättnad*, which is used for the same concept as *NCS-saturation* (Svensk Standard 2004). (Fig. 1) The comprehensive scientific presentation of the NCS (Hård et al. 1996 p 188), gives the following equation for *NCS-saturation*:[3]

$$m = c/(c+w) \quad \text{(m: NCS-saturation, c: chromaticness, w: whiteness)}$$

Colours that possess equal *NCS-saturation* constitute what is called a "shadow series", a term that we find similarly used in the Ostwald system (Ostwald & Birren 1969). They

---

[2] Wikipedia. http://en.wikipedia.org/wiki/HSL_and_HSV. Accessed 15.2.2015.

[3] In the comprehensive Swedish presentation of NCS (Hård & Svedmyr 1995), the NCS research team instead defines *mättnad* as m=c/w. This means that *m* can vary between 0 and ∞, which would give other figures in our discussion about *NCS-saturation* but not alter the principal conclusions.

display the perceived variation of a single coloured surface (or object) in an idealised progression from fully lit to totally shaded, approximating the perceived gradient of colour in a depiction of a round or cylindrical object in directional light.[4] Thus the concept of *NCS-saturation* does not (and does not claim to) refer to "vividness", but instead denotes a colour property that could rather be interpreted as "depth".
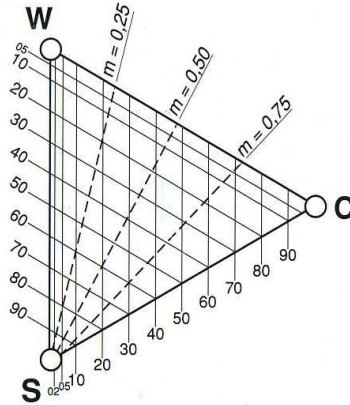


*Figure 1: Lines of equal NCS-saturation, from NCS atlas 2004. The lines in the atlas are not precisely drawn – according to the definition the line for m=0,50 should go from S to the nuance 0050 and the line for m=0,75 from S to the nuance 0075.*

Tryggve Johansson, who developed an earlier version of the natural colour system, also uses the concept of saturation (Swedish *mättnad*) in a similar way. He explicitly distinguishes between saturation and *colour strength* (Swedish *färgstyrka*), and uses *saturation* as a synonym for *depth*. He also presents the idea of *oversaturated* (övermättade) colours, by which he meant colours that are deeper than the colour that has maximum colour strength. Yellow colours cannot be oversaturated – there is no yellow colour deeper than the strongest one – whereas green, red and especially blue colours can increase in saturation beyond the most chromatic colour (Fig 2) (Johansson 1952 p4-6; Johansson 1965 p22-24)[5]. In pointing out this difference between colours of blue and yellow hue, Johansson implicitly acknowledges an observation that also influences everyday language. Colours with bluish hues are also called blue when they have a great amount of blackness, whereas yellowish colours with the same blackness are called brown or olive (Berlin & Kay 1991, Sivik & Hård 1984).

It is unfortunate that the same word – saturation – has been given these different and partly contradictory meanings. Further analysis of the concept of *NCS-saturation* also shows that it is not perceptually consistent, but rather a mathematical play with the numerical values of abstract parameters. For example, in the case of nearly black colours that can barely be distinguished visually, the *NCS-saturation* varies between the lowest (0) and highest (1) possible value (see table 1).

---

[4] It should, however, be noticed that the colour gradient of shading in real spatial contexts depends on the complex situation and cannot be simplified to a straight line in a theoretical model.

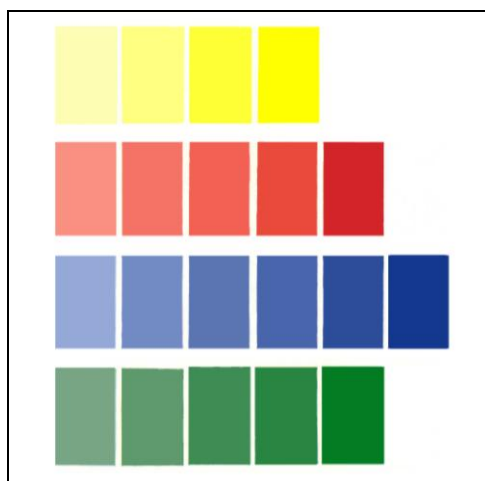[5] Also discussed in Hård et al. 1996 p181-183.

*Figure 2: An illustration from Johansson 1965 p22, with Johansson's caption: "Note the difference between colour strength and saturation. The most saturated colours are placed furthest to the right. Those with the highest colour strength are placed as number four from the left." (Our translation and reconstruction of pixelated figure).*

*Table 1. Calculated NCS-saturation for nuances very close to elementary black.*

| Nuance | Blackness (s) | Chromaticness (c) | Whiteness (w) | m= c/(c+w) | |
|--------|---------------|-------------------|---------------|------------|---|
| 9900 | 99 | 0 | 1 | 0/1 = 0 | On grey scale W-S |
| 9800 | 98 | 0 | 2 | 0/2 = 0 | On grey scale W-S |
| 9700 | 97 | 0 | 3 | 0/3 = 0 | On grey scale W-S |
| 9901 | 99 | 1 | 0 | 1/1 = 1 | On scale S-C |
| 9802 | 98 | 2 | 0 | 2/2 = 1 | On scale S-C |
| 9703 | 97 | 3 | 0 | 3/3 = 1 | On scale S-C |
| 9801 | 98 | 1 | 1 | 1/2 = 0,5 | |
| 9701 | 97 | 1 | 2 | 1/3 = 0,33 | |
| 9702 | 97 | 2 | 1 | 2/3 = 0,67 | |

The table reveals that the grey scale between white and black has *NCS-saturation* = 0. Here *NCS-saturation* coincides with *chromaticness* in a way that creates no conflict with any of the generic meanings of *saturation*. The scale of deep colours, between black and the maximally chromatic colour C, offers much more problems. Here the calculated *NCS-saturation* is maximal. Thus absolute NCS-saturation is a quality of all chromatic elementary colours, whereas white has zero saturation. The NCS-saturation of elementary black cannot be mathematically calculated, and in the graphical NCS model, black is the end point of all lines showing NCS-saturation; this simply makes no sense. Thus, the concept of *NCS-saturation* is misleading in two ways. First, the term *saturation* is not a good choice, as it inevitably leads to thinking about other colour qualities than those referred to by *NCS-saturation*. More serious, however, is the fact that NCS, which is based on colour

perception, introduces a variable that cannot be perceived, where the calculated values have no logical connection to perception and which gives a totally ambiguous value to the black elementary colour. This is not a matter of mere terminology - the concept of *NCS-saturation* would be as illogical and irrelevant to perception whatever it was called.

## 5. NCS DEEPNESS

In addition to *NCS-saturation*, the comprehensive scientific presentation of NCS includes a concept called *deepness* (Hård et al. 1996 p219). The term is tentatively suggested by the authors who point out that it may be ambiguous. Colours with deepness are characterized by a simultaneous resemblance to both black (S) and the maximal colour (C). Colours around the middle of the scale between S and C have the maximal deepness, according to this definition. Based on phenomenological analysis, the authors hypothesize that the deepness value (dv) can be calculated with the following equation:

$$dv = 40 \cdot s \cdot c/(w^2 + 1000)$$

This means that the nuance 5050 has maximal deepness = 100. Elementary black (S) and the maximal colour (C) both have deepness = 0, as does the white elementary colour. Lines of iso-deepness are shown red in Figure 3, which also shows lines connecting nuances with similar values of the analogically defined concepts greyness and clearness. The NCS authors call the three concepts "dual attributes". They mention that it is also possible to observe a corresponding category of colours that have simultaneous resemblance to two chromatic elementary colours. One example of such "dual attributes" is termed *orangeness*.
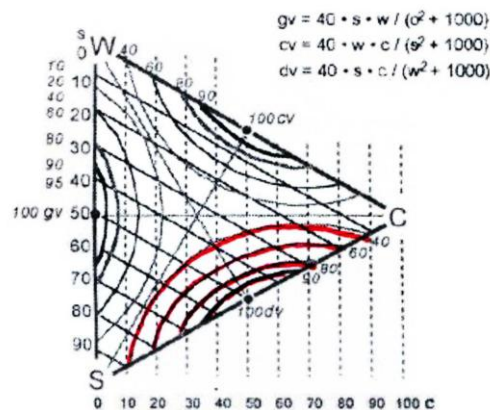


*Figure 2: Lines of equal deepness, from Hård et al.1996 (Marked with red by us).*

When looking at the colour triangle one can see some similarity between *NCS-deepness* and Tryggve Johansson's definition of *saturation*. For bluish hues, Johansson's maximally saturated (oversaturated) colour would approximately equal the nuance with *NCS-deepness* = 100. There is, however, an important difference: In Johansson's analysis, yellow colours cannot be oversaturated and the most saturated yellow nuance is the maximally chromatic one. In NCS, however, the concept of deepness is used irrespective of hue. Also Paul Green-Armytage (2002) indentifies a zone of "deep colours". Starting from the nuance triangle of NCS, he treats all hues in the same way, but his zone of "deep colours" does not fully coincide with *NCS-deepness*.

# 6. CONCLUSIONS

Colours can be perceived as deep, in a meaning that does not coincide with their chroma/ chromaticness. There are a number of attempts to define this quality and arrange it into the order of a colour system, and here the term *saturation* is often used. We see the need for further investigations of the perceived colour quality of depth.

The colour changes caused by successive shading are an interesting field of study, and in this NCS is a useful tool for documentation and analysis of observed phenomena. It is then important to see the system as a tool, not as a model, and not force the dynamics and complexity of real life into symmetry and linearity.

The NCS has solid foundations in human perception of colours. We understand the concept of *NCS-saturation* as a deviation from this approach and suggest that it is reconsidered and possibly excluded from the NCS's set of parameters.

# REFERENCES

Arnkil, H. (ed.) (2015). *Colour and Light - Concepts and confusions,* 2:nd edition. Aalto Univ. Art+Design+Architecture, https://shop.aalto.fi/p/208-colour-and-light/.

Berlin, B. & Kay, P. (1991). *Basic Color terms: Their Universality and Evolution.* Berkeley and Los Angeles.

Billmayer, F. W. Jr. & Saltzmann, M. (1981). *Principles of Color Technology*. Wiley.

Green-Armytage, Paul (2002). Colour Zones – Explanatory diagrams, colour names, and modifying adjectives. *9th Congress of the International Colour Association:* 861-864.

Hering, E. (1964). *Outlines of a Theory of the Light Sense* (Zur Lehre vom Lichtsinne. Wien 1878). Cambridge Mass.

Hård, A. & Svedmyr, Å.(1995). *Färgsystemet NCS. Tanke, tillkomst, tillämpning.* Färgantologi bok 1. Stockholm: Byggforskningsrådet

Hård, A, L. Sivik & G. Tonnquist (1996). "NCS Natural Color System - from Concepts to Research and Applications." *Color Research and Application* 21: 180-220.

Johansson, T. (1952). *Färg.* Stockholm

--- (1965). *Färgboken, färglära för praktiskt bruk*. Svenska Slöjdföreningen

Kuehni, R. (1983). *Color: Essence and Logic*. Van Nostrand Reinhold.

Ostwald, W. & F. Birren ( Eds.) (1969). *The Color Primer*. Van Nostrand Reinhold.

Sivik, L. & A. Hård (1984). *Namn på färger*. Färginstitutet, Färgrapport F24.

Svensk Standard (2004). *NCS Färgatlas SS 19102:2004*. Stockholm: SIS.

*Address: Prof. Karin Fridell Anter, Noreens väg 71, S-752 63 Uppsala SWEDEN*
*E-mails: karinfa@explicator.se, harald.arnkil@aalto.fi, ulf@klaren.se*

# Colour Education and Real Life Colour

**Ulf KLARÉN, Karin FRIDELL ANTER**
SYN-TES Nordic Interdisciplinary Network on Colour and Light

## ABSTRACT

In this paper, we address three problems of traditional colour education: (1) The idea that colour education must base itself on simplified cases as it is seen as impossible to analyse complex perception. (2) The consequent formulation of a traditional "colour knowledge" that is too abstract to relate to our real life experiences. (3) The misunderstanding that subjective experiences are valid only for the experiencing individual.

We claim that colour (and light) education must take its starting point in complex situations based on real life experience, that theoretical and descriptive concepts must apply to such situations, and that it is to a great extent possible to describe complex human experiences intersubjectively.

Our conclusions are based on findings and approaches of the interdisciplinary research project 'SYN-TES' (2010-2011) treating colour and light as a coherent field of knowledge (Fridell Anter et al 2012). SYN-TES is summed up in a book on colour and light for humans, in a spatial context (Fridell Anter and Klarén 2014).

## 1. COLOUR EDUCATION

In most cases colour education focuses on colour phenomena as such, and without taking into account the visual spatial experience. Colour education has no coherent field of knowledge. The content has often been determined by causal needs from different interest groups. For example, the fact that colour education has set out from surface colours in even and uniform light is a pragmatic response to the needs of artists or designers who regarded colours as a tool for pictorial art and for pattern design.

The lack of a holistic approach is in part obscured by abstraction of colour from its natural function in the living context. Artists and educators have been preoccupied by the thought of reducing colour to systems. It has been professionally important to have the use of systems describing mutual relationships between colours. However, useful for particular purposes, systematizing means that colours are represented by notations and colour samples and thus abstracted from their normal context. The nominal colours described in colour systems often are regarded as the "true" and constant colours beyond the accidental colours experienced in the complex world around. Separated from the complexity, a variety of colour phenomena might be clearly demonstrated, but with no connection to a complex spatial world they do not contribute to knowledge related to our every day experiences.

The physical theory describing perceived colours as caused by spectral power distribution also contributes to the notion of colour as something detached from the living context of the world. The Japanese philosopher Januchi Murata remarks that Newton's dark chamber is a device in which a light phenomenon that is inseparable from spatiality is made up into a light phenomenon that is independent of spatial constitution (Murata 2007: 82).

With simplifications – or limitations – of a similar kind, education on light is often restricted to a technical approach using concepts based on a theory on the human visual

systems' response to radiation, and to a large extent using physical measurements that cannot fully describe the complex dynamics of vision or the mutual nature of colour and light experiences.

To humans, the experiences of colour and light are mentally inseparable; colour and light together form our experience of space. Colours are an integral part of the human life-world; they are sensory qualities that are to be taken as "properties of the bodies which are actually perceived through these properties (Husserl 1970: 30). In this sense colours *are* the visual world and never appear isolated.

To conclude: The pedagogical problem of colour and light education is not too high a degree of complexity, but the opposite.

## 2. COLOUR AND LIGHT IN THE REAL WORLD

Colour and light education must take its starting-point from the human living and active relationship to the world around. Like all other living creatures, humans are naturally adapted to the surrounding world. We have our own specific perceptual ecological niche (Gibson 1979). Colour as such has no spatial extension, and colour separated from a spatial context is an abstraction; colour appearance without a connection to space is inconceivable. The human perceptual and cognitive systems – the mode of experience and the abilities to analyse and take stock of position in an ever-changing environment – are fundamental to human adaptation to the world around (Noë 2004: 1–3).

Perceptual adaptation is not limited to basic physiological reactions. It involves interplay between the individual and the world on many levels. These include the basic level of innate reactions (categorical perception), the level of perceptual understanding based on direct experience of the world, and the level of indirect cultural experience (Figure 1).
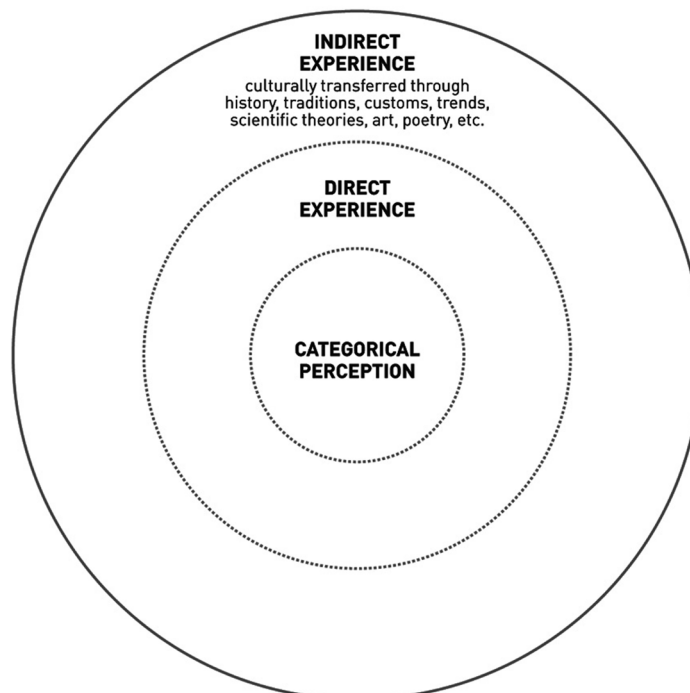


*Figure 1: Experience levels (Klarén 2012: 25-28).*

Colour and light experiences belong to the human perceptual niche and they have their distinctive features from this fact. They are properties of the world taken in relation to the perceiver or depend on both colour perceivers and their environment. (Thompson 1995: 177). Colour and light are natural, but non-physical (Noë 2004: 155). An absolute dichotomy between subjectivity and objectivity is thus hardly applicable to colour and light experiences.

The manifoldness of human colour and light experiences cannot be quantified or mapped in detail. But although our experiences are subjective by nature, our basic perceptual and mental conditions are functionally equal. Human experiences are largely intersubjective, and valid far beyond the individual. Each individual is a subject. However, by sharing and comparing experiences, individuals get a similar understanding of the world. When an external phenomenon is experienced and carefully described (in words and/or measurements) individuals can verify whether experiences of the phenomenon "fit" the description. This is the original core principle of empirical investigation. When it comes to colour and light experiences the only reality available to human senses is the human phenomenal world (Husserl 1936/1970:108-109).

## 3. A NEW PEDAGOGIC APPROACH

A pedagogy describing the coherent spatial interaction between colour and light calls for broad perspectives on aims and purpose of the human colour and light experience. Colour and light education should have its starting-point in phenomenology - in a wide sense of the word

It is possible to rationally describe and analyse colour and light within a complex context, but this requires other tools and concepts than those used in traditional colour and light education. People have a great tacit experience of colour and light in real life, and colour phenomena become clear and comprehensible only when they are discussed as part of a living everyday context, which is spatial by nature.

The interaction of colour and light in a living context may be successively analysed and understood by alternating systematic use of well-defined concepts and practice and reflection. There are as yet no widely applied concepts describing coherent spatial colour and light phenomena, and there is a great need for more research to develop useful methods and concepts. There are, however, a few approaches that have reached a certain spread. For example David Katz in the 1930s presented a number of concepts that names and defines appearance of colour in the spatial context, on surfaces, in transparency, in light sources, etc. (Katz 1935: 6f). *PERCIFAL - perceptual spatial analysis of colour and light* is a relatively late attempt to describe spatial colour/ light experiences (Klarén 2011).

Originally a method for visual evaluation of light presented by Anders Liljefors (Liljefors 2005), PERCIFAL is developed and pedagogically tested in the framework of the SYN-TES project (Klarén 2011). PERCIFAL aims at getting a firmer grasp of the total perceptual effect of colour and light through observation and concepts related to human experience, attention and reflection. Colour and light in the spatial context are described with eight well-defined concepts. The process resembles that of artists; working from the whole to the parts less essential details are sacrificed in favour of the overall impression. One can thereby describe important basic aesthetic and visually functional spatial qualities that are difficult to reveal by other means.

AIC2015 TOKYO - Color and Image

Colour and light education should aim at understanding colour and light phenomena as part of a greater whole, primarily developing the ability to focus attention towards important or relevant visual features in complex colour and light contexts, and – not least – acquiring relevant and well-defined concepts and put them in practice.

Colour and light pedagogy should be reflection, rather than reliance on isolated examples of elementary visual phenomena and abstract physical measurements.

## REFERENCES

Fridell Anter, K., C. Häggström, U. Klarén, and B. Matusiak. 2012. A trans-disciplinary approach to the spatial interaction of colour and light. In the proceedings of *CIE 2012 - International Commission of Illumination - "Lighting Quality and Energy Efficiency"*, Hangzhou, China.

Fridell Anter K., and U. Klarén (Eds). 2014. *Färg & Ljus. För människan – i rummet* (Colour & Light. For humans – in a spatial context). Stockholm: Svensk Byggtjänst. Forthcoming in English.

Gibson J.J. 1979 *The Ecological Approach to Visual Perception.* Hillsdale, NJ: Laewrence Erlbaum

Husserl, E.1936/1970. *The Crisis of the European Science and Trancendental Phenomenology.* Trans. David Carr Everston. IL: Northwestern Univ. Press

Katz, D.1935. *The World of Colour.* London: Routhledge.

Klarén U. 2011. *PERCIFAL – Perceptual spatial analysis of colour and light.* Background and study guidelines. SYN-TES report 3E. Stockholm: Konstfack. www.konstfack.se/SYN-TES

Klarén, U. 2012. Natural experience and Physical Abstractions – On epistemology of colour and light. In Arnkil H.(Ed.), K. Fridell Anter, U. Klarén. *Colour and Light – Concepts and confusions.* Helsinki: Aalto University. http://books.aalto.fi/p/208-colour-and-light/

Liljefors, A. 2005. *Lighting – Visually and Physically. Revised edition.* Stockholm: KTH Lighting Laboratory

Murata, J. 2007. *Perception, Technology, and Life-Worlds (Collection UTCP 1).* Tokyo: The University of Tokyo Center for Philosophy

Noë A. 2004. *Action in Perception.* Cambridge, MA: The MIT Press

Thompson, E. 1995. *Color Vision, A Study in Cognitive Science and the Philosophy of Perception.* London/New York: Routledge.

*Address:Ass.Prof.em Ulf KLARÉN, Metkroken 4, 193 41 Sigtuna, SWEDEN*
*E-mails: ulf@klaren.se, karinfa@explicator.se*

# Color Universes for the Chilean Heritage

Elisa CORDERO,[1] Eréndira MARTÍNEZ,[2]

[1] Instituto de Arquitectura y Urbanismo, University Austral of Chile

[2] Independent Designer

## ABSTRACT

The Government of the Libertador's Region in Chile, south of Santiago (the capital city), has decided to add value to its cultural heritage through the design of two new Interpretation Center buildings for the region. The first will shelter the 11,000 year old archaeological and paleontological site in a lagoon. The second project is related to the work of the famous "chamanto" poncho weavers, high-quality and beautiful woven pieces that received the Award for Excellence. A thorough color study was conducted in each place, including field visits, interviews, photographs, watercolor paintings, samplings and chromatic surveying. Theses colors should be used for the architecture, museography, and graphic art. Colors found were arranged into color universes specially created for each project. A color universe is a conceptual arrangement of colors related to its origin, ownership, culture, and space, among others. The full study, universes and their applications in the project's general image –from architecture to market products– are presented here.

## 1. INTRODUCTION

In 2013, the Government of the Libertador's Region in Chile, decided to design two new Interpretation Center buildings for the region, to add value to its cultural heritage. The O'Higgins Region is an exporter of mining products, in particular, copper and its derivatives. Its fertile soils have also favored the development of agriculture and agribusiness. The best wine that is produced in Chile, also comes from this region. But its touristic potential is not so much exploited, so the possible construction of these new centers are an excellent proposal to maximize its development.

These projects were designed by a team of architects, designers, anthropologists, engineers, and other professional most of them from the University Austral in Chile. They were delivered to the authorities of the Region in the hope they will get the means from the Chilean Government, to build them someday.

The architecture team entrusted each center with a study on color that includes the creation of color palettes to be used in the design of the architecture, museography, and graphic art. A thorough color study was conducted in each center, including field visits, interviews, photographs, watercolor paintings, samplings and chromatic surveying.Colors found were arranged into color universes specifically created for each project. A color universe is a conceptual arrangement of colors related to its origin, ownership, culture, and space, among others. These universes were then used to create the color palettes. The full study, universes and their applications in the project's general image –from architecture to market products– are presented here.

## 2. THE FIRST PROJECT: THE PALEONTOLOGICAL CENTER

The first project aims to shelter the 11,000 year old archaeological and paleontological site of the Tagua Tagua lagoon. In this place, bones of mastodons and other smaller mammals –including deer, horses, and rodents– have been found, as well as human remains belonging to an ancient extinct culture.

### 2.1 Methodology

The first project focused on the colors of the landscape, architecture, soil and museum pieces, mainly bones and arrow tips. Samples were taken of the land in different site locations and depths, where the bones were found, all with the NSC color palette. A study of the colors of the environment was also made, taking into account the landscape, architecture and objects.



*Figure 1: Colour survey of an arrow tip ca 10.000 BP (Elisa Cordero, 2013).*

### 2.2 Results

The colors found during field visits were arranged vertically, their place corresponding to the landscape in a geographical/spatial sense. At the top the colors of the sky and mountains; in the middle, architecture and objects; below, the land and the bones buried in it.This universe of colors was proposed to be used in the architectural, museographic and graphic design projects.

The architectural project offers a journey through the history of the place, starting with prehistory, in a showroom of bones found 13 meters deep and ending with recent history, in the ex-patrimonial house. The architects used the colors to create the atmospheres they needed in their showrooms. The graphic design team created their own color palettes from the color universe for brand design, paperwork and merchandising.
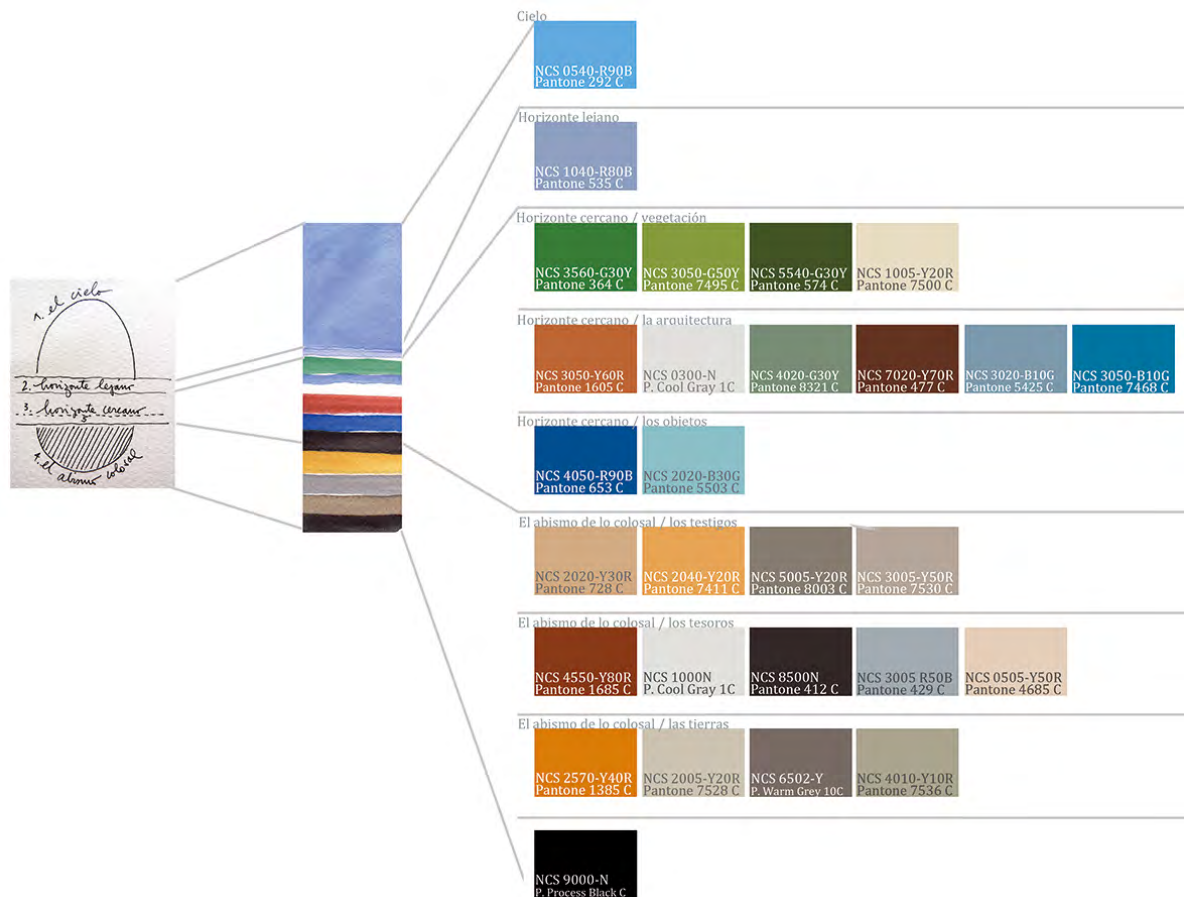
*Figure 2: Color universe created from the colours from landscape, architecture, soil and museum pieces, ordered in a vertical way (Elisa Cordero, 2013).*



*Figure 3: The Graphic Design uses colors from the color universe. Here, the logo and its possibilities (Eréndira Martínez, 2013).*

## 3. THE SECOND PROJECT: THE CHAMANTO CENTER

The second project is related to the work of the famous "chamanto" poncho weavers, beautiful high-quality woven pieces that received the Award for Excellence issued by Unesco in 2011. These master pieces are woven in the small village of Doñihue, of 15,000

people. Only women are authorized to do it, and the weaving technique is inherited from generation to generation in secret. The fabrication of one piece can take 6 months of lonely work, and they can be sold for around 5.000 dollars. The pieces are bought by country men who participate in a typical Chilean sport called "rodeo", where two men in horses must stop a young cow on a certain point inside a round corral. Many of these men are rich landowners, and the chamanto-poncho is an elegant and expensive dressing piece that displays their economic status and masculinity.

## 3.1 Methodology

This project focused on the colors of the threads used by weavers, and the colors of the landscape of Doñihue village. The colors of the ancient chamantos were studied in the "Museo del chamanto", some of which are up to 100 years old.

For current chamantos, the village weavers of Doñihue were sampled. The first step to approach the world of the weavers was to coordinate interviews to find out, for example, what meaning was given to the colors, which are the most common ones and how they decide the colors of each piece. Photos of the chamantos were taken as well as color samples and color surveys of the threads, parallel to the observation of the landscape, architecture and objects, studied through photos, sketches and color surveying.



*Figure 4: Color Survey with NCS of a Chamanto (Elisa Cordero, 2013).*

## 3.2 Results

The investigation showed that the designs are closely linked to country life, for they mostly represent flowers, fruits and animals. These elements were the basis for sorting colors in a geographical way (with the 4 cardinal directions) in this way: North, warm light: Yellow. South, cool light: Blue. East, rising sun: White. West, night: Black. In the center, the central valley of Chile, with its green fields and lands, split by the bright crimson of wine. From this scheme, the colors of the exterior are arranged within the project. Outside, each of the four corners of the architectural project dons one of the colors of the cardinal directions. Each room in the interior will also take on the color of each direction depending on its orientation.
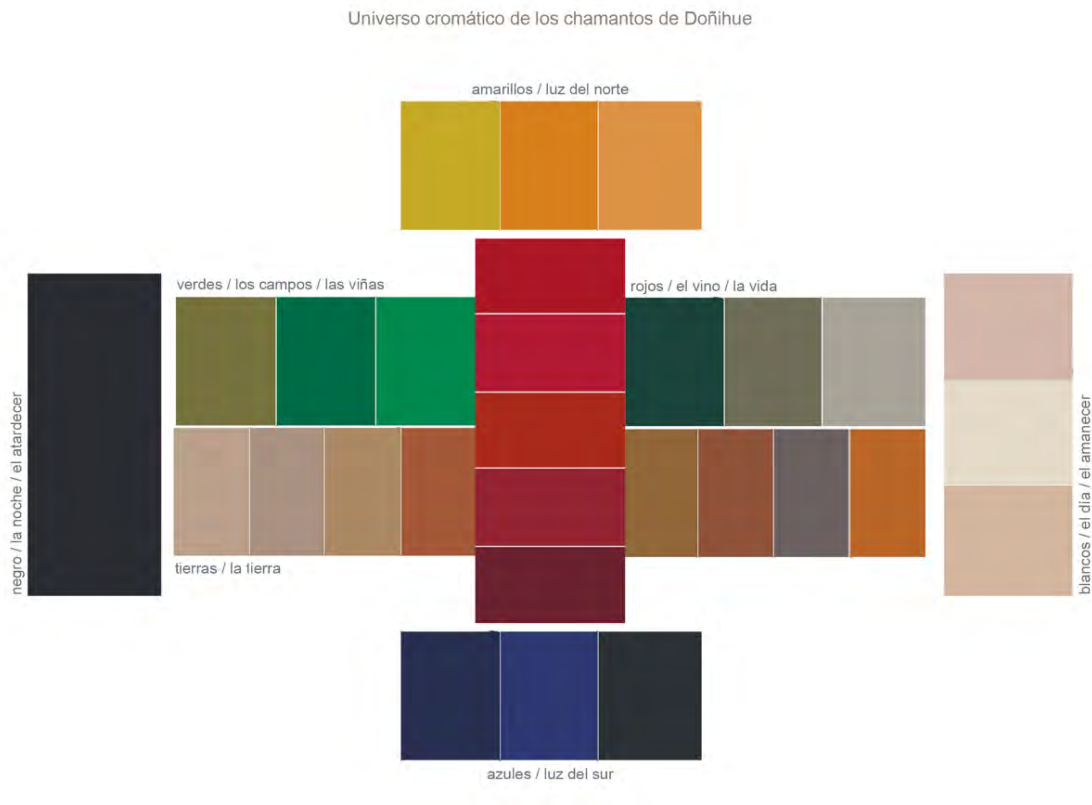
Universo cromático de los chamantos de Doñihue

amarillos / luz del norte

verdes / los campos / las viñas

rojos / el vino / la vida

negro / la noche / el atardecer

tierras / la tierra

blancos / el dia / el amanecer

azules / luz del sur

*Figure 5: Color universe created* on the colors of the threads and the landscape of Doñihue village, ordered in a geographical way *(Elisa Cordero, 2013).*



*Figure 5: The architecture Project used the color universe for the fassade (Institute of Architecture Archiv, 2013).*

The graphic design team created their own color palettes from the color universe for brand design, paperwork and merchandising.



*Figure 6: Some examples of the use of the color universo on graphic pieces (Eréndira Martínez, 2013).*

## 4. CONCLUSIONS

The assignment of the management team to create a color palette for the entire interpretation centers project was a challenge, because it was not only to create a useful palette, but to create an order that made sense to the project itself. This was achieved in both cases thanks to a deep study of the place where the project was to be deployed, which included space, landscape and social aspects (through interviews). The universe of colors is the temporal, spatial and social expression of a (current or past) historical moment, expressed through the language of colors. Because of these characteristics, is inextricably linked to the architectural project and other projects (graphic design, museology, landscaping) that make up the overall project.

*Address: Prof. Elisa CORDERO, Institute of Architecture and Urbanism,*
*University Austral of Chile, Faculty of Architecture and Arts,*

*Elena Haverbeck s/n, Isla Teja, Valdivia, CHILE.*
*E-mails: elisacordero@uach.cl, eremartinez@gmail.com,*

# FORSIUS' SECOND COLOUR ORDER DIAGRAM OF 1611 FROM THE ICONIC POINT OF VIEW

Verena M. SCHINDLER
Art and Architectural Historian, Zollikon
Atelier Cler Études Chromatiques, Paris
Chair of the Study Group on Environmental Colour Design (ECD) of the Association
Internationale de la Couleur (AIC)

## ABSTRACT

In her AIC 2009 paper the author demonstrated how important the cultural and historical context of colour order systems is for understanding them. This is especially the case for the colour order system of pastor, astronomer, mathematician, natural philosopher and astrologer Sigfrid(us) Aron(us) Forsius (ca. 1550–1624) that is illustrated by two diagrams in his *Physics, or a Description of the Qualities and Properties of Natural Things* of 1611. As the manuscript remained in the Archives of the Royal Library of Stockholm unpublished for more than 330 years until Johan Nordström published the transcription of the handwritten text in 1952, serious and critical debate of his work, and thus of his colour order diagrams, as well as its impact and acknowledgement previous to 1952 is non-existent. On the basis of printed evidence of his time, the author showed that Forsius' second diagram could perfectly be interpreted as a sphere, contradicting Kuehni and Schwarz's thesis (*Colour Ordered*, 2008) of a "linear" system. The present paper rejects Werner Spillmann's thesis (2001) that the colour order of Forsius' second diagram is incompatible with a sphere. The author bases her hypothesis on her own observations of the armillary sphere at the Globe Museum of the Austrian National Library in Vienna which show that Forsius' second scheme can be interpreted as a colour sphere. Hence, Forsius introduced a spherical colour system long before Otto Runge's Farben-Kugel (Colour Sphere) of 1810. These observations will be demonstrated with pictorial evidence. Further, Forsius' diagrams are considered in the context of contemporary colour theories such as those of François d'Aguilon (1566-1617), Athanasius Kircher (1602–1680) and Robert Fludd (1574–1637).

## 1. INTRODUCTION

### 1.1 Description of Forsius' colour diagram

First I'd like to describe Sigfrid(us) Aron(us) Forsius' second diagram in the possibly most neutral way. Figure 1 shows a geometrical form representing a circle. Within the circle, a straight vertical line is connecting two points of its cicumference as a diameter. Two curved lines either side of this vertical line connect the same two points on the top and the bottom. Small circles are set outside the circumference on the top and at the bottom. The one at the bottom is filled in with ink, and thus appears black. Five horizontal lines run across the circular form. The largest runs perpendicularly through the midpoint of the vertical line, thus through the center of the circle. Two horizontal lines further cut the upper semicircle in equidistant sections. Two other runs through the lower semicircle in the same way.

AIC2015 TOKYO - Color and Image

Handwritten colour names appear horizontally in the figure, with the exception of the four names (from left to right) 'red', 'yellow', 'green' and 'blue' that are midway between the top and the bottom, and going the length of both sides of the circumference and also the two curved lines. Further two colour names on the top left are written going along the interior side of the circumference.
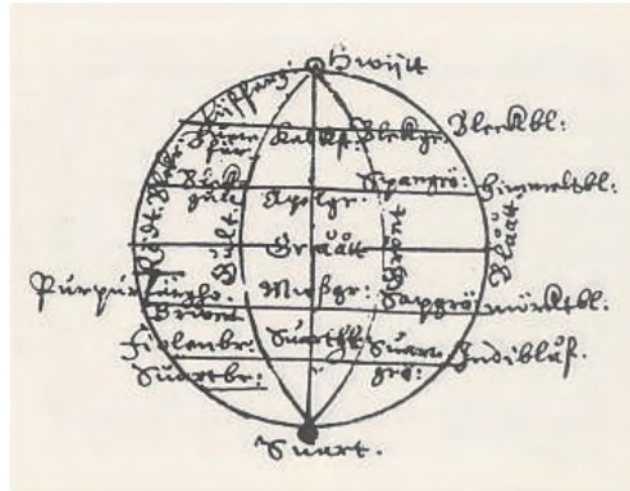


*Figure 1: Sigfrid Aron Forsius: Second colour order diagram, manuscript folio 421v of 1611.*

## 1.2 Forsius' manuscript

Forsius' drawing elucidates visually how colours organize in a geometrical form according to his philosophical ideas. It sounds amazing, but Forsius' diagramme seems to be one of the earliest showing visual evidence of the relationship between colours. The drawing appears in Book 9, Chapter VII entitled 'On vision' (Kiiskinen 2007: 355) of his manuscript on *Physics, or a Description of the Qualities and Properties of Natural Things* completed in 1611. The nine books on physics deal with principles of nature and are written in the grand tradition of Aristotle. Colour is discussed in the last chapter, which deals with the senses and is specifically related to the sense of sight or vision.

Forsius himself mentioned his manuscript for the first time in a dedication to his 1610 astrological prediction, dated August 1, 1609, and completed it in Stockholm in 1611. It was the first text on the topic written in Old Swedish and included 485r folio pages. After his death two attempts to publish it in 1626 and 1652 failed. Forsius' manuscript remained thus in the Archives of the Royal Library of Stockholm unpublished until Johan Nordström published the transcription of the handwritten text in 1952.

## 2. INTERPRETATION OF GEOMETRICAL FIGURE

### 2.1 On different interpretations since 1952

Concerning Forsius' scheme there is no agreement among scholars, whether the scheme is meant to be a linear system, or rather a sphere. Some researchers adhere to a three-dimensional interpretation (Feller and Stenius 1970), seen as a "World of Colours" (Hesselgren 1984: 220), however, the latter points at "some difficulty in making the perspective drawing of the sphere." This same argument will be taken up later (Kuehni

2003: 34–36) and Forsius' scheme will be put forward as a 'linear system' because of two reasons: "First, how to properly draw a transparent sphere was well known in the seventeenth century from several earlier books on perspective and geometry. Second, the text does not indicate that Forsius had a three-dimensional arrangement in mind." (Kuehni and Schwarz 2008: 45–46) More recently, Jones argues that "This model, if interpreted as three-dimensional, is surprisingly modern, (1) in its recognition of four primary hues and their complementarity, (2) in its use of the white-grey-black scale as a second parameter, and (3) in the introduction of a third dimension in which all the other colours fade to a central grey". Based on former articles (Spillmann 1993; Kuehni and Schwarz 2008), however, Jones concludes that "the weight of opinion now seems to favour a two-dimensional interpretation" (Jones 2013: 179).

## 2.2 Forsius' background

Forsius was a pastor, astronomer, mathematician, natural philosopher. When he began to write his 1611 manuscript, he was a professor of astronomy at the University of Uppsala (Sweden), where he lectured not only astronomy, but also geography and astrology (which also included meteorology and weather forecasts). It is important to note that in 1607 he was the first to publish an almanac calculating astronomical data of star positions at the local horizon for Stockholm and Åbo (Turku, in Finnish). In 1612, Forsius was appointed Royal Astronomer (Astronomus Regius) by King Gustav II Adolf, and in 1613 he was given the exclusive privilege of editing and printing almanacs. Forsius was a scientist of great knowledge, particularly in mathematics, and was called Sweden's first astronomer (Schindler 2009). This is especially significant contextually and historically for the interpretation of Forsius's scheme.

## 2.3 Armillary sphere

The author claims thus that such an armillary sphere was the basis of Forsius colour diagram. The armillary sphere is a device to determine celestial positions and demonstrate the motion of the stars around the Earth. Its name comes from the Latin *armilla*, since its skeleton is made of graduated metal circles linking the poles and representing the equator, the ecliptic, meridians and parallels. In Forsius' times, a ball representing the Earth (and later, the Sun) is placed in its center. Before the telescope was introduced in the 17th century, the armillary sphere was the prime instrument of all astronomers. In sum, a *sphera mundi* (armillary sphere) was the model and not a *mappa mundi* (globe) as in Philipp Otto Runge's *Farben-Kugel* of 1810 (Spillmann 2009: 40; Runge 1999).

## 2.4 A matter of perspective

Being an astronomer implies specific ways of drawing such an armillary sphere that can deffer from those of a painter. Circles can become straight lines depending of the point of view. Albrecht Dürer's *Nude Woman with Zodiac* is just one illustration of the fact that an armillary sphere could be composed of straight lines representing imaginary circles. As well, the symbol of the Portuguese Empire of the time gives much insight.

# 3. COLOUR ORDER

Some scholars base their arguments on the widely spread Aristotelian philosophy of the Middle Ages based on the four-colour theory (Parkhurst and Feller 1982: 226). The same authors also point at Alberti's six primary colours as the ancestor of Forsius' scheme. John Gage, however, notes a lack of coherence in the organization of colours, e.g., orange is located between yellow and black, and not between red and yellow (Gage 1997: 166). Another argument is put forward concerning the order of the four main colours. "A powerful argument against reading the Forsius diagram as a sphere has been put forward by Werner Spillmann. If the central horizontal line is to be read as a circle seen from the side, the colours are not in the right order." (Green-Armytage 2005: 349–351; Spillmann 2001)

The author bases her hypothesis on her own observations of the armillary sphere at the Globe Museum of the Austrian National Library in Vienna, which show that Forsius' scheme could be interpreted as a colour sphere. Looking from a specific angle, the colour order is changed in such a way that the order of the colours will constitute a hue circle corresponding to that of the NCS-System, flipped horizontally.
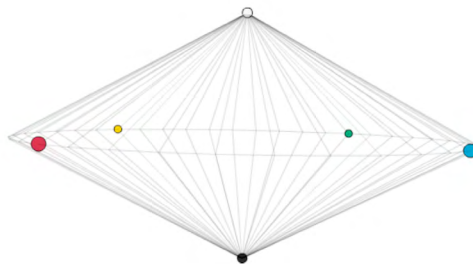


*Figure 2: NCS double cone from the navigator, flipped horizontally.*
*© http://www.ncscolour.com/en/natural-colour-system/*

## REFERENCES

Caivano, J. L. 1995. *Sistemas de orden del color,* Serie Difusión 12, Buenos Aires: Secretaría de Investigaciones en Ciencia y Técnica, Facultad de Arquitectura, Diseño y Urbanismo.

Feller R. L. and A. S. Stenius 1970. On the Color Space of Sigfrid Forsius 1611, *Color Engineering* 8(3), 48–51.

Forsius, S.A. 1611. *Physica,* Universitatis Upsaliensis 2, ed. Nordström, J. editor, Uppsala: Lundequist.

Gage, J. 1997. *Kulturgeschichte der Farbe: Von der Antike bis zur Gegenwart*, Ravensburg: Ravensburger Buchverlag.

Green-Armytage, P. 2005. *Colour, language, and design*, PhD thesis, University of Western Australia, Faculty of Architecture, Landscape and Visual Arts.

Hård A. 1969. Quality Attributes of Colour Perception (10:1), *AIC Color 69, Book of Abstracts of the 1st Congress of the Association Internationale de la Couleur*, Stockholm.

Hesselgren, S. 1984. Why Colour Order Systems? *Color Research and Application*, 9(4), 220–228.

Jones, W. J. 2013. *German Colour Terms: A Study in their Historical Evolution from Earliest Times to the Present*, John Benjamins.

Kiiskinen, T. 2007. *Sigfrid Aronus Forsius. Astronomer and Philosopher of Nature*, Frankfurt am Main: Europäischer Verlag der Wissenschaften Peter Lang GmbH.

Kuehni, R. G, 2003. *Color Space and Its Divisions, Color Order from Antiquity to the Present*, New York: A John Wiley.

Kuehni, R. G. and A. Schwarz 2008. *Colored Ordered, A Survey of Color Order Systems from Antiquity to the Present*, Oxford: University Press.

Parkhurst C. and R. L. Feller 1982. Who Invented the Color Wheel? *Color Research and Application* 7(3), 217–230.

Runge, P. O. 1999. *Farbenkugel: Konstruktion der Verhältnisse aller Mischungen der Farben zueinander und ihrer vollständigen Affinität (1810); mit Notizen zur Farbe und deren Briefwechsel mit Goethe*, Köln: Tropen-Verlag; Stuttgart-Bad Cannstatt:frommann-holzboog.

Schindler, V. M. 2009. Forsius' Colour Order System (1611): Its Cultural and Historical Context and its Impact on Contemporary Colour Culture, *Proceedings of the 11th Congress of the Association Internationale de la Couleur*, ed. by Dianne Smith, Paul Green-Armytage, Margaret A. Pope and Nick Harkness. CD. Sydney: Colour Society of Australia.

Schindler. V. M. 2009a. Forsius e i suoi diagrammi di ordinamento dei colori (1611), *Luce & Immagini* 14(4), 13–15.

Spillmann, W. 1993. Philipp Otto Runge—ancestor of the 20th century colour order systems. *Proceedings of the 7th Congress of the Association Internationale de la Couleur,* ed. by Antal Nemcsics and János Schanda, Budapest: Hungarian National Colour Committee and Technical University of Budapest, Vol. C14, 6–14.

Spillmann, W. 2001. Farbskalen, Farbkreise, Farbsysteme, Wallisellen: *Applica*, Special Issue.

Spillmann, W. (Ed.) 2009. *Farb-Systeme 1611-2007*, with texts by V. M. Schindler, S. Wettstein, et al., and an introduction by Karl Gerstner, Schwabe Verlag: Basel.

*Address: Verena M. SCHINDLER, Atelier Cler Etudes Chromatiques, 64 rue Vergniaud, 75013 Paris, FRANCE*
*E-mail: verenam.schindler@uzh.ch*

# Five Colours - A Study of Chinese Traditional Colour

Jie, XU

The School of Arts, Loughborough University

## ABSTRACT

This research gives an overview of Chinese traditional colour, and intends to investigate the characteristics and the principles of the Five Colours in a Chinese cultural context. This study may inspire the designers in contemporary graphic design field.

The Five Colours are the earliest and basic colours that recorded in Chinese history. It first appeared in the book Shu Ki (before 221 A.D.). 'Fully displayed in the Five Colours, so as to form the ceremonial robes; - it is yours to see them clearly' (translated by Legge. 1879). These representative samples can reflect the common characteristics of traditional colour usage. Therefore, this research focuses on the Five Colours, which are Red, Cyan, Yellow, Black and White.

The research context unites three independent and related fields of study: ontology of the Five Colours, colour theory, and the Five Colours in relation to the Five Elements: Red-Fire; Cyan-Wood; Yellow-Earth; Black-Water; and White-Metal.

The methodology includes: a literature review, quantitative data collection, correlation analysis, visual research and a case study.

The research shows that the original meaning of Five Colours derives from certain natural scenes that specifically refer to some substances, for example, the original meaning of black is refer to mark on a man's face. However, the colour names can become abstract nouns when they develop as the metaphors that refer to the different ideas. For instance, the extensional meaning corresponds to the Five Elements. The symbolisation of the Five Colours also extends the contents to associate with other concepts and sensations.

In addition, from the comparison with different colour system, the colours are not primary colours in modern chromatics classification. Instead the Five colours are close to the natural colour hue and the colour combination reflects the tones, which profoundly influences the Chinese traditional aesthetics.

In conclusion, colour can be discussed as a concept rather than just a visual element in the Chinese traditional cultural context. The philosophical 'balanced' thinking of the Five Elements applies the premier principle to the colour applications. Consequently, the concept of 'harmony' develops as the fundamental theory of Chinese traditional aesthetics.

## 1. INTRODUCTION

When I reviewed the traditional Chinese colours, which gives more imagination and evocation just by the colour names. For example, one of the colour called Xiangsi Hui (Warm Grey), which direct translated meaning is the grey of lovesickness. And the

subtleness of shades appears in traditional paintings and crafts are always appealing. Is there any principle of the colour application? To which extent graphic designer are using the five Chinese traditional colours and their meanings?

In the current graphic design research context, this subject has yet to be studied systematically. This research therefore complements the existent explorations of archaeology and social culture. Further, it may add or widen the horizon of historical and contemporary understandings of colour.

## 2. METHOD

The methods combine primary and secondary data collections. By using a systematic methodology, the original meanings and development of the Five Colours were examined from different aspects: etymology and chromatic. Attempt to restore and synthesise the concept of the Five Colours. The evidence potentially enables the answer of initial research question, which is there any principle of the colour application.

### 2.1 Sample Preparation

The study first focuses on the etymology of Five Colours from the Oracle (Xu Zhong Yu, 2006) (Fig. 1), which was the earliest hieroglyph, we see the description of the original story and the primary meanings attributed of the Five Colours. The diagram has been further extended with the definitions of the word class in linguistic.

| Oracle | Chinese Name | English Name | Word Class | Original Meaning |
|--------|--------------|--------------|------------|------------------|
|  | 黃 | Yellow | Abstract Noun, Adjective | The bulleye of target with mud |
|  | 赤 | Red | Abstract Noun, Adjective | A man dancing on the fire |
|  | 青 | Cyan | Abstract Noun, Adjective | The ore from coal mining |
|  | 黑 | Black | Abstract Noun, Adjective | A mark or stain on man's face |
|  | 白 | White | Abstract Noun, Adjective | Air from the mouth |

*Figure 1: Naming of Five Colours*

On the other hand, by using the principle of the Five Elements, which is the foundation of Chinese philosophy, to determine the Five Colours. The Five Elements: Metal, Wood, Water, Fire and Earth, are the summary of nature that known as a cyclical transforming system, which based on generating and overcoming, and reveal the law of the universe. According to the principle of association with the colours, it

demonstrates a series of chromatography that incurs the relationship of harmony and contrast colour presentations (Fig. 2).
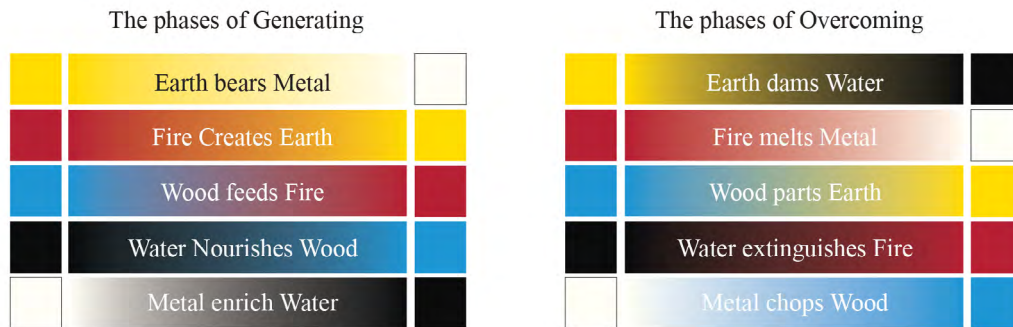


| The phases of Generating | The phases of Overcoming |
|---|---|
| Earth bears Metal | Earth dams Water |
| Fire Creates Earth | Fire melts Metal |
| Wood feeds Fire | Wood parts Earth |
| Water Nourishes Wood | Water extinguishes Fire |
| Metal enrich Water | Metal chops Wood |

*Figure 2: Phases of Five Colours*

As there is a tight cultural connection between China and Japan since ancient times. A well-documented Japanese traditional colour profile is a good case study of establishing a modus of naming, the classifying and determining any unique characteristics, as well as the way of research. The case study has selected 372 colours from Japanese traditional colours as the research samples, whereby each refers to a Chinese traditional colour.

## 2.2 Experimental Procedure

There are four main types of colour systems: RYB, RGB, CMYK and NCS, which contain both additive and deductive methods of colour mixing. The comparison of the samples reveals that the difference between Chinese traditional colour and other colour system in hue, value, and chroma by using Munsell colour theory (Fig. 3). The precise analysis visually demonstrates and determines the constitution and attribute of the Five Colours in chromatics. The five colours are not the primary colour and the tone is close to the natural colour classification.



Hue

*Figure 3: Colour Comparison Table*

According to the book The Yellow Emperor's Inner Classic (478 B.C.) the Five Colours represent the Five Elements and many other concepts (Fig. 4). Based on principle, a quasi-experimental test is designed to see, whether people can associate the colours with the associated ideas according to ancient theory.

| Five Colours | Five Elements | Five Directions | Five Seasons | Five Tastes | Five Senses | Five Emotions |
|---|---|---|---|---|---|---|
| Cyan | Wood | East | Spring | Sour | Sight | Anger |
| Red | Fire | South | Summer | Bitter | Touch | Happiness |
| White | Metal | West | Autumn | Spicy | Taste | Worry |
| Black | Water | North | Winter | Salt | Hearing | Fear |
| Yellow | Earth | Central | Seasons | Sweet | Smell | Sadness |

*Figure 4: Association of Five Colours*

## 3. RESULTS AND DISCUSSION

Through the oracle description it shows that the Five Colours original meaning derives from the live scene (Fig.1), which reflects that colour is the most expressive feature of the memory from the image. In this sense, imagery colour is a narrative form of visualisation.

Moreover, the Five Colours correspond to the Five Elements and other concepts in Chinese cultural context. The colour symbolism is to visualise the abstract concepts and ideas. The balanced and harmony principle of the Five Elements influences the usage of the Five Colours.

From the comparison of other colour system, there is no explicit evidence state that the Five Colours are the primary colours in modern chromatics. NCS colour has the most similar hue to the Five Colours. These 'natural' tones were considered as the basic colours in ancient Chinese pigment.

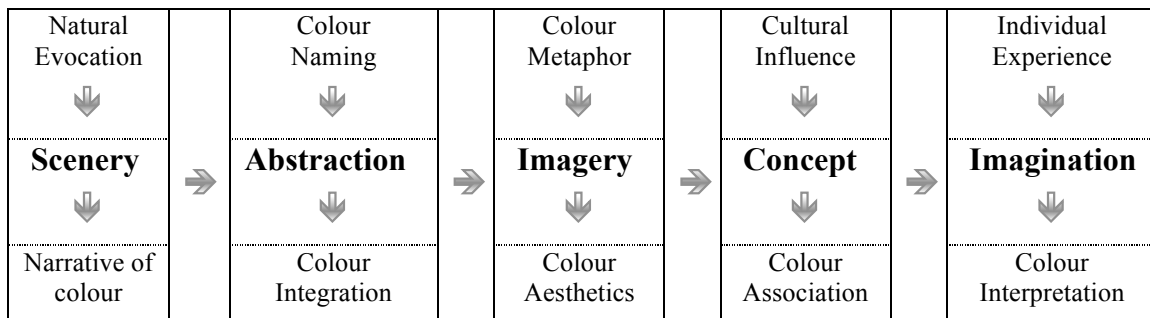| Natural Evocation ⬇ | | Colour Naming ⬇ | | Colour Metaphor ⬇ | | Cultural Influence ⬇ | | Individual Experience ⬇ |
|---|---|---|---|---|---|---|---|---|
| **Scenery** ⬇ | ⇒ | **Abstraction** ⬇ | ⇒ | **Imagery** ⬇ | ⇒ | **Concept** ⬇ | ⇒ | **Imagination** ⬇ |
| Narrative of colour | | Colour Integration | | Colour Aesthetics | | Colour Association | | Colour Interpretation |

*Figure 5: Chinese traditional colour mapping*

The mapping (Fig.5) shows the variation of the colour status in different stages. The earliest recognition based on the impression of a particular scene. This feature of memory was combined with psychological factors and extends the connotation meanings. The colour abstraction developed as a metaphor to refer to many other concepts when associated with certain cultural contexts. Eventually the colour symbolism allows the evocation of the imagination by individual experiences.

Additionally, the quasi-experiment test was invited 36 audiences from different countries, the result shows that most of the audience failed in the test to associate the Five Colours with other concepts according to the ancient rules. There is no direct map to today's world in the colour matching. Once set free from a given cultural

background, any interpretation will have a deviation according to the newly changed circumstances.

The limitations of the result, such as, language is inadequate in description of the colours, even it is a concrete noun, and the audience still has individual interpretation. One colour name may suggest a range of tones. I selected 327 samples to study the Japanese traditional colours, it shows that Japanese people uses more of the concrete nouns as colour names. In most of the cases, the colour naming denotes something in particular. Unlike Chinese tradition, the way that Japanese people divides colour into specific categories that avoid the distinction of colour as much as possible.

# 4. CONCLUSIONS

According to this paper, it shows that the cognitive bias of the colours derives from the process of abstract naming. There is no accurate term or parameter to quantify volume of colours. As colour can evoke different imaginings from different experiences, in this sense the way of interpreting colours is similar to that of interpreting images.

The ancient Chinese attributed a naturalistic manifestation to the colours. The Five Colours are therefore highly associated with the natural elements (Five Elements) and constituted an inner cyclical system, which generates and overcomes in the relationships of influencing each other. Furthermore, this belief that the nature law affected the moral, social and philosophical idea of Chinese traditional colour (Fig.6 , Fig.7).
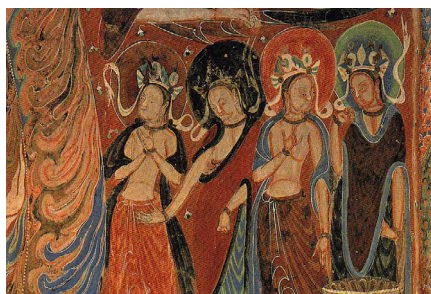


*Figure 6:  Mogao Caves Painting*

（*Cave 285, Wei Dynasty*)

*Figure 7: China Five Coloured Flag*

（ *1921-1928*）

Central to the research question, in order to decode the colour, it is imperative to understand the significance of a particular cultural dimension. Traditional Chinese colour which is combined with other disciplines and cultural contents,  negates the metaphor for the fixed cultural meanings. The 'balanced' thinking in philosophy of the Five Elements applies the premier principle to colour applications. Hence, the concept of 'harmony' was developed as the fundamental theory in Chinese traditional aesthetics.

Through the study of Chinese traditional colour, the enlightenment to the designers is that the colour has power of symbolism with its abstract form. The meaning of form refers to narratives, cultural contexts, and philosophical concept and so on. Therefore, colour is not only can be seen as a visual element but a symbolic image to visualise the abstract concepts or synesthesia other feelings. It implies that a good designer should be also a colourist who deeply understands the colour as a visual tool.

## ACKNOWLEDGEMENTS

## REFERENCES

RILEY, C. 1995. *Color Codes: modern theories of color in philosophy, painting and architecture, literature, music and psychology.* Hanover; London: University Press of New England.

ALBERS, J. 2013. *Interaction of Color.* 4th Ed. New Haven and London: Yale University Press

ANONYMOUS. 1996. *The Book of Songs.* translated by WALEY, A. New York: Grove Press,

VOLLMER, J. 1980. *Five Colours of the Universe: Symbolism in Clothes and Fabrics of the Ch'ing Dynasty (1644-1911).* China: The Gallery.

BURCHHARDT, T. 2009. *Foundations of oriental art and symbolism.* Indiana: World Wisdom, Inc.

XU, Z. S. 2006. *Oracle Dictionary.* Sichuan: Sichuan Publishing.

NI, M.S. 1995. *The Yellow Emperor's Classic of Medicine.* Boston: Shambhala Publications, Inc.

2015. Traditional colors of Japan. [online]. [viewed 20/10/14]. Available from: <http://irocore.com>

2013. Chinese Traditional Colors. [online]. [viewed 5/11/14]. Available from: <http://archive.today/TlsGt>

*Address: Johnny Xu Jie, The School of Arts, Loughborough University*
*Loughborough, LE11 3TU, United Kingdom*
*E-mails: j.xu4-14@student.lboro.ac.uk*

# Meeting New Challenges in Colour Tendencies in Norway

Kine ANGELO and Alex BOOKER,

Department of Architectural Design, Form and Colour, Faculty of Architecture and Fine Art, Norwegian University of Science and Technology (NTNU)

## ABSTRACT

A recent debate in the Norwegian press, and in part raised by the authors through the exhibition Colour in the City in Trondheim 2014, points to a dramatic change in the colour pallet used both in the repainting of existing buildings and as a dominant tendency in recent architecture. This is exemplified in a substantial shift towards an achromatic pallet. Jotun, the major provider of paint in Norway, has noted that 80% of the exterior paint sold in recent years has been white, grey, brown or black. This is counter to a long tradition of chromatic variation in both vernacular and 19th and 20th century architecture. Colour and materiality play an essential role in shaping our place and identity. Colour is information, it tells us about history, about status, about territories and functions. Previously distinct chromatic neighborhoods are being eroded and new property developments build without any chromatic character or differentiation. Area character as distinct architectural styles and chromatic qualities is an important contribution to the identity and differentiation in the urban environment; it provides both a means of identification, navigation affordance and generator of aesthetic atmospheres in the architectural gestalt. Place is more than a street number, it is an ensemble of qualities and relationships that make meaning; materiality and colour are the key component in this process. The scope of this paper will be an analysis of the drivers of this process from developer to the architect to the consumer with the intention of developing a colour program methodology that meets the pressures of increasing urban densification.
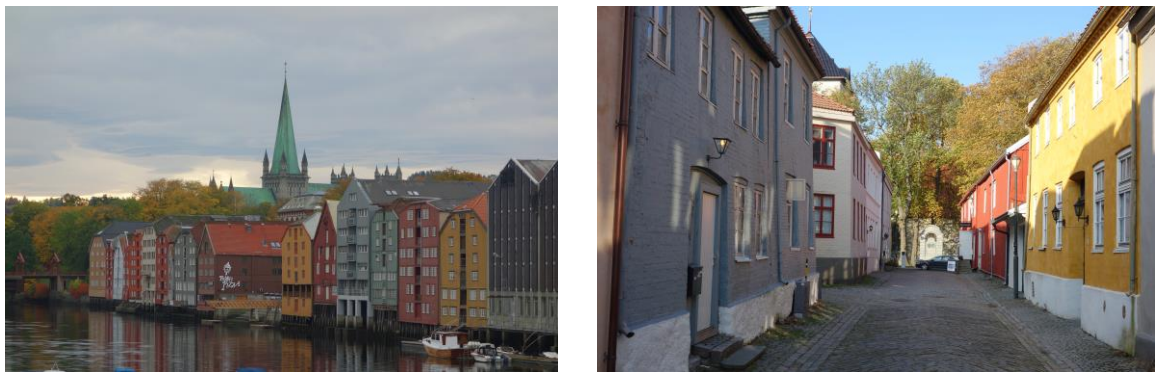
*Figure 1: The Waterfront Warehouses in Trondheim and neighboring area.*

## 1. INTRODUCTION

The city of Trondheim dates back over a thousand years, and the contempory building mass contains all the varieties of architectural styles, sizes and materials. But the image of Trondheim and its main identity is foremost associated with the remaining clusters of older wooden and plaster rendered buildings painted with pictorial colours in easily apprehended

AIC2015 TOKYO - Color and Image

relationships between hues and nuances. As of today, this is only a small element in the city's overall chromatic and material gestalt.

Colours in architectural context are the contextual result of the past and the present. Architectural colours are determined by variables of geography, such as culture, tradition, symbolic meaning and local resources. Other, time-related variables are preferences for a colour at a given period in history, the socio-political context and new technological advances. In short, the interactions of these variables have resulted in a present colour scheme of both governed regulations and ungoverned preferences and colour accessibility. However, none of these are perfectly or permanently consolidated, and all are susceptible to changes in patterns of use, of ownership and the tendencies of fashion; this last fifteen years exemplified by a drift from chromatic to a achromatic colour palette.
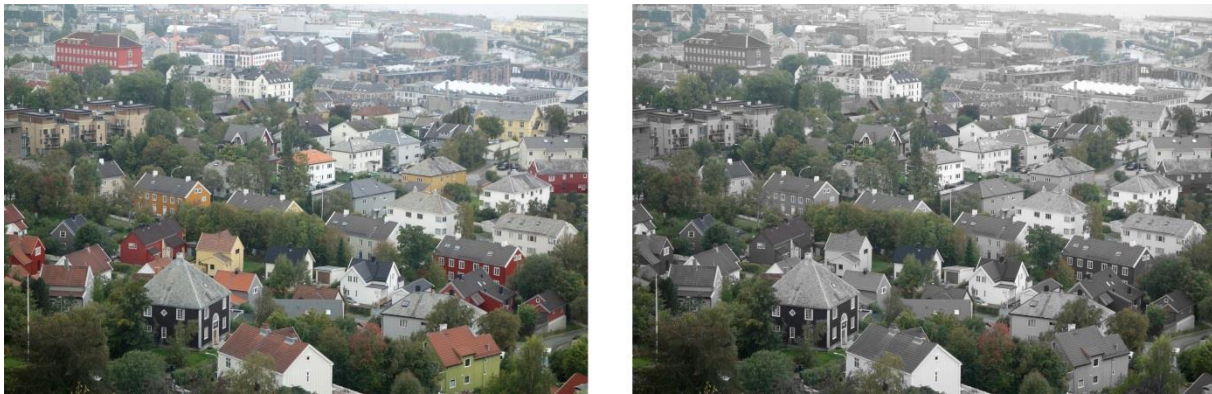


*Figure 2: The traditional chromatic colour palette of Trondheim is drifting towards achromatic colours (right picture is manipulated to show all houses in grayscale).*

A methodology is in general a guideline system used in a specific discipline for solving a task or a problem; i.e. methods, tools, techniques, rules and postulates. In proposing a methodology for the city of Trondheim it was therefor a priority to identify the main task or problem, in addition to finding out who may – and how to - implement them.

Buildings in Norway are regulated by two laws:
*1. Cultural Heritage Act:* The Act comprises buildings of conservation interest and buildings with conservation status, less than 10% of the buildings in the country.
*2. Planning and Building Act:* The Act mainly provides a framework for land use, transportation planning and the urban development, and comprises the buildings without conservation status or interest.

The responsibility and authority of building regulation in Norway is governed by elected councils in the Norwegian municipalities, and the methodology and the professional expertise involved varies a great deal within each municipality. Buildings with conservation status or interest have a well-founded methodology for dealing with architectural conservation, governed by people with an expertise within this field, but there is a lack of an overall colour methodology. The remaining 90% of the buildings are governed by regulations in the zoning plans and seldom includes any regulation of colour.

There is no existing archive showing if there has ever been a colour methodology for the city, and the material that does exist is fragmented and difficult to access. As the majority of the registered buildings in Trondheim are mostly in private ownership as residential houses or commercial buildings, and with a lack of a consistent colour methodology, the

colours chosen for the urban realm of Trondheim are mostly determined by the competence or fancies of the owners and the property developers.

In 2014, in co-operation with the Municipality of Trondheim[1], we initiated a pilot project for colour registration of a selected area in the city, with the intention of finding the contemorary city's colour pallet to create a public archive and a reference for both historic colours and as a basis for analyses of current tendencies and future colour methodology.

## 2. METHOD

The colour registration was restricted to the registration of the nominal[2] colours of the façades visible to the public, including cladding, foundation and most significant building components such as doors, window frames and window sashes. However, our perception of a façade colour is affected by several other variables, for example surrounding colours and texture and we registered the most basic information about the materials and textures of the façade surfaces in addition to the colour notations, i.e. if the wooden cladding has vertical or horizontal boards, or if the finish of the plaster renderings is fine or rough. Other variables that affect how we perceive a colour are but generally described in the overall userguide in the finished report (light conditions, human visual conditions and other variables).

### 2.1 Colour Registration

The colour reference system chosen for the colour registration was NCS - Natural Color System and Norwegian Standard since 1984. Each building was photographed, and the façade colours were scanned with a NCS colour scanner and notes down For the roof colours and multicoloured façades with an inherent material colour, such as slate tiles, bricks or prefabricated façade panels, we noted down the perception of the overall colour impression as one colour notation together with information about the material properties. The method for finding nominal and perceived colours of façades is well researched and documented by the Swedish architect and researcher Karin Fridell Anter [2].
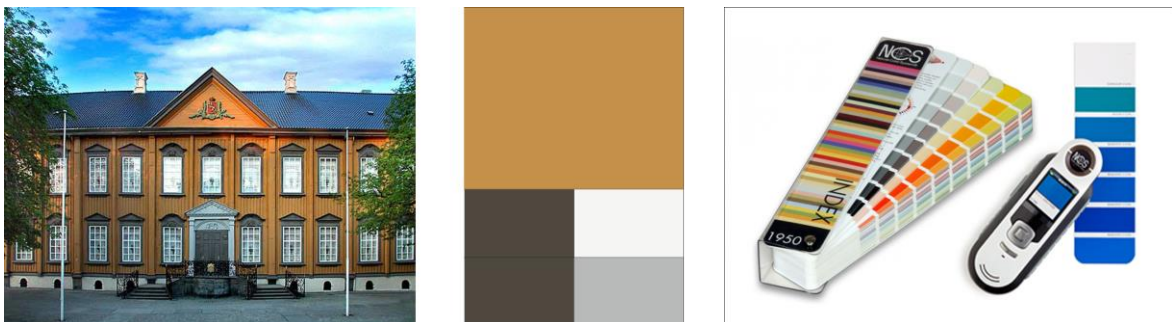


*Figure 3: Example of picture and colour palette of registered building (Stiftsgården), where the NCS notations were found using NCS Index and NCS Color Scan 2.*

[1] Office of Urban Planning in the Municipality of Trondheim.
[2] Karin Fridell Anter and Åke Svedmyr, *Färgen på huset*.
[3] Grete Smedal, *The Colours of Longyearbyen - An Ongoing Project*.

## 2.2 Public Archive

The material registered in the colour registration in this pilot project will be made publicly accessible through the Municipality of Trondheim in May 2015. The archive will provide an historical document of the colour palette of Trondheim as of today, and be a reference for both historical comparisons, present colour practice and tendencies, and used for future analyses. The archive can function both as inspiration and a guideline for the public in choosing colours for their buildings, provide information and knowledge about colours in an architectural context and give examples of traditional building articulation through the use of colour and its impact on perceived form and volume (for example, see figure 5).

## 3. RESULTS AND DISCUSSION

The NCS-system is commonly known and used as a colour reference system in Norway, but the system is not yet as commonly used as a tool for colour analyses and as a design tool. The method used in the pilot project was adopted from Norwegian interior architect Grete Smedals well established practice as a colour designer both nationally and internationally [3].

The system was also used as a tool for visual communication of the registered colours to show the colour palette of all registered colours in the pilot project. By plotting in the registered NCS notations in the NCS triangle (nuance) and NCS circle (hue), we can clearly identify the range of hues and nuances significant to the specific area or street, and communicate to the public what colours to choose from when repainting buildings or programming new buildings within the same area or street to stay within the contemporarely colour palette (see figure 4).
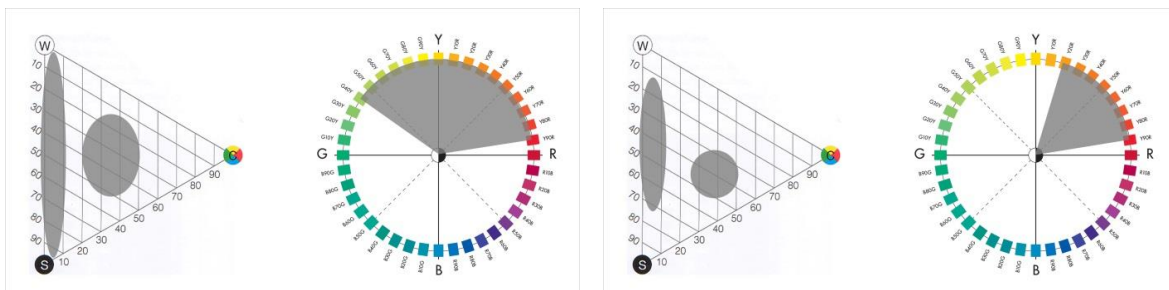


*Figure 4: Left: Colour palette of all colours in the pilot project. Right: Colour palette in one street (Kjøpmannsgata).*

However, we can speak of "area character" or "a coherent rhythm of buildings in a street" at micro and macro levels, but these characteristics are under pressure from the requirement for increased urban density, from radical shifts in architectural scale and proportion and not least from the often reflective surfaces of mass-production materials that in many cases offer very limited colour choice. These aspects are not discussed in this paper and will need further research before addressed and included in the current proposal for a colour methodology.

Another aspect of densification of the urban realm is that human colour vision was evolved to enable to distinguished object from background. The more complex the city becomes, there is an even stronger need for colour regulation to ensure a good hierarchy of colours and a good visual clarity.

AIC2015 TOKYO - Color and Image

# 4. CONCLUSIONS

Are colours in the urban realm of a private or public concern? The main design idea by using this methodology is that by identifying a colour palette for a city by colour registration of the facades, you can give the public the choice of choosing their own colours within the identified colour palette. In time, this data may be implemented in the city's Zoning Regulations and the Municipal Development Plan for a stronger effect to gain more control over visual clariry and the city's colour identity in a complex urban realm.

> The idea that colour should or could be controlled is anathema to many people, who regard it as one of their few remaining personal freedoms. Nevertheless, colour is already controlled in a significant number of ways that are taken for granted. Landowners still control large areas of town and country, and can dictate colour. Where individuals have relinquished control, government, institutions and public services have assumed control over civic design at many levels. Part of that control extends to colour, which is used in a variety of ways to express identity, impart information and in some cases to give warnings. But it is not clear who controls or coordinates these various uses. In principle many of the uses can be individually justified but the collective effect is often confused. There are two reasons for this: the sheer volume of uses, and the difficulties in achieving effective design and colour coordination between individuals and organizations. This is especially true where the former still believe that colour choice should be a personal matter. One solution is a design guide. (Michael Lancaster, *Colour in the Urban Context*)

By identifying the task of a proposed colour methodology to ensure a good visual clarity and the problem identified to losing the means to do so by a drift towards achromatic colours, we can propose a colour methodology to take back the city's image and identity. During the last year the discussion of colour in the media has fucused on whether to choose chromatic or achromatic colours, whereas the discussion should be directed to wich hue or nuance to choose, and how to use the colours in articulation of a building or the public realm.
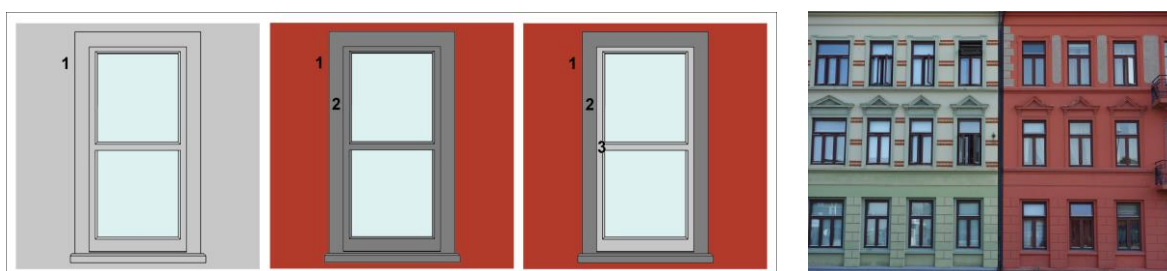


*Figure 5: Traditional threefold division of cladding (1), window frame (2) and window sash (3). The colour registration showed tendencies for building elements being reduced to fewer contrasting colours than originally designed or becoming completely monochrome.*

The limitations in the pilot project to a registration of colours only in parts of the city center of Trondheim does not give a full picture of the complexity of the city as a whole. The center has a stronger building regulation due to the fact that most of the buildings of concervations interest and regulation are situated in this area. The center also consists of more public buildings than the rest of the city and are therefore more easily regulated and controlled. But it has provided basis for a proposed colour methodology, by relatively simple means and possibility for a clear communication to the public.

The next, interesting possibility the colour registration gives a basis for will be to take the analyses further and include architectural styles, new cladding materials and building volume. For example, if a wooden building stands next to a modern construction made of concrete and glass, what would be a good hue and/or nuance combination to enrich both buildings?

## ACKNOWLEDGEMENTS

## REFERENCES

Drange, T. Aanensen, H.O. Brænne, J. 1992. Gamle trehus. Universitetsforlaget.
Fridell Anter, K. Svedmyr, Å. 2001. *Färgen på huset*. Byggforskningsrådet.
Lancaster, M. 2002. *Colour in the Urban Context.* The Institute of Historic Building Conservation (IHBC).
    URL: http://ihbc.org.uk/context_archive/75/urbancolour/colour.html
Smedal, G. 2009. *The Colours of Longyearbyen - An Ongoing Project*. Eget forlag.
Valberg, A. 2005  Light Vision Color, Chichester: John Wiley & Sons, Ltd.

*Address: Assistant Prof. Kine ANGELO, Department of Architectural Design, Form and Colour, Faculty of Architecture and Fine Art, Norwegian University of Science and Technology, Anton Getz vei 3, 7491 Trondheim, NORWAY*
*E-mails: kine.angelo@ntnu.no, alex.booker@ntnu.no.*

# The Image of the Color Red in Letters:
# A Study Based on the Historical Backgrounds of Russia and Japan

Sasha KRYSANOVA
Graduate School of Letters, Kansai University

## ABSTRACT

Color has been an important topic for thousands of years. In this research I will focus on the use of the color red in letters. The purpose of the survey is to discover the differences in point of view about color between Russia and Japan and to examine the traditional meanings of red in the two countries. The key points covered are the historical significance that people have attributed to this color. Use of the color red is prevalent all over the world. Red pigments were used for paintings on walls in caves, for graves, and in many other ways. It is obvious that people have a common perception of this color. But history also gives cultural meanings to colors. How they were symbolized in the past and some historical images of colors still influence the image of the color red today. For example, in Russia, red letters for celebrations are common. Red is associated with happy occasions, and is considered the color of strength and of life force. In contrast, in Japan this color can have positive meanings, but sometimes it is the color of *kegare,* a traditional concept of defilement. It is taboo to use the color red for letters in Japan. In this study, I will consider these different interpretations of the color red. This study is related not only to our lifestyles today, but to the cultural history of etiquette and manners in Russia and Japan.

## 1. INTRODUCTION

In Japan, writing letters or names in red is taboo. Using red letters is considered inauspicious. The following sentence about the appropriate color of ink was found in a book of manners.

> When you write letter of appreciation it is good manners to use black or blue ink (blue black which is almost black). A highlighter or pastel color ink is not suitable. Do not use red because it is the color of demand note or a letter of break off relations. Use dark black for celebration and light black for invitations or letter of appreciation (Tetsuo 2011: 22).

By searching on the internet with the keywords "write letter with red ink" in Japanese, we also can find many writings saying that it is good manners to not use red ink on letters or cards that you give to people. The reason, why people say to avoid this color were various. Mainly I could divide them into four categories.

1. On graves that are purchased while alive, the name of alive person is written in red.

2. Japanese warriors used red on a challenge.

3. Historically they would write the prisoner's name in red.

4. The rumor is that, if you write someone's name in red, his life will be shortened.

In all these reasons we can see inauspicious meanings of red letters. On the contrary, in Russia, those taboos are not seen. Moreover, red letters are frequently used in relation with celebrations. One example is red letters on celebration cards. In this survey, I compared frequency of using red letters on Russian and Japanese postcards related to celebrations. To measure the color red, I used the color cards "新配色カード199a". These cards are based on Practical Color Co-ordinate System which defines 2: R for red and 3: yR for yellowish red. The color numbers used are v2, v3 and dp2 for old cards (COLOR ENTERPRISE CO., LTD).

## 2. METHOD

At first, printed letters on birthday cards were compared. On Russian web site selling post cards (ЗАО"ПРАЗДНИК"), 63% of 48 cards had messages in red. On Japanese web site selling postcards (TOKYU HANDS INC), it was 12% of 221(9 % was in English). Secondly, I searched New Year cards. On Russian web site (ЗАО"ПРАЗДНИК"), 49% of 101 cards had messages in red. On Japanese web site (年賀.ORG.), it was 18% of 230 cards. Then, I observed the usage of red printed letters in the past( 19th and 20th centuries). Here, 19% of 880 Russian New Year Cards (Retropost. Ru.), 6% of 401 Japanese New Year cards (Ideafactory Corporation), had red letters. It is observed that Russian post cards have more red letters than Japanese. Also, on Japanese post cards a tendency was found, to use very limited quantity of red for letters. For instance, one phrase representing celebration and red for seals (name seals are not included in this research). On the other hand, in Russia, especially on current cards, not only is the main phrase but also (on many cards) long messages and wishes were printed in red. In addition, all hand written postcard that seems to written only with red ink, could found on the Russian web site which collecting old post cards for Easter (Россия в красках). For these reasons, it is possible to say that Russian people have different point of view for using the color red for letters.

## 3. RESULTS AND DISCUSSION

As red and blood is one of the highest association in many different countries including Russia and Japan, discussion will be focused on the image of blood in the two countries. Religions are very important factor considering this matter. In Japan, a traditional concept of defilement, *kegare*, existed. Tadao Kobayashi states that Japanese red color had two sides, positive and negative. On one hand, it was a color which had magical power, it could chase bad spirits away. Also it was used in festivals as a color of celebration. But, on the negative side, it was a minor, taboo color especially when it associated with *kegare* of blood. Blood from woman's childbirth and menstruation was called "*akafujyo*" (赤不浄) which means "red uncleanliness" (Kobayashi 2002). The Japanese folk customs dictionary "*Nihon minzoku daijiten*" also has an explanation of blood and *akafujyo*. In addition, the dictionary shows examples of customs related to this thought like "*Nagare-kanjyo* " (流れ灌頂) and "*Ketsubonkyo*" (血盆経). The first one is a custom of purify the soul of woman who died while giving childbirth. The red material was put on the riverside, and passengers sprinkled water on it. When the red color dissapeared, it was thought that the dead woman could rest in peace. "*Ketsubonkyo*" is blood pool sutra. It is said that this beliefe came from China. It says that the blood that woman sheds on giving birth and menstruation could cause defilement for other people which gets her into blood pool after her death (Hayashi 1999). Noboru Miyata indicates the relations beteween *kegare* of blood and historical

prohibition of eating meat. Also he clames that Buddhist "nonkilling" ethics is also an important factor. Furthermore, in Edo period, with growth of wet-rice farming, horses and cows became an indespensible labor saving device that discouraged people from eating them (Miyata 1996). From these reasons we can guess the gradual development of avoiding blood in Japan. In the Russian Orthodox religion, as in Western Europe, the color red associated with the Passion of Christ and His shed blood. On Easter, this color is used on Easter eggs and vestments. Perhaps it was the reason of using red letters on postcards related to Easter in Russia. Also, compare to Japan, Russia has a different history on relations with animals. People historically had various meats for eating and used the animals fur. Russia was known as one of the biggest fur trading countries since the medieval period. Fur was nesesarry to protect people from the cold climate, and it was an important property for country (Nishimura 2003). These historical backgrounds should have made the image of blood in Russia different from it in Japan.Of course, it does not mean that taboos related to blood do not existed in Russia. On this point, research will be continued.


## 4. CONCLUSIONS

In this study, it is observed that in Russian post cards related to celebrations, red letters were used more frequently than those in Japan. These differences are caused by various reasons including the ink problem and history of using color in writing. Here, I picked up the historical image of blood that is thought to be related to the color red in letters. As a conclusion, it seems that not only religion, but also the differences of life styles are involved. In future work, more data samples related to red letters will be collected.

## REFERENCES

Hayashi Hideo. 1999. *Nihon minzoku daijiten( 日 本 民 俗 大 辞 典 )*. Tokyo: Yoshikawakobunkan.

Kobayashi Tadao. 2002. Nihon no Shikakubunka wo yomu(日本の視覚文化を読む). *Kunizukuri to kenshu* (98): 28-31.

Miyata Noboru. 1996. *Kegare no minzokushi: Sabetsu no bunkateki yoin(ケガレの民俗誌 －差別の文化的要因)*. Kyoto: Jinbun Shoin.

Nishimura Saburo. 2003. *Fur in Mankind History( 毛 皮 と 人 間 の 歴 史 )*. Tokyo: KINOKUNIYA COMPANY LTD.

Tetsuo Shuichi ( ed.), 2011. *Croissant Special Edition: Chanto shita tegami to hagaki ga kakeru hon(クロワッサン特別編集[新装版]ちゃんとした手紙とはがきが書け る本)*.Tokyo: Magazine House, Ltd.

COLOR ENTERPRISE CO., LTD. Available online, www.sikiken.co.jp. Accessed: July 27, 2015.

ЗАО"ПРАЗДНИК". Available online, www.prazdnikcom.ru. Accessed: July 27, 2015.

Ideafactory Corporation. Available online, http://www.fuyuki-nenga.com/. Accessed: July 27, 2015.

Retropost. Ru. Available online. retropost.ru. Accessed: July 27, 2015.

TOKYU HANDS INC. Available online, http://hands.net/. Accessed: July 27, 2015.

年賀.ORG. Available online, http://www.nenga.org/. Accessed: July 27, 2015.

Россия в красках. Available online, http://ricolor.org/. Accessed: July 27, 2015.

*Address: Kansai University, 3-3-35, Yamate-cho, Suita-shi, Osaka, 564-8680,JAPAN*
*E-mail: k298324@kansai-u.ac.jp*

# Japanese Color Names Reflecting Dyeing:
# With a Focus on Their Color Terms in Brown Regions
# Including More than 100 Browns

Kohji YOSHIMURA,[1] Yuko YAMADA,[2] Stephen SHRADER[3]

[1] Department of English, Kansai Gaidai College
[2] Color Instructor, Illustrator
[3] Department of Foreign Languages, Kansai Gaidai University

## ABSTRACT

A variety of color terms such as *shijyu-hachi cha*, *hyaku nezu*, meaning "forty-eight browns, one hundred mouse colors," were used in the mid and late Edo period (A.D. 1651-1868) in Japan. At that time the most popular colors were browns, and the second most popular were mouse colors. Japanese color names for browns reflect Japan's *iki* aesthetic, and the defiant spirit of the Edo period people whose lives had become more affluent. The purpose of this paper is to show the main characteristics of Japanese color terms reflecting wood culture, i.e., dyeing, and 132 *cha*-named colors (despite the name 48). Color names based on the nomenclature of the forty-eight browns are used to refer to colors in Japanese fabrics, such as those for *kimono* in the 21st century. *Shijyu-hachi cha* (48 browns) embodies the *iki* aesthetic. For us, *iki* connotes the ability to live well with contradictory things by valuing how they complement and are a part of each other.

## 1. INTRODUCTION: "48 BROWNS" INCLUDING OVER 100 BROWNS

Among Japanese expressions for color terms, there is a famous phrase, *shijyu-hachi cha, hyaku nezu*, which means "forty-eight browns, one hundred mouse colors." As this expression suggests, from the mid to late Edo period (1651-1868) the most popular colors were browns, and the second most popular were mouse colors. Although not the focus of this article, the third most popular were indigos. Japanese color names for browns reflect Japan's *iki* aesthetic revealed in its color culture, and the defiant spirit of the Edo period people whose lives had become more affluent. Kunio Fukuda writes in his Dictionary of Strange Color Names (*Kimyo-na Siki-mei Jiten*, in Japanese, 1993: 13) that subdued, neutral colors matched the *iki* aesthetic, and that people favored color names with *cha* (tea) or *nezu* (mouse), hence the phrase *shijyu-hachi cha, hyaku nezu*. He argues that the number 48 was chosen because it sounded good, involved word play, and was lucky (p. 53). This paper will explain the existence through the years of 132 *cha*-named colors (despite the name 48), show that color names based on the nomenclature of the forty-eight browns are used in the 21st century in Japanese clothing as well as abroad, and additionally discuss the connotations of the number 48 in the phrase *shijyu-hachi cha* (48 browns).

## 2. A SUMMARY OF THE HISTORY OF BROWN DYE INGREDIENTS AND TEA PRIOR TO THE EDO PERIOD

Many Japanese color names reflect Japanese dyeing culture. The color name *cha-iro* (tea color) originated in the use of tea infusion as a dye during the Muromachi period (1336-1573). For example, *sencha-iro* (*sencha* is a type of green tea; *iro* means color) was a color

produced by dyeing with the infusion of *sencha* from refined buds of the tea plant. *Sencha* came to be widely drunk by commoners in the Edo period (1603-1868), and the color names incorporating *cha* became common as revealed in the phrase *shijyu-hachi cha, hyaku nezu*. Many of these color terms used interesting contrasts revealing the hidden resistance among the common people to the control of the ruling class. It is thought that the first use of the Chinese character for tea (茶) was in the "*Cha Jing*" (*The Classic of Tea*, or "*Chakyo*" 『茶経』 in Japanese), written around 760 by Lu Yu (Rikuu, 陸羽 in Japanese, 733-804) during the Tang Dynasty (618-907).

During the Nara period *tencha* (纏茶: half fermented tea) seems to have been brought to Japan from China by the Japanese envoy to Tang China. Actual tea production in Japan started in 805 when Saicho (最澄: 767-822) brought tea seeds from Tang China. Tea was presented to the Emperor. The courtiers of the Heian period (794-1185) began drinking tea in the form of tea-tasting competitions (*toucha*: 闘茶), and in the mid-Muromachi period (15th century) tea was a luxury item used in the tea ceremony. Among *samurai* and Buddhist priests tea was first drunk to ward off drowsiness. With the abandonment of the Japanese envoy to Tang China, tea declined in Japan; however, in 1191 Eisai (栄西:1141-1215) revitalized tea by bringing tea seeds and small tea plants from Southern Song China (1127-1279). From the late Heian to early Kamakura periods he had learned in China's Zen temples, which valued simplicity, the way of drinking tea that had developed from the Tang to Southern Song Dynasties.

The color names for browns before the Edo period did not use *cha* for their nomenclature. Heian period color names for browns included such terms as *kourozen* (黄櫨染), a yellowish brown dyed twice, but not using tea as a dye. It was a color forbidden to commoners. When the Edo period later came, some browns which had once been allowed only to the ruling class came to be permitted to the common people, which made them popular. The key point here is that it was the use of tea (*cha*) as a dye that caused this change, hence its wide popularity as a color name. Other browns of the Heian period, similar to *kourozen*, did not use tea as a dye. Another Heian color was *shira-tsurubami*, (白橡) a color produced from one of Japan's most ancient dyes, using the chestnut oak and acorns. Unlike *kourozen*, *shira-tsurubami* was actually prescribed for common people. *Aka-shira-tsurubami* (reddish *shira-tsurubami*), on the other hand, was reserved for high ranking officials only, and was produced with a dye based on madder (茜). *Ao-shira-tsurubami* (bluish *shira-tsurubami*) was used for everyday informal wear, but only by the Emperor. It was produced by cross-dyeing with *kariyasu* (*miscanthus tinctorius*) and lithospermum root. Unlike *shira-tsurubami*, *ao-shira-tsurubami* did not use chestnut oak, which was inexpensive and thought to be more appropriate for commoners. *Ki-tsurubami* was yet another brown color produced by dyeing with acorns and lye. Another color took its name from the Japanese word for cloves, *choji*. *Choji-zome* (丁子染) was produced in one of two ways. *Honzome* (本染) referred to *choji-zome* which was actually produced with expensive cloves, while *daiyou-zome* (代用染) referred to *choji-zome* which had been produced with red bayberry (楊梅) rather than cloves. *Choji-zome* was also called *kou-zome* (香染) or *koki-kou* (濃き香), and the *kou* in both of these color compounds refers to an aromatic wood. *Usu-kou*, also called *kou-iro*, was produced from lightly dyeing with cloves, and was light yellowish brown. The *kou* in its name comes from the use of incense as a dye. *Suou-kou* (蘇芳香) was similar to another color called *aka-kou* (a reddish variant

of *kou-iro*, explained above). *Suo-kachi* was similar to *suou-kou*, but of an even deeper brown. These were some of the many browns prior to the Edo period, and demonstrate how people back to the early days of Japan's history were sensitive to slight differences in color. While later in the Edo period people began to use terms incorporating *cha* to refer to browns, before the Edo period there were many distinct names for these colors.

In the Edo period color names with *cha* came to be widely used, but tea was not the only ingredient used in the production of these colors. Dyeing materials used in the Edo period included red bayberry, sappan, *kariyasu*, peels of *ume*, madder, turmeric, indigo, small dried sardines, and other things. The Edo colors *usu-cha* and *shira-cha* were similar to the Heian colors *shira-tsurubami*, *kou-iro*, and *usu-kou*. They were a pale brown, sometimes with a yellowish or reddish tint, similar to a beige. Dye produced with the peel of red bayberry was most loved from the early to mid-Genroku period (1688-1704), and became popular again in the Bunka-Bunsei period (1787-1843). *Kyara* denotes a type of high quality aromatic resin, but from the mid-Edo period *kyara-cha* referred to a dark yellowish brown produced by dyeing with something other than (the very expensive and rare) *kyara*. The Edo period government established the "Sumptuary Regulation," preventing farmers from living a life of luxury. By decree of this law, all people regardless of status were prohibited from wearing luxurious kimono. In 1642 this law prohibited the use of silk in *kimono* belts and neckbands, and in 1643 it prohibited the use of purple and reddish-pink. In 1663 this law was expanded to include the *samurai* and commoners. Although the people of that time followed the law in practice, the *iki* spirit included resistance to it.

## 3. "48 BROWNS" ACTUALLY INCLUDES 132 BROWNS

The origins of *cha-iro* (tea/brown color) names have many origins, including plants (*azuki* beans, Japanese white birch, mulberry, kelp, mandarin orange, willow, fallen leaves, and fruits such as persimmons and loquats), plant-based dyes (indigo, Japanese horse chestnut, and tea, among others), dyeing methods (*momo-shio*—*momo* literally means one-hundred, suggesting the large number of times something is dyed, while *shio* usually would mean salt, but when used in the context of dyeing refers to insertion into dye, and taken together means a deep color produced from multiple rounds of dyeing, i.e. *youkan-iro*, a brown produced with this method and named after a kind of sweet jelly of *azuki* beans), birds (sparrows, bush warblers, Japanese crested ibises, black kites, Eurasian siskins, and others), animals (mice, sea-otters, and so on), personal names (Enshu, Kempo, Shikan, Shikou, Souden, Danjurou, Baikou, Rikan, Rikyu, Rokou, Roshun, among others), place-names (Edo, Kishu, Tang, Momo-yama, etc.), furniture (such as *kawarake*, or unglazed earthenware), architecture (like *nando*, a storeroom), tools (such as *toishi*, a whetstone), spices (such as *choji*, cloves), aromatic trees and woods (such as *kyara*, a high-quality agarwood product that was deep brown, and agarwood itself), things related to fortunes and omens (such as *chitose*, meaning one thousand years; *takara*, treasure; *kin*, gold; *fuku-jyu*, long life and happiness; and *yama-buki*, here meaning a gold coin), symbols (such as the tea *ikou-cha*, which referred to a tea that had been drunk by people who held high social status—the *ikou* refers to this status—and symbolized the power they commanded, making it popular when it later came to be drunk by commoners), colors (red, blue, yellow, white, green, gray, and tea-brown), physical features (such as *okina-cha*, a near-white brown that takes its name from the gray hair of an *okina*, an aged man). In addition, there are browns that take their names from word play (such as *kobicha* (媚茶), a color name derived from

*kobu-cha*, or kelp brown, and also from the verb *kobiru*, meaning to butter someone up by fawning on them), from honorific expressions such as *omeshi-cha* (御召茶: a bluish, subdued brown named after a kind of high-quality *chirimen*, silk crepe-like fabric, loved by the 11th *shogun* Tokugawa Ienari, which subsequently came to be known as *omeshi*, itself is the honorific form of the verb "to wear"), and *bunjin-cha* (文人茶), which is an expression referring to fashionable and sophisticated people at that time (*bun* meaning literature, *jin* meaning people, and *cha* meaning tea, or people of tea and letters, such as the literati). Browns, unlike mouse colors, did not have color names that made reference to astronomical phenomena or river names. *Cha-iro* (茶色: tea color, brown) comes from the color of the drink tea, and includes 132 colors, which are typically divided into a three part classification system proposed by Nagasaki (1996), but which we have revised. Here we will explain his system and our modifications to it.

Nagasaki divided the browns into three categories, *aka-cha*, *ki-cha*, and *ao(midori)-cha*, which respectively mean red tea (brown), yellow tea, and blue (green) tea. He proposed this system based on different types of drinking tea, *ban-cha*, *sen-cha*, and *hiki-cha* (also known as *matcha*, thick green tea), and argued for this classification system noting that tea was used in the dyeing process. *Aka-cha* is a color category that he uses to describe colors similar to the drinking tea *ban-cha*, and they basically correspond to each other (but the first term represents the color category and the second term is the actual tea it is based on). Similarly, *ki-cha* is based on the tea type *sen-cha*, and *ao(midori)-cha* is based on *hiki-cha*. However, the fact is that while some of the browns are produced by dyeing with tea, some colors with the *cha* name use tea combined with other things, and some do not use tea at all. As part of our research we listed as many browns as we could find, and tried fitting them into Nagasaki's framework. We expanded the categories of his original proposed system by changing the names to better reflect a wider variety of browns, have added browns that were not in his original categories, and also added a fourth category of colors that include *cha* in the name, but are actually gray. Nagasaki himself did not attempt to fully list the *cha* colors in categories in this way.

Among the *ban-cha* colors, which Nagasaki called *aka-cha* (as do we; *aka-cha* means "red tea/brown"), are a total of 22 colors: *aka-cha*, *aka-koge-cha*, *azuki-cha*, *beni-ebi-cha* (紅海老), *danjyurou-cha*, *edo-cha*, *enshu-cha*, *kaba-cha* (which has three different Chinese characters with the same pronunciation, each counted as one color, 椛・蒲・樺), *kuri-ume-cha*, *kuri-kane-cha*, *kouetsu-cha*, *shikan-cha*, *shoujou-cha*, *suzume-cha*, *tangara-cha*, *tousei-cha* (当世), *toki-cha*, *momo-yama-cha*, *ume-cha*, and *usu-ume-cha*.

Nagasaki called the *sen-cha* category *ki-cha* when he referred to it as a color category name; however, we renamed it *ki-aka-kara-ki-cha*, which means "from yellow-red (tea brown) to yellow (tea brown)." It includes the following 30 colors: *bunjin-cha* (文人)*, cha-iro*, *cha-kasshoku*, *choji-cha*, *hiwa-cha*, *kaki-cha*, *kawarake-cha*, *ki-cha* (黄茶), *ki-kara-cha* (黄唐), *ki-gara-cha* (黄雀・黄枯), *ki-kara (ki-gare) cha* (木枯), *kishu-cha*, *kara-cha*, *kin-cha*, *kenpou-kuro-cha*, *ki-miru-cha*, *koge-cha* (焦茶), *kobi-cha* (媚茶), *koi-uguisu-cha* (濃鶯), *konbu-cha*, *kuwa-cha*, *mikan-cha*, *ran-cha* (欄茶), *shibu-cha/shibucha-iro*, *sen-cha/senji-cha-iro*, *senjicha-zome*, *takara-cha*, *uguisu-cha*, and *yamabuki-cha*.

Finally, Nagasaki has the *hiki-cha* category, which he calls *ao(midori)-cha* when he refers to the colors in it rather than the tea; we call this category *midori-kara-ao-cha* ("from green to blue" tea brown). It includes these 21 colors: *ai-tono-cha* (藍砥・藍礪), *ao-cha*

(青茶), *icou-cha* (威光・威公), *fukujyu-cha*, *gin-onando-cha* (銀御納戸茶), *jinkou-cha/tono-cha* (沈香茶・殿茶), *kusayanagi-cha*, *maccha-iro*, *ryoku-cha*, *omeshi-cha*, *sensai-cha/senzai-cha* (千歳・千哉・千才・仙斎・千載・仙歳), *shinsai-cha*, and *yanagi-cha*.

We are also proposing a new category of colors with *cha* in their name, but which are more gray than brown – the following 56 colors would previously have been organized under the system above, but we will be recategorizing them. The 7 dark grays formerly in the *aka-cha* category are *ebi-cha* (海老・蝦・葡萄), *ebi-kawa-cha*, *kuri-kawa-cha*, and *momo-shio-cha* (百塩・百入). Three grays formerly under *aka-cha* are *kara-cha* (唐茶, the *kara* comes from a Japanese way to refer to Tang, which came to mean "new, beautiful"), *souden-kara-cha*, and *souden-cha*. Two light grays that would have originally fallen into the *aka-cha* category are *toki-gara-cha* and *toki-cha*. The 15 colors originally in the *ki-aka-kara-ki-cha* category, but now in the new category include the following dark grays: *ochiba-cha*, *kara-cha/kare-cha* (枯茶), *kanze-cha*, *kogarashi-cha/kogare-cha/kikara-cha* (木枯), *kurokobi-cha*, *kuro-cha/kurocha-iro*, *kogarashi-cha*, *goku-koge-cha*, *susu-take-cha*, *miru-cha*, *su-miru-cha/su-miru-cha-iro*, *mukashi-kara-cha* (昔枯・昔唐), *rakko-cha,* and *rokou-cha*, the following 8 grays: *tono-cha* (砺・砥・礪), *nezumi-cha/nezu-cha*, *hai-cha*, *biwa-cha* (枇杷・琵琶), and *furu-cha*, and these 7 light grays: *awa-cha*, *usu-cha*, *usu-sira-cha*, *kuwa-iro-sira-cha*, *shigaraki-cha* (信楽), *shira-cha/shiro-cha* (白茶), and *rikyu-sira-cha* (利休白茶). From the *midori-kara-ao-cha* category, we are moving the 10 dark grays: *ai-koi-cha* (藍濃), *ai-kobi-cha* (藍媚), *ai-sumi-cha* (藍墨・相済), *ai-miru-cha* (藍海松), *onando-cha/nando-cha*, *sikou-cha*, *yanagi-susutake-cha* (柳煤竹), and *rikan-cha*, the 2 grays: *iwai-cha* (岩井) and *rikyu-cha*, and these 2 light grays: *baikou-cha* and *mamegara-cha* (豆殻). The colors listed so far were formerly divided into three categories, but we put them into a new category we call *kurai-hai-kara-akarui-hai-no-cha* (meaning dark gray to light gray cha/tea/browns). There are also three colors that did not fit into the original system: *okina-cha* (the *cha* color closest to white), *kara-take-cha*, and *roshun-cha*.

## 4. COLOUR TERMS OF "48 BROWNS" IN MERCHANDISE

The *cha* colors listed above are one aspect of Japan's traditional culture, which lives on in the fact that many of the *cha* colors continue to be used in Japan today, especially among specialists and in industry. Japan's *geisha* and *maiko* (teenagers who are in training to become *geisha*) are highly-trained professional entertainers and performers of Japan's traditional arts, who wear *kimono* that reflect Japan's color culture. Many of the terms introduced above are used to refer to colors in Japanese fabrics, such as those for *kimono*. The clothing for *kabuki* also makes use of fabrics using these colors. Another example is pottery, where some of the *cha* color terms are still used. Additionally, some shops are named after the colors. There has also been one example of how one of the colors has been used overseas – in 2011, the American company Fender produced a guitar at the request of a Japanese musician using the color *omeshi-cha*, which they named "grayish olive green."

## 5. CONCLUSION: THE CONNOTATION OF 48 IN "48 BROWNS"

The number 48 is traditionally a significant number in Japanese culture, and can be seen in other phrases such as *shi-jyu-hachi-no-seigan* (a phrase referring to the forty-eight wishes of the Amida Buddha), and *kuchiba-shi-jyu-hachi-shoku* (forty-eight decayed-leaves

colors). Although the phrase *shijyuhachicha, hyakunezu* (forty-eight browns, one-hundred mouse colors) states a clear number of colors, in fact the number of browns and mouse colors are both over one hundred. There are thus some questions about why these numbers were chosen in the first place, and why the number given for browns is smaller even though the actual list of color names is similar when we compare the browns and mouse colors. Kunio Fukuda (1993: 52-55) gives three reasons. First, he suggests that perhaps the number forty-eight is the same as the number of characters in a well-known poem which would have been even more widely known at that time, *Iroha*, which uses the Japanese syllabary and expresses Buddhist ideas. Second, he gives the possibility that forty-eight might have been chosen even though it was a bit different from the actual number because it involved some word play and sounded good, and this was seen as more important than accuracy. Third, he writes that the number might have been chosen for good luck, pointing out that the Chinese character for eight, 八, has a special additional meaning of good fortune and prosperity, and was often used to mean something similar to "a lot" regardless of the actual number of things being counted. Fukuda calls it the "magic number" of the Edo period, a part of Japanese culture carried on into modern society.

Interestingly, the number four traditionally has negative associations in Japan, since it sounds like the word for death; however, here it appears with the eight in forty-eight. The reason for this odd combination may be the interesting contrast it provides – one that would have been meaningful to people at that time, and today as well. It is the idea expressed in the yin and yang symbol (something that is good, for example, may contain the seeds or elements of its opposite). Aesthetically there is an enjoyment of putting opposites together which is revealed in the phrase, and is at the heart of the *iki* aesthetic. This can also be seen in the color terms themselves, which sometimes put opposites together (as in *ai-koi-cha*, in which the *ai* and *cha* are actually opposite colors). Earlier we mentioned the defiant spirit of the Edo people. The common people were resistant to the Sumptuary Regulation, and followed it outwardly but rejected it inwardly. This was revealed in the naming of the colors (i.e. the use of *cha* itself in naming the colors was a rejection of the Regulation). This reflects an aspect of Japanese culture referred to as *omote/ura*: outwardly saying one thing while internally thinking something else, and while this might be seen as being two-faced in English-speaking culture, it is not necessarily seen this way in Japan. Another interpretation of the 48 is that it embodies the *iki* aesthetic we have described – it was a kind of resilient and simultaneously restrained resistance to authority that took a sophisticated form in various aspects of life at that time. *Iki* connotes the ability to live well with contradictory things by valuing how they complement and are a part of each other, an outlook that is important to protect in the challenging world we live in today.

## REFERENCES

Fukuda, Kunio 1993. *Kimyo-na Siki-mei Jiten*, Tokyo: Seiga-Shobou.
Nagasaki, Seiki 1996, 2006. *Nihon-no Dento-Syoku: Sono Shiki-mei to Shiki-cho* (*The Traditional Colors of Japan*) (written in Japanese), Kyoto: Kyoto-Shoin.
Uchida, Hiroyuki 2008. *Teihon Wa-no Iro Jiten*, Tokyo: Shikaku Design Kenkyu-Sho.

*Address: Prof. emer. Kohji YOSHIMURA, Department of English, Kansai Gaidai College, 16-1, Nakamiya-Higashino-cho, Hirakata City, Osaka, 573-1001, JAPAN*
*E-mails: yoshim-k@kansaigaidai.ac.jp; yoshim-k@rk2.so-net.ne.jp*

AIC2015 TOKYO - Color and Image

# Assessing Glare Using LED Sources Having Different Uniformity Patterns

ShiNing MA[1], Yang YANG[1], Ming Ronnier LUO[1,2*], XiaoYu LIU[1,3], and BinYu WANG[4],
[1]State Key Laboratory of modern optical instrument, Zhejiang University, Hangzhou, China,
[2] Colour, Imaging and Design Research Centre, University of Leeds, UK
[3]College of science, Harbin Engineering University, Harbin, China
[4]Thousand Lights Lighting (Changzhou) Limited, Changzhou, China
*m.r.luo@leeds.ac.uk

## ABSTRACT

Glare has been a problem in lighting design because it can cause safety accidents and visual impairment. For LED source, the existing standards may not be suitable because of its high luminance intensity, small size and non-uniform distribution. In this work, an experiment was conducted to investigate the indoor LED discomfort glare. The physical parameters studied included luminance intensity, the size of LED matrix, the pattern of LED luminance distribution, the background luminance, and the LED positioned angle above the sight line. The results showed that the five parameters all had statistic significant effect on human sensation of glare. Finally,the visual glare was used to test two different glare models. The results domenstrated that there are still some rooms to improve the accuracy of the model, especially for the non-uniform LED patterns.

Keyword: LED, discomfort glare, UGR

## 1. INTRODUCTION

LED (light-emitting diode) lighting source has become the most important clean source because of its special characters such as energy-saving and long service life. More importantly, LED source can be tuneable whose luminance, chromaticity, spectrum and pattern can be adjusted with different application requirements. These strengths make it possible to be developed as intelligent lighting source to provide functionalisation, personalisation and with internet.

However, glare is a serious problem in LED lighting design due to its small size. It can cause visual fatigue and excessive glare which could result in safety accidents and visual impairment. Here the research is concentrated on indoor discomfort glare. For traditional lighting sources such as incadescent or fluorescent, Cai (2013) reported different vision models to describe indoor discomfort glare such as UGR, VCP, and BGI , while they can only be used in some restricted conditons such as medium area and medium luminance. The problem is that these glare indices cannot be used to precisely predict glare caused by LED which has high luminance intensity, small size and non-uniform distribution. As the LED is rapidly replacing traditional lighting source, it is necessary to evaluate LED lighting quality

especially the discomfort glare. With this in mind, CIE has established a Joint technical committee to investigate the prediction of glare for the non-uniform LED sources.

Over the past several years, several studies have been reported that many parameters exert strong impact on observer's perception of glare. Akashi et al. (2013) discovered that blue LED and cyan LED could have the lowest BCD luminance (borderline of comfort and discomfort) of discomfort glare compared with other colour's LED. By using fluorescent luminaires, Zhang et al. (2012) conducted a research on the effects of lighting source's color temperature on discomfort glare. Ayama et al. (2013) redefined the glare model UGR by calculating the luminance of LED glare source in HDR (high dynamic range) image and come up with the concept called 'effective glare luminance'.

Therefore, the purpose of the present research is to generate a glare viusal database and to analyse the relationship between lighting parameters and discomfort glare. Furthermore, it is still necessary to evaluate the existed indoor discomfort glare indices and improve them to some extent by analysing the collected data.

## 2. METHOD

### 2.1 Experimental Conditions

The experiment was carried out in an enclosed room without window. The apparatus is shown in Figure 1. LED elements were arranged in a four-by-four matrix, within an area of 16cm*16cm. These LEDs were Lambertian light source. The colour temperature of them was 4100K. The LED panel was placed on the background board covered with white cloth. The horizontal distance between observer's eyes and LED lighting source was 2.5 m. The distance between eye and computer display was 60 cm. The height of table was approximately 75 cm. For the display, the height was 32 cm and the width was 55 cm.

During the experiment, in order to simulate real working situation, the observers were asked to look horizontally at the computer display and enjoy the oil paintings presented randomly on the display. As for the subjective glare rating scale, Table 1 shows the detail.

Totally, there are twenty observers, eleven males and nine females in their twenties or thirties (the average age was 24 years) with normal colour vision, participated in the experiment.

### 2.2 Experimental Parameters

The experiment was divided into 2 parts. In Experiment 1, the effects of LED luminance intensity, the whole LED size, background luminance and LED positioned angle above the sight line were mainly investigated. Note that every bright LED has the same luminance in this experiment. LED luminance intensity corresponds to 5 levels (0.46, 1.65, 4.66, 9.57, and 16.79 cd) measured by PR670 (product of Photo Research). As the figure 2 shows, there were 3 matrices of LED sizes including 1*1, 2*2 and 4*4. There were two backgrounds (dark (0 lux) and bright (105 lux)). It had two LED positioned angles above the sight line, 10 degree and 20 degree.

AIC2015 TOKYO - Color and Image

Table 1. Subjective glare rating

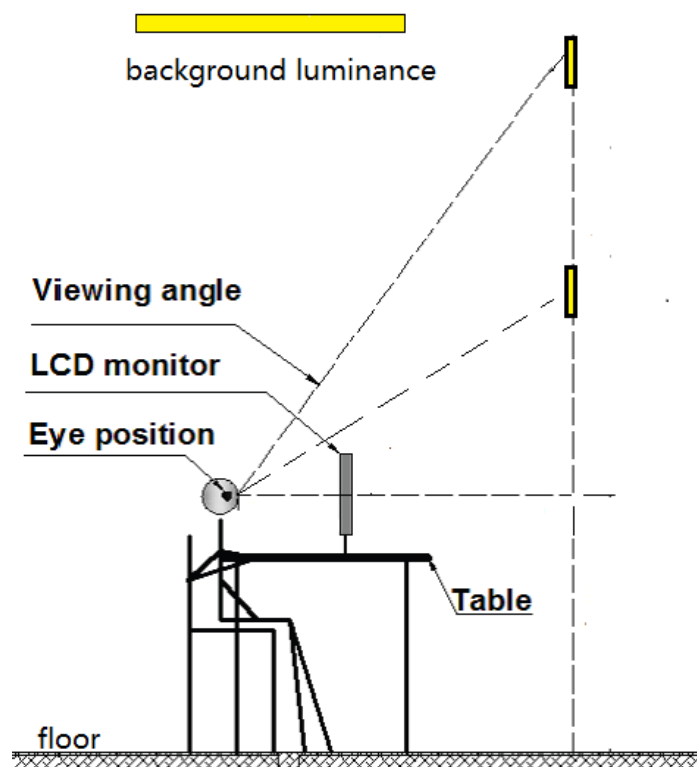| category | name |
|----------|------|
| 1 | imperceptible |
| 2 | just perceptible |
| 3 | noticeable |
| 4 | just uncomfortable |
| 5 | uncomfortable |
| 6 | just intolerable |
| 7 | intolerable |



Figure 1: Experiment apparatus

In Experiment 2, the pattern of LED distribution was changed so that the uniformity of glare source was varied. There were 12 kinds of LED patterns with different luminance distribution of LED panel while the LED luminance intensity was set the same (20.79cd). Shown in figure 3, the luminance contrast between outside part and inside part had 10 different levels. Another two patterns included 1*1 LED matrix and 4*4 LED matrix. Also in Experiment 2, LED positioned angle above the sight line and background luminance were set the same as Experiment 1.

Overall, there are 108 different lighting conditions in this experiment assessed by 20 observers, each one did twice. In each lighting condition, 20 observers visually assessed the glare. In total, 2160 estimations were made.
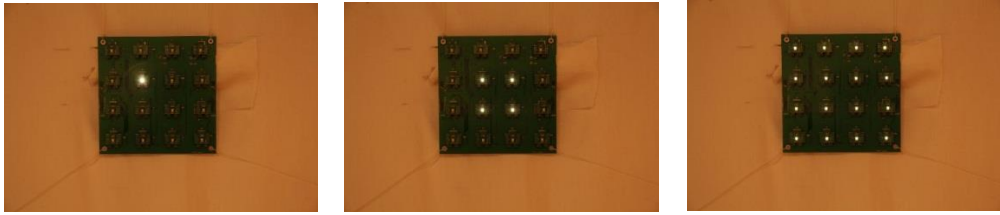
*Figure 2: LED matrix in experiment 1*
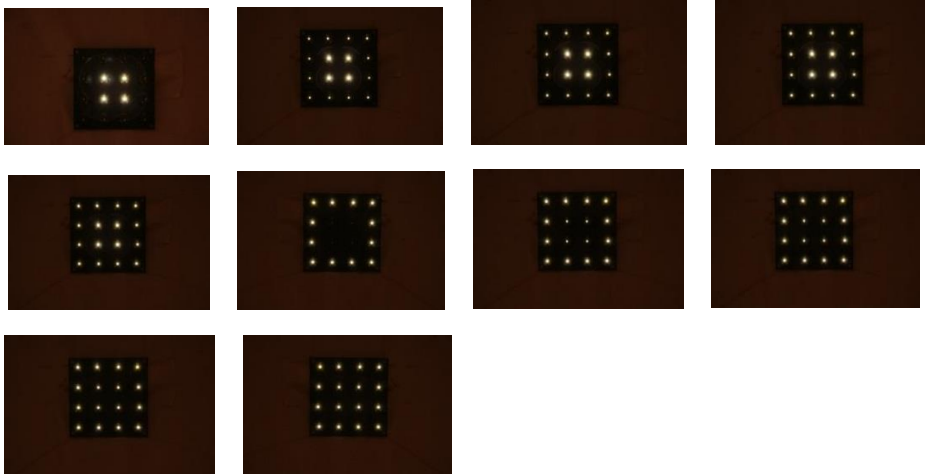


*Figure 3: LED pattern with different contrast level between outside and inside*

## 3. RESULTS AND DISCUSSION

### 3.1 Lighting Parameters on Perceived Glare

Statistical analyses were performed using SPSS version 16.0. For Experiment 1, the four parameters including LED luminance, matrix size, background luminance and LED positioned angle above the sight line. All had strong relationship with glare. After two-way factorial analysis of variance (ANOVA), it was found statistically significant interaction ($p=0$ and $p<0.05$) between glare rating score and all the parameters investigated in Experiment 1. For luminance, it is obvious that average glare rating score increases as the glare luminance increases. For the size of LED matrix, the glare rating score increases as the size increases. For background luminance, the sensation of glare in dark background is stronger than in bright background when other conditions are all the same. For the LED positioned angle above the sight line, the sensation of glare increases with the decrease of angle.

For Experiment 2, the most important parameter discussed here is the non-uniformity of LED lighting source. After two-way factorial analysis of variance (ANOVA), the results indicate statistically significant interaction ($p=0.002$ and $p<0.05$) between glare rating score and LED non-uniformity, or uniformity of LED pattern. Glare rating score increases with an increase of contrast between the inner and outer luminance. In other words, the discomfort glare increases as the increase of non-uniformity level.

AIC2015 TOKYO - Color and Image

## 3.2 Testing Models' Performances

Finally, the visual results were used to test UGR and BGI models. These were selected because the two models are known to have best performance in predicting the previous datasets (Cai, 2013). Parts 1 and 2 data represent the data from Experiments 1 and 2 respectively. Table 2 shows the predictive performance of the two models in terms of correlation coefficient (R value) for Part 1, Part 2 and combined data. Figure 4 plots the UGR predictions against the subjective ratings. It can be clearly seen that UGR model can predict Part 1 discomfort glare results better than those of Part 2. Figure 5 plots the BGI predictions against the subjective ratings. Similar to UGR model, BGI predicts Part 1 discomfort glare results better than those of Part 2. However, both models predict the combined data well, i.e. r values of 0.93 and 0.94 respectively. The results in Table 2 clearly indicate that both models gave good predictions to the combined data. They can predict better for Part 1 data than the Part 2 data. This implies that there is a room to improve the models in predicting the data having non-uniform LED patterns.
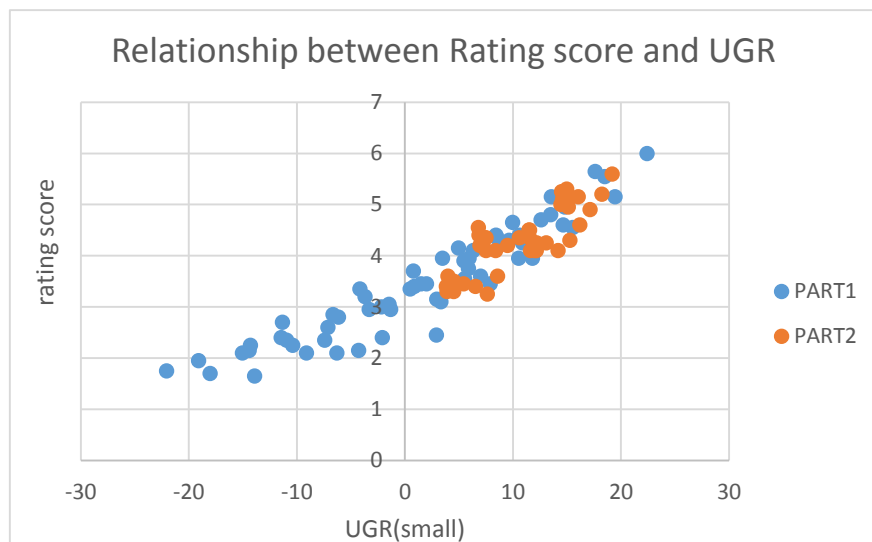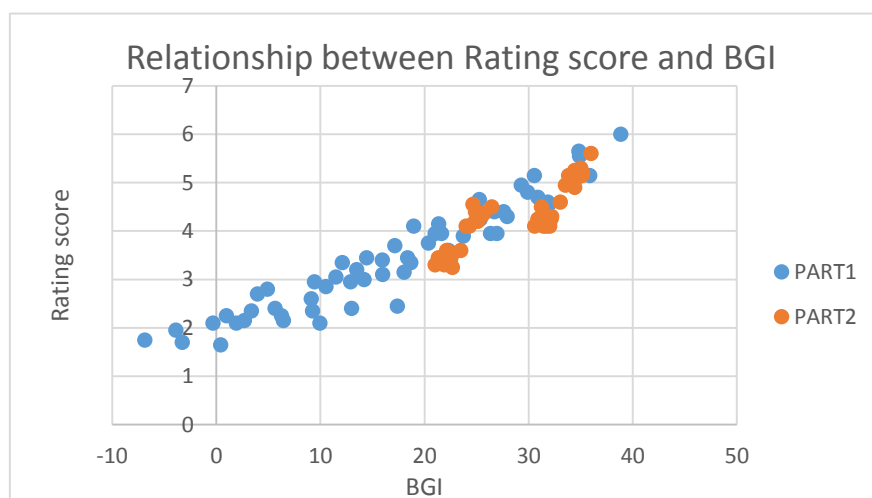


*Figure 4: Relation between UGR and glare rating score*



*Figure 5: Relation between BGI and glare rating score*

*Table 2. R value in different conditions*

|          | UGR  | BGI  |
|----------|------|------|
| Part 1   | 0.94 | 0.95 |
| Part 2   | 0.84 | 0.85 |
| Combined | 0.93 | 0.94 |

## 4. CONCLUSIONS

Two experiments investigating the relation between human sensation of glare and physical parameters of LED luminance, matrix size, background luminance, LED positioned angle above the sight line and non-uniformity were conducted. After data analysis, some important phenomena have been discovered. Firstly, all five parameters had significant impact on glare perception. Secondly, although UGR and BGI models can predict the combined glare data to some extent, there are still some rooms for improving in predicting non-uniform patterns. A new model is required by taking non-uniformity arrngments of LEDs into consideration.

## ACKNOWLEDGEMENTS

## REFERENCES

Akashi, Y., Asano, S., Kakuta, Y. (2013) Visual mechanisms of discomfort glare sensation caused by LEDs. In *Proceedings of CIE Centenary Conference: Toward a New Century of Light*: Paris, 327-330.

Ayama, M., Tashiroi, T., Kawanobe, S., Kimura-Minoda, T., Kohko, S., & Ishikawa, T. (2013) Discomfort glare of white LED sources of different spatial arrangements. In *Proceedings of CIE Centenary Conference: Toward a New Century of Light*: Paris, 119-122.

Cai, H., & Chung, T. (2013) Evaluating discomfort glare from non-uniform electric light sources. *Lighting Research and Technology*, 45(3), 267-294.

Zhang, J., Tu, Y., Liu, L., et al. (2012) The influence of correlated colour temperature of luminaire on overhead glare perception. In *Proceedings of CIE 2012: Lighting Quality and Energy Efficiency*: Hangzhou, 470-476.

*Address: Prof. M. R. Luo, Department of Optical Engineering, Zhejiang University,*
*No.38 in Zheda Road, Xihu district, Hangzhou, China*
*E-mails: M.R.Luo@leeds.ac.uk*

# Evaluation of the Performance of Different Colour Rendering Indices Employed in LEDs

Haiting GU,[1] Xiaoyu LIU,[1,2] Ming Ronnier LUO,[1,3] Binyu WANG,[4] Haiyan LIU,[4]
[1] State Key Laboratory of Modern Optical Instrumentation, Zhejiang University
[2] College of science, Harbin Engineering University
[3] School of Design, University of Leeds
[4] Thousand Lights Lighting (changzhou) Limited

## ABSTRACT

The goal of this study is to investigate the performance of various uniform colour spaces (UCSs) and colour rendering indices (CRIs) for evaluating colour rendering quality of light sources. An experiment was carried out to include colourful test samples and light sources of different types and correlated colour temperatures (CCTs). Ten observers participated to view identical samples placed in two cabinets under a pair of sources respectively, and judged their colour difference according to a grey scale. The results indicated that CAM02-UCS gave the best correlation with the visual results among all the UCSs tested. It was also concluded that all the colour fidelity indices gave similar performance and they outperformed colour preference indices in predicting the visual results.

## 1. INTRODUCTION

Colour Rendering Index (CRI) is one of the most important criterions. CIE-$R_a$ is the only internationally accepted measurement for evaluating the colour rendering properties of a light source. It was proposed by the International Commission on Illumination (CIE) in 1974 and has been widely employed in the lighting industry. However, recent studies have shown that perceived colour qualities of newer LED light sources are not well described by CIE-$R_a$. The problem may arise due to some drawbacks associated with CIE-$R_a$, such as the use of low saturated test samples, the outdated colour space and chromatic adaptation transform. Hence, various new CRIs have been developed to update the present CIE-$R_a$.

In order to recommend one CRI as a new method for measuring and specifying colour rendering, many researchers have focused on investigating the performance of new CRIs. Li et al. (2011) conducted an experiment using 15 coloured textile samples placed in two cabinets under five light sources, while observers evaluated the change of colour appearance of samples according to a grey scale. They concluded that an index based on CAM02-UCS gave the best performance. A similar experiment done by Sándor and Schanda (2006) also showed that CIECAM02 colour appearance model provided best correlation with visual conditions. Boissard et al. (2014) also performed the experiment using a paired comparison method and observers to assess several aspects of colour quality. Their results indicated that perceived colour differences were better dealt by the CIECAM02 Uniform Colour Space (UCS), naturalness was well described by colour fidelity indices and colourfulness was well described by gamut based indices.

This paper describes an experiment conducted in a dark room with an aim to evaluate the performance of existing UCSs and CRIs.

## 2. EXPERIMENTAL

### 2.1 Apparatus

Three viewing cabinets placed side by side were used in the experiment. The walls and bottom of these cabinets were painted in medium grey matt paint, which had CIELAB values of 53, 1.0 and 1.0 for L*, a* and b* values respectively measured under D65 and CIE 1964 standard colorimetric observer. One cabinet was a VeriVide cabinet, providing traditional light sources including fluorescent lamps and a tungsten bulb. Another one was equipped with a 16-channel LEDs illuminator named Telelumen Light Replicator, which was supplied by Telelumen Limited Liability Company in US. The third one was illuminated by a self-built tunable LED cluster. This LED cluster included 10 monochromatic LEDs and one white LED. Figure 1 plots their SPDs. The desired CCT, luminance level and CIE-$R_a$ value could be achieved by adjusting the intensity of each LED.
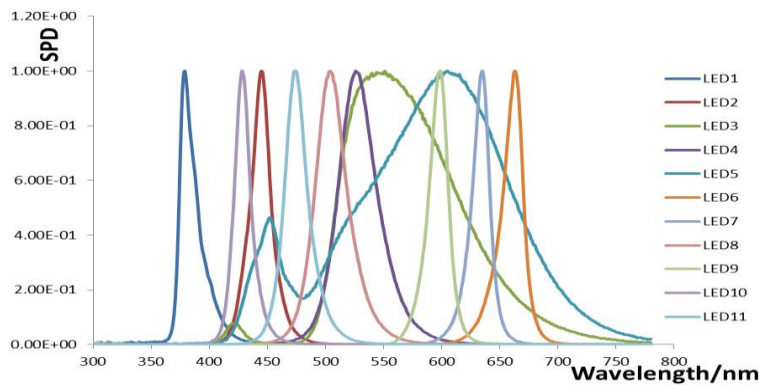


*Figure 1: SPDs of 11 LEDs.*

### 2.2 Pilot Experiment

The so-called 'test-sample method' adopted in this experiment requires observers to evaluate colour difference of identical samples illuminated by a reference and a test light source. Based on this, the grey backgrounds of two cabinets for adaptation should be visually alike. However, it was found that the bottom colour of two cabinets looked quite different while they had almost the same physical properties (CCT, luminance and chromaticity coordinates). The problem arises in part from the well-known shortcoming of $V(\lambda)$ function, or 2° $\bar{y}$ colour matching function, i.e. it has insufficient energy in the blue end of spectrum.

A pilot experiment was therefore conducted to match the grey background in the cabinet illuminated by reference light sources and that illuminated by test sources. Five observers participated in this visual matching experiment. Telelumen was adjusted accroding to each observer's assessments to obtain a visually matched reference light source.

Nine visually matched reference light sources were obtained. Afterwards, the matched two grey backgrounds under a pair of light sources were measured by a JETI Specbos 1211uv spectroradiometer (called TSR hereafter). Spectral measurements were carried out under 0°:45° geometry. Figures 2a and 2b plot the individual results of a target of 2850K in u'v' diagram calculated in 2° and 10° observers respectively. It can be seen that the points

are closer to the target in Figure 2b than in Figure 2a. This indicates that CIE 1964 or 10° standard colorimetric observer performed better than that of 1931 or 2°. In addition, the distance between 9 pairs of light sources in u'v' chromaticity diagram were calculated and the differences between the mean and each individual were averaged. This is known as MCDM (mean from colour difference of the mean) method. The MCDM values are 0.004 and 0.003 using 2° and 10° observers respectively. This is again confirmed that CIE 1964 standard colorimetric observer performed better than CIE 1931 standard one.
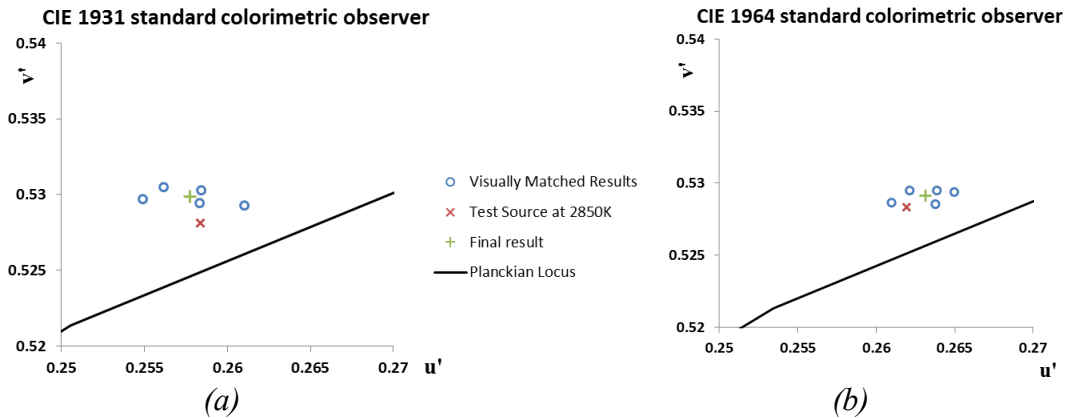


Figure 2: u'v' chromaticity diagram of visually matched results (a: 2°observer; b: 10°observer).

## 2.3 Experimental Setup and Method

Nine pairs of light sources were investigated in this experiment. Their SPDs were reflected from a white tile positioned in the center of the bottom of the cabinet and also measured by TSR under the same illumination/viewing geometry. Table 1 lists the engineering data of the 18 light sources at 3 CCTs (2850K, 4000K and 6500K). Note that all the reference light sources were set about 60 cd/m$^2$ luminance higher than their corresponding test light sources, in order to have a visual matched brightness of the bottom surface under a pair of light sources as found in the pilot experiment. This is mainly caused due to the diffuse test source and spot reference source used in the experiment.

Table 1. Colorimetric properties of the 18 light sources.

| Pair | Light sources | CCT(K) | Luminance (cd/m$^2$) | CIE-$R_a$ |
|------|---------------|--------|----------------------|-----------|
| 1 | Test/Reference source | 2814/2841 | 153/215 | 98/93 |
| 2 | Test/Reference source | 3955/3864 | 177/240 | 84/95 |
| 3 | Test/Reference source | 6280/6214 | 164/221 | 95/98 |
| 4 | Test/Reference source | 2812/2772 | 161/226 | 89/94 |
| 5 | Test/Reference source | 2829/2900 | 160/229 | 65/90 |
| 6 | Test/Reference source | 3960/3886 | 161/240 | 86/91 |
| 7 | Test/Reference source | 3953/3933 | 162/229 | 60/93 |
| 8 | Test/Reference source | 6308/6167 | 161/187 | 88/98 |
| 9 | Test/Reference source | 6322/5883 | 160/215 | 64/92 |

Thirty samples were chosen from various existing colour rendering sample sets, i.e. CIE-$R_a$, CQS and CRI2012. Figure 3 shows their distribution in CIELAB colour space,

which reveals that they gave a satisfactory coverage. All the samples had a size of 7.5 cm by 5 cm to subtend about 5° at the observers' eyes with a viewing distance of 50cm.
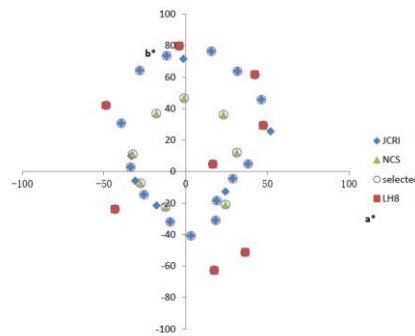


*Figure 3: Sample distribution in CIELAB colour space.*

Ten observers (5 male, 5 female) aged from 20 to 34 participated in the experiment. Before the experiment, they all passed the Ishihara colour vision test. Besides, they also took part in a small training session in order to be familiar with evaluation standards and to judge lightness, chroma and hue composition more accurately.

The whole experiment was carried out in a dark room without ambient light, as shown in Figure 4a. Before the start of experiment, observers were required to adapt to the dark condition for one minute. During this period, they were given an oral instruction of the experiment. Observers were then required to adapt to the grey backgrounds of two cabinets for one minute. In the experiment, according to a grey scale (see Figure 4b) placed in the cabinet of reference illuminant, observers reported colour difference in terms of grade values ranged from 1 (large difference) to 5 (no difference). Moreover, percentages of individual colour difference were also estimated, such as lightness difference, chroma difference and hue difference adding to 100. For each observer, the sequences of samples and light sources were all randomised.

In total, 12240 evaluations were accumulated, i.e. 4 questions × (30+4) samples × 9 pairs of sources × 10 observers.



*(a)*         *(b)*
*Figure 4: (a) Photo of experimental situation (b) A grey scale.*

## 3. RESULTS AND DISCUSSION

### 3.1 Observer Variability

Inter- and intra-observer variabilities were investigated in terms of the standardized residual sum of squares (STRESS) (García et al, 2007). A lower STRESS value indicates a smaller dispersion and better agreement. Inter-observer variability, which is also known as observer accuracy, was calculated between individual observer's results and mean

observer's results. Meanwhile intra-observer variability, which is also known as observer repeatability, was calculated between each observer's first and second evaluations for the four repeated samples. The results showed that a mean value of 36 ranged from 31 to 46, and of 34 ranged from 21 to 49 for the inter- and intra- observer variabilities, respectively. This implies that intra- is slightly smaller than inter- observer variability as expected.

In addition, observers showed poor performance under pairs of sources 1, 3, and 8. This was mainly caused by the high CIE-$R_a$ values for both the reference and test light sources. The higher the CIE-$R_a$ value of test light source, the smaller the perceived colour difference will be. It is well known that observers perform less consistently for assessing colour difference of small magnitude, which leads to high STRESS values consequently.

## 3.2 UCSs' performance

The raw data reported by observers in terms of grade values (1-5) were converted into visual colour difference ($\Delta V$) in CIELAB units via a fitted equation. Ideally, observers would find almost no lightness difference between two identical samples. However, it was found in the pilot experiment that observers required a higher luminance for the reference sources. Hence, the undesired visual lightness differences were calculated and removed from the total colour differences.

The visual chromatic differences obtained were employed to evaluate the performance of 4 different uniform colour spaces (UCSs), namely CIEU*V*W*, CIELAB, CIELUV and CAM02-UCS. Firstly, colour coordinates of 30 samples in different UCSs were calculated. Secondly, the colour differences between 30 sample pairs under each pair of light sources were calculated. These calculated colour differences ($\Delta E_i$) were then compared with the corresponding averaged visual colour differences ($\Delta V_i$) of ten observers. As mentioned earlier, 3 pairs of sources with high CIE-$R_a$ values were removed to make results more reasonable. Pearson correlation coefficient (r) was used to indicate the agreement between the calculated and visual colour differences. It was found that CAM02-UCS provided the best correlation, followed by CIEU*V*W*, CIELUV and CIELAB the worst, with r values of 0.58, 0.53, 0.52 and 0.34, respectively. The results indicate that CAM02-UCS gave the overall best performance on evaluating colour fidelity of light sources. This also agrees with the previous work reported by other researchers (Li et al, 2011; Sándor and Schanda, 2006).

## 3.3 CRIs' performance

Observers' visual data were also used to test different CRIs, which can be divided into two categories. One category includes colour fidelity based CRIs, namely CIE-$R_a$, CQS, CRI-CAM02UCS and CRI2012 and the other includes colour preference CRIs, namely FSCI, FCI, GAI and MCRI. The mean visual colour difference of 30 samples under each pair of light sources was used to represent visual data for that pair of sources. Afterwards, the obtained visual results were compared with different CRIs of each test light source calculated from its SPD. Table 2 summarizes the performance of each CRI in terms of pearson correlation coefficient values.

From Table 2, it can be seen that all the four colour fidelity based CRIs gave similar good performance in terms of r values ranged from 0.79 to 0.91. All the fidelity indices agreed better with the perceived colour difference than those of colour preference indices,

which gave quite poor correlations. Overall, CQS marginally outperformed the other colour fidelity indices. The results confirmed that colour preference based CRIs gave bad fit to the colour fidelity data.

*Table 2. Performance of different CRIs in terms of r values*

| CRI | CIE-$R_a$ | FSCI | FCI | GAI | MCRI | CRI-CA M02UCS | CQS | CRI2012 |
|---|---|---|---|---|---|---|---|---|
| r values | -0.908 | 0.100 | 0.404 | 0.479 | 0.028 | -0.862 | -0.909 | -0.792 |

## 4. CONCLUSIONS

A psychophysical experiment was carried out to investigate the performance of various UCSs and CRIs on evaluating colour fidelity of light sources. It is learned that a visual match of the grey backgrounds between the reference and test fields is strongly required. Also, the results obtained from the perception of colour difference reveal that test light sources with high CIE-$R_a$ values are not recommended to use, since observers are unable to scale small colour differences accurately and consistently.

It was found that CAM02-UCS correlated with visual results best among all the 4 UCSs tested. CIEU*V*W*, which is used to calculate CIE-$R_a$, and CIELUV also showed good performance with slightly lower correlations. On the contrary, CIELAB worked worst in predicting visual results.

In considering CRIs' performances, all the colour fidelity indices gave similar accuracy and outperformed colour preference indices in terms of r values. On the whole, CQS performed marginally better than the other three fidelity indices while MCRI showed worst prediction of visual results.

## REFERENCES

García, P. A., R. Huertas, M. Melgosa and G.H. Cui. 2007. Measurement of the relationship between perceived and computed color differences. *JOSA A*, 24(7): 1823-1829.

Jost-Boissard, S., P. Avouac, and M. Fontoynont. 2014. Assessing the colour quality of LED sources: Naturalness, attractiveness, colourfulness and colour difference. *Lighting Research and Technology*: 1477153514555882.

Li, C., M.R. Luo, G.H. Cui, and C.J. Li. 2011. Evaluation of the CIE colour rendering index. *Coloration Technology* 127(2): 129-135.

Sándor, N., and J. Schanda. 2006. Visual colour rendering based on colour difference evaluations. *Lighting Research and Technology* 38(3): 225-239.

*Address: Prof. Ming Ronnier LUO, State Key Laboratory of Modern Optical Instrumentation, Zhejiang University, 38 Zheda Road, Hangzhou,310007, CHINA*
*E-mails: m.r.luo@leeds.ac.uk*

# A Study on the Lighting of Bathroom for the Elderly

Jiyoung PARK,[1] Chanung JEONG,[2] Eunji SEO,[2] Jinsook LEE[3]

[1] Ph.D, Dept. of Architectural Engineering, Chungnam National University, Korea
[2] Master Course, Dept. of Architectural Engineering, Chungnam National University, Korea
[3] Professor, Dept. of Architectural Engineering, Chungnam National University, Korea

## ABSTRACT

In this study, I have come up with the luminance and color temperature that are appropriate for elderly people who are 65 or older, in the bathroom of houses that adopt direct LED light from the ceiling. To come up with a lighting environment in the bathroom space for the elderly, I combined the verified appropriate scope of luminance and color temperature with the analysis of the influence from the evaluation variables. As a result, the lighting environment in the bathroom space for elderly people who are 65 or older required the color temperature of 3000 K and the luminance of 400 lx.

## 1. INTRODUCTION

A bathroom is at once a space for satisfying the physiological needs of humans and a space for health care and rest. While its size is small compared to other units of a house, it accommodates a variety of behaviors. So, it requires sanitary and functional kind of lighting, and furthermore, since most bathrooms are closed without windows, the role of light looms even bigger. Moreover, as a bathroom registers the most accidents involving elderly people among all parts of a residential space and visual ageing follows health condition in influencing an elderly person's ability to perform activities of daily living, lighting should be applied while considering the visual characteristics of elderly people.

Also, the bathrooms for collective housing in Korea that is being sold or accommodating residents lately have direct light buried in the ceiling. And as LED has begun to be adopted for residential indoor lighting, studies should reflect such a trend for bathroom space.

Thus, in this study, I have come up with the luminance and color temperature that are appropriate for elderly people who are 65 or older, in the bathroom of houses that adopt direct LED light from the ceiling.

## 2. EXPERIMENTAL METHOD

The size of the bathroom space chosen for the experiment is 3000 (W) Χ 2000 (L) Χ 2000 (H) mm, and it includes a wash basin, a toilet, a bath tub, a mirror etc. The bathroom includes two pieces of direct light buried in the ceiling. The light chosen for the wash basin and the toilet is rectangular with the size of 1200 Χ 150 mm, while the round-shaped ones used for the center above the bath tub and above the center of the bathroom have a diameter of 150 mm, all adopting LED.

Four different levels of color temperature presented for the experiment are 3000 K, 4000 K, 5000 K, and 6000 K, while six levels of luminance used for it are 100 lx, 200 lx, 300 lx, 400 lx, 500 lx, and 600 lx. The color temperature was measured using a chroma meter (CL-200, Minolta) directly under the experimental light source, while luminance was measured as an average luminance for the bathroom space, in KS 5-point method, using an illuminometer (T-10, Minolta), at the height of 85 cm above the floor.
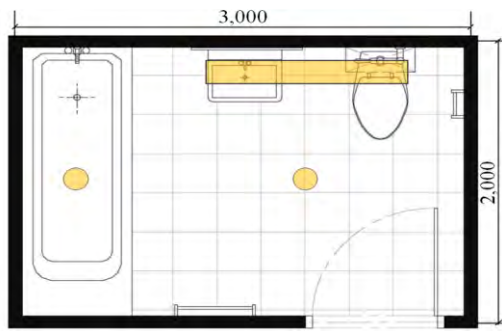
*Fig 1. Overview of the experimental space*



*Fig. 2. Composition of the experimental space*

*Table 1. Physical properties of the rectangular ceiling light and spectral distribution*

| Color temperature | CRI [Ra] | Spectral distribution |
|---|---|---|
| 3000 K | 80 |  |
| 4000 K | 79 |  |
| 5000 K | 77 |  |
| 6000 K | 75 |  |

*Table 2. Physical properties of the* round shaped ones *ceiling light and spectral distribution*

| Color temperature | CRI [Ra] | Spectral distribution |
|---|---|---|
| 3000 K | 78 |  |
| 4000 K | 81 |  |
| 5000 K | 81 |  |
| 6000 K | 80 |  |

The 15 subjects who participated in the experiment were at least 65 years old and below 86 (average age 75). To rule out the influence of any artificial light sources around including the daylight, the experiment was conducted in a windowless space and in sequential comparison. The subjects were instructed to adjust for 1 minute to the provided lighting environment and then verbally express the appropriateness (how bright) and preference (how much preferred) of the brightness on the 5-point scale (5 points for Very much so, 3 points for So-so (appropriate for brightness), and 1 point for Never), while the researcher recorded their responses on the evaluation sheet.

## 3. EXPERIMENT RESULTS AND ANALYSIS

The analysis of the group average for the category of 'Bright' is as shown in Fig 3. For all color temperature levels, respondents found it the most appropriate at 300 to 400 lx, found 500 lx somewhat bright, and found 600 lx very bright. And they found 200 lx somewhat dark and 100 lx very dark. In her study, Jinsook LEE (2014) saw that those respondents in their 20s or 30s found 300 lx the most appropriate as the brightness for general lighting in the bathroom space. When compared with the study that surveyed elderly people who are 65 or older, one can see that the group of respondents who are 65 or older comes close to the group of those in their 20s or 30s, thus preferring similar levels of brightness, or demands 100 lx or so more.

The analysis of the group averages in the evaluative category of 'Preferred' is as shown in Fig 4. 3000 K is highly rated in all categories compared to the other color temperature levels, and notably, 3000 K is the most preferred at 300 to 400 lx, now found to be the appropriate brightness. The study by Jinsook LEE (2014) showed that as the appropriate color temperature

for general lighting in the bathroom space, those in their 20s or 30s prefer 3000 K most. This agrees with the study involving the elderly who were 65 or older, and one sees that different age groups do not differentiate widely but share similar preference of color temperature.
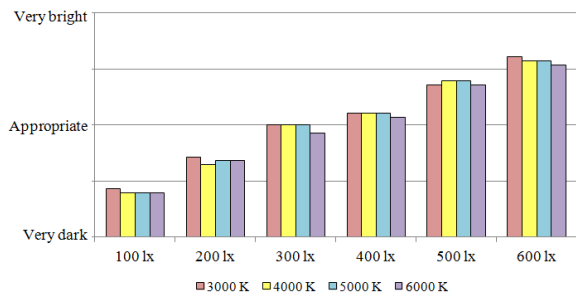


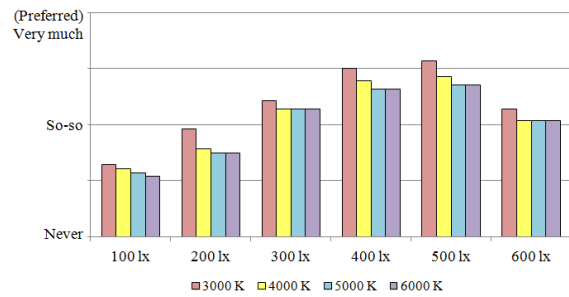*Fig. 3. Analysis of group averages in the evaluative category of 'Bright'*



*Fig. 4. Analysis of group averages in the evaluative category of 'Preferred'*

I performed H-test by Kruskal-Wallis to see if there exist any significant differences among the results of the luminance evaluation at the same color temperature. As a result, all came up with a statistical significance (p-value) of less than 0.05 (with a significance level of 5%), thus showing that there a significant differentiation with levels of luminance. Therefore, I think scrupulous consideration should be given to brightness in designing lighting environment for a bathroom space (Table 3).

*Table 3 . Test of statistical significance among levels of luminance at the same color temperature*

| Behavior | Type of lighting | Color temperature | Statistical significance (P) Bright |
|---|---|---|---|
| General | Direct light from ceiling | 3000 K | 0.000* |
| | | 4000 K | 0.000* |
| | | 5000 K | 0.000* |
| | | 6000 K | 0.000* |

\* : Significance level below 0.05,

I performed H-test by Kruskal-Wallis to see if there exist any significant differences among the results of the color temperature at the appropriate luminance. As a result, all came up with a statistical significance (p-value) above 0.05 (with a significance level of 5%), thus showing that there is no significant differentiation with levels of color temperature (Table 4).

*Table 4. Test of statistical significance among levels of color temperature at the appropriate luminance*

| Behavior | Type of lighting | Color temperature | Statistical significance (P) Preferred |
|---|---|---|---|
| General | Direct light from ceiling | 300 lx | 0.916 |
| | | 400 lx | 0.375 |

\* : Significance level below 0.05

For a quantitative analysis of the visual effects of the experimental variables, I performed multiple regression analysis to analyze the influence of different evaluation variables. The multiple and partial correlation coefficients obtained from the analysis are as shown on Table 5. Overall, correlation coefficient was minimum 0.5 and luminance registered the greatest influence.

'Preference' with regard to the color temperature and luminance of 'direct light from ceiling' registered a high correlation coefficient of R=0.9962 ($R^2$=0.9925). As for the scope of factors, luminance was 84.83%, thus registering bigger influence than color temperature. To look at the

quantity by category, respondents preferred 300 to 500 lx at the color temperature of 3000 K, with the greatest influence registered at 3000 K and 400 to 500 lx.

*Table 5. Influence of evaluation variables*

| Evaluation criterion | Multiple correlation coefficient ($R^2$) | Partial correlation coefficient (scope) | |
|---|---|---|---|
| | | Color temperature | Luminance |
| Preferred | 0.9925 | 0.916(0.300) | 0.996(1.678) |

$R^2$=0.9925

| Classification / Variable | Category | Number of samples | Standardized category quantity | Partial correlation coefficient | Variable scope | Variable scope quantity | Standardized category quantity distribution (-1.5 / 0 / 1.5) |
|---|---|---|---|---|---|---|---|
| Color temperature | 3000 K | 6 | 0.201 | 0.916 | 0.300 | 15.17% | 0.201 |
| | 4000 K | 6 | -0.014 | | | | |
| | 5000 K | 6 | -0.087 | | | | |
| | 6000 K | 6 | -0.099 | | | | |
| Luminance | 100 lx | 4 | -0.968 | 0.996 | 1.678 | 84.83% | |
| | 200 lx | 4 | -0.521 | | | | |
| | 300 lx | 4 | 0.179 | | | | |
| | 400 lx | 4 | 0.622 | | | | |
| | 500 lx | 4 | 0.709 | | | | 0.709 |
| | 600 lx | 4 | -0.021 | | | | |

*Fig. 5. Analysis of category-specific influence of different evaluation criteria*

## 4. CONCLUSIONS

To come up with a lighting environment in the bathroom space for the elderly, I combined the verified appropriate scope of luminance and color temperature with the analysis of the influence from the evaluation variables. As a result, the lighting environment in the bathroom space for elderly people who are 65 or older required the color temperature of 3000 K and the luminance of 400 lx.

## ACKNOWLEDGEMENTS

## REFERENCES

Jin-Sook, LEE. and Ji-Young, PARK. 2014. *Identifying the Appropriate Illuminance and Color Temperature of LED Lighting for Different Behaviors in Bathroom Space*, Journal of the Korea Society of Color Studies, 28(3), 179-188.

*Address : Jiyoung Park,  Dept. of Architectural Engineering, College of Engineering, Chungnam National University, 99 Daehak-ro, Yuseong-gu, Daejeon 305-764. Korea*
*E-mails: jiyoung1355@hanmail.net, chanwung2000@nate.com, sej4468@naver.com, js_lee@cnu.ac.kr*

# Sitting Posture Based Lighting System to Enhance the Desired Mood

Hyunjoo BAE,[1] Haechan KIM,[1] Hyeon-Jeong SUK[1]
[1] Department of Industrial Design, KAIST

## ABSTRACT

As a cue of desired mood, we attempted to identify types of sitting posture when people are involved in various tasks during their working hours. After having attached six pressure sensors and one distance sonsor to an office chair, we first recorded participants' postures while they took part in four different tasks. From the seven sensors, we gathered five sets of data related to the head, lumbar, hip, thigh pressure and the distance between the backrest and the body and then classified them. We derived four types of sitting posture that were mapped into the different tasks. In addition, we requested subjects to take poses that might be suitable for the each of the four task types. In this way, we tried to compare the matches between postures and tasks in natural setting with those in controlled situation. The comparison yielded no statistical significance and consequently, we moved on to the development of a posture based lighting system that manipulates the quality of office lighting and is operated by changes in one's posture. Facilitated by this system, color temperature ranging between 3000 K and 7000 K and illumination ranging between 300 lx and 700 lx were modulated. This study demonstrates how human emotion can interact with lighting mediated through physical behavior.

## 1. INTRODUCTION

There have been demands for higher qualities of daily life by extending the role of lighting system. LED lighting system in particular, has benefits to easily control its illumination and color temperature, offering users wide possibilities of desirable lighting environment. Thus, efforts are currently underway to investigate the optimal lighting environment to enhance the task productivity and emotional satisfaction. For example, some studies has conducted a study to determine the proper lightings for educational situation(Lee et al. 2013, Wessolowski 2014). As a cue of desired mood, physical behavior reacted to the user contexts have been studied such as automated posture analysis for detecting subject's interest level(Mota and Picard 2003). Especially when it comes to office, it is determined that sitting postures have high feasibility and can be detected robustly with sensing chair(Mutlu et al. 2007). In this regard, we aim to examine the feasibilities of sitting postures as a cue of desired mood. Also, we attempt to propose a posture-based lighting system focusing on office environment that provides optimal quality of lighting for different user contexts.

## 2. EXPERIMENTAL PLAN

In order to obtain the quantitative data when people have different sitting postures during their working hours, we planned an empirical study by attaching sensors to an office chair. Differently from thoroughly carried out studies on human ergonomics, we tried to reduce the number of sensors as much as possible while minimizing the loss of meaningful data. Moreover, we also intended to find a synergetic match between types of posture and those of task. Finally we anticipated to map out appropriate lighting contents unconsciously modulated by one's sitting postures.

AIC2015 TOKYO - Color and Image

## 2.1 Participants

A total of 10 college students participated and their average age was 21.50 years (SD = 1.78 years) Their average height of 167.30 cm and weight of 59.20 kg, and both genders were evenly recruited. In order to prevent abnormal sitting posture caused by poor eyesight, we acquired higher than 0.7 score in eyesight. Also participants should not have experience of having treatment for pain of neck, shoulder, legs or arms.

## 2.2 Experimental Setup

The experimental room was set up to resemble an office environment. Sitting postures on the office chair were observed while participants were taking part in the given tasks presented on computer monitor(Figure.1). To identify the postures, we attached six pressure sensors and one distance sensor to an office chair. To find the relevant locations of sensors we referred to the related research(Park et al. 2012) and then covered the chair with cotton fabric(Figure 1). While a participant was sitting we received signals from their head, lumbar, hip, thigh pressure and the signal of backrest-body distance at every 5 Hz. We transformed the signals into manageable data utilizing Arduino Processing. In addition, to measure the body angle, markers were attached on their joint of shoulder, hip and knee and the side view were recorded. The monitor was set to be center of the participants, and the distance between the monitor and the eyes was 50 cm. The chair's height was adjusted depending on the participant's height to keep 90 degree of knee angle. To reduce influence by lighting, the experiment was conducted under a constant illuminant (5000 K, 600 lux).
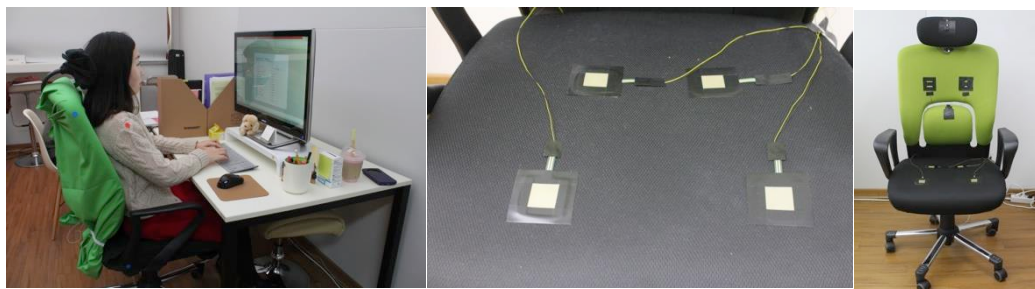


*Figure 1: Experimental environment and Sensor equipped office chair.*

## 2.3 Experimental Procedure

The empirical study involved two steps. In part 1, we observed participant's unconscious postures while they were working on the following four tasks: (1) memorizing words, (2) playing Tetris®, (3) reading magazine articles, and (4) relaxing. Memorizing words was for strong attention with high workload, while playing Tetris® game was considered as attentive but with low workload. Also, reading simple articles was associated with medium level of concentration as well as workload. As reading material we provided with six articles that were nor much informative. Finally, relaxing was expected to release participants from any types of tasks, and participants were listening to meditation music. In this way, the four tasks were carefully devised. Each task took seven minutes until completed and the tasks were given in random order(Figure 2). In part 1, participants were not informed that their posture was being recorded.

In part 2, on the other hand, the purpose of the experiment was revealed. Participants were asked to consciously take postures that best fit to the given task type. They sat in different positions approximately for 10 seconds and the request was repeated three times in random order(Figure 2).
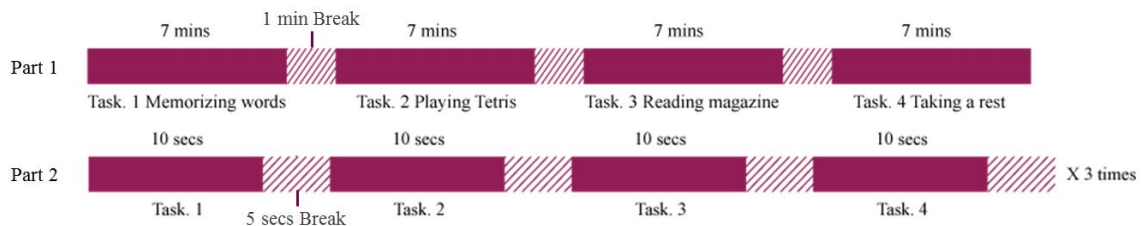
AIC2015 TOKYO - Color and Image

*Figure 2: Experimental process of part2.*

## 3. RESULTS AND ANALYSIS

### 3.1 Data Extraction

After having collected the data from both part 1 and 2, we focused on the replicated parts that appeared consistently. In part 1, when participants maintained certain posture for longer than 30 seconds, it was considered as one posture. We cropped out the 15 second-segment from the middle of the posture and then averaged them for each sensor value. Finally, a total of 45 segments (the number of observed postures which maintained longer than 30 secs) were collected from part 1, the unconscious sitting postures (Figure 3). In part 2, we applied the identical method but observed only 5 seconds. Since we requested to pose three times, we collected a total of 15 second-segment and then averaged them for each sensor value. Therefore, 40 segments (4 tasks × 10 participants) were collected from part 2, the conscious sitting postures (Figure 4).
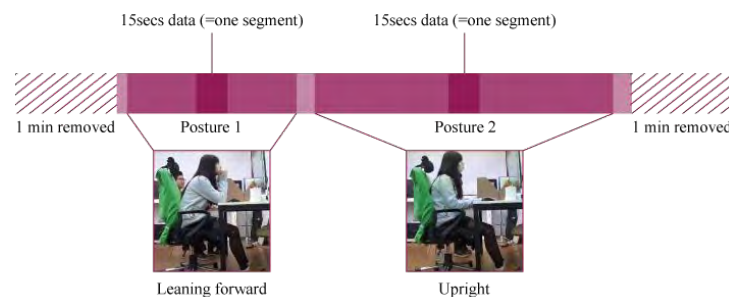


*Figure 3: Process of extracting data from part1.*
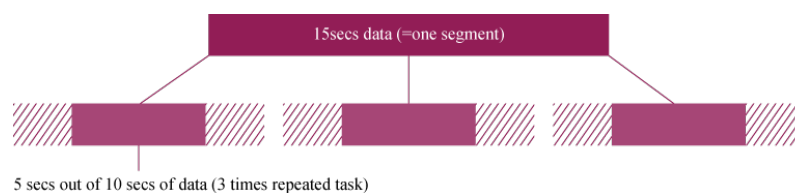


*Figure 4: Process of extracting data from part2.*

### 3.2 Classification of Sitting Postures based on the Sensor Values

Based on a total of 85 extracted posture segments, we classified them in following four kinds of postures: (P1) leaning forward (under 85 degree), (P2) upright (between 85 and 95 degree), (P3) upright with the lumbar supporting, (P4) leaning backward. We distinguished (P2) from (P3), because of different range of lumbar pressure. Furthermore, to confirm the statistical difference between posture types, we one-way independent ANOVA test based on the sensor values of each posture. The analysis yielded a statistical significance [$F_{(3,81)} = 22.033$, $p < .05$] indicating that each posture can be profiled with a noticeable difference. For example, backrest-body distance was significantly bigger than other postures while participants leaning forward. During upright with the lumbar supporting and

leaning backward, the lumbar pressure was significantly bigger than other postures. Subsequently, all 85 segments from observed postures could be classified in four posture types(Figure 5).
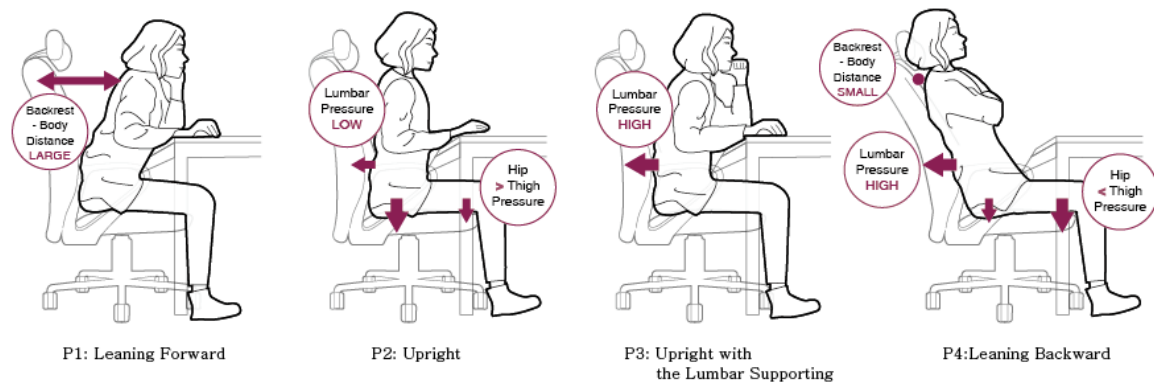


*Figure 5: Posture classification process and criteria.*

In addition, the Figure 6 illustrates the flow of signal processing to sort out the sensor signal into the corresponding postures.
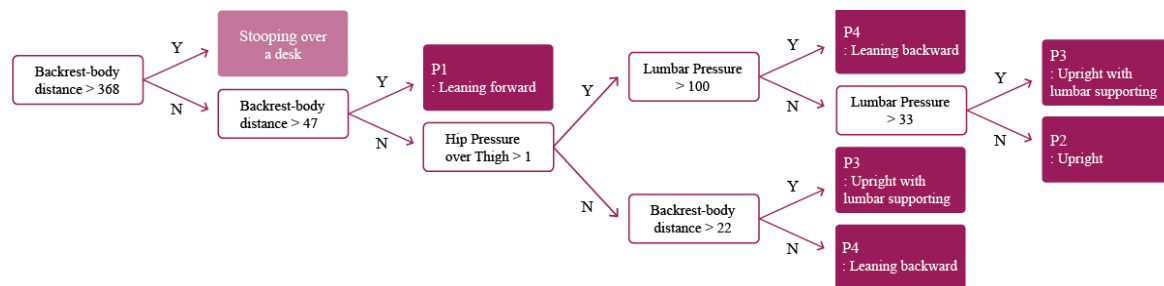


*Figure 6: Process of signal to be corresponded to one of the four posture types.*

### 3.3 The relationship between postures and tasks

Then we tried to explore whether the postures could be represent the user's task or not. Chi test was conducted to compare the frequency of observed posture types depending on unconscious and conscious tasks. Differently from anticipation, the difference between the unconscious postures in part 1 and conscious postures in part 2 did not show a statistical significance at an alpha level of 0.05 in each task. Therefore, the sum of posture frequency of both parts was used for statistical analysis (Table 1).

*Table 1. Posture frequency depending on task types.*

|  | P1 | P2 | P3 | P4 |
|---|---|---|---|---|
| (1) Memorizing Words | 11 | 6 | 3 | 3 |
| (2) Playing Tetris® | 7 | 7 | 5 | 2 |
| (3) Reading Articles | 4 | 5 | 11 | 2 |
| (4) Relaxing | 0 | 0 | 2 | 20 |

The results indicate that postures are influenced by the task. There was a significant association between the task types and the posture types [$\chi^2$ (9, N=85) = 62.087, p < .05]. While participants were memorizing words, leaning forward posture was most frequently observed. While playing game, leaning forward posture and upright posture were dominant identically. Whereas, during reading articles, upright with the lumbar supporting posture

AIC2015 TOKYO - Color and Image

was quite frequent. In addition, while relaxing, frequency of leaning backward posture was definitely higher than other postures. That is, people are unconsciously and consciously leaning forward when working intensively, whereas leaning backward during relaxing.

## 4. DISCUSSION

### 4.1 General Discussion

The empirical study showed sitting postures could be classified in posture types based on signals. Also, sitting postures appeared differently related to the concentration level of works. Since the postures reflect user's states, it can be used as a novel lighting control interface. To some disappointment, there was weak similarity between unconscious and conscious postures in memorizing words out of four task types. It could be assumed that that intensive working caused some tiredness and it affected on inconsistent tendency of postures. As such, to make more reliable posture sorting algorithm, accurate and stable signals of sensor should be collected. Also, more in-depth studies would be worthwhile to investigate the relationship between sitting postures and task types.

### 4.2 Application of posture based lighting system

Finally we developed a posture based lighting system that manipulates the quality of office LED lighting and is operated by changes in one's posture. As previous studies have revealed there are optimal combinations of color temperature and correlated illumination that can enhance people's affective experience. They demonstrated that higher color temperature (7500 K versus 3000 K) is more activating in the point of mental level (Deguchi and Sato 1992) and low color temperature lighting creates a lowering of central nervous system activity(Noguchi and Sakaguchi 1999). In addition, the efficiency of learning increases under high color temperature and high illuminance lighting, whereas the lighting of low color temperature and low illuminance was proper for relaxing(Lee et al. 2013, Wessolowski 2014). Consequently, for the concentration required activities, high color temperature - high illuminance lighting condition is needed to users, on the other hand, low color temperature - low illuminance lighting is suggested for relaxation.
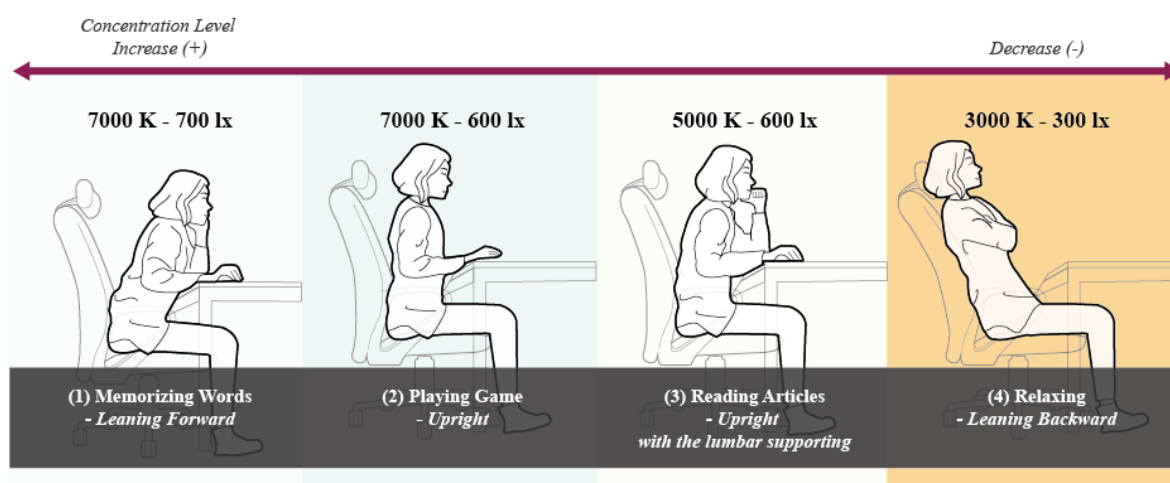


*Figure 8: Four scenarios of posture-based lighting system.*

Through the previous researches and the real demonstration under high rendering LED ambient lighting room, the modified illumination ranges between 300 lx and 700 lx, and correlated color temperatures range between 3000 K and 7000 K. After real-time posture classification by Arduino Processing, color temperature and illuminance of LED lighting

can be adjusted to offer desired mood of users. Thus, optimal lighting presets for each task can be produced by one's posture. Four representative lighting scenarios were generated as follow: (1) for the strong attention with leaning forward posture, 7000 K - 700 lx lighting will apply, (2) for the attentive task such as playing game with upright posture, 7000K - 600 lx lighting will apply, (3) for the medium level of concentration in daily life like reading, 5000K - 600 lx will apply, and (4) for the relaxation, 3000K - 300 lx lighting will apply. Ultimately, this system might increase intuitiveness and unobtrusiveness of lighting control interface for office environment. Furthermore, with the larger number of participants, more accurate posture classification algorithm should be developed. Also the verification experiment will be conducted in these posture-based lighting scenarios.

## 5. CONCLUSION

This study investigates the feasibility of posture classification based on simple sensor equipped chair. Through the experiment, it was determined that postures of users are related to different concentration level of tasks. Also, there is no significant difference between unconscious and conscious sitting postures from identical task. Wide possibility of automated indoor lighting system to provide desired mood using sitting postures was explored. The empirical findings of this research can be utilized for interaction between human emotion and lighting mediated through physical behavior.

## REFERENCES

Deguchi, Takatsugu, and Masahiko Sato. 1992. The effect of color temperature of lighting sources on mental activity level. *The Annals of physiological anthropology* 11 (1):37-43.

Lee, J, K Choi, N Na, and HJ Suk. 2013. LED Lighting for Educational Environment: Focusing on Math and Multimedia Based Tasks for 4th Grade Elementary School Students in South Korea. 12th Cogress of International Color Association AIC 2013, New Castle.

Mota, Selene, and Rosalind W Picard. 2003. Automated posture analysis for detecting learner's interest level. Computer Vision and Pattern Recognition Workshop, 2003. CVPRW'03, Villanova, 49-49.

Mutlu, Bilge, Andreas Krause, Jodi Forlizzi, Carlos Guestrin, and Jessica Hodgins. 2007. Robust, low-cost, non-intrusive sensing and recognition of seated postures. Proceedings of the 20th annual ACM symposium on User interface software and technology UIST 2007, Newport, 149-158.

Noguchi, Hiroki, and Toshihiko Sakaguchi. 1999. Effect of illuminance and color temperature on lowering of physiological activity. *Applied human science: journal of physiological anthropology* 18 (4):117-123.

Park, Jae Hee, Seung Hee Kim, Min Uk Kim, Hee Dong Han, Young Soo Shim, and Taeil Son. 2012. Measurement of Body Weight Distributions on a Seat Pan for Various Sitting Postures. *Journal of the Ergonomics Society of Korea* (Published online).

Wessolowski, Nino. 2014. Wirksamkeit von dynamischem Licht im Schulunterricht. Hamburg-Eppendorf: Universtitaet Hamburg.

*Address: Prof. Hyeon-Jeong Suk, Department of Industrial Design, KAIST*
*Bldg. N25, 291 Daehak-ro, Yuseong-gu, Daejeon, 305-701, KOREA*
*E-mails: bhjoo@kaist.ac.kr,kimhaechan@kaist.ac.kr,h.j.suk@kaist.ac.kr*

# Colour Lighting Based on Chromatic Strength

Toru KITANO, Tetsuji YAMADA, Kosuke OSHIMA
Iwasaki Electric Co., Ltd.

## ABSTRACT

In its technical report CIE 94: Guide for Floodlighting, the International Commission on Illumination (CIE) defines the recommended luminance for illuminating an object with white-colour light. However, it does not define recommended luminance for illuminating an object with coloured light. Accordingly, we conducted a matching experiment on the object illuminated with white-colour light and the object illuminated with coloured lights, for finding the luminance ratios when the both objects are perceived as having equal chromatic strength, and derived recommended luminance for colour lighting. As a result, we found that the recommended luminance for colour lighting can be expressed by a variable differing depending on the $u'v'$ chromaticity of the illuminated object. In addition, we conducted a verification experiment to confirm whether derived recommended luminance is utilized for actual lighting design. In detail, we conducted an experiment to confirm whether the object is equally conspicuous when the object is illuminated with different coloured lights to the identical chromatic strength. We verified that the recommended luminance for colour lighting can be utilized for actual lighting design.

## 1. INTRODUCTION

Emergence of full-colour LED lighting has increased opportunities to illuminate towers, bridges, monuments, etc. with vivid coloured lights. In its technical report CIE 94: Guide for Floodlighting, the International Commission on Illumination (CIE) defines the recommended luminance for illuminating an object with white-colour light such as mercury lamp and high-pressure or low-pressure sodium lamp as 4 cd/m$^2$ (poorly lit zones), 6 cd/m$^2$ (average zones) and 12 cd/m$^2$ (brightly lit zones) according to the brightness of the surroundings. However, it does not define recommended illuminance and luminance for illuminating an object with coloured light. As a result, it is impossible to easily calculate the quantity of light required for giving the suitable appearance.

Accordingly, we conducted a matching experiment on the object illuminated with white-colour light and the object illuminated with coloured lights, for finding the luminance ratios when the both objects are perceived as having equal chromatic strength, and derived recommended luminance for colour lighting.

## 2. DERIVATION OF THE RECOMMENDED LUMINANCE

### 2.1 Matching Experiment

Figure 1 shows a schematic diagram of experimental equipment. The subjects included 10 males and females in their 30s to 40s with normal colour vision.

To begin with, the subject sits in the chair in a dark room and observes black paper of luminance $L_B$ located in front for 5 minutes to adapt his/her eyes. As shown in Figure 1, the black paper is provided with two right and left circular holes opened symmetrically by the

center of the visual field beforehand, which are covered with the same kind of black paper during adaptation. There is a white wall ahead of the black paper, and the left portion of the wall viewed from the subject is uniformly illuminated with white-colour light of correlated colour temperature 5,000 K, and the right portion of the wall is uniformly illuminated with coloured light. A partition is installed at the center of the white wall so that right and left light will not be mixed.
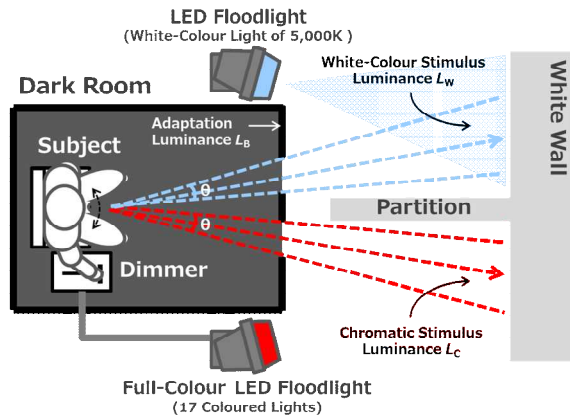


*Figure 1: Schematic diagram of experimental equipment.*

After the adaption, the black paper covering the holes is removed to present to the subject a stimulus by white-colour light (to be referred to as the white-colour stimulus) and that by coloured light (to be referred to as the chromatic stimulus) through the holes. When observing both stimuli, the subject was instructed to swing his/her face to the right and left to look at the center of the right and left stimuli. The subject was allowed to freely adjust the luminance $L_C$ of the chromatic stimulus with a dimmer at hand until he or she perceives as the strength equal to the white-colour stimulus of luminance $L_W$. The subjects were taught that the strength was a "concept combining brightness and conspicuousness." After matching was completed, the then luminance $L_C$ of the chromatic stimulus was measured and a different chromatic stimulus was presented again to make matching.



| No. | u' | v' | No. | u' | v' |
|---|---|---|---|---|---|
| 0 | 0.210 | 0.484 | 9 | 0.129 | 0.343 |
| 1 | 0.485 | 0.521 | 10 | 0.147 | 0.371 |
| 2 | 0.305 | 0.494 | 11 | 0.199 | 0.073 |
| 3 | 0.333 | 0.543 | 12 | 0.214 | 0.212 |
| 4 | 0.243 | 0.554 | 13 | 0.217 | 0.353 |
| 5 | 0.071 | 0.577 | 14 | 0.308 | 0.239 |
| 6 | 0.145 | 0.529 | 15 | 0.265 | 0.353 |
| 7 | 0.105 | 0.437 | 16 | 0.407 | 0.385 |
| 8 | 0.133 | 0.455 | 17 | 0.316 | 0.436 |
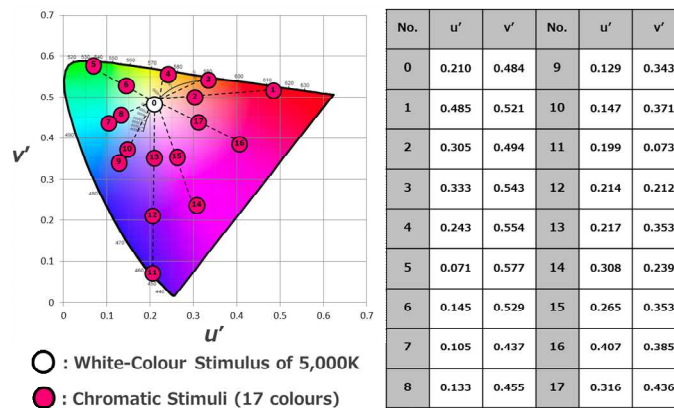
*Figure 2: u'v' chromaticity of the white-colour and chromatic stimuli.*

Figure 2 shows the *u'v'* chromaticity of the white-colour and chromatic stimuli. Totally 17 colours were used for the chromatic stimuli. Assuming the same 3 conditions as in the CIE94, 4, 6 and 12 cd/m$^2$, for the luminance $L_W$ of the white-colour stimulus, the then adaptation luminance $L_B$ was assumed to be 5% of $L_W$ (0.2, 0.3 and 0.6 cd/m$^2$, respectively). The viewing angle $\theta$ of the presented stimuli assumed 3 sizes of 5°, 15° and

AIC2015 TOKYO - Color and Image

30°. This viewing angle was determined, assuming a situation to view an illuminated object from near, medium and far distances. The matching experiment was conducted in 3 times for each different luminance $L_W$ of the white-colour stimulus, and matching was implemented 153 times in total (17 colours × 3 conditions × 3 sizes).

## 2.2 Experimental Results

Figure 3 shows the results of the $\log(L_W/L_C)$ values, that of the luminances $L_C$ of the chromatic stimuli perceived as equal strength to the white-colour stimulus at $L_W = 4$ cd/m$^2$ and $\theta = 5°$, in the form of a box plot. Nos. 1 to 17 in Figure 4 are common with Figure 2.
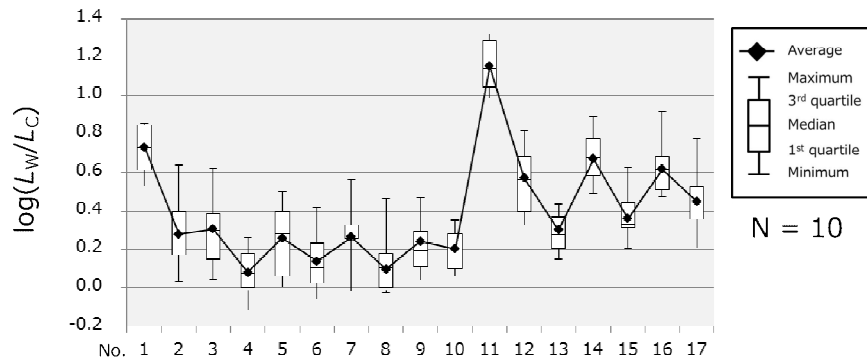


*Figure 3: Results of the log($L_W/L_C$) values.*

The $L_W/L_C$ ratios are proportional to the strength of that chromatic stimuli (to be referred to as the chromatic strength) and indicate that the chromatic stimuli are higher chromatic strength than the white-colour stimulus in case of $L_W/L_C > 1.0$, and they are lower chromatic strength than the white-colour stimulus in case of $L_W/L_C < 1.0$. According to Figure 3, the colour with the highest chromatic strength among Nos. 1 to 17 was No. 11, blue, and that with the lowest chromatic strength was No. 4, yellow. Also, among chromatic colours with the same dominant wavelength (for example, Nos. 11, 12 and 13), Figures 2 and 3 show that the one with higher excitation purity (No. 11 in this case) was the higher $L_W/L_C$ ratios, and higher chromatic strength. This phenomenon was the same as the Helmholtz-Kohlrausch phenomenon in which the brightness of a perceived colour changes when the excitation purity is increased. These results showed a similar tendency in the experimental results with the different luminance $L_W$ of the white-colour stimulus and different viewing angle $\theta$ of the presented stimulus.

As shown in Figure 3, the results of the $L_C/L_W$ ratios varied greatly among the subjects depending on the chromatic colours. If the recommended luminance for colour lighting is derived, assuming the average value of the $L_C/L_W$ ratios of the 10 subjects to be a representative value, the recommended luminance could be too low for about half of them. Accordingly, this study attempted to derive the recommended luminance for colour lighting, assuming the third quartile of the results to be the representative value of the $L_C/L_W$ ratios.

## 2.3 Derivation of the Recommended Luminance

The CIE recommends the empirical formulas (1) and (2) which compare the brightness of the luminance $L_1$ and $L_2$ of different colours. Formula (1) represents the brightness by a correction coefficient $f$ consisting of luminance and $xy$ chromaticity. When Formula (1)

AIC2015 TOKYO - Color and Image

holds, $L_1$ and $L_2$ are of the same brightness. When the $xy$ chromaticity is D65 (0.313, 0.329), $f = 0$ holds.

$$\log ( L_1 ) + f_1 = \log ( L_2 ) + f_2 \tag{1}$$

$$f = 0.256 - 0.184y - 2.527xy + 4.656x^3y + 4.657xy^4 \tag{2}$$

Then, it is assumed that the luminance $L_1$ of Formula (1) is the luminance $L_W$ of the 5,000 K white-colour stimulus, and that the luminance $L_2$ is the luminance $L_C$ of the chromatic stimulus. Furthermore, if $f = 0$ holds in case of the 5,000 K white-colour stimulus, Formula (1) can be expressed as Formula (3), using the new correction coefficient $f'$. Since $f' = \log (L_W/L_C)$ is allowed by deforming Formula (3), a regression Formula (4) for calculating the correction coefficient $f'$ was obtained by multiple regression analysis, assuming $\log (L_W/L_C)$ values obtained from the experimental results to be explained variables and variables consisting of the $u'v'$ chromaticity of the chromatic stimuli to be explanatory variables.

$$\log ( L_W ) = \log ( L_C ) + f' \tag{3}$$

$$f' = 1.023 - 2.79v' + 46.1u'v'^3 + 141u'^3v'^2 - 196u'^2v'^3 \tag{4}$$

$$L_C = L_W / 10^{f'} \tag{5}$$

If Formula (3) is deformed, the recommended luminance $L_C$ for colour lighting can be expressed by Formula (5). Now, suppose based on the CIE 94 that the recommended luminance $L_W$ for illuminating an achromatic object with 5,000 K white-colour light has 3 levels 4 cd/m$^2$, 6 cd/m$^2$ and 12 cd/m$^2$, the recommended luminance $L_C$ for colour lighting can be presented in Table 1. Figure 4 shows the relations between $10^{f'}$ values and $u'v'$ chromaticity coordinates. It is seen that the recommended luminance $L_C$ for colour lighting is a variable differing depending on the $u'v'$ chromaticity of the illuminated object.

*Table 1. Recommended luminance for colour lighting.*

| Brightness of the surroundings | Recommended luminance $L_W$ (White-colour light) | Recommended luminance $L_C$ (Coloured light) |
|---|---|---|
| Poorly lit zones | 4 [cd/m$^2$] | 4/10$^{f'}$ [cd/m$^2$] |
| Average zones | 6 [cd/m$^2$] | 6/10$^{f'}$ [cd/m$^2$] |
| Brightly lit zones | 12 [cd/m$^2$] | 12/10$^{f'}$ [cd/m$^2$] |
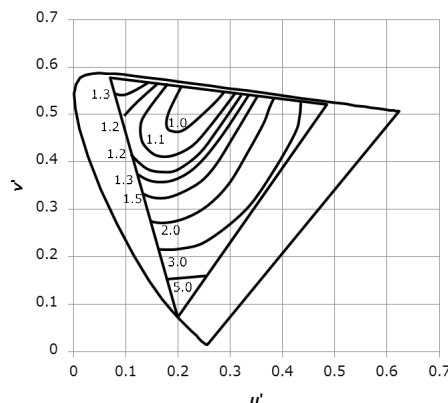


*Figure 4: Relations between $10^{f'}$ values and $u'v'$ chromaticity coordinates.*

AIC2015 TOKYO - Color and Image

# 3. VERIFICATION OF THE RECOMMENDED LUMINANCE

## 3.1 Verification Experiment

A verification experiment was conducted to see whether derived recommended luminance based on chromatic strength for colour lighting is utilized for actual lighting design. In detail, an experiment was conducted to see whether the object is equally conspicuous regardless of light colour when the object is illuminated with different coloured lights to the identical chromatic strength. The subjects included 6 males and females in their 20s to 40s with normal colour vision.
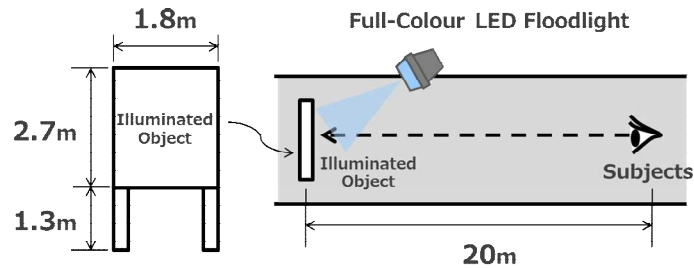


*Figure 5: Schematic diagram of verification experiment.*

The verification experiment was conducted on the factory campus passage at night. Firstly, a white wall sized to 2.7 m in length and 1.8 m in width was installed at the height of 1.3 m above the passage as an illuminated object as shown in Figure 5. And, the subjects were positioned 20 m away from the white wall. At this time, the viewing angle is $8°$ vertically $\times$ 5° horizontally. Next, using the full-colour LED floodlight used in the matching experiment, the white wall was alternately illuminated with white-colour light of correlated colour temperature 5,000 k (No. 0 in Figure 2) and coloured lights (Nos. 1, 3 to 5, 7 to 15, and 17 in Figure 2). The coloured lights used in the verification experiment were 14 colours optionally selected from all 17 kinds of coloured lights used in the matching experiment. When this is done, two patterns of lighting were performed; an equal-luminance lighting pattern to illuminate so that the overall luminance of the white wall will be 12 cd/m$^2$, and an equal-strength lighting pattern to illuminate so that the whole white wall will be $12/10^{f'}$ [cd/m$^2$] (the luminance of the white wall illuminated with white-colour light is same 12 cd/m$^2$). The subjects evaluated the impressions of all 14 colours in the two lighting patterns, respectively, using the 7-level evaluation scale (-3: Do not feel so strongly, -2: Do not feel so, -1: Do not rather feel so, 0: No opinion, 1: Rather feel so, 2: Feel so, 3: Feel so strongly), in response to the question, "Is the white wall illuminated with coloured light more conspicuous than when illuminated with white-colour light?"

## 3.2 Results and Discussion

Figure 6 shows the results of the verification experiment. The results are the average value of 6 subjects and shown in bar graphs with a standard error. In the equal-luminance lighting patterns in Figure 6, the evaluation results varied between -1 to 3 in all 14 colours. Particularly, the evaluation of No. 1 (red), No. 5 (green), No. 11 (blue) and No. 14 (purple) resulted in 2 or above. These results are generally consistent with those of the matching experiment. In the equal-strength lighting patterns on the other hand, the evaluation results concentrated between -1 to 1 in all colours except for No. 5 (green) in Figure 6. As

mentioned above, it was confirmed that if the object was illuminated to the identical chromatic strength, the object illuminated with white-colour light and coloured light respectively could be controlled to the same extent of conspicuousness. Because the white wall illuminated with No. 5 (green) coloured light is significantly more conspicuous than when illuminated with white-colour light, however, improvement of Formula (4) has to be also examined in the future. From a viewpoint of the characteristics of arranged illumination, however, it is presumed that illumination resulting in sufficient conspicuousness will not be a practical problem. Based on the above-mentioned results, the recommended luminance for colour lighting can be utilized for actual illumination design.
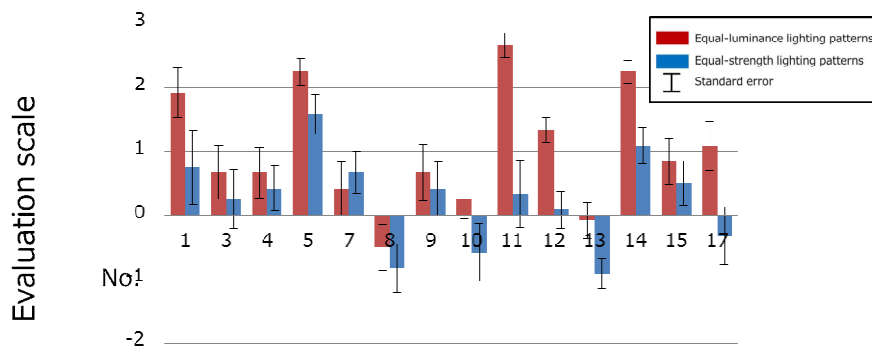


*Figure 6: Results of the impression evaluation.*

### 3. CONCLUSIONS

The matching experiment was conducted to obtain the luminance $L_C$ of the chromatic stimulus perceived as equal strength to the luminance $L_W$ of the white-color stimulus of the correlated colour temperature 5,000 K. Based on the obtained results of the $L_W/L_C$ ratios, the 3-level recommended luminance for colour lighting was derived as shown in Table 1. Since every colour has different chromatic strength, the recommended luminance for colour lighting is a variable to be calculated from the $u'v'$ chromaticity of the illuminated object. As shown in Figure 4, the blue colour region has the highest chromatic strength and the yellow colour region has the lowest. For this reason, the blue colour region is the lowest recommended luminance and the yellow colour region is the highest. It was verified whether the derived recommended luminance based on chromatic strength for colour lighting can be utilized for actual illumination design. The white wall was illuminated with 14 different colour light to evaluate its conspicuousness. As a result, the white wall illuminated with white-colour light and coloured light respectively could be controlled to the same extent of conspicuousness.

### REFERENCES

CIE 1993. *CIE 94 Guide for Floodlighting.*
Kaiser, P. K. 1986. Methods of heterochromatic brightness matching. *CIE J.* 5(2): 57-59.

*Address: Toru KITANO, Iwasaki Electric Co., Ltd., Bakurocho-daiichi Bldg. 2F, 1-4-16, Nihonbashi-bakurocho, Chuo-ku, Tokyo, 103-0002, JAPAN*
*E-mails: kitano-tooru@eye.co.jp, yamada-tetsuji@eye.co.jp, ooshima-kousuke@eye.co.jp*

# Influences to color constancy by wearing the optical dichromatic filter or the aged lens filter under static and rapidly-changed colored illuminations.

Mio HASHIDA,[1] Ippei NEGISHI,[2]  Keizo SHINOMORI,[2]
[1] Information Systems Engineering Course, Graduate School of Engineering, Kochi University of Technology
[2] School of Information, Kochi University of Technology

## ABSTRACT

Human beings have an ability to estimate an original color of an object regardless of color of a illumination, that is called as color constancy. There are many arguments about mechanisms of color constancy and it has not been confirmed yet. The color constancy also exists on red-green color deficient observers. Thus, in the process of investigating the mechanism, we tried to evaluate effects to color constancy by innate adaptation and learning in color deficiency and by the long-term adaptation in aging. We especially tried to estimate whether this evaluation could be made by measurement of the color constancy on a color normal observer wearing the functional filters; the optical dichromatic filter and the aged lens filter. The color normal observer wearing one of these filters would have simulated perception of dichromats or elder person, but he or she could not have the innate or long-term adaptation and learning.

We additionally used the rapidly-changed colored illumination to minimize the short-term adaptation (von Kries type of adaptation) in possible mechanisms of color constancy, especially at retina. Experimental conditions of this research would be the extreme case distorting the color constancy effect. By these reasons, this study would have the other purpose that we would be able to estimate the maximum difference of color constancy between dichromats, elderly people and young color-normal observers.

In this study, we performed two experiments. In Experiment 1, we performed categorical color naming by 11 basic colors for OSA Uniform Color Scales (558 chips) under one of illuminations; white, red and blue (about 17.5 cd/m$^2$) lights. The categorical color naming was made four times on one chip by three states; wearing no filter, the dichromatic filter, or the aged lens filter. In Experiment 2, we used 134 chips (at L=0 and L=1) under the rapidly-changed colored illuminations at 5 seconds interval and other conditions were identical with Experiment 1.

In Experiment 1, under the condition of wearing the dichromatic filter, we observed typical changes in the result of the categorical color naming that can be predicted by effects of the dichromat filter under each illuminant's colors and it means that we could not find any distortion of color constancy. Additionally, we found that almost no change in color constancy by wearing the aged lens filter, in the measurement by the categorical color naming. In Experiment 2, the result was almost the same with the result of Experiment 1. The accuracy of color constancy became worse, but tendency of color naming was almost the same between static and rapidly-changed colored illuminations.

The results of this study indicate that color constancy, at least as long as measured by the categorical color naming, is robust against the change of spectral distribution of

reflected lights from objects by filters and rapid change of illumination. It supports that color constancy strongly reflects the higher-order brain processing like estimation of illumination, rather than the simple short-term adaptation effect at retina.

# 1. INTRODUCTION

Color constancy is the phenomenon that we can still discern original color of object's surface even when the color of illumination light has been changed. Possible contributing factors for the color constancy are;

1.  Adaptation effect to cones and/or later processes (ex. von Kries type of adaptation)

2.  Illumination estimation and/or estimation of spectral reflectance of the object using visual environment of background (surroundings)

3.  Statistical estimation (Use of secondary statistics and/or Bayesian probability)

However, the mechanism of color constancy is still unclear though many researches have been conducted and many factors have been argued.

Previous study has been revealed that color constancy works on aged observers and color deficient observers, in limited conditions (Ma et al., AIC2012). We aimed to investigate color constancy of such observers, however, it was difficult to assemble sufficient number of them. Thus, we applied goggles with functional spectral filter simulating the color discrimination of dichromats or aged people to young people with normal color vision to measure color constancy. This method had the additional merit that the effect of long-term adaptation for congenital lack of one type of cones or age-related changes can be ignored. It would cause that the difference between normal and filter-simulated vision would reflect the worst and direct influences, meaning that the color constancy with these filters would help to reveal the mechanism of color constancy.

We additionally used the rapidly-changed colored illumination which changes illumination color in every 5 seconds in the order of Red-White-Blue-White- (or reversal order). Under this rapidly-changed colored illumination, we expected that the short-term adaptation (von Kries type of adaptation) in the possible mechanism of color constancy, especially at retina, would be minimized.

Overall, we expected that the experimental condition of this research would be the extreme case distorting the color constancy effect. By these reasons, this study would have the other purpose that we would be able to estimate the maximum difference of color constancy between dichromats, elderly people and young color-normal observers.

# 2. METHOD

## 2.1 Filters for experiments

One filter was the optical dichromatic filter, "Variantor (by Itoh Optical Industrial Co.)," which is the functional spectral filter simulating the color discrimination of dichromats for color normal observer. The other filter was the aged lens filter, "Simulation Filters of an Aged Human Lens (by Geomatec Co.)," simulating the age-related ocular lens density of 75 years old person for 32 years old observer. The color normal observer wearing one of

these filters would have pseudo-perception of dichromats or elder person, but he or she could not have the innate or long-term adaptation and learning.

## 2.2 Stimulus

We used three kinds of illumination lights (white, red and dark) of which luminance was set to the equal value (about 17.5 cd/m2) measured on a white calibration plate (CS-A5, Konica Minolta Co.Ltd.) placed on the 45-degree-angled stand in the booth. We measured luminance and the chromaticity coordinates of the illumination lights on the white calibration plate placed on the stand by luminance and color meter (CS-200, Konica Minolta Co.Ltd.).

- White; L=17.59 cd/m2, (x,y)=(0.317, 0.350)

- Red; L=17.39 cd/m2, (x,y)=(0.635, 0.349)

- Bue; L=17.23 cd/m2, (x,y)=(0.144, 0.069)

## 2.3 Subjects and apparatus

Subjects were four university students (two males and two females) of color normal. Color vision was evaluated by Ishihara color vision test, Standard Pseudoisochromatic Plates (SPP) and D-15 test.

The experiment was carried out in a stimulus presentation booth created by neutral color (gray) in the darkroom. We installed a LCD projector above the booth to make an arbitrary-colored illumination light and put the stand that was angled 45 degrees to place color chips in the booth. An experimenter sat next to the stimulus presentation booth and controlled the projector to change illumination light and recorded response of the color naming.

## 2.4 Experimental procedure

We conducted two experiments of categorical color naming in this research. In experiment 1, we performed categorical color naming by 11 basic colors (white, black, red, green, yellow, blue, brown, orange, purple, peach and gray) for Optical Society of America Uniform Color Scales (558 chips) under one of illuminations; white, red and blue (about 17.5 cd/m$^2$) lights. The categorical color naming was made four times on one chip by three states; wearing no filter, the dichromatic filter, or the aged lens filter. The color name and the number of the same color-name in 4 sessions were plotted on the coordinates of the OSA uniform color system (j-g axes). We performed this experiment for all combinations on each subject ; 558 color chips X 3 observation condition (without the filer, with the optical dichromatic filter and with the aged lens filter) X 4 sessions.

At first, the subject conducted the dark adaptation for 5 minutes in the dark room. Depending on the experimental condition, the subject wore the optical dichromatic fiter or the aged lens fiter. The experimenter turned on one kind of the illumination light from the CD projector, and the subject was adapted to the illumination light and the filter in 5 minutes. Then, the subject was asked to pick up one color chip and to place it on the stand (with black gloves). The subject performed the categorical color naming by 11 basic color terms.

In Experiment 2, we used 134 chips (at L=0 and L=1) of OSA Uniform Color Scales under the rapidly-changed colored illuminations at 5 seconds interval and the color naming was performed only when the illumination color was red or blue. Other conditions were identical with Experiment 1.

## 3. RESULTS AND DISCUSSION

### 3.1 Experiment 1

Figure 1 shows the normalized number of color chips using each color name. With no filter, blue illumination reduced green, yellow and red naming significantly. With the dichromatic filter, it tended to change response as reduction of the naming in pink, orange and yellow caused by the decrease of retinal illuminance and the less long wavelength component. With the aged lens filter, there was the reduction of green and orange naming under blue and red illumination, respectively.
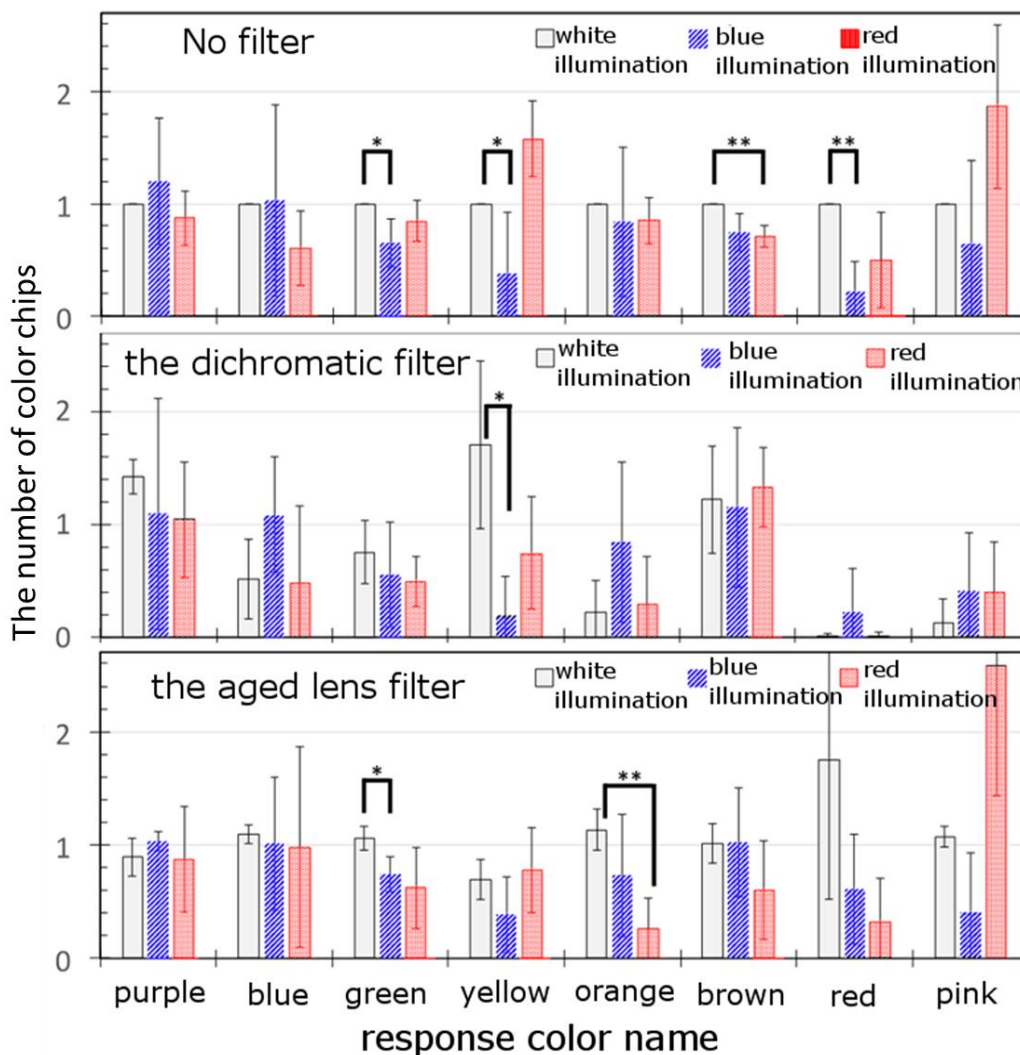


*Figure 1: The normalized color chips for each color response.*

AIC2015 TOKYO - Color and Image

In Experiment 1, under the condition of wearing the dichromatic filter, we observed typical changes in the result of the categorical color naming that could be predicted by effects of the dichromat filter under each illuminant's colors. No distortion of color constancy could be found. It means that the mechanism of color constancy should be composed by simple factors like color adaptation. Additionally, we found that almost no change in color constancy by wearing the aged lens filter, in the measurement by the categorical color naming.

## 3.2 Experiment 2

Figure 2 shows the number of color chips obtained the same (matched) response (using the same color name) between a certain illumination condition and white illumination.
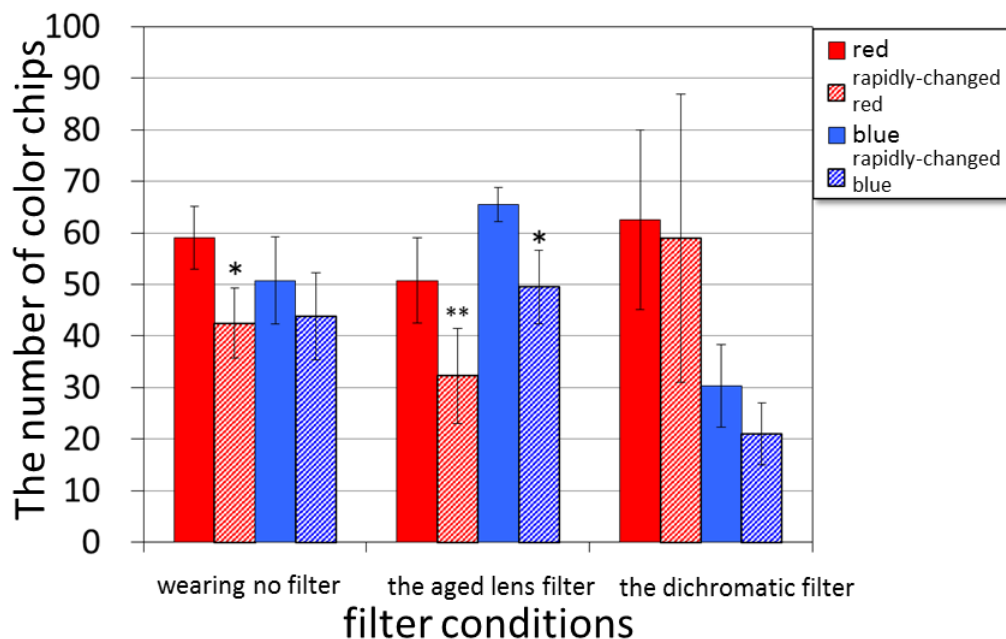


*Figure 2: The number is response of color was coincident with steady white illumination.*

In Experiment 2, the accuracy of color constancy became significantly worse with no filter and with aged lens filter conditions. The number of match response decreased when the rapidly-changed colored illuminations under red illumination in condition of wearing no filter and the aged lens filter. The effect of aged lens filter is minimum, observing the similar tendency in condition of wearing no filter and the aged lens filter. However, under the blue illumination, the result of the aged lens filter is more better than wearing no filter. Those reason is considered to the aged lens filter has property that decrease blue response a little.

On the other hand, this tendency was not much observed under the red illumination with the dichromatic filter. Although the number of match response was decreased overall when the illumination changes the rapidly-changed colored illuminations, but significant

decrease was not observed. It is considered that the property of the dichromatic filter which makes the reduced response of red.

However, tendency of the naming was almost identical even under such the rapidly-changed illuminations in all conditions compared to the static illumination. It means that adaptation of cone photoreceptor has to take only around 1 second, suggesting that the rapid processing obtained by learning, like spectral reflectivity estimation or statistical estimation, also contributes color constancy mechanism.

From the results of the experiments, two factors contribute to color constancy mechanism. One is early stage of visual processing like adaptation of cone photoreceptor or gain control of signal. The other is higher processing like spectral reflectivity estimation or statistical estimation. The reason why these factors contribute is still unclear and further researches are needed.

## 4. CONCLUSIONS

In Experiment 1, under the condition of wearing the dichromatic filter, we observed typical changes in the result of the categorical color naming that can be predicted by effects of the dichromat filter under each illuminant's colors and it means that we could not find any distortion of color constancy. Additionally, we found that almost no change in color constancy by wearing the aged lens filter, in the measurement by the categorical color naming. In Experiment 2, the result was almost the same with the result of Experiment 1. The accuracy of color constancy became worse, but the tendency of color naming was almost the same between static and rapidly-changed colored illuminations. From the results of the experiments, two factors contribute to color constancy mechanism. One is early stage of visual processing like adaptation of cone photoreceptor or gain control of signal. The other is higher processing like spectral reflectivity estimation or statistical estimation.

## REFERENCES

Ma, R., K. Kawamoto and K. Shinomori 2012. *Color constancy on red-green color deficient observers under illuminant change on confusion lines*, Conference Proceedings of AIC 2012 (T.R. Lee and J. Shyu eds.) 534-537.

*Address: Prof. Keizo SHINOMORI, School of Information, Kochi University of Technology, 185 Tosayamada-miyanokuchi, Kami-city, Kochi 782-8502, JAPAN*
*E-mails: 175083b@gs.kochi-tech.ac.jp, negishi.ippei@kochi-tech.ac.jp, shinomori.keizo@kochi-tech.ac.jp*

# Spectral functional filters for optical simulation of dichromats in color discrimination

Keizo SHINOMORI,[1] Kanae MIYAZAWA,[2] Shigeki NAKAUCHI[3]

[1] School of Information, Kochi University of Technology

[2] Itoh Optical Industrial Co., Ltd.

[3] Department of Computer Science and Engineering, Toyohashi University of Technology

## ABSTRACT

For dichromats, we should not use combinations of colors on such confusion lines for signs, indications, textbooks and other important notices. This concept was called as Color Universal Design. However, in many cases, it was not practical to measure all colors by a colorimeter, mostly because designers in color normal initially could not recognize problems in some color combinations. We though that if we would make the spectral functional filter to check the color combinations for dichromats, it would be more flexible, faster and easier to find initially-unexpected problems in color combinations.

Cone sensitivities of L- and M-cones, however, mostly overlap, and it was not possible to eliminate the stimulation of one type of cones by a spectral filter. Instead, we tried to simulate the ability of color discrimination defined by CIELAB color difference. We used 5745 modeled Munsell color chips under D65 illumination. The color difference was defined between each Munsell chip and the white starting point. In the next step, we assumed the spectrally band-pass filter which has two square-wave-shape peaks and three bottoms in its transmittance defined with 9 parameters. To simulate dichromat's color discrimination, from the spectral reflectance, we calculated LMS cone stimulations. We used the assumption that L- and M-cone stimulations always equal zero for protanope and deuteranope, respectively. Then, the tri-stimulus values were reversely calculated and we compared the CIELAB color differences between modeled protanope and deuteranope and each filter. The best filter was selected to minimize the "error" by changing 9 filter parameters under Genetic Algorithm. We successfully have made three kinds of the dichromatic filters even for commercial products ("Variantor" by Itoh Optical Industrial Co.); universal (U) type, protan (P) type and deutan (D) type. The U-type of the filter was designed to select worse case between P- and D-types in terms of color discrimination.

These filters were evaluated by Ishihara-plate, Standard Pseudoisochromatic Plates (SPP), D-15 and 100-hue test. As planned, results of SPP and 100-hue tests indicated that color normal observers wearing P- and D-type filters were evaluated as protanope and deuteranope, respectively, although the result of D-15 indicated that D-type filter were not significantly different with the result of no filter. The results with the universal filter indicated mixture and/or middle of protanope and deuteranope.

## 1. INTRODUCTION

Human has three types of photoreceptors called as cones. When we see objects in a bright environment, cones are used in visual dection processing. However, some people, classified as dichromats, do not congenitally have one type of cones and color discrimination using only that cone is theoretically impossible. Protanope and deuteranope do not have functioning L- and M-cones at retina, respectively, and additionally, it has been thought that they have no Red-Green opponency. Although there are some arguments

of color perception of dichromats, especially about perception of red and green, it has been well accepted that dichromats cannot discriminate colors on confusion lines in chromatic coordinates, corresponding the lost type of cones.

For the Color Universal Design. However, in many cases, it was not practical to measure all colors by a colorimeter, mostly because designers in color normal initially could not recognize problems in some color combinations. It was more practical to take digital pictures of scenes and to present them in modified colors converted by special software like UDing Simulator (TOYO INK). We made the spectral functional filter to check the color combinations for dichromats and it would be more flexible, faster and easier to find initially-unexpected problems in color combinations.

## 2. METHOD

### 2.1 Plan for spectral functional filters

Cone sensitivities of L- and M-cones, however, mostly overlap, and it was not possible to eliminate the stimulation of one type of cones by a spectral filter. Cone sensitivities of L- and M-cones, however, mostly overlap, and it was not possible to eliminate the stimulation of one type of cones by a spectral filter.

Instead, we tried to simulate the ability of color discrimination defined by CIELAB color difference. For that purpose, firstly, we defined the color set for evaluation. We used 5745-modeled Munsell color chips under D65 illumination. The modeled reflectance of each Munsell chip consisted of the offset reflectance function (as the average of 1239 Munsell chips) and three fundamental reflectance functions (obtained by principle component analysis) multiplied by three independent parameters for each chip. Here, we set the luminance factor Y to make $Y/Y_0$ equaled 0.1, meaning that Munsell Value was approximately 3.8. The color difference was defined between each Munsell chip and the neutral chip (N/3.8).

In the next step, we assumed the spectrally band-pass filter which has two square-wave-shape peaks and three bottoms in its transmittance. This spectral band-pass filter was defined with 9 parameters; two parameters for the transmittance of two square-wave-shape peaks, three parameters for the transmittance of three buttoms and four parameters for the boarder wavelengths of two square-wave-shape peaks. Filter effects were simply obtained by using the filter transmittance. To simulate dichromat's color discrimination, from the spectral reflectance, we calculated each Munsell chip's XYZ tri-stimulus values with CIE 1931 color matching function (Wyszecki and Stiles 1982) and obtained LMS cone stimulations by Smith-Pokony cone fundamentals (Smith and Pokorny 1975). We used the assumption that L- and M-cone stimulations always equal zero for protanope and deuteranope, respectively. Then, the tri-stimulus values were reversely calculated from LMS stimulations and used for color difference calculation. Finally, we compared the CIELAB color differences between modeled protanope and deuteranope. Figure 1 shows the CIELAB color difference of the 5745 modeled Munsell color chips under D65 illumination for color normal (Left panel), the modeled protanope (Center panel) and deuteranope (Right panel). Using these steps, the CIELAB color differences of each spectrally band-pass filter were also calculated. The best filters, defined as the best match to the color differences of thoretical protanope and deuteranope as shown in Figure 1, were selected to minimize the "error" by changing 9 filter parameters under Genetic Algorithm.
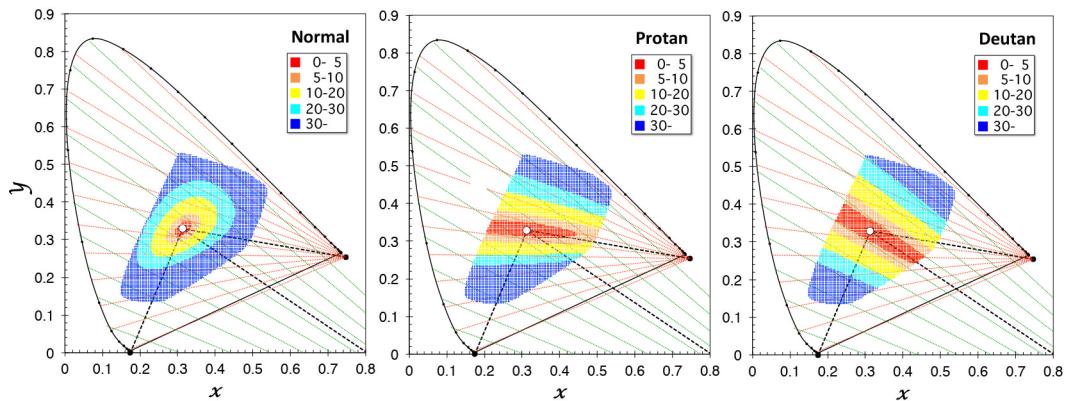
*Figure 1: CIELAB color difference of modeled Munsell chips for color normal, modeled protanope and deuteranope.*

For the purpose of the Color Universal Design. it can be more convenient to wear only one type of the spectral filter continuously. Thus, we defined "universal" type of dichromats as simulating worse color discrimination between protanope and deuteranope. In practical calculation, in the universal (U) type, color differences were defined as the worse value of theoretical protanopic and deuteranopic observers. Figure 2 shows the CIELAB color difference of the modeled Munsell color chips under D65 illumination with theoretically best protan (Left panel), deutan (Center panel) and universal filters (right panel). As expected, even the U-type of the filter was designed to select worse case between the P- and D-types in terms of color discrimination, the theoretical color differences was the about the middle of the P- and D-types because of the limitation of the filter transmittance with 9 parameters.
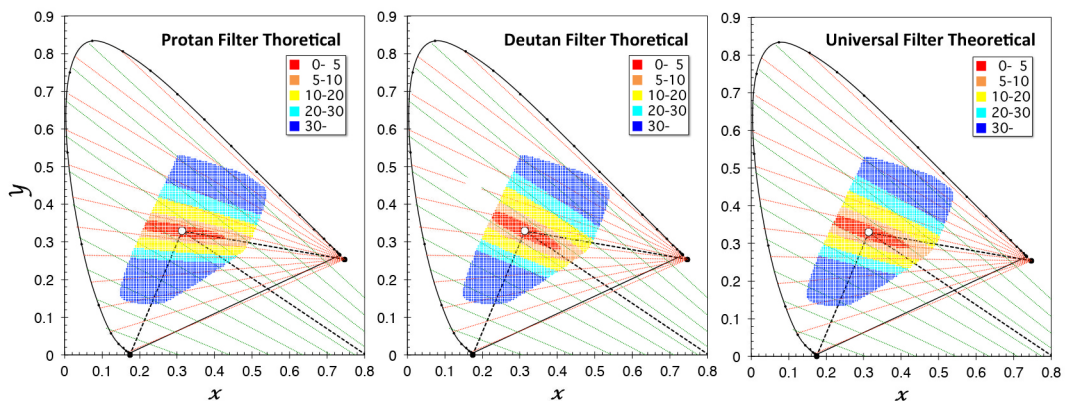


*Figure 2: CIELAB color difference of modeled Munsell chips with theoretically best protan, deutan and universal filter.*

We successfully have made three kinds of the dichromatic filters even for commercial products ("Variantor" by Itoh Optical Industrial Co.); universal (U) type, protan (P) type and deutan (D) type.

## 2.2 Evaluation of filters by traditional color tests

These filters were evaluated by traditional color vision tests; Ishihara-plate (38 plates edition), Standard Pseudoisochromatic Plates (SPP), D-15, Farnsworth-Munsell 100-hue test (FM 100-hue test) and 100 hue test (ND100) (Japan Color Enterprise Co.,Ltd.). ND100 is the new type of 100 hue test developed to measure more precise color discrimination with 100 color caps instead of 85 caps in FM 100 hue-test. In this sudy, only the result of FM100 would be presented. All color tests were performed in the light

booth (Macbeth Jadge II, x-rite Co.,Ltd.) under one Day-light (6500K) fluorescent lamp. The illuminance of the buttom of the booth was about 660 lux.

Fifteen observers (11 male and 4 female) in age from 20 to 22 years participated in Ishihara, SPP and D-15 tests. Six observers (4 amle and 2 female) from them also participated in FM 100 hue test and additional nine observers (3 male and 6 female) in age from 22 to 51 years participated to FM100. Two of additional observers in FM 100 hue-test were authors. All tests were performed by one eye which was selected by the observer.

## 3. RESULTS AND DISCUSSION

### 3.1 Evaluation of filters in terms of classification as dichromats

Test error scores of each color vision test were used to evaluate the ability of simulating color discrimination on dichromats by filters. The observer's test error score wearing each filter was obtained and compared to criteria of color vision test to classify dichromats. Figure 3 shows test error scores as the average of 15 observers for each color test with each filter type including with no filter condition. Error bars denote doubled standard error of the mean (2S.E.M.). In Figure 3, only not-statistically-significant difference was denoted by lines and n.s. and all other differences were statistically-significant (p <0.01).
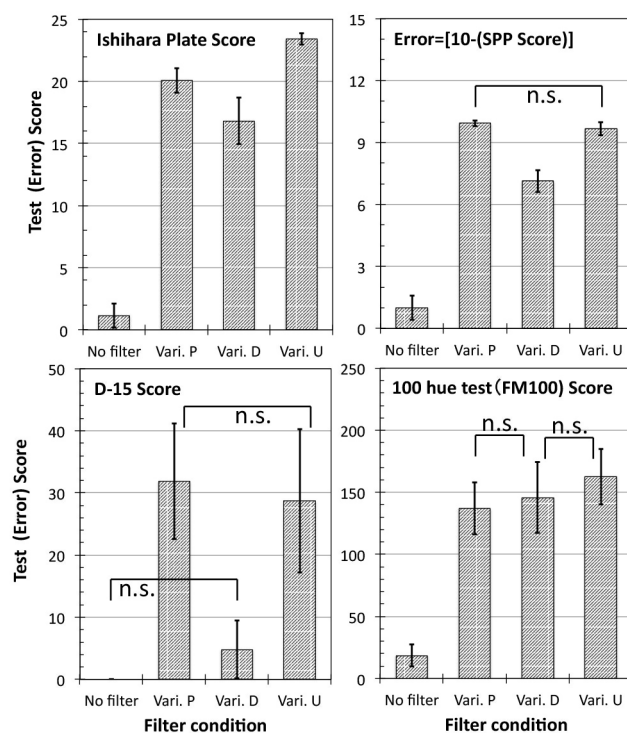


*Figure 3: Test error scores in Ishihara-plate, SPP, D-15 and FM 100 hue test.*

In the Ishihara plate test, one failed or unexpected recognition of a numeric number is counted as one error score and the worst score is 25. The criterion to doubt color deficiency on the observer is 4. All filters' error scores were enough high to judge as dichromats. In the SPP test, one correct answer is counted as one point and criterion of color vision normal is (more than) 8 points. For clarify of comparison with other tests, we calculated the test error score as [10 − SPP score], meaning that the error score more than 2 suggests dichromats. Again, all filters' error scores were enough high as dichromats. In both test, the score was significantly lower with the D-type filter compared to other filters.

In the D-15 test, test error score with D-type filter was not significantly different with the error score with no filter, meaning that D-type is simulating a weak dichromats or anomalous trichromats rather than strong dichromats. This result can be explained as the limitation of the spectral functional filter. As shown in Figure 1, assumption of the absence of M-cone response on deuteranope will make much less color difference compared to protanopes.  However, the spectral functional filter can make almost the same color difference between P-, D- and U-types of filters, causing that D-type filter effect can be recognized as "weak deuteranopic" compared to a real deuteranope.

Contrary, in the FM 100-hue test, there was no significant difference between P- and D-type filters.  The criterion of the FM 100-hue test estimated by Verriest et al. (1982) was 6.41±2.41(SD) as the average of left and right eyes in the age group of 20-29 years old. Error scores of all filters were significantly higher than the criterion.

## 3.2 Evaluation of filters in terms of protan/deutan classification

We also evaluated whether P- and D-type filters would be able to be classified as protanopic and deuteranopic observers, respectively, by the color tests. Ishihara-plate (38 plates edition) has 4 plates for protan/deutan classification (No.22-25). With P-type filter, correctly classification (one numeral seen) was 3.20 (80.0%) when the maximum is 4 and no classification (no numeral seen) was 0.47 (11.7%).  With U-type filter, the result was close to the P-type filter. Correctly classification was 3.40 (85.0%) and no classification (no numeral seen) was 0.47 (11.7%).

Contrary, with D-type filter, correctly classification was 0.13 (3.3%) and no classification was 0.07 (1.7%). In other cases, observers could see both numbers correctly. The result of the previous literature (Birch 1997) indicating that the protan/deutan classification plates were more effective for deuteranope than for protanopes. However, it was obtained by Birch's method (1997) in which one number, which was more clearer or brighter than the other, was selected as one number. Thus, this study's result of seeing both numbers was not strange and NOT meaning the failure of the D-type filter classification. Because we did not take this method for Ishihara protan/deutan classification plates, alternative measurement should be performed for the further study.

Distributions of errors in FM 100-hue test has also been used for protan/deutan classification (Fransworth 1943).  We refered protan (17 and 64), deutan(15 and 58) and tritan (5 and 46) axes used in FM 100-hue test scoring tool (v.3.0, Munsell Color Services Lab.). Figure 4 shows distribution of mean errors from 15 observers with filters. The P- and D-type filters were different and the U-type filter was mixture and/or middle of P- and D-type filters. One difference in the distribution between filters and dichromats should be mentioned that the distributions of filters were not showing high peak of errors at certain number of 100-hue test as frequently observed in dichromats (Fransworth 1943; Kinnear 1970). We expect that because the filters are not making confusion lines, which are caused by loosing signals from one type of cones, but making color discriminations more difficult, the errors distributed in many directions not a few directions.

## 4. CONCLUSIONS

By the idea of simulating the ability of color discrimination defined by CIELAB color difference, we successfully have made three kinds of the dichromatic filters even for commercial products ("Variantor" by Itoh Optical Industrial Co.); universal (U) type,

protan (P) type and deutan (D) type. These filters were evaluated by Ishihara-plate, Standard Pseudoisochromatic Plates (SPP), D-15 and 100-hue test. As planned, results of SPP and 100-hue tests indicated that color normal observers wearing P- and D-types filters were evaluated as protanope and deuteranope, respectively, although the result of D-15 indicated that D-type filter were not significantly different with the result of no filter. The results with the universal filter indicated mixture and/or middle of protanope and deuteranope.
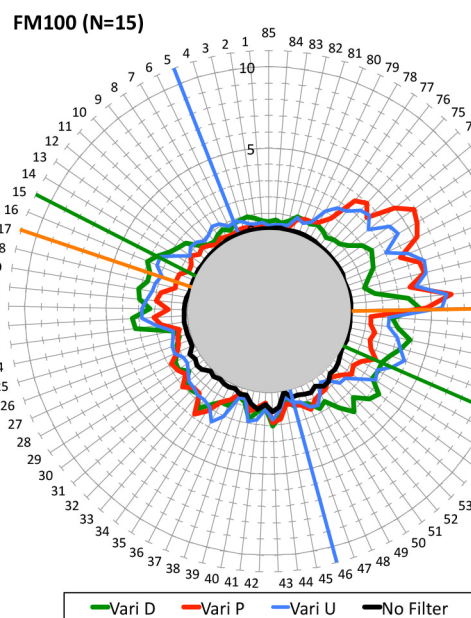


*Figure 4: Distribution of mean errors from 15 observers with filters.*

## ACKNOWLEDGEMENTS

## REFERENCES

Birch, J. 1997. *Efficiency of the Ishihara test for identifying red-green colour deficiency*, Ophthalmic and Physiological Optics, 17(5), 403-408.

Fransworth, D. 1943. *The Farnsworth-Munsell 100-hue and dichotomous tests for color vision*, Journal of the Optical Society of America 33(10), 568-578.

Kinnear, P.R. 1970. *Proposals for scoring and assessing the 100-hue test*, Vision Research 10, 423-433.

Smith, V.C. and J. Pokorny 1975. *Spectral sensitivity of the foveal cone photopigments between 400 and 500 nm*, Vision Research 15(2), 161-171.

Smith, V. C., J. Pokorny and T. Yeh 1993. *The Farnsworth-Munsell 100-hue test in cone excitation space,* Colour Vision Deficiencies XI (pp. 281-291). Springer Netherlands.

Verriest, G., J. van Laethem and A. Uvijls 1982. *A new assessment of the normal ranges of the Fransworth-Munsell 100-hue test scores*, American Journal of Ophthalmology 93 635-642.

Wyszecki, G. and W.S. Stiles 1982. *Color Science: Concepts and Methods, Quantitative Data and Formulae*. Hoboken: John Wiley and Sons.

*Address: Prof. Keizo SHINOMORI, School of Information, Kochi University of Technology, 185 Tosayamada-miyanokuchi, Kami-city, Kochi 782-8502, JAPAN*
*E-mails: shinomori.keizo@kochi-tech.ac.jp, k-miyazawa@itohopt.co.jp, nakauchi@tut.jp*

# What are Memory Colors for Color Deficient Persons ?

Jia-Wun Jian[1], Hung-Shing Chen[2] and Ronnier Luo[3]

[1]Graduate Institute of Color and Illumination Technology, National Taiwan University of Science and Technology, Taiwan

[2]Graduate Institute of Engineering, National Taiwan University of Science and Technology, Taiwan

[3]Department of Colour Science, University of Leeds, UK

## ABSTRACT

Color-deficient persons are unable to discriminate some specific colors and hence have great difficulties in their lives. The mechanism of memory color for color vision defect is less clear until now. The aim of this study is to realize what are perceived colors on the familiar objects for people with color vision deficiency (CVD), and buildup the rating database of memory color for color-deficient persons. The rating data was analyzed by modified bivariate Gaussian function. the high memorized area of normal color vision forms a smaller rating ellipses on CIE $u'_{10}v'_{10}$ chromaticity diagram, however the results of CVD would form different degrees of memory-color rating ellipses. By analyzing the rating results of memory colors for the chosen familiar objects, it is possible to determine the severity of CVD for a subject according to the distribution of the memory-color rating ellipses.

## 1. INTRODUCTION

Color vision deficiency (CVD) is a common functional defect. There are around 8% male and 0.2% female suffering from color vision deficiency in the world [1]. People with abnormal color vision are unable to discriminate some specific colors and hence suffering in their lives. Because cone cells are absent or the peak of sensitivity is shifted, people with CVD cannot sense some specific colors as the people with normal color vision [2].

Memory color can be categorized into short-term or long-term, depending on the delay between adaptation and reproduction [3]. In order to investigated the memory color effect for color vision deficiency, total 13 kinds of test images used in the experiment include the following familiar objects: apple (two types of red and yellow), lemon (two types of yellow and green), banana (yellow), orange (orange), tomato (red), leaf (green), sky (blue), strawberry (red), Asian skin (Asian facial skin) and cauliflower (milk white). All of the test objects are arranged in Table 1.

*Table 1. The test familiar objects*

| Name | (a) Banana | (b) Orange | (c) Yellow Lemon | (d) Cauliflower | (e) Asian Skin |
|------|------------|------------|------------------|-----------------|----------------|
| Image | | | | | |
| Name | (f) Strawberry | (g) Sky | (h) Tomato | (i) Green Leaf | (j) Green Lemon |
| Image | | | | | |
| Name | (k) Blueberry | (l) Yellow Apple | (m) Red apple | | |
| Image | | | | | |

## 2. METHOD

In this study, two kind of experiments were designed: CVD's memory color rating distributions of 13 familar objects were investagted (Exp-1) and their rating results were compared with normal color vision obsevers (Exp-2). A well-calibrated monitor (sRGB) was used to display the test images of familiar objects, and the visual assessment experiment was conducted in a dark room to find the degrees of the CVDs' memroy color.

### 2.1 CVD subjects

Eight subjects with deutan color vison were invited to join the experiment. As listed in Table 2, two of them are deuteranomaly (mild deutan; Sub.3 and Sub.8), and the other eight subjects are deuteranopia (strong deutan). All of the subjects are male and Taiwan-Tech college students. Subjects were asked to conduct two color vision tests to verify their degrees and types of color vision deficiency with Anomaloskope and Ishihara plate. All of the color vision tests were carried out twice, where "1$^{st}$" and "2$^{nd}$" in the table represent the diagnosing result of the 1$^{st}$ and 2$^{nd}$ time respectively.

*Table 2. Color vision diagnosing results of all subjects*

| Subject | Anormaloskope (1$^{st}$ / 2$^{nd}$) | Ishihara plate (1$^{st}$ / 2$^{nd}$) |
|---------|-------------------------------------|--------------------------------------|
| Sub.1 | Strong D / Strong D | Strong D / Strong D |
| Sub.2 | Strong D / Strong D | Strong D / Strong D |
| *Sub.3 | Strong D / Strong D | Mild D / Mild D |
| Sub.4 | Strong D / Strong D | Strong D / Strong D |
| Sub.5 | Strong D / Strong D | Strong D / Strong D |
| Sub.6 | Strong D / Strong D | Strong D / Strong D |
| Sub.7 | Strong D / Strong D | Strong D / Strong D |
| *Sub.8 | Normal / Normal | Strong D / Strong D |

## 2.2 Experimental Procedure

Before memory color rating experiment, subjects were asked to stay in the dark room for 1 minute, then the staff would turn on the program and select one of test image, each image was rendered into a large numbers (150~200) of different color objects, while keeping the luminance near constant (Fig. 1). According to each subject's mental capacity, score with the range between +1 and -1 was given whether the image colors were matched the subject memory or not. After finishing all memory color rating tests, the experiment rating results were further modelled by modified bivariate Gaussian function $R$ (Eq. (1)) [4, 5],
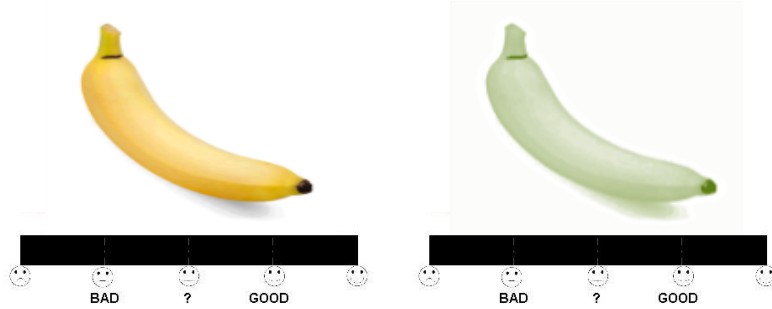


*Figure 1: Two examples of rendered different object colors.*

$$d\left(u'_{10}, v'_{10}\right) = \left\{\left[\begin{pmatrix} u'_{10} \\ v'_{10} \end{pmatrix} - \begin{pmatrix} a_3 \\ a_4 \end{pmatrix}\right]^T \begin{bmatrix} a_1 & a_5 \\ a_5 & a_2 \end{bmatrix}\left[\begin{pmatrix} u'_{10} \\ v'_{10} \end{pmatrix} - \begin{pmatrix} a_3 \\ a_4 \end{pmatrix}\right]\right\}^{\frac{1}{2}}$$

$$R\left(u'_{10}, v'_{10}\right) = a_7 + a_6 \cdot e^{-\frac{1}{2}d\left(u'_{10}, v'_{10}\right)^2}$$

(1)

where (u'$_{10}$, v'$_{10}$) means the use of CIE 1964 (10 degrees) Color Matching Functions in the calculation of u' v' chromaticity coordinate. The $d$(u'$_{10}$, v'$_{10}$) and $R$(u'$_{10}$, v'$_{10}$) are Mahalanobis distance and memory color rating at the (u'$_{10}$, v'$_{10}$) chromaticity coordinate respectively. Parameters a$_1$, a$_2$,.., and a$_7$ are the constants determined the observed data. The experiment flowchart is shown in Figure 2.
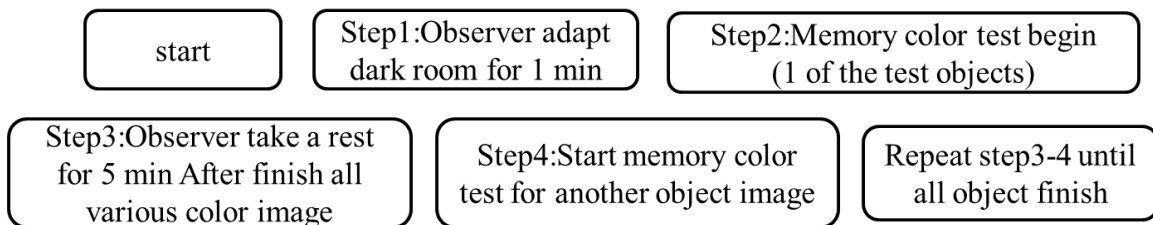


*Figure 2: Flowchart illustrating the sample process.*

# 3. RESULTS AND DISCUSSION

In Experiment 1, we collected the highest score data of all subjects, then draw the memory color rating distribution map of the mean values on CIE $u'_{10}v'_{10}$ chromaticity diagram. By plotting memory color rating distribution map, we could figure out what are memory colors of the people with deutan color vision perceived colors for the 13 familiar objects. Deutan memory color rating distribution map of mean values of all subjects are shown in Figure 2. In additions, Figure 3 shows the mean scores and all subject's highest scores plotted on $u'_{10}v'_{10}$ chromaticity diagram.

When analysing the experiment data, we used the Root Mean Square Deviation (RMSD) to calculate Inter- and Intra-observer variability. Intraobserver variability is each observer's first test and second test result data variation. And Interobserver variability is the difference between each test data and the average data, and the results of Inter- and Intra-observer variability are shown in Table 3. Besides, the color variations ($\Delta E^{*}_{u'10v'10}$) were calculated between individual $u'_{10}v'_{10}$ values and mean $u'_{10}v'_{10}$ values in Figure 3, and the result is shown in Table 4.
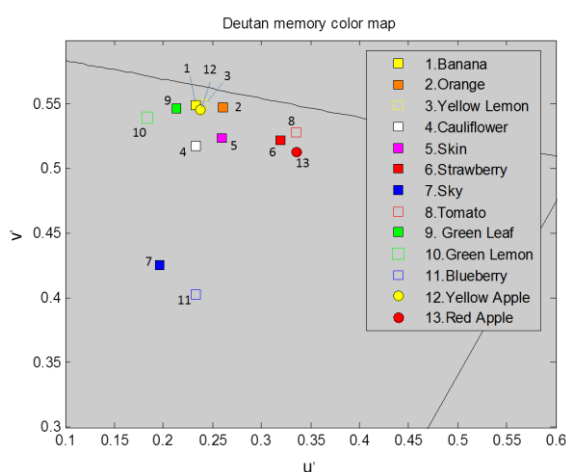


*Figure 3. Deutan memory color rating map of the 13 familiar objects in terms of mean data of the highest scores.*
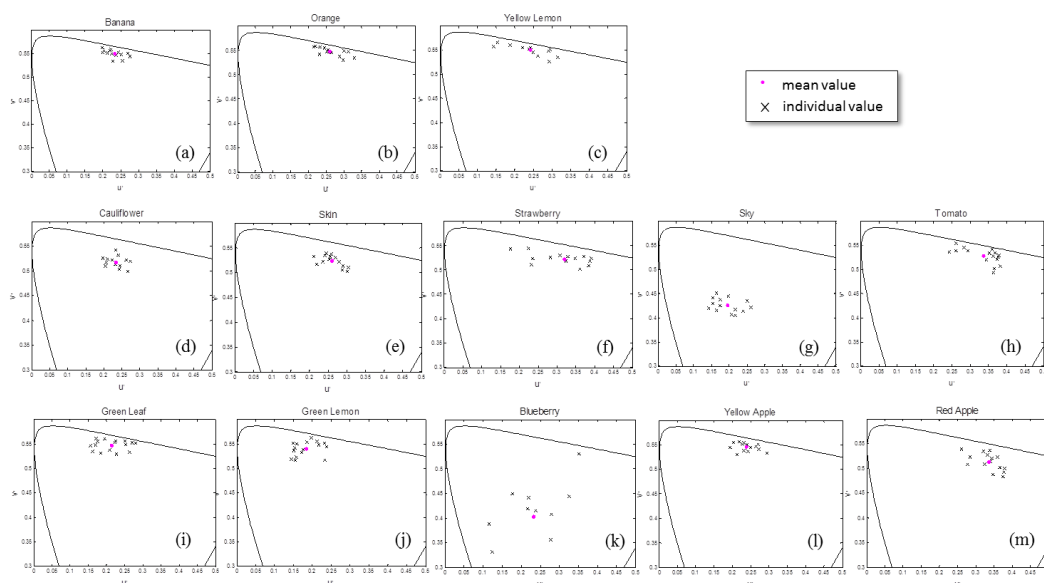
*Table 3 Inter- and Intra-observer variability of the rating data (for 13 familiar objects).*

| No. | 1 | 2 | 3 | 4 | 5 | 6 | 7 |
|---|---|---|---|---|---|---|---|
| Object | banana | Orange | Yellow Lemon | Cauliflower | Asian Skin | Strawberry | Sky |
| Inter-observer | 0.399 | 0.400 | 0.424 | 0.482 | 0.473 | 0.415 | 0.416 |
| Intra-observer | 0.456 | 0.448 | 0.476 | 0.435 | 0.476 | 0.353 | 0.415 |
| No. | 8 | 9 | 10 | 11 | 12 | 13 | |
| Object | Tomato | Green Leaf | Green Lemon | Blueberry | Yellow Apple | Red Apple | |
| Inter-observer | 0.425 | 0.531 | 0.576 | 0.485 | 0.462 | 0.496 | |
| Intra-observer | 0.475 | 0.561 | 0.662 | 0.453 | 0.526 | 0.473 | |

*Table 4 Color varivations $\Delta E^{*}_{u10v10}$ between individual u'$_{10}$v'$_{10}$ data and mean u'$_{10}$v'$_{10}$ data (for 13 familiar objects).*

| No. | 1 | 2 | 3 | 4 | 5 | 6 | 7 |
|---|---|---|---|---|---|---|---|
| Object | banana | Orange | Yellow Lemon | Cauliflower | Asian Skin | Strawberry | Sky |
| Color variation | 0.023 | 0.030 | 0.035 | 0.021 | 0.025 | 0.058 | 0.036 |
| No. | 8 | 9 | 10 | 11 | 12 | 13 | |
| Object | Tomato | Green Leaf | Green Lemon | Blueberry | Yellow Apple | Red Apple | |
| Color variation | 0.045 | 0.038 | 0.033 | 0.074 | 0.023 | 0.033 | |

In Experiment 2, we compare the memory color rating results between normal color visons and 2 degrees of deutan color visions (mild deutans and strong deutans). The test images for comparsion include 5 kinds of common familiar objects, which are strawbey, tomato, Asian skin, orange and banana. we anylized the rating scores of memory colors by modified bivariate Gaussian function, and draw the score distrubution ellepes on u'$_{10}$v'$_{10}$ chromaticity diagram, where the rating scores of normal color visons were retrieved from our earlier corrected memory color data (total 18 subjects; 12 males and 8 females; 2014), and their u'$_{10}$v'$_{10}$ rating ellipses based on score 0.0 and score 0.3 are shown in Figure 4.

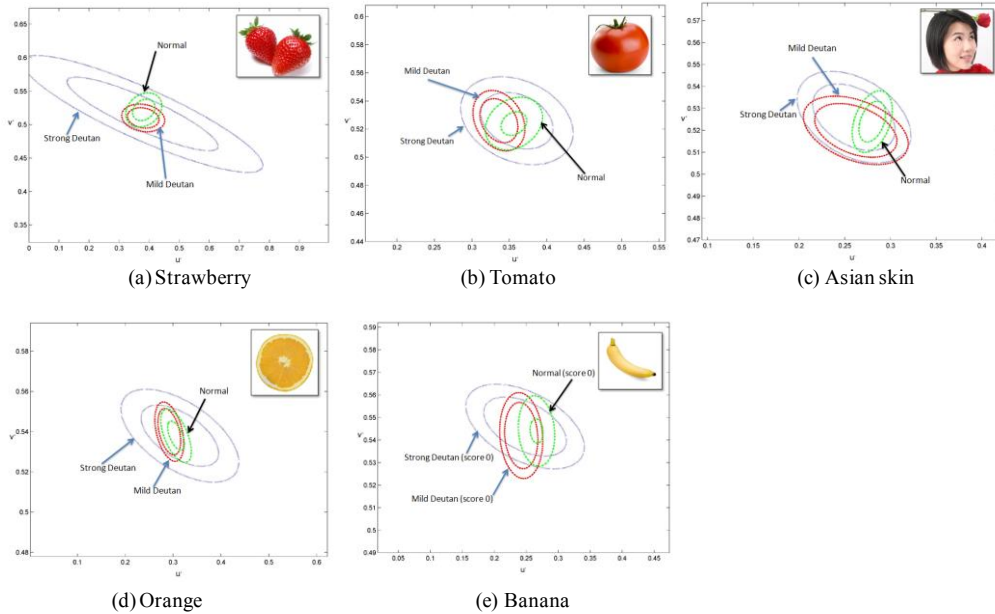(a) Strawberry     (b) Tomato     (c) Asian skin

(d) Orange     (e) Banana

*Figure 4. Memory color rating comparisons between normal color vision and deutan color vision, where outer and inner green/ red/ blue ellipses represent the rating boundaries of normal/ mild/ strong color visions corresponding to score 0.0 and score 0.3 respectively.*

## 4. CONCLUSIONS

In this study, memory color rating distribution map based on mild/ strong deutan color visions was investigated. The memory color rating results between normal color vison and deutan color visions (mild deutans and strong deutans) were compared. The modified bivariate Gaussian function was applied to form memory color rating ellipses of deutan color visions on $u'_{10}v'_{10}$ chromaticity diagram. The degrees of deutn color vision show stronger when the sizes of rating ellipses show bigger. This study could help us realize more about color vision mechanism between color vison deficieny and normal color vision. We hope this analysical results are beneficial to color vision deficiency's research. Our future works hope to add more subjects with different severities and color vision types to clarify memory color mechanism of abnormal color visions.

## REFERENCES

[1] A. Stockman, D. I. A. MacLeod, and N. E. Johnson , "Spectral sensitivities of the human cones," Journal of the Optical Society of America A, vol.10 (1993).

[2] P. Bodrogi, T. Tarczali, "Colour memory for various sky, skin, and plant colours: effect of the image context," Color Research & Application 26.4: 278-289 (2001).

[3] Rigmor C. Baraas, "Color Constancy of Red-Green Dichromats and Anomalous Trichromats," Visual Psychophysics and Physiological Optics. Vol. 51, No.4, pp. 2286-2293 (2010).

[4] Smet KA, Ryckaert WR, Pointer MR, Deconinck G, Hanselaer P, "Memory colours and colour quality evaluation of conventional and solid-state lamps," Opt Express (25): 26229-44 (2010).

[5] Kevin A.G. Smet, Yandan Lin, Balázs V. Nagy, Zoltan Németh, Gloria L. Duque-Chica,

Jesús M. Quintero, Hung-Shing Chen, Ronnier M. Luo, Mahdi Safi, and Peter Hanselaer, "Cross-cultural variation of memory colors of familiar objects," Optics Express, Vol. 22, Issue 26, pp. 32308-32328 (2014).

Postal address: 43, Keelung Road, Section 4, Taipei, Taiwan
E-mails: m10325005@mail.ntust.edu.tw, bridge@mail.ntust.edu.tw, m.r.luo@Leeds.ac.uk

# Establishment of a Model Colour Palette for Colour Universal Design

Kei ITO [1], TomomiTAKESHITA [2], Fumiko G OTO [2], Masafumi NISHIGAKI [2],
Teruo KOBAYASHI [3], MitsumasaHASHIMOTO [3], Yosuke TANAKA [4], Koichi IGA [4],
Shunsuke WATANABE [4], Koki OKAGAWA [4], Mitsuyoshi MAEKAWA [5]

[1] Institute of Molecular and Cellular Biosciences, University of Tokyo
[2] DIC Corporation (DIC Graphics Corporation, DICColour  Design, Inc.)
[3] Japan Paint Manufacturers Association (JPMA)
[4] NPO Colour Universal Design Organization
[5] Industrial Research Institute of Ishikawa

## ABSTRACT

Colour Universal Design (CUD) is a user-oriented design system to allow information to be conveyed accurately to people with diverse types of colour vision. Because of genetic variations or eye diseases, some people cannot easily distinguish certain combinations of colours. However, it is not practical to avoid all such combinations when painting graphic objects that require multiple colours, such as public signs, graphs and drawings, maps, and web pages. An alternative approach is to adjust the hue, saturation or brightness of each colour to maximise mutual separation. To achieve this, we organised a collaborative pr oject to establish a palette of least confusing colours with precisely defined colour values. We first asked people with common-type (normal) colour vision to classify several thousands of colour chips into groups of colour categories. We then asked colour-blind people to examine these chips and discard those that appear confusing. We finally asked colour-blind and low-vision people to examine and adjust the remaining colours to establish a set of colours that are most distinguishable from each other, and obtained a palette of 20 colours: nine vivid colours suitable for small objects such as signs, graphs  and characters, seven relatively pale colours for painting large objectssuch as maps and backgrounds , and four shades of achromatic colours that are least confusing with chromatic ones. Considering that colour-coded information in real life is presentedin three ways–painting, process colour printing and display panels– we fine-tuned colours and made suggested colour definitions in Munsell values, CMYK values with industry-standard profiles, and RGB values in sRGB colour space. The palette is being usedin a wide variety of pro ducts.

## 1. INTRODUCTION

About 8-10 % ofC aucasoid males and 4% of Asian males, as well as one in several hundreds of females are so called red-green colour-blind, who cannot discriminate certain combination of colours even if they are clearly distinguishable by the people with common-type colour vision. Depending on the problematic cone cells in the retina, they are classified as protan (problem in L cones) and deutan (problem in M cones). In addition, some of the people who suffer from low-vision also have difficulty in distinguish colours, because S cone cells, which accounts for only a few percent of the retinal cells, tend to disappear first by retinal diseases, causing tritan-like color vision.

The fact that colour-blind and low-vision people cannot distinguish certain colours does not necessarily mean that they cannot distinguish all the tones of colours in that category. The colours that are hard to distinguish by these people tend to lie on straight lines called

AIC2015 TOKYO - Color and Image

confusion lines on CIE xy charts (Pitt 1935, Figure 1). The colours appear much less confusing if they do not lie on the same confusion line. This is most exemplified by traffic lights. Even though colour-blind people have difficulty distinguishing red and green, few of them have problems with traffic lights, because red is deliberately shifted to yellowish and green to bluish colours, avoiding the combination that lie on a single confusion line.
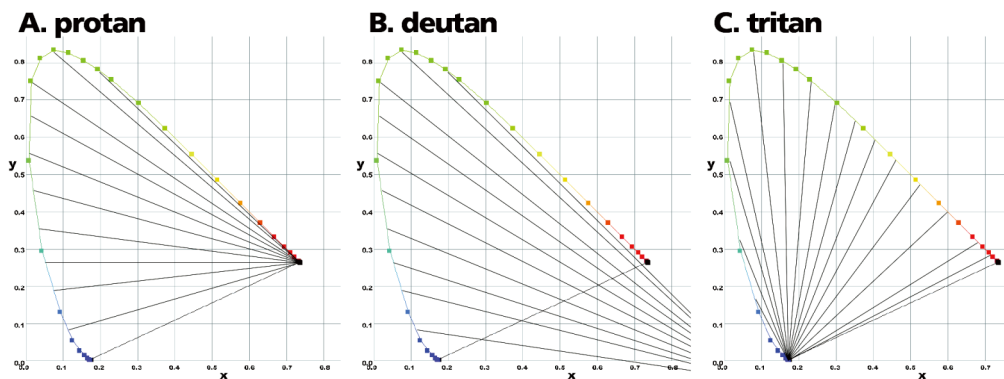


*Figure 1: Confusion lines of the three major types of colour blindness.*

Such fine-tuning of colours is a potentially promising way to provide information in many colours while keeping accessibility to diverse people. Although convenient algorithms for detecting potentially confusing colours have been established (Brettel et al. 1997) and are now implemented in popular graphic software such as Illustrator and Photoshop, fine-tuning of colours is not easy for designers who usually have only limited knowledge about the characteristics of various colour vision types.

For designers it should be most convenient, if they can have a palette of colours that are already fine-tuned for maximum distinction. To this aim we organised a collaborative project between research institutes (University of Tokyo and Industrial Research Institute of Ishikawa), leading company and industry association of the Japan's printing and painting industry (DIC Corporation and Japan Paint Manufacturers Association), and an NPO of colour-blind people that advises CUD (Colour Universal Design Organization).

## 2. METHOD

### 2.1 Sample Preparation

We used two types of colour sample chips that are *de facto* standards for ordering colours in Japan's printing and painting industry, respectively. The first is DIC Colour Guide library by DIC Corporation, which features 2,230 colours published in five volumes: Vol. 1 and 2 and Traditional Colours of Japan, France and China. The second set is the Standard Paint Colours by the Japan Paint Manufacturers Association (JPMA). The original set of JPMA samples feature 1,500 colours distributed evenly according to the Munsell colour system. Every two years, 600-700 colours are selected from this set and published as Standard Paint Colours. For fine-tuning colours for CMYK process printing, colour charts with various shades of cyan, magenta and yellow were specially made by DIC.

### 2.2 Experimental Procedure

Examination and selection of colours were performed in the form of "jamboree," where 10-15 people with various colour-vision types gather and examine colour samples together. This ensured quick comparison of conflicting colours by different types of people and fast

screening of alternative colours for the best possible compromise. All sessions were performed under D65 lighting.

## 3. RESULTS AND DISCUSSION

### 3.1 Selection of colours than can easily be called with distinct colour names

Humankind use colour names to describe the colours they perceive and to communicate with other people about colours. Although there are millions of colours, the ranges of colours whose names are difficult to describe are not suitable for presenting colour-coded information. Therefore we first selected the range of colours that are easy to be named.

Based on the consulting experience of the designers at DIC Colour Design Inc., we first selected 27 colour names. These included three achromatic colours (black, grey and white), 12 high-saturation colours that are often used for painting small objects, and 12 low- or middle-saturation colours that are often used for painting large objects (Figure 2).
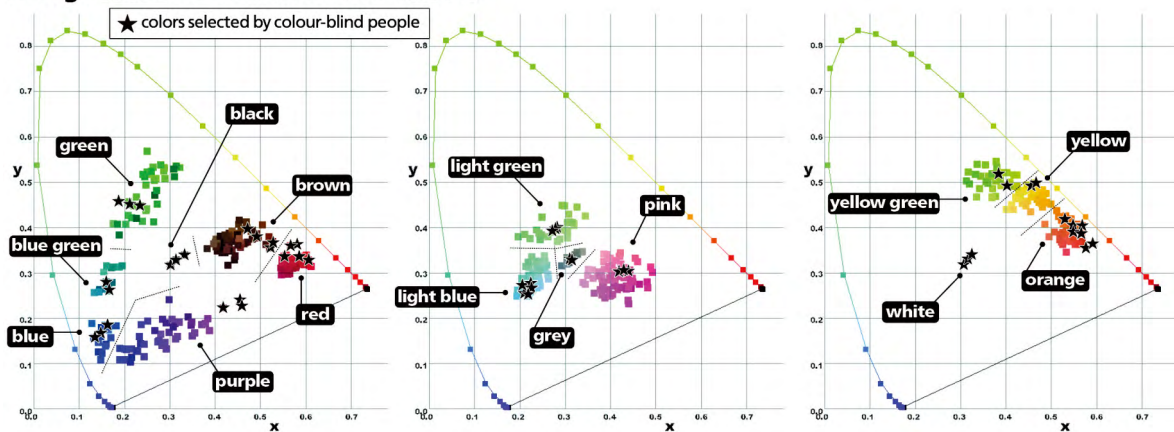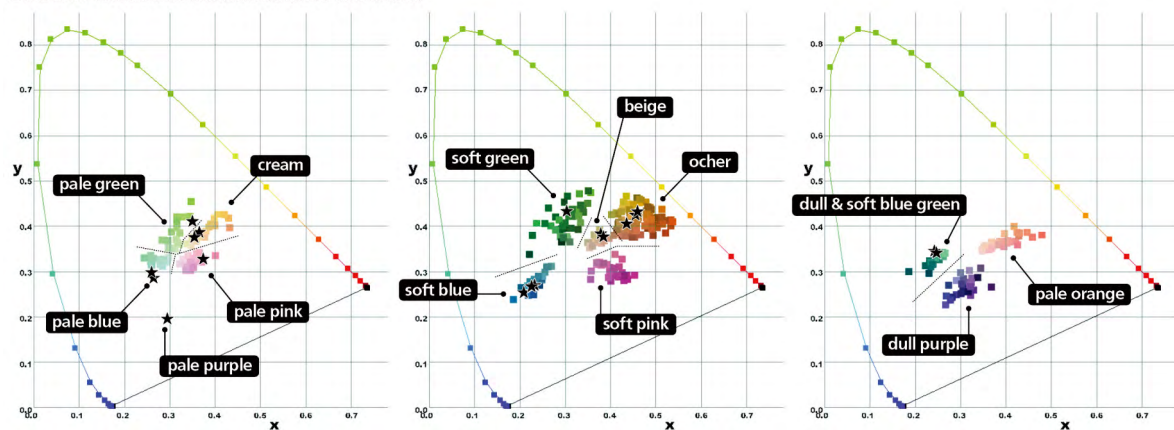


*Figure 2: Distribution of the colours for specific colour names
selected by common-type and colour-blind people*

We then asked five designers with common-type colour vision to categorise the 2,230 DIC Colour Guide sample chips. Only the chips whose colour names seem apparent were grouped, and the chips whose colour names were difficult to describe were discarded. As expected, the resulted groups of colour chips formed uniquely distributed clusters in the CIE xy colour space (coloured squares in Figure 2).

AIC2015 TOKYO - Color and Image

Although colour-blind people can also recognise colours using colour names, the range of colours described by a particular colour name is not the same as those used by common-type people. For example, some shades of red appear green or brown to colour-blind people, but certain range of red colours can distinctly be felt as red. To identify such range of colours for each colour category, we then showed the above sets of colour chips to a jury of colour-blind people (protanope and deuteranope) and asked to select the chips that they can recognise with the same colour name (Star symbols in Figure 2).

The results were striking but understandable. The ranges of colour chips selected by the colour-blind people were distributed at either side of the confusion lines. For example, only yellowish red chips that were above the confusion line connecting red and green were selected as red, and only the bluish green chips that were below that confusion line were chosen as green. Likewise, only reddish purple chips above the confusion line connecting purple and blue (for protanope) and purple and green (for deuteranope) were selected as purple. Bluish purple, including violet, were not selected because they appear confusing with blue (for protanope) or green (for deuteranope). Similarly, only yellowish pink was selected, because other ranges of pink appear confusing with light blue (for protanope) or light green (for deuteranope). Among the 27 sets of colour chips, colour-blind people were not able to select any chip for soft pink, pale orange and dull purple, because all the chips selected by the common-type people for these colour names appeared confusing with the chips of other colours by colour-blind people. Thus, we obtained a set of 24 colours.

## 3.2 Adjustment of colours for paint colours

The DIC Colour Guide is designed for special-colour printing that uses pre-mixed ink for each colour. Because commercial printing with tens of special-colour inks is not practical, we first developed a practical version of the colour palette for the JPMA Standard Paint Colours for painting industry, in which special pre-mixed colours are used more commonly. Because JPMA Colours are based on Munsell colour space, we first converted above-mentioned 24 ranges of colours to Munsell values. Because of the fewer number of sample chips, the JPMA Standard Colours lacked some of the colours that were found useful for clear distinction of colours. Most notably, it lacked the yellowish red between Munsell values R7.5 and R10. JPMA therefore made new colour chips at R8.75 specially for this project. It also made several other colours for bluish green. Using these, we were able to select 24 chips of the JPMA standard colours (Figure 3A).

The selected colours had a few problems when it would be used for practical applications. First, It had only one shade of grey even though in many cases different shades of grey are useful. Second, the number of low- and middle-saturation colours did not match the number of high-saturation colours. We therefore tried to increase the number of achromatic and low/middle-saturation colours by selecting candidate colours (Figure 3B). After examination by colour-blind people, colours that were hard to distinguish were deleted (x symbols), and the hue, saturation and brightness of some colours were adjusted for better distinguishability (white arrows), resulting in a set of 31 colours (Figure 3C).

So far, colour combinations that are difficult to distinguish for low-vision people had not been considered. It is not easy to set a model case of low-vision, because many eye diseases are progressive. We therefore asked people who suffered from retinal detachment or retinopathy of prematurity, whose symptoms in the retinae remain rather stable. In addition, we asked another person whose colour vision of one eye showed complete tritan characteristics for unknown reasons. After another session with both colour-blind and low-

vision people, many colours, especially those in the middle-saturation range, were determined confusing and had to be discarded (Figure 3D-1). In total 20 colours (nine high-saturation, seven low-saturation, and four achromatic colours) were selected eventually. Two remaining colours in the middle-saturation range (yellow and green) were designated as alternative colours that can be used instead of high-saturation colours.

## 3.3 Adjustment of CMYK values for process colour printing

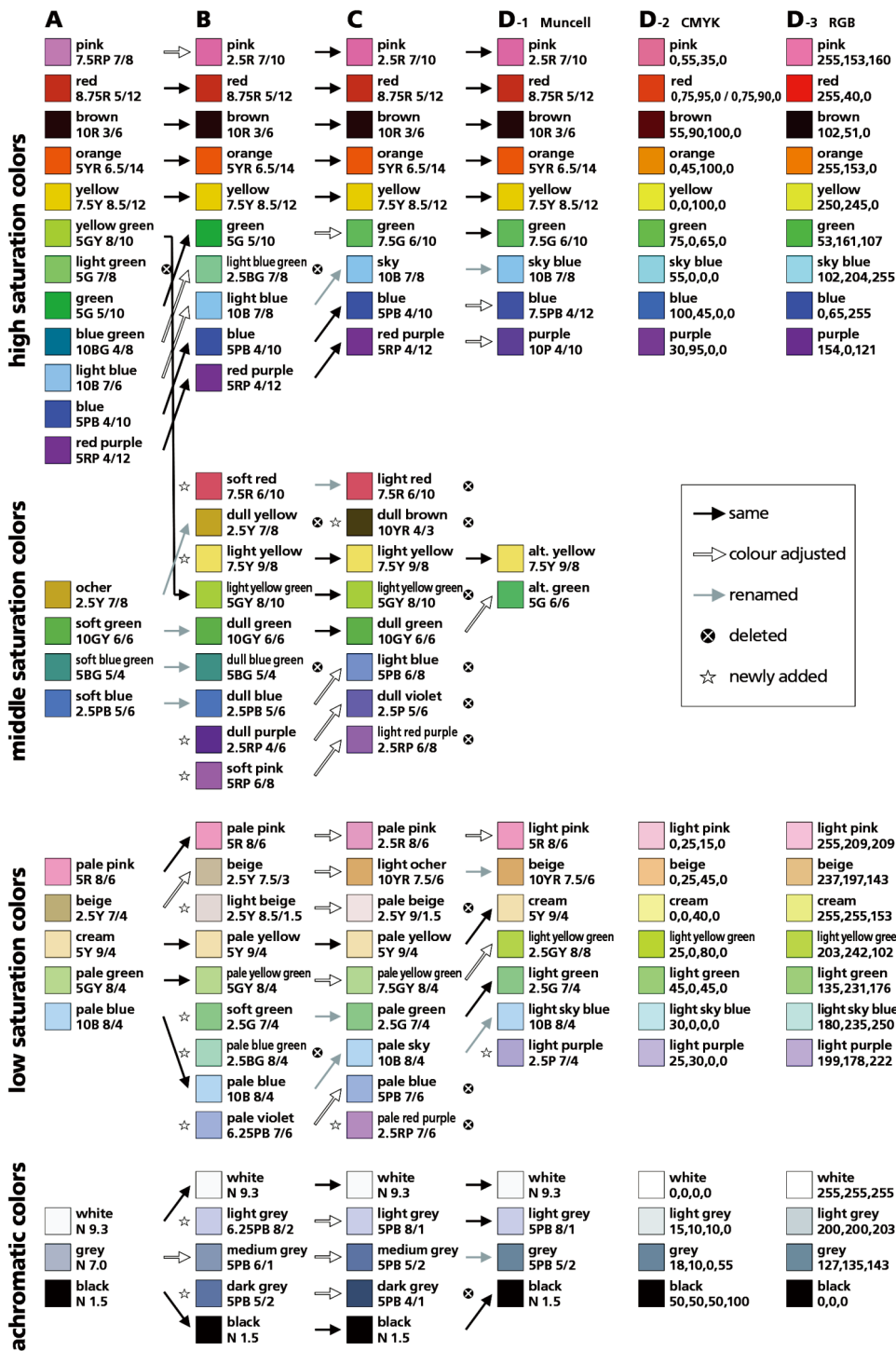Next, we made a similar colour palette for printing (Figure 3D-2). For practical multicolour print, we made the set for CMYK process-colour printing. Paint and print have rather different gamut. To make the best use of CMYK gamut, we adjusted each colour by making charts with varying levels of cyan, magenta and yellow and selecting the colours that are most distinguishable. To ensure consistency of reproduction, CMYK values were determined with precisely controlled profile (DIC Standard SFC_AM2.0), which is essentially similar to the industry standard Japan Color 2001 Coated printing profile.



*Figure 3. Colours for each version of the model colour palette*

### 3.4 Adjustment of RGB values for display panels

The final set of colour palette is for the displays of computers, mobile devices, TV sets, and digital signage. Most of these use LCD displays, where colours are defined with RGB values. Among the two industry-standard colour space for such displays –sRGB and Adobe RGB– we chose sRGB because (1) it is also the standard for Internet web sites and PDF documents, and (2) the latter is used only for specific purposes such as photography printing. Using a precisely calibrated LCD monitor, we adjusted each colour to make the best use of the specific gamut of the sRGB colour space (Figure 3D-3).

### 3.5 Application of the model colour palette

The JPMA, CMYK and GRB versions of the palettes were released in mid 2009, late 2009, and late 2011, respectively. To help choosing the most distinguishable colours, we provided for each set the lists of colours that are especially easy or relatively difficult to discriminate. A handbook was released in 2014 to provide detailed information of each colour set as well as the lists of recommended and unrecommended colour combinations.

Since its release, the colour palette is used by a wide variety of products including train line maps, signs in public spaces, graphs and drawings in the textbooks of elementary and high schools, as well as graphic interface of electronic devices. The colours were also reproduced for plastic materials of colour-coded trash boxes and buttons of TV remote controllers. With slight modification, the colours were also used for public information services such as colour-coded maps and alert charts for the web sites of the national meteorological agency, as well as tsunami hazard alert systems of TV broadcast networks.

### 4. CONCLUSIONS

The model colour palette provides for the first time a systematic way for conveying colour coded information that is least confusing for people with diverse colour vision types. By defining colours not with Yxy or L*a*b* values, which are mostly used only by scientists, but with industry-standard paint colour chips and CMYK and RGB values, the palette has become instantly useful for designers who shape the colour environment of the real world.

### REFERENCES

Brettel, H., Viénot, F. and Mollon, J. D. 1997. *Computerized Simulation of Color Appearance for Dichromats*, Journal of the Optical Society of America 14 (10) 2647–2655.

Pitt, F.H.G. 1935. *Characteristics of dichromatic vision,* Medical Research Council, Report of the Committee on the Physiology of Vision, XIV; Special Report Series, 200.

*Address: Prof. Kei Ito, Institute of Molecular and Cellular Biosciences,*
*The University of Tokyo, 1-1-1 Yayoi, Bunkyo-ku, Tokyo 113-0032, Japan*
*emails : itokei@iam.u-tokyo.ac.jp, ito@cudo.jp*

# Color Universal Design

Yasuyo G. Ichihara*1*2

1 Faculty of Informatics, Kogakuin University

2NPO Color Universal Design Organization (CUDO)

## ABSTRACT

The present study investigates the tendency of individuals to categorize colors. Humans recognize colors by categorizing them with specific color names such as red, blue, and yellow. When an individual having a certain type of color vision observes an object, they categorize its color using a particular color name and assume that other people will perceive the color in an identical manner. However, there are many variations in human color vision caused by photoreceptor differences in the eye, including red and green confusion. Thus, another person with a different type of color vision may categorize the color using another name. To address this issue, we attempt to determine the differences in the ranges of colors that people with different types of color vision categorize using particular color names. In the modern urban environment, most visual information, including warning signs and notice boards, is coded by color. Finding the common color categories among different types of color vision is an important step towards achieving Color Universal Design, a visual communication method that is viewer-friendly irrespective of color vision type. Herein we report on a systematic comparison between people with common (C-type) and deutan (D-type) color vision. Analysis of protan (P-type) color vision will follow in a subsequent report.

## 1. INTRODUCTION

In Japan, about 5% of men and 0.2% of women see color differently (so-called red-green confusion) than the general population, due to genetic differences. The percentage is higher in Europe and the United States; up to 10% of men in some countries. Visual information presented using various colors is generally easy to understand, but because of these differences in color vision, the use of colors can actually cause confusion. Modern society is filled with visual information comprising multiple colors, but the appearance of this information is often designed only with regard to people with the most common form of color vision. Designs employing certain ranges of colors can sometimes lead to ineffective communication or even accidents for the people who perceive colors differently. To avoid such misperceptions, the concept of "barrier-free color" or "color universal design" (CUD) has been advocated, with the goal of creating designs that are understandable regardless of the type of color vision.

Recently, computer software and glasses that provide a virtual experience of colors perceived by individuals with red-green confusion have become available, such as VisCheck, the CUD-proof function of Adobe Photoshop and Illustrator, and the Variantor glasses. However, these tools fail to indicate how individuals with different types of color vision recognize color categories.[1] In the present study, we compared the ranges of colors that people with common and red-green confusion color vision perceive when a particular color name is presented.

There are three major types of color vision: common (C-type), protan (P-type), and deutan (D-type). Individuals with P- or D-type color vision are often regarded negatively as being "colorblind",

color "anomalous" or having color vision "deficiency" compared to those with the "normal" C-type color vision. In order to avoid misleading impressions and promote more positive attitudes towards individuals with P- or D-type color vision, just two of the many types of genetic polymorphisms, we believe it is important to stem the use of words that are imbued with a negative connotation. We therefore refrain from using terms such as "normal", "anomalous", or "blind".

## 2. METHOD

### 2.1 Study Overview

Using a light source to fully render color properties, subjects were asked to classify color chips of 1,050 different colors into 20 color categories. Subjects were also asked to choose one color chip for each category that they felt was the most representative of the given color name. The 20 color category names included the 11 basic color names (white, black, red, green, yellow, blue, brown, orange, purple, pink, and gray) proposed by Berlin and Kay[1]. In order to analyze not only categories of high saturation colors but also low saturation colors, 9 additional color category names were used (beige, cream, yellowish-green, light green, blue-green, light blue, bluish-purple, purple, and reddish-purple. Considering that the ranges of colors covered by these names would occupy only discrete areas of the color space, we also made the "Color name unknown" category to avoid the risk of subjects feeling compelled to classify a color chip they had difficulty judging as belonging to a specific color category.

### 2.2 Subjects

Four subjects with C-type (trichromatic) color vision (Ishihara Test 38 plates – pass) and 4 subjects with complete deuteranope vision (strong D-type, Panel D15 test – fail). Color vision types were diagnosed at the Department of Ophthalmology, Jikei University School of Medicine.

Table 1. Subjects' characteristics

| Subject No. | Age (years) | Gender |
|---|---|---|
| C-type color vision No. 1 | 46 | Female |
| C-type color vision No. 2 | 21 | Female |
| C-type color vision No. 3 | 22 | Male |
| C-type color vision No. 8 | 21 | Male |
| D-type color vision No. 1 | 41 | Male |
| D-type color vision No. 2 | 66 | Male |

| D-type color vision No. 3 | 25 | Male |
|---|---|---|
| D-type color vision No. 4 | 62 | Male |

## 2.3 Test Equipment/Light Source

Standard lighting equipment: RW standard color viewer; color appraisal AAA fluorescent lamp (x=0.3425, y=0.3520, luminance=7,500 cd/m$^2$); measured with a luminance and colorimeter (CS-1000; Konica Minolta, Tokyo Japan).

## 2.4 Background Color

White (x=0.3370, y=0.3483, Y=62.18)

We first compared color perception with white and black backgrounds and observed a significant difference between the two. Considering that many colors used in public signs and printed materials, like magazines, are presented on bright rather than dark backgrounds, we chose the white background for subsequent tests.

## 2.5 Color Samples

We used the Toyo Color Finder (CF) with 1,050 color chips (size: 3.2 × 1.2 cm$^2$, colored area: 2.4 × 1.2 cm$^2$), a color sample book published by Toyo Ink Manufacturing Co., as the color samples for color category classification. The reasons for using the Toyo Ink chips include the following.

(1) They evenly cover a range of colors used in commercial printing. (2) A large quantity of precisely colored chips is readily available. (3) Considering the burden attributed to classifying colors and resolution over the entire color range, a quantity of about 1,000 colors was deemed appropriate. It typically took 2.5 hours for one subject to complete the entire task.

## 3. RESULTS

### 3.1 Color Perception Influenced by Background Color

We first asked the 4 subjects with C-type color vision to categorize colors on the black background (standard tabletop of the RW standard color viewer) and on the white background (a white sheet of paper placed on the color viewer tabletop). Some color chips were selected as a particular color when presented on the white background but not when presented on the black background, and vice versa. Selected color chips with significant differences between the different backgrounds are shown in Table 2.

Table 2. Selected color chip data using different background colors

| CF No. | XYZ-Y | Yxy-x | Yxy-y | Color category names | Number selected according to background |
|---|---|---|---|---|---|
| 10114 | 21.1 | 0.4702 | 0.3572 | brown | White – Black = 1 – 4 |
| 10845 | 12.35 | 0.4058 | 0.3922 | brown | White – Black = 0 – 3 |
| 10594 | 55.72 | 0.3763 | 0.3883 | beige | White – Black = 1 – 4 |
| 10220 | 78.62 | 0.3725 | 0.4043 | yellowish-green | White – Black = 3 – 0 |
| 10239 | 59.44 | 0.3713 | 0.463 | yellowish-green | White – Black = 4 – 0 |
| 10243 | 60.02 | 0.3588 | 0.4476 | yellowish-green | White – Black = 3 – 0 |
| 10645 | 36.76 | 0.2969 | 0.3871 | light green | White – Black = 3 – 0 |
| 10404 | 16.31 | 0.184 | 0.2348 | blue | White – Black = 3 – 0 |
| 10408 | 10.16 | 0.2116 | 0.2444 | blue | White – Black = 3 – 0 |
| 82 Purple | 6.29 | 0.2414 | 0.1485 | bluish-purple | White – Black = 1 – 4 |
| 10946 | 6.86 | 0.3223 | 0.3315 | black | White – Black = 1 – 4 |

## 3.2  Results of C-type Color Vision (Ishihara Test 38 plates – pass)

The color chips selected by all 4 subjects with C-type color vision presented for each color name are shown in Figs. 3-1 and 3-2. For white and blue-green, none of the color chips were unanimously selected by the 4 subjects. For white, this was most likely because the Toyo color chips contain essentially no ink that appears white; because it is made for printing on white printing paper, white ink is not required. For blue-green, midway between blue and green, this was most likely because blue-green may not be established as a definite color category even among individuals with C-type

color vision, at least in Japan; thus reflecting large differences based on the subjective experiences of individuals.

## 3.3 Results of D-type Color Vision (Panel D15 test – fail)

The color chips selected by all 4 subjects with D-type color vision are presented in Figs. 4-1 and 4-2. In addition, because of the wider variation among subjects with D-type color vision, colors selected by 3 of the 4 subjects are also shown in Figs. 5-1 and 5-2. For white, gray, green, purple, cream, yellowish-green, light green, blue-green, bluish-purple, and reddish-purple, there were no instances where all 4 subjects selected the same color chip. Of these, for white, light green, bluish-purple, and reddish-purple, even 3 of the 4 subjects did not select the same color chip. In addition, the color categories for brown and pink were broader than those for subjects with C-type color vision. Characteristically, the former (brown) extended to a dark yellow range, whereas the latter (pink) extended to a reddish-purple range.
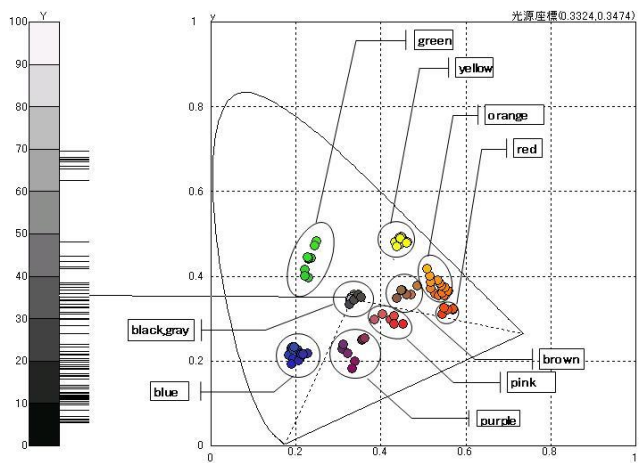


Fig. 3-1 Color chips selected by all 4 subjects with C-type color vision (basic colors)
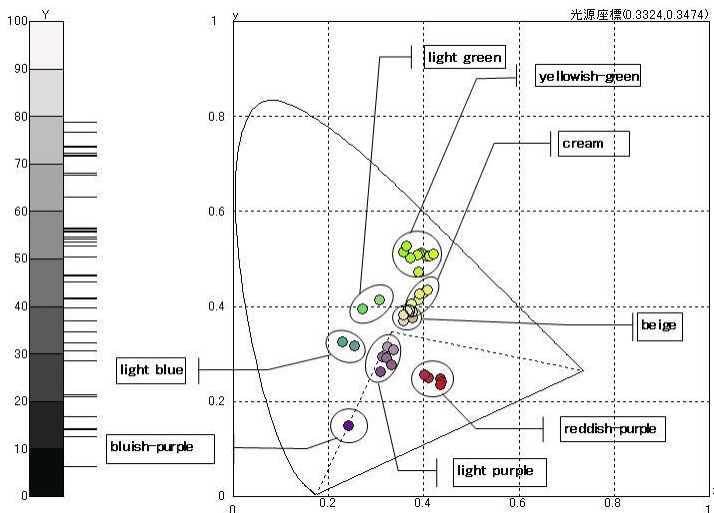


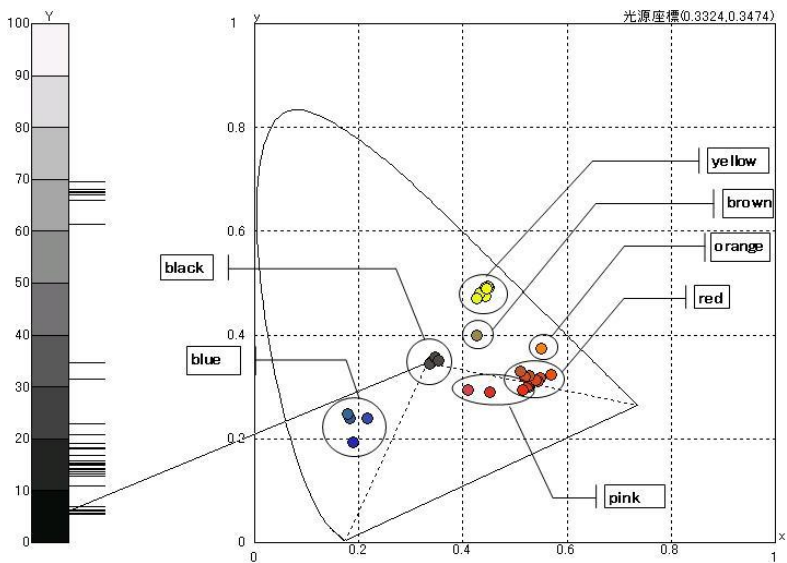Fig. 3-2 Color chips selected by all 4 subjects with C-type color vision (non-basic colors)

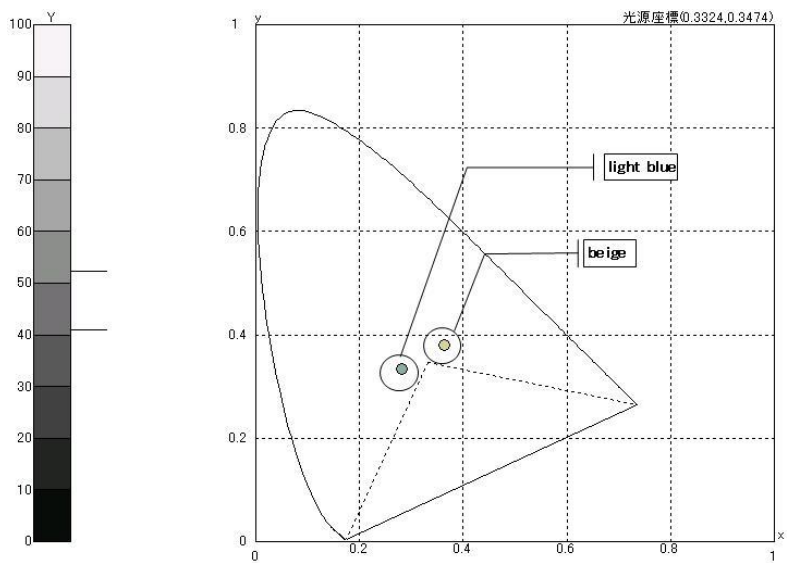Fig. 4-1 Color chips selected by all 4 subjects with D-type color vision (basic colors)



Fig. 4-2 Color chips selected by all 4 subjects with D-type color vision (non-basic colors)

Color categories for D-type subjects included beige and light blue.

## 3.4 Comparison of Color Name Recognition between Color Vision Types

Finally, we compared the color chips selected by subjects with C- or D-type color vision (color chips selected by at least 3 of the 4 subjects in each group, Fig. 6); those selected by subjects with C-type but not by those with D-type color vision (number of C-type subjects who selected the color vs number of D-type subjects who chose the chip differ by $\geq 3$ [4:0, 4:1, 3:0], Fig. 7); and conversely, color chips selected by D-type subjects but not by C-type subjects (Fig. 8).

As shown in Fig. 6, there were no color chips that were commonly selected for white, gray, blue-green, bluish-purple, light purple, and reddish-purple. For purple, only one color chip was selected in common. In particular, for light purple, purple, and reddish-purple, there were color chips commonly selected by most subjects with C-type color vision, but they were not commonly recognized as the corresponding color name by subjects with D-type color vision (Fig. 7).

Colors represented by these color chips must be used with caution when designing visual information, because they would not be perceived as the same color by individuals with different types of color vision. Colors selected commonly by D-type but not by C-type subjects included red in brown regions, brown in dark yellow regions, yellowish-green in yellow regions, yellow in yellowish-green regions, and pink in warm-color gray regions (Fig. 8). Usage of color tones in these regions may also impair effective color-based communication.

Moreover, some colors recognized unanimously by the C-type subjects were not recognized as the corresponding colors by subjects with D-type color vision. These include color chips of high saturation yellowish-green, high saturation brown, low saturation orange, bluish-purple, and green on the  confusion line with gray (Fig. 7).
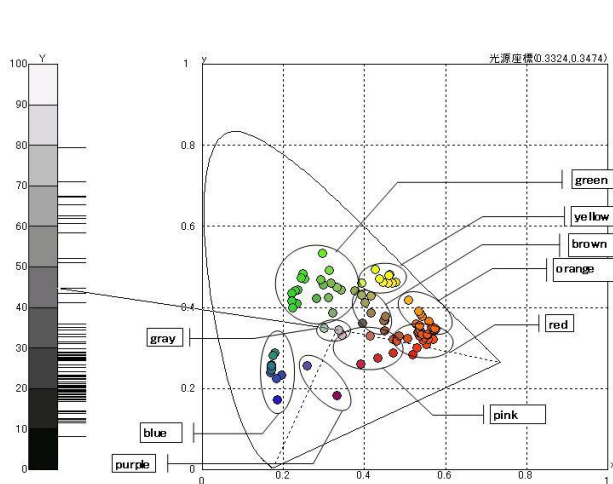


Fig. 5-1 Color chips selected by 3 of the 4 subjects with D-type color vision (basic colors)
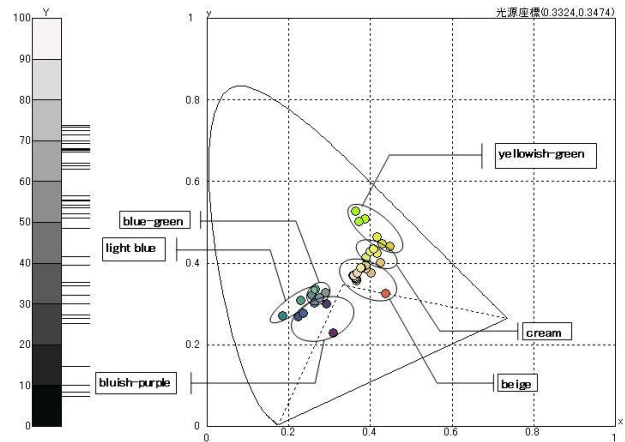


Fig. 5-2 Color chips selected by 3 of the 4 subjects with D-type color vision (non-basic colors)

AIC2015 TOKYO - Color and Image

Fig. 6 Color chips selected by 3 or more subjects with C- or D-type color vision

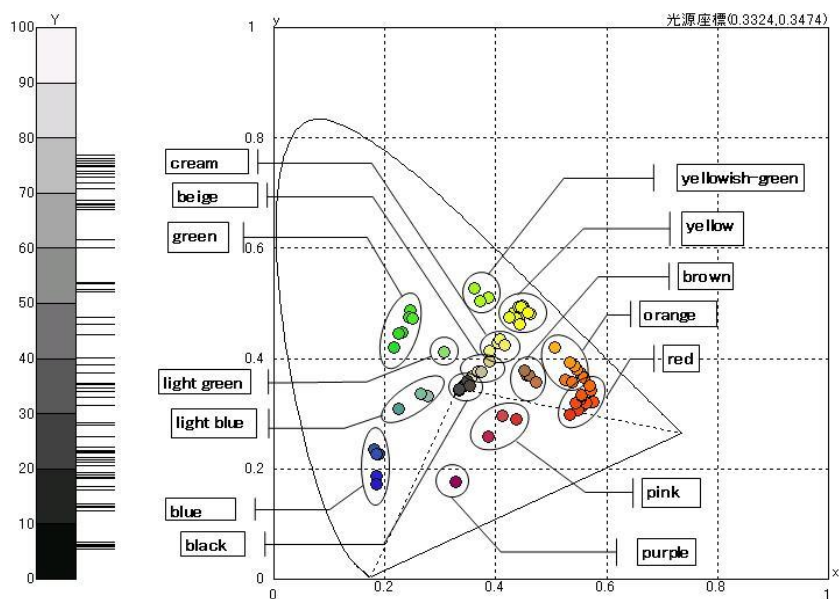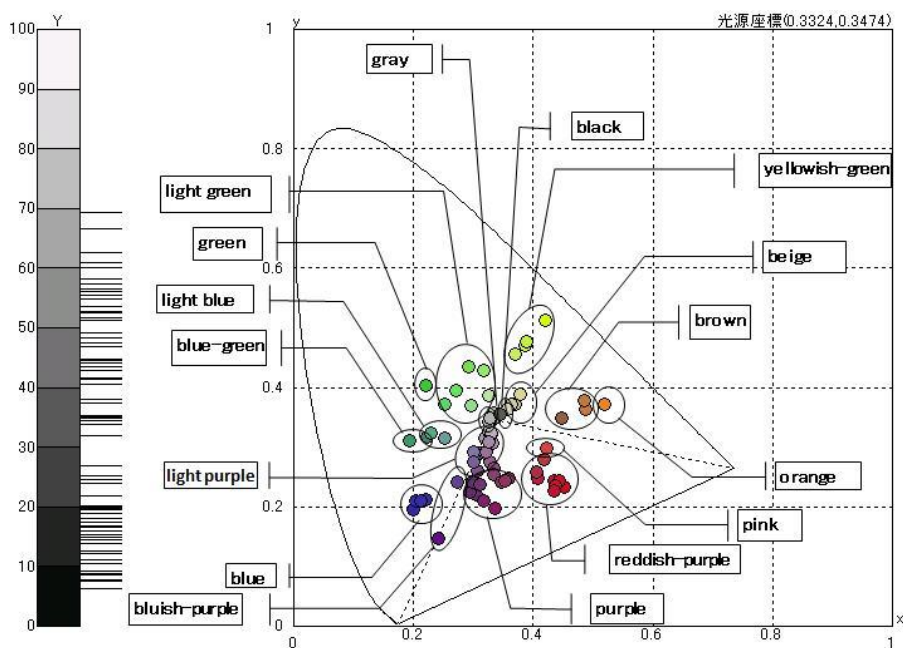(Colors that may possibly be used for color universal design)



Fig. 7 Color chips selected by subjects with C-type color vision but not by subjects with D-type color vision
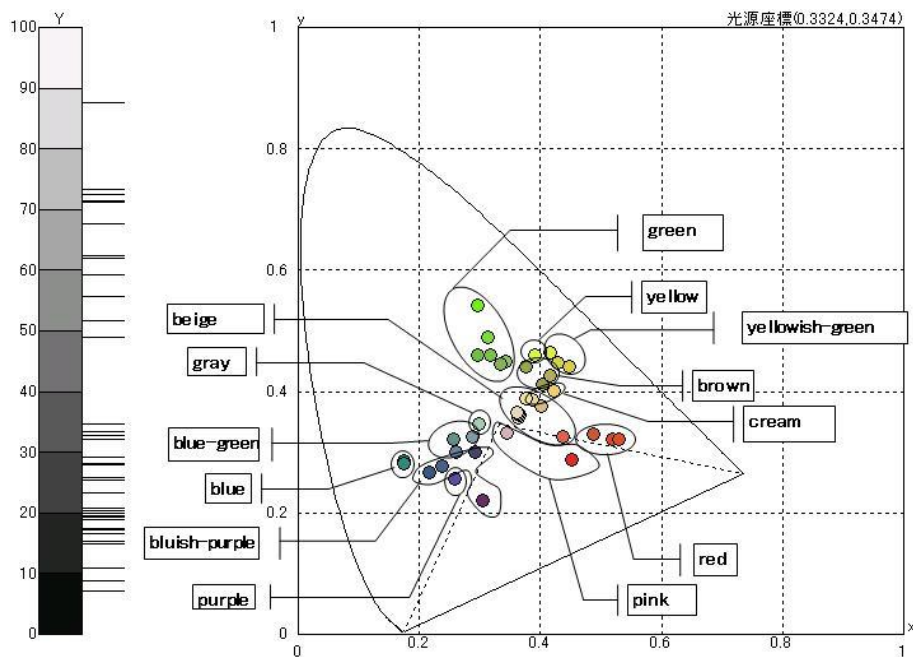
Fig. 8 Color chips selected by subjects with D-type color vision but not selected by subjects with C-type color vision

## 4. CONCLUSION AND FUTURE OUTLOOK

Our present study shows that color chips commonly selected by subjects with C- or D-type color vision exist for many color names. However, even for these colors, slight deviations in color tones may lead to color recognition using different color names. In future studies, data presented herein, combined with luminance information (reflectance Y or Munsell value) in the Yxy color space, will be compared three-dimensionally. In addition, the extent of individual differences and differences in the distribution of color tones felt to be most representative of a color name will be analyzed to further explore the differences in color category perception. An identical set of tests have already been conducted by 4 subjects with P-type color vision. Common and different features among C-, P- and D-type color vision will be analyzed in future studies.

Colors that are unanimously recognized as the same color name regardless of color vision type are good candidates for color universal design to facilitate color-name-based communication among individuals with different types of color-vision. Our study identified ranges of colors that are perceived differently depending on color vision type. Most notably, we identified ranges of colors that are perceived by individuals with C-type color vision with a certain color name but not by those with D-type color vision using the same color name. Such colors should be avoided when designing materials to be used in public places.

By replacing such colors with adjacent color tones that eliminate differences in color name recognition, color-coded designs that are difficult for those with different types of color vision to distinguish can be avoided.

## ACKNOWLEDGEMENTS

## REFERENCES

[1] Brent Berlin, Paul Kay [Basic Color Terms], Their Universality and Evolution (The David Hume Series) )(1969, 1991)

[2] Ichihara YG. Okabe M. Iga K.. Tanaka Y. Musha K. Ito K..,"Color Universal Design -The Selection of Four Easily Distinguishable Colors for all Color Vision Types- "EI2008 Color Imaging XIII:Processing, Hardcopy, and Application, SPIE Vol.6807 pp.6807O1~8 (2008)

[3] Ichihara Y.G., "Color constancy in Japanese Animation, EI2006 Internet Imaging", Color Imaging XI:Processing, Hardcopy, and Application SPIE Vol.6058 pp.60580c1~8 (2006)

[4] Ichihara Y.G. Nakadomari S,Takeuchi H,Satoru Miyauchi S,Kitahara K., "A fMRI Study of Color Related Visual Cortex V4- Retinex processing from the fMRI study on V4 -Artistic Research of coloured Picture Using Functional MRI", SPIE The International Society for Optical Engineering EI2002 Internet Imaging, Retinex40 SPIE Vol.4662 , 428 (2002)

[5] Ichihara YG,Nakadomari S,Takeuchi H,Satoru Miyauchi S,Kitahara K., "The difference between seeing a random colour dot picture and reading shapes from the same colour dot picture in the Ishihara pseudoisochromatic plates -Artistic research of coloured picture using functional MRI- ", AIC2001 Rochester Proceeding 2001 SPIE Vol.4421, 327-330, (2001)

[6] Ichihara YG., "What do you see in a digital color dot picture such as the Ishihara pseudoisochromatic plates? ", SPIE The International Society for Optical Engineering EI2001 Internet Imaging, vol. 4311, 419-426,(2001)

[7] Ichihara YG., "Suitable digital color palette (DPC) for individual human color vision sensitivity", SPIE The International Society for Optical Engineering EI2000 Internet Imaging, vol. 3964, 168-174,(2000 )

[8] K. Wakita and K shimamura, "SmartColor: disambiguation framework for the colorblind", In Assets '05:Proc. of the 7th international ACM SIGACCESS conference on Computers and accessibility, 158-165,(2

# An Investigation of the Appearance Harmony using Real Materials and Displayed Images

Midori TANAKA and Takahiko HORIUCHI
Graduate School of Advanced Integration Science, Chiba University, Chiba, Japan

## ABSTRACT

Color harmony has long been of interest to researchers in different fields who design the colors of various objects. When sensing harmony among actual objects, not only the harmony among the colors but also the appearance of harmony of the materials is an important consideration. In the previous study (Tanaka et. al., AIC2014), we investigated the appearance of harmony of various materials by conducting psychophysical experiments to collect quantitative data. In this study, we further investigated the appearance harmony using actual objects and rendered images and conducted the psychophysical experiments. Our results indicated that the sample pairs with similar reflection and texture patterns were viewed as harmonious, even though their materials were different. Furthermore, the appearance harmony of the materials was significantly affected by the subjects' reactions to the visual information of the displayed samples with/without monitor.

## 1. INTRODUCTION

Color harmony has interested researchers involved in color design based on various objects for a long time (e.g., Judd & Wyszecki, 1975; Hård, & Sivik, 2001; Burchett, 2002). By contrast, other traits related to harmony have not been investigated deeply in previous studies. The relationship between product identity and shape has been discussed (e.g., Bar & Neta, 2006; Nasser & Marjan, 2010; Ye, et al., 2014), but these studies investigated the preference for a single shape such as a kettle (Nasser & Marjan, 2010) or a chair (Ye, et al., 2014), whereas they did not consider two-shape combinations. Chen et al. investigated the relationship between preferences for color-pairs and shapes, but they did not discuss two-shape combinations. In the field of texture analysis, a single texture has been used in preference analyses. In 2014, Qiao et al. began the study of texture harmony (Qiao et al., 2014).

Recently, the analysis of material appearance has been studied actively. Most of these studies have focused on visual estimates of the specific properties of materials, such as glossiness, translucency, or roughness. According to experimental studies of material harmony, most of our empirical knowledge of harmony is based on specific material clusters in the actual field of industrial design, such as combinations of wood or stone used in architecture, or combinations of metals used in the car production. However, to the best of our knowledge, there have been no previous studies of the appearance harmony of materials.

Thus, in the present study, we investigated the appearance harmony of materials based on psychophysical experiments. Although numerous materials are mixed in the real world, the harmony among different materials has received little attention. In this study, we investigated the harmony across material categories.

## 2. EXPERIMENTAL STIMULI

### 2.1 Materials dataset

To investigate the perception of materials without being influenced by shape, we produced a dataset of 30 exemplars (size = 50 × 50 mm). The individual exemplars were selected from 10 material categories, i.e., stone, metal, glass, plastic, leather, fabric, paper, wood, ceramic, and rubber, thereby covering a wide range of material appearances. The materials are shown in Fig. 1. As noted by Albertazzi and Hurlbert (2013), color has a strong influence on perceptual qualities. However, it is difficult to collect uniform material exemplars of various hues, so we only collected exemplars with low saturation. In Fig. 2, the symbol "×" represents the location of each exemplar on the CIE xy chromaticity diagram. The number of exemplars in each material category was unequal because they were collected according to the differences in their surface properties. The material samples were used to generate 435 round-robin pairs, which were coupled arbitrarily and presented to the subjects, i.e., two samples each time.
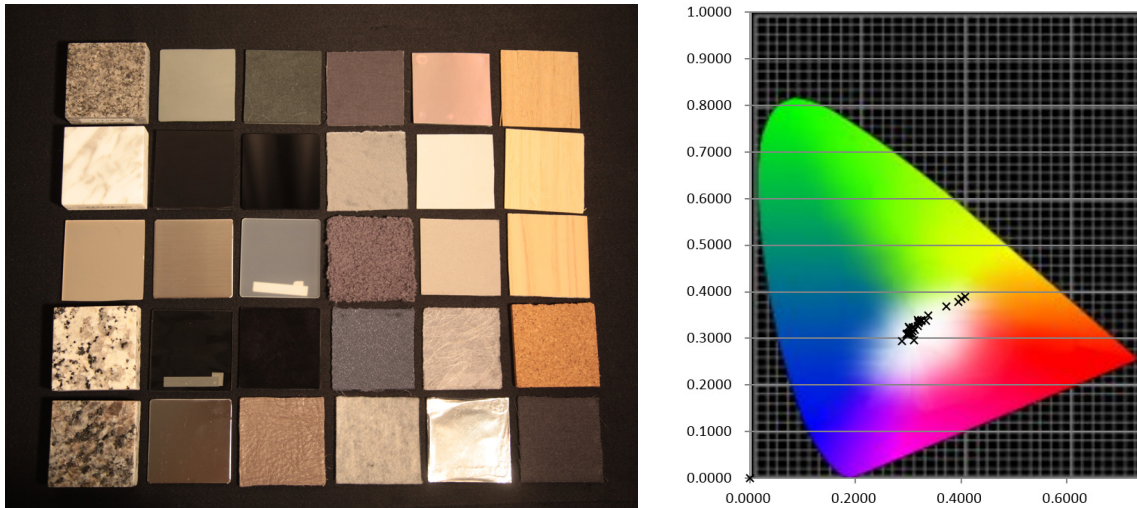


Fig. 1. Material dataset of 30 exemplars.   Fig. 2. Chrominance of the material samples.

### 2.2 Image dataset

We hypothesized that when materials are reproduced on a monitor, the following factors might strongly affect the perceptual harmony: intensity, color reproduction, and resolution. Thus, we constructed an imaging system to facilitate the accurate reproduction of the real-world display materials, where the camera system comprised an RGB camera and a standard lens. The camera used to obtain a linear camera output was a Canon EOS 5D Mark II, with a *sRAW2* image size of 2784 × 1856 pixels and a quantization level of 14 bits. We then prepared a color image dataset by capturing the materials which placed in a viewing booth. The output monitor was an Apple 15.4" MacBook Pro with Retina display, where the widescreen, LED-backlit IPS screen had a glossy finish, with a native resolution of 2880 × 1880 pixels and 220 pixels per inch. Using a calibration process, we verified that the intensity and chromaticity of the real materials and their images reproduced on the display were almost equivalent.

# 3. EXPERIMENTAL METHODS

We conducted two different experiments, as follows.

(1) Experiment A:

Sample pairs were placed such that their surfaces and viewing directions were perpendicular to the subject. In this experiment, subjects assessed the harmony or disharmony of each sample pair based on their two-dimensional surface appearance.

(2) Experiment B:

The static sample pairs used in Experiment B were photographed using a digital camera. Subjects assessed the appearance harmony or disharmony of each sample pair appeared on the images displayed on a calibrated monitor.

After dark adaptation for two 2 min, the subjects evaluated the pairs according to each experimental method. A forced-choice, 10-point scale was used to rate harmony-disharmony. The subjects determined the appropriate rating for each combination from 1 (disharmony) to 10 (harmony) and recorded them on answer sheets. In each experiment, 435 pairs were evaluated and over 30 pairs were then selected from the 435 pairs to confirm the reproducibility of the experimental results. The subjects were asked to wear gloves in order to avoid the possibility of tactile effects confounding their assessments. In each experiment, the subjects conducted the evaluation in a specified order and they changed the evaluation samples themselves. Five subjects participated in this experiment. All of the subjects were native Japanese with normal color vision.

# 4. EXPERIMENTAL RESULTS

## 4.1 Intra- and inter-participant variances

The intra-participant variance was calculated as the average variances in the ratings between the two sessions. The inter-participant variance was calculated as the average ratings for each of 435 pairs by five participants.

Table 1 summarizes the intra- and inter-participant variances in the ratings. The intra-subject variance was based on 30 samples, which were shown twice. The inter-subject variance in the right row of Table 1 shows the average variance of the ratings among 435 pairs. As shown in Table 1, we confirmed that the variance in the intra-subject ratings was less than the variance in the inter-subject ratings.

*Table 1. Variances in the Inter- and intra-participant ratings.*

| Experiment | Inter-var. | Intra-var. |
|:---:|:---:|:---:|
| A | 0.52 | 3.73 |
| B | 0.32 | 2.77 |

The observed variance had one notable feature, as shown in Table 1, i.e., the ratings in Experiment A varied among subjects, whereas the ratings in Experiment B were stable among subjects. This suggests that the richness of the real-world information was sensitive to the perceptual harmony ratings. These results show that the evaluations of appearance harmony using actual material samples differed from the surface appearance assessments obtained based on captured images.

## 4.2 Perceptual harmony ratings within and across the categories of materials

Table 2 summarizes the averaged perceptual harmony ratings for all subjects within the same material category and across different material categories in each experiment. As shown in Table 2, the ratings for sample pairs within the same material category were higher than the ratings across material categories. In all the experiments, the "Metal-Metal" pair had the highest harmony ratings. By contrast, the harmony ratings for "Leather-Leather" and "Paper-Paper" were categorized as perceptual disharmony. These results suggest that the perceptual harmony ratings depended on the materials, where two samples within the same material category could be perceived as having appearance disharmony. Interestingly, the harmony rating for "Paper-Metal" was higher than for "Paper-Paper". This indicates that the perceptual harmony of the pairs in different material categories could be higher than that of pairs within the same material category. Metal, plastic, ceramic and rubber shared the most harmony with each other across material categories. "Glass-Plastic" also had a high perceptual harmony rating. These results indicate that materials can be harmonized across material categories.

*Table 2. Averaged harmony ratings for the categories of materials.*

| Experiment | Within material | Across materials |
|------------|-----------------|------------------|
| A | 6.68 | 4.02 |
| B | 6.43 | 4.14 |

### 4.3 Changes in harmony between experiments

As shown in Table 2, the average ratings in Experiments A and B did not differ significantly. However, there were some notable differences between the experiments. For the pair of plastic and rubber, the average rating indicated harmony in Experiments A (7.60) and B (7.30). For the pair of glass and rubber, the average rating changed from disharmony in Experiments A (4.80) to harmony in Experiment B (6.80). In this case, the appearance of the material may have differed between the real objects and the displayed images.

Some of the ratings for each pair differed in the experiments. Table 3 shows the ratings and pairs that changed greatly between experiments. In Experiment B, the average ratings across all subjects changed by a maximum +4.8 (pair 6 and 13) from Experiment A to B. Pair 6 (chrome, metal) and 13 (gray calfskin, leather), as shown in Fig. 3(a), had low ratings in Experiment A because their surface properties differed greatly in appearance. However, this difference could not be perceived when this pair was displayed on the monitor in Experiment B. By contrast, the average rating across all subjects changed by a minimum of −5.2 (pair 12 and 14) from Experiment A to B. Pair 12 (pig suede, leather) and 14 (cotton, fabric) had a high rating in Experiment A because their surface textures and colors were similar. However, in Experiment B, a low rating was obtained due to the low resolution of the monitor, as shown in Fig. 3(b). In these cases, the material appearance may have differed between the real objects and the displayed images.

*Table 3. Harmony changes between experiments.*

| Experiment | Up (pair) | Down (pair) |
|------------|-----------|-------------|
| A→B | +4.8 (6-13) | -5.2 (12-14) |

*(a)*          *(b)*

*(a) Pair 6 (metal) and 13 (leather) , (b) Pair  14 (fabric) and 12 (leather)*
*Fig. 3. Pairs that changed significantly between experiments.*

## 4.4 Distributions of samples in the appearance harmony space

We performed a principal component analysis (PCA) of all the ratings across materials to facilitate the visualization of the distributions of material classes in the appearance harmony feature space. We created a $30 \times 30$ diagonal matrix where the lines and columns represented the 30 material samples. Each element in the matrix showed the average rating for a pair, where we assumed symmetry among the rating. The diagonal components were considered to be the maximum ratings because a diagonal showed the ratings for pairs of materials. We derived 30 dimensions and 30 PCs from the matrix. Therefore, materials with the same harmony properties had the same PC coefficients. In all of the experiments, the first three PCs accounted for almost 92% of the variance. It should be noted that the remaining 8% of the variance in the distribution was accounted for by the other 27 dimensions. Thus, regardless of the methods used to determine the appearance harmony among materials, we can obtain an approximation of the overall distribution simply by using the first three PCs.

Figure 4 shows the ratings for each sample projected onto the first two PCs where each image is color coded by its true class membership. The open circles indicate the average for each material class and the same color corresponds to the same material category. The observed distribution in the PC space has several key features. As shown in Figure 4(a), with the exceptions of wood and fabric, the material categories overlapped with each other in Experiment A. This indicates that the degree of harmony did not depend on the material clusters in a stationary state, unlike the objects that could be moved. Furthermore, most of the material categories overlapped with each other in Experiment B, as shown in Figure 4(b). This suggests that the degree of harmony did not depend on the material clusters in the displayed images.

## 5. CONCLUSIONS

We investigated the appearance harmony among various materials by conducting three psychophysical experiments using the following real materials and their displayed images. In Experiment A, the samples were placed such that their surfaces and viewing directions were perpendicular to the subject. In Experiment B, static sample images were displayed on a monitor. Based on the intra- and inter-participant variances, we found that the perceptual harmony ratings were sensitive to the richness of the information available in the real world. In addition, the ratings were sensitive to the reflectance properties obtained by tilting objects. However, the perceptual harmony ratings were insensitive to the poor information obtained from rendered images.

Based on subjective assessments, we confirmed that sample pairs with similar surface properties were viewed as harmonious, although the materials were different. Indeed, the

appearance harmony of the materials differed between static real samples and static images. The results of the PCA indicated that the degree of harmony did not depend on the material clusters in a stationary state and the displayed images.
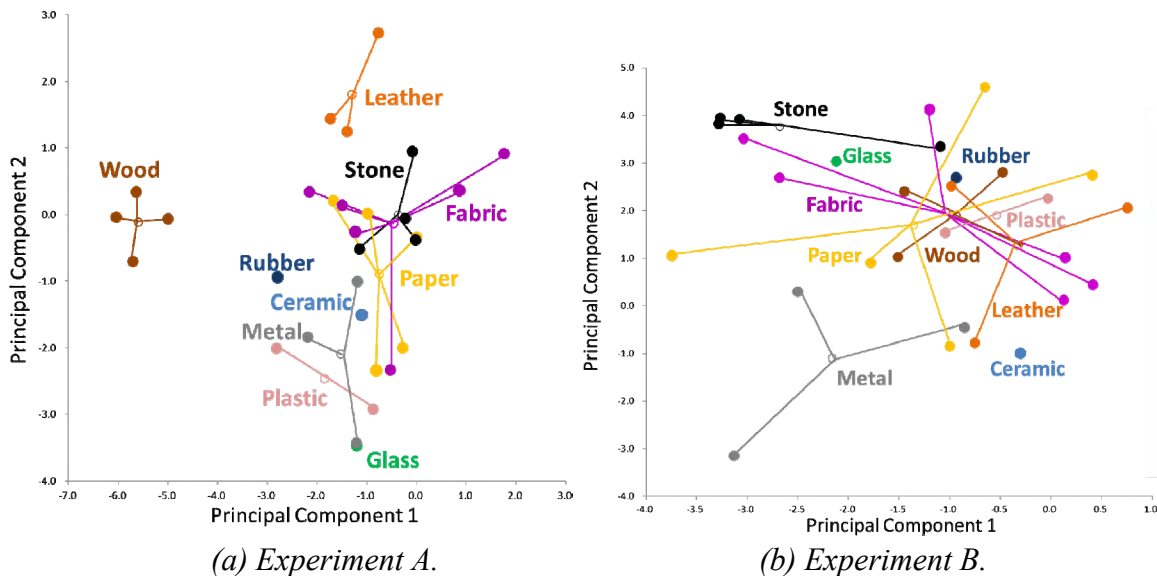


(a) Experiment A.           (b) Experiment B.

Fig. 4. Distribution of samples in the first two PCs.

## ACKNOWLEDGEMENTS

## REFERENCES

Bar, M. and M. Neta 2006. *Humans prefer curved visual objects*, Psychological Science 17 645–648.

Burchett, K.E. 2002. *Color harmony*. Color Res Appl. 27 28–31.

Chen, N., Tanaka, K., Matsuyoshi, D. and Watanabe, K. 2013. *Cross preference for color combination and shape*, Proc. Asia Color Association Conference, 98–101.

Hård, A. & Sivik, L. 2001. *A theory of colors in combination: A descriptive model related to the NCS color-order system*. Color Res Appl. 26 4–28.

Judd, D.B. & Wyszecki, G. 1975. *Color in Business*, Science and Industry, 3rd edition. New York: Wiley 390–396.

Nasser, K.M. & Marjan, T. 2010. *Design with emotional approach by implementing Kansei engineering—Case study: Design of kettle*, Proc. International Conference on Kansei Engineering and Emotion Research 625–632.

Qiao, X., Wang, P., Li, Y. and Hu. Z. 2014. *Study on a correlation model between the Kansei image and the texture harmony*, International Journal of Signal Processing, Image Processing and Pattern Recognition 7 73–84

Tanaka, M. and T. Horiuchi, 2014. *An Investigation of the Appearance Harmony of Materials*, Proc. AIC2014 Interim Meeting.

Ye, Y., Zhang Z. & He, R. 2014. *Study on design of chair shaping based on Kansei engineering,* International Journal of Scientific & Engineering Research 5 273–276.

*Address: Ms. Midori Tanaka, Graduate School of Advanced Integration Science, Chiba University, Yayoi-cho 1-33, Inage-ku, Chiba, 263-8522 JAPAN E-mails:midori_t@graduate.chiba-u.jp, horiuchi@faculty.chiba-u.jp*

# The Colour of Gold

Lindsay W. MacDonald

3DImpact Research Group, Faculty of Engineering, University College London

## ABSTRACT

The reflection from the surface of gold consists of both a body colour (dark and diffuse) and specular highlights (bright and metallic). Surface normals and albedo are calculated by regression over a subset of the intensity values from a set of images taken in an illumination dome. The specular component of reflectance is modelled as a Lorentzian function of radial angle from the specular peak direction. Rendering the surface by a model that adds diffuse and specular components at each pixel for any direction of incident illumination gives a good simulation of the appearance of the original object. It is shown how for gold this conforms to the Shafer dichromatic model of reflectance.

## 1. INTRODUCTION

There is nothing absolute about the colour of an object surface: it changes continually with illumination and orientation. So how can we define the colour of a surface? Given many images of the same object, even under the same light from many angles, what is the 'true' surface colour? Colorimetry specifies the colour of an object as the product of the illuminating power by the reflectance factor of the surface by the sensitivity of the observer, integrated over all wavelengths of the visible spectrum. This is the basis of the ubiquitous CIE system, but it relies on the assumption that the surface is perfectly matte so every point reflects the incident light equally in all directions, i.e. that it is perfectly Lambertian. In fact almost all real materials exhibit some angular dependence in the way they reflect light, and this behaviour must be taken into account when modelling the appearance of the object, by adding a gloss component to the underlying diffuse colour. The added light may appear as a sheen over the surface or as localised specular highlights, but its effect is to modulate the lightness and thereby change the colour stimulus.
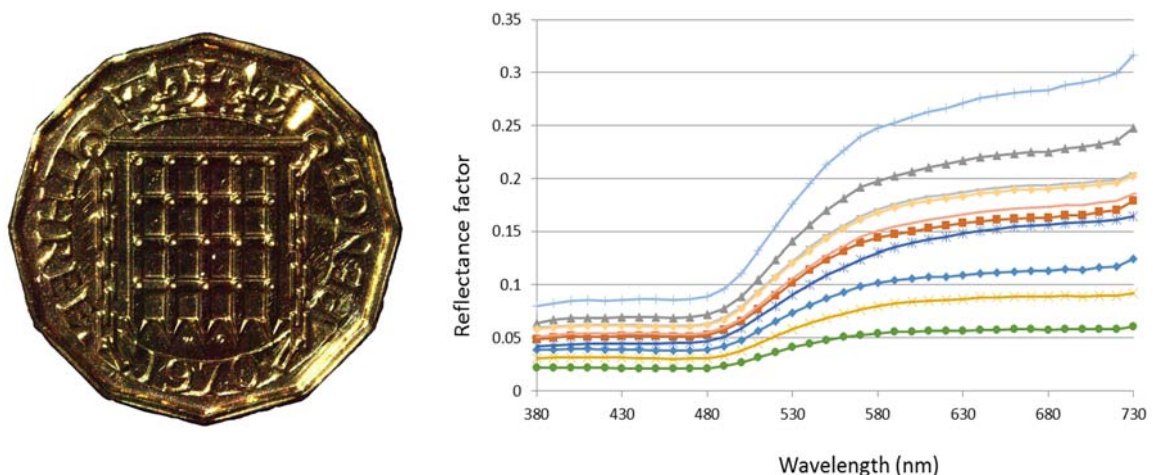


*Figure 1. (left) Reverse of gold-plated threepence; (right) Reflectance spectra of 10 measurements.*

This is especially true of gold, which combines glitter, specularity and sheen over a wide range of angles to give it a uniquely lustrous quality that sets it apart from ordinary materials.

To specify the colour of gold only by a single colorimetric triplet, or even by a single reflectance spectrum, would be dull indeed. As an example, a freshly gold-plated silver English threepence was selected as a test object and measured with an Xrite i1Pro spectrophotometer. The spectral reflectance distributions from 10 successive measure-ments are shown in Fig. 1. The characteristic rise in reflectance at 540nm corresponds to an energy band at 2.3 eV in pure gold where free electrons in the d-band can make the transition to unoccupied states in the conduction band (Saeger & Rodies, 1977). It is evident in the set of measurements that, although the shape of the curve remains the same, the magnitude of the reflectance varies by a factor of 5. This can be explained by the measurement geometry of the instrument, which is designed for measurement of flat surfaces, such as prints on paper, which may or may not be glossy. The 45° angle of incident light and 0° angle of view for the sensor ensures that the specular component of reflection is avoided. But when the instrument is removed and then brought back each time with the aperture in a different position over the relief surface of the coin, a different distribution of scattered light reaches the sensor and the reading changes. The majority of the variation in the measured colorimetric values is in the luminance, not the colour: in CIE 1931 chromaticity the range in $x,y,Y$ is [0.3988±0.0023, 0.4000±0.0013, 19.75±4.38] and in $L^*a^*b^*$ the corresponding range is [51.18±5.04, 44.79±0.04, 26.40±2.13].

## 2. DOME IMAGE PROCESSING

The dome imaging system at UCL enables sets of images of an object to be taken with illumination from different directions. A hemisphere of 104 cm diameter is fitted with 64 flash lights, calibrated so that the geometric centroid coordinates of every light source are known to within 3mm (MacDonald *et al*, 2015). A Nikon D200 digital camera at the 'north pole' captures a series of 64 colour images, each illuminated from a different direction and all in pixel register. This enables the object to be visualised from a fixed viewing angle, i.e. vertically from above, for many different angles of incident light. Image sets captured by the system can be visualised by the polynomial texture mapping (PTM) technique, which has numerous applications in archaeology and cultural heritage (Earl *et al*, 2010).
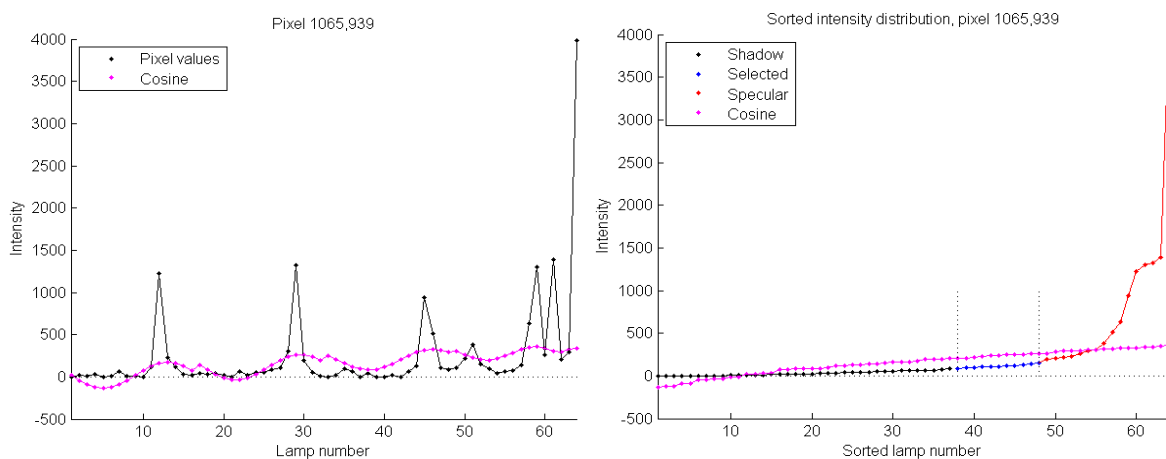


*Figure 2. Intensity distributions for a single pixel: (left) in lamp order; (right) sorted.*

The difficulty with gold, and indeed with all shiny and glossy materials, is that they reflect strongly in the specular direction. So in the vector of 64 intensity values for any pixel, there are a few values much larger than the others, corresponding to positions where the surface normal is close to the bisector of the angle between the illumination vector (toward the light) and the view vector (toward the camera). This results in images with high dynamic range

where a few pixels may be 100 times greater in value than the majority. In the dome, images are captured and processed as linear 16-bit per channel (range 0–65535), setting the lens aperture to *f*/11 to avoid over-exposure. Fig. 2 shows the intensity distribution for a single pixel on the rim at the upper left edge of the coin. One value is ~4000 and five are in the range 1000–1500 but most others are less than 200. The magenta curve shows what the intensities would be for a perfectly matte (Lambertian) surface with the same albedo and normal angle. It is clear that the specular peaks are much greater in intensity than the cosine, but all other values are lower. Thus the metallic gold surface is generally darker than the diffuse equivalent, except for a few bright highlights.
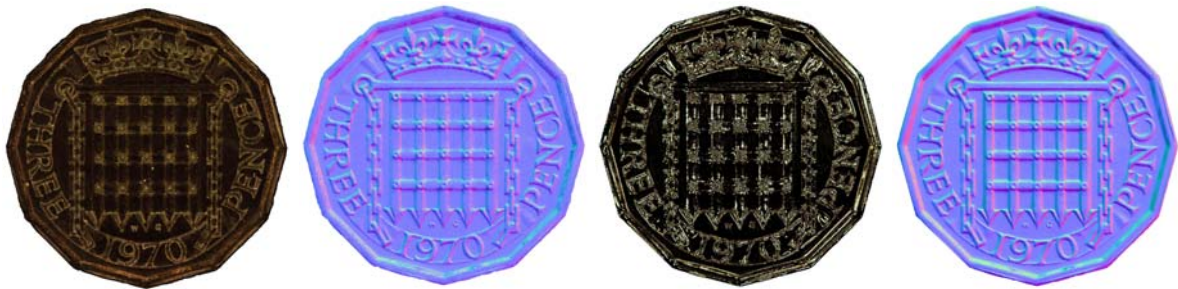


*Figure 3: Image components derived from processing the original set of 64 images: (left to right) albedo, normals, specular colour, specular normals.*

The processing method is to identify from the intensity distribution of a 3x3 pixel neighbourhood (9x64=576 values in total) a range of 100 values between the shadow and specular regions, which are taken to be representative of the non-specular 'body colour' of the object (the blue dots in Fig. 2 right). Then using the principle of 'shape from shading', a regression is performed on the corresponding lamp vectors to estimate the most probable direction of the surface normal at that pixel (MacDonald, 2014). The albedo is the magnitude of the normal vector, and its appearance is surprisingly dark (Fig. 3 left). The surface normals are represented in Fig. 3 by the standard false-colour coding with X values in red, Y in green and Z in blue. Note that the image set was taken with a Nikkor 200mm macro lens plus a 40mm extension ring, so the coin diameter of 21.0 mm spans 2060 pixels in the image. This means that the spatial resolution is 98 pixels/mm, i.e. 1 pixel represents 10.2 microns on the surface of the coin.
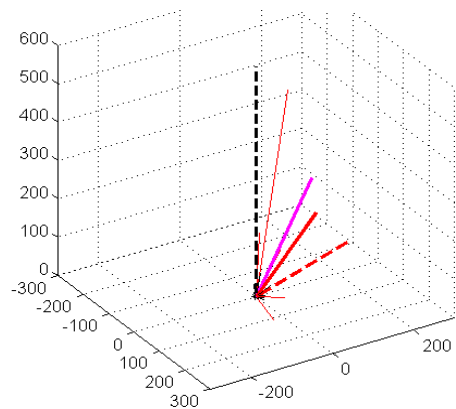


*Figure 4. Vectors for a single pixel, showing view vector (black), normal (magenta), ideal specular (red dashed) and computed specular (thick red).*

The second stage of processing is to determine the specular vector at each pixel, i.e. the direction of maximum specular reflectance. First the ratio, or specular quotient, is calculated between the actual intensity value and the diffuse component for each lamp. (This would be the black value divided by the magenta value for each of the 64 points in Fig. 2.) For semi-matte surfaces the quotient values are typically in the range 0.5 to 2.5, but for high gloss and shiny metallic surfaces they may be very large. In this case the maximum value over the image of the coin is 3,878 which is indicative of the high dynamic range of the imagery. To facilitate the computation, a compression function is applied to the quotient by a power function with fractional exponent. In this case an exponent of 0.5 (i.e. square root) has been used, giving a maximum

quotient value of 62.3. A weighted sum is made of all the normalised lamp vectors above a threshold of 0.2 and within 60° of the normal vector, using the magnitude of the quotient as the weighting factor. For the pixel in Fig. 2 there are five specular vectors, shown by the thin red lines in Fig. 4, with the result shown by the thick red line. One might suppose that the specular angle should be exactly double that of the normal, as it would be for a perfect mirror surface, but in fact there is a great deal of variation. This is caused not only by noise, but also by the fixed sampling positions on the dome. Moreover granularity and surface imperfections, such as scratches and dust, cause perturbations in the direction of the strongest reflectance. The scatter is clear when the specular angle wrt the Z axis is plotted against



*Figure 5. Specular vs normal angles for 10,000 random points in image.*

the normal angle for 10,000 points randomly selected throughout the image (Fig. 5). Instead of lying along the line of slope 2 they are spread over a wide range of angles, both greater than and less than the normal angle. The horizontal lines of red dots in the figure are computational artefacts, where the specular vector lies exactly toward the lamp, so they indicate the incident angles of the five lamp tiers in the dome at 10°, 27°, 45°, 63° and 80°.

The specular colour at each pixel is computed from the colours of the selected specular values, using the same weighting factors derived from the specular quotients. The resulting colour for the whole coin is shown in Fig. 2 (centre right) and it is apparent that the colour balance is slightly greenish, certainly less red than the albedo. The relationship can be explored by plotting corresponding values for a random selection of 10,000 points throughout the image area. In Fig. 6 albedo colours are shown as black dots and the specular colours as red dots in a normalised R,G,B cube. Also shown are lines representing the first principal component of each cluster of points, which tend in different directions. The albedo (body colour) is darker and on the red side of the neutral axis, whereas the specular colour is



*Figure 6. Specular vs albedo colours for 10,000 random points in image.*

lighter and on the green side of the neutral axis. Both are below neutral on the blue axis, meaning that both are yellowish. (Note that all images were taken with the Nikon camera white balance set to 'flash', not auto-white, and that the images were corrected to ensure that equal values of R,G,B would correspond to neutral grey, before the image processing was undertaken.) The two vectors in RGB colour space (denoted by the red and black lines in Fig. 6) may be considered as equivalent to the interface and body colours identified by Shafer (1985) in his proposal for a dichromatic model of reflection from a material surface.
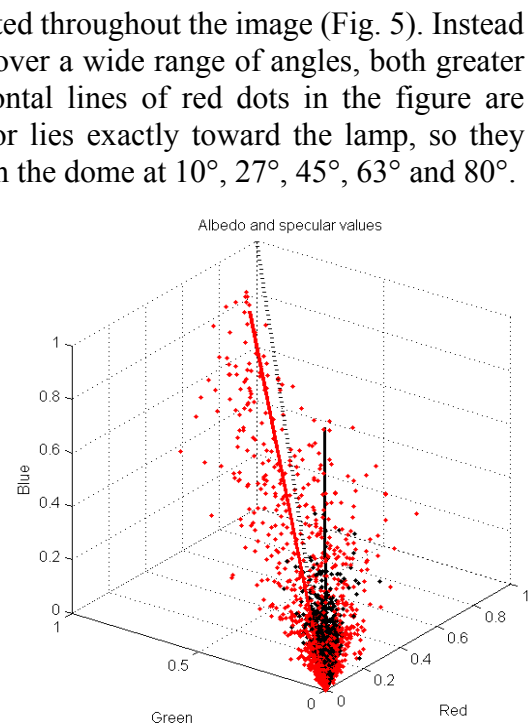
## 3. IMAGE RENDERING

The distribution of the specular quotient around the specular peak angle has been found for a variety of materials to be modelled well by a modified Lorentzian function (MacDonald, 2014), which takes the form of a curved peak plus a linear flank:

$$f(\omega) = \frac{p_a}{1+(\omega/p_s)^{p_e}} + \left(1 - \frac{\omega}{180}\right) \tag{1}$$

where $\omega = \text{acosd}(\mathbf{L} \cdot \mathbf{S})$ is the specular radial angle in degrees between the lamp vector and specular vector. Thus the distribution is characterised at each pixel in terms of three parameters: $p_a$ is the amplitude, $p_s$ is the scale and $p_e$ is an exponent. The flank is not fitted to the distribution of quotient values, but is assumed to be an invariant cone of value 1 at the apex and 0.5 at 90° from the specular vector. In this model the exponent $p_e$ of the peak term is not constant = 2, as for a standard Lorentzian, but can vary over the range 1-10. The parameters of the curve are determined for each pixel from the distribution of specular quotient values in the polar plane. The angle of the specular vector is translated to the centre of the plane, and the angles of all incident lamp vectors are translated by an equal amount. Delaunay triangulation is applied to the distribution of points on the polar plane; when plotted as a mesh in 3D, with quotient value on the Z axis, the distribution forms a polyhedral central peak surrounded by an irregular flank (Fig. 7).
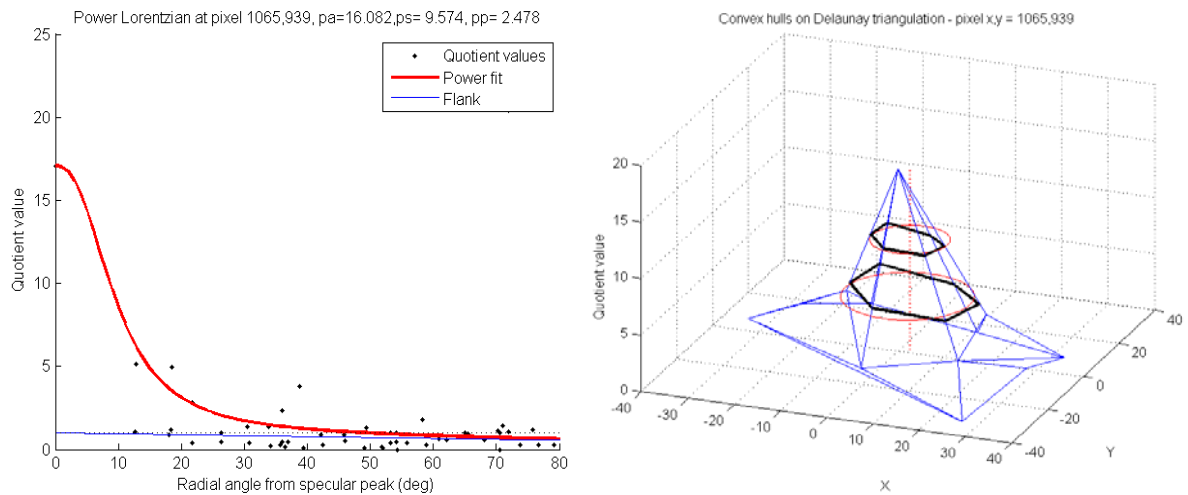


*Figure 7. (left) Lorentzian distribution of intensity as a function of radial angle;*
*(right) Profile modelled on the polar angle plane, fitting to Delaunay triangulation.*

The complete model for rendering images under a single light source adds the diffuse and specular terms:

$$A_m I = \mathbf{L} \cdot \mathbf{N} A_{rgb} + (f(\omega) - 1) S_{rgb} A_m / S_m \tag{2}$$

where $A_{rgb}$ is the albedo colour, $S_{rgb}$ is the specular colour, $A_m$ is the monochrome albedo (weighted sum of the R,G,B channels of $A_{rgb}$), and $S_m$ is monochrome specular intensity. This gives images that are realistic in appearance and a good match to actual photographs (Fig. 8). It is important to recognise that the specular reflection is not isolated at the specular peak angle, but extends over a wide range of angles. Without this broad flank in the specular reflectance distribution the rendering would be darker with scattered pinpoint highlights and would not be realistic.

AIC2015 TOKYO - Color and Image

Figure 8 juxtaposes the actual photographic image taken in the dome illuminated by lamp 60 with the image rendered by Eq. 2. Although not identical, the two are similar in terms of the overall tonality and distribution of highlights. Because the model is based on a continuous function of angle, images can be rendered for a virtual light source at any position in the hemisphere.



*Figure 8. (left) Photographic image for dome lamp 60; (right) image rendered with light from same direction.*

Thus the colour of gold can be represented as a sum of two components: a dark reddish-yellow 'body colour', the albedo corresponding to the diffuse reflectance from the material, plus a bright greenish-yellow highlight with a broad angular distribution around the specular peak. A more complete model would need to take into account the Fresnel effect, which causes the spectrum of the reflected light to flatten at angles of incidence greater than 70° (Cook & Torrance, 1982). This is confirmed by observations of gold materials in which the perceived colour changes from yellowish, when the incident light is normal to the surface, to whitish as the angle of incidence is increased (Okawaza & Komatsu, 2013). Conversely, multiple reflections from facets on the surface cause the spectrum of the reflected light to be multiplied and hence to appear darker and more saturated. When the object is diffusely illuminated, with incident light from many directions, the characteristic golden radiance suffuses the whole surface and brings it to life.

## REFERENCES

Cook, R.L. and Torrance, K.E. (1982). *A reflectance model for computer graphics*. ACM Transactions on Graphics, 1(1):7-24.

Earl G., K. Martinez and T. Malzbender (2010). *Archaeological applications of polynomial texture mapping: analysis, conservation and representation*, J. Archaeological Science, 37(8):2040-2050.

MacDonald, L.W. (2014) *Colour and Directionality in Surface Reflectance*, Proc. Conf. on Artificial Intelligence and the Simulation of Behaviour (AISB), April 2014.

MacDonald, L.W., A.H. Ahmadabadian and S. Robson (2015). *Determining the Coordinates of Lamps in an Illumination Dome*. Proc. SPIE Conf. on Optical Metrology, Videometrics, Range Imaging and Applications, Munich, June 2015.

Okazawa, G. and Komatsu, H. (2013). *Image statistics for golden appearance of a painting by a Japanese Edo-era artist Jakuchu Ito*. Proc. Computational Color Imaging Workshop (pp. 68-79). Springer.

Saeger, K.E. and J. Rodies (1977). *The colour of gold and its alloys*. Gold Bulletin, 10(1):10-14.

Shafer, S.A. (1985). *Using Color to Separate Reflection Components*, Color Research & Application, 10(4):210-218.

*Address: Dr Lindsay MACDONALD, 3DIMPact Research Centre,*
*Department of Civil, Environmental and Geomatic Engineering,*
*University College London, Gower Street, London, UK*
*E-mail: lindsay.macdonald@ucl.ac.uk*

# Preferred LED lighting for wood surfaces and colored surfaces

Markus REISINGER[1]

[1] Lucerne School of Engineering and Architecture

## ABSTRACT

The usage of Light Emitting Diodes (LEDs) as light sources in architectural lighting applications is quickly increasing. The present research addressed questions of material appearance by comparing effects of different LED-spectra. Preferred visual appearance is accessed for a set of 12 colors taken from the Natural Color System (NCS) catalog and a set of 8 types of wood surfaces. The results of this study demonstrates that certain hues fit better to lighting with higher correlated color temperature (cooler light) and other hues fit better to lighting with lower CCT (warmer light). Concerning the appearance of the wood surfaces the results are not fully conclusive. The observed reactions lead to the assumption that mainly hue determines the correlated light temperature of the LED light source that is preferred.

## 1. INTRODUCTION

The perceived atmosphere of an interior space is a whole of all consisting elements. Lighting as part of this constructed environment influences the visual appearance of objects and materials. A previous study (Lasauskaite Schüpbach, Reisinger and Schrader, 2015) evaluating lighting preferences for surfaces demonstrated that choice of the optimal lighting depends on the material and its typical characteristics. Light sources with a CCT of 3000K are preferred for red carpet and synthetic turf materials. For light blue flagstone and blue MDF materials light sources with 4000K CCT are preferred. Conversations with design experts, interior architects and architects are supporting the assumption to use warmer light for warm hues and cooler light for cooler hues. The first hypothesis tested is that people have clear preferences for warm or cold lighting, depending on the hue of the surface. Among lighting specialists it is well accepted that human skin and natural materials as wood surfaces suit better than others to judge lighting quality. The second part of the study is of explorative character and concerned with the appearance of different types of natural wood surfaces.

## 2. METHOD

In this study appearance of 12 color samples from the Natural Color System (NCS) catalog and 8 different types of wood are examined. Comparison is done side by side using two cabinets illuminated by LED light sources of different color temperature.

### 2.1 Materials

Two sets of materials are used to evaluate light preferences. The first set consists of 12 samples of NCS colors (NCS, Sweden). This are 4 highly saturated colors in yellow, red, blue, green and 4 saturated colors in hues exactly positioned in between. In the NCS hue

circle this 8 samples show equal distances and include the two major axes with the so called unique hues. The latter mentioned hues were additionally presented in pastel versions.



*Figure 1: Set of 12 NCS color samples.*

Precise technical characteristics of the used color samples are found in table 1.

*Table 1. Characteristics of the 12 color samples.*

| NCS-color tone | NCS lightness | CIE Yxy | | | CIE La*b* | | |
|---|---|---|---|---|---|---|---|
| | | Y | x | y | L | a* | b* |
| S0580-Y | 0.86 | 65.1 | 0.48 | 0.48 | 84.5 | 6.1 | 99.5 |
| S0580-Y50R | 0.62 | 34.5 | 0.55 | 0.40 | 65.4 | 46.6 | 69.0 |
| S1080-R | 0.32 | 11.7 | 0.57 | 0.32 | 40.8 | 58.3 | 28.9 |
| S3055-R50B | 0.3 | 10.6 | 0.30 | 0.21 | 38.8 | 33.6 | -27.9 |
| S1565-B | 0.45 | 21.6 | 0.18 | 0.24 | 53.6 | -24.7 | -36.3 |
| S2060-B50G | 0.48 | 24.0 | 0.20 | 0.34 | 56.1 | -45.6 | -9.6 |
| S1565-G | 0.52 | 26.9 | 0.25 | 0.45 | 58.9 | -53.4 | 19.5 |
| S0565-G50Y | 0.78 | 54.0 | 0.40 | 0.49 | 78.4 | -22.6 | 66.4 |
| S0520-Y50R | 0.86 | 67.8 | 0.38 | 0.36 | 85.9 | 13.6 | 22.8 |
| S0520-R50B | 0.85 | 67.7 | 0.31 | 0.31 | 85.8 | 7.6 | -8.6 |
| S0520-B50G | 0.88 | 73.3 | 0.29 | 0.33 | 88.6 | -14.2 | -2.9 |
| S0520-G50Y | 0.93 | 82.3 | 0.34 | 0.38 | 92.7 | -9.9 | 23.7 |

*Note.* CIE Yxy for 10° observer. La*b* reference light D65.

The second set consists of 8 types of wood surfaces: Fir, Staghorn sumac wood, Maple wood, Poplar, Red oak, Robinia, Beech wood and Plum wood. Color properties of these samples are described by their typical spectral reflection characteristics (see Fig. 2).
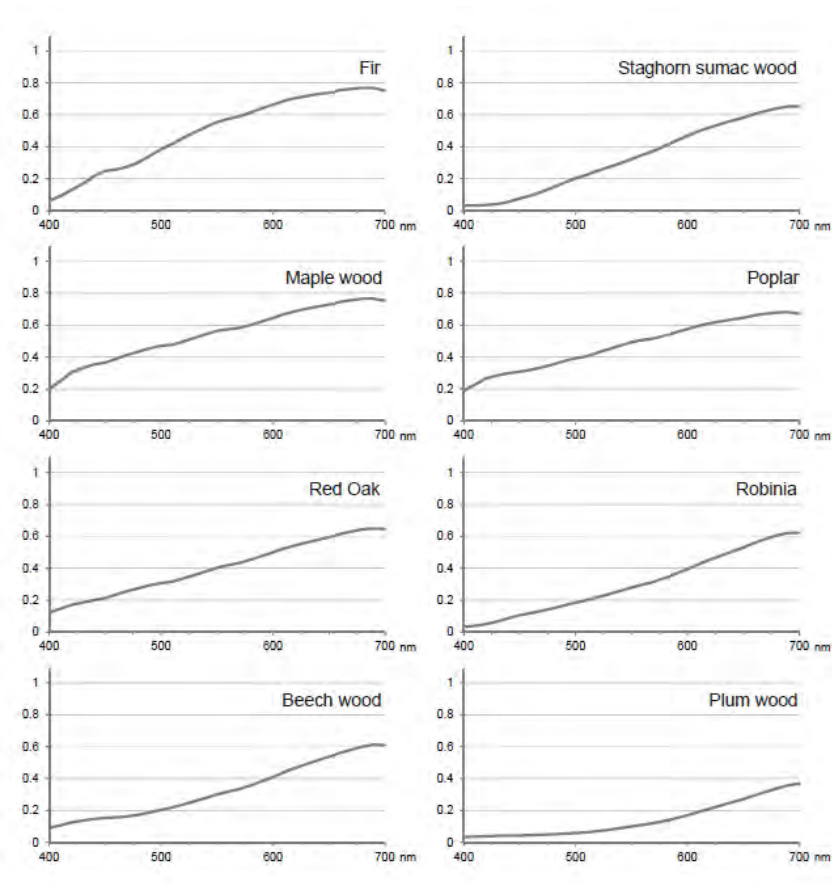
*Figure 2: Spectral reflectance curves for the 8 wood samples*

Visual preference is accessed by comparing visual appearance under two light conditions. Both scenes are illuminated with LED light sources: warm light with a CCT of approx. 3000K and cold light with a CCT of approx. 4000K. The Color Rendering Index (CRI) is for all used light sources (Xicato, USA) above 95. The average illumination level in both cabinets is 1400 lx. Measurements are done using a Illuminance Meter T-10 (Konica Minolta Sensing, Japan).



*Figure 3: Two lighting cabinets illuminated by LED light sources of different CCT.*

All participants assessed visual appearance by viewing the samples in front of a grey neutral background.

## 2.2 Procedure

27 interior architecture students (25 women: mean age 25 years) are participating in the experiment. None of the participants had color deficiency which is assessed with the Ishihara, 1999 color deficiency test. By performing a forced choice task participants expresses their preference for one out of two light conditions. The study design is within-persons (all participants are confronted with all experimental conditions).

## 3. RESULTS AND DISCUSSION

The light preferences for each of the 12 NCS samples are shown in Fig. 4. To address the question if materials are preferred under cold or warm light in a statistical manner, nonparametric two-tailed binomial tests are executed. Tests for light preferences on each of the materials are done with significance at 0.05 level using the IBM SPSS 22 statistical software package. The proportion of students' preferences is compared to 50% (chance level). The tests reveal, that participants have significant preference seeing red (NCS S1080-R) under the warm light condition, $P = 0.002$. The warm light is also preferred for purple color (NCS S3055-R50B), for the blue (NCS S1565-B) the cold light condition is preferred. However in both cases the difference from chance level only approached significance ($P = .052$). The proportion of preferences for other 9 materials does not significantly differ from the chance ($P > .12$).
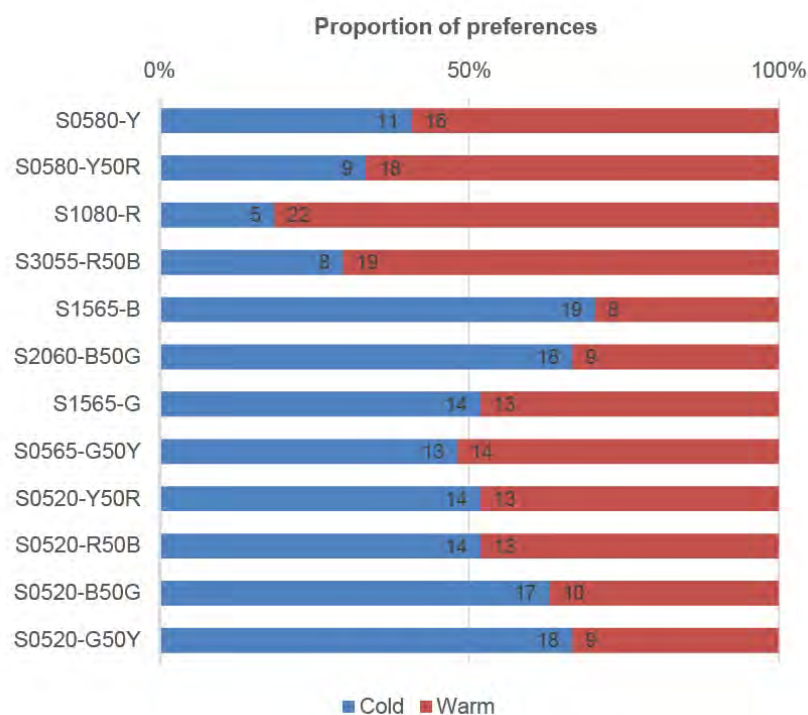


Figure 4: Preferences for appearance of 12 NCS color samples in coolish or warmish light.

The results for the 8 wood surfaces are summarized in Fig. 5. The descriptive percentage of light preference reveals that staghorn sumac wood is rather preferred in warm light condition, whereas appearance of robinia is preferred in cold light condition. Statistically are this differences not significant, but they point out that choice of wood type may ask for specific light considerations.
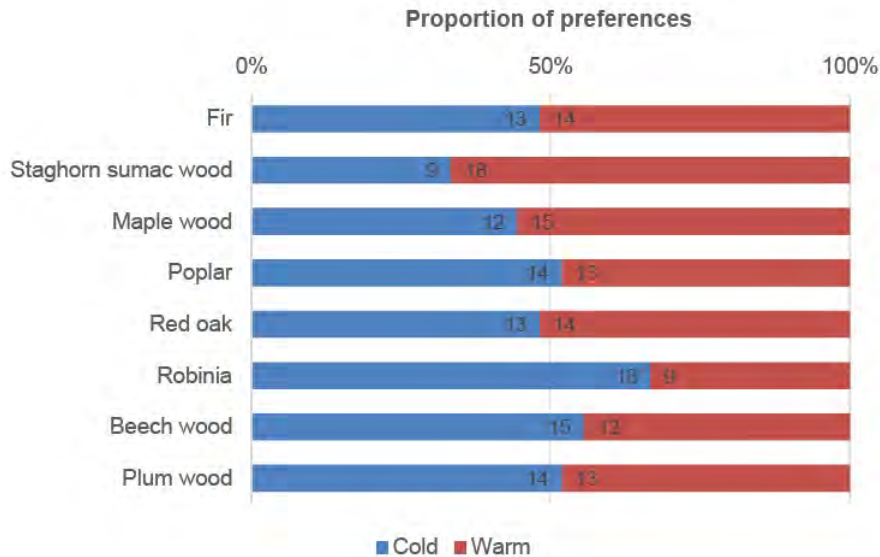


*Figure 5: Preferences for appearance of 8 wood samples in coolish or warmish light.*

.

## 4. CONCLUSIONS

The study confirmed that LED lighting with a CCT of 3000K is generally preferred for reddish hues. Light that fosters a cooler visual impression (CCT of 4000K) is generally preferred for bluish hues. Preferences for other hues and the pastel samples did not differ significantly from chance level. The explorative study about appearance of different wood types is not fully conclusive. Although it has shown that cooler light suit certain wood surfaces as robinia better, it cannot be explained by the measured spectral reflection characteristics. It can be assumed that for wood surfaces besides the reflection characteristics, respectively the hue, also grain, texture pattern and gloss might influence light preference.

In this study light sources with excellent color rendering characteristics are used, hence visual appearance for all samples is very close to the appearance under a CIE reference source. Although it is known from literature that visual preference of colors relates specifically to vividness and naturalness of its appearance (Bodrogi et. al., 2013), the use of LED types that emphasize vibrancy of colors is not considered for the reported experiment. All observed effects on preference thus can be attributed to the difference in correlated color temperature of the chosen LED light sources.

**REFERENCES**

Bodrogi, P., S. Brückner, T.Q. Khanh, and H. Winkler. 2013. *Visual Assessment of Light Source Color Quality*. Color Research & Application 38(1) 4-13.

Ishihara, S. 1999. *Ishihara's Tests for Colour Deficiency*. Tokyo: Kanehara & Co.

Lasauskaite Schüpbach, R., M. Reisinger, and B. Schrader 2015. *Influence of Lighting Conditions on the Appearance of Typical Interior Materials*, Color Research & Application 40(1) 50-61.

*Address: Markus REISINGER, Department of Interior Architecture, Lucerne School of Engineering and Architecture,*
*Technikumstrasse 21, 6048 Horw, SWITZERLAND*
*E-mail: m.reisinger@lightingresearch.eu*

# Development of a facial imaging system and new quantitative evaluation method for pigmented spots

Kumiko KIKUCHI,[1,2] Yuji MASUDA,[1] Tetsuji HIRAO,[1] Kiyoshi SATO,[1] Yoko MIZOKAMI,[2] Hirohisa YAGUCHI[2]

[1] Shiseido Research Center

[2] Graduate School of Advanced Integration Science, Chiba University

## ABSTRACT

The quantitative evaluation of skin color and skin chromophore distribution is important in dermatology, physiology, pharmacology, and cosmetic science. Various methods that evaluate facial pigmentation using image analysis have been proposed. These models provide visual information about the melanin distribution; however, the current methods cannot provide quantitative information on individual pigmented spots such as variation in size, shade of color, and distribution pattern. In this study, we describe our facial imaging system and pigment-specific image-processing techniques, and we also propose an image evaluation method that focuses on the analysis of individual pigmented spots on a wide area of the face. First, a facial imaging system that is equipped with an illumination unit and a high-resolution digital camera was developed. Facial images were captured and converted to *XYZ tristimulus values* from RGB values based on calibration using skin color chips. Next, to determine the melanin and hemoglobin concentration, we established pigment-specific image processing techniques based on relational expressions between *XYZ tristimulus values* and skin chromophore concentration. Finally, to obtain the features of individual pigmented spots in a cheek image, we established a simple object-counting algorithm that calculates spot size, colorimetric value, melanin concentration, and other features. Experimental results confirm that our system provides a reliable measurement with high precision and repeatability for skin color distribution on a wide area of the face. Applying the new methodology for individual pigmented spots to cheek skin images, the age-related changes of pigmented spots were clearly demonstrated. In conclusion, our techniques for skin color and individual pigmented spots allow us not only to determine the visual information about the melanin distribution, but also to understand the characteristics of individual pigmented spots on the face.

## 1. INTRODUCTION

The quantitative evaluation of skin color and skin chromophore distribution is important in dermatology, physiology, color science, and cosmetic science. Various studies have been conducted on the development of methods to evaluate facial pigmentation using image analysis (Tsumura, Haneishi, and Miyake, 1999; Masuda et al., 2001). These methods are based on the optical properties of light interaction with the components of the skin and provide visual information about the melanin distribution. However, such methods have not addressed in detail the quantitative information of individual pigmented spots, such as variation in size and colorimetric values or distribution patterns. In this study, we describe a facial imaging system that provides a reliable measurement for skin color distribution and pigment-specific image-processing techniques, and we also propose an image

evaluation method that focuses on the analysis of individual pigmented spot on a wide area of the face.

## 2. METHOD

This paper is organized as follows: Section 2 of the paper discusses the facial imaging system and algorithm that provide colorimetric values for skin, having high accuracy, simplicity, and reproducibility. It also proposes a pigment-specific image processing technique based on a relational expression between *XYZ tristimulus values* and skin chromophore concentration. Furthermore, it describes an object-counting algorithm that evaluates the individual pigmented spots. In Section 3, we performed validation tests of the imaging system and investigated the age-related changes of pigmented spots and skin color by applying the new methodology, and Section 4 concludes the paper.

### 2.1 Facial Imaging System and Quantification of Color Values

We developed a facial imaging system that consists of an illumination unit and a high-resolution digital camera (Figure 1). The illumination unit employs fluorescent lamps (FPL30EX-D; Toshiba, Tokyo, Japan) with a correlated color temperature of 6,700 K. The lamps were designed to provide diffuse illumination over a wide field of the subject's face to eliminate shadows and artifacts from specular reflections. Figure 2 shows the lightness distribution on a mannequin model, which indicates that the illumination unit is sufficiently accurate for analyzing facial skin color. A Canon CMOS digital photo-camera (EOS Kiss X3; Canon, Tokyo, Japan) containing of 4,500 (horizontal) × 3,000 (vertical) effective picture elements was used. It was equipped with a Canon lens (EF 35 mm F2; Canon, Tokyo, Japan). Facial images were captured with a neutral gray color chip (Murakami Color Research Laboratory, Tokyo, Japan) as the standard for color and brightness and stored as uncompressed tagged image file format (TIFF) images at a resolution of 1,500 × 1,500 pixels and 72 dots per inch (dpi).
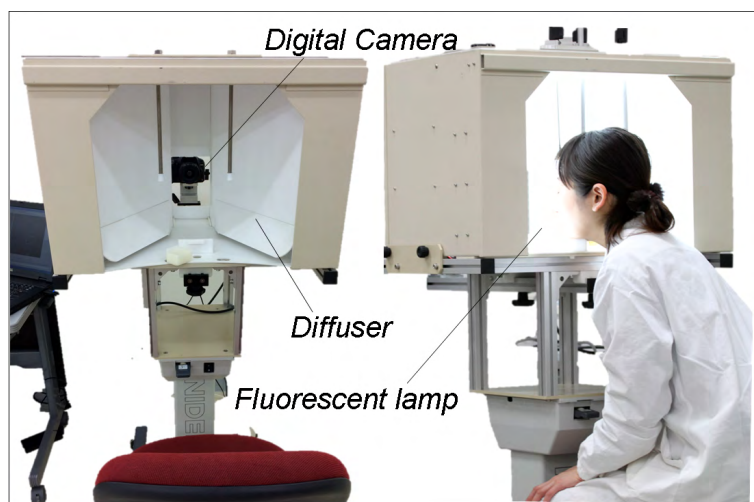


*Figure 1: Facial imaging system.*
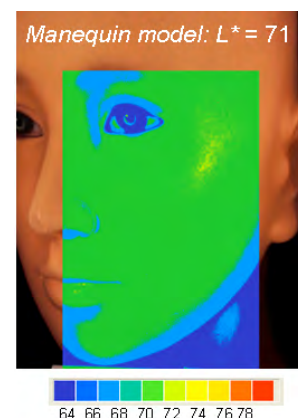


*Figure 2: Lightness distribution of a mannequin model.*

To ensure highly accurate conversion from linear RGB to *XYZ tristimulus values*, particularly in the skin color range, 100 color chips were selected based on experimentally acquired skin color data. Each color chip was captured by the imaging system to obtain all RGB color signals outputted from the camera and were measured with a contact-type spectrophotometer (CM-700d; Konica Minolta Sensing, Tokyo, Japan) to obtain the *XYZ*

*tristimulus values*. The RGB image information was converted into XYZ data using values obtained by multiple regression analysis. The conversion expressions are written as follows:

$$X = 0.001645R + 0.001116G + 0.000314B + 2.585143$$

$$Y = 0.001110R + 0.002080G + 0.000065B + 2.359088$$

$$Z = 0.000439R + 0.000610G + 0.002439B + 2.757769$$

Figure 3 shows the relationship between the *XYZ tristimulus values* measured using a spectrophotometer and the estimated values obtained from the digital camera data. In addition, values in the L*a*b* color space (1976 CIELAB) were calculated from the *XYZ tristimulus values* using this system.



*Figure 3: Comparison of XYZ values from a spectrophotometer and those converted from digital camera data.*

## 2.2 Conversion from XYZ Values to Skin Chromophore Concentration

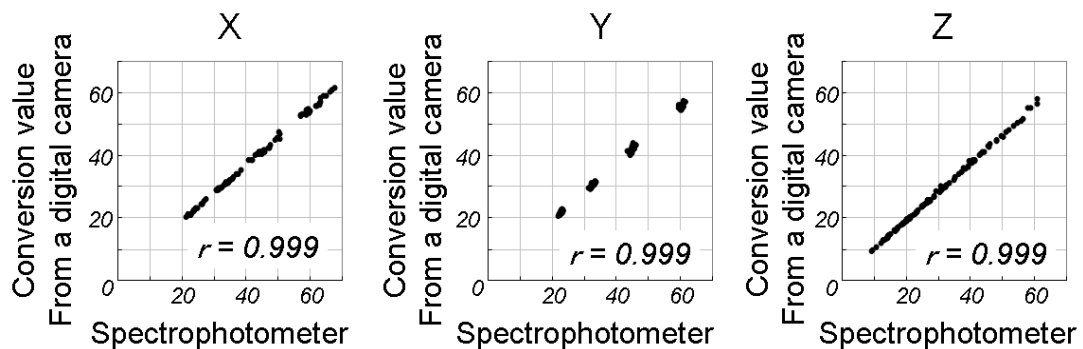To determine melanin and hemoglobin concentrations, we established pigment-specific image processing techniques based on relational expressions between *XYZ tristimulus values* and skin chromophore concentration. In previous studies, skin chromophore concentration (i.e., melanin and hemoglobin) was calculated from skin spectral reflectance (Shimada et al., 2000; Masuda et al., 2009). These studies suggested that the skin chromophore concentration could be calculated by a multiple regression analysis, assuming that the absorbance spectrum is a linear sum of the absorbance spectra of melanin, oxygenated hemoglobin, and deoxygenated hemoglobin. Here, we suggest that the concentration of melanin and total hemoglobin can be estimated from *XYZ tristimulus values* obtained from a color image. Spectral reflectance data from the cheeks of 60 women were obtained using a colorimeter. The *XYZ tristimulus values* were calculated from the spectral reflectance of the skin for an illuminant D65 and 2° visual field. In addition, the concentrations of melanin and total hemoglobin were calculated according to methods in the previous studies. A linear regression equation to predict the concentration of melanin was then determined using multiple regression analysis with the logarithm (base 10) of the inverse *XYZ tristimulus values* as independent variables and melanin concentration as a dependent variable. Similarly, we used regression to predict the hemoglobin concentration. The melanin and hemoglobin concentration were calculated according to the following equations.

$$\text{Melanin index} = -4.861\log_{10}(1/X) + 1.268\log_{10}(1/Y) + 4.669\log_{10}(1/Z) + 0.063$$

$$\text{Hemoglobin index} = -32.218\log_{10}(1/X) + 37.499\log_{10}(1/Y) - 4.495\log_{10}(1/Z) + 0.444$$

By fitting this equation to the XYZ images, we obtained the melanin and hemoglobin distribution images.

## 2.3 Detection and Quantification of Pigmented Spots

To quantify individual pigmented spots within a cheek image, we adopted an object-counting algorithm that enables us to calculate their size and colorimetric value. The melanin distribution images were used, and the regions of interest were manually selected. The algorithm for pigmented spot extraction consists of smoothing, binarization, region labeling, and candidate cropping. Various stages of this analysis are shown in Figure 4. In the smoothing step, images are processed using a Gaussian filter with a half-value width of 4.0 mm to correct the rough undulations of the surface (Figure 4(a)), and processed three times using a median filter of $5 \times 5$ pixels to remove spike noise (Figure 4(b)). After noise reduction, the melanin images are converted to binary images (Figure 4(c)) using a threshold optimized for the detection of pigmented spots. Furthermore, the connected-component labeling algorithm that gives each separate connected group of pixels a unique label is applied (Figure 4(d)) to calculate the number, sizes, and colorimetric values of the individual spots. Finally, spots are then identified as areas greater than 2 mm$^2$ to remove pores (Figure 4(e)).
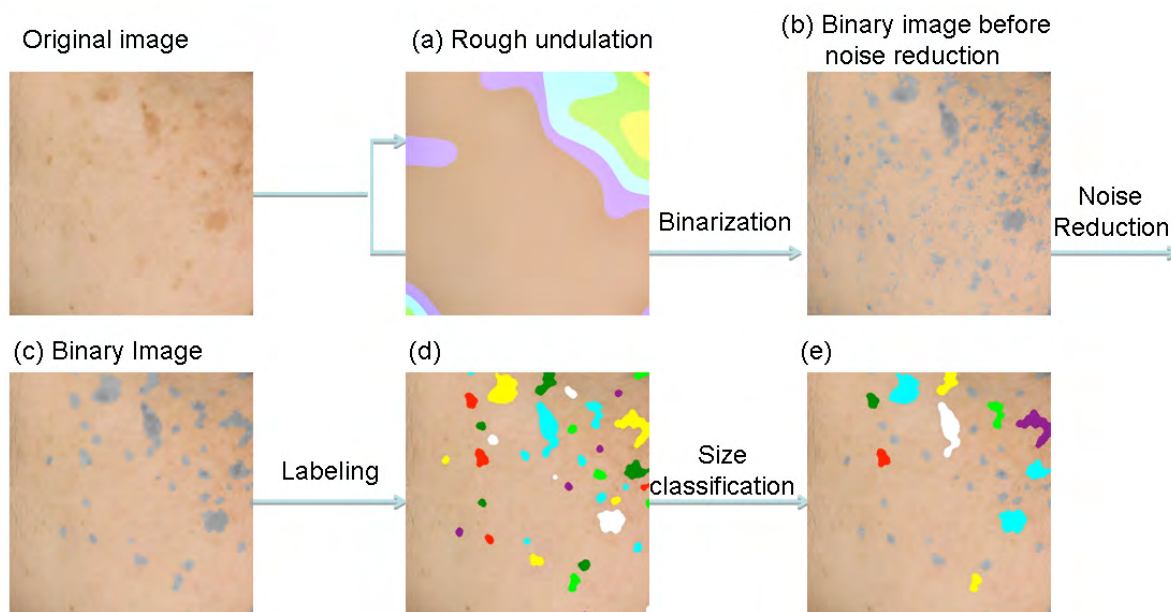


*Figure 4: Schematic flow of the image processing for pigmentation analysis.*

## 2.4 Method validation

To validate the accuracy of quantitative image analysis, the spectral reflectance of the cheek and lower eyelid of 32 Japanese women (age range 34–59 years; mean age 44.3 years) was measured using the contact-type spectrophotometer (CM-700d) with a probe head aperture of approximately 7 mm. At the same time, facial images of the same 32 subjects were obtained using the imaging system. In all facial images, regions of interest were selected in the same areas as those measured using the spectrophotometer. Melanin

concentration and L*a*b* values were calculated from the spectral reflectance, and the correlation between the two types of measurement system was determined.

## 2.5 Color Variation of Pigmented Spots Due to Aging

Applying the new methodology for skin chromophore and individual pigmented spot analysis to cheek skin images, we investigated the relationship between the characteristics of spot occurrence and age. Six-hundred and forty-three healthy Japanese women aged 20–80 years were enrolled in the study. They were classified into nine groups: 22 subjects in group A (20–24 years old), 76 in group B (25–29 years old), 76 in group C (30–34 years old), 76 in group D (35–39 years old), 76 in group E (40–45 years old), 76 in group F (45–49 years old), 76 in group G (50–54 years old), 76 in group H (55–59 years old), and 89 in group I (60–80 years old). Informed consent was obtained from all participants. Subjects washed their face and rested for 40 min under conditions of 23° C and 45% relative humidity.

## 3. RESULTS AND DISCUSSION

Figures 5(a)–(d) compare the values of the facial images of our system with those of the spectrophotometer for $L^*$, $a^*$, $b^*$, and melanin concentration in the cheek, respectively. The correlation coefficients between the spectrophotometer and facial images were higher than 0.900 for all parameters for the cheek. In addition, similar results were confirmed for the lower eyelids (data not shown). These results confirm that our system for facial imaging is sensitive enough to analyze not only colorimetric values but also melanin concentration with a good spatial distribution.
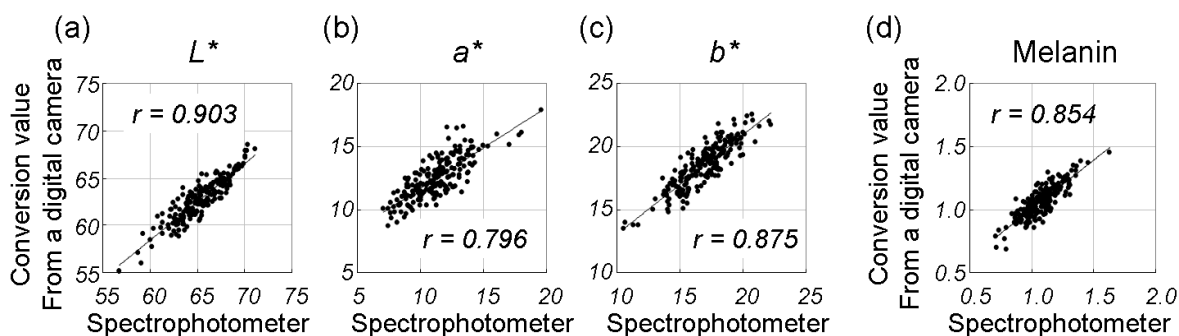


*Figure 5: Comparison between the facial imaging system and spectrophotometer results.*

The results of the cheek image analysis of 643 Asian women show that the proposed method is sufficiently sensitive to permit the measurement of colorimetric value, number, and size of individual pigmented spots. The differences of the parameters for each group were analyzed using one-way repeated analysis of variance. In this analysis, p-values less than 0.05 were assessed as statistically significant. Figure 6(a) shows that the number of spots per cheek on one side increased with age in a statistically significant manner (correlation coefficient of 0.613). The parameters of size and colorimetric values for spots on the cheek were plotted independently. The number of pigmented spots detected in the 643 women totaled 8,372. The size results indicate that there is a high probability of pigmented spots greater than 10 mm$^2$ in those older than 40 years (data not shown). Figure 6(b) shows that the colorimetric value $L^*$ of spots significantly decreased with age (correlation coefficient of −0.211). Figure 6(c) shows that the $C^*_{ab}$ of individual spots

significantly increased with age (correlation coefficient of 0.339). For the colorimetric value $h_{ab}$, no significant changes were observed (Figure 6(d)).



*Figure 6: Age-dependent spot changes: (a) number of spots per cheek on one side, values for (b) L\*,(c) C\*$_{ab}$, and (d) h$_{ab}$.*

## 4. CONCLUSIONS

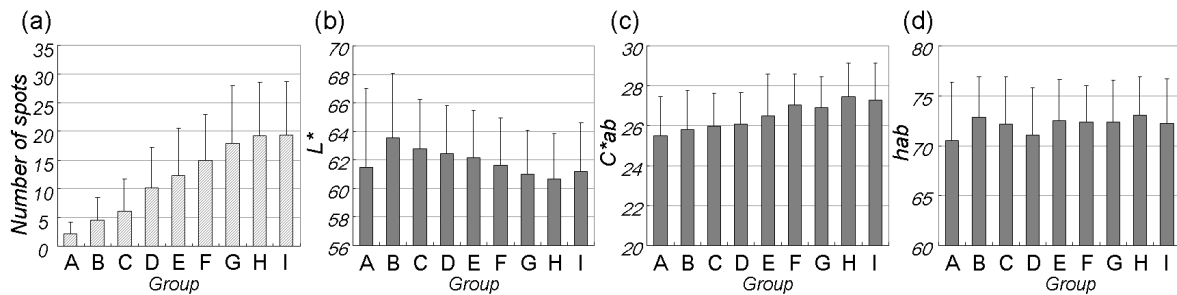Our techniques to determine skin chromophores and individual pigmented spots allow us not only to provide the visual information about the melanin distribution but also to understand the characteristics of various pigmented spots in a face. The results from our validation indicate that our system provides colorimetric data for skin that is highly accurate, simple to acquire, and reproducible. The data obtained in this study will be very useful for improving our knowledge about the aging of skin.

## ACKNOWLEDGMENTS

## REFERENCES

Tsumura, N., H. Haneishi, and Y. Miyake. 1999. Independent-component analysis of skin color image. *Journal of the Optical Society of America A* 16 (9): 2169-2176.

Masuda, Y., M. Takahashi, T. Sakamoto, M. Shimada, M. Itoh, and T. Yatagai. 2001. An innovative method to measure skin pigmentation. *Journal of the Society of Cosmetic Chemists of Japan.* 35: 325-332 (in Japanese).

Shimada, M., Y. Masuda, Y. Yamada, M. Itoh, M. Takahashi, and T. Yatagai. 2000. Explanation of human skin color by multiple linear regression analysis based on the modified Lambert-Beer law. *Optical Review* 7 (4): 348-352.

Masuda, Y., T. Yamashita, T. Hirao, and M. Takahashi. 2009. An innovative method to measure skin pigmentation. *Skin Research and Technology* 15 (2): 224-229.

*Address: Kumiko KIKUCHI, Shiseido Research Center, 2-2-1 Hayabuchi, Tsuzuki-ku, Yokohama 224-8558, JAPAN*

*E-mail: kumiko.kikuchi1@to.shiseido.co.jp*

*mizokami@faculty.chiba-u.jp*

*yaguchi@faculty.chiba-u.jp*

# Colour Preference and Harmony for Athletic Shoe Designs

Wei-Hsuan CHAO, Ji-Yuan HUNG, Chung-Chien LAN, Li-Chen OU
Graduate Institute of Color and Illumination Technology, National Taiwan University of
Science and Technology, Taiwan

## ABSTRACT

A psychophysical experiment was conducted using athletic shoes, a product commonly seen and used in our everyday activities, as an example to study colour preference and harmony. A total of 404 test images were generated from two original shoe images, one from Nike and the other from Adidas, each manipulated by varying the two-colour combinations of the shoe design, including the main colour of the shoe and the logo colour (i.e. the Nike tick and the Adidas stripes). Twenty observers with normal colour vision, including 10 males and 10 females, participated in the visual assessment. Each observer was asked to rate each shoe images using two 6-step semantic scales, like/dislike and harmonious/disharmonious. The experimental results show that the color preference rating relied strongly on the main colour of the shoe regardless of the logo colour, while the color harmony rating was affected not only by hue similarity but also lightness difference between the main colour and the logo colour.

## 1. INTRODUCTION

Colour preference and harmony have both been concidered the most essential factors in the design of colour combinations. The relationship between these two attributes of colour has been extensively studied. For example, Schloss and Pamer (2011) recently found that colour preference and harmony both tended to increase as hue similarity increases, while preference relies more strongly on component color preference and lightness contrast. Nevertheless, most existing studies of colour preference and harmony, including Schloss and Palmer's research as mentioned above, have used abstract, contextless colour patches as the stimuli in the experiments. It is still unclear whether the results can also apply to real-world product designs. To address this issue, athletic shoes, a product commonly seen and used in our everyday activities, were taken as an example in our study of colour preference and harmony.

Basic shoes of two brands, Nike and Adidas, were selected to generate the experimental images. Aims of the study included (1) using recoloured images in two athletic shoes as the stimuli, (2) using colours from real athletic shoes on the market to generate test images as the stimuli, and (3) the results would be analysed for the effects of hue and lightness difference on colour preference and harmony.

## 2. METHODS

For each shoe image, two areas were recoloured according to the following definitions: (1) the "logo colour" means the logo shown on the shoe (i.e. the Nike tick and the Adidas stripes); (2) the "main colour" means the main body of the shoe. Colour preference was defined as how much the observer liked the combination of the logo colour and the main colour. Colour harmony was defined as how well the logo colour and the main colour went together as shown in the shoe images.

For logo colours, we selected four tones, saturated (S), light (L), muted (M) and dark (D), each consisting five hues, red (R), yellow (Y), green (G), blue (B) and purple (P). For main colours, we only selected eight colours, containing four hues, each having two lightness levels, including saturated red (SR), light red (LR), saturated yellow (SY), dark yellow (DY), light blue (LB), dark blue (DB), light purple (LP) and dark purple (DP). All colour samples were shown in Figure 1.
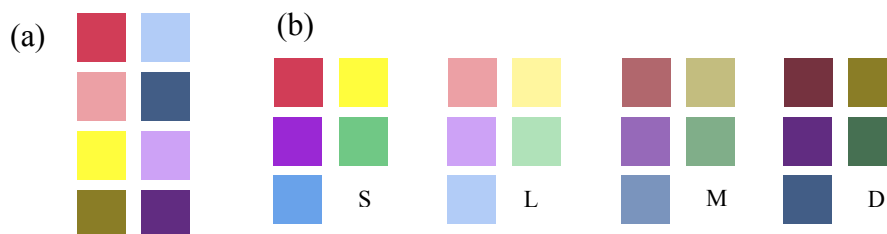


*Figure 1: Colour samples used in the experiment: (a) the main colours and (b) the logo colours.*

In the psychophysical experiment, we used 404 recoloured images of athletic shoes as the stimuli, presented on a calibrated computer display situated in a darkened room. The 404 images were generated from two original shoe images, one from Nike and the other from Adidas, each manipulated by varying the two-colour combinations of the shoe design, including the main colour of the shoe and the logo colour (i.e. the Nike tick and the Adidas stripes), as shown in Figure 2. Each of the two original shoe images were recoloured using 202 colour combinations, consisting of 152 pairs selected from CIELAB space to cover a wide variety of hue, lightness and chroma, and 50 colour pairs selected from real athletic shoes currently available on the market.



*Figure 2: schematic diagrams of Nike and Adidas.*

Twenty Taiwanese observers with normal colour vision, including 10 males and 10 females, participated in the visual assessment. Each observer was asked to rate each shoe images using two 6-step semantic scales, like/dislike and harmonious/disharmonious, as measures of colour preference and colour harmony, respectively.

## 3. RESULTS

### 3.1 colour preference for athletic shoes

Mean hues of main colur and main colour for preference ratings with Nike and Adidas athletic shoes in Figure 3, there were similar show that preference ratings is higher when dark blue (DB) as main colour with blue (B) as logo colour. When dark blue (DB) as main colour with some logo colour, it bring higher preference ratings. It was worth noting that dark blue (DB) with purple (P), the preference ratings was drop, the result was agree with original research. However, the dark yellow (DY) as main colour with any logo colour had lower preference ratings that everyone didn't like it. We surmise that dark yellow (DY) make disgusting that it look like excrement.

*Figure 3: Preference ratings for the hue of logo colours against each main colour.*

Preference ratings of Main colour in different hue difference in Figure 4. We can found that preference ratings of dark blue (DB) and light blue (LB) as main colour were higher than others, but the dark yellow (DY) as main colour had lower preference ratings. Again, proving that observers like blue colour much, instead yellow colour wasn't, especially dark yellow (DY).



*Figure 4: Preference ratings plotted against hue difference.*

Mean lightness of logo colour and different main colour for preference ratings in Figure 5. We can see that dark blue (DB) as main colour with different lightness as saturated (S), light (L), muted (M), that higher preference; instead, the dark yellow (DY) as main colour with different lightness as saturated (S) and light (L) had lower preference. Above all, dark blue (DB) and dark yellow (DY) in colour preference experiment, former was most like colour combination, another wasn't.
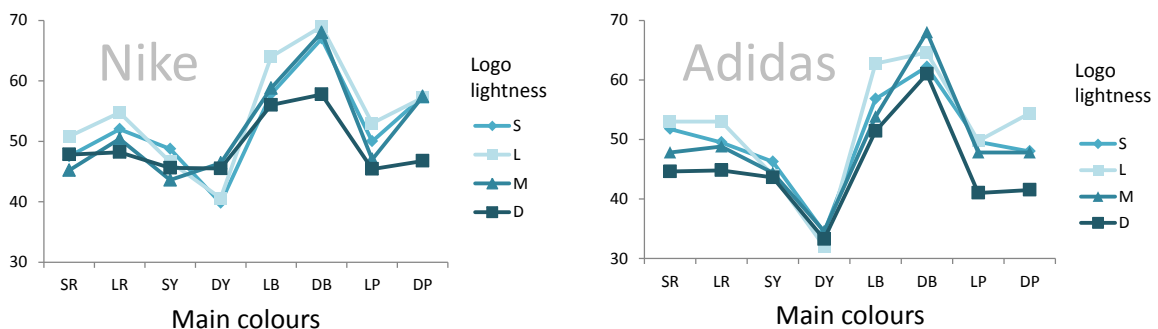


*Figure 5: Preference ratings for each lightness level of logo colours against each main colour.*

AIC2015 TOKYO - Color and Image

## 3.2 colour harmony for athletic shoes

Mean hues of logo colour and main colour for harmony ratings with Nike and Adidas athletic shoes in Figure 6. We can found harmony ratings is higher when light blue (LB) and dark blue (DB) as main colour with blue (B) as logo colour and dark yellow (DY) with yellow (Y). When dark yellow (DY) as main colour with purple (P) as logo colour, bring lower harmony ratings. In harmony ratings, we can found that the logo colour were similar with main colour, harmony ratings were higher, no matter the colour everyone like or not.
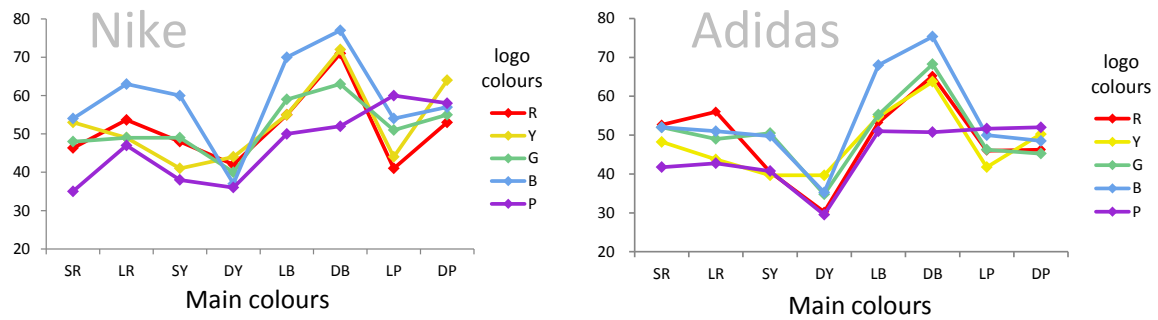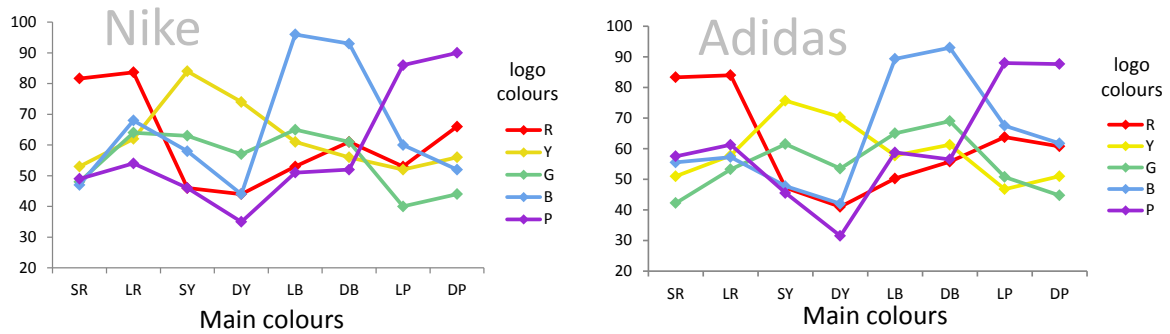


*Figure 6: Harmony ratings for the hue of logo colours against each main colour.*

Harmony ratings of main colour in different hue difference in Figure 7. Those pictures proved the hues difference less, the harmony ratings better. In other words, when main colour was similar to logo colour, the harmony was stronger.



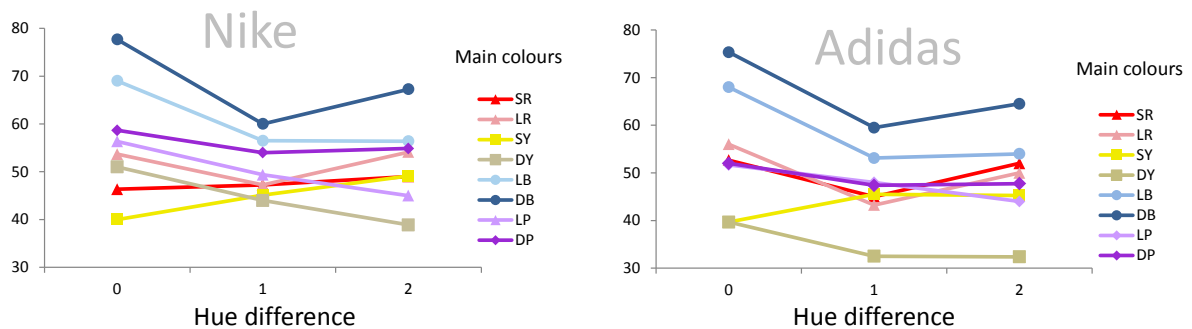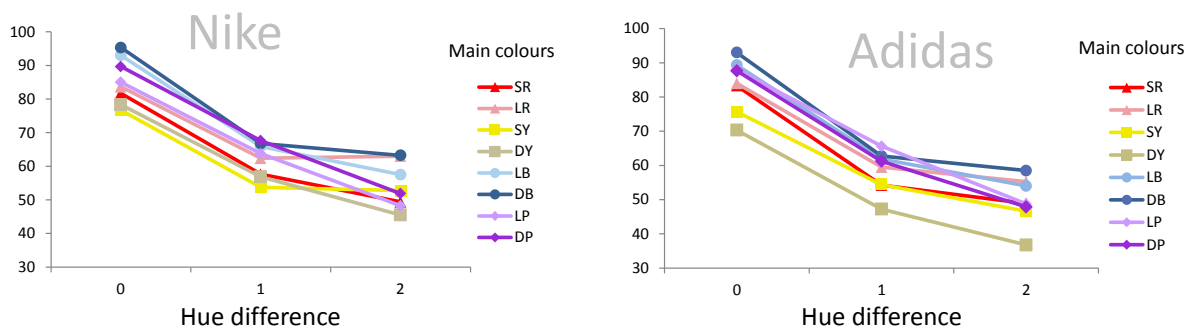*Figure 7: Harmony ratings plotted against hue difference.*

Mean lightness of logo colour and different main colour for harmony ratings in Figure 8. We can find that there were many peak values in those pictures, most in light (L), muted (M) as lightness of logo colour. That is, main colour with light (L), muted (M) as lightness as logo colour, the harmony ratings was better. However, when the dark yellow (DY) as main colour with light (L) as lightness as logo colour, the harmony ratings was lower. We surmised observers might influenced by preference.
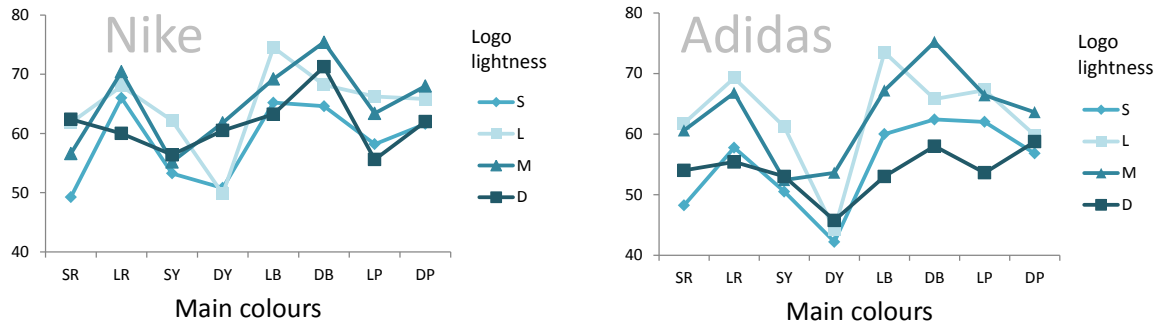
*Figure 8: Harmony ratings for each lightness level of logo colours against each main colour.*

## 4. CONCLUSION

Although all athletic shoes were comprised of main colours and logo colours (i.e. the logo colours in this study) in the experiment, the perceived color preference was affected mainly by the main colour of the shoe, while the perceived color harmony was affected not only by hue similarity but also by lightness difference between the main colour and the logo colour.

For colour preference, the blue tone was highly rated, while the yellow tone felt dull and dark and was thus not preferred. For colour harmony, the experimental results show that the smaller hue difference, the more harmonious. In addition, when the main colour with light (L), muted (M) as lightness as logo colour, the harmony ratings was better.

The results also show that shoe colors preferred by female observers tended to be liked by male observers, while shoe colors preferred by male observers were not necessarily liked by female observers. For colour preference, the two gender groups had a correlation coefficient of 0.63, however, high correlation between male and female data in terms of colour harmony, with a correlation coefficient of 0.83.

These results can help refine and clarify existing theories of colour preference and harmony based on contextless colour patches.

## AKNOWLEDGEMENTS

## REFERENCES

Schloss, K.B. and S.E. Palmer 2011. *Aesthetic response to color combinations:preference, harmony, and similarity*, Atten Percept Psychophys 73(2) 551-571.

*Address: Master. Wei-Hsuan CHAO, Graduate Institute of Color and Illumination Technology, National Taiwan University of Science and Technology, 43, Section 4, Keelung Road, Taipei, 10607, TAIWAN*
*E-mails: m10225009@mail.ntust.edu.tw*

# A study on silver metallic color preference
# - A comparison of responses by age and gender in Thailand –

Kamron YONGSUE[1], Mikiko KAWASUMI[2], Chanprapha PHUANGSUWAN[1], and Kanrawee TAWONPAN[1]

[1]Faculty of Mass Communication Technology, Rajamangala University of Technology Thanyaburi, Thailand
[2]Faculty of Science and Technology, Meijo University, Japan

## ABSTRACT

This paper describes the outcome of the research about the designing conditions for more attractive surface color of the silver metallic productos. It is significant for us to understand the customer's visual preference for each product in each nation. In this paper, we will show you the relationship between the surface colors of silver metallic products and the customer's desired feelings such as the feeling of "high-quality". Especially we will report the comparative results of observation by age and gender in Thailand.

## 1. INTRODUCTION

Thailand is one of the countries that have many factories of Japanese manufacturer such as cars, home appliances and textiles, and those products are popular for Thai people. We also can see many metallic colors here such as fridges and cameras. We are currently researching the relationship between the surface colors of silver metallic products and the desired feelings of the customer.

The visual appearance of a product is very important for the customers and the desired impression and color preference may be different by age and gender. In this research we would like to find out the attractive silver metallic color for Thai customers and compare these effects among age and gender.

## 2. METHOD

A questionnaire on the Web was used for our investigation and written both in Thai and in English. In previous survey, we investigated in English. But we translated it into Thai language this time in order to add the respondents who live in local region including elderly people. Figure 1 shows a part of our questionnaire. Computer graphics were used to represent the surface colors of metallic products. Their surfaces have slightly different silver metallic colors: reddish, yellowish, bluish, and so on, and each color was controlled in ten hues of the Munsell color system: **P**, **RP**, **R**, **YR**, **Y**, **GY**, **G**, **BG**, **B**, and **PB** as shown in figure 2. We set five target feelings: "clean / pure", "relaxing / comforting", "high-quality", "stylish / chic", and "favorite", which were chosen as the most important desired feelings by Japanese customers in previous study. The respondents answered with color that they felt was the most "high-quality", for example, for seven target products: a fridge, a television, a DVD player, a laptop computer, a digital camera, a smartphone, and a music player as shown in figure 3.

*Figure 1: A part of questionnaire.*



P    RP    R    YR    Y    GY    G    BG    B    PB

*Figure 2: Ten colored products.*

*Table 1: Target feelings.*

| In English | In Thai |
|---|---|
| Clean / pure | สะอาด / บริสุทธิ์ |
| Stylish / chic | มีรสนิยม / แฟชั่น |
| High – quality | คุณภาพสูง |
| Relaxing / comforting | ผ่อนคลาย / สะดวกสบาย |
| Favorite | ชื่นชอบ |



*Figure 3: Target products.*



*Figure 4: A scene of answering questionnaire.*

*Table 2: Respondents.*

| Age group \ Gender | Male | Female | Total |
|---|---|---|---|
| Teens ~ twenties | 62 | 75 | 137 |
| Thirties ~ forties | 40 | 59 | 99 |
| Over fifties | 34 | 51 | 85 |
| Total | 136 | 185 | 321 |

We requested that the screen size of a computer should be not less than twelve inches, because it may be hard to distinguish the differences among ten hues on a small display. The required time was about twenty minutes on average. However the elderly people took a lot of time over forty minutes. We instructed every question in Thai in the next seat and helped them to fill the answer sheets. Finally, more than three hundred persons have cooperated with us in Thailand, as shown in Table 2. We've compared the results among gender and three age groups: teen – twenties, thirties – forties, and over fifties.

## 3. COMPARATIVE RESULTS BY AGE AND GENDER

Our results are shown in Figures 5 by line graphs. The horizontal axis shows the Munsell hue: **P**, **RP**, **R**, **YR**, **Y**, **GY**, **G**, **BG**, **B**, and **PB**, and the vertical the percentage of choice for the hue. Different line types indicate the products: a fridge, a television, a DVD player, a laptop computer, a digital camera, a smartphone, and a music player. It shows the comparative results by five feelings for all Thai people.
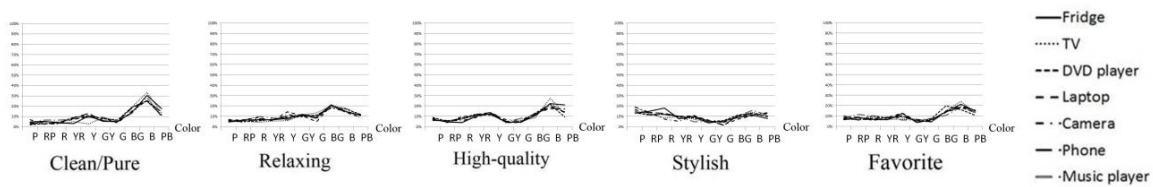


*Figure 5*: *Comparative results by feeling.*

We can see that most Thai selected Munsell **B** for the feeling of "clean/pure" and **BG** for the "relaxing". Also, they selected **B** and **YR** for "high – quality" and purplish silver for "stylish". In addition, we could confirm that "clean / pure" has the highest correlation with "favorite" (r = 0.75 ~ 0.92) for all product except a music player. "High-quality" also has high correlation with "favorite" for a fridge, a laptop, a computer, and a camera (r = 0.81 ~ 0.90).

Figure 6 shows the comparative results among three age groups. It became clear that most people under forties preferred bluish silver for the feeling of "clean / pure" in every product, , many elderly people preferred yellowish silver also, especially in the personal mobile product: a laptop computer, a camera, a smart phone, and a music player. As everyone knows, color appearance of an elderly person is difference from a young person by aging process of the lens. However we could not find out any difference clearly in a statistical analysis (p > 0.05) and also couldn't confirm a big difference between male and female, as shown in Figure 7.
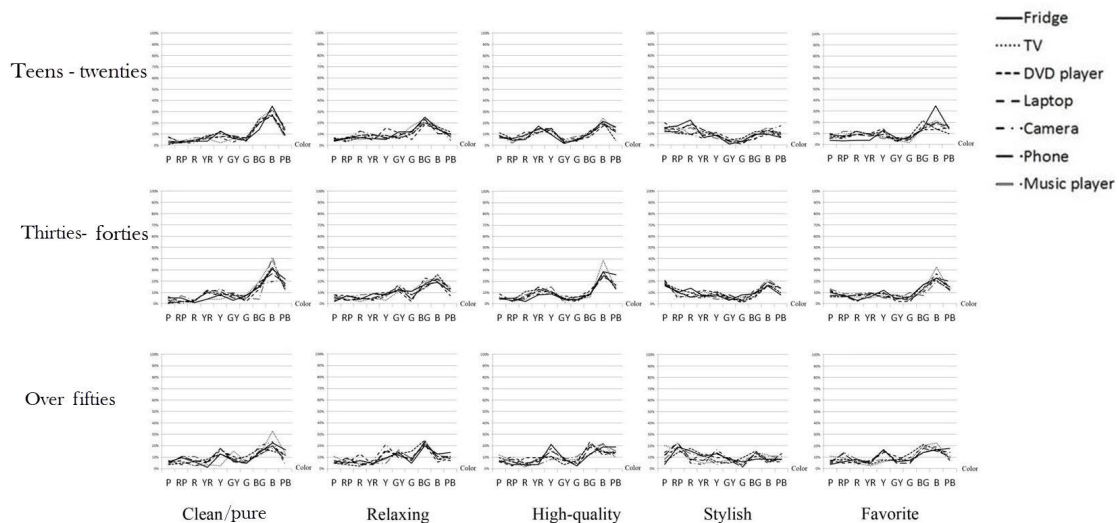


*Figure 6: Comparative results by three age group.*
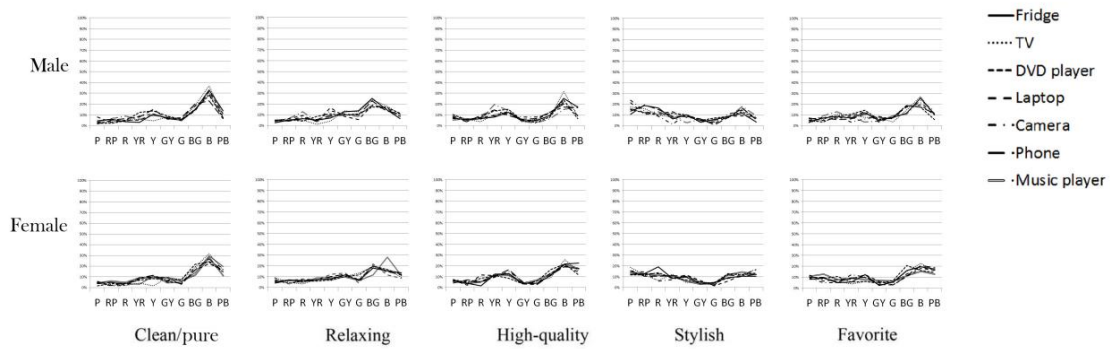
*Figure* 7: Comparative results by gender.

## 4. SUMMARY AND FUTURE PLANS

We've examined the silver metallic preference in Thailand and compared the results by three groups of age and gender. As the results, we could grasp the characteristic of Thai people's preference. For example, Thai selected **B** for the feeling of "clean/pure" and **BG** for "relaxing". The former is the same result as other countries, but the latter is difference from others.

Our next issue is to investigate by using other adjectives such as "modern", "creative / innovative", and "advanced", because Thai people chosen these adjectives as an important desired feeling for a metallic product. We plan to examine the relationship between these new adjectives and the surface colors.

## ACKNOWLEDGEMENTS

## REFERENCES

Saito, M., 1994. *A cross-cultural study on color preference in three Asian cities: Comparison between Tokyo, Taipei and Tianjin*. Japanese psychological Research 36(4): 219-232.

Xin, J.H., Cheng, K.M., Taylor, G., Sato, T., Hansuebsai, A., 2004a. *Cross-Regional Comparison of Colour Emotions Part I:Quantitative Analysis*. Color Research and Application 29(6): 451-457.

Xin, J.H., Cheng, K.M., Taylor, G., Sato, T., Hansuebsai, A., 2004b. *Cross-Regional Comparison of Colour Emotions Part II:Qualitative Analysis*. Color Research and Application 29(6): 458-466.

Kawasumi, M., 2013. *A Comparative Study in Asian Countries on Color Preference for Factory Products*. In Proceedings of the 1st Conference of Asian Color Association, ed. by Vichai Payackso. Thanyaburi: Rajamangala University of Technology Tanyaburi, 26-27.

Kawasumi, M., 2014. *A Comparative Study in Asian Countries on Color Preference of industrial products*. In *2nd* conference of Asian Color Association, ed. by Tien-Rein LEE. Taipei: Chinese Culture University, 268-271.

*Address: Kamron Yongsue,*
*Faculty of Mass Communication Technology,*
Rajamangala *University* of Technology Thanyaburi
39 Moo1, Rangsit-Nakhonnayok Rd. Klong 6, Thanyaburi Pathum Thani 12110
*Thailand*
*E-mails: ykamron@gmail.com, future@meijo-u.ac.jp*
*karamenn@gmail.com, ktawonpan@gmail.com*

# Effects on Impression of Taste in Color Stimuli

Masato SAKURAI, Yusuke MICHINAKA, Takahiro YOSHIKAWA
Department of Media Informatics, College of Informatics and Human Communication,
Kanazawa Institute of Technology

## ABSTRACT

To examine the effect on the impression of taste by color stimuli from the aspect of the three attributes of color (hue, lightness, and chroma) the impression of five basic tastes (sweetness, sourness, bitterness, saltiness, and umami) for the color stimuli were measured using the subjective evaluation. The color stimuli were uniformly selected from Munsell color system. In the results, the evaluation values increases with the regions between 5RP and 5YR on Munsell hue circle for the impression of sweetness and the regions between 5YR and 5GY on the hue circle for the impression of sourness. And in those hues, the evaluation value increases with the value of chroma. Therefore, the colors of reddish purple, red, and orange obtain the impression of sweetness and those of orange, yellow, and yellowish green give the impression of sourness with an increasing of the value of chroma. Dark achromatic colors obtain the high evaluation value in the impression of bitterness and its value increases with a decreasing of the value of lightness. Thus, the value of lightness affects the impression of bitterness.

## 1. INTRODUCTION

It is well-known that colors affect the impression of teste to humans. Previous studies have already reported that reddish purple, red, and orange colors highly obtain the impression of sweetness, yellow and green colors affect the impression of sourness, and grayish color highly obtains the impression of bitterness (Moga 1974, Kinoshita et al. 2010). And it is reported to associate the impression of sweetness with pink, orange, and red colors and to do that of sourness with yellow color as similar to the results of the above studies (Okuda et al. 2002). However, it is not clear how the three attributes of color – hue, lightness and chroma have an effect on the impression of the five basic tastes – sweetness, bitterness, sourness, saltiness and umami, from the point of view in the quantitative measurement. Also there are some literatures suggesting a connection, that colors for use in the food package enhance the willingness to buy a product when they are the impression close to actual food taste, then pass along information to become the criteria of judgment for buying (Kinoshita et al. 2010). So it seems to be the importance of investigating to the three attributes of color quantitatively. The purpose of this study is to examine the effect on the impression of taste by color stimuli from the aspect of the three attributes of color.

## 2. METHOD

### 2.1 Stimuli

Ten hues of the chromatic color (5R, 5YR, 5Y, 5GY, 5G, 5BG, 5B, 5PB, 5P, 5RP) and five of the achromatic color (N1, N3, N5, N7, N9) on the hue circle of Munsell color system were selected as the color stimuli in this experiment. In each hue of chromatic color,

twenty-five stimuli were regularly chosen with the values of Munsell Value and Chroma in Munsell notation. Thus, there were around 257 stimuli in total. Table 1 shows the stimuli used in this experiment. The stimuli were presented by 24-inch display (Dell, UP2414Q) placed in front of the observer and the viewing distance was 500 mm. They were displayed into the square at a visual angle of 15 deg in the center of the screen, and set N5 as the background color. Referring to the values of tristimuls values (*XYZ*) of Munsell color with $D_{65}$ light source in JIS Z 8721 (JIS 1993.), those colors were made. The mean value of $\Delta E_{ab}*$ in all the stimuli is 4.94 as shown in Table 1.

*Table 1. Stimuli in this experiment.*

| H | V | C | No. of colors | Ave. Δ *Eab** |
|---|---|---|---|---|
| 5R | 2 - 9 | 1 - 20 | 25 | 4.88 |
| 5YR | 2 - 9 | 1 - 16 | 25 | 5.36 |
| 5Y | 3 - 9 | 1 - 14 | 25 | 5.64 |
| 5GY | 3 - 9 | 1 - 14 | 26 | 5.35 |
| 5G | 2 - 9 | 1 - 20 | 25 | 4.93 |
| 5BG | 2 - 9 | 1 - 16 | 25 | 4.50 |
| 5B | 1 - 9 | 1 - 12 | 25 | 4.68 |
| 5PB | 2 - 8 | 1 - 16 | 25 | 4.42 |
| 5P | 2 - 7 | 1 - 28 | 25 | 5.04 |
| 5RP | 2 - 8 | 1 - 22 | 26 | 5.27 |
| N | 1 - 9 | | 5 | 1.23 |
| Total | | | 257 | 4.94 |

## 2.2 Procedure

After three minutes light adaption by the $D_{65}$ fluorescent lamps in experimental booth, the observers were asked to evaluate the impression of basic tastes (i.e. sweetness, sourness, bitterness, saltiness and umami) in stimuli presented, to each taste on a five-point scale (1: feel hardly, 2: feel slightly, 3: feel somewhat, 4: feel, 5: feel very much). The stimuli were presented randomly and the duration time was left to observer's discretion. The gray image of N5 was displayed as the inter-stimulus stimulus to remove the effect of the previous stimulus. In one session, the observer performed the evaluation of 257 times and three sessions were carried out for one observer. It was 771 times in total. Prior to the expriment, the observers had an enough time to practice for the evaluation.

## 2.3 Apparatus

The experimental booth was covered with a black curtain. It was illuminmated by the $D_{65}$ fluorescent lamps and the illumination of screen in the display was around 350 lx. The display was placed in front of the observer  and the viewing distance was 500 mm. The observers were asked to respond with the ten key when they evaluate the stimulus.

## 2.4 Observers

Twenty observers participated in this experiment. They were ten female and ten male students. They have the normal color vision.
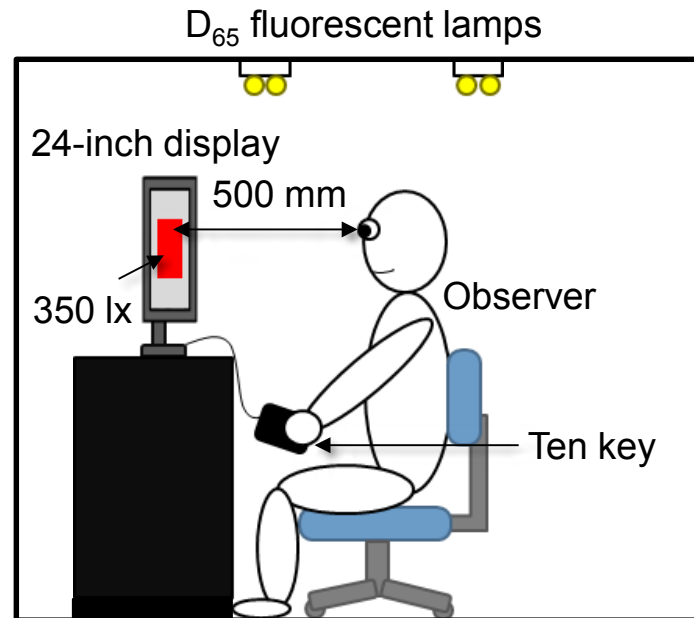


*Figure 1: Apparatus.*

## 3. RESULTS AND DISCUSSION

### 3.1 Effect of Hue

Figure 2 shows the results of the impression of five basic tastes (sweetness, sourness, bitterness, saltiness, and umami) on hue circle based on all the observers' responses. Figure 2 (a) – (e) indicate sweetness, sourness, bitterness, saltiness, and umami, respectively. The circumference in each panel represents the hue circle and each hue corresponds to the focal color in the hue used in this experiment (i.e. color of the highest chroma value in the hue). The radius indicates the subjective evaluation value in the experiment. In this figure the average values from all the observers' responses are connected.

As shown in this figure, particularly, the evaluation values increases with the regions between 5RP and 5YR in sweetness and the regions between 5YR and 5GY in sourness in Figure 2 (a) and (b), respectively. The colors of reddish purple, red, and orange obtain the impression of sweetness while those of orange, yellow, and yellowish green give the impression of sourness. For bitterness, saltiness, and umami in Figure 2 (c) – (e), the effects of hue are relatively small. On the other hand, N1 and N3 of achromatic colors obtain the high evaluation value in the impression of bitterness, and lightness affects the impression of bitterness as the mentioned in the next paragraph. The tendency of the results in hue effect corresponds to the results of previous studies (Kinoshita et al. 2010, Moga 1974, Okuda et al. 2002).
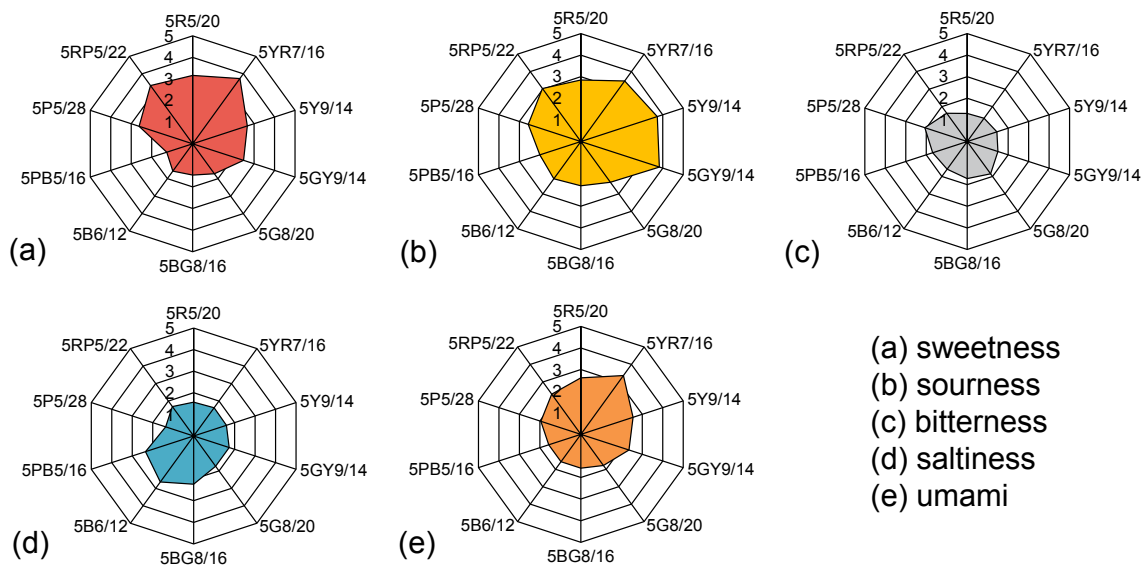
*Figure 2: Effect of hue in the average results of the impression of five basic tastes for ten focal colors (i.e. color of the highest chroma value in the hue) . (a): sweetness, (b): sourness, (c): bitterness, (d): saltiness, and (e): umami. The circumference and radius represent the hue circle and the subjective evaluation value, respectively.*

## 3.2 Effect of Lightness

Figure 3 shows the results of the impression of bitterness as a function with the value of lightness based on all the observers' responses. The horizontal and vertical axes indicate the value of lightness and the subjective evaluation value of bitterness, respectively. As the typical results, the average values of N, 5GY-/6, and 5G-/8 are plotted. In this figure, the evaluation value increases with a decreasing of the value of lightness in each color. It means that the value of lightness affects the impression of bitterness and it associates the impression of bitter with dark colors. This result corresponds to that of previous study (Kinoshita et al. 2010).
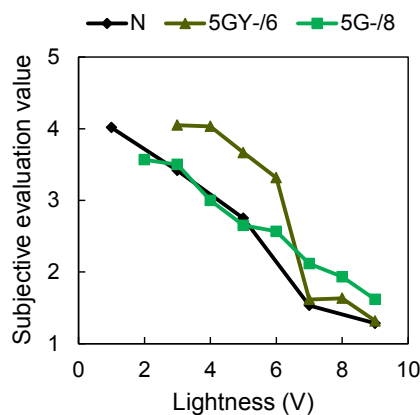


*Figure 3: Average results of the impression of bitterness as a function with the value of lightness for N, 5GY-/6, and 5G-/8.*

## 3.3 Effect of Chroma

Figure 4 (a) – (b) show the results of the impression of sweetness and sourness as a function with the value of chroma based on all the observers' responses, respectively. The horizontal and vertical axes indicate the value of chroma and the subjective evaluation value of sweetness and sourness, respectively. As the typical results, the average values of 5RP5/-, 5R5/-, and 5YR7/- are plotted in sweetness of Figure 4 (a) and those of 5GY9/-, 5Y9/-, and 5YR7/- are represented in sourness of Figure 4 (b).

In Figure 4 (a), the evaluation value increases with the value of chroma and then is saturated over 10 in the value of chroma in all the colors. It means that the value of chroma affects the impression of sweetness in reddish purple, red, and orange colors and it associates the impression of sweetness with high chroma value of those colors. In Figure 4 (b), the evaluation value increases with the value of chroma and then has a tendency saturated over 12 in the value of chroma in all the colors as well as the results of sweetness. It means that the value of chroma affects the impression of sourness in yellowish green, yellow, and orange colors and it associates the impression of sourness with the high chroma value in those colors. These results correspond to that of previous study (Kinoshita et al. 2010, Moga 1974, Okuda et al. 2002).
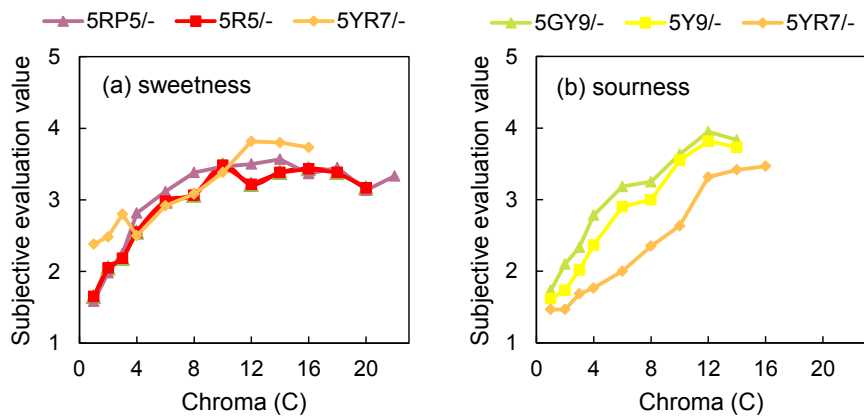


*Figure 4: Average results of the impression of sweetness and sourness as a function with the value of chroma. (a): sweetness for 5RP5, 5R5, and 5YR7 (b): sourness for 5GY9, 5Y9, and 5YR7.*

## 4. CONCLUSIONS

To examine the effect on the impression of taste by color stimuli from the aspect of the three attributes of color (hue, lightness, and chroma) the impression of five basic tastes for the color stimuli were measured using the subjective evaluation of five-point scale. The color stimuli were uniformly selected from Munsell color system. They included ten hues of chromatic colors and N of achromatic color. The value of lightness and chroma ranged from 1 to 9 and from 1 to 28, so that about 25 colors from each chromatic hues and 5 achromatic colors were selected and the total was 275 stimuli. The observers were asked to subjectively evaluate the impression of five basic tastes (sweetness, sourness, bitterness, saltiness, and umami) for the stimulus presented by the display using the five-point scale. In the results, the evaluation values increases with the regions between 5RP and 5YR on Munsell hue circle for the impression of sweetness and the regions between 5YR and 5GY on the hue circle for the impression of sourness. And in those hues, the evaluation value

increases with the value of chroma and then is saturated over 10 - 12 in the value of chroma. It means that the colors of reddish purple, red, and orange obtain the impression of sweetness while those of orange, yellow, and yellowish green give the impression of sourness with an increasing of the value of chroma. N1 and N3 of achromatic colors obtain the high evaluation value in the impression of bitterness. And the evaluation value increases with a decreasing of the value of lightness including 5G and 5GY stimuli. It means that the value of lightness affects the impression of bitterness and it associates the impression of bitter with dark colors.

## ACKNOWLEDGEMENTS

## REFERENCES

Japanese Industrial Standards (JIS) 1993. Colour specification−Specification according to their three attributes, JIS Z 8721 (in Japanese).

Kinoshita, T., K. Matsuda, and K. Ayabe 2010. Effects of taste image by three attributes of color, *Journal of Design Research Association* 54, 107-112 (in Japanese).

Moga, J.A. 1974. Influence of color on taste thresholds, *Chem. Senses Flavor* 1 (1), 115-119.

Okuda, H., M. Tasaka, A. Yui, and S. Kawazoe 2002. Correlation between the image of food colors and the taste sense −The case of Japanese twenties-, *Journal of Cookery Science of Japan* 35(1),  2-9 (in Japanese).

*Address: Masato SAKURAI (Dr. Eng.),*
*Department of Media Informatics,*
*College of Informatics and Human Communication,*
*Kanazawa Institute of Technology,*
*3-1 Yatsukaho, Hakusan, Ishikawa, 924-0838, JAPAN*
*E-mails: masato@neptune.kanazawa-it.ac.jp*

# The color image of dichromats and anomalous trichromats

Yuria NOGUCHI,[1] Muneo MITSUBOSHI,[2]
[1] Graduate School of Human Sciences, Kanagawa University
[2] Department of Human Sciences, Kanagawa University

## ABSTRACT

We measured color image of color vision deficients using SD scales, and compared the results with those of color vision normals. Eleven colors chips, 8 vivid color (red , orange , greenish-yellow , yellow green , bluish-green , greenish-blue , blue , purple) , and achromatic colors (white , gray, black ) were selected from the New Color Collections (199a) of the Japan Color Research Institute, and displayed on a black sheet .The size of stimulus was $3 \times 3$cm. Those colors were observed one by one by the participant through a square opening of black mask of the same size as stimulus to avoid mutual influence between adjacent colors. All the stimuli were observed under natural fluorescent lights with chromaticities of ( .364 , .379 ) and the average illumination was 842 lx . Four color vision deficients (one protan, one deutan , and two deuteranomats ) and 13 color vision normals participarted.

General tendency was that the point on each SD scale shifted towards right hand, i. e. negative image or affection, in color vision deficients.  For red, orange, and white colors, there existed several substantially different color images (SD scales) between color vision deficients and color vision  nomals. Image of blue, purple, gray, and black showed little difference  between  them.  Images  to  greenish-yellow  and  yellow green  were  slightly different.

In  terms  of  individual  images  (SD scales),  images  clustered  in  "activity ",  e.g. "crowded-lonely", "powerful-non powerful", or " showy-quite" were  much different for color vision deficients and color vision normals.

## 1. INTRODUCTION

There  have  been  much  data  concerning  how  color  vision  deficinets  recognize  color  and how differently they perceive colors from color vision normals (Graham & Hsia, 1958; Fletcher & Voke, 1985; Mitsuboshi & Hasegawa, 1987; CUDO, 2009; Noguchi, 2013). But little investigation has been made into how color vision deficients feel for colors, in other words, what kind of images they have to colors.

Many  studies  by  SD  method  in  the  past  show  that   there  are  generally  three  factors covering  images  to  colors;  i.e.  "evaluation",    "activity",   and  "potency"  (Oyama  et  al. 1965).  Such estimation  is, however, for color vision normals.

What  image  they  have  to  color  and  how  different  their  images  are  from  those  of  color vision normals are the scheme of the present report.

Color vision deficient may give same color name as color vision normals to a particular color, with different image  (Kawamoto  et al, 2008).  Images clustered in potency were largely  different in their participants.  Saito et al , 2010), on the other hand, reported that there was little difference in their images between color vision dificients and normals.

AIC2015 TOKYO - Color and Image

## 2. METHOD

### 2.1  Color Stimuli

Eleven color chips, eight vivid red , orange , greenish-yellow , yellow green , bluish-green , greenish-blue , blue , purple , white , gray (Gy-5,0), and black which were selected from the New Color Collections (199a) of the Japan Color Research Institute. Their size was of $3 \times 3$cm.  They were attached on  the black background paper.

All the stimuli were observed under natural fluorescent lights with chromaticities of ( .364 , .379 ) and the average illumination was 842 lx .

### 2.2  SD Scale

Figure 1 shows the SD scales used. These scales were evaluated with seven points.

| | |
|---|---|
| 1. light—dark | 11. beautiful—ugly |
| 2. elegant—vulgar | 12. calm—frivolous |
| 3. like—dislike | 13. monotonous—changeful |
| 4. get annoyed—mind | 14. plain—heavy |
| 5. natural—unnatural | 15. romantic—realistic |
| 6. amiable—not amiable | 16. modern—ancient |
| 7. warm—cool | 17. young—old |
| 8. crowded—lonely | 18. smart—rustic |
| 9. powerful—not powerful | 19. open—closed |
| 10. showy—quiet | 20. profound—light |
| | 21. clean—dirty |

*Figure 1: SD scales used.*

### 2.3  Participants

Paid experienced 2 male dichromats (1 protan and 1 deutan) and 2 male anomalous trichromats (deuteranomats) , ranging from 27 to 73 years old,  participated in this study. They were all recruited from CUDO organization. They had been tested their type of color vision at ophthalmological clinics

13 male and female color vision normals, who were all naive to this kind of color experiment and not paid, were also recruited so that their results can be compared. They had been tested their color vision by Ishihara Pseudoisochromatic Plates. They were all students of Kanagawa University at the age of around 20.

### 2.4 Experimental Procedure

11 colors of chips were observed one by one by the participant through a square opening of black mask of the size same as stimuli to avoid mutual influence between adjacent colors. The participants evaluated each 11 colors of images using 21 SD scales with 7 points.

## 3. RESULTS AND DISCUSSION

Figures 2 and 3 show SD average profile of the color vision deficients and color vision nomals for red and blue colors.  Red  is one of colors which showed remarkable difference

between color vision deficients and normals.   Blue is, on the other hand, one of colors which showed small differences.  Dotted and solid lines  indicate average results for color vision deficients and color vision normals respectively.

Table 1 shows the summary  of  individual images (SD scales) showing large difference , more than 2.0 points on each scale, between color vision deficients and normals in each color. Tha data for red and blue colors are excluded, which can be referred to Figures 2 and 3.
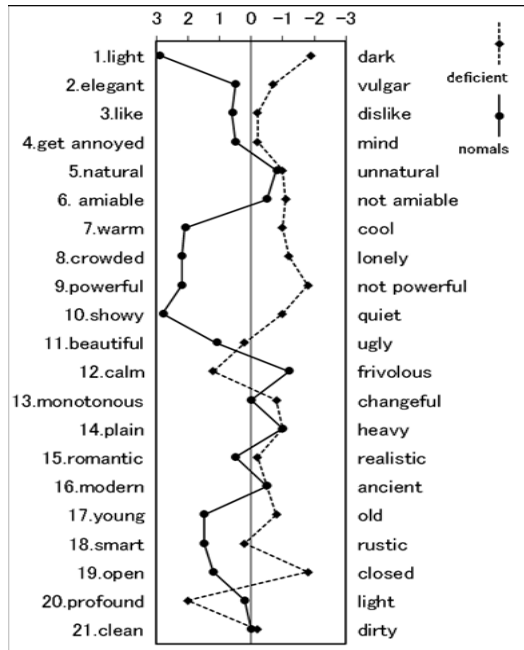


Figure 2:  Average image to red.          Figure 3: Average image to  blue.
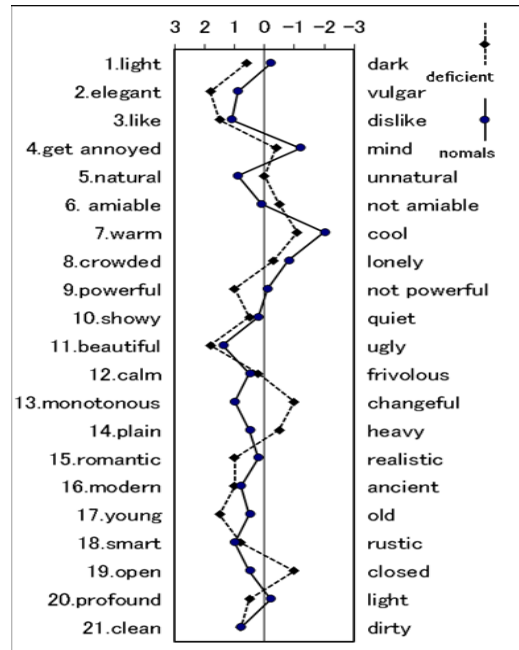
 Points on individual images (SD scales) shifted generally towards right hand in each scale, i.e. towards negative image or emotion in color vision deficients .

 For red color,   images of warm-cold, crowded-lonely, powerful-not powerful , and showy-quiet, all of which may be clustered into "activity",  shifted towards right hand in the color vision deficients. Images of romantic-realistic, modern-ancient,  which may be clustered into "modernness",  were similar between them .

 For blue color, images of monotonous-changeful and open-closed shifted towards right in color vision deficients. But, images of other scales are  generally analogous between them

 Table1 shows that orange color also give different image, more than red, to color vision deficients and nomals. That is predictable because orange and red are quite similar in their image for color vision normals (Oyama et al., 1965).  Many of images showing large difference were also from "activity ".  Both red and orange colors are not perceived "red" nor  "orange" as color vision normals do, but maybe look yellowish for them.  It seems natural to postulate that images to such colors differ for color vision deficients.

 It is, however, interesting that images for "narural-unnatural", "plain-heavy", or "modern-ancient" were little different between them despite of difference of appearance of color.  This result suggest that such images are created not by color, but other factors like brightness or shape.

It is predictably that images of blue or bluish colors did not show great difference between  color vision deficients and normals, for color vision deficients perceive blue color as "blue" (Graham & Hsia, 1958 ;  Mitsuboshi and Hasegawa, 1987) .

*Table 1: Scales showing large difference between color vision deficients and  color vision nomals in each color except red and blue.*

| Color | SD scale |
|---|---|
| Orange | amiable—not amiable |
| | warm—cool |
| | crowded—lonely |
| | powerful—not powerful |
| | showy—quiet |
| | plain—heavy |
| | young—old |
| | smart—rustic |
| | open—closed |
| yellow green | like—dislike |
| | beautiful-ugly |
| | plain—heavy |
| White | like—dislike |
| | amiable—not amiable |
| | calm—frivolous |
| | romantic—realistic |
| | smart—rustic |
| greenish-yellow | amiable—not amiable |
| | powerful—not powerful |
| | plain—heavy |
| | young—old |
| | smart—rustic |
| bluish-green | not greatly different |
| greenish-blue | not greatly different |
| Purple | not greatly different |
| gray | not greatly different |
| black | not greatly different |

The results that images to yellowish colors were rather different between color vision deficients and normals seem difficult to compromise with the hypothesis of their recognition of color,  since they both see the same "yellow"  color.  This may partly be explained by the fact that yellowish colors used in the present study included some green, like yellow green and greenish yellow, which is assumed to look different  from color vision normals.

Images by white were unpredictably different between color vision deficients and normals with those to gray and black little different.  It  is possible that  image by gray or black is essentially weak for both color vision deficients and normals.  Image by white is, on the other hand,  strong forming somehow difference between them.

## 4. CONCLUSIONS

Images to colors by color vision deficients are different from color vision normals depending color. General tendency was that the point on each SD scale shifted towards right hand, i. e. negative image or affection, in color vision deficients. For red, orange, and white colors, there existed several substantially different color images (SD scales) between color vision deficients and color vision nomals. But Image of blue, purple, gray, and black showed little difference between them. Images to greenish-yellow and yellow green were slightly different.

In terms of individual images (SD scales), images clustered in "activity ", e.g. "crowded-lonely", "powerful-non powerful", or " showy-quite" were much different for color vision deficients and color vision normals. Images of "narural-unnatural", "plain-heavy", or "modern-ancient" were, on the other hand, showed little difference between them. The latter suggest that such images are not created by color, but some other factors.

Thus we have to pay attention to difference in image between color vision deficients and normals when we construct color universal design.

## REFERENCES

Color Universal Design Organization(CUDO). 2009. *CUD* . Tokyo: Heart Publishing Co Ltd. (in Japanese).

Fletcher R. and J. Voke. 1985. *Defective Colour Vision fundamentals, diagnosis and management.* Bristol: Adam Hilger Ltd.

Graham, C. H. and Y. Hsia. 1958 The spectral luminosity curve for a dichromatic eye and a normal eye in the same person. *Proc. Natl. Acad. Sci.* 44, 46-49.

Kawamoto K. , Wake T. , and T. Yasuma. 2008. Identified color and impression of color deficiencies on color categorization, *The collection of papers of the Color Science Association of Japan, Supplement* 32:124-125. (in Japanese).

Mitsuboshi M and Hasegawa H. 1987. *Color vision, In Encyclopedia of Color, pp.170-247.* Tokyo: Asakura Publishing Co Ltd. (in Japanese).

Noguchi, Y. 2013. The effect of hatching on the word recognition of the color vision deficients using reaction time. *Bulletin of Human Sciences, Kanagawa University* 7: 5-17. (in Japanese).

Oyama, T., Soma, I., Tomiie, T., and H. Chijiiwa. 1965. A factor analytical study on affective responses to color. *Acta Chromatica* 1 (4):164-173.

Saito H. , Asano Y. , and M. Watanabe . 2010. The impression differences in color vision characteristics, *The collection of papers of the Color Science Association of Japan, Supplement* 34: 56-57. (in Japanese)

*Address: Yuria Noguchi, Graduate School of Human Sciences,*
*Kanagawa University, 3-27-1 Rokkakubashi, Kanagawa-ku, Yokohama, 221-8686, JAPAN*
*E-mails: r201370189ih@kanagawa-u.ac.jp*
*Address: Prof. Muneo Mitsuboshi, Department of Human Sciences,*
*Kanagawa University , 3-27-1 Rokkakubashi, Kanagawa-ku, Yokohama, 221-8686,*
*JAPAN*
*E-mails: mitsum01@kanagawa-u.ac.jp*

# Proceedings

## MCS Oral Papers

# Surface spectral reflectance estimation with structured light projection

Grzegorz MĄCZKOWSKI,[1] Krzysztof LECH,[1]  Robert SITNIK,[1]
[1] Institute of Micromechanics and Photonics, Warsaw University of Technology

## ABSTRACT

Several solutions were developed to reconstruct reflectance spectra of surfaces. Most of them focus on 2D acquisition of more than three spectral channels. The bands are separated by filtering the illumination spectrum or the light falling on the camera sensor. Recently more complex solutions have emerged, which combine the multispectral information with shape in 3D. We present a robust method of spectral reflectance estimation for points sampled on a 3D surface in a structured light projection system. The proposed solution does not need any additional hardware apart from the devices used in the classic structured light projection setup. It utilizes a calibrated color CCD camera and a DLP projector, which projects sine fringes in order to provide precise 3D point coordinates. Additionally, the projector is used as a light source for multispectral image capture by displaying uniform color fields. Simultaneous acquisition of the 3D shape information, as well as the multispectral data is possible in a single sequence of images. They are corrected for illumination non uniformity, ambient light and camera noise.

Two approaches are verified for the design of optimal projected hues. In the first one the saturated CMY fields are displayed. In the second approach three hues are found by an optimization algorithm which uses emission spectrum of the projector and quantum efficiency of the camera in order to minimize intensity variations between channels.

The presented method reconstructs a point cloud representing the surface with spectral reflectance estimated for each point. It uses the Wiener inverse method for the spectrum reconstruction. We provide evaluation of accuracy of the proposed method and show results of scanning painting samples created with different techniques, as an example application of cultural heritage digitization.

## 1. INTRODUCTION

Some very recent developments focus on spectrum reconstruction from minimal input data and no a priori information. They need two images of a scene, captured with different illuminants (Jiang and Gu 2012) or with and without a filter (Shrestha at. al. 2011). These methods provide robust solutions to multispectral imaging problem.

Recently also the 3D acquisition systems emerge, which combine shape information, encoded as a point cloud, with spectral or colorimetric data (Tonsho at. al. 2001, Mansouri at. al. 2007, Simon-Chane at. al. 2013). These achievements are innovative and promising in cultural heritage digitization, but they are also complex and expensive. On the other hand, they address the problem of angular reflectance properties of the 3D surface, which is important, but difficult to solve. In this work we take a different approach and propose a simple and low-cost solution, which enhances an ordinary 3D scanner with structured light projection (SLP) in order to equip it with spectral reflectance estimation capability at each registered point. Being aware of the hardware limitations and simplified acquisition model, which does not take into account illumination and observation directions with respect to the surface orientation, we propose the illumination optimization procedure. It improves the reflectance reconstruction results, providing a robust measurement method.

## 2. CONCEPT OF THE SETUP

The setup joins the concept of the structured light projection system, with additional acquisition step, which provides data for the spectral reflectance reconstruction.

### 2.1 3D scanner

The SLP system is built with a digital camera and a DLP projector, which provides active illumination. In our case the sine fringe projection technique is used. During the acquisition a set of images with shifted pattern, along with binary codes for the phase unwrapping, is captured. After automatic processing it yields a point cloud corresponding to the digitized surface. Normally each point in the cloud has assigned a color value, coming from one of the registered images, which was acquired with the projector displaying uniform white background. Such color information has relatively low quality, which is only slightly improved by adjusting the camera white balance. In the following study we propose to swap this data with the calibrated color map, derived from the estimated reflectance spectrum. Because in the image acquisition path just a single camera is used, there is one-to-one correspondence between the calibrated color value and the point in cloud and no additional texture mapping is necessary.

The tested setup features 2.8Mpix color, CCD camera and off-the-shelf FullHD DLP projector. It is calibrated with the method described in (Sitnik 2002), so that it has working volume of size 150x150x80mm and achieves resolution of 0.1mm, measured as the average distance between points in the captured cloud.

### 2.2 Spectrum reconstruction method

The multispectral methods for reflectance reconstruction need to operate on more than three, linearly independent spectral channels. Different methods and applications use diverse number of bands, either narrow or wide (Fischer and Kakoulli, 2006). Most of them use between six and ten channels, which is sufficient, when the appropriate algorithm for the reconstruction is chosen. The most widely used approaches include the Wiener inverse method and/or PCA-based one (Kang, 2006: 203). The former one uses signal and noise covariance in order to balance the inverse problem of increasing the dimensionality of the response from a few channels to the full spectrum sampled with a predefined resolution. The PCA-based methods use statistical information gathered from a large number of spectral samples in order to derive basis vectors, describing the set of samples.

In this work the Wiener inverse approach is used. The spectral filtering is realized by taking three images with a trichromatic camera, illuminated with different projected hues. This way nine channels can be captured with three acquisitions. Additionally each captured image is corrected for the camera noise and uneven illumination with the method described in (Mączkowski at. al. 2012).

## 3. DLP PROJECTOR MODEL

The available DLP projectors use mainly two kinds of light sources: tungsten lamps and LEDs. Both of these solutions are not ideal for faithful color reproduction and spectral reconstruction. Measurements of spectral response of sample off-the-shelf devices show, that their emission spectral power distribution (SPD) is very non-uniform, with high peak around blue region and much smaller power in the red region of the spectrum (Figure 1a). Especially LED-based projectors are a poor choice for the proposed application, because they often exhibit wide ranges with no, or very small emission, which gives no sensitivity

in these parts of the spectrum. Therefore in the further analysis the classic DLP projector, with tungsten lamp and filter wheel is used.

In order to take the advantage of the DLP projector in spectral measurements its characterization must be performed in order to find a relation between R, G and B values, which drive the output and produce the resulting SPD. For this purpose the spectral response $s_i(\lambda)$ in every channel of the projector was measured separately with a spectrophotometer. Additionally the total response, summed over the whole spectrum was measured at a range of supplied intensity levels between 100 and 250, with 10 levels interval. Based on this data a response model was found by least squares fitting of the power function to the intensity response. Based on the gamma coefficient found this way the final relation between input RGB values and the output SPD is derived as in Eq. 1.

$$S(\lambda)=s_R(\lambda)\left(\frac{R}{255}\right)^\gamma+s_G(\lambda)\left(\frac{G}{255}\right)^\gamma+s_B(\lambda)\left(\frac{B}{255}\right)^\gamma \tag{1}$$

The model was verified in two ways. In the first approach the hardware gamma correction was manually adjusted in the projector, so that two sets of responses for gamma 2.0 and 2.2 were collected. The model was found in both cases and the response was linearized. The resulting relations were identical, as is shown in Figure 1b, which proves that the model works for different gamma parameters.

In the second verification stage the reconstructed response was compared with the measured one for arbitrarily chosen RGB coefficients. The procedure was repeated for five different set of coefficients and in all cases the root mean square diffrence between the responses did not exceed 1%. Example pair of characteristics is depicted in Figure 1c. In the whole reasoning the assumption is made, that the $\gamma$ coefficient is the same for all channels and does not change with wavelength. Furthermore, the emission spectrum is considered constant for the whole illuminated area, so that differences between pixels are neglected.
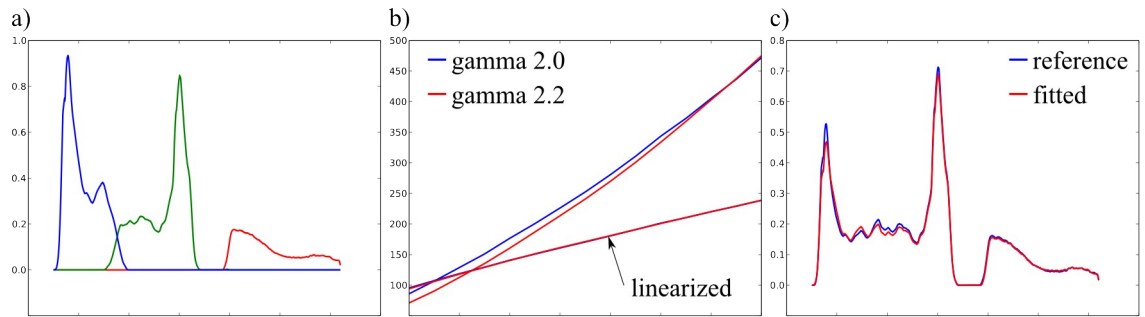


*Figure 1: Spectral analysis of the DLP projector: a) response in channels R, G and B; b) results of response linearization; c) reconstruction of the SPD for R239, G228, B176.*

## 4. OPTIMIZATION OF THE ACQUISITION PARAMETERS

Optimization of the acquisition parameters requires an image registration model, which describe how the spectral channels' intensity is captured. It equals the total irradiance $S_l(\lambda)$, emitted by a light source in the band $l$, filtered by the surface spectral reflectance $r(\lambda)$ and the detector sensitivity $D_k(\lambda)$ in the channel $k$, integrated over the visible spectrum (Eq. 2).

$$I_{kl}=\int D_k(\lambda)S_l(\lambda)r(\lambda)d\lambda \tag{2}$$

Input multispectral signal comprises of all combinations of light source spectral bands and camera channels. In this study the camera channels are equivalent to R, G and B spectral sensitivity of a CCD matrix with the Bayer color filter. For simplification the

attenuation of the optical system is not considered separately, however the 8bit quantization of the intensity, resembling the actual camera behavior is taken into account.

The light source bands are chosen from three different hues, displayed by the DLP projector. It can be observed, that the pairs with projected red hue and captured blue channel and vice versa will likely produce low imaged intensity and low signal to noise ratio. To avoid this the cyan, magenta and yellow hues are displayed as the primary colors, so that relatively even exposure in all channels and high signal level is achieved.

The method of DLP bands selection is based on a simulation, which finds the solution minimizing the root mean square error between the reference and reconstructed spectral reflectance for different projected colors. The displayed hues are changed by manipulating the proportions between the nominal cyan, magenta and yellow channels. The procedure uses the model from Eq. 2 to calculate the camera response in each band. Spectral characteristics of the ColorChecker target patches are used as a set of reference reflectances $r(\lambda)$. Light source emission spectrum in channel $l$ is calculated from the displayed $C_l M_l Y_l$ with the projector model from Eq. 1, and the detector sensitivity corresponds to the camera color channel $k$. Once the camera response in each band is found for the reference color patches, the Wiener inverse spectrum reconstruction model is established. Afterwards it is used to recover reflectance spectra of another set of representative samples, which come from spectrophotometric measurements of painted surfaces.

In the initial attempt a non-linear solver was employed to find the optimal sets of CMY coordinates of the projected hues, which give the best results of the spectral reconstruction of the chosen samples. Unfortunately, the model proved to be not sensitive enough for the channels parametrization. To overcome this problem another approach was proposed. Because the parameter space is only three-dimensional and in practice can be sampled in only 256 levels, corresponding to the possible color values displayed by the DLP in each channel, it was possible to calculate the objective function for different parameters combinations. The error function was defined as the total RMS error of spectrum reconstruction for 24 representative samples, drawn from measured reflectances.
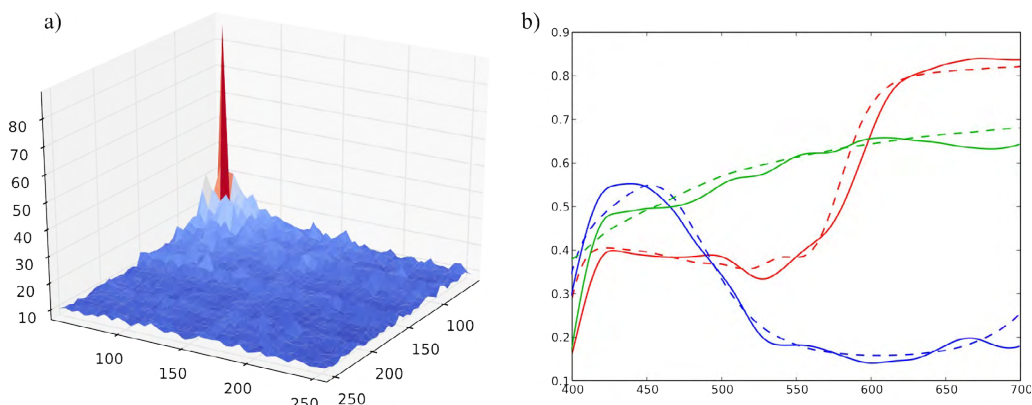


Figure 2: a) Slice of the spectral reflectance reconstruction error function on the $R_l G_l$ plane, for the parameter B = 245; b) example spectrum reconstruction results for three samples.

The three dimensional grid of the projected color samples was chosen as the domain for evaluation of the error function.The sampling was made in the range between 50 and 255, with the step of 5 levels for each of the nominal CMY channels. Fig. 2a depicts the plot of the CM slice of the objective function for Y = 245. It clearly shows, that for intensities above a certain threshold, the error variations are very small. It means that the spectrum reconstruction performance does not depend much on the projected intensities, unless they are lower than a border value. The data evaluation shows, that the threshold equal to 150 is sufficient. Additionally it proves that the overall accuracy of the spectral reflectance

reconstruction is determined by the shape of the light source SPD, rather than by proportions of its subranges.

Fig. 2b presents simulated reconstruction of spectral curves for three exemplary samples. Their reference characteristics, indicated by the dashed lines, come from real reflectances, measured by a spectrophotometer.

## 3. EXPERIMENTAL RESULTS

The reflectance spectrum reconstruction, based on the acquisition with structured light projection, was verified experimentally. The 3D scanner was set in the laboratory, where it was shielded from light sources other than the DLP projector. Three illumination patterns with cyan, magenta and yellow hues were used as lighting for in the multispectral acquisition.

The ColorChecker Passport target was captured as a point cloud. The color patches were extracted by a semiautomatic segmentation of the 3D data, so that an average value was found for each patch in every band. These data served as input for calculation of the Wiener inverse model of the spectrum reconstruction. The model was verified with measurement of the same color target and a set of painted samples, which did not took part in the model estimation. Additionally the setup was used to scan two paintings' reproductions, made in different techniques. The first one was the fragment of V. van Gogh impasto on canvas and the other was a limestone wall painting with an antique theme. The 100x100mm samples were digitized as point clouds with the resolution of 100 points per square millimeter. Fig. 3 shows point clouds with reconstructed color and spectral curves recovered in chosen places, along with their RMS and GFC error metrics (Imai at. al. 2002).
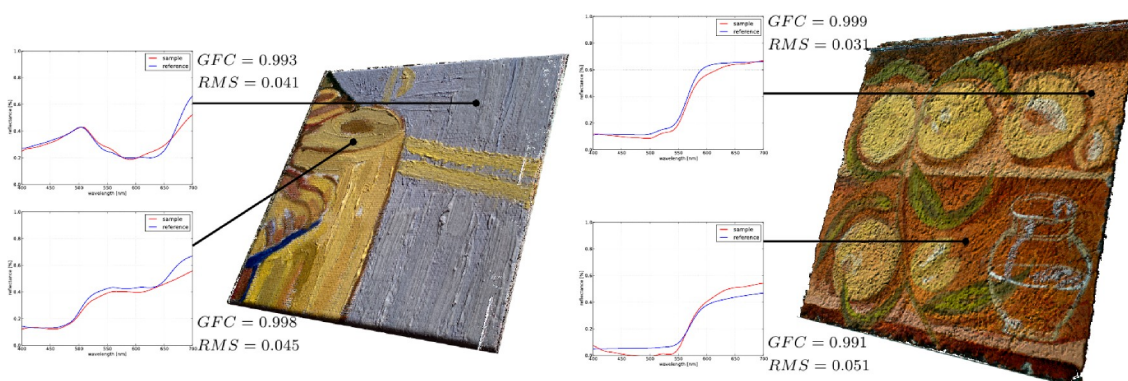


*Figure 3: Measurement results of the painting samples.*

## 4. CONCLUSIONS

The presented work shows a successful fusion of the shape measurement method with structured light projection, with the spectral reflectance estimation. It provides a starting point for further analysis of such integrated solutions, which open new possibilities in cultural heritage digitization.

The analysis leads to a conclusion that, having a flexibility of choice of the projected colors, they can be adjusted to achieve the same exposure in all acquired band images. This way the signal to noise ratio and quantization errors are similar and easier to compensate for. Moreover, the linear model of intensity registration provides data giving very accurate spectral reconstruction, which is generally not achievable in practice. This means, that the experimental factors such as noise, uneven illumination, ambient light and camera non-

linearity play important role in the reconstruction accuracy and elimination of them should provide better spectral reflectance reconstruction.

## ACKNOWLEDGEMENTS

## REFERENCES

Fischer, C. and I. Kakoulli. 2006. Multispectral and hyperspectral imaging technologies in conservation: current research and potential applications. *Reviews in conservation*, 7: 3-16.

Imai, F. H. and M. R. Rosen, and R. S. Berns. 2002. Comparative Study of Metrics for Spectral Match Quality. In *The First European Conference on Colour Graphics, Imaging and Vision*, 492-496.

Jiang, J. and J. Gu. 2012. Recovering spectral reflectance under commonly available lighting conditions. In *IEEE Computer Vision and Pattern Recognition Workshops (CVPRW)*, 1-8.

Kang, H. R., 2006. *Computational Color Technology*. Washington: SPIE Press.

Mansouri, A. and A. Lathuilière, F.S. Marzani, Y. Voisin, and P. Gouton. 2007. Toward a 3d multispectral scanner: an application to multimedia. *IEEE Multimedia* 14(1): 40-47.

Mączkowski, G. and R. Sitnik, and J. Krzesłowski. 2012. Data Acquisition Enhancement in Shape and Multispectral Color Measurements of 3D Objects, In *Image and Signal Processing*. 7340, 27-35.

Shrestha, R. and A. Mansouri, and J. Hardeberg. 2011. Multispectral imaging using a stereo camera: concept, design and assessment. *EURASIP Journal on Advances in Signal Processing*. 2011(57).

Simon-Chane, C. and R. Schütze, F. Boochs, and F. S. Marzani. 2013. Registration of 3D and multispectral data for the study of cultural heritage surfaces. *Sensors*. 13: 1004-1020.

Sitnik, R, 2002. *A fully automatic 3D shape measurement system with data export for engineering and multimedia systems*. PhD thesis, Warsaw University of Technology.

Tonsho, K. and Y. Akao, N. Tsumura, and Y. Miyake. 2001. Development of goniophotometric imaging system for recording reflectance spectra of 3D objects. In *Proc. SPIE 4663, Color Imaging: Device-Independent Color, Color Hardcopy, and Applications VII*, 370-378.

*Address: Grzegorz MĄCZKOWSKI, Institute of Micromechanics and Photonics, Warsaw University of Technology, Św. Andrzeja Boboli 8, Warsaw, 02-525, POLAND E-mail: g.maczkowski@mchtr.pw.edu.pl, lech@mchtr.pw.edu.pl r.sitnik@mchtr.pw.edu.pl*

# Multispectral Imaging System based on Tuneable LEDs

Muhammad SAFDAR,[1] Ming Ronnier LUO,[1,2] Yuzhao WANG,[1] Xiaoyu LIU[1,3]
[1] State Key Laboratory of Modern Optical Instrumentation, Zhejiang University, Hangzhou, China
[2] School of Design, University of Leeds, Leeds, UK
[3] College of Science, Harbin Engineering University, Harbin, China

## ABSTRACT

A modified multiplexed illumination based multispectral imaging system was proposed using RGB camera and LED illumination, which used RGB camera and different combinations of RGB LEDs. The system was developed, optimised for its performance and compared with a commercial hyperspectral imaging system which uses line-scan and Push-Broom technology developed by Isuzu Optics. The Isuzu system was tested first by capturing different targets and its performance was found excellent. Three optimal combinations each of 3 LEDs (one from each of red, green and blue regions) were selected to illuminate the scene. Three exposures of RGB camera were used to estimate the 9-band spectral image of the scene using linear regression method. Some further improvements were made like optimization of camera spectral sensitivities, uniformity correction of exposures and adaptively assigning different weights to different LEDs and training samples. With these improvements the performance of the system was improved by about 50%. The sytem was tested by using four different target charts for training and testing. For different trainnig and testing sets, the performance of the system was lacking behind Isuzu system by 1 $\Delta E_{00}$ units which is obvious because of using low intensity LEDs. It can be concluded that the developed system is self-illuminated, energy efficient, easily realisable, cost effective and  fast in acquisition.

## 1. INTRODUCTION

Multispectral imaging is preferred over conventional RGB imaging because of high color accuracy, non-metameric match and is not limited to visual range. Typically, multispectral imaging systems are developed using filter wheel, filter array, stereo camera or monochrome camera with multiplexed illumination which are expensive and time consuming methods. Much attention has been paid to the multiplexed LED illumination based systems during last decade because of their robustness, high switching capability and cost effectiveness (Shurestha 2013). Spectral imaging has wide spread applications including heritage and culture (Cotte 2003), biometrics (Rowe 2005), astronomy (Rosselet 1995), remote sensing (Swain 1978), medical imaging (Everdell 2009) and many others.

Many different methods of multispectral imaging have been proposed already and are available in literature. Multispectral imaging based on multiplexed LED is of prime interest in this paper (Tominaga 2012). In such a system, n different LEDs are illuminated in a sequence and the scene is captured under each light using a monochrome camera in result of which n band spectral image is obtained. Such a system has been used in several applications including film scanner (Shurestha 2012), biometrics (Rowe 2005) and medical imaging (Everdell 2009). Other types include filter wheel based, tuneable filter (Hardeberg 2002, Shurestha 2011) and filter array (Baone 2000, Miao 2006) based systems.

In State of the art multiplexed illumination based system, n band multispectral image is obtained by using n LEDs and n number of exposures of monochrome camera. While in modified multiplexed illumination based system, three LEDs, one from each of red, green and blue regions are illuminated at a time and RGB camera is used to capture the scene. So in this way, n band spectral image can be obtained by n/3 number of exposures (Shurestha 2013).

In the Current work, modified multiplexed illumination based system has been developed and some improvements have been made including uniformity correction, optimization of camera spectral sensitivity functions, and assigning optimal weights to different LEDs used as well as to training samples. The developed system was tested by using different training and testing color targets including four different charts named MCCC- Classic, MCCC-SG, DigiEye Digitizer and Oil Painting Pigments. Its performance was compared with a commercial hyper-spectral system (Hyper-spectral Microscope with EMCCD camera, VNIR-400~900nm) by Isuzu Optics. The commercial system uses line-scan and push-broom technology which is fast and robust comparing with typical filter based systems. This section is followed by method, results and discussion, and conclusions drawn in the end.

## 2. METHOD

In this paper, modified multiplexed illumination system was devleoped, improved and its performance was compared with a commercial hyper-spectral system. A commercialy available 16 channel LED illuminant, each channel of which is computer controlable, was used to illuminate the scene. Nine LEDs were selected out of sixteen, three from each of red, green and blue regions. The selected nine LEDs are narrow band, lying within and covering more less the whole visible range of 400-700nm (Figure 1). One combination of three LEDs, one from each region, was illuminated at a time and scene was captured using Canon 5D Mark II camera with RGB sensors. Three optimal combinations of LEDs were selected which give the minimum color difference. Four different color charts were used for training and testing (Figure 1). A computer system was used to synchronise illumination and capture. So the system is simple, self illuminated and computer controlled. The schematic daigram is shown below (Figure 2).

For each light the scene was captured once using Canon 5D Mark-II camera. These three exposures were used to estimate the 9-band spectral image of the scene using linear regression method. In this method, the reflectance values were back predicted using SPDs of the LEDs used, spectral sensitivities of the camera and reflectance values of the training set of samples measured using Data-Color SF600. Some further improvements were made like optimization of camera spectral sensitivities, uniformity correction of exposures and adaptively assigning different weights to different LEDs and training samples. With these improvements the performance of the system was improved by more than 50% of that of original for initial test done using MCCC-Classic. Main errors are caused by acquisition noise due to non-uniform and low intensity of the LED sources used. The performance of the developed system was compared with a commercially available hyper-spectral system. The commercial system was first tested by comparing its results with reflectance data measured using Data-Color SF600. The performance of the commercial system was found excellent. The Isuzu Optics used line-scan and push-broom technology to develop a hyper-spectral imaging system. The performance of both systems was measured using latest CIE

color difference formula named CIEDE2000 (Luo 2001). Our developed system's performance was lacking behind Isuzu's system by about 1 $\Delta E_{00}$ units.
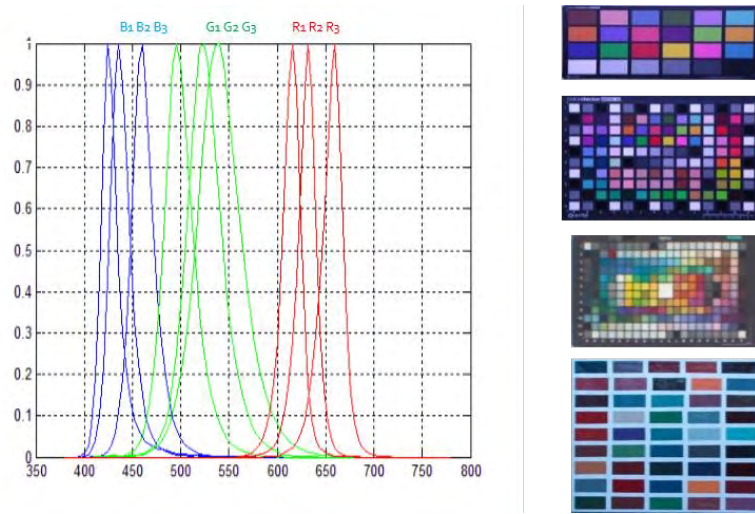


Figure 1: SPDs of selected 9 LEDs and four color charts used for training and testing.
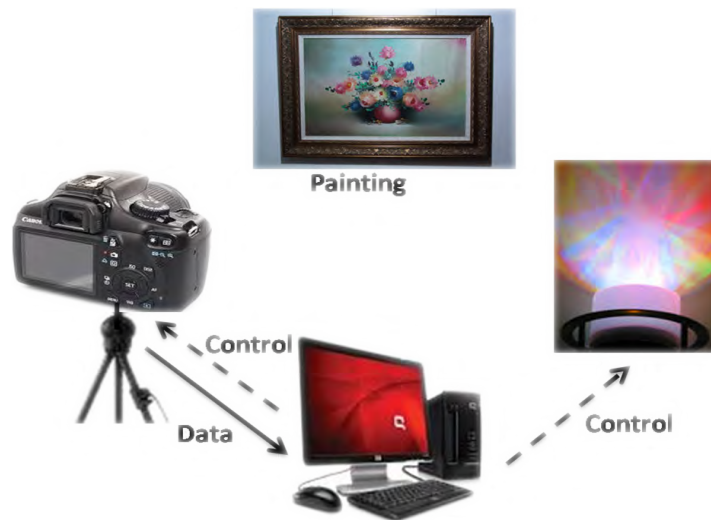


Figure 2: Schematic diagram of developed system.

## 3. RESULTS AND DISCUSSION

Both systems were tested by comparing results with measured reflectance data using Data-Color SF600. The results of Isuzu's system were found very close to the measured reflectance values and hence its perfromance was found excellent. The developed modified multiplexed illumination system was improved by introducing some modifications. The camera spectral sensitivities were optimized using an adaptive algorithm. The captured RGB images were stored in raw data form and then uniformity was corrected by using a unifrom white board. The uniformity corrected real matrices were then used to back predict reflectance data of each pixel. Different weights were adaptively assigned to SPDs of selected 9 LEDs. And in the same way different weigts were assigned to reflectance vectors of different training samples. The black level was also adjusted. In result of these

improvements the performance of developed system was improved by about 50% compaing with original system. The performance of developed system was compared with Data-Color measurements and Isuzu's system as well. The performance of developed system was found lacking behind Isuzu's system by 1 CIEDE00 units. The results of developed system for four different training and testing targets are shown in Table 1. Oil paiting pigments chart was only used for self prediction because it does not include grey patches. First column respresents training sets while all other columns repesent testing results against four test targets. The results were presented in terms of color difference between measured and estimated reflectance calculated using CIEDE2000 formula. The developed system reduces acquisition time by 5 times because of fast switching capability of LEDs and computer control. The use of RGB camera is more convinient and its focus and resolution can be set by user. Moreover, such a system costs much less comparing with state of the art technology.

*Table 1. Summary of the results of developed system for different trinig and testing sets.*

| Charts | MCCC-Classic | MCCC-SG | DigiEye-DigiTizer | Oil Paintig Pigments |
|---|---|---|---|---|
| MCCC-Classic | 3 | 4.4 | 4.5 | 3.5 |
| MCCC-SG | 3.0 | 2.8 | 3 | 3.7 |
| DigiEye-DigiTizer | 2.9 | 3.2 | 2.5 | 3.8 |
| Oil Paintig Pigments | X | X | X | 3.9 |

As for different traning and testing samples the color defference is less than 3 on everage, so the improved multiplexed illumination spectral imaging system can give acceptable results for real time applications (Song 2000). Some paintings were also captured using develped system and images were found close to those captured using commercial system.

## 4. CONCLUSIONS

A modified multiplexed ilumination system was developed using tuneable LEDs and RGB camera. The developed system was then improved by optimising SSFs, applying uniformity correction, and adaptively asigning different weights to different SPDs of LEDs and different training samples. Dark levels were also adjusted adaptly. It was found that the performance of developed system improved after above mentioned modifications. The improved system is much faster and cost effective comparing with state of the art spectral imaging systems.

The performance of commercial system was also tested which was found excellent. The developed system was compared with the commercial one. The developed system was lacking a bit behind commercial system in terms of performance but was found more faster and cost effective. The developed system can be used for many applications including

biometrics, medical imaging and especially for culture and heritage. It can be concluded that the developed system is self-illuminated, energy efficient, easily realisable, cost effective and  fast in aquisition.

More work is being carried out to use high intensity and more uniform LED pannel and the expected results using the current method are less than 2 $\Delta E_{00}$.

## REFERENCES

Baone G. A., and Qi H. 2000. De-mosaicking Methods for Multispectral Cameras Using Mosaic Focal Plane Array Technology. The 8th International Symposium on Multispectral Color Science 6062 75-87.

Cotte P., Dupouy M. 2003. CRISATEL High Resolution Multispectral System. In PICS 161-165.

Everdell N. L., Styles I. B., Claridge  E., Hebden J. C., and Calcagni A.S. 2009. Multispectral Imaging of the Ocular Fundas Using LED Illumination. Novel Optical Instrumentation for Biomedical Applications IV, SPIE Proceedings 3771.

Hardeberg J. Y., Schmitt F., and Brettel H. 2002. Multispectral colour image capture using a liquid crystal tuneable filter. Optical Engineering, 41(10) 2532-2548.

Lou M. R., Cui G., and Rigg B. 2001. The Development of CIE 2000 Color Difference Formula: CIEDE2000, Color Res. App., 26(5) 340-350.

Miao L., Qi H., Ramanath R., and Snyder W. 2006. Binary Tree Based Generic De-mosaicking algorithm for Multispectral Filter Array. IEEE Transactions on Image Processing 15(11) 3550-3558.

Rowe P. K., Nixon K. A., and Corcoran S. P. 2005. Multispectral Fingerprint Biometrics. Proc. of 6th Annual IEEE Information Assurance Workshop (IAW) 14-20.

Rosselet A. C., Graff W., Wild U. P., Keller C. U., and Gschwind R. 1995. Persistent Spectral Hole Burning Used for Spectrally High-Resolved Imaging of the Sun. Imaging Spectrometry, SPIE Proc. 2480.

Shurestha R., and Hardeberg J. Y. 2013. Multispectral Imaging Using LED Illumination and An RGB Camera. Proc. of 21st CIC, 8-13.

Shurestha R., Mansouri A., and Hardeberg J. Y. 2011. Multispectral Imaging Using a Stereo Camera. EURASIP Journal on Advances in Signal Processing 2011(1).

Shurestha R., Hardeberg J. Y., and Boust C. 2012. LED based Multispectral Film Sacanner for Accurate Color Imaging. The 8th International Conference on Signal Image Technology and Internet based Systems 811-817.

Song T., and Luo R. 2000. Testing Color Difference Formula on Complex Images Using a CRT Monitor. The 8th Color Imaging Conference (IS&T), 44-48.

Swain P. H., and Davis S. M. 1978. Remote Sensing: The Quantitative Approach. Mcgraw-Hill, New York., 1978.

Tominaga S., Horiuchi T. 2012. Spectral imaging by synchronizing capture and illumination. J. of Opt. Soc. Am. A, 29(9) 1764-1775.

*Address: Prof. Ming Ronnier Luo, State Key Laboratory of modern optical instrumentation, Zhejiang University, Hangzhou, China*
*E-mails: msafdar87@zju.edu.cn，  m.r.luo@leeds.ac.uk，  wangyuzhao@zju.edu.cn，*
*wangflxy@zju.edu.cn*

# Evaluation of Hyperspectral Imaging Systems for Cultural Heritage Applications Based on a Round Robin Test

Sony George, Irina Mihaela Ciortan, Jon Yngve Hardeberg
The Norwegian Colour and Visual Computing Laboratory
Gjøvik University College, Gjøvik, Norway

## ABSTRACT

There has been an increasing interest in using spectral imaging for cultural heritage applications as it provides valuable scientific knowledge on the materials and techniques employed by the artist. In order to select the suitable device for various kinds of applications in the cultural heritage sector, it is necessary be able to evaluate the diverse set of available spectral imaging devices. The resulting spectral images are influenced by several device parameters (sensor characteristics, spectral sensitivity, spectral range, noise, dynamic range, optics, data formats) and imaging conditions (illuminant intensity and spectral power distribution, imaging geometry, illuminant non-uniformities etc.). This paper describes the details and preliminary results of a Round Robin Test (RRT) conducted to ensure the quality and comparability of measurements performed by different spectral imaging laboratories involved in cultural heritage imaging. The present RRT is considered as an external spectral image quality assurance tool in cultural heritage applications. Results from this RRT will be used to standardize spectral imaging procedures, and also to determine certain characteristics of reference materials which are useful for accurate documentation and analytical studies.

## 1. INTRODUCTION

The study of the paintings and other artworks that represent the cultural heritage is key to effective and adequate restoration and conservation procedures. Spectral imaging has been proved as a promising technology to perform scientific documentation and analysis of cultural heritage objects (Liang, 2012, Hardeberg et al. 2014). This non-invasive technique was found useful for achieving several objectives. Even though the general classification of spectral imaging is based on the number of bands – multispectral and hyperspectral systems, spectral imaging devices vary according to the technology used for capturing the data. This includes the sensor, electronics, optics and the imaging conditions also. Thus, the spectral characteristics of the same object acquired with different setups might vary.

The spectral imaging techniques have been initially developed in the remote sensing domain and later adopted in many other disciplines (Martinez et al. 2002). Many of the imaging systems used in the cultural heritage imaging are not designed to be applied in this domain, but they are adapted for this purpose. Due to this reason, the imaging systems has to be studied to understand the sensor characteristics, imaging geometry, reference objects which generate high quality data in cultural heritage sector. The EU funded COST action COSCH, Colour and Space in Cultural Heritage, is one of the initiatives that aim to investigate and enhance the use of spectral imaging for cultural heritage objects.

A Round Robin Test is a widely accepted tool to study the influence of various parameters, which may vary between individual laboratories and instruments. In this exercise, the same test objects was circulated among the participating laboratories and measured by different instruments to evaluate the quality of the data. This RRT has been conducted as a part of the European project COSCH and more than 16 laboratories have been participating in this programme. Each participating laboratory uses one or more imaging systems. Five test targets has been chosen for this RRT and each of these objects has different typologies which represent commonly used elements in cultural heritage imaging. The test targets includes a Spectralon wavelength calibration standard, X-Rite ColorChecker Classic, X-rite white reference, a painted panel reconstructed with medieval Tuscan technique, and an antique Russian icon on copper. The main discrepancy between the instruments might be caused by the different sub components, which has been used to build the acquisition setups, and the processing workflow. One of the main objectives of this RRT is to identify these elements and to recommend solutions to form an inter-instrument and inter-lab agreement.

Analysis of the hyperspectral data from two imaging systems to understand the quality in terms of image noise has already reported (Vitorino et al. 2015). This paper describes methodologies and preliminary results of the hyperspectral image data obtained by three of the participating laboratories.

## 2. METHOD AND MATERIALS

One of the most important factors that influences the result of any round-robin test practice is the choice of test targets. Utmost care has been taken to choose the targets, which replicate the common reference targets used while performing the spectral acquisition of cultural heritage objects. Details of the test targets are explained briefly in the following section.

### 2.1 Test Targets

**Test target 1: Spectralon reference.** The Spectralon® multi-component wavelength calibration standard is one of the most commonly used reference standards to keep track of the reflectance/absorbance of the measured object. Spectralon is impregnated with a combination of three rare earth oxides (holmium oxide, erbium oxide, dysprosium oxide), is a stable and chemically inert reflectance standard, commonly used for establishing the accuracy of the wavelength scale of reflectance spectrophotometers. Spectralon has a size of 90mm of diameter, and opaque, homogenous, smooth surface, and exhibits sharp absorptions at specific wavelengths span over UV-VIS-NIR region of the electromagnetic spectrum. This object was selected as one of the reference objects in this RRT in order to assess the wavelength accuracy and the spectral resolution of each spectral system.

**Test target 2: X-rite ColorChecker Classic.** The X-Rite® ColorChecker Classic target is a twenty-four patch color chart with standard colors which are the representation of true colors of natural matter (such as skin, foliage and sky), additive and subtractive primary colors, various steps of grey, and black and white. Each square patch has a size of 40mm and total size of 279.4mm x 215.9mm. The ColorChecker is a very commonly used item for conventional photography and also as a standard color reference to evaluate color

reproduction processes, to guarantee that the information obtained is valuable and represents the true colors of the object that has to be studied and documented (Berns 2001).

**Test target 3: X-rite White Reference.** The ColorChecker® white balance target is a spectrally neutral reference standard to deliver accurate white reproduction. White balance reference is used to measure the light distribution in the objects location and it guarantees precise, uniform, neutral white under any lighting condition.



Figure 1. RRT test objects (a) Spectralon reference (b) ColorChecker Classic  (c) White balance  (d) Painted panel (e) Icon

**Test target 4: Painted panel.** In addition to the above listed reference targets, a painted panel is also included in the test objects. The panel was reconstructed by Elena Prandi and Marina Ginanni (Restoration Laboratories of the Soprintendenza SPSAE e per il Polo Museale della città di Firenze, Italy), in order to reproduce the medieval Tuscan technique as described by Cennino (1954). This panel was made in a wooden support and includes several layers of different pigments and underdrawings. The painted panel was included in the RRT items to evaluate the relevant spectral region for pigment analysis and to unveil underdrawings especially in the NIR region.

**Test target 5: Icon**. Test targets 1-4 were mainly proposed as reference objects for spectral imaging in cultural heritage. However, it is also desirable to study the current challenges in this field, which arises when dealing with objects of different properties like metallic or glossy surfaces. This will help to form best practices for imaging such items. A Russian icon, "Virgin of Kazan" dated 1899 owned by Lindsay MacDonald (University College London, UK) was chosen as a test target. The icon is in the form of a colored image printed on copper plate, with wooden support as the substrate. Due to the metallic plating, the illuminant generates specular reflections, which often reduces the quality of imaging. The aim of including this icon in this RRT is to understand the imaging

instruments response to such challenging objects and investigate ways to address such issues.

## 2.2 Experimental Procedure

The same set of test objects was circulated among the participating laboratories. Each participant was provided with the general instructions of the test and performed the image acquisitions in the same manner they usually work with their instrument. Details of the spectral instrument and the image acquisition conditions have been collected with a Test report form. Basic processing steps were requested to be performed by every laboratory in order to get the object spectral reflectance data. Ground truth data for the test objects was measured using point spectrometers and used as reference for comparison for the data sets.

## 3. RESULTS AND DISCUSSION

In the present paper, we discuss the comparison between three sets of hyperspectral image data obtained from three laboratories. As shown in Table 1, the instrument specifications are different in several aspects and also the original purpose of not all these spectral systems are for cultural heritage imaging.

Spectral image quality highly depends on the end objective and the application domain. Defining attributes for every application is a challenging task (Shrestha et al. 2014). Most of the existing studies are in the remote sensing domain and are mostly related to the accuracy in classification. For cultural heritage applications, a standard has not been well established to evaluate the spectral imaging systems. In Table 2, a set of quality specifications is proposed. The values in the table are given for the three laboratories and hyperspectral imaging systems presented in the current study, but the attributes are meant to be a standard of quality that will be extended to all the imaging systems involved in the Round Robin Test.

*Table 1. Details of the hyperspectral imaging systems.*

| Participant | No of bands | Wavelength (nm) | Imaging geometry | Spatial resolution | Bit depth | Original purpose of system |
|---|---|---|---|---|---|---|
| Lab 1 | 61 | 400-1000 | 0- 45 | 275 ppi | 16 bit | Measurement and color control of spatially complex patterns |
| Lab 2 | 160 | 400-1000 | 0- 45 | 150 ppi | 16 bit | Airborne applications |
| Lab 3 | 450 | 400-900 | 0- 45 | 300 ppi | 12 bit | Art scanning |

Table 2. Quality specifications of the 3 hyperspectral systems

| Class of attributes | System Attributes | Lab 1 Pushbroom Hyperspectral Imaging System VIS-NIR | Lab 2 Hyperspectral Camera | Lab 3 Line Scanning Spectral System |
|---|---|---|---|---|
| System Attributes | Spatial sampling | 275 ppi | 150 ppi | 300 ppi |
| | Spectrum coverage | Visible + near infrared (400-1000nm) | Visible + near infrared (400-1000nm) | Visible + near infrared (400-960nm) |
| | Number of bands | 61 | 160 | 450 |
| | Band separation | ~10 nm | ~3.7nm | ~1.25nm |
| | Number of bits | 18 | 12 | 16 |
| Set-up Information | Position of the target | Horizontal | Horizontal | Vertical |
| | Complexity | Medium | Medium | Medium |
| | Portability of the system | Low | Low | Low |
| | Cost | High | High | High |
| Post-processing | File format | .tif | Proprietary | .cub |
| | Compatibility with ENVI | No | Yes | Yes |

It is noted that spectral data obtained from Lab 3, resulted in least spectral and colorimetric error compared with data from Lab 1 and Lab 2. This imaging system has better spectral and spatial resolution with 450 bands and 300 ppi. Since this system has originaly designed for art scanning applications, close range scanning might have resulted in better spectral data. Painted panel was made by mixing different materials and the spectral measurements was performed at visually similar spatial locations in the same bands. The imhomogeneity in painted material might have caused slightly higher values in RMSE compared to the ColorChecker. The overall trend of error metrics of spectral data from the 3 instruments is comparable.

In addition to the quality system specifications in Table 2 and the spectral and color accuracy metrics in Table 3 and Table 4, a set of image quality attributes has been defined to be taken into consideration as well in the final report of quality evaluation for the RRT Test objects, ColorChecker and Painted panel spectral images are compared spectrally and colorimetrically. In this analysis, measurements performed with a point spectrometer are considered as the ground truth. The metrics Root Mean Square Error and the CIELAB color difference are computed to quantify the spectral and the colorimetric quality respectively. The attributes refer to the quality of the image captured by the spectral

systems, in terms of image sharpness, uniformity, noise and specularities that characterise the spectral digital captures of the cultural heritage objects studied in the RRT. The proposed attributes will be analysed in future work.

*Table 3. RMSE and CIELAB color difference computed for the each of the 24 patches of the Color Checker, between the values measured with the three imaging systems and the ground truth data.*

| Color Checker Patch | | 1 | 2 | 3 | 4 | 5 | 6 | 7 | 8 | 9 | 10 | 11 | 12 | 13 |
|---|---|---|---|---|---|---|---|---|---|---|---|---|---|---|
| Lab 1 | RMSE | 0.11 | 0.12 | 0.02 | 0.03 | 0.09 | 0.10 | 0.12 | 0.09 | 0.09 | 0.05 | 0.11 | 0.11 | 0.04 |
| | CIELAB diff | 8.24 | 5.44 | 1.43 | 9.54 | 4.11 | 6.28 | 17.76 | 7.77 | 11.55 | 3.90 | 13.61 | 17.34 | 9.93 |
| Lab 2 | RMSE | 0.05 | 0.03 | 0.05 | 0.02 | 0.01 | 0.05 | 0.07 | 0.03 | 0.04 | 0.04 | 0.02 | 0.09 | 0.03 |
| | CIELAB diff | 1.33 | 1.54 | 1.76 | 2.22 | 1.43 | 6.38 | 6.89 | 4.52 | 2.18 | 4.14 | 3.59 | 7.42 | 6.41 |
| Lab 3 | RMSE | 0.01 | 0.01 | 0.01 | 0.01 | 0.01 | 0.01 | 0.01 | 0.01 | 0.01 | 0.01 | 0.01 | 0.01 | 0.01 |
| | CIELAB diff | 2.31 | 1.84 | 1.03 | 1.46 | 1.54 | 1.94 | 2.19 | 2.25 | 1.20 | 1.42 | 2.68 | 2.00 | 0.69 |
| Color Checker Patch | | 14 | 15 | 16 | 17 | 18 | 19 | 20 | 21 | 22 | 23 | 24 | **Mean** | |
| Lab 1 | RMSE | 0.11 | 0.11 | 0.14 | 0.10 | 0.04 | 0.14 | 0.05 | 0.02 | 0.02 | 0.01 | 0.01 | **0.08** | |
| | CIELAB diff | 15.12 | 15.55 | 17.42 | 12.03 | 6.84 | 6.88 | 5.55 | 4.25 | 3.21 | 4.03 | 4.81 | **8.86** | |
| Lab 2 | RMSE | 0.02 | 0.02 | 0.03 | 0.08 | 0.03 | 0.14 | 0.09 | 0.04 | 0.02 | 0.04 | 0.02 | **0.04** | |
| | CIELAB diff | 5.37 | 3.52 | 2.18 | 3.07 | 5.93 | 7.72 | 2.86 | 0.93 | 2.14 | 2.67 | 3.65 | **3.74** | |
| Lab 3 | RMSE | 0.01 | 0.02 | 0.02 | 0.02 | 0.01 | 0.02 | 0.01 | 0.01 | 0.01 | 0.01 | 0.01 | **0.01** | |
| | CIELAB diff | 2.11 | 2.18 | 1.51 | 2.84 | 3.28 | 0.43 | 0.51 | 0.40 | 0.69 | 0.34 | 1.20 | **1.58** | |

*Table 4. RMSE and CIELAB color difference computed for the each stripe of the Painted Panel, between the values measured with the three imaging systems and the ground truth data.*

| Painted Panel | | 1 | 2 | 3 | 4 | 5 | 6 | 7 | 8 | 9 | 10 | 11 | 12 | Mean |
|---|---|---|---|---|---|---|---|---|---|---|---|---|---|---|
| Lab 1 | RMSE | 0.04 | 0.03 | 0.12 | 0.14 | 0.12 | 0.11 | 0.03 | 0.02 | 0.06 | 0.05 | 0.08 | 0.02 | **0.07** |
| | CIELAB diff | 6.52 | 4.20 | 11.18 | 12.96 | 15.15 | 15.94 | 7.08 | 5.92 | 8.70 | 7.19 | 6.48 | 7.57 | **9.08** |
| Lab 2 | RMSE | 0.04 | 0.01 | 0.09 | 0.04 | 0.07 | 0.12 | 0.06 | 0.04 | 0.02 | 0.02 | 0.21 | 0.04 | **0.06** |
| | CIELAB diff | 1.87 | 3.15 | 3.61 | 7.16 | 7.19 | 7.23 | 8.96 | 2.57 | 4.37 | 5.35 | 6.39 | 4.29 | **5.18** |
| Lab 3 | RMSE | 0.01 | 0.01 | 0.01 | 0.01 | 0.02 | 0.01 | 0.00 | 0.01 | 0.01 | 0.01 | 0.02 | 0.01 | **0.01** |
| | CIELAB diff | 3.73 | 4.97 | 5.56 | 3.54 | 2.31 | 0.83 | 0.78 | 1.00 | 1.05 | 1.99 | 1.01 | 4.39 | **2.60** |

## 4. CONCLUSIONS

In this paper we have presented the preliminary analysis of hyperspectral data generated from a Round Robin Test. In addition to the technical comparison of spectral imaging systems, a quantitative evaluation of the image data has also been performed for three laboratories. In future work, this quality analysis will be extended to the full set of multispectral and hyperspectral devices involved in the RRT and more metrics will be added towards an in-depth evaluation.

## ACKNOWLEDGEMENTS

## REFERENCES

Berns, R.S. (2001) The Science of Digitizing Paintings for Color-Accurate Image Archives: A Review. *Journal of Imaging Science and Technology*, 45(4), 305-325

Cennino, C (1954). Il Libro dell'Arte (The Craftsman's Handbook), translated by D. V. Thompson. Dover, New York.

Hardeberg, J.Y., et al. (2015) Spectral Scream: Hyperspectral Image Acquisition and Analysis of a Masterpiece. To appear in Public paintings by Edvard Munch and some of his contemporaries. Changes and conservation challenges, Tine Frøysaker, Noëlle Streeton, Hatmut Kutzke, Biljana Topalova-Casadiego and Françoise Hanssen-Bauer, eds., Archetype Publications, London, UK

Liang, H. (2012) Advances in Multispectral and Hyperspectral Imaging for Archaeology and Art Conservation. *Applied Physics A: Materials Science & Processing*, 106(2), 309-323

Martinez, K. et al.: (2002) Ten Years of Art Imaging Research. *Proceedings of the IEEE*, 90(1), 28-41

McCamy, C.S. et al. (1976) A Color-Rendition Chart. *Journal of Applied Photographic Engineering*, 2(3), 95-99

Shrestha, R. et al. (2014) Quality evaluation of spectral imaging: Quality factors and metrics. *Journal of the International Colour Association*, 12:22–35.

Vitorino, T. et al., (2015) Accuracy in Colour Reproduction: Using a ColorChecker Chart to Assess the Usefulness and Comparability of Data Acquired with Two Hyper-Spectral Systems. *Computational Color Imaging, Lecture Notes in Computer Science 9016, 225-235*

*Address: Dr. Sony George, The Norwegian Colour and Visual Computing Laboratory*
*Faculty of Computer Science and Media Technology, Gjøvik University College*
*P.O. Box 191, N-2821 Gjøvik, Norway, http://www.colourlab.no*
*E-mails: sony.george@hig.no, jon.hardeberg@hig.no, irina.ciortan@gmail.com*

# Spectral Gigapixel Imaging System
# for Omnidirectional Outdoor Scene Measurement

Motoki HORI, Naoto OSAWA, Keita HIRAI, Takahiko HORIUCHI, Shoji TOMINAGA
Graduate School of Advanced Integration Science, Chiba University

## ABSTRACT

This paper presents a system for acquiring spectral gigapixel images of omnidirectional outdoor scenes. The system is constructed using two programmable high-speed RGB video cameras with telephoto lenses and a programmable rotating table. The captured image size is 2048 × 1088 pixels, and the camera can capture images at a rate of more than 100 frames per second. The telephoto lens covers a horizontal angle of 14.5° and a vertical angle of 10.8°. The rotating table can be automatically controlled by a computer. It can rotate 360° in the horizontal plane and 180° in the vertical plane. Two different types of color filters are mounted on the two RGB video cameras for multi-band image acquisition. By combining these color filters with the camera sensitivities, we can obtain six-channel spectral sensitivity functions. Then, spectral power distributions can be recovered from the captured six-band images by using the Wiener estimation algorithm. From the experimental results, the average RMSE in the proposed system is estimated to be 0.01427. For achieving gigapixel omnidirectional images, we capture the images for 60 horizontal and 21 vertical directions. Then we synthesize a gigapixel omnidirectional image by combining the above captured 1,260 images. This synthesized image covers a spherical field of 360° and comprises approximately 1.9 gigapixels (60000 × 32000 pixels). As a result, our spectral gigapixel image makes it possible to view the omnidirectional details, and also to reproduce accurate spectral power distributions in the scene.

## 1. INTRODUCTION

Omnidirectional imaging is a useful technology for landscape archiving applications such as Google Street View (Anguelov, 2010) and "Aftermath of the 2011 Tohoku earthquake and tsunami" (A project by The University of Tokyo and Tohoku University) (Sakurada, 2013). In addition, omnidirectional images are currently being applied to virtual experiences through head mounted display systems (Hale, 2014). Hence, it is clear that omnidirectional imaging has been widely used in our daily life.

A variety of omnidirectional imaging systems have also been developed. For example, a camera system with mirrors and panorama stitching algorithms using multiple images are well-known approaches (Szeliski, 2010). For covering 360° spherical field of view, recently a Ladybug camera system has been utilized (PointGrey Research, Ladybug5, 2014). This system has six cameras for synthesizing an omnidirectional image.

For high-quality omnidirectional scene archiving, it is also important to achieve accurate scene spectral information and high-resolution images. In other words, the technology of a spectral gigapixel imaging system for omnidirectional natural scenes is significant for the next-generation natural scene archiving. So far the imaging systems were developed separately through spectral imaging, gigapixel imaging, and omnidirectional imaging and had different applications. In addition, some integrated systems with above two functions were also proposed for specific purposes. For examples, a 360° omnidirectional gigapixel imaging system has been developed by using a telescopic camera and an automatically-

controlled rotating table (Gigapixel Panorama Photo, 2013). In our previous work, we had developed a system for acquiring spectral images for time-lapse omnidirectional natural scenes (Hirai, 2014). However, there are no imaging systems for acquiring spectral, gigapixel and omnidirectional images concurrently.

In this paper, therefore, we present a system for acquiring spectral gigapixel images of omnidirectional outdoor scenes. In general, a gigapixel image is generated by combining huge amount of images that are captured using telephoto lenses. Then, we capture more than one thousand multi-band images for generating a spectral gigapixel image of an omnidirectional outdoor scene. For realizing this capture, we develop a system using two programmable high-speed RGB video cameras with telephoto lenses and a programmable rotating table.

## 2. PROPOSED SYSTEM AND IMAGE SYNTHESIS

### 2.1 Proposed Imaging System

Figure 1 shows the proposed imaging system for acquiring spectral gigapixel image of omnidirectional scenes. Our system consists of two programmable high-speed RGB video cameras with a telephoto lens, and programmable rotating table. Two different types of color filters are mounted on the two video cameras.

The video camera is a Baumer HXG20 with an image size of 2048 × 1088 pixels and a bit depth of 12 bits, which can capture images over 100 frames per second (fps). The cameras also have liner response characteristics. This specification of the camera is enough for reducing the acquisition time. The lens is Kowa telephoto lens, which covers a horizontal angle of 14.5°and a vertical angle of 10.8°. The rotating table is CLAUSS RODEON VR station HD, which can be automatically controlled by a computer and allow 360° movement in the horizontal plane and 180° in the vertical plane.

Two different types of color filters (KODAK No.34A, FUJIFILM SP-18) are mounted on the two color video cameras for six band image acquisition. Figure 2 shows the overall spectral sensitivity functions of the proposed imaging system. We reconstruct spectral power distributions (color signals) from the six-band images based on the Wiener estimation algorithm.
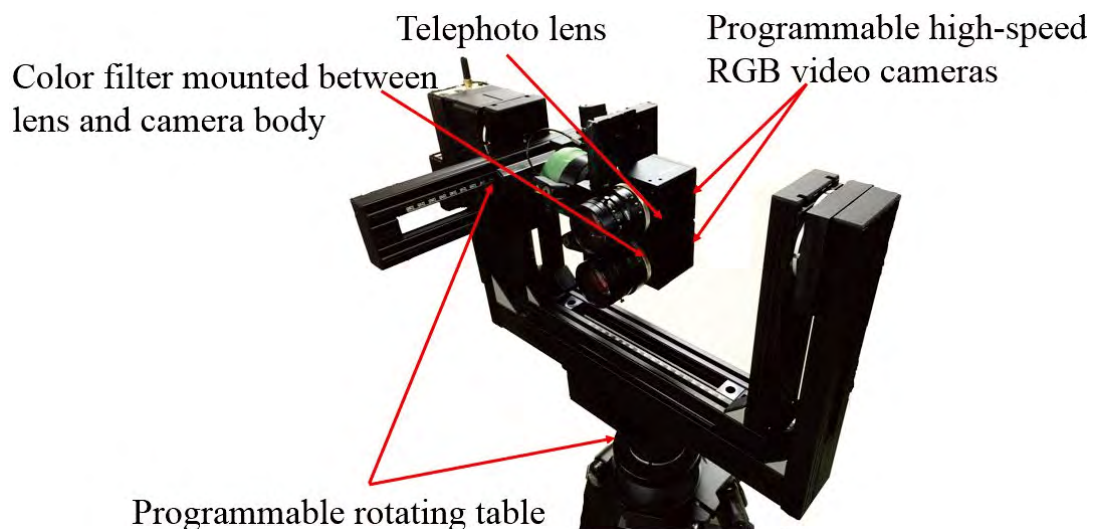


*Figure 1: Proposed system for acquiring gigapixel image of omnidirectional scenes.*
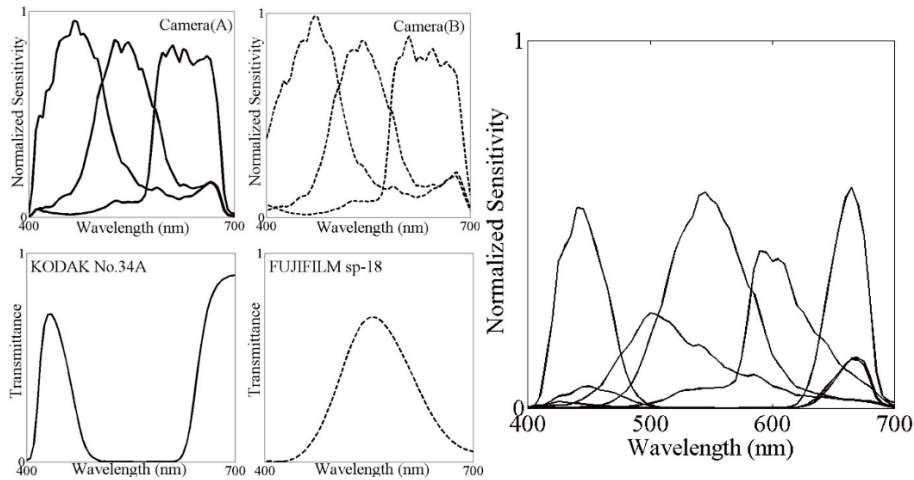
*Figure 2: Spectral sensitivity functions spectral of the proposed six-band imaging system.*

## 2.2 Image Synthesis

Figure 3 shows the flowchart for synthesizing a spectral gigapixel image of an omnidirectional scene. In our measurement system, we capture HDR images in 1260 directions (60 images in the horizontal plane and 21 images in the vertical plane). Each HDR image is generated by combining fifteen low dynamic range (LDR) images captured at 15 different exposure times.

Because the original images are captured using the stereo camera system, there is a disparity (displacement) between images captured using KODAK No.34A filter and Fujifilm SP-18 filter. Hence, we have to completely align the two images for the combined six-band images such that there is no registration error. We have implemented the Phase Only Correlation (POC) technique (Takita, 2003) for image registration.

Then, all captured images are transformed into the polar coordinate system (Szeliski, 1997) for representing the omnidirectional images. For synthesizing an omnidirectional image, we utilize a total of 1260 images. The use of the programmable rotating table allows us to control and record the horizontal and vertical directional angles of each captured image. In other words, the relative polar coordinates can be determined for the polar coordinate images. Then, we can simply synthesize an omnidirectional image from the 1260 polar coordinate images based on the recorded directional angles.

Finally, we recover the spectral images from the six-band images based on Wiener estimation technique (Hirai, 2012). The Wiener estimation is well known and widely utilized for recovering spectral information from noisy observations.
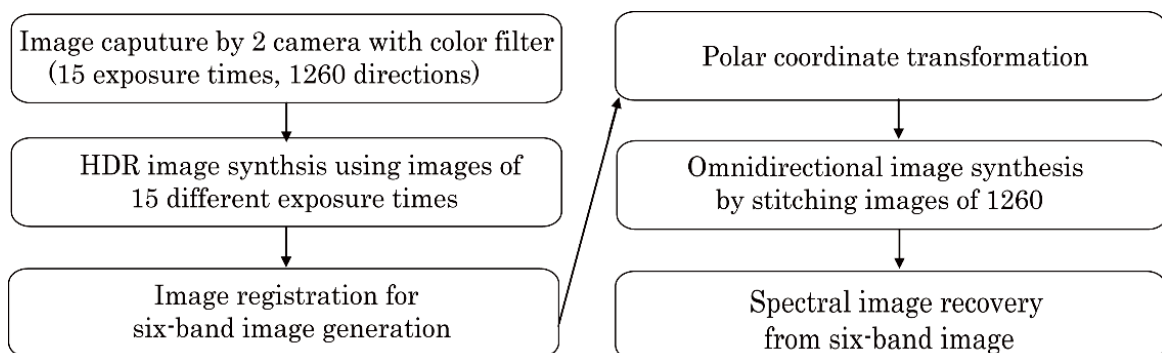


*Figure 3: Flowchart for a spectral gigapixel image of an omnidirectional scene.*

## 3. RESULTS AND DISCUSSION

Table 1 summarizes the performance of the proposed system. The six-band images are acquired using two color video cameras with two different types of color filters. In our image acquisition system, we require no filter exchange because we employ multiband imaging based on stereo one-shot technique. An omnidirectional image is synthesized from 1260 images. The pixel size is approximately 1.9 gigapixels. However, our system requires a higher acquisition time for capturing more than 1000 images.

*Table 1. Summary of the configurations and performances of the proposed system.*

| Number of channels | Six-bands |
|---|---|
| Filter exchange | Not required |
| Multi-band technique | Stereo one-shot |
| Photographing direction | 1260 directions: 60 horizontal and 21 vertical |
| Pixel size | Approx. 1.9 gigapixels (60000 × 32000) |
| Total acquisition time | Approx. 2 hour 17 min |
| Acquisition time for each directional image | Approx. 5 seconds (including both capturing and rotating processes) |

For resolution comparison, we compare the proposed system with the conventional system (Hirai, 2014). Figure 4 shows the comparative rsults. The resolution of the conventional system is 7260 × 3630 pixels. The conventional system focuses on temporal resolution (acquisition time) rather than spatial resolutions, because the conventional system had been developed for acquiring time-lapse spectral images of omnidirectional natural scenes. As shown in Figure 4, we can see the details of distant objects.
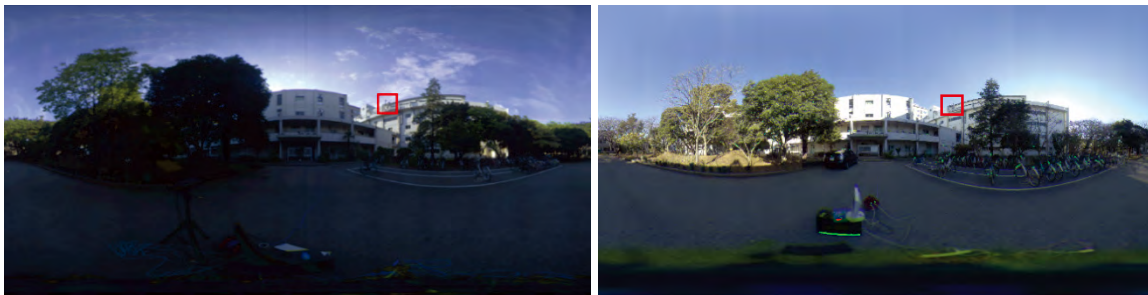


*(a) Conventional system (7260×3630 pixels)*   *(b) Proposed system (60000 × 32000 pixels)*

*(c) Close-up of the red square in (a)*   *(d) Close-up of the red square in (b)*
*Figure 4: Resolution comparison between the conventional and proposed system.*

AIC2015 TOKYO - Color and Image

Next, for validating the accuracy of the recovered spectral power distributions, we compare the estimated results with the ground truth. In this experiment, we estimated spectra of X-rite ColorChecker under D65. The ground truth data was measured by a spectrophotometer. Figure 5 shows the estimation results of the spectral power distributions. The average normalized RMSE shown in Figure 5 is 0.0147, and the average ΔE is 1.315. The results show that the proposed system can estimate the spectral power distribution accurately. In addition, the proposed system has the ability to reproduce accurate color and spectra of omnidirectional scenes in high resolution.



*(a) ColorChecker No.13:blue*  *(b) ColorChecker No.14:green*

*(c) ColorChecker No.15:red*  *(d) ColorChecker No.16:yellow*

*(e) ColorChecker No.17:magenta*  *(f)ColorChecker No.19:white*
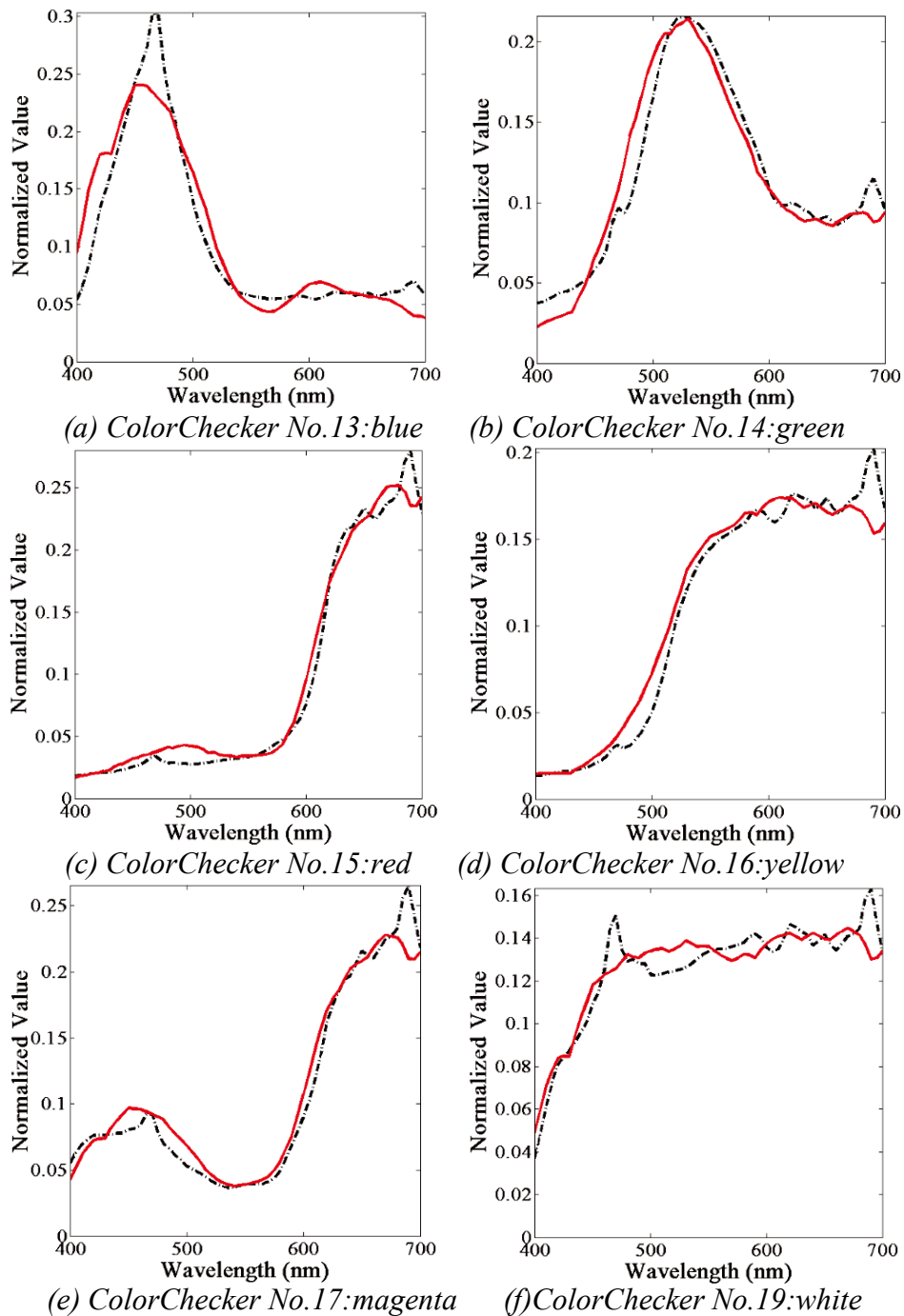
*Figure 5: Estimation result of spectral power distributions of the selected six colors: blue, green, red, yellow, magenta, and white.( Red line : actual value , Black line : estimation)*

## 4. CONCLUSIONS

This paper proposed a spectral gigapixel imaging system for omnidirectional outdoor scene measurement. The system was constructed using two programmable high-speed RGB video cameras with telephoto lenses and a programmable rotating table. Next, we generated gigapixel images from 1260 directional images. We also recovered spectral information from six-band images. As a result, an approximately 1.9 spectral gigapixel image of an omnidirectional scene was realized. We also showed the proposed system could accurately provide spectral power distributions of an omnidirectional scene (RMSE: 0.01427, ΔE: 1.315).

As future work, the acquisition time of the proposed system should be reduced. Another issue is the optimal color filter selection for acquiring accurate spectral information of an omnidirectional natural scene.

## ACKNOWLEDGEMENTS

## REFERENCES

Anguelov, D., C. Dulong, D. Filip, C. Frueh, S. Lafon, R. Lyon, A. Ogale, L. Vincent, and J. Weaver. 2010. Google Street View: Capturing the world at street level. *Computer*, 43(6):32-38.

Sakurada, K., T. Okatani, and K. Deguchi. 2013. Detecting Changes in 3D Structure of a Scene from Multi-view Images Captured by a Vehicle-mounted Camera. In *CVPR2013, Proceedings, 26th IEEE CVPR*, 137-144.

Hale, S., and M. Stanney. 2015. *Handbook of Virtual Environments: Design, Implementation, and Applications, Second Edition*. Florida: CRC Press.

Szeliski, R. 2010. *Computer Vision: Algorithms and Applications. Texts in Computer Science*. Berlin: Springer Science & Business Media.

Point Grey Research. Ladybug5, http://wwx.ptgrey.com//Products/Ladybug5/. Accessed: February 27, 2015.

Gigapixel Panorama Photo, http://360gigapixels.com/petrin-prague-photo/. Accessed: February 27, 2015.

Hirai, K., N. Osawa, T. Horiuchi and S. Tominaga. 2014. An HDR Spectral Imaging System for Time-Varying Omnidirectional Scene. In *ICPR2014, Proceedings, 22nd IEEE ICPR*, 2059-2064.

Takita, K., T. Aoki, Y. Sasaki, T. Higuchi and K. Kobayashi. 2003. High-accuracy Subpixel Image Registration based on Phase-only Correlation. *IEICE Trans. Fundamentals*, vol.E86-A, no.8, 1925-1934.

Szeliski, R., and H. Y. Shum. 1997. Creating Full View Panoramic Image Mosaics and Environment Maps. In *ACM SIGGRAPH 97*, 251-258.

Hirai, K., and S. Tominaga. 2012. A LUT-based Method for Recovering Color Signals from High Dynamic Range Images. *Proceedings, IS&T/SID's Twentieth CIC*. 88-93.

*Address: Motoki Hori, Graduate School of Advanced Integration Science, Chiba University, Yayoi-cho 1-33, Inage-ku, Chiba, 263-8522, JAPAN E-mails: aaca2805@chiba-u.jp, hirai@faculty.chiba-u.jp, horiuchi@faculty.chiba-u.jp*

# HANDHELD HYPERSPECTRAL IMAGING SYSTEM FOR THE DETECTION OF SKIN CANCER

Xana DELPUEYO,[1] Meritxell VILASECA,[1] Santiago ROYO,[1] Miguel ARES,[1] Ferran SANABRIA,[1] Jorge HERRERA,[1,2] Francisco J. BURGOS,[1] Jaume PUJOL,[1] Susana PUIG,[3] Giovanni PELLACANI,[4] Jorge VÁZQUEZ,[5] Giuseppe SOLOMITA,[6] Thierry BOSCH[7]

[1] Centre for Sensors, Instruments and Systems Development (CD6), Technical University of Catalonia (UPC), Terrassa, Spain.
[2] Instituto Tecnológico Metropolitano (ITM), Medellin, Colombia
[3] Hospital Clínic i Provincial de Barcelona, Barcelona, Spain
[4] Università di Modena e Reggio Emilia, Modena Italy
[5] Carril Instruments, S.L., Barcelona, Spain
[6] Mavig GmbH, Munich, Germany
[7] Institut National Polytechnique de Toulouse (INPT), France

## ABSTRACT

Skin cancer detection is currently carried out using visual inspection through the dermoscope. Later, histological examination with a surgical extraction of the lesion is required for a complete and precise diagnosis. In this study, a new handled tool based on a hyperspectral system is proposed as a means of obtaining objective color and spectral information of the lesions to help in the diagnosis of skin cancer. The system includes light-emitting diodes (LEDs) as a light source as well as a digital camera. Preliminary images taken with the system and the corresponding results indicate the usefulness of the system. The prototype presented in this study will be integrated in the near future in a multiphotonic platform, including also 3D images, blood flow analysis and confocal microscopy, for in-vivo imaging of skin cancer lesions as a diagnosis service.

## 1. INTRODUCTION

Skin cancer represents one in three of all cancers worldwide and its incidence in Europe, USA and Australia is increasing rapidly. The melanoma, which only represents 4% of all skin cancers, is the most aggressive one causing the greatest number of deaths (Kuzmina et al., 2011). About 90% of skin cancers are caused by ultraviolet light from daylight or tanning booths. The World Health Organization estimates that 60,000 people die every year for sunlight excess: 48,000 from melanoma and 12,000 from another type of skin cancer. On the other hand, the survival rate in 5 years really increases if the pathology is detected and treated early.

Nowadays, visual inspection through the dermoscope is the technique most widely used by dermatologists for the detection of skin cancer. It consists of a handheld device with a magnifying lens and a white and uniform illumination field. The light is often polarized to remove specular reflection from the skin surface to obtain information of deeper layers. Dermoscopy allows the specialists identifying different structures, patterns and colors of the skin lesions suggesting if they are benign (seborrheic keratosis, haemangiomas, lipomas, warts) or malignant (melanoma, basal cell carcinoma). This is confirmed by a histological examination later on requiring a surgical extraction of the lesion, which is the

gold standard for clinicians. By means of this procedure, a lot of false positives are still obtained and thus, the direct annual costs of diagnosis and treatment of skin cancer are high (Braun et al., 2005).

In order to improve the detection and diagnosis of skin cancer, in the last years color and spectral imaging technology have started to be used to enhance and analyze color and spectral properties of skin. They are caused by chromophores such as melanin, hemoglobin, water etc., which might differ among skin lesions of different etiologies.

In this context, some prototypes such as those developed by Spigulis et al. (Bekina et al., 2012), Kapsokalivas et al. (Kapsokalivas et al., 2013), and also some commercial devices such as the SIAscope V system (Emery et al., 2010), have already been proposed as a means of improving skin cancer diagnosis. However, most of them only use three spectral bands in the visible range (typically three colour RGB channels) and additionally another one located at the near infrared range.

For the reasons exposed above, in this study we propose a new handheld hyperspectral system with more spectral bands for the diagnosis of skin cancer, trying to improve the results obtained with the existing devices. In this work, we present the methodology carried out to setup and characterize the whole system, including the protocol followed in order to select the most suitable spectral bands to detect skin cancer lesions. Furthermore, the first results corresponding to real lesions analyzed at a clinical site are also presented. This work is within the framework of the European Project DIAGNOPTICS "Diagnosis of skin cancer using optics" (ICT PSP seventh call for proposals 2013), the aim of which is developing a multiphotonic platform including hyperspectral and 3D techniques, blood flow analysis and confocal microscopy for in-vivo imaging of skin cancer lesions as a diagnosis service (Ares et al., 2014). These technologies are envisaged to improve the detection ratio and the evaluation of the prognosis of skin cancer at earlier stages, compared with the conventional approach used nowadays.


## 2. METHOD

### 2.1 System design and components

The system developed has a cylindrical shape of about 10 cm in length, 7.5 cm of width and a weight of 0.5 kg. It includes a 12 bit-depth monochromatic camera and an objective lens, which allows recording skin lesions at 4 cm with a 15x20 mm field of view as their size is usually smaller.

A ring light source including light-emitting diodes (LEDs) with different spectral emissions within the visible and near infrared range (400 nm to 1000 nm) was designed to illuminate the sample. This illumination source was located onward of the objective lens to avoid the light of the LEDs reaching the sensor directly. The spectral bands of the system were chosen according to the spectral properties and absorption peaks of the skin chromophores and also taking into account market availability of LEDs. In order to obtain a uniform field of illumination on the sample and enough energy to acquire spectral images with low exposure times, 32 LEDs were finally included in the light source.

Moreover, two polarizers allow changing the degree of polarization of light and thus obtaining information from different skin depths. Specifically, the first polarizer is located

in front of the LEDs and the second in front of the objective lens. Light polarization can be changed into 3 different positions: 0º - parallel polarizers, 45º and 90º - crossed polarizers.

The first prototype developed, which is a light, compact and ergonomic device to be used at a clinical site, is shown in Figure 1. The handheld hyperspectral head can be placed on a base between measurements, making all the procedure comfortable for the physician. Moreover, this base has also a storing function as the power supply and the electronic boards and other parts of the system are placed inside.



*Figure 1: Different views of the handheld hyperspectral system.*

Furthermore, the base also incorporates a calibrated sample resembling the light human skin that can be sheltered from external agents like dust by positioning it in the "in" and "out" positions (Figure 2). This sample is used in the preliminary calibration of the system that is done every day before starting measurements and that will be a key step when computing spectral results from the images acquired (see next section).



*Figure 2: View of the base of the handheld hyperspectral system with the calibrated sample in the "out" and "in" positions, respectively.*

## 2.2 Software development

A specific software was developed for controlling all components of the system (camera and LEDs), allowing for its proper operation. The software (Borland Builder C++) included autoexposure algorithms for adjusting the exposure time of each spectral band taking into account the LED emission level and also the typical reflectance and absorption properties

of the skin. It also includes security controls avoiding LEDs to be switched on if the program is not running. A user interface was also developed for its use at a clinical site. A complete acquisition lasts 40 seconds approximately.

An additional software implemented in Matlab® was created to process all the images of the lesions. It included calibration algorithms as a means of computing reflectance values, chromaticity coordinates, colour differences etc., which might enhance subtle differences between benign and malignant lesions enabling a better diagnosis.

## 3. RESULTS AND DISCUSSION

Figure 3 shows spectral images obtained with the developed system corresponding to a common nevus lesion at different spectral bands between 400 nm and 1000 nm, and different degrees of polarization. As it can be seen, the degree of polarization allows removing the specular reflection of the skin surface (0º), obtaining information from deeper layers (90º), basically in the case of short (blue) wavelengths. This is important as for instance, melanomas can grow deeper than other lesions.
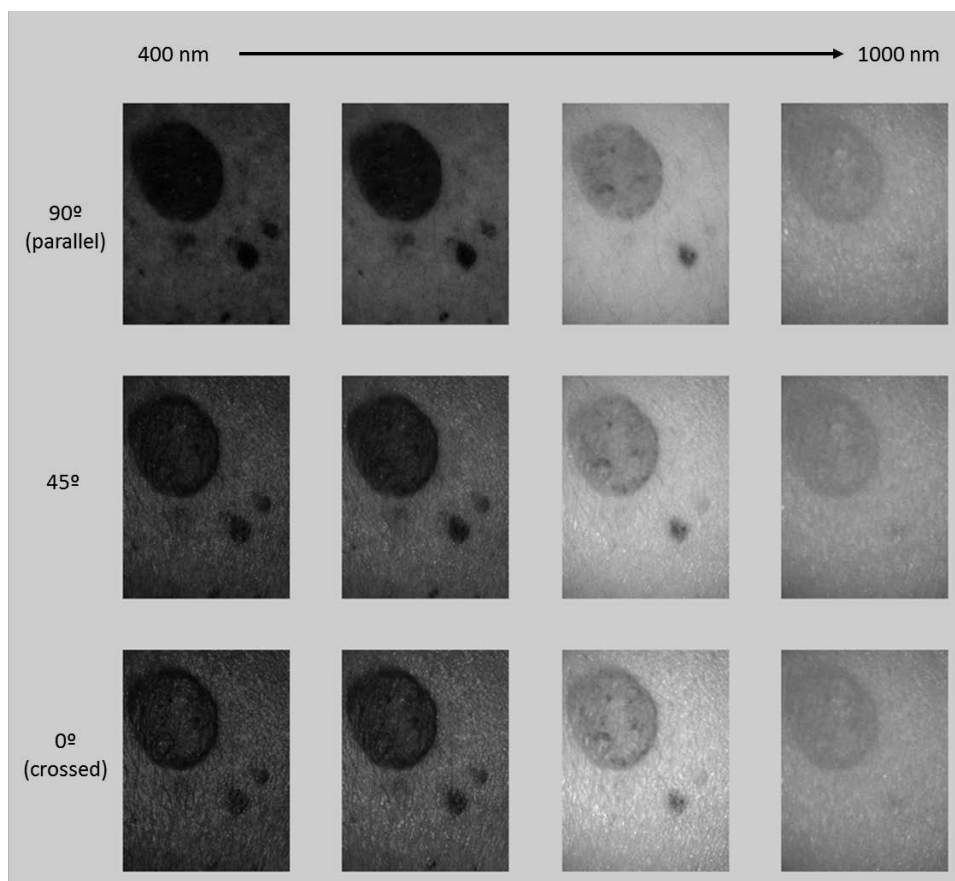


*Figure 3: Images of a benign lesion (common nevus) obtained with the system using different spectral bands and three degrees of polarization (0º, 45º, 90º).*

Figure 4 shows the spectral reflectance curves computed from two different areas of a skin sample: one corresponding to common skin and the other to a nevus. As it is shown the reflectance curves associated to each of them differ completely. As it was expected, nevus had lower reflectance values because its higher amount of melanin absorbs more light.
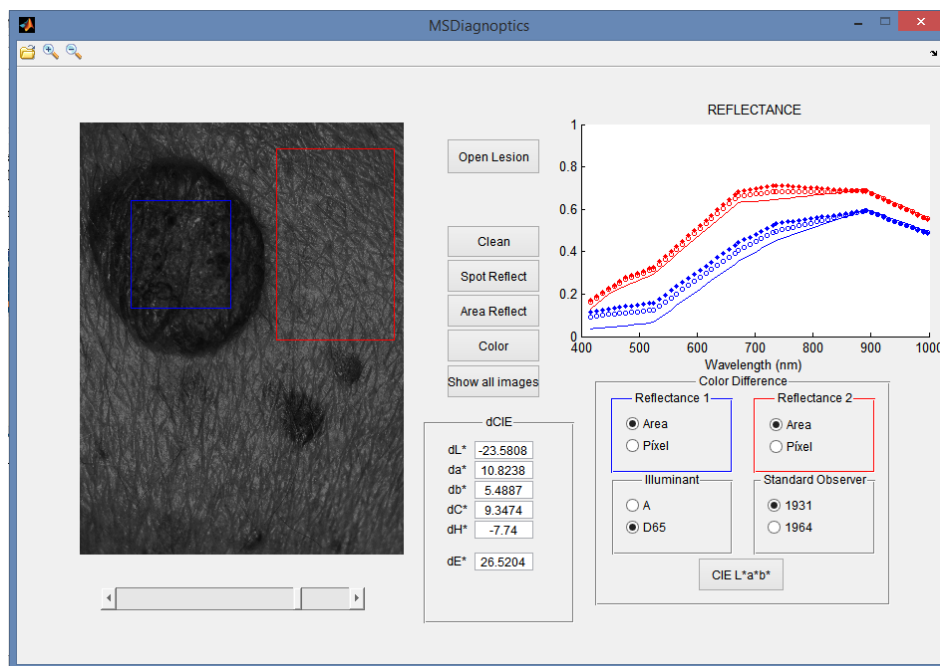
*Figure 4: Spectral reflectance of common skin (red area) and common nevus (blue area)*

## 4. CONCLUSIONS

In this study, a first prototype of a handheld hyperspectral system with several spectral bands in the visible and near infrared ranges of the electromagnetic spectrum for improving the diagnosis of skin cancer was presented. The developed system allows obtaining precise spectral information from the skin lesion analysed with a high spatial resolution in a fast and easy way. The use of LEDs as a light source enabled to build a system with reduced size and cost.

Current work is focused on the acquisition of images from a great variety of skin lesions in a clinical environment, including benign and malignant lesions (Hospital Clínic i Provincial de Barcelona, Spain), as well as the development of algorithms to obtain more reliable and objective diagnosis, helping dermatologists in their daily clinical practice. Skin lesions can be generally categorized according with their clinical presentation, taking into account different easily recognizable aspects, including from shape to colour. Therefore, it is expected that this last one will be a key in the diagnostic procedure as spectral reflectance profiles obtained with the new system will be related with the lesion etiology.

## REFERENCES

Ares, M., Royo, S., Vilaseca, M., Herrera, J.A., Delpueyo, X., Sanabria, F., 2014. Handheld 3D Scanning System for In-Vivo Imaging of Skin Cancer. In the 5$^{th}$

*International Conference on 3D Body Scanning Technologies, Proceedings,* ed. by Hometrica Consulting. Switzerland: 231-236.

Bekina, A., Diebele, I., Rubins, U., Zaharans, J., Derjabo, A., Spigulis, J., 2012. *Multispectral assessment of skin malformations using a modified video-microscope,* Latvian Journal of Physics and Technical Sciences 49(5), 4-8.

Braun, R.P., Rabinovitz, H.S., Oliviero, M., Kopf, A.W., Saurat, J.H., 2005. *Dermoscopy of pigmented skin lesions,* Journal of the American Academy of Dermatology 77(2), 104-110.

Emery J.D., Hunter, J., Hall, P.N., Watson, A.J., Moncrieff, M., Walter, F.M., 2010. *Accuracy of SIAscopy for pigmented skin lesions encountered in primary care: development and validation of a new diagnostic algorithm,* BMC Dermatology, 10(9), 1:9.

Kapsokalyvas, D., Bruscino, N., Alfieri, D., de Giorgi, V., Cannarozzo, G., Cicchi, R., Massi, D., Pimpinelli, N., Pavone, F.S., 2013. *Spectral morphological analysis of skin lesions with a polarization multispectral dermoscope.* Optics express 21(4), 4826-40.

Kuzmina, I., Diebele, I., Jakovels, D., Spigulis, J., Valeine, L., Kapostinsh, J., Berzina, A., 2011. *Towards noncontact skin melanoma selection by multispectral imaging analyasis,* Biomedical Optics Express 16(6), 060502.

*Address: MSc Xana Delpueyo,*
*Centre for Sensors, Instruments and Systems Development (CD6). Technical*
*University of Catalonia (UPC), Rambla Sant Nebridi 10, Terrassa, 08222, SPAIN.*
*E-mails: xana.delpueyo@cd6.upc.edu, mvilasec@oo.upc.edu, santiago.royo@upc.edu*

# Empirical Disadvantages for Color-Deficient People

Joschua SIMON-LIEDTKE[1] and Ivar FARUP[1]

[1] The Norwegian Colour and Visual Computing Laboratory, Gjøvik University College

## ABSTRACT

Trichromatic color vision in humans evolved most likely because it provides behavioral advantages in assisting attentional mechanisms, object recognition and, possibly, also detection of emotion states in other humans. Behavioral experiments, namely visual search and object recognition experiments, with normal-sighted observers have shown to support these hypotheses. We argue that the same types of experiments can be used to show that trichromacy does indeed give a behavioral, empirical measureable advantage before dichromacy or anomalous trichromacy by comparing behavioral responses of normal-sighted observers to color-deficient observers. More precisely, we suggest the use of visual search experiments to measure attentional responses, sample-to-match and object recognition tasks to measure objection recognition, and emotion detection to measure emotional responses. We furthermore implemented a visual search task to measure the performance of the attentional mechanism that showed that for the given experiment normal-sighted observers do indeed have an advantage over color-deficient observers.

## 1. INTRODUCTION

Trichromatic vision is based on the response of photosensitive receptors on the retina of the human eye, so-called *cones*, with sensibilities to light of different wavelengths. Color-deficient people typically have either reduced sensibility for one of the cones or lacking one of the cones altogether. Consequently, this will lead to a decreased ability of distinguishing certain colors. Color-deficient people truly encounter certain problems in daily life both in natural settings – for example when picking berries, determining whether a steak is raw or well-done etc–, and especially in social settings where color coding is heavily used in communication – for example when reading geographic and public transportation maps. More severely, they are excluded from certain professions that rely heavily on different colored signals, like pilots, train conductors etc. However, behavioral disadvantages of color-deficient people in natural and social settings is still only marginally researched. More specifically, two main questions remain: What is the behavioral advantage of trichromatic color vision in comparison to dichromatic color vision? And are there measurable behavioral differences between normal-sighted and color-deficient observers?

Studies suggest that color influences behavioral responses in the field of attention, object recognition, and interpretation of emotional states. Firstly, Treisman and Gelade (1980) proposed the feature-integration theory of attention stating that visual attention can be split up in a pre-attentive early state and a later stage. Color is used especially in the first stage to make elements "pop out" depending on their color contrast. Secondly, Bramão et al. (2012) suggested that colors helps to support object recognition at different states of visual processing. Thirdly, Changizi, Zhang, and Shimojo (2006) suggested that trichromatic color vision is used to better discriminate changes in skin spectra that arise to signal emotions, for example in socio-sexual contexts, and/or may indicate danger.

The previously mentioned research have in common that the hypotheses have been tested only on normal-sighted observers using both colored and black-and-white images showing

that normal-sighted observers react faster and more accurate to colored than to black-and-white images. In this paper, we argue firstly that the same methodologies can be used to measure empirical differences between normal-sighted and color-deficient observers supporting the hypothesis that trichromatic color vision manifests an evolutionary advantage for attentional mechanism, object recognition and emotion detection over dichromatic or anomalous trichromatic vision. More precisely, we suggest the use of behavioral experiments involving visual search, object recognition, object identification, object class identification and emotion detection tasks for colored images to empirically measure disadvantages and advantages of color-deficient observers over normal-sighted observers. Secondly, we implemented a visual search experiment – the Visual Search Daltonization Evaluation Method (ViSDEM) – that is used to compare response times and accuracies for tasks involving the attentional mechanism of normal-sighted and color-deficient observers. We found out that color-deficient observers have indeed a slight behavioral disadvantage over normal-sighted observers.

## 2. BACKGROUND AND METHODOLOGY

Behavioral responses related to attention of trichromats, further called normal-sighted observers, and anomalous trichromats or dichromats, further called color-deficient observers, can be measured by visual search experiments as introduced by Treisman and Gelade (1980). In the basic implementations, the observer has to identify a target stimulus, like a symbol, object etc., among a number of distractors that differ in size, shape, color etc. In another experimentation design that we proposed (Simon-Liedtke, Farup and Laeng 2015), the observer is shown different natural images and a question/task related to the content of the image. The observer is then asked to answer as fast and as accurate as possible for each picture. For both experiments, response times (RTs) and accuracies (ACCs) of the answers are recorded, and analyzed by comparing RTs and ACCs of normal-sighted and color-deficient observers. We assume that according to our previously discussed hypothesis the normal-sighted observers will be able to respond faster and more accurately than the group of color-deficient observers.

Bramão et al. (2012) identified several object recognition experiments to access performance of color vision on object recognition. Images of different objects are shown to the observers, and the participant are asked to answer to certain questions. In the object verification task the observer has to state whether an object or a non-object is shown, in the category verification task the observer has to state whether the object is natural or artificial, and in the name verification task the observer has to state the correct name of the object. RTs of each observation were recorded and analyzed. We suggest implementing the same setup to compare performances of normal-sighted and color-deficient observers. Namely, we suggest the use of the object verification task, the category verification task, and the name verification tasks with colored objects, for which the RTs and ACCs are recorded. If our hypothesis about trichromatic vision is true, we assume that normal-sighted observers will be able to identify objects faster and more accurately than color-deficient observers.

The analysis of emotion detection through skin identification has to-date not yet been conducted. Thus, we propose an emotion detection experiment similar to the one that Adolphs *et al.* (2000) conducted based on the experiments to evaluate the universality of facial expressions proposed by Ekman (1999). Images of people imitating different facial expressions are shown to participants that are asked to name the emotional state that the expressions are meant to represent. Since the influence of emotion detection has to yet been analyzed to-date, the experimentation has to be conducted in two stages. In the first

stage, normal-sighted and color-deficient observers are shown different images of facial expressions both colored and grayscale from males and females belonging to different emotion categories. In the second stage, only colored images are presented to both normal-sighted and color-deficient observers. For both stages we record the RTs and ACCs of the observations. If color vision in general and trichromatic color vision in particular facilitates emotion detection as expected, we expect, firstly, that observers in both groups will react faster and more accurate for the colored images than for the grayscale images, and, secondly, that for colored images normal-sighted observers will react faster and more accurate than color-deficient observers.

## 3. IMPLEMENTATION

To-date, we implemented a visual search experiment to analyze influence of color on attentional mechanism for normal-sighted and color-deficient observers: The method is originally designed to evaluate daltonization methods, and is called Visual Search Daltonization Evaluation Method (Simon-Liedtke, Farup and Laeng 2015). Fortunately, the results can also be interpreted in order to support for the previously discussed hypothesis that normal-sighted observers have a slight empirical measurable advantage to color-deficient observers. In our experiment, the observer looks at a range of images, for each of which we define certain tasks. The task consists of a statement, which the observer has to agree, respectively disagree to. The statement is connected to colors of objects, people etc. in the image like for example "The feather in the image has the same color hue as the background." or "There is green powder in the image." We conducted the experiment with 23 observers, of which 10 were normal-sighted and 13 deutan color-deficient, and we used 7 different sets of images. For more details on the implementation, please check our previous paper (Simon-Liedtke, Farup and Laeng 2015). We analyzed the confidence interval of the ACCs for both observer groups, and compared the medians of RTs for both groups according to a Mood's median test.

## 4. RESULTS AND DISCUSSION

Figure 1 shows both RTs and ACCs of both normal-sighted and color-deficient observers. The median RT for the group of normal-sighted group is much lower than for the group of color-deficient observers. A Mood's median test revealed a p-value of $4 \cdot 10^{-6}$ indicating that the medians of both populations are indeed significant different. The confidence interval (CI) of the ACCs for the group of normal-sighted observers is much higher than the CI of the ACCs for the group of color-deficient observers. Both observations agree with the assumptions we made prior to the experiment, namely that color-deficient people react less accurate and slower than normal-sighted observers. In other words, the results indicate that color-deficient people do indeed have behavioral disadvantages connected to their attentional system, and that these differences are indeed measureable with our proposed methodology based on visual search tasks.

## 5. CONCLUSIONS

We proposed a range of behavioral experiments through visual search, object identification and emotion detection tasks in order to test the hypothesis that trichromatic color vision provides evolutionary advantage for attention, object recognition and emotion detection. We suggest that color-deficient observers will respond slower, and less accurate to these tasks when compared to normal-sighted observers. Furthermore, we implemented a visual

search experiment that shows that deutan color-deficient observers do indeed react slower and less accurate than color-deficient observers in a visual search experiment measuring attentional reactions.
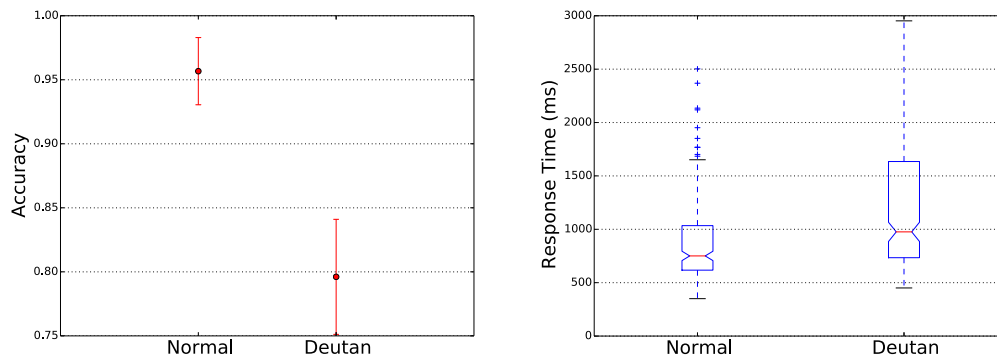


*Figure 1: Accuracies (ACCs) and response times (RTs) of the visual search experiment for normal-sighted and deutan color-deficient observers indicating that color-deficient people do indeed react less fast and less accurate than normal-sighted observers. The median RTs of both groups are significant different according to the Mood median test.*

## ACKNOWLEDGEMENTS

## REFERENCES

Adolphs, Ralph, Hanna Damasio, Daniel Tranel, Greg Cooper, and Antonio R. Damasio. 2000. A role for somatosensory cortices in the visual recognition of emotion as revealed by three-dimensional lesion mapping. In *The Journal of Neuroscience*: 2683–2690.

Bramão, Inês, Luís Faísca, Karl Magnus Petersson, and Alexandra Reis. 2012. The Contribution of Color to Object Recognition. In *Advances in Object Recognition Systems*: 73–88.

Changizi, Mark A., Qiong Zhang, and Shinsuke Shimojo. 2006. Bare skin, blood and the evolution of primate colour vision. In *Biology letters*: 217–221.

Ekman, Paul. 1999. Facial expressions. In *Handbook of Cognition and Emotion*: 301–320.

Simon-Liedtke, Joschua T., Ivar Farup and Bruno Laeng. 2015. Evaluating color deficiency simulation and daltonization methods through visual search and sample-to-match: SaMSEM and ViSDEM. In *Proceedings of SPIE/IS&T Electronic Imaging 9395, Color Imaging XX: Displaying, Processing, Hardcopy, and Applications*. San Francisco, CA, USA.

Treisman, Anne M. and Garry Gelade. 1980. A feature-integration theory of attention. In *Cognitive Psychology*: 97–136.

*Address: Joschua Thomas Simon-Liedtke, The Norwegian Colour and Visual Computing Laboratory, Gjøvik University College, Teknologivegen 22, 2815 Gjøvik, Norway*
*E-mails: joschua.simonliedtke@hig.no*

# Spectral reflectance recovery using natural neighbor interpolation with band-divided linear correction

Tzren-Ru Chou[*] and Tsung-Chieh Sun,
Dept. of Graphic Art and Communications,
National Taiwan Normal Univ., Taiwan, R.O.C

## ABSTRACT

In this paper, we proposed an accurate recovery method of object spectral reflectance using the traditional natural neighbor interpolation, shortly named as NNI, with band-divided linear correction. Our method consists of two stages of recovery procedures. First, the NNI interpolation was used to construct the spectral reflectance from the real samples of color checkers. Secondly, the spectra resulting from NNI were further fine-tuned according to the difference between its sRGB color under illuminant of $D_{65}$ and the original input one of ground true. Some experiments were performed to evaluate the performance of the proposed method. The 1269 checker spectra from Munsell book was used as the test samples under the training samples from Macbeth 24 color checkers. The largest color difference was 1.4869, and the average one was 0.0726. The experimental results showed that the proposed method was very accurate for the recovery of spectral reflectance.

## 1. INTRODUCTION

The purpose of this study is to obtain a precise estimation of the spectral reflectance. Essentially, such a recovery problem was usually to transform the RGB channel values into a spectrum to simulate the reflectance of an object. There were many previous works for the reconstruction of spectral reflectance, for instance, principle component analysis (PCA) (Fairman and Brill 2004), PCA modification (Lee et al. 2012), interpolation (Abed et al. 2009), such as hybrid methods (Kim et al. 2012), others like regression analysis (RA) (Harifi et al. 2008) (Amiri et al. 2014) or based on metamerism (Chou and Lin 2012).

PCA is a classical method for the reconstruction of spectral reflectances with good performance, but the value of estimation is out of the range from 0 to 1. This unnaturalness phenomenon may lead to an unexpected result during the reconstruction. On the other hand, the interpolation may establish more natural results (Amidror 2002), but could suffer from the extrapolation for the scatter data, such as the samples of color checkers. Further studies were needed to solve these shortcomings.

This paper proposed a new interpolation method with much more accuracy. The NNI was the basic reconstruction model. Eight additional pre-determined spectra were imposed for the corners of the sRGB color space to guarantee all the test samples in the gamut spanned by the known samples. And then, the traditional NNI were further fine-tuned according to the color difference under the illuminant of $D_{65}$. Three pre-specified wavelengths, denoted S, M, and L, were selected as the control points to adjust the spectral curve toward the correct direction.

The reminder of this paper is divided into three sections. Section 2 is our method in full details. Section 3 is our experiment results and discussion. Finally, the conclusions are drawn in Section 4.

## 2. METHOD

The method consists of two stages of the recovery procedures. First, the NNI interpolation was used to construct the spectral reflectance from the real samples of color checkers. Eight additional pre-determined spectra were imposed for the corners of the sRGB color space, named virtual extreme spectra, to guarantee all the test samples in the gamut spanned by the known samples (Figure 1).
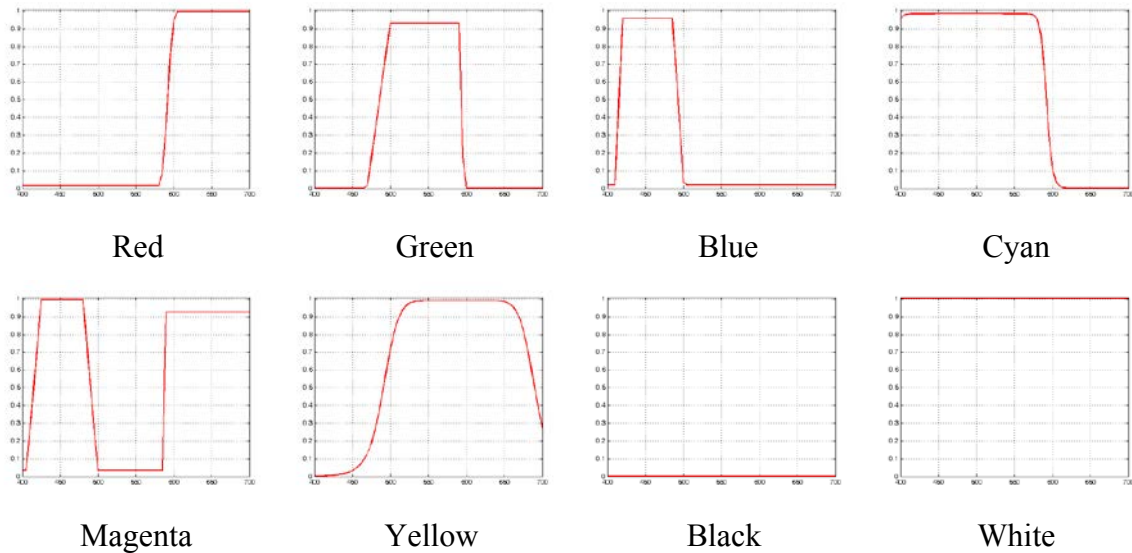


| Red | Green | Blue | Cyan |

| Magenta | Yellow | Black | White |

*Figure 1: Eight additional pre-determined spectra*

### 2.1 Method of natural neighbor interpolation

The natural neighbor interpolation developed by Robin Sibson is based on Voronoi tessellation of a discrete set of spatial points. In this method, the scattered points are used to form many tetrahedra in 3D space, and an interpolation model is performed within each tetrahedron (Amidror 2002). For example, we simulated a color x in the sRGB space to get the spectral reflectance. The x1, x2, and x3 in Figure 2 are the data of training samples with their RGB values are (255, 30, 30), (210, 150, 110), and (254, 200, 100), respectively. The color point x will be interpolated to the right place according to the RGB values as shown in Figure 2. The following diagram illustrates that the new Voronoi polygon is separated from the polygon formed by the neighbor color x1, x2, and x3. Then, the interpolating weight of x affected from each neighbor point can be determined according to the proportion of the partition volumes.
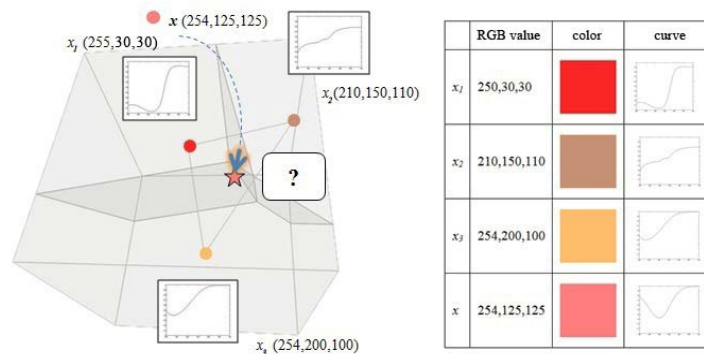


*Figure 2: The interpolating model of NNI*

## 2.2 Band-divided linear correction model

The spectra resulting from NNI were further fine-tuned according to the difference between its sRGB color under illuminant of $D_{65}$ and the original input one of ground true. Three pre-specified wave lengths, denoted S, M, and L, were selected as the control points to correct this NNI spectrum approaching to a new one with less color difference. The x-axis values of three control points are 465nm, 550nm and 610nm, selected by the nearest dominant wavelength of blue, green and red in the sRGB gamut (Bergquist 2012). This correction was composed of 4 piecewise linear transformations related to 4 bands from 400nm to S, from S to M, from M to L, and from L to 700nm respectively as shown in Figure 3. We can get more accurate spectrum by solving the matrix as following equation (1). Equation (2) shows its expansion of the matrix form.

$$\begin{bmatrix} \Delta R \\ \Delta G \\ \Delta B \end{bmatrix} = \begin{bmatrix} c1 & c2 & c3 \\ c4 & c5 & c6 \\ c7 & c8 & c9 \end{bmatrix} * \begin{bmatrix} \Delta h_s \\ \Delta h_m \\ \Delta h_l \end{bmatrix} \qquad (1)$$
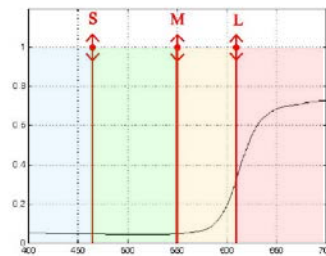


*Figure 3: The L, M, and S control points*

$$\Delta R = c1 * \Delta h_s + c2 * \Delta h_m + c3 * \Delta h_l$$

$$\Delta G = c4 * \Delta h_s + c5 * \Delta h_m + c6 * \Delta h_l \qquad (2)$$

$$\Delta B = c7 * \Delta h_s + c8 * \Delta h_m + c9 * \Delta h_l$$
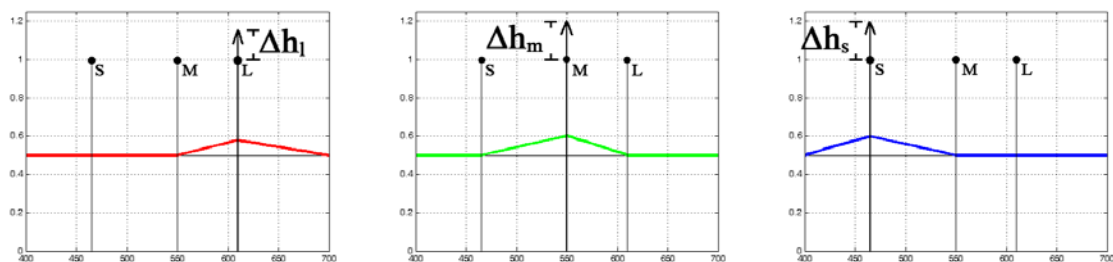


*Figure 4 Changes of spectral curve after pulling the L, M and S control points*

Figure 4 illustrates an example of the band-divided linear correction. Firstly, assuming the original spectrum is flat with its reflectance of 0.5, the control point L is pulled up of $\Delta h_l$. The $\Delta h_l$ will lead to the linear transformation of the spectrum, denoted by the red line, during both bands from M to L, and from L to 700, with the change of $\Delta R$ about 0.0784.

The control points of M and S behave in the same manner, and are denoted by the green and blue lines in Figure 4, respectively.

The following presents the formulas for the correction of the spectra due to the changes of $\Delta h_l$, $\Delta h_m$, and $\Delta h_s$. The wavelength is represented by the discrete form of 61 values from 400nm to 700nm with the interval of 5nm. The linear correction is formed by 4 connected bands, from 400nm to S, from S to M, from M to L, and from L to 700nm.

1. If the x-axis value of point (x, p) is in the range between x-axis value of 400nm and S, the coordinate (x, p') on the spectral curve is calculated by equation (3) from the original one (x, p). $X_S - X_{400}$ means the separating distance between the control point S and (400nm, 1.0), that is, the point of the highest reflectance at 400nm.

$$p' = p(1 + \Delta h_s) * \frac{x}{X_S - X_{400}} \tag{3}$$

2. If the x-axis value of point (x, p) is in the range between x-axis value of S and M, the coordinate (x, p') on the spectral curve is calculated by equation (4) from the original one (x, p). $X_M - X_S$ means the separating distance between the control point S and M.

$$p' = p(1 + \Delta h_m) * \frac{x}{X_M - X_S} + p(1 + \Delta h_s) * \frac{(X_M - X_S) - x}{X_M - X_S} \tag{4}$$

3. If the x-axis value of point (x, p) is in the range between x-axis value of M and L, the coordinate (x, p') on the spectral curve is calculated by equation (5) from the original one (x, p). $X_L - X_M$ means the separating distance between the control point M and L.

$$p' = p(1 + \Delta h_l) * \frac{x}{X_L - X_M} + p(1 + \Delta h_m) * \frac{(X_L - X_M) - x}{X_L - X_M} \tag{5}$$

4. If the x-axis value of point (x, p) is in the range between x-axis value of L and 700nm, the coordinate (x, p') on the spectral curve is calculated by equation (6) from the original one (x, p). $X_{700} - X_L$ means the separating distance between the control point L and (700nm, 1.0), that is, the point of the highest reflectance at 700nm.

$$p' = p(1 + \Delta h_l) * \frac{(X_{700} - X_L) - x}{X_{700} - X_L} \tag{6}$$

## 2.3 Sample Preparation and Experimental Procedure

The simulating system was implemented in MATLAB® R2012 with Multi-Parametric Toolbox. The dataset consisting of 1269 spectra of Munsell book and 24 color samples of Macbeth color checkers with 8 sRGB extreme spectra were used in our experiments. All the reflectance data were fixed between 400 and 700nm of the interval of 5nm. The result of recovery spectra was evaluated by $\Delta E_{2000}$ color difference formula under illuminants $D_{65}$ for CIE1931 standard observer. Figure 5 shows the experimental scheme.
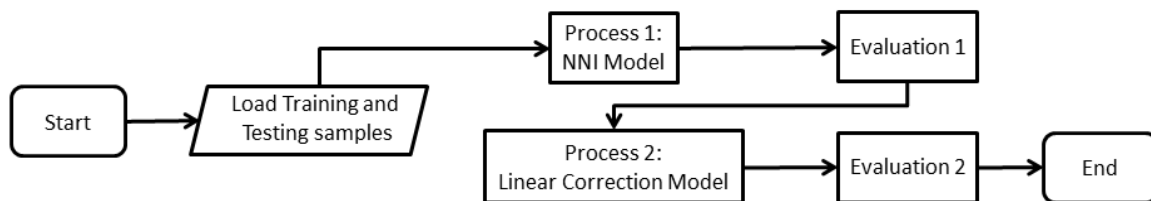


*Figure 5: Flowchart of the experimental scheme*

AIC2015 TOKYO - Color and Image

# 3. RESULTS AND DISCUSSION

Three experiments were performed to evaluate the performance of the new NNI with eight pre-defined spectra and the additional correction stage. At first, the 1269 checker spectra from Munsell book was used as the test samples under the training samples from Macbeth 24 color checkers. The largest color difference of $\Delta E_{2000}$ was 1.6366 based on the illuminant of $D_{65}$, and the average difference was 0.0915. And, the color differences were further improved, if the band-divided correction was adopted. Then, the largest $\Delta E_{2000}$ was 1.4869, and the average difference was 0.0726. In addition, the entire gamut of sRGB was also evaluated. The spectra recovered from the specified RGB channel values lead to the largest color difference was 1.6671 and the average one was 0.0315 under the illuminant of $D_{65}$, based on the training samples of Macbeth color checkers. The largest difference was 1.4915, and the average one was 0.0126, based on the training samples of Munsell book checkers. These experimental results showed that the proposed method was very accurate for the recovery of spectral reflectance.

# 4. CONCLUSIONS

In this paper, we proposed a new method to reconstruct the spectral reflectance of object. This new solution proposed not only gives more accurate results, but also avoids the extrapolation problem causing by the phenomena out of gamut. It is worth mentioning that our reconstructed reflectance ranges from 0 to 1, and it matches the phenomenon in the natural world. The method we proposed is successful to prevent the situation of improper data. Finally, the estimated spectral reflectance could be quite useful in various fields of color research, such as spectral camera designing, automatic white balancing, and digital lighting, etc.

# REFERENCES

Amidror, I. 2002. Scattered data interpolation methods for electronic imaging systems: A survey. *Journal of Electronic Imaging, 11*(2): 157–176. doi: 10.1117/1.1455013

Abed, F.M., Amirshahi, S.H. and Abed, M.R. 2009. Reconstruction of reflectance data using an interpolation technique. *Journal of the Optical Society of America A, 26*(3): 613-624. doi: 10.1364/JOSAA.26.000613

Amiri, M.M. and Amirshahi, S.H. 2014. A hybrid of weighted regression and linear models for extraction of reflectance spectra from CIEXYZ tristimulus values. *Optical Review, 21*(6): 816-825.

Bergquist, J. 2012. Display with arbitrary primary spectra. *SID Symposium Digest of Technical Papers, 39*(1): 783-786. doi: 10.1889/1.3069786

Chou, T.R. and Lin, W.J. 2012. Optimal estimation of spectral reflectance based on metamerism. In *Proceeding of SPIE-IS&T Electronic Imaging 2012*, 8292, 829213-829213-10. doi: 10.1117/12.907606

Fairman, H.S. and Brill, M.H. 2004. The principal components of reflectances. *Color Research and Application, 29*(2): 104–110. doi: 10.1002/col.10230

Harifi, T., Amirshahi, S.H. and Agahian, F. 2008. Recovery of reflectance spectra from colorimetric data using principal component analysis embedded regression technique. *Optical Review, 15*(6): 302-308. doi: 10.1007/s10043-008-0049-1

Lee, M.H., Park, H., Ryu, I. and Park, J.I. 2012. Fast model-based multispectral imaging using nonnegative principal component analysis. *Optics Letters, 37*(11): 1937-1939.

Kim, B., Han, J. and Park, S. 2012. Spectral reflectivity recovery from the tristimulus values using a hybrid method. *Journal of the Optical Society of America A, 29*(12): 2612-2621. doi: 10.1364/JOSAA.29.002612

Munsell Color Science Laboratory. 2011. Useful Color Data. Available online, http://www.rit.edu/cos/colorscience/resources.php. Accessed: Oct 29, 2014.

University of Joensuu Color Group n.d. Spectral Database. Available online, https://www.uef.fi/fi/spectral/spectral-database. Accessed: Oct 29, 2014.

*Address: Prof. Tzren-Ru Chou, Department of Graphic Art and Communications, National Taiwan Normal University, No.162, Sec. 1, Heping East Road., Taipei, Taiwan*
*E-mails: trchou@ntnu.edu.tw,*

# Evaluation of gastrointestinal tissue oxygen saturation using LEDs and a photo detector

Yoshitaka MINAMI,[1] Takashi OHNISHI,[2] Koki KATO,[3]
Hiroyuki WASAKI,[3] Hiroshi KAWAHIRA,[2] Hideaki HANEISHI [2]
[1] Graduate School of Engineering, Chiba University
[2] Center for Frontier Medical Engineering, Chiba University
[3] Departure of Information and Computer Engineering,
Kisarazu National Collage of Technology

## ABSTRACT

Accurate diagnosis of gastrointestinal viability in the reconstructive and resection surgery is strongly required to avoid anastomotic leak. Realization of quantification of gastrointestinal viability is really desirable. In this paper, we propose a method for estimating the tissue oxygen saturation ($StO_2$) of gastrointestinal organ using some LEDs in NIR region and a photo detector. We determine an organ absorbance model equation based on the Beer-Lambert law and estimate $StO_2$. However, the absorption coefficients of tissues in organs are unknown. First, we apply the nonnegative matrix factorization to the organ absorbance data obtained in advance to retrieve the absorption coefficients of each tissue. Furthermore, we define the band-based absorption coefficients that are suitable for emission characteristics of the LEDs to correct the error due to the LED bandwidth. Using the band-based absorbance coefficients, we re-defined the organ absorbance model equation. Then we estimate concentrations of organ tissues and calculate $StO_2$ by the ratio of oxygenated hemoglobin concentration and de-oxygenated hemoglobin concentration. Using transmittance spectra obtained in animal experiments, we simulated the performance of the proposed method and found that good estimation results will be obtained.

## 1. INTRODUCTION

Anastomotic leak leads to prolongation of hospitalization and increases postoperative morbidity, resulting in the increase of patient burden. Thus, correct determination of gastrointestinal viability at the time of anastomosis is very important. The determination is performed by visual inspection of surgeon now (Murai et al, 2013). However, the criterion of determination is neither quantified nor unified. Therefore, a quantitative method for viability determination of intraoperative organ is required (Urbanavicius et al, 2011).

As one of the quantification methods for organ viability determination, pulse oximeter is prevalent (La Hei et al, 2001). It can measure the oxygen saturation in artery blood. The measured value is sometimes expressed as $SpO_2$ because it utilizes pulsation. In contrast, it cannot measure that in veins and microcirculations that have no strong pulsation. Thus, the pulse oximeter is not suitable for evaluating viability of distal gastrointestinal organ.

In MCS2014, we presented a method for estimating the tissue oxygen saturation ($StO_2$) of gastrointestinal organ by near infrared (NIR) region spectroscopy. We performed animal experiments and obtained successful estimation results. However, a bulky setup for measurement is not suitable for clinical use.

In this paper, we investigated the feasibility of a more compact setup using several spectral bands of LEDs in NIR region and a photo detector. We first constructed a method, then predicted the performance of the proposed setup through computer simulation using transmittance spectra obtained in animal experiments.

## 2. METHOD

### 2.1 Outline

We build an organ absorbance model equation based on the Beer-Lambert law and estimate StO$_2$ by calculating the ratio of concentrations between oxygenated hemoglobin (HbO$_2$) and de-oxygenated hemoglobin (Hb). However, there are various light-absorbing materials other than blood in organs. Therefore, a model equation considering their influences is required. Thus, we model organ absorbance $A_{spectral}(\lambda)$ using absorption coefficients $\varepsilon(\lambda)$ and amounts $C$ as

$$A_{spectral}(\lambda) = \varepsilon_{HbO_2}(\lambda)C_{HbO_2} + \varepsilon_{Hb}(\lambda)C_{Hb} + \varepsilon_{other}(\lambda)C_{other}. \tag{1}$$

Here, $\varepsilon_{other}(\lambda)C_{other}$ represents the influences of scattering and/or absorption by tissue other than blood. Spectral characteristics of the third term, $\varepsilon_{other}(\lambda)$, are unknown although oxygenated and de-oxygenated hemoglobin absorption coefficients, $\varepsilon_{HbO2}(\lambda)$ and $\varepsilon_{Hb}(\lambda)$, are already known.

Futhermore, as we assume to use several specral band of LEDs, we need to modify the wavelenth based model given by Eq. (1). In the proposed method, StO$_2$ is estimated as show in Fig. 1. In the preparation step, the absorption coefficients for LED wavelengh bands are estimated using the specral data. This is performed only once. In the intraoperative step, StO$_2$ is intraoperatively estimated using measured absorbance.
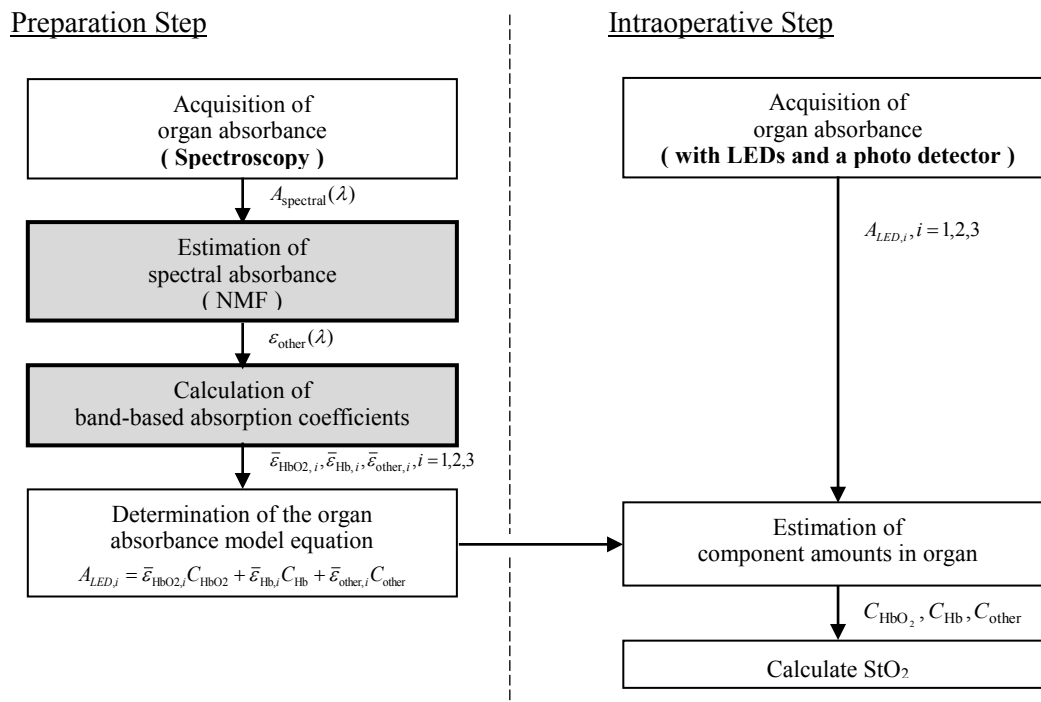


*Figure 1: Flowchart of the proposed method.*

AIC2015 TOKYO - Color and Image

## 2.2 Details of each step

As mentioned above, a simple system using LEDs can not use the wavelngth based model given by Eq. (1). In the preparation step, first of all, the spectral transmittance are measured. Then absorption coefficients $\varepsilon(\lambda)$ and amounts $C$ are estimated. Then, using the amounts $C$, known spectral emittance of LED, spectral sensitivity of the sensor, the absorbtion coefficients for LEDs are calculated. In the intraoperative step, a simple matrix operation output the amounts $C$ from the obained data. Detailed procesdure is given below.

(1) *Estimateion of spectral absorbance*

In the preparation step, we obtain the $n$ transmittance spectra in advance and calculate absorbance by Eq. (2).

$$A^{(k)}(\lambda) = -\log \{T^{(k)}(\lambda)\}, \ k = 1,...,n \ . \tag{2}$$

Here, $A^{(k)}(\lambda)$ and $T^{(k)}(\lambda)$ represent $k$-th absorbance and transmittance, respectively. Using these learning data, we estimate $\varepsilon_{\text{other}}(\lambda)$ by nonnegative matrix factorization (NMF) (Lee et al, 1999, 2001) that is a kind of blind source separation method.

NMF represents a given matrix by a weighted sum of two nonnegative matrices. We decompose the absorbance matrix $\mathbf{A}$ into two nonnegative matrices, $\mathbf{C}$ and $\mathbf{E}$, as

$$\mathbf{A} = \mathbf{CE} \ . \tag{3}$$

Here $\mathbf{C}$ and $\mathbf{E}$ correspond to the amount of components for each subject and absorption coefficients of components in organs, respectively (Galeano et al, 2013) (Pauca et al, 2006). We call $\mathbf{C}$ and $\mathbf{E}$ as amount matrix and absorption coefficient matrix, respectively. Fig. 2 shows a schematic diagram of NMF. We use absorption coefficients of oxygenated and de-oxygenated hemoglobin as the known information. Separation number is three in this time. Thus we obtain the absorption coefficients and the amounts of each component from the learning organ absorbances.
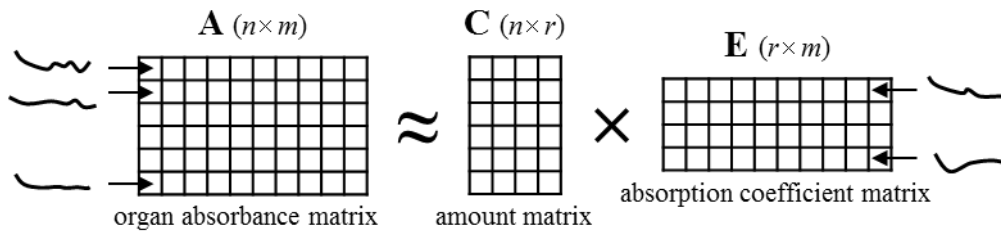


*Figure 2: Schematic diagram of NMF.*

(2) *Calculation of band-based absorption coefficients*

We assume a band-based model similar to Eq. (1) as

$$A_{\text{LED},i} = \bar{\varepsilon}_{\text{HbO}_2,i}C_{\text{HbO}_2} + \bar{\varepsilon}_{\text{Hb},i}C_{\text{Hb}} + \bar{\varepsilon}_{\text{other},i}C_{\text{other}}, \ \ i = 1,...,m \ . \tag{4}$$

Here, $A_{\text{LED},i}$ and $\bar{\varepsilon}_i$ represent the absorbance measured by $i$-th LED and a photo detector and the band-based absorption coefficients, respectively.

Absorbance of $k$th sample measured with $i$-th LED and the photo detector, $A^{(k)}_{LED,i}$ is represented as

$$A_{LED,i}^{(k)} = -\log \frac{\int_\lambda I_{LED,i}(\lambda) \times T^{(k)}(\lambda) \times S(\lambda)d\lambda}{\int_\lambda I_{LED,i}(\lambda) \times S(\lambda)d\lambda}, \ k=1,...,n, \ i=1,...,m. \tag{5}$$

Here, $I_{LED,i}(\lambda)$ and $S(\lambda)$ represent the spectral emission charactersitic of *i*-th LED and the spectral sensitivity of the sensor, respectively. These functions are assumed to be known. $T^{(k)}(\lambda)$ represents the transmittance spectra of *k*-th sample organ measured in the preoperative step. So $A_{LED,i}^{(k)}$ can be calculated.

Since we have $\{A_{LED,i}^{(k)}\}$ and the amounts $\{C_{HbO2}^{(k)}, C_{Hb}^{(k)}, C_{other}^{(k)}\}$ now, we represent Eq. (4) as a matrix form as

$$\mathbf{A}_{LED} = \mathbf{C}\overline{\mathbf{E}}. \tag{6}$$

Here, $\overline{\mathbf{E}}$ represents the band-based absorption coefficient matrix.

Using simulated absorbance $\mathbf{A}_{LED}$ and amounts of each component $\mathbf{C}$ calculated by NMF, we estimate $\overline{\mathbf{E}}$ as

$$\overline{\mathbf{E}} = \mathbf{C}^+ \mathbf{A}_{LED}. \tag{7}$$

Here, $\mathbf{C}^+$ represents a pseudo inverse matrix of $\mathbf{C}$.

The intraoperative step is conducted as follows. If the number of LED bands *m*=3, $\overline{\mathbf{E}}$ becomes a 3x3 matrix. So by multiplying the simple inverse matrix by the measured three values, the amounts of three components are obtained. If there are more than three LED bands, a least square method is applied to dermine $C_{HbO2}$, $C_{Hb}$ and $C_{other}$. Then, we estimate the $StO_2$ by the ratio of obtained $C_{HbO2}$ and $C_{Hb}$.

## 3. SIMULATION EXPERIMENTS & RESULTS

In this paper, we simulated the performance of the proposed method using transmittance spectra of swine small intestines. Using Eq. (5), we simulated absorbances obtained with three LEDs and a photo detector intraoperatively, and estimated $StO_2$ by applying proposed method. As a light emitting device, we assumed three LEDs made by Revox Inc. that have peak at 630, 690, 890 nm, and with a full width at half maximum (FWHM) of 20, 25, 45 nm, respectively. A photo detector made by Hamamatsu Photonics K. K. was assumed as a light receiving device.

### 3.1 Material

We measured small intestine absorbances of swine from 600 to 950 nm at 5 nm intervals. The measurement experiments were performed with prototype probe that consists of a compact spectrometer and a halogen light. Fig. 3 shows representative photos and some absorbances taken during the animal experiments.
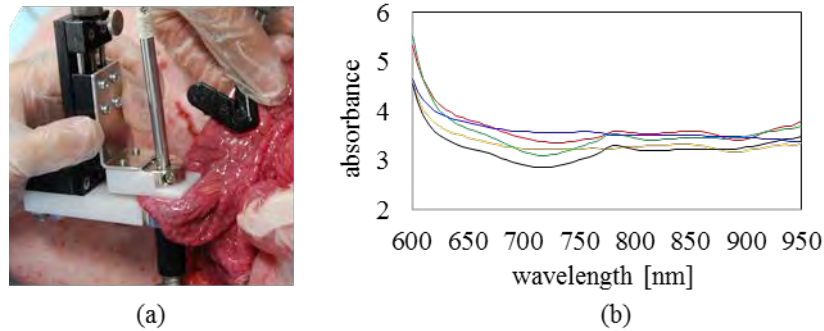
*Figure 3: (a) Represent photo of animal experiment.*
*(b) Some examples of obtained spectra data.*

We have three kinds of measurement data. First one is for determination of the model equation. We have 32 spectra. Second one is for comparison with pulse oximeter. As a reference value, we measured oxygen saturation with a pulse oximeter. The measurement is performed in large vessel region of small intestine that had pulsation. We have 29 spectra and reference values. Last one is for evaluation of changes in the blood circulation state. We ligated the small intestine and created a poor blood circulation state. Thereafter we continued to obtain transmittance spectra of five intestines for three minutes at 20-second intervals after ligation.

### 3.2 Results

Fig. 4 shows $StO_2$ estimation results where (a) and (b) show comparison with reference value and $StO_2$ reduction for ligated intestines, respectively. In the comparison with pulse oximeter value, $StO_2$ was estimated with 2.4 % of average error and 8.4 % of maximum error, and we confirmed the linearity between estimated value and pulse oximeter value. Then, the capability of $StO_2$ estimation for various blood circulation state was confirmed. Furthermore, we confirmed the decrease of $StO_2$ with elapsed time after ligation for all time-dependent absorbance data of ligated intestines. From these experiments, the possibility of $StO_2$ monitoring in intraoperative organ was suggested by our proposed method using the simple setup.
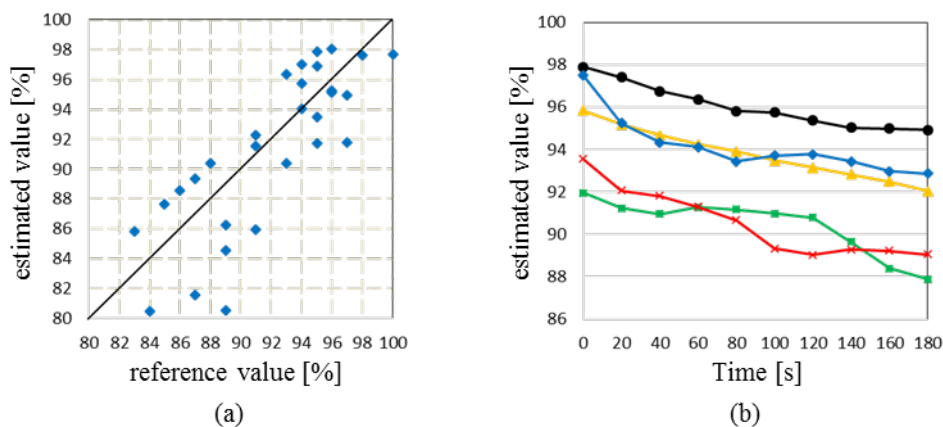


*Figure 4: (a) Comparison with pulse oximeter. (b) Estimation results to ligated intestines.*

# 5. CONCLUSIONS

We proposed a $StO_2$ estimation method of intraoperative organ using a simple setup with some LEDs and a photo detector, and simulated the performance of the proposed method using spectra absorbance of swine small intestines. We confirmed the linearity between estimated value and reference value measured with a pulse oximeter, and achieved average error 2.7 %, maximum error 8.4 %. In the estimation experiment of ligated intestines, the reduction of $StO_2$ due to ligation was evaluated by our proposed method. Thereby, the possibility of $StO_2$ monitoring for intraoperative organs with a simple setup using three LEDs and a photo detector is suggested.

As a future work, we will prototype an actual equipment and evaluate our proposed method by applying to more swine small intestines in various blood circulation state.

# ACKNOWLEDGEMENTS

# REFERENCES

Murai, K., H. Kawahira, and H. Haneishi. 2013. Improving color appearance of organ in surgery by optimally designed LED illuminant. *IFMBE Proc*. 39: 1010-1013.

Urbanavicius, L., P. Pattyn, D.V. Putte, and D. Venskutonis. 2011. How to assess intestinal viability during surgery: A review of techniques. *World J Gastrointest Surg.* 3(5): 59-69

La Hei, E.R. and A. Shun. 2001. Intra-operative plus oximetry can help determine intestinal viability. *Pediatric Surg. Int.* 17: 120-121

Lee, D.D., and H.S. Seung. 1999. Learning the parts of objects by nonnegative matrix factorization. *Nature* 401: 788–791

Lee, D.D., and H.S. Seung. 2001. Algorithms for non-negative matrix factorization. *Adv. Neural Process.*

Galeano, J., R. Jolivot, F. Marzani, and Y. Benezeth. 2013. Unmixing of human skin optical reflectance maps by Non-negative Matrix Factorization algorithm. *Biomedical Signal Processing and Control* 8: 169– 175

Pauca, V.P., J. Piper, and R.J. Plemmons, 2006. Nonnegative matrix factorization for spectral data analysis. Linear Algebra and Its Applications 416: 29–47

*Address: Mr. Yoshitaka MINAMI, Graduate School of Engineering, Chiba University, 1-33 Yayoi-cho, Inage-ku, Chiba, 263-8522 JAPAN E-mails: y_minami@chiba-u.jp, t-ohnishi@chiba-u.jp, k.kato1060@gmail.com, wasaki@j.kisarazu.ac.jp, {hk, haneishi}@faculty.chiba-u.jp*

# Proceedings

## Poster Papers

# COLOUR IMAGE, FASHION DESIGN AND IDENTITY

Dr. Larissa NOURY, Paris, France

«Couleur-Espace-Culture» / «Colour-Space-Culture»

The Colour, Art and Fashion design concerns the Harmonies of color associations of textile and other materials used for couturier's aesthetic project. It is an illustration of collaboration of artists and couturiers on the harmonies of color associations in order to create a personal style and marque or brand identity. They were more closely tied at the turn of the 20th century than they are today. Artists did not see the difference between creating an original work of art, such as a painting, and designing a textile pattern that would be reproduced many times over. Each was a valid creative act in their eyes. There are a lot of vivid illustrations of the centuries-long love affair between fashion and art of color.

## Fashion and identity

Beginning from the 19th century major changes both emerge in the role of fashion and in the place of art in society. Growing affluence and new social structures gradually turned both fashion design and art of color into ways of expressing personal taste and identity.

Our study raises a historic panorama of the colour in the fashion design during the XXth century, highlighting certain symbolic movements such as the Art nouveau, the Russian avant-garde, the modernism, pop art or the kinetic art. It lists the colour's harmonies for modern fashion design and describes the tools, ranges, palettes, techniques which allow personalizing a dress with fantasy and subtlety.

Art has often been a major source of inspiration for dress designers of XXth century: we remind some creations by Paul Poiret, Sonia Delaunay, Liza Schiaparelli, Coco Chanel, Yves Saint Laurent and Givenchy. In their practice art of color is in fashion image.

This connection between art and fashion is obvious from the end of XIXth century. Nowadays, the collaboration between artists and fashion designers continues. The personal artist's inspiration of French colorist Larissa Noury comes from her own color harmonies of tactile painting, from within. Jean Marie Pujol, couturier who worked with Dior and Yves Saint Laurent at the time, designed several dresses to be painted by coloriste and designer Larissa Noury. Their unique collection of painted dresses means to perpetuate the art and fashion marriage in order to create an original color image.

## Belle époque / Belle Epoch

The synthesis of practical considerations and of an aesthetic natural forms and lines is characterized by colour palettes of great richness. Modern times influences a great deal the development of fashion design and produced a profusion of the polychromy in it.

The large selection of paintings by Claude Monet and Pierre-August Renoir, Giovanni Boldini, Auguste Toulmouche, James Tissot, Jean Beraud and Alfred Stevens, – visual artists, who reflected the best on the fashion style of Belle Epoch, – is an example of what

could be called fashion inspiration in fine arts. Artworks were created in realistic manner and do not have even a touch of stylization typical of modern art. Figures depicted in these paintings are precise and realistic. However, it would be fair to say that style itself is the subject matter instead of a particular model. Fashion is the main theme and inspiration for these paintings.

After a visit to the workshop in Vienna the avant-garde fashion designer Paul Poiret combined the idea of mixing art and fashion in his Parisian practice. He opened a Martine school (1911), a place which was also attractive for artists. He then employed Parisian artists such as Lepape, Ibibe, and Erte for fashion illustrations. He employed the artist Raoul Duffy to design fabric prints and to invent tissues. He went to art galleries and showed his artistic sensibilities by preferring Impressionist paintings at a time when they were new and unappreciated by the public. Poiret became very interested in modern art and said, "I have always liked painters. It seems to me that we are in the same trade and that they are my colleagues." The couturier considered himself firstly as an artist.

## Russian constructivisme & suprematisme

The Russian avant-gard in Art and Design (1915-35) deserves to be mentioned. The word "revolution" has become a slogan for fashion design as well. The Russian constructivists defined the chromatic surfaces as fundamental coloured elements where the straight lines, the rectangular forms, the principal colors (yellow, red, blue, black and the white) are used to make a unified and inexistent on Nature composition.

Varvara Stepanova, Alexandre Rodchenko, Liubov Popova and others show their creativity through re-energizing new forms and meaning in art and dress design. The strong and independent colour, the uniformity of geometrical shapes and the lack of forces of gravity, - all those elements forms a kind of representation of an ideal cosmos. The key fragments of Russian revolutionary creativity still glow like radium, living on futuristic art and design into the imaginations of some most influential couturiers of the 20th and 21st century's. Christian Dior's Haute Couture was inspired by Malevich's painting in 2002.

## Simultaneous Contrasts & Sonia Delaunay.

In the 1920s, abstract painting inspired a variety of fabric designs by successful designer and artist Sonia Delaunay. Married to Robert Delaunay and a close friend with artists like Mondrian, Arp, Vantongerloo and Kandinsky, she was a member of the contemporary artistic avant-garde in her own right. It was her own abstract paintings that she translated into rhythmic designs composed of squares, lines, circles, diagonals and colour planes. In all, Delaunay created over 2,000 of these fabric designs, around 200 of them produced especially for fashion house Metz & Co in Amsterdam.


## Surrealism & Elsa Schiaparelli

Fashion designer Elsa Schiaparelli, Coco Chanel's main rival in the 1920s and '30s, produced clothing and hats heavily influenced by Surrealism. Her sweaters incorporating knitted ties or sailor collars were a sensation and she worked in close cooperation with artists like Salvador Dalí and Jean Cocteau. An example of her work with Dalí is her famous lobster dress and the original design of the very imaginative patterns such as the 'shoe hat' and surrealistic shoes and gloves. Dali said: **"Surrealism is destructive, but it destroys only what it considers to be shackles limiting our vision".**

**Art deco & Coco Chanel**

The designer's passionate interests inspired her fashions. Her apartment and her clothing followed her favorite color palette, shades of beige, black, and white, which composes a bases for style of art deco. Elements from art deco design, her art collection and even theatrical interests provided themes for her collections. The ornament of the dress, in both pattern and color palette, resembles the Asian lacquered screens which the designer loved and collected. The convergence of Art Deco line, the modernist impulse was married with pure form and Japanese's potential.

**Art of Neoplasticism**

Piet Mondrian changed the face of modern art. His influence extends to painting, sculpture, graphic design, and fashion. In search of plastic harmony he introduced a universal language of shapes and primary colors that goes beyond the painting, Mondrian was the central figure and the most famous of the De Stijl movement. This style was baptized as neoplasticism and intended to achieve real objectivity by releasing the work of art from its dependence on the momentary individual perception and temperament of the artist. Yves Saint Laurent has created his famous dress with Mondrian's colour composition.

Yves Saint Laurent, Diane Von Furstenberg, Nike, Moschino, Kara Ross, Christian Louboutin, Vans also used the codes of Neoplasticism. They proclaimed a new polychrome design "neo-plastician" who applies sharp and pure colors in their achievements. They intend to propose a theory of a relationship between design and painting, like "a place of modern painting in architecture". Théo van Doesburg defined the chromatic surfaces coloured as fundamental elements where the straight lines, the rectangular shapes, the principal colors (yellow, red, blue, black and the white) are used to make a unified composition.

In the 1950s, **Mrs Carven** produced a special designs dresses inspired by Optic illusion, and since then the emergence of Minimalist art has given rise to a widespread taste for sober, often asymmetrical designs. Not only paintings but also sculpture inspired couturiers for a news creation. **Mrs Grès** was known as a sculptor of fabric, since she used to create long, draped Grecian-style dresses with delicate pleats. Her favorite fabric was silk jersey and her signature was cutout gowns which would leave parts of the skin exposed. The perfect construction of her designs would always bring out a sophisticated feel of classical antiquity and 'extreme purity'. Her clients included 20th century fashion icons such as the Duchess of Windsor, Jacqueline Kennedy and Grace Kelly. Madeleine **Vionnet** was known as the "architect among dressmakers". Her vision was all about comfort and fluidity in movement. Her name is associated with the 'bias cut' which she introduced in order to help accentuate the natural curves of the female body. Inspired by ancient Greek art, the French designer remains known for her Grecian-style dresses and revolutionary clothes, worn by stars such as Marlene Dietrich and Greta Garbo.

Since the Second World War there has been frequent interaction between art, architectural design and fashion. Le Corbusier **was the designer of Minimalism.** He was one of the principal actors of the rationalist modern and purist movement with his slogan "Order. Reason. Purity. Truth. Structure. Bleaching". But he was also one of the first architects that

organized and classified the color in the scale of environmental polychromy. **Minimalist in fashion is** a case of André Courrèges who has opened his own couture house in 1961. He wanted to "modernize the women." From there, he created the futuristic collections, with clean and original shapes. He was then nicknamed "Le Corbusier of fashion."

### Pop-art , op-art & hippie culture in fashion

The emerging hippie culture rejected the dictates of Paris haute couture, adopting instead an eclectic, highly individual look, mixing vintage and ethnic clothing with fashions inspired by contemporary psychedelic Pop art, nature, fantasy, and ethnographic art For instance Jean-Charles de Castelbajac was inspired by Andy Warhol and his **Pop-art** "Campbell's Soup" painting , he has always been inspired by contemporary art; he brings a joyful colour pallet from BD, cartoons, art graphics in his collection. **Op-art** produces at the spectator a physiological and psychological optical effect in environmental design and fashion.The artists as Victor Vazarely, Yvaral, Cruz Diaz and other representatives of "Optical Art" continue to influence modern fashion design and modern life today. Especially artists of "Op Art" inspired the fashion and interior design created by fashion designer Jean-Paul Gaultier.

The creativity work of Friedrich Hundertwasser remains before all that of a painter and a designer fighting against the austerity and the monotony of the industrial design. The unusual achievement of Hundertwasser with application of colour material and the use of irrational geometrical forms is a demonstration of kind of spatial contrasting harmony.

In 2007, Christian Dior designed a unique piece: hand painted and enhanced with spectacular embroidery Manteau Suzurka-San. Dior Haute Couture was inspired by The Great Wave of Kanagawa, emblematic work of Japanese artist Hokusai. Focusing on the relationship between art and creations of the house of Dior, we can say that the original works have been in one way or another influenced by different artists.

During his whole existence Yves Saint Laurent revolutionized fashion and gave the woman her freedom of movement that has inspired artists, poets and painters. "The profession needs an artist to exist," he said. He loved paintings, especially those of as Matisse, Mondrian, Braque, Picasso, and Van Gogh. Saint Laurent paid tribute in 1988 to Georges Braque, whose famous birds seem to fly stuck to the bride's dress. Then he designed a jacket inspired by "The Iris" of Van Gogh. It took 800 hours to sow the whole Van Gogh image. Flakes, tubes, seed beads, ribbons were all embroidered by hand to make the effects and lighting as it was on the canvas. Yves Saint Laurent, a veritable artist influenced in some way other couturiers.

Nowadays, fashion designs have increasingly been regarded as autonomous works of art. Some creations by designers like Jean-Paul Gauthier have been inspired by "futurism" and use the "tromp-l'oeil" effect. For instance stylish French can-can dress has been inspired by the "Moulin rouge" dancer. And we can see some kind of butterfly as a "camouflage" for his new fashion collection. The fashion house of "Martin Margiela" has been inspired by quotations from Frank Llloyd Wright, paintings of Gauguin and graphic codes of pop art that were transposed on dresses in an open way; yet fashion-art chemistry worked well together. Faces are covered with the now famous masks in combination with a kind of cap and remind us of motifs between science fiction and oriental legacy; sham tattoos on the tissue placed directly on the skin were hallucinating and sexy. Art of green fashion design

show us the tendency to the ecological way of thinking. The very famous botanist Patrick Blanc, world known for his green wools & fashion designer Jean-Paul Gauthier have created a "green" wedding dress in 2002.

The latest movement is a combination of light & urban design as well as light and fashion design. Renowned for its distinctive colour palettes and creative designs **Franck Sorbier** used just two designs and stunning visual effects to narrate a medieval French fairytale on the runway in Paris. The Haute Couture Autumn/Winter 2012/2013 collection retold the 17th century story: Donkeyskin, a widowed king set on marrying his own daughter, who escapes his clutches by demanding a series of impossible gowns, the colour of the sky, moon or sun. "The collection is a bridge between the past, the present and what the future could be," explained Franc, who had teamed up with software giant Intel for the high-tech side of the project.

All these examples show us that the variety of colour harmony in art and actual fashion design is a true colour 3D conception, with nuances and details, with specific colour codes and combinations, constantly changing in space and time. We can distinguish 4 colour associations or fundamental groups: "Colour", "Value", "Nuance" and "Mixed"; Inside of each group different components lose their own characteristics to the profit of a global perception. We can distinguish also 24 complementary intermediate colour groups (colour will be expressed on *NCS – Natural Colour System*).

These families of colours reflect their global impressions and comply with the laws of *"gestalt theory"*.

Aleatory : Values of hue, saturation and brightness are pulled at random in every action.

Antagonistic achromatic: Two opposite values of tints on the achromatic axes with various brightness levels.

Antagonistic chromatic: Two opposite values of tints on the chromatic circle with various brightness and saturation levels.

Bichrome: Two values of tints in right angle on the chromatic circle with various brightness and saturation.

Camaïeu: Colours of close tints on the chromatic circle with various brightness and saturation.

Partial contrast: Two tones with diverse brightness and saturation which binds a gradation between these two values.

Degrading: Continuous progression between two colours, both in tint and in saturation or in brightness.

Progression moving: Progression between two colours, in very distinctive ways as a step of colours in a staircase.

Fusion: Two colours merge gradually into a third whose colour is in the middle of the first two but the saturation is lower if the shades are remote.

Equally chromatic: Unity of tint, diverse saturation and brightness.

Equally bright: Unity of brightness, variations of tints and saturation.

Equally saturated: Unity of saturation, variations of tints and brightness.

<u>Isolated:</u> A colour in opposition of tint, saturation and brightness compare to a neutrality of the background.

<u>Monochromatic:</u> A colour with very close variations of saturation or brightness.

<u>Multicolored:</u> Multicolour is a complete harmony of all chromatic colours that are completed by the Neutral.

<u>Neutral:</u> A simple gradient from black to white. The harmony is very common in contemporary art, fashion design & architecture.

<u>Nuanced:</u> Low saturated group and close colours in brightness.

<u>Progression in saturation:</u> Unity of tint and brightness, progress in saturation.

<u>Polychromatic:</u> Composition of different chromatic colours.

<u>Quadrichromatic :</u> Four colours in right angles on the chromatic circle, degraded by saturation and by brightness.

<u>Tone in the tone:</u> The same colour tone which is corresponding to the different materials play some kind of contrast.

<u>Trichromatic:</u> Three colours in an equilateral triangle on the colour wheel, gradient in saturation and brightness.

<u>United:</u> The combination of very close colours in relief materials which give us a unique colour perceived from a long distance.

<u>Translucent:</u> Luminous effect of colour composition due to transparency of used materials.


**Tactile colour & Haute Couture**

My inspiration as a colorist and designer comes from my own painting, from within. Jean Marie Pujol, couturier who worked with Dior and Yves Saint Laurent at the time, designed several dresses to be painted using my technique to perpetuate the union of art and fashion. With this personal style we created a series of hand painted dresses presented during exhibitions and international events. An evolution of coloured strata in constant transformation, beauty of nature, the interaction of forms and images... It is towards this universe of harmony that I invite you. Everything lies in the pondering of both visual and tactile beauties which conceal thus a created space. A perception an eye discovers which is then transfigured and transformed by the feeling of touch.

« Beauty has as many meanings as man has moods.
Beauty is the symbol of symbols.
Beauty reveals everything, because it expresses nothing.

When it shows us itself, it shows us the whole fiery-colored world. »

 Oscar Wilde, 1890


This type of art, beyond the visible, enriches us by its power and its self-fulfilment.


*Address : Dr. Larissa NOURY, « Couleur-Espace-Culture »/ « Colour-Space-Culture »*

*14 rue de la Chapelle, 75018 Paris, France.* E-mails: larinoury@gmail.com

www.larinoury.fr **,** www.CEC.larinoury.fr

# Contemporary Art and the Unfoldings of Colour

Laura CARVALHO[1]

ProCor Brazilian Colour Association

School of Arts and Communication, University of São Paulo, Brazil

## ABSTRACT

Contemporary art legitimates colour by leading it away from the traditional techniques of painting, and it transgresses platforms by thinking about new modalities of image: it puts the spectator and the space as central elements of the chromatic experience. Colour is the sensation given by the image – and the latter is no longer assimilated from traditional constituents (canvas, paint) – in installations and urban interventions. The passengers on streets and avenues are captured by the unexpected, and colour is inserted within the city's landscape as a sensorial input to be perceived. From the 60's onwards, the role of colour on the realms of contemporary visuality has been deeply rethought by art. Carlos Cruz-Diez (Venezuela), Hélio Oiticica (Brazil) and Daniel Buren (France) are leaders of this conceptual turning point: they established new chromatic formulations for installations and urban interventions; they made colour a way of awaking within the spectator the everyday sensitivity and the attention to the landscape.

## 1. INTRODUCTION

The 20th century was determinant for the colour judgement on the realms of art and culture. Modern art emancipates colour as a pictorial element, it deposes *mimesis* from its well-privileged field and it begins to consider the chromatic material within the domain of subjectivity. Contemporary art, on the other hand, evaluates the modern perspective, takes away from colour its character of personal expression in order to create new parameters – more objective and impersonal ones – on the way it turns into image.

It is not possible to accompany the fast transformation of the colour role in the art of the 20th century without taking into account Marcel Duchamp's legacy to the contemporary art (Temkin 2008). The French artist, through *readymade*, articulates his critique to the institutionalization of the work of art and the primacy of the object made by the artist: painting, its auratic dimension and its disarticulation with the social dynamics. Duchamp incorporates everyday objects – the common, the ordinary ones – in the field of artistic production in order to depose the handicraft character of art and its exclusive relation with the artistic genius.

---

[1] Laura Carvalho is Brazilian colour researcher and production designer for the cinema. Graduated on Audiovisual Arts by the University of São Paulo and Master of Arts in Theory and Aesthetics of Cinema by the same institution. Her academic research establishes a parallel between colour, cinema and visual arts, notably modern and contemporary art. Such academic research has brought results presented in conferences in Brazil and overseas, including countries as Spain (2012) and United Kingdom (2009, 2010). Presently works as production designer and scenographer for film, performance and theatre.

Duchamp was not notably a colour artist, but the debate he engendered resounds on the way colour was taken in within art from the decades of the 50's and 60's. The manufactured or industrial colour assumes certain distance from its handicraft process of production; the tube paints are replaced by those found at stores not dedicated to the artistic production, such as the masonry and automotive paints. At that moment, there was not a disarrangement between the artistic practice and the everyday life elements, and colour enters the world of art as a present element in the real world.

As for the installation and urban intervention - the focus of this text - the artists validated Duchamp's methodology on a two-folded way: not only did they question the museum as a space which endorses the value of art, but they also thought about the way of inserting art into the contemporary visual culture, through colour and urban landscape.

Hélio Oiticica, Carlos Cruz-Diez and Daniel Buren (having considered the different contexts they developed their work) stand out in their use of colour in the poetics of the expanded field (Krauss 1979), taking here the famous term coined by Rosalind Krauss. They do not move away from their personal preferences for determined shapes or shades – as, for instance, Buren's stripes, Cruz-Diez's geometry and Oiticica's primary colours -, however, they dimension their aesthetical choices according to their colours, materials and the design found in the field of industrial production.

That does not mean that those artists' visual scheme is a submission to the world of capitalist production; instead, through colour release in 3D space, Oiticica, Cruz-Diez and Buren adopted a critique to the institutional spaces of art and the way the everyday experience neglects our vision. For them, colour shows space in its social nature.


## 2. HÉLIO OITICICA

The Brazilian artist develops his journey along with his search for solving artistic problems through colour. Oiticica not only stands out in the Brazilian contemporary production, as well as he is one of the best developers of colour within a prism that takes into consideration the debates occurred around art and the insertion of his project into an underdeveloped context, such as the Brazilian one.

For him, colour needed to get out from the screen frame and reach space projection. This colour dodge aimed at dismantling the traditional art categories, as painting and sculpture. Throughout the years, this artist created a series of projects, identified by specific names: Núcleo (core), Penetrável (penetrable), Parangolé (colorful costumes made of fabric and plastic) and Bólide (fireballs). Let us focus on the Penetrable series, especially the *Magic Square* series.

From architectonic scale, *Magic Square#5* (1978, Figure 1) searches the spectator's involvement through colour. Nine brick 4,5 X 4,5m squares constitute ample coloured walls simulating labyrinths. Colour embodies the work structure; masonry paints cover the square faces, whose nuances may vary among white, magenta, blue, red, orange and yellow. Other elements from the industrial universe are used in the work, such as acrylic blue.

Oiticica, with this bold arrangement, assumes the hybrid qualities of the work, flirting with painting, sculpture and architecture. In Magic Square#5, the labyrinth structure enables the public to go through the colour fields, to walk on its walls, to learn on them, to observe the

blue light that passes through the acrylic board, to pay attention to the landscape that involves the installation. The device he created reaffirms the project collective character. The word "square" takes at least two different meanings: the first, allusive to the architectonic dimension of the work (in relation to the fixed measured squares) and the other that relates to the public square space and its relation with the surroundings, making the installation prone to promote meetings among people and to promote the encounter between people and their surroundings.



*Figure 1: Hélio Oiticica, Magic Square#5, 1978*

The big dimensional work is clearly an exogenous element to the landscape it is inserted in (as it is the case of *Magic Square#5*, located at Tijuca Forest in Rio). Through colour, the walls stand out from their surroundings and activate the public's sensorial experience, carrying out a physical and social dimension of the work. It is physical because it demands the audience's bodily presence inside the installation, and it is social because the spectators walk around its labyrinths and they are invited to free themselves away from the dull and anti-creative everyday life (Pedrosa 2004), in order to acquire a new experience through art. The formal set projected by Oiticica opens up a magical dimension, as if the installation were from a fantastic nature inside a landscape that notably does not belong to it.

Hélio's project mixes intellectuality and intuition, this chromatic arrangement distances itself from a symbolic propensity of colour, denying possible associations between colour and its cultural meaning. The artist deeply debates the importance of colour on the social net where the installation in fixed in. The palette he searches is not the painter's one, not the architect's one, but it is a visual data which presents itself independently, lightly and loosely, and it is able to grab the spectator in a universe of sensations.

## 3. CARLOS CRUZ-DIEZ

In the Latin-American context and its situation in the international art, the Venezuelan Carlos Cruz-Diez has a relevant development of colour in the 3D field. He begins from a careful study of colours in the realm of science, graph art and painting, moved by the curiosity in associating scientific research and artistic production in the search for new industrial materials to be inserted in his works.

From easel painting to designer and illustrator, Cruz-Diez persisted on the way colour might be registered as an image. Thus, his extensive career deals with diverse materials (cardboard, wood, aluminium, plastic, LED light bulbs, etc.) adapted to specific aesthetic

assumptions. For having this diversity of materials that enable a range of concepts, his art meets kinetic art, geometrical art, constructive art, expanded cinema and site specific.

Comparably to Oiticica and Buren, Cruz-Diez also presents himself opposed to the symbolic associations of colour, not conditioning it to a mythical character of interpretation. What he proposes is for colour to be emancipated from its cultural charge in order to be recreated according to the spectator's experience. Colour is a live and mutant organism, whose acknowledgement depends on people's interaction with his work, as if our vision were also something unstable to be transformed. His investigation of colour resulted in the study of added, subtracted or reflected colour and it took him to create some series of works: Adición Cromática (chromatic addition), Inducción Cromática (chromatic induction), Fisicromía (physichromia), Ambientación Cromática (chromatic environment) and Cromosaturación (chromosaturation).

Chromatic Addition is founded upon the concept of colour irradiation, when two colours get in touch and optically generate a third one. Some determining works of Chromatic Addition merge into Chromatic Environment: for instance, when the phenomenon of irradiated colour is present in urban shapes, in the zebra crossing (Figure 2) – a feature that used site specific experience in many different countries – or yet in panels or floorboards associated to the airport architecture (*Pisos y muros de Color Aditivo en el hall central del aeropuerto*, Caracas, 1974).



*Figure 2: Carloz Cruz-Diez, Chromatic Addition – Liverpool One, 2014.*

Chromatic Induction, on the other hand, is based on the phenomenon of post-image or retinal persistence. Linear structures capture the complementary colour and thus the presence of colour is given both physically (primary colour) and virtually (complementary). Once more, the zebra crossings, under the effect of Chromatic Induction, enter as an efficient visual resource in the integration of art and urban space.

At last, Chromosaturations promote a physical colour experience. They stimulate ways of thinking, seeing and acting. Cruz-Diez made this series throughout decades and kept modifying its shapes and support, either in transparent material constructions or using LED light bulbs. He made, for example, projects in the city of Paris, *Chromosaturation pour une allée publique* (1969), which enabled the collective experience of colour through an installation in the urban environment. A simple event such as this one invites the passer-by to turn into a prospective public, a spectator that is capable of exploring their perceptive domains about the installation space and about the urban space on which the work was

constructed. As a whole, Cruz-Diez's efforts, throughout his vast production, is on a social dynamics of colour, by promoting an individual and collective experience that reconditions man's vision and makes him recognize the power of his look.


## 4. DANIEL BUREN

The French artist assumes *readymade* as a new repertoire of the contemporary visual culture. Buren does not nullify Duchamp's critical position; he just reconfigures art from his observation of the consumer society. The artist sets the repetition of shape (the famous white-and-colour stripes of 8,7cm, his identity mark) in different support, making the work merge into the landscape of the city and to its emphatic symbolic production of the mass culture.

Buren attributes the creation of this visual tool, the so-called stripes, to the observation of the fabric found at the Market in Saint-Pierre, Paris. These are meaningless signs, from an apparent neutrality and immutability. His colours also do not share a culturally given symbolism or a prescribed emotional charge. These are his projects named *Affiches Sauvages* (developed from 1968, Figure 3) and *Papiers Collés* (from 1969), bold proposals that carried out the discussion around image in the urban space, its banality in relation to the social life events.



*Figure 3: Daniel Buren, Affiches Sauvages, 1968.*

His method consists of gluing those works to walls as if they were mere posters, reproductive and ordinary ones, in which the artist's identity remains anonymous. The works merge in the visual assortment, characteristic of the contemporary society. The more palatable it could seem at first, the arrangement of colourful stripes created by Buren sieves aggressiveness, even present in the title of the series: "wild posters".

The urban intervention is a gesture of visually modifying a given reality, without asking for permission to any public or private institution in order to do so. Both series are nor exempt from ambiguity: along with their mimesis in a set of information, the works are intentionally glued and they make their presence in the own visuality of the contemporary culture on a non-institutional way. Actually, they are not marketing work because they had not been created by a marketing agency and they are not worthy the title of work of art (in the auratic and bourgeois sense of the term) because the artist remains anonymous and refuses the museum as a cultural privileged space of art.

AIC2015 TOKYO - Color and Image

Buren proposes a break in the everyday normality and demands from the spectator the attention to the uninteresting, the observation of the disintegration of the stripes as his authorial mark and of his artistic genius. He refuses painting as an aesthetic resource and little by little transforms his works in objects of the common world (which might be flags, towels, posters, etc.). Despite the apparent static shape of his works, they accompany an external spatial transformation; they are entangled in the architectonic, economic and political set of the city. The artist gives visibility to the urban architecture and he makes the museum invisible as an institution space of art (Rorimer 2002).

## 5. CONCLUSION

One of the most important premises of contemporary art in relation to colour was putting the artist as an observer of the social reach of the art from the dynamics it establishes with the urban space. In spite of having come from different contexts whose works get connected in debates of different theoretical perspectives, Oiticica, Cruz-Diez and Buren reintegrate colour into art: both architecture and colour as ways of the contemporary visual culture. The works invalidate the museums as official places of art and they take off their symbolic value associated to meanings of cultural nature. The movement from colour to space – both in installation and in the city – transforms the everyday experience into an aesthetic experience. For them, colour, art and life do not diverge, they merge in the attempt of re-establishing and updating the public's eye over the everyday events.

## REFERENCES

Batchelor, D. 2008. *Colour - Documents of Contemporary Art*. Whitechapel Gallery/The MIT Press.

Buren, D. 2009 (1969-70). Beware!, *Art in Theory, 1900-2000*. Blackwell Publishing 861-867.

Cruz-Diez, C. 2009 (1989). *Reflections on Color*. Juan March Foundation/Cruz-Diez Foundation.

Jimenez, A. 2014. *Carlos Cruz-Diez Conversa com Ariel Jimenez*. Cosac Naify.

Krauss, R. 1979. *Sculpture in the Expanded Field*, October, spring 31-44.

Machado, T. 2011. *O Efeito Beaubourg na Perspectiva de Daniel Buren*, Angelus Novus (2) 142-161.

Oiticica, H. 1960-61. *Vários Escritos*. Itaú Cultural.

Pedrosa, M. 2004 (1961). Os projetos de Hélio Oiticica, *Acadêmicos e Modernos*. EDUSP 341-343.

Rorimer A. 2002. *Daniel Buren, From Painting to Architecture*, Parkett 66 61-68.

Salzstein, S. 1995. *Autonomia e Subjetividade na Obra de Hélio Oiticica*, Novos Estudos CEBRAP (41) 150-160.

Temkin, A. 2008. "Color shift", *Color chart: Reinventing Color, 1950 to Today*. The Museum of Modern Art 16-27.

*Address: Laura CARVALHO, ProCor Brazilian Colour Association and University of São Paulo, Caio Prado Street, 207, São Paulo,01303-001,BRAZIL*
*E-mails: contato@lauracarvalhoarte.com, laura.carvalho.h@gmail.com*
*Website: lauracarvalhoarte.com*

# Comparison of Slovene color identities by researchers A. Trstenjak and M. Tusak with colors on Slovenian municipality flags

Vojko POGACAR,
Faculty of Mechanical Engineering, University of Maribor

Abstract

Combinations of specific forms and colors represent most effective method to distinguish between different identities. When forms (objects, items) are similar or even identical, then only colors remain most reliable discriminatory factor.

Medieval time in Europe were mainly dominated by the general illiteracy and forms of visual identities such as shields, coats of arms and flags, which were important to unambiguously distinguish the different actors - especially when they have emerged as opponents in fighting or games, or any expression of belonging, labeling property, possession, etc. In 11th century, when designing coats of arms and flags, a series of disciplines from heraldry, vexillology, sfragistics, insigniology, iconology emerged, which were applied among philosophical sciences at that time. However, today they are complementary Sciences of Art History.

The aim of this paper is to present colors, appearing on Slovenian municipality flags and to compare them with the findings on Slovenian color preferences by psychologist Anton Trstenjak 40 years ago and by psychologist Max Tusak around 20 years ago.

In last fifty years Slovenia gained a multitude of new flags appeared due to new municipalities on the basis of local features or attractions which were designed in accordance with modern trends in design. On the other hand, part of the municipal flags represent the heritage of the past, their historical traditions and well-known local attractions, etc. These "older" flags are generally based on heraldic and vexillological principles.

The three studies were done in different time frames, separated by decades. Psychologist Anton Trstenjak presented the color preferences of Slovenian population on a sample of 1,000 students in secondary schools. Psychologist Max Tusak, who worked with Anton Trstenjak, has carried out two decades later, a similar survey on a sample of students in four different types of secondary schools. In the third study, decades later, we made a research of the colors on Slovenian municipality flags, which represent color preferences of population in a given environment. Some structural analysis of color histograms was performed to find out representation of the colors in the flags. The results were given into the Periodic color model to comparatively analyse current state and illustrate the changes. In final study we found a lot of differences and changes over time in color preferences among decades, but we found also exception, mostly concerning similar preferences with color blue.

## 1. INTRODUCTION

Combinations of specific forms and colors represent most effective method to distinguish between different identities. When forms (objects, items) are similar or even identical, then only colors remain most reliable discriminatory factor.

Medieval time in Europe were mainly dominated by the general illiteracy and forms of visual identities such as shields, coats of arms and flags, which were important to unambiguously distinguish the different actors - especially when they have emerged as opponents in fighting or games, or any expression of belonging, labelling property, possession, etc. (Stanic, R. and Jakopic, T. 2005). In 11th century, when designing coats of arms and flags, a series of disciplines from heraldry, vexillology, sfragistics, insigniology, iconology emerged, which were among philosophical sciences applied at that time. However, today they are complementary Sciences of Art History.

In last fifty years, Slovenia gained a multitude of new flags appeared due to new municipalities on the bases of local features or attractions (Heimer Z. 2005), which were designed in accordance with modern trends in design. On the other hand, part of the municipal flags represent the heritage of the past, their historical traditions and well-known local attractions, etc. These "older" flags based on vexillology and heraldic principles, but the semantic undertones bearing important messages for the study of today's Slovenian identity.


## 2. METHOD

The aim of this paper is to present colors, appearing on Slovenian municipality flags and to compare them with the findings on Slovenian color preferences by famous Slovenian psychologist Anton Trstenjak 40 years ago and by psychologist Maks Tusak around 20 years ago. Although the three color studies were done separated by decades in different timeframe, they show us that the most preferred common color through all times were blue. In a comparison of all three investigations, we would like to bring some conclusions in relationship to Slovenian identity background through aspects of color symbolism and psychological frames of color language.

### 2.1 Samples of Anton Trstenjak

Anton Trstenjak was PhD in philosophy and theology, beside that he was ordained a priest in 1931 in Maribor. He was one of the first Slovene, who made deeper researches in a field of color. All mentioned facts were in that times of deep socialism politically inappropriate and also life dangerous. Governmental behaviour was suspicious in most of scientific researches in which they haven't have a proper control and knowledge what they mean and for what purpose they are done. They were too afraid of "bad western influences" which could spoil our society and out of such trivial reasons many of his colleges were imprisoned for many years. So, it is important to know in what kind of circumstances were done this first research of Slovenian color preferences. He made his research on a sample of 1.000 younger Slovenian students from secondary schools, among 15 to 22 years old, 500 male, 500 female, 500 citizens and 500 from province. The research was supported by adequate questionnaire, based on colors of clothing and fashion. To make the research frame more real and understandable, he posed a questions like: 1. Which color is generally referred favourite at all? 2. Which color is the most prefered in clothes? 3. Which color is the most unpleasant at all? 4. Are they in the choice of colors (clothes) follow fashion or their own, irrespective of fashion? 5. Have they prefer a single or multi-colored dress? 6. Are they prefer to dress abstract (geometric) or specific image-like, that they represent something? 7. Do they like the color changes, regardless of whether the new color is "his" or just fashionable?

This last question is particularly important because it is one of the main characteristics of each mode, precisely in the fact that rotational dictate of someone else always affect individual taste.

In general, the research examined the popularity and unpopularity of colors. In making this determination, an important difference arises whether it is a personal preference of color or for its applied use. For example, someone who likes red color will not buy a red coat, but something more socially acceptable. In clothing, therefore we get completely different results. Trstenjak draw attention to this duality that, personal color preferences differ from socially consensual. These colors are then located in the field among indifferent colors. Under such, just a little bit simplified interpretation, we can better understand the respond to colors, based on individual emotional level with a difference of social consensus and rational selected colors on the other side (Trstenjak A. 1996: 310-322).
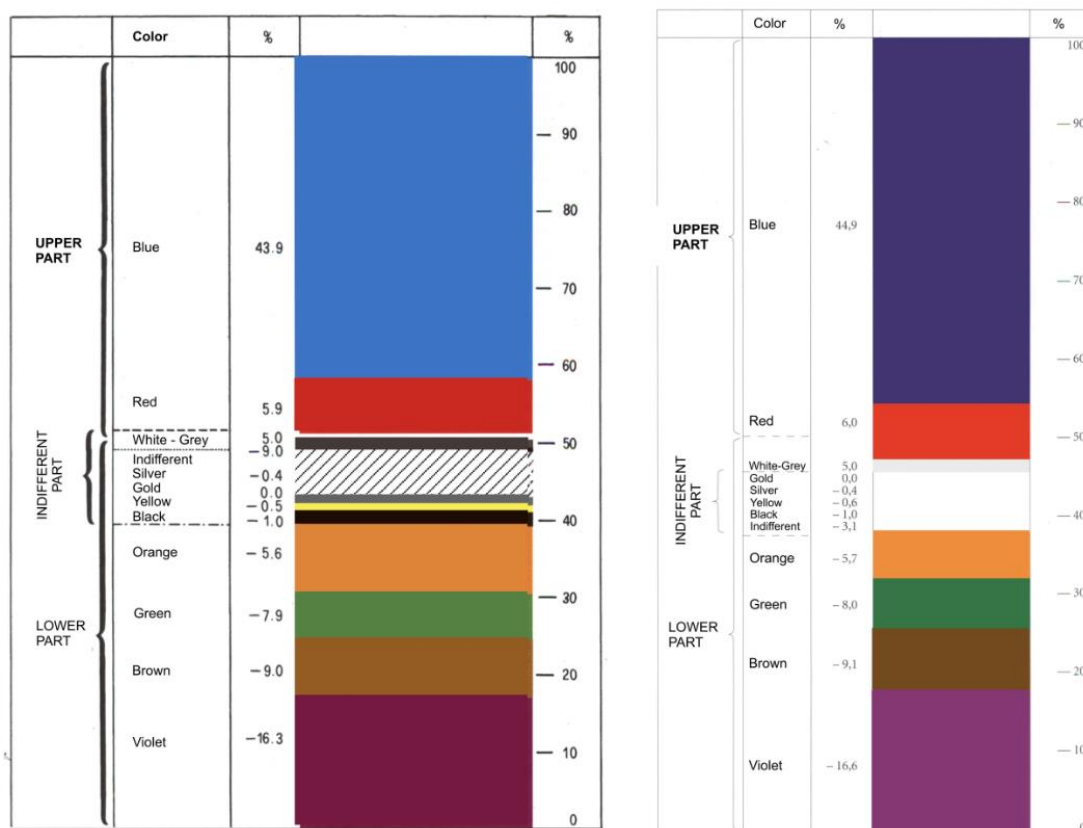


*Figure 1: Color preferences of Slovenian student population by A. Trstenjak (left table) was done in 1975, first published in 1979 and second (right table) in 2001 by M. Tusak. The differences in printed colors are evident. It is also obvious that the colors were meant more in symbolic as in colorimetric sense (Trstenjak A. 1996: 312, Tusak, M., 2001: 87-118).*

Trstenjak research was done around 1975 and presented in his book Psychology of colors, edited in 1979. As the research based on his questionnaire, we may suppose that each participant had slightly individual interpretation of exact colors tone, what means, that colors were understood wider, more loose and generally. Confirmation of this thesis can be found in the presentation of his results (Figure 1), when Trstenjak was still alive. The table in Figure 1 was first presented in his book as a blue color, closer to Cian - that time called Process blue. In second edition Cian turn to much deeper blue, closer to Blue out of RGB system. Also the other colors changed, but for further analyses it is not so important for us.

## 2.2 Samples of Maks Tusak

Psychologist Maks Tusak, who worked some time with Anton Trstenjak, also continued his research in the frame of improved Trstenjak's methodology. Two decades later in 1995 he carried out a similar survey on a sample of four different types of population on secondary and one elementary school in amount of more than 4000 participants. He also used the similar or even the same questionary method, and the results presented in Figure 2 also showed general similarities to Trstenjak's research. Tusak results of research are published in 2001 and presented on eight tables: 1st refer to male students and 2nd to female students of gymnasium, 3rd to male students 4th to male students of technical school, 5th to male students and 6th to female students of vocational schools and 7th and 8th to male end female of elementary school.
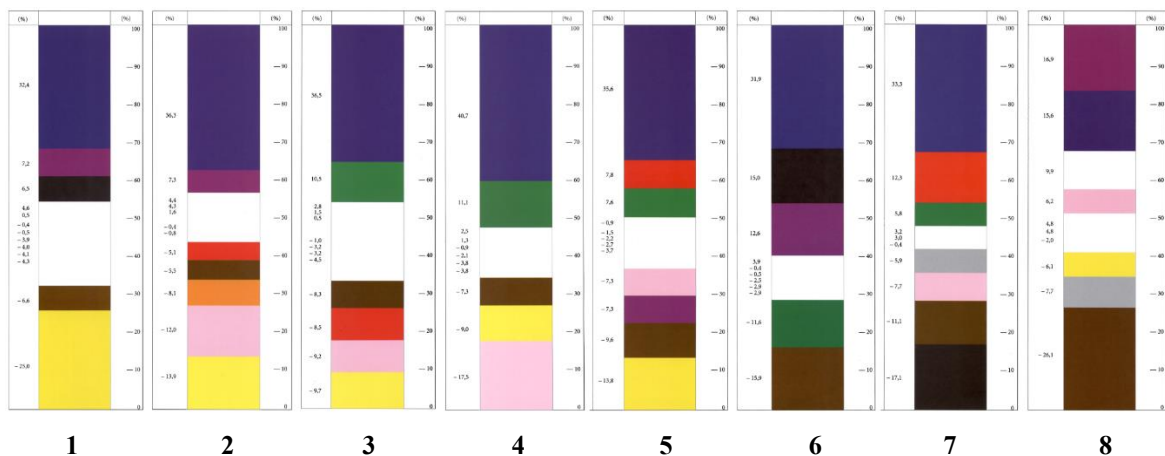


*Figure 2: Color preferences of Slovenian elementary and secondary school's population by Maks Tusak performed in 1995 and published in 2001.* (Tusak M. at all. 2001: 87-118.)

In all 8 tables in Figure 2 it comes out that the Blue is the most prefered, except at last one, where the Blue color is on second place, but general amount of Blue and Violet together figure as common positive opposition to unlike brown (Tusak M. at all. 2001: 87-118.).

## 2.3 Color samples of Municipality flags

A decade later in year 2005, we made a research of the colors on 193 Slovenian municipality flags, which represent color preferences of population in a given environment. It was published in (Pogacar V., at all. 2006: 6 f.). The research of Trstenjak and Tusak present as well positive as negative and indifferent color preferences, but our research was focused only on positive part. Technically based or research on structural and histogram analysis of colors on municipality flags. We presumed that the part of historic flags as leftovers of the heritage were already peoples identity out of habit. On the other hand, we have a multitude of newly created municipalities with flags, which are also selected consensually in accordance with the criteria of the wider local community and, in principle, reflect a consensual color identity. Perhaps the colors of the flags even more accurate represent personal color preferences, because they are not tied to any pragmatic use, but linked with symbolic and presentational level. Our result was also in accordance with previous researches of Trstenjak and Tusak: the average of Slovenians most prefered color is Blue, but an additional important conclusion comes out in this research, that the Green appeared as second most prefered color and it takes almost a half part of positive

side. That way is clearly expressed tendency, which can be noticed as wide spreaded in nowadays Slovenia. These slightly trends were noticed in some parts of Tusak's research by pupils of technical and partly in vocational and elementary schools (Figure 3).
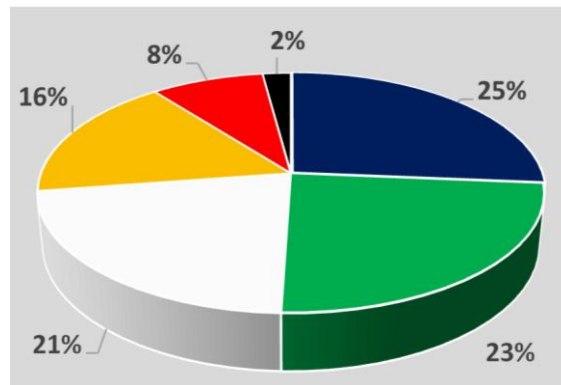


*Figure 3: The everage of used colors on Slovenian municipality flags shows on the first place the same result as the previous researches of Trstenjak and Tusak, but in second place was ranked the green, which is no surprise since this is observed also in the nowadays Slovenian daily lives.*

## 3. RESULTS AND DISCUSSION

In final study we found a lot of differences and changes over the time in color preferences among decades, but we found also exception, concerning to similar preferences in color Blue. But the most important changes in our opinion, appeared on the second place with Green and probably white. Green means the other half stated at the positive side of the color identity and its importance is increasing with the growth of Slovenian self-esteem. To interpret the pragmatic side of this thesis, we used our previous developed PCM (Periodic Color Model) (Pogacar V. 2005 and 2007), where we can analyse and compare symbolic meanings of prefered colors and future trends. All three research results given into PCM showed the general color tendencies (Figure 4).
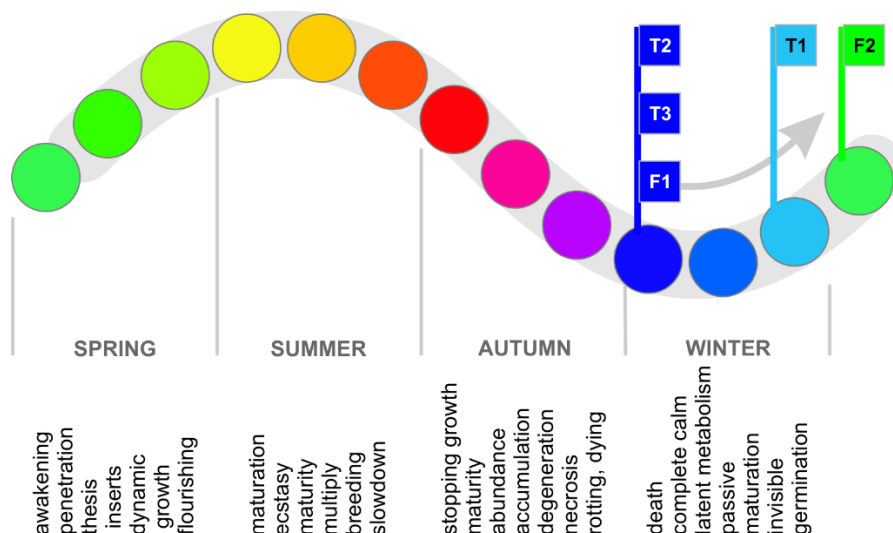


*Figure 4: The interpretation in Periodic Color Model is shown general tendencies of the Research of Trstenjak (T1), (T2) and of Tusak (T3) and of Flags (F1). The Flag color*

AIC2015 TOKYO - Color and Image

*(F2) on the second place shows probably in which direction goes general color preferences in Slovenia nowadays.*

## 4. CONCLUSIONS

And finally, all in research identified trends are already noticed in nowadays manifestations in sport disciplines and also on many other fields, mostly related to Slovenian state identity (Figure 5). But on the other hand, our State's flag doesn't reflect our research conclusions at all, because it was selected under the pressure of time in a year of liberation (1991), when Slovenia separated from former Yugoslavia. This flag is clearly reflecting a heritage and conception of previous times.



*Figure 5: The pictures tell more than a thousand words: color identification through Slovene dresses on Olympic games in Sochi 2014 already confirmed predictions of our results in research.*

## REFERENCES

Heimer Z. 2005. *Slovenian municipal flags.* http://zeljko-heimer-fame.from.hr/hrvat/si-obc01.html

Pogacar V. 2005. Colors in relationship to time cycles. In AIC 2005: Proceedings, ed. by J.L. Nieves and J. Hernandez-Andres. Granada, Spain. 1449-1452.

Pogacar V. 2007. *The principles of Dynamic Color Model development.* Book of. In AIC 2007: Proceedings, Hangzhou, China, 14-17.

Pogacar V., A. Skrbinek, D. Zimsek. 2006. Colors of the national symbols. In 37th ISNT [and] 2nd ISNG [and] 7th IS of SCA. *Proceedings,* ed. by B. Simoncic et al. Ljubljana: Faculty of Natural Sciences and Engineering, 6 f.

Stanic, R. and Jakopic, T. 2005. *Osnove heraldike in istovetnostni simboli slovenskih občin.* Ljubljana: Lecnik.

Trstenjak A. 1978. *Človek in barve.* Ljubljana: Delavska univerza Univerzum.

Trstenjak A. 1996. *Psihologija barv.* Ljubljana: Institut Antona Trstenjaka.

Tusak M. 2001. Psihologija barve. In *Interdisciplinarnost barve vol. 1.* (Monograph DKS). ed. by S. Jeler and M. Kumar. Maribor: Društvo koloristov Slovenije, 87-118.

Address: Prof. Vojko POGACAR, Lab for Product Design, Faculty of Mechanical Engineering, University of Maribor, Smetanova 17, 2000 Maribor, SLOVENIA
E-mail: vojko.pogacar@um.si

# A Comparison of Color Schemes and Images in the Package Design of Sweets in the US and Japan

Kyoko HIDAKA

Faculty of Art and Design, Tama Art University

## ABSTRACT

This study compares the color schemes and design of packages of sweets in the US and Japan from the viewpoint of the cultural history of color. To visualize this comparison, color charts representing typical Japanese and American sweets packages are presented. The central aim of the comparison is to clarify cultural differences in color that characterize appetizing sweets, between the US and Japan. The research method was as follows: I purchased a total of 120 items, 20 items each of hard candy, chocolate, and chewing gum sold nationally, both in the US and Japan in 2013-14. Using ColorMunki Design of X-Rite, I measured the color scheme of these packages and listed the data in the form of color charts. These data are significant in revealing the fundamental cultural differences in the package design in these nations, a valuable insight for the field of international marketing and graphic/package design. Generally, there is a strong tendency for Japanese sweets packages to use a warm and light color scheme, whereas American ones apply a vivid multicolor scheme. Japanese sweets manufacturers produce various novelty items that promote seasonal and regional marketing, whereas American mass-produced sweets and its coloring are generally aimed at children and their dreams. Therefore, the color scheme of and the images on packages of US sweets resemble American comics.

## 1. INTRODUCTION

This paper compares the color schemes of the package design of sweets in the US and Japan from the the cultural history of color perspective. To visualize this comparison, color charts representing typical Japanese and American sweets packages are presented. The main objective of this paper is to clarify the cultural differences in color that characterize appetizing sweets between the US and Japan. Hues in the color scheme of these package designs are primarily examined.

Sugita reported that colors that infants see everyday largely influence the human color sense[1]. The development and innateness of color sense is still the subject under discussion. Even so, I hypothesized that the color scheme of the packaging of sweets can be a root cause of forming color culture since human beings habitually see packages of sweets from childhood. The result of this comparison can expose the cultural distinction in the color perspective and will be valuable in international marketing when exporting Japanese sweets. As precedence research, Birren published a series of books on color and consumer psychology[2]. Kawasome presented a paper examining the relation between food color and

---

[1] Sugita, Y. 2010.

[2] Birren, F. 1961.

human appetite. Iyenger, in her book, *Art of Choosing,* wrote on the issue of how people choose color.

## 2. METHOD

The research method was as follows. I purchased 120 items: 20 items each of hard candy, chocolate, and chewing gum sold nationally, both in the US and Japan in 2013-14. The names of stores were Wegmans, ACME, and Hudson News in New York and New Jersey; and 100 Lawson, Aeon, and Okashi-no-Machioka in Tokyo and Kanagawa. Both in the US and Japan, retail stores displayed an average of 18-30 competing products on the same shelves.

Using ColorMunki Design of X-Rite, I measured the color scheme of these packages and listed the data in the form of color charts. I selected 100 representative colors, including 5 colors each from 20 items. Then I sorted these 100 colors into Munsell's 10 hues: red, orange, yellow, yellow-green, green, blue-green, blue, blue-purple, purple, and red-purple, in addition to achromatic grayscale, including white, gray, and black. Figures 1-6 represent the hues of hard candy, chocolate, and chewing gums, which are frequently used.

For reference, I compare the typical colors of the sweets packages in the US and Japan in Munsell notations and RGB variables (Figure 7 and Tables 1-3).

Moroever, as an example of the cultural image influencing color, I mention one case of sweets package and American comics (Figures 8-9).
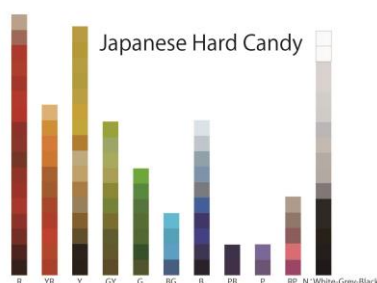
## 3. COLOR SCHEMES

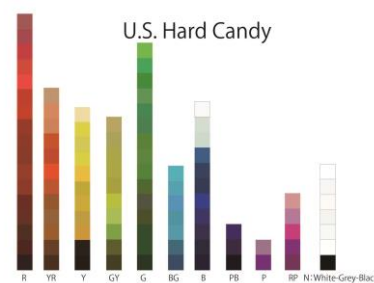### 3.1. Hard Candy



Figure 1: Japanese Hard Candy.



Figure 2: US Hard Candy.

Figure 1 shows that Japanese hard candy packages tend to use warm hues, such as red to yellow and light gray; however, they use less green to purple. The use of warm hues and grayish colors gives bright and soft impression overall. Furthermore, the Japanese data show middle ranges of value and chroma.

Figure 2 shows the similarity with the Japanese data, which also use warm hues. However, there are two differences: first, there is no use of gray, and second, there is frequent use of green. The tendency of not using gray in the US hard candy packages makes it look very colorful and vivid. The US hard candy uses low value (brightness) and high chroma (vividness).
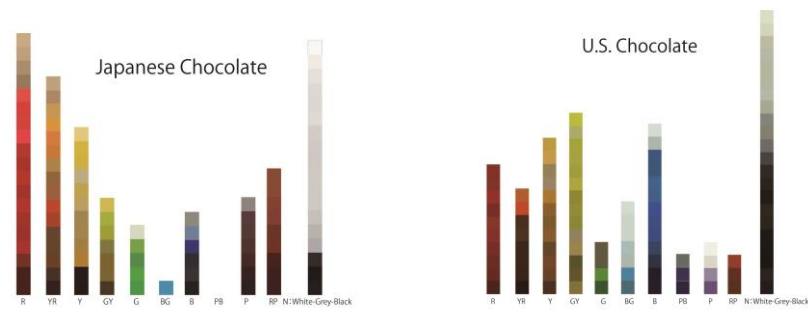
## 3.2. Chocolate



*Figure 3: Japanese Chocolate.*      *Figure 4: US Chocolate.*

Figure 3 shows that the colors frequently used in Japanese chocolate packages are red, brown (orange and red-purple low in value and chroma), black, and light gray. Moreover, they use gold frequently for product logos. Red, brown, black, and gold are four hues that seem to be typical colors for Japanese chocolate. In Japan, black reminds bitterness and red reminds sweetness. Additionally, brown is in between red and black; to make brown hue, people mix these two colors. Typical products such as Glico's Pocky and Lotte's Ghana milk chocolate also use red packages. The bitterer taste and more cacao ingredients the products have, the darker are the hues of the package from brown to black.

In contrast, Figure 4 displays the frequent color scheme in the US. They use brown, dark gray, yellow-green, and blue. The Hershey chocolate currently uses brown in red-purple hue and silver gray. American traditional chocolate snacks, such as Milky Way and Reese, use orange and green, which are not found in the Japanese color scheme.
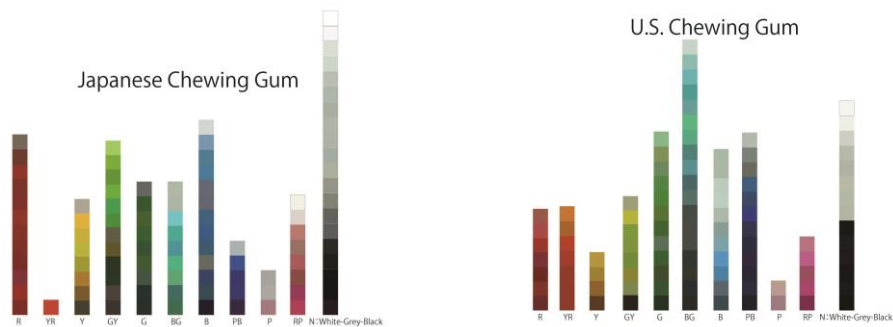
## 3.3. Chewing Gums



*Figure 5:Japanese Chewing Gums.*      *Figure 6: US Chewing Gums.*

Both Japanese and US chewing gums frequently use yellow-green to blue-purple and silver (gray) for their packages. These hues represent cool, refreshing sensation of menthol flavor. On the contrary, they scarcely apply orange and brown for their overall background. Figure 5 shows that the most frequent hue in Japan is silver (gray). Japanese chewing gums use metallic colors and do not apply many hues to give an impression of a cool, sharp feeling. Black is also often used to express a sharp stimulus. Moreover, Japanese have an image of healthiness in green color. A unique Japanese chewing gum flavor is Japanese plum, and its red packaging reminds one of ripe plum.

AIC2015 TOKYO - Color and Image

American chewing gums use more blue-green than those of Japanese. In terms of value, Japanese chewing gums use high to medium range of colors, whereas the American package applies low range of colors. Furthermore, Figure 6 shows that the use of orange in the US is more frequent than in Japan.

## 4. BLUE COLORED SWEETS AND PACKAGE

Quoting the article from Birren, Kawasome reported that blue food reduces appetite[3]. It seems that previous research papers have spread such stereotype to the public, especially package designers and food manufacturers. Therefore, food packages in Japan frequently use warm colors, such as red, which is confirmed in this study. However, in the US, even though "blue" and "fluorescent color" in food rarely exists naturally, this survey found that these colors are widely used in both the packaging and food.

## 5. RESULTS AND DISCUSSION

### 5.1. The Typical Packaging Colors of the US and Japan



*Figure 7: Typical Colors in Packages.*

This section compares the typical colors from the result of this survey and examines the cultural distinction. Figure 7 illustrates a list of typical colors used in packages, sequenced from the first to fifth place. The left column is of the Japanese hard candy, chocolate, and chewing gum, and the right column is of the US. Comparing these three types of sweets, the divergence of hue is remarkable, particularly in chocolate.

In Japanese packages, the illustrative images of fruits, green tea, or milk are often used to inform and evoke these flavors. Accordingly, the colors of these items reflect the color of the packages. In Japan, the use of color in packages of long sellers, basic items versus seasonal, limited, or regional novelties are poles apart. The seasonal, limited ones use more drastic color schemes, whereas the long sellers do not often change the design and colors.

American package design generally applies colors in high chroma and low value. Unlike Japanese, American sweets tend to use illustrative images of contents rather than ingredients. Seasonal and limited novelties are also popular in the US, but it seems that these are rather event based, such as Halloween, Easter, and Christmas with its symbolic colors[4].

---

[3] Okuda, H., Tasaka, M., Yui, A., and Kawasome, S. 2002.

[4] Red & green for Christmas, yellow & pink for Easter, and orange & black for Halloween.

*Table 1. Comparison of the Typical Colors of Hard Candy in Japan and the US.*

| Japan | Munsell (HVC) | RGB | USA | Munsell (HVC) | RGB |
|---|---|---|---|---|---|
| 1 | 6.6R 4/11 | 179: 57: 44 | 1 | 7.6R 4/12 | 195: 67: 45 |
| 2 | 4.9Y 6/7 | 187: 158: 66 | 2 | 1.9G 4/6 | 72: 134: 82 |
| 3 | 3.5YR 5/9 | 213: 122: 57 | 3 | 9.2R 4/10 | 197: 83: 46 |
| 4 | N 8.0 | 207: 205: 199 | 4 | 4Y 7/9 | 234: 187: 65 |
| 5 | 1GY 6/7 | 153: 161: 60 | 5 | 1.2B 6/5 | 88: 161: 176 |

*Table 2. Comparison of the Typical Colors of Chocolate in Japan and the US.*

| Japan | Munsell (HVC) | RGB | USA | Munsell (HVC) | RGB |
|---|---|---|---|---|---|
| 1 | 6.2R 4/11 | 180: 57: 50 | 1 | N7.0 | 180: 181: 159 |
| 2 | 8.6YR 5/5 | 173: 130: 72 | 2 | 0.2GY 6/7 | 164: 163: 59 |
| 3 | 6.7R 1/3 | 72: 35: 29 | 3 | 1YR 1/1 | 49: 38: 32 |
| 4 | N8.0 | 207: 199: 195 | 4 | 7.6PB 3/8 | 65: 81: 142 |
| 5 | N1.0 | 32: 28: 24 | 5 | 7.3YR 4/5 | 137: 96: 47 |

*Table 3. Comparison of the Typical Colors of Chewing Gum in Japan and the US.*

| Japan | Munsell (HVC) | RGB | USA | Munsell (HVC) | RGB |
|---|---|---|---|---|---|
| 1 | 5.1GY 7/1 | 176: 181: 168 | 1 | 9.2G 4/3 | 82: 129: 117 |
| 2 | 1.7PB 3/4 | 66: 96: 124 | 2 | 8GY 3/4 | 69: 98: 50 |
| 3 | 9.2GY 5/8 | 78: 140: 59 | 3 | 1.3P 2/2 | 56: 54: 74 |
| 4 | 3.3R 3/7 | 128: 50: 40 | 4 | 7.9RP 5/9 | 188: 93: 136 |
| 5 | 9GY 3/4 | 61: 92: 49 | 5 | 1.2GY 7/1 | 183: 185: 169 |

## 5.2   American Comics and Sweets Package

The mass-produced snacks and sweets sold in American supermarkets and convenience stores are mostly for children, and its coloring is generally aimed at children and their dreams. Professor Story of University of Minnesota pointed out a tendency to use toys and cartoon characters for food advertisement to make children recognize brands[5]. In particular, M&M (Figure 8), Kellogg's cereal, and Oreo cookies use this marketing strategy[6].

---

[5] Story, M., and French, S. 2004.

[6] Ibid.
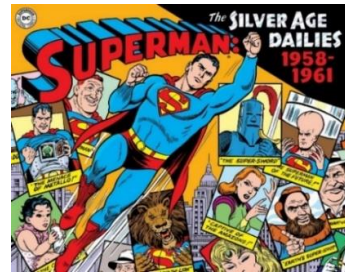
*Figure 8: M&M Pretzel flavor in 2013.*



*Figure 9: "Superman: Silver Age Dailies Vol. 1: 1959-1961" the Library of American Comics, 2013, Superman TM and © DC Comics, Inc.*

Thus, it is predictable that the color scheme of these snacks and sweets packages resemble toys and cartoons. In Figure 9, Superman's color, which are blue, green, and red shows similarity to the one used in the US sweets. In Japan too, children purchase sweets because of bonus toys and the popular anime cartoon characters that are seen on the package. Yet, the colors of Japanese toys and cartoons may not be as vivid as those of the US.

# 6. CONCLUSIONS

The packages of long seller sweets can become the evidence of color sense in every country. In Japan, warm and light colors are used in the basic long sellers, and color scheme variations are seen in seasonal, regional, and limited items. In the US, marketing to children and color scheme of American comics deeply influence the design and colors of sweets packages. Humankind forms the color culture by looking at these items on a daily basis since childhood.

# ACKNOWLEDGEMENTS

# REFERENCES

Birren, F. 1961. *Color Psychology and Color Therapy*, University Books.

Iyengar, S. 2010. *The Art of Choosing*, Grand Central Publishing.

Okuda, H., Tasaka, M., Yui, A., and Kawasome, S. 2002. *Correlation between the Image of Food Colors and the Taste Sense: The Case of Japanese Twenties*, Journal of Cookery Science of Japan 35(1), 2-9.

Story, M. and French, S. 2004. *Food Advertising and Marketing Directed at Children and Adolescents in the US*, International Journal of Behavioral Nutrition and Physical Activity 1-3.

Sugita, Y. 2010. *Experience in Early Infancy for Color Perception*, Journal of the Color Science Association of Japan 34(2) 164-167.

*Address: Dr. Kyoko HIDAKA, Department of Graphic Design, Faculty of Art and Design*
*Tama Art University, 2-1723 Yarimizu, Hachioji-shi, Tokyo, 192-0394, JAPAN*
*E-mail: kh2017@nyu.edu*

# Human monochromatic impressions on multichromatic / colorless phenomena and concepts

Ayana DEGUCHI[1], Akira ASANO[1], Chie MURAKI ASANO[2*], Katsunori OKAJIMA[3]
[1]Faculty of Informatics, Kansai University
[2]Faculty of Human Ecology, Yasuda Women's University
[3]Faculty of Environment and Information Sciences, Yokohama National University

## ABSTRACT

This research experimentally investigates human association of colorless or abstract concepts and phenomena with a single color. This association is called *affinity* between concepts/phenomena and colors in this research. The respondents of the experiments were asked to express various colorless or abstract concepts and phenomena, presented by words, by a single color based on their impressions. The reason why the color was selected is also asked. According to the experimental results, it is found that there exists a color or a category of colors selected by most of respondents for each of several concepts and phenomena. The reasons answered for such concepts and phenomena indicate that the color is selected because most of the respondents agree with an association of the concept or phenomenon with a common concrete object, and the color derived from the object is selected. The model of color affinity is also applied for the selection of a single color for expressing a multichromatic phenomenon, and the existence of the affinity is observed through the experiments.

## 1. INTRODUCTION

Color is a human perception of a physical property of light. It indicates that a color perception is caused by actual stimuli of light with a distribution of spectra (Gonzalez and Woods, 2008). However, it is observed that humans often visualize even abstract or shapeless concepts and phenomena with some colors in mind, by an association of the concepts or phenomena with concrete objects containing some colors. For example, it is usual in Japan that the concept "spring season" is visualized with pink color, which is derived from cherry blossoms.

It is observed in the above example that a concept or a phenomenon can be associated with a color through the relationships between the concept/phenomenon and an intermediate object and between the intermediate object and the color. We call the relationship *affinity* between a color and a concept/phenomenon in this research, as shown in Fig. 1. High affinity indicates a tight relationship, that is, most of people select a common single color for a concept/phenomenon. In case of the above example, the affinity between the concept "spring" and the color "pink" is high if most people agree with associating spring with pink color. There have been a lot of research works on the association of color with concepts (Elliot and Maier, 2014), whereas our experiments investigate the association of concepts with colors.

The model of color affinity is also applicable not only to abstract concepts but also to multichromatic objects. We consider the situation that one is asked to express a multichromatic object, which is shown not by actual things or photos but by words. If one color is preferred
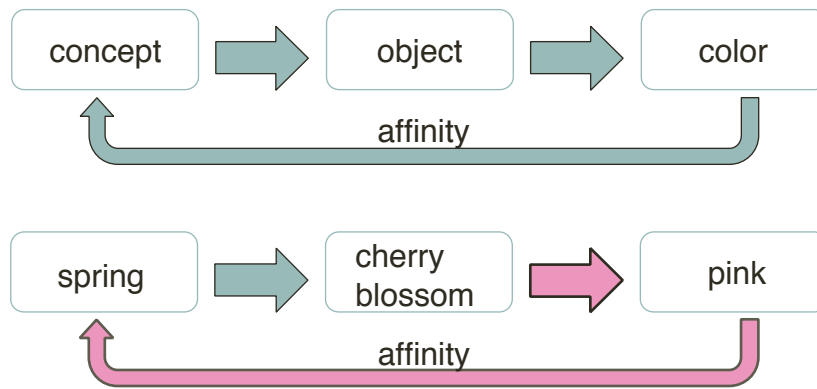
---

*Fig. 1. The model of color affinity.*

to express the color of multichromatic objects, the affinity between the color and the object in mind is high. For example, the rainbow has a continuous spectrum of colors. If a color is significantly preferred to express the rainbow when the respondents are asked to express the rainbow in mind by one color, the affinity between the color and the rainbow is high. It is expected that there are cultural characteristics.

We experimentally investigated the applicability of the model of color affinity for several abstract and colorless concepts/phenomena, and a multichromatic object. The respondents of the experiments were asked to express various colorless or abstract concepts, for example "summer," "Internet," etc., and a multichromatic phenomenon, "rainbow," presented by words, by a single color based on their impressions. The reason why the color was selected was also asked. We carried out the experiments for more than 100 respondents in Japan.

It is observed through our experiments that several concepts/phenomena have high affinity with specific colors, and some have high affinity to specific color categories. The intermediate objects are also observed in these cases. The result for the multichromatic phenomenon, "rainbow," indicates that all colors in the spectrum is not evenly selected and the affinity with a specific color is observed. It is shown by an additional experiment that the affinity is influenced by the background color and the arrangement of color stripes in the rainbow.

## 2. EXPERIMENTS

Our experiments are based on questionnaires for respondents. The respondents of the experiments are restricted to those who have mainly lived in Japan, in order to control the dependence on culture and circumstance. The following words, which were in Japanese in the experiments, were presented to each respondent. These words indicate colorless and/or abstract concepts and phenomena, and one multichromatic phenomenon, "rainbow."

*Abstract concepts and phenomena*
    "spring", "summer", "Internet", "dream", "winter", "time",

*Colorless phenomena*
    "water", "hot water", "air", "wind"

*Multichromatic phenomena*
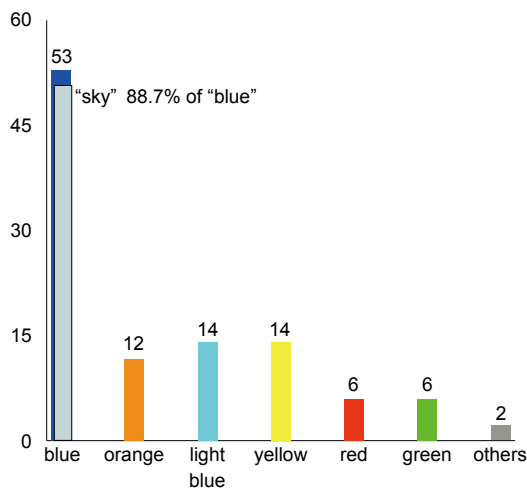    "rainbow"

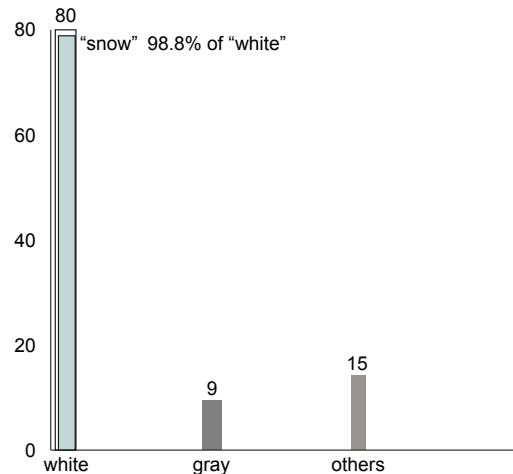*Fig. 2. Result for "summer."*　　　*Fig. 3. Result for "winter."*

The respondents were requested to answer a color in mind by a word for expressing each of the presented words. The answer was strictly restricted to a word expressing one single color. The respondents were also requested to answer the reason why the answered was selected for each of the concepts and phenomena. The number of the respondents is 107, and most of them are university students in Osaka, middle western city of Japan. Some of them are "friends" of Akira Asano, one of the authors, on Facebook, living in Japan.

## 3. RESULTS AND DISCUSSION

We show the results of the experiment for several concepts and phenomena where interesting characteristics on the affinity were observed.

### 3.1 "summer"

Figure 2 shows the number of respondents who answered each color to the concept "summer." The number on each bar indicates the number of respondent who answered each color. The result shows that 49.5% of the respondents answered "blue" to "summer." According to the reasons answered by the respondents, 88.7% of the respondents selecting "blue" associated "blue" with "sea" or "sky." It is observed that the affinity between "summer" and "blue" is high, and the intermediate object in the color affinity model is "sea" and "sky."

### 3.2 "winter"

Figure 3 shows the number of respondents who answered each color to the concept "winter." The result shows that 76.9% of the respondents answered "white" to "winter." According to the reasons answered by the respondents, 98.8% of the respondents selecting "white" associated "white" with "snow." It is observed that the affinity between "winter" and "white" is very high, and the intermediate object in the color affinity model is "snow."

The participants are mainly from around Osaka, middle western city of Japan. Since it snows only several days in one winter in this region, the winter scenery in this region is usually not white, but rather brown because of the defoliation of trees. The impression may be not from their actual experience but from their knowledge.
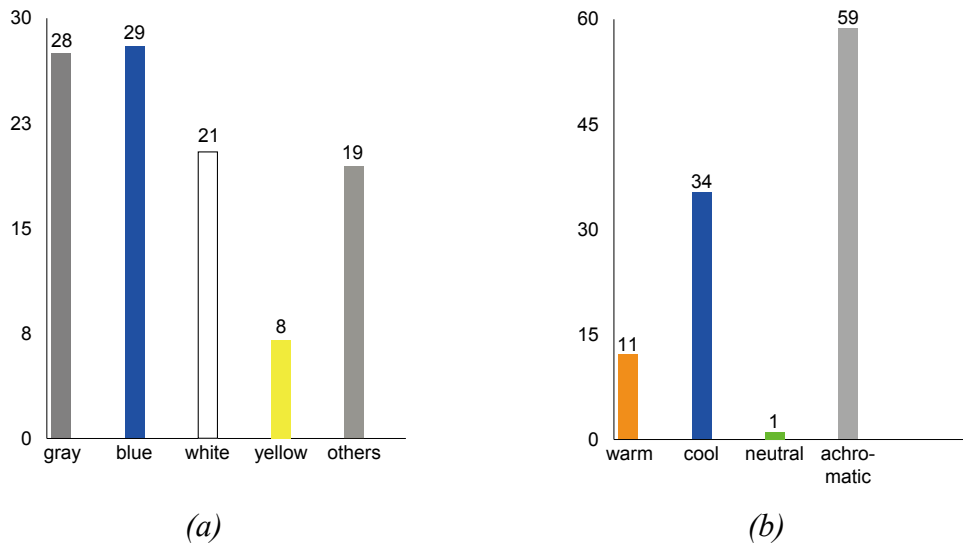
*Fig. 4. Results for "Internet." (a) preferred colors. (b) another categorization.*
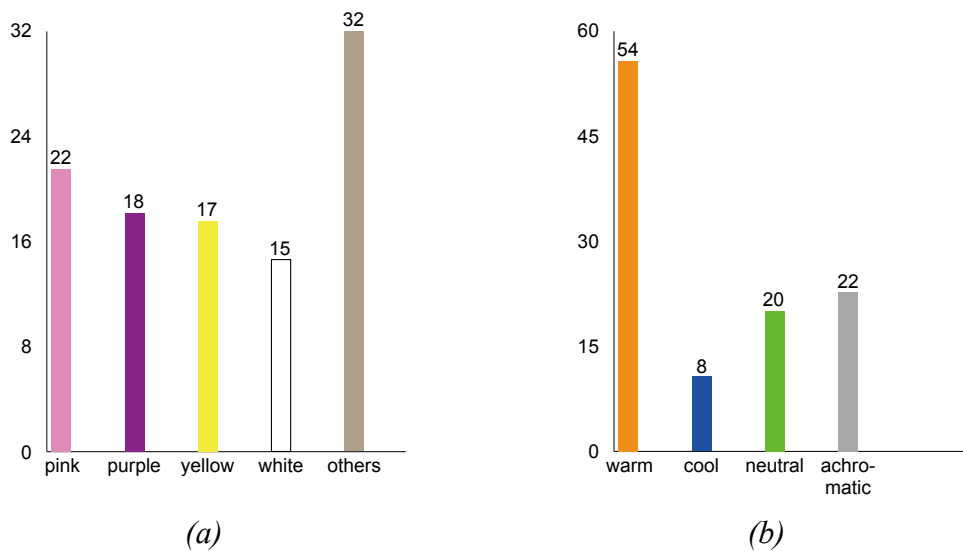


*Fig. 5. Results for "dream." (a) preferred colors. (b) another categorization.*

### 3.3 "Internet"

Figure 4(a) shows the number of respondents who answered each color to the concept "Internet." It indicates that no specific color is closely related to this concept, and no affinity between "Internet" and any color is observed. Figure 4(b) shows the result by categorizing the answered colors into warm, cool, neutral, and achromatic colors. It shows that 56.2% of the respondents selected achromatic colors to express "Internet." The reasons answered by the respondents selecting achromatic colors were mainly negative impressions, for example "network crimes," "mixture of good and bad things," and "complex chaos." It suggests that a concept related to negative idea may be associated with achromatic colors.
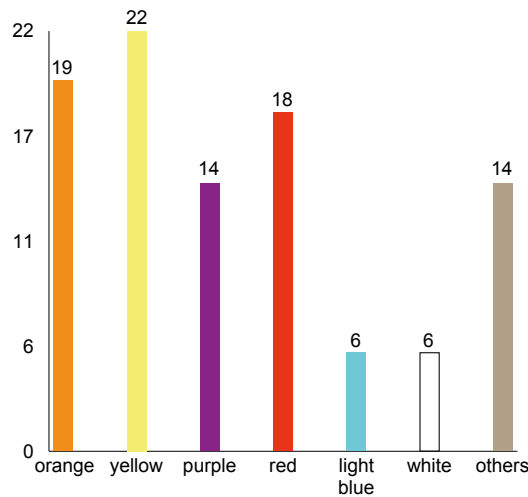
*Fig. 6. Results for "rainbow."*

### 3.4 "dream"

Figure 5(a) shows the number of respondents who answered each color to the concept "dream." It indicates that no specific color is closely related to this concept, and no affinity between "dream" and any color is observed. Figure 5(b) shows the result by the categorization similar to Fig. 4(b). It shows that 51.9% of the respondents selected warm colors to express "dream." The reasons answered by the respondents selecting warm colors were mainly positive impressions, for example "brightness" and "hope." It suggests that a concept related to positive idea may be associated with warm colors.

### 3.5 "rainbow"

Figure 6 shows the number of respondents who answered each color to the multichromatic phenomenon "rainbow." No affinity to any specific color is observed, but orange, yellow, purple, and red are preferred. The reasons answered by the respondents selecting warm colors were mainly "significant," "impressive," and "beautiful in the background blue sky." The reasons for "purple" were mainly "significant," "impressive," "purple is on the edge of the rainbow." Such answers as "The rainbow is watched in the cool sky" were found as the reason for cool colors.

It is interesting that none of the respondents answered "green," except one answer of "yellow-green," although green is physically obviously observed in the spectrum of the rainbow. We assumed a hypothesis that green is difficult to remember because the contrast between green and the background blue sky, and that between green and adjacent colors. A photo of the actual rainbow is shown in Fig. 7 for reference. We carried out two small experiments to confirm the hypothesis. We showed respondents 1) a color stripe similar to the rainbow with blue background on a display, and 2) the same color stripe with orange background, and asked which color was remembered best. The results was that warm colors were preferred in case 1), whereas in case 2) some respondents answered that blue and green were easy to memorize. We also showed a rearranged color stripe where green was between red and orange, and asked the same question. The result was that some respondents answered that blue and green were easy to memorize, also in this case. These results suggests that the results depend on contrasts among neighboring colors.

AIC2015 TOKYO - Color and Image

*Fig. 7. Actual rainbow*[1].

## 4. CONCLUSIONS

This research considers a model of color affinity, which means the association of an abstract or colorless concept/phenomenon with a color via an intermediate concrete object. We experimentally investigated the applicability of the model to several concepts and phenomena. We also investigated the applicability to a multichromatic object. We expect that further investigation of colors derived from concepts and phenomena may yield the inverse relationships, i. e. concepts or phenomena derived from colors.

The dependence of color affinity on each culture is an interesting problem. When we asked university students in Thailand to express the rainbow in one single color, 12 of 37 students selected green. The result was different from our experiments in Japan, and it is said that green is preferred in a lot of situations in Thailand.

## REFERENCES

Gonzalez, C. and Woods, R. E. 2008. *Digital Image Processing, Third Edition, Chapter 6.,* Pearson Education.

Elliot, A. J. and Maier, M. A. 2014. *Color Psychology: Effects of Perceiving Color on Psychological Functioning in Humans,* Annual Review of Psychology, 65, 95-120.

*Address: Prof. Akira Asano, Facutly of Informatics, Kansai University*
*Ryozenji-cho 2-1-1, Takatsuki, Osaka 569-1095, JAPAN*
*E-mail: a.asano@kansai-u.ac.jp*

---

[1] Photographed by Akira Asano in Kansai University Takatsuki Campus, Osaka, Japan, on Apr. 4, 2014.

# How to create a colour education that fosters price-winning design students

Ivar JUNG

Department of Design, Linnaeus University, Sweden

## ABSTRACT

This paper has the objective to describe a price-winning approach to colour education. The colour education of today is an important building block for all future design. If we can provide our students with state of the art colour education we will get the best future design when it comes to the use of colours. That will include all kinds of design e.g. graphic design, architecture and product design.

In 2014 there was a national competition called *Prisad Färg* (Award-winning Colour) organized by Swedish Colour Centre Foundation that celebrated its 50 years anniversary. The competition was open to all students of design, architecture, fine art, graphic design and advertisement. Design students from the product design programme at the Linnaeus University won no less than two out of three awards.

The subject of colour is introduced very early in the programme. Students of product design have two weeks of colour theory and workshops in their first semester. In this basic theoretical course the students get to know different colour systems and the advantage of using systems to think, visualise and communicate colour. In the workshops they can train their eyes and skills in mixing and combining colours with different amount of complexity. The workshop ends with a task where students explore the colour language in different contexts and cultures. This lays a ground for four more weeks of colour projects with a exploratory approach. The students phrase their own colour questions and seek answers through research and visual colour representations. In the second year students progress to understanding different contexts of colour. The students continue with light theory and light projects for five more weeks and then proceed with light and colour in space contexts for another five weeks. The three-fold strategy: early introduction, emphasis on colour and continuous progression, has proved to be successful.

## 1. INTRODUCTION

Colour education is not a priority issue for the main part of Swedish design and architectural education. The competition, *Awarded-winning colour*, was in itself an attempt to emphasize the importance of colour education on a university level as a seed for advanced future colour design and colour research.

To express yourself you need a language. Colour is an important part of the language of visual communication. It is used more or less consciously in the fields of art, design, architecture and visual media. If we regard colour as a media for communication we need to provide our design students with the best tools for using that language. The more skilled the students are in the language of colour, the more they use it and also dare to make advanced colour design. An uncertain and unskilled designer tend to use only "safe" colours and colour combinations and can not use the variety of possibilities in the language of colour to create an excellent design.

## 2. SYSTEMATIC COLOUR EDUCATION

The aim of colour education at the product design BA programme at Linnaeus University, Sweden is to provide the students with skills to concisely use colour as a tool to make a more efficient design.

To discuss colours students normally use our everyday language and use traditional colour names. However, in order to engage in a professional discussion about colours the spoken language has to be complemented with an efficient and precise vocabulary. Therefore one of the first steps is to provide the students with a common language regarding colours. At Linnaeus University, we have found the NCS colour system (Hård et al 1996) a helpful tool for communication about colour and colour combinations. One of the great advantages with this system is that it allows students to visualise the relations between colours in a visual system consisting of the colour wheel and colour triangles. The same basic structure is also found in other colour systems as e.g. Munsell. NCS is also useful for the students to discover that the naming of colours regarding hue, and perceived amount of blackness, chromaticness and whiteness is a tool for making cognizant colour combinations.

The students learn that there is a variety of different colour systems used for different purposes and in alternative contexts. They learn about Munsell, Pantone, CIELab, CMYK, RGB and how they are related. The main language used in the learning program is the NCS system, mainly because it is clearly based on human perception, easy to understand for students and easily communicated. The design students appreciate the visual representation, which helps them to work with colours in a systematic way.

The foundation of understanding of colour systems makes it is easier for students to proceed to understand different theories regarding colour combinations. The students explore in theory and practice different principles of colour combinations such as complementary colours, likeness and contrasts regarding chromaticness, hue, blackness and whiteness. The students make colour combinations of increasing complexity in workshops and write down their analyses and reflections. At first they have to make their colour work physical with gouache and acrylic colours to give the students a sense of the colour pigments and materiality of colour. The next step is to explore the possibilities of working with colour in the digital world in different computer programmes.


## 3. COLOUR AND CULTURE

To explore the language of colour the students, on their second week of colour education, are given sixteen different words such as "warm", "cold", "young", "old" that they are asked to express with colour chords consisting of three chosen colours in a given form. This can be compared with a musical chord consisting of three notes. The colour chords are organized on the wall in groups where all chords made from one of the words are clustered together. In this way it is possible to see if there is a common colour language for those words (Figure1). The result is that certain words have a clear likeness when it comes to the chosen colours, while other words have a wider variety. This is a good opportunity for starting a discussion and exploring if there is such a thing as a common colour language and to what extent it is primarily cultural, contextual or individual. To explore these matters the students have to research the use of colours in different contexts, such as art, design, packaging, architecture and visual communication. They also look into the use of colours in different parts of the world, in different cultures and in different historical

contexts. This gives a broad understanding of the use of colours and colour combinations in different cultural contexts.



*Figure 2: Students analysing their colour chords from different words*

The three-week-long theoretical and practical block evokes new questions for the students. These are channelled into an individual research question that the student will explore theoretically and practically for further three weeks. The result is presented to the group and also documented in an individual workbook where the teachers can follow the students individual work process, which includes reflections and further questions raised during the project.

## 4. LIGHT AND SPACE

In the second year the students are supposed to gain a deeper understanding of the perceived colour in relation to light and space. Students explore/observe their perception of colour in different environments and spaces and systematically write down and discuss their observations. The students learn how the perceived colour changes under the influence of different light and spatial conditions. The students build models where they make experiments with light and colours. They also make full-scale experiments with different light sources and different lighting design before they make their own design of a lamp and build it as a functioning prototype. This creates knowledge of the complexity of the relation between perceived colour and the contexts. The basic theory can be found in books but students also need to explore and see how colours in light and space are really perceived and experienced in the real context, to be able to have a full understanding of the impression of light and space on colours.

AIC2015 TOKYO - Color and Image

To ensure that the students will practice and use their colour skills throughout their entire study period they are asked to present and motivate the chosen colours in every project they do. That helps them always remember that the aspects of colour are as important as any other design aspect when it comes to the visual expression.

## 5. COLOUR RESEARCH

It is important to connect the colour education to current colour research. In the library the students can find literature with colour research to inspire them and inform them, but the students are also used as subjects in various colour studies, both in the lecturers' own projects and in studies carried out by researchers from other universities. In one of the design department's own research studies, 20 students compared perceived colours in glass with 1950 NCS opaque colour charts (Figure 2) and also with NCS colour charts on a computer screen (JUNG et al 2011). In another international linguistic study, 20 students participated and listed Swedish colour names to be compared to colour names in ten other languages. This student participation creates an interest and understanding of colour research. It also shows the dignity and variety of the field of colour. Participation points out the possibility for a future career in research, which may be about questions identified during their colour education that have not yet been answered.
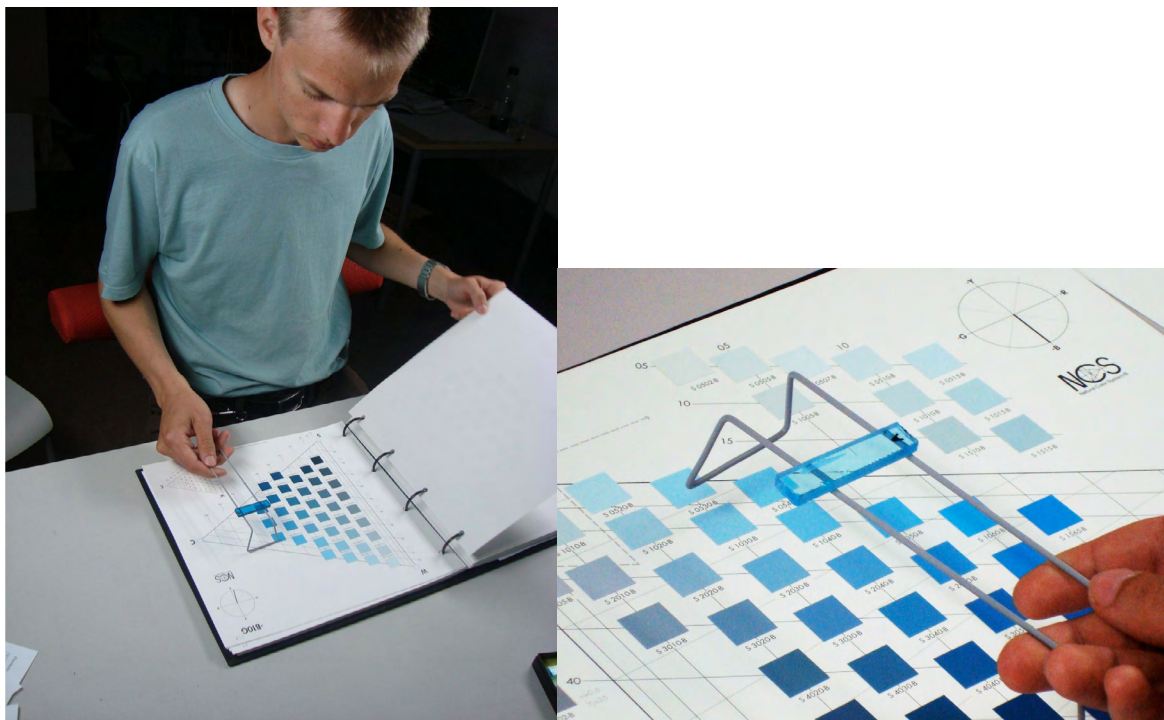


*Figure 2: Student participating in research study, perceived colour in glass.*

## 6. CONCLUSIONS

It is essential to introduce colour at an early stage of the BA programme. This means that the students are considering colour as a part of their design and a part of the visual expression. If not introduced early, colour will just be something added to the design at the end and not an integrated part of the design process. Students have different skills and levels of experiences when it comes to colour when they arrive on the programme. This emphasises the need for learning and practicing a colour system, which can be a language that helps the student to think about and communicate colour in a precise way. The introduction of colour systems in general and NCS in particular creates a possibility for students to visualise and understand the relations between colours in their future work. The conclusion is that it is the clear strategy for colour education that is repeatedly implemented throughout the entire programme that fosters award-winning students.

## REFERENCES

Bimler, D. L., M. Uusküla 2014, *The map is the itinerary: Cognitive color space reconstructed from listing data for 11 European languages Perception* **43** ECVP Abstract Supplement, page 68.

Hård, A., L. Sivik and G. Tonnquist. 1996a. NCS, Natural Color System – from Concept to Research and Applications. Part I. *COLOR research and application* 21(3): 180-205.

Hård, A., L. Sivik and G. Tonnquist. 1996b. NCS, Natural Color System – from Concept to Research and Applications. Part II. *COLOR research and application* 21(3): 206-220.

Jung, I., P. Jokela, P. Brandt, and O. Victor. 2012. *What is the colour of a glass of wine? Color in food: Technological and Psychophysical Aspects*. Boca Raton: CRC Press. 35-41.

Jung, I., P. Jokela, P. Brandt, and O. Victor. 2011. *Percieved colour in transparent materials and objects*. In *AIC 2011 Interaction of Colour & Light in the Arts and Sciences, Midterm Meeting of the International Colour Association, Zurich, Switzerland, 7–10 June 2011: Conference Proceedings, CD,* edited by Verena M. Schindler and Stephan Cuber. Zurich: pro/colore, 2011.

*Address: Senior lecturer Ivar JUNG, Department of Design,*
*Linnaeus University, S-391 82 Kalmar, SWEDEN*
*E-mail: ivar.jung@lnu.se*

# INFLUENCE OF ODORS FUNCTION AND COLORS SYMBOLISM IN ODOR-COLOR ASSOCIATIONS: COMPARATIVE STUDY BETWEEN RURAL AND URBAN REGIONS IN LEBANON

Léa NEHMÉ[1], Reine BARBAR[2], Yelena MARIC[3] and Muriel JACQUOT[4]

[1]LIBio (Laboratoire d'Ingénierie des Biomolécules), Université de Lorraine, 2 avenue de la Forêtde Haye, BP 172, 54505 Vandoeuvre-lès-Nancy, France.
[2]Departement of Food Science, Faculty of Agricultural and Food Sciences, Holy Spirit University of Kaslik, Lebanon, P.O.BOX 446, Jounieh, Lebanon
[3]myrissi, 24-30 rue Lionnois, BP 60120, 54003 Nancy Cedex
[4]Innovative Crossmodal Interactions Modeling (InnoCIM), ENSAIA, Université de Lorraine, 2 av. de la Forêt de Haye, 54500 Vandoeuvre-lès-Nancy, France

## ABSTRACT

The purpose of this study was to assess the intra-cultural impact on the relationship between odor and color on one hand, and on the parameters of the smell on the other hand, within the same country, Lebanon, unlike the preliminary studies that evaluated the cultural effect between two different countries. To assesss this intra-cultural effect, sensory analyzes were performed on 200 subjects in two campus of the Holy Spirit University: two regions were considered, Zahleh campus representing the rural community, and Kaslik campus representing the urban community. The experiment was based on a set of 24 odors, some of them are internationally recognized, others nationally, and some of them are mainly recognized in the rural area. Statistical analyzes revealed anintra-cultural impact, given the existence of significant differences for some odors: shallots score the biggest difference, where it is more recognized in the urban area and more familiar, and they link it to brown color while at Zahleh it is linked to black color. Caramel, smoke, orange blossom, molasses and *Jellab* (the last two being purely national odors) also show significant differences in color choice between the two regions. Similarly, scores of familiarity, of intensity, pleasantness and edibility indicate some differences for few odors. These sensory analyzes have shown for the first time in Lebanon the impact of habits, environment and lifestyle on the relationship between odor and color, between rural and urban areas.

## 1. INTRODUCTION

According to UNICEF (2012) the definition of 'urban' varies from country to country, and, with periodic reclassification, can also vary within one country over time, making direct comparisons difficult. An urban area can be defined by one or more of the following: administrative criteria or political boundaries (e.g., area within the jurisdiction of a municipality or town committee), a threshold population size (where the minimum for an urban settlement is typically in the region of 2,000 people, although this varies globally between 200 and 50,000), population density, economic function (e.g., where a significant majority of the population is not primarily engaged in agriculture, or where there is surplus employment) or the presence of urban characteristics (e.g., paved streets, electric lighting, sewerage). The task of defining urban population has always been particularly challenging. The United Nations itself recognizes the difficulty of defining urban areas globally, stating that, "because of national differences in the characteristics that distinguish urban from rural

areas, the distinction between urban and rural population is not amenable to a single definition that would be applicable to all countries" (UN, 1998). Rural areas are usually defined as "what is not urban" (UN, 1998 and 2004), and so inconsistencies in the definition of what is urban lead to inconsistencies in characterizing what is rural. In Lebanon , Kaslik area is considered as urban, due to the fact that the definition given by the UNICEF for urban cities is applicable on it. While Zahleh is considered as rural.

Crossmodal correspondence is one of the terms that have been used to describe the tendency that people have to associate certain features, or stimuli across the senses (Spence, 2011).

Throughout the years the relationship established between different senses attracted the attention of researchers, in particular the relationship between vision and hearing. While the intermodal correspondence between vision and olfaction has been less studied, it has been proven that this relation is consistent and durable. Various studies highlighted those facts: subjects noted the same results when the same sensory analysis were repeated after two years (Wada *et al.,*2012 ; Maric & Jacquot, 2013).

Previous studies showed that people tend to match basic tastes with a host of other non gustatory stimuli such as color (Spence *et al.,* 2010) or shapes (Spence and Deroy, 2014). On the other hand growing number of studies started to investigate cross-cultural differences in the way in which people match gustatory information with non gustatory ones. For instance, Levitan *et al.* (2014)investigated color-odor association between 6 different cultural groups. While Velasco *et al.* (2014) studied the color-flavor association between 3 different countries.  Wan *et al.* (2014) showed cross-cultural differences in crossmodal correspondences between basic tastes and visual features between 4 countries.Maric *et al.*investigated in 2012 cross cultural differences between Lebanese and French populations.

These cross cultural studies have been carried out from two points of views: to understand cultural differences in food acceptance and preference (Yeh *et al.,* 1998) and to evaluate the effect of individual experience and knowledge of odors and colors, on odor and color perception, in order to understand how olfactory stimuli or visual stimuli influence psychology and behavior (Hudson & Distel, 2002). But while these studies evaluated the cross-cultural differences, rare are the studies focusing on the differences in one culture (one country).

The aim of the present study is to focus on the intra-cultural effect within the same country, Lebanon. The intra-cultural differences related to habits, environment and lifestyle between Zahleh (rural area) on one side and the urban area Kaslik on the other, were investigated in orderto analyze their impact on the odor-color association, on familiarity, pleasantness and edibility. The effect of the geographic area of residence can stimulate potential differences between the perception of the color-odor relationship among those residents in rural and urban areas in Lebanon.

## 2. METHOD

### 2.1 Sample Preparation

*Participants:*

Two hundred participants, aged between 18 and 60 years were recruited for these experiments, 100 from the rural area of Bekaa and 100 from the urban area of Kaslik in Lebanon.For the coastal region of Kaslik, subjects were either students or employees of the Holy Spirit University of Kaslik. In Zahleh participants were either students or residents of the region of Zahleh. Taking into consideration the differences between residents in both areas: Zahleh residents usually live, study and work in Zahleh so they are practically growing on the rural traditions of their area, where they are more engaged in agriculture and more familiar with the Lebanese "*mouneh*", which is a Lebanese word used to describe the fact of preserving food. *Mouneh* is prepared during the summer months in order to be consumed during the harsh days of winter. The main purpose is to transform foods that perish into foods with long shelf life, durable, lasting throughout a whole season. While Kaslik citizens are less familiar with these traditions.All subjects were naive about the stimuli. It was recommended not to wear perfume on the day of the experiment nor to eat or drink coffee 30 minutes before the session.The subjects were also tested for abnormalities of vision using the Ishihara test.

*Olfactory Stimuli:*

18 natural food and floral odors were chosen as olfactory stimuli. Our selection aimed firstly, to cover a wide variety of odors related to food and drinks, and secondly, to raise the intra-cultural differences of the same color-odor association for national aromas. To evaluate the level of the relationship between odors and colors, we chose two similar odors (peppermint*vs.* chlorophyll; lime *vs.* lemon).All odors were presented in a single aromatic intensity, except for the smell of plum (yellow fruit Mirabelle, specialty of the French Lorraine region), which was presented twice, with two different intensities. The samples were preparedby injecting 1 ml of each odor in a small piece of cotton placed in a little opaque glass vial. No visual factor was therefore present.

The samples were identified by three-digit codes and refrigerated between each two sessions. Samples were placed at room temperature 15 minutes before the analysis.The samples of international odors (rose, violet, orange blossom, lavender, cucumber, wild strawberry, lime, lemon, pineapple, smoked, shallot, caramel, chlorophyll, peppermint, mirabelle (high intensity), mirabelle (low intensity)) were purchased from the laboratories Mathé (Maxville, France), using the corresponding essential oils, while the two national odors (pomegranate molasses, *jellab*) were prepared in the Holy Spirit University of Kaslik campus. They were purchased directly from the products of the market (Kasatlé Chtoura brand).

*Visual stimuli:*

24 different color patches (4cm in diameter) were presented in a color chart. This color chart consisted of a white A3 size page containing twenty-one color patches arranged in circle from red to purple, and three achromatic colors (white, grey, black) presented separately in the lower left corner. Each color patch was identified by a code (one capital letter and one figure). Color charts were printed on coated paper. The print was calibrated to ensure consistent colors between participants. L*a*b coordinates were measured for each color chip by means of a Datacolor system (Pantone® ColorVision™ Spyder Master Suite Spectro), and converted in L*C*H* (Lightness, Chroma, Hue) coordinates, to get the exact position in the CIELAB color space (Figure 1).
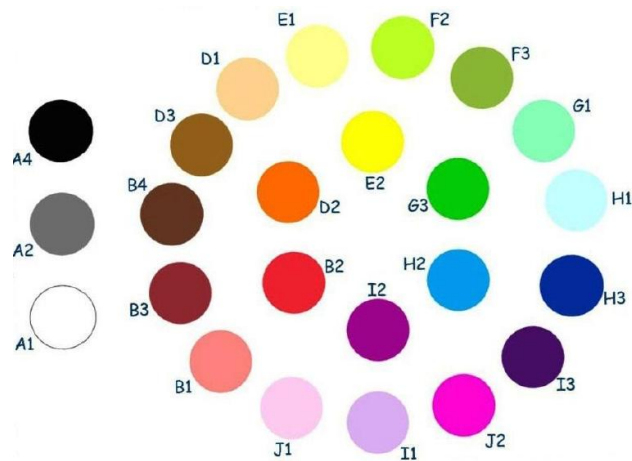
*Figure 1:the color chart used in sensory analysis*

## 2.2 Experimental Procedure

*Task location and procedure:*

In each area, sessions were conducted in sensory testing facilities with separated booths. Each testing booth had white walls and standardized white light source. After completing the Ishihara Color Vision test, each subject was presented with the olfactory stimuli in a random order, and with the color chart. For each olfactory stimulus, participants were asked to open the glass bottle and smell its content orthonasally. Afterwards, participants were instructed to select among the 24 color patches one color that they felt closely matched the odor. After having made their choice, they rated the difficulty of odor-color association and the odor perceived intensity, familiarity, pleasantness, and edibility. Participants were not required to name the odors they smelled.

*Data analysis:*

All data were processed by SPSS 16.

## 3. RESULTS AND DISCUSSION

### 3.1 Relation between odor and color

**Choice of color for each odor:**

The results revealed that the participants of each area did not choose colors uniformly but rather tended to choose some colors over others when matching the odors. Indeed, all 18 olfactory stimuli led to significant preferences in the choice of color ($p < .05$ in all cases) in both areas.

Among the odors tested for the study, six indicated a significant difference in the choice of a color for a specific odor, between the two areas of Kaslik and Zahleh: caramel ($p=0.04<0.05$), shallot ($p=0.00<0.05$), orange blossom($p=0.00<0.05$),smoked ($p=0.01<0.05$), pomegranate molasses ($p=0.035<0.05$) and *jellab* ($p=0.036<0.05$).

For both Zahleh and Kaslik residentswe could note that the participants have registered in their majority the light brown color (or honey-color) as being the color of caramel but the difference lies in the choice of both purple and yellow color in Kaslik and brown color in Zahleh (Khi-Square=29.78, dl=21, p= 0.04<0.05)

Shallot registered a significant difference (Khi-Square= 39.36, dl=17, p=0.00<0.05) in the choice of associated colors between Zahleh and Kaslik. Zahleh residents tend to choose black and grey colors while Kaslik residents tend to choose the browncolor.

Orange blossom registered a significant difference (Khi-Square= 46.88, dl=23, p=0.00<0.05) in the choice of odors among both areas (Figure 2). So there is a relationship between the choice of color for orange blossom odor and the regions (urban *vs.* rural) where participants of the urban area of Kaslik have chosen in their majority the white color and more frequently the color pink, whereas in Zahleh the majority chose pink and gray colors.
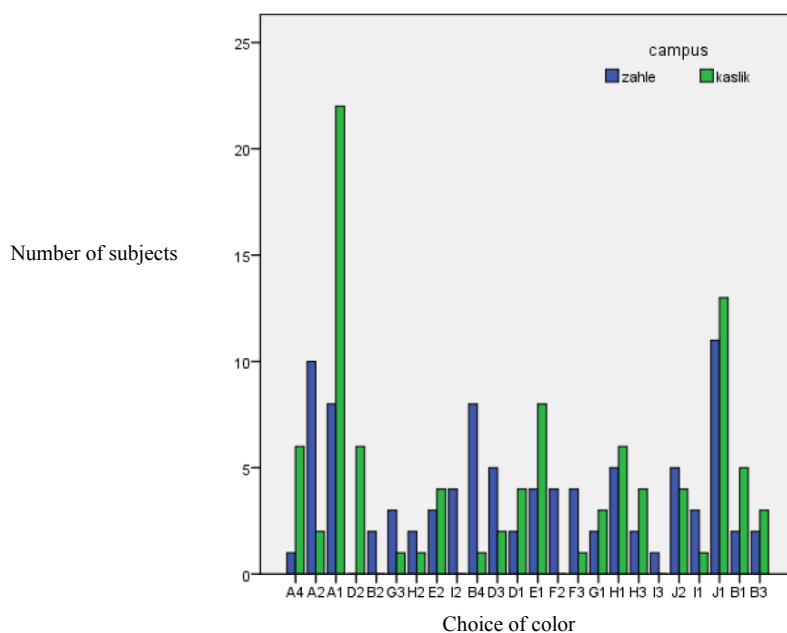


*Figure 2:Graph representing the difference in the choice of color for the smell of orange blossom between Zahle and Kaslik*

Smoke odor indicated a significant difference between the twolocations and the choice of color (Khi-Square= 34.11, dl=19, p=0.01<0.05). The most dominant color given by subjects of Kaslik is brown while in Zahleh the choice of color is more diversified tending to black and gray.

Pomegranate molasses recorded a significant difference (Khi-Square= 33.25, dl=22, p= 0.035<0.05). Zahleh subjects selected the color brown while Kaslik citizens selected in their majority the white color followed by the light pink.

*Jellab* displayed a significant difference (Khi-Square= 33.521, dl=23, p=0.036<0.05). The majority of participants in urban area of Kaslik selected the white color. While the participants of Zahleh selected pink, purple and red colors.


**Difficulty of associating a color with an odor in the two areas:**

Three odors registered difficulty of association with a color. They revealed a significant difference between the difficulty of association and the two areas: Pineapple; Peppermint; Chlorophyll.

AIC2015 TOKYO - Color and Image

Participants of Kaslik area found it more difficult (than Zahleh participants) to associate a color for these 3 odor samples: Pineapple (Khi-Square= 4.554, dl=1, p=0.033<0.05), peppermint (Khi-Square=3.910, dl=1, p=0.048<0.05) and chlorophyll (Khi-Square=3.910, dl=1, p=0.048<0.05).

## 3.2 Odor Parameters

**Odor intensity :**

The only significant difference was found for the odor of cucumber. Data analysis indicates that the mean intensity chosen by participants in Zahleh area is 5.60, superior to the mean in Kaslik which is 4.03. Moreover, the difference between the two regions is significant. So there is a relationship between the region and the average intensity detected for cucumber odor.

**Odor familiarity:**

Among the odors, data analysis detected significant differences in odor familiarity between Zahleh and Kaslik for 4 odor samples: Shallot, smoked, *jellab* and mirabelle (high intensity).

The mean value of familiarity parameter of shallot for Zahleh is 5.77 which is inferior to Kaslik (7.05). And there is a significant difference between the 2 areas (t-test= -2.163, dl=192, p=0.031<0.05) which indicates that Kaslik citizens tend to find shallot odor more familiar than Zahleh participants.

The mean value of familiarity score for smoked odor in Zahleh is 6.44 inferior than the mean in Kaslik (7.81). In addition, there is a significant difference between the two regions (t-test= -2.32, dl= 184, p=0.021<0.05). Therefore there is a relation between the area and the familiarity for the smoked odor. Kaslik participants found smoked odor familiar while in Zahleh the answers were heterogenic, some participants found it familiar while others did not.

*Jellab* odor shows a mean value of familiarity of 6.90 in Zahleh and of 5.62 in Kaslik with a significant difference (t-test= 2.338, dl= 188, p= 0.020<0.05). Residents in Zahleh found*jellab* odor more familiar than those living in Kaslik.

Mirabelle (high intensity) registered a mean familiarity score of 6.62 in Zahleh and of 7.68 in Kaslik. In addition significant difference was found between familiarity and area (t-test= -2.075, dl= 189, p= 0.039<0.05). Mirabelle (high intensity) was found to be more familiar in Kaslik.

**Odor pleasantness :**

Shallot registered the only significant difference among the 2 regions (t-test= -2.806, dl=186, p=0.038<0.05). Data analysis recorded a mean value for pleasantness for Zahleh residents (1.93) inferior to Kaslik (2.95). Kaslik citizens registered shallot odor as more pleasant.

**Odor edibility:**

Four odorsscored a significant difference between Zahleh and Kaslik concerning their edibility: shallot, rose, lime and mirabelle (low intensity).

The difference between the two variables, area and odor edibility for shallot was registered as significant (Khi-Square= 5.602, dl=1, p= 0.018<0.05). That indicates the presence of a

relation between odor edibility and area of living. Kaslik residents still finds it more edible than Zahleh residents.

Rose odor samples registered a significant difference between the two variables area of living and odor edibility (Khi-Square=7.681, dl=1, p=0.0006<0.05). Both areas tend to describe it as edible. But Kaslik residents tend to find it more edible than Zahleh participants.

Significant difference was found in lime odor between the two variable odor edibility and area of living (Khi-Square=4.638, dl =1, p= 0.031<0.05). Both regions tend to consider lime odor as edible but Kaslik residents describe it as more edible than Zahleh residents.

The difference between odor edibility and region for mirabelle (low intensity) was found to be significant (Khi-Square=4.058, dl=1, p=0.034<0.05). Both regions tend to describe it as edible, but Kaslik residents tend to describe it as more edible.


## 3.3 General discussion

Among the 18 odor samples used in this study, shallot odor revealed the most striking difference between Kaslik and Zahleh. Residents of urban area (Kaslik) find shallot odor familiar, more pleasant, more edible and link it to brown color in comparison with Zahleh residents who linked it to black color. This could be due to the fact that shallot is usuallymore planted and consumed in urban areas, because it is sensitive to cold weather and need warm weather to grow. Therefore Kaslik residents find it more familiar and pleasantthan Zahleh residents which explain their choice of the black color.

In their study, Maric, Barbar and Jacquot (2012) found a significant difference between Lebanese and French participants in the attribution of a color to orange blossom odor.In Lebanon, orange blossom is associated to traditional Lebanese desserts and sugar pastries products, with color associations of white and pink.In France, this odor is more associated with hygiene products justifying the shades of bluechosen by the participants, typical color for non-food items. According to their study culture-dependent experiences affect our capacity to use, identify, like and consume odors. Thus odor-color associations can be similar or different among countries. When we recognize odors that seem familiar, semantic association is made upon the choice of colors. Even if subject is not able to identify exactly an odor, he might still beable to categorize it, for example, as a floral or fruity odor, edibleor non-edible odor.Both usage and association models affect odor-color associations revealing the complexity and multi-dimensional aspects of this linkage. In Lebanon orange blossom registered a significant difference between the residents of rural and urban areas, rural residents attributed first pink color followed by grey color, while urban residents attributed white color followed by pink color. Orange blossom is widely used in the Lebanese food, specifically pastries. The color of its extract is light pink color, which explain the use of the pink color in both areas. Orange blossom is used as well as a beverage mainly in urban areas, it is called by the Lebanese white coffee (café blanc) which can explain the choice of white color by Kaslik residents. The choice of grey color in Zahleh is due to its use in case of faintings to awaken people up. This relation with an unpleasant event justifies the choice of the grey achromatic color.

Smoked odor registered a significant difference as well in the choice of colors: Zahleh residents attributed to it the brown color for reminding them of the barbecue odor, while Kaslik residents associated it to black color for reminding them the pesticide odor and fuel combustion odor.

For the caramel smell almost the same odors were selected, but the difference lies in the fact that at Kaslik, 10 participants from 97 noted a clear purple color for caramel. Fact that has not been registered for Zahleh participants. Choosing clear purple color for caramel by Kaslik residents could be as a result of the use of the caramel flavor in sweets and candies, that are colourful and exist in urban areas supermarkets and rarely at the small stores of rural areas.

For national odors (*jellab* and pomegranate molasses) rural residents were able to detect easily these odors in comparison with urban residents. Due to the fact that these products are mainly produced in the Lebanese mountains, where the residents following the traditions prepare grapes, dates and pomegranate syrups to use them during winter and the cold season, when these fruits are rarely present. And they include them as well in food: *jellab* is usually drank during the fasting period and pomegranate molasses are used in Lebanese dishes like *fattouch*.

Concerning the rest of the odor samples, interesting remarks could be made. For chlorophyll odor, participants in urban area tend to link it with white color or light green for it reminds them of mint flavoured chewing-gum. While in Zahleh participants linked it to green color for it reminds them ofmint plants that areusually widely planted in the Lebanese mountains.

What seemed obvious was the difficulty that the subjects had in trying to connote a precise color to an odor,without guessing the origin of this aroma.Indeed, all subjects were trying to guess the smell, to imagine the object, then to link it to a specific colorwhich is consistent with the results of Morrot, Brochet & Dubourdieu study (2001).For odors they have not recognized, they scored directly "yes" to the question of the difficulty of association. For example, it was difficult to connote a color to the smell of peppermint and the smell of mint chlorophyll in both regions, but this was more acute for the region of Zahleh (rural), taking into consideration that both of these smells are extremely known in urban areas, because of their use in candies, food, gums and even fragrance and detergent. It wasn't the case for the smell of ananas that registered a difficulty of association to a color in both regions but was more common in Kaslik.

The smell of wild strawberry reminded participants in both rural and urban areas, the smell of *shisha* or Lebanese *hookah*, which explain the choice of both purple and red colors given that tobacco used to prepare the shisha is red colored.

In addition participants detected unpleasant odors faster than pleasant ones. It has been noticed that participants disliking an odor detected it easily when these odors where in some cases undetectable by other participants.

On the other hand molasses, registered lower rate of pleasantness in Zahleh, while familiarity rate was higher than in Kaslik, and the color chosen by the majority is dark brown, more appropriate than the white color given by the subjects in Kaslik. A question arises here, why residents of the rural area would note a low rate of pleasantness for molasses while it is used in their daily culinary traditions dishes. Let us not forget, however, that the samples of the two national odors, *jellab* and molasses, have not been taken from essential oil extract, but they were prepared directly from the product of the market, which is why after having opened the sample several times, the smell had become so slight that some subjects had difficulties to detect it. Always talking about the intensity of the odor,we noticed a significant difference in the score of intensity for the smell of cucumber, it was noted more intense in Zahleh.

Concerning edibility rates, subjects that could not detect the odor noted it directly as non-edible. Rose and lime odors were considered more edible, more familiar and more pleasant in Kaslik. This indicates a linear relation between edibility and pleasantness. The more the odor is edible, the more it is considered as pleasant.

One of the hypotheses that could explain these observations is that the residents of the rural area recognize more easily the smell of flowers. Due to the fact that it reminds them of gardening and green space in their area, while subjects living in the urban area recognize the smell of flowers as an ingredient used in pastries, gum and food products in the market.

## 4. CONCLUSIONS

The purpose of the present study was to evaluate the intra-cultural effect on the relation between odor and color. Past studies highlighted cross cultural effects on odor-color associations, where according to Maric, Barbar and Jacquot (2012) the construction of odor- color correspondences proved to be culture-dependent: If participants of different countries, have the same usage purpose for a product they will associate it to similar colors. If not, significant differences will be revealed as it was the case for orange blossom.

The present study aims to emphasize the intra-cultural effect within the same country. The Lebanese residents tend to have different color-odor association between rural and urban area. Taking into consideration that Lebanon is a small country of 10452 km$^2$ the current study proved the effect of culture, not only internationally but also within the same country,in terms of environment, intra-cultural and culinary habits and ease of access to more local productions,on the relation between odor and color, and its effect on odor parameters.

## REFERENCES

Hudson, R., and Distel, H. 2002. The individuality of odor perception. In Rouby, C., Schaal, D., Dubois, D., Gervais, R., and Holley, A. (Eds.), *Olfaction, taste and cognition, Cambridge*, London: Cambridge Press.

Levitan, C., Ren, J., Woods, A., Boesveldt, S., Chan, J., McKenzie, K., Dodson, M., Levin, J., Leong, C., and Van den Bosch, J. 2014. Cross-Cultural Color-Odor Associations. Available online at Plosone, http://journals.plos.org/plosone/article?id=10.1371/journal.pone.0101651.

Maric, Y., and Jacquot, M. 2013. Contribution to understanding odour-color associations. *Food Quality and Preference* 27: 191-195.

Maric, Y., Barbar, R., and Jacquot, M. 2012. As pink as an orange blossom odour: a French-Lebanese cross-cultural study. In *AIC Color 2012*, Proceedings, Interim Meeting of the International Colour Association.

Morrot, G., Brochet, F., Doubourdieu, D. 2001. The Color of Odors. *Brain and Language* 79: 309-320.

Spence, C. 2011. Crossmodal correspondences: A tutorial review.*Attention, Perception & Psychophysics* 73: 971-995.

Spence, C., and Deroy, O. 2014. Tasting shapes: A review of four hypothesis. *Theoria Historia Scientiarum* 10: 207-238.

Spence, C., Levitan, C.A., Shankar, M. U., and Zampini, M. 2010. Does Food Color Influence Taste and Flavor Perception in Humans? *Chemosensory Perception* 3: 68–84.

UNICEF. 2012. available at http://www.unicef.org/sowc2012/pdfs/SOWC-2012-DEFINITIONS.pdf

United Nations. 1998. *Principles and Recommendations for Population and Housing Censuses*. Revision 1. Series M, No. 67, Rev. 1 (United Nations publication, Sales No. E.98.XVII.8).

United Nations. 2004. World *Urbanization Prospects, the 2003 Revision*. United Nations Publication sales No. E.04.XIII.6


Velasco, C., Wan, X., Salgado-Montejo, A., Woods, A., Onate, G., Mu, B., and Spence, C. 2014. The context of color-flavor associations in crisps packaging: a cross cultural study comparing Chinese, Colombian, and British consumers. *Food Quality Preference* 38: 49-57.

Wada, Y., Inada, Y., Yang, J., Kunieda, S., Masuda, T., Kimura, A., Kanazawa, S. and Yamaguchi, M.K. 2012. Infant visual preference for fruit enhanced by congruent in-season odor. *Appetite*58: 1070-1075.

Wan, X., Velasco, C., Michel, M., Mu, B., Woods, A.T., and Spence, C. 2014. Does the shape of the glass influence the cross modal association between color and flavor ? A cross cultural comparison. *Flavor* 3: 3.

Yeh, L.L., Kim, K.O., Chompreeda, P., Rimkeeree, H., Yau, N.J.N., and Lundahl, D.S. 1998. Comparison in use of the 9-point hedonic scale between Americans, Chinese, Koreans, and Thai. *Food Quality and Preference* 9: 413-419.

# Differences of generation dependences of preferences between colors and styles in women's fashion

Chie MURAKI ASANO[1*], Kanae TSUJIMOTO[1], Akira ASANO[2], Katsunori OKAJIMA[3]
[1]Faculty of Human Ecology, Yasuda Women's University
[2]Faculty of Informatics, Kansai University
[3]Faculty of Environment and Information Sciences, Yokohama National University

## ABSTRACT

This research investigates generation dependence of preferences in fashion, and shows differences of dependences between colors and styles of dresses. It has been assumed that the tendency of age independence is found not only in the fashion-style but also in the color preference of fashion. In this paper, we investigated the preference of twenties students and their mothers, who are generally forties, in the fashion-style and color of fashion. As a result, a significant difference was confirmed in the fashion style between the student generation and the mother generation, especially in the taste of characteristic parts. However, the tendency of color preferences are found different from what have been assumed; Although it has been usually believed that elderly women prefer dark and dull colors, young students also preferred dark colors, while their mothers preferred dull colors to dark tone, according to our surveys for winter cloths. The mothers also preferred bright colors, especially in summer cloths, similarly to young students.

## 1. INTRODUCTION

It has been widely accepted that the preference of colors in fashion is different by the age group (Beke et al., 2008). However, it is said that the preference in fashion of forties' women has recently become less different from it of twenties. The fashion trends and their transitions were clear and charismatic leaders of fashions appeared successively in 1970s and 80s, when the forties' women were young. On the contrary, there are a lot of fashion trends simultaneously, and main stream of fashion trends in the whole society and their transitions are unclear in the 21st century. It may be the reason why the preferences have become less different between forties' and twenties' women.

It has been assumed the tendency of age independence is found not only in the fashion-style but also in the color preference of fashion. In this paper, we investigates the preference of twenties students and their mothers, who are generally forties, in the fashion-style and color of fashion. It examines precisely what kind of the preferences has really become less different. The research will be utilized for marketing in fashion industries.

As a result, a significant difference was confirmed in the fashion style between the student generation and the mother generation, especially in the taste of characteristic parts. However, it was shown that any significant difference was not confirmed in the color preferences, although some difference was observed. It has been usually said that elderly women prefer dark and dull colors, however, according to our surveys, young students also preferred
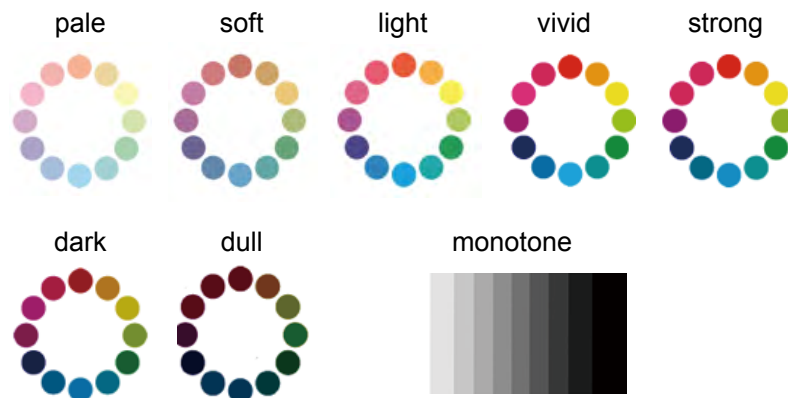
---

*Fig. 1. Example of hue circle for each tone.*

monochromes, especially in autumn-winter dresses. Mothers group also preferred bright colors, especially in spring-summer ones, similarly to the young students.

## 2. METHODS

The participants of our survey were 200 female university students and 60 of their mothers in Japan. We made a questionnaire on the preferences of colors and styles of dresses. The questionnaire sheet was written in Japanese.

Preferences of colors were surveyed not by selecting hues but by selecting from the following words indicating tones in the PCCS color system: pale, soft, light, vivid, strong, dark, and dull tones, and monotone. This is because it has been assumed that the generation dependence of color preferences is mainly on vividness or dullness and the target of our survey is confirming this assumption (Baucom and Grosch, 1996). Preferences of hues depend higher on each person than on generations. The example of the hue circle for each tone was presented on the questionnaire sheet, as shown in Fig. 1.

Preferences of styles were also surveyed on the details of the tops and the bottoms, e.g. shapes and lengths of skirts, sleeve lengths, etc. These style were explained by illustrations on the questionnaire sheet. Preferences on spring-summer and autumn-winter dresses were separately surveyed.

## 3. RESULTS AND DISCUSSION

We show the results of the surveys for preferences of styles and colors by young women and their mothers. For the sake of the limitation of paper length, some parts of styles showing significant generation differences are selected.

### 3.1 Materials

We surveyed preferences of materials, selected from cotton, hemp, wool, silk, cupra, rayon, tencel, nylon, polyester, and acrylic fibers, which are usually used for textiles. Each respondent selected one material from the list for each of summer and winter cloths. Figures 2(a) and (b) show the preferences in summer and winter cloths, respectively. Figure 2(a) indicates that hemp is preferred by young women to their mothers for summer cloths, while cotton is preferred by the mothers to the young women. It may be because hemp is difficult to handle
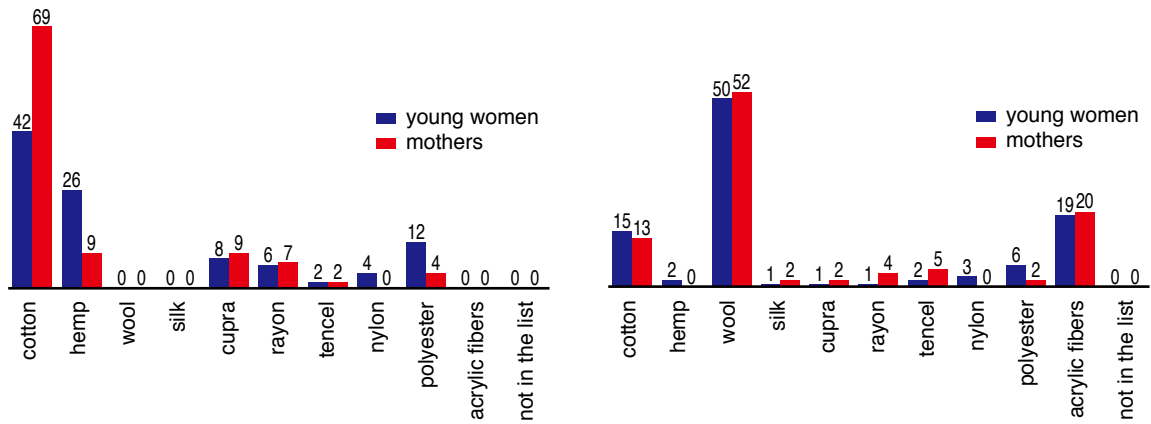
(a) summer cloths.       (b) winter cloths.

Fig. 2. Preferences of materials (%).
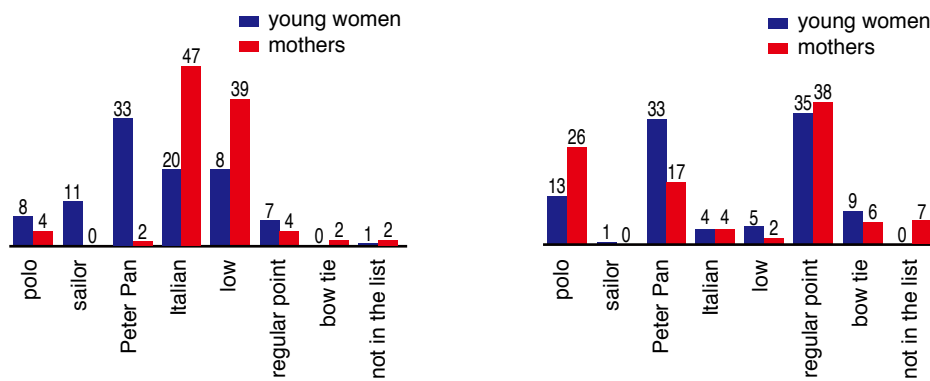


(a) summer cloths.       (b) winter cloths.

Fig. 3. Preferences of collar shapes (%).

in home laundry and it has not been preferred by the mothers group, but its wrinkles caused by laundry process are rather preferred as a kind of fashion by young women. Figure 2(b) indicates that the preferences of winter cloths are similar for young women and their mothers.

**3.2 Collar shapes**
We surveyed preferences of collar shapes, selected from polo, sailor, Peter Pan, Italian, low, regular point, and bow tie collars. Figures 3(a) and (b) show the preferences in summer and winter cloths, respectively. Figure 3(a) indicates that the preferences of Peter Pan collar by young women and their mothers in summer cloths are significantly different. Since Peter Pan collar is a narrow-necked style, it may be considered uncomfortable by the mothers. Italian and low collars, which are preferred by the mothers, are low-necked styles. Figure 3(b) indicates that the difference of the preferences of Peter Pan collar is similar in winter cloths. The opposite difference appears in polo collar in winter cloths.

**3.3 Colors**
Figure 4(a) and (b) show the results of the survey of color preferences in summer and winter cloths. Color tones instead of color hues were surveyed, as explained in Section 2. Figure

AIC2015 TOKYO - Color and Image
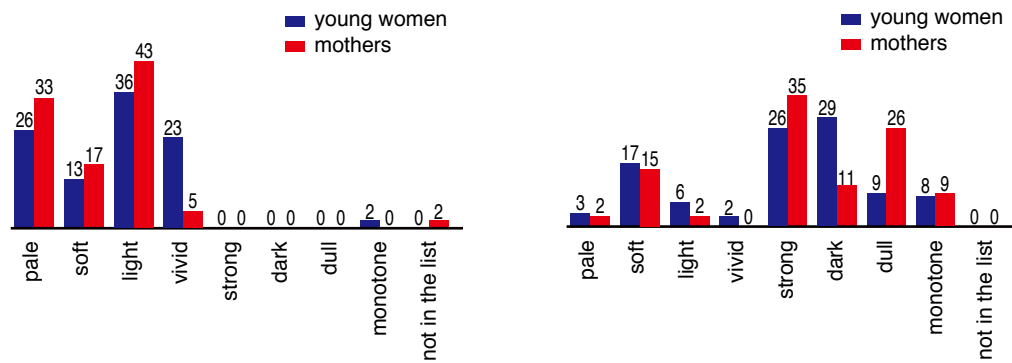
(a) *summer cloths.*  (b) *winter cloths.*

*Fig. 4. Preferences of colors (%).*

4(a) shows that the majorities of the preferences both by young women and their mothers in summer cloths are almost similar, and the only difference is found in vivid color. Neither dark nor dull tone were selected by any of the young women or their mothers, although it has been usually believed that elderly women prefer dark and dull tone. Figure 4(b) shows that the only differences in winter cloths are found in dark and dull colors. Young women preferred dark colors, while their mothers preferred dull colors, according to our survey. This is also different from the above assumption for elderly women.

## 4. CONCLUSIONS

Although it has been assumed that the tendency of age independence is found not only in the fashion-style but also in the color preference of fashion, our research has shown that a significant difference is confirmed in the fashion style between the student generation and the mother generation, especially in the taste of characteristic parts. However, the tendency of color preferences are found different from what have been assumed; Although it has been usually believed that elderly women prefer dark and dull tone, young students also preferred dark tone, while their mothers preferred dull tone to dark tone, according to our surveys for winter cloths. The mothers also preferred bright tone, especially in summer cloths, similarly to the young women. The results, as well as further survey and investigations, will help business strategies of fashion industry.

## REFERENCES

Beke, L., Kutas, G., Kwak, Y., Sung, G. Y., Park, D. S., and Bodrogi, P. 2008. *Color preference of aged observers compared to young observers,* Color Research and Application, 33(5), 381-394.

Baucom, A. H. and Grosch, R. J. 1996. *Hospitality Design for the Graying Generation: Meeting the Needs of a Growing Market,* John Wiley & Sons.

*Address: Prof. Akira Asano, Facutly of Informatics, Kansai University*
*Ryozenji-cho 2-1-1, Takatsuki, Osaka 569-1095, JAPAN*
*E-mail: a.asano@kansai-u.ac.jp*

# Effect of Color Appeared in Signage to Identify Gender of Thai

Chanida SAKSIRIKOSIL[1]*, Kitirochna RATTANAKASAMSUK[2] and Ploy SRISURO[1]

[1]Department of Advertising and Public Relations Technology, Faculty of Mass Communication Technology, Rajamangala University of Technology Thanyaburi,Thailand.
[2] Color Research Center, Faculty of Mass Communication Technology, Rajamangala University of Technology Thanyaburi,Thailand.

## ABSTRACT

This research aimed to study the effect of color appeared in signage to identify gender of Thai people. Colors used in this study were light blue and dark blue, identified as male; red and pink, as female and black as neutral color. Two symbols, as for male and female, were in aforementioned five colors. So the total was ten images. These symbol images were showed within 2 seconds. The subjects were 50 Rajamangala University of Technology Thunyaburi students. For the first evaluation, the subjects assessed the color of the symbols whether or not that color was identified as male or female. For the second evaluation, the subjects assessed the details of the symbols whether or not they were male or female. Then these two evaluations were compared. The results showed that the factor that most affecting gender identification was the details in the symbols. Color appeared in symbol is not relevant to gender identification in this experiment.

## 1. INTRODUCTION

Color is what we all see because it has physical properties. The color is what we see with our eyes. It also tells a story or information to human and creature. These data, such as food, are very important to our life. Creatures differentiate color of plants and animals so they can tell what can or cannot be eaten. Or they can tell the time from the color of the sky. Even the color can also be used to differentiate the human tribes, such as black is represent Africans, yellow for Mongoloid in Asia, and white for Caucasian in West and Scandinavian. (Pungrassamee and Ikeda 2008)

Colors are involved in our daily, considering the various appliances we use. Humans have known to use color since the old days, for example, the painted images on cave walls hundred years ago. Colors are around us as we are learning today. Colors are used to identify the ripe fruit that can be eaten or not. In addition, it also used to convey the meaning of writing, such as the color used in traffic signs on the road (Tangkijviwat 2014)

Red sign means danger. Yellow means caution. Green, often seen on the road, means harmless. Therefore, green has been used for many things, such as, in medical condition or to convey the emotion.

Colors are often used for designing advertising media in order to create the beauty and the eye-catching material, as well as it is used to convey the meaning of the typography in order to make the audience easily understand the message. (Itsadul 2007)

From the aforementioned reason, colors are very useful for daily life and also affect the interpretation. They can be conveyed without a written text and can easily be interpreted and understood. Therefore, this research was to study the influence of the color of the

symbols that affect the classification of male and female of Thailand. Colors in Thailand have not been used as a standard to represent female and male. Unlike many other countries, such as Japan, colors are used to convey the meaning of female and male, such as red is used for lady's room and black or blue is used for men's room. In this study, the researcher chose dark blue and light blue as the color identified as male, red and pink as female and black as neutral.

## 2. METHOD

Female and male symbols were presented on a monitor placed inside an experimental room. Ten symbols were created by the combination of two gender (female and male) and five different colors (dark blue, light blue, black, red and pink) as shown in Table 1. These symbols were presented on a white background as shown in Figure 1. The room illuminance was kept constant throughout the experiment. The viewing distance is fixed at 30 cm. 50 undergraduate students of Faculty of Mass Communication Technology were participated in this experiment.

*Table 1. Chromaticities of color symbols.*

| Colour name | Y | x | y |
|---|---|---|---|
| Red | 35.6 | .527 | .339 |
| Pink | 34.7 | .416 | .217 |
| Black | 3.63 | .286 | .312 |
| Drak blue | 33.0 | .154 | .121 |
| Light blue | 42.5 | .186 | .187 |
| White | 200 | .295 | .326 |

The experiment started by asking the subject to enter in the experimental room and adapt to the room illumination for 2 minutes. A symbol image was presented to the subject one at a time. Each symbol was displayed for 2 seconds. Then, the symbol was disappeared and replaced by gray background in order to make the observer ready for the next assessment.

There were two tasks for each subject. For the first task, the subject was asked to identify if that symbol represent the female or male. In case of the second task, the observer was asked to identify if that color of the symbol represent the female or male.
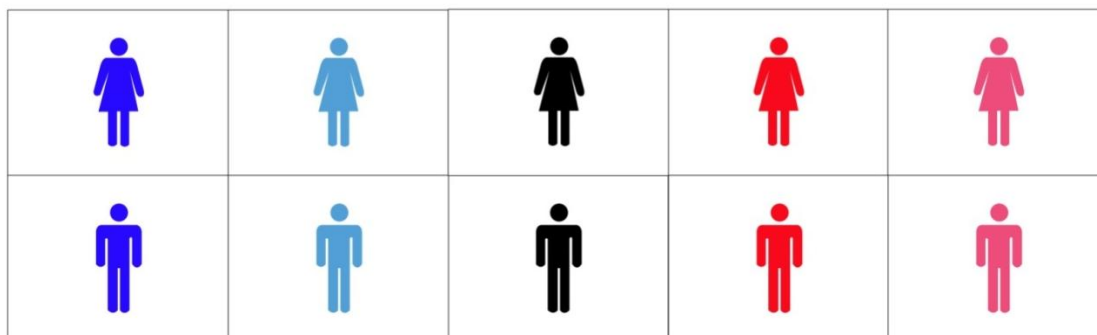


*Figure 1: Color and symbol used in the study*

AIC2015 TOKYO - Color and Image

## 3. RESULTS AND DISCUSSION

The result of the first task was shown in Figure 2. Almost all the Thai subject could correctly identify the gender of symbol even though that symbol was created in any colors. The results implied that color appeared in symbol has no effect on gender identification in this experiment.
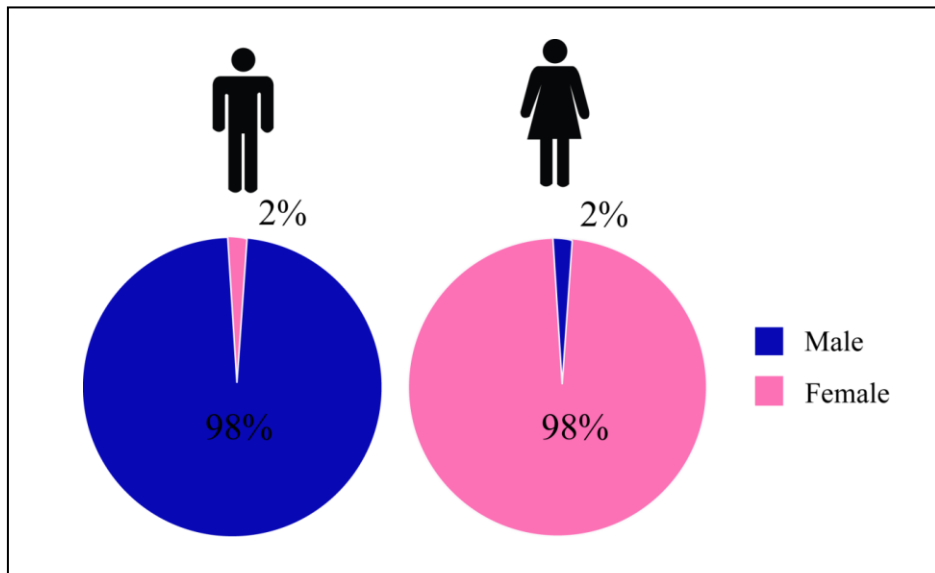


*Figure 2: Gender identification by Symbol's details*

The results from the second task were shown in Figure 3. We hypothesized that red and pink should associate with female identification, whereas blue and light blue should associate with male identification. Our results seemed to follow our hypothesis. 86% of Thai thought that pink was strongly represented the female and 60% of Thai associated red color with female. In case of male, dark blue and light blue associated with male by 74% and 54% respectively. However, color which strongly associated with male was neutral color like black.

If the saturation of color is considered, it seems that low saturation color such as light blue and pink obtained higher female identification than the vivid color. According to the hypothesis, red was represented female. However, 24% of the subject thought that it was represented male and 16% thought that it was represented both gender.

This concludes that, for Thai, even though there was some association between color and gender. But this association was not relevant to the gender identification in symbol. It was possibly due to no usage of color code to express gender in Thailand. Unlike some countries, for example, Japan, the male toilet symbol is generally blue or black and the female toilet is generally red. We expected that the obtained result would be different if the subjects were Japanese who are familiar to the color coding for gender identification in their daily life. Further experiment is required to confirm this expectation in the future.
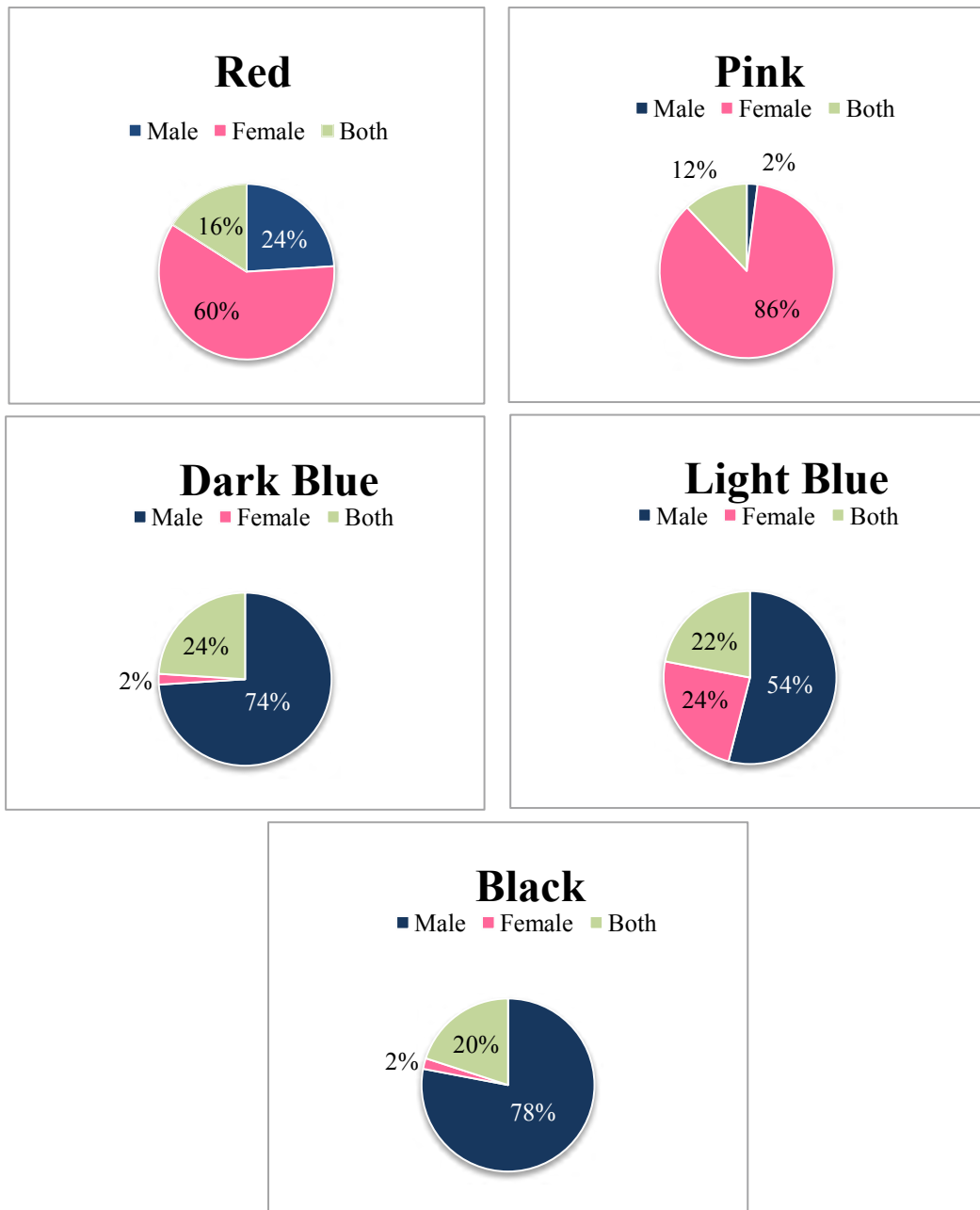
## Red

Male ■ Female ■ Both

- 24% Male
- 60% Female
- 16% Both

## Pink

Male ■ Female ■ Both

- 2% Male
- 86% Female
- 12% Both

## Dark Blue

Male ■ Female ■ Both

- 74% Male
- 2% Female
- 24% Both

## Light Blue

Male ■ Female ■ Both

- 54% Male
- 24% Female
- 22% Both

## Black

Male ■ Female ■ Both

- 78% Male
- 2% Female
- 20% Both

*Figure 3: Gender identification by Symbol's color*

## 4. CONCLUSIONS

The study found that the factor influencing gender identification in Thailand was the detail of the symbol but not the color of the symbol. From the first task, the subject correctly identified gender of the symbol. The subject also had the answers in the same direction whether the symbols were alternately colored. In the second task, the subject had different opinions when asked to identify the gender after seeing the color of the symbol. Almost the subjects agreed that pink was represented as female. Blue and black were represented as male. However, this association was not relevant to the gender identification in symbol.

AIC2015 TOKYO - Color and Image

## ACKNOWLEDGEMENTS

## REFERENCES

Ludwig, C. and others. 2010. *Adult age differences in the Color Stroop Test*, Archives of Geriatrics 51,  135-142.

Itsadul, P. 2007. *Vector Graphic in Printed Advertising,* Thammasart University, Bangkok.

Pungrassamee, P., and Ikeda, M. 2008. *Colr and Color Vision,* Chulalongkorn University Press, Bangkok.

Jewbang, T. 2007.  *Learning Theory of Colour,* O.S .Printing House. Bangkok .

Tangkijviwat, U. 2014. *Color Science & Technology [PowerPoint Slides]*, Rajamangala University of Technology Thanyaburi.

*Address: Chanida Saksirikosol, Department of Advertising and Public Relations,*
*Rajamangala University of Technology Thanyaburi,*
*39 Rangsit-Nakhonnayok Klonghok Thanyaburi Pathumthani, THAILAND*
*E-mails: dadahz69@gmail.com,chanida_69@hotmail.com,*

# Development of three primary-color transparent cubes for learning subtractive color mixing visually

Keiichi MIYAZAKI
Cubics Design

## ABSTRACT

Since the principle of subtractive color mixing is more difficult to understand than additive color mixing, we have developed a teaching materials to learn the subtractive color mixing visually[1]. Teaching materials are three types of transparent cube with three colored surfaces, and one big color mixing transparent cube composed of eight stacked cubes. By making full use of the optical design, three types of cube is devised to be interesting in appearance and rainbow-colored beauty of color mixing. The process of making one big cube by stacking eight cubes, is devised to be able to enjoy the color mixing like solving the puzzle.

## 1. INTRODUCTION

It is said that young people have been lost interest in science, efforts to improve the learning motivation by fun experience, with facilities such as RiSuPia[2], have been made. If you try to learn the color science, usually, it is necessary to learn a variety of terminology and definitions related to visual characteristics as well as physical optics.

The purpose of this study is to provide teaching materials that can experience the fun and beauty of color for learning the subtractive color mixing used for printing or photo reproduction.

For example, building blocks of Cubicus[3](Figure 1(1)), because it has both beautiful appearance and puzzle features likes contemporary art, is very attractive as the teaching materials for visual learning. Therefore, by developing a new teaching materials for learning a subtractive color mixture incorporating the art puzzle elements, we want to make learn color mixing visually.
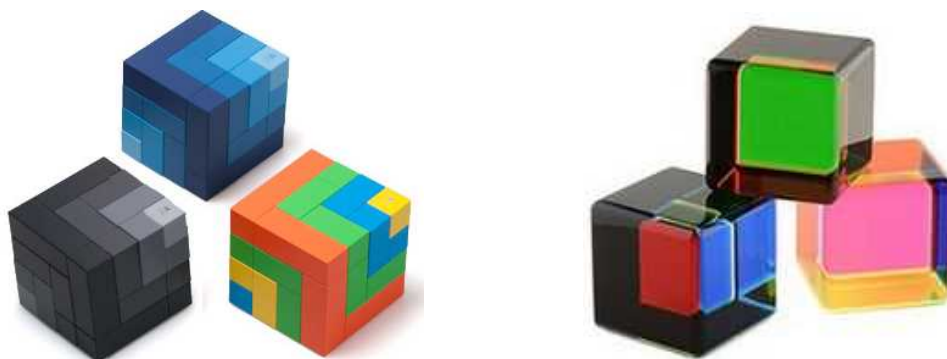


*Figure 1: (1)Cubicus of Neaf            (2)Vasa Cubes of VASA*

# 2. METHOD

## 2.1 Color Mixing by Transparent Cube

Building blocks made of opaque plastic timber is not suitable for teaching materials of subtractive color mixing. However, if the transparent cube is used, such as Vasa Cubes[4] in Figure 1 (2), by making use of two parallel faces or two adjacent surfaces, it is possible to express the subtractive color mixing as shown in Fig. 2 (1). Each of the two color mixing, is referred to as the parallel surface color mixing(PCM) and the adjacent surface color mixing(ACM). When two transparent cubes are stacked as shown in Fig. 2 (2), it is also possible to represent the subtractive color mixing.



*(1)Color mixing by one cube*          *(2) Color mixing by two cubes*
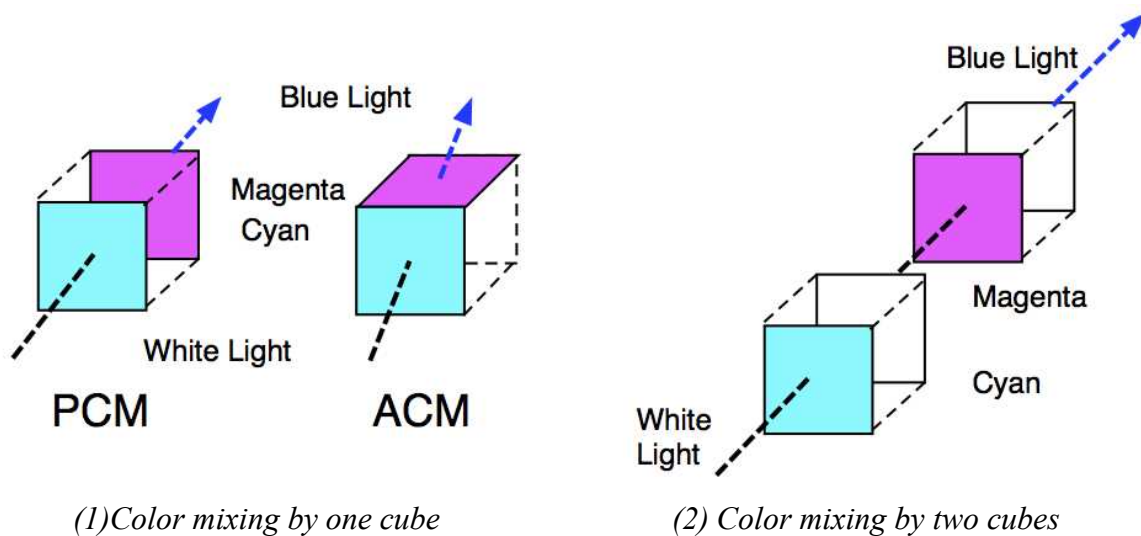
*Figure 2: Subtractive color mixing by transparent cube*

## 2.2 Tri-Mixing Color Cube

Since the cube has six faces, it is possible to represent the three sets of PCM information per cube as shown in Figure 3. Thereafter, a transparent cube with information of three sets of PCM is referred to as a tri-mixing color cube. It is possible to represent additional color mixing by the combination of some tri-mixing color cubes placing two or more cubes as shown in Figure 2 (2).
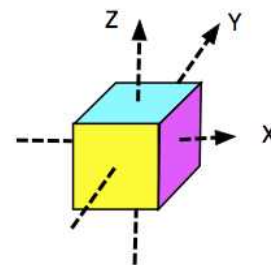


*Figure 3:Tri-mixing color cube*

## 3. Results and Discussion

### 3.1 Mixing Color of PCM-CUBE and ACM-CUBE

Using the six faces of the cube (from 1-6 dice surfaces), tri-mixing color cubes assigned the CMY to the arrangement of the PCM and ACM were shown in Figure 4. Comparing the number of colors that could be observed at the same time, PCM-CUBE(with three

different mixing color pairs of PCM) had 6 colors, and ACM-CUBE(with three different mixing color pairs of ACM) had four colors. Considering the cause of the difference at looking of cubes, and decomposing the cube to check the placement of the CMY, gave a good opportunity to be interested in subtractive color mixing.
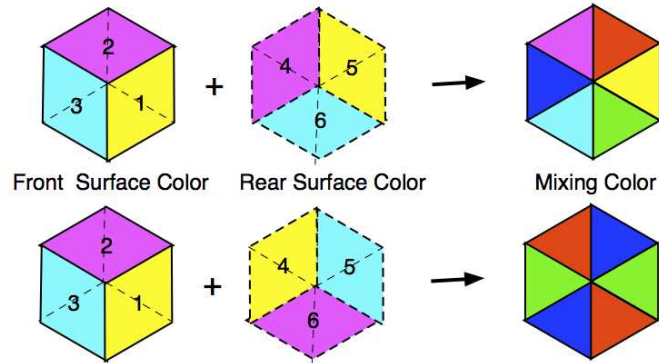


*Figure 4:Surface color and mixining color of PCM(upper) and ACM(lower) CUBEs*

## 3.2 Unexpected Color Mixing

In color mixing by stacking tri-mixing color cube, unexpected color mixing(UCM) occured in an oblique direction as in Figure 5, and UCM becomes the noise of stacking color mixing. Since the cause of the UCM was mainly ACM, in order to reduce ACM, a solid transparent cube was experimentally
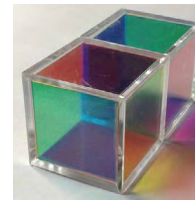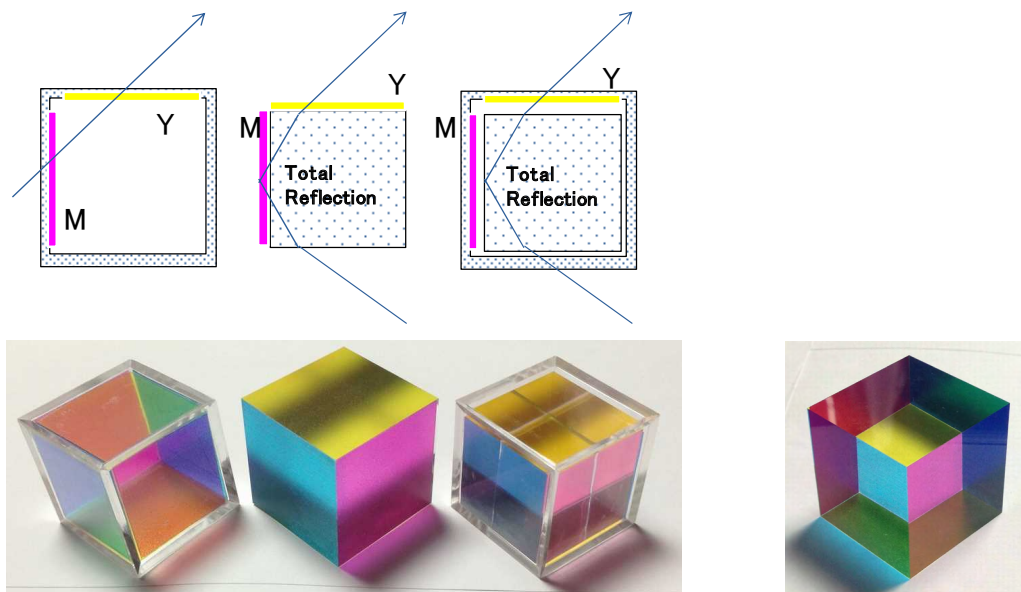


*Figure 5 : An example of  UCM*



*(1)  Box(ACM)    (2)Solid-FrontView    (3)Box&Solid        (2)Solid-RearView*

*Figure 6:Optics(upper figure) and appearance(lower figure) of cubes in Table 1*

put inside the ACM-CUBE in Figure 6(1). And then, ACM of box and solid type in Figure 6(3) was nearly invisible by the total reflection of internal transparent solid cube.

## 3.3 Transparent Color of Tri-Mixing Color Cube

Transparent color with three types of tri-mixing color cube was summarized in Table 1. Row (3) in Table 1 had no ACM(no RGB) even viewed from any direction, and didn't occur UCM, then we called this type of tri-mixing color cube as tri-primary color cube. Row (2) in Table 1, as shown in Figure 5(2:Rear View), had a colorful and beautiful ACM.

*Table 1.Transparent color of tri-mixing color cube[No. is same as Figure 6]*

| No. | Optical Structure (Dice※ Number) | Front 1 | 2 | 3 | Rear 6 | 5 | 4 | Parallel 1→6 6→1 | 2→5 5→1 | 3→4 4→3 | F→R 1→4 | 1→5 | 2→4 | 2→6 | 3→5 | 3→6 | R→F 4→1 | 5→1 | 4→2 | 6→2 | 5→3 | 6→3 |
|---|---|---|---|---|---|---|---|---|---|---|---|---|---|---|---|---|---|---|---|---|---|---|
| PCM | Box | Y | M | C | C | Y | M | G | R | B | R | YY | MM | B | G | CC | R | YY | MM | B | G | CC |
| (1) | | Y | M | C | Y | M | C | YY | MM | CC | G | R | B | R | B | G | G | R | B | R | B | G |
| (2) | Solid | Y | M | C | – | | | Y | M | C | Y | Y | M | M | C | C | G | R | B | R | B | G |
| (3) | Box & Solid | Y | M | C | – | | | Y | M | C | Y | Y | M | M | C | C | C | M | C | Y | M | Y |

※1→2 means viewing from 1 to 2 direction

## 3.4 Stacking Tri-Primary Color Cubes

An interesting example of stacking color mixing was stacking up the RGB tri-primary color cube from eight CMY tri-primary color cubes. When stacking eight CMY tri-primary color cubes, CMY tri-primary color cubes changed to one large RGB tri-primary color cube by subtractive color mixing, as shown in Figure 7(1). Furthermore, when replacing four CMY tri-primary color cubes to RGB tri-primary color cubes, as shown in Figure 7(2), color of whole cube changed to BLACK.
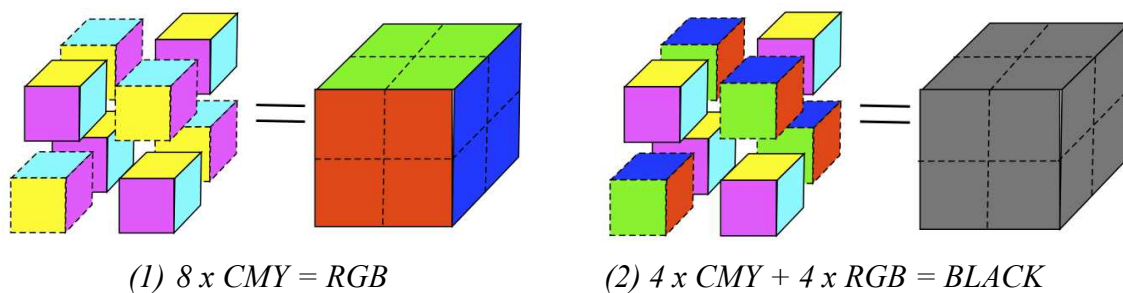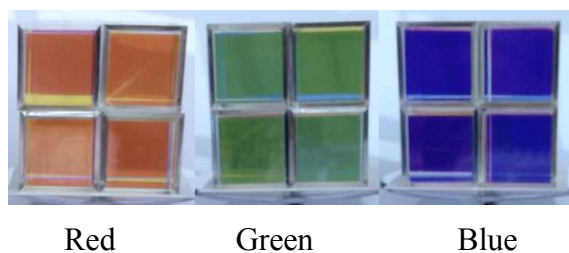


*(1) 8 x CMY = RGB*    *(2) 4 x CMY + 4 x RGB = BLACK*

*Figure 7: Arrangement of stacking eight cubes to one bigger cube*

The image obtained by observing actual RGB cube stacked by eight CMY cubes from three directions was shown in Figure 8. It could be seen that the UCM does not occur.

Red          Green          Blue

*Figure 8: One big RGB cube without UCM*
*resulting from the stacking method of Figure 7(1)*

## 4. CONCLUSIONS

Tri-mixing color cubes which can be observed CMYRGB six colors simultaneously, and a method for building one RGB cube by stacking eight CMY tri-primary cubes have been developed. Next, we will promote use of tri-mixing and tri-primary color cubes at schools to teach the subtractive color mixing, and to verify the validity as a teaching material.

## ACKNOWLEDGEMENTS

## REFERENCES

[1] Keiichi Miyazaki, 2014, J. Color Sci. Assoc. Jpn., 38(6), in Japanese.
[2] RiSuPia, http://www.panasonic.com/global/corporate/center/tokyo/risupia.html
[3] Mikado Koyanagi, 2004, Edu-toy - NAEF and European Wooden Toys, in Japanese.
[4] Vasa Mihich, 2007, VASA

*Address: Keiichi Miyazaki, Cubics Design*
*1-16-3 Sakae-cho, Odawara-shi, Kanagawa, 250-0011, JAPAN*
*E-mail: mgg02366@nifty.com*

# Multicolor LED Lighting Device with a Microprocessor for Demonstrating Effects of Lighting on Color Appearance

Takashi NAKAGAWA[1]

[1] Faculty of Information Engineering, Fukuoka Institute of Technology

## ABSTRACT

The author has assembled multicolor LED lighting devices to demonstrate effects of lighting on color appearance. The most recent device, containing eight color LEDs and three white LEDs, is controlled by a microprocessor Arduino MEGA to realize flexible lighting conditions. In this paper, the author first describes the employed LEDs and discusses the importance of variety of LEDs that enables variety of light spectrum. He then describes and compares two versions of multicolor lighting devices he has assembled and shows that the equipment of a microprocessor greatly enhances the usability in the demonstration of color experiments.

## 1. INTRODUCTION

There are phenomena that can be demonstrated with lighting devices: metamerism, additive color mixture, color rendering, etc. Performance of LED lighting apparatus depends on the assortment of LED colors. However, wavelength ranges of available LEDs are restricted to those of mass production. Recently, power LEDs of various colors are available in chips. So, the author has fabricated multicolor lighting devices with chip LEDs.

## 2. LEDS

The lighting devices were made with Philips LUXEON Rebel chip LEDs: deep red (DR, $\lambda_D$ = 655nm at 350mA), red (R, $\lambda_D$ = 627nm), red orange (RO, $\lambda_D$ = 617nm), amber (A, $\lambda_D$ = 590nm), green (G, $\lambda_D$ = 530nm), cyan (C, $\lambda_D$ = 505nm), blue (B, $\lambda_D$ = 470nm), royal blue (RB, $\lambda_D$ = 448nm), cool white (CW, 6500K), neutral white (NW, 4100K), and warm white (WW, 3100K). Figure 1 shows the package outline. Light is emitted through the dome lens on the top surface. There are a thermal pad and two electrical contact pads on the bottom surface.
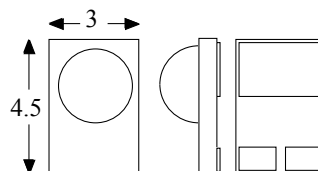


*Figure 1. Package outline.*

Figure 2 shows the relative spectrum power distributions of color LEDs and neutral white LED (cited from the supplier's data sheets). There is a vacant range of wavelength between blue and cyan as well as green and amber.

Figure 3 is the chromaticity diagram of LEDs. Trianguar marks in the outer area indicates color LEDs, and marks in the inner area indicates white LEDs.
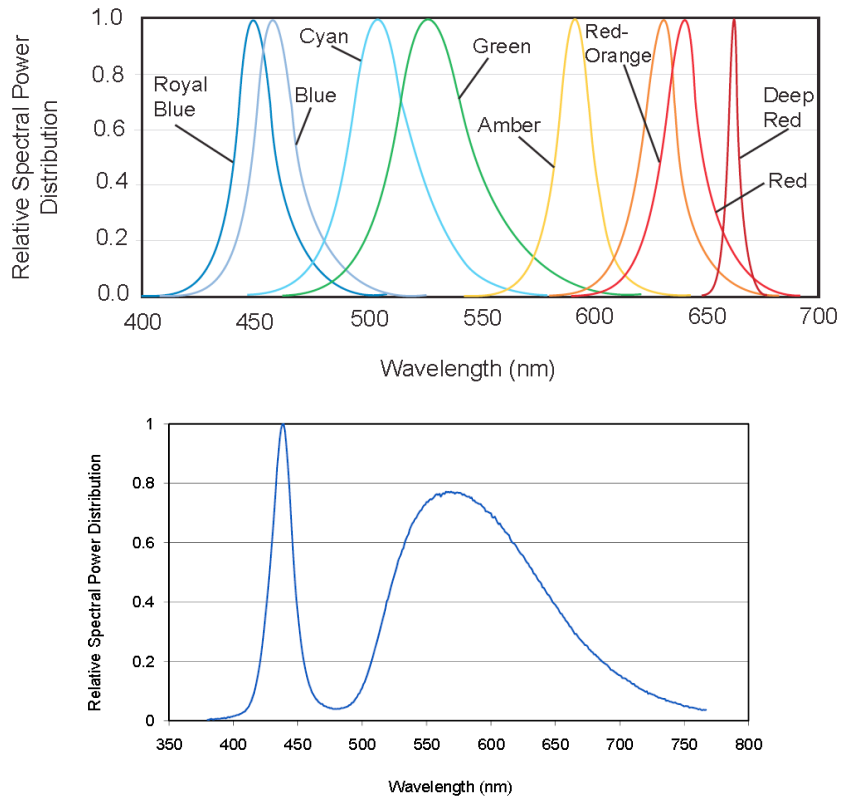
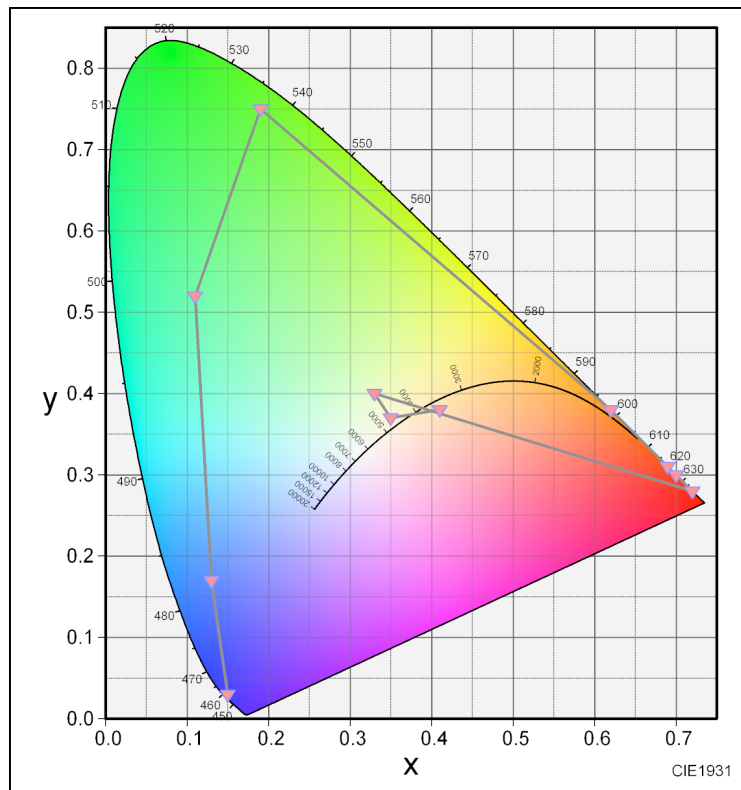*Figure 2. Relative spectrum power distributions of LEDs.*



*Figure 3. chromaticity diagram of LEDs.*

AIC2015 TOKYO - Color and Image

It is well known that the chromaticity coordinate (x,y) of the color light L produced by summing three color lights $L_1$ $(x_1,y_1)$, $L_2$ $(x_2,y_2)$, $L_3$ $(x_3,y_3)$ can be calculated as a weighted average of $(x_1,y_1)$, $(x_2,y_2)$, $(x_3,y_3)$ where the weights are sums of color tristimulus values. In other words, it is possible to produce a color light L by summing three color lights $L_1$, $L_2$ and $L_3$, if the chromaticity coordinate (x,y) of L is inside of the triangle $L_1L_2L_3$ on the xy chromaticity diagram.

From Figure 3, it is obvious that there are many different combinations of three LEDs that can produce the same white color. For example, by using LEDs B, C and A, the color of neutral white LED can be obtained, whereas the same color can be also obtained by using RB, G and DR. To demonstrate this phenomenon, LED powers must be finely adjusted. This is possible by using Arduino MEGA.

Although the white color lights produced by the above three different ways (a) lighting NW, (b) lighting B, C and A, and (c) lighting RB, G and DR, have the same chromaticity coordinate (x,y), their spectrum power distributions are different. This difference causes the difference of body colors of two objects with different spectral reflections. Thus, our lighting device can be used to demonstrate metamerism and color rendering property of light.

Therefore, it is important that the lighting device has many LEDs of different colors.

## 3. THE LIGHTING DEVICES WITHOUT MICROPROCESSORS

Figure 4 shows the lighting devices without microprocessors. Each of them contained pairs of 8 color LEDs. Their fabrication was easy because wiring was simple: each color was simply switched ON or OFF. Yet they were useful for demonstrating metamerism.
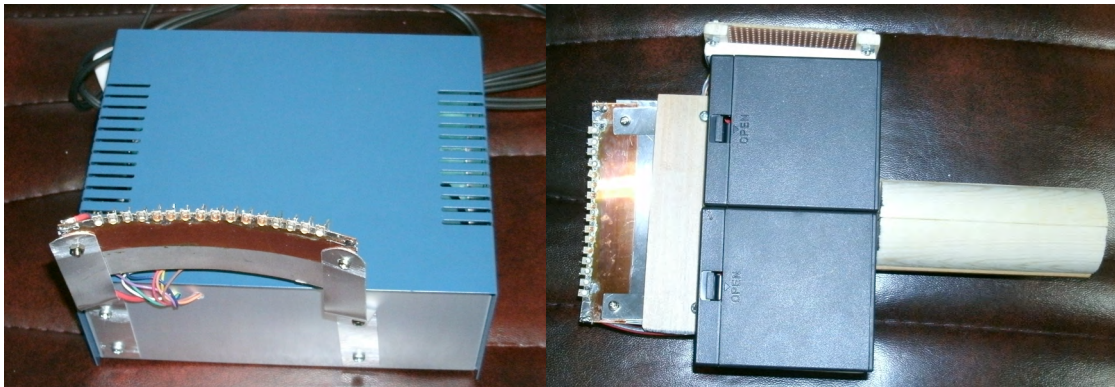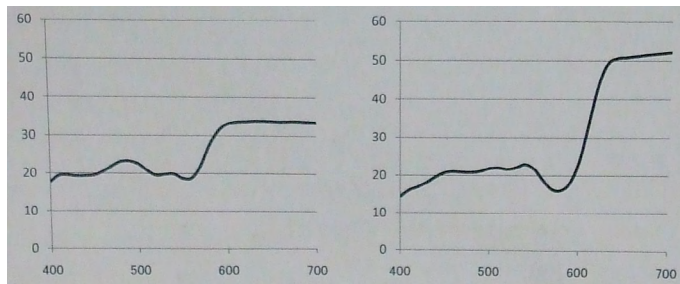


*Figure 4. An AC driven lighting device (left) and a portable one (right).*



*(a) under the daylight*

*(b) lighted with green and amber*

*Figure 5. Spectral reflectance of a metameric pair.*    *Figure 6. Color appearances.*

Figure 5 shows the spectral reflectance of a metameric pair sheet provided by the manufacturer. Figure 6 shows their photographs under the daylight (a) and under the mixture of green and amber LED lights. We see in (b) that the left sheet appears brown while the right sheet appears green. This difference of color appearance can be explained using their spectral reflectance and the spectral power radiation of LEDs.

There is a problem in soldering chip LEDs. Chip LEDs are weak to the high temperature over 300°C. Therefore, the author used a temperature-controlled soldering iron for wiring and a temperature-controlled hot plate for the soldering of chip thermal pads to the radiation plate. Figure 7 shows the schematic diagram of the reflow technique where the chip has been previously attached to a supporting card paper and the radiation copper plate has been previously covered with solder.
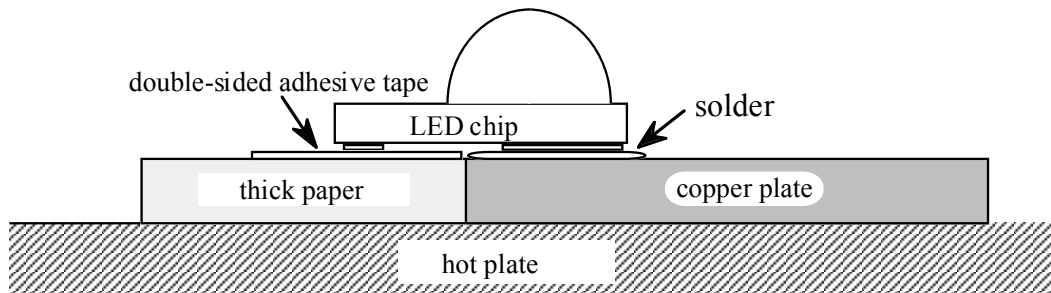


*Figure 7. Soldering thermal pads of an LED chip on the radiation plate.*

## 4. THE LIGHTING DEVICE WITH A MICROPROCESSOR

To freely control radiation levels of LEDs, the author employed an Arduino Mega 2560 microprocessor with 54 digital I/O pins of which 15 provides 8-bit PWM output. Figure 8 shows the outline of the electrical connection. PWM outputs to control LED lighting drive two subsystems: FETs that drive LEDs and the bar graph display units. A bar graph display unit is composed of a 10-segment LED bar graph display and its driver IC. These units are employed to display the radiation spectrum.
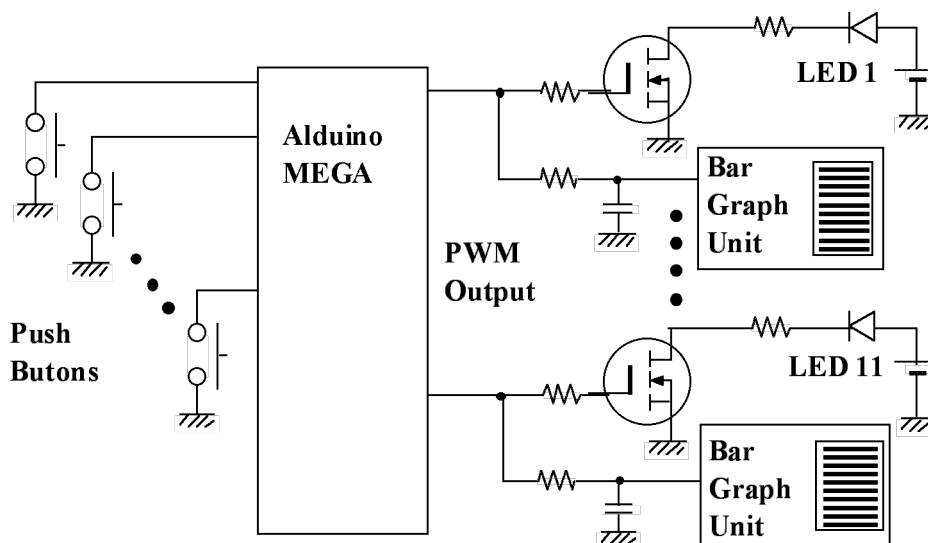


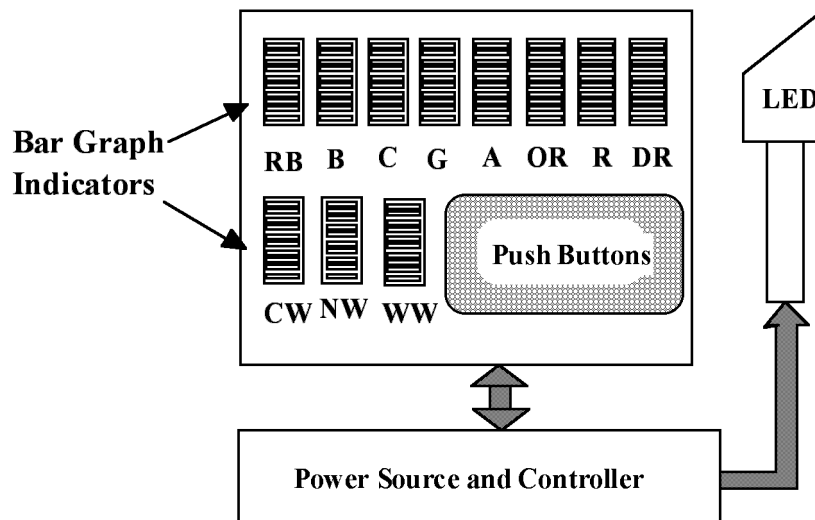*Figure 8. The outline of electrical connection.*

*Figure 9.  Rough composition of the lighting device.*

Figure 9 shows the rough composition of the system. Power source and Arduino is contained inside a metal case, push buttons and bar graph indicators are on the surface of the case. The light radiation unit is connected to the power and controller unit case.

## 5. THE OPERATION OF THE LIGHTING DEVICE

With Arduino MEGA, various modes of operation can be realized. Some modes are as follows: (1) single LED lighting,  (2) sequential lighting of  single LEDs, (3) LED combination lighting,  (4) sequential combination lighting, (5) On site adjustment of LED lighting, (6) Registration of the adjusted lighting and recalling.

With this flexibility, we can make various modes of demonstration. For example, we can show that the same color can be obtained with different combinations of primary colors, we can demonstrate metamerism and we can check color rendering.

## 5. CONCLUTION

By using multiple color LEDs, we can make lighting devices to demonstrate various color phenomena, and the ability of flexible demonstration is greatly enhanced by controlling with microprocessors.

## REFERENCES

Takashi, Nakagawa: *Multicolor LED Lighting ApparatusFabricated to Demonstrate Metamerism*, Proceedings of ACA 2013, pp.118-120.

*Address: Takashi NAKAGAWA, Kokubu 3-15-12, Dazaifu-shi, Fukuoka-ken, 818-0132, JAPAN*
*E-mails:nakagawa@fit.ac.jp, na32ka@yahoo.co.jp*

# The Effect of Environment Colour on Behavioural Inhibition.

Nicholas CICCONE, Stephen WESTLAND School of Design, University of Leeds, UK

## ABSTRACT

The interplay between colour and behavioural inhibition (a trait of impulsivity) has yet to be researched despite the growing interest and activity in the field of impulsivity and behavioural inhibition (Webster and Jackson, 1997). The implications of gaining a better understanding of this area will help improve crime prevention strategies, the use of colour in marketing, the design of environments and product development. For example, in Japan and, recently, in the UK blue lights have been installed on railway platforms to discourage suicide attempts. However, the robustness of research into the veracity of claims about colour and impulsive behaviour remains to be tested.

This study addresses this by conducting a preliminary experiment in this area. Participant's behavioural inhibition was measured using reaction times gained from a computer based Go No-Go signal task within in a pop up colour studio. The luminance and chroma of the lighting environment was kept constant but the hue was manipulated between red, blue and green using a 24-bit LED stage lighting system; a white control lighting environment was also used. Results obtained through one way and mixed design ANOVA's found that: In the red light participants task reaction times were significantly faster than under white light. Highly impulsive participants showed significantly slower reaction times under all conditions except for green where a significant interaction was found. Additional work is underway to replicate the preliminary study using more advanced psychophysical techniques.

Keywords: *Colour, Impulsivity, Environment, Go no-go task, Crime prevention, Marketing.*

## 1. INTRODUCTION

For the purpose of this study impulsivity will be seen as reduced executive function and Inhibitory control (Logan, 1997). Behavioural Inhibition is the ability to suppress a pre-potent response (Nigg, 2000). Logan (1997) investigated if the inability to inhibit a pre-potent responses was a reflection of true impulsive behaviour through a stop signal task. It was found that go-signal responses were unaffected by impulsivity levels, but stop-signal tasks took longer with more impulsive subjects. Evidence indicates that in normal cohorts behavioural measures of inhibitory control are accurately related to represent levels of impulsivity (Enticott, 2006).

There are two main paradigms used when explaining the neurologically arousing effect of colour. The process is either; a learned or associated response (Grossman, 1999) or the result of the activation of an internally innate mechanism (Adams, 1973; Hupka, 1997).

An associative response to colour is caused by past experiences which effect an individual's physiological arousal, a process known as 'associative learning'. An unpleasant (fear) stimulus could be paired to a particular colour for example red with blood and pain. After

AIC2015 TOKYO - Color and Image

several similar associations future exposures to that colour elicits the same neurological response to the paired stimulus but with only the colour being present (Bierley, 1985).

The general consensus on arousal caused by innate mechanisms is that the effect of the colour is dependent on where it falls within the colour spectrum (see figure 1). Longer light wavelength colours (yellow, orange and red) result in greater neuronal activation whereas shorter wavelengths (green and blue) have a sedative effect (Wright & Rainwater 1962).



**Figure 1**: Colour spectrum with wavelengths (nm).

Neural activity has been associated with behavioural arousal and inhibitory control relating to individual differences in impulsivity. An fMRI study found a "positive correlation with activation (arousal) in the bilateral ventral amygdala, parahippocampal gyrus, dorsal anterior cingulate gyrus (BA 32), and bilateral caudate" to impulsivity. In addition to this there was a negative correlation when activation was seen in the dorsal amygdala and ventral prefrontal cortex (BA 47). This suggests that impulsivity is indeed influenced by the level of corticolimbic arousal (Brown, 2006).

Interestingly an effect has been found in relation to physiological arousal and impulse buying. A stimulating store environment was found to cause a momentary loss of self-control increasing instances of impulse purchases (Mattila and Wirtz 2008). These findings are consistent with psychology studies which highlight that over-stimulation or high arousal lessens a person's self-regulation (Baumeister *et al.*; 1998).

## 2. METHOD

A white pop-up studio was erected in a colour neutral room (white and black items only) with a marked x position for light positioning from behind the participant. A laptop equipped with Inquisit (by Millisecond Software version 4) and the Go/No Go experiment code installed on it with a touchpad was placed at a comfortable height for the participant to see the screen. A light emitting diode (LED) RGB capable light was used for colour accuracy and low temperature emission and placed in a position behind the participant facing towards the marked X. A Chroma meter displaying the International Commission on Illumination (CIE) was used to ensure similar luminosity levels within the popup studio in each condition while changes were made to the chroma (see figure 2).



**Figure 2**: The four colour conditions.

## 2.1 Procedure

Participants entered the pop up studio and were instructed to sit at the desk and read the participant pack. This consisted of an information sheet about the general nature of the project, a consent form, the Ishihara colour deficiency test and the Barratt Questionnaire. An acclimatisation period of at least 10 minutes passed before the experiment began. The experiment file was then run on a laptop. Subjects were given adequate time to read the instructions and had an opportunity to ask any questions before the test was completed. The experimenter then turned on the LED light to the relevant colour setting for the participant and trial number. The main room light was then switched off and the participant was instructed to begin the task. After the first sets of trials were complete the experimenter changed the light to the second colour setting. The subject then completed the task for a second time. This process was then completed for each of the colour conditions. On completion of the last Go/No-Go task the main lights were turned on before the LED light was switched off. The participant were then given a full debrief of the purpose of the experiment thus concluding the test phase of the research.

## 2.2 PARTICIPANTS

This study used 27 participants (12 females and 15 males) with an average age of 20.9 years. Opportunity sampling was used to recruit individuals. Participants were screened to check: (i) They had had no previous experience in a similar study or any in-depth prior knowledge of colour research in the area being studied. (ii) That no one suffered from either claustrophobia or epilepsy. (iii) Normal colour perception through the use of the Ishihara test of colour perception deficiency (Ishihara 1917). (iv)That there was no high risk individual that may be suffering from impulsivity based pathologies using the Barratt Impulsivity Scale (Barratt 1959).

## 2.3 THE GO NO-GO TASK

The Go No-Go Task used in this study is a simplified version of the test used by Fillmore (2003). It measures impulse control by the level of ability shown by an individual to inhibit a behavioural response. The task consists of 200 trials, 50 in each condition (white, red, blue, green light) and took approximately 20 minutes to complete. The participant was shown a pre-target stimuli with a 60% chance of a go signal (black circle) and a 40% chance of a no go signal (black circle).

## 3. RESULTS AND DISCUSSION
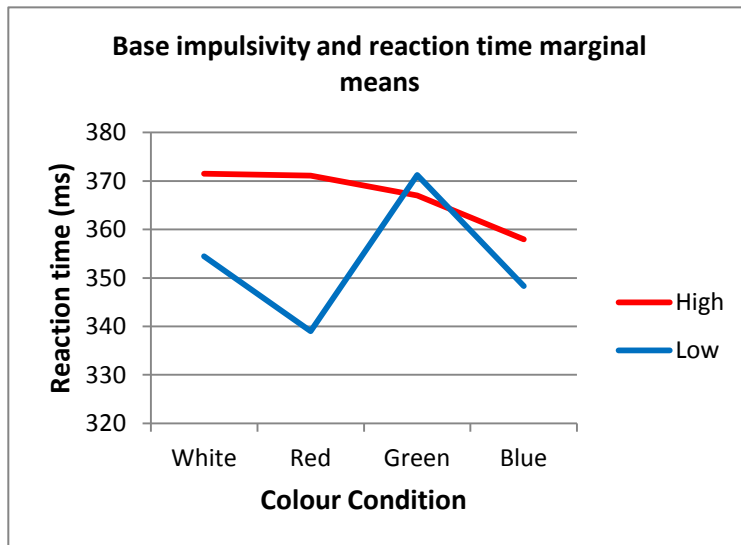
### 3.1 PAIRED SAMPLE T-TEST
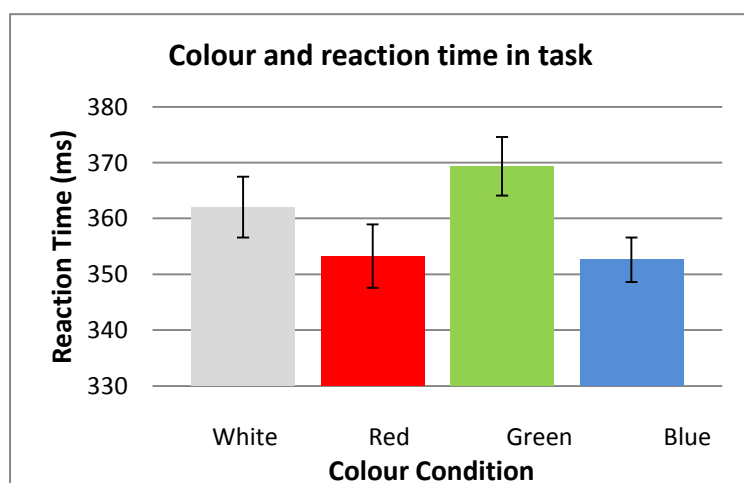


A paired sample T-Test found a significant effect of colour and Go No-Go task reaction times between white (M=362.03, SD=28.3) and red (M=353.3, SD=29.5); t(26)2.25, P=.033.

AIC2015 TOKYO - Color and Image

## 3.2 MIXED ANOVA



**Base impulsivity and reaction time marginal means**

The sample was split into two groups; low and high base impulsivity determined from The Barrett Impulsivity Questionnaire (a score over 70 was considered high). A significant main effect of colour was found $F(2.23, 55.72) = 4.59$, p = .012 and a significant interaction between colour and impulsivity $F(2.23, 55.72) = 4.84$, p = .009 . The Mauchley test for spherecity was significant p=.036 so a Greenhouse-Geisser correction was used.

## 4. Conclusions

Colour has previously been demonstrated to manipulate level of psychological arousal increases of which have been linked to greater impulsivity. Kosslyn (2003) found increases in physiological arousal and glandular responses when exposed to the colour red. The pituitary gland stimulates the adrenal medulla releasing epinephrine causing a higher psychological state with peaked behaviour and emotional responses (Fuller, 1982). Long wavelength colours have also been found to cause greater general neuronal activation compared to shorter wave length ones which have a sedative effect (Wright and Rainwater, 1962). Theories linking increased arousal to increased impulsivity include the one-dimensional concept (Eysenck, 1982; Doux, 1996) and the three-dimensional arousal model (Boucsein, 1992; 1997). If these theories are correct than red would be expected to cause increased impulsivity and thus a lower level of behavioural inhibition however this was not supported by the findings the T-Test showed significantly faster reaction times in the red light condition (M=353.3, SD=29.5); t(26)2.25, P=.033) compared to the control condition white (M=362.03, SD=28.3. This may suggest that the increased neuronal activation and arousal caused by red had a counteractive effect on the negative effect on the test caused by increased impulsivity. Faces of a competitor that are red are an indicator of testosterone levels related to anger and aggressiveness (Changizi, 2009). This combined with research associating colour within the context of evaluating threat (Elliot, 2009; 2007. Moller, 2009; Mathews, 1985) demonstrates the importance of red as a threat signal in humans. The human perceptual system assigns resources based on importance of the stimuli (Bishop, 2008) and this could be an explanation for these results however further research is needed to investigate the interaction between attention and impulsivity and effectiveness of behavioural inhibition.

Highly impulsive subjects had generally slower reaction times across the lighting conditions, compared to those of low base impulsivity. This was expected as in previous studies lower impulsivity has been associated with generally faster reaction times across colour conditions (Derefinko et al. 2008). Whereas highly impulsive participants have slower response times . A study of ADHD (a condition characterized by high impulsivity) found that typically

participants had more errors and slower inhibition compared with controls (Roberts, Milich, 2011).

The faster reaction times in the red condition in those with low impulsivity can be explained through arousal theories (Kosslyn, 2003; Fuller, 1982, Wright and Rainwater 1962, Eysenck, 1982; Doux, 1996, Boucsein, 1992; 1997) and the selective processing of threat cues discussed previously (Elliot, 2009; 2007. Moller, 2009; Mathews, 1985). Red causes a higher level of alertness and therefore causes increases in attentional controls thus a faster response can be made without necessarily increasing impulsivity.

In contrast there was an interaction seen in reaction times and green light in those with low impulsivity. Under arousal theory states that impulsivity may be due to physiological under-arousal when in a state of rest than greater increases in arousal when stimulated (a rebound effect; Corr, 1995). This could support the interaction. The colour green is commonly associated with go & safe (McShane, 1999) It is possible that this memory schemata made through previous memory consolidation (Tse, 2007) negatively interacted with the stop signals. Rapid error-prone processing was used because of the cognitive matching between green and go when under green light (Dickman, 1990). More cognitive resources and time were therefore needed to correct this conflict.

The faster reaction times in the blue condition may be the result of reduced impulsivity through the relaxing effect of the colour. Anecdotally participants reported after the study that during the blue condition they felt calm. The sedative effect of blue has been previously reported by Wright and Rainwater (1962) notably this could have caused these faster reaction times through decreases in impulsivity levels however this still needs further investigation.

# REFERENCES

Adams, F.M. and Osgood, C. E. (1973).”A Cross-Cultural Study of the Affective Meanings of Color”, Journal of Cross Cultural Phychology 4 (2).

Barratt, E. S. (1959). Anxiety and impulsiveness related to psychomotor efficiency. Perceptual and Motor Skills, 9(2), 191-198 doi: 10.2466/PMS.9.3.191-198

Baumeister, R., Bratslavsky, E., Muraven, M., & Tice, D. (1998). Ego depletion: Is the active self a limited resource. Journal of Personality & Social Psychology, 74(5), 1252–1265.

Bierley, C., McSweeney, F. K., & Vannieuwkerk, R. (1985). Classical conditioning of preferences for stimuli. *Journal of Consumer Research*, 316-323.

Bishop, S. J. (2008). Neural mechanisms underlying selective attention to threat. *Annals of the New York Academy of Sciences*, *1129*(1), 141-152.

Boucsein, Wolfram (1992), Electrodermal Activity. New York, London: Plenum Press.

Boucsein, Wolfram (1997), "Aktivierung," Handbuch Arbeitswissenschaft, eds. Luczak, Holger and Walter Volpert, Stuttgart: Schaeffer-Poeschel, 309-312.

Brown, S. M., Manuck, S. B., Flory, J. D., & Hariri, A. R. (2006). Neural basis of individual differences in impulsivity: contributions of corticolimbic circuits for behavioral arousal and control. Emotion, 6(2), 239.

Changizi, M. A. (2009). The vision revolution: How the latest research overturns everything we thought we knew about human vision. Dallas,TX: BenBella Books.

Corr, P. J., Pickering, A. D., & Gray, J. A. (1995). Sociability/impulsivity and caffeine-induced arousal: Critical flicker/fusion frequency and procedural learning. Personality and Individual Differences, 18(6), 713-730.

Derefinko KJ, Adams ZW, Milich R, Fillmore MT, Lorch EP, Lynam DR. (2008). Response style differences in the inattentive and combined subtypes of attention deficit/hyperactivity disorder. Journal of Abnormal and Child Psychology, 36, 745-758.

Dickman, S. J. (1990). Functional and dysfunctional impulsivity: personality and cognitive correlates. *Journal of personality and social psychology*, *58*(1), 95.

Doux Le, Joseph (1996), The Emotional Brain: The Mysterious Underpinnings of Emotional Life, New York: Simon & Schuster. PP.11-27

Elliot, A. J., Maier, M. A., Binser, M. J., Friedman, R., & Pekrun, R. (2009). The effect of red on avoidance behavior. Personality and Social Psychology Bulletin, 35, 365–375.

Elliot, A. J., Maier, M. A., Moller, A. C., Friedman, R., & Meinhardt, J. (2007). Color and psychological functioning: The effect of red on performance attainment. Journal of Experimental Psychology: General, 136, 154–168.

Enticott, Peter G.; Ogloff, James R.P.; Bradshaw, John L. (2006). "Associations between laboratory measures of executive inhibitory control and self-reported impulsivity". Personality and Individual Differences 41 (2): 285–94. doi:10.1016/j.paid.2006.01.011.

Eysenck, M. W. (1982). Attention and arousal: Cognition and performance. New York: Springer-Verlag.

Fillmore MT, Rush CR, Marczinski CA (2003).Effects of d-amphetamine on behavioral control in stimulant abusers: the role of prepotent response tendencies Drug and Alcohol Dependence, 71, 143-152.

Fuller, R. W. (1982). Pharmacology of brain epinephrine neurons. Annual review of pharmacology and toxicology, 22(1), 31-55.

Grossman, R.P. and Wisenblit, J. Z. (1999), "What we Know about Consumers Color Choices", Journal of Marketing Practice Applied Marketing Science, 5 (3) pp.77-89.

Hupka, R. B., Zaleski, Z., Otto, J., Tarabrina, N. V. (1997), "The Colors of Anger, Envy, Fear, Jealousy: A Cross Cultural Study", Journal of Cross-Cultural Psychology 28 (2), pp. 155-172.

Ishihara, S. (1917). Test for Coiour-Blindness. Tokyo: Hongo Harukicho.

Kosslyn, S. M. & Thompson, W. L. (2003), "When in Early Visual Cortex Activated During Visual-Mental Imagery Theory and Meta-Analysis", Psychological Bulletin 129 (5), pp. 722-747.

Logan, Gordon D.; Schachar, Russell J.; Tannock, Rosemary (1997). "Impulsivity and Inhibitory Control". Psychological Science 8 (1): 60–4. doi:10.1111/j.1467-9280.1997.tb00545.x. JSTOR 40062847.

Mathews, A., & MacLeod, C. (1985). Selective processing of threat cues in anxiety states. Behaviour research and therapy, 23(5), 563-569.

Mattila, A and Wirtz, J (2008), "The Role of Store Environmental Stimulation and Social Factors on Impulse Purchasing," Journal of Services Marketing, Vol. 23, No. 1, 562-567.

McShane, C. (1999). The origins and globalization of traffic control signals.Journal of Urban History, 25(3), 379-404.

Moller, A. C., Elliot, A. J., & Maier, M. A. (2009). Basic hue-meaning associations. Emotion, 9, 898–902.

Nigg, Joel T. (2000). "On inhibition/disinhibition in developmental psychopathology: Views from cognitive and personality psychology and a working inhibition taxonomy". Psychological Bulletin 126 (2): 220–46. doi:10.1037/0033-2909.126.2.220. PMID 10748641.

Roberts W, Fillmore MT, Milich R (2011). Separating automatic and intentional inhibitory mechanisms of attention in adults with Attention-Deficit/Hperactivity Disorder .Journal of Abnormal Psychology, 120, 223-233.

Tse, D., Langston, R. F., Kakeyama, M., Bethus, I., Spooner, P. A., Wood, E. R., ... & Morris, R. G. (2007). Schemas and memory consolidation. Science,316(5821), 76-82.

Webster, Christopher D., and Margaret A. Jackson, eds. *Impulsivity: Theory, assessment, and treatment.* Guilford Press, 1997.

Wright, B., & Rainwater, L. (1962). The meaning of color. Journal of General Psychology, 67, 89-99.

## CONTACT

Nicholas Ciccone: ps10n2c@leeds.ac.uk

Stephen Westland: S.Westland@leeds.ac.uk

# Influence of light incident angle and illuminance intensity on visual comfort and clarity

Yinqiu YUAN, Li-Ching CHUO, Hsin-Pou HUANG, and Ming-Shan JENG

Green Energy and Environment Research Laboratories, Industrial Technology Research Institute, Taiwan

## ABSTRACT

This study focused on the influence of the combination of light source position and illuminance intensity on visual comfort for reading/writing. Two psychophysical experiments were conducted in a darkened room, 34 Taiwanese participated as the observers in both experiments. Each of them was asked to perform tasks of writing and reading in varied experimental lighting conditions. Evaluations of lighting quality were made by each observer. The results show that the position of the LED light had a strong impact on the observer response in terms of comfort. Although there was no significant difference in visual clarity between the three tested illuminance levels, 900lx was rated the most comfortable and was mostly preferred among the three illuminance levels.

## 1. INTRODUCTION

A wide variety of factors can affect visual comfort evaluation in an illuminated room, such as illuminance intensity, the correlated colour temperature (CCT), illumination uniformity, glare, colour rendering quality and so on. Enormous efforts have been made in investigating the influence of these factors on perceived visual comfort. For example, Lee (2011) found that the performance of visual accuracy in reading E-paper was best at ambient illumination of 1500lx. Xu and Zhu(1990) found that visual performance decreased as the illumination of display increased. Isono (2004) and his colleagues found that in terms of visual fatigue, there was no significant difference in reading electronic materials and conventional paper materials. Viewing difference and angle can also influence visual comfort. According to Shieh and Lee (2007), it was found that, in reading paper materials, the best viewing distance was at 360mm, which is less than the distance 500mm in reading E-paper. In terms of the effect of viewing angle, Shieh and Lee (2007) reported that the display screen tilted at 29.51 below horizontal eye level was evaluated the most comfortable for reading. Although the previous research findings provided evidence that light source was importance for visual satisfaction, there has been few study to investigate the influence of the combination of light source position and illuminance intensity.

To address the issue, the presented research conducted two psychophysical experiments to investigate the relationship between perceived visual comfort and positions of light source, as well as the effect of illuminance intensity.

## 2. METHOD

To address the issue, two psychophysical experiments were conducted in a darkened room, with a size of 42cm (height) by 222cm (width) by 230cm (depth). Thirty-four Taiwanese (including 17 males and 17 females) participated in both experiments. Half of the

observers were over 175cm and the other half below 165cm.  All of the observers have passed the Ishihara test for colour deficiency.  A same wall-mounted LED lamp was used for  providing experimental lights in both experiments.

## 2.1 Sample Preparation

To investigate the influence of light incident angle on visual comfort in Exp-1, a wall-mounted directional LED luminaire with fixed CCT of 4000K and illuminance of 500lx was used as experimental light.  The position of the lamp can be varied horizontally by changing the angle of an adjustable folding arm that supported the lamp. This resulted in 7 angles of incident light on the writing panel: -24.45, -22.50, -14.40, 0, 14.40, 22.50 and 24.45 degrees, in which the negative angle values mean that the incident light came from the right side above the observer, and positive angle values mean the light came from the left side.  Figure 1 shows the lighting conditions under each of the seven experimental incident angle of light.
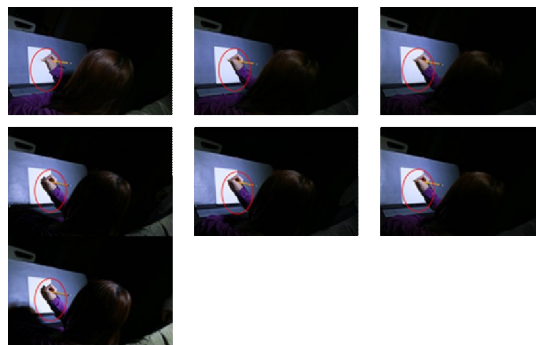


*Figure 1: Lighting conditions caused by the 7 experimental incident angles of light.*

The  light  intensity  of  600lx,  900lx  and  1200lx  were  selected  as  experimental illuminance levels (measured at the centre of reading panel) in Exp-2.  The incidental light angle was fix at 24.50 during the experiment.  The same group of observers took part in the experiment to evaluate visual comfort, preference and clarity for the tested light intensities.

## 2.2 Experimental Procedure

In Experiment 1, each observer performed a writing task on a matt ISO paper placed on a flat panel, with a tilt angle of 45 degrees, lit by a wall-mounted directional LED luminaire with fixed CCT of 4000K and illuminance of 500lx.  This luminaire was positioned above the observer's head and adjustable to achieve varied incident angle of light.  In the experiment, 7 angles of incident light on the writing panel were generated including -24.45, -22.50, -14.40, 0, 14.40, 22.50 and 24.45 degrees.  During the experiment, the observer was allowed to adjust the viewing distance between his/her body and the writing panel as preferred.  The observer was asked to perform a writing task on the panel under each experimental incident angle and give rating for each angle in terms of visual comfort.

In Experiment 2, the incidental light angle was fix at 24.50 which was found the most comfortable angle in Experiment 1.  The illuminance intensity of the lamp can be adjusted by a DC power supply at 600lx, 900lx and 1200lx.  The same group of observers performed a reading task on the same paper and the same panel as in Experiment 1.  Each

observer was asked to evaluate visual comfort, preference and clarity to each of experimental illuminance.

## 3. RESULTS AND DISCUSSION

The significance of influence by gender, observer's height, viewing distance and incident angel of light on visual comfort was analysed using ANOVA. Table 1 shows the results. It is clear that among the four factors, light incident angle had the most significant influence on visual comfort with p-value of 5.13E-12. In terms of significance of effect by gender, observer's height and viewing distance, the results of ANOVA indicate no significant effect was caused by neither of the three factors, with p values being far less than 0.05, Table 1 shows the detailed figures. This suggests that the position of light source can dramatically affect induced visual comfort. Figure 2 demonstrates the trend of the influence. Positive angles means the experimental light source was placed at the observer's left hand side, while negative angles were those of right hand oriented. The perceived visual comfort was found to increase as the angle of incidence becomes larger and larger, indicating a tendency that the observers (all right-handed) felt more comfortable when the lamp was situated on the left hand side than on the right hand side.
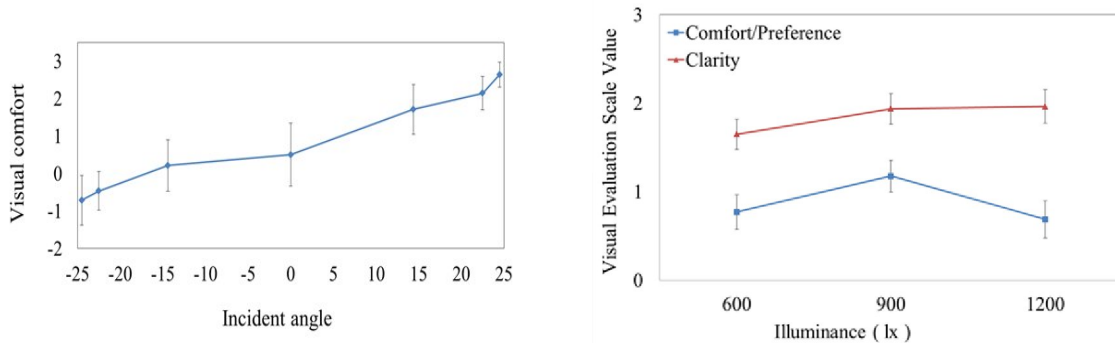


*Figure2*: *Effect of incident angle on visual comfort*    *Figure 3*: *Influence of illuminance intensity on visual comfort/preference and clarity*

In terms of the influence of illuminance intensity on visual comfort, preference and clarity, there was no significant difference between 600lx, 900lx and 1200lx. However, 900lx was rated the most comfortable and preferred intensity among the three tested illuminance levels. In addition, little gender difference and height difference was found in judging visual comfort, preference and clarity affected by illuminance intensity.

*Table 1. ANOVA results for the significance of gender, observer's height, viewing distance and incident angel of lighting for the impacts on visual comfort*

| Dependent Variable： Visual comfort | Source | Gender | Height | Viewing distance | Incident angle |
|---|---|---|---|---|---|
| | Mean Square | 1.143 | 1.829 | 0.008 | 16.104 |
| | F | 0.561 | 0.898 | 0.004 | 7.905 |
| | p | 0.457 | 0.347 | 0.996 | 5.13E-12 |

AIC2015 TOKYO - Color and Image

## 4. CONCLUSIONS

The experimental results show that the position of the LED light had a strong impact on the observer response in terms of comfort. The perceived visual comfort was found to increase as the angle of incidence becomes larger and larger, indicating a tendency that the observers (all right-handed) had higher visual satisfaction when the lamp was situated on the left hand side than on the right hand side. Although there was no significant difference in visual clarity between the three tested illuminance levels, 900lx was rated the most comfortable and preferred among the three illuminance levels. This indicates that uncomfortable illuminance does not necessarily cause a decline in visual clarity. The research result is useful for lighting design in indoor environments.

## REFERENCES

Isono, H., S. Takahashi. , Y. Takiguchi. and C. Yamada. 2004. Measurement of Visual Fatigue from Reading on Electronic Paper. In  IDW 2004,Proceedings,ed. by Niigata. Niigata Convention Center, 1647-1648.

Lee, D. S., Y. H. Ko. , I. H. Shen. and C. Y. Shen. 2011. Effect of light source, ambient illumination, character size and interline spacing on visual performance and visual fatigue with electronic paper displays. Journal of  Displays 32:1-7.

Shieh, K. K. and D. S. Lee. 2007. Preferred viewing distance and screen angle of electronic paper displays. Journal of  Applied Ergonomics 38:601-608.

Xu, W.and Z. Zue. 1990. The effects of ambient illumination and target luminance on colour coding in a CRT display. Journal of  Ergonomics 33:933-944.

*Address: Dr. Yinqiu YUAN, Green Energy and Environment Research Laboratories, Industrial Technology Research Institute, No.195, Sec. 4, Zhongxing Rd., Zhudong Township, Hsinchu County 310, TAIWAN*
*E-mails: AlinaYuan@itri.org.tw, lichingchuo@itri.org.tw, itri451595@itri.org.tw, msjeng@itri.org.tw*

# Colour Terms in the Interior Design Process

Douha Y ATTIAH, Vien CHEUNG, Stephen WESTLAND and David BROMILOW
School of Design, University of Leeds

## ABSTRACT

Colour is a very important topic that interior designers need to consider. Considerable research has been conducted in the area of colour application in interior design; in this study we are concerned with colour terms in interior design, mainly the terms designers use and know about. Fifteen interior designers with varied professional backgrounds, but based in the Middle East (Saudi Arabia, Dubai, Bahrain, Lebanon, Egypt, and Turkey), were interviewed. Previously we reported that fourteen out of fifteen designers stated that colour thinking and decision making take place at the early stages of their design processes; eight of them reported that colour takes place in the first step when meeting clients and starting the project (Attiah *et al.*, 2014). This study documented 137 terms which the fifteen designers use whilst brainstorming and working on a design project; subsequent analysis of these terms could form a basis for understanding how interior designers communicate the abstract properties of colour as part of their design processes. In this paper we show how the 137 terms were categorised according to a framework of four categories of colour terms: emotional, descriptive, cultural and functional. In addition, seventeen words (scientists names and technical terms), which are widely used in colour science (such as: CIELAB, Saturation, Itten) were shown to the designers; their knowledge was shown to be incomplete.

## 1. INTRODUCTION

The field of interior design is an interdisciplinary practice that is concerned with the creation of interior environments to articulate identity and atmosphere through the manipulation of spatial volumes, placements of specific elements, and dealing with special surfaces (Coates *et al.*, 2009). Colour is an important element for both 2D and 3D surfaces of the interior, thus it plays a big role in the aesthetical success or failure of the interior. For this purpose, we are trying to look at the possibilities of enhancing better colour schemes for interiors through enhanced colour communication; hypothesising that some minor execution problems may be due to lack of technical knowledge and ineffective colour communication between designers themselves, designers and public (clients), designers and less-experienced designers, and contractors or working people.

## 2. METHOD

### 2.1 Case Studies

Prior to approaching designers we analysed (Figure 1) three different semi-public interiors in the UK and their colour schemes. The analysis considered colours in every aspect of each interior (colour in lights, materials, and surfaces, etc.) and how all these appear together in the final analysed space. We found that the terms we used in the study need to be categorised for a better discussion, thus we have assigned groups where we found the terms could fall onto four groups: *Cultural, Descriptive, Emotional,* and *Functional*. Table 1 shows the description of each group.

*Figure 1: Three different semi-public interiors in the UK: restaurant (left), hotel lobby (middle) and bar (right).*

*Table 1: Four groups of colour terms category.*

| Groups | Descriptions | Examples |
|---|---|---|
| Cultural | When the colour is used in the interior to depict a certain era or when the colour is inspired or used to show a cultural background. | • renaissance<br>• modern |
| Descriptive | When a scientific colour term or name is used to describe a colour. | • hue<br>• shade |
| Emotional | When the colour is used in the design to convey or leave a certain impact on users' feelings. | • warm<br>• cosy |
| Functional | When the colour is used in the space to create a specific effect such as to make the ceiling higher. | • deep<br>• enlarging |

## 2.2 Interviews

A semi-structured individual interview approach was conducted to try to find out what designers really think, and to prevent designers impacting on each other (as in a focus group). A total of 15 designers were recruited from different cultural backgrounds, age groups, working experiences, and places of work around the Middle East. The duration of each interview was 45-120 minutes for each participant. Data were both qualitative and quantitative and in this study the focus will be on two of the fourteen interview questions, which are described in Sections 2.2.1 and 2.2.2.

2.2.1 Collecting terms

*Name terms you always use in your daily design life/career describing colour choices/decisions/schemes?*

Designers freely expressed the terms that they usually use in their daily professional lives. A total of 137 words were collected (Attiah *et al.*, 2014). The analysis included counting the usage frequencies for frequently-used terms and categorising the terms according to the four groups in Table 1.

## 2.2.2 Testing knowledge

*What do you know about each given term/name. Summarise what you know about each? If not familiar cross the word out.*

Designers were given a sheet of seventeen colour terms (Table 2) and asked to write what they know about each. They were free to cross out what they believe they do not know. For each completed term the responses were categorised as being complete but with ambiguous description (CA), correct but incomplete (P), correct (C) or incorrect (X). Table 3 shows an example for one of the designer's responses.

*Table 2: Seventeen colour terms.*

| Munsell | Colour intensity | Ostwald | Newton | Hue | Colour saturation |
|---------|------------------|---------|--------|-----|-------------------|
| Chroma | Itten | Colour lightness | NCS | CIELAB | Colour value |
| Pantone | RAL system | Colour vividness | Colour temperature | Colour harmonies | |

*Table 3: An example of colour terms answer sheets.*

| Colour terms | Answers | Category |
|--------------|---------|----------|
| Munsell | --- | Do not know |
| Colour intensity | The saturation level of the colour | CA |
| Ostwald | --- | Do not know |
| Newton | --- | Do not know |
| Hue | Black-white shade | X |
| Colour saturation | The intensity of the shade | CA |
| Chroma | --- | Do not know |
| Itten | --- | Do not know |
| Colour lightness | Lighter shade | X |
| NCS | --- | Do not know |
| CIELAB | --- | Do not know |
| Colour value | Within the same colour shades | P |
| Pantone | Graphic design; like RAL | P |
| RAL system | Used a lot with contractors | X |
| Colour vividness | Darker shade | X |
| Colour temperature | Cold vs warm colour | C |
| Colour harmonies | How colours work together | C |

## 3. FINDINGS AND DISCUSSION

### 3.1 Collected terms

The 137 words were analysed for similarity and 76 unique terms were collected. Table 4 lists the 76 terms and their usage frequncies. Warm/cool was the most mentioned term with a frequency of 10.

Table 4: *Collected terms and their usage frequencies (terms with a frequency greater than 4 are highlighted yellow; terms with a frequency greater than 2 are highlighted grey).*

| | | | | | | | |
|---|---|---|---|---|---|---|---|
| accent | 2 | contrast | 3 | harmony | 3 | renaissance | 1 |
| achromatic | 2 | country | 1 | Honest | 1 | saturation | 1 |
| active | 1 | cozy | 2 | hue | 3 | shade | 5 |
| analogous | 2 | dark | 1 | maroon | 1 | shocking | 1 |
| armani beige | 1 | daylight | 1 | metallic | 2 | sophisticated | 1 |
| artificial | 1 | earth tones | 3 | modern | 1 | split complementary | 1 |
| babies | 1 | elegant | 1 | monochrome | 4 | stressful | 1 |
| beiges | 1 | family of colours | 1 | moody | 1 | strong | 2 |
| bold | 2 | fashionable | 2 | mustard | 1 | tetrad | 1 |
| bright | 2 | feminine | 1 | natural | 5 | tint | 4 |
| Brown-scale | 1 | fire | 1 | neutral | 7 | tone | 2 |
| champagne | 1 | flashy | 2 | office/formal | 1 | tone down | 1 |
| childish | 1 | fresh | 1 | pale | 1 | transparent | 1 |
| chroma | 1 | funky | 3 | pastel | 6 | trendy | 2 |
| classic | 1 | gipsy | 1 | posh | 1 | triad | 1 |
| colour scheme | 3 | green design | 1 | powerful | 1 | ultra bright / neon | 1 |
| comfort | 1 | grey-scale | 1 | pewter | 1 | value | 2 |
| complementary | 3 | Happy | 1 | refer to samples | 1 | warm/cool | 10 |
| contemporary | 1 | harmonies | 1 | relaxing | 1 | youth | 1 |

## 3.2 Categorised terms

Table 5: *Categorised terms in the Descriptive, Emotional, Cultural and Functional groups and their usage frequencies (terms with a frequency greater than 4 are highlighted yellow; terms with a frequency greater than 2 are highlighted grey).*

| Descriptive | | Descriptive | | Emotional | | Cultural | | Functional | |
|---|---|---|---|---|---|---|---|---|---|
| accent | 2 | maroon | 1 | active | 1 | classic | 1 | comfort | 1 |
| achromatic | 2 | metallic | 2 | babies | 1 | contemporary | 1 | cozy | 2 |
| analogous | 2 | monochrome | 4 | bold | 2 | country | 1 | elegant | 1 |
| armani beige | 1 | mustard | 1 | childish | 1 | fashionable | 2 | feminine | 1 |
| artificial | 1 | natural | 5 | comfort | 1 | funky | 3 | fresh | 1 |
| beiges | 1 | neutral | 7 | cozy | 2 | gipsy | 1 | green design | 1 |
| bold | 2 | pale | 1 | elegant | 1 | modern | 1 | office/formal | 1 |
| bright | 2 | pastel | 6 | fresh | 1 | renaissance | 1 | sophisticated | 1 |
| brown-scale | 1 | pewter | 1 | funky | 3 | trendy | 2 | | |
| champagne | 1 | refer to samples | 1 | happy | 1 | youth | 1 | | |
| chroma | 1 | saturation | 1 | honest | 1 | | | | |
| colour scheme | 3 | shade | 5 | moody | 1 | | | | |
| complementary | 3 | strong | 2 | posh | 1 | | | | |
| dark | 1 | tetrad | 1 | powerful | 1 | | | | |
| earth tones | 3 | tint | 4 | relaxing | 1 | | | | |
| family of colours | 1 | tone | 2 | shocking | 1 | | | | |
| fire | 1 | tone down | 1 | sophisticated | 1 | | | | |
| flashy | 2 | trasparent | 1 | stressful | 1 | | | | |
| grey-scale | 1 | triad | 1 | strong | 2 | | | | |
| harmonious | 1 | ultra bright / neon | 1 | warm/cool | 10 | | | | |
| harmony | 3 | value | 2 | | | | | | |
| hue | 3 | warm/cool | 10 | | | | | | |

54% of the filtered terms were categorised as *descriptive* according to Table 1. Table 5 summarises the categorised terms. All the fifteen designers included *descriptive* terms. *Functional* terms such as *green design* and *formal* were mentioned the least (10% of the terms were categorised as *functional*). 24% of the terms were categorised as *emotional* and 12% as *cultural*. 44 terms were descriptive, 20 were emotional, 10 were cultural, and 8 were functional. Some terms were put in more than a category, for example: *bold*, *warm/cool*, and *strong* can be both *descriptive* and *emotional*.

### 3.3 Technical colour terms

Table 6 shows the seventeen colour terms and a summary of the frequency responses in each of the categories: complete but with ambiguous description (CA), correct but incomplete (P), correct (C) and incorrect (X).

*Table 6: Summary of responses from technical colour terms.*

| Colour terms | CA | P | C | X | Do not know |
|---|---|---|---|---|---|
| Munsell | 0 | 2 | 3 | 0 | 10 |
| Colour intensity | 9 | 0 | 0 | 5 | 1 |
| Ostwald | 0 | 1 | 1 | 0 | 13 |
| Newton | 0 | 2 | 2 | 2 | 9 |
| Hue | 0 | 0 | 5 | 6 | 1 |
| Colour saturation | 6 | 0 | 0 | 6 | 0 |
| Chroma | 1 | 0 | 0 | 2 | 9 |
| Itten | 0 | 1 | 1 | 0 | 13 |
| Colour lightness | 1 | 4 | 1 | 9 | 0 |
| NCS | 0 | 0 | 0 | 0 | 15 |
| CIELAB | 0 | 0 | 0 | 1 | 14 |
| Colour value | 0 | 3 | 3 | 4 | 5 |
| Pantone | 0 | 1 | 5 | 3 | 6 |
| RAL system | 0 | 0 | 3 | 1 | 11 |
| Colour vividness | 1 | 1 | 1 | 5 | 7 |
| Colour temperature | 0 | 0 | 12 | 2 | 1 |
| Colour harmonies | 0 | 0 | 13 | 0 | 2 |

As shown in Table 6, the terms that received the most correct responses were colour temperature (12 out of 15) and colour harmonies (13 out of 15). Most other terms wee poorly understood. The least known terms were: NCS, CIELAB, Itten and Ostwald (15, 14, 13 and 13, respectively, out of 15 do not know). Ambiguity was shown mainly between colour saturation and intensity.

In terms of the four groups in Table 1, this study has shown that designers in the Middle East mostly use descriptive colour terms in their daily profession. However, their technical knowledge of colour terms and names, was found to be weak or incomplete in all but a few cases. This does not mean that the knowledge on all colour terms in this study is necessary for achieving well-chosen colour schemes. The findings therefore show a potential need for better technical colour knowledge in relation to design in the region.

# 4. CONCLUSIONS

Paterson (2003) suggested that any attempt to define or describe colour by means of words is doomed to failure; whereas we believe that an efficient verbal communication and knowledge on colour can result in better interior setups consequently. Although some of the colour terms in this study (such as Itten, Ostwald and Newton) may not have an impact on the colour choices in the design process, and indeed we previously found that most of these designers prefer to get inspired when thinking of the colours than sticking to a theory (Attiah *et al*, 2014), good technical knowledge on precise colour descriptions such as intensity, saturation and hue will enable effective colour communications. This study led us to rethink if designers' knowledge needs to be rethought of in the region, and if we can suggest a framework for designers for better colour and design discussions using the resulted categories (Table 2). A future study can include comparing Middle-East participants' results and Western designers' (for example, in the UK and USA).

## REFERENCES

Attiah, D.Y., Cheung, V., Bromilow, D. and Westland, S. 2014. *Colour planning in the interior design process*, Proceedings of The Second Conference of Asia Color Association, 187-191, Taipei, Taiwan.

Coates, M., Brooker, G. and Stone, S. 2009. *The Visual Dictionary of Interior Architecture and Design*. AVA publishing.

Paterson, I. 2003. *A Dictionary of Colour*. Thorogood publishing Ltd.

*Address: Douha Attiah, School of Design, University of Leeds, Leeds LS2 9JT, UK*
*E-mails: sd10dya@leeds.ac.uk, t.l.v.cheung@leeds.ac.uk,*
*s.westland@leeds.ac.uk, d.bromilow@leeds.ac.uk*

# Effects of Classroom Wall Color on Students

Fazıla DUYAN,   Rengin ÜNVER
Faculty of Architecture, Yıldız Technical University

## ABSTRACT

It is a known fact that properties of physical environment act as stimulus and affects student's behavior and learning performance. The physical environment factors playing significant roles in achievement and reaching educational goals are size, heat, sound, light, color. In this paper, the results of an experimental research study which investigates preferences of 8-10 years-old subjects on their classroom's wall colors will be presented. Five colors (5R 7/8, 5Y 7/8, 5G 7/8, 5B 7/8, 5P 7/8) were selected by using Munsell Color System. The students have had lessons under different wall color in five weeks. The preferences of students were collected by surveys for each wall color.

## 1. INTRODUCTION

Effects of stimuli generated by physical properties such as volume, dimensions, temperature, sound, color and light on occupants emotions, behavior and performance is a well-known fact. In this respect, the effect of color, as one of the primary physical environmental elements of classrooms where the majority of learning takes place, on students is obvious. Therefore, a research project entitled "The Effect of Lighting and Color Schemes on Student's Performance in Classrooms of Primary School" had been initiated. This research has been supported by Yıldız Technical University Scientific Research Projects Coordination Department. Project Number: 2013-03-01-DOP01. The project consists of three basic stages.

- Determination of students' personal and classroom wall color preferences using color samples,
- Determination of students' preferences by painting classroom walls,
- Determination of the effect of classroom wall colors on student performance.

In this paper, studies to determine classroom wall color preferences of student groups between the ages of 8-10 by means of applying different colors on classroom walls, which is the second stage of the research project, will be explained. The findings made at this stage of the research will enable data gathering that would be instructive providing students with more pleasing educational environments, in terms of "surface color" which is one of the physical environmental elements.

## 2. METHOD

Procedures followed, on the second stage of "The Effect of Lighting and Color Schemes on Student's Performance in Classrooms of Primary School" research project, by painting classroom walls to determine 8-10 ages student preferences can be briefly listed as follows:

- Selection of the primary schools.
- Identification of classroom wall colors and application on the walls.
- Determination of classroom color preferences through surveys.
- Assessment of survey results.

The research has been conducted with different socio-cultural and economic backgrounds, in two elementary schools, one of which is a state school and the other is a private school at same location in Istanbul. 18 girls and 25 boys from the Private School, 21 girls and 13 boys from the State School, in total 77 students have been participated. All students were tested for color vision deficiencies prior to participation using Ishihara color vision test. In order to prevent the color of classroom equipment influencing the color of the walls, benches and panels were wrapped with dark medium gray (N 5/0) clothes and classroom cabinets covered with cartons of the same color. The lamps that were used in the present luminaries had been replaced with fluorescent lamps with higher color rendering index (Ra). Colors that were selected for the study had been applied on the walls for 5 consecutive weeks. The surveys were carried out on 10th March-11st April 2014. Students underwent their education in a different wall colors each week and preference surveys were conducted at the end of each week.

## 2.1. Identification of classroom wall colors

Results, obtained from the survey conducted to determine classroom color preferences at the first stage of the project, were used in the second stage. Value and chroma for selected colors remained constant and hue has changed according to Munsell Color System. Five wall colors that were going to be used in research on the second stage of the project are red (5R 7/8), yellow (5Y 7/8), green (5G 7/8), blue (5B 7/8) and purple (5P 7/8).

## 2.2. Application of Determined Colors and Preference Tests

Chosen five colors were applied to the classrooms during weekends and students were trained for the duration of the week. On the last day of the week (Friday) students were given a classroom wall color preference survey. In order to rate participant's preferences, a ten step Likert-type scale was used, ranging from 0 (disliked) to 9 (strongly liked). The sample pictures are shown in Figure 1 and 2.



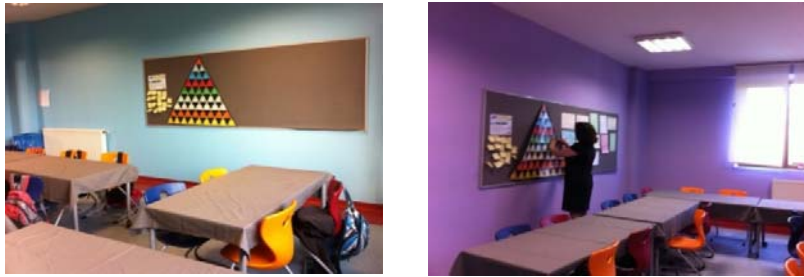*Figure 1: Red, Yellow and Green Classroom*

*Figure 2: Blue and Purple Classroom*

## 2.3. Assessment of Survey Results

Data collected from surveys to determine preferences of student groups 8 to 10 years of age on colors applied to classrooms are studied in five groups as given below:

- Girls (private and state)
- Boys (private and state)
- Private school (girl and boy)
- State school (girl and boy)
- All students (girl and boy; private and state school)

Scores are given in terms of ratings from 0 to 9 on Likert-type scale as the average responses of students and shown in Table 1:

*Table 1. Preference Scores of Students*

|  | GIRLS | BOYS | PRIVATE SCHOOL | STATE SCHOOL | TOTAL |
|---|---|---|---|---|---|
| **RED 5R 7/8** | 6,62 | 5,61 | 4,74 | 7,74 | 6,06 |
| **YELLOW 5Y 7/8** | 6,10 | 6,82 | 6,44 | 6,47 | 6,45 |
| **GREEN 5G 7/8** | 7,00 | 7,34 | 6,42 | 8,12 | 7,17 |
| **BLUE 5B 7/8** | 7,54 | 8,53 | 8,12 | 7,91 | 8,03 |
| **PURPLE 5P 7/8** | 7,95 | 6,37 | 6,53 | 7,97 | 7,17 |

**Girl preference results:** In both schools girls have stated their classroom wall color, all five color pretty close to each other. The purple wall color was preferred the most and the yellow the least (Table 1 and Figure 3).

**Boy preference results:** Red turned out to be the least preferred color in both schools, whereas blue turned out to be the most preferred. Second to the most preferred color was green wall color. Red was the least favored wall color (Table 1 and Figure 3).

**Private school (girl+boy) preference results:** As seen in Table 1 and in Figure 4, private school students liked the color blue the most. Average rating given by students to color blue is 8,1. Blue wall color is followed by purple (5P 7/8), yellow (5Y 7/8) and green (5G 7/8.) Red wall was the least liked color among students with a rating of 4,47 points (Figure 4).

**State school (girl+boy) preference results:** Color preferences at the State school, green took the first place, followed by blue, purple and red with close scores (8,12 to 7,74 points). The least preferred color was yellow with 6,47 points (Table 1 and Figure 4).
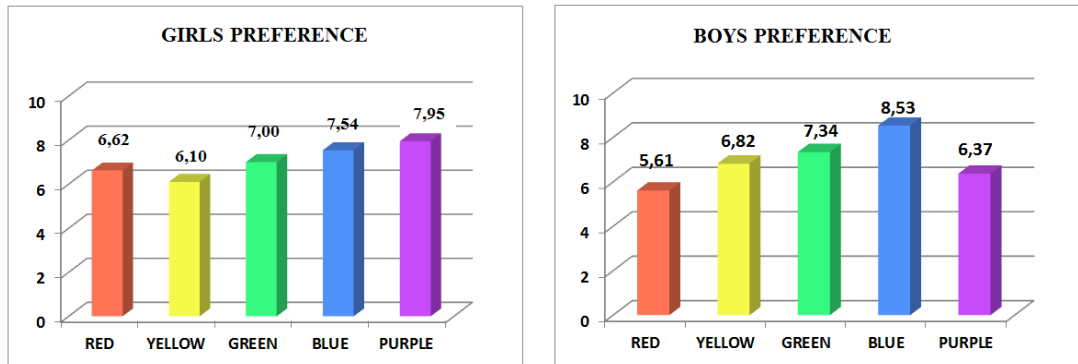


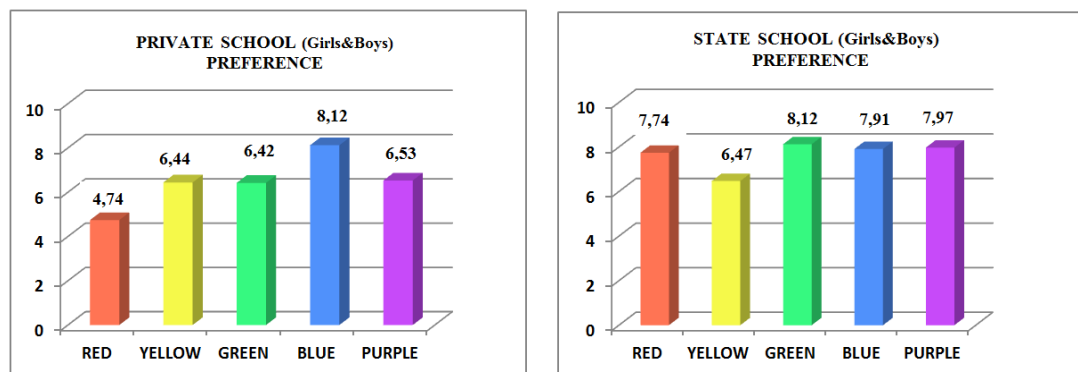*Figure 3: Female and Male Classroom Wall Preference Results*



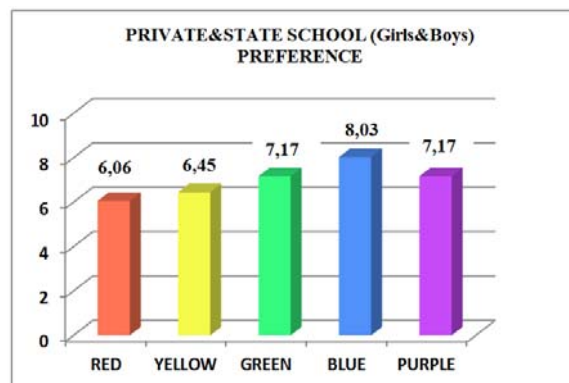*Figure 4 : Private and State School (Girl&Boy) Classroom Wall Preference Results*



*Figure: 5. Total Classroom Wall Preference Results*

**All students (boy&girl; private school & state school) preference results:** The preference results for all the students participated are seen in Table 1 and Figure 5. According to these results blue with a score of 8,03 is the most preferred color. Blue is

followed by purple and green with the same score of 7,17. The least preferred color is red with a score of 6,06.

## 3. CONCLUSION

In order to determine 8-10 years old students' classroom color preferences, five different colors were applied each week successively and a survey was conducted each week. Collected data was evaluated by gender (girls and boys), by school (private and state) and by sum of both gender and schools. Results could be summarized as follows:

- In both schools, purple was preferred the most and yellow the least by girl students. While blue is the most preferred and red is the least preferred color among boys. Girls rated blue with a high score that is close to purple's.
- On school basis, while private school students liked the blue most and red the least, state school students preferred green the most and yellow the least. State school students rated red higher in contrast to private school students.
- Blue is the most preferred color in both private and state schools and by both genders while red is the least preferred color.

In this research where student preferences are gathered, the highest inclination had been towards blue in every group. In this research conducted with 3rd grade elementary school students, it has been concluded that participants are most pleased studying in an environment painted blue (5B 7/8).

In order to enable the primary school students to receive education in a happier environment, the results from the first stage of the project and from the consequent similar studies should act as a guideline for the school headmasters and designers who have an important role in classroom color prefer all.

## REFERENCES

Baytin, Ç., A. Kıran, M. Tunbiş 2005. Colour Preferences in Architectural Design Studious. *Architectural Science Review*, University of Sydney, 48(4) 317-328.

Schloss, K. B., E. D. Strauss, S. E. Palmer 2013. Object Color Preferences, *Color Research and Applications,* 38(6) 393-411.

Park, J. G. P. 2014. Correlations between Color Attributes and Children's Color Preferences, *Color Research and Applications*, 39 (5) 452-462.

Wang, H., R. R. Randall 2008 Computer Classroom Wall Colour Preference and They Relationship with Personality Type of College Students, *Colour, Design & Creativity*, 4 (2) 1-13.

*Address: Prof. Dr. Rengin Ünver, M.Sc Fazıla Duyan,*
*Yıldız Technical University, Faculty of Architecture, Unit of Building Physics,*
*34349, Beşiktaş-Istanbul, TURKEY,*
*E-mails: faziladuyan@gmail.com, renginunver@gmail.com*

# A Study on the Evaluation Process of Facade Colour Parameters

Esra KÜÇÜKKILIÇ ÖZCAN, Rengin ÜNVER
Yıldız Technical University

## ABSTRACT

Contemporarily, many material alternatives for facades has been emerged due to the improvements in the building and material technology along with the increased painting opportunities. Thus an excessive range of façade colours appear in cities causing inharmonious colour appearances and colour pollution in settlements. To avoid any inappropriate situations due to colour pollution in the design process, building façade colours should be determined considering factors such as architectural and environmental (natural and built) features as well as colour perception. Therefore, a systematic façade colour design approach for various scales including all the stages has been developed as a Research Project at Yıldız Technical University. This paper basically prepared with the aim of introducing the developed façade colour design approach which is constituted of several stages, mainly includes a detailed analysis of the first stage of the Research Project.

## 1. INTRODUCTION

Façade colour is one of the most important factors affecting the architecture of the building and the appearance, image / identity of the settlements. Therefore, any decision about the façade colour of a building changes the appearance and image of both the building and its environment. Contemporarily, many material alternatives for facades has been emerged due to the improvements in the building and material technology along with the increased painting opportunities. Furthermore, in the design process façade colour is being determined according to the likes, preferences and personal desires of architects, occupants, employers, etc. without caring the environmental parameters and colour perception factors in practice. Thus, an excessive range of façade colours appear in cities causing inharmonious colour appearances and colour pollution in settlements.

To avoid any inappropriate situations due to colour pollution in the design process, building façade colours should be determined considering factors such as architectural and environmental (natural and built) features as well as colour perception. But in practice, complex relationships of related factors constitute a major problem for the colour designers, architects, etc.

There are a range of important studies examining the façade colour design and the effects of related environmental and perceptional factors but the holistic approaches for the whole façade colour design process are very limited. Therefore, a systematic façade colour design approach for various scales including all the stages of urban master colour plan has been developed as a Research Project entitled "An Aproach to Façade Colour Design". This research has been supported by Yıldız Technical University Scientific Research Projects Coordination Department. Project Number: 2013-03-01-DOP02. This paper basically prepared with the aim of introducing the developed façade colour design

approach which is constituted of several stages, mainly includes a detailed analysis of the first stage of the Research Project.

## 2. APPROACH FOR FAÇADE COLOUR DESIGNING

While preparing urban colour plans, general criteria involving the whole settlement and appropriate colour designs need to be done. Colour planning criteria show similarities for all settlements. But every settlement has a unique architecture, natural and built environments, total area, population, building intensity and distribution, and these particularities show diversities from each other. Various particularities of the settlements create differences in generating urban colour plans. When considering these varieties, for considerably big, complex and constantly evolving cities like Istanbul, preparing master colour plans involving all the buildings in the city, requires very detailed and hard work.

In this research project, which began following these informations, it is needed to improve an Approach for Façade Colour Designing in preparing urban master colour plans. The project has been started with determining the main procedures for the urban colour planning process according to the Approach for Façade Color Designing. Therefore, Approach for Façade Color Designing is thought to consist of four basic phases. These phases are listed as:

a. Determining regions (district, quarter, neighborhood, square/street) and buildings of the settlement that have priority in making the colour design.

b. Making the environmental colour analysis of urban regions and buildings

c. Determining and evaluating the particularities affecting the colour perception of urban regions and buildings

d. Making colour proposals for urban regions and buildings

Since this paper is limited, only the first one of the above mentioned phases is explained in details.

## 3. DETERMINING REGIONS AND BUILDINGS THAT HAVE PRIORITY IN COLOUR DESIGNING

Although colour planning criteria are similar in new and current settlements, since the particularities of the current settlements are various and independent from each other, it is difficult to determine the colour planning criteria and this requires more detailed studies. Therefore, particularly in big settlements, beginning with the determination of regions and buildings having priority in colour designing and creating an evaluation system to fasten the process would be useful in colour planning preparations. But, determining this priority depends highly on many factors as socio-cultural structure, economic structure and aesthetic features. In this study, assuming that the main role in cityscape is obtained by buildings, the priority in colour designing is thought to be determined by "effects of urban regions and buildings on cityscape".

For this purpose, an evaluation system called "Degrees of Affecting the Cityscape" (DAC) has been created in order to determine the regions and buildings having priority in colour designing. This evaluation system helps measuring the building and the region it is part of. After setting the evaluation system in general, some criteria regarding the features

of regions and buildings that affect the cityscape are determined. Subsequently, a questionnaire (public survey) has been realized in order to measure the influence degrees of the regions and buildings on the cityscape and prioritize these criteria.

## 3.1 The Evaluation System on Measuring Influence Degrees of Regions and Buildings on Cityscape

The flow diagram of the evaluation system for determining the degrees of affecting the cityscape is fundamentally set from urban scale to building scale (from macro scale to micro). However, after many examinations, it is found that the environmental factors in the phases from urban scale to neighbourhood scale are very different from the factors in the phases from neighbourhood scale to building scale. Therefore, the influence evaluation system (DAC) is limited within neighbourhood scale and building scale (from middle scale to micro) and presented in Figure 1.

After setting the evaluation system in general, some criteria regarding the features of regions and buildings that affect the cityscape are determined. Some literature examinations are made for the criteria in question, and after these examinations, criteria regarding effective regions and buildings in cityscape are determined and evaluated in details. In this context, the main criteria determined to establish the neighborhood, square/street, road, building ect. Having priority in colour designing process, are handled in two main groups as region scale and building scale (Table 1). Nine criteria for each group, thus totally 18 criteria, and subcriteria for each criterion, are generated.
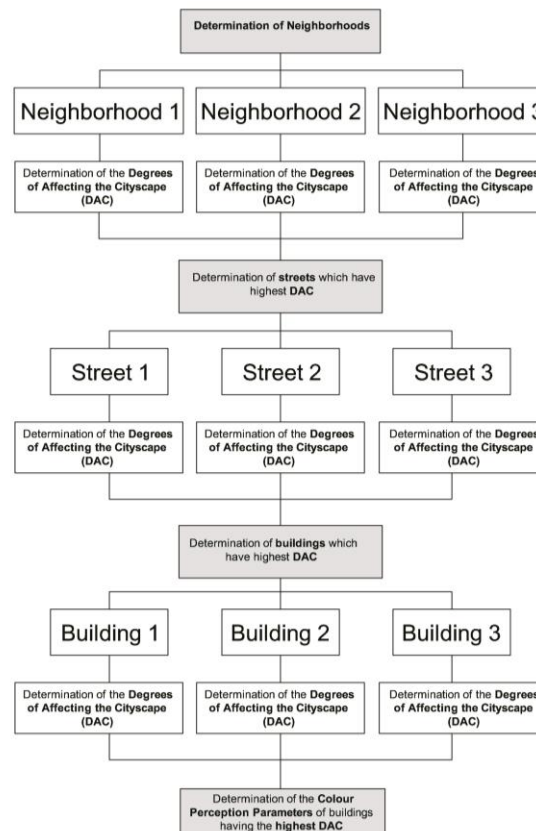


*Figure 1: The phases of the fundamental method about determining the degrees of affecting on cityscape of urban regions and buildings*

*Table 1. Criteria regarding the groups : region scale and building scale*

| Basic Criteria for region Scale | | Basic Criteria for Building Scale | |
|---|---|---|---|
| 1 | Architectural qualification | 1 | Architectural qualification |
| 2 | Building heights | 2 | Effect on environmental scape-Height |
| 3 | Effect on environmental scape | 3 | Effect on environmental scape-Width |
| 4 | Function | 4 | Function |
| 5 | Presentational effect | 5 | Presentational effect |
| 6 | Symbolic quality | 6 | Symbolic quality |
| 7 | Location in the city | 7 | Location |
| 8 | Topography | 8 | Façade material |
| 9 | Building intensity | 9 | Building colour |

### 3.2 Survey Study

In order to determine the degrees of affection of regions and buildings on cityscape via the criteria decided to establish the prior regions and buildings in colour designing and presented in Table 1, a public survey has been realized.

There are totally 24 questions in this questionnaire. In the questionnaire, under every question regarding city region, building and environmental factors, there are various criteria and each participant has been asked to answer the question by rating every criterion based on Liekert Scale. In five degrees rating prepared according to Liekert Scale, expressions as "not effective at all, a little effective, effective, fairly effective, very effective" are used and each expression is related to a point, such as "not effective at all – 1 point; a little effective – 2 points; effective – 3 points; fairly effective – 4 points; very effective-5 points".

The participants are mostly architects and city planners as well as other professions which are closely involved in the subject. Information about age, education status, profession and etc. are given in Table 2.

*Table 2. The quantity and percentage (proportion) regarding personal information of the participants of the questionnaire*

| Personal Information | | Quantity/Number |
|---|---|---|
| **Sex** | Female | 61 |
| | Male | 39 |
| **Age** | 22-40 | 73 |
| | 40-55 | 17 |
| | 55-70 | 10 |
| **Education status** | University degree | 29 |
| | Master | 38 |
| | PhD | 33 |
| **Profession** | Architect | 67 |
| | Civil Engineer | 12 |
| | City planner | 10 |
| | Other | 11 |

Results obtained by the questionnaire are separately analysed and numerically evaluated for each question and criterion. Since the basic criteria are high in number, and thus not so easily evaluated directly, in evaluating the basic criteria the "method of factor analysis" through the SPSS 15.0 Computer Statistics Program has been used. The analysis for region and building scales are separately realized for each basic criterion. In order to determine the basic criteria on building scale, a four factor groups' analysis has been made with the evaluation of all the participants. In this four factors group analysis, in the 1st factor group there are respectively criteria of façade material and colour; in the 2nd factor group there are respectively quality, height, presentational effect; in the 3rd factor group there are respectively architectural qualification and location in the city; in the 4th factor group there are function and effect on environmental scape-width.

Following these results, in order to determine the regions and buildings that have priority in façade colour designing, basic criteria present in the 1st and 2nd factor groups of the region and building scales are decided to be taken into consideration. Speaking more clearly, basic criteria given in Table 3 are determined as the most effective features of regions and buildings that have affects on city/urban region scape and within the Evaluating System created for determining the regions and buildings that have priority in façade colour designing, subcriteria of these basic criteria are used to evaluate the degrees of affecting the cityscape.

*Table 3. Basic Criteria to be Used for Determining the Influence Degrees of Regions and Buildings on Cityscape*

| **Region Scale** | **Building Scale** |
|---|---|
| Building heights | Façade material |
| Building intensity | Colour |
| Topography | Symbolic quality |
| Function | Effect on environmental scape-Height |
| Architectural qualification | Presentational effect |

In order to determine the degrees of affection the cityscape by regions and buildings, the points given for subcriteria of the basic criteria in the questionnaire are summed, then divided by the number of the participants and thus the points according to Liekert Scale are obtained for each criterion. The features of urban regions and buildings shall be evaluate according to the points obtained and the priority in colour designing for these regions and buildings shall be done according this grading system.

## 4. CONCLUSION

A successful colour design can be obtained by examining appropriately each scale of the city, streets, squares, urban regions and the city itself, examining natural and built environments, many factors and data regarding visual perception and colour planning. In this context, colour master plans for every settlement should be prepared following the basic colour planning criteria.

Within the research project entitled "Approach for Façade Colour Designing", of which general features and its first phase are presented in this paper, in the preparation of colour master plans process, studies relevant apparoach for façade colour designing are still going

on. Other data obtained in several phases of the approach, are going to be presented in subsequent publications.

## REFERENCES

Küçükkılıç Özcan, E. and Ünver, R. 2014. *Yerleşimlerde Yapı Yüzü Renk Tasarımına Yönelik Bir Yaklaşım Önerisi*, Mimarlık Dergisi 379 60-65 (in Turkish).

Buether, A. 2014. *Colour Design Principles Planning Strategies Visual Communication*, An Edition Detail Book Institut für Internationale, ISBN 978-3-920034-96-6.

Ünver, R. and Dokuzer Öztürk, L. 2002, *Toplu Konutlarda Yapı Yüzü Renk Tasarımında Temel İlkeler ve Öneriler*, Yıldız Teknik Üniversitesi Araştırma Fonu Bitirme Raporu, Proje No: 99-03-01-02 (in Turkish).

*Address: M.Sc Esra KÜÇÜKKILIÇ ÖZCAN, Prof. Dr. Rengin ÜNVER*
*Yıldız Technical University, Faculty of Architecture, Unit of Building Physics*
*34349, Beşiktaş, Istanbul, TURKEY*
*E-mails: esrakucukkilic@gmail.com, renginunver@gmail.com*

# Correlation between Personal and Classroom color Preferences of Children

Rengin ÜNVER,  Fazıla DUYAN
Faculty of Architecture, Yıldız Technical University

## ABSTRACT

The appearance and perception of colors make a strong impact on us in our daily lives. Our emotions, actions, perceptions, performances and health are influenced by colors of the environment. The color preferences of people differ based on the objects they use and spaces they live in. As people age, their tastes and choices evolve in years, which results in a change in their color preferences. In the related literature, there are various studies about color preferences but subjects of these studies are usually adults and children's color preferences studies are limited.

In this context, a research has been realized to investigate the correlation between the personal and classroom wall color preferences of children. 74 girls and 78 boys, in total 152 corresponding to the age group of 8-10 have participated in the survey. In the study, 10 hues having different values and chromas, in a total of 84 different colored samples were used and "personal color preferences" and "classroom wall color preferences" of children were determined through a survey. This paper aims to explain the method and findings of the research.

## 1. INTRODUCTION

Educational environments, especially classrooms where students spend a large part of the day have a significant impact on students' lives. As other physical components in an environment, it is a fact that colors of classroom affects students' performance and behaviors. However, classroom colors are determined by school managers or designers and students' preferences and opinions are not considered.

Therefore, in 2013, a research project entitled "The Effect of Lighting and Color Schemes on Student's Performance in Classrooms of Primary School" was started. This research has been supported by Yıldız Technical University Scientific Research Projects Coordination Department. Project Number: 2013-03-01-DOP01. The project was constructed in three parts; determination of personal and classroom wall color preferences of students using colored samples, determining personal and classroom wall color preferences of students using colored samples, determining students preference of the painted classroom walls in different colors and determining the effect of classroom wall colors on performance of students.

This paper presents the findings of the first step of this research project, which consists of the studies conducted for determining personal and classroom wall color preferences of students' in the age group of 8-10, using colored samples.

## 2. METHOD

The method of the first step of the research entitled "The Effect of Lighting and Color Schemes on Student's Performance in Classrooms of Primary School" can be summarized follows:

- Selection of the primary schools.
- Identification of the colors that are used in the personal and classroom color preferences.
- Determination of individual and classroom color preferences through surveys.
- Evaluation of survey results.

Two primary schools (private and state) in the same district of Istanbul were selected. The students in the private school have better social, cultural and economic conditions than the public school. 33 girls and 38 boys from the private school, 41 girls and 40 boys from state school, in total 152 students participated. Before the survey, the color vision deficiencies of the students were tested using an Ishihara Color Vision Test. The surveys were carried out in their classrooms on 1-13rd December 2013. Each student had spent approximately 20 minutes for the surveys. Average illuminance (daylight+artificial lighting) level on the working plane in the classrooms was 350-450 lux. The desks were covered with a matt grey cloth.

## 2.1. Identification of the Colors that are used in the Personal and Classroom Color Preferences.

84 colors selected for the determination of students color preferences in the survey was constructed taking into consideration findings from the first survey that was realized in 2012 with 119 (60 girls, 59 boys) students (Duyan and Unver, 2013). Principally, Hue, value and chroma dimensions of selected colors were determined by using Munsell Color System.

*Tablo 1. Munsell Color System Notations for Colors.*

| HUE (Munsell) | VALUE/SATURATION | | | | HUE (Munsell) | VALUE/SATURATION | | |
|---|---|---|---|---|---|---|---|---|
| **5R (5R)** **RED** | 9/2 | | | | **5BG (55)** **BLUE-GREEN** | 9/2 | | |
| | 8/2 | | | | | 8/2 | 8/4 | |
| | 7/2 | 7/6 | 7/10 | | | 7/2 | 7/6 | 7/8 |
| | 6/2 | 6/6 | 6/10 | 6/12 | | 6/2 | 6/6 | 6/8 |
| **5YR (15)** **ORANGE** | 9/2 | | | | **5B (65)** **BLUE** | 9/2 | | |
| | 8/2 | 8/6 | 8/8 | | | 8/2 | 8/4 | |
| | 7/2 | 7/6 | 7/10 | 7/12 | | 7/2 | 7/6 | 7/8 |
| | 6/2 | 6/6 | 6/10 | | | 6/2 | 6/6 | 6/8 |
| **5Y (25)** **GREEN** | 9/2 | 9/6 | 9/10 | 8/12 | **5PB (75)** **PURPLE-BLUE** | 9/2 | | |
| | 8/2 | 8/6 | 8/10 | | | 8/2 | 8/6 | |
| | 7/2 | 7/6 | 7/10 | | | 7/2 | 7/6 | |
| | 6/2 | 6/6 | | | | 6/2 | 6/6 | 6/10 |
| **5GY (35)** **GREEN-YELLOW** | 9/2 | 9/6 | 8,5/10 | | **5P (85)** **PURPLE** | 9/2 | | |
| | 8/2 | 8/6 | 8/10 | | | 8/2 | 8/4 | |
| | 7/2 | 7/6 | | | | 7/2 | 7/6 | 7/8 |
| | 6/2 | 6/6 | | | | 6/2 | 6/6 | 6/8 |
| **5G (45)** **GREEN** | 9/2 | | | | **5RP (95)** **RED-PURPLE** | 9/2 | | |
| | 8/2 | 8/6 | | | | 8/2 | 8/6 | |
| | 7/2 | 7/6 | 7/10 | | | 7/2 | | |
| | 6/2 | 6/6 | 6/10 | | | 6/2 | | |

In this context, in terms of hue, 10 hues (5R, 5YR, 5Y, 5GY, 5G, 5BG, 5B, 5PB,5P, 5RP) having different values and chroma, in a total of 84 colors were decided to use. Lower values were not selected in the previous survey (2012) by the students, therefore 6 and upper values were used in this survey. Chroma of colors were determined between 2 and 10 or 12 which are followed each other four step. For equal size in perceptual color differences, 1:4 was used as the ratio of units for value and saturation in the study according to the recommendations in the literature. Thus, values were selected as 6,7,8,9

and saturation determined as 2, 6, 10 or 12. The Munsell notations of the colors are given in Table 1.

Colored samples which were used in the study were generated using gouaches. Then the samples were measured by spectrophotometer. The colored samples were prepared in two different dimensions (Small: 3,5 x 3,5 cm; Big: 7x7 cm). The small size samples were pasted and grouped on grey cartons (N 5/0, size A4) for the same hue and 10 different hue pages were arranged. The big size colored samples were pasted on grey cartons (N 5/0, size B5) and 84 different samples were obtained. Some examples of the colored samples used in the surveys are given in Figure 1.
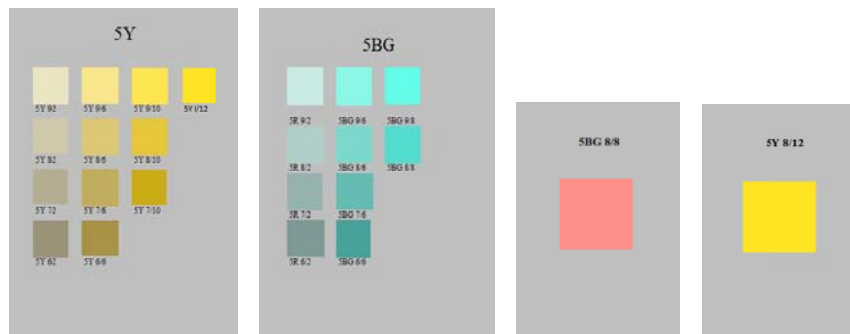


*1a: Hue page samples*          *1b:Big sized samples*
*Figure 1: Color Samples*

## 2.2.    Determination of Personal and Classroom Wall Color Preferences

Two-step process for determining the color preference was carried out. In the first step, 10 different Hue pages (size: A4) were shown to the subjects and asked to choose one color from each Hue pages and to note on the survey page. In the following step the chosen samples were presented as Big size (7x7 cm, B4) and the subjects were asked to select their most favorite color. This process was repeated both personal color and classroom wall color preferences (Figure 2).



*Figure 2:  Pictures from Survey*

## 3.   EVULATION of SURVEY RESULTS

The data obtained from surveys were examined in three parts; girls, boys and total (girl& boy).

### 3.1. Results of Personal Color Preferences

**Girls Personal Color Preferences:** The first preference of 74 girls in total on the personal color are 5P 7/8 purple (11%) and 5RP 8/9 red-purple (11%). Second most preferred colors are 5P 6/8 purple and 5R 7/8 red at the same rate (9%). Third preferred color is 5BG 7/8 blue-green. According to the results, girls tend to the red, purple as shown in Figure 3.

**Boys Personal Color Preferences:** Boys prefer strongly 5B 6/8 blue in 21%. Then they prefer 5BG 7/8 blue-green, 5PB 6/10 purple-blue and 5R 6/12 red at the same rate (8%). Based on the results, boys tend to the bluish colors.
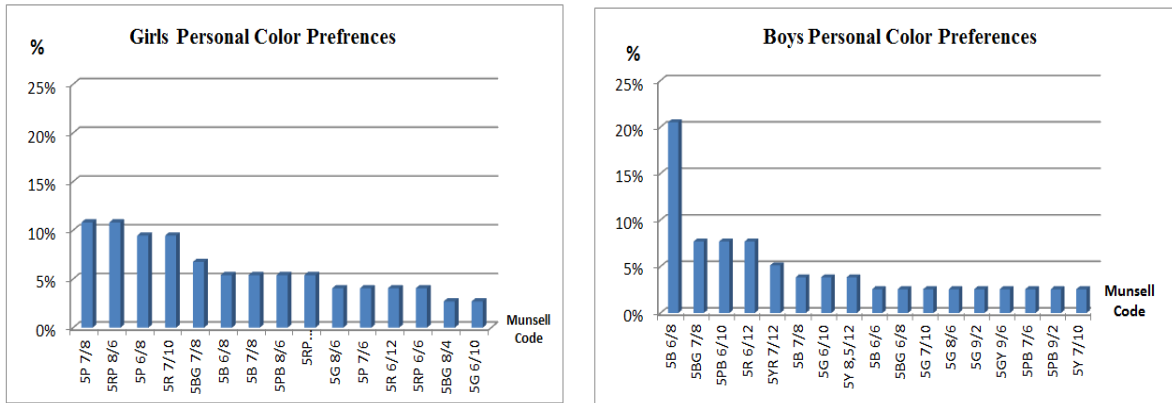


*Figure 3: Girls and Boys Personal Color Preferences*

**Girl and Boy Students Personal Color Preferences:** In total, both genders prefer mostly 5B 6/8 at 13% rate. The second most preferred color is 5BG 7/8 blue-green (7%) and the third one is 5R 6/12 red (6%). Girls prefer 5B 6/8 blue at a 5% rate. The blue color BG 6/8 was the first most preferred color because it was selected by a high rate of boys.
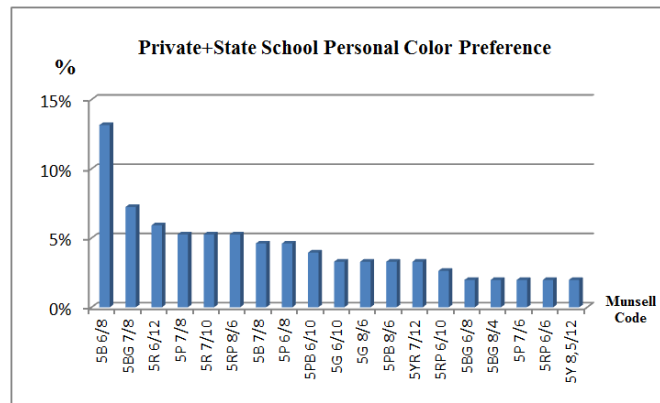


*Figure 4: Personal Color Preferences (Private & State)*

### 3.2. Results of Classroom Wall Color Preferences

**Girls Classroom Wall Color Preferences**: Classroom wall color preference of girls are in respectively 5 RP 6/10 red (8%), 5GY 8/10 green-yellow (5%), 5P 7/8 purple (5%) and 5RP 9/2 red-purple (5%).

AIC2015 TOKYO - Color and Image

**Boys Classroom Wall Color Preferences:** Most preferred color of boys for classroom wall color of boys is 5B 6/8 blue (12%). Second preferred colors are 5B 7/8 blue (6%) and 5YR 7/12 orange (6%).
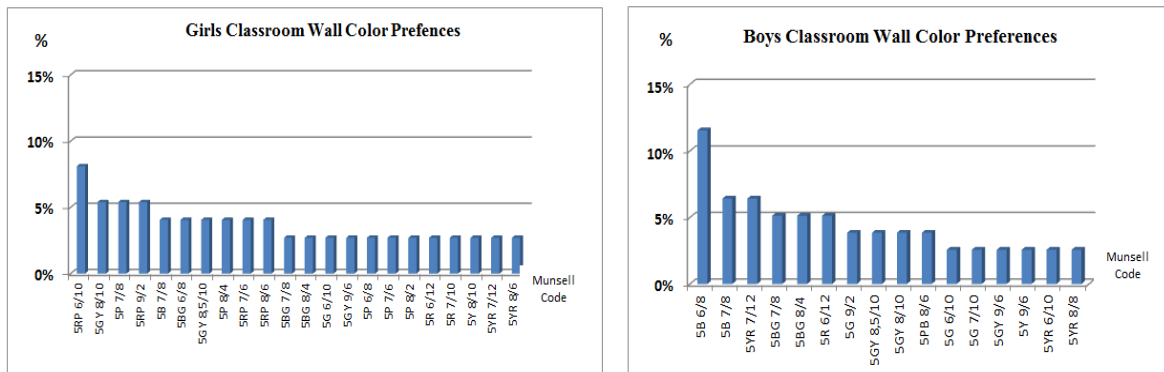


*Figure 5: Girls and Boys Classroom Wall Color Preferences*

**Girls and Boys Students Classroom Wall Color Preferences:** As shown in Figure 6, a total of 152 students' most preferred wall color is 5B 6/8 at the 6% rate. 5B 7/8 blue, 5GY 8/10 green-yellow, 5RP 6/10 red-purple and 5YR 7/12 orange follow to 5B 7/8 blue at the 5% rate.
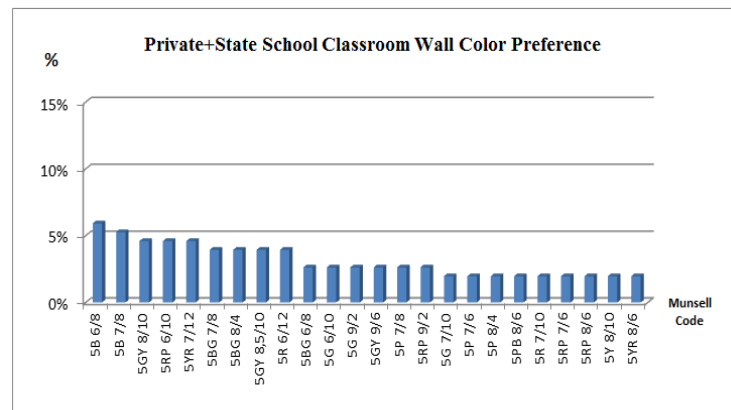


*Figure 6: Girls and Boys Classroom Wall Color Preferences*

## 4. CONCLUSION

The first, second and third preferences on the personal and classroom wall color results are given in Table 2 as girls, boys and total. According to the findings, girls prefer mostly red, purple hues on personal color preference. Whereas, boys prefer strongly blue. As personal color preference, both of the two genders preferences focus in blue

As classroom wall color preference, girls focus in order to red-purple, green-yellow, purple and red-purple. Boys significantly tend to 5B 6/8 blue as wall color preferences. Second preferred colors are 5B 7/8 blue and 5YR 7/12 orange sharing at the same rate. In total (girls and boys), the first preferred color is 5B 6/8 blue where the high rate of boys choosing this color is a determinant. The second, preferred color is shared between 5B 7/8, green-yellow, red-purple and orange.

*Table 2: Distribution of the Preferences on the Individual and Classroom Colors.*

| Preference | PERSONAL | | | | | | | | | | | | CLASSROOM WALL | | | | | | | | | | | |
|---|---|---|---|---|---|---|---|---|---|---|---|---|---|---|---|---|---|---|---|---|---|---|---|---|
| | GIRLS | | | BOYS | | | TOTAL | | | GIRLS | | | BOYS | | | TOTAL | | |
| | Munsell Code | Color | % | Munsell Code | Color | % | Munsell Code | Color | % | Munsell Code | Color | % | Munsell Code | Color | % | Munsell Code | Color | % |
| **1.** | 5P 7/8 | | 11 | 5B 6/8 | | 21 | 5B 6/8 | | 13 | 5RP 6/10 | | 8 | 5B 6/8 | | 12 | 5B 6/8 | | 6 |
| | 5RP 8/9 | | 11 | | | | | | | | | | | | | | | |
| **2.** | 5P 6/8 | | 9 | 5BG 7/8 | | 8 | 5BG 7/8 | | 7 | 5GY 8/10 | | 5 | 5B 7/8 | | 6 | 5B 7/8 | | 5 |
| | 5R 7/10 | | 9 | 5PB 6/10 | | 8 | | | | 5P 7/8 | | 5 | 5YR 7/12 | | 6 | 5GY 8/10 | | 5 |
| | | | | 5R 6/12 | | 8 | | | | 5RP 9/12 | | 5 | | | | 5RP 6/10 | | 5 |
| | | | | | | | | | | | | | | | | 5YR 7/12 | | 5 |
| **3.** | 5BG 7/8 | | 7 | | | | 5R 6/12 | | 6 | | | | | | | | | |

As a result of the findings, in both personal and classroom wall color preferences, girls liked to warm color like red, purple hues. The boys tended to blue (5B 6/8) in both personal and classroom wall color preferences. In total, the students preferred 5B 6/8 blue as a first color in both personal and classroom wall color preferences. Consequently, it can be said that there is a parallel correlation between personal color preference and classroom wall color preference of students.

**REFERENCES**

Baytin, Ç., A. Kıran, M. Tunbiş 2005. Colour Preferences in Architectural Design Studious. *Architectural Science Review*, University of Sydney, 48(4) 317-328.

Duyan F., R. UNVER 2013. A Study on Individual and Classroom Color Preferences of Children between the Ages of 8-10. *In AIC Color 2013, Proceeding*s, ed.

Schloss, K. B., E. D. Strauss, S. E. Palmer 2013. Object Color Preferences, *Color Research and Applications,* 38(6) 393-411.

Park, J. G. P. 2014. Correlations Between Color Attributes and Children's Color Preferences, *Color Research and Applications*, 39 (5) 452-462.

Wang, H., R. R. Randall 2008 Computer Classroom Wall Colour Preference and They Relationship with Personality Type of College Students, *Colour, Design & Creativity*, 4 (2) 1-13.

*Address: Prof. Dr. Rengin Ünver, M.Sc Fazıla Duyan,*
*Yıldız Technical University, Faculty of Architecture, Unit of Building Physics,*
*34349, Beşiktaş-Istanbul, TURKEY,*
*E-mails: renginunver@gmail.com, faziladuyan@gmail.com*

# Research on the Coexistence of Color between Buildings and Exterior Advertising that Create a Cityscape
## ~ focusing on the Okamoto district of Kobe ~

Yoshihumi TAKAHASHI[1], Ikuko NARITA[2]
[1]Hosei University Graduate School of Regional Policy Design
[1]Couwa Sign Co. Ltd.
[2]Sense Up Planning. Ltd

**ABSTRACT**

In line with the Landscape Act of 2004, the Exterior Advertising Code was revised. At the same time, a new principle was put into place which includes not only improving aesthetic and scenic beauty but also the overall creation of a more favorable cityscape. There are a number of issues addressed by the Exterior Advertising Code, such as illegal signboards, restrictions on surface area, as well as delaying the rules to adjust to rapid growth in technology. Furthermore, in order to improve the cityscape, there is an increase in color restrictions being placed throughout the country. Indeed, many municipalities have implemented restrictions on color of high chroma for signboards. But could the solution be that simple? There should be a way to create an even better and more attractive cityscape by incorporating the colors of exterior advertising. Therefore, we reconsidered and studied the possibilities of a coexistence between the colors of buildings and exterior advertising. The survey was conducted by focusing on a mixed commercial and residential area in the Okamoto district of Kobe, Japan. We conducted a fact-finding survey on the colors of buildings and exterior advertising in the district, as well as a meeting with the Beautiful City Okamoto Council that drew up "The Exterior Advertising Rules and Guidelines." As a result, we found out that with respect to the regional style of the buildings throughout the entire district, some cityscapes are actually being harmonized with the colors of signboards.Therefore, it is conceivable that the colors of signboards do not prevent a landscape from forming scenic beauty, yet rather become an important factor for beautification. This form of cityscape was even supported by the the local residents themselves, who led the town planning over many years to formulate the guidelines for conforming the colors of exterior advertising.

## 1. INTRODUCTION

In line with the Landscape Act of 2004, the Exterior Advertising Code was revised. At the same time, a new principle was put into place which includes not only improving aesthetic and scenic beauty, but also the creation of a more favorable cityscape. According to Article 2 in the Exterior Advertising Code, the exterior advertising is "displayed outside in public permanently or a certain period of time and is presented on signboards, standing signboards, billboards, noticeboards, buildings and other structures and those similar thereto. "The Exterior Advertising Code itself does not contain detailed regulations. Thus, specific regulations are mostly determined by each municipality. This can be observed as a preceding example of decentralization. (Koide and Anpu 2007: 9-15). Once local authorities have become a part of landscape administrative bodies, they are then allowed to set up regulations on exterior advertising independently. This enables them to adapt suitable advertising in accordance with the local characteristics of their region. There is a lack of accumulated

research on the standard measurements regarding the control of exterior advertising. Therefore, even the municipalities that have a positive attitude towards the utilization of exterior advertising for the improvement of the cityscape find themselves in a cycle of trial and error. On top of this, there are a number of conflicting issues regarding exterior advertising, such as illegal signboards, restrictions on surface area that do not take regional character into account, as well as delaying the adjustment of rules in accordance with rapid growth in technology. In regards to colors, there is an increasing number of color restrictions placed throughout Japan with the aim to create a more satisfactory cityscape. A number of areas have implemented restrictions on color of high chroma for signboards. But could the solution be that simple? There should be a way to create an even better and more attractive cityscape by incorporating the colors of exterior advertising. Therefore, we reconsidered this principle and studied the possibilities of a coexistence between the colors of buildings and exterior advertising. The investigation was conducted in the Okamoto district of Kobe, the area of the Beautiful City Okamoto Council that drew up "The Exterior Advertising Rules and Guidelines" and have been taking an active part in utilizing exterior advertising for beautification.

## 2. METHOD

The study method we performed involves a quantitative color analysis of the Okamoto district of Higashinada-ku, Kobe-shi. Based on the results from the survey, we examined how the coexistence of colors between buildings and exterior advertising influence the quality of cityscape color. We also studied the initiatives of the local residents who led town planning over many years in order to formulate the guidelines for conforming the colors of exterior advertising. Lastly, for the survey of the actual color condition, we employed a visual colorimeter supervised by Japan Color Research Institute. The survey was then conducted from 10:00 to 15:00 in August, 2014.

## 3. RESULTS

### 3-1 Community Development of the Beautiful City Okamoto Council

The Beautiful City Okamoto Council was formed on September, 1982. According to the community development agreement of Okamoto district, the area includes the entire area of 1-chome Okamoto, Higashinada-ku, Kobe-shi and a part of 5-chome Okamoto and 3-chome Kitamachi, Honzan. The Beautiful City Okamoto Council established rules such as, "Community Development," to form a community that allows citizens to play a part in making decisions about their own city. It has been over thirty years since the establishment of the council and the cityscape in Okamoto has shown a dramatic change.

In recent years, the soaring land prices have accelerated the increase in national chain stores, while the number of privately-owned local shops continues to decline. This is indeed the case in Okamoto city, whose cityscape of common signboards is being infiltrated by the growing number of stores that are putting up unnecessarily gaudy and thoughtless signboards with harmful colors. Due to these factors, in 2009 the authorities of Okamoto city began research for the formation of "The Exterior Advertising Rules and Guidelines for Okamoto." This set of rules was finally approved at the 32nd general meeting in 2014.The rules outline that signboards are an indispensable element of what construct the cityscape. This also explains that signboards that harm the beautiful landscape are unsuitable for the city and will be restricted under the rules.

Moreover, "The Exterior Advertising Rules and Guidelines for Okamoto" aims to increase suitable signboards for the overall image of Okamoto. Attractive signboards should enhance the city's charm so that citizens will be even more proud of their city – in turn, this would eventually make the city more appealing for outside visitors as well.

There are three keywords that symbolize the universal elements and essential values of the city of Okamoto. These are the following: open sky, Mt. Rokko, and stories told by unique paved stones. Naturally, colors significantly influence these images. Considering these aspects, Okamoto city determined the suitable colors for exterior advertising as a way to maintain its fine cityscape. The city took on the positive challenge to place the colors of signboards in a way where they can coexist with the founding characteristics of the city.

Through the hearing surveys provided, various measures have been taken, such as the publishment of the quarterly magazine, "Beautiful Town Okamoto," and a signboard contest that follows with the purpose of drawing up "The Exterior Advertising Rules and Guidelines." These were all conducted to specifically visualize how the city should appear. The hearing surveys revealed that it takes steady efforts and enthusiasm to achieve successful community development.

### 3-2   The color investigation result of the Okamoto district

We performed the color investigation of the Okamoto district. We analyzed it with the quantitative investigation into outer wall (79 places) of the building and outdoor advertising goods (219 places) and grasped the characteristic of the color.

### 1) The color investigation result of buildings

We measured the color of the outer walls of 79 buildings. As a result, a building of the hue of YR and Y accounts for 60%. About the value, 8-9, 50% and less than 3 are 7%. About the chroma, 1-3, 63% and 4-6, 14% and 7-13, 0% and 14 are 1%. Achromatic color accounts for 22%, but black isn't and white is 13%. There are a lot of YR and Y of the high value and the low chroma overall. Light beige, white and gray of the high value are admitted the local color of this district.
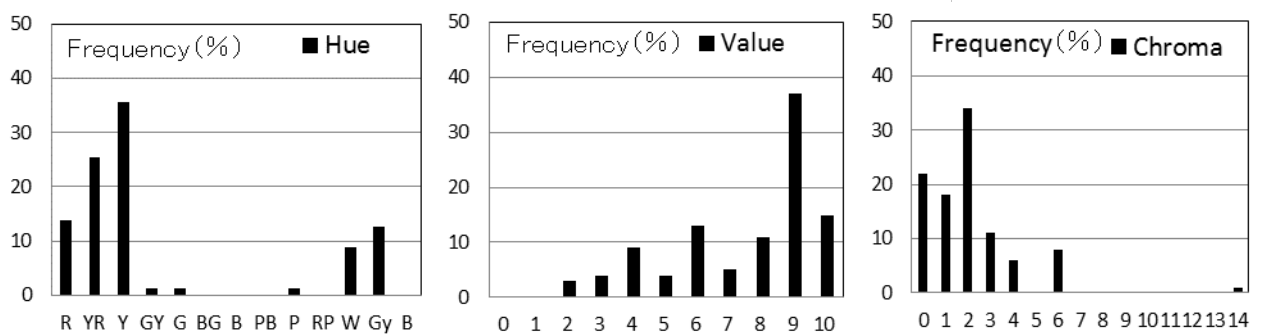


*Figure 1: Color distribution map of buildings*

## 2) The color investigation result of exterior advertising

We measured the color of exterior advertising goods of 219 places. As a result, it was white (29.2%) that there was the most. It accounts for 47.5% only by achromatic color. There are a lot of R (14.6%) and YR (8.7%) by chromatic color. Low and medium value is 43.9%. The medium and high chroma accounts for 35.1%. There are a lot of achromatic color, vivid red and orange for the feature of the overall color.
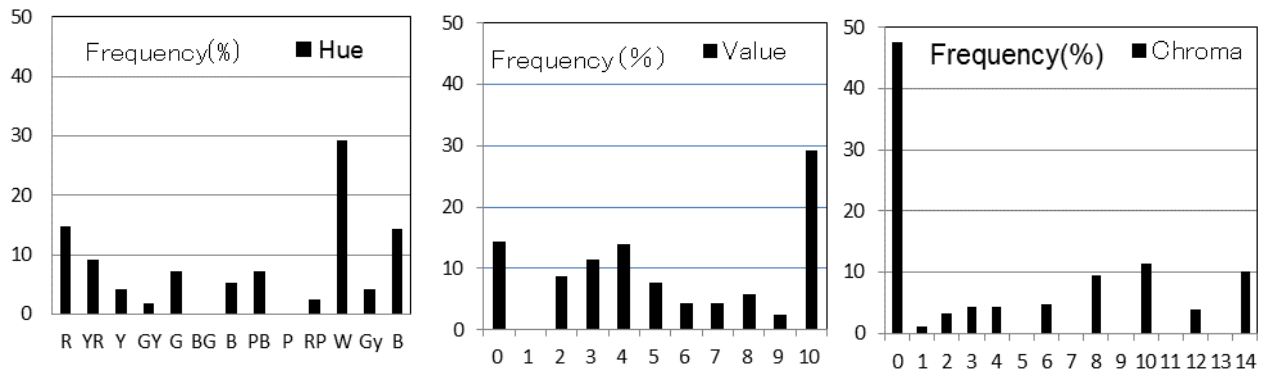


*Figure2: Color distribution map of the exterior advertising goods*

## 3) The features of the colors in Okamoto district

We found out that the local color of the building is admitted clearly. A commercial store and housing are intermingled in this Okamoto district. We can think a possibility that the color of the exterior advertising goods influences the quality of the color landscape in this whole district is high. A color of medium-high chroma is used for most of colors of the outdoor advertising goods backed by the white that is a local color.

Because the use area of those colors is small, the color of the outdoor advertising goods is accent color. In the Okamoto district we can recognize it to be a local color including the color of the outdoor advertising goods as well as buildings.

## 4. CONCLUSION

In the Okamoto district, the signboard colors harmonize with the building colors that were already established in the whole city over the years. That means exterior advertising colors have naturally and successfully created a part of the cityscape without becoming detrimental. We can conclude that this achievement was only made possible through the tremendous effort put forth by the local initiatives of The Beautiful City Okamototo Council, who have successfully made an ideal city come true.

AIC2015 TOKYO - Color and Image

# REFERENCES

Koide K, and H, Anpu. 2007. *Munincipal Activities for Exterior Advertising and Hereafter*. Urban City + Design. 26 : 9-15.

*Address: Yoshihumi TAKAHASHI,*
*Hosei University Graduate School of Regional Policy Design,*
*Couwa Sign Co. Ltd.,*
*2-19-11 Matsugaoka, Nakano-Ku,Tokyo, 165-0024, JAPAN,*
*E-mails: ytaka0502@gmail.com*

# Colour management in the colour design process

Per JUTTERSTROM
NCS Colour AB

## ABSTRACT

Colour management in the colour design process in all manufacturing industries are changing due the development in technology and the change of needs from the end customers. With todays widely available colour measurement technology there are no secrets when it comes to the colour shades used by different industries as well as paint companies. Also with the higher demands from the end customers to expect the availability of any colour they want, the number of colours are escalating for different products in general, and for the coatings industry in particular, with number of colours exploding in the paint companies databases often with the consequences that colours are more or less visual identical but having different names.

By taking a more holistic approach to the management of colours in the colour design process and using a scientific system as a platform there are many benefits when it comes to make the colour design process more efficient and by doing that to save time and money in the management of colours. The starting point in that process is how to make a useful analysis of existing colours, both with digital applications as well as visual adjustments and comparisons with other colours on the market with the aim to develop a range that can deliver all the colours that is necessary for a market success.

This will also result in quality improvements and a more understandable offering of the colour range to the end customers.

This paper will present some case studies examining the importance of this holistic approach in the colour design process and how that result can be developed into more useful colour collections.

## 1. WHAT IS COLOUR?

According to my built in dictionary on this computer where this paper is written, colour is "the property possessed by an object of producing different sensations on the eye as a result of the way it reflects or emits light". We can all agree that colour is a visual sensation, that it makes us able to navigate in our daily life, orientate and make social statements by picking certain colours for our clothes, our homes, our cars or any other items.

## 2. NEED FOR COLOUR SYSTEM

Since colour is something that we as a human beings can see, a colour system should be based on visual perception. There are several systems for colours on the market, some of them based on colour research in different professional areas, not only in technical meanings, but also historical, social and psychological, physical etc., while others are basically collections based on purely commercial aspects or spun from technical processes

AIC2015 TOKYO - Color and Image

such as tinting colours in different substrates.

Colour systems can be described by their purpose and can be divided into different levels of sophistication. The most basic of the colour systems are simply different collections of colours. The German RAL Classic is a clear example of such a "system", or to be more precise - a collection of colours. RAL is a collection of popular colours that are frequently used in the industrial area. Each colour has an unique four digit number to identify them (e.g. RAL 1003 etc.), however this number does not tell or give the user any added information about the actual colour, it is just an identification. Other collections such as British Standard could be added to this category.

The next level includes the system that has a production driven purpose. This could be tinting systems for tinting machines, or RGB for computers, Pantone for print etc., where colours also gives the information how it is mixed.

The most sophisticated level of colour systems are those based on colour perception and on scientific research. NCS (Natural Colour System) is one of those systems, the American Munsell is an other one and also, the no longer on the market, DIN (Deutsche Industrie Norm) system. Common for those systems are that they are all visually based, with a spectrum that covers the colour space and with some kind of logical steps where the relation of the colours can be described. This is also reflected in their way to notate the colours. There is actually a correlation between the name and the actual colour we can see.
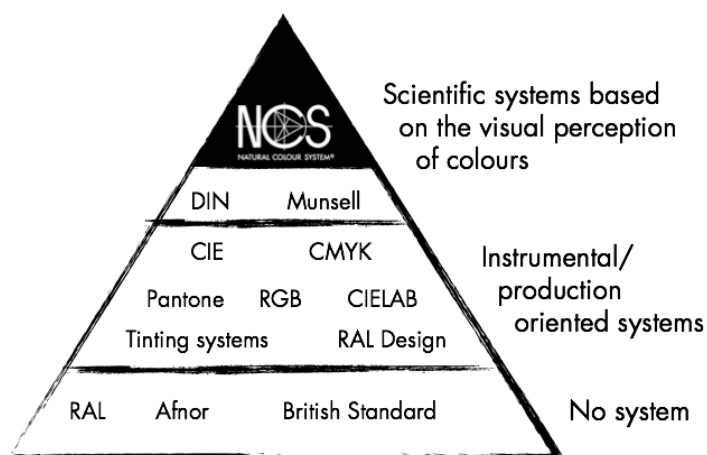


*Figure 1. To illustrate the different levels for colour systems and collections on the market.*

## 3. THE HOLISTIC APPROACH

With the globalized economy of today with the demand of quicker design processes and with outsourced production of the products to foreign countries the management of colours are more critical than ever.

Since there is no international standard for colours and manufacturing companies and industries are competing with the colour range on the market, the management of the colours are usually a big part of the design and production process. For manufacturing of products the colours are usually the most difficult part to manage when it comes to

accuracy and consistency. Often with the result that the "same" colour appears different due to different materials and application techniques.

For the paint industry this often results in overlapping colours, e.g. colours that are basically the same but with different names and notations, which also creates a situation where it is difficult to manage the issues of, colour accuracy and consistency in the production. It also makes it difficult to get a holistic view from marketing, sales and production point of view.

## 4. CASE STUDIES

By taking a holistic approach in the design process and using a visual based colour system, the management of colours can be done in a more simplified way, no matter if there are just a few colours for a range of products or a more extensive range for a paint industry.

### 4. 1. Product manufacturer

A manufacturer of household goods used to have 50 different colours for their range of products. The products were produced in different materials and applications such as powder coating, industrial coating, plastics, vinyl etc. with the result of difficulties to manage the wide range of colours and materials in terms of accuracy and consistency.

By comparing the used colours with the colours from competitors on the market and make an analysis and illustrate this in a visually based colour system, the company were able to reduce the number of colours from 50 down to only 6 but with a maintained strong offering to the market in terms of good and useful colours. It also made them able to differentiate from the competitors and make huge savings in the management process of their colour range.
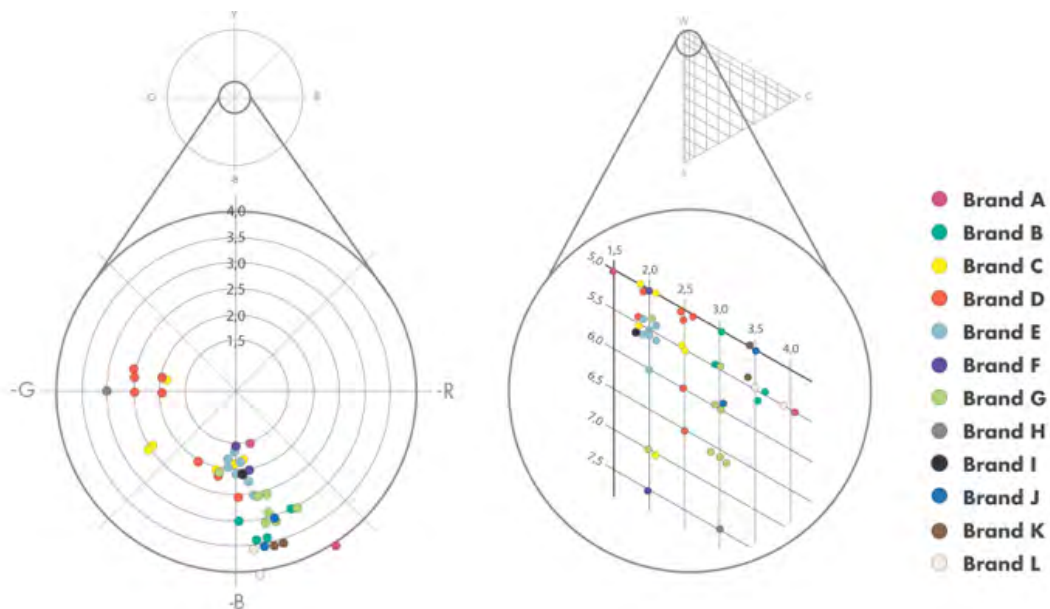


*Figure 2. Comparisons for different producers of household goods and how the colours are located in the NCS colour system*

## 4. 2. Paint producer

With the introduction of automatic tinting machines in the decorative coatings business, the options for the customer have dramatic increased in number of shades.

As a walk in customer in a paint shop, we expect the shop to be able to present and instant deliver a wide range of different shades. We also expect to be guided with colour sample material so we can see with our own eyes how the final colour will look like. Sometimes we also bring a piece of painted material that we would like to find the very same colour for, or a colour that goes well with it. Because of the possibilities in the modern tinting technology and the implementation of information technology, paint shops can carry thousands of formulas for different shades and quality of products. Not only for the brand that the shop sell, but also for other common colour collections on the market with competitors selections etc.

A mid sized decorative paint producer in the Middle East took the decision a few years ago to update their colour range and to get away from the clutter and overlapping colours in their tinting system. The primarily used fan deck was the Nova colour card with approx. 2000 colours with some additional influx from other fan decks such as British Standard, RAL, NCS, competitors etc. resulting in a database with more than 5000 formulations. The aim was be better represented in the colour space and cover more areas and give the end customer a better range of colours that is considered to be richer even though the number of colours are less.

By taking all the these different colours and using a visual based colour system as NCS, the ground work was to illustrate the range of the colours and identify areas where there were overlapping colours as well as areas with missing colours.

By mapping all the colours all those areas were easily identified and it made it possible to refine the colour range in a more efficient way.
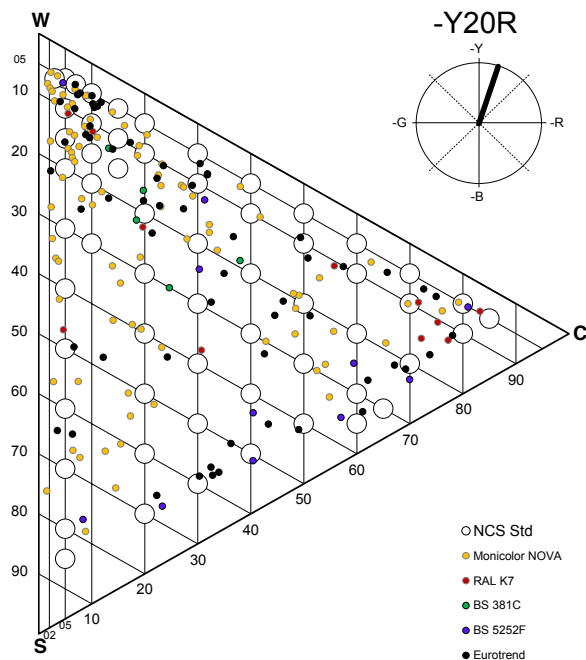


*Figure 3: Different colour cards measured and notated into a visual colour system that gives the ability to see the correlation between the colours and how they actually are related.*

By then identify the most important areas, a new range of colours could be developed that meet the demand from the market as well as create a more useful range.
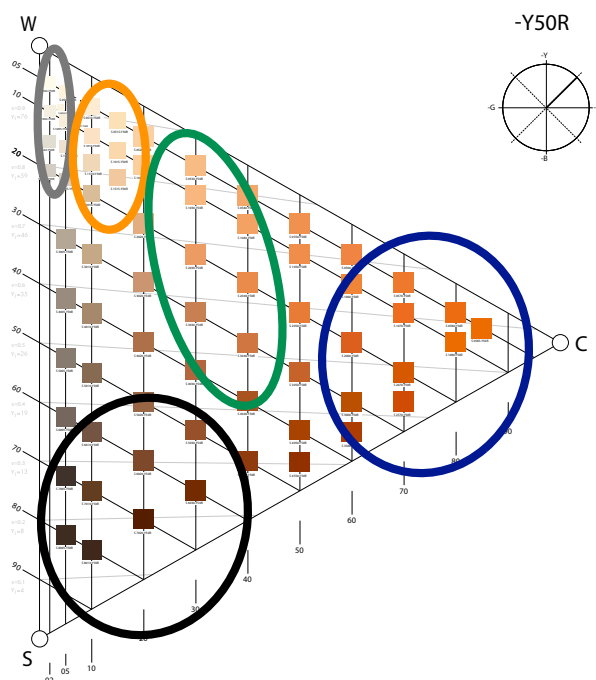


*Figure 4: Areas that needed to be included in the new range.*

This work ended up in a new collection with 915 colours, all carefully selected and with an even distribution in the colour space, eliminating overlaps and creating a more comprehensive range for the market.

By making this reduction, this paint producer was able to increase their efficiency and cut time and costs in the handling of different formulations.

## 5. CONCLUSIONS

Modern technology in the productions process gives infinity possibilities of different colour shades on manufactured products or in paint. However, from both a customer point of view and for the management of the production and handling for the producer, the huge number of colours will not really add any benefits in the end. Instead customers are more helped with less clutter and a more balanced colour range.

Customers want more options, but they also need guidance and a straight offer for their colours.

The challenges manufacturing industries as well as the coatings industry is to optimize their offering, by using advanced technical systems but also to benefit from colour systems based on visual perception – since colour is something we all can see.

# REFERENCES

SIS (Swedish Standards Institution). 2004. *NCS Colour Atlas, Swedish Standard SS 019102*, Stockholm.

Hard A, Sivik L, Tonnquist G. 1996. NCS Natural Color System – from Concept to Research and Applications, Part I and II. *Color Reserach & Application*, Volume 21, Number 3, June 1996.

Bergström B. 2008. *Colour Choices – A practitioner´s guide to colour scheming and design*. Formas.

Hard A, Sivik L. 1977. Distinctness of Borderline Related to the Natural Color System. In *Proc of the 3rd AIC Congress, Color 77, Bristol*: Adam Hilger Ltd.

Hard A, Sivik L. 1978. Distinctness of Border as a Measure of Color Contrast - Effects of background color and border length. Report to BFR.

Hard A, Sivik L, 1983. Distinctness of border -A concept for a uniform color space. *Fackskrift nr F27*. Scand. Color Inst, Stockholm

Hard A, Sivik L, 1986. Distinctness of border: An alternative concept for a uniform color space. *Color Research and Application*, Vol.11, No.2.

Hard A, Sivik L, 1976. Distances between Colours - A Comparison of Different Structures, *Göteborg Psychological Reports*, Vol. 6, No. 7. (also in Edberg, G. (ed) Gruppen för Arkitekturpsykologi Symposium, nr 4, KTH, Stockholm, 1974.)

Hard A, Sivik L. 1977. Methodological Studies of Color Changes Due to Distance and lighting: Direct Assessment Using the Natural Color System. In *Proc of the 3rd AIC Congress, Color 77, Bristol*: Adam Hilger Ltd.

*Address: Per Jutterstrom*
*NCS Colour AB, PO Box 49022, 100 28 Stockholm, Sweden*
*E-mail: per.jutterstrom@ncscolour.com*

# Exploring combinations of color patterns in Nature

Akemi YAMASHITA,[1] Naoko TAKEDA,[2]
[1] Okayama Prefectural University
[2] Tecnológico de Monterrey

## ABSTRACT

In recent years the philosophy of Biomimicry is increasing, Nature is a result of many years of evolution, provides us an infinitely rich combination of wisdom and beauty. Observing, exploring and imitating Nature's best strategies we can obtain innovating ideas to solve any kind of needs and problems. That is why many researchers of any field of science and art base their studies on its creations.

We find the Lepidoptera (butterfly and moth) egg, caterpillar and its metamorphosis from pupa to adult, a source of inspiration with a great potential for achieving results to be applied in product and graphic design.

The focus of this research is the study of some species that have bright colors to flaunt in the context they are, in the other hand some that pass unnoticed by its neutral colors. Information as the color and graphic patterns of egg, larvae, pupa and butterflies and moths are collected from many source to obtain a comparative graphical table of pattern color combination. The objective is to design a palette of color patterns as a tool useful to do original creations for graphic and industrial design products, convenient for daily life and suitable to different environments as hazardous, quiet, modern, classical, cheerful, sporting to mention some. In this occasion we design some foldable umbrellas and their covers.

## INTRODUCTION

Through the development of technology, in these days, the population living in artificial environment as cities is increasing, away from Nature. The coexistence with animals, plants, insects, is more and more difficult. It is reflected as a recent incident in Japan, covers for elementary school notebooks that had been featured with photographs of insects for long time, have been recalled because they are no longer familiar to children, even more they are considered as ugly beings.

One fundamental principle of nature is the optimization of resources, obtaining more with less. Specialists consider that Nature respond with functions according to the context that defines them, in the most economical manner. So, in nature there are no coincidences, every form, structure, movement, texture, odor, color, reaction has a reason.

Butterflies and moths are just an example of what marvelous the Nature is, of course the complete metamorphosis they undergo, but also the birth of larva from egg, their transformation to caterpillar and then to pupa.

Lepidoptera is one of the most widespread and widely recognizable insect orders in the world. In Japan exist around 5800 variations of butterfly and moth, around 3 hundred are butterflies and the remainder are moths. This project illustrates the scope of some of those lepidopteras color patterns, which provide a wide variety combination of designs and colors many of them difficult to imagine, that is why these invites us to deepen a research on them. The environment around lepidoptera is the reason of their motives, to camouflage or to draw attention to one objective: survive.

Within this body of information we can infer that the pattern and the color combination of each stage of lepidopteran species have a reason to be as the way as they are. Even there are still remaining many unknowns to discover, scientific around the world are discovering interesting features about their colorations useful to be apply on the development of design products.

## 2. METHOD

1. Selection of the Lepidoptera inhabiting in Japan.
   We select the most common Lepidoptera species to analyze, as Namiageha (Asian swallow tail) and others that have interesting patters and colors.
2. Observation and analysis of each step of transition
   We observe some species from egg until adult: colors, patterns, textures, movement, feeding, the transition when casting of the skin, pupa and silk.
   Common swallow tail butterfly, known as Namiageha in Japanese, lay a individual brilliant yellow and spherical egg on the host plant (citrus like mandarin and oranges or Japanese peppers plants), most of the cases on the underside of the leaf to protect them from the predators like bees. The egg become dark and transparent before larva get out, larva has as first food the egg's shell. The aspect of the larva is textured with thorns, black body with white spots. They transform to green caterpillar as mimicking the color of the host plant. The color of pupa could be green or brown. The wings of the butterfly are striped black and white with small orange and blue circles as accent colors.
3. Revise printed literature and web information
   The most of butterflies and moths after mating have a host plant where they lays eggs, the plant will be the food of larvae during caterpillar's instars until reach fully mature, and then develop into a pupa, chrysalis in the case of butterflies and cocoon for moths. Butterfly and moth are cover by scales throughout their bodies and wings, over millions of years of evolution, result a wide range of patterns and colorations from drab to brightly colored and complex-patterned.

Namiageha principally mimics in the following aspect:
- In the first stage of larvae is mimicking bird droppings, showing that are not taste good.
- Caterpillar turns green color as the host plant. The two eyes like spot are mimicking the face of a snake or a cat, which are enemy of the birds. Those eyes are oval conformed by 3 colors, black, red (warning color) and in the middle a white line like iris (exactly as the cat eyes).
- The larva chooses the place to become a pupa, the texture, odor, the diameter or the branch influence to become a green or brown chrysalis.
- In the adult stage, the shape of the back wings have an elongation as swallows have, near presents an orange dot, those characteristics are mimicking a face in backwards to deceive the enemy.

4. Conformation of color scheme. See 2.1
5. Development of patterns. See 2.2
6. Application in a product design See Result and Discussion.

## 2.1 Conformation of color scheme

Table 1 shows roughly the analysis of the colors and patterns of Lepidoptera.

| | Scientific name | Japanese name | Larval food | egg Pattern | egg color | Larvae or Caterpillar Pattern | Larvae or Caterpillar Color scheme | Pupa or Chrysalis Pattern | Pupa or Chrysalis Color scheme | Adult Pattern | Adult Color scheme |
|---|---|---|---|---|---|---|---|---|---|---|---|
| 1 | *Parantica sita* | Asagimadara | *Asclepiadaceae* | | | | | | | | |
| 2 | *Papilio xuthus* | Namiageha | *Zanthoxylum piperitum* | | | | | | | | |
| 3 | *Byasa alcinous* | Jacouageha | *Aristolochiaceae* | | | | | | | | |
| 4 | *Lycaena phlaeas* | Benishijimi | *Polygonaceae* | | | | | | | | |
| 5 | *Araschnia burejana* | Sakahachichou | *Boehmeria spicata* | | | | | | | | |
| 6 | *Polygonia c-aureum* | Kitatcha | *Humulus japonicus* | | | | | | | | |
| 7 | *Argyreus hyperbius* | Tsumagurohyoumon | *Viola* | | | | | | | | |
| 8 | *Cyrestis thyodamas* | Ishigakechou | *Ficus* | | | | | | | | |
| 10 | *Zophoessa callipteris* | Himekimadarahikage | *Sasa nipponica* | | | | | | | | |
| 11 | *Choaspes benjaminii* | Aobaseseri | *Meliosma rigida* | | | | | | | | |
| 12 | *Monema flavescens* | Iraga | *Diospyros kaki Thunb.* | | | | | | | | |
| 13 | *Parasa sinica* | Kuroshitaaoiraga | *Quercus acutissima* | | | | | | | | |
| 14 | *Parasa lepida* | Hiroheriaoiraga | *Zelkova serrata* | | | | | | | | |
| 15 | *Milionia zonea* | Kiobiedashaku | *Podocarpus macrophyllus* | | | | | | | | |
| 16 | *Malacosoma neustrium* | Obikareha | *Prunus mume* | | | | | | | | |
| 17 | *Saturnia japonica* | Kususan | *Castanea crenata* | | | | | | | | |
| 18 | *Lymantria dispar* | Maimaiga | *Quercus acutissima* | | | | | | | | |
| 19 | *Cucullia Maculosa* | Haiirosedakamokume | *Artemisia indica var.maximowiczii* | | | | | | | | |
| 20 | *Hebomoia glaucippe* | Tsumabenichou | *Crateva religiosa* | | | | | | | | |
| 21 | *Idea leuconoe* | Oogomadara | *Parsonsia laevigata* | | | | | | | | |
| 22 | *Damaus genutia* | Sujigurokabamadara | *Cynanchum boudieri* | | | | | | | | |
| 23 | *Arichanna gaschkevitchii* | Hyoumonedashaku | *Pieris japonica* | | | | | | | | |
| 24 | *Macroglossum passalus* | Negurohoujakku | *Daphniphyllum teijsmannii* | | | | | | | | |
| 25 | *Papilio protenor* | Kuroageha | *Zanthoxylum piperitum* | | | | | | | | |

*Table 1. Colors and Patterns of some Lepidoptera*

Table 2. shows in detail the study of color and pattern which were conducted for Namiageha from egg to adult stages and the host plant.

| Larval food | egg | Larvae: shed their shell about four times as they grow | Larvae: 5th instar larvae | pupa: pupation | pupa: last instar | newly-emerged butterfly | newly-emerged butterfly | adult |
|---|---|---|---|---|---|---|---|---|
| | process of growth | | | | | | | |
| | Color Scheme | | | | | | | |

*Table2. Color and Pattern of Namiageha from egg to adult stage.*

AIC2015 TOKYO - Color and Image

## 2.2 Development of patterns

In the section on Results and Discussion are described the results obtained of the development of some analyzed patterns.

## 3. RESULTS AND DISCUSSION

The developed patterns were applied on a common product as an umbrella (parasol), wich are used in the daily life.

This is the first step of the project, that is why Namiageha was chosen as main sample to develop new patterns. On the figure 1 are shown three variations of motives developed from the same Namiageha butterfly. Above in the figure are the inner of the hind wings, applied to the inside of the umbrella, below are the outside of the hind wings applied to the outside of the umbrella. Each pair represent one umbrella.
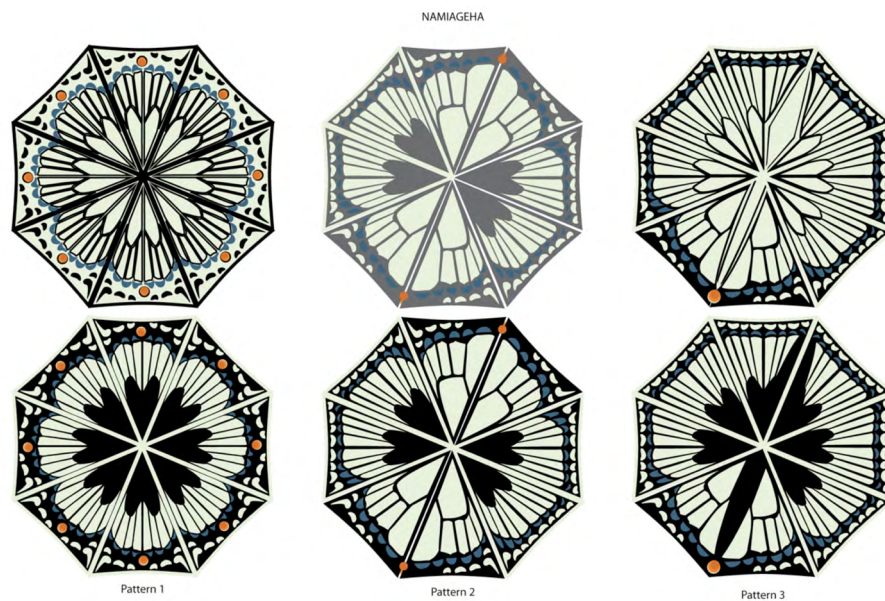


*Figure 1: Patterns apply to canopy cloth of umbrella inspired by Namiageha's butterfly, both side of the hind wings.*

As metaphor of the transition from larva to pupa, a reversible cover for the foldable umbrella was designed, one side  refers to the green larva, and the reverse side to pupa in two colours as the Namiageha chrysalis could become. Fig. 2
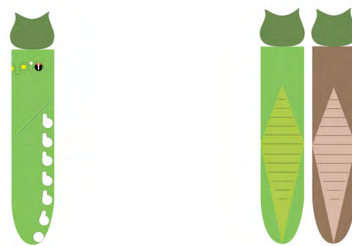


*Figure 2: Patterns inspired by Namiageha's caterpillar and chrysalis*

Others samples of lepidoptera attractive in their different stages were developed. The figure 3 shows Iraga (Monema flavescens) moth, Sujigurokabamadara (Danaus genutia) and Aobaseseri (Choaspes benjaminii) butterflies.
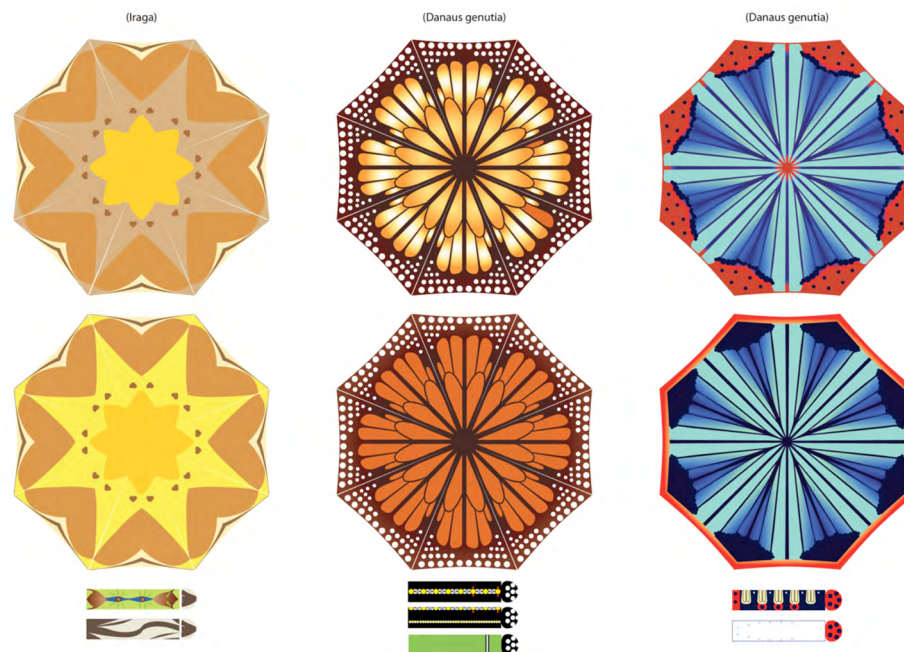


*Figure 3: Patterns inspired by others butterfly and moth both side of the hind wing, caterpillar and pupa*

Consider that it is the first step, the graphics resulting until now, have been applied to the design of umbrellas for women, this is the first stage of the project. The theme chosen for them, was striking, with the same principle further applications could be develop as an umbrella for emergency, umbrellas for children, signals. So well, camouflage in the context is also a intersanting issue to be developed.

The pattern could be applied also to products like parachute, glider, tarp, architecture, outdoor wear, traffic safety equipment and soon.

On the other hand, it is our intention continue developing the palette of colors and designs, considering more butterflies and strengthening aspects of camouflage and mimicry.

## 4. CONCLUSIONS

The wide variety of lepidoptera is an endless source of useful patterns for design development. Inspired by only one butterfly we can get several variations, if we take in account that there are more than 5,000 species only in Japan, we can infer that it is possible to get at least 5000 graphic patterns. We consider that the color scheme obtained is a potential tool, useful to develop different design depending the needs and the context in which the product will be used.

## ACKNOWLEDGEMENTS

## REFERENCES

1) Ruxton,G and Sherratt, T 2005. *Avoiding Attack: The Evolutionary Ecology of Crypsis*, Warning Signals And Mimicry

2) Harman, J 2013. *The Shark's Paintbrush Biomimicry and How Nature is Inspiring Innovation*, Japanese version.

3) Ruse, M 2003. *DARWIN and Design*, Harvard University Press.

4) Yasuda,M 2010. *The Handbook of Japanese Caterpillar* vol.1, bunichi Co.Ltd.

5) Yasuda,M 2010. *The Handbook of Japanese Caterpillar* vol.2, bunichi Co.Ltd.

6) Futahashi, R and Fujiwara, H. 2008. *Juvenile Hormone, Regulates Butterfly Larval Pattern Switches*, Science 22, Vol. 319 no. 5866 p.1061.

7) Fujiwara, H. 2007, *Nisete Damasu Gitai no Fushigi na Sekai*, DOJIN Sensho  2

8) Yamaguchi, J et al, 2013  *"Periodic Wn1 expression in response to ecdysteroid generates larval spot markings on caterpillar"*,  Nature Communications Online Edition. Recuperated on 2015-02-22

http://www.nature.com/ncomms/journal/v4/n5/abs/ncomms2778.html

9) Ueyama, S.  *"Osaka-shi to sono shuhen no Cho"*  27 September 2014

http://butterflyandsky.fan.coocan.jp/index.html

*Address: Prof. Akemi Yamashita, Department of Visual Design, School of Design, Okayama Prefectural University, 1-1-1 Kuboki, Soja, 711-1197, JAPAN*
*Prof. Naoko Takeda, Department of Industrial Design, School of Art and Design, Tecnologico de Monterrey, Puebla, Mexico.*
*E-mails: yamashita@dgn.oka-pu.ac.jp, naoko@itesm.mx,*

# Visual Impressions Induced by Colours of Facial Skin and Lips

Mei-Ting LIU, Hsing-Ju HUNG, Wen-Ling DENG, Li-Chen OU
Graduate Institute of Colour and Illumination Technology, National Taiwan University of
Science and Technology, Taiwan

## ABSTRACT

Two psychophysical experiments were conducted to investigate visual impressions induced by colours of facial skin and lips. The first experiment focused on the effect of facial skin tone. The visual impressions were measured in terms of bipolar scales including active/passive, vibrant/dull, healthy/unhealthy, extraordinary/common, cute/not-cute, sexy/not-sexy, natural/unnatural, sensible/insensible, beautiful/ugly, young/old, delicate/strong, innocent/worldly and like/dislike. A total of 75 skin tones were tested using the face images, assessed by 35 observers with normal colour vision. The face images were presented on a 27-inch liquid crystal display (LCD) with a display luminance of 79 cd/m$^2$, situated in a darkened room. The experimental results show that the lightness of skin tone had little effect on all scales studied. There was a strong effect of hue on the impression of skin tone for all scales. The second experiment used face images with 3 skin tones and 45 lip colours, resulting in 135 combinations, as the stimuli, each assessed by 30 observers with normal colour vision. The experimental results show that observers' impression was significantly affected in terms of "beautiful/ugly", "extraordinary/common", "vibrant/dull" and "delicate/strong". The lightness, chroma, and hue of lip colours were all found to have significant effects on all scales. Male and female observers were found to agree with each other in terms of "harmonious/disharmonious" while they had different responses in "delicate/strong ".

## 1. INTRODUCTION

Facial expression is the most direct and honest reflection of a person's emotions. Interactions between two human beings often begin with the observations of each other's faces, which have this unparalleled ability to immediately convey the emotional states of the persons. To a certain degree, faces could even reveal what kind of person someone is. Using the information gathered through observing the faces, a person could make different choices in his or her approach to other human beings.

There have been studies into visual impressions of skin tones and make-ups. For instance, B. Fink et al. (2008) tracked the observers' eye gaze while they viewed images of varied skin colour distribution. It shows that skin colour distribution is highly correlated with age, health conditions, and attractiveness. Y. Yuan et al. found in 2011 that there are differences between male and female observers' responses in "attractiveness", "cooperativeness", and "masculinity" while using virtual face images for skin tones research. Zeng and Luo found in 2011 that the preferred skin tones for Oriental and African faces were more reddish than real skin tones. In addition, varied from the lightness of skin tone, the observers' preferences for chroma and hue of skin tone were different.

In recent decades, computer animation is developed rapidly. Virtual characters have been seen more and more in a wide range of applications in daily life. In order to enhance the realistic of virtual characters, it is important to use the suitable facial make-up to show

the personality of the characters. According to the analysis of experimental results in present research, design guidelines can be provided to computer animation and other related industries.

The aims of present research include:

- To investigate the connection of virtual character's skin tone and observers' visual impressions.

- To investigate the connection of virtual character's make-up and observers' visual impressions.

- To realise the interaction of the colours on the face.

- To give different colour collocation for individual virtual character.

## 2. METHOD

The present research had two parts. The first part was aimed to investigate visual impressions induced by facial skin tone. The second part was to investigate visual impressions induced by facial colours including colours of facial skin and the lips. The visual impressions were measured in terms of bipolar scales including active/passive, vibrant/dull, healthy/unhealthy, extraordinary/common, cute/not cute, sexy/not sexy, natural/unnatural, sensible/insensible, beautiful/ugly, young/old, delicate/strong, innocent/worldly and like/dislike. These scales were selected on the basis of a questionnaire survey conducted before the main experiment. There were 35 observers (including 10 females) in the first experiment to conduct the questionnaire.

### 2.1 Experiment condition

The liquid crystal display (LCD) used in this research was EIZO ColorEdge CX270, which was calibrated to sRGB by X-rite i1 Pro. In order to present the right experimental colour, the display used the GOG model for colorimetric characterisation. Both of the experiments used the same LCD situated in a darkened room.

The reference white for the first experiment had a luminance of 78.76 cd/m$^2$, of which the chromaticity coordinates (x, y) was (0.3083, 0.3291). The reference white for the second experiment had a luminance of 81.92 cd/m$^2$, with chromaticity coordinates of (0.3092, 0.3277). The visual distance was about 1 metre for the first experiment and 0.5 metres for the second experiment.

### 2.2 Observers

Observers of both experiments were students of National Taiwan University of Science and Technology, aged from 22 to 29 years. There were 35 observers (including 19 females) participated in the first experiment. In the second experiment, among the 30 observers (including 14 females) were 19 observers taking part in both experiments. All of the observers passed the Ishihara test for colour deficiency.

### 2.3 First experiment

The experimental images were 5*5 in size, and were put together for every 25 images presented against a mid-grey background. Each image was framed with the reference white. Between any two slides, there was a full-screen slide with mid-grey background for

at least 1 second to avoid the afterimage effect. The observers had no time limit to evaluate each test image using the 13 scales.

## 2.4 Second experiment

According to the results of the first experiment, the highest score of combination of chroma and hue in "natural/unnatural" was picked up, which had $C^*_{ab}=36$, $h_{ab}=45$ degrees. Colours with lightness values of 50, 60 and 70 corresponded to the light, medium, deep tones.

A total of 95 lip colours, which were acquired in terms of tristimulus values from our market research using a spectrophotometer Xrite-962. These were then converted into CIELAB values. Based on these 95 colours, a total of 135 colours were selected systematically from CIELAB space were selected for recolouring the lips in the experimental facial images.

Five semantic scales were used in the second experiment, of which two, "beautiful/ugly" and "extraordinary/common", were selected according to the Principal Component Analysis (PCA) results. The other three scales, "vibrant/dull", "delicate/strong" and "harmonious /disharmonious" were selected on the basis of the component loading results.

## 3. RESULTS

The results of the first experiment converted the data on the basis of the categorical judgment method to determine the scale values. Figure 1 shows the scale values of "natural/unnatural" plotted against hue angle.
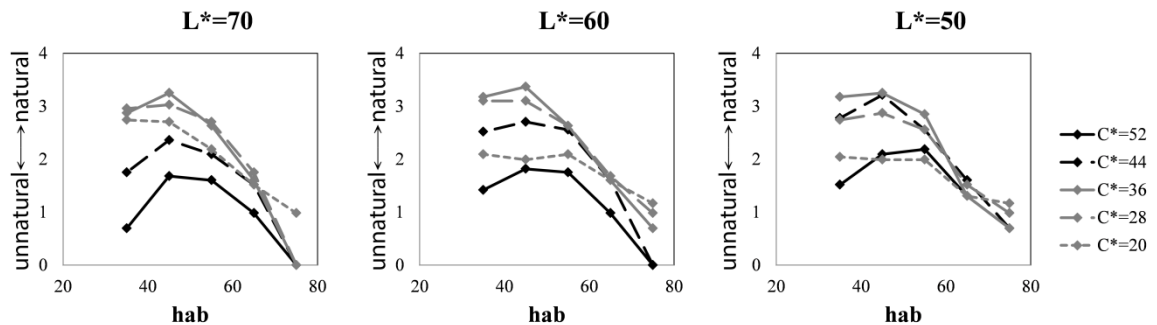


*Figure 1: the scale values of "natural/unnatural" in the first experiment*

All the other scales show trends similar to the graphs. ANOVA was conducted to see whether there was any influence of lightness on each scale. According to the results, the lightness of skin tone had little effect on all scales, and the hue of skin tone had significant effects on all scales except vibrant/dull and sexy/not sexy. No matter what the lightness of skin tone was, observers preferred the reddish skin tone for chroma values of 20, 28 and 36. Observers preferred orange skin tone for chroma values of 44 and 52.

The second experiment was to investigate the influence of lightness of skin tone in terms of the 5 semantic scales. No matter what the lightness of skin tone was, the higher the chroma of lip colour was, the higher the scale value was for all scales. In other words, if the chroma of lip colour that virtual character used was higher, there were more chances for observers to have the association with the 5 scales, "beautiful/ugly",

"extraordinary/common", "vibrant/dull", "delicate/strong", and "harmonious /disharmonious".

Except "extraordinary/common", when the lightness values of skin tone were 50 and 60, the variability of chroma of lip colour had no significant effect on scale values. In addition, no matter which chroma of lip colour coordinate, the scale values were the lowest for lip colours with a lightness value of 70.
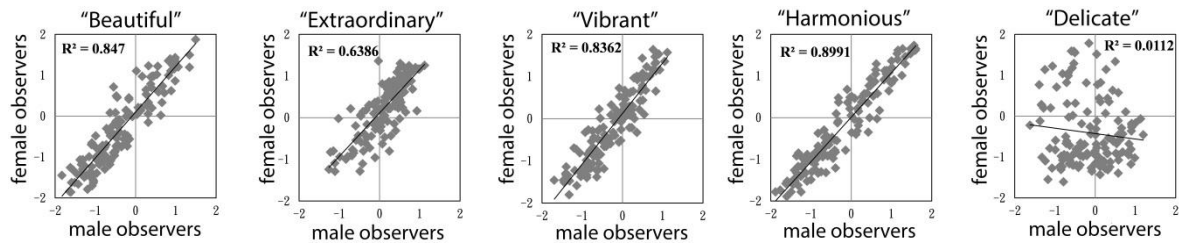


*Figure 2: comparisons between male and female observers in the second experiment*

According to figure 2, the comparisons of male and female observers, "delicate/strong" show a wide spread in the scatter graph. The result suggests that the image which felt delicate for male observers did not felt so for female observers. Figure 3 shows that female results show larger variability than male in rating different images. This suggests that male observers were not as sensitive as female observers in terms of visual impressions of skin tones and lip colours.
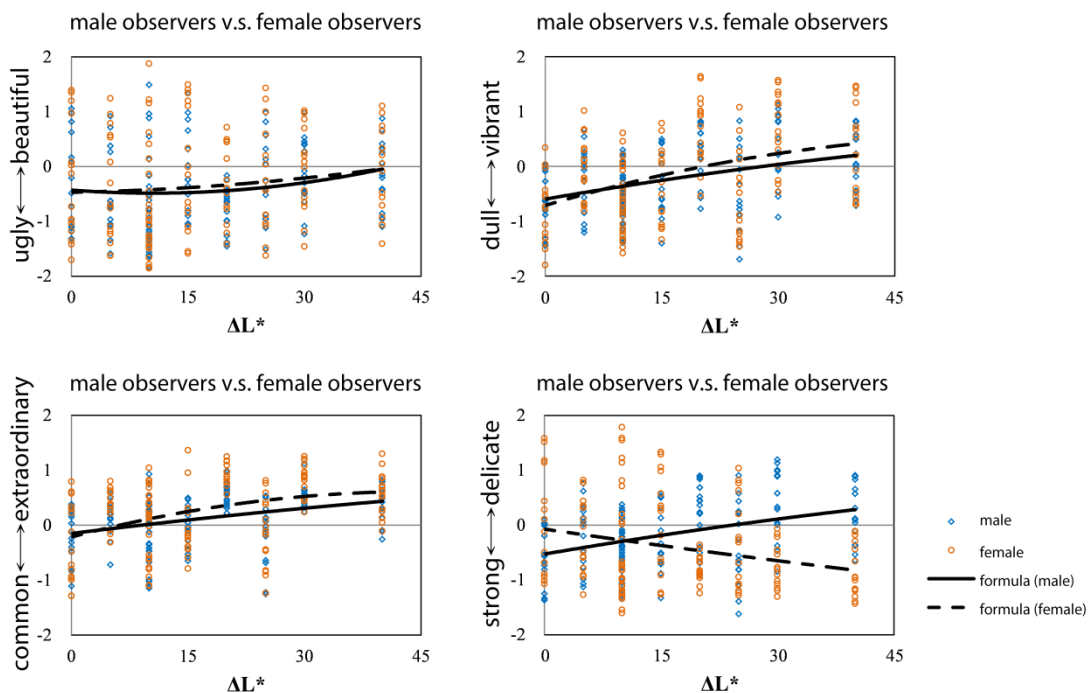


*Figure 3: comparisons of "delicate/strong" between male and female observers*

According to the comparison of the two experiments using ANOVA, there were strong difference in the values of "beautiful/ugly", "extraordinary/common", "vibrant/dull", and "delicate/strong" between whether a virtual character had make-up or not. Another result was that the lightness, chroma, and hue of lip colour had significant influence on all scales. In addition, there was significant interaction between the lightness and hue of lip colour in "extraordinary/common" and "vibrant/dull". There was also significant interaction

between the chroma and hue of lip colour in "harmonious /disharmonious" and "vibrant/dull".

For skin tones with a lightness value of 50, the lightness of lip colour would need to be higher for the facial image to feel more beautiful and more harmonious. For those with lightness of 60, the lip colours with lightness of 45 were found to be the most beautiful and most harmonious. For skin tones with lightness of 70, observers tended to associate the virtual character's face with being ugly, dull, strong and disharmonious for lip colours with a lightness value of more than 70.

## 4. CONCLUSION

Ou and Luo (2006) have developed a two-colour harmony model based on contextless colour patches. This quantitative model was tested using the current experimental data, i.e. the CIELAB values of the skin and lip colours used in Experiment 2. As figure 4 shown, the test result shows a correlation coefficient of only 0.0045, indicating poor predictive performance of the colour harmony model for colour combinations of facial skin and the lips in a facial image.
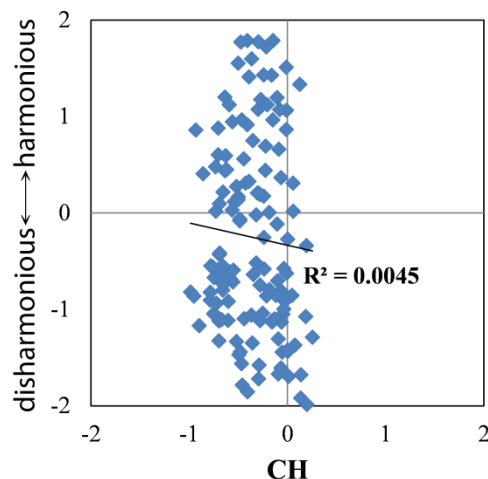


*Figure 4: the colour harmony model by Ou & Luo v.s. the result of the present research*

The virtual characters used in the computer simulation of the experiments were based on Southeast Asian females. It is thus recommended that, for a more comprehensive investigation of facial skin colours, virtual characters of various races and genders be used in future studies. Additionally, the races and cultural backgrounds of the observers should also be included as factors in order to compare any discrepancies between the visuals and different groups of observers. All of the observers in the experiments were between the ages of 22 to 29 years, making it difficult to eliminate the possibility that age might by one of the factors influencing the results of the study.

## AKNOWLEDGEMENTS

## REFERENCES

Egges, A., S. Kshirsagar, N. M. Thalmann. 2003. A model for personality and emotion simulation. Knowledge-Based Intelligent Information and Engineering Systems. *Lecture Notes in Computer Science* (Vol. 2773) : 453-461.

Fink, B.,P.J. Matts, H. Klingenberg, S. Kuntze, B. Weege, K. Grammer. 2008. Visual attention to variation in female facial skin colour distribution. *Journal of Cosmetic Dermatology* (Vol. 7, No. 2) : 155-161.

Yuan, Y., L. C. Ou, M. R. Luo. 2011. Gender differences in social perception for skin tones. Proceedings of AIC Midterm Meeting, Interaction of Colour and Light in the Arts and Sciences.

Zeng, H., M. R. Luo. 2011. Colour and tolerance of preferred skin colours on digital photographic images. *Colour Research and Application* (Vol. 38, No. 1) : 30-45.

Ou, L. C., M. R. Luo. 2006. A colour harmony model for two-colour combinations. *Colour Research and Application* (Vol. 31, No. 3) : 191-204

*Address: Graduate Institute of Color and Illumination Technology,*
*National Taiwan University of Science and Technology, Taiwan*
*E-mails: blueh919@gmail.com, b9934036.ntust@gmail.com,*
*fd70517@gmail.com, lichenou@mail.ntust.edu.tw*

# International Comparison of Uses of Color for Pictograms

Yuki AKIZUKI,[1] Michico IWATA,[2] Hirotaka SUZUKI[3]
[1] Faculty of Human Development, University of Toyama
[2] Faculty of Science and Engineering, Setsunan University
[3] Faculty of Engineering, Kobe University

## ABSTRACT

Pictogram is a square including representative figure which indicates function or purpose of the facility. These pictograms are used in countries with different languages spoken, so although with different degrees of recognition, they are able to make people understand the space intuitively. Our study therefore conducts comparative survey on colors of pictograms in order to grasp the possibilities for pictograms to be attached to certain images pertaining colors, and to establish basic data for designing signs. We surveyed on colors of pictograms at international public facilities in 14 cities in 7 countries. The results of Toilet-Pictogram indicates tendency that European countries use achromatic colors without gender difference, and China uses multiple colors. All of pictograms of Unisex-Toilet use one same color, without differentiating genders. Gender image attached to particular color for pictogram is only seen in Japan, not elsewhere. In order to design signs in international perspectives, it is important to consider differences of culture, religion gender as well as color image.

## 1. INTRODUCTION

Japan enacted Basic Act for Promoting a Tourism-Oriented Country in 2007, which considers tourism one of the major growing industries in the 21st century, and tries to accept more foreign visitors. Recently, major stations and airports put signs in two languages  (Japanese and English), and guideboards in tourist destination such as Kyoto are now also written in the two languages. But many cities still have Japanese only signs, which cause trouble for foreign visitors to use facilities or move around.

Pictogram is a square including representative figure which indicates function or purpose of the facility. ISO7001:2007, "50 passenger/pedestrian Symbol Signs" developed by American Institute of Graphic Arts, and JIS Z8210:2002 standardize various pictograms, and new pictograms are being proposed as needed.  These pictograms are used in countries with different languages spoken, so although with different degrees of recognition, they are able to make people understand the space intuitively. They are useful in constructing urban building space becoming more and more international. JIS Z9103 is applied to pictograms for fire preventive equipment and evacuation signs, but other pictograms tend to have white background and black foreground internationally. On the other hand, in Japan, pictograms for toilets have distinct tendency of color (blue for men, red for women). There are various ways to use color for pictograms.

Our study therefore conducts comparative survey on color of pictograms in order to grasp the possibilities for pictograms to be attached to certain images pertaining color, and to establish basic data for designing signs.

## 2. METHOD

In 2008 and 2009, we surveyed on color of pictograms at international airport terminals, major railway stations, city halls, museum/historical buildings, major commercial centers, hotels, and parks in 14 cities in 7 countries. One spot of one facility is the subject, and if there is a pictogram, its background and foreground color are measured on the spot by visual photometry using a color chart (Figure 1) based on PCCS color coordinate system. Table 1 shows the correspondence with Mansell color system and PCCS color system.
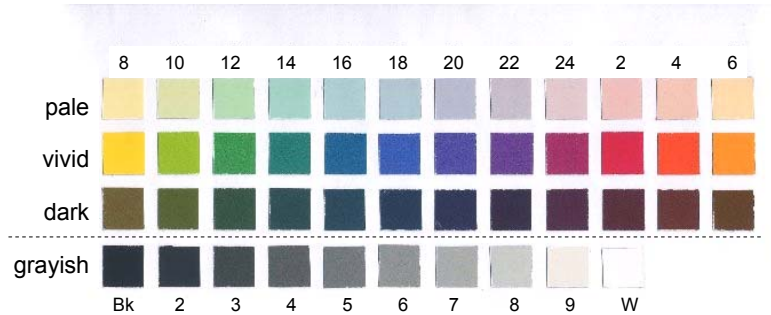


*Figure 1. Color Chart based on PCCS color coordinate system.*

*Table 1. Correspondence table with Mansell color system.*

| | pale (p) | | | vivid (v) | | | dark (dk) | | | grayish(g) | |
|---|---|---|---|---|---|---|---|---|---|---|---|
| 2 | 4R | 8 / | 3.5 | 4R | 4.5 / | 14 | 4R | 2.5 / | 6 | Bk | N1.5 |
| 4 | 10R | 8 / | 3.5 | 10R | 5.5 / | 14 | 10R | 3 / | 6 | 2 | N2.0 |
| 6 | 8YR | 8.5 / | 3.5 | 8YR | 7 / | 14 | 8YR | 3.5 / | 6 | 3 | N3.0 |
| 8 | 5Y | 9 / | 3 | 5Y | 8 / | 13 | 5Y | 4 / | 5.5 | 4 | N4.0 |
| 10 | 3GY | 8.5 / | 3 | 3GY | 7 / | 12 | 3GY | 3.5 / | 5 | 5 | N5.0 |
| 12 | 3G | 8 / | 3 | 3G | 5.5 / | 11 | 3G | 3 / | 4.5 | 6 | N6.0 |
| 14 | 5BG | 8 / | 3 | 5BG | 4.5 / | 10 | 5BG | 2.5 / | 4.5 | 7 | N7.0 |
| 16 | 5B | 8 / | 3 | 5B | 4 / | 10 | 5B | 2.5 / | 4.5 | 8 | N8.0 |
| 18 | 3PB | 7.5 / | 3 | 3PB | 3.5 / | 12 | 3PB | 2 / | 5 | 9 | N9.0 |
| 20 | 9PB | 7.5 / | 3 | 9PB | 3.5 / | 12 | 9PB | 2 / | 5 | W | N9.5 |
| 22 | 7P | 7.5 / | 3 | 7P | 3.5 / | 12 | 7P | 2 / | 5 | | |
| 24 | 6RP | 8 / | 3 | 6RP | 4 / | 13 | 6RP | 2.5 / | 5.5 | | |

## 3. RESULTS AND DISCUSSION

### 3.1 Color for Toilet-Pictogram

Table 2 shows the results of used color combinations for Toilet-Pictgram country by country. We collected 56 data at 25 male's toilets and 31 female's toilets. The results indicates a tendency that European countries use achromatic colors without gender difference, and China (Hong Kong, Macau and Taipei) uses multiple colors.

We also surveyed 33 unisex toilets in 5 countries. The results is shown in Table 2. 27 toilets use pictograms including both male and female symbols, and 6 toilets use only the letters "WC". All of them use one same color, without differentiating genders. In Japan, unisex toilets usually have pictogram with two different colors for each symbol. But these survey results show colors are not tied to symbol's meaning internationally.

17 toilets for disabled people were surveyed in 5 countries, and the results are shown in Table 2, too. In Japan, green color is often used for the pictgram of disabled-accessible

facilities.　However there are no green pictgram for disabled-accessible toilet in any country, and there are some red pictgram for it in China.
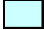
*Table 2. Color Combinations for Toilet-Pictgram.*

**（1）Toilet-Pictogram for Male**

| figure | ground | Germany | Switzerland | Austria | UK | Sweden | Finland | China |
|---|---|---|---|---|---|---|---|---|
| Red | Yellow | | | | | | | |
| Red | Gray | | | | | | | |
| Red | White | | | | | | | |
| Yellow | Yellow | | | | | 1 | | |
| Blue | Gray | | | | | | | 1 |
| Blue | White | | | | | 3 | | 2 |
| Black | Yellow | | 1 | | | | | |
| Black | Green | | | | | | 1 | |
| Black | Gray | 3 | | | | 1 | | |
| Black | White | 1 | | 1 | | | 2 | 2 |
| Gray | Gray | | | | | | | 1 |
| White | Red | | | | | | | 2 |
| White | Yellow | | | | | | | |
| White | Blue | | | | | | 1 | |
| White | Black | | | | 1 | | | |
| White | Gray | 1 | | | | | | |

**（2）Toilet-Pictogram for Female**

| figure | ground | Germany | Switzerland | Austria | UK | Sweden | Finland | China |
|---|---|---|---|---|---|---|---|---|
| Red | Yellow | | | | | | | 1 |
| Red | Gray | | | | | | | 1 |
| Red | White | | | | | | | 1 |
| Yellow | Yellow | | | | | | 1 | |
| Blue | Gray | | | | | 3 | | 1 |
| Blue | White | | | | | | | |
| Black | Yellow | | 1 | | | | | |
| Black | Green | | | | | | 1 | |
| Black | Gray | 4 | | | 1 | | | |
| Black | White | 2 | | 1 | | | 2 | 2 |
| Gray | Gray | | | | | | | |
| White | Red | | | | | | | 2 |
| White | Yellow | | | | | | | 2 |
| White | Blue | | | | | 3 | | |
| White | Black | | | 1 | | | | |
| White | Gray | 1 | | | | | | |

☐ chromatic pictogram　　■ achromatic pictogram
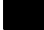
**（3）Toilet-Pictogram for Unisex**

| figure | ground | Germany | Switzerland | Sweden | Finland | China |
|---|---|---|---|---|---|---|
| Red | White | | | | | 1 |
| Yellow | Blue | | 1 | | | |
| Yellow | Black | | | | | 1 |
| Green | White | 1 | | | | |
| Blue | Green | | | 1 | | |
| Blue | Gray | | | | | 1 |
| Blue | White | | | | | |
| Black | Yellow | 3 | | | | |
| Black | Blue | | | | | 1 |
| Black | White | 5 | | 1 | 1 | |
| Gray | Black | | | 2 | | |
| White | Red | | | | | 1 |
| White | Yellow | | | | | 1 |
| White | Green | | | | 1 | 2 |
| White | Blue | | | | 3 | 2 |
| White | Black | | | 1 | | 1 |
| White | Gray | 1 | | | | |

**（4）Toilet-Pictogram for disabled people**

| figure | ground | Germany | UK | Sweden | Finland | China |
|---|---|---|---|---|---|---|
| Red | White | | | | | 1 |
| Yellow | Blue | | | | | |
| Yellow | Black | | | | | |
| Green | White | | | | | |
| Blue | Green | | | | | 1 |
| Blue | Gray | | | | | |
| Blue | White | | | 2 | | |
| Black | Yellow | | | | | |
| Black | Blue | | | | | |
| Black | White | 4 | | 1 | | |
| Gray | Black | | | 1 | | |
| White | Red | | | | | 1 |
| White | Yellow | | 2 | | | |
| White | Green | | | | | |
| White | Blue | | | | 2 | 1 |
| White | Black | | 1 | | | |
| White | Gray | | | | | |

☐ chromatic pictogram　　■ achromatic pictogram

## 3.2 Color for Emergency-Pictogram

Coloring of emergency evacuation sign is regulated by ISO and JIS. Among 74 pictograms of emergency in this survey, 88% pictograms have the color combination of white figure and green (3G5.5/11.0) background, whether it is at an exit or in a passage. In Japan, the color combination of the passage evacuation signs is reversed (with green figure and white background). Same arrangement is seen in 6 cases in only China (Taipei and Hong Kong).

AIC2015 TOKYO - Color and Image

Therefore it suggests that the color combination difference in passage evacuation signs is only seen in East Asia region including Japan. Also, 2 cases in China (Hong Kong and Macau) use non-safety color for emergency evaluation pictogram, 5B8.0/3.0 and 5Y4.0/5.5.

Among 34 pictograms of fire equipment, 90% pictograms use ISO regulated red (10R5.5/14.0) figure and white background. But 4 cases in China use other colors.

## 3.3 Most Frequently-Used Color for Pictogram

The frequently-used colors are examined with all 438 cases. The results shows in Figure 2. The most frequently-used color as figure is white (252 cases) and then black (103cases), these two explain 80% results. For background, the most frequently-used color is again white (100cases) but the second is 3G5.5/11.0 (70cases) followed by 3PB3.5/12.0 (61cases) and black (42cases). Considering that 3G5.5/11.0 is designated color for emergency evacuation signs, 3PB3.5/12.0 might be the most popular color for chromatic background. For the two color combination, the most frequent one is black figure and white background. The most chromatic combination is white figure and 3PB3.5/12.0 background, which is typically seen in airports and stations. Figure 3 shows some typical examples.
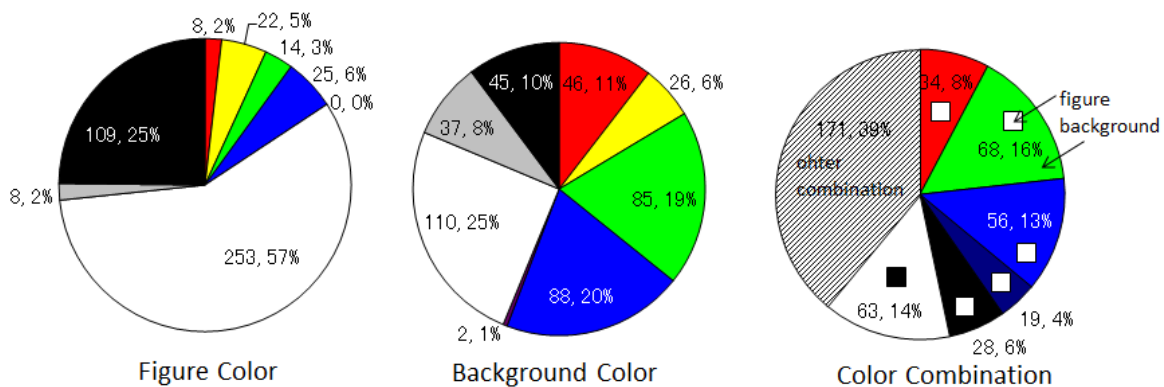


Figure 2. Frequently-Used Color for Pictograms.



Figure 3. Typical Example for Color Combination of Pictgram.

## 4. CONCLUSIONS

Gender image attached to particular color for pictogram is only seen in Japan, not elsewhere. In order to design signs in international perspectives, it is important to consider differences of culture, religion gender as well as color image. On the other hand, as our study shows there is some common tendency of color use.

It is useful to accumulate data further, to realize ideal sign designing to support space recognition.

And then, our survey finds some pictograms not honoring ISO color regulation. In order to ascertain that pictogram functions as common language, and to let them function for safety, further action will be called for to eliminate such cases.

## ACKNOWLEDGEMENTS

## REFERENCES

ISO7001:2007. *Graphical symbols - Public information symbols*.
JIS Z8210: 2002. *Public Information Symbols*.
JIS Z9103: 2005. *Safety Colours – General specification*.

*Address: Associate Prof. Yuki AKIZUKI, Faculty of Human Development,*
*University of Toyama,3190 Gofuku, Toyama, 930-8555, JAPAN*
*E-mails: akizuki@edu.u-toyama.ac.jp, michico@led.setsunan.ac.jp,*
*hirotakasuzuki@people.kobe-u.ac.jp*

# The Influence of Colour on the Perception of Cartographic Visualizations

Zbyněk ŠTĚRBA,[1] Jan D. BLÁHA[2]

[1] Department of Geography, Masaryk University in Brno, Czech Republic
[2] Department of Geography, J. E. Purkyně University in Ústí nad Labem, Czech Republic

## ABSTRACT

The contribution provides an overview of the ways colour is used in cartographic visualizations and how it affects perception of these visualizations. Colour is generally considered as the most important graphic variable for expressing spatial information in cartographic visualizations. Through appropriate use of colours, the content of a map can be significantly accentuated, which enhances its legibility and comprehensibility profoundly. Appropriate use of colours is a very important factor in many cartographic applications, such as emergency management tools, in which cartographic visualization helps to transfer the required information effectively. A well-chosen colour scheme with appropriate contrasts is the best way to depict the overall character of an area or a phenomenon. The present paper describes the most significant approaches to colour use in cartography, which can be of immense help when communicating information to map users.

## 1. INTRODUCTION

When creating cartographic products, the form of depiction of the map's content is one of the primary outcomes of a cartographer's work. At the same time, the way various map symbols are depicted is a factor which is most likely to influence users' interpretations of the map. Different means of cartographic information transmission evolved gradually, but the greatest boom came with the development of thematic cartography, whose methods provided extra space for invention in the design of cartographic symbology.

The classic text in the field of cartographic symbology is Jacques Bertin's Semiology of Graphics (Sémiologie Graphique). The book, published in 1967, was the first to define basic cartographic means of expression, also referred to as graphic variables. Apart from the feature's position on the map, which represents the spatial location itself, external characteristics of a symbol can be described through various variables communicating different types of information. These variables, co-indicators of a symbol's content, include size, intensity, shape, orientation, structure and colour (among others).

Out of these, colour is generally considered as the most important graphic variable for expressing spatial information in cartographic visualizations. Colour can be used to display a relatively large amount of information in a single map without reducing the map's legibility and comprehensibility. Colour can also be easily combined with other variables, increasing their communication potential. Finally, in both thematic and topographic maps, colour is one of the principal enhancers of aesthetic quality, making the map much more visually attractive.

## 2. METHOD

Cartographic products are generally very powerful tools for communicating visual and spatial information. Through appropriate use of colours, the content of each map can be significantly accentuated, increasing the map's legibility and comprehensibility rapidly. Conversely, use of inappropriate colours and colour combinations can significantly undermine users' perception of the visualized information. Colour is used as a communication means in most elements and symbols within a map. Therefore, it both helps to communicate cartographic information and increases the legibility of the map and its aesthetic quality (Bláha, 2011). Hence, colours and colour contrasts influence the aesthetics of a map and the user's emotional response, as well as the map's usability.

Colour perception is definitely influenced by physiological, psychological, and other subjective factors. It is therefore always necessary to consider specific contexts in which the map will be used, such as light conditions (outdoor v. indoor use, etc.), type of cartographic product (analogue v. interactive map), map size (or display size of the display device), typical situations in which the map will be used, as well as potential cultural specifics (Bláha, 2013). Chesneau et al. (2005) argue that colours are able to elicit emotional responses that might significantly influence decision-making in map users. This effect is stronger in colour than in any other graphic variable. Drápela (1983) also views colour as a specific means of expression occupying a special position among cartographic variables and points out different aspects which should be considered when using colour effects in map design. Krygier & Wood (2005) describe several examples of inappropriate colour use in maps and emphasize the counterproductive impact of inappropriate colours on map legibility, which may manifest especially as erroneous or slow map interpretation. Inappropriate colour use also involves employment of inadequate colour ranges for displaying qualitative and quantitative data. On the other hand, use of appropriate colours and colour combinations can increase overall comprehensibility and legibility of the map substantially.

### 2.1 Colour contrast

An important thing to consider when designing map products is the contrast between different colours. This is because the effect of colours in maps – just like in any other graphic visualization – always depends on their combinations with other colours. Colour contrast can greatly enhance effective representation of the target information. A well-applied palette of contrasting colours is a perfect means of depicting the overall character of an area or a phenomenon, as the perceiver can immediately see the spatial distribution as well as the quantity and quality of different features on the map. Appropriately selected contrasts intensify the perception of the figure and the ground through dividing the map field into "layers" representing base and extension information (see Stachoň et al., 2013). As Krygier & Wood (2005) point out, contrast must be taken into consideration in any map design. It is therefore necessary to choose colours carefully to make them suitable for a particular background. Colours that are chosen arbitrarily and carelessly may produce uneven contrasts, which, in turn, may result in ambiguous perception of some of the features on the map, which become semantically indiscernible and unclassifiable.

In general, contrast refers to a situation when a clear difference can be observed between two juxtaposed objects or phenomena (Itten, 1987). Hence, contrast can result from differences in size, temperature or – in this case – colour. These observed differences are

always relative because they arise through comparisons between two or more objects. Perception of colour and colour contrasts is a largely subjective process, which makes it hard to quantify or describe in detail. In the past (especially since the early 19th century), a relatively large number of authors commented on the issue of colour contrast (for overview, see Chesneau et al., 2005). However, it was not until Johannes Itten[1] that colour laws were finally formulated with sufficient objectivity, and principles of colour perception postulated which are often used in cartography to this day. Itten's principles systematically and explicitly define and describe seven basic types of contrasts observable in colour perception: contrast of hue, light-dark contrast, cold-warm contrast, complementary contrast, simultaneous contrast, contrast of saturation, and contrast of extension (for more detail and examples, see Bláha & Štěrba, 2014).

It has to be noted that, in reality (and all the more on the map), the above contrast types complement and mingle with each other and therefore cannot be treated as completely separate variables. For example, simultaneous contrast especially affects areas which also show the contrast of extension. Extension (relative area size), in turn, tends to influence colour saturation and colour lightness. On the other hand, the perception of colours as cool or warm, particularly with regard to their function as depth cues, is mostly independent of relative area size. All of this indicates that there might be certain hierarchy among different contrast types. Map design, just like visual arts, uses the law of cool and warm colours. When reading a map, similarly coloured (cool or warm) areas create an impression of similar depth, independent of area size. This effect is even more marked in cartography than in visual arts, where contrasts were originally studied. An impression of depth can also be achieved through the contrasts of saturation and light and dark, which is why figure elements on the map should always be depicted in deep and dark colours. When applied appropriately, the effects of individual contrasts will be multiplied.

Design of cartographic symbology should follow certain rules which are implicitly contained in the above principles. There are also other methods of increasing contrast that can be used to enhance the distinctness of particular features on the map. For example, Kennely & Steward (2010) design chloropleth maps with additional shading within the individual categorized polygons to create an illusion of a (pseudo)three-dimensional visualization. This effect enables further differentiation of individual elements within the same interval, adding new information represented – thanks to the impression of plasticity – by the polygon's "height". To a certain extent, this impression is also enhanced by appropriate choice of colour contrast – i.e. if features representing greater values are depicted in intensive and more saturated colours, there will be a stronger perception of ground features (polygons representing low values) and figure features (polygons representing high values). Obviously, a similar method could be used to visualize qualitative phenomena, namely to accentuate the contrast between warm and cool colours. Adequate choice of colour combinations and contrasts should, naturally, be also directed by the purpose for which the map is designed.

---

[1] Johannes Itten (1888 – 1967) was a Swiss designer, expressionist painter and theoretician closely associated with the arts and architecture group *Bauhaus*. He was especially interested in colour theory and studied the impact of colour on visual perception.

## 2.2 Effect of colour on the perception of a map

Colour perception, in general, is a very complex process. Apart from the properties discussed above, this is also caused by the fact that individual colours create different impressions in different people. Moreover, colour perception is strongly influenced by the context, i.e. colour properties of the surrounding objects as well as other external factors (Kryger & Wood, 2005).

MacEarchen (2004) notes that cartographers harnessed the knowledge of individual differences and variation in colour perception, and of the way people interpret cartographic information differently depending on the employed colour combinations, relatively early in the past. The best illustration is the cartographic visualization of elevation layers by means of hypsometric tints. This convention, established by Karl Peucker[2] in the late 19th century, is used in various analogous forms in atlas designs to this day (Thrower, 2008). The principle of this method consists in the fact that perception of distance (or depth) varies with changing colour tints or hues. This creates an impression of depth perspective and facilitates the process of information transmission. For example, hues of long wavelengths (orange and red) are perceived as closer on the map than hues of short wavelengths (blue and green). This phenomenon is often employed in spectral ranges (or, more often, their parts) used in cartographic visualizations. As specified by Imhof (2007), this stereoscopic effect does not result directly from physiological processes, but arises from a psychological illusion that is formed in people's minds. It is also advisable that similar colour ranges additionally involve the cold-warm contrast, which amplifies the overall impression of distance. Hence, colour ranges that include cool colours as well as warm colours (e.g. red – orange – light blue – dark blue) show particularly good properties in cartographic products.

Drápela (1983) describes the effect of colour, especially colour excitability, on the expression of positive and negative qualities of a phenomenon. "Calm" colours include shades and tints of yellow, blue and green. These colours create the most placid impression in people. "Excitable" colours, on the other hand, are represented by the other pole of the spectrum, namely by the red colour. The colour which is considered most excitable is non-spectral purple, which is physically composed of light with the shortest and longest wavelength (red and blue). This effect is probably caused by an increased struggle of the visual system to form a sharp image of purple-coloured objects on the retina. These properties are partly used – in analogy with traffic conventions – also in emergency maps to display potential hazards (see Konečný et al., 2011).

Cartographers who design maps are sometimes limited by various rules, standards and other conventions whose meaning is largely historical. Adherence to these rules is usually implicitly required by the user, and any deviations might lead to incorrect interpretations of the cartographic material. Such general conventions are summarized, for example, by Robinson et al. (1995), who find it natural that green colour represents areas covered by vegetation, brown colour indicates mountain ranges and yellow colour is used to depict areas with poor moisture supply (dry land, areas without vegetation cover, etc.). Besides mere conventionality, however, these expectations are fuelled by the connotations evoked by different colours, i.e. associations they tend to produce in most people (e.g. blue suggests moisture and cold, brown is associated with soil, etc.). Apparently, conventions

---

[2] Karl Peucker (1859 – 1940) was an Austrian theoretical cartographer.

such as these should be observed especially in maps designed for the general user. The more specialized a map is, the more its design should adhere to the rules and standards typical for that particular domain. As another example, Vasilev (2006) discusses how habitual practices of colour use in maps may vary due to regional or national differences. Apart from several, mostly topographical features (*blue* for bodies of water, *green* for forests and *brown* for mountains), individual colours may imply different meaning in different geographical areas. This could be caused not only by differences in culture and cultural traditions, which may produce different emotional impacts of a particular colour on the individuals, but also by differences in actual colour perception characteristic of the context or environment in which the cultural community lives. Finally, colours can also be perceived differently due to variations in individual dispositions.

## 3. CONCLUSIONS

In cartography, appropriate use of colours plays a crucial role in effective communication of the target information. A well-chosen colour scheme with suitable contrasts provides the best way of depicting the overall character of an area or a phenomenon. For these reasons, appropriate use of colours is especially important in domains such as emergency management where cartographic visualisations are extremely helpful in obtaining all of the needed information. Colour can be a very effective tool for displaying emergency situations. It can be used to depict possible hazards, ongoing events, or the current state of restoration processes in the afflicted areas. However, it must be noted that the domain of emergency management cartography tends to be particularly affected by conventions in colour use, which might be very limiting for cartographers designing these types of products.

In general, cartographic products for emergency management are employed by users who need to obtain the target information as quickly as possible, with a substantial level of accuracy. Decisions based on unclear cartographic visualisations could lead to misunderstandings that may finally turn into weighty losses. Through the employment of adequate colour contrasts, one can achieve optimum differentiation between the figure (most important) and the background (less relevant) information. This effect helps to significantly increase the efficiency and effectiveness of perception of the target information, which has a strong impact on the overall usability of a map.

## ACKNOWLEDGEMENTS

## REFERENCES

Bláha, J. D. (2011). Aesthetic Aspects of Early Maps. In Ruas, A. (ed) *Advances in Cartography and GIScience. Vol. 1, Selection from ICC 2011 Paris*, 53–71.

Bláha, J. D. (2013). Cultural Aspects of Cartographic Creation: Use of Mental Maps in Cross-cultural Research. In *Proceeding of 26th ICC Dresden*, 1–15.

Bláha, J. D., Štěrba, Z. (2014). Colour Contrast in Cartographic Works Using the Principles of Johannes Itten. In *Cartographic Journal*: 51(3), 203-213.

Chesneau, E., Ruas, A., Bonin, O. (2005). Colour Contrasts Analysis for a better Legibility of Graphic Signs on Risk Maps. In *22nd International Cartographic Conference 9-16 July* [online], A Coruna, 2005, 10 s,

Drápela, M. V. (1983). *Vybrané kapitoly z kartografie*, 1. vyd., SPN Praha, Brno, 1983, 128 s.

Imhof, E. (2007). *Cartographic Relief Presentation*, 1. vyd., 2007, ESRI Press Redlands, 416 s., ISBN 978-1-58948-026-1.

Itten, J. (1987). *Kunst der Farbe: subjektives Erleben und objektives Erkennen als Wege zur Kunst*, Maier, Ravensburg.

Konečný, M. et al.(2011). Dynamická geovizualizace v krizovém managementu. Brno: Masarykova univerzita, 379 p. ISBN 978-80-210-5858-3.

Krygier, J., Wood. D. (2005). *Making Maps: a Visual Guide to Map Design for GIS*, 1. vyd., New York: Guilford Press, 2005, 303 s., ISBN 1593852002.

MacEachren, A. M. (2004). *How Maps Work: Representation, Visualisation and Design.* New York: The Guilford Press, 2004, 513 s., ISBN 0-89862-589-0.

Robinson, A. H., Morisson, J. L., Muehcke, P. C., Kimerling, A. J., Guptill, S. C. (1995). *Elements of Cartography*, 6. vyd., Wisley&Sons, 1995, 664 s., ISBN 0-471-55579-7.

Stachoň, Z., Šašinka, Č., Štěrba, Z., Zbořil, J., Březinová, Š. and Švancara, J. (2013). 'Influence of Graphic Design of Cartographic Symbols on Perception Structure', *Kartographische Nachrichten*, 63(4), pp. 9.

Thrower, N. J. W. (2008). *Maps & Civilization: Cartography in Culture and Society*, 3. vyd., The University of Chicago Press, 2008, 352 s., ISBN 978-0-226-79974-2.

Vasilev, S. (2006). Cartographical Symbolic. In *International Conference on Cartography and GIS* [online], Borovetz, 2006.Gage, J. 2008. *Signs of Disharmony: Newton's Opticks and the Artists*, Perspectives on Science 16(4) 360-377.

*Address: Zbyněk Štěrba, Ph.D., Department of Geography, Faculty of Natural Sciences, Masaryk University, Kotlářská 2, Brno, 611 37,Czech Republic*
*E-mails: zbynek.ste@gmail.com, jdg@seznam.cz*

# Evaluation of colour appearances displaying on smartphones

X. Gao [1*], E. Khodamoradi [1], L. Guo [2], X. Yang [2], S. Tang [3], W. Guo [3], Y. Wang [3]

[1] Department of Computer Science, Middlesex University, London, NW4 4BT, UK
[2] Department of Information Science, Fuzhou University, Fuzhou, China
[3] Biomedical Engineering Center, Fudan University, Shanghai, China

*Corresponding Author:  Prof. Xiaohong Gao, x.gao@mdx.ac.uk*

## ABSTRACT

Despite of the limited size and capacity of a mobile phone, the urge to apply it to meet quotidian needs has never been unencumbered due to its appealing appearance, versatility, and readiness, such as viewing/taking pictures and shopping online. While a smartphone can act as a mini-computer, it does not always offer the same functionality as a desktop computer does. For example, the RGB values on a smartphone normally cannot be modified nor can white balance be checked. As a result, performing online shopping using a mobile phone can be tricky, especially when buying colour sensitive items. Therefore, this research takes an initiative to investigate the variations of colours for a number of smartphones while making an effort to predict their colour appearance using CIECAM02, benefiting both phone users and makers. The paper studies models of Apple iPhone5, LG Nexus 4, Samsung, and Huawei, by capitalising on comparisons with a CRT colour monitor that has been calibrated under the illuminant of D65, to be in keeping with the usual way of viewing online colours. As expected, all the phones present more colourful images than a CRT does.

## 1. INTRODUCTION

A smartphone is  a mobile  phone with   more  advanced  computing  capability  and connectivity than basic feature phones, offering functionalities of typically  personal assistance, media player, digital camera, and a GPS navigation unit in addition to the basic calling/receiving facilities. At present, the global smartphone audience has reached 1 billion consumers [eMarkter] and expects to arrive at 1.75 billion by the end of 2014.  As such, mobile sales are not only focusing heavily on smartphones, but also on the more affordable option of feature phones that do not have an operating system. As a result, mobile penetration has surpassed 100% in many regions of the world, including North America, Western Europe, Central and South America, Central and Eastern Europe, and the Middle East [WeAreSocial]. Among those smartphone users, about half of them go online by using the phone regularly. Table 1 lists the top 10 most popular smartphones on the market.

*Table 1. Top 10 smartphone list as of May 2014 [Counter].*

| Rank | Brand | Model |
|------|-------|-------|
| 1 | Apple | iPhone 5s |
| 2 | Samsung | Galaxy S5 |
| 3 | Samsung | Galaxy S4 |
| 4 | Samsung | Note 3 |

| 5  | Apple   | iPhone 5c       |
|----|---------|-----------------|
| 6  | Apple   | iPhone 4S       |
| 7  | Xiaomi  | MI3             |
| 8  | Samsung | Galaxy S4 mini  |
| 9  | Xiaomi  | Hongmi Redrice  |
| 10 | Samsung | Galaxy Grand 2  |

One of the unexpected by-products of smartphones remains in the field of digital photography. It appears that more photos are taken by using Smartphones than normal cameras. For example, the Apple iPhone 5 is currently the most popular 'camera' on Flickr.com [Flickr]. As a direct result, large amount of money are being investigated by mobile developers to create photo apps in an attempt to satisfy the demands of 'serious' camera phone photographers.

While using smartphone to perform everyday activities, colour remains one of the key factors, in particular in online shopping. Similar to any other digital device, a phone represents a digital image in a RGB colour space. Therefore when an image is to be processed, it is usually firstly converted into the colour space of, say, hue, lightness and colourfulness. In this way, the dependency of RGB space on hardware devices can be circumvented, i.e., a colour in one device usually does not appear nor measure the same as the one in another device even with the same RGB values in both devices. This is because the range of R, G, or B values are manually set to be the same (such as [0, 255] for an 8-bit computer) for all devices regardless their physical measurements. On the other hand, hue, colourfulness and lightness, space agrees more with human vision theories. To further improve the fitness between users' perception and retrieved results, CIE has recommended a colour appearance model CIECAM02 to predict colours appear on any media under a number of viewing conditions [Moroney]. Stemmed from Hunt's early colour vision model [Luo (a) 1993, Luo (b) 1993 ] employing a simplified theory of colour vision for chromatic adaptation together with a uniformed colour space, CIECAM02 can predict the change of colour appearance as accurately as an average observer under a number of given viewing conditions. In particular, the way that the model describes a colour is reminiscent of subjective psychophysical terms, i.e., hue, colourfulness, chroma, brightness and lightness.
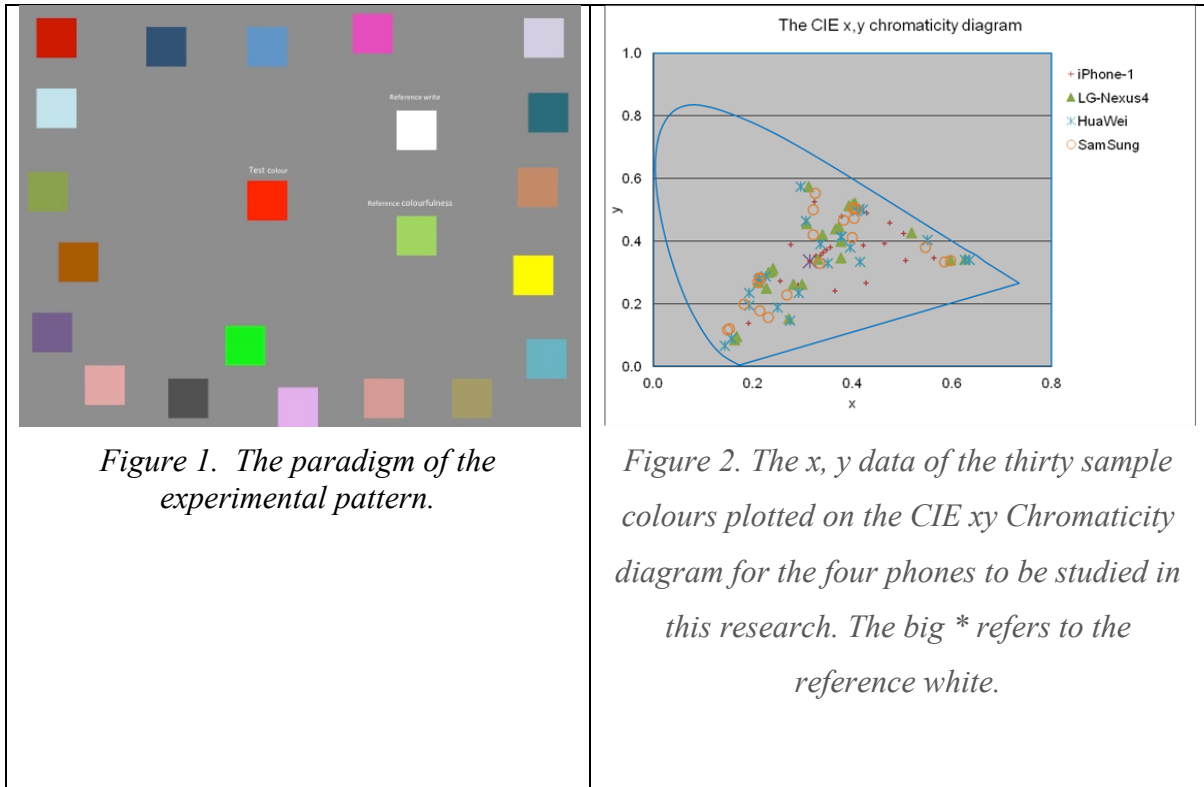
To begin with, CIECAM02 takes into account of measured physical parameters of viewing conditions, including tristimulus values (X, Y, and Z) of a stimulus, its background, its surround, the adapting stimulus, the luminance level, and other factors such as cognitive discounting of the illuminant. The output of the colour appearance model predicts mathematical correlates of perceptual attributes.

With regard to the representation of the colour appearance of an image, in this investigation, the perceptual colour attributes of lightness (*J*), colourfulness (*M*) and hue (*H*) are employed.

## 2. METHOD

Thirty test colours are randomly selected from the Munsell colour book while making an effort to cover as much CIE 1931 colour space as possible. Psychophysical experiments are then carried out on both 19" CRT colour monitor with its illuminant calibrated to D65 and mobile phones. As illustrated in Figure 1, each test colour is placed at a centre against a grey background (with 20% of luminance of reference white) and surrounded by the reference white, reference colourfulness and surrounding colours. The test field in the

centre subtends a visual angle of $2^o$ at a viewing distance of ~60cm. Ten subjects with normal colour vision are selected to conduct the experiments using the technique of magnitude estimation which they have been trained in advance to apply skilfully. Specifically, for each test colour, each subject is asked to estimate its appearance in terms of lightness, colourfulness and hue contents verbally that are then recorded by an operator sitting nearby.
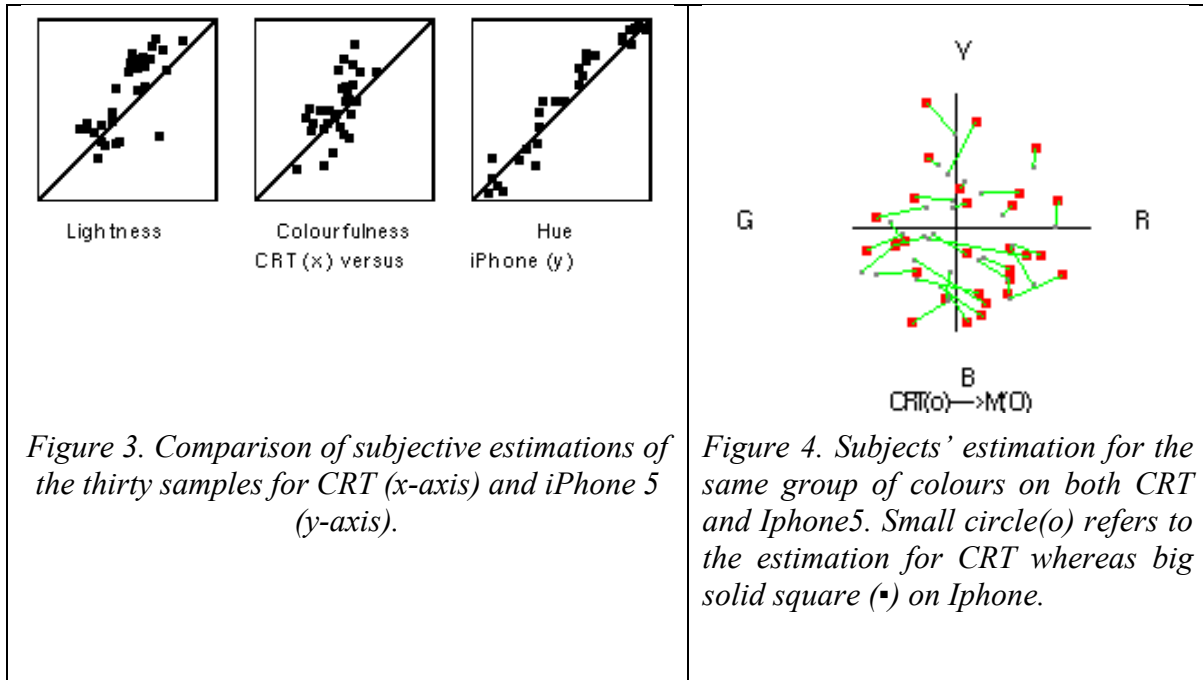


*Figure 1. The paradigm of the experimental pattern.*



*Figure 2. The x, y data of the thirty sample colours plotted on the CIE xy Chromaticity diagram for the four phones to be studied in this research. The big \* refers to the reference white.*

In addition, each colour on each phone has been measured using a colour meter CS-100A, simulating subjects' viewing position. Specifically, the reference white, reference colourfulness, and background are measured at least 3 times, e.g., at the beginning, the middle and the end of the colour sample sequence, to check the repeatability of the phone. In total, 6 phones, including three iPhone5, one Huawei, one SamSung, and one LG Nexus4, are measured and estimated. The same work is also performed on the CRT monitor, Philips Brilliance 201B. The measured data are presented in a CIE xy Chromaticity diagram as illustrated in Figure 2.

## 3. RESULTS AND DISCUSSION

### 3.1 iPhone

Three handsets of iPhone 5 are investigated in this paper. Figure 2 compares the subjects' estimation results between CRT and iPhone 5 where correlation coefficient (r) values are 0.76, 0.62 and 0.96 respectively for Lightness, colourfulness, and hue estimations.

For lightness, the estimation on mobile iphones tends to be 16% more than that on CRT mornitors, whereas 11% increase of colourfulness for mobile phones is evidenced. In Figure 4, a hue-colourfulness plot is presented, where small circles (o) represent the colours from CRT and big square (□) from iPhone5.

*Figure 3. Comparison of subjective estimations of the thirty samples for CRT (x-axis) and iPhone 5 (y-axis).*



*Figure 4. Subjects' estimation for the same group of colours on both CRT and Iphone5. Small circle(o) refers to the estimation for CRT whereas big solid square (▪) on Iphone.*

## 3.2 Modelling of Iphone appearance using CIECAM02

Since the colour appearance model CIECAM02 is developed for the media of CRT, refection and transparency, it may not be well equipped to predict smartphones. After the setting of environmental parameters to 'dim' condition where F =0.9, c = 0.59, and Nc=0.90 to compensate lightness differences between CRT and iPhone, the comparison results are given in Figure 6 for the three phones, where colourfulness is adjusted according to Eq. (1).

$$Colourfulness\_smartphone = 1.8 * Colourfulness\_CIECAM02. \qquad (1)$$
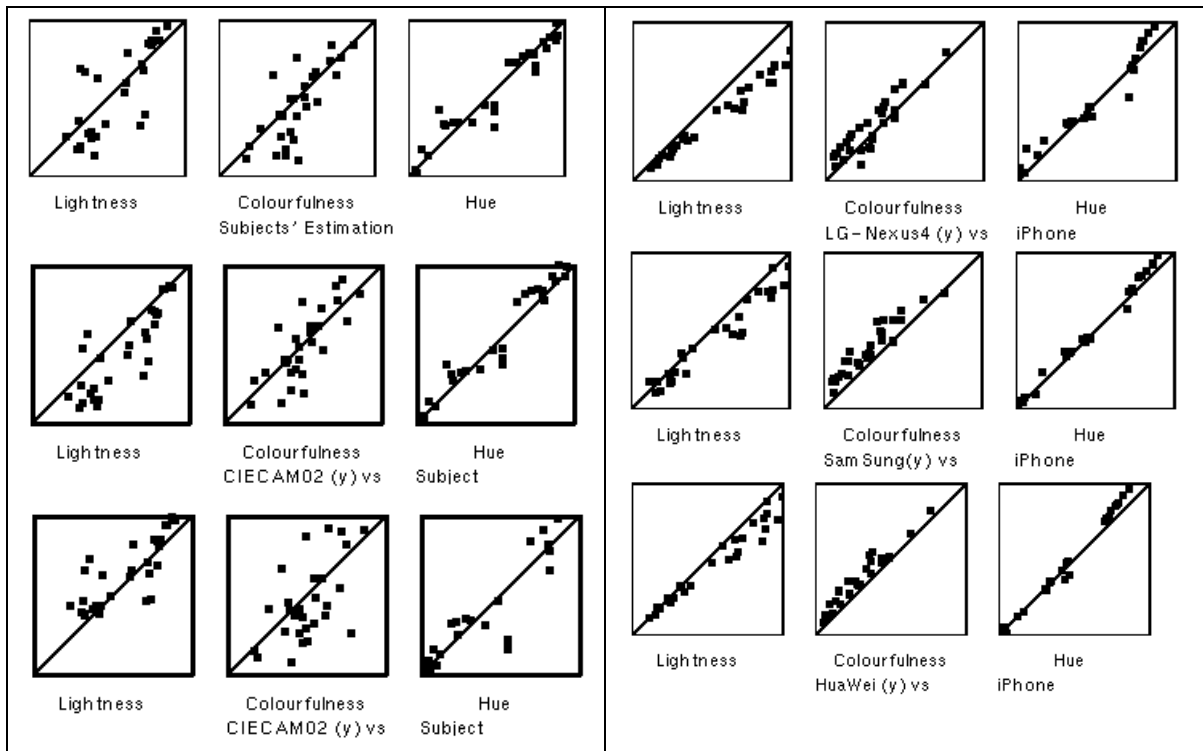
AIC2015 TOKYO - Color and Image

It can be seen that after the correction using Eq. (1), the modified CIECAM02 can predict smartphones accurately.

## 3.3 Comparison with other smart phones

After the modelling of iphones using CIECAM02, a number of other smartphones are evaluated as well, including, a LG-Nexus4, SamSung, and HuaWei. Figure 7 presents the comparison results by the calculations using CIECAM02 for all the phones, whereas Figures 8 demonstrates a colour checker depicted on these phones.
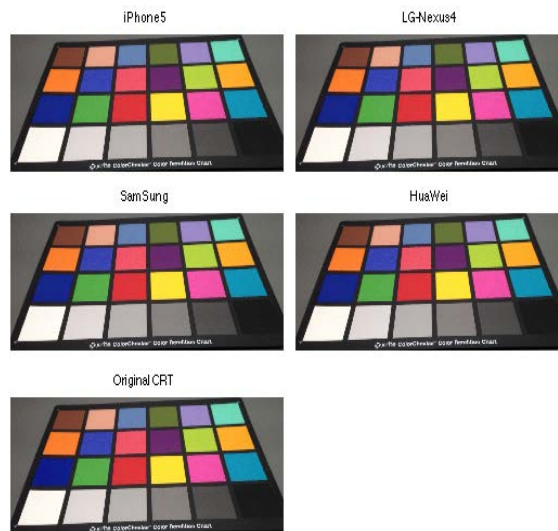


*Figure 8. Colour checker depicted using four phones and CRT*

When comparing with the other smartphones, in terms of hue, all three phones tends to be more reddish for purplish colours than those displayed on an iPhone, whereas the rest maintains near the same. With regard to lightness, for lighter colours, all three phones unanimously appear darker than on iPhones with LG-Nexus being the darkest with 25% darker, whereas 18% and 16% darker are evidenced for HuaWei and SamSung respectively. However, the opposite phenomenon occurs when it comes to the representation of colourfulness. All three phones of LG-Nexus4, SamSung, and HuaWei appear more colourful than those displayed on an iPhone. For example, the colours on a LG-Nexus4 phone appears systemically 10% more colourful than those depicted on an iPhone. In addition, for both HuaWei and SamSung phones, they appear again to be 17% and 22% more colourful, especially for colourful samples, the tendency presenting across all three phones. Since these findings are based on only one phone of each type, future study will focus on the investigation of large samples with more similar phones.

# 4. CONCLUSIONS

With 85% smartphone users perform their everyday tasks [Salesforce] using the device due to its ability and connectivity, smartphone continues to revolutionize how people perform their everyday activities. It is expected that this work will contribute to this revolutionary and complement users with some information when they perform online shopping buying colour incentive goods.

In summary, in terms of the measurement on each phone, encouragingly, the variations among the same kind of phones are insignificant with less than 3 ΔE CIELAB units. In addition, when comparing with subjects' hue estimations, all phones and the CRT monitor appear to have similar hue values, indicating that the hue values have been well reserved on those phones although some variations among phones are observe red. However, when it is viewed on a phone, a colour appears to show at variance with colourfulness by appearing much more colourful. Furthermore, the correlation coefficient (r) for CIELUV L* are 0.963, 0.959, 0.960, and 0.940 for iPhone, LG Nexus4, HuaWei and SamSung respectively, and are 0.890, 0.876, 0.761, and 0.764 respectively for CIELUV C* when comparing with the counterparts on the CRT monitor. Therefore, the iPhone tends to be the best with fewer scatterings. To predict a colour on a mobile phone using CIECAM02, the predictions rest on a number of environmental parameters settings, e.g., f = 0.9, c = 0.59, and nc = 0.90, which gives closer results with less scattering. Consequently, for an image with truthful colour to be displayed on a mobile phone, the forward and reverse model of CIECAM02 will have to be applied. Specifically, for iPhone5, nearly half of the colourfulness predicted by CIECAM02 need to be factored into. Further studies are in place to take more number of phones into consideration.

## REFERENCES

Counter Point Research, http://www.counterpointresearch.com/top10. Retrieved in February 2015.

eMarkter, http://www.emarketer.com/, retrieved in February, 2015.

Flickr: https://www.flickr.com/cameras. Retrieved in February, 2015.

Luo MR, Gao XW, Phodes PA, Xin HJ, Clark AA, Scrivener SAR, Quantifying colour appearance - Part IV., Transmissive media, *Color Research and Application*, vol. 18, 1993, pp. 191-206.

Luo MR, Gao XW, Phodes PA, Xin HJ, Clark AA, Scrivener SAR, Quantifying colour appearance - Part III., Supplementary LUTCHI colour appearance data, *Color Research and Application*, vol. 18, 1993, pp. 98-113.

Moroney N, Fairchild MD, Hunt RWG, Li C, Luo MR, Newman T, The CIECAM02 Color Appearance Model, *In IS@T/SID Tenth Color Imaging Conference*, 2002, pp. 23-27.

Salesforce: www.salesforce.com , retrieved in February 2015.

We are social, http://wearesocial.net/, retrieved in February, 2015.

# Colour Management for High Dynamic Range Imaging

Keith D. M. FINDLATER
School of Design, University of Leeds

## ABSTRACT

High dynamic range (HDR) composite images can be used to create photo-realistic and hyper-real images. Parameters including contrast ratios and tone mapping functions are used to control HDR image processing. However, the dynamic range of real world scenes is highly variable and digital cameras need to be characterised for different scenes. This research aims to investigate and compare colour management processes and image processing between standard and HDR image capture. It will also assess the advantages of HDR images by revealing perceived differences and to ascertain the boundaries where HDR imaging becomes a significantly advantageous process to use.

The proposed research method initially sets up an optimised camera characterisation using standard capture of a scene in controlled lighting conditions. The subject luminance range will then be extended beyond the dynamic range of the camera sensor through experimentation by controlling illumination and the subject using calibrated digital colour test charts. HDR capture techniques will then be employed to create composite images from multiple exposures and single images, from which colour reproduction can be assessed in comparison with the original scene. This process will be used for a range of types of scenes using natural and artificial light sources.

This research aims to extend existing methods of colour management to the HDR domain, to develop new methods if necessary, and to ascertain to whom colour management of HDR Images would be beneficial.

## 1. INTRODUCTION

An illuminated scene will have numerous defining characteristics that will affect the production of images captured by a camera. In photography, these are captured using a lens system and recorded onto either photo-sensitive silver halide film or electronic digital sensors. These camera systems have different design specifications for capturing varying types of scene, for example, by introducing interchangeable lenses and sensor formats to change the shape and angle of the photographed scene (Allen *et al.*, 2011).

The subject luminance ratio is the luminance range of a scene between the darkest shadow and the brightest highlight. A digital camera sensor or photographic film will be capable of recording a limited range of subject reflectances as a tonal range. The sensitivity is optimised for specific types of photography, varying from low level light to very bright scenes. The sensor is exposed to the scene for a period of time through a lens with a measured aperture. This exposure is set so that the sensor records the full tonal values of the subject. This process has been optimised by camera manufacturers so that a photographer can capture a desired image by arranging a scene along with camera settings and control of image or film processing to capture a desired image.

For a brightly illuminated scene, the range of reflectances of a subject can be too great for the tonal range of the captured image. This results in clipping, where tonal detail in the brightest highlights and darkest shadows are recorded as maximum and minimum image

tones. The photographer has the option to accept this result, or attempt to reduce the subject luminance range by changing the lighting conditions, exposure control or image processing, to meet a desired outcome.

High Dynamic Range imaging is a field of research into ways of increasing the range of reflectances that a camera sensor can capture of a subject. The limiting factors include the dynamic range of the sensor and display or the reflectance range of the printed image. However, the commercial and consumer use of digital cameras is widespread using basic sRGB colour gamut for online, digital and printed platforms.

Colour management is the process of adjusting an image to account for differences between various image capture and display devices to ensure colour fidelity. For conventional imaging, methods for colour management have been extensively studied and various solutions are available (Westland *et al.*, 2012). However, much of HDR imaging has been to generate aesthetically pleasing images rather than to obtain colorimetrically accurate ones. This research aims to extend existing methods of colour management to the HDR domain, to develop new methods if necessary, and to ascertain to whom colour management of HDR Images would be beneficial.

## 2. PROPOSED WORKFLOW

The two components of this research involve investigating colour characterisation methods for cameras and then combining this with methods for generating HDR images. Once a workflow is established then more detailed research can begin into the nuances of comparative performance between single captured images with HDR images of different types of natural and artificial scene.

### 2.1 Sample Preparation

For standard camera characterisation, a digital reflective colour chart is normally used as a reference target to generate measured data for a scene under controlled uniform lighting conditions. The known CIE colour coordinates of the patches in the chart and their corresponding captured camera RGB values can be used to constrain a model that can predict CIE values given RGB values.

For HDR imaging, it is not clear that the colour patches in the standard colour charts have a high-enough dynamic range. A test scene needs to be created where the subject luminance range is extended beyond the dynamic range of the camera sensor by controlling illumination and the subject using calibrated digital colour test charts. One solution could be based on having two adjacent reflective colour test charts that fill the image capture area. Localised controlled lighting would be introduced so that, for example, one colour test chart is much brighter than its adjacent. Once optimized, this would be the starting point for creating a controlled test target for the characterisation of HDR images. Another possibility is to use self-luminous display targets.

The advantage of a controlled scene, such as the DigiEye System, is to be able to produce repeatable results for analysis. However, the ultimate aim would be to compare the capture of normal and HDR images under variable natural daylight and artificial light sources.

## 2.2 Camera Characterisation for a Display

The first stage is to establish a standard digital imaging workflow from a real scene to display output. This optimised workflow will be the camera characterisation for a display using standard capture of a scene in controlled lighting conditions.

This process uses principles of additive colour mixing using Grassman's Laws and the 1931 CIE system. The RGB values of the camera image are converted into XYZ values. These values are then converted and outputted to sRGB values or other colour space used by the display.

Once the camera is characterised for a display for a standard image, the same can be used for subsequent HDR captured images.

## 2.3 High Dynamic Range Image Capture

Many sensors in digital SLR cameras capture 12-bit RAW or 8-bit Jpeg files in a single image, corresponding to a dynamic range of exposure values of up to 9 stops between the brightest highlight and the darkest shadow. Firstly, the digital SLR camera will be characterised for display for a fixed colour target under uniform and constant illumination. This would be used for comparison with subsequent HDR images captured of a reference scene with a large subject luminance range.

High Dynamic Range images can be captured using different methods.

The Multiple Exposures Technique is where a sequence of images is captured with incremental changes in exposure time of a fixed scene from a fixed viewpoint (Nightingale, 2012). The number of images and the choice of exposure times are variable and this will be researched to produce a optimised HDR capture process. The resulting component images are merged into a single HDR image using a computational tone mapping process. The alternative method is to capture a single image using a sensor with an extended dynamic range capture capability.

The resulting HDR images will be assessed for colour fidelity by comparing the image colour data with the scene reference data, resulting in the characterisation of HDR images for display. Analysis of the differences between different Multiple Exposures Techniques and tone mapping processes will also be made. Differences between Standard Colour Capture and High Dynamic Range Imaging will be investigated for a variety of types of illuminated scene.

McCann & Rizzi found that glare occurs when a bright object in a scene reduces contrast everywhere within the field of view of the camera. The effect of glare increases with greater dynamic range, so this research would be looking to observe any limits to any corresponding increased colour fidelity (McCann & Rizzi, 2012).

Other limiting factors would include the performance of the imaging sensor, also optical limits in acquisition and visualisation. Other results would include comparison of colour fidelity on single and multiple exposure for scene capture.

A practical issue will be to override the automated proprietary functions in the chosen camera's firmware to provide experimental RAW data for analysis.

Initially for this research, the tone mapping functions will be used for creating photo-realistic HDR composite images only for comparison with standard digital characterisation for a display.

## 3. CONCLUSIONS

As mentioned earlier, the purpose of this paper is to outline the early stages of my PhD research into Colour Characterisation for High Dynamic Range Imaging. This paper will raise awareness and help refine my research plans by attending AIC Tokyo 2015.

The emphasis of my initial research will be to establish a workflow for the Colour Characterisation of HDR images. The differences and merits of HDR imaging techniques including Multiple Exposure techniques, sensors with extended dynamic range capture capability and tone mapping functions will be investigated.

Experimental data will also be collected to see whether observers notice a significant improvement between the resulting colours between captured standard and HDR images for different scenes. This will help see how successful the HDR imaging processes have been.

Other areas of investigative research will include comparisons of colour characterisation for different HDR tone mapping functions; the success of HDR characterisation for different types of scene using Natural and Artificial Light Sources.

Ultimately, my research aims to determine a number of questions. What are the best conditions for using HDR imaging for colour reproduction? What situations are best served by using colour reproduction for HDR imaging? What are the benefits and advantages of HDR imaging? Within what boundaries is HDR imaging a better process to use and for what applications? At what point will people significantly prefer viewing HDR images for different subject matter? What archival storage implications are there for HDR imaging?

## ACKNOWLEDGEMENTS

## REFERENCES AND BIBLIOGRAPHY

McCann, J.J., Rizzi, A. 2012. *The Art and Science of HDR Imaging (First Edition)*. Wiley, Chichester.

Westland, S., Ripamonti, C., Cheung, V. 2012. *Computational Colour Science using MATLAB (Second Edition)*. Wiley, Chichester.

Nightingale, D. 2012. *Practical HDR – A complete guide to creating High Dynamic Range images with your digital SLR (Second Edition)*. ILEX, Lewis.

Allen, E., Triantaphillidou, S. et al. 2011. *The Manual of Photography (Tenth Edition)*. Focal Press (Elsevier), Oxford.

*Address: Keith D. M. FINDLATER, School of Design,*
*The University of Leeds, Leeds, West Yorkshire, LS2 9JT. ENGLAND U.K.*
*E-mails: sdkdmf@leeds.ac.uk, keith@keithfindlater.com*

# Development of a Wide-Gamut Digital Image Set

Stephen WESTLAND, Qianqian PAN, Yuan LI, Soojin LEE
School of Design, University of Leeds, UK

**ABSTRACT**

A great many imaging devices are consistent with the sRGB colour space. However, wide-gamut display devices exist that conform to colour spaces that have wider gamuts such as Adobe (1998) RGB. There is a shortage of standard image sets that contain colours that are outside of the sRGB gamut. Such images could be useful, for example, for testing various performance metrics in wide-gamut display systems. The purpose of this work is to develop a wide-gamut image set and make it widely available on the internet for the imaging community. Three digital SLR cameras were used to capture a large number of images that contained saturated colours. The colour space of the cameras was set to Adobe RGB and the file format was set to record raw. The images were converted to 48-bit TIFF images in the Adobe colour space and on average had about 18% of their pixels outside of the sRGB gamut. MATLAB was used to process the images and to ascertain the proportion of pixels that were outside of the sRGB gamut in each case. Images have been made available on a website – in both raw and tiff formats – and are categorised according to their colour and also according to the description of the objects for which the pixels are out of gamut. Example, object classifications include textiles, jewellery, arts, plants, foodstuffs and electronics. A total of 100 wide-gamut images were selected and have been made available to the community.

## 1. INTRODUCTION

Trichromacy is a crucial concept in colour imaging. The majority of digital cameras capture colour using three sensors, usually referred to as RGB, that capture different wavelength properties of the scene. Digital cameras often output images in a standard colour space known as sRGB (Süsstrunk *et al.*, 1999). The sRGB colour space has a gamut that is illustrated in Figure 1 by the black solid lines. The vast majority of image display devices also conform, at least approximately to the sRGB colour space so that they have a limited colour gamut. The vast majority of consumer images are defined in the sRGB colour space.

However, some capture and display devices are based on other colour spaces and one of the most common of these is the Adobe 1998 RGB space (Süsstrunk *et al.*, 1999). This colour space encompasses about 50% of the colours in CIELAB and improves on the gamut of sRGB in the green-cyan colours in particular. The Adobe RGB colour gamut is illustrated by the white lines in Figure 1. As can be seen the major difference between the two colour spaces is the chromaticities of the green primary which, for the Adobe space, is much more saturated. Images that contain colours that are outside of the sRGB colour space are referred to as wide-gamut images. There is some need to have standard wide-gamut images that can be widely available to the scientific community because these can be used to evaluate, for example, properties of so-called wide-gamut devices. With the widespread use of commercialised wide-gamut displays, the demand for wide-gamut content is increasing (Murakami *et al.*, 2013). The majority of LCD displays are based on the sRGB colour gamut whereas AMOLED displays support the Adobe RGB colour space;

based on an analysis of gamut volumes, AMOLED displays have been shown to be able to display 60-80% more discernible colours than the LCD displays (Li *et al.*, 2014). Wide-gamut images can also be useful for evaluating gamut-mapping algorithms (Langendijk *et al.*, 2009).

There have been several approaches to collect wide-gamut images. One approach is to use a spectral camera because this can capture a very wide colour gamut (Murakami *et al.*, 2013) or, alternatively, a multispectral camera (Murakami *et al.*, 2012). However, spectral cameras can be expensive, bulky and sometimes require extensive calibration and these constraints make them not so suitable for capturing images outdoors. A second approach has been to artificially expand the gamut of existing sRGB-specified images. However, in this paper we use consumer-grade digital SLR cameras that have the capacity to record images in Adobe RGB colour space. The aim of the work is to capture a large number of naturally occurring images that contain pixels that are outside of the sRGB colour gamut and to make these images widely available to the community for use.
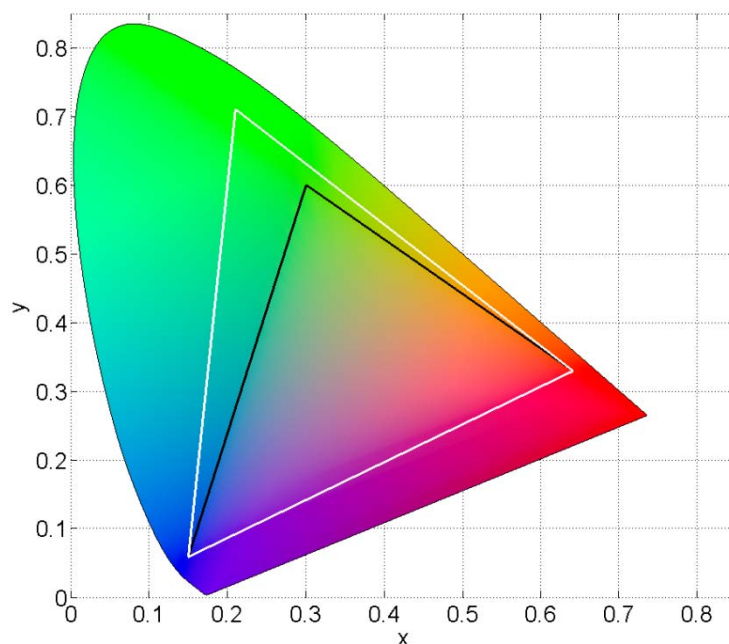


*Figure 1: CIE 1931 chromaticity diagram showing the gamut of sRGB (black line) and Adobe 1998 RGB (white line).*

## 2. METHOD

Three different digital SLR cameras were used to capture the images. Table 1 lists the cameras and their settings.

Images were captured as raw files and converted to 16-bit TIFF files with the Adobe sRGB colour space. Note that some images were captured in portrait mode and others were captured in landscape mode.

AIC2015 TOKYO - Color and Image

*Table 1: Details of the camera files used in the work.*

| Device Name | Colour Space | File Type | Conversion File Type | Image Size |
|---|---|---|---|---|
| Nikon D90 | Adobe RGB | RAW | 16-bit TIFF | 4288 × 2848 |
| Nikon D7000 | Adobe RGB | RAW | 16-bit TIFF | 4298 × 3264 |
| Canon EOS 100D | Adobe RGB | RAW | 16-bit TIFF | 5184 × 3456 |

## 2.1 Image Processing and Selection Criteria

A large number of images were captured and these were processed and then selected to produce a set of 100 images with content outside of the sRGB gamut. A MATLAB program was therefore written to analyse each image. The first step was to convert the raw image to 16-bit Adobe RGB TIFF files. This was done using Corel PaintShop Pro (in the case of the Nikon images) and Canon Image Browser EX (for the Canon images). The second step was to convert from Adobe RGB to CIE XYZ, using the linear transform

$$\mathbf{T} = \mathbf{MC}$$

where $\mathbf{T}$ is a matrix of $3 \times N$ XYZ values (where $N$ is the number of pixels in the image), $\mathbf{C}$ is a matrix of $3 \times N$ linear RGB values, and $\mathbf{M}$ is the $3 \times 3$ matrix thus:

$$\mathbf{M} = \begin{bmatrix} 0.57667 & 0.18556 & 0.18823 \\ 0.29734 & 0.62736 & 0.75290 \\ 0.27230 & 0.07069 & 0.99134 \end{bmatrix}$$

The linear RGB values were obtained from the camera RGB values according to the equation

$$C(i,j) = \left((D(i,j) + 0.055)/1.055\right)^{2.199}.$$

for channel $i = 1$ to 3 and pixel $j = 1$ to $N$ and where $D(i, j)$ is the 16-bit RGB value normalized to the range 0-1 for channel $i$ and pixel $j$. The third step was to convert from XYZ values to sRGB values. The normalized XYZ values $\mathbf{T}$ were converted to linear sRGB values using the matrix equation

$$\mathbf{S} = \mathbf{AT}$$

where $\mathbf{T}$ is a matrix of $3 \times N$ normalised XYZ values, $\mathbf{S}$ is a matrix of $3 \times N$ linear sRGB values, and $\mathbf{A}$ is the $3 \times 3$ matrix thus:

$$A = \begin{bmatrix} 3.2406 & -1.5372 & -0.4986 \\ -0.9689 & 1.8758 & 0.0415 \\ 0.0557 & -0.2040 & 1.0570 \end{bmatrix}$$

The proportion of pixels that were outside of the sRGB gamut was calculated as being thr proportion of pixels for which either $A(1, j)$, $A(2, j)$ or $A(3, j)$ was less than zero or greater than 1 at this stage. However, for display and subsequent storage as sRGB values the linear values A were processed thus

$$RGB(i,j) = 1.055 S(i,j)^{1/2.4} - 0.055$$

if $S(i, j) > 0.0031308$ and otherwise

$$RGB(i,j) = 12.92 S(i,j).$$

Figure 2 shows the flowchart of the colour-imaging workflow.
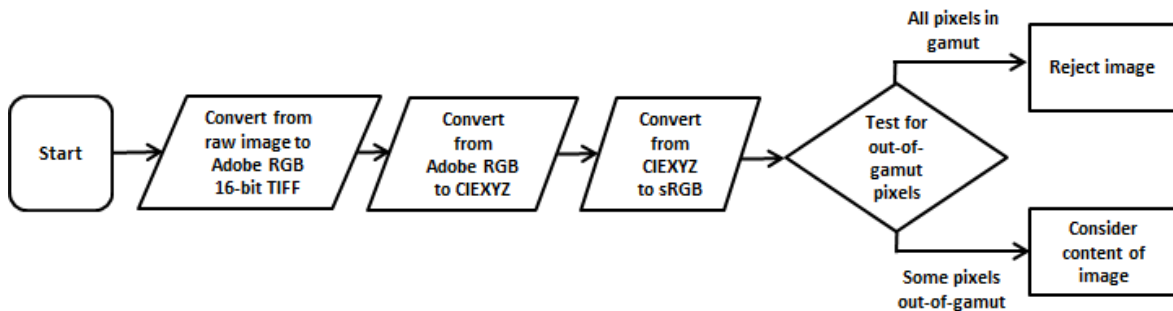


*Figure 2: Flowchart illustrating workflow.*

The approach of using an Adobe RGB camera system to obtain the images means that only colours that are blue, green, yellow and orange can be captured that are outside of the sRGB gamut. This is because the gamut boundaries of the two RGB systems in the red-magenta-blue region are the same (see Figure 1). A wide variety of content was aimed for including natural (precious stones, animals, plants, food) and manmade (light, textiles, plastics/paints, modern).

## 3. RESULTS AND DISCUSSION

Figure 3 illustrates some example output from the image processing described earlier. The left-hand upper pane shows the original image (as an sRGB representation) and the left-hand lower pane highlights the pixels that are out of the sRGB gamut (in this image pixels that are inside the gamut are darkened and the out-of-gamut pixels retain their original colour). The yellow colours of the flowers, for example, are out of gamut. The right-hand pane shows a CIE chromaticity diagram and the chromaticities of every pixel in the image. The sRGB and Adobe RGB gamuts are shown as white triangles. It is clear that some of the pixels in the yellow region are out of gamut. However, recall that gamuts are three

dimensional and the out-of-gamut pixels have been identified as those that are outside of the three-dimensional sRGB gamut (as described in the Methods) and are highlighted in pink in the right-hand image. Note that in this example some pixels that are inside the sRGB triangle are actually out of gamut. In Figure 3, it can be seen that 43.8% of the pixels for this particular image were out of gamut. On average the images had about 18% of their pixels outside of the sRGB gamut with the minimum and maximum being 1% and 82% respectively.
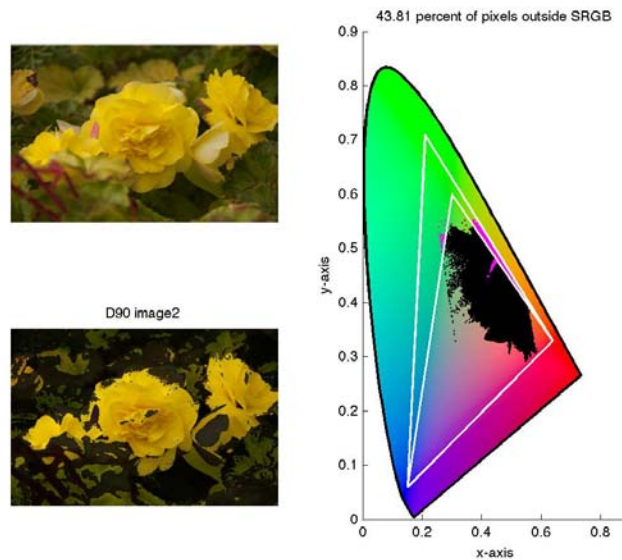


*Figure 3: Flowchart illustrating the sample process.*

As can be seen in Table 2, the number of images with out-of-gamut blue, green, yellow and orange components was 47, 43, 29 and 12 respectively; these numbers sum to more than 100 because some images contained two or more different colours that were outside of the gamut. Blue and green colours were most prevalent. In terms of categories, animal and jewelry were the most difficult to obtain.

*Table 2. Summary of images included in the final database.*

|  |  | blue | green | yellow | orange |
|---|---|---|---|---|---|
|  | jewellry | 2 | 0 | 0 | 0 |
| natural | animal | 0 | 0 | 1 | 0 |
|  | plants | 0 | 5 | 4 | 2 |
|  | food | 4 | 5 | 7 | 3 |
|  | light | 3 | 6 | 5 | 3 |
| manmade | textiles | 6 | 1 | 3 | 1 |
|  | dyeing | 17 | 11 | 4 | 3 |
|  | modern | 15 | 15 | 5 | 0 |

The images are publically available at the following website which has been developed to support the images and their use within the scientific community - http://widegamutimages.wordpress.com/.

# 4. CONCLUSIONS

A total of 100 images have been captured with pixels that are outside of the sRGB gamut. On average the images had about 18% of their pixels outside of the sRGB gamut with the minimum and maximum being 1% and 82% respectively. The image contents represent a wide variety of subject matter including natural (precious stones, animals, plants, food) and manmade (light, textiles, plastics/paints, modern) objects. The images

The colour space of the cameras was set to Adobe RGB and the file format was set to record raw. The images were converted to 48-bit TIFF images in the Adobe colour space and on average had about 18% of their pixels outside of the sRGB gamut. MATLAB was used to process the images and to ascertain the proportion of pixels that were outside of the sRGB gamut in each case. Images have been made available on a website – in both raw and tiff formats – and are categorised according to their colour and also according to the description of the objects for which the pixels are out of gamut. Example, object classifications include textiles, jewellery, arts, plants, foodstuffs and electronics. The images have been made freely available to the scientific community for download.

# REFERENCES

Süsstrunk, S., Buckley, R. and Swen, S. 1999. *Standard RGB Color Spaces*, Proceedings of the 7th IS&T Color Imaging Conference, 127-134.

Murakami, Y., Yamaguchi, M. and Ohyama, N. 2013. *Dictionary-Based Estimation of Spectra for Wide-Gamut Color Imaging*, Color Research and Application, **38** (2), 120-129.

Li, Y., Westland, S., Pan, Q. and Cheung, V. 2012. *Methods to assess the relative number of discernible colours for displays*, Proceedings of the 22nd IS&T Color Imaging Conference, 189-194.

Langendijk, E.H.A., Hotz, A.S. and Hinnen, K.J.G. 2009. *Wide Gamut Color Mapping and Image Enhancement using Image Segmentation*, Proceedings of the 17th IS&T Color Imaging Conference, 181-185.

Murakami, Y., Iwase, K., Yamaguchi, M. and Ohyama, N. 2008. *Evaluating Wide Gamut Color Capture of Multispectral Cameras*, Proceedings of the 16th IS&T Color Imaging Conference, 189-194.

.

*Address: Prof. Stephen WESTLAND, School of Design, University of Leeds, Woodhouse Lane, Leeds, LS2 9JT, UK E-mails:s.westland@leeds.ac.uk,texqp@leeds.ac.uk*

# Construction of display profiles using simplicial maps and application to color reproduction of displays

Masashi YAMAMOTO,[1] Jinhui CHAO[1, 2]
[1] Graduate School of Science and Engineering, Chuo University
[2] Faculty of Science and Engineering, Chuo University

## ABSTRACT

In this paper, we present an algorithm for color device calibration based on 3D-LUT using tetrahedral interpolation for displays. In particular, instead of test in which tetrahedron an input point lies, we proposed a fast algorithm to build a tetrahedron which contains an arbitrary input point for non-uniform grids. Performance of the proposed method is evaluated with color difference for single color inputs and natural images.

## 1. INTRODUCTION

To achieve a uniform color reproduction between different devices, a framework for color management and device calibration proposed by ICC using device profiles has been widely used e.g. Green (2010). Currently, most color devices are furnished with a profile by the device manufactures. Certain commercial software of profile making are also available.

However, variations exist between individual devices even by the same manufactures or due to device aging. The profile often describes device characteristics by a product of three 1D (usually monotonous) functions which is a rough approximation of a 3D nonlinear map. It might be useful for CRT but not enough for e.g. LCD displays with highly nonlinearity.

A solution is to use 3D look-up table (3D-LUT) in particular tetrahedronal interpolation. Lee(2005), Barsotti(2014), Kang(1996). However, besides a large number of measurements required, there seemed no efficient way to test which tetrahedron for a non-uniform grid an input point lies before to apply the inversion transformation. Existing approaches repeat try-and-error to test if the point is contained in a tetrahedron turned out to be inefficient.

In this paper, we present 3D-LUT calibration of displays using tetrahedronal interpolation in terms of simplicial maps. This formulation provides a conceptually clearer description of device calibration. The algorithm is different from existing approaches based on 3D-LUT using tetrahedral interpolation in the way to determine which tetrahedron an input point lies in. Instead of try to test if the point lies in a tetrahedron, we directly build a tetrahedron which contains the input point.

The following three implementations of the proposed method with different computational costs are investigated: 2D maps of the chromaticity plane, 3D maps of the color space which compensate chromaticity and brightness simultaneously, and (2+1)D maps which compensate chromaticity and brightness separately. The (2+1)D version shown to be a reasonable trade-off between performance and cost.

The proposed method and commercial profile makers are compared in terms of quantitative color difference between input and output colors. Besides, natural images are also used as

input data for subjective comparison. Both experiments confirmed effectiveness of the proposed method.

## 2. PROPOSED METHOD

### 2.1 Simplicial linear maps and convex combination

A $m$-simplex is a $m$-D polytope which is the convex hull of its $m+1$ vertices $x_1,\ldots,x_{m+1}$:

$$S = \{x = a_1 x_1 + a_2 x_2 + \ldots + a_{m+1} x_{m+1}, \ a_i \geq 0, \ \sum_{i=1}^{m+1} a_i = 1\}$$

E.g. a 2-simplex is a triangular, a 3-simplex is a tetrahedron. A set of points in $R^n$ can be regarded as a collection of simplices or a simplicial complex.

Here $a = (a_1, a_2, \cdots, a_m)^T$ are called convex or barycentric coordinates of $x$ with respect to $\{x_i\}$, which can be obtained as follows including the inverse of an $m \times m$ matrix $X$.

$$a = X^{-1}(x - x_{m+1}), \ X = (x_1 - x_{m+1}, \ldots, x_m - x_{m+1}) \tag{1}$$

E.g. m = 2 and m = 3, denote $x_i = (x_{i1}, \cdots, x_{im})^T$,

$$\begin{pmatrix} a_1 \\ a_2 \end{pmatrix} = \begin{pmatrix} x_{11} - x_{31} & x_{21} - x_{31} \\ x_{12} - x_{32} & x_{22} - x_{32} \end{pmatrix}^{-1} \begin{pmatrix} x_1 - x_{31} \\ x_2 - x_{32} \end{pmatrix} \tag{2}$$

$$\begin{pmatrix} a_1 \\ a_2 \\ a_3 \end{pmatrix} = \begin{pmatrix} x_{11} - x_{41} & x_{21} - x_{41} & x_{31} - x_{41} \\ x_{12} - x_{42} & x_{22} - x_{42} & x_{32} - x_{42} \\ x_{13} - x_{43} & x_{23} - x_{43} & x_{33} - x_{43} \end{pmatrix}^{-1} \begin{pmatrix} x_1 - x_{41} \\ x_2 - x_{42} \\ x_3 - x_{43} \end{pmatrix} \tag{3}$$

A point $x$ lies insides the $m$-simplex if and only if all its barycentric coordinates $a_i \geq 0$.

A map $y = f(x)$ is a linear simplicial map if $f(x_i) = y_i, i = 1, \cdots, m+1$ and when $x = \sum_i a_i x_i$, $y = f(x) = \sum_i a_i y_i$. The linear simplicial maps then can be used to approximate $C^0$-class or continuous maps.

Characterization of a device is to produce a profile or a forward model as a map $p$ from a device color space to the PCS or vice versa. Then calibration of the device is basically to apply the inverse map of $p$ on the input color in PCS to compensate or correct the characteristics of the device in order to obtain a truthful color reproduction. E.g. for a display, the profile is measurements of the output RGB values for certain target colors in PCS. Such a forward map $p$ is approximated by a linear simplicial map in 3D-LUT and the inverse map $p^{-1}$ by tetrahedronal interpolation. Then an input $x$ is first transformed to $z = p^{-1}(x)$ of which the output $p(z) = p \circ p^{-1}(x) = x$ reproduces the input faithfully.

The inverse $f^{-1}$ of a linear simplicial $f$ such that $x = f^{-1}(y)$ is also linear simplicial, which can be calculated as follows.

Given a point $y$, one needs first to find a simplex in which the point lies. Denote the vertices of the simplex as $y_1, \ldots, y_{m+1}, y_i = f(x_i)$. The second step is to calculate the barycentric coordinates $b_i$ of $y$ with respect to $y_i$ such that $y = \sum_i b_i y_i$. The inverse map is then given by

$$x = f^{-1}(y) := \sum_i b_i x_i \qquad (4)$$

Since $f(x) = \sum_i b_i f(x_i) = \sum_i b_i y_i = y$, the map (4) does give the inverse image of $y$.

## 2.2 Test if a point is inside a tetrahedron

In order to calculate the inverse map, a 3D-LUT requires to find the tetrahedron in which the input point $x$ lies. This is however non-trivial for non-uniform grid which is the typical case for device calibration.

It is usually done by choosing a tetrahedron whose vertices are closted to $x$. Then calculate the convex coordinates $a_i$ and check if the convex inclusion conditions $a_i \geq 0$ are satisfied. If not one needs to try another tetrahedron. In fact, since trials have to be repeated to avoid the cases shown in Figure 1(a), these calculations seemed to be the most time-consuming step in the 3D-LUT processing.

There are also other ways e.g. Amidror. I. (2002) to test if the straight line connecting $x$ with a point lie in the tetrahedron intersects a face of the tetrahedron. $x$ lies insides when there are no such a intersection for all 4 faces of the tetrahedron. However since the calculation to test the above intersection in a face or a triangular requires as the first step to calculate the convex coordinates of $x$ with respect to the tetrahedron, this method seemed to be less efficient than direct application of the convex inclusion condition.

## 2.3 A new method to build a tetrahedron containing a point

Firstly, we reduce all 3D processings to 2D ones since calculations of barycentric coordinates and convex inclusion for triangulars are much easier than for tetrahedrones. Secondly, instead of repetition of test in which tetrahedron the input point lies, we directly produce a tetrahedron which contains the point without try-and-error.

To explain the idea, assume that an input point $x = (\alpha, \beta, \gamma)^T$ is given. Then one can draw a line $\lambda$ through $x$ in parallel to one coordinates axis e.g. $X_1$. Here we used $X_1$ as the $L$ values in the CIELUV space. This line will intersect with two triangulars near to $x$. (We omit the lucky case when the line intersects a vertex or grid point of the triangulars.) In particular, the projections of the two triangulars onto the plane $[X_2, X_3]$ of the 2nd and the 3rd coordinates, which are two triangulars again will contain the projection $(\beta, \gamma)$ of the input point $x$ onto $[X_2, X_3]$. Search for these two triangulars is easy since it is virtually in the $[X_2, X_3]$ plane among the grid points whose the 2nd and the 3rd coordinates are close to $(\beta, \gamma)$ We di this for the $L$ levels below and about $\alpha$.

Then we chose the desired tetrahedron with vertices of one of triangulars, e.g. $\langle x_1, x_2, x_3 \rangle$ and $x_4$ as the intersection point of the line $\lambda$ with the other triangular. (See Figure 1(b)).

In fact, the barycentric coordinates of the intersection $w$ between the line $\lambda$ and the triangular $\{x_1, \ldots, x_3\}$ can be found the following 2D calculation.

Denote $x_i = (x_{i1}, x_{i2}, x_{i3})^T$

$$w = c_1 x_1 + c_2 x_2 + (1 - c_1 - c_2) x_3 \tag{5}$$

$$\begin{pmatrix} c_1 \\ c_2 \end{pmatrix} = \begin{pmatrix} x_{12} - x_{32} & x_{22} - x_{32} \\ x_{13} - x_{33} & x_{23} - x_{33} \end{pmatrix}^{-1} \begin{pmatrix} x_2 - x_{32} \\ x_3 - x_{33} \end{pmatrix} \tag{6}$$
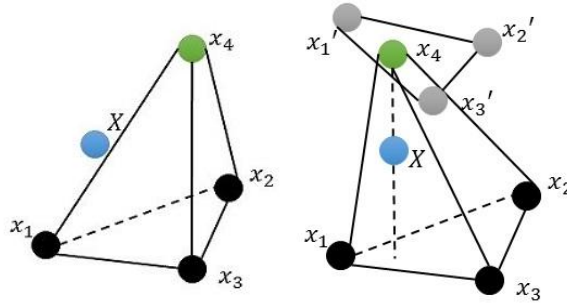


*(a) $x_4$ is an invalid vertex*     *(b) $x_4$ as intersection of a line through X*

*Figure 1: Build a tetrahedron containing a point X*

Notice here that the inverse image of $w$ under the profile map is the convex combination with the same barycentric coordinates of the inverse images of $x_i$.

## 2.4 Algorithm

The algorithm for display calibration with PCS as CIELUV space is described as follows:

Step 1: Build the profile or forward map by measurement on a display for target colors. The data are averaged among three measurements;

Step 2: For an input color $x = (\alpha, \beta, \gamma)^T$, for $L$ levels below and above $\alpha$, find the two triangular including $(\beta, \gamma)$ in $[u^* v^*]$ plane;

Step 3: Draw the line $\lambda$ along $L$ axis and find the fourth vertex $x_4$ by (6) therefore build the tetrahedron containing $x$;

Step 4: Calculate the convex coordinates of the input color $x$ with respect to measured data by eq.(3);

Step 5: The inverse map (4) was applied to input color data as a preprocessing for color reproduction.

This algorithm is applied in three stages in the order of increasing complexity: firstly to $u^* v^*$ plane in CIELUV which we called 2D correction, secondly $u^* v^*$ and $L$ axis separately which we called (2+1)D correction and finally the CIELUV space which we called the 3D correction.

## 2.5 Environment

Measurements and photos of the displays were all taken in a darkroom. CA-210 by KONICA MINOLTA was used as the colorimeter and each colorimetry value was obtained from average of three measurements. The target colors are consisted of 695 sample points on CIELUV space derived from 113 lattice points on the $u^*v^*$ chromaticity plane and 11 levels of brightness as $L = 25, 30, \ldots, 75$. Furthermore, color difference between input color data and measured color data was evaluated by the distance $\Delta E$ in CIELUV space. E.g. for

$$a = (L_a, u_a, v_a) \text{ and } b = (L_b, u_b, v_b), \ \Delta E = \sqrt{(L_a - L_b)^2 + (u_a - u_b)^2 + (v_a - v_b)^2} \ .$$

## 3. EXPERIMENTAL RESULT

Experiments on single color input and natural image are conducted for evaluation.

The table 1 shows the result applying the proposed method on 695 target colors. The color difference between input color and output color measured on display are shown for colors under calibration. The proposed method is compared with Spyder4Elite, a commercially available ICC profile maker. The proposed methods provided very closer reproduction of the input in 2D, (2+1)D and 3D cases. In Figure 2, we show the photos of two displays both showing the same color input twice on top and bottom. The top images are without calibration and the bottom were calibrated color. The improvement of agreement between the two displays can be easily observed.

*Table 1: Comparison of color difference on displaying single color input*

|  | Spyder4Elite | 2D calibration | 3D calibration | (2+1)D calibration |
|---|---|---|---|---|
| Average ΔE | 16.415 | 7.255 | 1.712 | 3.361 |
| Standard Deviation | 7.806 | 1.039 | 1.245 | 1.938 |
| Max ΔE | 38.440 | 11.646 | 10.577 | 16.606 |
| Min ΔE | 1.070 | 4.147 | 0.200 | 0.284 |
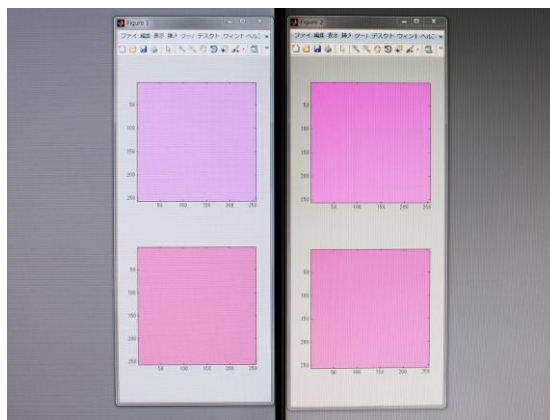


*Figure 2: Comparison of the outputs of a single color input before and after calibration*

Result of applying proposed method to natural images are shown in Figure 3.



*Figure 3: Comparison of a natural image before and after calibration*

## ACKNOWLEDGEMENTS

## REFERENCES

Green, P. 2010. *Color Management Understanding and Using ICC Profiles.* New Jersey: Wiley.

Kang, H.R. 1996. *Color Technology For Electronic Imaging Devices*. Washington: SPIE.

Aristova, A. 2010. Smoothness of color transformations. Available online, hdl.handle.net/11250/144133. Accessed: January 21, 2015.

Barsotti, J, T. Schulte. 2014. Display Profiling Solutions A Report On 3D LUT Creation. Available online, www.spectracal.com/Documents/White%20Papers/Display%20Profiling%20Solutions.pdf. Accessed: January 23, 2015.

Lee H.C. 2005. *Introduction to Color Imaging Science*. Cambridge: Cambridge University Press.

Amidror, I. 2002. Scattered data interpolation method for electronic imaging systems: a survey. *Journal of Electronic Imaging* 11(2): 157-176.

Yamamoto, M., J. Chao. 2014. Construction of display profiles using simplicial maps and application to color reproduction of displays. In *Proceedings of 29$^{th}$ SIP SYMPOSIUM*, IEICE Japan: Kyoto, 393-398.

*Address: Prof. Jinhui CHAO, Faculty of Science and Engineering, Chuo University, 1-13-27, Kasuga, Bunkyo-ku, Tokyo, 112-8551, JAPAN E-mails: a10.7tb8@g.chuo-u.ac.jp, jchao@ise.chuo-u.ac.jp*

AIC2015 TOKYO - Color and Image

# "Psycolorsynthesis": An Introduction of 10-Color Communication Method

Chiori OHNAKA
Office Color Palette

## ABSTRACT

"Psycolorsynthesis" is a newly developed concept derived from psychosynthesis. While harmonizing one's plural selves to attain integration of the personality is what Assagioli (1965) calls psychosynthesis, this paper shows that colors can play a critical role to attain this integration. 10-color communication method is introduced to demonstrate that colors enhance the awareness of self as well as others' understandings. And this awareness brings about personality integration. The method applies colors as an effective medium for people to express themselves regardless of their social status and contexts. The method calls for a workshop with a group of 8 to 12 people, and let each of them use a set of color cards (normally about 200 colors). It consists of two modules: communication with self by making a color identification data (ID) arranged from 10 selected favorite colors and communication with others by giving 2 colors to other participants as a gift.

Data collected from more than 300 workshop participants identify that approximately 80% of them show clear correlations between 10 self-selected favorite colors and colors received from others as a gift. In addition, workshop observation suggests that communication with a medium of colors clearly enhance relaxed interactions among participants and result in becoming aware of self and others. 10-color communication method demonstrates that the power of colors can overcome risks, worries, and fears that
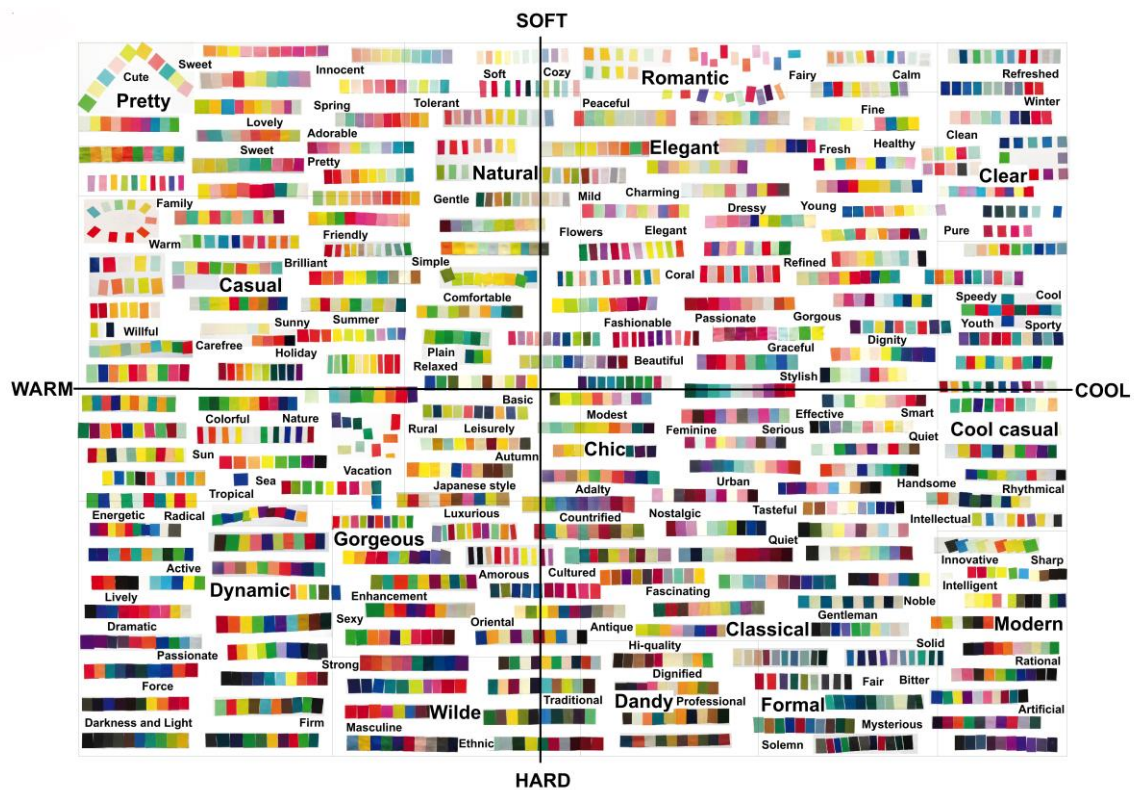
Figure1

people have deal with when they attempt to share their inner-colors. When colors applied to people as their representations, each color-ID (representing each person) is unique and distinctive, for which nobody can say better or worse compared with others' color-IDs (representing other persons). This communication method can effectively be applied to improve the practices of social activities such as recruiting and counseling.

# 1. INTRODUCTION

This paper introduces a new color communication method and shows, with the evidence of collected data, that the method can be an effective way for enhancing the awareness of self as well as others' understandings. In 10-color communication method that this paper introduces, colors are used as representations of one's multiple aspects of inner-selves (hereafter "inner-colors"). While mutual understanding is the essential goal of communication, few can actually understand self, let alone understand others. To begin with, one may not necessarily express one's feelings and thoughts freely due to socially expected norms and/or conflicting interests that one might have vis-à-vis others. This paper shows that colors enable people, regardless of their social status and contexts, to express themselves through inner-colors freely and to gain self-confidence The data collected from the communication workshops show that this straightforward method not only develops the awareness of self and others' understandings but also and more importantly provides participants with self-synthesizing and healing experiences. In this regard, this method can be named "psycolorsynthesis" after psychosynthesis (Assagioli, 1965).

The paper firstly explains the two modules of 10-color communication workshop and color-IDs, followed by the results of the workshop to show features of color-IDs and remarkable findings of color correlations. The paper then suggests how 10-color communication can potentially be effective when applied to social practices such as recruiting and counseling.

# 2. METHOD

The method calls for a workshop with a group of 8 to 12 people, and let each of them use a set of color cards[1]. It consists of two modules of communication as follows.

## 2.1 Module1: Communication with self

For the first module, each participant is asked to select 10 favorite colors, cut them squarely from the provided color card set, paste the selected 10 color pieces on a sheet straightly in his/her own favorite arrangement with glue. A frequently asked question is if selected color cards shall be arranged in order of his/her preference. And its answer is to arrange straightly as one feels the color-ID the most beautiful. This method specifically uses 10 colors for the following reason; while beautiful color combinations are two-color, three-color, four-color, five-color, and six-color combinations, a ten-color-ID can contain combinations such as 2-2-2-2-2, 3-3-4, 5-5, 6-4, 2-2-2-4, and so forth. Thus, not only mere color combinations but also groupings of the combinations show the feature of one's personalities and patterns.

---

[1] "Color Cards 199a " produced by Japan Color Enterprise Co., LTD contains 199 selected colors based on Practical Color Co-ordinate System(PCCS) and better serves for this workshop.

Once color-IDs are made, participants take a close look at each of their color-IDs that are sticked on a board, express in words whatever they intuitively sense and feel for each color-ID. Words can be nouns, adjectives, and short sentences. For example, "I feel bright like Sun shine." When participants express in words for each color-ID, each participant takes notes what others say about his/her own color-ID.

## 2.2 Module2: Communication with others

For the second module, each participant selects two colors that most fit the image of each of other participants, and then cut the two colors in square and give them to the participant as a gift. In this way, everybody receives two colors each from other participants. Each participant pastes all the received color squares on a sheet as he/she likes. Then, again, participants take a close look at each of the sheets sticked on a board, express in words for each of the sheets. When participants received colors and then received words for collected colors, participants realize how they are perceived by others. Finally, participants take out their own color-ID sheets and gifted color-square sheets from the board, and compare and analyze these two sets of colors.

## 3. RESULTS AND DISCUSSION

### 3.1 Color-IDs representing diverse inner-colors

In Module1, when participants expressed their feelings for each color-ID, they could talk freely as if they were playing a game. Participants shared many inspiring words to enjoy this process. On the other hand, when a participant took his/her turn to receive words from others, the participant realized that each word received from others was a representation of him/her-self. Through receiving many words, each participant becomes aware of one's inner-selves.

Color-IDs on Figure 1 are 188 (65 men and 123 women in the age range of between 20s and 50s) sample results collected from Module1 color communication workshops conducted for Japanese. Presented words for color-IDs mean that popular words that the owners of color-IDs received from other participants. This figure shows that they are all unique, different, and extremely diverse[2]. Yet, careful observation offers some tendencies.



Figure2

Color-IDs of women tend to be found in areas with presented words such as "Cute," "Pretty," and "Casual," while those of men are found in areas with "Dynamic," "Classical, "Cool. Having said that though, color-IDs for both women and men can be found any areas in the figure. Thus, one cannot identify men/women from color-IDs.

---

[2] Total possible combination is more than $10^{29}$, while the total world population is about $10^{10}$.

Figure3

Color-IDs on Figure 2 are collected from 20 female university students. Looking at these color-IDs, people imagine words in mind. Women are likely to express their feelings in words. At beginning, theorists might feel not at ease finding words, yet colors gradually relax them to utter words as they feel. Some people are rather reserved to express their feelings. For this color communication workshop, however, it was observed that the bulk of participants were comfortable to express their feelings in words about presented color-IDs. As far as their topic was color-IDs, they seemed not to have any hesitation to share their feelings. Color-IDs are independent from their social positions and have an affinity for intuitive feelings. Participants apparently felt at home. They were talkative and open-minded as they enjoyed pleasant interactions. Many participants said that this communicative interactions to express and receive feelings each other were a healing experience.

Color-IDs on Figure 3 are collected from 20 men. Which color-IDs are atttrative for you? What do you imagine persons making these color-IDs? Because color-IDs are simple and visual, anybody can participate in sharing feelings. Through color-IDs, people appreciate the diverisity of people's identities.

### 3.2 Comparing and analyzing results of Module1 and Module2

Figure 4 shows 15 color-IDs (from Module1) and corresponding 15 sets of colors that each participant received from others (from Module2). The 15 participants consist of 13 female university students, a lecturer, and a professor. The more colors one receives from others, the more one can understand one's inner-colors that are reflected on one's appearance. While vividness and brightness of one's inner-colors may change according to the time place, occasion and physical condition to some extent, their hue basically remains more or less the same. As one practices this workshop several times, one can realize one's inner-colors' patterns. One's preference, ways of thinking, and behavioral patterns are reflected in one's color arrangement. The comparison between one's own color-ID and colors received from others remarkably shows that many of them have resembling compositions to a great extent. This result suggests that one's inner-colors, which are practically invisible, are actually appearing outside oneself, and thus, others can sense one's inner-colors from one's appearance and express them in colors with a significant degree of accuracy.

Experiencing this remarkable result leads participants to astonishingly realize that their inner-colors are visualized by others. One can become aware of inner-colors of others, which people would not expect to be aware of. Inner-colors, which one thinks that one may hide as far as one does not express, can actually be aware of by others through one's appearance, atmosphere, behavior, voices, etc. When the impression of color-ID differs from that of colors one receives, the difference suggests that one have an unrecognized inner-colors that others can visualize. Does that mean that one does not realize one's own appealing selves? Or does one show a different image of selves to others? This, in any

event, provides one with a valuable opportunity to become aware of selves through realizing how one is perceived by others.

Through this workshop, participants understand that color-IDs make their invisible subconscious mind visible. This experience makes each participant begin to become his/her own self-counselor. That one can visualize one's inner-colors through one's color-ID provides an opportunity for the one to critically reflect oneself for personal growth. Participants also become aware that people have intuitive abilities to read "invisible." This is not supernatural power. People have intuition to read others' inner-colors. Colors can convey one's inner-selves to others.

### 3.3 Practical applications

(1)*Recruiting*: 10-color communication method can benefit both recuiting companies and applicants because it removes unnecessary biases from recruiting processes. Computer based recruiting methods that analyze one's expected performance based on sexes, ages, academic background, working histories, obtained licenses, etc. tend to only appreciate talents appeared on selected aspects of abilities. Semantic differential (SD) method, which has widely been applied in a broad range of practices, tends to strengthen dichotomies such as good-bad, strong-weak, superior-inferior, and to develop unnecessary hierarchy due largely to its linear relationships. It would be fine to apply SD method for analyzing the tendency of personalities. However, applying SD method for recruitment may be problematic as people who happen to be allocated at the top of the unnecessary hierarchy are selected despite the fact that it does not necessarily make sense.



Figure 4

This may obvioulsy result in mismatched recruiting due to the lack of matching personalities to expected yet unwritten subtle tasks that a given job position requires. In contrast, complementary and neighboring color relationships of a color wheel, and the theory of color harmony never creates hierarchy. The concept of color harmony suggests creativity from mixing colors and mutual enhancement from complementary colors.

Analyzing his/her color-ID that is obtained through 10-color communication method, his/her personal features can much accurately be understood. The power of colors can eliminate unnecessary hierarchical biases. Thus, taking visualized inner-colors in account when matching a person to a specific job works for the benefit of both recruiting companies and applicants through sound selection processes.

(2)*Counseling*: 10-color communication method can effectively be applied to personal counseling. People naturally arrange colors in a way they feel beautiful. Through this arrangement, one is coordinating to harmonize plural selves inside. This coordination is what Assagioli (1965) calls psychosynthesis. The process of becoming aware of self through the color communication workshop resembles psychosynthesis that asserts "the direct experience of the self, of pure self-awareness …. is true." While Assagioli (2007) emphasizes the possibility of progressive integration of the personality, 10-color communication method contributes to the awareness of self as well as others, which, in turn, brings about the integration of the personality. In this regard, this 10-color communication method can be called "psycolorsynthesis."

## 4. CONCLUSIONS

The author conducted 10-color communication workshops for a total of more than 300 people. The paper has shown that this method contribute to become aware of self and others' understandings. Specific findings from the workshops and collected data are follows: (1) color-IDs can represent inner-selves of people, (2) results of color-IDs show that they are all unique, distinctive, and extremely diverse, (3) about 80% of sample data showed clear correlations between color-IDs and received colors, (4) one's inner-colors, which are invisible, is actually appearing outside oneself, and therefore, others can sense one's inner-colors from one's appearance and express in colors with a significant degree of accuracy, (5) 10-color communication method can enhance participants to actively engage in communicative interactions with other participants, (6) through communication with a medium of color-IDs, participants can overcome risks, fears, and worries that they face when they attempt to share their inner-selves, (7) the method provides an opportunity for participants to reflect their own inner-colors in a way they can use for their personal growth, (8) the method has significant potential to make recruiting and counseling more effective.

## ACKNOWLEDGEMENTS

## REFERENCES

Assagioli, Robert. 1965. *Psychosynthesis*. Penguin books.
Assagioli, Robert. 1973. *The Act of Will*. Synthesis Center Press.

*Address: Chiori Ohnaka, Office Color Palette*
*Ariake1-4-11-203, Koto-ku, Tokyo, 135-0063, JAPAN*
*E-mail: chiori@officecolorpalette.com*

# Perceptually inspired gamut mapping between any gamuts with any intersection

Javier VAZQUEZ-CORRAL, Marcelo BERTALMÍO
Information and Telecommunication Technologies Department, Universitat Pompeu Fabra,
SPAIN

## ABSTRACT

Gamut mapping transforms the color of an input image within the range of a target device. A huge amount of research has been devoted to two subproblems that arise from this general one: gamut reduction and gamut extension. Gamut reduction algorithms convert the input image to a new gamut that fits inside the one of the image , i.e. the gamuts' intersection is equal to the target gamut, while gamut extension algorithms convert the input  image to a gamut that embodies the original image gamut, i.e. the gamuts' intersection is equal to the source gamut. In contrast to the two aforementioned cases, very little attention has been paid to the most general problem, where the intersection of source and target gamut is not equal to one of the two gamuts. In this paper we address this most general problem of gamut mapping between any two gamuts presenting any possible intersection. To deal with this problem we unify the gamut extension and gamut reduction algorithms presented in Zamir –et al- (Zamir 2014), which are based in the perceptually inspired variational framework of Bertalmío –et al- (Bertalmío 2007) that presents three competing terms; an attachment to the original data, a term for not-modifying the per-channel image mean (i.e. not modifying the white point), and a contrast enhancement term. In particular, in this paper we show how by defining a smooth transition on the contrast enhancement parameter over the chromaticity diagram we can simultaneously reduce the input gamut in some chromatic areas while increasing it in some other without introducing neither color artifacts nor halos.

## 1. INTRODUCTION

Gamut mapping is defined as the modification of the gamut of an input image to make it fit into a destination gamut. This problem is usually divided into two sub-problems that are treated separately: gamut reduction and gamut extension. The former is when the destination gamut is smaller than of the original image. This situation occurs both in the printing industry where images must be carefully mapped to those colors that are reproducible by the different inks and in the cinema industry where cinema footage needs to be passed through a gamut reduction method in order to be displayed on a television screen (Kennel 2007). Conversely, gamut extension is devoted to the case where the destination gamut is bigger. This is currently needed for state-of-the-art cinema projectors which are able to display a wider variety of color than those obtained by cameras.

There exist a huge number of gamut reduction algorithms and just a few gamut extension algorithms in the literature and we refer the reader to the book of Morovic (Morovic 2008) for a detailed explanation of them. Gamut reduction algorihms are usually divided into two classes: global (or non-local, non-adaptive) and local (or adaptive). Global methods involve point-to-point mapping of colors from source to target gamut. In contrast, local methods share two important properties of human perception: i), they better preserve the

color gradient between two out-of-gamut colors instead of mapping them to the same in-gamut color and ii), two out-of-gamut colors with identical lightness and chromaticity map to two different in-gamut colors depending on their spatial context in the image. Recently, Zamir -et al- (Zamir 2014) presented a local method that is based on a perceptually based contrast reduction of the colors. This method was also modified to take into consideration the saliency of the original image (Vazquez-Corral 2014). Regarding gamut extension, the simplest method consists of simply taking any GRA and use the one-to-one mapping in the reverse direction to perform gamut extension, as Morovic comments in his book. Other methods that exist in the literature are (Kang 2003, Kim 2004, Laird 2009). Recently, Zamir -et al- showed how that by modifying the contrast parameter on their reduction method, a gamut expansion method was obtained (Zamir 2014, Zamir 2015).

In this work we do not focus on any of these two particular problems, but in the most general one: the case where the intersection between the two gamuts is not one of them (this intersection is the destination gamut in case of the reduction, and the image gamut in case of the extension). In particular, we explain how we can introduced some locality in the algorithms of Zamir -et al- in order to simultaneously perform reduction on those parts of the original image that exceed the destination gamut whilst performing extension on those parts of the image that are in the surface of the image gamut but far from the destination gamut. In particular, we will show the ability of this method to harmonize different images.

The paper is organized as follows. In the next section we explain the Zamir -et al- methodology. Later on, we explain how we introduce locality which allows us to extend or reduce each of the parts of the image. Results are presented in section 4. Finally in section 5 we sum up the conclusion of this work.

## 2. ZAMIR –ET AL- METHOD

Zamir –et al- (Zamir 2014) method is a modification of the perceptually-inspired image energy functional defined in Bertalmío -et al- (Bertalmio 2007). In particular, the image energy functional considered is Zamir –et al- is

$$E(I) = \frac{\alpha}{2} \sum_x (I(x) - \mu)^2 - \frac{\gamma}{2} \sum_x \sum_y w(x,y)|I(x) - I(y)| + \frac{\beta}{2} \sum_x (I(x) - I_0(x))^2$$

(1)

where α and β are constant and positive weights, γ is a constant and real weight, I is a color channel (R, G or B), w(x,y) is a normalized Gaussian kernel of standard deviation σ, $I_0$ is the original image, μ is the mean average of the original image, and I(x) and I(y) are two intensity levels at pixel locations x and y respectively.

The resulting evolution equation for the previous functional can be expressed as

$$I^{k+1}(x) = \frac{I^k(x) + \Delta t \left( \alpha \mu + \beta I_0(x) + \frac{\gamma}{2} R_{I^k}(x) \right)}{1 + \Delta t(\alpha + \beta)}$$

(2)

where the initial condition is $I^{k=0}(x) = I_0(x)$. The function R $_{I^k}$(x) indicates the contrast function:

AIC2015 TOKYO - Color and Image

$$R_{I^k}(x) = \frac{\sum_{y \in \Im} w(x,y) s\left(I^k(x) - I^k(y)\right)}{\sum_{y \in \Im} w(x,y)} \qquad (3)$$

where x is a fixed image pixel and y varies across the image domain. The slope function s() is a regularized approximation to the sign function, which appears as it is the derivative of the absolute value function in the second term of the functional; in (Bertalmio 2007) they choose for s() a polynomial of degree 7.

Zamir –et al- presented the importance of the weighting parameter of the contrast term (γ) for the gamut mapping problem. In particular, they showed that for γ smaller than 0, the gamut of the image was reduced, while for γ bigger than 0, the gamut of the image was extended. Moreover, they also showed that the smaller the value of γ, the smaller the gamut of the resulting image.

Zamir –et al- therefore chose a set of γ values smaller than 0 for creating a gamut reduction algorithm and a set of γ values bigger than 0 for creating a gamut extension algorithm. They, however, did not try study the case of selecting both negative and positive values of the γ parameter for the same image, in order to obtain a more general gamut mapping algorithm. This problem is the one we are tackling in this paper. In the next section we explain how given an input image and a target gamut (coming from a different image or from a display) a local γ value for each image pixel can be obtained, allowing the method to perform reduction in some parts of the image and extension in the others.

### 3. LOCAL CONTRAST COEFFICIENTS

To start with let us shed some light in the situation we will face. Let us call $Y_1$ the gamut of the image to modify and $Y_2$ the gamut we want to obtain. When plotting these gamuts in the chromaticity diagram three different regions will be presented. The first region will be the one where both gamuts intersect, and we denote it as Φ. The second region will present those colors in the input image that are not presented in the destination gamut. We call this region Ψ. Finally, the last region, that will call Ω, will be formed by the colors present in the destination gamut that are not present in the input image. Therefore, our goal is to reduce section Ψ while at the same time increasing section Φ to cover the section Ω. In other words, we want to reduce those colors presented only in the input image, while at the same time, expanding colors of the input image presented in the destination gamut to cover the full destination gamut. An illustration of the aforementioned procedure can be found in Figure 1.

Mathematically, we will proceed as follows to obtain the γ value corresponding to each chromatic color. First, we erode the region Φ to obtain the core region of the intersection between the two gamuts.

$$\Phi_{er} = \Phi \oplus D_\tau \qquad (4)$$

where $D_\tau$ is a disk of radius τ.

Then, we define those points where we want to perform a bigger reduction, i.e., the points of section Ψ that are at a further distance of Φ, and we will give them a value that depends on the minima gamma we consider ($\gamma_{min}$). In particular, if we call Γ the map of the
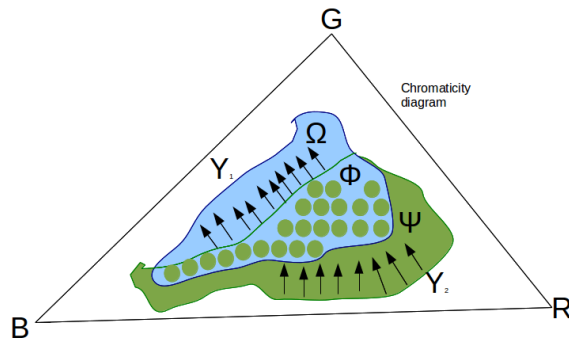
*Figure 1: Explanation of the different regions found in our problem. See first paragraph of section 3 for details.*

different gammas presented in the chromaticity diagram, and we call z any point presented in the chromaticity diagram, we obtain

$$\Gamma(z) = \left\{ \gamma_{min} \cdot \frac{d(z, \Phi_{er})}{\max_{\hat{z} \in \Psi}(d(\hat{z}, \Phi_{er}))} \right\} \; if \; z \in \Psi \, and \; \frac{d(z, \Phi_{er})}{\max_{\hat{z} \in \Psi}(d(\hat{z}, \Phi_{er}))} < \delta_1 \quad (5)$$

where all the values obtained will be negative.

Later, we look for the points in $\Phi$ that are in the border with respect to $\Omega$. These points are the ones where we want to perform a bigger expansion to cover the region $\Omega$. Their value will be based on the maxima gamma we consider ($\gamma_{max}$).

$$\Gamma(z) = \left\{ \gamma_{max} \cdot \left( 1 - \frac{d(z, \Omega)}{\max_{\hat{z} \in \Phi}(d(\hat{z}, \Omega))} \right) \right\} \; if \; z \in \Phi \; and \; \frac{d(z, \Omega)}{min_{\hat{z} \in \Phi}(d(\hat{z}, \Omega))} < \delta_2$$
$$(6)$$

where all the values obtained will be positive.

Finally, we look for the points we want to keep static when performing our method.

$$\Gamma(z) = 0 \; if \; z \in \Phi_{er} \tag{7}$$

Once all these different values have been defined in the matrix $\Gamma$, all the rest of the values are obtained by interpolation. Finally, for each pixel of the input image, its gamma value is obtained by searching its correspondence in $\Gamma$.

## 4. RESULTS

Figure 2 shows a result of our method. In the upper row of the figure we show the input image (left), the image from where we obtain the reference gamut (right) and the result of our method (center). In the bottom row we present: i) left: the gamut intersection between the images, where the red region represents $\Phi$, the yellow region represents $\Psi$, and the blue region $\Omega$ represent, ii) center: the map of $\Gamma$, and iii) an image with the gammas used at each pixel. We would like to fix the reader attention both in the sky and in the sand, where our method is able to match the colors of the original image to those of the reference one. The parameters used in this image are $\delta_1$=0.25, $\delta_2$= 2, $\sigma$=3, $\gamma_{max}$ =0.3, and $\gamma_{min}$ =-0.75.
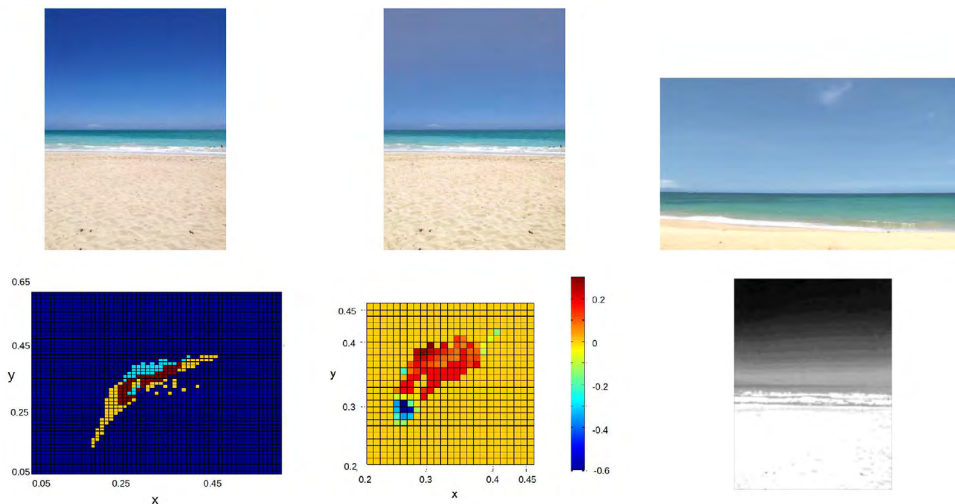
*Figure 2: Results of our method. Upper row: Input image (left), Reference image (right) and our result (center). Bottom row: the gamut intersection between the images, where the red represents Φ, yellow represents Ψ, and blue represents Ω (left) , the map of Γ, (center) and the gammas at each pixel (right).*

More results are presented in Figure 3, where we show the input image (left), the reference image from where the gamut is obtained (right), and our result (center). Again, we want to notice our ability to match the original image to look closer to the reference image. In thefirst case, we see how the white color has tent to the yellow of the reference image, while the blue has got the electric tone of the tub. In the second image, the orangish background has been moved towards the red of the reference image. Finally, in the last one, blue of the sky has been modified as there have been also modified other regions of the input image to look greener.

## 5. CONCLUSIONS

In this work we have presented a modification of Zamir –et al- algorithms in order to perform full gamut mapping, i.e., to being able to simultaneously reduce gamut of colors in some parts of the image while extending the colors in some other parts. The results presented are promising. Some future lines to improve our results may be the consideration of the full 3D gamut (a first attempt is presented in Figure 4) and the search of further applications such as semantic transfer.

## ACKNOWLEDGEMETS

## REFERENCES

M. Bertalmío, V. Caselles, E. Provenzi, and A. Rizzi. 2007. *Perceptual color correction through variational techniques.* IEEE Transactions on Image Processing, 6(4):1058–1072.
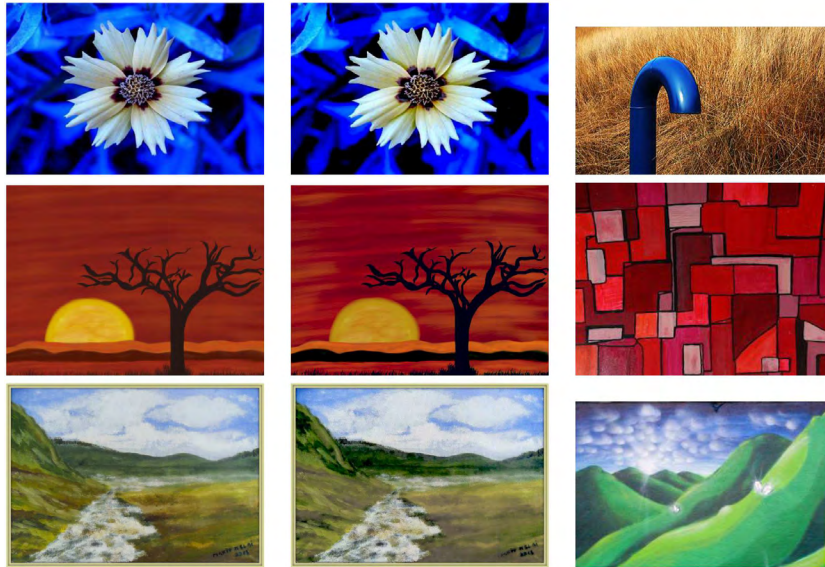
*Figure 3: Results of our method. Left: original image. Right: reference image. Center: Our result*



*Figure 4: Example of the 3D case for our method. Left: original image. Right: reference image. Center: Our result*

B. H. Kang, J. Morovic, M. R. Luo, and M. S. Cho. 2003. Gamut compression and extension algorithms based on observer experimental data. ETRI journal, 25(3):156–170.

G. Kennel. 2007. *Color and mastering for digital cinema: digital cinema industry handbook series*. Taylor & Francis US.

M. C. Kim, Y. C. Shin, Y. R. Song, S. J. Lee, and I. D. Kim. 2004. *Wide gamut multi-primary display for hdtv*. In Proc. of CGIV, pages 248–253.

J. Laird, R. Muijs, and J. Kuang. 2009. *Development and evaluation of gamut extension algorithms*. Color Research & Application, 34(6):443–451.

J. Morovic.2008. *Color gamut mapping,* Wiley.

J. Vazquez-Corral, S.Zamir, and M. Bertalmio. 2014. *Considering saliency in a perception inspired gamut reduction algorithm*. Is&T Color and Imaging Conference (CIC2014).

S. Zamir, J. Vazquez-Corral, and M. Bertalmio. 2014. *Gamut mapping in cinematography through perceptually-based contrast modification*. Selected Topics in Signal Processing, IEEE Journal of, 8(3):1–1

S. Zamir, J. Vazquez-Corral, and M. Bertalmio. 2015. *Gamut Extension for Cinema: psychophysical evaluation of the state of the art and a new algorithm*. IS&T/SPIE Electronic Imaging.

Address: Dr. Javier Vazquez-Corral, and Dr. Marcelo Bertalmío, Information and Telecommunication Technologies Department, Universitat Pompeu Fabra, Roc Boronat 138, 08018 Barcelona, Spain

E-mails: {javier.vazquez,marcelo.bertalmio}@upf.edu

# Color Correction Operation for 3D Scanning Models

Kai-Lin Chan[1], Lin Lu[2], Tzung-Han Lin[1], Hung-Shing Chen[1,2],

Chia-Pin Cueh[3], and Kang-Yu Liu[3]

[1] Graduate Institute of Color and Illumination Technology, National Taiwan University of Science and Technology

[2] Graduate Institute of Electro-optical Engineering, National Taiwan University of Science and Technology

[3] Printing Technology Research Institute, Taiwan

## ABSTRACT

Color performance of 3D scanning model depends on color quality of the range images of a 3D object. In this study, color correction operation for 3D scanning models was established, which was composed of 2D color correction and 3D luminance correction Firstly, 2D color correction was executed, which contains lighting uniformity correction, gray balance correction and camera color correction. After 2D color correction, each range image is correction by 3D luminance correction considering its 3D depth information. A direct color measuring method using a 2D colorimeter is used to capture precise color information of the reference ColorChecker and the 3D object, which can apply to the proposed color correction operation.

## 1. INTRODUCTION

Nowadays, 3D scanner is capable of acquiring more realistic 3D objects. However, the color correction of 3D scanning models is still a challenging topic. The precise color reproduction of a 3D object highly depends on lighting conditions, material properties and geometrical shapes. To improve the color reproduction abilities of 3D object, we develop practice color correction operation for 3D scanning models by means of the using of 2D color correction and 3D luminance correction.

We initially fabricate a color 3D scanner based on a laser and a stereo camera, and we carry out the software for calculating 3D models. Likewise, this 3D scanner consists of a turntable with motor control unit, for rotating a 3D object to specific positions, and several LED white light bulbs. All the signal of construction is delivered by Arduino unit (Figure 1). During the 3D scanning process, eight range images of a 3D object are obtained and further integrated into one using digital 3D model [1].

Since color information of the scanning model is determined by the combination of all range images, the practice solution of the 2D color correction is useful for solving the color information. However, these color-calibrated 2D range images are still affected by 3D depth information of a 3D object. Therefore, another practice solution is to perform the 3D luminance correction. It is expected that the scanning model could make duplicate object achieve the same as the realistic object by means of the total color correction solution.
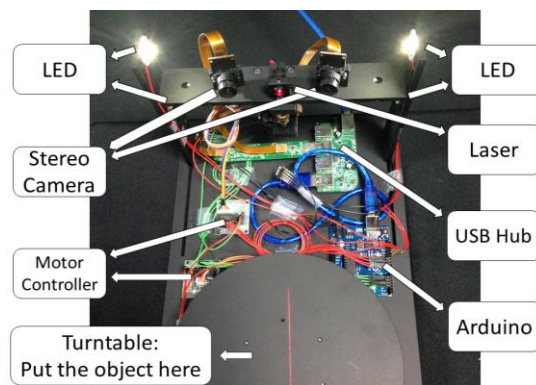
*Figure 1: 3D scanner construction*

## 2. METHOD

A 3D scanning system was developed in our laboratory. The 3D scanner is designed for scanning the object and taking the range images of the object by a set of stereo camera. Besides, the equipment and tools used in this study are arranged in Table 1.

*Table 1: The equipment and tools in this study*

| No | Item | No | Item | No | Item |
|---|---|---|---|---|---|
| 1 | Topcon UA-1000A  | 2 | X-rite ColorChecker Passport  | 3 | 3D printed Ball  |
| 4 | X-rite SpectraLight III  | 5 | X-rite White Balance Card  | | |

In a 3D scanning process, we capture a color image, and then scan the object to obtain a series of full-color range images. To obtain a completed shape, the scanned object is rotated to eight specific positions by a turntable. Finally, all range images are merged into one solid model. However, in the merge process, the overlapped region may have duplicated vertexes and colors. To simplify the algorithm, we store the RGB color values for each vertex instead of for each polygon. To decide the reasonable color information of a vertex, we blend the colors which are from the projection positions of all visible images. In

practice, the colors of all vertexes are set white after all scanned range images are merged. In this study, our developed color correction operation for 3D scanning models composes of 2D color correction and 3D luminance correction.

## 2.1  2D Color Correction

As mentioned above, the colors of the scanning models cover eight range images for a 3D object. Therefore, 2D color correction of scanning models depends on the calibrating colors of each range image. The standard ColorChecker was used, and its tristimulus values of 24 color patches emitted by $D_{65}$ simulator in the light cabinet was measured by a 2D colorimeter (Topcon UA-1000A), which are regarded as the reference color values during 2D color correction process (Figure 3).
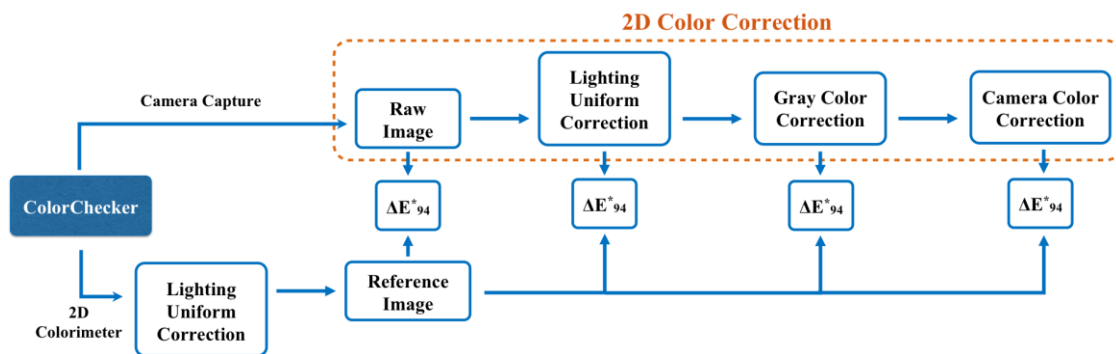


*Figure 2: Schematic of 2D color correction*

## Lighting Uniformity Correction

Since the illuminant in light cabinet possibly irradiates on the white board non-uniformly in the beginning, the luminance distribution on ColorChecker would have the similar phenomenon. Due to the non-uniform luminance, the luminance and color information of a 3D object should not be reproduced accurately. To solve this problem, luminance uniformity should have a high priority at the first step for calibrating image. A uniform white board is placed at the same position of the object. When the background white was captured by a camera, its 8-bit RGB values can be converted to CIExyY. The Y distribution represents the lighting distribution of a range image. According to its original Y distribution, the inverse luminous mask (brightness compensating mask) can be designed to compensate the uniformity of a digitalized image. The original digital image was also converted to CIExyY. Its luminous distributions carry the entrywise product with the brightness compensating mask, then a digitalized image with lighting uniformity correction would be achieved.

## Gray Balance Correction

The captured raw images look greener than normal one if the camera has no color calibration. To confirm this problem, the example of RGB tone curves was plotted using the six gray-scale patches on ColorChecker, as shown in Figure 3(a). At each luminance level, the green signal values are higher than red and blue signal values. Therefore, it is necessary to adjust RGB tone curves to the similar curve shape (Figure 3(b)).
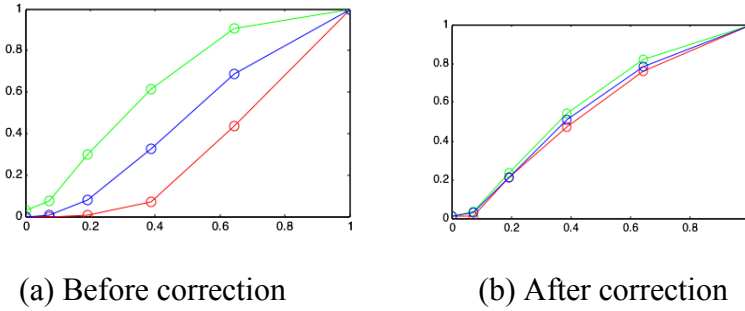
(a) Before correction        (b) After correction

*Figure 3: Gray-scale tone curves before and after gray balance correction*

**Camera Color Correction**

After gray balance correction, the corrected image is only calibrated for gray-scale colors. The other colors on ColorChecker could be still error in comparison with the reference values. Therefore, we try to use polynomial regression to perform  camera color correction. It is helpful for resolving an unknown matrix by two groups of known matrices by Eq. 1. If [A] and [B] are the known matrices, and [T] is the unknown matrix. Then [T] can be found by using Eq. 2. $[A]^T$ is transpose of [A], and $[A]^{-1}$ is the inverse of [A]. When the tristimulus values [X Y Z] of each range image's pixel with gray balance correction are set as the [A], and the target value is set as the [B]. Therefore, the computed [T] can make the tristimulus values of the input image be close to the target values.

$$[A] * [T] = [B] \tag{1}$$

$$[T] = ([A]^T * [A])^{-1} * [A]^T * [B] \tag{2}$$

Furthermore, [A] could be written by the forms of the 1st order regression in Eq. 3, or the 2nd order regression in Eq. 4 as follows.

$$[A]= [X, Y, Z, K] \text{  for 1st order regression} \tag{3}$$

$$[A]=[X^2, Y^2, Z^2, XY, YZ, XZ, X, Y, Z, K] \text{  for 2nd order regression} \tag{4}$$

Here, [B] is defined as [X Y Z], where XYZ are the vectors of the tristimulus values, which are translated from the 8-bit RGB values of an image according to sRGB standard, and K is the constant [2].

## 2.2  3D Luminance Correction

Before resolving the luminance problem caused by 3D depth of a real object, 2D color correction is necessary first. Then lightness difference $(\Delta L^*)$ is computed for checking the performances of the 3D luminance correction. Finally, all range images with 3D luminance correction are projected again to form the new 3D object using 3D scanning model (Figure 4). Firstly, the representative luminance values on the surface of a 3D object under the specific lighting condition were measured by a 2D colorimeter. The luminance values of 37 training points were chosen to obtain reference luminance values by using a 2D colorimeter capturing (Figure 5(a)). On the other hand, the luminance values at the same 37 positions on the captured range image after 2D color correction were computed (Figure 5(b)). Then the 2nd order regression similar to Eq. 1 was used to compute the correcting luminance values of the test image. Matrices [A] and [B] are described by Eq. 5, where Y means the luminance value.

AIC2015 TOKYO - Color and Image

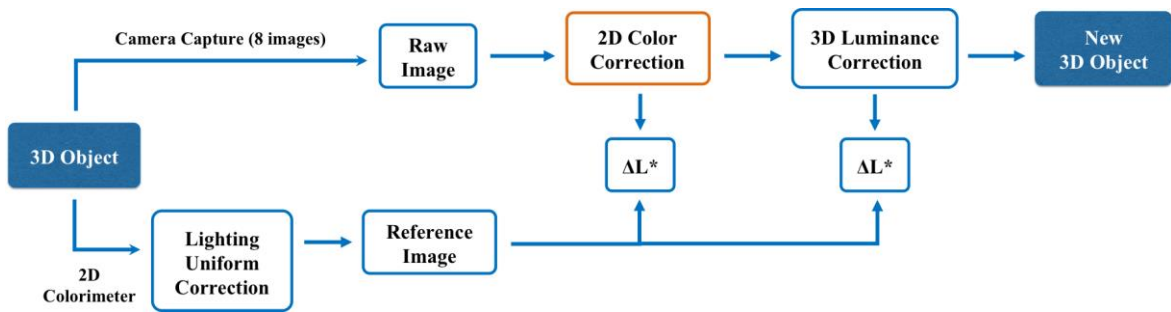$$[A] = [Y, Y^2]; \quad [B] = [Y] \tag{5}$$



*Figure 4: Schematic of 3D luminance correction*



(a) Raw image      (b) Image after camera color correction

*Figure 5: Training points for measuring luminance values*

## 3. RESULTS AND DISCUSSION

The computed range images based on 2D color correction, which covered from raw image to camera color correction, are arranged in Table 2. Besides, the computed range images based on 3D luminance color correction are also arranged in Table 3.

*Table 2: Images at 2D color correcting stages and color difference values*

| Stage | ColorChecker | 3D Ball | $\Delta E^*_{94}$ |
|-------|--------------|---------|-------------------|
| Raw Image | | | 43 |
| Luminance Uniformity Correction | | | 34 |
| Gray Balance Correction | | | 22 |

| | | | |
|---|---|---|---|
| 1st Order Regression |  |  | 10 |
| 2nd Order Regression |  |  | 6 |
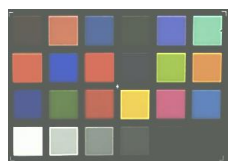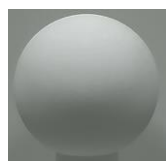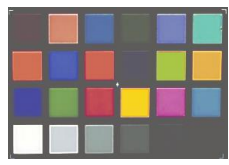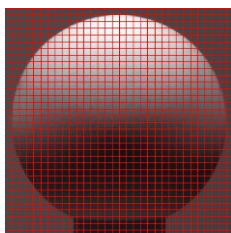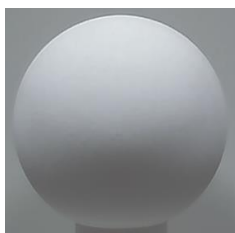
*Table 3: Images of 3D luminance correction and the lightness difference ($\Delta L^*$)*

| | Reference 2D Colorimeter | 2D Color Correction | 3D Luminance Correction |
|---|---|---|---|
| Image |  |  |  |
| $\Delta L^*$ | -- | 14 | 5 |

## 4. CONCLUSIONS

Color correction operations for 3D scanning system were developed, which made reproduced colors of a 3D object much better than non-calibrated colors. A direct color measuring method using a 2D colorimeter is used to capture precise color information of the standard ColorChecker and the 3D object, which can apply to the proposed color correction operation. The mean $\Delta E^*_{94}$ values were reduced from 43 to 6 after 2D color correction, and the mean $\Delta L^*$ values were reduced to 5 after 3D luminance correction. Future work is to correct not only 3D depth luminance but also the color shift problem of a real 3D object during 3D scanning process.

## REFERENCES

[1] T. H. Lin, "Resolution adjustable 3D scanner based on stereo cameras," Asia Pacific Signal and Information Processing 2013, Kaohsiung, Taiwan, 2013.

[2] R.W.G Hunt and M. R. Pointer, Measuring Colour, 4th Edition, 2011

*Postal address: Graduate Institute of Color and Illumination Technology,*

*No.43, Sec. 4, Keelung Rd., Da'an Dist., Taipei 106, Taiwan*

*E-mails: M10325002@mail.ntust.edu.tw, zmes159753@gmail.com, thl@mail.ntust.edu.tw, bridge@mail.ntust.edu.tw, james@ptri.org.tw, terryliu@ptri.org.tw*

# Correcting for induction phenomena on displays of different size

Marcelo BERTALMÍO
Universitat Pompeu Fabra, Spain

## ABSTRACT

In this work we introduce a model for visual induction based on efficient coding and which elaborates on a previous approach. We show that this new model is able to qualitatively replicate psychophysical data on visual induction, and we propose a method by which an image can be pre-processed in a screen-size dependent way so that its perception, in terms of visual induction (i.e. ignoring the color capabilities of the displays), may remain constant across displays of different dimensions.

## 1. INTRODUCTION

In visual perception, induction designates the effect by which the lightness and chroma of an stimulus are affected by its surroundings. When the perception of an object shifts towards that of its surround the phenomenon is called assimilation; in the opposite case, when the perception of an object moves away from that of its neighborhood, we talk about contrast. Visual induction manifests itself both in achromatic and chromatic form, and the ocurrence of assimilation or contrast is determined by the spatial frequency of the stimulus (Helson 1963, Fach and Sharpe 1986), with assimilation being associated to large spatial frequencies and contrast to lower ones. There is evidence of neural activity at V1 that correlates with visual induction phenomena (Pereverzeva and Murray 2008).

A common observer looks at images on displays of vastly different sizes, from cinema screens to mobile phones, and in general the usual viewing distance is not proportional to screen dimensions. For instance, a comfortable distance to view a 50 inch TV screen may be 10 feet, or 120", whereas for a mobile phone screen of 5 inches the usual viewing distance is around 15" (Heinonen 2013). This difference in the ratio of screen size over viewing distance implies a different angle of view for each screen, and therefore a change in the spatial frequency of the image content when viewed on different displays. As a consequence, the visual induction phenomena will also change from one screen to another: the same image may show significant assimilation effects when displayed on a screen, and less assimilation or even contrast when displayed on another.

In a recent work (Bertalmío 2014) we proposed a neural activity model which was able to predict lightness induction. It is in the form of the Wilson-Cowan equations (Wilson and Cowan 1972), that model the activity of neural populations along time and represent interactions with the use of a sigmoid function:

$$\frac{\partial a(x,t)}{\partial t} = -\alpha a(x,t) + \gamma \sum_{y} \omega(x,y) S(a(y,t)) dy + \beta h(x,t) \qquad (1)$$

where **a** is the activity, x and y are cortical positions, t is time, w is a spatial summation kernel that decreases monotonically with distance, S is a sigmoid function in the range [0,1], **h** is an external input, and α, β,γ are constants. The work by Wilson and Cowan is

very influential and has been used extensively for many different problems in computational neuroscience. Regarding vision in particular, Wilson and Cowan point out that their model reproduces several visual perception phenomena, including edge enhancement.

Bertalmío et al. (2007), in an image processing context, proposed the following evolution equation to perform local histogram equalization:

$$\frac{\partial a(x,t)}{\partial t} = -\alpha(a(x,t) - \frac{1}{2}) + \gamma \sum_y w(x,y)s(a(x,t) - a(y,t)) + \beta(h(x,t) - a(x,t)) \quad (2)$$

where **a** is an image channel (R,G or B), x and y are pixel coordinates, t is the evolution parameter, 1/2 is the target global mean average, w is a spatial summation kernel, s is a sigmoid function in the range [-1,1], **h** is the original image channel, and α,β,γ are constants. In this method, the input image **h** is processed by running the above evolution equation (with initial condition **a**=**h**) until steady state: the output image will be **a** at the last iteration step, when the evolution has stopped.

We can see then that this evolution equation has the form of the Wilson-Cowan equations, linking them to efficiency of representation, color constancy and the Retinex theory (Bertalmío et al. 2009, Bertalmío and Cowan 2009) and other visual perception phenomena. But as a limitation we must note that this method always increases contrast, so it's incapable of reproducing assimilation, as shown in Figure 1.
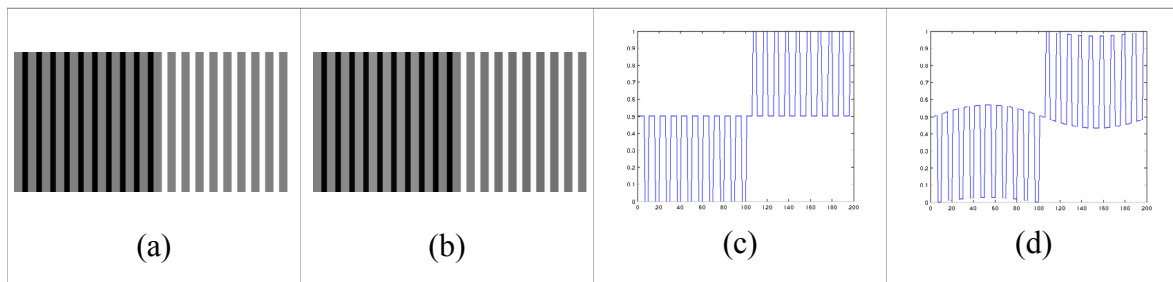


*Figure 1: (a) Original image, example of lightness assimilation: the grey bars have all the same value but appear different over black and white backgrounds. (b) Result of applying the model of (Bertalmío et al. 2007) to image (a). (c) Profile of a line from image (a). (d) Profile of a line from image (b): notice how the model of (Bertalmío et al. 2007) actually emulates lightness contrast rather than assimilation. Figure taken from (Bertalmío 2014).*

It was in order to overcome this issue that we recently proposed (Bertalmío 2014) the following modification:

$$\frac{\partial a(x,t)}{\partial t} = -\alpha(a(x,t) - \mu(x,t)) + \gamma(1 + (\sigma(x,t))^c) \sum_y w(x,y)s(a(x,t) - a(y,t)) + \beta(h(x,t) - a(x,t))$$

$$(3)$$

where μ(x) is a Gaussian average, σ(x) is the local standard deviation and c is a global, fixed parameter. Results now show both assimilation and contrast, and the model is related to efficient coding by performing (local) histogram equalization, spectrum whitening and contrast enhancement. But the aforementioned changes to the 2007 model, specifically multiplying the contrast term by a weight depending on the local standard deviation, don't fit too well with the basic postulates of Wilson and Cowan's theory.

Our contribution in this work will then be to introduce a new model for visual induction that, while still based on efficient coding and the aforementioned approaches, is now able to comply better with the theory of Wilson and Cowan as well as to qualitatively replicate

AIC2015 TOKYO - Color and Image

psychophysical data on assimilation and contrast results, both on achromatic and chromatic data. Finally, we will propose a method by which an image can be pre-processed in a screen-size dependent way so that its perception, in terms of visual induction (i.e. ignoring the color capabilities of the displays), may remain constant across displays of different dimensions.

## 2. METHOD

### 2.1 Proposed model

Going back to the generalized form of the Wilson-Cowan equations used in Bertalmío et al. (2007)

$$\frac{\partial a(x,t)}{\partial t} = -\alpha(a(x,t) - \frac{1}{2}) + \gamma \sum_y w(x,y)s(a(x,t) - a(y,t)) + \beta(h(x,t) - a(x,t))$$

(4)

we replace the target global mean average 1/2 with μ(x), which is a local average:

$$\frac{\partial a(x,t)}{\partial t} = -\alpha(a(x,t) - \mu(x,t)) + \gamma \sum_y w(x,y)s(a(x,t) - a(y,t)) + \beta(h(x,t) - a(x,t))$$

(5)

The value for μ(x,t) is computed by a convolution with a kernel K obtained as a weighted sum of two Gaussians, a wider one with less weight and a narrow one with larger weight, as shown in Figure 2.
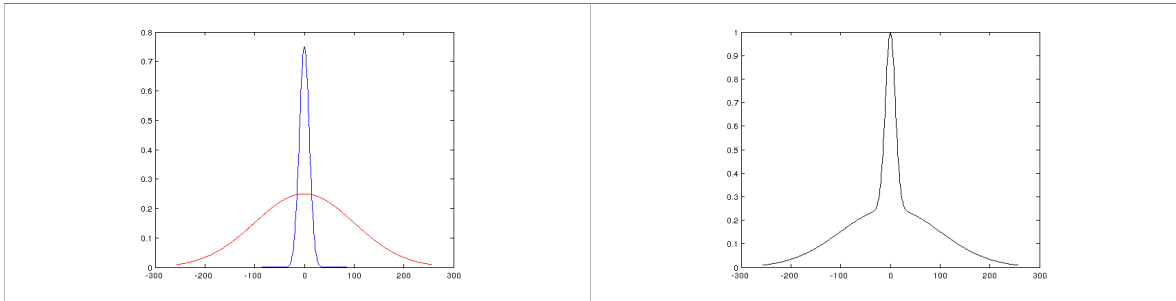


*Figure 2: Left: scaled Gaussians. Right: resulting kernel K for computing the local mean.*

The model given by Eq. (5) now complies with the basic postulates of Wilson-Cowan. Again, how we apply it in practice to an input image **h** is by running Eq. (5) to steady state, with **a**=**h** as initial condition, and the output will be the image **a** at the last iteration. The results thus obtained show both assimilation and contrast, as it can be seen in Figure 3 and Figure 4. We want to point out that all these achromatic and chromatic induction results have been obtained with the same set of parameter values and kernel sizes, i.e. the change from assimilation to contrast is only due to the spatial content of the images since the model is fixed.

### 2.2 Pre-correcting for changes in induction

With Eq. (5) we can qualitatively replicate the psychophysical results of the induction experiments of both (Helson 1963) for achromatic stimuli and (Fach and Sharpe 1986) for chromatic images. In both cases, observers were presented with stimuli consisting of

gratings, identical bars over a uniform background, and reported the strongest assimilation effects for the largest spatial frequencies (thinnest bars); the strength of the effects would decrease with the increase in bar width, turning into contrast effects for wide bars. Using Eq. (5) we obtain the same type of results, as the green induction vs. bar-width plots in Figure 5 show.
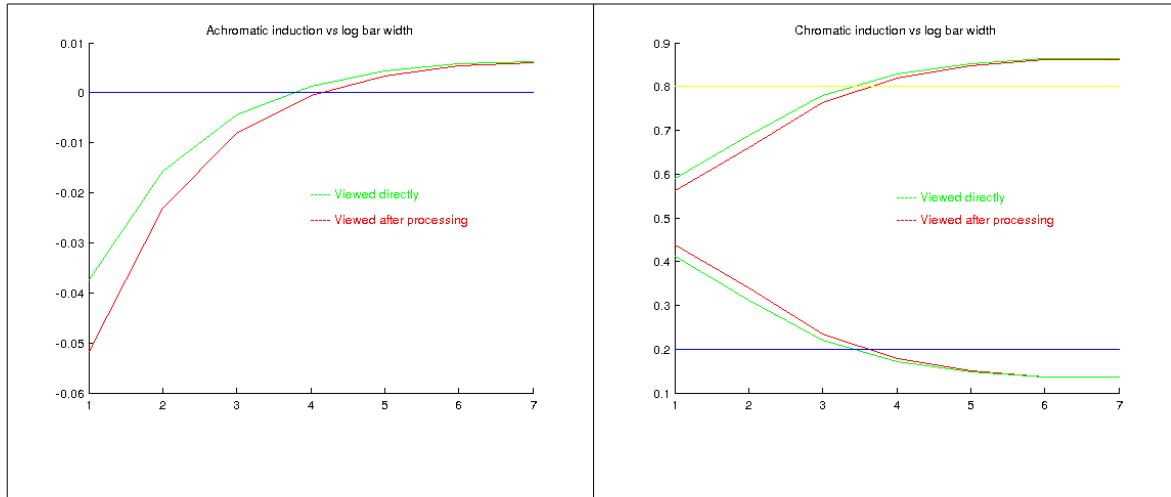


*Figure 5: Predicting induction phenomena and correcting for changes in screen size. Left: achromatic grating, assimilation below blue line, contrast above blue line. Right: yellow-blue grating; top plots correspond to yellow, and yellow line separates assimilation from contrast effects; bottom plots correspond to blue, and blue line separates assimilation from contrast effects. Images in this figure approximate the plots of both (Helson 1963) for achromatic stimuli and (Fach and Sharpe 1986) for chromatic images, which were obtained through psychophysical tests.*

Now for pre-correcting for changes in induction what we would need is the following. Given an image I, and with the correct choice of parameters, Eq. (5) will predict the induction effects that will be observed when looking at said image on a screen. If we now move away from the screen or, equivalently, look at the image on a screen of smaller size, the spatial frequencies of the image will increase and therefore Eq. (5) will predict a shift towards assimilation effects. Then what we would want to have is a pre-processing technique that applied to I produces an image I' whose induction vs. bar-width plot moves to the right. This would imply that the same induction effects would be seen by looking at I on the large screen as by looking at I' on the small screen. It turns out that what we need to do as pre-processing is simply to run the same Eq. (5) but with a different choice of parameters: giving more weight to (and reducing the standard deviation of) the Gaussian of kernel K which has smaller width, and reducing the value of the parameter β, which sets the strength of the contrast term. Example of plot shifts produced with this technique can be seen in red in Figure 5.

## 4. CONCLUSIONS

We have presented a method, related to neural models of vision and efficient coding in the visual system, that is able to qualitatively replicate psychophysical data on visual induction. We have also proposed a technique by which an image can be pre-processed in a screen-size dependent way so that its perception, in terms of visual induction, may remain constant across displays of different dimensions. These are very preliminary results, and currently we are working towards an accurate and automatic determination of all

AIC2015 TOKYO - Color and Image

parameters involved, extensive testing on natural as well as artificial images and a full psychophysical evaluation.
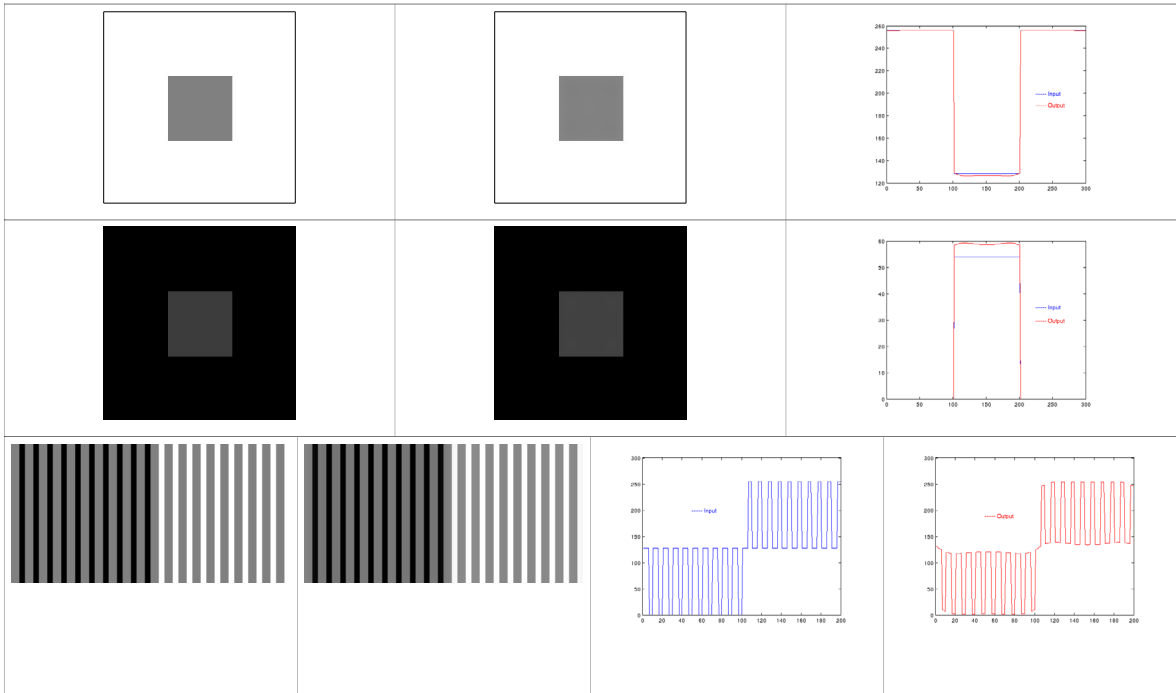


*Figure 3: Achromatic induction examples. Top and middle rows: contrast. Bottom row: assimilation. In each row the first image is the input and the second image is the output result of applying our model.*
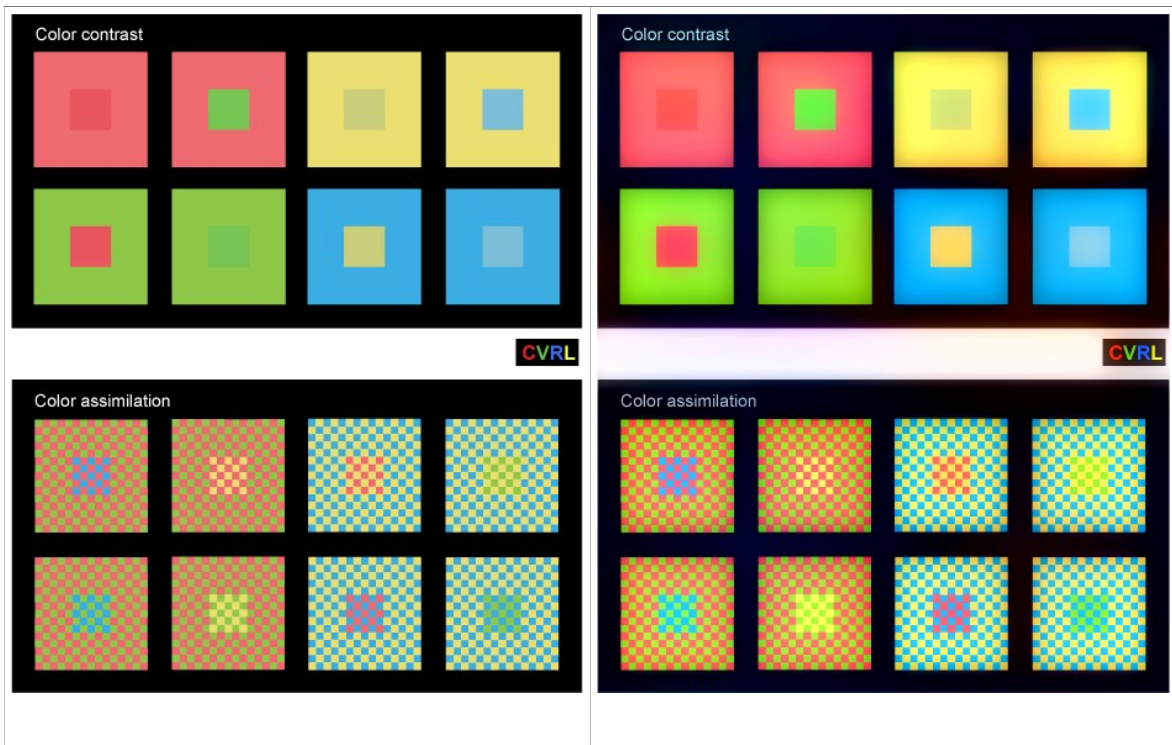


*Figure 4: Chromatic induction examples. Left: input. Right: output from our model. Original figure from (Stockman and Brainard 2009).*

## REFERENCES

Bertalmío, M., Caselles, V., Provenzi, E., & Rizzi, A. (2007). Perceptual color correction through variational techniques. *Image Processing, IEEE Transactions on, 16*(4), 1058-1072.

Bertalmío, M., Caselles, V., & Provenzi, E. (2009). Issues about retinex theory and contrast enhancement. *International Journal of Computer Vision, 83*(1), 101-119.

Bertalmío, M., & Cowan, J. D. (2009). Implementing the Retinex algorithm with Wilson–Cowan equations. *Journal of Physiology-Paris, 103*(1), 69-72.

Bertalmío, M. (2014). From image processing to computational neuroscience: a neural model based on histogram equalization. *Frontiers in computational neuroscience*, 8.

Fach, C., & Sharpe, L. T. (1986). Assimilative hue shifts in color depend on bar width. *Perception & psychophysics*, 40(6), 412-418.

Heinonen, C. (2013). http://referencehometheater.com/2013/commentary/image-distance-is-everything-4k-and-hidpi-displays/

Helson, H. (1963). Studies of anomalous contrast and assimilation. *JOSA*, 53(1), 179-184.

Pereverzeva, M., & Murray, S. O. (2008). Neural activity in human V1 correlates with dynamic lightness induction. *Journal of Vision*, 8(15), 8.

Stockman, A., & Brainard, D. H. (2009). Color vision mechanisms. The Optical Society of America Handbook of Optics, 3rd edition, Volume III: Vision and Vision Optics. New York: McGraw Hill.

Wilson, H. R., & Cowan, J. D. (1972). Excitatory and inhibitory interactions in localized populations of model neurons. *Biophysical journal*, 12(1), 1-24.

*Address: Prof. Marcelo BERTALMÍO, Department de Tecnologies de la Informació i les Comunicacions, Universitat Pompeu Fabra, Roc Boronat 138, 08018 Barcelona, SPAIN*
*marcelo.bertalmio@upf.edu*

# KANSEI evaluation of color images presented in different blue primary displays

Toshiya Hamano,[1] Takashi Fuseda,[1] Tomoronori Tashiro,[2] Tomoharu Ishikawa[1]
Hiroyuki Shinoda,[3] Kazuhiko Ohnuma,[4] Keisuke Araki,[2,5] Miyoshi Ayama[1]
[1] Graduate School of Engineering, Utsunomiya University
[2] Center for Optical Research & Education, Utsunomiya University
[3] College of Information Science and Engineering, Ritsumeikan University
[4] Graduate School of Engineering, Chiba University
[5] Canon Inc.

## ABSTRACT

Recently, Rec.ITU-R BT.2020 has been published, and the new era for a super-wide color gamut has been started. It is generally accepted that the wider the color gamut, the better the color reproduction performance of the display. However, few have been reported on the comparison of color gamut from image preference or naturalness point of view. Among the three primaries, blue primary is considered to affect most on the color tone or color shade. Therefore, to investigate the best blue primary for color display from KANSEI-evaluation point of view, evaluation experiment was carried out using four different blue primaries of 430nm, 450nm, 470nm, and 480nm. Before the experiment, test image selection was carried out. Color distributions of more than 2620 images were analyzed based on our categorical color database, and 15 color images are selected as the test images from them. In the experiment, the test image was projected by the 2 projectors, one was for blue signal and the other one was for the red and green signals. Interference filters of λp = 430nm, 450nm, 470nm, and 480nm were inserted in front of the projection lens of the B projector to achieve different blue primaries. Images from the two projectors were carefully superimposed. Evaluation experiments were carried out with 2 luminance levels of 60 cd/m$^2$ for 430nm, 450nm, 470nm, and 480nm, and 170 cd/m$^2$ for 450nm, 470nm, and 480nm. The semantic differential method was used to quantify subjective evaluations of images using 14 adjective pairs. Results of the 4 blue primaries comparison, 430nm, 450nm, and 470nm blue primaries showed similar performance except for the skin color image. Results of the 3 blue primaries comparison, 470nm showed the best performance.

## 1. INTRODUCTION

Rec.ITU=R BT.2020 has been published in 2012. Its primary colors are 630nm, 532nm, and 467nm(ITU 2012). It is a new standard for broadcasting a super-high vision such as 4K or 8K in the future. In general, it has been considered that the wider color gamut is the better one. Performance of color gamut is usually assessed by how much of the spectrum reflectivity data of the real existence object can be reproduced (Masaoka et al. 2010). However, few have been reported on the comparison of color gamut from image preference or naturalness point of view. Evaluations using these words are called KANSEI-evaluation. "KANSEI" has the meaning called "mental sense of subjectivity" in Japanese. It is a higher order function of the human brain.

Among the tree primaries of R, G, and B, blue primary is considered to affect most on the color tone or color shade of image. Therefore, to investigate the best blue primary for color display from KANSEI-evaluation point of view, evaluation experiment was carried out using four different blue primaries of 430nm, 450nm, 470nm, and 480nm.

## 2. METHOD

### 2.1 Test images

Color distributions of more than 2620 images were analyzed based on our categorical color database (Ashiguchi 2009), and 15 color images are selected as the test images from them. Each pixel of image is labelled as a certain color category among 14 categories as shown in the right-hand side of Figure 1, using the color conversion from (RGB) to (L*a*b*) via (XYZ). In the categorical color database proposed by Ashiguchi et al., L*a*b* color space is gridded and each grid is labelled with one color among 14 categories. Using this categorical color database, all pixels of an image are divided into 14 color categories, and then the pixel ratio for each of color categories are calculated. In the next step, the image is denoted as one of the 15 groups shown in Table 1, according to the criterion shown in the right column of Table 1. Figure 1 shows the example of "blue image" , of which pixel ratios are indicated in the right-hand side.

*Tabe 1    Criterion of the color group of image from pixel ratios of categorical colors*

| Group | Criterion | Group | Criterion |
|---|---|---|---|
| red | red > 40% | yellow-green | yellow + green > 60% |
| green | green > 40% | red-blue | blue + light blue + red > 60% |
| blue | blue + light blue > 40% | pink | pink > 40% |
| yellow | yellow> 40% | purple | purple > 40% |
| orange | orange > 40% | multi-colors | all color categories < 25% |
| red-green | red + green + orange > 60% | monochromatic | black + dark gray + gray + light gray + white > 80% |
| blue-green | blue + light blue + green > 60% | | |
| yellow-blue | blue + light blue + yellow > 60% | skin | Images of human face and skin |

| red | 0% |
| blown | 0% |
| pink | 0% |
| orange | 0% |
| yellow | 0% |
| green | 6% |
| blue | 5% |
| light blue | 74% |
| purple | 0% |
| black | 0% |
| dark gray | 5% |
| gray | 1% |
| light gray | 0% |
| white | 8% |

*Figure 1: The image and the analysis data of the image.*

## 2.2 Experimental environment

Figure 2 shows the experimental apparatus of two projectors that project images. Test images were projected by the 2 projectors, one is for blue signal and the other one is for the red and green signals. Interference filters of λp = 430nm, 450nm, 470nm, and 480nm were inserted in front of the projection lens of the B projector to achieve different blue primaries. Projection from two projectors has been neatly matched. White balance of different blue primary conditions was set nearly the same chromaticity coordinates by inserting proper ND filters in front of the two projectors as well as adjusting the gain control. Figure 3 indicates color gamuts of different blue primaries in the CIE 1976 u'v' chromaticity diagram. Evaluation experiments were carried out with 2 levels of average luminance, 60 cd/m2 for 430nm, 450nm, 470nm, and 480nm, and 170 cd/m2 for 450nm, 470nm, and 480nm.

Average distance of vision is about 150cm. The size of the presented image is 42 × 58cm, visual angle is 16°×22°.



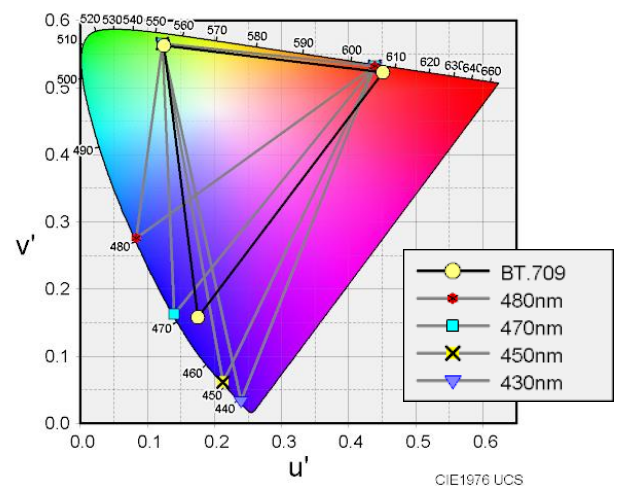*Figure 2: Two projectors that project images*



*Figure 3: Color gamuts of different blue primaries. Solid line denotes bt.709.*

## 2.3 Experimental Procedure

Tabel 2 shows 14 adjective pairs used in the experiment. "Unappetizing - Delicious" was used only in the images of foods and drinks. These word pairs were chosen from previous studies on the assessment of color image quality (Ayama et al. 2010, Kishimoto et al. 2011). The observer entered the experiment booth, and adapted to a dark environment for five minutes. Then test image was presented with one of the 4 or 3 blue primaries. Blue primary is changed every five pieces. The observer was instructed to evaluate each test image by indicating a score between two bipolar adjectives, on a seven-point scale from -3 to 3. There was no time limit for observer to see each image and make judgement. Fourteen observers participated in the 4 primaries experiments, while 17 observers in the 3 primaries experiments.

*Table 2. Adjective pairs used in KANSEI evaluation*

|  | negative | positive |  | negative | positive |
|---|---|---|---|---|---|
| 1 | Dark | Bright | 8 | Mundane | Impressive |
| 2 | Pale color | Deep color | 9 | Unnatural | Natural |
| 3 | Weak contrast | Strong contrast | 10 | Discomfort | Comfort |
| 4 | Dirty | Beautiful | 11 | Calm | Powerful |
| 5 | Blurry | Clear | 12 | Flat | Chiseled |
| 6 | Plain | Showy | 13 | Dismal | Cheerful |
| 7 | Dislike | Like | 14* | Unappetizing | Delicious |

*used only in the images of foods and drinks

## 3. RESULTS AND DISCUSSION

Figure 4 shows rating score of each evaluation word pair in the experiment using 4 and 3 different blue primaries, in the left-hand and right-hand side, respectively. Each point denotes the average of all observers' scores. Results of the 4 blue primaries experiment, 430nm, 450nm, and 470nm blue primaries showed similar performance for each evaluation word. 480nm blue primary is a remarkably bad result. Results of the 3 blue primaries comparison, 470nm showed the great result than 450nm.
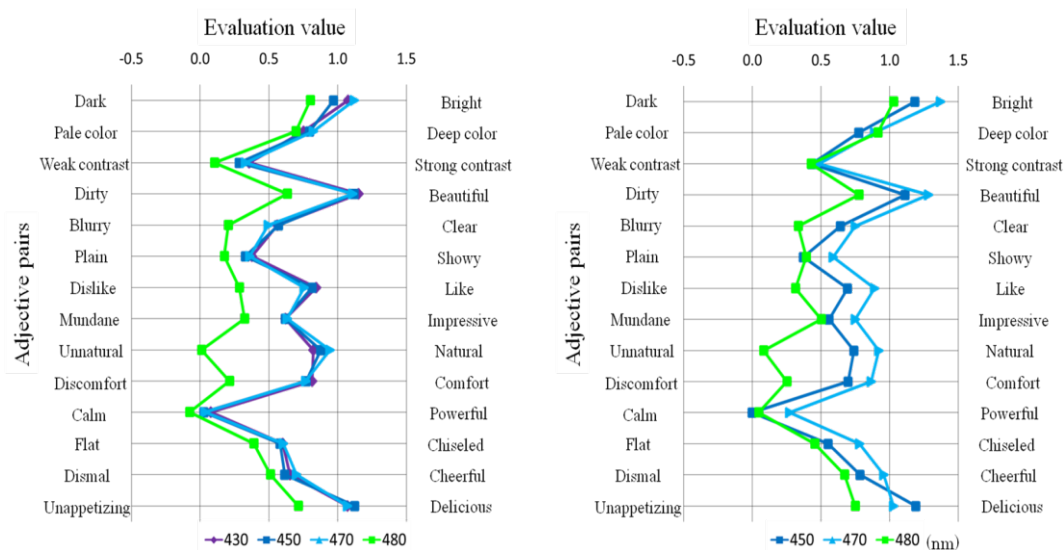


*Figure 4: Left: Rating score of each evaluation word pair in the experiment using 4 different blue primaries. Right: The same figures using 3 different blue primaries.*

AIC2015 TOKYO - Color and Image

In order to see the effect of different blue primaries more clearly, difference between the maximum and the minimum values of the evaluation word pairs were calculated for each of the test images. We found that effect of blue primary is relatively clearly indicated in the results of the following 5 adjective pairs of "Pale color vs Deep color", "Dirty vs Beautiful", "Dislike vs Like", "Unnatural vs Natural", and "Discomfort vs Comfort" in the results of the 4 blue primaries. "Dirty vs Beautiful" changes into "Dark vs Bright" in the results the 3 blue primaries. A average scores of these evaluation words were calculated.

Figure 5 shows average scores of the selected adjective pairs (1,2,7,9, and 10 in Table 2) for "purple", "red-blue", "blue", "blue-green", "yellow-blue", and "skin" images in the 3 blue primary experiments. As shown in the figure, 470nm showed the best performance, while 480nm showed the worst. Generally, marked difference of evaluation was found in the bluish, greenish, and purple images, while no difference was observed in other color images such as red, yellow, and pink, etc.
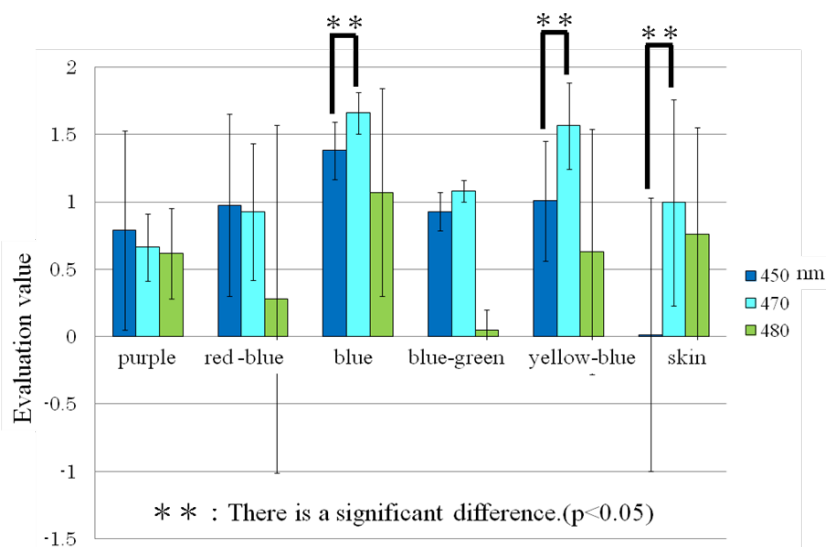


*Figure 5: Average results of subjective evaluation of 6 color images in 5 adjective pairs (1,2,7,9,and 10 in Table 1) in the 3 blue primary experiment.*

## 4. CONCLUSIONS

It was shown that 470nm blue primary showed the best performance for 15 test images in the KANSEI evaluation using 13 to 14 adjective pairs in the 3 blue primary experiment. It is suggested that the choice of the blue primary in the BT2020 is appropriate from the KANSEI-evaluation point of view.

A serious comment would be given to this study that the test images are chosen from the stock photos that are usually optimized in the color gamut of ITU-R BT.709-5 (ITU 2004) often called as sRGB. Among the blue primaries used in this study, 470nm is the closest to the blue primary of sRGB. If a picture is taken by a color camera with 430nm blue primary, the color signals are optimized, and displayed using the same blue primary, then the evaluation results of 430nm might be the best. Relation between the best color gamut from KANSEI-evaluation point of view and the selection of blue primary in the steps of taking a picture, optimization of color signal, and displaying the image, is the future issue. It is worth noting that for the "purple" image, 450nm showed the best performance in the 3 blue primary experiment as indicated in Figure 5, and 430nm blue primary showed the best

score in the 4 blue primary experiment. This suggests that colors in the display stage is the most important for the image assessment from KANSEI-evaluation point of view.

## ACKNOWLEDGEMENT

## REFERENCES

Ashiguchi, T., T. Yaguchi, K. Kijima, 2009. Application of categorical colors to area segmentation for road image, *Electronic Imaging 2008, Color Imaging XIV,Proceedings of SPIE*, 7241:.72410K-1-27410K-8,

Ayama, M., T. Shirakawa, T. Shimizu, H. Oguro, M. Sato, T. Eda, T. Ishikawa, and M. Kasuga. 2010. Kansei evaluation of color image - Influence of screen size, brightness and saturation contrast-, *Kansei Engineering*, 9 (2): 177-187

Kishimoto, Z., M. Kanazawa, Y. Murakami, M. Yamaguchi, H. Haneishi, N. Oyama. 2011. Analysis of psychological factors in high-fidelity color image reproduction system, *Image Electronics Journal*, 40 (6): 1017-1026

Masaoka, K., Y. Nishida, M. Sugawara, and E. Nakasu. 2010. Design of Primaries for a Wide-Gamut Television Colorimetry., *IEEE transactions on broadcasting*, 56 (4): 452-457.

ITU. 2004. Parameter values for the HDTV standards for production and international programme exchange. In Recommendation ITU-R BT.709-5

ITU. 2012. Parameter values Ultra-high definitiontelevision systems for production and international programme exchange. In Recommendation ITU-R BT.2020

*Address: Toshiya Hamano, Graduate School of Engineering, Utsunomiya University,*
*7-1-2 Yoto, Utunomiya,Tochigi,321-8585, JAPAN*
*E-mails: mt146647@cc.utsunomiya-u.ac.jp*

# New Proposal for Advanced Measurement Technology for Image Clarity

Hideo Kita, [1] Shigeo Suga, [1] Jack A. Ladson[2]
[1]SUGA Test Instruments Co., Ltd.
[2]Color Science Consultancy

## ABSTRACT

Evaluation of object surface structure traditionally involves the assessment of optical properties known as Gloss[1] and Haze[2]. More recently an advanced optical property of surfaces, known as Image Clarity, has gained major importance because Image Clarity provides an accurate assessment of the optical property of an object, while the traditional properties do not. The optical phenomenon of Image Clarity exists in both the reflection and transmission modalities for opaque and transparent products. We have evolved the design of instruments used to measure this phenomenon by using a narrow, diffraction limited optical beam and a CCD array as a detector. Results are obtained by analyzing the surface optical transfer function which uses Fast Fourier Transforms[3] for computational speed.

This optical surface evaluation technique affords several improvements over previous technologies[4]. This analytical technique allows assessment of the classical appearance properties and new appearance methods and metrics. Classically, the traditional appearance properties are gloss, haze, orange-peel and image clarity. Further, the measurement time of the new instrument is more rapid than bench top instruments allowing for near real-time measurement as well as continuous monitoring of moving plastic sheets or other processes in need of continuous examination. Both short and long wave surface phenomena are assessed with equal accuracy, and both precision and accuracy are improved by the new design. The rapidity of measurements affords a manufacturer the opportunity to assess the impact on surface quality of the product by controlling parameters in the manufacturing process.

Correlation is obtained with traditional assessments; such as gloss and haze. Additionally, the advanced technique correlates with visual product assessments. The fact that the new design is smaller and lighter than previous instruments provides the very important property of portability and usability to the instrument. The device is the latest in solid-state technology, ensuring reliability.

End users come from processes that require control of the quality of surface reflectance or transmittance and maintaining of product quality. These are industries and applications, such as; automotive enamels, coated surfaces, displays, films, glasses, material

---

1 ASTM D 523, Standard Test Method for Specular Gloss, ASTM International, West Conshohocken, PA

2 ASTM D 1003Standard Test Method for Haze and Luminous Transmittance of Transparent Plastics, ASTM International, West Conshohocken, PA

3 http://mathworld.wolfram.com/FastFourierTransform.html

4 ASTM D5767-95(2012) Standard Test Methods for Instrumental Measurement of Distinctness-of-Image Gloss of Coating Surfaces, ASTM International, West Conshohocken, PA

smoothness, paper processing, paper smoothness, painted panels, photographic hard reproduction media photographs, plated surfaces, plastics, polished surfaces, printed materials, surface texture and other industries where quality of surface structure or the quality aspects of components appearance is important.

# 1. INTRODUCTION

The method and apparatus for detecting certain surface phenomenon, such as, but not limited to, gloss, sheen, crazing, blistering, mud-cracking, cratering, haze, fog, orange-peel, distinctness of image[5] and texture of various frequencies is presented. The apparatus consists of a collimated beam illuminating the surface to be analyzed. A knife edge, commonly referred to as a slanted edge in image analysis, interrupts the reflected beam whose local intensities are captured by a Digital Still Camera containing a CCD/CMOS array. The images are scanned in the time domain and transformed to frequency domain using Fast Fourier Transforms (FFT). Certain frequency patterns prove to be associated quantitatively with certain of the mentioned appearance degradation phenomenon.

# 2. APPEARANCE MEASUREMENT

The appearance of an object is attributable to many factors. In this article, we concern ourselves with the appearance attributes that are associated with color appearance. The attributes of color are lightness, hue and chroma. The attributes of appearance are related to the optical surface structure. Gloss is classically used in many industries to evaluate surface appearance of an object. However, soon one discovers that gloss does not correlate with visual appearance and surfaces with the same gloss have totally different appearances. This issue was first addressed by Richard Hunter[6] in the 1980's. Hunter discovered that the appearance of an object is related to the spread of a light beam reflected from an object or transmitted through an object. Quantifying the spatial deviation of a light beam from a perfectly un-deviated beam at various spatial frequencies allows us to see deviations in surface structure that are consistent with appearance attributes; such as, gloss, DOI, orange peel and other optical imperfections caused by a less than perfect optical surface.

# 3. SAMPLE PREPARATION

The importance of proper sample preparation cannot be over stated. Sample conditioning is appropriate and necessary. We condition the sample before sample measurement. This typically involves the necessary time for allowing sufficient time for the sample(s) to stabilize in the measurement environment. The measurement environment is defined in ASTM[7], as; condition the test specimens at 23 ± 2°C [73.4 ± 3.6°F] and 50 ± 5 % relative humidity, Rh, for not less than 40 hours prior to test, in accordance with Procedure A of ASTM Standard Practice D618[8] . Samples are prepared in exactly the same manner each time they are collected before measurement.

---

5 ASTM D5767-95(2012) Standard Test Methods for Instrumental Measurement of Distinctness-of-Image Gloss of Coating Surfaces, ASTM International, West Conshohocken, PA

6 Hunter Lab, www.hunterlab.com, Model Dorigon II DOI/Haze Meter

7 ASTM International, West Conshohocken, PA

8 ASTM Standard Practice D 618.- Procedure A, ASTM International, West Conshohocken, PA

## 4. SELECTING SAMPLES

Select sample(s) that are representative of the entire batch should be selected for appearance measurement. Choose samples that are truly representative of the materials collected. For statistical analysis collect samples from various sources or differences in location at different times. These are the guidelines that we follow in our selection protocol.

1. The sample must also be representative of production and the attributes that are of interest. If samples are non-representative of the batch or are spoiled, damaged, or irregular, then the sample measurement may introduce a bias into the colour appearance measurement chain.

2. Choose a sample randomly.

3. Examine the sample to ensure that it is representative of production. This methodology will avoid biasing the results.

4. Follow the corporate SOP for handling instructions.

5. If sampling procedures are adequate, a different sample selected from the same batch should result in comparable measured values.

## 5. APPARATUS

An illustrative schematic diagram of the apparatus appears in Figure 1. A CCD camera is focused on the film surface to be analyzed. A knife edge interrupts the beam reflected from the surface under analysis from a collimated light source. The distance between the camera and the surface under analysis is slightly variable and under operator control because different optical surface phenomena will be found at different focal depths. The pixels of the image will be raster scanned across the image of the knife edge and Fast Fourier Transform (FFT) used to convert from time (spatial) domain to frequency domain. Certain patterns in the frequency domain act as fingerprints for certain characteristic surface degradation phenomena.
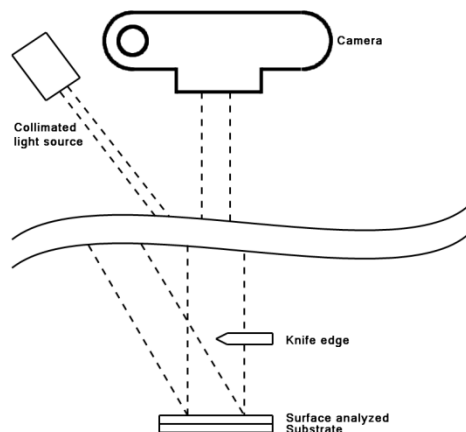


*Figure 1: Schematic diagram of the apparatus*

The variability in measurement angle relative to the sample and the light source allows measurements to be made in reflection and transmission and other intermediate angles. Other intermediate angles are useful for identifying different surface structures attributable to different optical effects.

This design implementation uses the slanted edge in accordance with ISO12233[9] . The slanted edge significantly reduces the aliasing that commonly occurs in high density linear array detectors. A linear dimensional array is used to compute the discrete derivative along the slanted edge. These data are combined to create a one-dimensional edge spread function. This over sampling produces an accurate assessment of the spatial frequency factor, SFR. Noise produces a bias in the SFR. However, when the data from the array are combined this significantly reduces the electronic and optical noise. We also use noise smoothing algorithms to reduce the influence of noise to an acceptable limit.
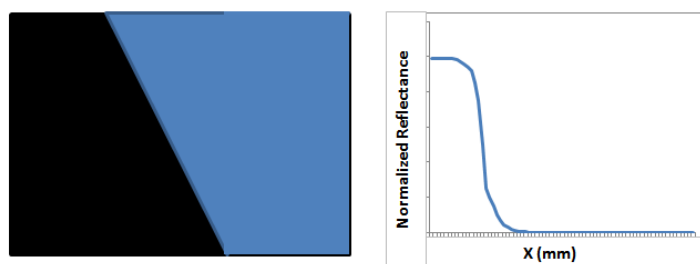


*Figure 2: Slanted edge and data*

In addition, certain characteristic patterns emerge from various depths within the fractured film itself. Therefore, it is necessary that the camera maintain a narrow focal plane and the focal plane is moved to various levels within the fractured film by mechanically changing the length of the specimen to camera axis by amounts proportional to a fraction of the film's thickness. This variance accommodates another feature of the method that the analysis may be accomplished without resort to variation of relative angles between camera, specimen, and the illumination.

## 6. METHOD

### 6.1 Standardization

Standardization of the photometric scale is accomplished by scanning a black polished glass representing zero (0) followed by scanning a white polished glass, representing full scale (100%).

### 6.2 Test Scan

Images are captured using physical and optical conditions identical with those of the standardization. Images are scanned along the entire x-axis if the image across the specimen perpendicular to the axis of the knife edge. In most cases, a single scan contains insufficient data to obtain repeatable results. In this case we form a histogram at each x-pixel location and combine data from the array. The histographic function is treated as the time domain function and submitted to FFT for analysis. The results in the frequency domain are then compared to scans of known specimens and experimental conditions. Here we show the acquired data and its corresponding modulation Transfer Function as a result of applying the image analysis transform.

---

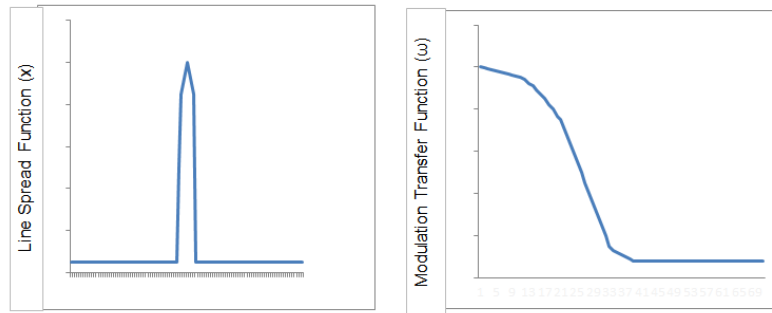9 International Organization for Standardization, ISO Central Secretariat, Chemin de Blandonnet 8, CP 401, 1214 Vernier, Geneva, Switzerland,  http://www.iso.org/iso/home/store.htm

*Figure 3: Line Spread Function and Moduration Transfer Function*

## 7. RESULTS

By examining the data and applying algorithms we have minimized the sources or error which may introduce a bias into the modulation transfer function.

The image quality fundamental standards; such as, Orange Peel, Gloss, and other surface structural phenomenon, serve as crucial ground-truth information for evaluating Image Quality algorithms. Specifically, to quantify how well our Image Quality algorithm can predict the fundamental effect values from a particular analysis technique. We evaluate the algorithm's performance in terms of three performance criteria recommended by the Video Quality Experts Group (VQEG) [141][10]: (1) prediction accuracy, (2) prediction monotonicity, and (3) prediction consistency.

The prediction accuracy will be quantified and evaluated by measuring how well the algorithm's predictions correlate with known established standards values and by measuring the average error between the algorithm's predictions and those values. The Pearson correlation coefficient (PPMCC) and the root-mean-squared error (RMSE) are used to evaluate the performance.

## 8. CONCLUSIONS

Our experimental data show that this method of analysis provides increased analytical sensitivity, and discrimination and classification of various surface effects. These data in turn allow the user to perfect and control their manufacturing process where the appearance of high quality surfaces is important.

## ACKNOWLEDGEMENTS

## REFERENCES

PS Burns - IS&T PICS, 2002 Refined Slanted-edge Measurements for Digital Camera and Scanner Testing

Monie, S. A.; Stief, B. C.; Krupkin, N. V.Evaluation of Glossy Inkjet Papers Using Distinctness of Image (DOI) Measurement, NIP & Digital Fabrication Conference,

---

10 Arthur Webster, U.S. Dept. of Commerce, NTIA/ITS, Boulder, Colorado U.S.A.,Email: webster@its.bldrdoc.gov

2003 International Conference on Digital Printing Technologies. Pages 458-910., pp. 763-768(6)

Ming-Kai Tse*, David Forrest and Eugene Hong, An Improved Method for Distinctness of Image (DOI) Measurements,

*Address: Hideo Kita, Calibration Dept, SUGA Test Instruments Co., Ltd.,*
*5-4-14, Shinjuku, Shinjuku-ku, Tokyo, 160-0022, JAPAN*
*E-mails: kita@sugatest.co.jp*

# Analysis of color appearance of metallic colors and pearlescent colors using multi-angle spectrophotometer

Yu-Wen Chiu[1], Hung-Shing Chen[2], Chia-Pin Cueh[3], Kang-Yu Liu[3]

[1] Graduate Institute of Color and Illumination Technology, National Taiwan University of
   Science and Technology, Taiwan
[2] Graduate Institute of Optical-Electronic Engineering, National Taiwan University of
   Science and Technology, Taiwan
[3] Printing Technology Research Institute, Taiwan

## ABSTRACT

Many industrial products and packages use metallic or pearlescent inks to produce special effects. However, there is little specific comparison on special-effect inks and traditional inks to signal their feature difference. Using RAL color charts as examples, this paper provides three types of ink materials (solid, pearlescent and metallic colors) to discuss their appearances under varying illumination types and measurement geometries. The viewing angle-dependent color samples are measured using multi-angle spectrophotometer under different illuminating and measurement geometries. In addition, solid color samples with two levels of gloss coatings are also measured to analyze their color appearances.

## 1. INTRODUCTION

During the last few decades, there has been a rapid growth of special-effect performances due to the development of effect inks and post-processing technologies. The special effects generated by using metallic and pearlescent inks allow the creations of different fantastic optical effects. For examples, traditional inks only produce selective absorption and scattering, which show monotone color perception, and uniform appearance effect with independent observation angle, so called solid color. On the other hand, pearlescent inks can create special interference effect because they are composed of multi-layer structure, i.e., high refractive metal oxides coated low refractive mica flakes, leading to color change with different observation angles. Furthermore, metallic inks are usually generated by shinny and thin metal flakes, which tend to lie parallel to the surface and create highly specular reflection (Figure 1). Their appearances could vary with the illumination geometries and viewing conditions[1-3]. Because color appearances of ink materials with effect coating could vary with the viewing geometries and illumination geometries, the use of multi-angle spectrophotometer is necessary in the quantification of angle-dependent color appearances.
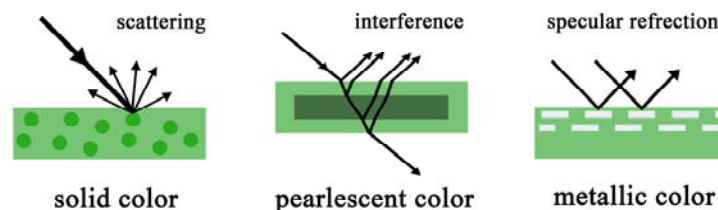


*Figure 1: Optical effects of solid, pearlescent and metallic inks*

In addition, it is well known that gloss coating has a notable effect on surface appearance. The spike of specular lobe reflection locates in the specular angle region, where the lightness and chroma extremely change. The shape of specular spike is lower and broader in matte materials than in glossy one. Matte surface appears higher lightness and lower chroma than the corresponding glossy surface[4]. Recent researches have explored the characteristics of special color appearance, and the surface appearance issues related to illumination and viewing conditions also pay more attentions[1-2]. Our objective in this study is to measure appearances of different ink materials and different gloss levels through multi-angle spectrophotometer.

## 2. METHOD

The method to carry out this study was using multi-angle spectrophotometer, BYK-mac instrument from BYK Gardner (Figure 2), which can objectively measure total appearance under different viewing angles and lighting conditions. The lighting conditions include directional illumination and diffused illumination. Under directional illumination, color appearance including CIELAB values is assessed at given 45° lighting angle and viewing under six aspecular angles -15°/ 15°/ 25°/ 45°/ 75°/ 110°. The aspecular angle is the viewing angle measured from the direct specular direction. Positive angle means in direction towards incident illumination, negative angle means away from incident illumination (Figure 3). Besides, sparkle grade is assessed under directional incidence angle 15°/ 45°/ 75° and observed from the normal direction. Under diffused illumination, graininess is evaluated from the normal direction[5] (Figure 4).
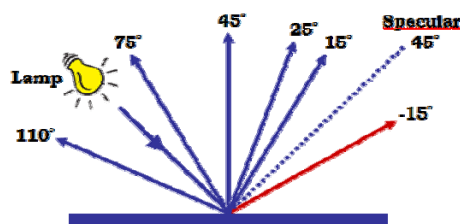


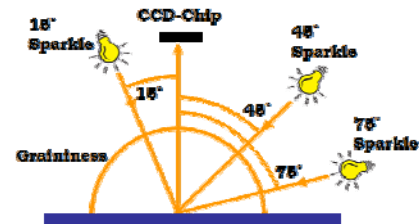Figure 2: BYK-mac instrument

Figure 3: Color measurement geometry

Figure 4: Effect measurement geometry

### 2.1 Experimental Design

In order to investigate the appearances of different ink materials and gloss levels in the particular illuminating conditions and viewing geometries, we measured a series of samples using a multi-angle spectrophotometer, BYK-mac. CIELAB values and the effect parameters including sparkle grade and graininess were analyzed. This study consisted of two experiments, Experiment 1 (Exp-1) of which was intended to elicit the appearance of three type of ink materials including solid, pearlescent and metallic effects varied with different lighting and measurement geometric conditions. Experiment 2 (Exp-2) focused on color changes of solid colors regarding two levels of gloss impressions, gloss and semi-matte (Figure 5).
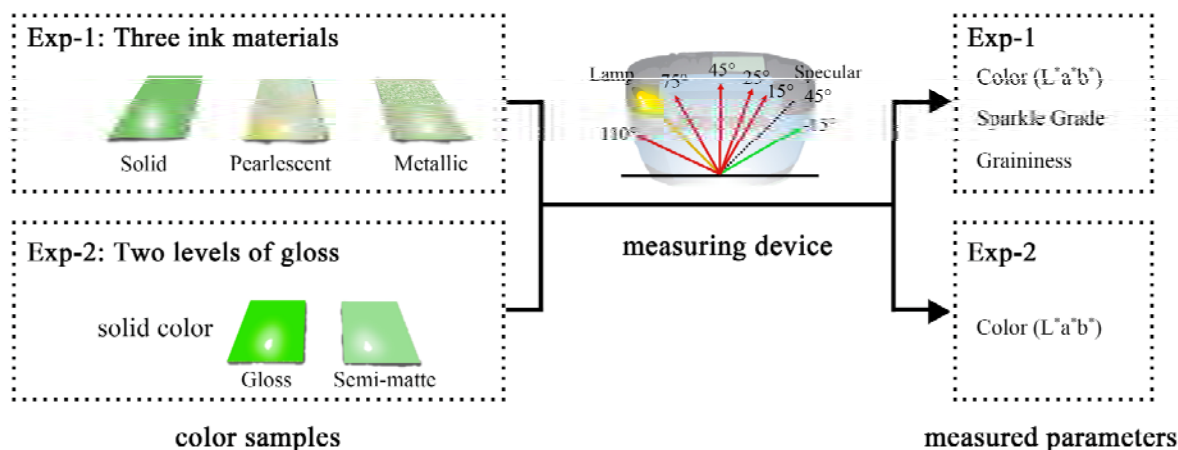
*Figure 5: Experimental schematic*

## 2.2 Sample Preparation

For Exp-1, total eight solid, eight pearlescent and eight metallic color samples were prepared. Colors of samples included red, orange, yellow, green, blue, violet, light grey and dark grey. For Exp-2, considering gloss as a specific appearance attribute, two levels of gloss in the solid color samples so called semi-matte and gloss samples were prepared. The solid color samples with gloss used in Exp-2 are the same as Exp-1. All color samples were chosen from the RAL color system. Solid and pearlescent colors were chosen from the RAL CLASSIC K5 collection, and metallic colors were chosen form RAL EFFECT E4 collection. The list of test samples is showed in Table 1.

*Table 1: The list of color samples*

| Exp | Exp-1, Exp-2 | Exp-2 | Exp-1 | Exp-1 |
|---|---|---|---|---|
| Ink type | Solid color | | Pearlescent color | Metallic color |
| Gloss level | gloss | semi-matte | gloss | gloss |
| Red | RAL 3020 Traffic red | | RAL 3032 Pearl ruby red | RAL 450-M |
| Orange | RAL 2009 Traffic orange | | RAL 2013 Pearl orange | RAL 410-M |
| Yellow | RAL 1023 Traffic yellow | | RAL 1036 Pearl gold | RAL 270-M |
| Green | RAL 6024 Traffic green | | RAL 6035 Pearl green | RAL 220-M |
| Blue | RAL 5017 Traffic blue | | RAL 5025 Pearl gentian blue | RAL 640-M |
| Violet | RAL 4006 Traffic purple | | RAL 4011 Pearl violet | RAL 570-M |
| Light grey | RAL 7042 Traffic grey A | | RAL 9022 Pearl light grey | RAL 110-M |
| Dark grey | RAL 7043 Traffic grey B | | RAL 9023 Pearl dark grey | RAL 840-M |

## 3. RESULTS AND DISCUSSION

### Experiment 1: Appearances of Ink Materials

The $a^*b^*$ loci for eight color samples with three ink materials (solid, pearlescent and metallic colors) in $a^*b^*$ color plane are illustrated in Figures 5(a) through 5(c). For solid colors, the measured color values of aspecular viewing angle -15° are close to the $a^*b^*$ center. With the aspecular angle increases, $a^*$ and $b^*$ values increase. In case of pearlescent colors, chroma changes with measuring angle are significant and become greyish as measuring angle become larger. No significant trend was uncovered in metallic color samples.

The L*C* loci for eight color samples of three ink materials in L*C* color plane are illustrated in Figures 5(d) through 5(f). The measurement results showed that lightness (L*) of all samples becomes larger with measuring angle accordingly up to specular direction. The lightness change is dramatic in pearlescent and metallic colors. In case of solid color samples, chroma changes with measuring angle are significant and become larger as measuring angle become larger. In contrast, chroma changes in pearlescent color samples with measuring angle are significant and become smaller as measuring angle become larger.

On the other hand, the measured effect parameters of sparkle grade and graininess are showed in Figure 6. The solid color samples have little sparkle effect because they are made by traditional solid inks. The pearlescent colors and metallic colors are made by metallic flakes which enable to generate grainy shining effects. In particular, the metallic samples appear with larger flake size, are more significant in the sparkle and graininess effects.
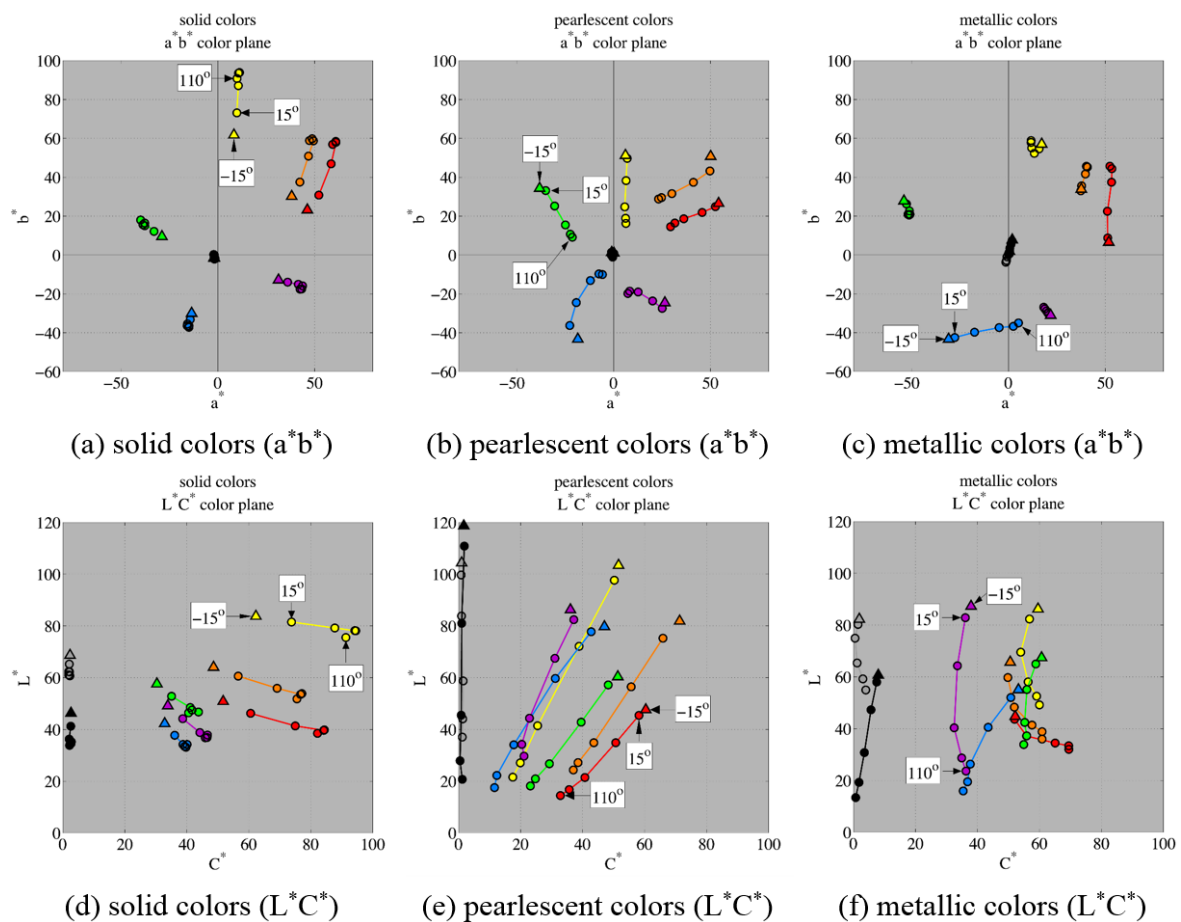


(a) solid colors (a*b*)        (b) pearlescent colors (a*b*)        (c) metallic colors (a*b*)

(d) solid colors (L*C*)        (e) pearlescent colors (L*C*)        (f) metallic colors (L*C*)

*Figure 5: The LAB color values of three different ink colors (in a\*b\* / L\*C\* planes)*
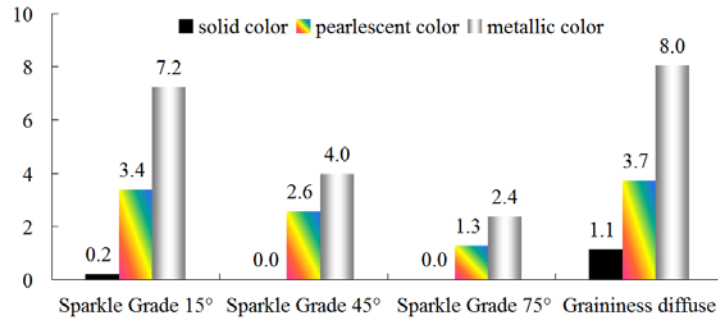
*Figure 6: The effect parameters of three different ink colors*

**Experiment 2: Solid Color Appearances Regarding Gloss Levels**

The $a^*b^*$ loci of eight solid color samples with two levels of gloss (gloss and semi-matte) in $a^*b^*$ plane are illustrated in Figure 7. For semi-matte colors, the measured color values of aspecular angle -15° and 15° are closer to the $a^*b^*$ center than the glossy colors. Far from the specular region, the measured color values of gloss samples and semi-matte samples are rather identical. The $L^*C^*$ loci of the solid color samples with two levels of gloss are illustrated in Figure 8. As expected, the main impact of gloss coating was the lightness value close to the aspecular angle of -15°, 15°. The lightness value of the semi-matte surface was higher than the gloss one, while the chroma value of the semi-matte surface was lower than the gloss one.
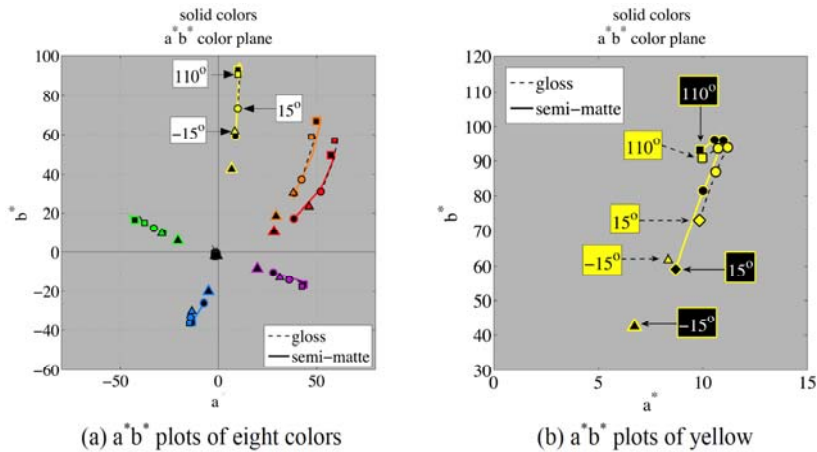


(a) $a^*b^*$ plots of eight colors

(b) $a^*b^*$ plots of yellow

*Figure 7: The $a^*b^*$ plots of two surface processing*



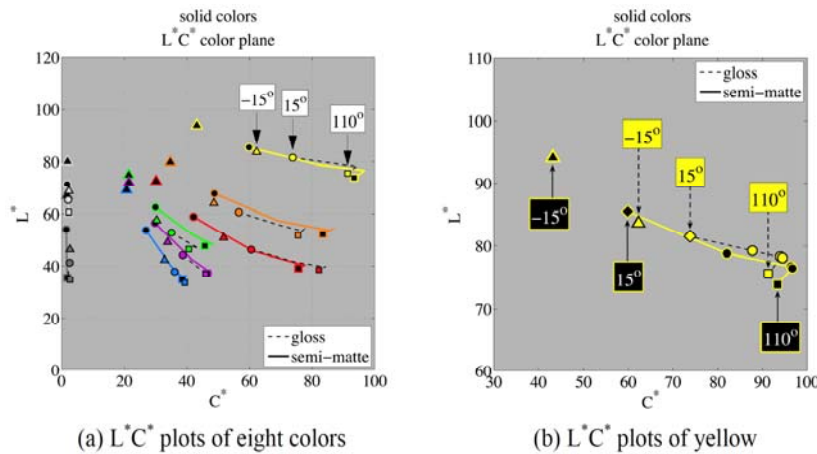(a) $L^*C^*$ plots of eight colors

(b) $L^*C^*$ plots of yellow

*Figure 8: The $L^*C^*$ plots of two surface processing*

# 4. CONCLUSIONS

The viewing angle-dependent color samples with solid, pearlescent and metallic colors are measured using multi-angle spectrophotometer under different illuminating and measurement geometries. In addition, the solid color samples with 2 levels of gloss coatings are also measured to analyze their color appearances. The analysises in this paper are performed using a multi-angle spectrophotometer to obtain CIELAB color values and the effect parameters (sparkle grade and graininess). Experimental evaluation results show color appearances of three type ink materials (solid, pearlescent and metallic colors) are quite different. Besides, the main impact of gloss coating is the lightness value close to the aspecular angle of -15°, 15°. From the comparison of solid color samples between gloss type and semi-matte type, semi-matte surface appears higher lightness and lower chroma than glossy one. Our current implementation uses RAL color charts, but the development of special-effect inks technology is diversity. Our future work is to implement more ink materials to realize more multi-angle color performance of special-effect inks.

# REFERENCES

1. Cramer, W.R., Gabel, P.W., 2001, *Measuring Special Effects*, Paint & Coating Industry, 9, p.36-46.
2. M. E. Nadal and T.A. Germer, 2002, *Colorimetric characterization of pearlescent coatings*, Proc. SPIE 4421, p.757–760.
3. McCamy CS., 1996, *Observation and measurement of the appearance of metallic materials. I. Macro appearance*, Color Res Appl, 21, p.292–304.
4. Mikula, Ceppan, et al., 2003, *Gloss and Goniocolorimetry of Printed Materials*, COLOR research and application, 28, p.335-342.
5. "BYK-Gardner Digital Catalog, 2013", from http://www.byk.com/en/support/instruments/download-catalog.html

*Address: Prof. Hung-Shing Chen, Department of Optical-Electronic Engineering, National Taiwan University of Science and Technology, 43, Keelung Road, Section 4, Taipei, Taiwan*
*E-mails: M10325003@mail.ntust.edu.tw, bridge@mail.ntust.edu.tw, james@ptri.org.tw, terryliu@ptri.org.tw*

# HDR imaging – Automatic Exposure Time Estimation A novel approach

Miguel A. MARTÍNEZ,[1] Eva M. VALERO,[1]  Javier HERNÁNDEZ-ANDRÉS,[1] Javier ROMERO,[1]

[1] Color Imaging Laboratory, University of Granada, Spain.

## ABSTRACT

Digital imaging of common scenes can be a very challenging task if the scene radiances present a high dynamic range (HDR). HDR imaging techniques are applied to overcome this issue. The most popular technique is based in the combination of differently exposed low dynamic range (LDR) images. However there is a lack of a robust method for determining either the amount of LDR pictures needed, or their exposure time settings, without any prior knowledge of scene content. In a recent publication, we proposed a novel method for estimating the set of exposure times (bracketing set) needed to capture the full dynamic range of HDR scenes including daylight skies. Now we extend the applicability of this method to any imaging system or application (scientific, industrial or artistic). The proposed method is adaptive to scene content and to any camera response and camera configuration (raw, jpeg, etc). Our method works on-line, since the exposure times are estimated as the capturing process is ongoing. Therefore, it requires no a-priori information about scene content. The resulting bracketing sets are minimal for the scene being captured. The user can set a tolerance for the maximum percentage of pixel population that is underexposed or saturated. We can use this method separately for each color or spectral channel. This method can thus also be used for multispectral imaging systems.

## 1. INTRODUCTION

The use of HDR imaging techniques converts our digital camera in a tool for measuring the relative radiance outgoing from each point of the scene, and for each color channel. This final HDR image is called HDR radiance map. In order to generate it, we need to know the relationship between camera response values and relative irradiance impinging on the sensor (which is proportional to the radiance outgoing from the scene). This relationship is represented by the camera response function (CRF), which is easily calculated as proposed by Debevec and Malik (2008).

Merging different low dynamic range (LDR) images into a HDR radiance map using the CRF, is a very well known technique widely used in many imaging fields from photography to scientific or industrial applications. However, when the captures take place, there is no method that allows us to determine either how many LDR shots are going to be needed or what exposure times to be used, without having any prior knowledge of the radiance content of the scene being captured. Authors care the most about optimizing the signal to noise ratio (SNR) of the resulting HDR radiance map, rather than controlling the number of shots and the final total exposure time. For this purpose, they assume known information about scene content before starting the capturing process, like known illuminant or radiance levels, or they assume a camera with linear CRF (Granados et al. (2010), Hirakawa and Wolfe (2010), Gallo et al. (2012)). Their bracketing set selection is based in finding an intermediate exposure time, and increasing and decreasing it for the contiguous shots a fixed number of stops (Stunpfel et al. (2004), Bilcu et al. (2008)). Other authors capture a

large number of exposures, and afterwards select which ones to use for an optimal SNR reconstruction (Hassinoff et al. (2010), Gallo et al. (2012)). Only Barakat et al. (2008), proposed a method for finding minimum bracketing sets for any given camera. They studied the radiance ranges covered by their camera using every exposure time setting available on it. Afterwards, they selected only those exposure times that covered the full dynamic range of the camera with some overlap, eliminating redundant shots that do not add any new radiance range to the final HDR image. To make this method adaptive to scene content, they included a stopping condition if they found no underexposed or saturated pixels respectively. This way they are limiting their capturing possibilities to usually 4 or 5 possible exposure times, and they do not control the SNR of the resulting HDR radiance map.

In this work we extend the applicability of the proposed method from natural scenes with daylight skies to any general or particular HDR imaging application. Numerical results of a different set of HDR radiance maps generated for daylight outdoors scenes, and a comparison with the method proposed by Barakat et al. (2008), are shown and explained in Martínez et al. (2015). Here we captured a set of 24 HDR scenes including both outdoors (with and without sky) and also indoors scenes, and also both in very bright and very dim lightning conditions.

We aimed for a method that can be used for any camera, whether it is linear or not. We wanted it to be adaptive to scene content and also to work on-line, as the capturing process is ongoing, without the need of being fed with any information about the scene. We also wanted the method to be tunable. The default configuration is to find a minimum bracketing set for the given camera and scene. However this would also mean reduced SNR compared to captures with larger number of shots and longer exposure times. Therefore, the user can tune the balance between shorter captures or higher SNR levels. We also included a parameter to bound the radiance range to be captured if we are not interested in recovering the full dynamic range, neglecting the extreme low or high radiances present in the scene (deep shadows or brilliant highlights).

We compared the SNR performance of our method, using 5 different tunning conditions (AEE-A to AEE-E), against the best SNR case that our camera can achieve. The latest case is called the ground truth (GT), and it is an HDR radiance map generated using every available exposure time that our camera offers (optimal SNR case).

## 2. METHOD

We present here the results obtained using a consumer camera model Canon EOS 7D working in sRGB jpeg mode (non linear). Nonetheless, the method was successfully tested as well in two linear scientific cameras (monochrome Retiga 1300 and RGB Retiga 1300C working in raw mode), yielding similar results as the ones presented here (Martínez et al. (2015)).

Our Canon camera was driven from a laptop computer via USB interface. The method proposed was implemented using Matlab and worked on-line. For the generation of GT images we just captured all 55 available exposure times in the camera.

Our method uses an initial shot as starting point. It can be any exposure time, as long as the resulting LDR image has some useful pixels (neither underexposed nor saturated). A good initial exposure time is the one implemented in the auto-exposure setting of most consumer cameras. If the camera used does not implement this function, then any intermediate exposure time would work good.

Once this image is captured, we calculate its cumulative histogram. This cue will give us information of the pixel populations which were correctly exposed in this first shot. The idea of using cumulative histograms to control sensor responses to pixel populations in the scene was taken from Grossberg and Nayar (2002), who originally used it to select pixel populations for CRF estimation.

We will consider at this point two sensor response levels: low (Lo) and high (Hi). Our algorithm will consider underexposed any sensor response that is below Lo level, and saturated whatever is above Hi level. This way, the user can tune the method. If Lo and Hi levels are set very close to the extreme sensor response values (say 0 and 255 for 8 bits data), the overlap between consecutive shots will be minimal, yielding thus a minimum bracketing set as output. If otherwise the Lo and Hi levels are selected far from these extremes, then the redundancy between consecutive shots will increase and the SNR of the resulting HDR radiance map will be higher at the cost of more shots and longer total exposure time.

So if thanks to the cumulative histogram of the image, we know the sensor responses at the Lo and Hi limits ($DC_{Lo}$ and $DC_{Hi}$), and we also know the CRF, and the exposure time used ($\Delta T_0$), we can determine the relative irradiance values ($E_{Lo}$ and $E_{Hi}$) for the areas of the image which lie just in the limits of the correct exposure, as shown in equation 1:

$$E_{Lo} = \frac{CRF^{-1}(DC_{Lo})}{\Delta T_0} \quad E_{Hi} = \frac{CRF^{-1}(DC_{Hi})}{\Delta T_0} \tag{1}$$

Now the aim is to find new exposure times, that shift the sensor responses corresponding to these irradiance values, to the opposite limit (Lo or Hi) that they were found in. For this purpose now we determine that the new longer and shorter exposure times ($\Delta T_{longer}$ and $\Delta T_{shorter}$), are calculated as shown in equation 2:

$$\Delta T_{longer} = \frac{CRF^{-1}(DC_{Hi})}{CRF^{-1}(DC_{Lo})} \cdot \Delta T_0 \quad \Delta T_{shorter} = \frac{CRF^{-1}(DC_{Lo})}{CRF^{-1}(DC_{Hi})} \cdot \Delta T_0 \tag{2}$$

When the new exposure times are estimated, the algorithm will order to the camera, to acquire new pictures using them. For the new LDR images captured, the same procedure will be followed to find longer and/or shorter exposure times if needed. The stopping condition for this process would be to check in the cumulative histograms of the new LDR images captured, if the pixel population above Hi level or below Lo level is below some threshold percentage set by the user (zero for full range).

## 3. RESULTS AND DISCUSSION

We captured a set of 24 indoors and outdoors HDR scenes using our method. In every scene captured, the full dynamic range was recovered successfully, except for the case of direct sunlight, like figure 1. We see all its LDR exposures and the tone-mapped version of its HDR radiance map generated. We can also see the cumulative histograms of each LDR

image. In figure 2, some other HDR tone-mapped radiance maps are shown, corresponding to outdoors and indoors scenes where the irradiance levels were lower than daylight skies'.

In order to study the SNR performance of the proposed method for different tuning conditions, we created a controlled illumination indoors scene to avoid illumination changes during the experiment. This is important because during the whole capturing process we need no changes in the radiance conditions coming from the scene to happen. This is a key factor to consider the irradiance on the sensor as a constant and not as a variable. With natural illumination this radiance stability is not controllable. We generated 6 sets of 10 HDR radiance maps. 5 of them were generated using our method with different tuning conditions (AEE from A to E). The other one was generated using all available exposure times in the camera (GT).
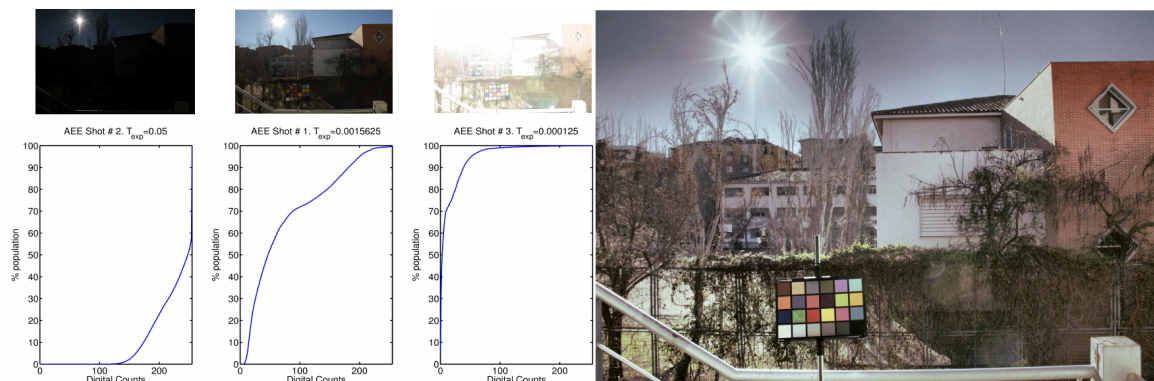


*Figure 1: LDR images and histograms, and tone-mapped HDR radiance map.*

*Table 1. Numerical results of SNR study.*

| Condition | Lo level | Hi level | # of shots | $\Sigma\Delta T$ (s) | SNR (dB) | std(SNR) |
|-----------|----------|----------|------------|----------|----------|----------|
| AEE A | 3 | 252 | 3 | 8.313 | 23.82 | 2.42 |
| AEE B | 5 | 250 | 3 | 21.31 | 25.81 | 2.94 |
| AEE C | 10 | 245 | 3 | 30.2504 | 26.62 | 6.68 |
| AEE D | 30 | 225 | 4 | 30.252 | 28.14 | 3.45 |
| AEE E | 55 | 200 | 6 | 31.468 | 28.55 | 4.57 |
| GT | X | X | 55 | 151.4308 | 31.38 | 6.52 |

Numerical results are shown in table 1. We can see the total number of shots, total exposure time, average SNR and standard deviation of SNR and the Lo and Hi levels tuned.

As we can see, the minimum bracketing set achieved to recover the full dynamic range of the scene happened when setting the Lo and Hi levels close to the 8 bits sensor responses extremes. As we move these levels further from the extremes of the range, the number of shots and/or the total exposure time increase, and so does the average SNR. This is

expected as for longer exposure times the signal is higher as well as because higher number of shots means to average more LDR images thus reducing the noise to a lower level.

In figure 3 we can see the HDR radiance map of the HDR indoors scene generated, as well as the SNR histograms of each of the tuning conditions tested.



*Figure 2: Tone-mapped HDR radiance maps of outdoors and indoors scenes.*

These results prove the ability of the proposed method to recover full range HDR radiance maps for any lightning condition, finding minimal bracketing sets, as well as the ability to control the balance between total exposure time (number of shots) and SNR. Therefore, for each application, the user can decide if faster acquisitions are more important or higher SNR are key factor, sacrificing capture speed.
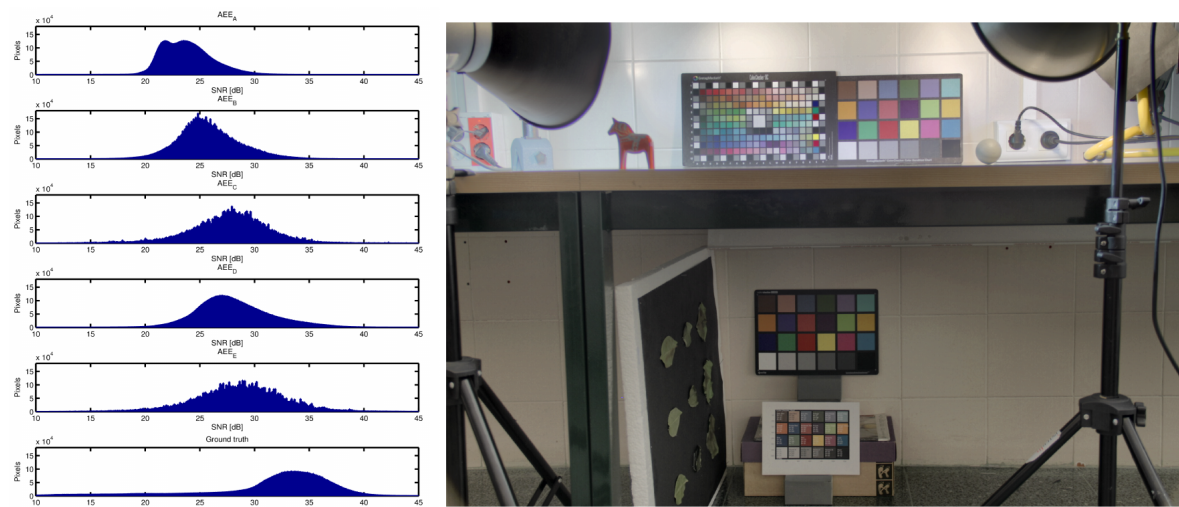


*Figure 3: SNR histograms and tone-mapped HDR radiance map of indoors scene.*

## 4. CONCLUSION

We have extended the applicability of a recently proposed method for estimating the bracketing set needed for a HDR radiance map capture via multiple LDR exposures. Our method adapts to any camera whatever camera response function has, as well as to any scene content. There is no need to know any information about scene content prior to the capture. Only a first exposure of the scene where some pixels are neither underexposed nor saturated is sufficient. We have captured several HDR scenes and in all of them the full dynamic range was covered except for direct sunlight.

We have also tested the ability of our method to be tuned in order to increase the SNR performance, at the cost of increasing also the total exposure time. We have seen how the

more shots the method adds to the capture, the more similar the SNR performance is with the optimal one achievable by the camera.

The proposed method is therefore suitable for HDR imaging in any application, artistic, industrial or scientific, independently of the number of spectral channels or camera response function that the imaging system has.

## ACKNOWLEDGEMENTS

## REFERENCES

Debevec, P. and Malik, J. 2008. Recovering high dynamic range radiance maps from photographs. In ACM SIGGRAPH 2008 proceedings 31.

Granados, M. Ajdin, B. Wand, M. and Theobalt, C. 2010. Optimal HDR reconstruction with linear digital cameras. In IEEE Conference on Computer Vision and pattern recognition 215-222.

Hirakawa, K. and Wolfe, P. J. 2010. Optimal exposure control for High Dynamic range imaging. In IEEE International Conference on Image Processing 3137-3140.

Gallo, O. Tico, M. Manduchi, R. Gelfand, N. and Pulli, K. 2012. Metering for exposure stacks. In Computer Graphics Forum 31, 479-488.

Stumpfel, J. Tchou, C. Jones, A. Hawkins, T. Wenger, A. and Debevec, P. 2004. Direct HDR capture of the sun and sky. In Proceedings of the 3rd International Conference on Computer Graphics, Virtual Reality, Visualization and Interaction in Africa 145-149.

Bilcu, R. C. Burian, A. Knuutila, A. and Vehvilainen, M. 2008. High Dynamic Range imaging on mobile devices. In the 15th IEEE International Conference on Electronics, Circuits and systems 1312-1315.

Hassinoff, S. W. Durand, F. and Freeman, W. T. 2010. Noise-optimal capture for high dynamic range photography. In IEEE Conference on Computer Vision and Pattern Recognition 553-560.

Barakat, N. Hone, A. N. and Darcie, T. E. 2008. Minimal-bracketing sets for high-dynamic-range image capture. In IEEE Transactions on Image Processing 1864-1875.

Martínez, M. A. Valero, E. M. Hernández-Andrés, J. 2015. Adaptive exposure estimation for high dynamic range imaging applied to natural scenes and daylight skies. Applied Optics Vol. 54, No. 4, B241-B250.

Grossberg, M. D. and Nayar, S. K. 2002. What can be known about the radiometric response from images?. In Computer Vision ECCV 189-205.

*Address: MSc. Miguel Ángel Martínez, Color Imaging Laboratory, Department of Optics, Faculty of Sciences. University of Granada 18071, Granada, SPAIN. E-mails: martinezm@ugr.es, valerob@ugr.es, javierha@ugr.es.*

# Real-time Green Visibility Ratio Measurement

Motonori DOI [1], Akira KIMACHI [2], Shogo NISHI [2]

[1] Department of Telecommunications and Computer Networks,
Osaka Electro-Communication University
[2] Department of Engineering Informatics, Osaka Electro-Communication University

## ABSTRACT

The green visibility ratio is one of the important indices for urban environment assessment. The green visibility ratio is defined as the ratio of vegetation green in an image. The green area is usually detected manually. There is a product for automatic green visibility ratio measurement, which measure the green visibility ratio using color information only. Some artificial green objects often exist in the urban scene. Therefore, the discrimination of the vegetation green from other green objects is required for automatic green visibility ratio measurement. This paper presents a new method for the detection of vegetation green area based on the brightness changes in vegetation area. The experimental results showed the feasibility of the proposed method. We implemented a prototype system of the real-time green visibility ratio measurement by using the proposed method.

## 1. INTRODUCTION

There are some indices for urban environment assessment, such as the green plot ratio (Ong 2003) or the green visibility ratio (Ohki 2009). The green visibility ratio (GVR) is often used by Japanese local governments. The GVR is defined as the ratio of vegetation green in an image. The green area is usually detected manually. There is a product for automatic GVR measurement (Takizawa 2013), which measures the GVR using color information only. Some artificial green objects often exist in the urban scene. Therefore, the discrimination of the vegetation green from other green objects is required for automatic GVR measurement.

This paper presents a method for vegetation green area detection and a real-time GVR measurement system by using the proposed method. The vegetation green detection method is based on the analysis of color and image texture.

## 2. VEGETATION GREEN VS. NON-VEGETATION GREEN

Vegetation green and non-vegetation green have different characteristics in images. Natural vegetation green is defined as green colors observed in leaves of trees and grasses. Leaves are interlaced and have shades and shadows. Vegetation green areas exhibit large brightness changes caused by the shades of leaves, as shown in a sample scene in Figure 1, which contains bamboo leaves and a green chalkboard. These brightness changes in green areas allow humans to correctly identify vegetation areas.

In contrast, non-vegetation green areas arise from artificial green objects such as signboards, in an outdoor natural scene. These green areas usually exhibit uniform color or

AIC2015 TOKYO - Color and Image

only small color variation. For example, the chalkboard in Figure 1 is recognized as a uniform surface with a certain color.

## 3. IMAGE PROCESSING FOR DETECTING BRIGHTNESS CHANGE

We define the vegetation green area as a green color area that undergoes frequent brightness changes. A simple, but effective, image processing technique for detecting brightness changes is edge detection because in image processing edges are defined as a local structure with large brightness changes and thus often related to object contours. The result of edge detection for the image in Figure 1 is shown in Figure 2, which represents the intensity of edges in grayness. The area of bamboo leaves produces many edges, whereas the chalkboard yields few edges associated with letters and attached sheets.

Edges are detected by differential operators in general. The most popular differential filter is the Sobel filter, which consists of two operators for detecting vertical and horizontal edges. Figure 3 shows these operators with the size of 3 pixels square. In the



*Figure 1: A picture containing vegetation green (bamboo leaves) and non-vegetation green (a green chalkboard).*



*Figure 2: Edges extracted from Figure 1, with gray values denoting edge intensities.*

| 1 | 0 | -1 |
|---|---|----|
| 2 | 0 | -2 |
| 1 | 0 | -1 |

(*a*) *Vertical edge filter*

| 1 | 2 | 1 |
|----|----|----|
| 0 | 0 | 0 |
| -1 | -2 | -1 |

(*b*) *Horizontal edge filter*

*Figure 3: Sobel edge filters.*

case of vertical edge detection, the differential in pixel values between the leftmost and the rightmost pixels in the 3x3 neighborhood of a target pixel is calculated. In general, the outputs of vertical and horizontal edge detection are combined.

## 4. AUTOMATIC DETECTION OF VEGETATION AREA

We propose a method for detecting vegetation areas by edge detection and subsequent image processing. The scheme of the method is shown in Figure 4.

First of all, the image of a scene is captured. Then, from the captured image, green color pixels are detected as those with a high G ratio and low R and B ratios to the sum of R, G and B values of the pixel. Meanwhile, edge pixels are detected with the Sobel filters for the G channel of the image, and assigned a flag "1". The vegetation green pixels are then detected by AND operation between the green color pixel and the flag of edge pixels. Next, the vegetation green pixels are binarized. The vegetation area has some holes by non-uniformity of the texture. Therefore, recursive dilation and erosion operation is done for closing holes in the vegetation green area. Finally, the ratio of the number of pixels in the vegetation area to those of all pixels in the image is calculated.

## 5. EXPERIMENTS

We conducted experiments for evaluating the effectiveness of the proposed method. We took several pictures containing trees and artificial green objects in urban scenes as shown in Figure 5. The size of these images was 816 x 612 pixels. The vegetation areas were detected from these images.

Figure 6 shows the green color areas in Figure 5, that was determined by the ratios of R,G and B. When a pixel had the ratios of R and B larger than 0.4 and that of G smaller than 0.35, it was regarded as a non-green color pixel. Moreover, the green colors close to
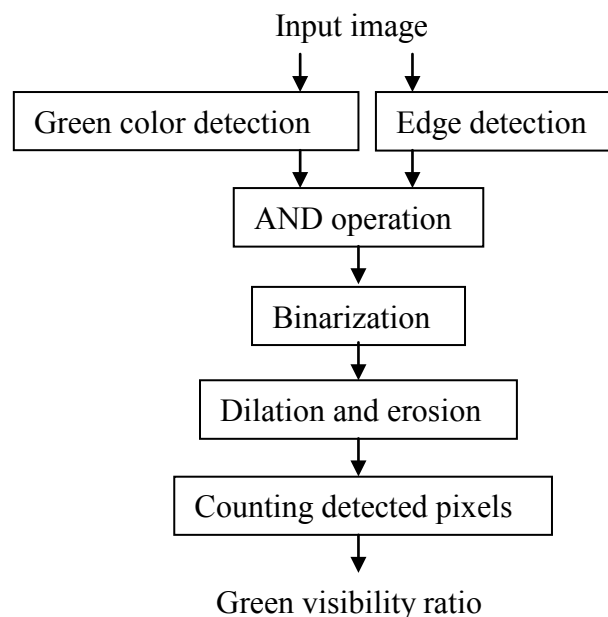
*Figure 4: Scheme of vegetation green area detection.*

white or black were also regarded as non-green. In Figure 6, non-green color pixels are painted in white. Detected green color areas in both images contain both vegetation green and artificial green. In this experiment, we used a simple color detection procedure. Even if we use more complicated color detection method, the detected vegetation green area will contain artificial green in some cases.

The results of the vegetation detection are shown in Figure 7, which depicts the vegetation areas as white. Successive operations of three dilations, six erosions and three dilations were applied for closing holes. These result images show that the proposed method detects correct vegetation areas of trees and leaves from the complicated scene.
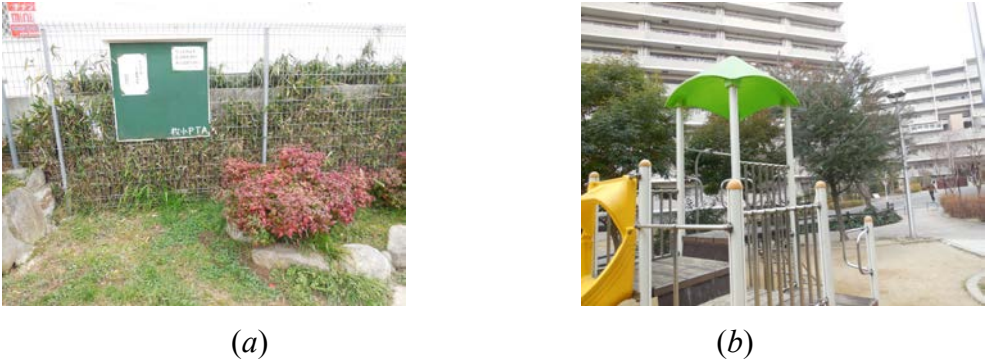


(a)                                    (b)

Figure 5: Pictures for evaluation



(a)                                    (b)

Figure 6: Green color areas detected from pictures in Figure 5.
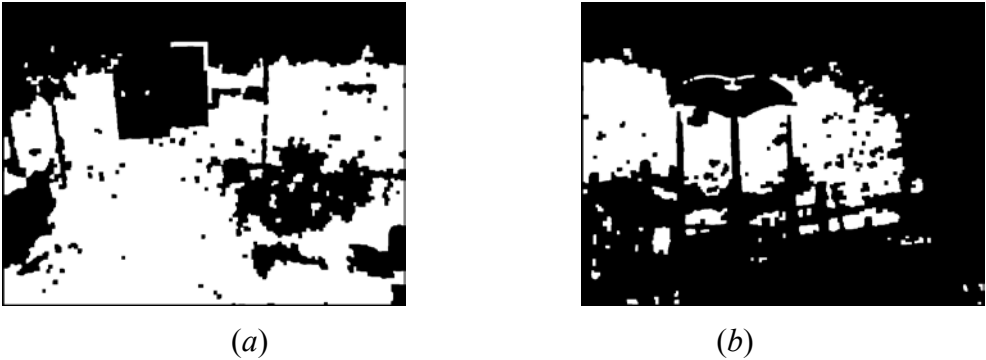


(a)                                    (b)

Figure 7: Results of vegetation area detection for pictures in Figure 5.

AIC2015 TOKYO - Color and Image

Artificial green objects, which also appeared in the image, are nearly completely eliminated, though some part of object contours are wrongly detected. The GVRs were 41.3% for Figure 7 (a) and 24.0% for Figure 7 (b).

## 6. IMPREMENTATION

We implemented a prototype system for real-time GVR measurement by the proposed method. The system consists of a laptop computer (Mouse Computer W170HN, CPU: Intel Core i5-2450M 2.50GHz, Memory: 8GB) and a USB camera (Logicool HD Pro Webcam C920). The size of the input images was VGA (640 x 480 pixels). We developed the system by using Microsoft Visual Studio 2010 and the Open CV library, which is an open source library for computer vision programming.

Figure 8 shows a part of the PC monitor image during real-time processing. The left window shows the input image and the right shows the detected vegetation area and its GVR, 21.9% in this scene. The frame rate was about 5 fps.

## 7. CONCLUSIONS

This paper has proposed a method for vegetation green area detection from complicated scenes consisting of leaves and artificial green objects. The method detects green color areas with brightness fluctuation, which appear in leaf areas of images. The brightness fluctuation is detected as edges by the Sobel filters. We conducted experiments with images containing trees and artificial green objects. The experimental results show the correct detection of tree areas and thus demonstrate good feasibility of the proposed method. We implemented a prototype system for real-time GVR measurement by the proposed method. The system detected vegetation green areas and calculated GVR at a frame rate of 5 fps.
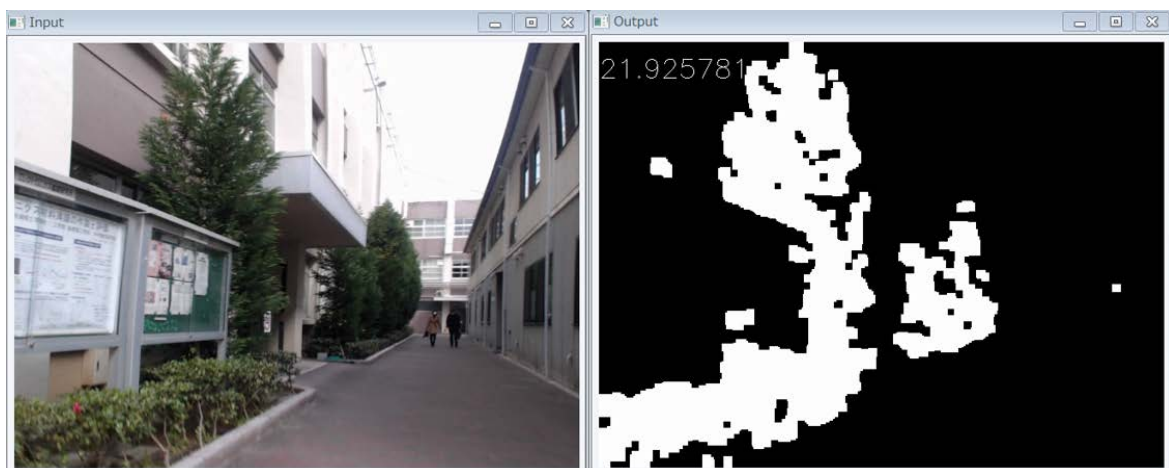


*Figure 8: Screen shot of real-time processing.*

# REFERENCES

Ohki. T., et al., 2009. Proposal of the Green Landscape Evaluation Method That adopts Each View Angle Green Visibility Ratio, In *the 23rd Conference on Environmental Information Science*, 367-372. (in Japanese, with English abstract)

Ong. B. L., 2003. Green plot ratio: an ecological measure for architecture and urban planning, *Landscape and Urban Planning* 63: 197-211.

Takizawa. S., et al., 2013. Development of an instrument for the urban-green measure, In *the 44th Annual Meeting of Color Science Association of Japan*, 314-315. (in Japanese)

*Address: Motonori Doi, Department of Tele-Communication and Computer Networks,*
*Osaka Electro-Communication University,*
*18-8 Hatsu-cho, Neyagawa, Osaka 572-8530, JAPAN*
*E-mails: doi@isc.osakac.ac.jp, kima@oecu.jp, s-nishi@isc.osakac.ac.jp*

# Evaluation of 20 p/d-safe colors used in image color reduction method for color deficient observers

Takashi SAKAMOTO

National Institute of Advanced Industrial Science and Technology (AIST)

## ABSTRACT

This manuscript describes an evaluation of the safe colors used in the author's previous study on color vision deficiency. In my previous manuscript, a color reduction method especially designed for protan and deutan color vision deficiency (commonly known as red-green color blindness) was proposed. This method enables the replacement of protan- and deutan-confusion colors in target images with preliminarily selected protan- and deutan-safe (p/d-safe) colors. In this study, the chromaticity distribution of 20 p/d-safe colors is analyzed and evaluated using the CIELAB color space and a quasiuniform color space theoretically derived from the LMS (the response of the long, medium, and short cones of the human eye) color space. The results of the evaluation are described in this manuscript taking into consideration the uniformity of the chromaticity distribution of 20 p/d-safe colors, the color distance between each color, and the image processing utility of the color reduction implemented as a look-up table. The results of this study suggest that the chromaticity distribution of the 20 p/d-safe colors and the number of colors applied for the proposed color reduction method have to be optimized.

## 1. INTRODUCTION

A color vision deficiency such as protan and deutan defects occurs when the cells in the human retina fail to function normally or lack one or more types of cone cells. In many cases, the dysfunction is caused by specific genetic factors that affect a considerable number of people. In Japan, for example, approximately 5% of males and 0.2% of females suffer from either protan or deutan defects. Globally, more than 200 million people suffer from some form of congenital color vision deficiency. Such people have difficulty distinguishing particular sets of colors. For example, protan and deutan observers confuse red with green, deep-red with black, pink with sky blue, blue-green with gray, and pea-green with yellow. These particular sets of colors are called confusion colors.

A congenital color vision deficiency is caused genetically and is currently incurable by means of surgery and other medical procedures, visual training, or electrotherapy. The most reasonable and effective means to assist those suffering from a color vision deficiency is to improve their visual environment using imaging devices (e.g., TVs, projectors, electronic bulletin boards, PC monitors, and smartphones). An image color enhancement is the most effective method to replace sets of colors that cause color confusion in color deficient observers.

Sakamoto (2015) proposed an image enhancement method using image color reduction that enables protan and deutan observers to distinguish between confusion colors. The proposed method is based on a simple color mapping and does not require a complex computation. This method is significant for its simplicity and use of a unique color palette. The color palette comprises 20 protan- and deutan-safe (abbreviated to p/d-safe) colors and was originally proposed by Ito et al. (2013). Ito and his colleagues have not intended to

AIC2015 TOKYO - Color and Image

apply their color palette to photographic and image processing. In contrast, Sakamoto (2015) proposed the idea that a color palette consisting of preliminarily selected p/d-safe colors is applicable to the color reduction processing of photographic images. Sakamoto (2015) found that a color reduction method using 20 or less p/d-safe colors is effective for replacing confusion colors and enhancing a target image for protan and deutan observers.

Sakamoto (2015) also described a few problems related to the color selection of the p/d-safe colors. Twenty or less colors may be unsuitable for high-definition color image processing because there are too few colors to replace, and the image degradation caused by the color reduction was noticeable in the color processing results. The most appropriate and effective solution for this may be to increase the number of colors used in a p/d-safe color palette. If so, the chromaticity distribution of the colors in the p/d-safe color palette must be analyzed and optimized to avoid color confusion.

This manuscript describes an evaluation of the 20 p/d-safe colors used in Sakamoto (2015) and shows the analysis results of the uniformity of the chromaticity distribution of 20 p/d-safe colors, the color distance between 20 p/d-safe colors, and the utility of the color reduction implemented as a look-up table.

## 2. METHOD

### 2.1 Twenty p/d-safe colors

Twenty p/d-safe colors for protans and deutans were proposed by Ito et al. (2013). These colors consist of nine vivid and strong colors, seven soft and pale colors (excluding two alternative low-saturation colors), and four achromatic colors. These colors are selected on the basis of visual tests for protan and deutan observers such that they are easily identified, classified, and distinguished from each other by protan and deutan observers. However, Ito et al. (2013) did not describe a chromaticity distribution of the 20 p/d-safe colors. Figure 1 shows these 20 colors, their index numbers, and the sRGB [IEC 61966-2-1:1999 standard RGB color space (1999)] tristimulus values for each color, as defined in Ito et al. (2013).
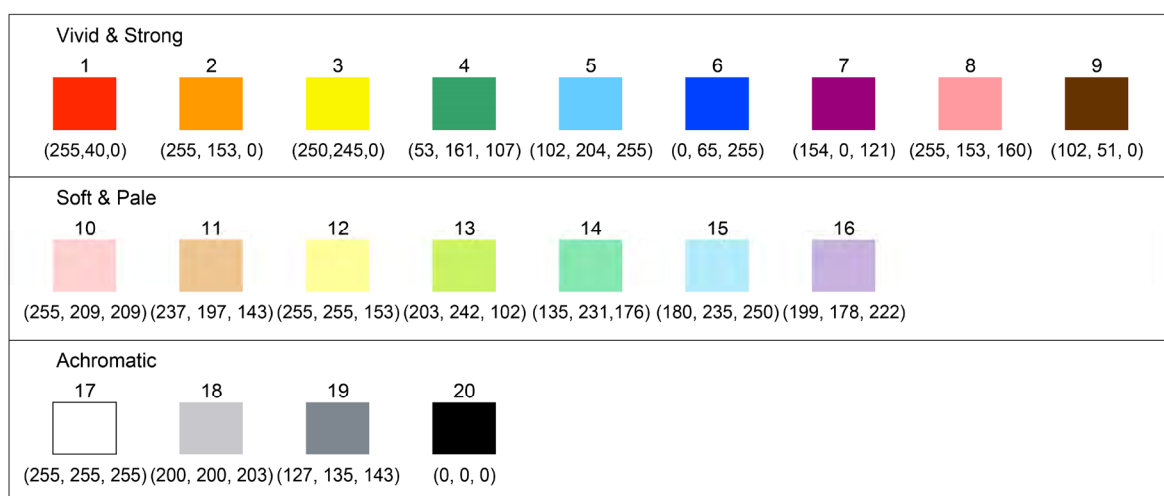


*Figure 1: Twenty p/d-safe colors, their index numbers, and sRGB tristimulus values.*

## 2.2 Simulation of protanopia and deuteranopia

Protanopic and deuteranopic color vision under the Joint ISO/CIE Standard Illuminant D65 (1999) condition is simulated according to the method proposed by Brettel et al. (1997). This study replaces the transformation matrix used in Brettel et al. (1997) with a Hunt–Pointer–Estevez matrix, as documented in Hunt (1995). This alternative matrix is used because the original matrix of Brettel et al. (1997) does not consider the illuminant D65 and sRGB color space.

Protanopic and deuteranopic simulated images are calculated as follows [with regard to the color spaces, sRGB, XYZ, and LMS are documented in Hunt (1995), Brettel et al. (1997), and IEC 61966-2-1 (1999)]: (1) the sRGB coordinates of the target image are converted into XYZ tristimulus values based on the reference document; (2) the XYZ tristimulus values are converted into LMS coordinates; (3) the LMS coordinates are modified according to the reduction in the cone types in the human retina, e.g., protanopia can be expressed by means of the M and S axes of the LMS coordinates; (4) the modified LMS coordinates are back-converted into XYZ tristimulus values; and (5) the sRGB coordinates of the simulation image are calculated from the XYZ tristimulus values.

## 2.3 CIELAB and $L^{\#}M^{\#}S^{\#}$ color spaces

The chromaticity distribution of the 20 p/d-safe colors and their protanopic and deuteranopic simulated colors are examined and analyzed using CIELAB, which is a perceptually uniform and standard color space [CIE 1976 color space, as documented in Hunt (1995)]. The lightness L* represents the darkest black at zero and the brightest white at 100. The a* and b* axes represent the degrees of chromaticness, and acromatic colors at a* = 0 and b* = 0.

The CIELAB color space represents a color difference by its Euclidean distance between colors. CIELAB can evaluate color differences perceived by observers with normal color vision but cannot deal with color differences perceived by observers with protan and deutan defects immediately. To deal with protanopic and deuteranopic color differences, the CIELAB values of protanopic and deuteranopic simulated colors must be known. Brettel et al. (1997) may be utilized for this purpose, but this procedure lacks precision because the simulation method is only an approximation of protanopic and deuteranopic views.

To avoid the approximation related to the protanopic and deuteranopic simulation, this study utilizes the LMS color space that can deal with and indicate protanopic and deuteranopic views of colors immediately in the form of tristimulus values. However, there remains another issue with the color differences in that the LMS color space is not perceptually uniform. In order to overcome this issue, this study proposes a new perceptually quasiuniform color space $L^{\#}M^{\#}S^{\#}$ and utilizes it for an analysis of the chromaticity distribution of the 20 p/d-safe colors. $L^{\#}$ is nonlinear transformation of the L axis of the LMS color space, and it is obtained by using the same nonlinear formula for the L* axis of the CIELAB color space. $M^{\#}$ and $S^{\#}$ are also obtained using a similar procedure for the M and S axes of the LMS color space.

# 3. RESULTS AND DISCUSSION

## 3.1 Chromaticity distribution analysis using CIELAB

Figure 2 shows the chromaticity distribution map of the 20 p/d-safe colors along the a* and b* axes. Black squares represent views of normal color vision, red circles represent simulated views of protanopic color vision, and blue triangles represent simulated views of deuteranopic color vision. The solid lines and filled dots represent the vivid and strong colors that are indicated as No. 1 to No. 9 in Figure 1. The dashed lines and open dots represent the soft and pale colors that are indicated as No. 10 to No. 16 in Figure 1. Achromatic colors (No. 17 to No. 20) are not indicated in Figure 2.

Figure 3 shows the chromaticity distribution map of the 20 p/d-safe colors along the L* and b* axes. Black squares, red circles, and blue triangles represent the same color vision categories as shown in Figure 2. Additionally, the green diamonds and solid lines represent the achromatic colors that are indicated in Figure 1 as No. 17 to No. 20. The other solid lines and filled dots represent vivid and strong colors, and the dashed lines and open dots represent soft and pale colors that are in the same color categories as in Figure 2.
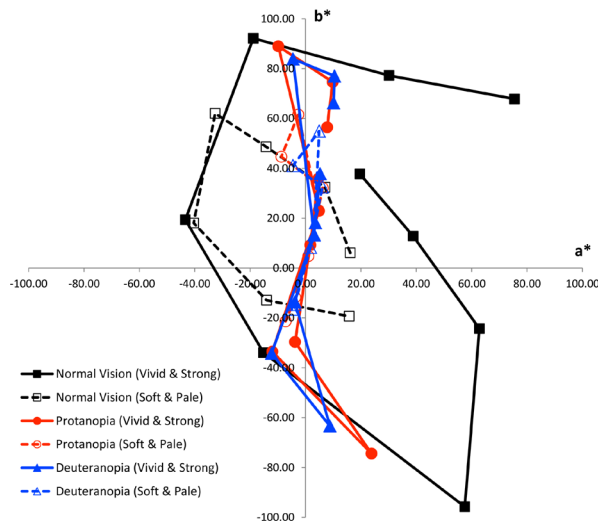


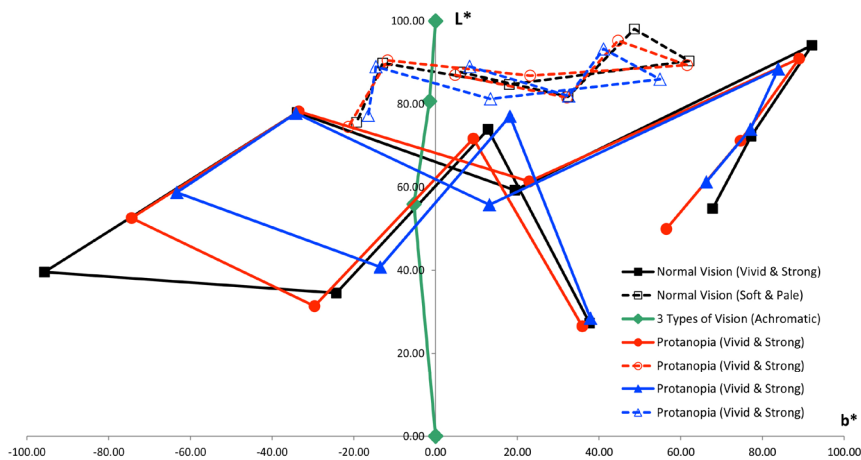*Figure 2: Chromaticity distribution map of the 20 p/d-safe colors along the a\* and b\* axes.*



*Figure 3: Chromaticity distribution map of the 20 p/d-safe colors along the L\* and b\* axes.*

AIC2015 TOKYO - Color and Image

Figure 2 suggests that protanopic and deuteranopic observers can hardly perceive color differences along the a* axis. From Figure 3, we know that protanopic and deuteranopic observers can distinguish between 20 colors using the L* and b* axes. In addition, we know that vivid and strong colors have longer color distances between each other than soft and pale colors, which suggests that soft and pale colors are more difficult to distinguish amongst each other. Figure 2 also suggests that achromatic color No. 18 has lower color distances between it and soft and pale colors such as No. 10, No. 15, and No. 16, which suggests that pale gray (No. 18) may be confused with pale pink (No.10), pale blue (No. 15), and pale violet (No. 16).

## 3.2 Chromaticity distribution analysis using $L^#M^#S^#$

Figure 4 shows the chromaticity distribution maps of the 20 p/d-safe colors; the left-side distribution map describes protanopic views of colors using the $M^#$ and $S^#$ axes, and the right-side distribution map describes deuteranopic views of colors using the $L^#$ and $S^#$ axes. Black squares represent the vivid and strong colors that are indicated as No. 1 to No. 9 in Figure 1. Green circles represent the soft and pale colors that are indicated as No. 10 to No. 16 in Figure 1. Achromatic colors (No. 17 to No. 20 in Figure 1) are represented by blue triangles, and the dashed lines represent the ideal achromatic line (equal-energy line). The red circles will be used in further discussion.
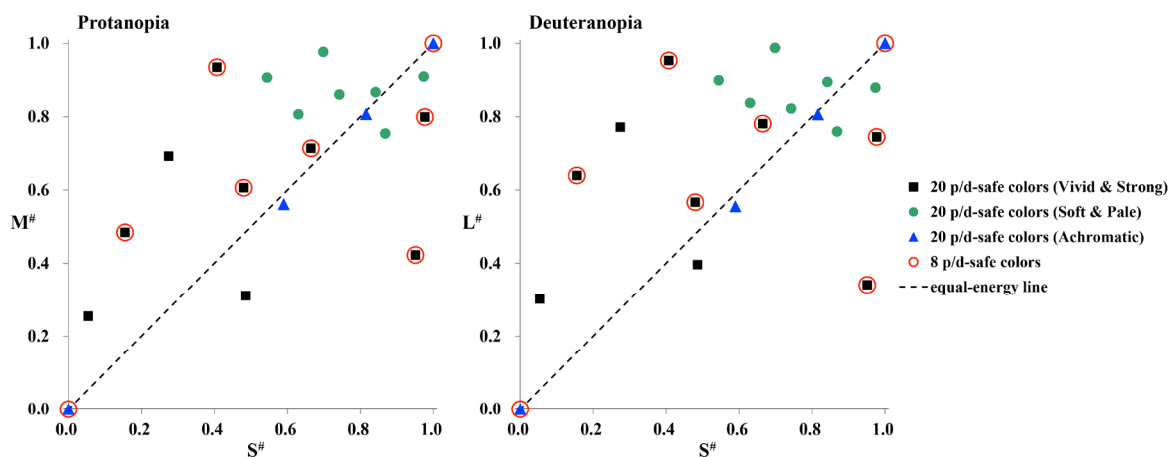


*Figure 4: Chromaticity distribution map of the 20 p/d-safe colors using $L^#$, $M^#$, and $S^#$.*

Figure 4 suggests that vivid and strong colors have longer color distances between each other than soft and pale colors, which suggests that soft and pale colors are more difficult to distinguish amongst each other. Figure 4 also suggests that achromatic colors such as pale gray (No. 18) and gray (No. 19) have lower color distances between them and the other chromatic colors such as green (No. 4), pale pink (No. 10), pale green (No. 14), and pale violet (No. 16).

Figure 3 and Figure 4 also suggest that the 20 p/d-safe colors include few low-lightness colors, so the number of colors should be increased, and low-lightness colors such as deep blue and deep green should be utilized for the p/d-safe color palette. On the other hand, the number of soft and pale colors seems to be too high to distinguish between them. Soft and

pale colors and gray may be redesigned to have uniform color differences between each color.

## 4. CONCLUSIONS

This study evaluated the chromaticity distribution of the 20 p/d-safe colors used in Sakamoto (2015). The evaluation revealed that the 20 p/d-safe colors had a lopsided distribution in the CIELAB and proposed $L^{\#}M^{\#}S^{\#}$ color spaces. The number of soft and pale colors may be too high to distinguish between them, and the number of low-lightness colors may be few, thereby allowing for an increase in the number of colors.

Eight p/d-safe colors, as indicated by the red circles in Figure 4, are easy to use in image color processing, and these eight colors have sufficient color differences between them. Therefore, these eight colors and the other color sets comprised of a few pale and dark colors, and gray colors may enable the construction of an appropriate p/d-safe color palette for the image color reduction method.

## ACKNOWLEDGEMENTS

## REFERENCES

Brettel, H., F. Vienot, and J. Mollon. 1997. Computerized simulation of color appearance for dichromats. *Journal of the Optical Society of America A* 14 (10) 2647–2655.

Hunt, R. W. G. 1995. *The Reproduction of Colour*. Wiley.

International Electrotechnical Commission. 1999. *IEC 61966-2-1:1999 Multimedia systems and equipment - Colour measurement and management - Part 2-1: Colour management - Default RGB colour space - sRGB*, Geneva, Switzerland. International Electrotechnical Commission.

Ito, K., Japan Paint Manufacturers Association, DIC Corporation, Color Universal Design Organization, Maekawa, M. 2013. *Color Universal Design Color Set Guide Book 2013*. Taisei-sha (in Japanese).

Joint ISO/CIE Standard. 1999. ISO 10526:1999/CIE S005/E-1998. *CIE Standard Illuminants for Colorimetry*. International Organization for Standardization.

Sakamoto, T. 2015. Image color reduction method for color-defective observers using a color palette composed of 20 particular colors. *Proc. SPIE* 9395 (939514) 1–6.

*Address: Dr. Takashi SAKAMOTO, Human Technology Research Institute, National Institute of Advanced Industrial Science and Technology (AIST), AIST Central 2, Umezono 1-1-1, Tsukuba, Ibaraki, 305-8568, JAPAN E-mail: takashi-sakamoto@aist.go.jp*

# Silkscreen Printing on Cotton Fabrics with Soil Colorant

Somporn JENKUNAWAT[1], Pratoomtong TRIRAT[2] and Kulthanee SIRIRUK[3]

[1] Faculty of Agricultural Technology, RMUTT

[2] Faculty of Mass Communication Technology, RMUTT

[3] Phanomwan Technology College, Thailand

## ABSTRACT

Recently, there is an increasing interest in natural or eco-colorants. Soils are natural colorants that have been used since ancient times before synthetic colorant quickly replace them. In this study 3 types of soil: black-, yellow- and red soils were used as sources of colorants of silkscreen ink for printing on cotton fabrics. Soil colorants were prepared by grinding soil into fine powder, then dissolved with water and left overnight for sedimentation. The supernatant liquid was discarded and the sediment was collected as soil colorant. Soil colorants were mixed with water based silkscreen medium for silkscreen inks. Physical properties of 3 types of silkscreen inks from soil colorants were measured. The result showed that density of silkscreen ink of black soil, red soil and yellow soil colorant were 1.02, 0.53 and 0.75 and the CIE (L*a*b*) values were L* = 47.79, a* = 7.57 b*= 19.54; L* = 72.18, a* = 17.88 b*= 27.55; L* = 72.26, a* = 15.18 b*= 38.91, respectively. Silkscreen inks from soil colorants were printed on cotton fabrics with the resolution of image printed at 30 LPI. The printed cotton fabrics were measured for halftone, dot gain, density, and wash-resistant. The results showed that silkscreen ink printed on cotton fabrics gave good quality line at 1-6 points for every soil colorant. The halftone was 10-50 per cent for red- and yellow soil while black soil halftone was 10-40 per cent. Densities of printed cotton fabrics before washing were 1.02, 0.53 and 0.75 for black-, red- and yellow soil, respectively. After washing printed cotton fabrics for three times the results showed that densities were changed to 0.99, 0.52 and 0.73, respectively. Dot gain of black soil at 10 - 20 per cent showed normal dot gain and gave a good printing quality but dot gain more than 60 per cent appeared solid ink density. While red- and yellow soil dot gain was 10-40 per cent showed normal dot gain and gave a good printing quality but dot gain more than 70 per cent showed solid ink density. In addition, quality of printed cotton fabrics not only depends on printing ink but also the worker has to have printing experience.

## 1. INTRODUCTION

Soil is the most important natural resources. The differences of soil when we looking is colors. In agriculture soil color means the fertile of the soil but for painter or artist soil colors were used as coloring agents. Soil series in Thailand was report including soil color (Boonsompopphan et al, 2008). The identification of soil series also showed the difference of soil color and properties. Blavet et al (2002) reported that the mean angular hue and mean redness rating of a soil are significantly linked to annual soil waterlogged rate. Hyun Jin Jeong studied her master degree on soil as fabric dyes. She collected 45 different soils across South Korea and United Kingdom and categorize them into seven different color families. Jeong apply soil-based paint directly to fabric (Earth dyeing, 2014). Trirat et al (2014) and Chotaku et al (2014) reported used soil dyes for colored handmade paper and

printing ink, respectively.  Nowadays, environmental have been more concerned especially toxic materials.  Authors aim to reduce the use of harmful chemicals by replacing it with a friendly natural material that can be easily obtained such as the soil to replace chemical colorants.

## 2. METHOD

Three types of soil color were collected from the areas of Pathumthani province: red, yellow and black soil.  Soil colorants were prepared by drying and grinding soil into fine powder.  To make soil colorant, 100g of soil powder was added into 500 ml of clean water and mixed well by the blender. The mixture was filtered through muslin sheet to remove debris, and the mixture was left overnight for sedimentation. The supernatant liquid was discarded and the sediment is collected as soil colorant.  Soil colorant was mixed with water based silkscreen medium for making silkscreen ink by adding 75 ml of soil colorant into 100 ml of water-based resin, and the mixture was mixed well by hand.  Prepare screen frame by using T48 screen.  Silkscreen inks from soil colorants were printed on cotton fabrics with the resolution of image printed at 30 LPI by using square-shaped rubber with the off contract of 3.0 mm.  Printed cotton fabrics were measured for density, CIE-L*a*b* values, dot gain, the quality of silkscreen printing ink from soil colorants on cotton fabric.  Printed cotton fabric was test for wash resistant by using washing machine with the ratio of detergent and water at 15g: 5L.  The printed cotton fabric was washed for three times.  Printed cotton fabric was washed for 5 minute and then rinsed with water for another 5 minutes, after that they were dried by sun light and density was measured after drying.

## 3. RESULTS AND DISCUSSION

The density and CIE L*a*b* of silkscreen ink were shown in tables 1.  The result showed that density of silkscreen ink of black soil, red soil and yellow soil colorant were 1.02, 0.53 and 0.75 and the CIE (L*a*b*) values were L* = 47.79, a* = 7.57 b*= 19.54; L* = 72.18, a* = 17.88 b*= 27.55; L* = 72.26, a* = 15.18 b*= 38.91, respectively.  The quality of silkscreen printing ink on cotton fabric showed that all types of colorants gave the line size from 1-6 point.  The screen dot of water-based screen printing ink of red soil at 10 per cent was not appeared (Table 2).  Similarly to yellow soil that could print only 7 percent while the black ink had 36.8 per cent.  Water-based screen printing of black soil had dot gain from 10 per cent, but from 30 per cent it gave higher dot gain up to 80.8 per cent.   When compared at 10 per cent, the black ink had more dot gain than red and yellow ink about 26 per cent. The results revealed that water-based screen printing ink able to print on figure with big screen dot or line printing.  All type of soil colorants gave line printed of 1-6 point and area of halftone of black soil was 10-40 per cent while red and yellow soil had 10-50 per cent (Table 3).

*Table 1. The density and CIE L*a*b* of silkscreen printing ink on cotton fabric from 3 types of soil.*

| Soil type | Density | CIE L*a*b* | | |
|-----------|---------|------|------|------|
|           |         | L*   | a*   | b*   |
| Black     | 1.02    | 47.79 | 7.57  | 19.54 |
| Red       | 0.53    | 72.18 | 17.88 | 27.55 |
| Yellow    | 0.75    | 72.26 | 15.18 | 38.91 |

AIC2015 TOKYO - Color and Image

*Table 2. The dot gain of silkscreen printing ink from 3 types of soil on cotton fabric.*

| Screen dot (per cent) | Black soil | Red soil | Yellow soil |
|---|---|---|---|
| 10 | 36.8 | 0.0 | 7.0 |
| 20 | 64.1 | 21.0 | 32.1 |
| 30 | 80.8 | 40.1 | 51.0 |
| 40 | 85.9 | 66.9 | 58.2 |
| 50 | 90.0 | 73.3 | 82.1 |
| 60 | 93.8 | 83.4 | 84.8 |
| 70 | 93.8 | 92.0 | 90.5 |
| 80 | 93.9 | 94.1 | 97.1 |
| 90 | 98.3 | 99.4 | 99.0 |
| 100 | 100.0 | 100.0 | 100.0 |

*Table 3. Line size and area of halftone of cotton fabric printed with silkscreen printing ink from 3 types of soil.*

| Soil type | Line size (Point) | Area halftone (per cent) |
|---|---|---|
| Black | 1-6 | 10-40 |
| Red | 1-6 | 10-50 |
| Yellow | 1-6 | 10-50 |

Printed cotton fabrics were measured for density and then were washed for wash resistant. It was found that density was slightly decreased from before washed. Densities of printed cotton fabrics before washing were 1.02, 0.53 and 0.75 for black-, red- and yellow soil, respectively. After washing printed cotton fabrics for three times the results showed that densities were changed to 0.99, 0.52 and 0.73, respectively (Table 4).

*Table 4. The density of silkscreen printing ink from 3 types of soil on cotton fabrics before and after washing.*

| Soil type | Before washing | First washing | Second washing | Third washing |
|---|---|---|---|---|
| Black | 1.02 | 1.01 | 1.00 | 0.99 |
| Red | 0.53 | 0.53 | 0.52 | 0.52 |
| Yellow | 0.75 | 0.74 | 0.74 | 0.73 |

# 4. CONCLUSIONS

Different types of soil gave different color.  Silkscreen printing ink from soil colorants gave a good printing quality on cotton fabric.   The result revealed that water-based screen printing ink able to print on figure with big screen dot or line printing.  The results showed that silkscreen ink printed on cotton fabrics gave good quality line at 1-6 points for every soil colorant. The halftone was 10-50 per cent for red- and yellow soil while black soil halftone was 10-40 per cent.  Dot gain of black soil at 10 - 20 per cent showed normal dot gain and gave a good printing quality but dot gain more than 60 per cent appeared solid ink density.  While red- and yellow soil dot gain was 10-40 percent showed normal dot gain and gave a good printing quality but dot gain more than 70 per cent showed solid ink density.  Densities of printed cotton fabrics before washing were 1.02, 0.53 and 0.75 for black-, red- and yellow soil, respectively.   After washing printed cotton fabrics for three times the results showed that densities were changed to 0.99, 0.52 and 0.73, respectively.

## REFERENCES

Blavet, D., J.C. Leprun, E. Mathe and Pansu M.  2002. Soil colour variables as simple indicators of the duration of soil waterlogging in a West African catena.  17th WCSS, 14-21 August 2002, Thailand. 1333-1-1333-11.

Boonsompophan, B., T. Vearasilp, T. Attanandana and R.S. Yost.  2008.   Field identification of soil series-enabling Thai farmers share experience and knowledge. *Soil Science,* Vol.173, No.10:736-744.

Chotaku, S., P. Trirat , K. Siriruk.  2014.  Water-Based Screen Printing Ink by Soil Dyes on Cotton Fabric for Community Products.  AIC 2014: 312-314.

Jeong, Hyun Jin.  2014.  *Earth dyeing*.  Online:www.ecouterre.com/soil-as-fabric-dye-earth-dyeing-hits-pay-dirt/.  Access: 25 May, 2014.

Trirat, P., S.  Jenkunawat and V. Songcharoen.  2014.  Dyeing paper by soil colorants for produce packaging paper. *Journal of the color science association of Japan,* Vol.38, No.3: 276-277.

*Address:  Somporn JENKUNAWAT, Faculty of Agricultural Technology,*
*Rajamangala University of Technology Thanyaburi, 39 Moo 1,*
*Rangsit-Nakornayok Road., Klong 6, Thanyaburi,*
*Pathumthani 12110, Thailand*
*E-mails: sompornjen@gmail.com*

# Estimation of the Environment Illumination Color Using Distribution of Pixels

**Noriko YATA, Yuki ARAI, Yoshitsugu MANABE**
Graduate school of advanced integration science, Chiba University

## ABSTRACT

Techniques for estimating the illumination color of the imaging environment from an image are needed. This paper proposes a new technique to estimate the illumination color by examining pixel distributions in a characteristic space for each of the objective surfaces. A two-dimensional log-chromaticity differences space of the differences between logarithms of R and G, and B and G is used as a space of amount of characteristic. The proposal method to estimate the color of illuminations is a clustering of the characteristic values for each color temperature using support vector machine. In this study, the distributions of target pixels correspond to the surfaces of objects under different illumination conditions are plotted in the characteristic space. The training data are obtained from images of seven colors objects. In the results of the verification experiment for test data, the rate of correct estimation is 86.5 %. It can be expected to improve the illumination estimation accuracy through using combinations of different colors.

## 1. INTRODUCTION

We can perceive the colors of objects impervious to changing the illumination light in everyday life. On the other hand, colors of pixels in images depend on the surfaces conditions of the objects and the environment illuminations. It is difficult to determine which factor is cause of the changing color of pixels. The problem can be solved by performing the estimation of an illumination color and surface conditions of objects from a image. White patch retinex and gray world algorithm and others have been proposed as algorithms for representing the colors of objects without depending on the illumination light conditions. These algorithms are not performed an appropriate illumination estimation when white point is not present in the image or the scene has partial colors (Ebner 2007). The purpose of this study is to estimate the correlated color temperatures of the illumination light of the shooting environment from a single image that has partial color without white point.

## 2. METHOD OF CORRELATED COLOR ESTIMATION

The proposal method estimate the illumination color by clustering the pixel distribution in a feature space for each characteristic of the surfaces of objects. We focused on the log-chromaticity differences (LCD) that is proposed for shadow removal in images (Finlayson and Hordley 2001) as suitable features for the clustering. The method uses the LCD values in two-dimensional axes as the differences between the logarithm of R and G ($\log (R/G)$), and B and G ($\log (B/G)$) that represent colors of each pixel. The distribution of pixels color under various illuminations in LCD space is shown in Figure 1.

The method to estimate the correlated color temperatures of illuminations is a clustering of the LCD values for each color temperatures using support vector machine (SVM). The four values of $\log (R/G)$, $\log (B/G)$, angular coordinate in LCD space, and brightness obtained from target pixels are used to perform clustering for each image by SVM.
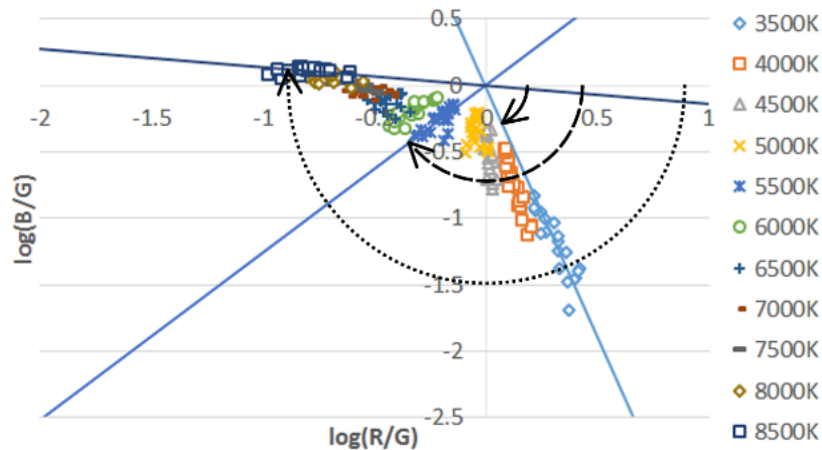
AIC2015 TOKYO - Color and Image

*Figure 1: The distribution of pixels color and angular coordinate in LCD space.*

## 3. EXPERIMENTATION AND RESULTS

### 3.1 Data preparation for Experiment

Illumination lights were configured to capture images for correlated color temperature estimation in the following way. The illumination lights was generated based on the spectral radiance of each color temperature using a spectral light source device. The actual spectral distributions and color temperatures of the illumination lights were measured using a spectral irradiance meter, and the measured values were defined as correct color temperatures of the illumination lights. In this study, the illumination light color temperatures of eleven types were set in 500 K increments of 3500 K to 8500 K for training data, and 24 types for test data. The correct classes and the color temperatures of the training data and the test data shown in Table 1.

The images of cylindrical papers with shading under controlled illuminations in dark room were used as test data for the experimentation. The colors of objects are seven types of white, gray, blue, green, orange, purple and yellow. The target pixels are taken from place of change to the shade from the bright part of the object, avoiding the specular reflection regions.

### 3.2 Verification Accuracy and Application to Color Correction

The results of estimation by proposed method are described follow. In the results of the verification experiment for the test data, the number of the estimated classes matched to the correct color temperatures has been 21 of 24 illumination conditions, and the rate of correct estimation has been 86.5 %. The proposed method has estimated the wrong class in three conditions of 3801 K, 7616 K, and 8136 K. Although our proposed method could not perform appropriate estimation for the three test data, all of these have been classified next to the correct class.

The color temperatures of the illumination lights were estimated using the images of new objects and the illuminations with different color temperatures with training data. The objects were cloth of four colors. Color corrections of the images were performed based on the estimated color temperatures, and the results were compared with white patch retinex (WPR) method. The examples of the color correction results are shown in Figure 2. Images shown in Figure 2 (a) and (d) are image before color correction, and the color temperatures of each image are 3285 K and 8597 K. Images shown in Figure 2 (b) and (e) are the results

*Table 1. Correct classes and the color temperatures of the data.*

| Correct class | Color temperatures of training data (K) | Color temperatures of test data (K) |
|---|---|---|
| 3500 | 3548 | 3289 |
| 4000 | 4055 | 3801 |
| 4500 | 4489 | - |
| 5000 | 4955 | 4939, 5009, 5093, 5161 |
| 5500 | 5552 | 5432, 5634 |
| 6000 | 6011 | 6106, 6207 |
| 6500 | 6512 | 6416, 6527, 6595, 6680 |
| 7000 | 6985 | 7091, 7096, 7098 |
| 7500 | 7496 | 7443, 7616 |
| 8000 | 7915 | 7885, 8114, 8136 |
| 8500 | 8485 | 8431, 8572 |



*(a) Original image A (3285K)*    *(b) Proposed method for A*    *(c) WPR for A*

*(d) Original image B (8597K)*    *(e) Proposed method for B*    *(f) WPR for B*
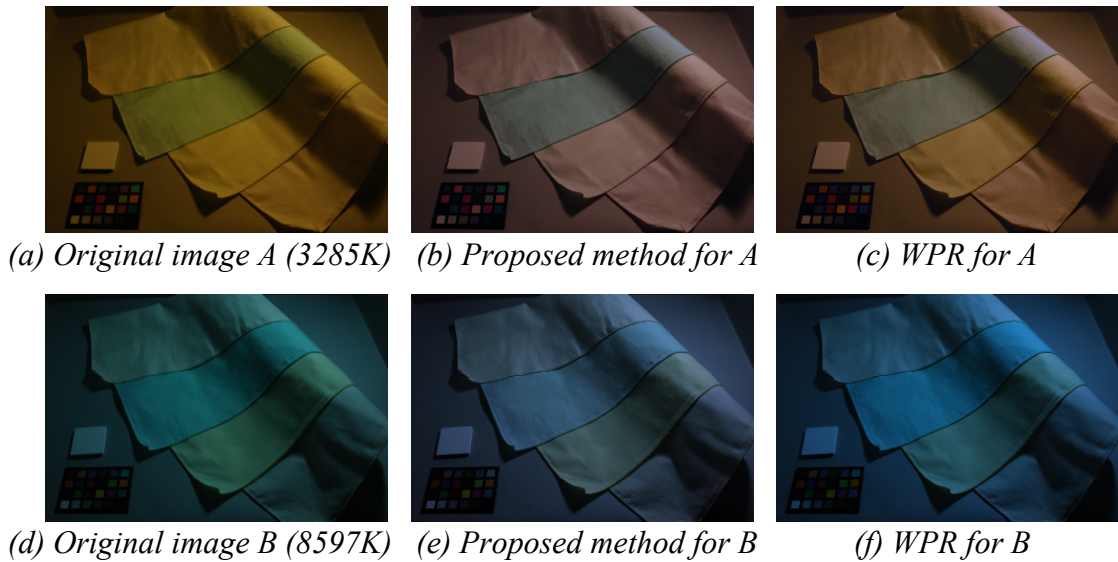
Figure 2: The results of color corrections.

of our proposed method. Images shown in Figure 2 (c) and (f) are the results of WPR which use the information of white point. It can be seen that these images had been corrected from bluish or yellowish by both methods. The color differences $\Delta E^*_{ab}$ between the corrected images and the reference image were compared to quantitatively evaluate the color correction result by the proposed method and WPR. The reference was corrected image of the illuminated by 6382 K light. The differences were calculated on 24 colors of

*Table 2. The mean color differences of ColorChecker.*

| Color temperatures of original images (K) | Proposal method | WPR |
|---|---|---|
| 3285 | 12.24 | 15.02 |
| 4051 | 12.57 | 13.61 |
| 4492 | 13.13 | 13.01 |
| 5001 | 10.25 | 10.58 |
| 5608 | 7.14 | 6.62 |
| 6085 | 5.07 | 3.67 |
| 7102 | 3.69 | 3.84 |
| 7671 | 6.46 | 6.61 |
| 8156 | 7.10 | 8.07 |
| 8597 | 8.60 | 9.39 |

ColorChecker (x-rite). The mean color differences of ColorChecker shown in Table 2. The maximum value of the color difference of the proposed method has been smaller than that of WPR. The color differences of 5608K and 6085K however have been larger because the color temperatures of the estimated classes were incorrect in these conditions.

## 4. CONCLUSIONS

The new technique to estimate the illumination color was proposed in this paper. It was performed by examining the pixel distribution in a feature space for each characteristic of the surfaces of objects. The proposed method has shown better results than the WPR in verification of the accuracies of the estimated classes and the colors of corrected image.

It can be expected to improve the estimation accuracy using combinations of different colors objects to obtaining training data. Moreover, it is necessary a verification under illumination light such as fluorescent lamps and LED lights because neither of the training data and the test data was obtained from images taken in the same environment using the spectral light source device.

## REFERENCES

Ebner, M. 2007. *Color Constancy*. New York: John Wiley and Sons.
Finlayson, G.D. and S.D. Hordley. 2001. Color Constancy at a Pixel. *Journal of Optical Society of America A* 18(2): 253-264.

*Address: Noriko YATA, Graduate school of advanced integration science,*
*Chiba University, 1-33, Yayoi-cho, Inage-ku, Chiba-shi, Chiba 263-8522, JAPAN*
*E-mails: yata@chiba-u.jp, manabe@faculty.chiba-u.jp*

# A Spectral Reflectance Measurement System for Human Skin by Using Smartphone

Seungwan HONG, Norihiro TANAKA, Kosuke MOCHIZUKI

Faculty Business and Informatics, Nagano University

## ABSTRACT

This paper describes a method for estimating the spectral reflectance of human skin based on multi-spectral imaging by using a smartphone. A spectral reflectance of human skin is very useful for a health care and beauty in cosmetic fields. By this system, anyone can measure spectral reflectance of human skin with smartphone and color chart. First, we develop a multi-spectral camera model of a smartphone for describing a light reflection process of a smartphone camera system. A camera of the smartphone has an automatic exposure and an automatic white balance function. The camera output (RGB) is modeled with spectral reflectance of human skin, spectral distribution of illumination, camera sensitivity and time parameter in the visible wavelength [400–700 nm].Second, we propose a simplified method for estimating spectral reflectance using a smartphone camera based on the multi-spectral camera model. We assumed that the spectral reflectance of a human skin surface can be described as linear combination of some basis functions. On the assumption that the system conversion matrix from the camera output to spectral reflection is estimated based on statistically analysis of tuple of spectral reflectance and camera outputs (RGB).Generally, smartphone camera has an automatic exposure and an automatic white balance function. The exposure and white balance is fixed correctly with a color chart. Third, we implement a position detection method for improving accuracy of human face and color chart position calibration. In the results, we can estimate spectral reflectance in arbitrary part of the human face. Finally, to confirm accuracy of the proposed method, we measured spectral reflectance of human face with a smartphone. The estimation results were compared with direct measurement of spectral reflectance with spectrophotometer. Consequently, it was possible to obtain the estimation results of spectral reflectance of human skin with high precision.

## 1. INTRODUCTION

Smartphone is useful as color device at any time. And also, because computer and digital color camera is implemented in the smartphone, the smartphone may be considered a color device for easily performing multi-spectral imaging. However it is difficult to estimate spectral information from the color image by the smartphone[1]. The camera of smartphone has an automatic exposure and automatic white balance function. These functions destabilize of estimating spectral information form the image.

   In this study, we develop a method for estimating spectral reflectance of human skin from the smartphone. The human skin surface has inhomogeneous reflection properties and spectral reflectance. This paper will describe a method for estimating the spectral reflectance of human skin based on multi-spectral imaging by using smartphone. First, we develop an automatic detection system for color chart and human face in an image taken by smartphone. The system is developed based on machine leaning method[2]. The color information of color chart and geometry of face position in the image are used for calibrating camera

characteristics and image recognition. Second, we proposed method for estimating spectral reflectance of human skin using smartphone. Finally, to confirm the feasibility of our method, we demonstrate the spectral estimation system for the smartphone.

## 2. DETECTION OF COLOR CHART AND HUMAN FACE

In this study, we need to know the position of the color chart and face in the measured image. Haar Feature-based Cascade Classifier method[2] is used as face detection and recognition system. And also, the method is used for the detection of color chart position. Haar Feature-based Cascade Classifier method is a sort of machine learning method. The machine learning can be carried out by using the learning data suitable for detection of color chart and human face. Firstly, to train Classifier, collect positive and negative samples from images that have notable features. Then, obtain several numbers of weak classifier by combining the features. Haar Feature-based Cascade Classifier method is not using a single strong classifier but using several weak classifiers in serial order for detecting an object. At first, low recognition rated classifier is applied on detecting a face. Then, gradually raise the rate of classifier to narrow the error range. This method can save time and memory for recognizing object during detection. In this project, 244 positive samples and 3000 negative samples are used for training color chart. As a result 7 weak classifiers are generated and the classifier detects color chart from an image by cascade method.

## 3. CAMERA MODEL OF THE SMARTPHONE

In order to estimate spectral reflectance using smartphone, the image data taken by smartphone is modeled based on multi-spectral reflectance[1][3]. Generally, the camera of the smartphone has an automatic exposure and an automatic white balance function. The camera output is modeled in visible wavelength[400-700nm] as

$$
\begin{bmatrix} R \\ G \\ B \end{bmatrix} = \int_{400}^{700} E(\lambda)S(\lambda) \begin{bmatrix} r_r(\lambda,t) \\ r_g(\lambda,t) \\ r_b(\lambda,t) \end{bmatrix} d\lambda .
\tag{1}
$$

$E(\lambda)$ is the spectral distributions of light sources. $S(\lambda)$ is the spectral reflectance of the objects. $r_r(\lambda,t), r_g(\lambda,t), r_b(\lambda,t)$ are, respectively, the spectral sensitivity functions of sensor RGB. $t$ is time parameter.

## 4. ESTIMATION METHOD OF THE SPECTRAL REFLECTANCE

In this study, we use two cameras[3]. The first one is the camera system which calibrated to remove influence of spectral sensitivity and illumination environment beforehand. The second one is uncalibleted camera of spectral sensitivity and illumination environment. As for the model, sensitivity properties change in time $t$. We measure a k-colored color chart in calibrated camera. The camera output of the calibrated camera assumes it matrix $\mathbf{\Lambda}_C$ of $3 \times k$. The camera output of the uncalibrated camera assumes it matrix $\mathbf{\Lambda}_U(t)$ of $3 \times k$ including sensitivity change t by automatic exposure and white balance of the camera. We can describe the relations of the camera output of both in the next expression using color conversion matrix $\mathbf{T}$.

$$\Lambda_C = T(t)\Lambda_U(t) \tag{2}$$

We estimated $T$ as $T(t) = \Lambda_C \Lambda_U^+(t)$ using pseudo inverse matrix $\Lambda_C$ of matrix $\Lambda_C$. In this study, we get conversion matrix $T(t)$ in time $t$ by measuring a color chart becoming the standard at the time of photography at the same time. We can calculate heaviness coefficient matrix like the next expression when We express an image of uncalibrated camera of number of the pixels n then in matrix $C_U$ of $3 \times n$. If this $W(t)$ can be calculate, the spectral reflectance can be estimate.

## 5. EXPERIMENTAL RESULTS

The proposed method was applied to estimate of spectral reflectance of human skin. We used a Motorola Atrix4G phone as the smartphone. Machine learning system is implemented with Open CV libraly. Figure 1 shows estimation results of the experiment. Figure 1(a) shows human face and color chart detection results. The red square is face detection result. The Green squire and red circles are color chart and color patach detection results. Figure 1(b) is estimation results of spectral reflectance. The blue line is the graph of estimation results and red squire in the red cirlce is estimation area of spectral reflectance.



(a) face and color chart detection    (b) estimation results of spectral reflectance
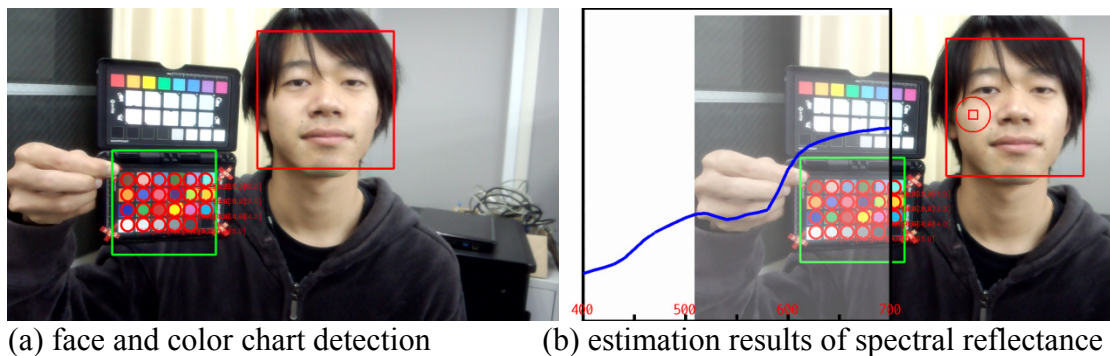
*Figure 1. Estimation results*

## 6. CONCLUSIONS

In this paper, we have developed a method for estimating spectral reflectance of human skin from the smartphone. The human skin surface has inhomogeneous reflection properties and spectral reflectance. This paper described a method for estimating the spectral reflectance of human skin based on multi-spectral imaging by using smartphone. First, we developed an automatic detection system for color chart and human face in an image taken by smartphone. The system is developed based on machine leaning method. The color information of color chart and geometry of face position in the image are used for calibrating camera characteristics and image recognition. Second, we proposed method for estimating spectral reflectance of human skin using smartphone. Finally, to confirm the feasibility of our method, we demonstrate the spectral estimation system for the smartphone.

## ACKNOWLEDGEMENTS

## REFERENCES

[1] S. TOYA, N. TANAKA and J. WOO: Estimation of Human Skin Properties using Smartphone, International Colour Association (AIC), 2012.

[2] P. VIOLA and M. JONES, Rapid object detection using a boosted cascade of simple features, Computer Vision and Pattern Recognition(CVPR), 2001.

[3] N. TANAKA, H. ARAI, J. WOO: Color Image Rendering of Human Skin Based on Multi-spectral Reflection Model, Vol. 36, suppl., pp.242-243, 2012.

*Address: Faculty of Business and Informatics, Nagano University, 658-1 shimonogo, ueda-shi, Nagano 386-1298,Japan*
*E-mails:holyidea0824@yahoo.co.jp, n-tanaka@nagano.ac.jp, k-mochiduki@nagano.ac.jp*

# Colour Management for High Quality Reproduction on Uncoated Papers

Maja STRGAR KURECIC, Lidija MANDIC, Ante POLJICAK, Diana MILCIC
Faculty of Graphic Arts, University of Zagreb

## ABSTRACT

The goal of this research was to establish the consistent and predictable workflow from the screen to the print on uncoated paper, taking into account specific constraints of the substrate and the reproduction process. The substrate is a major factor in determination of the attainable full-tone density and affects the reproducible color contrast, which both have a large impact on overall print quality. The specific restrictions on uncoated paper are determined by a rough surface on which there is always a large dot gain, reduced relative printing contrast compared to a print on coated paper, as well as the reduced gamut of colors that can be reproduced. By implementing color management ICC profiles characterized for specific uncoated printing substrate and by conducting proposed correction methods in the prepress, as well as optimizing the thickness of ink in printing, it is possible to achieve high quality color reproduction.

In the experimental part of this work special test target was designed and printed in offset on three different types of uncoated paper and one type coated paper. The test target was composed of ten types of color strips for instrumental measurements of dot gain, relative printing contrast, raster tonal value, full-tone density, etc. In addition, a photograph for visual assessment of prints was included. To be able to objectively compare the color differences of prints, spectrophotometric measurements of color strips were also made and analyzed.

## 1. INTRODUCTION

In recent years, the appeal of uncoated paper has undergone a dramatic image change in the eyes of designers and printers, contributing to the growing demand for uncoated stock. There is a wide range of high quality uncoated paper on the market today, available in many different textures, colours, weights and finishes. Because of their tactile properties and natural surface, uncoated paper creates a much stronger impression and lasting value compared to coated paper. On the other side, coated paper has an advantage in the standardised reproduction process and achieves higher quality printing results. The challenge is to ensure that uncoated print results are able to match the performance of colour prints on coated paper.

Each production step and each production device in the reproduction workflow can be a source of error. Figure 1. shows typical production steps of prepress to print where colour and tone value variations can occur.

The two main reasons of colour differences are the tone value increase (dot gain) and overprint changes (colour balance). On uncoated paper, the ink dots are absorbed slowly into paper surface and dots expands in size (dot gain). This makes the dots less sharp and colours slightly dull. Without proper corrections and compensations in the prepress the images printed on uncoated paper look darker, with colours not as clean, saturated and

bright as they could be. Also, dark areas often lose details and have low contrast. Incorrectly done prepress can affect the stability in the press, prolonged ink drying times and problems like set-off and smearing, both in press and in binding.
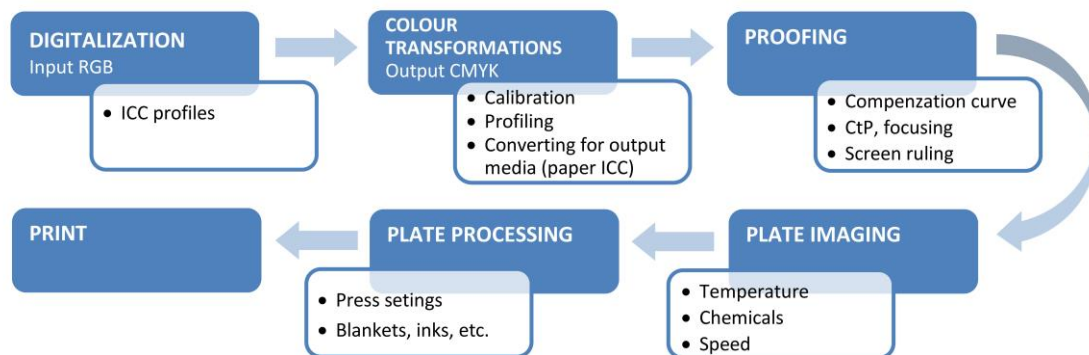


*Figure 1: Production workflow*

To keep the digital reproduction under control it is essential to regularly record and evaluate the colour and tone value variations. The most important things when printing on uncoated paper are: minimizing the dot gain and controlling the ink density. The tone value progression (RTV) should be checked in at least ten different halftone steps from 0% - 100% in every process colour. Also, 2- and 3-color overprint should be checked for controlling the grey balance. The transfer processes between different phases of prepress and printing is described by characteristic tone curve. It contains a great amount of information about the tone gradations from paper colour to solid tone. A distinction is made between characteristic tone curves for printing plates, proofs and printing.

Implementing Colour Management into the production workflow makes the exchange of colour data more consistent and predictable. The first step towards the standardisation of reproduction process is calibration of all equipment used in the graphic chain. That means taking it to a chosen operating state and ensuring that it remains in this state. Second step is characterization (profiling) which quantifies the colour space, colour gamut, or colour behaviour of the particular device under known conditions. When all devices are both calibrated and characterized it is possible to convert colours back and forth depending on the need and production workflow. This could be soft or hardcopy proofing.

## 2. METHOD

In the experimental part of this work a special test target was developed and printed in sheet fed offset machine on three different types of uncoated paper and one type coated paper.

### 2.1 Test Target Development

Special test target was developed for the process control and for evaluation of print quality on uncoated papers. Target consists of control elements for checking most important parameters by instrumental measurements and by visual control (Figure 1). The size of the target is adjustable to the standard formats of offset printing machines. All elements of the test target were designed in Adobe InDesign and Adobe Photoshop applications. File conversion was made with output Fogra Uncoated 29 profile.
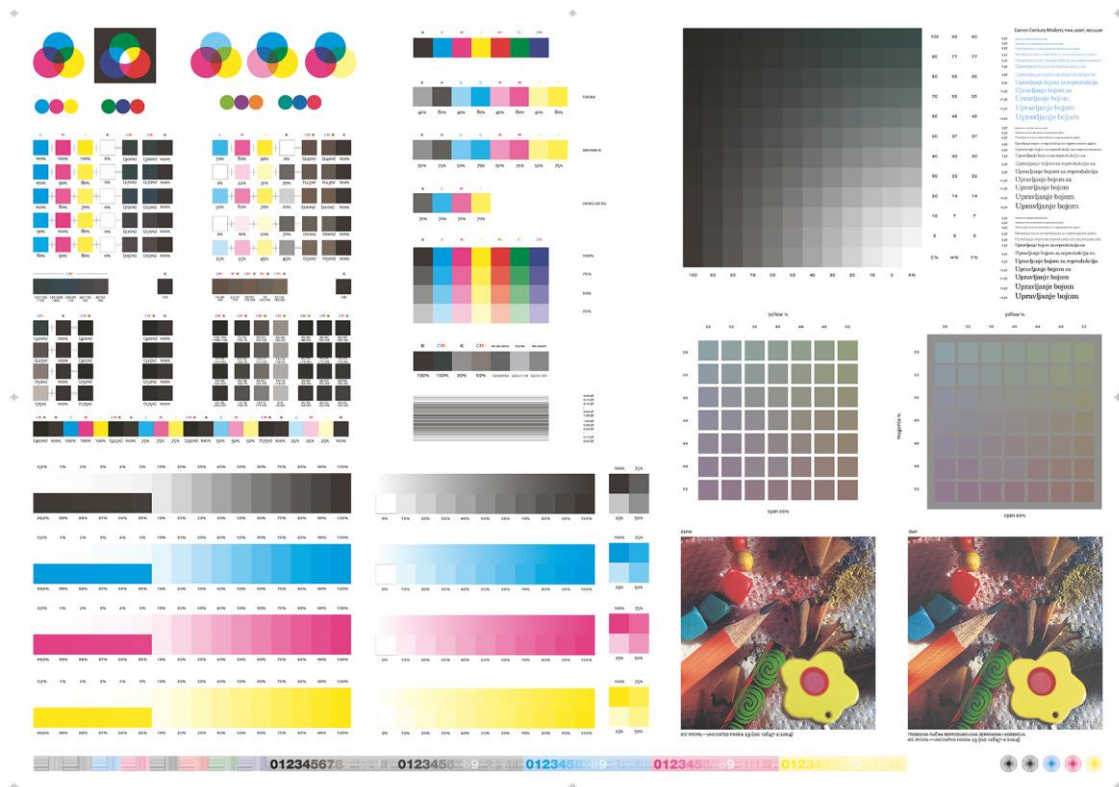
*Figure 1: The test target*

Each element of the test target was designed to higlight a particular aspect of the printing process. The main elements were: colour patches with primary colours in different combinations and with different RTV values, and with different UCR and GCR shares, patches with tone values from 0% - 100% in ten different halftone steps in every proces colour and the strip with continious tone, strip with minimal (0,5% - 5%) and maximal (99,5% - 95%) RTV, four color matrix for visual assessment of grey balance, photos reproduced with standard and custom profile, typographic elements from 2pt - 18pt, etc.

## 2.2 Preparing and Printing Test Target

The rasterization process was done with Harlequin Navigator RIP, Version 9. Offset plate (Thermostar P970) was exposed and processed with CTP system Luescher Xpose! 230 Thermal. Target was printed with Heidelberg Speedmaster 74-4-P3-H sheetfed offset machine. Offset ink used was Inkredible Resista (Michael Huber-Munchen). Coated paper used was Artic volume white (150 g/m$^2$). Three different uncoated papers used were: Munken Lynx (170 g/m$^2$), Munken Pure (170 g/m$^2$) and Maestro print (140 g/m$^2$).

## 2.3 Measurement Procedure

Spectral measurement of colour paches were conducted using Gretagmacbeth Eye-one Pro spectrophotometer in accordance with the ISO 13655 standard. The illumination corespond to D50, measurement geometry was 0/45, 2° observer. For process control during the print run black backing was used and dry ink was measured. For visual observation of prints Gretagmacbeth The Judge II light testing box was used under standard illuminant D50. The parameters observed were: coloure balance (colour tone), image gradation (lighter/darker), contrast range (high/low contrast) and register.

## 3. RESULTS AND DISCUSSION

Due to the large amount of results obtained, here will be presented only those that show the greatest differences in reproduction between different types of paper. Some of the results obtained by spectral measurement are shown in the Tab 1, Tab 2, and Fig 2.

*Table 1. CIELAB colour values for solid tones of primary and secondary colours for offset printing on two paper types (one coated and three uncoated papers) compering to standard ISO 12647 values.*

| Paper type | ISO 12647 (PT 2) | | | Arctic Volume White 150 g/m² | | | ISO 12647 (PT 4) | | | Maestro Print 140 g/m² | | | Munken Lynx 170 g/m² | | | Munken Pure 170 g/m² | | |
|---|---|---|---|---|---|---|---|---|---|---|---|---|---|---|---|---|---|---|
| | L* | a* | b* | L* | a* | b* | L* | a* | b* | L* | a* | b* | L* | a* | b* | L* | a* | b* |
| K | 16 | 0 | 0 | 21 | 1 | 1 | 31 | 1 | 1 | 36 | 1 | 2 | 36 | 1 | 3 | 36 | 1 | 4 |
| C | 54 | -36 | -49 | 58 | -34 | -50 | 58 | -25 | -43 | 63 | -24 | -43 | 63 | -25 | -40 | 63 | -27 | -36 |
| M | 46 | 72 | -5 | 50 | 75 | -5 | 54 | 58 | -2 | 56 | 58 | -5 | 57 | 59 | -2 | 57 | 57 | 0 |
| Y | 88 | -6 | 90 | 89 | -4 | 96 | 86 | -4 | 75 | 89 | -4 | 77 | 90 | -4 | 79 | 90 | -3 | 80 |
| R | 47 | 66 | 50 | 48 | 69 | 45 | 52 | 55 | 30 | 53 | 56 | 29 | 54 | 56 | 30 | 55 | 55 | 31 |
| G | 49 | -66 | 33 | 51 | -63 | 31 | 52 | -46 | 16 | 56 | -44 | 22 | 57 | -43 | 23 | 57 | -42 | 24 |
| B | 20 | 25 | -48 | 27 | 22 | -45 | 36 | 12 | -32 | 40 | 11 | -30 | 40 | 12 | -27 | 40 | 9 | -26 |
| W_paper | 92 | 0 | -3 | 92 | 1 | -4 | 92 | 0 | -3 | 90 | 1 | -6 | 91 | 1 | -2 | 91 | 0 | 4 |

*Table 2. Density values for quarter tones measured on prints (dry ink) printed on two paper types (one coated and three uncoated papers).*

| Paper type | Arctic Volume White 150 g/m² | | | | Maestro Print 140 g/m² | | | | Munken Lynx 170 g/m² | | | | Munken Pure 170 g/m² | | | |
|---|---|---|---|---|---|---|---|---|---|---|---|---|---|---|---|---|
| RTV % | 100 | 75 | 50 | 25 | 100 | 75 | 50 | 25 | 100 | 75 | 50 | 25 | 100 | 75 | 50 | 25 |
| K | 1,25 | 0,65 | 0,30 | 0,13 | 1,04 | 0,68 | 0,41 | 0,24 | 1,05 | 0,69 | 0,41 | 0,23 | 1,04 | 0,67 | 0,39 | 0,22 |
| C | 1,00 | 0,53 | 0,26 | 0,10 | 0,86 | 0,58 | 0,37 | 0,22 | 0,85 | 0,57 | 0,37 | 0,21 | 0,85 | 0,57 | 0,36 | 0,20 |
| M | 1,06 | 0,60 | 0,29 | 0,12 | 0,90 | 0,62 | 0,38 | 0,22 | 0,90 | 0,64 | 0,39 | 0,23 | 0,89 | 0,63 | 0,39 | 0,22 |
| Y | 0,88 | 0,48 | 0,23 | 0,08 | 0,83 | 0,53 | 0,31 | 0,18 | 0,83 | 0,54 | 0,34 | 0,20 | 0,85 | 0,56 | 0,36 | 0,23 |
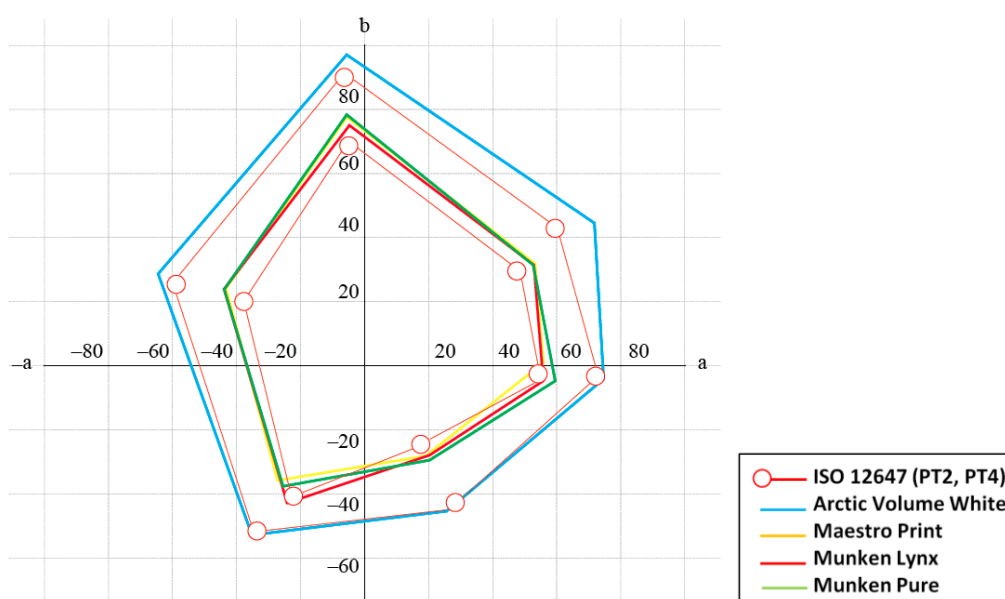


*Figure 2: Comparison of colour gamut obtained on different types of paper plotted in CIELAB diagram.*

AIC2015 TOKYO - Color and Image

Even though the numbers show that the print on uncoated papers does have a smaller densities and reduced colour gamut, our eyes can percieve the image to be similar to the orignal through good procesing. This research show that image adjustments made in prepress can improve percieved quality of prints on uncoated papers. Image adjustments should be conducted in the controled conditions on calibrated monitor by applying the simulation of paper colour and the output device profile. The paper type settings, together with an ICC profile, is fundamental to the whole process of prepress. It is recommended to adjust the density of an image by adjusting tone curves. By reducing the mid-tones and three-quarter tones by 12-15% the dot gain could be compensated. Also, important parts of an image should not involve tone values that lie outside the printable tone value range. Printable tone range for uncoated paper is from 4% for highlights dots to 85% for the darkest shadows. Total ink coverage (TIC) must be decreased to suit uncoated paper. It should not be over 280%. Too high TIC without proper curve compensation can result in ink set-off and drying problems. It is important to check that the ICC profile has the correct TIC value. By using the Under Colour Removal (UCR) or Gray Component Replacment (GCR) methods when defining the separations it is possible to reduce the TIC without detracting from the image's quality and achieving a more even degree of inking. Also, screen ruling should not be too high. Recommendation is to use 80-120 lpi for high bulk paper and 133-150 lpi for low bulk paper.

## 4. CONCLUSIONS

Offset printing is an unstable printing process and there is high potential for saving costs and time by standardisation. By folowing the propositions of the graphic industry printing standard ISO 12647 for adjustments acording to five predefined paper types and by using paper ICC profile depending on the output media, it is posible to secure and stabilise the reproduction process and printing quality. But, even though using the ICC profiles will help in many ways, it must be stated that every profile will have some level of generalization. In some cases, when high quality level is required, the specific (custom) profile, that will handle a specific offset press and a specific paper quality, should be used. It implies fine-tuning the system by customizing curves for particular paper/ink/print conditions.

The research show that well-planed and prepared separations are crucial for the quality of the print on uncoated paper. Adjustments made in the prepress, concerning the dot gain, contrast, saturation, colour balance and total ink coverage, sets the main quality level on the end results. The only thing that can be optimized during printing, if needed, is ink film thickness. Uncoated paper needs more ink to reach the same density as on a coated paper. A general recommendation for uncoated paper is to lower ink density to avoid over inking. But, if the prepress is done correctly and the total ink coverage is low (250-260%), the ink density can be kept relatively high without the risk of over inking. This will provide more colourful image.

## ACKNOWLEDGEMENTS

**REFERENCES**

ISO 12647-1:2004 Graphic technology - *Process control for the production of half-tone colour separations, proof and production prints - Part 1: Parameters and measurement methods.*

ISO 12647-2:2004 Graphic technology - *Process control for the production of half-tone colour separations, proof and production prints - Part 2: Offset lithographic processes.*

ISO 13655:2009 Graphic technology - *Spectral measurement and colorimetric computation for graphic arts images.*

ISO 13656:2000 *Graphic technology - Application of reflection densitometry and colorimetry to process control or evaluation of prints and proofs*

*Address: Assistant Prof. Maja STRGAR KURECIC, Department of Graphic Design and Image Reproduction, Faculty of Graphic Arts, University of Zagreb, Getaldiceva 2, 10000 Zagreb, CROATIA*
*E-mails: mstrgar@grf.hr, lmandic@grf.hr, ante.poljicak@grf.hr, diana.milcic@grf.hr*

# A Real-Time Multi-spectral CG Rendering Method for Building with Scene Illumination

ChihiroSAKURAI, NorihiroTANAKA,  Kosuke MOCHIZUKI

Faculty Business and Informatics, Nagano University

## ABSTRACT

This paper describes a real-time CG rendering method for building with scene illumination data. However, the multi-spectral scene rendering method with high accuracy scene illumination information needs a huge amount of calculation processing time. Therefore, we improve rendering performance of multi-spectral rendering system with omnidirectional illumination data. First, we develop a scene rendering system with multi-spectral reflection model include multi-spectral omnidirectional illumination data. The illumination data is measured with fish-eye lens and digital camera. The illumination data is generated as multi-spectral omini-directional image. Second, to reduce the time for rendering processing of scene illumination, we develop a real-time rendering method for implementing to Graphics Processing Unit (GPU). Moreover, we render a building with a rendering method based on Image Based Lighting (IBL). To improve rendering performance, we develop a multi-spectral irradiance map from the multi-spectral omni-directional image for GPU. Finally, to confirm validity of the proposed method, Nagano university campus is rendered by proposed method. And also, we compared CG reproduced image to the real scene.

## 1. INTRODUCTION

In the fields of digital archive of buildings, walk-through rendering method is required. To walk around various places with viewing landscape, we develop a rendering method for buildings with scene illumination. The scene illumination is very important for object color[1]. The rendering method need to render precise lighting, shading, gross and soft shadow et al. in the real scene illumination [2]. For the realistic rendering, the system needs to calculate illumination distribution characteristics in the scene and light reflection process on an object precisely[3][4]. Moreover, it is important that the CG rendering system can reproduce scene illumination precisely[5]. By the conventional RGB-based rendering technique, it is difficult to calculate scene illumination precisely. Because multi-spectral information is physical data peculiar to an object, the multi-spectral data is independent of color device such as a camera.

This paper describes a real-time CG rendering method for building with scene illumination data. However, the multi-spectral scene rendering method with high accuracy scene illumination information needs a huge amount of calculation processing time. Therefore, we improve rendering performance of multi-spectral rendering system with scene illumination data. We develop a scene rendering system with multi-spectral reflection model include multi-spectral scene illumination data. The illumination data is measured with digital camera.

Second, to reduce the time for rendering processing of scene illumination, we develop a real-time rendering method for implementing to Graphics Processing Unit (GPU). And

also we develop a data compression algorithm for multi-spectral data for improving resolution and performance. Finally, to confirm validity of the proposed method, Nagano university campus is rendered by proposed method. And also, we demonstrated walk-through in the campus scene.

## 2. DIGITAL ARCHIVE METHOD

### 2.1 Measuring Structure

In this study, we need a real-time rendering speed for providing the presence that a user experiences. To render a high quality CG image of a structure while reducing the number of polygons, we develop rendering system for digital archivine of structures. To efficiently display 3D CG of structure with high accuracy using required minimum measured data by performing required minimum 3D vertex measurement. The dimension of the structure is measured by using laser distance meter. And also, the equipment such as furniture in the room is measured by using digital camera. The size of equipment is measured by using measure and image data. To make up for 3D vertex data shortage, the texture mapping is used for describing object surface material.Figure 1 shows measurement scene of interior dimensional size of the building and its equipment in the room. Figure 1(a) shows laser measurement of internal dimention of buildings. Figure 1(b) is measurement process of equipment in the room. The equipment is measured 3D verstex as 3D shape and its texutre image. It is synthesized for each measurement data to generate a composed CG data of the equipment.



(a) Interior dimention of building      (b) Equipment in the room
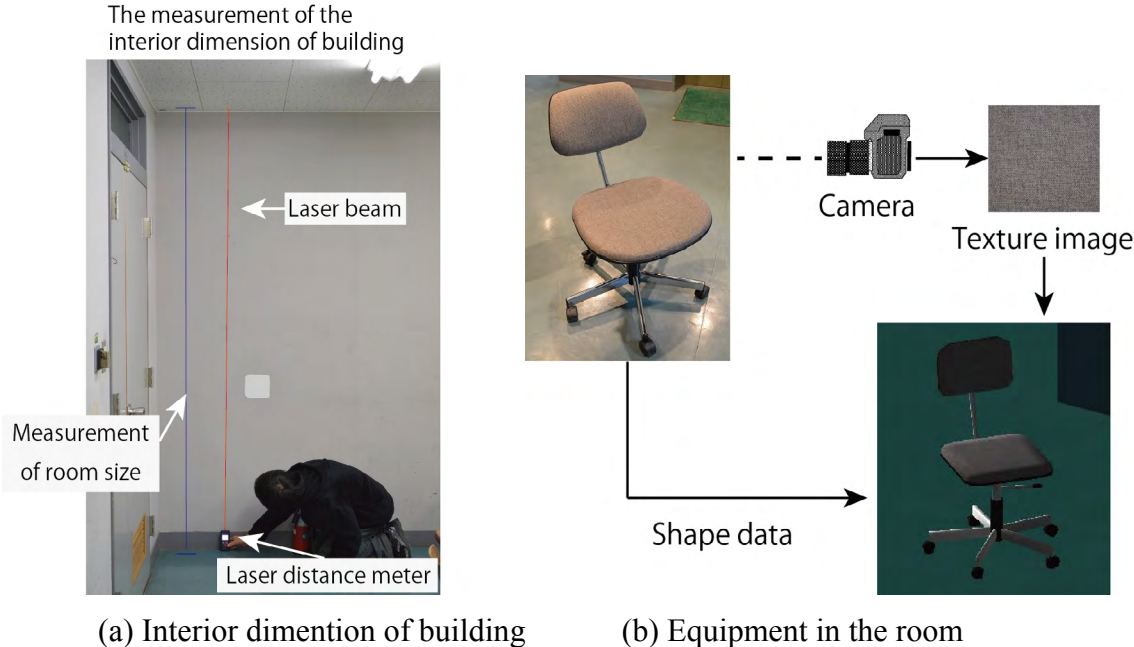
*Figure 1. Measurement of the building and equipment*

## 2.2 Multi-spectral model

Figure 2 shows scene illumination in a building. In this study, he scene illumination is described as spectral distribution of light source and object surface reflectance. We propose a method for estimating spectral distribution based on statistical method with color patches and a spectrophotometer. In this method, we assume that principal illumination in the scene consist of one type light source. We described the spectral information as 61 dimensional vector that is sampled at 5nm intervals in the visible light wavelength region (400-700nm). To estimate the spectral distribution of light source in the scene illumination, we developed multi-spectral camera model. In the model, the estimated spectral distribution $\mathbf{e}$ is described as

$$\overline{\mathbf{e}} = \rho \mathbf{M} \tag{1}$$

where $\rho$ is camera output. $\mathbf{M}$ is $3 \times 3$ translation matrix. $\Lambda$ and $\mathbf{P}$ are $61 \times m$ matrix of m-tuple spectral distribution and $3 \times m$ matrix of $m$-tuple camera outputs, respectively. $\mathbf{t}$ is $61 \times 3$ matrix of camera sensitivity. The relation of these matrixes is described as $\mathbf{P} = \Lambda \mathbf{t}$. We estimated $\mathbf{t}$ as $\mathbf{t} = \Lambda^{+} \mathbf{P}$ using pseudo inverse matrix $\Lambda^{+}$ of matrix $\Lambda$. Then, $3 \times 1$ matrix $\mathbf{e}$ of the spectral distribution of light source can be estimated as $\mathbf{e}^{T} = \rho^{T} \mathbf{t}^{-1}$ using inverse matrix $\mathbf{t}^{-1}$ of $\mathbf{t}$. The translation matrix $\mathbf{M}$ is described as $\mathbf{t}$.
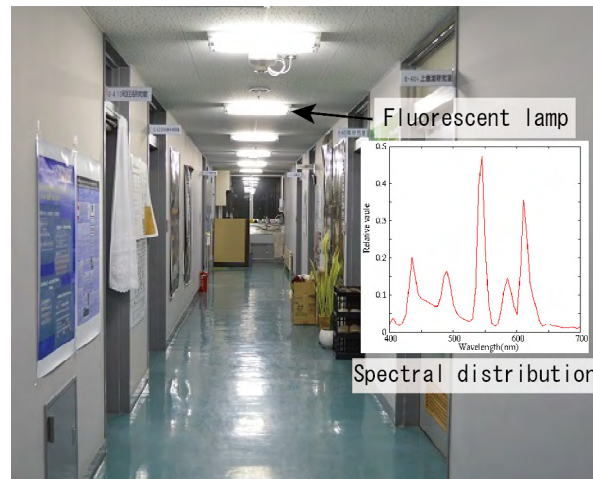


*Figure 2. Multi-spectralscene illumination in the building*

## 3. RENDERING METHOD

Figure 3 shows proposed multi-spectral rendering system. The multi-spectral real-time rendering system was developed for digital archive data for the building. In this system, the rendered CG image is based on multi-spectral image rendering. The CG images are precisely created under an ambient light environment in the scene. The system is developed as interactive walk-through system in the building. And also, the whole scene is modelled as multi-spectral scene light reflection model. In this study, the color signal of the visual system is calculated from the reflection model and illumination map. Therefore, the object color is calculated from the color signal and CIE color matching function $\overline{x}(\lambda), \overline{y}(\lambda), \overline{z}(\lambda)$ as a tristimulus value (CIE XYZ), which is computed as follows.

$$\begin{bmatrix} X \\ Y \\ Z \end{bmatrix} = \int_{400}^{700} S(\lambda)E(\lambda) \begin{bmatrix} \overline{x}(\lambda) \\ \overline{y}(\lambda) \\ \overline{z}(\lambda) \end{bmatrix} d\lambda \qquad (2)$$

The tristimulus value is independent of any display device. To render the RGB value precisely, we must calibrate the display device. The device RGB of the color display is obtained from the XYZ value via a transformation matrix and gamma correction, which collectively specify the intrinsic values of the display device. These values are estimated by measuring the corresponding relationship between the tristimulus and device RGB values, with a spectral radio photometer (TOPCON TECHNOHOUSE SR-3A-L1). The proposed method is implemented on a GPU, assuming a color monitor as the display device.
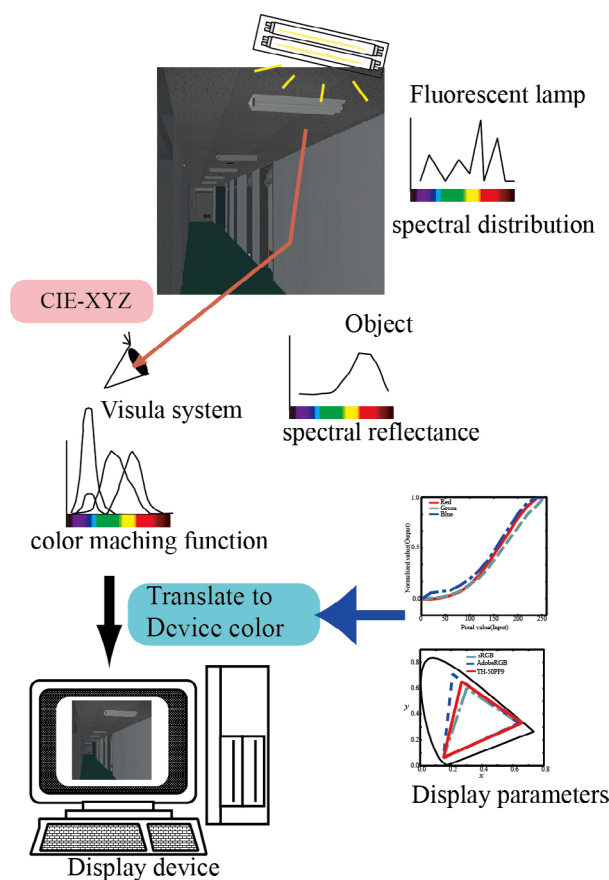


*Figure 3. Multi-spectral rendering system with scene illumination data.*

## 4. EXPERIMENTAL RESULTS

The proposed method was applied to digital archive of Nagano university campus. Once all vertex and texutre datas were estimated, we could reproduce the object in 3D CG of campus scene. Thus, we rendered the object shown in Figure 4. We have compared the reproduced CG with the picture of the real scene. Figure 5 shows rendering results at various location in Nagano University.

AIC2015 TOKYO - Color and Image

*Figure 4.Renderingu results(comparison between Original Scene and Reproduced CG)*



*Figure 5. Rendering results at various location in f Nagano University.*

## 4. CONCLUSIONS

This paper described a real-time CG rendering method for building with scene illumination data. We improved rendering performance of multi-spectral rendering system with scene illumination data. The multi-spectral scene rendering method with high accuracy scene illumination information needs a huge amount of calculation processing time. First, we proposed method reducing 3D shape data without lowering image quality. Second, to reduce the time for rendering processing of scene illumination, we develop a real-time rendering method for implementing to Graphics Processing Unit (GPU). Finally, to confirm validity of the proposed method, Nagano university campus is rendered by proposed method. And also, we compared CG reproduced image to the real scene.

## REFERENCES

[1] C. C. Chiao, T. W. Cronin, and D. Osorio, "Color signals in natural scenes: Characteristics of reflectance spectra and effects of natural illuminants", J. Opt. Soc. Am. A 17, 218,2000.

[2] P. E. Debevec," Rendering Synthetic objects into real scenes:bridging traditional and image-based graphics with global illumination and high dynamic range photography", Proc. Of SIGGRAPH 98, pp.189-198,1998

[3] N. Tanaka, K. Mochizuki and J. Woo, "A Real-time Rendering Method of Art Objects Based on Multi-spectral Reflection Model", Proc. of IASDR, 4 pages,2009.

[4] N. Tanaka, K. Mochizuki: A digital archive method based on multispectral imaging with goniometric multiband camera,The Bulletin of Japanese Society for the Science of Design. 61(3) 35-44 2014.

[5] C. Iwasaki, N. Tanaka: A CG Reproduction Method of Human Skin under Omni-directional Illumination,Proceedings of International Association of Societies of Design Research (IASDR) 2013

*Address: Prof. Norihiro TANAKA, Faculty of Business and Informatics,*
*Nagano University, 658-1 Shimonogo,Ueda,  Nagano,386-1298 , JAPAN*
*E-mails: j13033cs@nagano.ac.jp,k-mochiduki@nagano.ac.jp, n-tanaka@nagano.ac.jp*

# Color mapping between a pair of similar facial images with and without applying cosmetics

Lin Lu, Hung-Shing Chen, Neng-Chung Hu

Graduate Institute of Electro-optical Engineering, National Taiwan University of Science and Technology, Taiwan

## ABSTRACT

The aim of this study is to develop an automatic facial makeup technology, which can make a raw facial image reproduce the preferred cosmetic colors according to the chosen facial color template. The developed facial makeup method named Facial Color Morphing Algorithm (FCMA). Discriminative Response Map Fitting (DRMF) was also introduced to find the main facial organs (e.g. eyes, nose, mouth etc.) and the face outline. The facial image was divided by a series of triangles according to the facial feature points detected by DRMF. In addition, affine transformation and bilinear interpolation are applied to perform facial skin-color mapping between the test image and the morphing image. The simulated results indicate that our developed algorithm works well in representing preferred facial colors.

## 1. INTRODUCTION

An image-dependent color palette will be a better choice to achieve high image quality for displays (Chen et. al., 2014). However, it is difficult to analyze facial color differences between two similar facial images. In this study, image morphing technology (Howard Anton, 2005) is applied to map facial colors between the pair of faces which have a little different shapes. Besides, Discriminative Response Map Fitting (DRMF) (Asthana A. et al., 2013) is used to find the feature points of a human face. The aim of this study is to develop an automatic facial makeup technology, which can make a raw facial image reproduce the preferred cosmetic colors according to the chosen facial color template. The experimental schematic is shown in Figure 1.
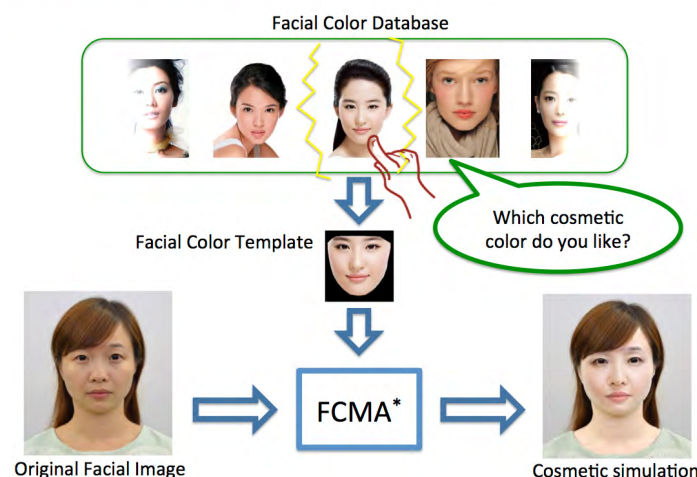


(FCMA: Facial Color Morphing Algorithm)

*Figure 1: Experimental schematic*

# 2. METHOD

Figure 2 demostrates the experimental flowchart in this study. The test image is defined as a raw image without cosmetics, and it is desired to make up her new face according to the chosen facial color templates. The simulated makeup results are mainly achieved by our developed algorithm, named Facial Color Morphing Algorithm (FCMA).
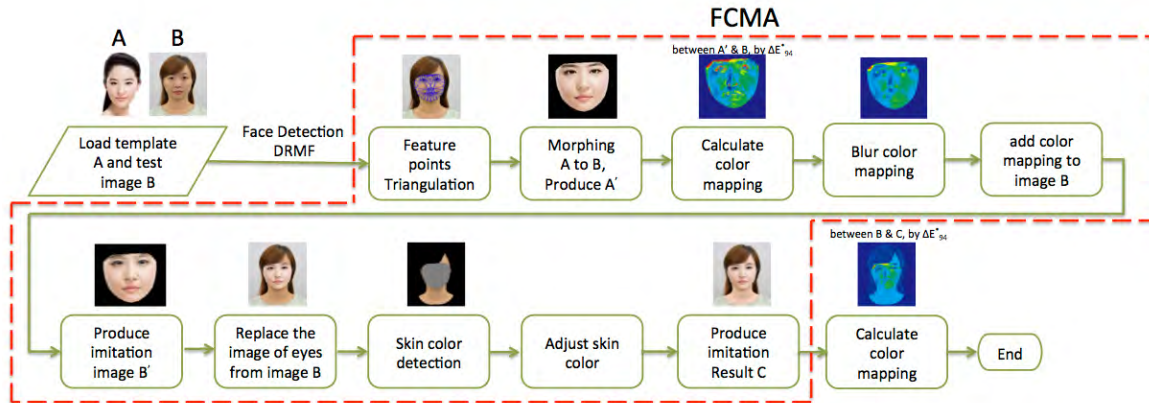


*Figure 2: Experimental flowchart*

## 2.1 Test Image and Facial Color Template

A test image, which is the raw face of a young woman without makeup (Figure 3(a)), is inputted into the FCMA. Also two template images with cosmetics of the young models are found from the website, which are seen as facial color templates (Figure 3(b)-3(c)). It is hoped to makeup the test image more pleasant to approach a similar skin color appearance to the chosen facial color template.
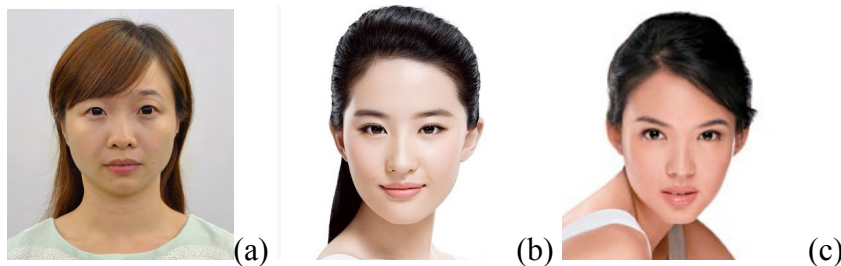


*Figure3: Test image and template images; (a) test image,(b) and (c) facial color templates*

## 2.2 Face Detection and Transformation

DRMF was applied to execute the facial feature point detection for the test image and the template image, respectively. As shown in the example of Figure 4(a), the red points represent the feature points of a facial image found by DRMF. It can be observed that most of the feature points almost cover the main facial organs (e.g., eyes, nose, mouth etc.) and the face outline.

When the feature points of the test image and the template image were found by DRMF, we let all feature points in an image produce feature line connections between a pair of the nearest points, and these feature lines do not cross each other. Finally, an image can be divided into a series of polygon grouped with many triangles (Figure 4 (b)) by face triangulation. Notice that numbers and orders of inner triangles between the test image and the template image should be equal.
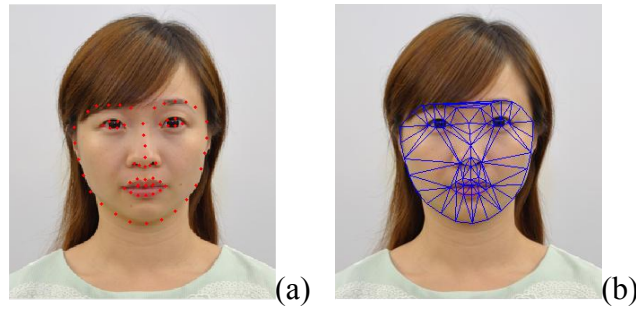
AIC2015 TOKYO - Color and Image

*Figure 4. Face detection; (a) feature points in test image (b) face triangulation*

## 2.3 Image Morphing

Image morphing is performed in the template image mainly, which concept is based on affine transformation (Figure 5(a)). When a triangle T₁ in one image has three vertices $V_1, V_2, V_3$ and the point $V$ is in T₁, then it can be expressed by Equation 1. Therefore, the coefficients $(C_1, C_2, C_3)$ can be expressed by a triangle T₂ in the other image, which vertices $W_1, W_2, W_3$ can also satisfy Equation 2. So the point $W$ inside the triangle T₂ can be determined by the coefficients$(C_1, C_2, C_3)$. The point $V$ and point $W$ have a unique relation in affine transforming process.

$$\begin{cases} V = C_1 V_1 + C_2 V_2 + C_3 V_3 \\ \quad C_1 + C_2 + C_3 = 1 \\ \quad\quad C_1, C_2, C_3 > 0 \end{cases} \tag{1}$$

$$W = C_1 W_1 + C_2 W_2 + C_3 W_3 \tag{2}$$

When all triangles in an image are computed by affine transformation, then image morphing is finished. The morphing example is shown in Figure 5 (b). The left part is the original image, and the right part is the morphing result. Note that they have the same facial shape of the test image, but different facial colors at this stage.



*Figure 5: (a) Triangulation and interpolation, (b) Images before and after affine transformation*

During image morphing processing, the calculated (x, y) position at point $W$ in Figure 5(a) calculated may not integer value. If the point W is selected as the position with the nearest calculated integer value, it could lead a morphing result unsmooth. Therefore, bilinear interpolation is suggested to solve this problem. As shown in Figure 6, bilinear interpolation based on four nearest points was used to perform interpolation points of all mapped RGB pixels (see Eq. 3). It is expected that the morphing image become smoother. In Equation 3, $x_i$ and $y_i$ mean the location of a pixel needed to interpolate. The combinations of $x_1$, $x_2$, $y_1$ and $y_2$ are the locations of four points which are nearest $(x_i, y_i)$. $f(x, y)$ means the RGB values located on z axis corresponding to the position $(x, y)$.
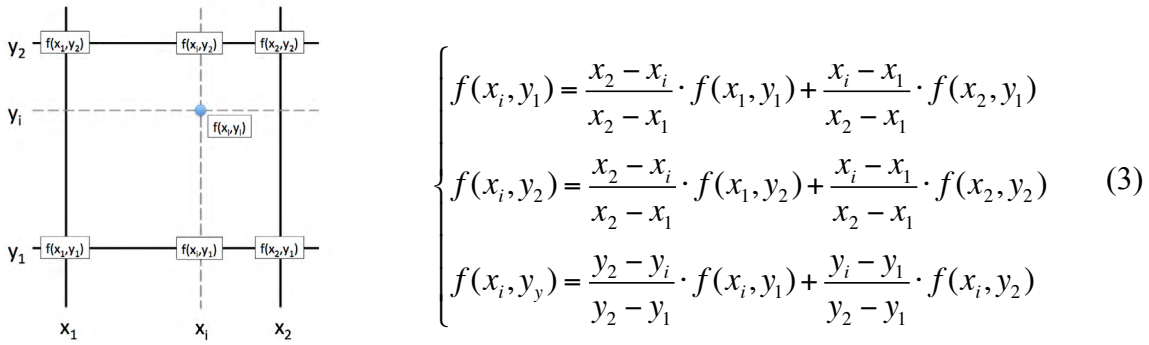
$$f(x_i, y_1) = \frac{x_2 - x_i}{x_2 - x_1} \cdot f(x_1, y_1) + \frac{x_i - x_1}{x_2 - x_1} \cdot f(x_2, y_1)$$

$$f(x_i, y_2) = \frac{x_2 - x_i}{x_2 - x_1} \cdot f(x_1, y_2) + \frac{x_i - x_1}{x_2 - x_1} \cdot f(x_2, y_2) \qquad (3)$$

$$f(x_i, y_y) = \frac{y_2 - y_i}{y_2 - y_1} \cdot f(x_i, y_1) + \frac{y_i - y_1}{y_2 - y_1} \cdot f(x_i, y_2)$$

*Figure 6: Bilinear Interpolation*

## 3. RESULTS AND DISCUSSION

As shown as the example in Figure 7, which are the results based on affine transformation and DRMF, but with two kind of interpolation methods. The left part is the nearest interpolation, and the right part is bilinear interpolation. We can observe that the edges of eyes and mouse are not smooth in the left images, but smoother edges appear in the right images. Therefore, the morphing images using bilinear interpolation are suggested in this study.
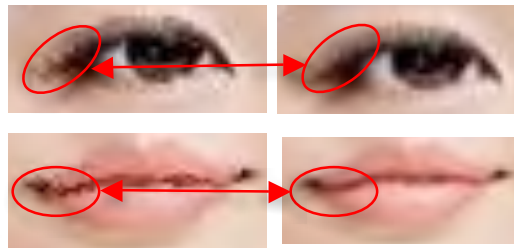


*Figure 7 : Image interpotation comparisons; the nearest interpolation (left part) and bilinear interpotation (right part)*

Image color differrences were calculated by $\Delta E^*_{94}$ color different formula between the test image and the morphing image. Referring to sRGB standard, the 8-bit RGB values of all image's pixels were transformed into XYZ tristimulus color space, then their XYZ value were transformed into $L^* a^* b^*$ color space. When a test image and a morphing image are compared (Figure 8), the color difference map indicates there is a large area with $\Delta E^*_{94}$ range of 0 to 5. However, there are several coutour areas with larger color different values (e.g., $\Delta E^*_{94} > 7$). Therefore, coutour smoothing is necessay to solve this problem.



*(a)*        *(b)*        *(c)*
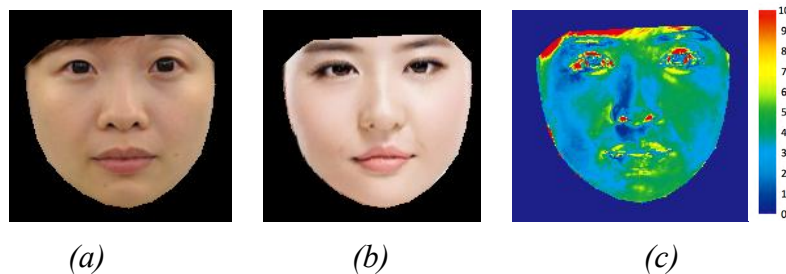
*Figure 8 : Facial color mapping results : (a) test image, (b) morphing image, (c) color differeence map*

As shown in Figure 9, the sub-images (a), (c) and (e) are the results before smoothing in $\Delta L^*$, $\Delta a^*$ and $\Delta b^*$ channel respectively, and (b), (d) and (f) are the results after

smoothing in $\Delta L^*$, $\Delta a^*$ and $\Delta b^*$ channel respectively. We can observer that $\Delta L^*$, $\Delta a^*$ and $\Delta b^*$ channels before smoothing have a little strong contours. Therefore, the Gaussian blur filter is introduced into the initial morphing result to smooth large color differences in the coutour area. The $\Delta L^*$, $\Delta a^*$ and $\Delta b^*$ channels after smoothing show much smoother results than the ones before smoothing. Then the smoothed $\Delta L^*$, $\Delta a^*$ and $\Delta b^*$ channels are added to the original $L^*$, $a^*$, $b^*$ channels again to restore a new facial image. Note that the eyes parts in a new face are still kept the same as the origial. Finally, Table 1 arranges the results that test facial image mapped by two facial template colors, which are (a) test image, (b) template color image, (c) color mapping result, (d) optimized mapping image and (e) color difference map.



| (a) | (b) | (c) | (d) | (e) | (f) |
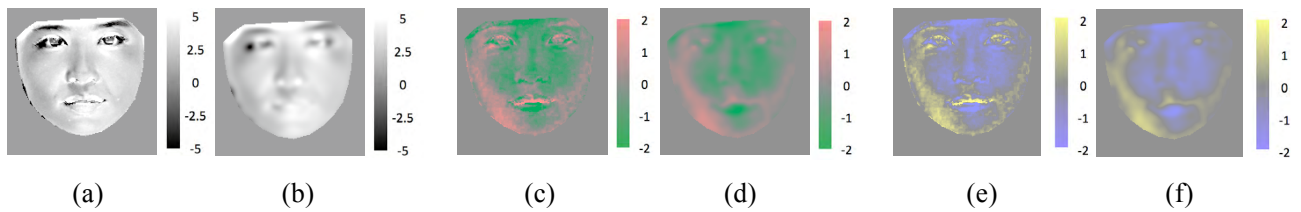
*Figure 9: $\Delta L^*$, $\Delta a^*$ and $\Delta b^*$ channels; (a), (c) and (e) are before smoothing, (b), (d) and (f) are after smoothing*

*Table 1: Facial color mapping results*

| (a) Test image | (b) Templete color | (c) Color mapping result | (c) Optimized image | (d) Color difference map |
|---|---|---|---|---|
|  |  |  |  |  |
| |  |  |  |  |

## 4. CONCLUSIONS

In this study, we developed an automatic facial makeup technology named Facial Color Morphing Algorithm (FCMA), which can make an original facial image without makeup reproduce the preferred cosmetic colors according to the facial color template database. Discriminative Response Map Fitting (DRMF) was also introduced to find the main facial organs (e.g. eyes, nose, mouth etc.) and the face outline information. In addition, affine transformation and bilinear interpolation was applied to perform facial skin-color mapping between the test image and the morphing image. The simulated results indicate that our developed algorithm works well in representing preferred facial images.

## REFERENCES

Hung-Shing Chen, Shih-Han Chen, Yen-Hsiang Chao, Ronnier Luo and Pei-Li Sun, "*Applying Image-based Color Palette for Achieving High Image Quality for Displays*," Color Research and Application, Volume 39, Issue 2, pp. 154-168. 2014.

Howard Anton, 2005, *"Elementary Linear Algebra, 9th Edition "*, *Warps And Morphs,* New York : John Wiley & Sons.

Asthana A., S. Zafeiriou, S. Cheng and M. Pantic, CVPR 2013, *Robust Discriminative Response Map Fitting with Constrained Local Models*.

Address: Master. Lin LU, Graduate Institute of Electro-optical Engineering, National Taiwan University of Science and Technology, 43, Section 4, Keelung Road, Taipei, 10607, TAIWAN

E-mails: M10219005@mail.ntust.edu.tw, bridge@mail.ntust.edu.tw,

nchu@mail.ntust.edu.tw

# The consistent color appearance based on the display-referred

Yasunari KISHIMOTO,[1] Hitoshi OGATSU,[1] Hirokazu KONDO[2]
[1] Key Technology Laboratory, Fuji Xerox Co., Ltd.
[2] Imaging Technology Center, FUJIFILM Corporation

## ABSTRACT

We report the results of testing of our hypothesis that using the largest gamut display as a reference and by producing colours to printers with different color gamuts, the use of a 'consistent color appearance' rendering including color and tone reproduction produces optimal results. The results obtained by two subjective assessments indicate that 'consistent color appearance' for various gamut sizes, from multi-color inkjet with a wide color gamut to newsprint with a narrow color gamut. 'Consistent color appearance' will provide an automatic process which enhances value of future digital printing.

## 1. INTRODUCTION

In recent years, printing for applications such as advertising and presentations are working to improve their quality and to reduce their color variation. This includes the use of color standards such as JapanColor, and the certification body. However, color differences between the target color gamut of the color standard and each output color gamut has been a problem as users can not fully utilize the color reproduction capability of wide color gamut printers and in addition them can not appliy to a narrow gamut printer. As shown in Fig. 1 and Fig. 2 (Case 2) the input images in the traditional offset print workflow (ISO 12647-2) are restricted to a standard color gamut such as JapanColor for color matching with the use of a print reference (ISO 22028-1). The characterized reference printing conditions (CRPCs, CGATS.21-2 2013) were specified as standard seven printing conditions from multi-ink wide color gamut printing to coldset inks for newspaper printing (narrow color gamut). These are intended as the basis for similar looking color for a variety of printing systems with print reference. They pay particular attention to gray balance and operational stability to produce similar results. Johan Lammens (2004) reported that the CMYK input images should apply color re-rendering following color rendering to the intended printing system for effective use across a variety of printing systems. In some cases it is important for a variety of printing systems to have a display reference and cross-media reproduction is often used as shown in Fig. 2 (Case 3). The International Color Consortium (ICC) has developed the concept of 'consistent color appearance' which should have a balance between color matching and consistent tone reproduction across multiple devices. Similar concepts are being studied in CIE Reportership R8-13 that it is include ITU-R BT. 2020 wide gamuts (Andreas Kraushaar 2013, Paul Sherfield 2013, CIE 156 2004). Furthermore, when preparing advertising for multiple media, the color gamut of different reproduction systems such as signage displays, inkjet or offset printing, the designer or prepress process involves making color adjustment of each color reproduction manually.
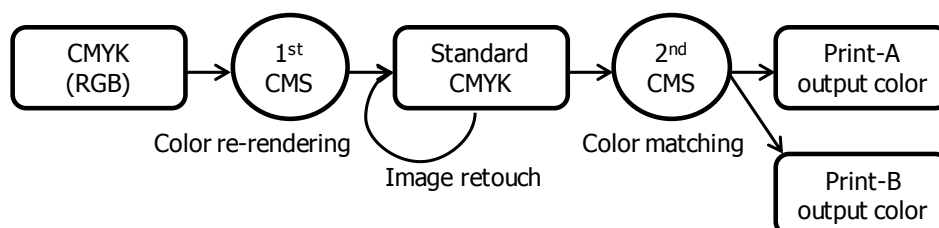


*Figure 1: Examples of a standard traditional printing workflow based on CMYK print-referred.*
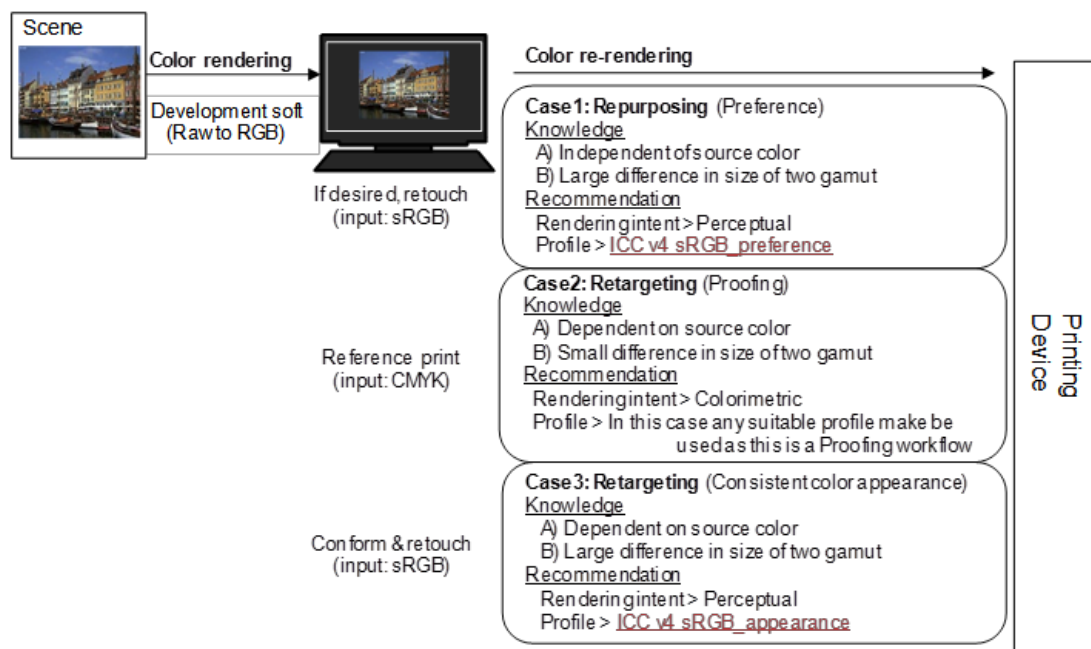
*Figure 2: ICC color re-rendering as described in the ICC White Paper 42 update (2014).*

This approach achieves a similar look between the display reference and the prints. Few reports are available on achieving a similar look between the display reference and prints from a variety of printing systems. This paper describes the results of an investigation of consistent color appearance. When color reproductions show highest similarity between the display reference and each print, and across the set of prints, when viewed under a common viewing condition they have by definition a 'consistent color appearance'. Similarity is judged by subjective assessment.

## 2. METHOD

We built the following hypothesis to test whether consistent color appearance is achieved based on a display reference. When display reference and outputs of respective printer have a similar looking image (color and tone) in a common viewing condition based on the common color reproduction aims (re-targeting of the display reference), outputs of all printer have a similar look. First, fundamental output colors corresponding to a limited number of common target colors (input color) are obtained by a full search of the colors on the reference images the can be produced by each printer. The number of colors is affected by the performance of experimental redering. Second, the new retargeting rendering is developed from fundamental output colors in each printing condition. Finally, we examined whether the same output was chosen as the preferred rendering by two subjective assessments.

### 2.1 Repeating subjective assessment and development of new retargeting rendering

The subjective assessment verified the closeness of appearance between the display reference image and all available print sample and judged its closeness of appearance. The reference images were selected as s set of images that covered the input color space. In addition, the assessment was limited to the relationship of a set of key image colors. New guidelines were made for fundamental output colors based on the result of the assessment. Common target colors were added as appropriate until the appearance of the two images looked similar. We repeated the process of making new print samples from fundamental output colors using the new guidelines and conducting this assessment until we judged the appearance of the image to be the nearest possible. This experiment was repeated even when multiple color gamuts of different printer and paper combinations.

As a result, we obtained a set of common target colors for multiple gamuts, and as shown in Fig. 3 and used these to develop a new retargeting rendering. The rendering is composed of two steps: (1) generate common appearance between the display reference and prints without considering gamut limitations (the common color reproduction), and (2) to control influence of the gamuts. In the common color reproduction, the relative Y matching (Rel.-Y) can maintain colors of highly sensitive color for skin tones, gray balance and so on with different output systems and paper types. Except for color close to the display white point, the effect of the Rel.-Y is superior to ICC absolute colorimetric reproduction and ICC relative colorimetric reproduction (ISO 15076-1 20124), because the luminance of display white point is close to the luminance of the paper white point in the viewing environment condition. This confirmed from not only our experimental data but also some market data. If the colors close to the white point in display system become out of gamut colors using Rel.-Y, they are adjusted in the consistent color rendering.
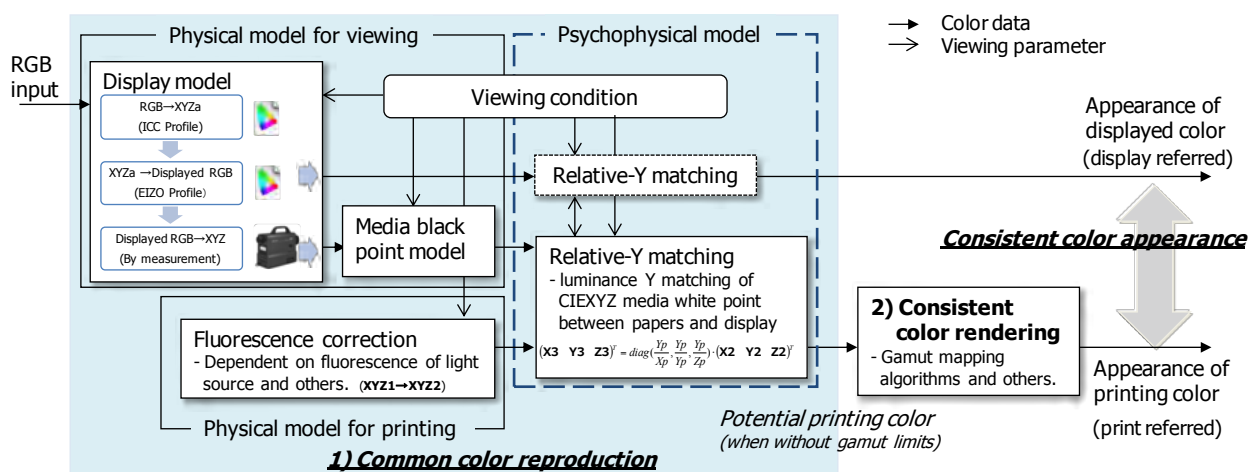


*Figure 3: Schematic diagram showing a new retargeting rendering for 1) the common color reproduction without gamut limits, and 2) consistent color rendering. Using the relative-Y matching (Rel.-Y) equation, Xp, Yp, and Zp is the white point CIEXYZ; X2, Y2, and Z2 is the input CIEXYZ; X3, Y3, and Z3 is the Rel.-Y generated CIEXYZ.*

## 2.2 Verification Experiment

The verification examined by using two subjective assessments (Table 1, 2). The first assessment was to rank the closeness of the appearance of the images on standard gamut in comparison with the display reference, and second assessment was to rank the closeness of the appearance of the images between images on standard gamut output and image on wide gamut output.

*Table 1. Assessement conditons.*

| | |
|---|---|
| Test subject | 20 persons. |
| Environment condition | ISO 3664 P2 conditon. |
| Display | EIZO CG221. |
| Test image | 4 images (ISO 12640-4 SCID, high chroma image, portrait, and landscape). |
| Subjective assessment method | 7 rank order scales (mentioned in Table 2). |

*Table 2. Print sample output conditions.*

| Color gamut | 2 gamuts (Standard print, wide gamut by multiple-ink inkjet). |
|---|---|
| Paper | 2 papers (plain paper, inkjet proofing paper). |
| Sample output | 7 samples as combination of 3 methods (Commercial ICC profile builder, default condition of the each printing systems, and proposed rendering) and 2 printers (above-mentioned gamuts). |

## 3. RESULTS AND DISCUSSION

As shown in Fig. 4, assessment of the average score of 4 images is divided into two groups. The group having a low degree of closeness of appearance with the reference image is a default condition used with factory setting on a commercial printing system. The group that has a high degree of closeness were made by a commercial ICC profile builder. It is suspected that in some cases closeness of appearance is achieved using the same algorithm for different printers. The proposed rendering showed the best result where the appearance of the image was judged to be the closest to display reference. Thus it is possible to achieve consistent color appearance by making the print output where the appearance of the image is close to the display reference.
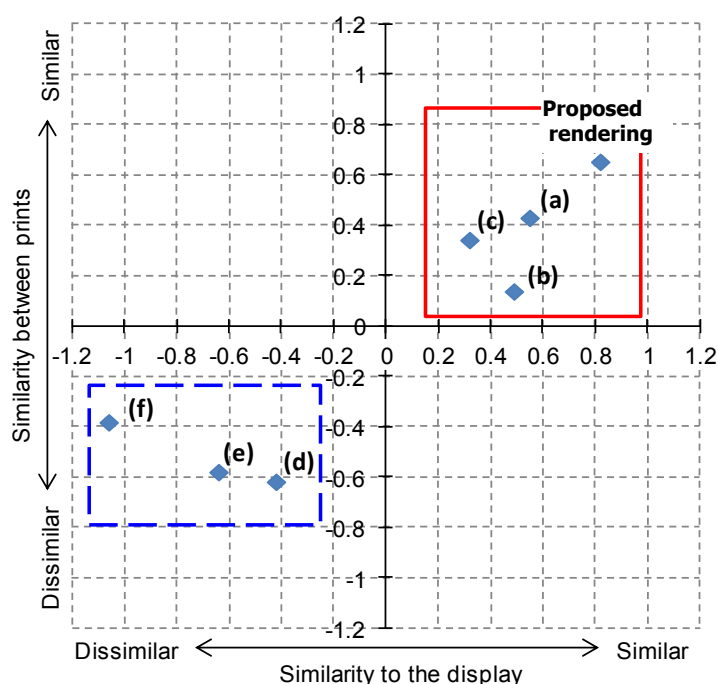


*Figure 4: The results from the experiment. The (a), (b) and (c) is a condtion of a commercial ICC profile builder, the (d), (e) and (f) is a condition using a printer with color gamut corresponding to each print output.*

## 4. CONCLUSIONS

In traditional printing workflow based on CMYK print reference there was a limitation that the full colour reproduction capability of a printing system cannot be used Furthermore, when producing advertising materials on multiple media designer or prepress process must control each color to look for similar colors and the display reference becomes important. Consistent color appearance aims to achieve similar output between the display reference and the prints on a variety of printing systems. We developed a new retargeting rendering by acquiring basic target color data using repeated subjective assessment. The rendering showed the result that the continuity (a color and tone) of the image was close visually between the display reference and the prints of two printing systems. Our results have demonstrated that the consisitent color appearance is feasible.

## REFERENCES

ISO 3664:2009. *Graphic technology and photography -- Viewing conditions.*

ISO 12640-4:2011. *Graphic technology -- Prepress digital data exchange -- Part 4: Wide gamut display-referred standard colour image data [Adobe RGB (1998)/SCID].*

ISO 12647-2:2013. *Graphic technology -- Process control for the production of half-tone colour separations, proof and production prints -- Part 2: Offset lithographic processes.*

ISO 13655:2009. *Graphic technology -- Spectral measurement and colorimetric computation for graphic arts images.*

ISO 15076-1:2010. *Image technology colour management -- Architecture, profile format and data structure -- Part 1.*

ISO 22028-1:2004. *Photography and graphic technology -- Extended colour encodings for digital image storage, manipulation and interchange -- Part 1: Architecture and requirements.*

ANSI CGATS.21-2 2013. *CRPCs*, http://www.idealliance.org/downloads/iso-15339-reference-print-conditions-2011 .

CIE 156:2004. *Guidelines for the Evaluation of Gamut Mapping Algorithms.*

Lammens, J. Morovic, J.Nielsen, M. Zeng, H 2004. *Adaptive re-rendering of CMYK image data*, CGIV 2004 Final Program and Proceedings (5) 454-458.

International Color Consortium 2014. *Using the sRGB_ICC_v4_appareance.icc profile,* ICC White Paper 42 http://www.color.org/profiles/srgb_appearance.xalter and http://www.color.org/whitepapers.xalter

Andreas Kraushaar 2013. *Common Appearance - Introduction, Concept and Overview*, ICC Frankfurt Graphic Arts Color Experts' Day, http://www.color.org/events/frankfurt/Kraushaar_ICCFrankfurt2013_CommonAppearance.pdf .

Paul Sherfield 2013. *Common Color appearance*, ICC Frankfurt Graphic Arts Color Experts' Day, http://www.color.org/events/frankfurt/Sherfield_ICCFrankfurt2013_Common_Appearance.pdf .

*Address: Yasunari KISHIMOTO, Key Technology Laboratory, Research & Technology Group, Fuji Xerox Co., Ltd., 430 Sakai, Nakai-machi, Ashigarakami-gun, Kanagawa, 259-0157, JAPAN*
*E-mails: Y.Kishimoto@fujixerox.co.jp, ogatsu.hitoshi@ fujixerox.co.jp, hirokazu.kondo@fujifilm.com*

# The study of museum lighting:
# the optimum lighting and colour environment
# - the proposal for the colour quality index -

Yuki NAKAJIMA, Takayoshi FUCHIDA,
Graduate School of Joshibi University of Art and Design

## ABSTRACT

The purpose of this study is to develop the new calculation method to evaluate the colour rendering values taking illuminance into consideration based on the subjective experiments. We carried out the experiments to examine subjectively impression of the test colour samples (the two-colour samples, the multicolour sample and the picture samples) under various light sources and illuminance. The results showed that subjective colour feelings were influenced by illuminance as well as the spectral power distributions of light sources, and also subjective impression depended on the hue of colour samples, especially on whether the sample contained red. It was also found that subjective impression could be evaluated by "colour quality" such as subjective vividness and brightness by factor analysis. We defined "the colour quality index" called Gx and Rxi to evaluate the new colour rendering properties representing illuminance-effects and hue-effects. It was confirmed that the new index Gx and Rxi correlated practically subjective results.

## 1. INTRODUCTION

The lighting environment of a museum must be carefully controlled not to give any damage against deterioration of artworks. The CIE publication (157: 2004) recommends illuminance and a limiting exposure time to control of damage to artworks by optical radiation. In case of the exhibition of Japanese paintings for example, illuminance is regulated to constrain under 50 lx not to give colour fade damage as less as possible.

The present ISO/CIE standard recommends for museum lighting that General Colour Rendering Index *Ra* is better than 80. However, *Ra* does not include illuminance effects. The calculation method taking into consideration of illuminance does not exist at present. Low illuminance means the decrease of inherent colour appearance of artworks because artworks will lose brightness and colourfulness at low illuminance. As known as the Hunt-effects, chromatic objects look more vivid when illuminance increase, on the other hand they look darker and dull when illuminance decreases.

We clarified on the previous paper that *Ra* would not be sufficient when colour rendering properties were evaluated at low illuminance, and showed that the colour rendering properties at very low illuminance could be evaluated by Gamut Ratio (Nakajima et al. 2013, Nakajima et al. 2014). As for the relationship between colour rendering properties and chromatic samples whether the sample contained red, Rea (Rea et al. 2008) and Wei (Wei et al. 2014) showed the importance of red.

The purpose of this study is to clarify colour rendering properties at low illuminance and also to try to develop the new calculation method to evaluate the colour rendering values taking into consideration of illuminance based on the subjective evaluation experiments.

## 2. METHOD

The two types of experiments were performed by a haploscopic viewing method. The evaluation booth (Figure 1) separated at the center was used. The different light source was installed at the top of the each box. The wall of the booth was painted in matted gray (N6). The observer evaluated subjective colour feelings of the test colour samples of the test side compared with colour feelings of those of the reference side by Semantic Differential method. Figure 2 shows the eleven adjective pairs and the seven categorized scale. Ten females observers in the experiment 1 and 17 females observers in the experiment 2 were participated.
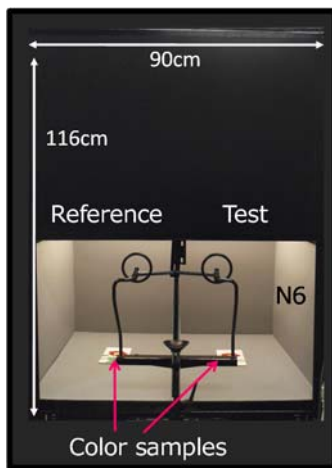


*Figure 1:*
*The evaluation booth.*

| No. | (—) ←→ (+) | No. | (—) ←→ (+) |
|-----|-------------|-----|-------------|
| 1 | dirty-beautiful | 6 | heavy-light |
| 2 | uncomfortable-comfortable | 7 | dark-bright |
| 3 | muddy-clear | 8 | cool-warm |
| 4 | sober-flashy | 9 | dislike-like |
| 5 | passive-active | 10 | dull-vivid |
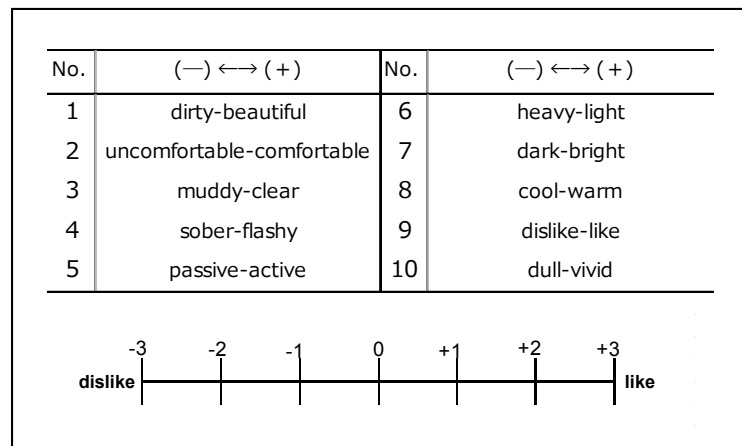
*Figure 2: the adjective pairs and the seven categorized scale.*

### 2.1 The reference and the test lighting

The reference light source was the fluorescent lamp specially designed for a museum lighting (FL-EDL: $Ra$96, 3060 K). The four types of test light sources were used in the two experiments, the two fluorescent lamps (FL-EDL: $Ra$96, 3060 K and FL-WW: $Ra$55, 3460 K), and the two LED lamps (LED-RGB: $Ra$21, 3050 K and LED-BY: $Ra$84, 3060 K). LED-RGB composed of the combination of red, green, blue LEDs had the special effect emphasizing saturation of colour. LED-BY composed of blue-LED and yellow phosphor had the effects rendering object colour dull. Table 1 shows the specifications of light sources, and Figure 3 shows the spectral power distributions of the test and the reference light sources. Illuminance of the test side was set at 700 lx and 10 lx respectively at the table top of the booth, and the illuminance of the reference side was fixed at 700 lx.

*Table 1: The specifications of the light sources.*

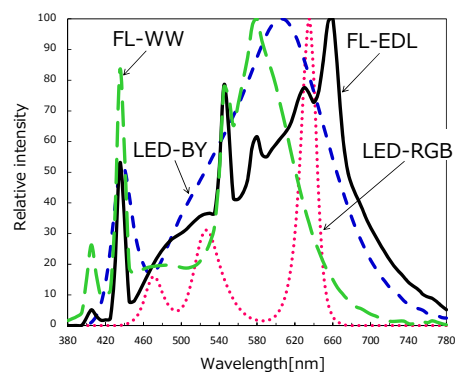| Light sources | | CCT | $Ra$ |
|---------------|---------|------|-----|
| Reference | FL-EDL | 3060 | 96 |
| Test | FL-EDL | 3060 | 96 |
| | LED-BY | 3060 | 84 |
| | FL-WW | 3460 | 55 |
| | LED-RGB | 3050 | 21 |



*Figure 3: The spectral power distributions of the light sources.*

## 2.2 Test colour samples

The seven kinds of the test colour samples (the two-colour pairs, the multicolour sample, the picture samples) were used in the experiment 1 (Figure 4). The test colour samples were categorised in two groups, red-include and red-exclude. The muti-colour sample was made up of the mineral pigments and the gold leaf for Japanease-style arts.
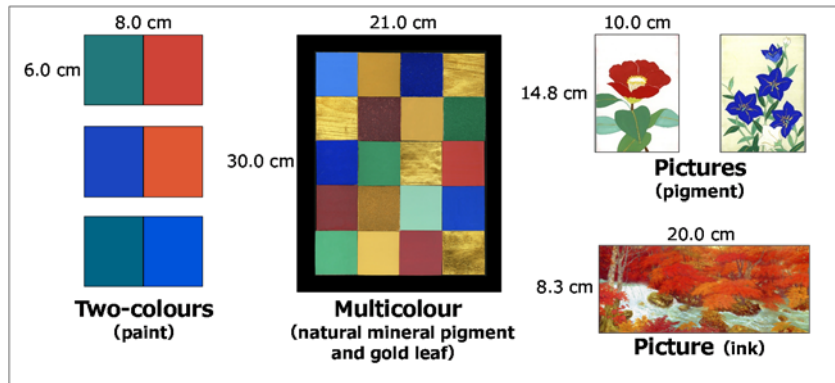


Figure 4: The test colour samples in the experiment 1.

The nine test colour samples were used in the experiment 2 (Figure 5). The original sample (Japanese painting by the artist Meiji HASHIMOTO）was selected by the reason that the sample did not include red at all. The each test sample had the small leaf images (green-yellow-yellow red-orange-red-red purple-blue purple-blue) sprinkled in the original image as addition. The hue angle of the leaf image, the spectral reflectance of the leaf image was shown, and the $a_M b_M$ coordinates (CIECAM02: Colour Appearance Model) was shown in Figure 5, Figure 6, and Figure 7.



| Hue | Original | Green | Yellow | Yellow Red | Orange | Red | Red Purple | Blue Purple | Blue |
|---|---|---|---|---|---|---|---|---|---|
| Image | | | | | | | | | |
| Hue angle | | 133 | 95 | 39 | 28 | 20 | 355 | 347 | 265 |

Figure 5: The test colour samples in the experiment 2.
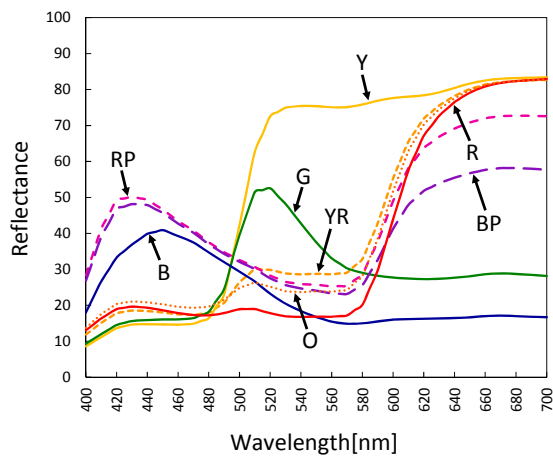


Figure 6: The spectral reflectance of the leaf images.
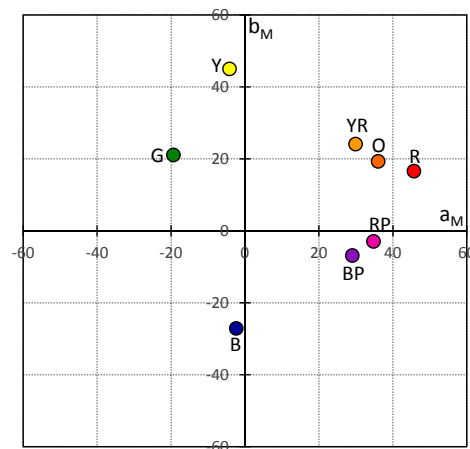


Figure 7: the $a_M b_M$ coordinates (CIECAM02) of the leaf images.

AIC2015 TOKYO - Color and Image

# 3. RESULTS AND DISCUSSION

## 3.1 Results of the experiment 1

Figure 8 shows the subjective evaluation profiles for the colour samples. As shown in Figure 8, the results of the subjective experiment were divided into two groups, the results of the red-include samples and those of the red-exclude samples. In the results of the red-include samples, it was clearly shown that the subjective impression under LED-RGB and those under the other test lamps were different. However in the results of the red-exclude samples, the subjective results were not different for the test lamps.

To examine which colour was most influenced when the observer evaluated the subjective evaluation of the test colour samples, the observer was asked two questions, one was which colour the most attention was when you judged the evaluation, and the other was which colour the most difference from the reference colour was. As shown in Figure 9 (a), the observer's judgement for the most attention colour was "red" regardless of illuminance and the light sources. On the other hand, the observer's evaluation for the most different colour from the reference colour varied by illuminance and the light sources shown in Figure 9 (b). The results suggested that "red" was the most important in colour rendering terms.
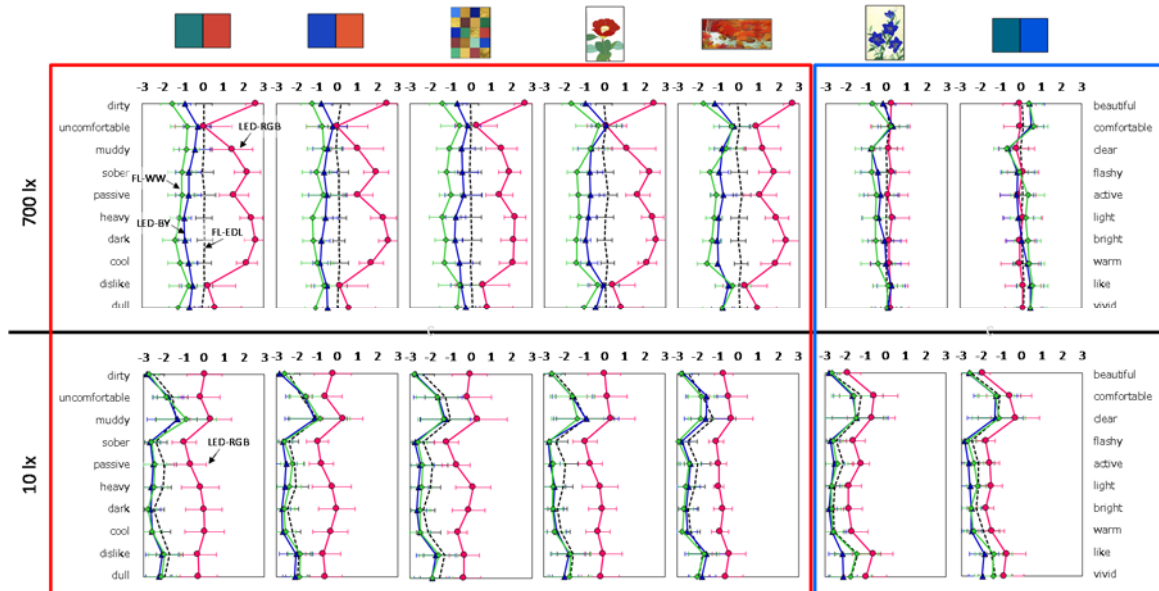


*Figure 8: The subjective evaluation profiles of the colour samples.*



*(a) the most attention color*          *(b) the most different colour from the reference*
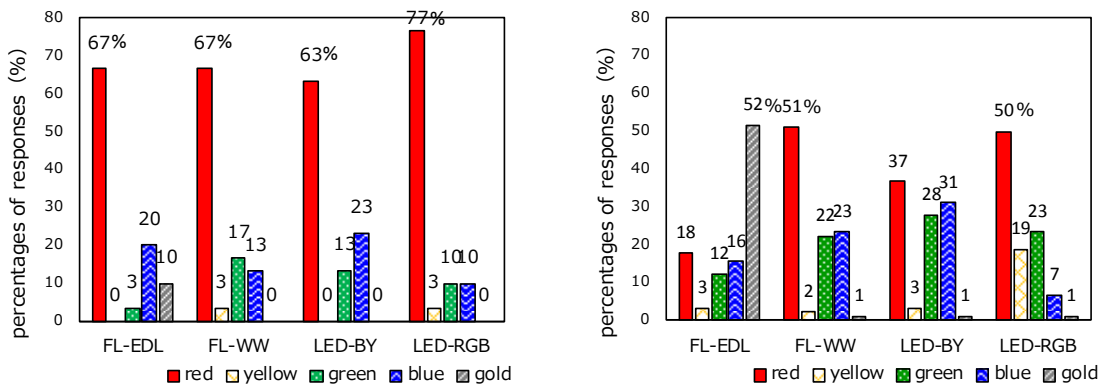
*Figure 9: Percentages of observer's responses to two questions at 700 lx.*

## 3.2 Results of the experiment 2

The evaluation structure when impression of colour samples under various illuminations were sujectively observed was analysed by factor analysis. Factor analysis revealed the two main factors "color quality" and "preference". Figure 10 shows that the relationship between the subjective evaluation results for each factor and the hue angle of the leaf image by CIECAM02, and the relationship between ΔM and the hue angle. ΔM shows the difference between the colourfulness (M) under the test light source and that under the reference light sources. The results of "colour quality factor" were different from those of "preference factor" and it was clearly shown that the subjective impression of "colour quality facor" depended on the hue angle of the test colour, especially had the peak at about hue angle 20° (red) under LED-RGB and LED-BY. On the other hand, in the case of preference factor did not change for the hue angle as well as the test light sources. The results showed that the subjective feelings could be evaluated by "colour quality" of the colour samples such as vividness, brightness, flashyness, clearness and activeness.
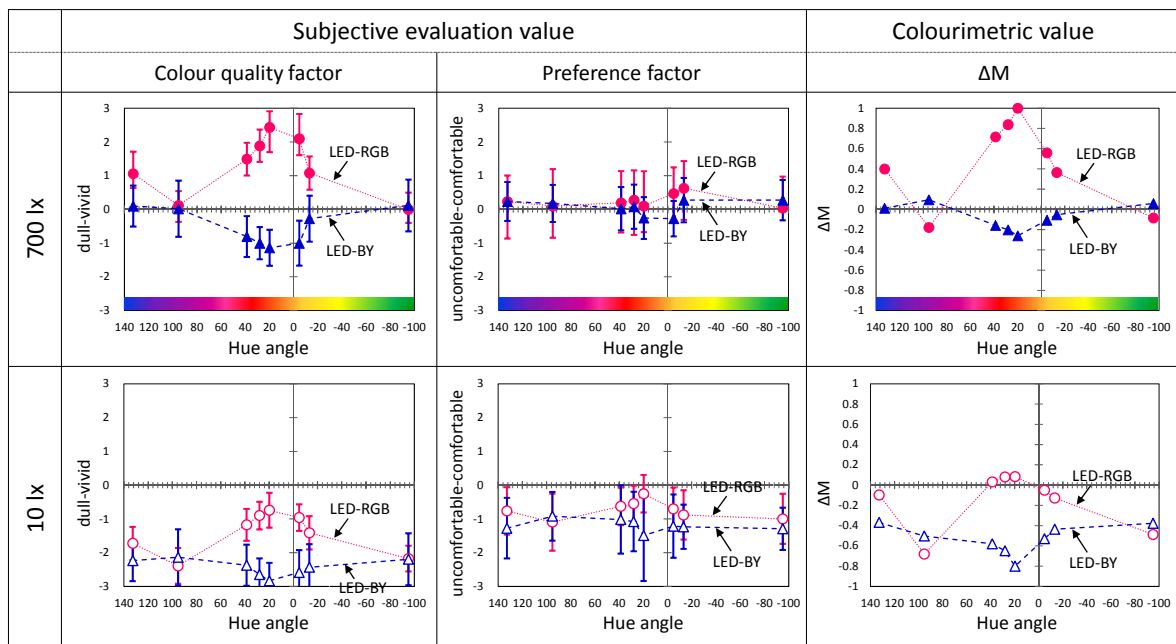


*Figure 10: The relationship between the subjective evaluation results, ΔM and the hue angle.*

As shown in Figure 10, the results of the subjective evaluation of "colour quality factor" were very similar with those of the colorimetric ΔM. It was clearly shown that "colour quality feeling" could be explained by the colorimetric ΔM.

Figure 11 shows that ΔM correlates closely with the subjective evaluation results of colour quality factor. The results suggested that the subjective evaluation results of colour quality factor could predict by ΔM based on colorimetric colourfulness.
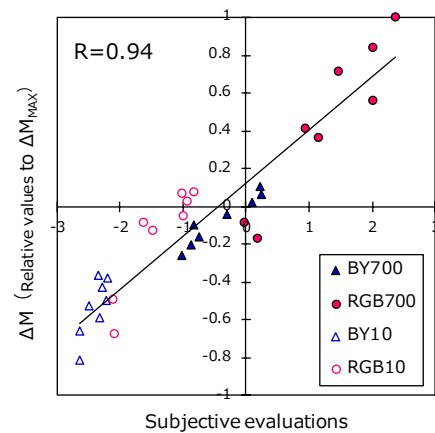


*Figure 11: The relationship between ΔM and the subjective evaluation results.*

### 3.3 Colour Quality Index (Gx and Rxi)

We defined "colour quality index" called Gx and Rxi to evaluate colour rendering properties taking into consideration of illuminance-effects as well as hue-effects based on the subjective evaluation results of the experiment 1 and the experiment 2.

3.3.1 The test colour samples and the reference light source

The saturated 20 colours made by Japan Colour Research Institute were used for the calculation of Rxi and Gx as the test color samples. Figure 12 and Figure 13 show the spectral reflectance and the $a_M b_M$ coordinates of CIECAM02 (FL-EDL, 700 lx).

The reference light source was FL-EDL specially designed for a museum lighting (3060 K, *Ra*96). The illuminance of the reference lighting was set at 700 lx for the calculation.
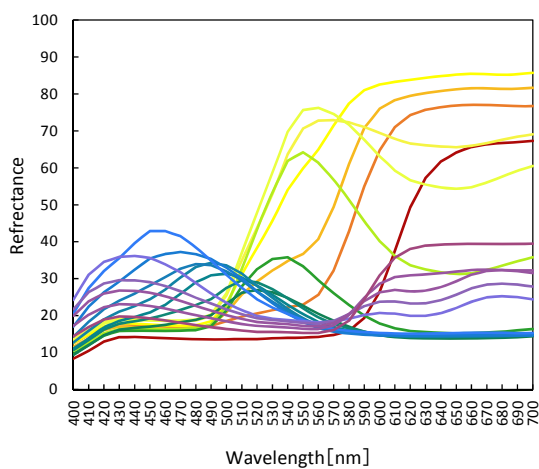


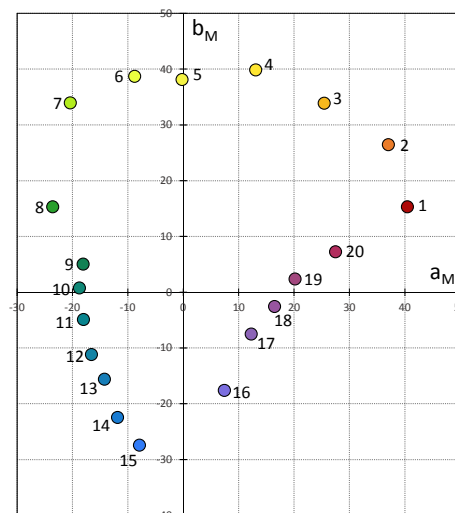*Figure 12: The spectral reflectance of the test colour samples.*



*Figure 13: The $a_M b_M$ coordinates of the test colour samples.*

3.3.2 Rxi

Gx is the colour quality index showing the subjective impression not for the individual test colour, but for the overall test colour samples. Gx is calculated by the ratio between the gamut of the test colour samples under the test light source and the that of the reference light source.

$$\text{Rxi} = 100 + 100 \cdot \left( \frac{M_{iT(E)} - M_{iR(E)}}{M_{iR(E)}} \right) \quad (i=1\sim20) \tag{1}$$

where $M_{iT(E)}$ is M of the test colour sample i under the test light source and any illuminance. $M_{iR(E)}$ is M of the test colour sample i under the FL-EDL and 700 lx.

Figure 14 shows the relationship between the color quality index (Rxi) and the subjective evaluation for colour quality by the experiment 2. These Rxi values were calculated by the test color samples chosen hue angle close to the hue angle of the test color samples (see Table 2). Rxi was correlated to the subjective results (R=0.94).

AIC2015 TOKYO - Color and Image

*Table 2: The hue angle of the test color samples and the leaf images.*

| No of TCS | 8 | 5 | 2 | 1 | 19 | 18 | 15 |
|---|---|---|---|---|---|---|---|
| Hue angle | 147 | 90 | 36 | 21 | 7 | 351 | 254 |

↕

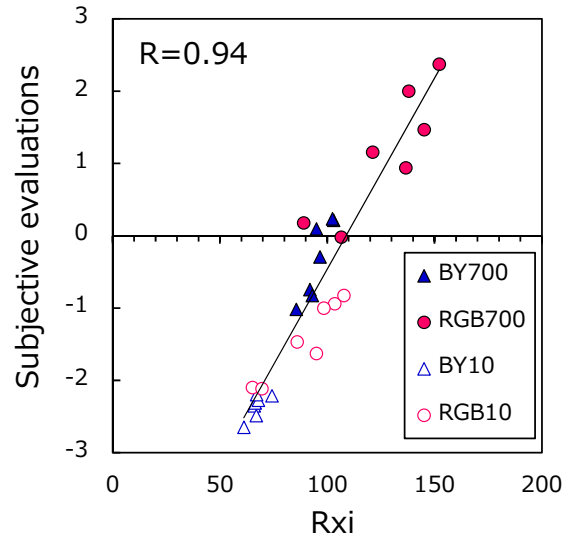| Leaf images | G | Y | YR | R | RP | BP | B |
|---|---|---|---|---|---|---|---|
| Hue angle | 133 | 95 | 39 | 20 | 355 | 347 | 265 |





*Figure 14: The relationship between Rxi and the subjective evaluation results.*

### 3.3.3 Gx

Gx is the colour quality index showing the subjective impression not for the individual test colour, but for the overall test colour samples. Gx is calculated by the ratio between the gamut of the test colour samples under the test light source and the that of the reference light source by Equation 2.

$$Gx = 100 \cdot \left(\frac{G_{T(E)}}{G_{R(E)}}\right) \quad (2)$$

$$a_{xi} = a_{Mi} \cdot W_{hi} \quad (i=1\sim20) \quad (3)$$

$$b_{xi} = b_{Mi} \cdot W_{hi} \quad (i=1\sim20) \quad (4)$$

$$W_{hi} = \frac{R_{xi}}{100} \quad (i=1\sim20) \quad (5)$$

where $G_{T(E)}$ is th gamut area of the test colour samples under the test light source at the illuminance E lx. $G_{R(E)}$ is the gamut area of the test colour samples under FL-EDL at 700 lx. In addition, the $a_M b_M$ coordinates under the test light source were calculated with the weighting coefficient $W_{hi}$ by Equation 3 to Equation 5. $W_{hi}$ was defined at the test colour samples No.1~No.3 (reddish colours), No.9~No.11 (greenish colours)
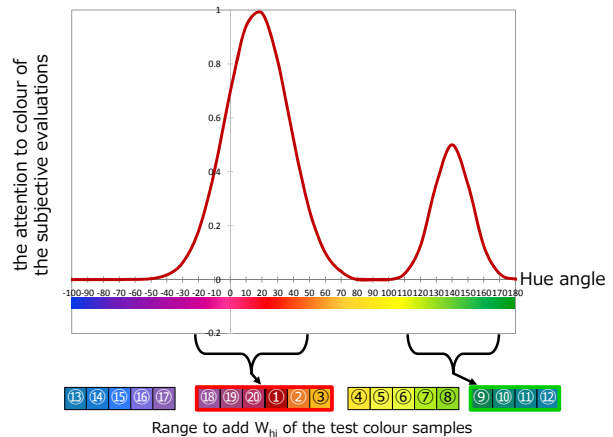


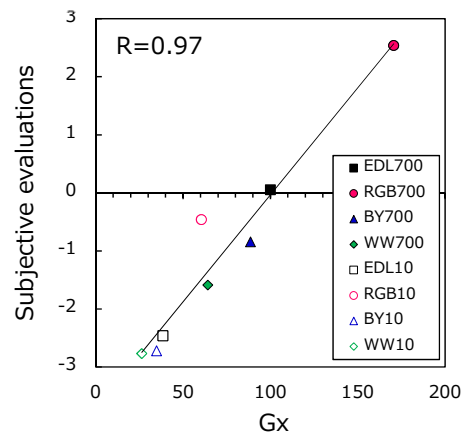*Figure 15: The relationship between the attention colours and the corresponding test colors.*



*Figure 16: The relationship between Gx and the subjective evaluation results.*

and No.18~No.20 (reddish colours) by the hue dependency of the subjective evaluation results as shown in Figure 15.

Figure 16 shows the relationship between Gx values and the subjective evaluation results by the experiment 1.  As shown in Figure 16, Gx correlated very closely to the subjective evaluation results (R=0.97).

## 4. CONCLUSIONS

The colour quality indices Gx and Rxi supplementing *Ra* especially when evaluated at low illuminance were defined to represent the new colour rendering properties which could explain illuminace effects as well as hue dependency of the test colour sample. It was shown that Gx and Rxi correlated to the subjective evaluation of the test colour samples under various light sources. These new indices could be expected to use practically.

## ACKNOWLEDGEMENTS

## REFERENCES

Publ. CIE 157 : 2004. *Control of damage to museum objects by optical radiation*.

Hunt, R.W.G. 1952. *Light and dark adaptation and the perception of colour*, J. Opt. Soc. Am. 42(3) 190-199.

Nakajima, Y. and Fuchida, T. 2013. *Affective evaluation  on  color samples illuminated by LED illumination ～influence of illuminance level*, CIE2013 Paris Conference.

Nakajima, Y. and Fuchida, T. 2014. *Development of a new calculation method of color rendition taking illuminance into consideration*, CIE2014 Malaysia Conference.

Rea, M.S. and Freyssinier-Nova, J. P. 2008. *Color rendering : A tale of two metrics*, Color Res. Appl. 33(3) 192-202.

Wei, M., Houser, K.W., Allen, G.R. and Beers, W.W. 2014. *Color Preference under LEDs with Diminished Yellow Emission*, LEUKOS, 10(3) 119-131.

*Address: Yuki Nakajima, Graduate School of Joshibi University of Art and Design, 1900 Asamizodai, Minami-ku, Sagamihara-shi, Kanagawa, 252-8538, JAPAN E-mails: limesun.yn@gmail.com,  fuchida11001@venus.joshibi.jp*

# Developing Test Targets for Color Management of Full Color Three-dimensional Printing

Yu-Ping SIE,[1] Pei-Li SUN,[1]  Yun-Chien SU,[1] Chia-Pin CUEH,[2] Kang-Yu LIU[2]
[1] National Taiwan University of Science and Technology
[2] Printing Technology Research Institute, Taiwan

## ABSTRACT

To evelate color fidelity of a 3D printer, several targets with different shapes and measurement methods were designed in this research, including Multi-direction Color Target which tests the color on different orientations, TC 2.83 C5 Target which can generate ICC profile rapidly with i1 Profiler, and 729-color Target which is material-saving and it use a DSLR to quickly calibrate its colors. The influence of different surface normals and post-processing methods also have been evaluated. Our experimental results show the color variations of different orientations are noticible and the color accuracy of top direction can be improved by applying 3D color LUTs with interpolation.

## 1. INTRODUCTION

The development of 3D printing technology has accelerated over the past few years (Stanic and Lozo, 2012). However, only few products can make full color models (Xiao, Zardawi, Noort and Yates, 2013). In traditional two-dimensional (2D) printing, color target is applied to estimate the color performance and make color management work. If we apply the same method to 3D printing, some problems will be encountered. For example, 3D printing can produce 3D objects with curved surfaces, which have various surface normals towards different directions (Jackson et. al, 2006). The same RGB input show different colors in different orientations. To optimize its color quality, it's necessary to develop new methods to evaluate the color characteristics of a 3D printer. The efficiency of 3D printing color management must be considered because of high-cost in materials and low-speed in printing.

## 2. METHODS

In this research, several targets with different shapes and measurement methods were designed. Each target was developed based on different purposes including color evaluation of different surface directions, compatibility of commercial color measuring tools such as X-rite i1 Publish Pro 2, evaluating colors and generating ICC profile (ICC, 2012) with limited material and process time.

### 2.1 Target Design

**Multi-direction Color Target** is designed to estimate color performance of surfaces in 26 directions (Figure 1). The target is combined with 13 pieces in different surface directions, like a puzzle, and each piece has two sides with several color patches on it. The biggest piece, which is printed on top and bottom, has 225 color patches for general color management. The 225 colors consist of 6-level RGB and 9-level grayscale. The other pieces have 4 or 14 color patches and can represent the color differences in various surface

AIC2015 TOKYO - Color and Image

normals. 4 pieces are consist of CMYK colors, and they are rotated for evaluating the color quality of 8 corner directions. 8 pieces of 14-color patches are consist of CMYKRGB primary colors and mid-tone CMYKRGB colors, and they are rotated for evaluating the color quality on 16 different directions, including front, back, right, left, and other 45 degrees oblique angle directions. The size of each color patch is 9×9 mm$^2$, and each pecies has 4.5 mm interval. The target can be measured by X-Rite i1 Publish after combined the 26 pieces in a correct order. In our model, the target is designed as a puzzle. Each piece has a unique shape to avoid mistakes in combining the pieces.
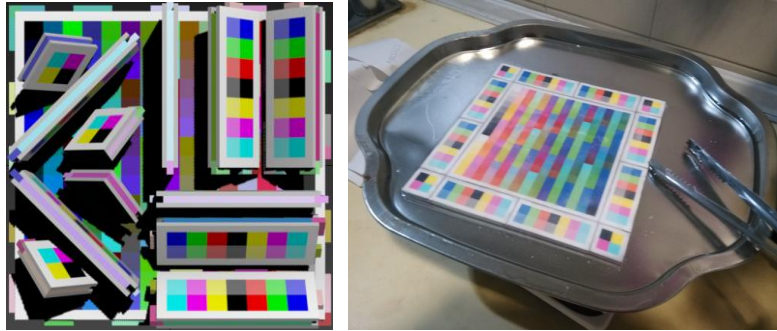


*Figure 1: Multi-direction Color Target. The left figure shows the arrangement of each pieces in modeling software Autodesk 3DsMax. Each piece is arranged to face particular direction. The right figure shows a real target after the assembling.*

TC 2.83 C5 Target was designed by X-rite. It is a RGB-based test chart, which arranged 283 color patches in C5 size and can be measured by X-Rite i1 Pro 2 spectrometer with a handheld scanning ruler and generates ICC profile rapidly and simply.
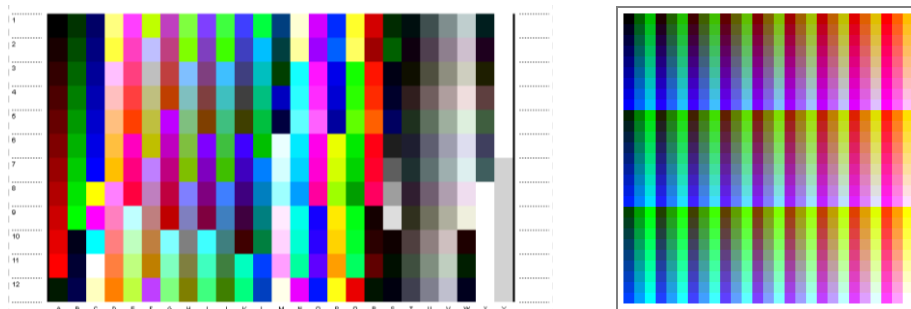


*Figure 2(left): TC 2.83 C5 Target. Figure 3(right): 729-color Target. Both height and width of the target are 10 cm. The color patch set in RGB values from top-left to bottom-right is (0, 0, 0), (0, 0, 31), (0, 0, 63)…, (255, 255, 223) and (255,255,255), which is a set of 9-level RGB values. The size of each color patch is 0.35 × 0.35 cm.*

729-color Target has 729 color patches in small area (10x10 cm). 729-color patches are consist of 9-level RGB colors, which is proper to RGB printer. It designed to be a material-saving target. However, because of the size of color patches, it cannot be measured directly by any spectrophotometer. Thus, it is necessary to design a process to measure the color patches by a calibrated DSLR camera. Taking a photo of the target and ColorChecker passport in a viewing booth simultaneously, the RGB values in particular light source can be read and applied to color management.

## 2.2 Modeling and Printing

The targets was modeled with Autodesk 3DsMax. The models are exported into VRML format and attached with PNG files for texture mapping, which are supported by 3D

Systems Projet 460 Plus Color 3D printer. The printer support RGB 3-channel color input and have CMY inkjet heads to print full-color 3D model. All of the glue-jet and the material of model which is gypsum-like powder are made by 3D Systems. The color inkjet heads are provided by HP.

## 2.3 Post-Processing

The models printed by Projet 460 Plus still need post-processing to enhance the purity of color and strength of material. To investiage the differences between various post-processing methods, some often-used coating material like Color-bond™, salted water, and paraffin wax were tested. These post-processing methods are detialed as follows:

The processing of Color-bond™ is to coat some "z-bond 90" on the model. The liquid infiltrates the model and coagulates. It is the most recommented method of post-processing because it can make the 3D model stronger and more colorful. To make sure that the color patches won't be influented by hand processing, we skipped scrubbing the targets by sandpaper which is a often-used process to make model surface flatter and more colorful.

Salted Water post-processing is also recommented. To make salted water, it is need to mix up epsom salt and water with 1:6 ratio. Spray  salted water on the model and wait for it to be dried. The process called "Water Cure." The material become weak after sprayed salted water, so it is necessary to put the model carefully before it dried.

Paraffin Wax is also a material for post-processing, which is cheap and has good color performance. To melt the paraffin wax, it is needed to heat it until 60 to 70 degrees. Put the model into melted paraffin wax to infiltrate the model. Take the well-infiltrated model out and wait for cooled. The model will be a little swallowed after processed, but doesn't make influence on color measuring.

# 3. RESULTS AND DISCUSSION

To evulating the color performance of 3D printer, we made some process to measure the color patches for every targets we designed. For Multi-direction Color Target and TC 28.3 C5 Target, we used X-rite i1 to measure the color patches. The color differences between different surface normals were found to be visible by human eyes. We also tested 3 kinds of post-processing methods including Color-bond™, salted water and paraffin wax using the Multi-direction Color Target.

For the color patches on 729-color Target, we designed a process to obtain the CIELAB values of 729 color patches from measured spectra or XYZ stimulus data of ColorChecker and RGB image taken with camera in the light booth. For building an ICC profile for 3D printer with a fast and materal-saving method, we developed a program to make a 3D Look-Up-Tables (LUTs) for 729-color Target. To evaluate the LUTs, we read the B2A1 and A2B1 tables generated by i1 Profiler using TC 2.83 C5 Target. Both the TC 2.83 C5 Target and 729-color Target are Color-bond™ processed.

## 3.1 Color Difference across Different Orientations

For the Multi-direction Color Target, which combined 13 pieces, can be measured by X-rite i1. We also can connect X-rite i1iO and set patch numerial as 21 by 21 array to measure all of them automatically. After we measured the spectra for every color patches,

we divided the color patches into 26 groups, which represent different surface direction. Calculating the XYZ values from spetral data with ASTM D50 Veneble sheet, the color patches on the target can be evaluated.

To analyze color difference on different surface normal, we regard the color patches on top (+z direction) surface as the standard color and compare the color differences of the other color patches with the same RGB inputs. Figure 4 shows the average color differences on each surface normal and average differences on L*, a* and b* in the Color-bond[TM] post-processed Multi-direction Color Target. Figure 5 compares color differences between CMYK colors. The mean and maximum color difference is up to 6.71 and 22 $\Delta E_{00}$ (CIE, 2012) respectively, which is noticible by human eyes. Color differences on different surface normal are mostly depended on the differences of lightness, and happened in black color which mixed by equal amount of cyan, magenta and yellow inks. The differences were caused by many different sources, such as moving direction of inkjet heads, asporbsion of the powder, dust, and force of gravity. Color image quality of 3D printing can be improved if we take the color variations across different orientations into account.
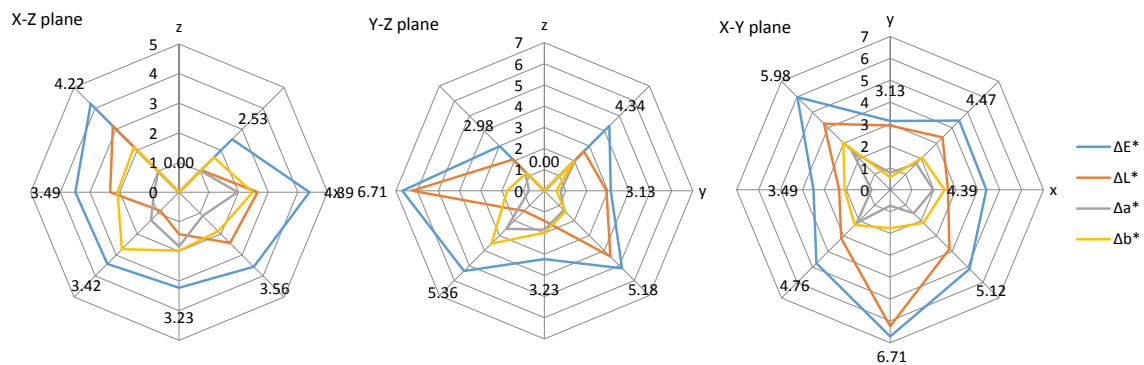


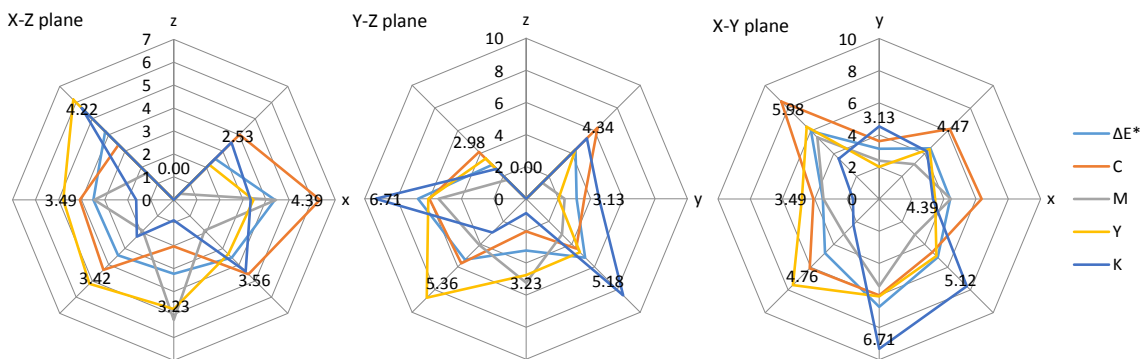Figure 4: Average color differences on each surface normal and average differences on L*, a* and b*.



Figure 5: Average color differences on each surface normal and color differences on CMYK colors.

## 3.2 Color Difference on different post-processing method

Post-processing plays an important role on not only material strength but color performance. To compare the effects of post-processing, we printed 4 sheets of Multi-

direction Color Target and applied non-post-processed, Color-bond^TM, salted water and paraffin wax respectively. Figure 6 shows the color differences between CMYKRGB colors in sRGB color space and printed target. Color performance on non-post-processed target is pale, while post-processed targets show better color density. Paraffin wax processed target has similar effect with Color-bond^TM. It means we also can get good color quality with the low-cost method.
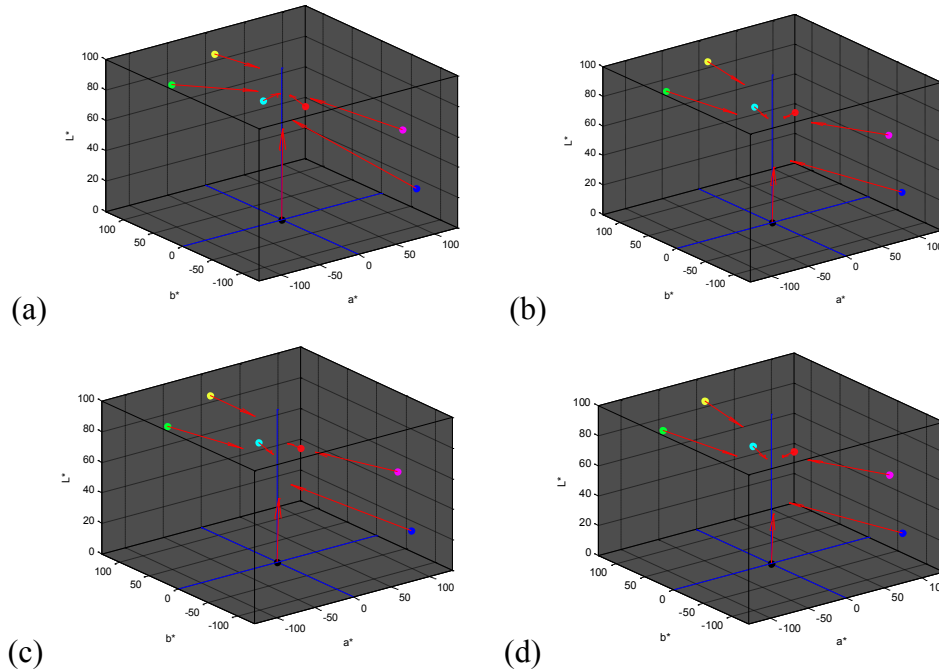


*Figure 6: Color difference of CMYKRGB colors in (a) non-post-processed, (b) Color-bond^TM, (c) salted water and (d) paraffin wax.*

### 3.3 Build look-up-tables with 729-color Target

The method to measure color patches from 729-color Target was different with the other targets. We put the target and a ColorChecker Passport into a light tooth (SpectraLight III) under D65 light source, and took a RGB photo with digital camera Canon EOS 5D Mark II (Figure 7a). The spectra or XYZ stimulus data of 24 colors on ColorChecker Passport were measured by Topcon SR-UL1R spectrometer.
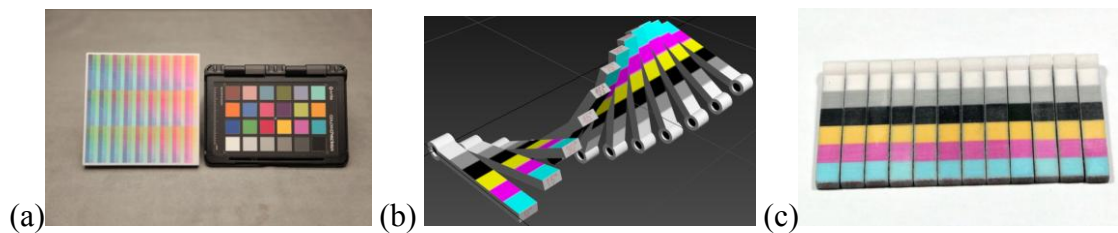


*Figure 7: (a)729-color Target with ColorChecker Passport under SpectraLight III light booth.(b)3D model of Multi-angle Color Target. (c) Visual Comparison of target (c).*

The purpose of measuring the color patches is to build an ICC Profile for 3D printer. Reading the RGB values of 729 colors from the target and 24 colors from the ColorChecker, the XYZ stimulus values of 729 color patches can be calculated by a polynomial regression with the measured spectra or XYZ stimulus data of 24 colors on

ColorChecker Passport and transform into CIELAB color space. We made a BtoA1 LUTs (Lab to RGB) in ICC profile from the LAB values of 729 color patches, and calculated the inverse LUTs as A2B1 (RGB to Lab) with tetrahedral interpolation. Applying the LUTs to colors in gamut of 3D printer, we can obtain similar output colors as the LUTs in ICC profile generated via TC 2.83 C5 Target. The mean and maximum color errors for the top surface were 2.8 and 9.5 $\Delta E_{00}$ in its in-gamut inverse transform. It is much better than no color management where the mean and maximum errors were 11.5 and 30.8 $\Delta E_{00}$ respectively.

We also developed some other test targets for evaluating image and object quality of a color 3D printer. Figure 7b is an example. The Multi-angle Color Target is printed in 12 different angles. Once we put all 12 pieces together, the user can visually compare the difference of CMYKGy primary colors in different printing angles (see Figure 7c).

## 4. CONCLUSIONS

In this work, we developed 3 types of test targets to evaluate color performance of a 3D printer. It was found that color performance changes along with different surface directions and post-processing methods. We also built ICC-based 3D LUTs in a material-saving way. Establishing different processes for 3D printing is important to make color management well and efficiently. In the future, we can keep on finding other factors which cause color differences in 3D printing, and make a complete color management system for 3D printers.

## ACKNOWLEDGEMENTS

## REFERENCES

CIE Central Bureau, Vienna 2012. *Colorimetry – Part6: CIEDE2000 colour-difference formula,* CIE DS 014-6/E:2012

Jackson R. et al. 2006. *Methods and Systems for Producing a Desired Apparent Coloring Through Rapid Prototyping,* EU patent, EP#1558440-B1

ICC, *Specification ICC.1:2010. Image technology colour management — Architecture, profile format, and data structure,* International Color Consortium.

Stanic, M. and B. Lozo, *Color and Permance Issues in 3D Ink-jet Printing,* MIPRO2010

Xiao, K., Zardawi, F., Noort R. and Yates, J. M. 2013. *Development of Skin Colour Reproduction using 3D Colour Printing*, 12th International AIC Congress, 1805-1808.

*Address: Yu-Ping SIE, Graduate Institute of Color and Illumination Technology,*
*National Taiwan University of Science and Technology,*
*43, Section 4, Keelung, Taipei, 10607, TAIWAN*
*E-mails: m10225006@mail.ntust.edu.tw*

# The Effect of Training Set on Camera Characterization

Semin OH,[1] Youngshin KWAK[1], Heebaek OH[2]

[1] Human and Systems Engineering Department, Ulsan National Institute of Science and Technology

[2] Aclover Co. Ltd

## ABSTRACT

It is well known that the performance of the camera characterization model is strongly affected by the training set used to extract the model parameters. In this study, the effect of training color types (color paper vs. LCD monitor) on the camera characterization model performance is investigated. As training sets, 'Patch set' and 'Monitor set' were prepared. For 'Patch set', 114 color patches in Macbeth Colorchecker and Gretagmacbeth Colorchecker-SG chart were displayed in the viewing booth illuminated with D65 simulator and each color was measured with spectroradiometer and also with the camera. In the case of 'Monitor set', 150 colors were shown on the wide-gamut LCD monitor in a dark room covering around Adobe RGB color gamut. Similar to 'Patch set', each color was measured using a camera and the spectroradiometer at the same position. The performance test results showed that each model predicts the training data set well but the performance is significantly deteriorated when different type of data set was used. This result clearly indicates that the observer metamerism between CIE standard observer and camera sensors should be considered when three channel camera is used to measure color.

## 1. INTRODUCTION

These days there are many attempts to use a camera as a color measurement device, which requires camera characterization model. It is well known that the performance of the camera characterization model is strongly affected by the training set used to extract the model parameters. Training sets used in previous researches mostly consisted of paper-based colors (Kobus and Brian 2001; Vien et al 2004; Vien and Stephen 2005). However, if monitor colors are used as a training set, more various colors with high chroma can be generated to characterize a camera. In this study, the effect of a training set on the camera characterization model performance is investigated by using two different training sets, 'Patch set' and 'Monitor set'.

## 2. METHOD

For all measurement, Toshiba Teli CCD camera was used. Its resolution is 1280x960 and camera gamma was fixed to 1. For the comparison with camera measurement value, spectroradiometer CS-2000 was used. As a camera characterization model, simple 3x3 matrix was used since the camera RGB values showed the linear relationship with the luminance of the measured color.

As training sets, 'Patch set' and 'Monitor set' were prepared. For 'Patch set', 114 color patches in Macbeth Colorchecker and Gretagmacbeth Colorchecker-SG charts were shown

in the viewing booth illuminated with D65 simulator and each color was measured with spectroradiometer and also with the camera. Below figure shows the measurement settings for 'Patch set' (Figure 1). The illuminance in the center of viewing booth was 1090 lux and luminance of reference white was 278.22 cd/m$^2$. The chromaticities of the color patches were mostly distributed within the range of sRGB gamut (Figure 3a).



*Figure1: Measurement settings for 'Patch Set'.*

In the case of 'Monitor set', 150 colors were shown on the wide-gamut LCD monitor in a dark room covering around Adobe RGB color gamut (Figure 3b). The luminance of the peak white was 262.74 cd/m$^2$. Similar to 'Patch set', each color was measured using a camera and the spectroradiometer at the same position. Figure 2 shows the measurement settings for 'Monitor set'.
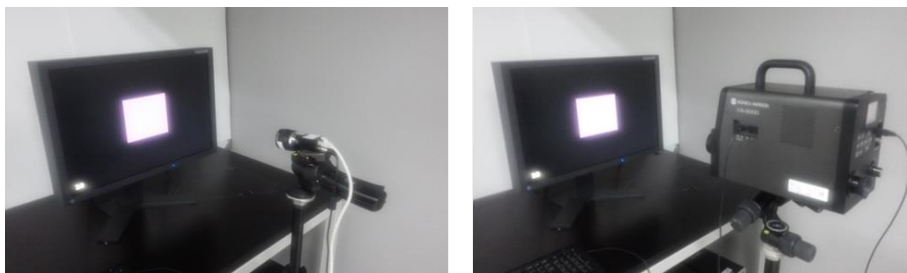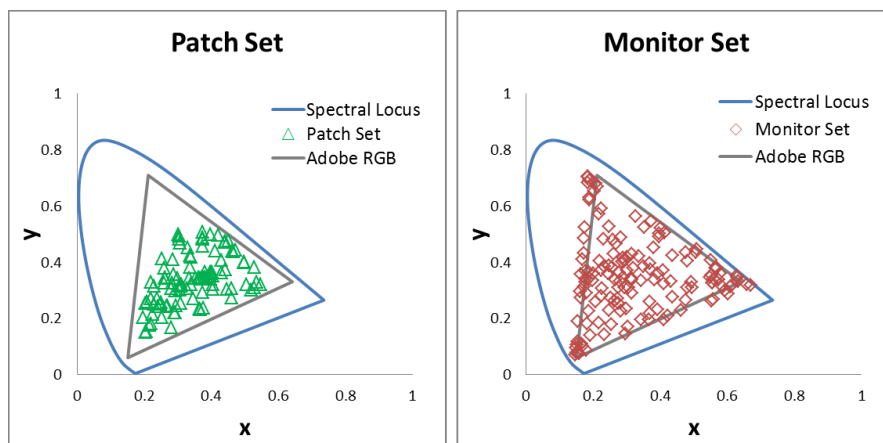


*Figure2: Measurement settings for 'Monitor Set'.*



(a)        (b)

*Figure 3: Chromaticity coordinates of '(a) Patch Set' and '(b) Monitor Set'*

# 3. RESULTS AND DISCUSSION

To optimize the model parameters, 'Patch Set' and 'Monitor set' were used seperately by minimizing the CIELAB $\Delta E^*_{ab}$ values between the measured and the predicted CIELAB values. For CIELAB calculation, the white color in the viewing booth was used as the reference white since that color showed the highest luminance. Then, the performances of two camera characterization models obtained using two different data set were evaluate using the same data sets.

*Table 1. the Performance Test Result.*

| $\Delta E^*_{ab}$ | Patch Model | Monitor Model |
|---|---|---|
| Patch Set | $1.38 \pm 1.22$ | $11.48 \pm 11.08$ |
| Monitor Set | $13.58 \pm 12.14$ | $4.05 \pm 2.24$ |

As shown in Table 1, each model predicts the training data set fairly well but the performance is significantly deteriorated when different data set was used. This result implies that the type of color stimuli − color paper or monitor color − affects the camera characterization model's significantly.

To evaluate the effect of type of the color stimuli more directly, trisimulus values of MCC chart colors except neutral colors were reproduced on the monitor and then measured using both the camera and the spectroradiometer. Figure 4 compares the spectrums of 'Patch Set (MCC)' and 'Monitor Set (MCC)'. The CIELAB color difference between the patch and the monitor was around 1.5 $\Delta E^*_{ab}$. Therefore the main difference between two data sets was the spectral characteristics not the tristumulus values XYZ.
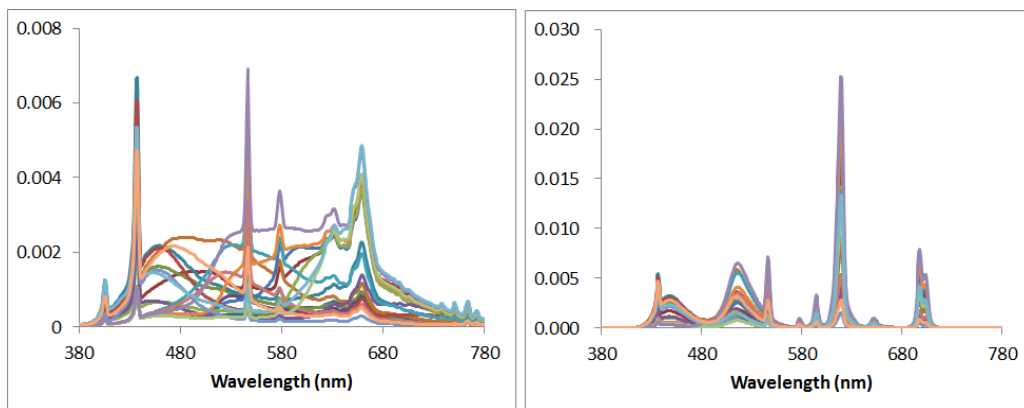


*Figure 4: Spectrum of 'Patch Set (MCC)' and 'Monitor Set (MCC)'*

To visualize how the CIE standard observer and the camera tested in this study see the test colors differently, chromaticity coordinates, xy and rg, were calcuated using CIE XYZ and camera RGB values. As shown in Figure 5, RGB values are very different between two data sets while XYZ values are similar to each other. It clearly indicates that the observer metamerism should be seriously considered when three channel camera is used to measure color.
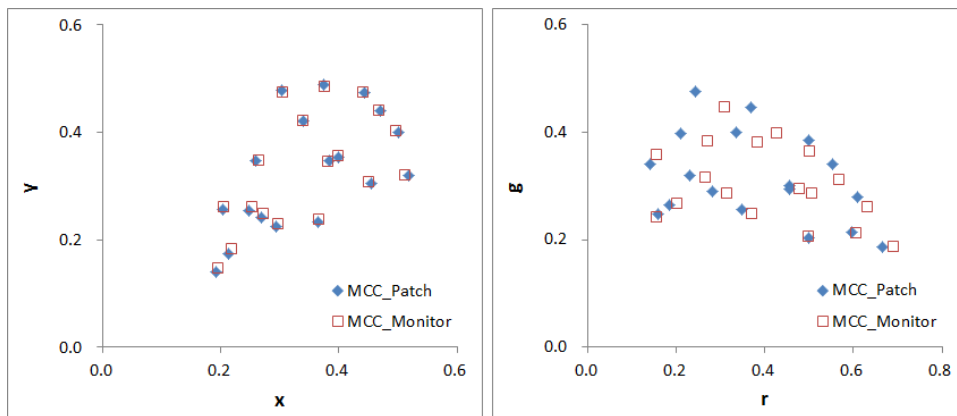
AIC2015 TOKYO - Color and Image

*Figure 5: CIE xy and Camera rg chromaticity coordinates of 'Patch Set (MCC)' and
'Monitor Set (MCC)'*

## 4. CONCLUSIONS

The effect of training color types (color paper vs. LCD monitor) on the camera characterization model performance is investigated. As training sets, 'Patch set' consisting of 114 color papers and 'Monitor set' consisting of 150 colors generated using LCD monitor were prepared. Then each color was measured using a camera and the spectroradiometer at the same position to develop the camera characterization models.

The performance test results showed that each model predicts the training data set fairly well but the performance is significantly deteriorated when different data set was used. This result indicates that the observer metamerism between CIE standard observer and three channel camera sensors is quite serious. Therefore, different camera characterization model should be used depnding on the spectral characteristics of data sets.

## REFERENCES

Kobus Barnard and Brian Funt 2001. *Camera Characterization for Color Research*, Color research and application 27(3) 152-163.

Vien Cheung, Stephen Westland and Mitch Thomson 2004. *Accurate Estimation of the Nonlinearity of Input/Output Response for Color Cameras*, Color research and application 29(6) 406-412.

Vien Cheung and Stephen Westland 2005. *Characterization of trichromatic color cameras by using a new multispectral imaging technique*, Journal of Optical Society of America A 22(7) 1231-1240.

*Address: Prof. Youngshin Kwak, Human and Systems Engineering Department
UNIST, Banyeonri, Eonyangeub, Uljugun, Ulsan, SOUTH KOREA
E-mails: smoh@unist.ac.kr,yskwak@unist.ac.kr, ohb@aclover.co.kr*

# Reproducing the Old Masters:
# A study in replicating dark colours with inkjet printing

Melissa OLEN,[1] Joseph PADFIELD[2]

[1] Centre for Fine Print Research, University of the West of England

[2] Scientific Department, The National Gallery, London

## ABSTRACT

This paper presents work carried out to extend the available range of printable dark colours by incorporating the use of alternative direct channel and multiple pass printing techniques not usually employed within current inkjet printing workflows. These methods aim to improve the colour match between the colours measured within printed reproductions and those measured within paintings in the collection of the National Gallery, London. For this study, a number of colour measurements were taken from the dark paint passages of one particular National Gallery painting, *The Supper at Emmaus*, by Michelangelo Merisi da Caravaggio. Reproductions of the painted colours were printed using the alternative printing techniques, along with traditional inkjet print reproduction workflows. The colour of various printed reproductions were then measured and compared with the original measurements taken from the painting. The results of this comparison show that the proposed alternative direct channel and multiple pass printing techniques are capable of producing a range of dark colours which more closely matched the original paint passages.

## 1. INTRODUCTION

One of the major difficulties in producing inkjet reproductions of Old Master paintings is the accurate replication of the colours found within dark paint passages. Reproducing these very dark colours is normally achieved by mixing the available coloured inks with high proportions of black. However, this high concentration of black ink tends to dominate the printed passages, leading to a smaller perceivable gamut of printed dark colour and the original subtle variations seen in the painted colours being perceptively lost. Reproducing the colour of dark paint passages in old master paintings, using inkjet printing, can be very difficult. Limited sets of inks and media obviously restrict the print process in its ability to replicate the vast number of colours and surface qualities observed in paintings.

In order to investigate the practical application of direct channel and multiple pass printing methods described in previous research undertaken by the authors (Olen, Padfield, & Parraman 2014), this paper examines how well a selection of colours measured from a suitable target painting in the National Gallery, London, can be reproduced. Containing a range of dark paint passages, *The Supper at Emmaus*, by Michelangelo Merisi da Caravaggio, was chosen as a target painting for this research. While difficult to accurately print, the colours in the dark paint passages of this target painting can be easily distinguished under normal viewing conditions. This paper presents measurements and evaluation of the alternative printing methods based upon six of the measured paint passages. This research aims to investigate the potential benefits of incorporating these alternative printing techniques into future reproduction workflows, expanding the available gamut of darker colours and improving the overall colour accuracy of inkjet printing in fine art reproduction.

## 2. METHOD

For this evaluation measurements were gathered from both the target painting, *The Supper at Emmaus*, and from a series of colour patches printed using a Canon iPF8400 multichannel inkjet printer.

To ensure the safety of the target painting and to avoid disrupting public access the colour measurements needed to be carried out before the National Gallery opened, utilising a Konica Minolta CS1000a Spectroradiometer, which allowed for measurements to be taken without touching the surface of the painting.

Alternatively, measurements of prepared colour charts, produced with the Canon inkjet printer, could be taken outside of the public galleries using a handheld X-Rite i1Pro spectrophotometer, allowing for faster measurement of many more patches. Testing and analysis was undertaken to ensure consistent and comparable results were achieved with both devices.

### 2.1 Measurement of Target Painting

For each measurement, the spectroradiometer was placed on a tripod directly in front of the painting, roughly perpendicular to the surface and a portable D50 light bank was placed to the side at an approximate forty-five degree angle. For each sampled area a white control measurement was taken of a white calibration tile before and after the actual colour measurement. This allowed the measured spectral reflectance of the colour to be divided by the averaged whites in order to obtain an illuminant independent measurement. The six colours sampled from the Caravaggio target painting include the red in Christ's drapery, the green of his disciple's shirt, the blue in the pitcher on the table, and a sample of the black, yellow, and red in the table cloth. The location of each measurement is depicted by a white dot in Figure 1.



*Figure 1: Location identification of each colour measurement taken of Michelangelo Merisi da Caravaggio's 'The Supper at Emmaus.'*

### 2.2 Experimental Procedure for Matching Inkjet Colour

To evaluate the capabilities of the Canon inkjet printer using direct channel and multiple pass printing capabilities the authors first designed a custom colour chart composed of a range of near neutral dark colours. The Canon printer was selected for the study, controlled with the Caldera VisualRIP+, with which the cyan, magenta, yellow, red, green, blue, and

black ink channels can be controlled independently. Whilst the printer can use all seven channels to generate a single colour, to keep the number of reference samples manageable for this study the chart was limited to include up to three colours, plus black. For each four colour combination, variations were included where each colourant, or a set of two colourants, decreased in coverage in ten percent intervals. While the chart did not sample the entirety of the shadow region of the printer's gamut, it provided close approximations from which further refinement could be applied. In total the chart consisted of 2,290 colour patches, each with a unique colourant combination. This chart was printed in multiple passes through the printer, where one colour was printed onto the paper with each pass. In this instance, the sequence in which the colours were printed was kept consistent for all patches.

The spectral reflectance curves of all of the 2,290 reference patches were compared with the spectral reflectance curves measured for the six paint passages. Using the adjusted spectral reflectance of the painting measurements as reference, the root-mean-square (RMS) error for each of the patches was calculated, as this method has been shown to be an accurate measurement of spectral differences (Viggiano 2004). This allowed for the identification of the closest approximation that best replicated the spectral distribution of the reference colour. Table 1 depicts the colourants, and their percentage of coverage, present in the patches with the smallest deviation from each of the sampled painting colours. Several of the colourant combinations follow the common approach of subgrouping colourants using only analogous colours (Sharma 2003: 370), such as the red drapery of Sample 1, which contains magenta, red, and black. However, in the case of sample 3, the blue pitcher, the calculations identified the colour patch containing both cyan and red as having the best approximation. While this reflectance was later found to have a spectral redundancy to a combination of unequal percentages of CMYK, it was also noted that redundancies do not occur for all non-analogous subgroupings. Therefore the data set continues to employ triadic and analogous-complimentary subgroupings where the selected colourants span across the gamut.

*Table 1.Percentage of ink colourant combinations for approximate colour matches.*

| Sample | Cyan | Magenta | Yellow | Red | Green | Blue | Black |
|---|---|---|---|---|---|---|---|
| 1 : Red Drapery | | 70 | | 100 | | | 100 |
| 2 : Green Shirt | | | 80 | | 80 | | 100 |
| 3 : Blue Pitcher | 70 | | 100 | 70 | | | 100 |
| 4 : Black in Cloth | | | | 50 | 50 | | 100 |
| 5 : Yellow in Cloth | | | 60 | 60 | | | 100 |
| 6 : Red in Cloth | | 40 | | 100 | | | 100 |

For comparative analysis a smaller chart was also prepared containing the six reference measurements from the painting converted to L*a*b* colour values. This chart was printed four times following suggested, as well as common, colour management workflows using custom ICC profiles. Two were printed using the control of Adobe Photoshop and the Canon printer driver, and two were processed through the Caldera VisualRIP+ using its CMYKRGB mode. For each of these two workflows, one set of prints was produced using the absolute colorimetric rendering, as recommended by Frey and Farnand (Frey & Farnand 2011) for cultural heritage reproduction, and the second set was printed using

perceptual rendering, which is typically found useful for images requiring a remapping of the dynamic range to maintain detail information (BS ISO 15076-1:2010).

## 3. RESULTS AND DISCUSSION

The spectral reflectances of the collected painting references, direct channel / multiple pass print, and colour managed samples can be seen in Figure 2. For all six of the samples the method of direct channel / multiple pass printing produces a better match to the reference than the colour managed print samples. While this is partially to be expected due to the potential limitations of a colorimetric workflow compared to a spectral one (Morovič et al. 2012), it can be further attributed to the direct channel / multiple pass method's ability to produce colour that is unattainable through the current implementation of either of these workflows. With the ability to apply colours in layers, the direct channel / multiple pass method generates a higher density in the final colour output, which can be seen here as the method's spectral reflectances fall below the other inkjet printed samples. Furthermore, the ability to utilise non-customary combinations of colourants allows for increased control over the hue for each of the dark samples, creating a closer approximation to the reference measurement from the painting.
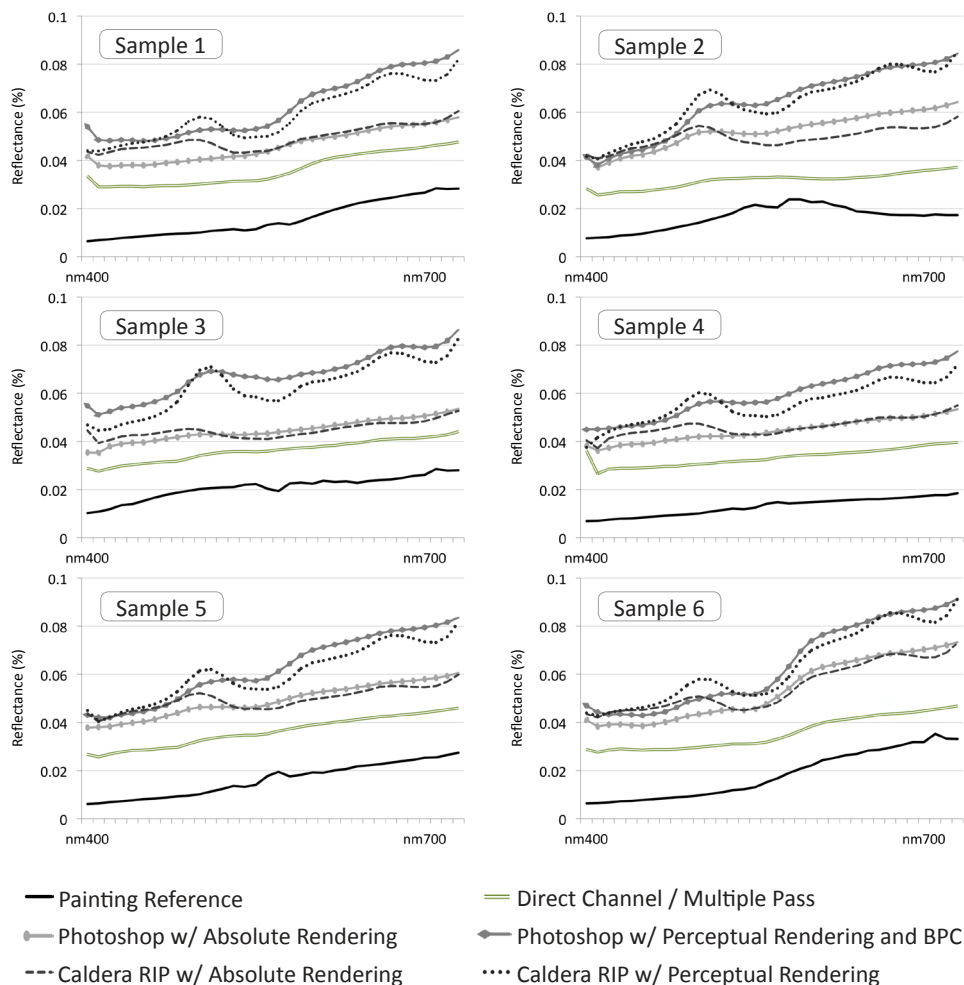


*Figure 2: Spectral reflectances of direct channel / multiple pass print and colour managed samples shown against the reflectances of the painting for all six sampled colours.*

Calculation of the root-mean-square error between the reference measurement of the painting and the printed samples shows that the direct channel / multiple pass printing method outperforms the colorimetric workflows more significantly in some cases compared to others, as can be seen in Figure 3. In the instances of Samples 1 and 3, the difference between the direct channel / multiple pass print and the colour processed through Adobe Photoshop and the Canon printer driver with absolute colorimetric rendering are relatively small, especially when considering the RMS error present in the direct channel / multiple pass method. However, when considering the overall improvement in colour reproduction, the benefits of this printing method can be seen.
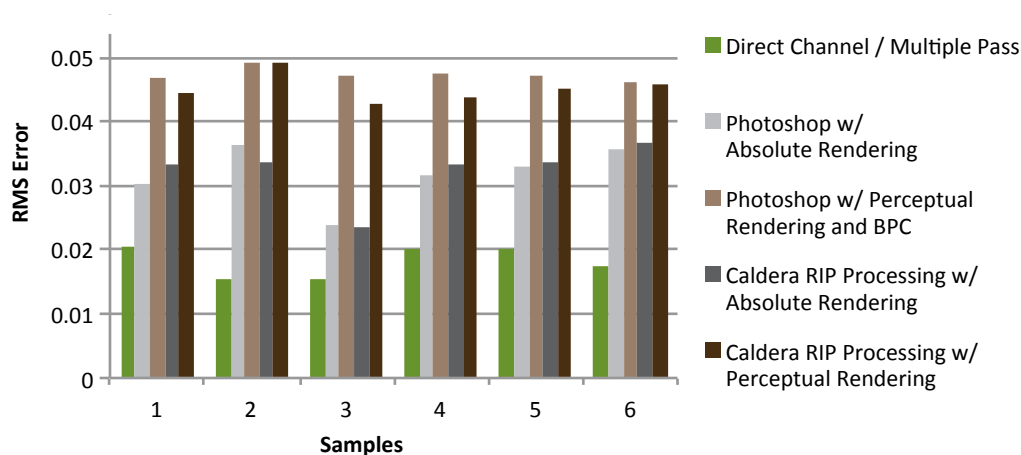
*Figure 3: Chart of root mean square errors against painting reference measurements.*

## 4. CONCLUSIONS

In this paper a working method has been shown for evaluating the capabilities of direct channel and multiple pass printing to better reproduce colours in the dark passages of Old Master paintings, using Caravaggio's *The Supper at Emmaus* as an example. It has also been shown the direct channel / multiple pass print method obtains increased colour accuracy compared to common colorimetric workflows, and achieves greater density and spectral distribution.

While the results of this study are promising, further research and refinement of this process is required. The data set in the test colour chart is limited and would benefit from a secondary search of more closely related colour patches. Also, the greatest discrepancy between the adjusted spectral reflectance from the painting and the colour reproduction is in the darkness of the colour. Limitations of the substrate used in the study could have attributed to the inability to achieve the same dark values as the original painting. Further investigation into alternative media and/or varnish coatings will be beneficial.

## ACKNOWLEDGEMENTS

AIC2015 TOKYO - Color and Image

# REFERENCES

Olen, M., Padfield, J., and Parraman, C. 2014. *Reproducing the old masters: applying colour mixing and painting methodologies to inkjet printing*, Proc. SPIE 9015 Color Imaging XIX. doi:10.1117/12.2040647.

Viggiano, JA. 2004. *Metrics for Evaluating Spectral Matches: A Quantitative Comparison*, Proc. Conference on Colour Graphics, Imaging and Vision. pp. 286-291.

Sharma G. 2003. *Digital Color Imaging Handbook*. CRC Press.

Frey, F. and Farnand, S. 2011. *Benchmarking Art Image Interchange Cycles: Final Report 2011,* Rochester Institute of Technology.

BS ISO 15076-1:2010: *Image technology colour management. Architecture, profile format and data structure*. Based on ICC.1:2010 2010, British Standards Institute.

Morovič, P., Morovič, J., Arnabat, J., García-Reyero, J.M. 2012. *Revisiting Spectral Printing: A Data Driven Approach*, Proc. 20th Color and Imaging Conference. pp. 335-340

*Address: Melissa Olen, Centre for Fine Print Research, School of Art and Design,*
*University of the West of England, Bower Ashton Campus,*
*Kennel Lodge Rd, Bristol, BS3 2JT, UK*
*E-mail: melissa.olen@uwe.ac.uk*

# A New Metric for Evaluating the Closeness of Two Colors

Yasuki YAMAUCHI, Yusuke IIDA, Yuki KAWASHIMA, Takehiro NAGAI
Graduate School of Science and Engineering, Yamagata University

## ABSTRACT

Color difference metrics such as CIEDE2000 and CIE76 are suggested to use when the color differences are relatively small. We would also need a new metric which can well express large color differences. Evaluating the difference of two colors would be equivalent to evaluate how close those two colors are. Instead of directly comparing the color difference/closeness, it would be also possible to compare colors with some intervening color. In this study, we try to propose a new metric based on the hypothesis mentioned above. We assume that each color has several "corresponding colors", which give the impression or the appearance of that color to be identical or at least similar. If those colors form a trend-line, it would be way to make a new metric by describing how far a given color would be from this trend-line. We call a series of the color on the same trend-line "consistent color". In Experiment 1, we tried to find consistent colors for 12 reference colors. In order to find a trend line of consistent color for each reference color, a subject changed the test color on the surface of a given gamut until the test color appeared the most similar, or closest to the reference color. By fitting the closest colors of different gamut, we could obtain the trend line for consistent color appearance. Then, we tried magnitude estimation experiment to evaluate how close the displayed colors were to a given test color. Although there seems to be many issues to be solved, from our preliminary experiment, we would say that it is possible to judge how consistent a presented color is to the reference color, which may lead to define a new metric.

## 1. INTRODUCTION

In order to estimate the difference of colors, metrics describing color difference such as CIEDE2000 and CIE76 are widely used. They are suggested to use when the color differences are relatively small. When it comes to evaluate two colors whose color difference, such as lightness and saturation, are large, we would need a new metric which can well express their differences. Evaluating the difference of two colors would be equivalent to evaluate how close those two colors are. Instead of directly comparing the color difference/closeness, it would be also possible to compare colors with some intervening color.

In this study, our final goal is to propose a new metric based on the hypothesis mentioned above. We assume that each color has several "corresponding colors", which give the impression or the appearance of that color to be identical or at least similar. If those colors form a trend-line, a new metric to be proposed should describe how far a given color would be from this trend-line. We call a series of the color on the same trend line "consistent color". This concept is close to that proposed in ICC as the term "common color appearance". A new Reportership TC8-13 has been just started its activity in CIE, aiming to validate this concept.

As the first step, we need to find consistent colors. As Experiment 1, we tried to find consistent colors for several reference colors. In order to find a trend line of consistent

AIC2015 TOKYO - Color and Image

color for each reference color, we need several different color gamut whose surface will cover differently. We used several CRPCs (Characterized Reference Printing Condition) proposed by CGATS. A subject could change the test color on the surface of a given CRPC until the test color appeared the most similar, or closest to the reference color. By fitting the consistent colors of different CRPCs, we could obtain the trend line for consistent color appearance.

Secondly, we tried to verify our concept with magnitude estimation experiments as a preliminary experiment to evaluate how close the displayed colors are to a given test color.

## 2. METHOD

### 2.1 Apparatus

The experiments were conducted in a booth whose walls were covered with black velvet. A schematic view of the apparatus is shown in Figure 1. A fluorescent light (Toshiba, N-EDL, CCT 5000K) lit the inside the booth in order to prevent subjects from dark adaptation. The illuminance of the booth was approximately 100 lx. An LCD monitor (NEC MultiSync LCD-PA241W, 24.1 inch), controlled with Psychtoolbox, was placed in front of the subject in order to present stimuli. The gamut of this monitor covered almost the entire Adobe RGB space. The distance between a monitor and a subject was approximately 80 cm. Subjects could move their head freely. The adjustment of the test color was conducted with a trackball and a keyboard.
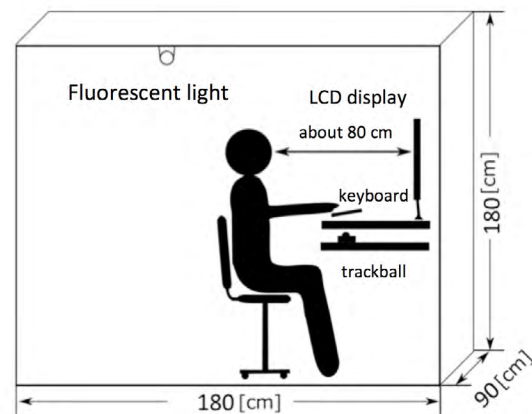


*Figure 1: Experimental setup*

### 2.2 Stimuli

In Experiment 1, 36 reference colors were used in total in the experiment, 3 different luminance levels for 12 different hues. The hues were chosen as those of CUSPs of three primaries (RGB) and their mixtures (CMY), and also those of the midpoints between 2 contiguous colors of RGBCMY. They are shown in Figure 2, which is represented on CIECAM02 a*-b* plane.

As for the luminances of the stimuli, the luminances of RGBCMY and their midpoints were used, which will be referred to as "middle range". Two other conditions were used in the experiment:
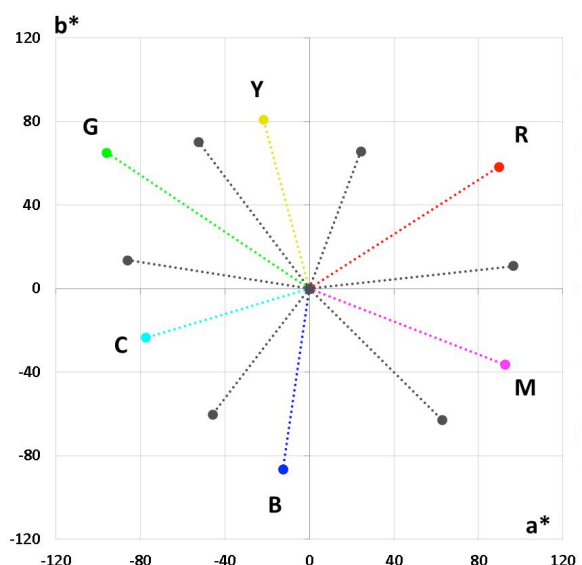


*Figure 2: 12 different hues used in the experiment*

1) "high-range", whose luminances were the midpoints between each of 12 reference colors and that of white, and 2) "low-range", whose luminances were the midpoints between each of the reference colors and that of black.

We adopted three different CRPCs: CRPC7, CRPC5 and CRPC3. Adobe RGB space was used to display the reference colors. Their size projected on a*-b* plane are shown in Figure 3.

The test stimulus was the color on the surface of one of the CRPC, which are controlled by the manipulation of the trackball and the keyboard.
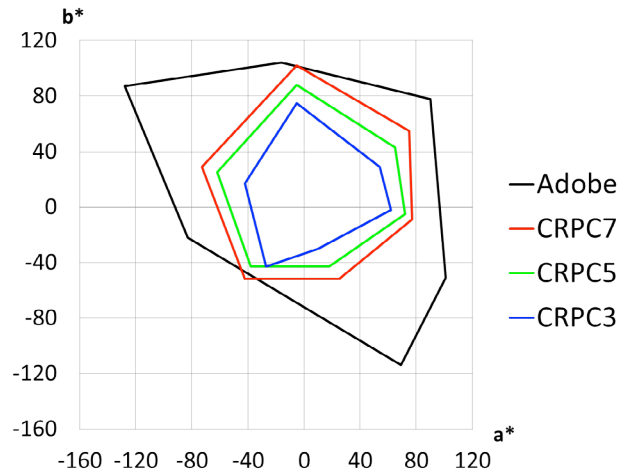


Figure 3: Color gamuts used in the experiment

All the squares extended 2 deg, with a separation of 1 deg. The background was fixed to gray.

The reference colors which were shown during the setting increased as the difference of the color gamuts became larger (multiple reference method). In this method, the corresponding color of CRPC 7 was first searched. Then, the corresponding color of CRPC 5 was explored. Here both the reference color and the corresponding CRPC7 color were displayed in a row. Schematic diagram of the stimulus presented to the subjects is shown in Figure 4.
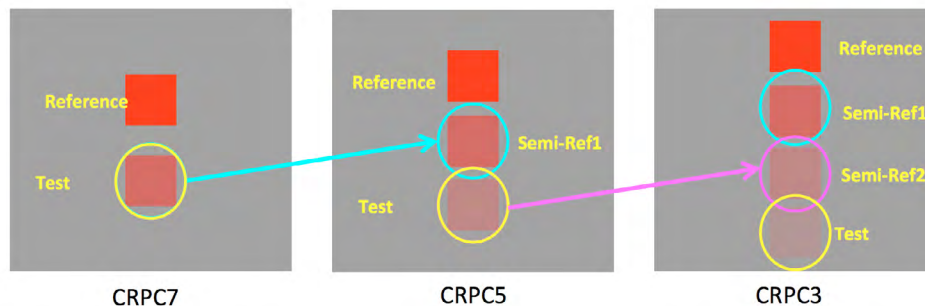


Figure 4: Multiple reference method used in the expeirment

In the next step (Preliminary Experiment 2), we showed one of the series of the reference colors: reference color and three colors of different CRPCs, in a row. The test color, which were apart from the trend line were shown below the row. We used three different colors of the same saturation (C*) for each side of the trend-line. The subject answered the score how different the test color is from the trend line, e.g. the subject rated "0" when the test color was on the trend-line.

## 2.3 Procedure and subjects

After adapting for 3 minutes under the fluorescent light in the booth, the experiment was started.

In each trial, a test stimulus and the reference color ( or the reference colors in some conditions of 3) ) was displayed on a monitor. The hue and their luminance range used in that trial was randomly selected. By controlling a trackball, the subject could change the color to move along the surface of a given color gamut. Each trial started when the subject hit any button on the keyboard. The stimulus was presented continuously. There was no restriction in time for observing stimuli.

As mentioned above, in the preliminary Experiment2, a trial was consisted of rating a test color displayed on the screen. The stimulus was continuously presented to the subject until the rating was completed.

10 color normal male subjects participated in the experiment. All the subjects were naïve for the purpose of the research.

## 3. RESULTS AND DISCUSSION

The results of the experiment are shown in Figure 5. Left and right panel refers to the luminance condition of "middle range" and "low range", respectively. They are shown in a*-b* color plane. The results are the mean values obtained from all the subjects. Solid circles are the reference colors (Adobe RGB). Solid squares, diamonds, and triangles indicate the results obtained from CRPC7, CRPC5 and CRPC3, respectively. Error bars show the standard deviation among the subjects.

Dashed lines shows the equal hue angle trends relative to the reference colors. If the consistent colors show the same trends to the equal hue, they should line up on the same line.

As clearly shown in the figures, the consistent colors of several colors have more or less the same hue angle, i.e. they line up on the same line. The colors of the 1st quadrant of the middle range and the yellow of all the ranges are the distinct results among them.
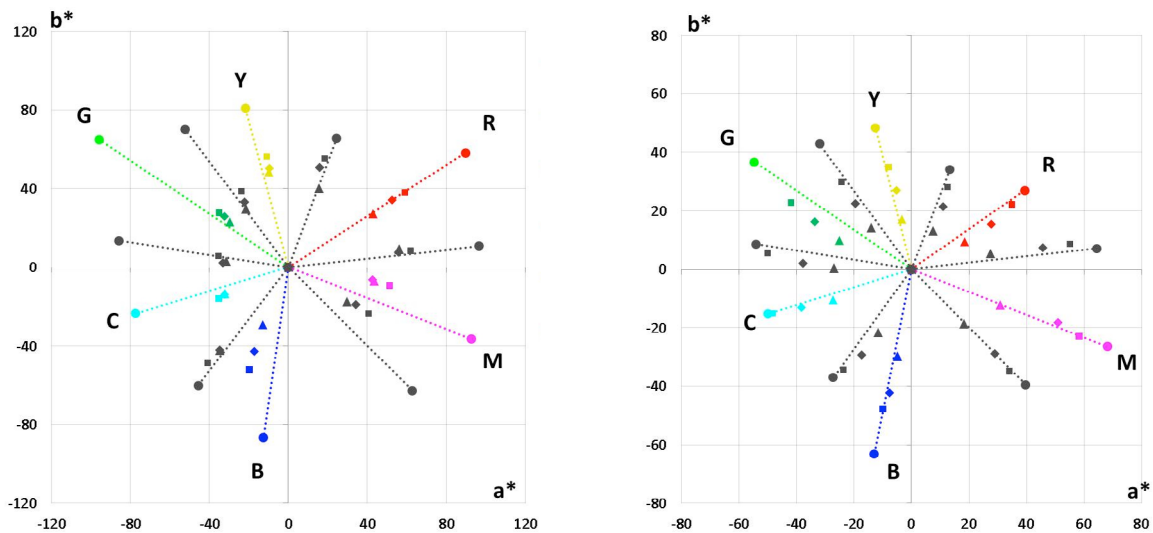


*Figure 5: Consistent color trends of 12 colors (Left: "Middle range", Right: "Low range" )*

As for the consistent color of the blue, the colors of intermediate saturations were apart from the hue angle of the reference color. The tendency was similar to that reported by

Hung(1995), which was investigating the constant hue loci of several colors. It means that our subjects conducted an experiment with the judgment of the hue for the primary criteria.

The results of the preliminary experiments showed that in some hues, the subjects rated higher rates to the test colors which are further from the trend line. However, the results were dependent on the subjects and colors. Some subjects, however, did not show such a clear trends.

## 4. CONCLUSIONS

In our research, we tried to propose a new metric which can well describe the difference of two colors with the concept of the consistent color. So far, we haven't come to the stage for proposing a new metric, but we could obtain the trend-lines of the color which give the similar or the "close" appearance to the reference color. This might be a way of verifying the concept of the consistent colors. Moreover, the trend-lines showed a similar behavior as the constant hue loci. This finding indicate that when the judgment of the closeness of the color should be done, hue is the primary factor in its process.

Although we haven't obtained a clear result, we could show a possibility to evaluate the difference of the color apart from the consistent color loci quantitatively. In order to verify the concept, we need to explore our experimental conditions more in detail. We are expecting our findings will lead to propose a new metric that can be used to express the difference of the colors.

## REFERENCES

CIE 2001, CIE Publication No. 142-2001, Central Bureau of the CIE

CGATS, https://www.npes.org/programs/standardsworkroom/ cgatstechnicalstandards.aspx

Zhu, S.Y, Luo, M.R. and Cui, G.H. 2002, *New experimental data for investigating uniform color spaces*, Proc. SPIE 4421, 9th Congress of the International Colour Association, 626

Hung, P. and Berns. R.S 1995, *Determination of constant Hue Loci for a CRT gamut and their predictions using color appearance spaces*, Color Research & Application 20 (5) 285-295.

*Address: Prof. Yasuki YAMAUCHI, Department of Informatics, Graduate School of Science and Engineering, Yamagata University, 4-3-16 Jonan, Yonezawa, Yamagata, 992-8510, JAPAN*
*E-mails: yamauchi@yz.yamagata-u.ac.jp, tkk25057 @st.yamagata-u.ac.jp, kawashima.yu@yz.yamagata-u.ac.jp,tnagai@yz.yamagata-u.ac.jp*

# Image and Color Space Clustering for Image Search

Akinobu HATADA,[1]

[1] Graduate School of Human Sciences, Kanagawa University, Japan.

## ABSTRACT

Image search is one of application like Google internet search. But normally internet search engine use text context, not image. Google provides image search system, today. It seems recognize image as what it is and generate text key word as search key. Final search result is web page list, and image list of same theme. For example, Eiffel tower image is given as search source, it report Eiffel tower web page and list of Eiffel tower picture. It seems searching picture that contains same subject in source image.

Image search by image is yet another thema. (Abhinav Shrivastava, etal, 2011) is a quite similar research as previous case. Abhinav approach is by way of massive caliculation. (Hatada, 2014) report more simple approach by way of pre-caliculated index data, that based on color region on image.

Search speed is a big value for search engine. Nobody never look up Google if it spend one hour for every searching request. Image searching. It means caliculation in searching phase should light. In other hand, making index data for each searching target is easy to allowing spend time.

In this study report indexed data by color information and image clustering approach as image search application.

## 1. INTRODUCTION

Image search like Web page search is one of interest application. Today, what we call web search is "full text search" in strictly. It search web page by text key word, and search result is sorted by certain order, which called ranking (Brin and Page, 1998). Today, Google provides image search service (Google Search by Image). User is able to having an experiment of search by image at Google site, today. It seems searching picture that picture including same major content of source picture. For example, searching by picture of Eiffel tower; try to show web page of Eiffel tower or picture which include Eiffel tower.

Either case of text, image or voice, search engine is includes data analysing unit, characteristic data storage, data matching unit and ranking unit. Data analysing method is most important unit, because it determines search engine's character or capability. For example, data analysing method is definitively different between text data case and image data case.

One of popular image characteristic data is vector data. Vector data is line of subject edge in image. Usually many numbers of vector data is generated by single image. This style of search engine would suitable to subject recognition. In above case, pick up a word "Eiffel tower" from Eiffel tower's picture is required subject recognition. Once text word is provided, search system can find web page by its key word. If text word is not appeared by image, search engine could search by vector data itself. Vector data is comparable and matching process is able to developing.

(Abhinav etal, 2011) is also uses this kind of data. As their presentation, it seems pretty good result. But it requires massive calculation in searching process.
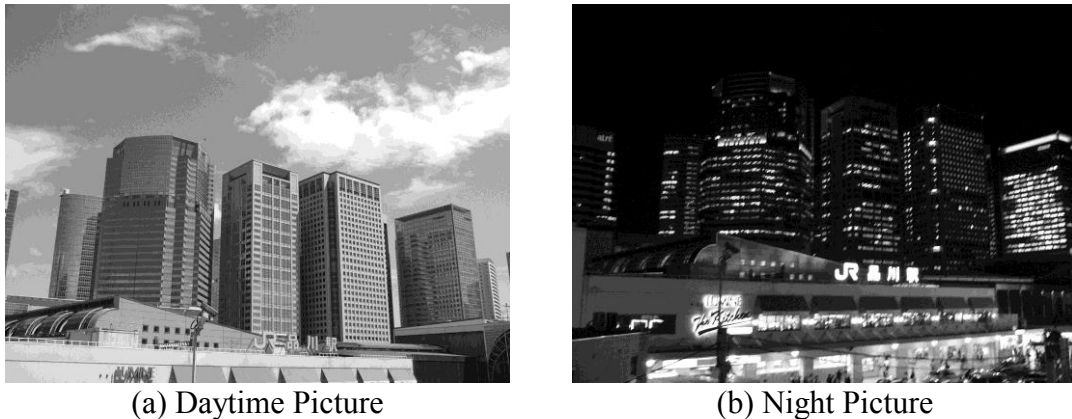


(a) Daytime Picture          (b) Night Picture

*Figure 1: Tow Pictures Takes Same Place and Different Time.*

Figure 1 shows two pictures. These picture takes same place and simular angle, but different times. These picture includes same contents like buildings. According my observation, many people don't think these are simular picture, as far as these are including same content. This fact means that content in picture is not key point of evaluating landscape. If two picture have same vector dates, it is not galantee they are simular. By this observation, our research effort developed by color information.

## 2. METHOD

In previous study, filling region is employee as characteristic data. In this study, clustering data is improved as characteristic data. All of images are normalized to 1024 x 768 size and rotation.

### 2.1 Characteristic Data

Characteristic data from image is using filling region information. Filling region is an area that determined by flood filling algorithm (Figure 2). In previous experiment, image colors are reduced 64 from 16 million of it. Filling region is simple and provided useful information as characteristic data. It is not include position data. It means image rotation is not matter about in phase of image search, but it claimed that important data is missing.
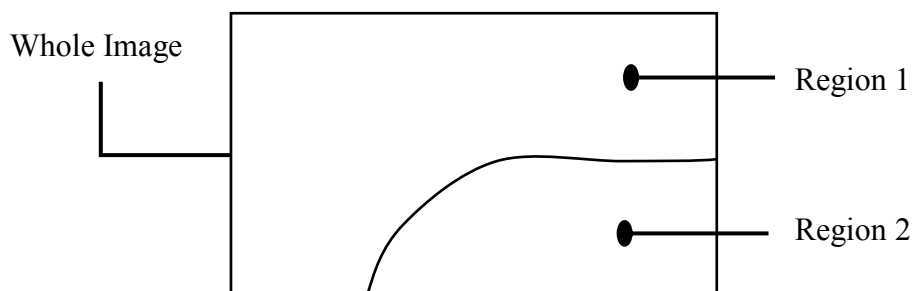


*Figure 2: Filling Region.*

Cluster a kind of concept that representing some vector space. It includes clustering point in analysing data space(Figure 3).
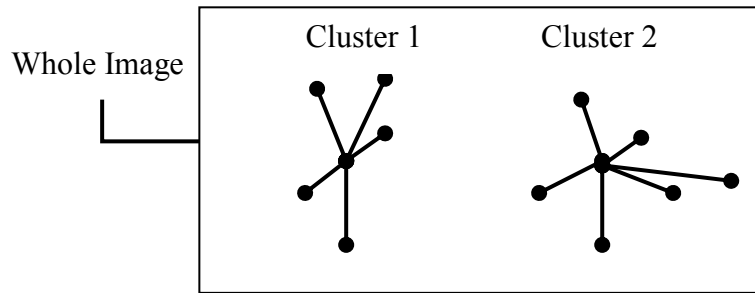


*Figure 3: Cluster.*

## 2.2 Clustering Approach

Around clustering study, K-means algorithm and its application is one of major topics, that reported by (Steinhaus, H., 1957) or (MacQueen, J. B., 1967) etc. There are also a lot of study is easy to found in imaging processing research area. A point of those studies is, how makes clusters well. In original K-means algorithm should provide number of initial cluster, and it takes large effect to clustering result. (YAMAMOTO and MURAKAMI, 2003) tried to calculate number of cluster according image data. This study also uses color data. Actually, it uses color distance as cluster combining threshold. But their experiment includes several ad-hoc methods to integrate clusters, i.e. omitting small clusters. It also not disclosing how many cycle is required until K-means loop.

Avoiding problem of loop cycle evaluation, and ad-hoc small cluster omitting issue, this study improve yet another approach. In point of view of vision psychology, human eye is sensitive to lightness rather than colour hue. Actual example is shown in Figure 4. It shows edge of colour image (a) and grey scaled edge (b).



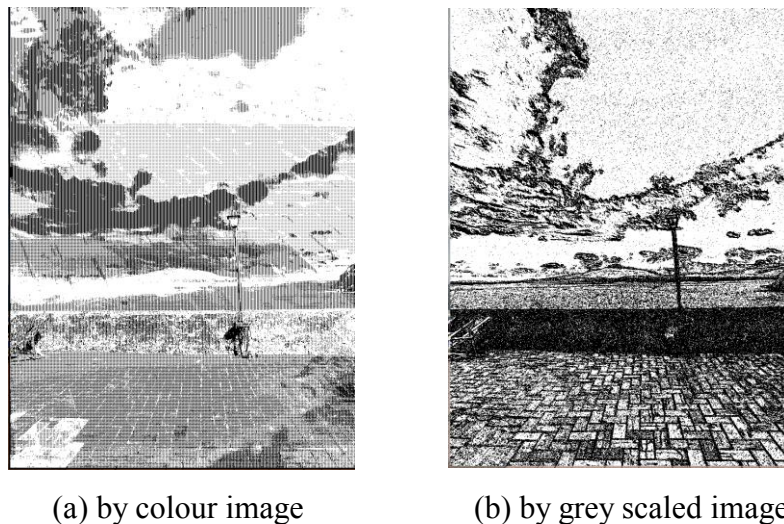(a) by colour image        (b) by grey scaled image
*Figure 4: Edge Example.*

Edge data from colour image is noisy than grey scaled data. Then this study employee grey scaled data as bases of image clustering. Grey scale is 8 steps and it is decided adapted to image data. In additionally, reduce less than 1% area cluster is processed.

In result of it, 322 sample landscape data converted about 20 clustered data (Figure 5).

| "GrayScale", | "x", | "y", | "Count" |
|---|---|---|---|
| 177, | 57, | 117, | 12716 |
| 250, | 152, | 260, | 55718 |
| 255, | 486, | 97, | 98754 |
| 250, | 301, | 277, | 20636 |
| 129, | 40, | 293, | 9749 |
| 177, | 96, | 594, | 20664 |
| 0, | 971, | 496, | 10386 |

*Figure 5: Generated Cluster Data (Sample).*

## 2.3 Scoring

Matching score is calculated according (exp.1). Comparing source cluster and destination image's clusters and pick up most neighbor cluster and takes a differential.

$$De = k \sum_{Color} \frac{1}{(R1 - R2)^2 + 1}$$  **(exp.1)**

De: Differential value of two images
k: adjustment value.
R1 and R2 is number of region in two images.

## 3. RESULTS AND DISCUSSION

Sample result is shown at Figure 6. Search trial shows some interesting result.For example, a case of Figure 6 hit similar composition of image. In previous study, search result did not care about this kind of effect.
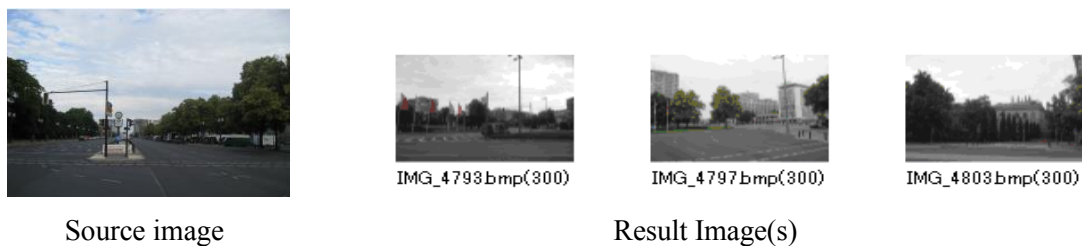


Source image                                         Result Image(s)

IMG_4793bmp(300)    IMG_4797bmp(300)    IMG_4803bmp(300)

*Figure 6: Sample Search Result.*

## 4. CONCLUSIONS

This trial shows some interesting result, but it is not enough. In this study, clustering seems to good idea of including location data to charateristic data. But grey scale information may not enough as search key. Color data should concern about cluster property in future study.

## REFERENCES

Abhinav Shrivastava, Tomasz Malisiewicz, Abhinav Gupta, Alexei A. Efros, 2011, *Data-driven Visual Similarity for Cross-domain Image Matching*, ACM Transactions on Graphics (TOG) - Proceedings of ACM SIGGRAPH Asia 2011 ,Volume 30 Issue 6, December 2011, Article No. 154

Akinobu Hatada, 2014, *Image comparing by color information*, ACA2014 Proceedings, 140-143

Brin, S.; Page, L., 1998, *The anatomy of a large-scale hypertextual Web search engine*. Computer Networks and ISDN Systems 30: 107–117.

Steinhaus, H., 1957,. *Sur la division des corps matériels en parties*. Bull. Acad. Polon. Sci. (in French) 4 (12): 801–804

MacQueen, J. B., 1967, *Some Methods for classification and Analysis of Multivariate Observations*, 1. Proceedings of 5th Berkeley Symposium on Mathematical Statistics and Probability. University of California Press. pp. 281–297

Kyuuich YAMAMOTO and Shinichi MURAKAMI, *A Study on Image Segmentation by K-Means Algorithm*, Report of Information Processing Society of Japan [Audio-Visual combined information processing] 2003(125), 173-178, 2003-12-18, Information Processing Society of Japan

*Address: Akinobu Hatada, Graduate School of Human Sciences, Kanagawa University*
*3-27-1 Rokkakubashi Kanagawa-ku Yokohama, 221-8686, JAPAN*
*E-mails: r201270904ui@kanagawa-u.ac.jp*

# Restoration of color appearance by combining local adaptations for HDR images

Yuto KUBO,[1] Takao JINNO,[1] Shigeru KURIYAMA[1]
[1] Toyohashi University of Technology

## ABSTRACT

Image colors are often degraded due to saturation or fade-out for the scenes illuminated by colored lightings. This research improves such degradation for high dynamic range (HDR) images that can fully capture the brightness and chroma at high bit-depth. The dynamic range should be compressed to fit that of ordinary color monitors, and color appearance model (CAM) is widely used for authentically reproducing colors in compressions. This model can take the feature of human visual system that can adaptively perceive colors according to the brightness within a local area. This adaptation model, however, is inapplicable to an image including both brightly- and dimly-lit areas. We propose a method of combining such local adaptations for different brightness on a single image. Our method enables unified color restoration for HDR images while retaining the global consistency of brightness variations, and its effectiveness is experimentally demonstrated for the indoor scene illuminated by a color LED.

## 1. INTRODUCTION

With popularization of color LED lightings, accurately restoring the chromaticness of captured images become important for demonstrating their effectiveness, which may be utilized for lighting design, advertisement, etc. Most of ordinary digital cameras, however, lack the capability in color restoration, owing to the insufficient dynamic ranges of their image sensors.

HDR images can fully capture the scene radiance at high bit-depth, and displaying them on ordinary monitors of lower bit-depth requires compressing their dynamic range. The range compression based on iCAM06 (Kuang 2007) can reproduce the color appearance. Since the scenes including glaring colored light source have very wide dynamic range, iCAM06 cannot sufficiently restore the colorfulness owing to its limited compression rate.

Our previous study (Kubo 2014) divides an input HDR image into the areas of lights and surroundings, for separately compressing their dynamic ranges. It can reproduce the color appearance for each image region whose dynamic range is lower enough for accurate restoration. This approach, however, often causes a contrast inversion along the boundary of areas to which different adaptation parameters are set. This paper therefore proposes the dynamic range compression by introducing a local adaptation of white point with a bilateral filter. This can reproduce the local color appearance of an HDR image on an ordinary low dynamic range (LDR) image, without causing any contrast inversion.

## 2. DYNAMIC RANGE COMPRESSION

Methods of dynamic range compression are roughly categorized as the following types:

(a) Non-linear function whose global parameter is changed for a whole image, which can retain brightness gradients without causing any contrast inversion

(b) Non-linear function whose parameters are changed for each pixel, which can preserve the details of the scene

(c) Non-linear function based on the color appearance model (Kuang 2007) (Reinhard 2010)

where the last category is most suitable for our target, especially, those based on the iCAM06 model.
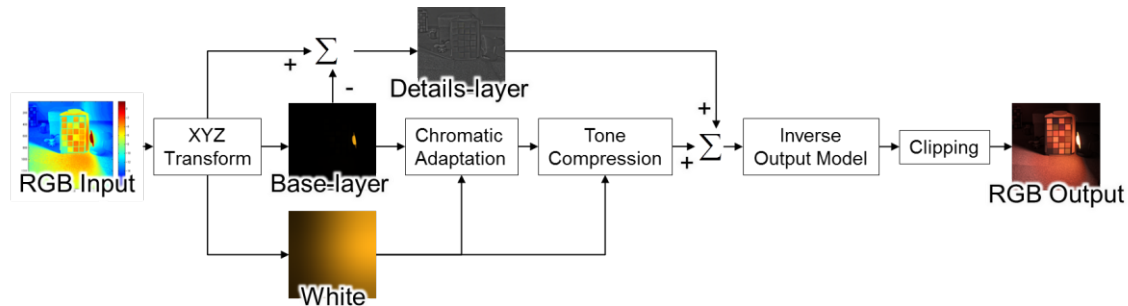


*Figure 1: Flowchart of iCAM06.*

## 2.1 iCAM06

Human visual system consists of many non-linear response functions and adaptations for maximizing sensing performance against real world of very wide dynamic range, and many range compression algorithm for HDR image is developed by imitating this functionalities.

The iCAM06 was developed for HDR image rendering by extending iCAM framework (Johnson 2003) that can reproduce the color appearance based on CIECAM02 (Moroney 2002). The CIECAM02 predicts the color appearance attributes from the tristimulus values; this process, however, cannot be suited to compress the dynamic range of the HDR image into LDR one. The iCAM06 introduces an empirical range clipping mechanism by rounding off the values outside the 1th and 99th percentile. Although this clipping is suitable for most of the HDR scenes, color degradation is inevitable for the scenes including very wide dynamic range, e.g. the scene including both dim regions and colored lights, as shown in Figure 2.

Figure 1 shows the flowchart of the iCAM06. The iCAM06 separates the HDR image into the details-layer and the base-layer, and compresses only a wide dynamic range of the base-layer based on the Retinex theory (Rahman 1997) by applying a tone compression. The tone compression consists of cone and rod response functions, which have local adjustments according to an adaptation luminance map. This map is estimated by filtering the input HDR luminance using a Gaussian kernel whose standard deviation is 5 (Kuang 2004).
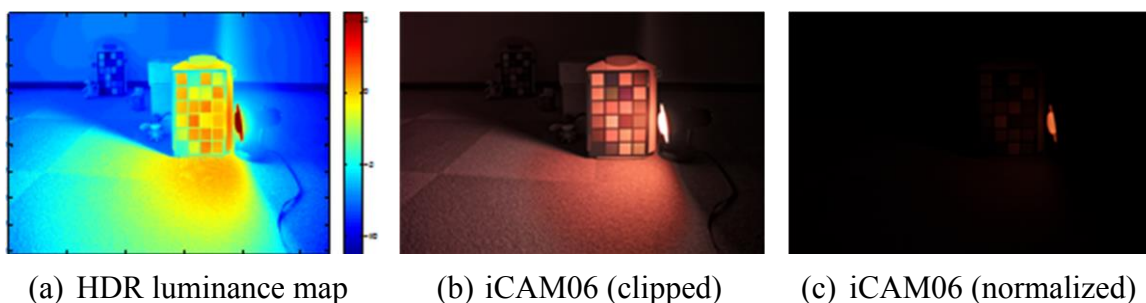


(a) HDR luminance map      (b) iCAM06 (clipped)      (c) iCAM06 (normalized)

*Figure 2: Range compression for a colored light.*

## 2.2 Effect of iCAM06

Figure 2 shows (a) brightness distribution, (b) the clipped effect of iCAM06, and (c) the normalized effect without clipping, for HDR scene including a colored lighting. Figure 2(b) shows that the colorfulness of the lighting is faded out due to the effect of clipping, whereas it is retained in Figure 2(c). This demonstrates the insufficiency of the range compression rate of iCAM06 for very wide dynamic range scenes.

Figure 3 shows a converted image with iCAM06 and its adaptation luminance, which reveals that the emitted light strongly affects the adaptation white for a whole image. This suggests that restoring the colors of lighting and surrounding areas requires stronger compression of the dynamic range in a separate manner, by using more local adaptation.

## 3. METHODOLOGY

Our target is to reproduce the color appearance when converting HDR images into LDR ones, which can be attained by more locally changing the adaptation luminance in the iCAM06.

Narrowing the field of view (i.e. decreacing the standard deviation of Gaussian filter) is effective for reducing the chromatic degradation of the lighting area; it, however, causes a halo effect on the boundary against the surrounding and brightens the black colored objects of low reflectance in unnatural ways. For improving these defects, the edge-preserving smoothing operation with a bilateral filter is applied to calculate the local adaptation. This filter is comnputed at the input luminance I of each pixel p as

$$\text{BF}\big[I_p\big] = \frac{1}{W_p}\sum_{q \in S} G_{\sigma_s}(\|p - q\|)G_{\sigma_r}\big(|I_p - I_q|\big)I_q, \tag{8}$$

$$G_\sigma(x) = \frac{1}{2\pi\sigma^2}\exp\left(-\frac{x^2}{2\sigma^2}\right), \tag{9}$$

where $\|p - q\|$ denotes the Euclidean distance of pixel coordinates, $|I_p - I_q|$ denotes the luminance difference, and $W_p$ is the normalization term. Both $G_{\sigma_s}$ and $G_{\sigma_r}$ denote the normal distribution function whose standard deviations representing a view field size $\sigma_s$ and masking effect $\sigma_r$ are adaptively controlled for avoiding halo effect. We found that a bilateral filter can yield the local adaptation more effectively than that is yielded with a Gaussian filter.

## 4. EVALUATION

### 4.1 Experimental setup

We investigated the effects of the dynamic range compression of iCAM06, whose tone compression (Section 2.1) uses our adaptation luminance, for the scenes illuminated by a red LED bulb (CIE xy chromaticity: x = 0.62, y = 0.33) against various values of $\sigma_s$ and $\sigma_r$.

As a quantitative evaluation, we calculated the differences between reference chromaticity $(u_r^{'}, v_r^{'})$ and mean chromaticity $(u', v')$ for each pixel of the output image, where the references are obtained by measuring with a color illuminometer at the following locations:

(A) a white patch of the front chart as shown in Figure 4A.
(B) a white patch of the rear chart as shown in Figure 4B.
(C) the area of the red colored bulb.

The resolution and the range ($\max(I) - \min(I)$) of the input image were $2736 \times 1824$ and $6.47$, and $\sigma_s$ and $\sigma_r$ were determined as $\sigma_s = \min(height, width)/s$ and $\sigma_r = (\max(I) - \min(I))/r$, respectively.
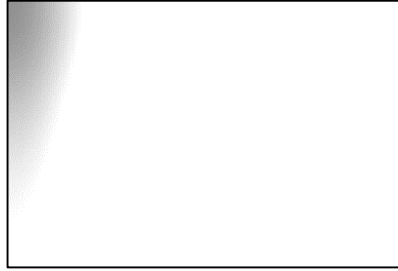


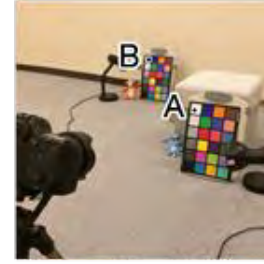*Figure 3: Resulting image with iCAM06 (left) and its clipped adaptation luminance (right).*

*Figure 4: Experimental environment.*

## 4.2 Observation

Figure 5(a) shows the converted images with our method and Figure 5(b) shows the corresponding adaptation luminances. The results with small $\sigma_s$ can preserve the color of the red colored bulb but causes the halo effects at the front chart and the bulb and reducing the global contrast. Our method can, however, reduce the halo effects by setting smaller $\sigma_r$ as shown in the upper row of Figure 5(a). Unfortunately, our mtehod also unnaturally brightens the black colored objects as shown in Figure 5. This negative effect is caused by neglecting the reflectance components for bilateral filtering. We solved this problem by extending the bilateral filter to a cross bilateral filter with a Lighting or Shading map, which is obtained by intrinsic image estimation algorithms.

Figure 6 shows the chromatic differences of our method against the iCAM06, sampled at three areas whose brightness are middle (A), low (B) and high (C). The difference is lower in images restored with our method than those obtained with the iCAM06, where our local adaptation effect is relatively noticeable at the areas (B) and (C). The color reproducibility of the iCAM06 is promoted at the area (A) because the middle brightness area is not affected by clipping or weak range compression.

Consequently, we have found that our method can restore local color appearance more accurately by setting $\sigma_s$ and $\sigma_r$ by smaller values. These settings, however, decrease a global contrast of the output image, because of the trade-off between the color reproducibility and the global contrast. This paper does not evaluate the chromatic differences for the lower reflectance areas, where (A) and (B) are the higher reflectance areas and (C) is the light bulb area. We should measure the reference chromaticity with a spectral radiance meter at the various reflectance areas for more accurately evaluating the chromatic differences.

## 5. CONCLUSION

This article has proposed a color restoration scheme for the scenes of very wide dynamic range caused by colored lightings. Our method calculates the local adaptation white more effectively with the bilateral filter, and adaptively utilizes iCAM06 to reproduce the color appearance of HDR images.

We should improve the remapping mechanism for lower reflectance areas by introducing more accurate quantitative evaluation for color reproducibility of various reflectance areas.

It is also challenging task to restore colors for the scenes illuminated by many lightings of different colors. Our future work also includes psychological experiments in actual lighting environments or with various color monitors.
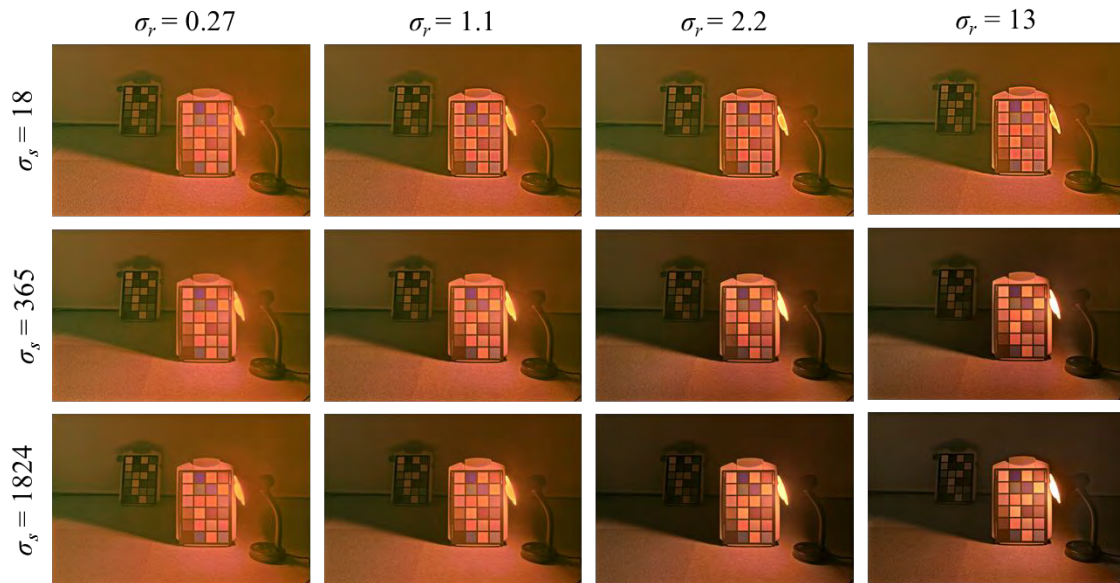


(a) Converted images for various parameters
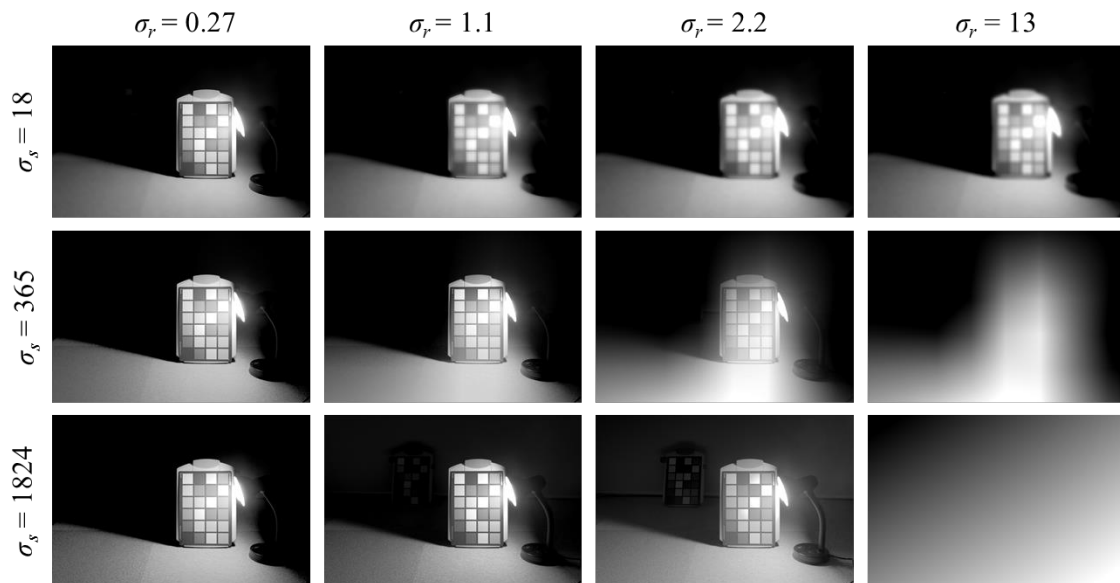


(b) Adaptation luminance (clipped)

*Figure 5: Output images and adaptation luminacnes.*

## REFERENCES

J. Kuang, G.M. Johnson and M.D. Fairchild 2007. iCAM06: *A refined image appearance model for HDR image rendering*, Journal of Visual Communication 185, pp406–414.

E. Reinhard, G. Ward, S. Pattanaik, P. Debevec, W. Heidrich and K. Myszkowski 2010. *High Dynamic Range Imaging Acquisition, Display, and Image-Based Lighting*, Morgan Kaufmann, pp91–118.

N. Moroney, M.D. Fairchild, R.W.G. Hunt, C. Li, M.R. Luo and T. Newman 2002. *The CIECAM02 Color Appearance Model*, IS& T/SID 10th Color Imaging Conference pp23–27.

Z. Rahman, D.J. Jobson and G.A. Woodell 1997. *Multi-Scale Retinex for Color Image Enhancement*, Proc. International Conference on Image Processing 3 pp1003–1006.

J. Kuang, H. Yamaguchi, G.M. Johnson and M.D. Fairchild 2004. *Testing HDR image rendering algorithms*, Color Imaging Conference pp315–320.

Y. Kubo, T. Jinno and S. Kuriyama 2014. *Color Restoration of Color Lighting Effects*, 47th Annual Conference of IEIJ, 8-20.

(A) white patch of the front chart

(B) white patch of the rear chart

(C) light bulb

(upper row) chromatic differences when setting the various $\sigma_r$ against the fixed $\sigma_s$

(A) white patch of the front chart

(B) white patch of the rear chart

(C) light bulb

(lower row) chromatic differences when setting the various $\sigma_s$ against the fixed $\sigma_r$
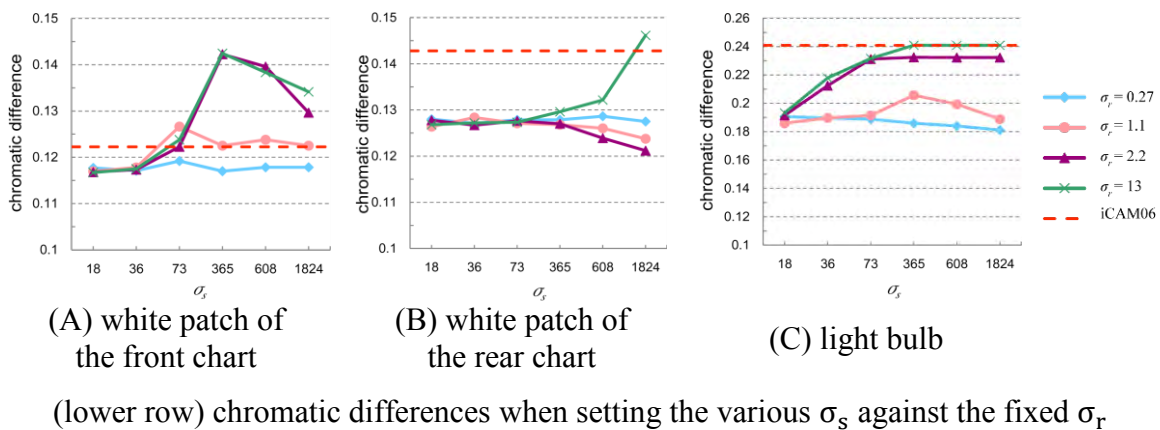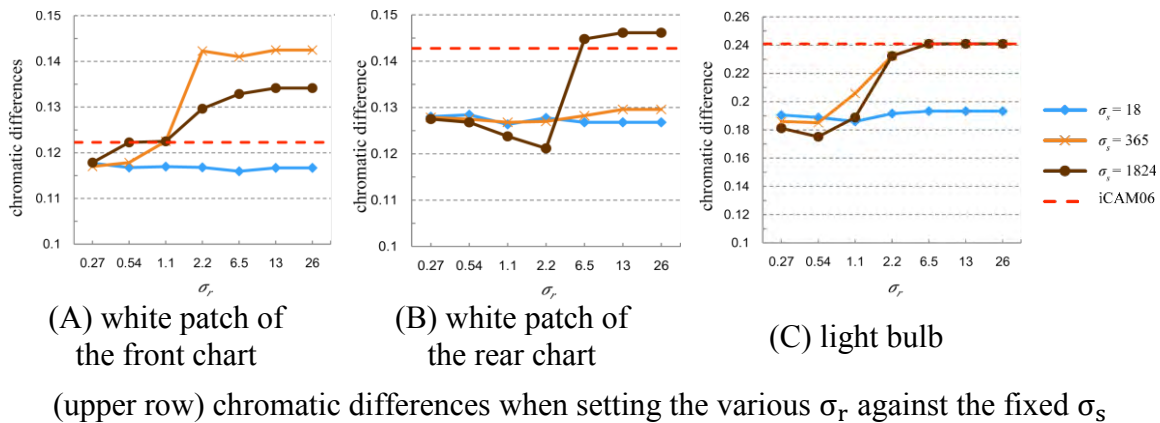
*Figure 6: Chromatic difference against measurement.*

*Address: Assistant Prof. Takao JINNO, Department of Computer Science and Engineering, Toyohashi University of Technology, 1-1 Hibarigaoka Tenpaku-cho, Toyohashi, Aichi 441-8580, JAPAN.*
*E-mails: kubo@val.cs.tut.ac.jp, jinno@cs.tut.ac.jp, sk@tut.ac.jp*

# Image Quality index for perceiving three-dimensional effect in mobile displays

Chun-Kai CHANG, Hirohisa YAGUCHI, Yoko MIZOKAMI
Graduate School of Advanced Integration Science, Chiba University

## ABSTRACT

This article mainly describe two color indices, one is image quality index for color ($IQI_{\text{color}}$) for evaluating image qualities of color and sharpness. Another is image quality index for 3D perception ($IQI_{\text{3D}}$) for evaluating depth perception. The result shows $IQI_{\text{color}}$ represents perceived that image color qualities sufficiently and $IQI_{\text{3D}}$ provides an easy way to discriminate the depth effects between heterogeneous displays.

## 1. INTRODUCTION

Recent years, with the rapid development of technology in mobile displays, from traditional cell phones to brand-new smart phones, wider-gamut, higher resolution and higher contrast mobile displays have appeared on the market. In such cases, we could perceive that they have three-dimensional effects but in different levels. In order to understand the differences in perceiving these effects between mobile displays, and precisely estimate in which condition mobile displays perform it well, we consider two indices. One was for evaluation of image quality index of color and sharpness, the image quality index for color $IQI_{\text{color}}$, another was for evaluation of depth perception, the image quality index for depth perception $IQI_{\text{3D}}$.

## 2. METHOD

First, we prepared nine mobile displays, including one AMOLED tablet, one LCD tablet, four AMOLED phones and three LCD phones. Table 1 illustrates each basic specification.

The $IQI_{\text{color}}$ and $IQI_{\text{3D}}$ are both specified with chromatic contrast and luminance contrast that are the common factors in the color clarity of display. The procedures of obtaining colorimetric specifications are shown below.

Step 1. Basic color patches, R, G, B, C, M, Y, W and Bk were presented on each display by using 4% pattern which length and width were one fifth of display size, and measured with a Konia Minolta CS-2000 spectroradiometer.

Step 2. The luminance and the tristimulus values *X*, *Y*, and *Z* of color patches are measured with a Konica Minolta CS-2000A spectroradiometer in dark room at 1 lux.

Step 3. *XYZ* were transferred to the lightness *J*, the colorfulness *M*, and the hue *h* of the CIECAM02, then transferred to *a'* and *b'* of the CIECAM02-UCS.

Step 4. The color volumes and luminance contrast of the display were calculated.

Table 2 illustrates the *x,y* chromaticity coordinates and the maximum and minimum luminance in R, G, B and W color patches.

**Part 1: Image quality index for color ($IQI_{\text{color}}$)**

In chromatic contrast, we defined a relative color volume in the CIECAM02-USC color space (Luo et al., 2006) using the volume color gamut efficiency (Inui, 2000) which can be described as volume of display color gamut divided by volume within optimal color. As

AIC2015 TOKYO - Color and Image

the volume within optimal color is 2,334,000 in CIELAB unit (Inui, 2000), the relative color volume in CIECAM02-USC ($RCV_{CAM02\text{-}USC}$) unit can be simply described as follow,

$$RCV_{CAM02\text{-}USC} = (\text{Volume of display color gamut}) / 2{,}000{,}000 \qquad (1)$$

In luminance contrast, we used luminance ratio as a luminance contrast index instead of usual Michelson contrast. Although the luminance of black in AMOLED displays is approaching to 0, we defined our contrast ratio index ($CRI$) as 8 log unit for some facilitating calculation reasons as follows,

$$CRI = \log (L_{max} / L_{min}) / 8 \qquad (2)$$

The image quality for color and luminance contrast could be represented as a function of color volume and contrast ratio as following equation.

$$IQI_{color} = (RCV_{CAM02\text{-}USC} * CRI)^{1/2} \qquad (3)$$

*Table 1. Each basic specification of mobile display*

|  | Display size (inch) | Diagonal size (inch) | Number of pixels | Resolution (ppi) |
|---|---|---|---|---|
| AMOLED phone 1 | 4.91 x 2.8 | 5.7 | 1920 x 1080 | 386 |
| AMOLED phone 2 | 4.32 x 2.45 | 5.0 | 1920 x 1080 | 441 |
| AMOLED phone 3 | 4.40 x 2.49 | 5.1 | 1920 x 1080 | 432 |
| AMOLED phone 4 | 4.17 x 2.37 | 4.8 | 1280 x 720 | 306 |
| LCD phone 1 | 4.13 x 2.34 | 4.8 | 1280 x 720 | 308 |
| LCD phone 2 | 5.07 x 2.84 | 5.9 | 1920 x 1080 | 373 |
| LCD phone 3 | 4.29 x 2.45 | 5.0 | 1920 x 1080 | 443 |
| AMOLED tablet | 8.85 x 5.49 | 10.5 | 2560 x 1600 | 288 |
| LCD tablet | 7.6 x 5.77 | 9.7 | 2048 x 1536 | 264 |

*Table 2. Chromaticity coordinates of mobile displays*

| Display primaries | ($x,y$) Chromaticity coordinates | | | | Luminance (cd/m$^2$) | |
|---|---|---|---|---|---|---|
|  | R | G | B | W | White $L_{max}$ | Black $L_{min}$ |
| AMOLED phone 1 | (0.655, 0.336) | (0.223, 0.722) | (0.144, 0.043) | (0.299, 0.328) | 395.37 | $7 \times 10^{-5}$ |
| AMOLED phone 2 | (0.665, 0.334) | (0.223, 0.724) | (0.142, 0.045) | (0.301, 0.331) | 316.37 | $6 \times 10^{-5}$ |
| AMOLED phone 3 | (0.662, 0.337) | (0.227, 0.711) | (0.141, 0.046) | (0.302 0.320) | 440.58 | $3 \times 10^{-5}$ |
| AMOLED phone 4 | (0.668, 0.331) | (0.213, 0.724) | (0.140, 0.051) | (0.303, 0.325) | 254.16 | $8 \times 10^{-4}$ |
| LCD phone 1 | (0.635, 0.331) | (0.302, 0.557) | (0.149, 0.061) | (0.293, 0.293) | 465.03 | $5 \times 10^{-1}$ |
| LCD phone 2 | (0.637, 0.335) | (0.303, 0.610) | (0.155, 0.066) | (0.311, 0.344) | 438.61 | $5 \times 10^{-1}$ |
| LCD phone 3 | (0.648, 0.342) | (0.265, 0.645) | (0.153, 0.037) | (0.300, 0.327) | 401.25 | $1 \times 10^{-1}$ |
| AMOLED tablet | (0.660, 0.339) | (0.237, 0.709) | (0.141, 0.048) | (0.303, 0.319) | 350.71 | $6 \times 10^{-5}$ |
| LCD tablet | (0.641, 0.338) | (0.305, 0.609) | (0.154, 0.048) | (0.306, 0.322) | 389.56 | $3 \times 10^{-1}$ |

**A visual experiment of image quality**

In this experiment, excepting 2 tablet displays for size reasons, we prepared 7 mobile displays, and carried out a visual evaluation of image quality by a paired comparison method using three natural images called "Wineglass", "Wool" and "Harbor" from SHIPP (Standard High Precision Picture) data shown in Figure 1 (a)-(c). Each image was selected for a particular purpose as follows,

Wineglass: tone reproduction of light and neutral color.

Wool:color reproduction of high chroma image.

Harbor: evaluation of image processing for fine detail of geometrical structure.



(a) Wineglass (b) Wool (c) Harbor (d) Venice

(e) Wine & Table (f) Houses (g) Trees (h) Swan

*Figure 1. Test images*

Visual image quality performance is provided by Z-scores from the experiment. The Z-scores represent the image quality as a distance from mean in terms of standard deviation. Table 3 shows the final result of calculation in image quality indices and Z-scores from a visual experiment for image quality. Figure 2 shows the Z-score of each device in three images, and the error bars indicate standard deviation. When using mobile displays, our impression of image would also be affected by the modulation transfer function (MTF) of display indirectly, we consider another formula to explain this result instead of Equation (2) as describe below,

$$IQI_{\text{total}} = (RCV_{\text{CAM02-USC}} * CRI * RI)^{1/3} \tag{4}$$

Where the resolution index *RI* is given by the following Equation. The number of 582 ppi corresponds to the limit of retinal resolution for visual acuity 2.0 at the viewing distance of 30 cm, are regarded as normalization base. Table 3 shows pixel per inch (ppi) and resolution index (*RI*) for mobile displays.

$$RI = ppi\,/\,582 \tag{5}$$

Although Equation (4) shows a good relationship between the three parameters, we tried to develop a total image quality index with weighting coefficients as following equation. From least square method, the weighting coefficients $w_{\text{CV}}$ , $w_{\text{CR}}$ and $w_{\text{R}}$ as 0.2, 0.4 and 0.4 respectively, perform the highest correlation between $IQI_{\text{total}}$ and Z-score as shown in Figure 3.

$$IQI_{\text{total}} = w_{\text{CV}}\, RCV_{\text{CAM02-USC}} + w_{\text{CR}}CRI + w_{\text{R}}RI \tag{6}$$

**Part 2: Image quality index for 3D perception ($IQI_{\text{3D}}$)**

In this part, 3D depth effect will be verified by two psychophysical experiments, a paired comparison method and an observers' subjective evaluation. Comparing to $IQI_{\text{color}}$, we added two tablet displays and reduced one LCD phone from the experiment. Test images called "Venice", "Wine & Table", "Houses", "Trees" and one short movie "Swan" are also shown in Figure 1 (d)-(h). Total 15 observers with normal visual acuity participated in this experiment.

**(a) The method of successive categories**

AIC2015 TOKYO - Color and Image

In this session, the observers were asked to evaluate the depth perception of displays directly in 5 stages, by using the method of successive categories in binocular and monocular visions in a dark room. The successive categories are shown in Figure 4.

**(b) The method of paired comparison**

We carried out a paired comparison method to evaluate depth perception for 6 mobile displays, totally 15 combinations. Observers answered which mobile phone presented stronger 3D effect in each image and movie.

*Table 3. Image quality indices and visual evaluation result*

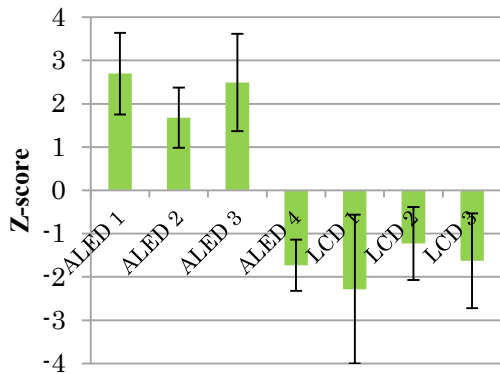| Device | RCVCAM02-USC | CRI | RI | $IQI_{total}$ | Z-score |
|---|---|---|---|---|---|
| AMOLED phone 1 | 0.811 | 0.837 | 0.664 | 0.763 | 2.698 |
| AMOLED phone 2 | 0.811 | 0.840 | 0.757 | 0.801 | 1.680 |
| AMOLED phone 3 | 0.857 | 0.886 | 0.742 | 0.823 | 2.491 |
| AMOLED phone 4 | 0.760 | 0.686 | 0.526 | 0.637 | -1.730 |
| LCD phone 1 | 0.513 | 0.363 | 0.526 | 0.458 | -2.284 |
| LCD phone 2 | 0.503 | 0.364 | 0.642 | 0.503 | -1.227 |
| LCD phone 3 | 0.703 | 0.372 | 0.761 | 0.594 | -1.626 |



*Figure 2. Visual image quality results of paired comparison method of $IQI_{color}$*
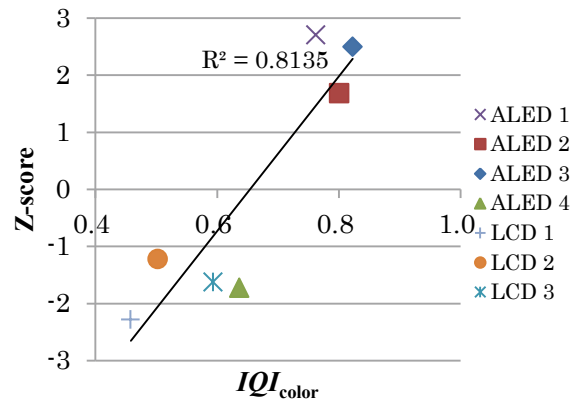


*Figure 3. The relationship between $IQI_{total}$ & Z-score*
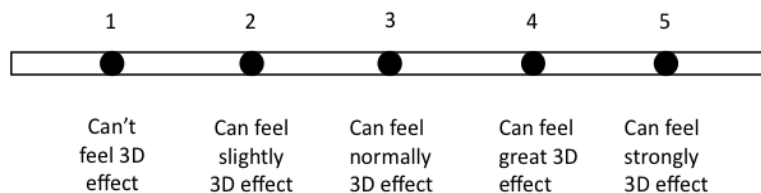


*Figure 4. Category of 3D perception*

As Part 1, after completing above experiments, an image quality index for depth perception will be established. It would be considered that the feeling of depth could be affected by color volume, luminance contrast, resolution and display size. We have already defined the color volume and the contrast ratio as Equations (1) and (2), but we use pixel per degree (ppd) instead of pixel per inch in resolution index as follows,

$$RI_{retina} = ppd / 100 \tag{7}$$

The number of 100 comes from rough number of cones in a visual angle of one degree in a foveal retina. Display size are also be defined as a field size in retina as follows,

$$RDS_{retina} = [(\text{Display size in degree}) / 1440]^{1/2} \tag{8}$$

The number of 1440 comes from a full visual field with binocular vision, 48º by 30º. Both of the display resolution in retina, $RI_{retina}$ and the display size in visual angle, $RDS_{retina}$ depend on the viewing distance. As the same way, we derive $IQI_{3D}$ as Equation (6).The weighting coefficients $w_{CV}$ , $w_{CR}$, $w_R$ and $w_{DS}$ are 0.3, 0.3, 0.2 and 0.2, having a high correlation with Z-score. Table 4 shows the $IQI_{3D}$ result of each mobile display.

$$IQI_{3D} = w_{CV}\, RCV_{CAM02\text{-}USC} + w_{CR}CRI + w_{RS}\, RI_{retina} + w_{DS}\, RDS_{retina} \qquad (9)$$

*Table 4. IQI_{3D} evaluation results*

| Device | $RCV_{CAM02\text{-}USC}$ | CRI | $RI_{retina}$ | $RDS_{retina}$ | $IQI_{3D}$ |
|---|---|---|---|---|---|
| AMOLED phone 1 | 0.811 | 0.837 | 0.837 | 0.470 | 0.752 |
| AMOLED phone 2 | 0.811 | 0.840 | 0.926 | 0.413 | 0.763 |
| AMOLED phone 3 | 0.857 | 0.886 | 0.909 | 0.420 | 0.789 |
| AMOLED phone 4 | 0.760 | 0.686 | 0.639 | 0.399 | 0.642 |
| LCD phone 1 | 0.513 | 0.363 | 0.645 | 0.395 | 0.471 |
| LCD phone 2 | 0.503 | 0.364 | 0.792 | 0.481 | 0.515 |
| AMOLED tablet | 0.834 | 0.840 | 0.623 | 0.864 | 0.800 |
| LCD tablet | 0.562 | 0.382 | 0.574 | 0.825 | 0.563 |

## 3. RESULTS AND DISCUSSION

Figure 5 and Figure 6 shows the results of psychophysical experiments in $IQI_{3D}$. In Figure 6, we normalized the successive categories from 0 to 1. We can see the all AMOLED displays have a high preference than LED displays. Finally, we conducted a one-way ANOVA in each result of the experiments, showing some of differences reach their significant levels as shown in green shaded cells in Table 5 and Table 6. The results indicated the threshold is 0.09 when observers can discriminate 3D depth effect easily. As the same way in Table 6, the base rate of subjective evaluation can be earned from the difference ratio in $IQI_{3D}$ and subjective evaluation is 0.9158, thus we can know roughly how much the subjective 3D depth feeling will be according to $IQI_{3D}$ value.
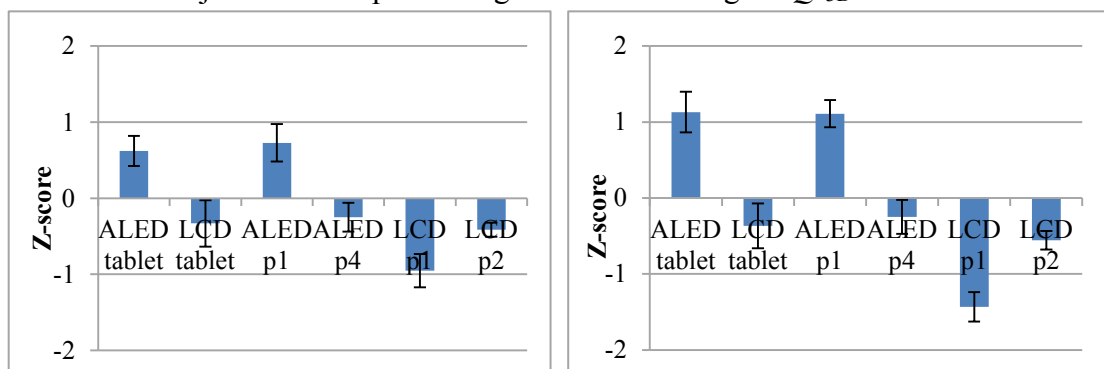


*Figure 5. Visual image quality obtained by paired comparison method,*
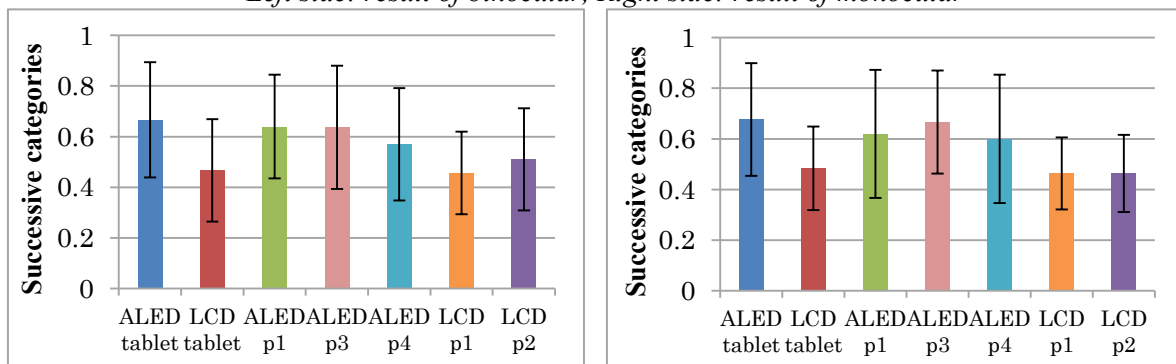*Left side: result of binocular, Right side: result of monocular*



*Figure 6. Visual image quality obtained by successive categories experiment*
*Left side: result of binocular, Right side: result of monocular*

AIC2015 TOKYO - Color and Image

| ALED p1 | ALED p3 | ALED p4 | LCD p1 | LCD p3 | ALED tablet | LCD tablet |

*Table 5. The differences of $IQI_{3D}$ in paired comparison*

| | ALED p1 | ALED p4 | LCD p1 | LCD p3 | ALED tablet | LCD tablet |
|---|---|---|---|---|---|---|
| ALED p1 | 0 | -0.110 | -0.280 | -0.227 | 0.275 | -0.189 |
| ALED p4 | 0.110 | 0 | -0.170 | -0.117 | 0.158 | -0.078 |
| LCD p1 | 0.280 | 0.170 | 0 | 0.053 | 0.328 | 0.091 |
| LCD p3 | 0.227 | 0.117 | -0.053 | 0 | 0.275 | 0.038 |
| ALED tablet | -0.048 | -0.158 | -0.328 | -0.275 | 0 | -0.237 |
| LCD tablet | 0.189 | 0.078 | -0.091 | -0.038 | 0.237 | 0 |

*Table 6. The differences of $IQI_{3D}$ in subjective evaluation*

| | ALED p1 | ALED p3 | ALED p4 | LCD p1 | LCD p3 | ALED tablet | LCD tablet |
|---|---|---|---|---|---|---|---|
| ALED p1 | 0 | 0.037 | -0.110 | -0.280 | -0.227 | 0.048 | -0.189 |
| ALED p3 | -0.037 | 0 | -0.147 | -0.317 | -0.264 | 0.011 | -0.226 |
| ALED p4 | 0.110 | 0.147 | 0 | -0.170 | -0.117 | 0.158 | -0.078 |
| LCD p1 | 0.280 | 0.317 | 0.170 | 0 | 0.053 | 0.328 | 0.091 |
| LCD p3 | 0.227 | 0.264 | 0.117 | -0.053 | 0 | 0.275 | 0.038 |
| ALED tablet | -0.048 | -0.011 | -0.158 | -0.328 | -0.275 | 0 | -0.237 |
| LCD tablet | 0.189 | 0.226 | 0.078 | -0.091 | -0.038 | 0.237 | 0 |

## 4. CONCLUSIONS

We developed image quality index for color ($IQI_{color}$) for evaluating the image qualities of color and sharpness, and image quality index for 3D perception ($IQI_{3D}$) for evaluating depth perception. In $IQI_{color}$, we found that as bigger values displays had, the better image qualities were perceived. In $IQI_{3D}$, there are the same tendencies with $IQI_{color}$ in perceiving 3D depth effect. The results also suggest that the $IQI_{3D}$ difference of 0.1 could cause an easily perceptible difference of depth between different displays.

## REFERENCES

Mark D. Fairchild, 2013. *Color Appearance Models, 3rd Ed.* Wiley-IS&T, Chichester, UK

Masao Inui, 2000. The Quantification of Color Gamut Efficiency, *J. Soc. Photogr. Sci. Technol. Japan,* 63, 277-281.

M. Ronnier Luo, Guihua Cui, and Changjun Li, 2006.Uniform Colour Spaces Based on CIECAM02, *Color research and application* 31(4): 320-330.

Society for Information Display (SID) 2012.Information Display Measurements Standard ver.1.03, 82-84

*Address: C.-K. CHANG, Graduate School of Advanced Integration Science, Chiba University, 1-33 Yayoicho, Inage-Ku, Chiba, 263-8522, Japan*
*E-mail:hibadina0520@yahoo.com.tw*
*yaguchi@faculty.chiba-u.jp, mizokami@faculty.chiba-u.jp*

# Imageries of Edible Souvenirs Evoked by Colours and Visual Textures of Packages

Shuo-Ting WEI

Department of Visual Communication Design, TransWorld University, Taiwan

## ABSTRACT

The current study aims to investigate the relationship between imagery and appearance of packing papers for edible souvenirs in terms of colours and visual textures. To achieve this, an experiment of categorical judgments was carried out. 25 observers provided integers from 1 to 7 to show their opinions for 100 stimuli with 12 different textures. The 20 bipolar scales of imagery were assessed for each stimulus. The results showed that only the imagery of roughness was significantly influenced by texture. For the effect of colour on imagery, we found that packing papers with light colours are more likely to be considered soft and relax. Red and orange were considered warm and friendly colours, whereas cyan and blue were associated with cool and unfriendly. The 20 imageries for the appearance of packing papers can be explained using 4 principal imageries. They explained 80.41% of total variations.

## 1. INTRODUCTION

In the recent few years, Taiwan's travel industry has witnessed a surge in tourist numbers and the spending by tourists in souvenirs has increased accordingly. This has led to a larger yet more competitive market of tourism souvenirs, i.e., commemorative merchandise associated with a location to provide tourists a memento of their visit and to encourage an opportunity for a return visit. Thus, seeking approaches to highlight features and to create a unique identity (e.g., product feature, brand images…etc) for tourism souvenirs has received a great deal of attention from package designers. Among many aspects, colors and visual textures of packaging materials are two essentials of design that conveys product features and brand images. In this study, we aim to examine the relationship between imagery and appearance of packing papers for edible souvenirs in terms of colours and visual textures.

Many of the relevant studies regarding the imagery of colour, or colour emotion, tended to agree that imagery of heat, i.e. warm and cool, is highly associated with hue. The imageries of hardness (i.e. hard and soft) and weight (i.e. heavy and light) are associated with lightness. Activity and clearness, on the other hand, tend to be associated with chroma (Kobayashi, 1981; Sato et al., 2000; Ou et al., 2004; Lee & Lee, 2005; Gao et al., 2007). In the recent years, the relationship between colour and imagery was proved to be impacted by visual textures. Lucassen et al. (2011) investigated the influence of texture on the imagery of colours. They concluded that texture cannot be ignored in colour emotion studies as they found that the imagery of hardness is fully determined by texture, and in decreasing extent for masculine–feminine, heavy–light, and warm–cool. Simmons & Russell (2008) also found that the imagery of pleasantness was impacted by texture. People tended to feel unpleasant for colour samples with textures. The extent of unpleasantness was determined by types of textures.

## 2. METHOD

Visual assessments using the categorical judgment method (Torgerson, 1958) were conducted to obtain psychological responses with regard to imageries of packing papers. The experimental settings and procedures are described below.

### 2.1 Stimuli Preparation

A hundred of packing papers were selected in this study as the materials for stimuli preparation. As shown in Figure 1, the papers include 12 different textures. Each texture has multiple colours from 1 to 21. These papers are frequently used in graphic design and package design. Figure 2 shows the CIELAB values of the 100 papers, which gives a good coverage in $a^*$-$b^*$ plane. The reason why colours of lightness below 20 were missing is because surfaces of the papers are matt, which naturally produces diffuse reflection of light. The packing papers were presented in a form of 20*12*4 cm$^3$ boxes in the experiment as visual stimuli, as shown in Figure 3. This was to simulate the papers being seen in the context of souvenirs.



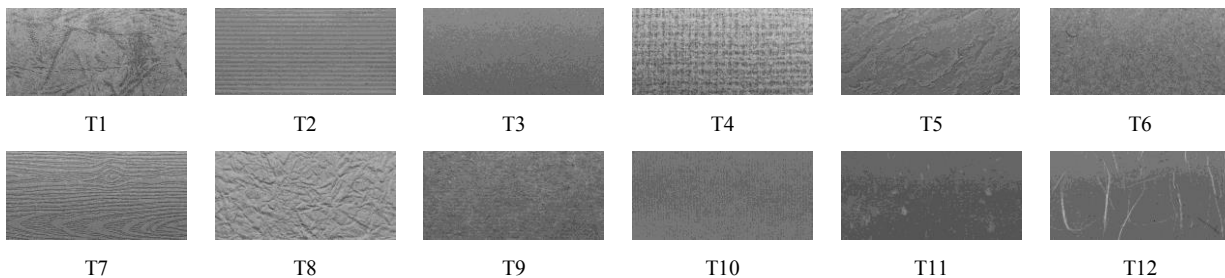| T1 | T2 | T3 | T4 | T5 | T6 |

| T7 | T8 | T9 | T10 | T11 | T12 |

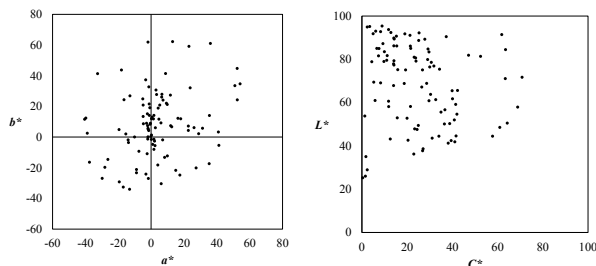Figure 1 The 12 textures of packing papers examined in this study.



Figure 2 The colours of packing papers in CIELAB (a) $a^*$-$b^*$ plane and (b) $L^*$-$C^*$ plane.
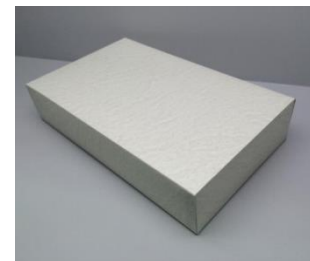
Figure 3 An example of the visual stimuli

### 2.2 Scales of Imagery

Twenty bipolar scales of imagery were used in this study to measure observers' opinions about appearance of packing papers in terms of colour and texture. These scales includes heavy – light, complex – simple, natural – artificial, rough – smooth, local – international, active – passive, dislike – like, old – new, romantic – realistic, casual – formal, realistic – exaggerated, fresh – overdue, hard – soft, relax – serious, cheap – expensive, warm – cool, friendly – unfriendly, delicious – insipid, plain – gorgeous and loose – tight. These scales are relevant to package design (e.g. romantic – realistic), colour appearance (e.g. warm–cool), texture appearance (e.g. rough – smooth) or food souvenir (e.g. delicious – insipid). They were chosen by five package designers using KJ method, i.e. affinity diagram.

Integer eget neque ac ex lobortis consequat. Morbi non eros arcu. Donec convallis sem et augue cursus, vel rutrum orci sollicitudin. Quisque vel nulla felis. Sed scelerisque mollis consectetur. Integer lacinia nec ex nec consectetur. Phasellus finibus sollicitudin volutpat. Nunc eget nibh lacus. Vivamus commodo convallis turpis, et dignissim ex suscipit id. Phasellus lorem massa, auctor nec porttitor a, dignissim id tellus. Nam laoreet ut ante vitae pulvinar. Proin est ipsum, iaculis sit amet ipsum nec, mattis hendrerit nisi. Quisque nec orci sed metus interdum molestie sit amet vitae arcu. In hac habitasse platea dictumst. Sed volutpat lectus at lorem vehicula blandit. Donec fermentum ligula sit amet augue finibus ornare congue a purus.

## 2.3 Observers

Twenty five observers participated in this study, including 13 females and 12 males. All of them were undergraduate students at the TransWorld University, Taiwan. All of them major in graphic design. The ages of these observers ranged from 20 to 22 with an average of 21. All observers passed the Ishihara test to ensure normal colour vision.

## 2.4 Experimental Procedures

The experiment was carried out in a dark room. The visual stimuli were presented in a viewing cabinet and illuminated using D65. The observers were seated approximately 30cm from the near edge of the viewing cabinet. During the experiment, the observers provided integers from 1 to 7 to show their opinions for the 100 stimuli. The 20 bipolar scales of imagery were assessed for each stimulus. The whole experiment was divided into 4 sessions of equal numbers of assessments. The observers completed the 4 sessions within two weeks.

## 3. RESULTS

### 3.1 Consistency of Responses

The consistency of observers' responses was firstly investigated by examining intra- and inter-observer agreements using the measure of *root mean square* (RMS). For intra-observer agreement, the results revealed that most of the RMSs between repeated assessments were around 1 unit with the mean RMS of 1.07 units for female observers and 1.08 units for male observers. This indicates high intra-observer agreement, as the differences between repeated assessments for both male and female were around 1 category of the 7-category measurement scale.

In the case of inter-observer agreement, the mean values of RMS were 1.37 for female and 1.33 for male observers. This indicates that the differences between individual observers' responses and the responses of the majority were less than 1.5 categories of the 7-category measurement scale, suggesting reliable inter-observer agreement.

### 3.2 Gender Differences

Gender differences were investigated using the measure of *root mean square* (RMS, see equation 1), too. It was found that the RMS value is 0.92, which is slightly smaller than 1 unit of the 7-category measurement scale. This suggests small differences of experimental

results between female and male observers. Hence, the imageries of the visual stimuli were determined by mean scores of the 25 observers' raw data.

### 3.3 The Influence of Textures

The results of the stimuli with beige and cyan colours were selected to analyse the influence of textures. We found that only the imagery of rough – smooth was significantly influenced by texture. Figure 4(a) illustrates the results of rough – smooth against 9 different textures with error bars of 95% confidence interval. Dots and crosses denote beige and cyan samples, respectively. The figure shows that the texture of flax (T4) and texture of kneaded paper (T8) were considered rough textures ($p<.05$). Although in average the texture of wood (T7) was considered rough, the results did not significantly lower than the score 4.

Hard – soft, the scale that was concluded by Lucassen et al. (2011) to be fully determined by texture, did not show the same result in the current study. As shown in Figure 4(b), most of the 9 textures were considered soft for both beige and cyan colours. In addition, beige colour looked much softer than cyan colour ($p<.05$) for the stimuli with the textures of T2, suggesting that colour influences the imagery of hard – soft.
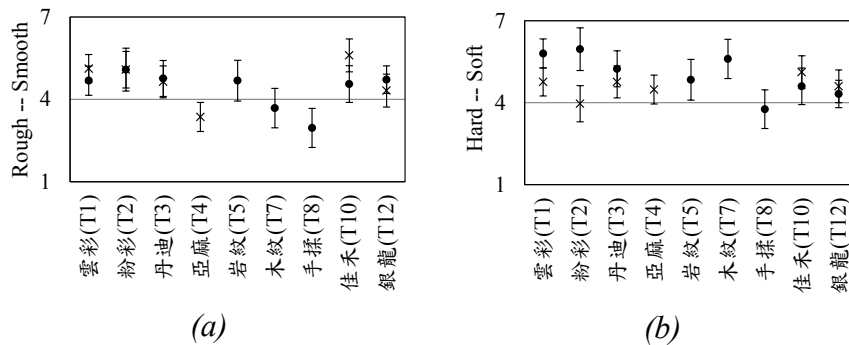


*(a)*        *(b)*

*Figure 4 (a) Roughness and (b) hardness scores of the 9 textures with beige (dots) and cyan (crosses) colours.*

### 3.4 The Influence of Colours

The influence of colours was examined in terms of lightness, hue and chroma. We found that some scales of imagery were affected by lightness and chroma. However, Chroma of packing papers neither correlated well with the scales of imagery nor showed any clear nonlinear trend.

The scales of heavy – light, hard –soft and relax – serious were highly correlated with lightness. The correlation coefficients R equals .88, .74 and -.80, respectively. This suggests that packing papers with light colours are more likely to be considered soft and relax no matter what kind of texture is used. Figure 5 shows the scatter plots of hue against the scales of warm – cool and friendly – unfriendly. It was found that both scales of imagery were associated hue with clear nonlinear trends. Red and orange were considered warm and friendly colours, whereas cyan and blue were associated with cool and unfriendly.
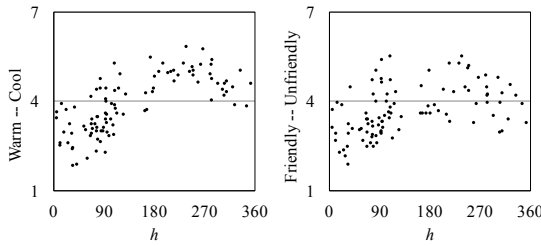
*Figure 5 the scatter plots of hue angle against warm – cool and friendly – unfriendly.*
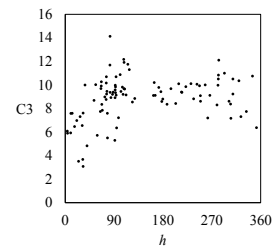


*Figure 6 the scatter plot of hue angle against the component C3.*

## 3.5 Principal Imageries

Principal Component Analysis (PCA) was carried out to investigate whether there is any underlying principal component that can be used to explain the experimental results of the 20 scales of imagery. As a result, 4 principal components were found and they explained 80.41% of total variations. The components and the included scales of imagery are given in Table 1. Component C1 was highly correlated with lightness of packing papers (R = -.84). C2 and C3 were moderately with yellowness-blueness (i.e. $b^*$) and Chroma, respectively (R = -0.51 and -0.63). The scatter plot of C3 against hue also revealed a clear nonlinear trend as shown in Figure 6. No clear trend was found between the component C4 and colour attributes.

*Table 1 The 4 principal components and their relevant imageries.*

| Components | C1 | C2 | C3 | C4 |
|---|---|---|---|---|
| Scales of imagery | complex – simple | cheap - expensive | realistic - exaggerated | warm - cool |
| | rough – smooth | loose - tight | romantic - realistic | friendly - unfriendly |
| | dislike – like | natural - artificial | active - passive | delicious - insipid |
| | old – new | hard - soft | | fresh - overdue |
| | local - international | plain - gorgeous | | |
| | heavy - light | relax - serious | | |
| | casual - formal | | | |

## 4. CONCLUSIONS

This study aims to investigate the imagery of packing papers for edible souvenirs. More specifically, we examine the relationship between imagery and appearance of packing papers in terms of colours and visual textures. To achieve this, visual assessments using the categorical judgment method were conducted to quantify psychological responses with regard to imageries of packing papers. A hundred packing papers with the 12 different textures were visually assessed by the 25 observers using the 20 bipolar scales of imagery. The results revealed that only the imagery of rough – smooth was significantly influenced by texture. For the effect of colour on imagery, we found that heavy – light, hard –soft and relax – serious were highly correlated with lightnes, suggesting that packing papers with light colours are more likely to be considered soft and relax. The scales of warm – cool and friendly – unfriendly were associated with hue angle. Red and orange were considered warm and friendly colours, whereas cyan and blue were associated with cool and unfriendly. Chroma of packing papers neither correlated well with the scales of imagery nor showed any clear nonlinear trend. The results of PCA suggest that imagery of packing papers for edible souvenirs can be adequately explained using 4 principle imageries.

## ACKNOWLEDGEMENTS

## REFERENCES

Gao, X., Xin, J., Sato, T., Hansuebsai, A., Scalzo, M., Kajiwara K., Guan, S., Valldeperas, J., Lis. M., and Billger, M. 2007. Analysis of Cross-cultural Color Emotion, *Color Research and Application* 32: 223-229.

Ishihara, S. 2003. *Ishihara's tests for colour deficiency. 38 Plates Edition.* Tokyo: Kanehara Trading.

Kobayashi, S. 1981. The Aim and Method of Color Image Scale. *Color Research and Application* 6: 93-107.

Lee, Y. and Lee, J. 2005. The Development of an Emotion Model Based on Colour Combinations. *International Journal of Computer Studies* 30: 122-136.

Lucassen, M.P., Gevers, T., Gijsenij, A. 2011. Texture Affects Color Emotion, *Color Research and Application* 36: 426-436.

Ou, L., Luo, M. R., Woodcock, A. and Wright, A. 2004. A study of Colour Emotion and Colour Preference Part I: Colour Emotions for Single Colours, *Color Research and Application* 29**:** 232-240.

Sato, T., Kajiwara, K., Hoshino, H. and Nakamura, T. 2000. Quantitative Evaluation and Categorizing of Human Emotion Induced by Color, *Advances in Color Science and Technology* 3: 53-59.

Simmons, D. and Russell, C. 2008. Visual Texture Affects the Perceived Unpleasantness of Colours. *Perception* 37, ECVP Abstract Supplement, 146-146.

Torgerson, W.S. 1958. *Theory and methods of scaling*. New York: John Wiley & Sons.

*Address: Dr. Shuo-Ting Wei, Department of Visual Communication Design, TransWorld University, No.1221, Zhennan Rd., Douliu City, Yunlin County 640, Taiwan*
*E-mail: tim.stw@gmail.com*

# A Study of the preference and orientation of
# "the sense-oriented"

Takashi INABA

Nippon Color & Design Research Institute Inc.

## ABSTRACT

To decide the color of the product, it is desirable to reflect the preference of the users. When only one or two color use is permitted for a new product, it is important to choose novel and distinguishable colors. In order to achieve this, we offer a method to identify individuals with strong interest in colors, design, art and trends as "sense-oriented", and refer to them as an index upon determining the colors of products.

The "sense-oriented" females, obtained through a survey of 1,440 subjects, wish others to consider them as fashionable figures, and prefer the elegant and classy image. Moreover, they hold a preference for high-quality materials, brilliant colors such as red and gold, and cold colors with hues of B and BG. They are also enthusiastic consumers and set a high value on texture.

## 1. INTRODUCTION

Upon deciding the color of a product, it is important to reflect the users' color needs. When it is possible to have color variations for a single product, the colors can be set for each user group with different needs. If that is not the case, it is a common solution to choose a popular color among the general population which consequently results in a situation where many products have the same color, which leads to the lack of distinction and novelty.

The introduction of the method to identify individuals who actively adopt new colors and using their preferred colors on new products will bring novel colors to the market, which could potentially lead other users to follow and consume those colors. The process is to first select people with strong interest in colors and design, then within that group determine individuals who are interested in the field of that product, who will then serve as the index for the target as color leaders.

In this research, as the primary step, people with strong interest in colors, design and trends were selected, then were compared to those who lack interest in the subject area for color and image preference.

## 2. METHOD

The survey was conducted online on 1,440 male and female subjects, ages ranging from 18 to 69 years old. The questionnaire consisted of two parts: Part 1 Questionnaires to research the awareness of colors, design, art and trends, and Part 2 Questionnaires to research color preference by presenting visuals.

20 questionnaires, such as "Have you confidence in your sense of color ? ", "Do you often go to the event or exhibitions of art and design ?" and "Do you buy cheaper thing even

AIC2015 TOKYO - Color and Image

though that is not your favorite color and design ? ", were set to select out individuals with strong interest in colors, design and trends. The subjects answered the questionnaires on a 5 point scale.

In the questionnaire to research the preference by presenting visuals, 48 colors selected from Hue & Tone system were used in order avoid bias (Figure 1).
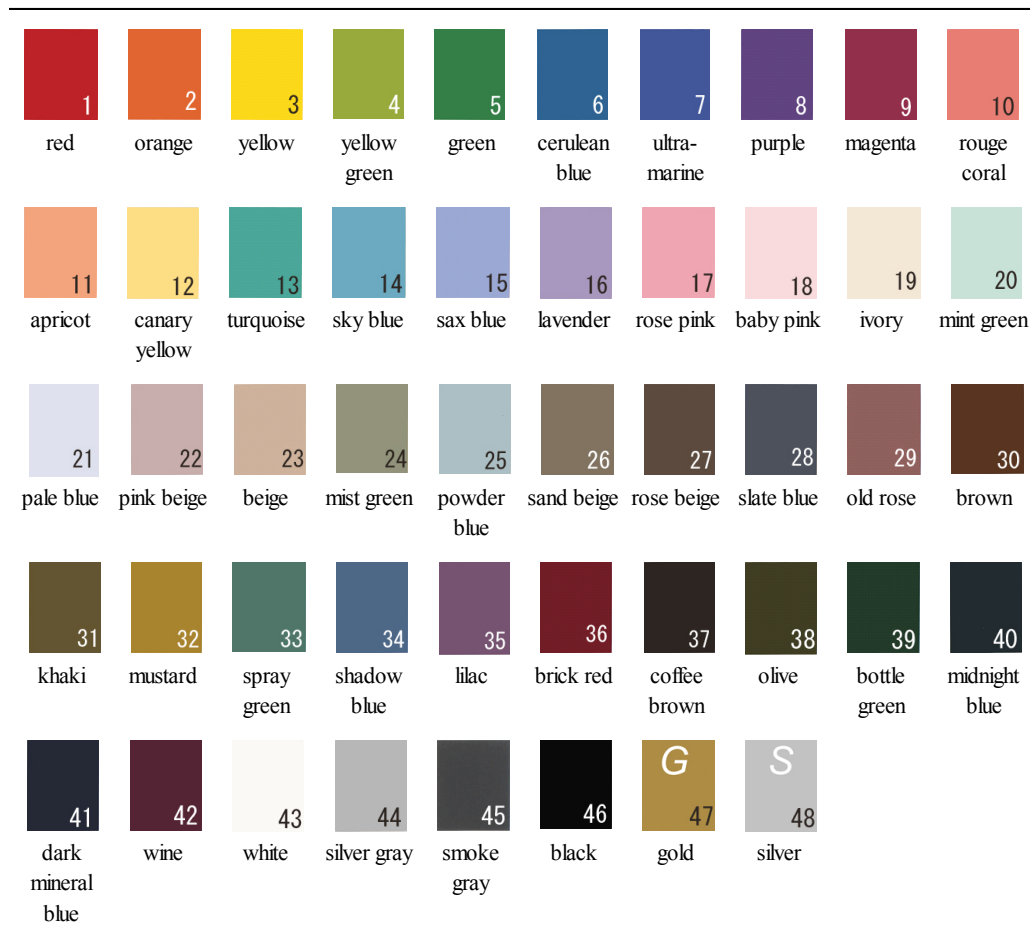


*Figure 1: Color Samples.*

## 3. RESULTS AND DISCUSSION

Factor analysis was performed on the data from the questionnaires on colors, design, art and trends (maximum likelihood method, Promax factor rotation with Kaiser's normalization). Pattern matrix is shown in the Table 1.

Factor 1 indicates the acquisition of information, such as familiarity with events regarding design and art, and the knowledge of trend colors and designs. Factor 2 indicates the actual actions taken, such as adopting colors and designs into their daily lives or how much they put emphasis on colors and designs upon purchasing items.

Cluster analysis was then conducted. As a result, 1,440 subjects were divided into four clusters. Regarding the component ratio, Cluster 1 is the smallest at 15.6% whereas Cluster 2 is the largest at 35.0% as shown in Table 2. Figure 2 presents the cluster center of each cluster.

*Table 1.  Pattern matrix(Factor analysis).*

| | FACTOR | |
|---|---|---|
| | 1 | 2 |
| Do you know "Milano Salone","Tokyo Designer's Week" ? | 0.977 | -0.250 |
| Do you often go to the event or exhibitions of art and design ? | 0.910 | -0.140 |
| Are you engaged in color and design on business (or study) ? | 0.873 | -0.173 |
| Do you have a favorite designer of product or fashion ? | 0.863 | -0.024 |
| Are you well informed of art and design ? | 0.845 | -0.028 |
| Do you often watch TV programs, Web sites, magazines on art and design ? | 0.828 | 0.012 |
| Do you know the latest trendy colors ? | 0.780 | 0.043 |
| Do you like finding the information of trends about color and design in magazines or on the Internet ? | 0.582 | 0.230 |
| Do your family or friends ask you for advice how to use colors ? | 0.548 | 0.322 |
| Do you often go to fashionable shops and town ? | 0.508 | 0.325 |
| Do you pay attention to a new package of beverage, confectionery and foods ? | 0.417 | 0.317 |
| Do you buy cheaper thing even though that is not your favorite color and design ? | -0.474 | 0.830 |
| Do you think color and design enrich people's life ? | -0.090 | 0.786 |
| Do you know the color that suits yourself ? | -0.003 | 0.719 |
| Are the colors and design of your clothes and room coordinated by your own taste ? | 0.077 | 0.701 |
| Do you like making the coordination of fashion or interior ? | 0.181 | 0.695 |
| Do you want to buy a product that nobody has the similar design ? | 0.030 | 0.658 |
| Do you often buy a product because you are attracted by its color and design ? | -0.036 | 0.643 |
| Do you check the color of your clothes and accessories so that it won't be the same with others around you ? | 0.173 | 0.612 |
| Are you praised for the color coordination of your clothes and accessories ? | 0.229 | 0.611 |
| Do you like going window-shopping or looking display of products ? | 0.256 | 0.562 |
| Have you confidence in your sense of color ? | 0.265 | 0.543 |
| Do you try to use the colors that match to the season ? | 0.264 | 0.540 |
| Can you explain the good points of the product design that you chose ? | 0.444 | 0.453 |
| Do you want to use trendy colors into your daily life ? | 0.336 | 0.401 |

Cluster 1 holds a positive position for both Factor 1 "information" and Factor 2 "actions", which indicates that Cluster 1 considers their sense, interests in colors, design and trends, to be essential. They were categorized as "sense-oriented". Cluster 2 regards sense as an important factor, though not as much as Cluster 1, therefore were categorized as "semi sense-oriented". Cluster 3 and Cluster 4 were identified as "average" and "low-interest", respectively. Regarding the component ratio of sex, Cluster 1 had the highest female ratio, whilst Cluster 4 had the highest male ratio.

*Table 2.  Component ratio.*

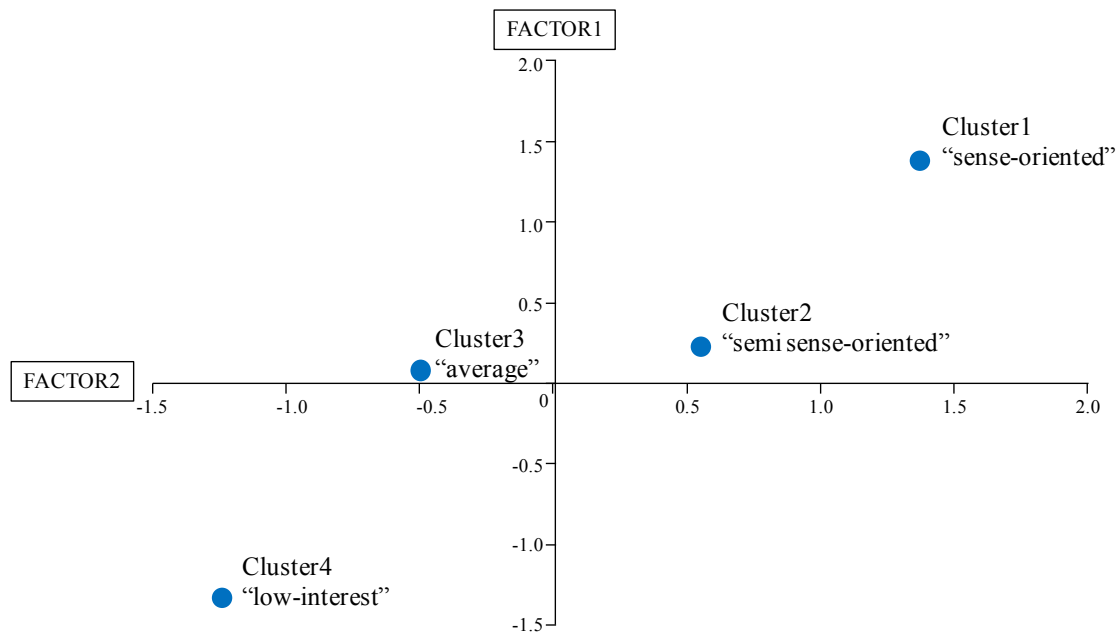| | | % |
|---|---|---|
| Cluster1 | "sense-oriented "(sensibility as important ) | 15.6% |
| Cluster2 | "semi sense-oriented" ( sensibility a little ) | 35.0% |
| Cluster3 | "average" | 26.9% |
| Cluster4 | "low-interest" | 22.5% |
| | | N=1440 |

*Figure 2: Cluster score matrix.*

A comparison was then performed between Cluster 1 "sense-oriented" and the other clusters for color and image preferences. Since color preference differs by gender, the analysis was separately performed on males and females. The following is the result of the female subjects.

Figure 3 presents the result of individuals from the "sense-oriented" cluster and individuals from other remaining clusters choosing a single favorable color. Additionally, a Chi-squared test was performed to investigate the presence of a significant difference between the two groups. As a result, there was a significant difference in turquoise, red and gold (P<0.01), and lavender, white, ultra marine, mint green and dark mineral blue (P<0.05).
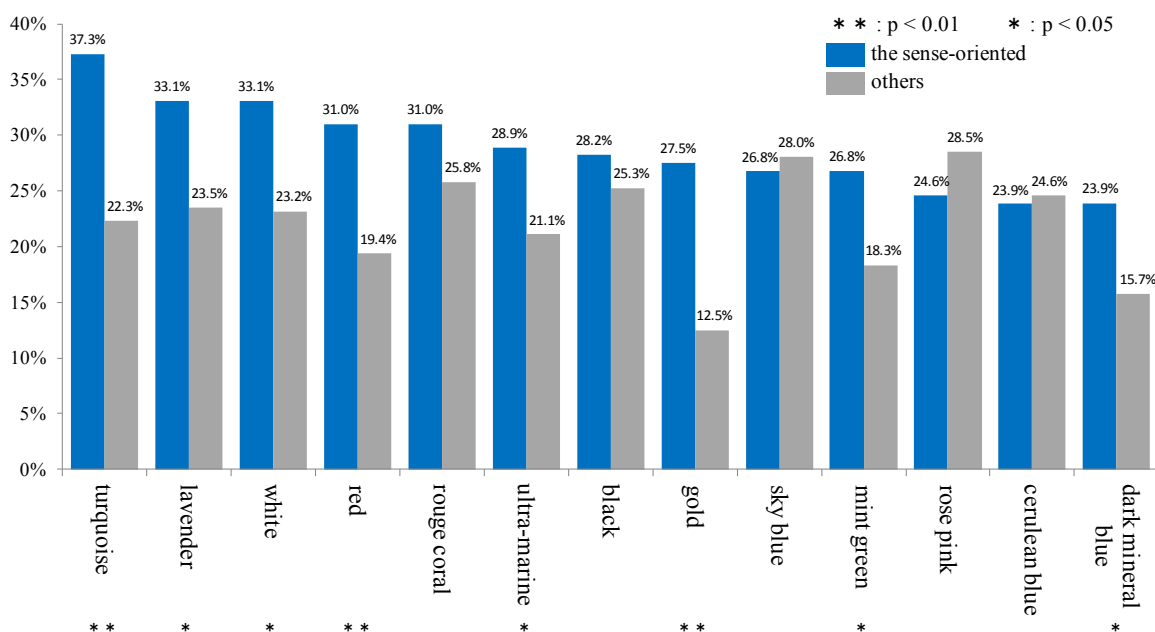


*Figure 3: Color Preferences.*

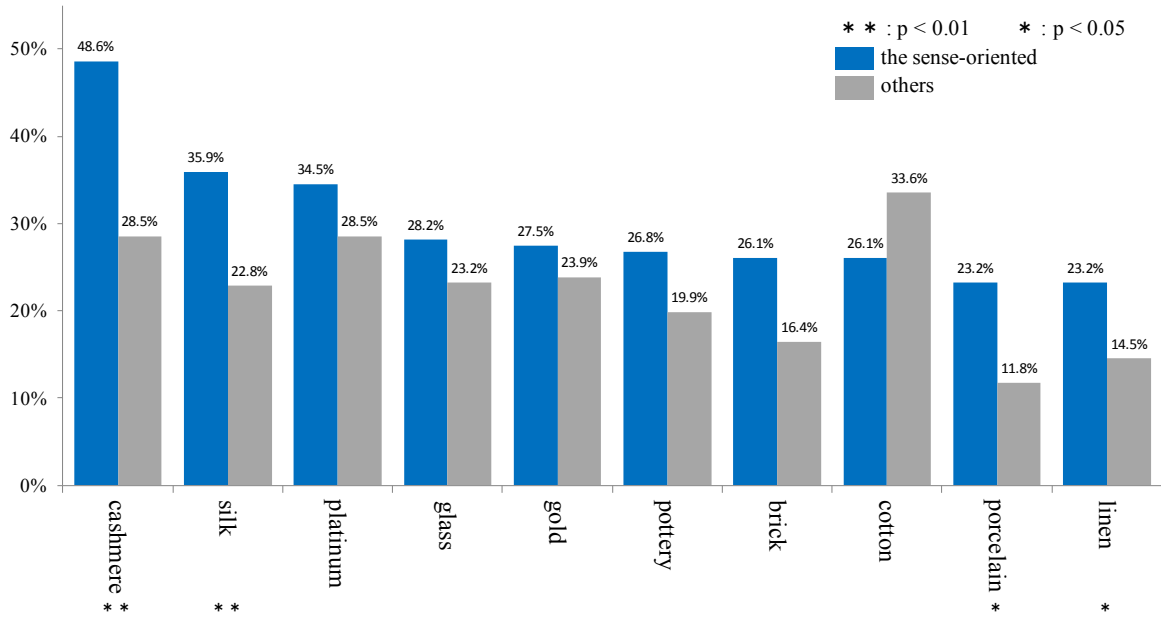Moreover, in the material category, cashmere and silk were P<0.01, and porcelain and linen were P<0.05 (Figure 4).



*Figure 4: Material Preferences.*

When the subjects were asked to choose a favorite image word, elegant (P<0.01), and refined, polished and feminine (P<0.05) presented a significant difference (Figure 5).
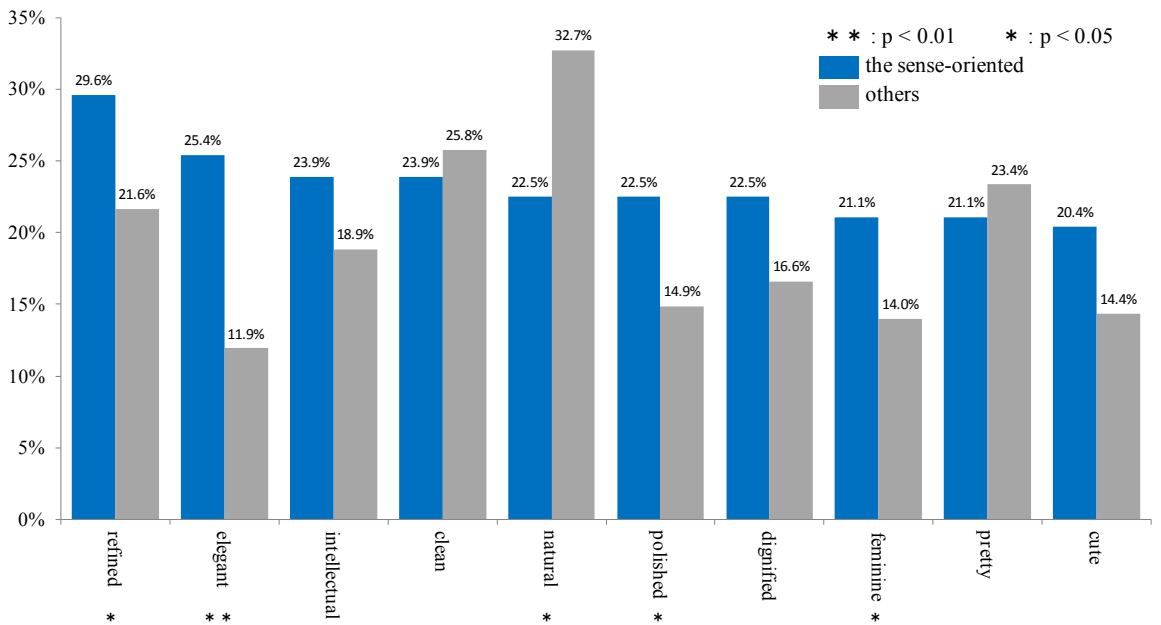


*Figure 5: Favorite Image Word.*

In the questionnaire on how they wish to be viewed by others, fashionable, person with good taste and intelligent (P<0.01), and polished (P<0.05) presented a significant difference.

In the questionnaire regarding their perspective on purchasing, there was a significant difference (P<0.01) between "sense-oriented" and others in the following:

I love shopping (sense-oriented 36.6%, others 23.9%)
I buy items I like even if it is slightly out of my range (35.9%, 18.9%)
I put a high value on the sense of touch and the texture upon purchasing (35.2%, 17.0%)
The country of origin of the product is significant to me (33.1%, 15.2%)
I will put emphasis on the design if the price is the same (30.3%, 15.9%)
I am confident in my judgment to choose a good product (27.5%, 10.9%)
I have my own preference for specific brands and companies (23.2%, 8.1%)

The above results indicate that the "sense-oriented" females desire to be viewed as fashionable and favor elegant and polished images. Regarding their perspective on purchasing, they are proactive buyers with specific preference for the countries of origin of the product and the brands. Moreover, their value on not only the appearance of the product but also the texture of it became apparent as they favored high quality materials such as cashmere and silk.
They favor vibrant, brilliant colors such as red and gold, along with colors in several tones which give out a cool impression such as turquoise, ultra marine, mint green and dark mineral blue.


# 4. CONCLUSIONS

By presuming that it is crucial to reflect user preference upon deciding the best color for a product, the method to select individuals with strong interest in colors, design and trends among product users, and using their preference as an index to select colors and designs for products was presented.

A survey was conducted on 1,440 subjects, with questionnaires to evaluate the subjects' value on their sense, and questionnaires to study their favorite colors and materials, which was then used to select a "sense-oriented" group. The results indicated that the "sense-oriented" females value their sense, quality and elegance, and have high buying intention. Furthermore, when compared to females in the non-"sense-oriented" groups, they favor brilliant warm colors with high saturation, and cold colors in various tones which convey a cool impression.

In this manner, the efficacy has been partially verified regarding the method to refer to "sense-oriented" females as an index to select product colors in the process of product development.

*Address: Takashi INABA, Nippon Color & Design Research Institute Inc.,*
*3-5-2 Hongo Bunkyo-ku, Tokyo, 113-0033, JAPAN*
*E-mails: inaba@ncd-ri.co.jp*

# Color Preference Measured by Paper-Format Implicit Association Test

Shinji NAKAMURA,[1] Aya NODERA[2]
[1] Faculty of Child Development, Nihon Fukushi University
[2] Faculty of Human Culture and Sciences, Fukuyama University

## ABSTRACT

In a history of research concerning color preference, preference judgment has been measured via explicit behaviors, such as verbal report or so on. In many recent psychological studies, however, it has been indicated that expressed attitude measured with explicit methods often differs from underlying implicit attitude. In the present studies, we tried to analyze an implicit attitude toward color, using implicit association test (IAT). Paper-and-pencil style IAT (paper-IAT) makes us enable to execute psychological experiments simultaneously in a massy group to collect preference data from considerable number of participants. In a paper-IAT, the participants were asked to manually tick a list of discrimination targets (printed on paper). We can assess relative implicit color preferences by calculating differences of number of the items that the participants could make judgments. 234 undergraduate participants took part in paper-IAT experiments to measure relative preference between red and green, blue and yellow, and also black and white. Target colors were presented by either color names or object names which can easily make the participants recall specific colors. Two separated IAT experiments were repeated with an interval of five weeks. Results of psychological experiments indicated that correlations between implicit color preference measured by IAT and explicit color preference measured by visual analogue scale (VAS) were significant in chromatic color evaluations (red-green and yellow-blue), but not in the case of achromatic color (white-black). It was also shown that correlations between two repeated IATs were significant. These results suggested that paper-IAT holds a considerable reliability in measuring relative implicit color preference, and we can utilize it for measurements of color preference in a group experiment.

## 1. INTRODUCTION

Color preference has been one of the biggest concerns in the color sciences for long years. The color preference has been measured by various methods in accordance with the researcher's interest. In most cases, the methods in measuring color preference would be based on the participants' explicit behavior, such as verbal report or so on. Typically, an investigator may simply ask the participants to select their most preferred or hated color from a set of candidate colors. In many recent psychological studies, however, it has been indicated that explicitly expressed attitude often differs from underlying implicit attitude. Thus, in the present investigation, we tried to analyze implicit attitude toward color, using implicit association test (IAT; Greenwald et al, 1998). IAT is recognized as one of the most conventional methods in measuring implicit attitude in psychological studies. In IAT, participants discriminate target words into two criteria. In the condition where two psychological concepts which are mutually associated with each other are paired in discriminatory criteria, the participant's reaction is facilitated (reaction time is reduced),

and vice versa in the condition where the psychological concepts without implicit association are paired. IAT utilizes differences of reaction time in categorical judgment in order to measure participants' implicit attitude without their conscious and arbitrary indication.

In our previous reports, we tried to measure implicit associations between specific color combinations (red-green and white-black) and psychological concepts of pleasantness /unpleasantness, and found that significant positive correlations between IAT scores and explicitly measured color preference (by visual analogue scale [VAS]) in the case of chromatic color (red-green), but not in the achromatic case (white-black) (Nakamura & Nodera, 2014). The previous experiments employed four different styles of target color presentation, namely color name, color patch, object name and object picture. Correlations of IAT scores across the different targets were considerably high, indicating that IAT can be reliable and quite stable in measuring participant's implicit color preference.

The previous investigation successfully demonstrated that IAT can be utilized as one of the possible implicit measurements concerning the participant's color preference. On the other hand, conventional IAT measurement requires considerable test durations in isolated individual experiments. It makes researchers difficult to collect data from mass participants and grab general tendencies concerning color preference in specific groups. In the present studies, we tried to measure the participants' implicit color preference using paper-and-pencil style IAT (paper-IAT; Lemm et al, 2008). It makes us enable to execute psychological experiments simultaneously in a massy group to collect preference data from considerable number of participants. In a paper-IAT, the participants were asked to manually tick a list of discrimination targets (printed on paper), instead of a computer-based key pressing in the case of conventional IAT.

## 2. METHOD

Before participating IAT sessions, the participants' explicit color preferences were measured with visual analogue scale (VAS). In VAS session, the participants answered degree of preference/hate towards six colors (white, black, red, green, blue and yellow), by drawing slash ("/") on line whose ends were correspond to "completely dislike (0)" and "completely like (100)." In IAT session, they were participated in IAT trials measuring implicit associations between pleasantness/unpleasantness and targeted colors. Target color combinations were red-green, blue-yellow or white-black. IAT sheets were supplied to the participants. Each sheet was composed by 20 rows and three columns of target words, belonging to either the following four categories; target color1, target color2, pleasant and unpleasant (see figure 1). The target color was presented as 1) color name or 2) object name. In both cases, the target color was presented in Japanese with Chinese character. Table 1 indicates the objects employed in the object name conditions to represent the target colors. Pleasant and unpleasant words were also presented as nouns which represent the target concepts (e.g., happiness, peace or fortune for pleasant, and misery, pollution or evil for unpleasant words, in Japanese with Chinese character).

The participant's task was to discriminate and categorize the word, and tick a check mark at corresponding box (either left or right) located both sides of each target word. They executed two discrete discriminations simultaneously; colors and pleasant/unpleasant. Time limitation for discrimination in each sheet was 20 seconds. In a case of red-green evaluation, for example, two IAT sheets were employed. The participants were requested to

| GOOD or RED | | BAD or GREEN |
|:---:|:---:|:---:|
| ☐ | war | ☑ |
| ☐ | leaf | ☑ |
| ☑ | post | ☐ |
| ☐ | green | ☑ |
| ☐ | grass | ☑ |
| ☑ | apple | ☐ |
| ☑ | red | ☐ |
| ☑ | red | ☐ |
| ☐ | green | ☑ |
| ☑ | fortune | ☐ |
| ☐ | misery | ☑ |
| ☑ | peace | ☐ |

Figure 1 Sample of Paper-IAT sheet employed in the experiment. The participants were required to check the left box for "red" or "good" target and the right box for the "green" or "bad" target. In a real sheet, there were 20 rows and 3 columns of target words, and the color name and the object name were tested in a different trial.

Table 1 Objects employed in object-name IAT trials

| color | object | | | |
|---|---|---|---|---|
| red | tomato | apple | post | strawberry |
| green | melon | leaves | grass | (green)pepper |
| blue | earth | space | sea | sapphire |
| yellow | banana | lemon | dandelion | sunflower |
| white | rice | snow | tofu | rabbit |
| black | ink | tire | coal | (black)seaweed |

check "red" and pleasant words (and "green" and unpleasant words) at the check box located in same side in one of the sheets, and "green" and pleasant ("red" and unpleasant) were paired in the other one. The participants who exhibited greater implicit associations of psychological concept of pleasantness with the red, rather than with the green, can make more discrimination in the red-pleasant sheet than the green-pleasant sheet, and vice versa for the participants who implicitly preferred the color green. Thus, we can assess relative implicit preference between red and green, by differentiating numbers of checked items between two sheets.

Both VAS and IAT sessions were repeated with interval of 5 weeks (Test1 and Test2) in order to examine reliability of paper-IAT as an implicit measurement for color preference. The participants were undergraduate students. 275 students were participated in Test1 and 282 students were participated in Test2. 234 students who took part in both tests were set to be subjects to the following analyses (76 male and 158 female, ages ranged from 18 to 23). In this study, VAS and IAT scores were calculated for explicit and implicit indices which would represent relative color preference between red and green, blue and yellow or white and black. VAS scores were accomplished by difference between two raw VAS values divided by sum of them. IAT scores were also defined by difference of numbers of checked items between two target colors, divided by sum of them; e.g., in a case of red-green evaluation, scores were indicated by (red-green)/(red+green). With the standardization by sum of raw values, we can archive relative measurements avoiding the effects of general variations of the raw values. Both for VAS and IAT scores, positive values were assigned to relative preference to red, blue or white. Thus, score 0 means that there was no difference of preference, greater positive score means that the participant's greater preference in red, blue or white, and vice versa for negative value. We obtained three VAS scores (three color combinations; red-green, blue-yellow and black-white) and six IAT scores (three colors and two color presentations [color name and object name]) from each participant in each test.

# 3. RESULTS AND DISCUSSION

Table 2 indicates Peason's coefficiates of correlation between Test1 and Test2 for both VAS and IAT scores. VAS scores demonstrated quite high correlations ranging from 0.69 to 0.75 for each color combination. For IAT scores, correlations were relatively low as compared with VAS, but still significant and considerable with regard to the numerous participants took part in this investigation (ranging from 0.36 to 0.46). Thus, IAT scores obtained in this experiment can be a reliable measrement for implicit color preference, exhibiting a certain range of robustness against repeating tests with interval of five weeks.

Table 2 Coefficients of correlations between Test1 and Test2

|  | red-green | blue-yellow | white-black |
|---|---|---|---|
| VAS | 0.69 | 0.75 | 0.73 |
| color-name IAT | 0.36 | 0.40 | 0.39 |
| object-name IAT | 0.45 | 0.42 | 0.46 |

Table 3 Coefficients of correlations between VAS and IAT scores

| Test1 | red-green | blue-yellow | white-black |
|---|---|---|---|
| VAS-ColorName | 0.37 | 0.32 | 0.15 |
| VAS-ObjectName | 0.32 | 0.37 | 0.11 |
| ColorName-ObjectName | 0.28 | 0.31 | 0.30 |

| Test2 | red-green | blue-yellow | white-black |
|---|---|---|---|
| VAS-ColorName | 0.36 | 0.28 | 0.06 |
| VAS-ObjectName | 0.29 | 0.32 | -0.03 |
| ColorName-ObjectName | 0.32 | 0.34 | 0.29 |

Table 3 indicates correlations between VAS and IAT (both for color and object names) in Test1 and Test2. In red-green and blue-yellow evaluations, VAS and IAT were mildly correlated (from 0.28 to 0.37). Implicit color preference mesured by paper-IAT and explicit preference measured by VAS were consistent with each oterh in the case of evaulation for chromatic color combination, suggesting shared underlying foundations for both types of preferences. On the other hand, in white-black evaluation, correlations bween VAS and IAT were not significant and quite low (from 0.03 to 0.15).

This might be due to the fact that IAT scores were slightly biased toward white preference, whereas there were no such biases in VAS scores. This means that the participants who explicitly reported black preference exhibited black avoidance in implicit measurements, and sugests that there would be some discontinuities between explicit and implicit measurements of achromatic color preference. Table 3 also indicates correlation btween color-name IAT and object-name IAT. Coefficients supposed to be in medium range (from 0.28 to 0.34) evinced that the discrimination targets presented by either the color name or the object name successfully elicited identical psychological concept concerning color to the participants.

Above mentioned results in this research were generally consistent with our previous investigation employing conventional computer-based IAT. Thus, we can conclude that paper-IAT can be used as cost effective alternative with less equipment requirments and applicable for mass group experiments in measuring implicit color preference.

# 4. CONCLUSIONS

The current investigations tried to apply paper format IAT (paper-IAT) as implicit measurement of color preference. Psychological experiments indicated that paper-IAT exhibited a considerable reliability and mild but significant correlations against

conventional and explicit measurments of color preference (VAS) in the case of chromatic color evaluations.  Thus, we can utilize it for measurements of implicit color preference in a group experiment.

## REFERENCES

Greenwald, A. G., McGhee, D.E., and Shwarz, J.L.K. 1998. Measuring individual differences in implicit cognition: The implicit association test. *Journal of Personality and Social Psychology,* 74(6): 1464-1480.

Lemm, K. M., Lane, K. A., Sattler, D. N., Khan, S. R., and Nosek, B. A. 2008.  Assessing Implicit Cognitions with a Paper-Format Implicit Association Test.  In M. A. Morrison & T. G. Morrison (Eds.), *The psychology of modern prejudice* (pp. 123-146).  Hauppauge, NY: Nova Science Publishers.

Nakamura, S., and Nodera, A., 2014. Implicit association test can be applied for measuring color preference. *The 2nd Conference of Asia Color Association, Conference Proceedings* p.77-81.

*Address: Shinji Nakamura, Faculty of Child Development,*

*Nihon Fukushi University, Okuda, Mihama-cho, Aichi, 470-3295*

*JAPAN*

*E-mails: shinji@n-fukushi.ac.jp, nodera@fuhc.fukuyama-u.ac.jp*

# SSVEP response study for low semantic images

Syntyche Gbèhounou,[1] Enrico Calore,[2] François Lecellier,[1] Alessandro Rizzi,[2] Christine Fernandez-Maloigne[1]

[1] Department SIC of XLIM Laboratory, UMR CNRS 7252; Poitiers, France
[2] Dipartimento di Informatica, Università degli Studi di Milano, Milan, Italy

## ABSTRACT

In this paper, we have studied the relation between Steady-State Visual-Evoked Potentials (SSVEP) responses, the emotion valence and some low level images features. In the literature numerous papers refer to this kind of study made on IAPS (Lang, Bradley, & Cuthbert, 2008). This database is dedicated to emotion study and it contains many images carrying a strong semantic. From the experiences on this dataset, the amplitude, latency and topography of the SSVEP response have been proven to be correlated to the arousal and valence of the shown pictures. Our aim is to test if this conclusion can be extended for low semantic images: could SSVEP response also be used to study the affective content of natural images that were not specially created to elicit emotional responses?

We chose 12 images from our new database SENSE (Studies of Emotion on Natural image databaSE) developed for this kind of task. From the obtained results we can confirm that for the considered natural images, there is a clear and strong correlation between the pictures and the SSVEP response elicited in the observers.

## 1. INTRODUCTION

An Evoked Potential (EP), in the context of EEG signals, is an electrical potential elicited by the presentation of a stimulus that can be recorded from the nervous system. In particular, in the case of non-invasive EEG recordings, it can be acquired from an electrode positioned on the surface of the scalp. Visually Evoked Potentials (VEP) are EP aroused by a visual stimulation and Steady-state VEP (SSVEP) are a particular case of VEP. The stimulus is presented multiple times at a frequency at least higher than 3.5Hz, but more commonly higher than 6Hz. Then, a periodic response called SSVEP can be observed in the recorded scalp EEG signal, in particular in the occipital brain region, where the visual cortex resides. The SSVEP response have been studied deeply in the field of vision research starting from the seventies (Regan, 2009) and it is still considered in the fields of cognitive neuroscience and clinical neuroscience. Moreover in the last years it has been adopted widely for the implementation of Brain-Computer Interfaces (BCI) (François-Benoît Vialatte, 2010) and various researches are being conducted to provide applications for new Human-Computer Interactions (HCI) systems.

In the literature, multiple evidences exist suggesting the SSVEP response not being only a mechanical reaction of the brain to a flickering stimulus, it is known to be modulated by the user's attention and affective state (Yee Joon Kim, 2006) (Paolo Toffanin, 2009). In particular, in these works, flickering pictures from the International Affective Picture System (IAPS) (P.J. Lang, 2008) have been shown to a group of users during the acquisition of their EEG. These studies conclude that the amplitude, latency and topography of the SSVEP response are correlated to the arousal and valence of the shown pictures.

The aim of our research is to test if the SSVEP response could be used to study the affective content also of natural images that were not specifically created to elicit emotional responses. In fact, the majority of the studies is done on IAPS which is a semantic image set.

The rest of the paper is organized as follows: we describe in Section 2 the considered database and evaluation protocol. We present in Section 3 the results of our different analysis and we conclude and provide some future works in Section 4.

## 2. EXPERIMENTAL METHOD

### 2.1 Description of the database

Our studies were made on a natural and low semantic image database called SENSE (Studies of Emotion on Natural image databaSE) (Syntyche Gbèhounou, 2013). In this paper, "low-semantic" means that the images do not induce a strong emotional response. This dataset is composed of 350 images such as animals, food and drink, landscapes, historic and touristic monuments as shown in Figure 1.
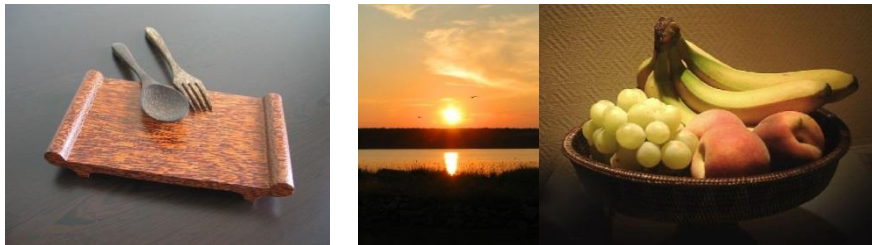


*Figure 1: Some images from the database SENSE we used.*

The images of SENSE are assessed according to the nature and power of their emotional. For the nature, that corresponds in part to the valence, observers had choice between "Negative", "Neutral" and "Positive" and the power varies from "Low" to "High". The nature rating corresponds to the emotion valence information.

For our evaluations we only recorded the SSVEP response of 12 colored images from SENSE. They were chosen according to the percentage of observers that defined the final nature of the emotion in order to consider conclusive images.

### 2.2 The test description

During the tests, we recorded the EEG of the 4 participants looking at the 12 colored images. The participants to our tests were volunteer and did not receive a financial reward.

The images are evaluated during three trials and presented in a pseudo-random order. For each trial, an image was displayed for 8s and flickering at 10Hz. After displaying the image to assess, a black image is displayed for 5s.

The EEG was recorded from 4 electrodes positioned on the occipital area on Pz, POz, PO3 and PO4 location according to the 10-20 system as shown in Figure 2.

We studied different correlation between the SSVEP responses recorded across different trials and observers to be sure that there is a significant modulation of the response due to the pictures content.
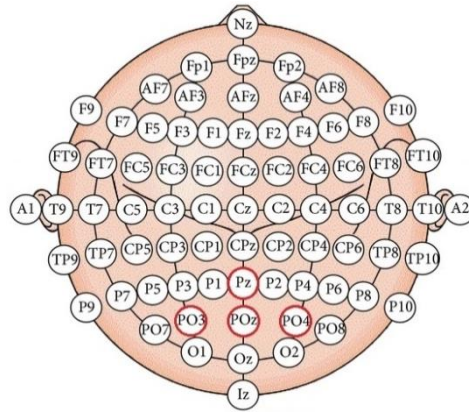
*Figure 2: 10-20 system with the four location we considered.*

## 3. RESULT ANALYSIS AND DISCUSSION

In particular we looked for a correlation between the intensity of the SSVEP response of 4 subjects computed with a relatively novel state-of-the-art technique (O. Friman, 2007) (Zhu, 2011).

To study the potential correlation we used the Pearson's correlation computed by PSPPIRE software[1].

At first, we evaluated the correlation between the computed SSVEP responses and the pictures across different trials and observers to be sure that there is a significant modulation of the response due to the pictures content. We had two configurations:

1. We computed the SSVEP response for the whole displaying duration (8s) using the "Minimum Energy" algorithm (O. Friman, 2007);

2. We computed with the same algorithm the SSVEP response for each second of viewing and then averaged it.

The results are presented in the Table 1 for the first configuration and in Table 2 for the second one. The SSVEP response used is the mean value for the duration considered.

*Table 1. Correlation between the trials the complete duration of SSVEP response recording: the duration time is equals to 8s*

|  |  | Trial 1 | Trial 2 | Trial 3 |
|---|---|---|---|---|
| **Trial 1** | Pearson' Coef | 1 | **0.56** | **0.49** |
|  | Significance | - | **0** | **0** |
| **Trial 2** | Pearson' Coef | 0.56 | 1 | **0.40** |
|  | Significance | 0 | - | **0** |
| **Trial 3** | Pearson' Coef | 0.49 | 0.40 | 1 |
|  | Significance | 0 | 0 | - |

Regarding the results in the tables 1 and 2 (the Person's coefficients and the significance values $\leq 0.05$) we reject the null hypothesis of correlation between the three trials for both configurations. Moreover, for the second one a stronger correlation has been found

---

[1] https://www.gnu.org/software/pspp/tour.html

between trials. This confirms, at first, that the SSVEP responses we have computed are consistent and correlated to the pictures.

*Table 2. Correlation study in the second configuration: the duration time is equals to 1s*

|  |  | Trial 1 | Trial 2 | Trial 3 |
|---|---|---|---|---|
| **Trial 1** | Pearson' Coef | 1 | **0.62** | **0.61** |
|  | Significance | - | **0** | **0** |
| **Trial 2** | Pearson' Coef | 0.62 | 1 | **0.68** |
|  | Significance | 0 | - | **0** |
| **Trial 3** | Pearson' Coef | 0.61 | 0.68 | 1 |
|  | Significance | 0 | 0 | - |

To complete this study, we compute the average luminance, the energy of Gabor features and the emotion valence for each image. Then we analysed the possible correlation between them and the SSVEP response for the images selected. The idea is to try to study the potential link between the SSVEP response and these low level features in order to better understand and analyze the emotional impact of images.

The energy of Gabor features is based on Gabor filters (S.E. Grigorescu, 2002) which are directly related to Gabor wavelets. The two-dimensional Gabor filter is defined by the function $g_{\lambda,\Theta,\varphi}(x,y)$ as the multiplication of a cosine/sine (even/odd) wave with a Gaussian window, as follows:

$$g_{\lambda,\Theta,\varphi}(x,y) = \cos(2\pi\frac{x'}{\lambda} + \varphi)\exp(\frac{-x'^2+\gamma^2 y'^2}{2\sigma^2}), \tag{1}$$

with $x' = x\cos\Theta + y\sin\Theta$ and $y' = y\cos\Theta - x\sin\Theta$.

For Gabor features, we considered 12 different angles $\Theta \in [0,\pi[$ every $\frac{\pi}{12}$ and 2 phases $\varphi \in \{0, -\frac{\pi}{2}\}$, leading to 24 filters. We chose an isotropic Gaussian ($\lambda = 1$) with standard deviation $\sigma = 0.56\lambda$. This choice is justified by the properties of the visual cortex that can be model with Gabor filter as said Grigorescu and al. (S.E. Grigorescu, 2002).

The energy of Gabor features is the combination of the results of the 12 filtering for each phase.

The luminance and the energy of Gabor features given in the tables 1 and 2 are the average for the values computed for each pixel. Considering the obtained results, we cannot conclude to a correlation between the SSVEP responses recorded and the low level features chosen. The result for the second trial and the average value of SSVEP response through the whole test is not relevant. This probably comes from the selected images which, on the contrary of IAPS ones does not provoke a strong emotion. We also think that more observers must be suitable and the correlation with other features could be tried as well, since the most important features may not have been in the tested set. Moreover, using more EEG electrodes and more complex signal processing techniques, to take into account the SSVEP response propagation from the occipital to the parietal and frontal areas of the cerebral cortex, as proposed in (Gary Garcia-Molina, 2013), more information about the valence and/or arousal of the emotion involved in the SSVEP response elicitation could be deduced. It is in fact demonstrated that the modulation of the SSVEP response, due to the user's affect state, changes across different scalp locations in correlation with the arousal and valence of the emotion (Kemp A. H., 2002).

*Table 3. Correlation study between the emotion valence, the luminance, Gabor energy and the SSVEP responses of the images used for our tests: Duration time t=1s. The average SSVEP response presented in this table corresponds to the mean response compute through the tree trials.*

|  |  | Valence | Luminance | Gabor energy |
|---|---|---|---|---|
| **Trial 1** | Pearson' Coef | -0.15 | 0.14 | 0.13 |
|  | Significance | 0.30 | 0.33 | 0.39 |
| **Trial 2** | Pearson' Coef | -0.17 | 0.12 | 0.08 |
|  | Significance | 0.25 | 0.43 | 0.61 |
| **Trial 3** | Pearson' Coef | -0.03 | 0.04 | 0.09 |
|  | Significance | 0.82 | 0.80 | 0.53 |
| **Average** | Pearson' Coef | -0.13 | 0.12 | 0.11 |
|  | Significance | 0.34 | 0.43 | 0.44 |

*Table 4. Correlation study between the emotion valence, the luminance, Gabor energy and the SSVEP responses of the images used for our tests: Duration time t=8s. The average SSVEP response presented in this table corresponds to the mean response compute through the tree trials.*

|  |  | Valence | Luminance | Gabor energy |
|---|---|---|---|---|
| **Trial 1** | Pearson' Coef | -0.16 | -0.24 | 0 |
|  | Significance | 0.27 | 0.10 | 1 |
| **Trial 2** | Pearson' Coef | 0.07 | **-0.33** | 0.13 |
|  | Significance | 0.65 | **0.02** | 0.36 |
| **Trial 3** | Pearson' Coef | 0.01 | -0.07 | -0.10 |
|  | Significance | 0.95 | 0.63 | 0.51 |
| **Average** | Pearson' Coef | 0.23 | -0.27 | 0.02 |
|  | Significance | 0.11 | 0.06 | 0.87 |

### 3. CONCLUSIONS

From this study we can confirm that for the used natural images there is a clear and strong correlation between the pictures and the SSVEP response elicited in the observers.

On the other side, we cannot at this stage identify which are the main image features modulating the SSVEP response; a clear statistical significance could be reached performing the experiment on a higher number of subjects and/or using a higher number of images.

Due to the kind of our database, it could be interesting also to plan new evaluations with the aid of an "eyetracker" to study during the observation duration the change in the SSVEP response according to the gaze region.

### REFERENCES

François-Benoît Vialatte, M. M. (2010). Steady-state visually evoked potentials : focus on essential paradigms and future perspectives. *Progress in neurobiology, 90*(4), 418-438.

Gary Garcia-Molina, T. T. (2013). Emotional brain–computer interfaces. *International Journal of Autonomous and Adaptive Communications Systems, 6*(1), 9-25.

Hovagim Bakardjian, T. T. (2011). Emotional faces boost up steady-state visual. *NeuroReport, 22*(3), 121–125.

Kemp A. H., G. M. (2002). Steady-State Visually Evoked Potential Topography during Processing. *NeuroImage, 17*(4), 1684-1692.

O. Friman, I. V. (2007). Multiple Channel Detection of Steady-State Visual Evoked Potentials for Brain-Computer Interfaces. *IEEE Transactions on Biomedical Engineering, 54*(4), 742-750.

P.J. Lang, M. B. (2008). *International affective picture system (IAPS): Affective ratings of pictures and instruction manual. Technical Report A-8*. University of Florida.

Paolo Toffanin, R. d. (2009). Using frequency tagging to quantify attentional deployment in a visual divided attention task. *International Journal of Psychophysiology, 72*(3), 289-298.

Regan, D. (2009). Some early uses of evoked brain responses in investigations of human visual function. *Vision Research, 49*(9), 882–897.

S.E. Grigorescu, N. P. (2002). Comparison of texture features based on gabor filters. *IEEE Transactions on Image Processing, 11*(10), 1160 – 1167,.

Syntyche Gbèhounou, F. L.-M. (2013). Can Salient Interest Regions Resume Emotional Impact of an Image? *Lecture Notes in Computer Science , 12*(4), pp. 515-522.

Wang Shangfei, W. G. (2013). Analysis of Affective Effects on Steady-State Visual Evoked Potential Responses. *Advances in Intelligent Systems and Computing, 194*, 757-766.

Yee Joon Kim, M. G. (2006). Attention induces synchronization-based response gain in steady-state visual evoked potentials. *Nature neuroscience, 10*(1), 117-125.

Zhu, G. G.-M. (2011). Optimal spatial filtering for the steady state visual evoked potential :BCI application. *5th International IEEE/EMBS Conference on Neural Engineering*, (pp. 156-160).

# MY OWN COLOURS
### KRISTIINA NYRHINEN

"The nature has always been the most important source for the art in Finland."

Is this the truth or is it a cliché or a mantra that we Finns keep on repeating, while we have the opportunity to tell someone about our art.

The truth is that we as a country have a large surface, but we are small in population. The countryside surrounds every city, even the capital is close to the nature. It takes less than an hour to be on the fields and forests alone or enjoy solitude on the small island nearby.

In my generation almost everyone has roots in the countryside, grandparents and relatives still live there. Also many families living in the city have a little summer cottage somewhere in the woods, isolated by the lake.

I lived my childhood in the countryside by a large lake. The changes of the four seasons were easy to observe there. The first signs of the spring were seen in the lighter colours and brightening light. Suddenly the ice disappeared and the lake was blue and glittering again.  Also in the autumn when the funny scratchy noise was heard from the lake as a fanfare before the first cold night and a very thin ice was formed on the lake. The winter had come.

Now I live and work in a city close to the capital but still in the forest.  I can't feel the changes of the seasons so easily and clearly as before. I've grown to know the seasons inside me and I can see its influence in my artwork. I don't know the trees and vegetable world very good but I enjoy the atmosphere and the colouring of the forest and meadows.

My early work, the huge, transparent textiles, in the public buildings was highly influenced by the big lake near my home and water in general. I've used water like materials and shades to reflect the rich palette of the water.

In my childhood I've looked my mother planting and watering plants in the garden. From her garden she harvested vegetables for the table and flowers for the eyes.. And now in three years time I have a small patch of land of my own where I care for my peonies and lilies. Now my textile works have changed a lot. I've studied flower petals, how they grow and fade away. And I've noticed that the form becomes more exciting and the colours become darker. I reflect the garden of my mothers in my art, the hues of blue, red and yellow. I work with the metaphor of ageing and fading-out.

I have focused in three main ideas in my poster: the nature, water and ageing and fading-out.

My earliest memories from my childhood are the short moments in the nature; I'm walking on a small path feeling the sun on my face and wind blowing and carrying the small grains of sand to my cheeks. I remember the colour and the shape of the sunspot on the wooden floor of my home when I'm sitting there with my colouring box. In wintertime when the lake was

covered with ice and snow I used to ski there and wonder about the ultramarine shadows of the bushes. The lake was a great source of imagination. It had a huge amount of shades all around the year, ranging from clear blue to depressing grey to almost violent black, and all hues had a strong influence to the people who lived nearby.

All the other memories of my childhood consist memories of colours and sense of the materials. Through my eyes and the sense of touch the observation has been carved to my memory. Now, thinking back to my textile works I've realised my aim was to reach for the "golden" days of the free and happy childhood. I'm trying to build the solid scenery of my lost childhood what my adultery has separated for good.

In my textile work colour and material are equals. In my art the colour and the material unite essentially. When I begin to create and sketch something new, colour and material come hand in hand. I choose the material that brings out the best intensity in colours and brings the best result in realising the idea. The works for the public buildings have the special demands, concerning mostly materials and techniques the sustainability in general. I never compromise concerns the colours, I worked as long it took to find the best among the colour samples.

Transparency has always been characteristic in my work, either they are huge in close relationship with the architecture or tiny mini textiles. The lightness and many layers in textiles with different shades and different impressions seen from different angles always gives me great pleasure and satisfaction that only textile art can give.
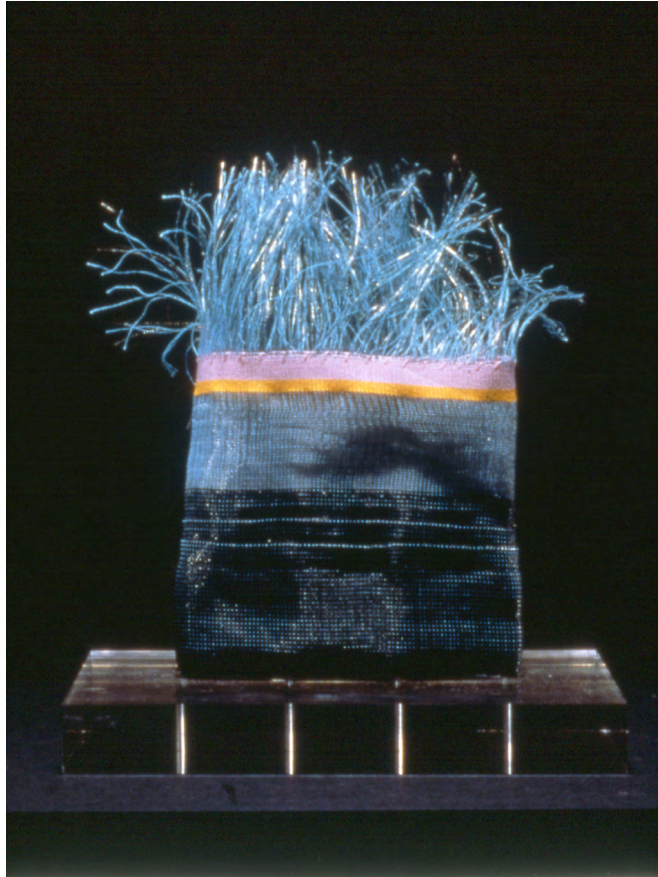
I have to agree on the hypothesis that nature plays a great role in importance for the Finnish artist. My main goal is not to imitate the nature, but use it as a source and a key to my memory to catch the significant moments and emotional incidents in my life.

**Water**



Myyrmäki Church, Textile Art Work by Kristiina Nyrhinen.
Architect Juha Leiviskä 1984

**Nature**



"The Wind in The Willows"

Contact:

Textile Artist

Kristiina Nyrhinen

Kristiina.nyrhinen@gmail.com

Suvikuja 3 A 10,

02120 Espoo

FINLAND

# Hue and Tone Effects
# on Color Attractiveness in Mono-Color Design

Uravis TANGKIJVIWAT, Warawan MEKSUWAN,
Color Research Center, Rajamangala University of Technology Thanyaburi

## ABSTRACT

In the marketing world, color of a product play an important role to catch a customer's attention. Althought a colorful object is more powerful to be attractive, a mono-color design is considered as competitor due to eco-anxiety. This research, hence, examined the influence of hue and tone on color attractiveness. Thirty-three color chips were chosen from the Munsell notation varying in hues and chromas. The results showed a vivid color was more attractive. In addition, warm colors were greater to draw attention than cool colors. Color appearance mode also affected to color attractiveness. Colors appearing in light source color mode and unnatural ojbect color mode were attracted. Furthurmore, we found that perceived color attributes related to color attractiveness.

## 1. INTRODUCTION

One cannot deny the fact that nowadays there are serious competitions in the market. Marketing practitioners know that a product's color may play an important role in a consumer's purchase decision (Grossman, 1999). About 62-90 percent of the assessment is based on color alone. So, prudent use of colors can contribute not only to differentiating products from competitors, but also to influencing moods and feelings –positively or negatively- and therefore, to attitude towards certain products (Singh, 2006). For building up a market share, designers must be created products which are interesting and attract the customer's attention.

One of the important roles for catching a customer's attention is to color attractiveness of product package. It indicates a characteristic that which product can be distinguished most clearly among various products. It said to be that a colorful package attracts a subject's attention and to arouse the desire to consume in marketing (Shun, 2001). Regarding the environmental conservation matter, ecological design, eco-design, seeks to conform to the environment and substantially reduce material consumption. Monochromatic design in printing has been noted as alternative technique as eco-design. Amount of ink on substrates for this design is less than that for color printing in the printing process. Moreover, this design reduces the printing troubles and cost of a product. Although monochromatic design seems to conform to eco-design, the color attractiveness is required for a product design. It would like to know how to catch customer's eyes with the monochromatic design. Several factors are said to be responsible for color attraction for instance differences in age, gender, culture and so on (Radeloff, 1990; Zellner, 2010). The major aim of this study, hence, is to investigate the effect of monochromatic color on attractiveness.

## 2. METHOD

### 2.1 Experimental Setting

As shown in Figure 1, the apparatus was composed of two rooms separated by a wall with a $1^\circ$ square aperture (T). The subject's room was covered inside with white wallpaper of about N9 and illuminated by daylight type fluorescent lamps ($FL_S$). The intensity of the lamps was adjusted by a light controller. The room illumination was measured by an illuminometer ($I_S$) placed on a shelf below the aperture at distance of 44 cm. Many objects such as artificial flowers, dolls, books, and dolls were put into this room. Color chips to serve as the test stimuli were attached to a rotating wheel placed in the test chart's room. They were also illuminated by adjustable daylight type fluorescent lamps ($FL_T$).
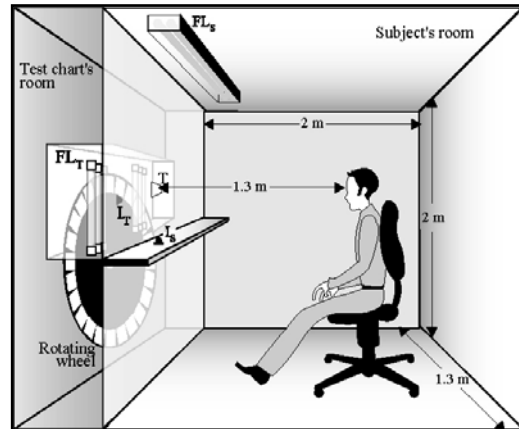


*Figure 1: Schematic diagram of the apparatus*

### 2.2 Color Stimuli and Conditions

Thirty-three color chips selected from the Munsell Color notation were used as the test stimuli. The color chips included one achromatic color (N5) and eight hues (5R, 5YR, 5Y, 5GY, 5G, 10BG, 10B, and 5P) varied in different chromas (2, 5, and 8). The Munsell value of all color chips was 5. The experimental conditions were composed of the combination of subject's room illuminance levels (50 and 500 lx) and test chart's room illuminance levels (500 and 700 lx).

### 2.3 Subjects

Five subjects ranging from 22 to 27 years in age took part in this experiment. All subjects had normal or corrected-to-normal visual acuity. They were screened for color deficiencies using the Ishihara plate.

### 2.2 Experimental Procedure

The subject sat in subject's room and looked at the test stimuli through the aperture from a distance of 130 cm. There were three tasks for each subject. In the first task, the subject was asked to assess the degree of color attractiveness for each color by using the scale which was divided into 6 levels, as -3 (do not attract) to +3 (extremely attract). The word "attractiveness" here means salient or conspicuous, which is to get attention of viewers. In the second task, the subject judged the color appearance mode of each color chip as object color mode (OB-mode), unnatural object color mode (UN-mode), and light source color mode (LS-mode). And the last one, the subject was asked to assess the amount of chromaticness, whiteness, and blackness for each color chip base on the NCS. These three components have 100% in total. Within each session, 16 or 17 color chips were randomly presented under four conditions to make 96 or 102 judgments. Each subject has done three

sessions per condition. No time limits were set for making the judgments. Subjects were tested individually.

## 3. RESULTS AND DISCUSSION

For each color chip, the attractiveness scores for the five subjects were averaged. As shown in Figure 2, the mean score for each color chip is plotted against different Munsell chromas. Results showed that the higher the chroma of the color chip, the higher the attractiveness score, regardless of hues. For instance, the mean score of chroma 2, 5, 8 and maximum under $I_S50:I_T500$ condition are -0.1, 1.1, 2.0, and 2.7, respectively. Therefore, it was found that the vivid color attracts subject's attention. The same tendency occurred in all conditions. Our result agreen well with previous researches. Tanaka *et al.* (2000) proposed that chroma is linearly correlated to attractiveness. In our results, moreover, warm colors such as 5R, 5YR, 5Y and 5P were greater to draw attention than cool colors. Many previous researches reported that warm colors are considered arousing (Bellizzi and Hite, 1992; Cahoon, 1969) and active (Madden *et al.*, 2000; Richards and David, 2005), and lead to higher levels of anxiety (Jacobs and Suess, 1975). Tanaka *et al.* (2000) suggested that the closer the hue of a color to red was, the more salient the color would be.
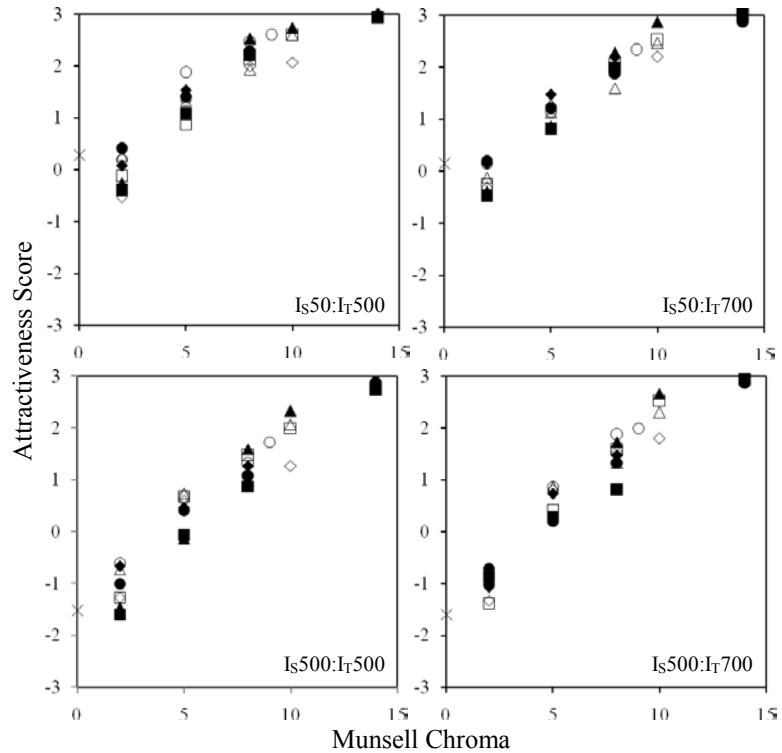


*Figure 2: The attractiveness score from average result across all subjects by plotting against Munsell chroma for different Munsell hues; 5R(◆), 5YR(●), 5Y(■), 5GY(▲), 5G(◇), 10BG(○), 10B(□), 5P(△), N5(✕).*

Because a perception of color varies in a different illuminations, an effect of color apperance mode on attractiveness was considered. The color apperance mode judgment accummulated from all subjects were expressed in term of the color apperance mode index ($i_{CAM}$) by following equation:

$$\text{Color appearance mode index } (i_{CAM}) = \frac{-1(N_{OB}) + 0(N_{UN}) + 1(N_{LS})}{N_{OB} + N_{UN} + N_{LS}} \quad ,(1)$$

where $N_{OB}$, $N_{UN}$, and $N_{LS}$ are the numbers of response in OB mode, UN mode, and LS mode. If $i_{CAM} > 0.5$, the color chip is classified in LS mode; if $i_{CAM} < -0.5$, UN mode; and if $-0.5 < i_{CAM} < 0.5$, OB mode.

*Table 1. Mean and Standard Deviation of the attractiveness score across eight hues.*

| | $I_S50:I_T500$ | | $I_S50:I_T700$ | | $I_S500:I_T500$ | | $I_S500:I_T700$ | |
|---|---|---|---|---|---|---|---|---|
| Chroma | Mean | SD | Mean | SD | Mean | SD | Mean | SD |
| 2 | -0.1 | 0.26 | -0.1 | 0.34 | -1.1 | 0.38 | -1.0 | 0.25 |
| 5 | 1.1 | 0.24 | 1.3 | 0.31 | 0.4 | 0.34 | 0.6 | 0.29 |
| 8 | 2.0 | 0.21 | 2.2 | 0.21 | 1.2 | 0.25 | 1.5 | 0.32 |
| Maximun | 2.7 | 0.31 | 2.7 | 0.30 | 2.2 | 0.56 | 2.5 | 0.43 |

Note. For each chroma, *n* = 120

In Figure 3, the mean attractiveness score for the color chips that appeared in the LS and UN modes were higher than those in OB mode. This showed that color that appeared in LS and UN modes paid attention to viewers. In a light source color and unnatural object color modes, subjects perceived color too bright than adjacent surrounding. The bright color with dimmed background is an outstanding color. This result agrees with previous results. Tanaka *et al.* (2000) reported that background has an influence over color attractiveness. However, Mackiewicz (2007) noticed that a color of background had a little effect on viewers' ratings of the attractiveness of color combinations.

Next, possible correlations between color attractiveness and perceived color attributes were determined. The elementary color naming method was used to assess the perceived color attributes of the color chips in three color appearance modes. The amounts of the perceived color attributes were expressed as average values across all subjects for each color chip under each condition. In Figure 4, the attractiveness scores were plotted against perceived chromaticness, whiteness, and blackness. As shown in Figure 4 (a) and (b), it was found that the perceived blackness significantly related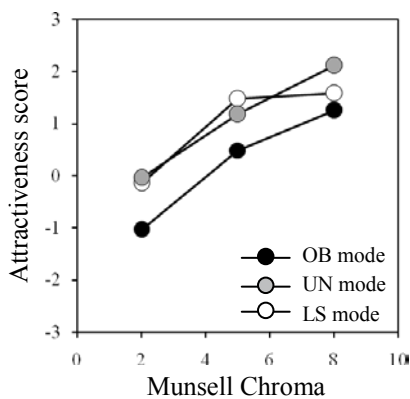 to the attractiveness score as negative correlation in OB mode (-0.854) and perceived whiteness in UN mode and LS mode (-0.879 and -0.889) as shown in Table 2. On the other hand, the attractiveness score increased with increasing perceived chromaticness as shown in Figure 4. There was a significant correlation between the perceived chromaticness and the attractiveness score in all color appearance modes. This result corresponded with the results of Munsell chroma. This showed that both physical chromaticness and perceived chromaticness have an influence over color attractiveness. Our result indicates that the color attractiveness may be described as the perceived color attributes.



*Figure 3: Mean color attractiveness plotted against Munsell chroma for different color appearance modes.*

*Table 2. Pearson correlation coefficients between attractiveness score and perceived color attributes.*

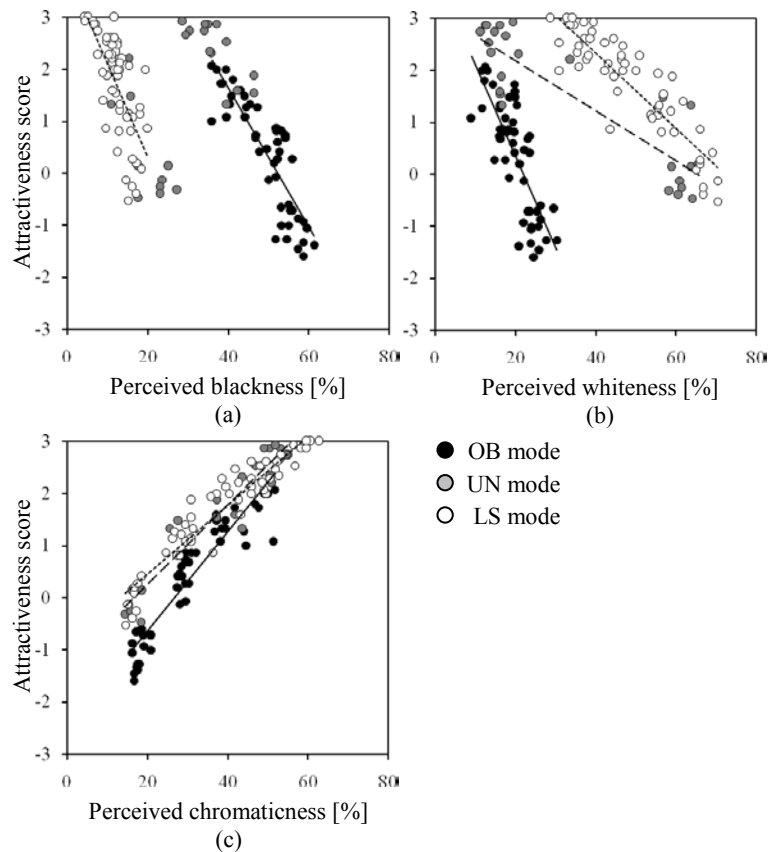| | OB mode | UN mode | LS mode |
|---|---|---|---|
| Perceived chromaticness | 0.924 | 0.960 | 0.948 |
| Perceived whiteness | -0.785 | -0.879 | -0.889 |
| Perceived blackness | -0.854 | 0.490 | -0.698 |

AIC2015 TOKYO - Color and Image

*Figure 4: Scatter plot of attractiveness score and perceived color attributes:*
*(a) perceived blackness, (b) perceived whiteness, and (c) perceived chromaticness.*

## 4. CONCLUSIONS

In this study, thirty-three color chips varying in hues and tone were assessed under four conditions covered three color appearance modes. Findings showed that color with high chroma yielded higher attractiveness scores and warm color is to get attention of viewers. In a comparison among three color appearance modes, the color attractiveness in the unnatural object color mode and in light source color mode were significantly higher than those in the object color mode. Furthermore, the color attractiveness was significantly related to the perceived color attributes. They play a role as underlying mechanism on the determination of color attractiveness. Thus, it may be possible to use these components as a scale for predicting color attractiveness on the different color appearance modes. Our empirical finding delivers the idea to choose a proper hue and tone to get more attractiveness in mono-color design. However, this study is limited in color stimulus and a small number of subjects. In further research other factors are required for instance color combinations, tone combinations, a great number of subjects, circumstances, and so on.

**REFERENCES**

Bellizzi, J.A., and Hite, R.E. 1992. *Environmental color, consumer feelings, and purchase likelihood.* Journal of Psychology and Marketing 9(5) 347-363.

Cahoon, R.L. 1969. *Physiological arousal and time estimation.* Journal of Perceptual and Motor Skills 28(1) 259-268.

Grossman, R.P. and Wisenblit, J.Z. 1999. *What we know about customers' color choiese,* Journal of Marketing Practice: Applied Marketing Science 5(3) 78-88.

Jacobs, K.W., and Suess, J.F. 1975. *Effects of four psychological primary colors on anxiety state.* Journal of Perceptual and Motor Skills 41(1) 207-210.

Madden, T.J., Hewett, K., and Roth, M.S. 2000. *Managing images in different cultures: A cross-national study of color meanings and preferences.* Journal of International Marketing 8(4) 90-107.

Mackiewicz, J. 2007. *Perceptions of clarity and attractiveness in power point graph slides.* Journal of Technical Communication 54(2) 145-156.

Radeloff, D.J. 1999. *Role of color in perception of attractiveness.* Journal of Perceptual and Motor Skills 71(1) 151-160.

Richards, A., and David, C. 2005. *Decorative color as a rhetorical enhancement on the World Wide Web.* Journal of Technical Communication Quarterly 14(1) 31-48.

Shun, L.Y. 2001. *The effects of store environment on shopping behaviors: Acritical review.* Journal of Advances in Consumer Research 28(1) 190-197.

Singh, S. 2006. *Impact of color on marketing,* Journal of Management Decision 44(6) 786-789.

Tanaka, S., Iwadate, Y. And Inokuchi, S. 2000. *An attractiveness evaluation model based on the physical features of image regions,* In Pattern Recognition, *Proceedings,* ed. by A. Sanfeliu. Barcelona, 793-796.

Zellner, D.A., Lankford, M., Ambrose, L. and Locher, P. 2010. *Art on the plate: Effect of balance and color on attractiveness of, willingness to try and linking for food.* Journal of Food Quality and Preference 21(5) 575-578.

*Address: Uravis TANGKIJVIWAT, Color Research Center,*
*Rajamangala University of Technology Thanyaburi,*
*39 Rangsit-Nakornayok Rd., Klong Hok, Thanyaburi, Pathumthani 12110 THAILAND*
*E-mails: uravis_t@yahoo.com*

# A study on silver metallic color preference
# -A comparison of responses between Japanese and Thai people-

Mikiko KAWASUMI[1], Kamron YOUGSUE[2], Chanprapha PHUANGSUWAN[2],
Kanrawee TAWONPAN[2], and Ken NISHINA[3]

[1] Faculty of Science and Technology, Meijo University, Japan
[2] Faculty of Mass Communication Technology, Rajamangala University of Technology Thanyaburi, Thailand
[3] Department of Techno-Business Administration, Nagoya Institute of Technology, Japan

## ABSTRACT

This paper describes the outcome of the research on the comparative studies in Asian countries on silver metallic color preference of industrial products. We are doing research on the relationship between the customers' impression and the color of a products' surface. In this revised survey, we increased the number of the respondents in a wide range of age, and then compared the results between Japanese and Thai people. We could confirm the previous results in detail and some interesting topics were newly found.

## 1. INTRODUCTION

Japanese industries export various products such as cameras, games, laptops, etc., and those products are very popular in overseas markets. We've researched the designing conditions for more attractive surfaces of the industrial products in cooperation with a material manufacture. It is significant for us to understand the customers' visual preference for each product in each nation. The appearance of a product is one of the important factors for the customers' visual impressions. What kind of impression do you desire for metallic products? And what kind of silver metallic color do you prefer for each product? The desired impression and color preference of the customers may be different by age, gender and nationality. Manufacturers hope to develop the attractive metallic silver with a tint according to the customers' preference. In this survey, we've prepared every question of our questionnaire in Thai language in order to increase Thai respondents who live in local region including local elderly people. I'll show you the comparative results between Japanese and Thai people.

## 2. METHOD

A questionnaire was used for our investigation and written in Japanese, Thai, and English. Figure 1 shows a part of our questionnaire on the Web. Computer graphics were used to represent the metallic surface products such as a fridge and a DVD player. Those have slightly different silver colors: reddish, yellowish, bluish, and so on, and each of color was controlled in ten hues of the Munsell color system: **P**, **RP**, **R**, **YR**, **Y**, **GY**, **G**, **BG**, **B**, and **PB** (Figure 2). We set five target feelings: "clean / pure", "relaxing / comforting", "stylish / chic", "high-quality", and "favorite" as shown in Table 1, which were chosen as the most important feelings for the metallic product by Japanese customers in our previous investigation. We translated these English adjectives to Thai language carefully. The respondents answered with the color that they felt was the most "clean / pure", for example, for seven target products: a fridge, a television, a DVD player, a laptop computer, a digital camera, a smartphone, and a music player (Figure 3). Also, we asked other many questions such as the preference of gold / silver, the most important desired feelings, etc.

Figure 1: A part of questionnaire.

Table 1: Five target feelings.

| in Japanese | in English | in Thai |
|---|---|---|
| 清潔感のある | Clean / pure | สะอาด/บริสุทธิ์ |
| スタイリッシュな | Stylish / chic | มีรสนิยม/แฟชั่น |
| 上質な | High-quality | คุณภาพสูงสุด |
| 落ち着いた | Relaxing / comforting | ผ่อนคลาย/สะดวกสบาย |
| 好きな | Favorite | ชอบ |



Figure 2: Ten colored products.



Fridge    TV    DVD player

Laptop    Camera    Smart phone    Music player

Figure 3: Seven target products.

Table 2: Number of respondents.

| Nation | Male | Female | Total |
|---|---|---|---|
| Japan | 213 | 207 | 421 |
| Thailand | 136 | 185 | 321 |
| Total | 349 | 392 | 742 |
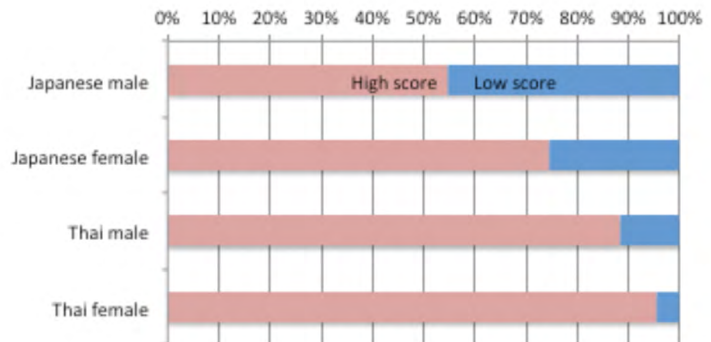


Figure 5: Percentage of persons with high color consciousness.



Rajamangala University of Technology Thanyaburi



Department of Social Welfare Development Center for Older Persons

Figure 4: Scenes of answering questionnaire.
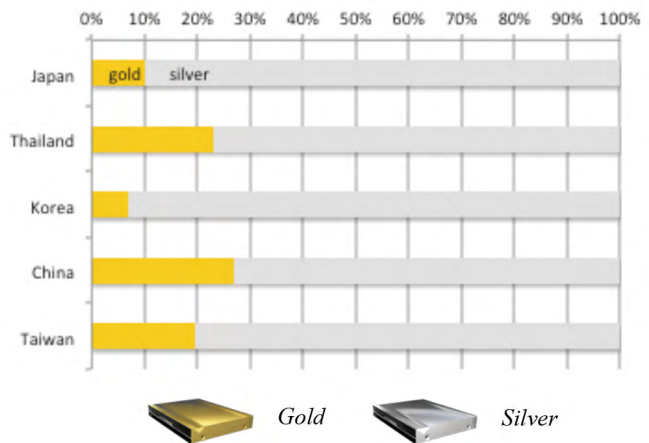


Figure 6: Which do you prefer, gold or silver?

AIC2015 TOKYO - Color and Image

We requested that the screen size of a computer should be not less than twelve inches, because it may be hard to distinguish the differences among ten hues on a small display. The required time was about twenty minutes on average for the people under forties. It took a lot of time over forty minutes for elderly people, because we instructed every question in their mother tongue in the next seat and wrote down each answer on the paper sheet, as shown in right side of Figure 4. We formed small groups, and several participants (3 – 6 persons) could answer at the same time. Finally, more than seven hundred persons from Japan and Thailand have cooperated with us in total (Table 2). Japanese people participated in Japanese questionnaire, and Thai people joined in Thai or English.

## 3. RESULTS AND DISCUSSION

Firstly, we newly found from other additional questions that Thai people's color consciousness is very high in comparison with Japanese, as shown in Figure 5. In Figure 6, you can see that most people prefer silver metallic color for the industrial products, though Thai people prefer gold more than Japanese. The necessity of more investigation about silver metallic color could be confirmed.

Figure 7 shows our main results, the comparative results for five feelings between Japanese and Thai people. The horizontal axis shows ten hues of the Munsell color system, and the vertical the percentage of choice for the hue. Different line types indicate seven target products. As the result, it became clear that both nationalities preferred the bluish silver color as the feeling of "clean / pure" in every product. Especially, Munsell **B** had the largest followers in both nations, and **BG** was also higher in Japan. Many Thai people selected **BG** in every product for "relaxing / comforting", in contrast, many Japanese selected **YR** and **B**. Also, Japanese and Thai people were similar in the tendency for "high-quality" and different for "stylish / chic".

Table 3 shows the correlation between "favorite" and other four feelings. We could confirm that "favorite" has strong correlations with "clean / pure" and "high-quality" in every product in Thailand. On the other hand, in Japan, you can see that it has a little bit strong correlation with "clean / pure" and "stylish" only in family-use products such as a fridge, a TV, and a DVD player.
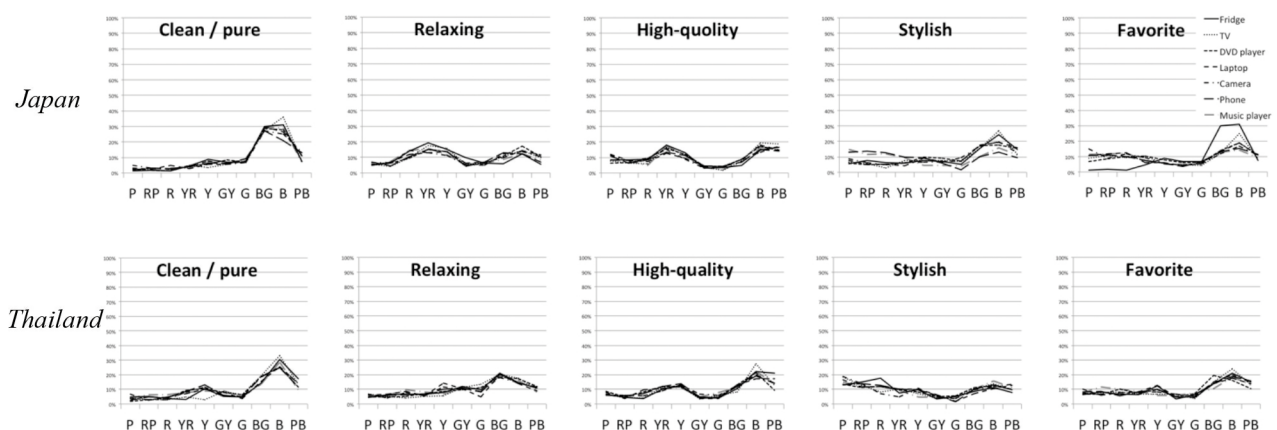


*Figure 7: Comparative results between Japan and Thailand*

*Table 3: Correlation coefficient between "favorite" and other four adjectives.*

Japan

| | Clear / pure | Relaxing | High-quality | Stylish / chic |
|---|---|---|---|---|
| Fridge | 0.51 | 0.02 | 0.06 | 0.51 |
| TV | 0.61 | 0.15 | 0.31 | 0.69 |
| DVD player | 0.65 | 0.57 | 0.57 | 0.59 |
| PC | 0.37 | 0.16 | 0.41 | 0.41 |
| Camera | 0.25 | 0.21 | 0.31 | 0.36 |
| Smart phone | 0.29 | 0.05 | 0.16 | 0.57 |
| Music player | 0.18 | 0.02 | 0.05 | 0.20 |

Thailand

| | Clear / pure | Relaxing | High-quality | Stylish / chic |
|---|---|---|---|---|
| Fridge | 0.92 | 0.28 | 0.84 | 0.01 |
| TV | 0.85 | 0.32 | 0.67 | 0.19 |
| DVD player | 0.75 | 0.62 | 0.56 | 0.19 |
| PC | 0.75 | 0.33 | 0.90 | 0.14 |
| Camera | 0.88 | 0.46 | 0.81 | 0.12 |
| Smart phone | 0.75 | 0.35 | 0.77 | 0.26 |
| Music player | 0.59 | 0.15 | 0.56 | 0.50 |

*Table 4: Top ten of desired feeling for the metallic products*

Japan

| 1 | 上質な (High-quality) |
|---|---|
| 2 | シンプルな (Simple) |
| 3 | 清潔な (Clean) |
| 4 | スタイリッシュな (Stylish) |
| 5 | スマートな (Smart) |
| 6 | 上品な (Elegant) |
| 7 | 高級な (Luxurious) |
| 8 | 美しい (Beautiful) |
| 9 | 落ち着いた (Comforting) |
| 10 | カッコイイ (Cool) |

Thailand

| 1 | Fine-quality |
|---|---|
| 2 | Clean |
| 3 | Comforting |
| 4 | Modern |
| 5 | High-quality |
| 6 | Stylish |
| 7 | Smart |
| 8 | Luxurious |
| 9 | Creative |
| 10 | Classic |

In addition, we asked about the important desired feelings for the metallic products by using adjectives at the ending of our questionnaire. Table 4 shows the top ten of adjectives that the respondents chose. Many Thai and other ASEAN people chose "modern" as the important desired feeling. But it is not included in the top twenty in Japan. We need to additionally examine the silver color preference that Thai people feel is the most "modern".

Moreover, we examined how much the response was affected by his/her "birthday color" in Thailand, because Thai people have his/her own special color depending on birthday that based on an ancient Buddhist wisdom. However those were not found to have a correlation.

## 4. CONCLUSIONS

We've examined the relationship between the customers' desired feelings and the surface colors of metallic products by an online survey, and our questionnaire was written in mother tongue for Japanese and Thai people. As the results, we could compare the characteristic of preference between two nations and some interesting topics were found. For instance, they have difference tendencies in "relaxing / comforting" and "stylish / chic".

The results from this survey are very useful for a manufacturer to fit the design concept in each nation. It is necessary for us to continuously analyze the data from cultural and social points of view and link to predict the customers' preference in future.

## ACKNOWLEDGEMENTS

## REFERENCES

Saito, M., 1994. *A cross-cultural study on color preference in three Asian cities: Comparison between Tokyo, Taipei and Tianjin.* Japanese psychological Research 36(4): 219-232.

Xin, J.H., Cheng, K.M., Taylor, G., Sato, T., Hansuebsai, A., 2004a. *Cross-Regional Comparison of Colour Emotions Part I, Part II: Quantitative Analysis.* Color Research and Application 29(6): 451-457, 458-466.

Kawasumi, M., 2013. *A Comparative Study in Asian Countries on Color Preference for Factory Products.* In 1st Conference of Asian Color Association, Proceedings, ed. by Payackso V., Thanyaburi: Rajamangala University of Technology Tanyaburi, 26-27.

Kawasumi, M., 2014. *Comparative studies in Asian countries on color preference of industrial products.* In 2nd conference of Asian Color Association, Proceedings, ed. by Tien-Rein LEE. Taipei: Chinese Culture University, 268-271.

*Address: Mikiko Kawasumi,*
*Faculty of Science and Technology, Meijo University*
*1-501 Shiogamaguchi, Tempaku-ku, Nagoya 468-8502 JAPAN*
*E-mails: future@meijo-u.ac.jp, ykamron@gmail.com, karamennn@gmail.com,*
*ktawonpan@gmail.com, nishina@nitech.ac.jp*

# COLORS' RELATIONS TO OTHER THINGS
# IN MY WORKS

Helena LUPARI

Textile artist

Board member of Finnish Color association

Senior lecturer emerita (School of Arts, Design, and Architecture, Aalto University

Department of Textile Arts)

I see my works in textile art as traveling through colors, shapes and materials. First I thought that technique was most important (I discovered how I can weave twelve layers´ fabrics).
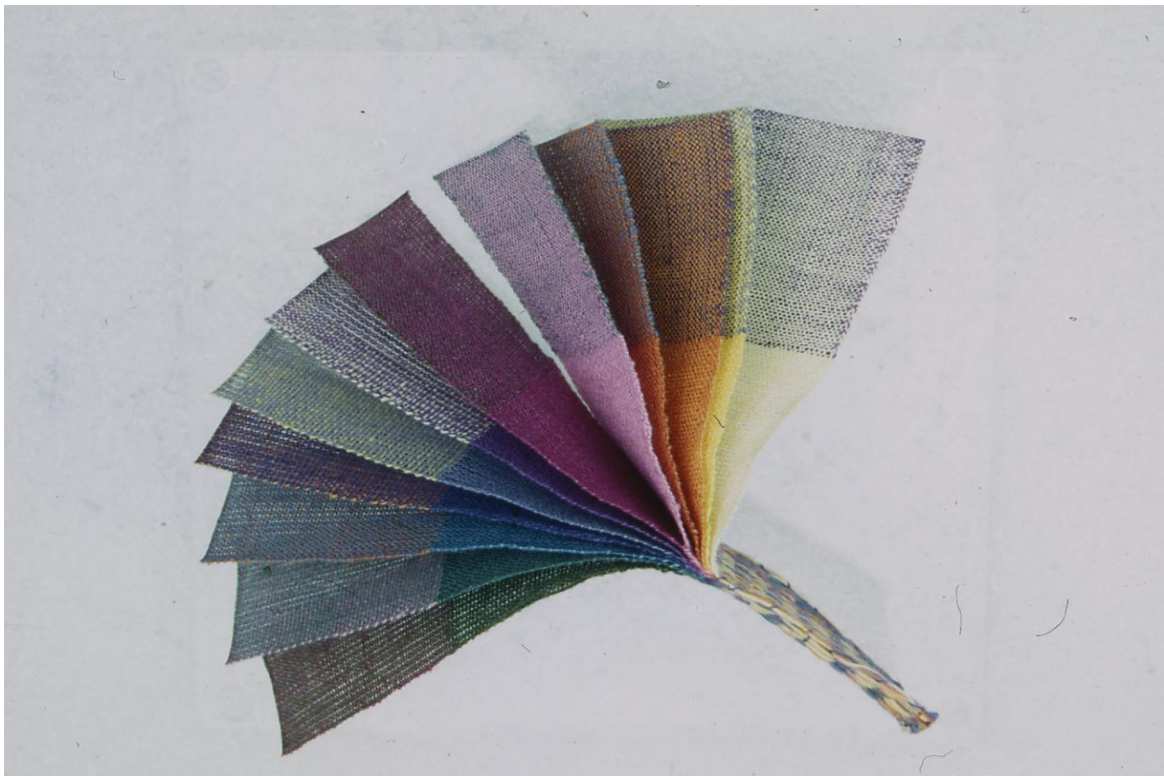


Now I'm more interested in how to get the color, the sculptural shape, the material and the light work well together, to give an emotional experience.

Making textile art is an endless way of questions:

How much I can think of myself, my ideas, my wishes, other people and all the demands of the commercial point of view. As for colors, everyone has his or her own color taste. Should I and can I give new experiences of it and what is the ultimate meaning of my work.
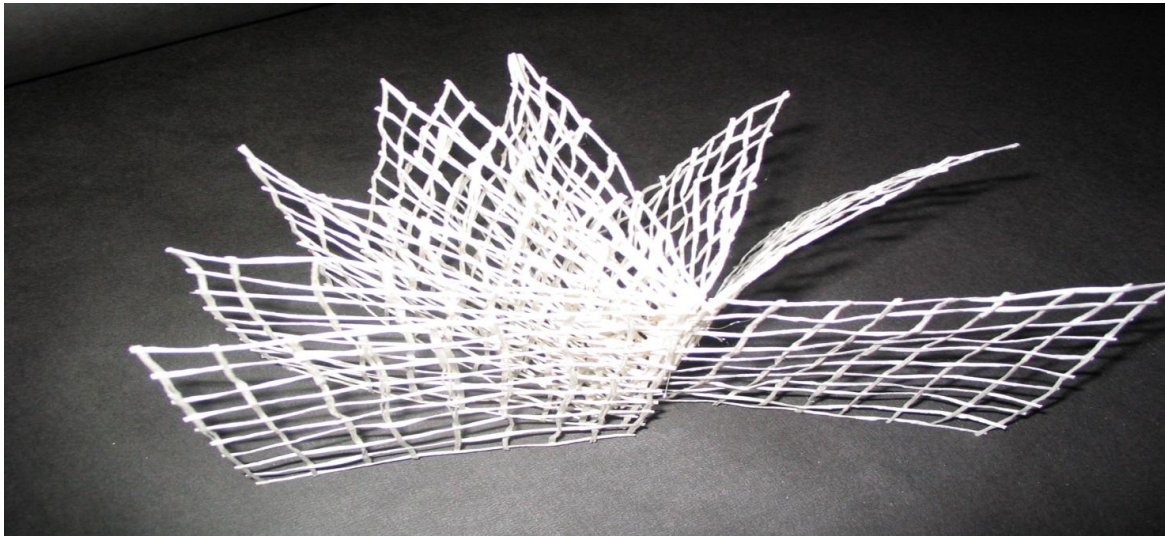


The art piece must be so strong that it takes its space where ever it will have its role in the future and the co-operation with the environment. How important is the color right now? Does it shout or whisper? Both shouting and whispering could be strong items. And the emotional point of view! Is it white clean and pure or black, dark or silent? For me the color is the first thing I see in an art piece. It opens the work.



It calls or draws you away.

I'm fascinated in architectural bridges. They lead you somewhere and at the same time they combine you with someone. They inspire me and when the structure is strong the color must support it like material does too. I found the Japanese flat silk yarn so sensitive and strong at the same time. I dyed it and it took the color precisely the way I wanted.
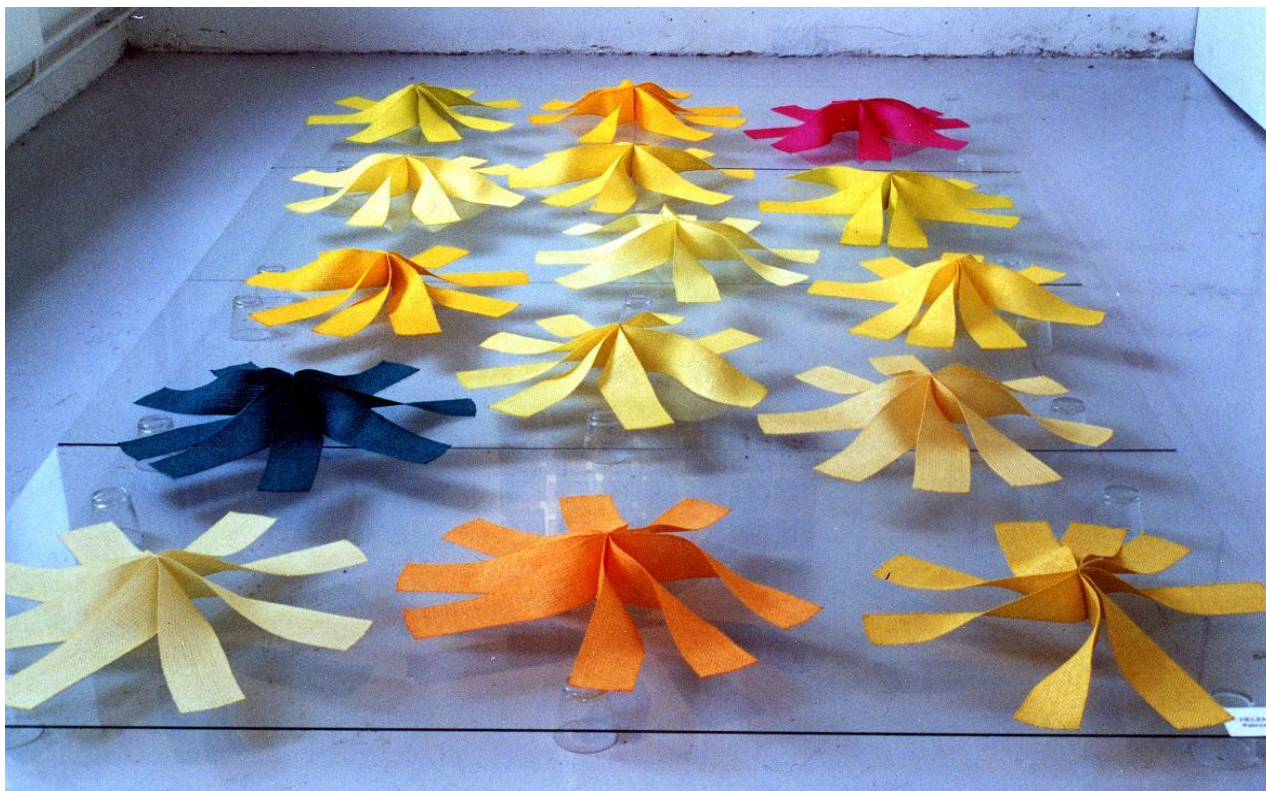


In textile Art there are so many ways to use color as a tool.

The color combinations are most demanding, can you make the colors alive and interesting new versions.

The right color gives more to the material but you can also kill the feeling.

The best thing in colors is that it is like poetry, you just have to let your imagination be free.

*Address: Senior lecturer emerita Helena LUPARI,*
*Jokitie 12 C, 00780, Helsinki, FINLAND*
*E-mail: helena.lupari@kolumbus.fi*

# Color Preference of Preschoolers: Compared to Adults' Surmise

Wei-Chun HUNG, Pei-Li SUN, Li-Chen OU
Graduate Institute of Color and Illumination Technology, National Taiwan University of Science and Technology

## ABSTRACT

The aim of this study is to investigate the color preferences of young children aged 4~5 and to compare with the viewpoint of adults in color preferences of the children. Based on the truth that preschoolers receive minor influence from environment comparing with adults, it's interesting to know as if adults' opinions agree with the young children'. The effects of gender and the association of objects also were analyzed. In this study, 15 color samples were chosen to produce color patches, mini T-shirts and candy-shaped packaging as test samples. The experimental results show there are gender differences in the preschoolers' color preferences. Age and the association of objects also influence the color preferences. Adults chose stereotype colors – pink for girls and blue for boys – especially in guessing the preschoolers' favorite color patches. However, the preschoolers prefer wide range of colors including neutral colors.

## 1. INTRODUCTION

Previous studies show that color preference of human varies across different culture (Choungourian, 1968), gender (Hurlbert and Ling, 2007), age (Taylor, Schloss, Palmer, and Franklin, 2013), race and educational background (Schloss, Strauss and Palmer, 2013). Personal experience and personality also would affect the choice of preferred colors (Palmer, and Schloss, 2010). In addition, the preference could be object dependent (Schloss, Strauss and Palmer, 2013). For example, an individual would prefer black shoes but dislike a black wash machine.

"Girls wear pink and boys wear blue" is one of gender stereotypes nowadays. However, before the 1920s, parents dressed infants and toddlers, girls and boys alike, in white dresses, suggesting that color and dresses were not used to distinguish between girls and boys (Chiu et al., 2006). Gender identity imposed by the parents might play an important role on the pink frilly dresses of girls (Ruble, Lurye, Zosuls, 2007). It is interesting to know the color preference of patches and dresses across different genders and different ages. The results will be useful for designing learning materials for children.

## 2. METHOD

A series of psychovisual experiments were conducted to investigate the preferred colors of preschoolers. Young adults also participated to the experiments for comparing the results. Three types of objects including color patch, T-shirt and candy-shaped packaging were used for preferred color selection. The independent variables of the experiments were Gender, Object Type, and Age Group.

AIC2015 TOKYO - Color and Image

## 2.1 Test Samples

In the experiments, every participant must select one of 15 colors to be his/her favorite color for each test session. The 15 colors include pure red (R), orange (O), yellow (Y), green (G), blue (B), purple (P), black (K), gray (Gy), white (W), plus six additional colors selected from Angela Wright's Personality Type 1 Morning Light Color (Wright, 1998) which is common used to produce children's products. It contains pink (LR), light orange (LO), light yellow (LY), light green (LG), light blue (LB) and light purple (LP). These six colors are relatively brighter and less saturate. 45(=15*3 repeated) color patches were printed out on uncoated papers using an inkjet printer and then folded them manually as the color patches, the mini T-shirts and the candy-shaped packaging respectively as shown as Figure 1.



*Figure 1: Test samples: (a) color patches, (b) mini T-shirts, and (c) candy packaging*

## 2.2 Experimental Setup

The experiments were conducted under a dark room. The participants were asked to fully adapt to the dark surround in front of a LED light booth with about 835 lux illuminance for two minutes. After the adaptation, the participants were asked to choose their preferred color of a set of samples inside the light booth. The participants divided into two age groups. The preschoolers include 19 children (10 male and 9 female) aged 4 to 5 from a kindergarten in Taipei. And the adults include 15 postgraduate students (9 males, 6 females) aged 23 to 25 from our university. All of them passed Ishihara color vision test. Each of them has to answer a questionnaire. The preschoolers have three sessions for choosing favorite color patch, mini T-shirt and candy packaging sequentially. However, the adults have four sessions including two sessions to choose their own favorite color patch and mini T-shirt, and two sessions to guess the favorite colors of boys and girls. Figure 2 show the sequence of answering the questionnaire of each test session for either the preschoolers or the adults.



*Figure 2: The sequence of answering the questionnaire for different test session.*

# 3. RESULTS AND DISCUSSION

## 3.1 Gender Differences of Preschoolers

We would like to know whether the preschoolers have gender differences in color preferences. The preferred colors of the preschoolers for color patches listed in descending order are: pink, light green, light blue, light yellow, gray, white, light purple, red, purple, and blue (see Figure 3). Pink (34%) and light green (30%) are the most favorite colors for the girls and the boys respectively. Furthermore, the boys selected light blue (20%) as the second favorite color whereas the girls selected light yellow (22%) as the second. In comparison with the two genders, none of the boys like pink as their favorite color whereas girls are not interesting in green, but girls rank light blue (11%) as their third favorite color. Boys are interested in red more than girls and girls prefer light yellow more than boys. Light blue, gray, and white are favorite colors for both boys and girls. In general, the preschoolers prefer bright colors with low chroma. In summary, there are significant gender differences in preschoolers' color preferences based on Chi-square test on 4 color groups (pink, light blue, neutral colors and all the others).
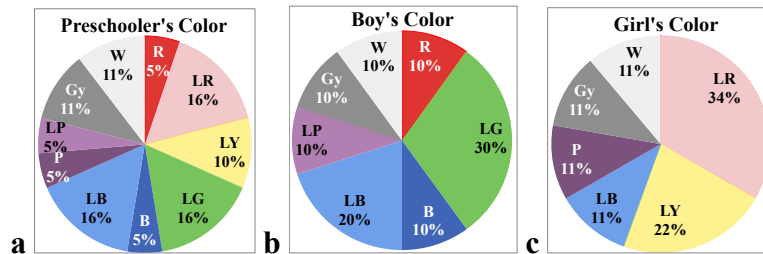


*Figure 3: Color (patch) preference: (a) preschoolers, (b) boys, and (c) girls.*

## 3.2 Preschoolers vs. Adults

We also would like to know whether age influenced the choice of favorite colors. The preferred colors of the adults listed in descending order are: light blue, pink, light green, red, orange, light orange, yellow, light yellow, green (see Figure 4). Pink (33%) and light blue (45%) are the most favorite colors for the females and the males respectively. It confirms the stereotype colors for the two genders. Furthermore light blue are favorite for both males and females. In compared with the preschoolers (referring to Figure 3), adults also preferred light color. However, the latters are not interested in neutral colors. Adult has the same tendency as the preschoolers that males do not like pink whereas females are not interesting in green. In the top three chosen colors (light blue, light green and pink), adults and preschools are the same. Moreover, adults like orange and preschoolers like purple and neutral colors. Regardless of age, females like pink (adult and preschooler both are 34%) and warm color, males like cool color more. Surprisingly, some preschoolers are interest in neutral color, and none of them like orange color. Light blue was preferred by all genders and age groups. In short, there are some age differences in color preferences.
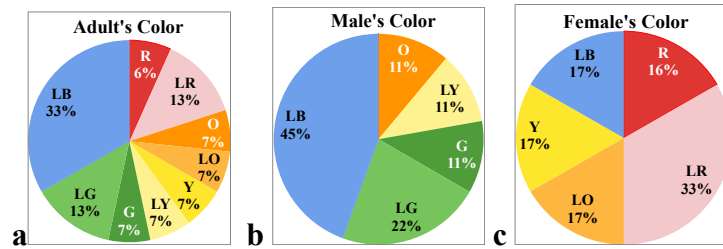
AIC2015 TOKYO - Color and Image

*Figure 4: Color (patch) preference: (a) adults, (b) males, and (c) females.*

The results of Chi-square test show insignificant differences between the proportional distributions of boy and girl subjects in color preference of warm and cool colors. Conversely, there is significant difference between the proportional distributions of male and female ($\chi2$ =5.402, d.f. =1, p=.041). (see Figure 5)
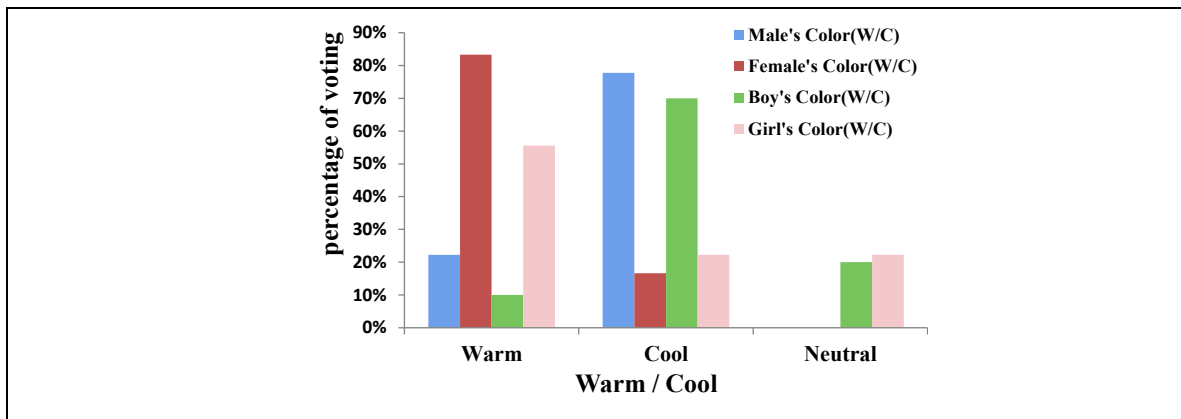


*Figure 5:Color preferences (Warm/Cool) of males and females, boys and girls*

*in percentage of each group.*

## 3.3 The Impact of Object Type

We are interested to know if object type influencing the color preference significantly. Color preferences of different group of participants on T-shirts and candies are shown in Figure 6. As we can see, the boys prefer a T-shirt in black (30%) but the girls more like a T-shirt in white (23%). It seems that children like neutral colors when buying a T-shirt. Their secondary choice was light blue. The red, pink and orange are top three preferred colors of the candy packaging among the preschoolers. Boys like orange (20%) and girls like red (45%)and pink (44%) in choosing a candy. The result implies color and taste has some connection. A red or pink candy might taste sweeter in participants' memory. It should be a psychological effect. The results of Chi-square test show that the color preference of patch (p=0.001) and candy packaging (p=0.002) of the preschoolers have significant gender difference but T-shirt doesn't (p=0.09) at 95% confidence level. In terms of the effect of object types in the preschooler group, only T-shirt versus candy packaging for girls (p=0.003) have significant different color preferences. Moreover, in the adults group, color patch and T-shirt of both males and females show significant preferance differences. The males prefer a light blue T-shirt (45%) whereas the females like a red T-shirt (33%).
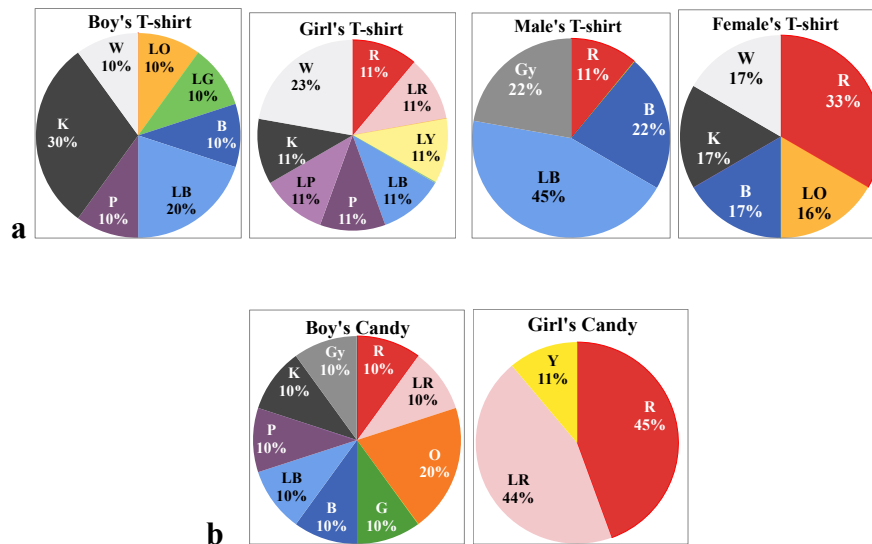
*Figure 6: Color preference between objects. (a) T-shirts and (b) candies.*

## 3.4 Adults' Surmise

We are also interested to know how accurate is the adults' surmise on preschoolers' color preferences on different type of objects. A comparison between Figure 3 and 7a confirms that adults picked stereotype colors for the preschoolers especially in guessing the preschoolers' favorite color patches. 73.3% adults surmised that the girls like Pink and 47% adults surmised that the boys like Blue (or light blue). The results are a little bit different from the preschoolers' shown in Figure 3. In reality, preschoolers chose more color categories such as gray and white. On the other hand, adults' surmise on the preschoolers' preferred T-shirt colors are quite inaccurate. The adults think the girls like light pink but in reality, the girls like a wide range of colors including white, black and purple (Figure 6a). The adults also think boys like light colors especially in light yellow and green. However, the boys prefer black instead of the light yellow.
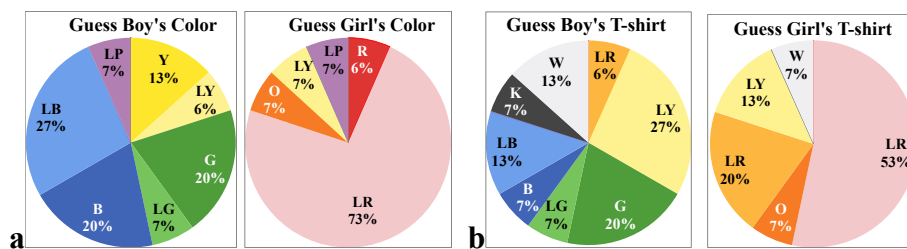


*Figure 7: Adults' surmise on: (a) favorite color patch, and (b) favorite T-shirt color of the preschoolers.*

## 4. CONCLUSIONS

This study aims to explore the color preferences of preschoolers and to compare with the viewpoint of adults in color preferences of the children, and the effects of gender, age and the association of objects also were investigated. The results show there are gender differences in the preschoolers' color preferences. Age and the association of objects also influence the color preferences to some degree. Adults chose stereotype colors – pink for

AIC2015 TOKYO - Color and Image

girls and blue for boys – especially in guessing the preschoolers' favorite color patches. However, the preschoolers prefer wide range of colors including neutral colors. We hope the results can break the gender stereotypes, prompt product designers to rethink the color usage for children and let children select more neutral and variety of colors for their everyday life.

## ACKNOWLEDGEMENTS

## REFERENCES

Chiu, S.W., Gervan, S., Fairbrother, C., Johnson, L.L, Owen-Anderson, A.F.H., Bradley, S.J, Zucker, K.J. 2006. *Sex-dimorphic color preference in children with gender identity disorder: A comparison in clinical and community controls*. Sex Roles, 55, 385-395.

Choungourian, A. 1968. *Color preferences and cultural variation.* Perceptual and Motor Skills, 26(3), 1203-1206.

Hurlbert, A. C., and Ling, Y. 2007. *Biological components of sex differences in color preference*. Current Biology, 17(16), R623 – R625.

Karp, E. M., and Karp, H. B. 1988. *Color Associations of Male and Female Fourth-Grade School Children*, The Journal of Psychology, 122 (4), 383-388.

Palmer, S. E. and Schloss, K. B. 2010. *An ecological valence theory of human color Preference*, Proceedings of the National Academy of Sciences USA 107(19), 8877 – 8882.

Ruble D.N., Lurye L.E., Zosuls K.M. 2015. *Pink frilly dresses (PFD) and early gender identit*y. Princeton Report on Knowledge, http://www.princeton.edu/prok/issues/2-2/pink_frilly.xml.

Schloss K.B., Strauss E.D., Palmer S.E.2013. *Object Color Preferences*. Color Research & Application 38(6), 393-411.

Taylor, C., Schloss, K., Palmer, S.E., and Franklin, A. 2013.*Color preferences in infants and adults are different*, Psychonomic Bulletin & Review 20(5), 916-922.

Wright, A. 1998. *The Beginner's Guide to Colour Psychology*, Colour Affects Ltd.

Ruble, D.N., Lurye, L.E., Zosuls, K.M. 2015. *Pink frilly dresses (PFD) and early gender identit*y. Princeton Report on Knowledge, http://www.princeton.edu/prok/issues/2-2/pink_frilly.xml.

Wright, A. 1998. *The Beginner's Guide to Colour Psychology*, Colour Affects Ltd.

*Address: Wei-Chun HUNG, National Taiwan University of Science and Technology, No.43, Sec. 4, Keelung Rd., Da'an Dist., Taipei 10607,Taiwan E-mails:m10325009@mail.ntust.edu.tw*

# Influence of the typical color in object memory task

Mikuko SASAKI, Yasuhiro KAWABATA

Department of Psychology, Graduate School of Letters, Hokkaido University

## ABSTRACT

This paper presents the results of a study on changes in color memory. We presented colors from two adjacent color categories to participants, and found that color memory may change in the direction towards the typical color of each object when two object images of the same color are presented. On the other hand, no significant differences between the color conditions were found for objects that do not have a typical color. These results suggest that knowledge about an object's color may affect the recognition and categorization of the color.

## 1. INTRODUCTION

When people see the color of an object, they recognize it using their accumulated knowledge. Many studies have discussed the role of color in object memory (Tanaka, Weiskopf & Williams, 2001; Nagai & Yokosawa 2006). The color of an object is categorized immediately, and stored with its shape and texture in the memory trace. If the hue of an object is typically within a particular range, these information is stored with other knowledge of the object. As the color yellow comes to mind when one hears the word "lemon," colors that are strongly associated with objects are referred to as typical colors. Delk and Fillenbaum suggested that the knowledge of an object's typical color could indeed affect an object's color perception (Delk and Fillenbaum, 1965). Moreover, several studies have reported that when objects are presented in their typical colors, recall performance is higher than when objects are presented in non-typical colors (Ratner & McCarthy, 1990). In general, it is thought that objects presented in their typical color are stored in greater detail than are objects without a typical color. However, the accuracy of color memory based on typical color might be rather low. In addition, Mitterer and Ruiter (2008) reported that observers use knowledge of an object's color to recalibrate their color categories. But the role of typical color in color categorization is not enough discussed. Thus, the present study examines whether the degree of association object and its color influences categorization.

## 2. METHOD

In this experiment, we used as stimuli colors that are difficult to clearly categorize as (e.g., intermediate colors of red and orange). Images of two objects that have a typical color and an image of an object without a typical color were presented in the same color. We compared the amount and direction of change in memory for each condition. We additionally examined whether color categories determined by using color chips are the same as when determined using object images. From these results, we consider the effect of typical color on categorization of color memory.

### 2.1 Participants

A total 68 students (67 Japanese, 1 Chinese, 28 male, 40 female, average age = 20.3 $\pm$ 1.3) participated in this experiment.

## 2.2 Stimulus

In the memory task, 18 photo images of familiar objects were prepared as stimuli. These images were classified into an A, B, or C condition depending on the color property of the objects (Figure 1). Conditions A and B consisted of objects that have a typical color. The typical colors of the objects in conditions A and B were adjacent, such as red and orange. If the image in condition A was a tomato, for example, condition B was a persimmon. There were 6 pairs of stimuli in conditions A and B. The objects classified into condition C did not have a typical color. In addition, the three object conditions were presented with two color conditions of consisting of colors intermediate from the typical and non-typical colors of objects A and B. The objects and their typical colors are listed in Table 1. Participants performed two of these six conditions. In addition, 7 color selection charts were created for each condition (Figure 2). In each chart, the correct color and six other neighboring colors were indicated: three neighboring colors clockwise from the correct on the Mansell hue ring were selected, and three colors counterclockwise from correct color on the Mansell Hue ring were selected. The color difference $\Delta E$ (the L*a*b* color space) between each chart was about 13.6 on average. In the color categorization task, 48 colors, including the same color used in the memory tasks and those on the color charts, were selected as stimuli for assessing color categorization.

*Table 1. Stimulus objects of the 3 object conditions.*

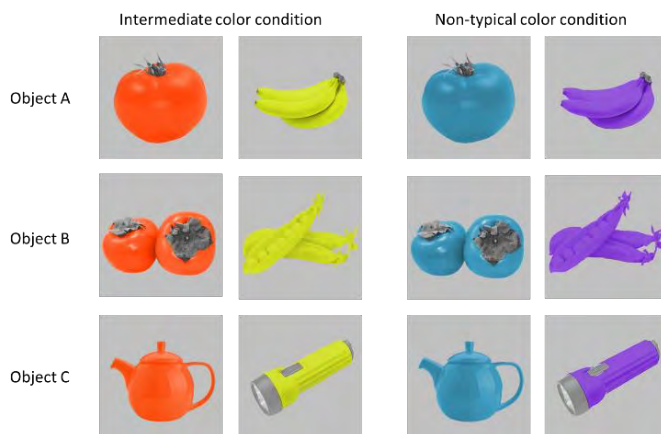|  | Red-Orange | Orange-Yellow | Yellow-Light green | Green-Blue green | Blue-Violet | Purple-Red purple |
|---|---|---|---|---|---|---|
| Object A | tomato | orange | banana | cucumber | grape | eggplant |
| Object B | persimmon | lemon | peas | ramune bottle | blueberry | red radish |
| Object C | tea pot | cap | flash light | polo shirt | camera | ribbon |



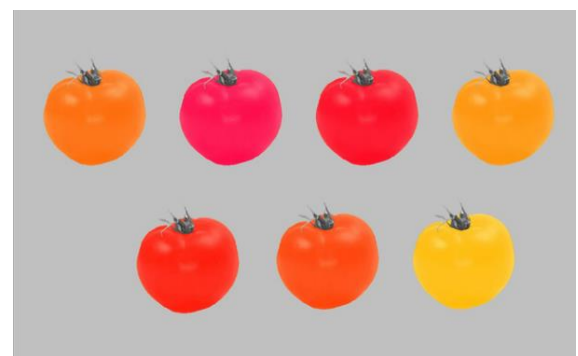*Figure 1. Example of stimulus images.*



*Firure 2. Example of a screen in color recognition task.*

## 2.3 Experimental Procedure

After instruction, participants began the memory task. All images were displayed on 24.1-inches LCD screen. The observation distance to the screen was 80 cm, and the view angle

was 5-7 degrees. In this task, color images appeared for 2 sec each at the center of the screen, and the participants observed the image. A total of 12 color images were presented. Next, participants completes a 5-10 min interference task in which they subtracted two-digit numbers or practiced typewriting. After this interference task, all participants began the object recognition task. In the recognition task, participants were asked to select the object they observed during the memory task from the object list and mark it with a check. There were 24 object names, including the correct answer, on the list. Following this, the participants were asked to choose the color of the objects observed during the memory task. At first, grayscale images were displayed for 2 sec. Next, seven images of the same shape but painted in different colors were presented. These seven images appeared in random positions. The participants were instructed to indicate which object were same color as that presented during the memory task by clicking on the image with an optical mouse. When they clicked the mouse, the next trial began. There were a total of 12 trials. Then, participants were instructed to classify 48 color chips of the color category. The 48 color chips (3 cm × 3 cm) were singly presented at random, and participants were to indicate whether the presented color applied to any color category on the screen (see Figure 3). Nine color names and frames were presented on the screen, and participants were to move the color chips using the mouse. The color categories that were prepared in advance were red, orange, yellow, yellow-green, green, light blue, blue, purple, and brown. Participants were allowed to create a new category if they did not think any of the displayed categories were accurate. The experiment concluded following the color category task.
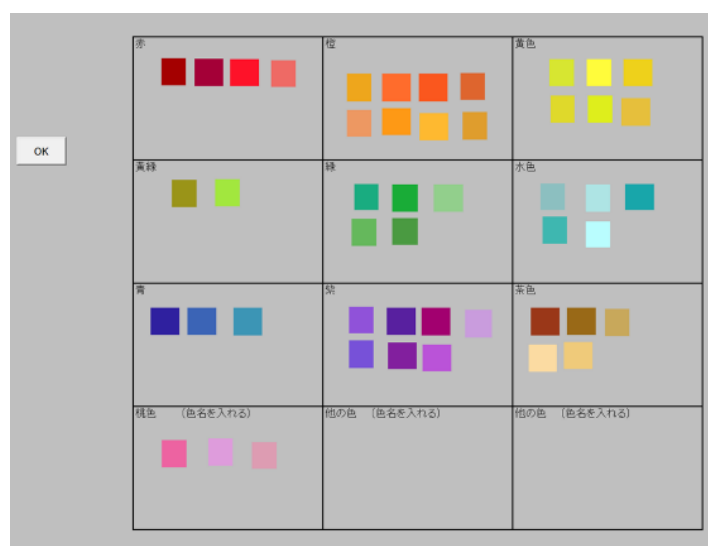


*Figure 3. A screen example after color categorization task.*

## 3. RESULTS AND DISCUSSION

To compare recognition of object names across the conditions, we calculated the number of correct objects participants selected from the list. The average of correct rates for each condition were compared in a 3 (object: object A, B, C) × 2 (color: intermediate vs non-typical) ANOVA. There was a significant effect of object [$F_{(2, 130)} = 3.26$, $p < .05$]. Object A (93.6%) was associated with a significantly higher percentage of correct answers than was object C (85.8%). If an object was presented in a color close to the typical color of object A,

recognition of the object name was better than objects without a typical color. Thus, when an object is associated with color, its color information facilitates recognition of the object.

Next, we investigated recognition of the object color rather than the object name. From the results of the recognition task, it was examined whether the selected color changed in either direction and how far it shifted from the stimulus color. The differences between the 12 selected colors and 12 stimulus colors were calculated using the L*a*b* color space. Change in direction was calculated as + changes clockwise on Mansell hue circle, and - changes in the counter-clockwise direction. The amount of change in each trial was analyzed AVOVA. There was a significant effect of color [F (1, 130) = 6.7, p < .05] (Figure. 4). Analysis results of the average change in direction did not indicate any significant effects of color and object, but did show a significant interaction [F (2, 130) = 7.16, p < .01]. Examination of the simple main effects revealed that in the close color to the typical color of objects A and B, the changes in direction were significantly different between objects A and B (p < .001), and objects A and C (p < .001). In addition, in the intermediate color condition of objects A and B, there was a clear change in direction relative to the non-typical color condition. The left side of Figure 4 indicates that in the object B condition, the direction changed to clockwise, and in the object A condition, it changed to counterclockwise. In addition, we calculated the number of different category cases between the stimulus color and the selected color in the color categorization task. Results of the $\chi 2$ test showed a significant difference between objects that have typical color and objects that do not have a typical color (p < .05). This suggests that when the participants viewed an object with a color close to the typical color, they selected a color belonging to a different category of the color they saw in the memory task. Thus, information regarding the typical color of an object influenced color category boundaries.
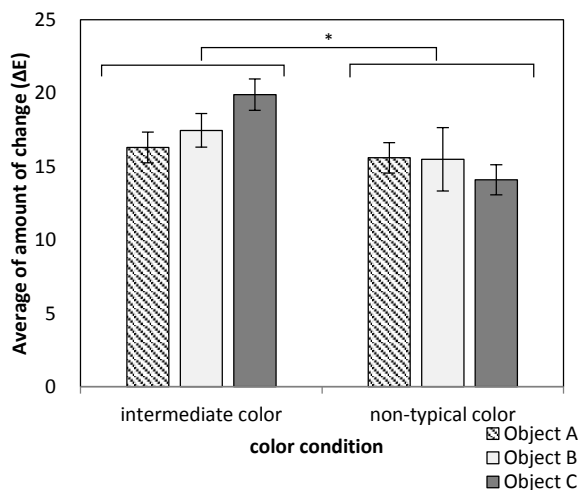


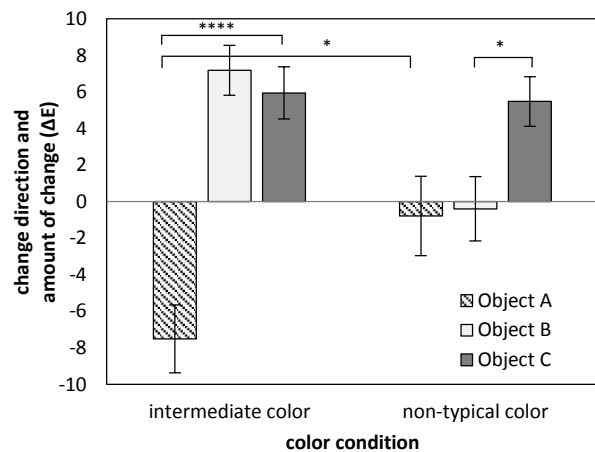Figure 4. difference between stimuli color and selected color.



Figure 5 change direction and amount of change.

## 4. CONCLUSIONS

From these experiments, it has become clear that human color memory shifts to its own typical color of the object when 2 objects of a different typical color are painted with an

intermediate color. Moreover, the present results suggest that in the case of objects that do not have a typical color, color condition does not impact memory. It is suggested that the strength of an association between an object and its color involves the accuracy of color memory. Further, it is possible that information regarding the representative color does not necessarily promote accuracy of detailed color memory. In the object condition that have a typical color, the participants often selected a color that belong a different category from a stimulus color's one. Colors close to an object's typical color promote readjustment of color category boundaries when recognizing the object.

## REFERENCES

Delk, J.L., & S. Fillenbaum. 1965. Differences in perceived color as a function of characteristic color. *American Journal of Psychology* 78: 290–293.

Mitterer, H., J.P. Ruiter. 2008. Recalibrating Color Categories Using World Knowledge. *Psychological Science* 19(7): 629-634.

Nagai, J., K. Yokosawa. 2006. Color diagnosticity or category: Which determines the role of color in visual object recognition?. *The Japanese Journal of Cognitive Psychology* 3(2): 181-192.

Ratner, C., & J. McCarthy. 1990. Ecologically relevant stimuli and color memory. *Journal of General Psychology* 117: 369-377.

Tanaka, J., D. Weiskopf, & P. Williams. 2001. The role of color in high-level vision. *Trends in Cognitive Sciences* 5: 211–215.

*Address: Mikuko SASAKI & Yasuhiro KAWABATA,*
*Department of Psychology, Graduate School of Letters, Hokkaido University,*
*Kita 10 Nishi 7, Kita-ku, Sapporo, 060-0810, JAPAN*
*E-mails: sasaki-m@let.hokudai.ac.jp, kawabata@let.hokudai.ac.jp*

# Neural basis of color harmony and disharmony based on two-color combination

Takashi IKEDA,[1] Naoyuki OSAKA[2]
[1] Graduate School of Engineering, Osaka University
[2] Graduate School of Letters, Kyoto University

## ABSTRACT

Prior to functional imaging study, individual color harmony scores were determined by rating experiment. Each participant rated 351 two-color combinations stimuli presented against a gray background on a 9-point scale. Based on the results, we made individual data sets for each participant to optimise the subjective experience of color harmony and disharmony; then we selected 30 stimuli in each class according to highest, middle, and lowest scores. We conducted functional magnetic resonance imaging to determine the brain regions activated by harmonious and disharmonious color combinations in comparison to neutral combination. Each participant was instructed to rate a stimulus on a 3-point scale. During the presentation of Harmony stimuli, we found that the left medial orbitofrontal cortex was activated, while, bilateral amygdala and right inferior frontal gyrus were activated under the presentation of Disharmony stimuli. To quantify the relationship of two colors, we introduced five indexes based on CIELAB color space, i.e. difference in lightness ($\Delta L^*$), mean lightness ($meanL^*$), difference in chroma ($\Delta C^*$), mean chroma ($meanC^*$), and difference in hue ($\Delta H^*$). This experiment revealed that there were no significant differences between Neutral and Harmony stimulus combinations, however, Disharmony stimulus had significant differences in $\Delta L^*$, $meanL^*$, $meanC^*$ and $\Delta H^*$ in comparison to Harmony or Neutral. We found that color disharmony depended on perceptual properties of the actual stimulus. Taken together, our findings suggest that color disharmony depends on its stimulus properties and unconscious neural processes mediated by the amygdala, whereas color harmony is harder to discriminate based on color characteristics and is supported by processing aesthetic value within the medial orbitofrontal cortex.

## 1. INTRODUCTION

To make our daily lives more comfortable, we tend to gravitate toward harmonious color combinations. This can be seen in the clothing combinations we select, and so on. Research on color harmony theory has a long history. Theory of Colours, a book published by Goethe in 1810, established a wheel describing principal components of colors, which are consisted of three primary (yellow, red, and blue) and three secondary colors (orange, green, and violet); it was thought that harmonious relationships existed between colors that were opposite (complementary) each other on this wheel (Von Goethe 1970). Additionally, Munsell (1907) developed a color order system that was based on three perceptual properties: hue, value (lightness), and chroma. More recent study has focused on how to generate harmonious color combinations based on hue, chroma, and lightness using CIELAB to quantitatively assess differences in uniform color space (Ou and Luo 2006).

Previous studies revealed that color harmony could be predicted by these three properties. However, the neural mechanisms which underlie the aesthetic and emotional aspects of color, specifically harmony or disharmony, are still poorly understood. It is known that

color information is first processed on the retina followed by higher visual cortices (McKeefry and Zeki 1997). Since, color harmony has been reported to exert a pleasing effect (Judd and Wyszecki 1963), brain regions activated by harmonious or disharmonious color combination should be able to process both perceptual and affective, in particular aesthetic aspects of color. Moreover, disharmonious color combinations might elicit an opposite, negative emotion.

Previous studies have indicated that color harmony can be influenced by many factors such as shape, size, the number of colors, and the relative positions of colors in a combination (Hård and Sivik 2001, Burchett 2002). Therefore, in the current study, we first examined the association between perceptual properties and color-harmony score with 351 color combinations presented against a gray background. The use of different pairs of color combinations allowed us to assess the relationship between two colors and the three perceptual properties: lightness, chroma, and hue. We then conducted functional magnetic resonance imaging (fMRI) to examine the brain regions which were activated during the presentation of harmonious and disharmonious combinations compared with the neutral stimuli. This method appears to be the simplest way to examine the neural correlates of aesthetic preference of color.

## 2. METHOD

### 2.1 Participants

Eighteen participants (6 females and 12 males, aged 19–30) attended the fMRI study All participants had normal or corrected-to-normal vision, and none had a history of neurological or psychiatric disorders. Moreover, none of the participants had any special experience with art or color design. We used Ishihara plates for the color vision test under a fluorescent light simulating D65 illuminant. Written informed consent was obtained from all participants, the experiments were conducted in accordance with the ethical guidelines of the Declaration of Helsinki, and all methodology was approved by the Committee of Medical Ethics, Graduate School of Medicine, Kyoto University.

### 2.2 Experimental Procedure

In the fMRI experiment, participants viewed stimuli on a screen projected (U2-X2000, PLUS Corporation, Japan) through a mirror attached to the head coil. Earplugs were used to reduce the noise from the MRI scanner. We calibrated the projector using a luminance colorimeter (CS-100A, Konica Minolta, Japan). We made a color palette that contained 27 colors (six hues across four tones and three achromatic colors, see Figure 1). These colors were chosen from the Practical Color Co-ordinate System (PCCS: developed by Japan Color Research Institute), which has been determined to be suitable for making harmonious color combinations.

From the results of the preliminary experiment, we made individual data sets for each participant to optimise the subjective experience of color harmony and disharmony; we selected 30 stimuli in each condition according to highest, middle, and lowest given scores individually.

The fMRI experiment was conducted in a 3-T MRI scanner (Trio, Siemens, Germany). A forehead strap and form pads were used to reduce head motion. Functional images were taken with a gradient echo echo-planar pulse sequence (TR = 2500 ms, TE = 30 ms; flip angle = 90°, voxel size = 3 mm × 3 mm × 3 mm; 36 axial slices). To minimise signal loss

in the orbitofrontal cortex caused by local susceptibility gradients, we used a tilted acquisition sequence at 30° to the AC-PC line (Deichmann et al. 2003). Following the acquisition of functional images, anatomical T1-weighted images (MPRAGE sequence, voxel size = 0.94 mm × 0.94 mm × 1 mm, 208 slices) were collected.
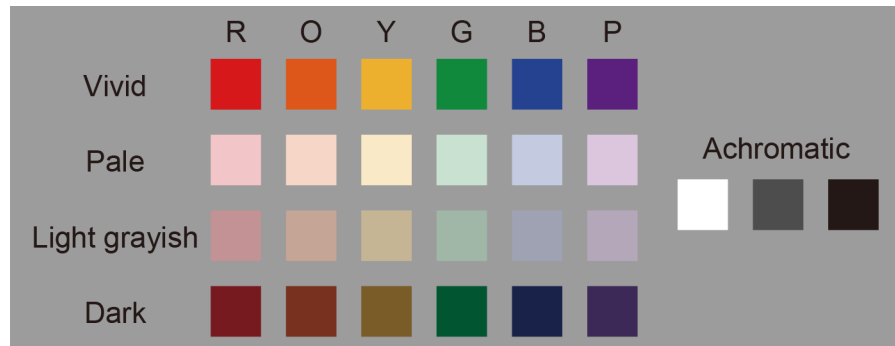


*Figure 1: Color pallet used in this experiment.*

Following the presentation of a black fixation cross (for 1000 ms), participants were instructed to rate a stimulus on a 3-point scale (1 = disharmony, 3 = harmony) within 2500 ms by pressing three buttons on the response box in their right hand. After the rating, we set a pseudo-randomised inter-trial interval (2000, 2500, or 3000 ms) before starting the next trial. Participants rated for 180 trials (30 stimuli × 3 data sets × 2 repetitions) and 60 catch trials in which they had to press any button as soon as the black fixation point turned white. All trials were presented in a pseudo-randomised order.

## 2.3 Image Processing and Analysis

Image processing and analysis were performed using SPM8 (Wellcome Department of Cognitive Neurology, London, UK) running on MATLAB (MathWorks Inc., Sherborn, MA, USA). First, we conducted slice acquisition timing correction to functional images. These images were realigned to the mean image for correction of head movement. T1-weighted anatomical images were then normalised to the MNI space, and its parameter was applied to normalise the realigned functional images. Images were then smoothed with an isotropic Gaussian kernel of 6-mm full width-half maximum, and low-frequency noise was removed using a high-pass filter (time constant 128 s).

Individual analysis was performed with a fixed effect model. Statistical parametric maps were calculated to identify voxels with event-related BOLD signal changes using the general linear model (GLM). Trials were classified into three conditions (Harmony, Neutral, and Disharmony) by the responses of each participant during functional scanning. Each event defined as the onset of a stimulus presentation was convolved with a canonical hemodynamic response function (HRF) to provide regressors for the GLM. Head movement parameters calculated in the realignment step and onsets of the catch trials convolved with HRF were included in this model as regressors of no interest. Lastly, contrast images for 'Harmony vs. Neutral' and 'Disharmony vs. Neutral' were run through a second-level *t*-test to make statistical maps at the group level. The statistical threshold was set at *p* < 0.001 (uncorrected).

# 3. RESULTS AND DISCUSSION

Table 1 shows activated regions during presentation of Harmony and Disharmony stimuli when compared to Neutral stimuli as baseline. During the presentation of Harmony stimuli, we found that the left medial orbitofrontal cortex (mOFC) was activated, while, bilateral amygdala and right inferior frontal gyrus were activated under the presentation of Disharmony stimuli (Figure 2). These results are reported as MNI coordinates.

*Table 1. Activated areas in each contrast.*

| Contrast | Anatomical label | BA | Coordinates | | | Z | k |
|---|---|---|---|---|---|---|---|
| | | | x | y | z | | |
| Harmony > Neutral | Medial Orbitofrontal Cortex | 10/11 | -4 | 56 | -2 | 3.53 | 9 |
| Disharmony > Neutral | Cerebelum | | 22 | -44 | -36 | 5.53 | 57 |
| | Inferior Frontal Cortex | 45/47 | 50 | 32 | -2 | 4.26 | 33 |
| | Hippocampus | | -20 | -38 | 10 | 4.15 | 27 |
| | Amygdala | | -10 | -4 | -14 | 4.07 | 24 |
| | Precentral Gyrus | 6 | 56 | -4 | 36 | 3.91 | 57 |
| | Amygdala | | 20 | -8 | -20 | 3.78 | 14 |
| | Anterior Cingurate Cortex | 32 | -6 | 48 | 14 | 3.71 | 24 |
| | Middle Temporal Cortex | 39 | 46 | -56 | 20 | 3.70 | 21 |
| | Cerebelum | | -14 | -50 | -32 | 3.68 | 33 |
| | Superior Temporal Cortex | 39 | 46 | -32 | 20 | 3.57 | 41 |
| | Celeberum | | 14 | -38 | -32 | 3.56 | 14 |
| | Middle Temporal Cortex | 38 | -60 | -8 | -20 | 3.53 | 15 |
| | Inferior Frontal Cortex | 45 | 42 | 22 | 12 | 3.45 | 14 |

(BA : Brodmann Area)
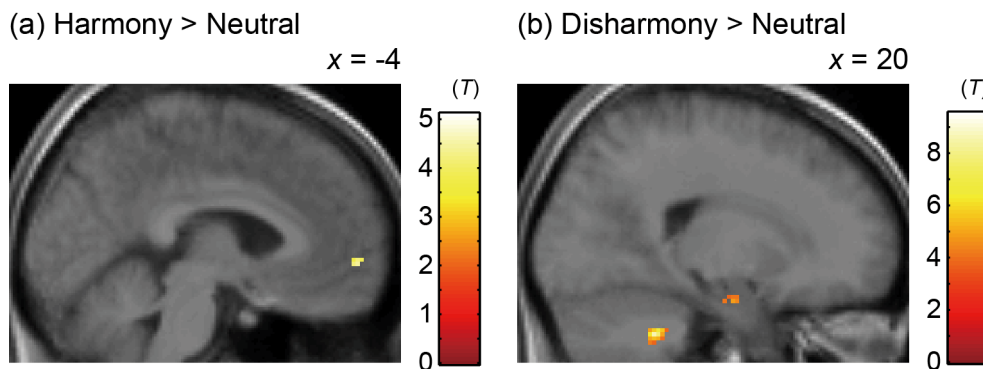


*Figure 2: Statistical parametric maps rendered on a slice of T1-weighted image.*

The fact that harmonious stimuli combinations activated the mOFC was consistent with previous studies showing that this region was activated when individuals felt an aesthetically pleasing experience in the musical context (Blood et al. 1999) and the visuo-spatial context (Kawabata and Zeki 2004, Vartanian and Goel 2004, Ishizu and Zeki 2011). Therefore, activation of the mOFC is not restricted to experiences of color harmony, but is involved in various aesthetic experiences regardless of modality.

We also found that disharmonious stimuli combinations activated bilateral amygdala and several cortical regions including the right IFC, anterior cingulate cortex, and middle/superior temporal cortex. It is well established that the amygdala plays an important role in evaluating the biological significance of affective visual stimuli. This subcortical region has been shown to activate when emotionally negative stimuli are presented, and furthermore, the activation of the amygdala might involve unconscious processing of affective visual stimuli (Pessoa and Adolphs 2010).

To quantify perceptual properties of two colors, we introduced five indexes made from CIELAB color space, i.e. difference in lightness ($\Delta L^*$), mean lightness ($meanL^*$), difference in chroma ($\Delta C^*$), mean chroma ($meanC^*$), and difference in hue ($\Delta H^*$) (Note: we avoided using mean hue since we determined it to be an unsuitable index; for example, the mean hue of red and green is yellow). From the results of one-way ANOVAs, we determined that main effects of $meanL^*$ [$F_{(2,34)} = 24.44$, $p < 0.001$], $\Delta L^*$ [$F_{(2,34)} = 14.08$, $p < 0.001$], $meanC^*$ [$F_{(2,34)} = 13.02$, $p < 0.001$], and $\Delta H^*$ [$F_{(2,34)} = 23.04$, $p < 0.001$] were significant; however, the main effect of $\Delta C^*$ [$F_{(2,34)} = 1.10$, $p = 0.344$] was not significant. Additionally, multiple comparisons using Shaffer's modified Bonferroni procedure revealed that there were significant differences between Disharmony and Neutral, and between Disharmony and Harmony ($p < 0.05$; Figure 3). However, there were no significant difference between Neutral vs. Harmony ($p > 0.05$) in any indexes. Perceptual characteristics of disharmonious stimuli were different from those of neutral and harmonious stimuli. This results suggest that disharmonious combination can be determined by perceptual characteristics, including darkness, saturation, and complementary color combination.
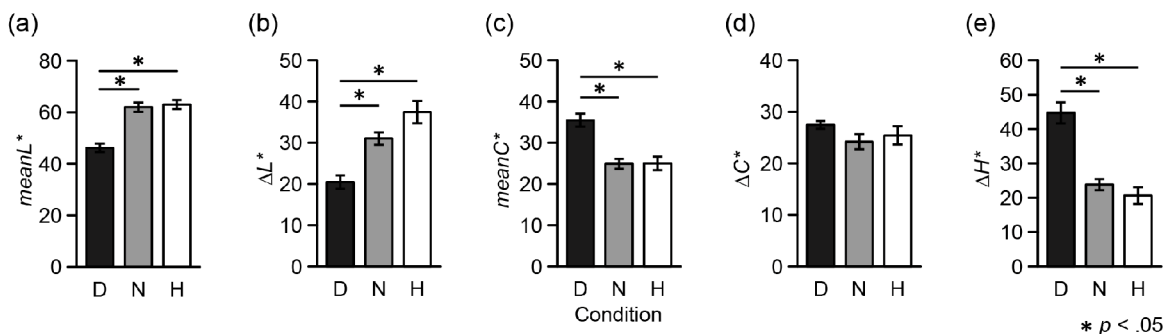


*Figure 3: Five indexes of color combination stimuli across the three conditions.*

Previous studies have treated the scoring of color harmony as a bipolar single scale; however, the results of our fMRI experiments suggest that color harmony contains two processes. First, color disharmony depends on the stimulus itself and the unconscious neural process that is mediated by the amygdala. In contrast, color harmony is hard to determine based on color characteristics alone, and this is supported by processing aesthetic value within the mOFC.

## 4. CONCLUSIONS

Harmonious color combination was represented in mOFC. However, amygdala was activated by a disharmonius color combination, which was easily determined by perceptual

characteristics in the CIELAB color space. A bipolar single scale on color harmony might consist of independent neural mechanisms.

## ACKNOWLEDGEMENTS

## REFERENCES

Blood, A. J., R. J. Zatorre, P. Bermudez and A. C. Evans (1999). Emotional responses to pleasant and unpleasant music correlate with activity in paralimbic brain regions. *Nature Neuroscience* 2 (4): 382-387.

Burchett, K. E. (2002). Color harmony. *Color Research and Application* 27 (1): 28-31.

Deichmann, R., J. A. Gottfried, C. Hutton and R. Turner (2003). Optimized EPI for fMRI studies of the orbitofrontal cortex. *Neuroimage* 19 (2 Pt 1): 430-441.

Hård, A. and L. Sivik (2001). A theory of colors in combination - A descriptive model related to the NCS color-order system. *Color Research and Application* 26 (1): 4-28.

Ishizu, T. and S. Zeki (2011). Toward a brain-based theory of beauty. *PloS One* 6 (7): e21852.

Judd, D. B. and G. Wyszecki (1963). *Color in business, science, and industry*. New York, Wiley.

Kawabata, H. and S. Zeki (2004). Neural correlates of beauty. *Journal of Neurophysiology* 91 (4): 1699-1705.

McKeefry, D. J. and S. Zeki (1997). The position and topography of the human colour centre as revealed by functional magnetic resonance imaging. *Brain* 120: 2229-2242.

Munsell, A. H. (1907). *A color notation*. Boston, MA, Geo. H. Ellis Co.

Ou, L. C. and M. R. Luo (2006). A colour harmony model for two-colour combinations. *Color Research and Application* 31 (3): 191-204.

Pessoa, L. and R. Adolphs (2010). Emotion processing and the amygdala: from a 'low road' to 'many roads' of evaluating biological significance. *Nature Reviews: Neuroscience* 11 (11): 773-783.

Vartanian, O. and V. Goel (2004). Neuroanatomical correlates of aesthetic preference for paintings. *Neuroreport* 15 (5): 893-897.

Von Goethe, J. W. (1970). *Theory of colours*. Cambridge, MA, MIT Press.

*Address: Takashi IKEDA, Ph.D., Graduate School of Engineering, Osaka University, 2-1 Yamadaoka, Suita, Osaka, 565-0871, JAPAN*
*E-mails: tikeda@ams.eng.osaka-u.ac.jp, nosaka@bun.kyoto-u.ac.jp*

# Psychological hue circle of blind people and development of a tactile color tag for clothes

Saori OKUDERA, Ken SAGAWA, Yuko NAKAJIMA, Natsumi OHBA,
Shoko ASHIZAWA
Department of Clothing, Faculty of Human Science and Design,
Japan Women's University

## ABSTRACT

Totally blind people have a strong interest in color though they are not able to see it. Women, in particular, like to know the color of their clothes and enjoy color coordination of their wear. In order to meet this need, psychological mechanism of color identification of blind people was investigated and a method to convey color information was developed by means of the tactile sense.

In the study of investigating color identification of the blind who has no experience of seeing color in his/her life, psychological distances (or distinctness) among a total of 10 fundamental colors (red, orange, yellow, … etc.) were measured in a 5 point scale from "very far" (point 5) to "very close" (point 1). From these perceptual distances and using the MDS (multi-dimensional scaling) method, a possible placing of those 10 colors was derived. The result obtained when averaged over 16 subjects was that the 10 fundamental colors showed a clear hue circle with exactly the same order of colors as those obtained for the sighted people.

On the basis of this experimental result, a tactile tag designed with a hue circle was developed in which ten small tactile dots were lined up on a circle each representing fundamental color with one bigger dot or hole to show the color for identification. Tactile experiments were done also to confirm the appropriate size of the color circle and a tactile dot size. And finally, a color tag was developed from a few materials (acrylic button, embroidery, and artificial leather) and was attached to a T-shirt for the field test which showed successful color identification by blind people.

## 1. INTRODUCTION

Color is one of the important information in our daily life not only for functional means such as traffic signals for safety but also for some emotional purpose like ladies' fashion. Unfortunately totally blind people are not able to use and enjoy those color information. This study was triggered by a request from a blind lady that she would like to know by herself the color of clothes she is wearing.

In order to develop a method to meet her request, a few questions were raised: (1) what is the effective way to let her know the color; voice or Braille or some other means, (2) how the blind person, the congenitally blind person in particular, understands the color, (3) what is the feasible way to apply the method to clothes.

The 2nd question is most interesting in color science, and some studies were already done (Shepard and Cooper, 1992; Shinn and Ohmi, 2012). Those studies provided us some important insight about the color recognition of the blind people. However, it was difficult

to draw any definite conclusion and this lead us to the need for carrying out a new experiment which give us a directly useful result for developing a method for conveying color information to blind people.

In addition to this scientific interest, we were clearly aware that this type of study should extend to the level practically useful. This means the development of a color tag that can be attached to clothes. Tactile marking was one possible way to develop and the suitable design for this was investigated.

## 2. HUE CIRCLE OF BLIND PEOPLE

In order to investigate the identification and psychological representation of color in totally blind people, particualry in those who have never seen the color from the birth (congenitally blind), an experiment was carried out in which the psychological distances or distinctness of any two colors were scaled in 5 points scale, and by applying the multi-dimensional scaling (MDS) to those scaled distance data, the scheme of color of blind people was investigated.

### 2.1 Experiment

A total of 10 fundamental colors addressed in Munsell hue circle, such as red(R), orange(YR), yellow(Y), green-yellow(GY), green(G), blue-green(BG), blue(B), pueple-blue(PB), purple(P), and red-purple(RP), were selected as test colors and any two-colors combination was made by those fundamental colors and presented verbally to the subject who was totally blind. The subjet was asked how those two colors were considered different or close to each other.
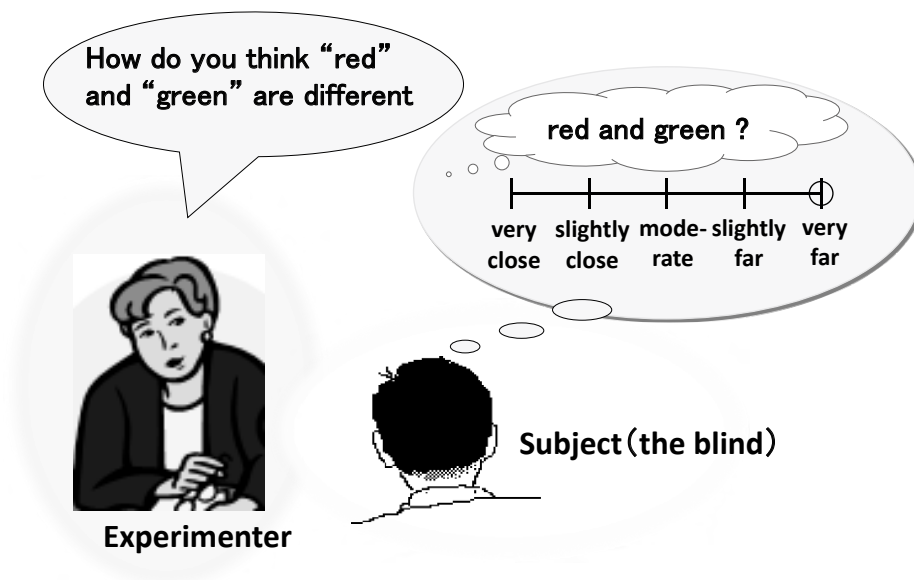


*Figure 1: Experimental procedure to evaluate the psychological difference of two colors*

Figure 1 illustrates this procdure. The experimenter picked up any of two colors among 10 fundamental colors and asked the blind subject the difference of those two colors. The

subject estimated the difference from his/her own understanding of those colors and responded the difference in 5 points scale from very close (point 1) to very far (point 5). For example, as shown in Figure 1, if he/she regarded red and green are very different he/she gave the answer of "point 5, very far". This procedure was repeated for one subject until a total of 45 pairs of colors were presented.

A total of 16 subjects, all totally blind, participated in the experiment. Ten subjects are congenitally or almost congenitally blind, and the remaining 6 subjects lost their sight at ages between 5 to 18 years old and have clear experience of seeing color. Male and female were just evenly balanced.

## 2.2 Results and discussion

The data were originally obtained in a form of 10 x10 matrix for all the combination of 10 colors and a half of the matirx was entered by data avoiding the same entry in the matrix. These data, individual or averaged over 16 subjects, were analyzed by the MDS method to seek for the best possible placement of those 10 colors to satisfy the numerical relationships reported by subjects among the colors. The MDS analysis was done for each individual data as well as for the averaged one.

Figure 2 shows the result obtained for the averaged distance data for the 10 test colors. Two dimentional space is mathematically sufficient to discribe the relationships of the colors and in this space the ten test colors were reasonbly placed as shown in Figure 2. It is clear that the 10 colors form a beautiful circle with the color order exactly same as normal color vision. It is noted that the hue circle obtained by MDS only expresses the relationships among colors and, therefore, the direction of the color order, such as clockwise or unticlockwise, does not matter.
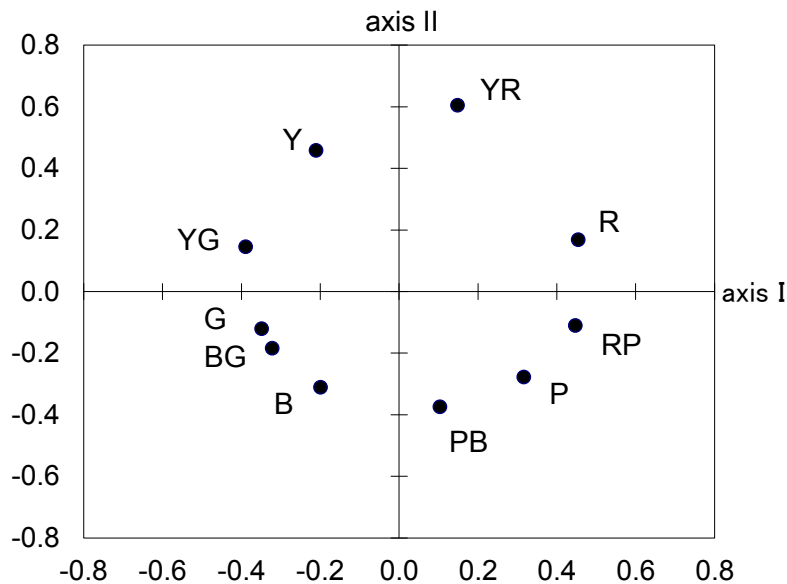


*Figure 2: Placing of 10 test colors in a two dimensional space obtained from psychological distances of the colors and analyzing with the MDS method*

Although the averaged data shows a clear circle as shown in Figure 2, it is not all the 16 subjects who exhbits such a clear hue circle. As shown in Figure 3(b) as an example, some subject did not show the hue circle, while some other subject exhbited a clear hue circle more or less as shown in Figure 3(a) as an example. Three subjects failed to show the hue circle, while the remaining 13 subjetcs showed it. It was found that those subjects who did not show a clear hue circle were all male and they had not been interested in color at all in his/her daily life and they ware mostly the blackish colors selected by their families. This means that the blind people take and understand the color information from their daily conversation which contains much of color terms, and if they have no interest in getting such color informaiton the concept of hue cirlce does not seem to be establsihed.

Previous studies on the color representation of the blind (Shepard et al, Shin et al) mostly indicated that the hue circle was not established or understandable by the blind. On the contrary the present study, being based on relatively larger number of subjects, showed that the hue circle or at least the relationship of colors of hue cirlce was understandable by blind people except for some cases.
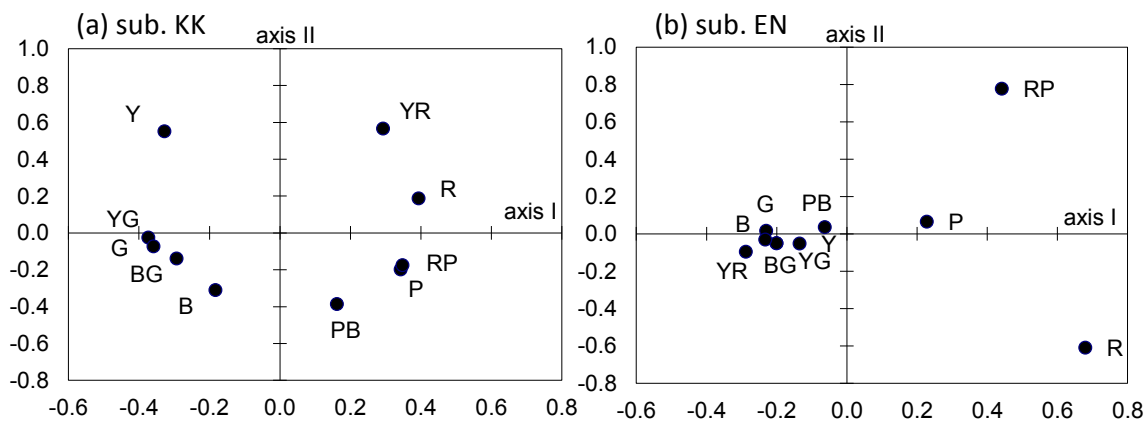


*Figure 3: Two typical example of color placing obtained by MDS for the blind subjects showing (a) a clear hue circle, and (b) no hue circle*

## 3. DESIGN AND DEVELOPMENT OF COLOR TAG FOR COLOTHES

Being based on the experimental results described above, a tactile tag for clothes was designed so as to inform color information to the blind. As shown in Figure 4, the tactile tag consists of a total of 10 small tactile dots which forms a circle and each dot represents a fundamental color of a hue circle. With red at the top and placing orange, yellow, green-yellow, etc in clockwise until it comes to the red-purple, and by enlarging or making a hole for one of the ten dots (in case of green, see Figure 4) it is possible to tell a blind person the color of clothes which the tag indicates through touching the dot or the hole. At the center of the circle three achromatic colors, white, gray, and black, are placed, and if the color is pale or desaturated, an inner circle is used.

Tactile experiment was also done to confirm the appropriate size of the circle and the dot.

Finally, we made a set of test tags from a few different materials (acrylic button, embroidery, and artificial leather) and attached them to T-shirts of different colors. Figure 5 shows some examples of the tag of each material and T-shirts the tags attached. Ten blind people participated in the color identification experiment of T-shirts color with the tactile tags. They showed almost perfect performance in identifying colors of the T-shirts (93 %

AIC2015 TOKYO - Color and Image

correct). The feeling of touch on the tag was also evaluated by psychological experiement and the result was also satisfactory. Among those test tags, the acrylic button was found to be the best for identifying color, and the artificial leather for tactile feeling.
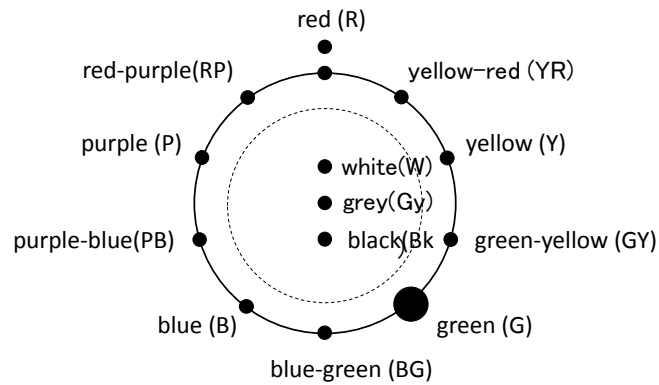


*Figure 4: A color tag designed for representing color for the blind by tactile dots*
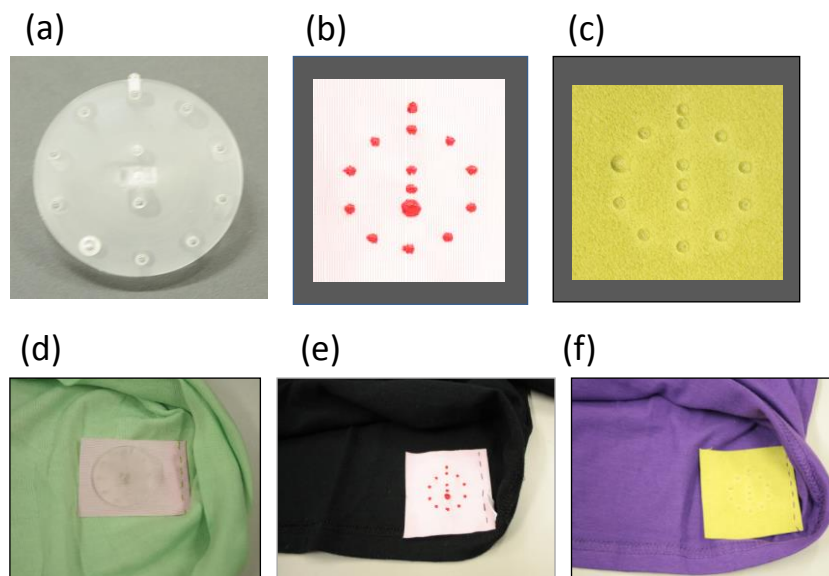


*Figure 5: A color tag actually developed and attached to T-shirts. (a) and (d) are acrylic button, (b) and (e) are embroidery, and (c) and (f) are artificial leather.*

## 4. CONCLUSION

Through psychological scaling experiment on color distinctness of blind people and analysing those data by multi-dimentioanl scaling (MDS), the relationships among fundamental colors were found to be nearly same for blind people as those for people with normal color vision. This means that hue circle was quite reasonable to tell the color to the blind people. A tactile color tag which has a hue circle made by ten tactile dots

representing fundamental colors with three dots at the center representing achromatic white, grey, and black colors, was developed for informing blind people the color of their clothes. The successful test results of color identification by the tag confirmed that the idea of tactile color tag with the hue circle was very useful.

## ACKNOWLEDGEMENTS

## REFERENCES

Shepard, R.N. and Cooper, L.A. 1992. Representation of colors in the blind, color-blind, and normally sighted, Psychological Science, 3(2), 97-103.
Shin E. and Ohmi G. 2011. Color Vocabularies and Their Cognitive Contents in the Congenitally Blind, 35(3), 203-211.

*Address: Dr. Ken SAGAWA, Department of Clothing, Human Science and Design,*
*Faculty of Human Science and Design, 2-8-1, Mejirodai, Tokyo 112-8681, JAPAN*
*E-mails: sagawa@fc.jwu.ac.jp*